Roussos Dimitrakopoulos
Editor

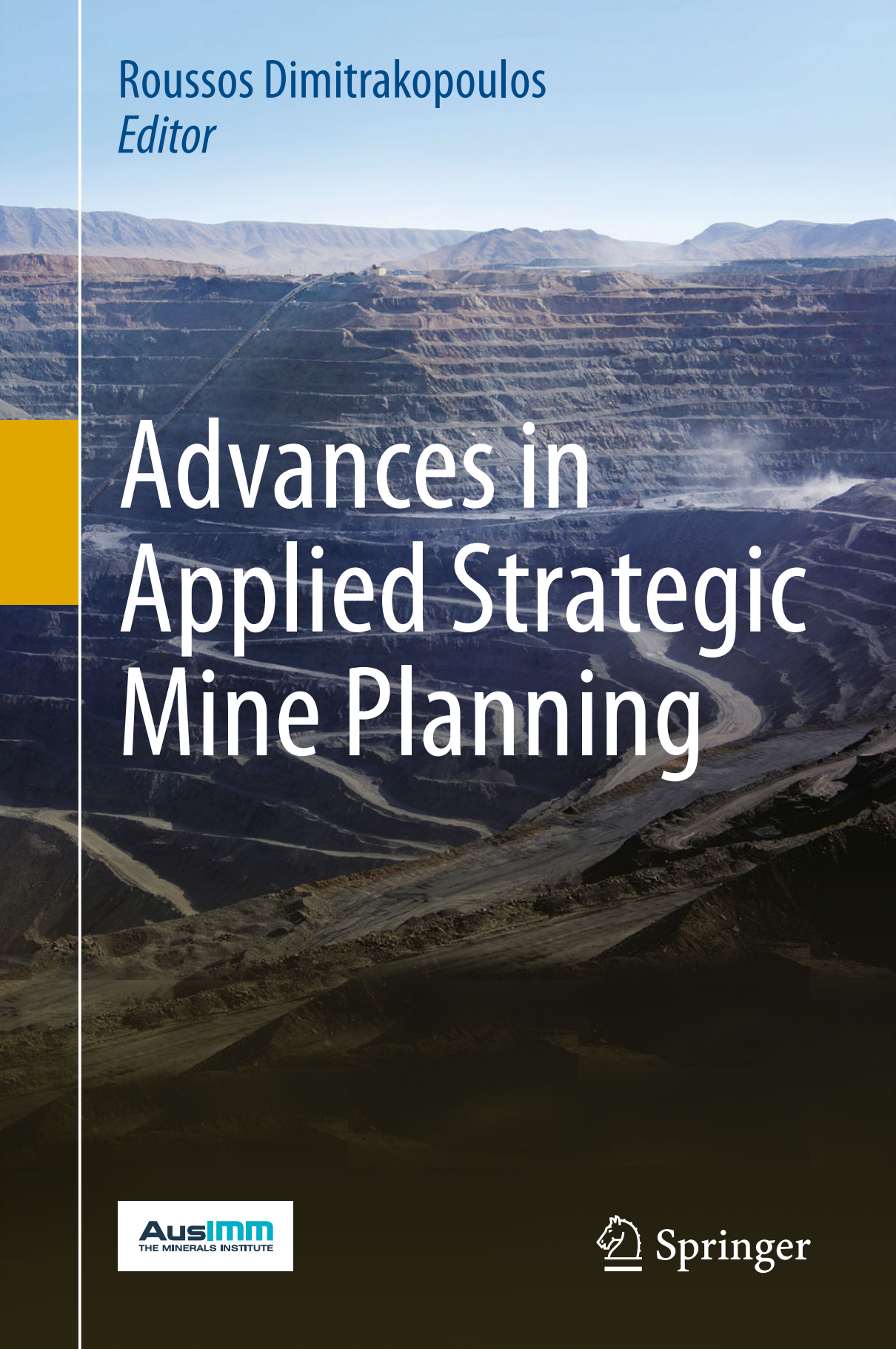

Advances in Applied Strategic Mine Planning

AusIMM
THE MINERALS INSTITUTE

Springer

Advances in Applied Strategic Mine Planning

Roussos Dimitrakopoulos
Editor

Advances in Applied Strategic Mine Planning

AusIMM
THE MINERALS INSTITUTE

Springer

Editor
Roussos Dimitrakopoulos
COSMO—Stochastic Mine Planning Laboratory
Mining and Materials Engineering
McGill University
Montreal, QC
Canada

ISBN 978-3-319-69319-4 ISBN 978-3-319-69320-0 (eBook)
https://doi.org/10.1007/978-3-319-69320-0

Library of Congress Control Number: 2017956314

Cover illustration: Andrey N. Bannov/shutterstock

Printed on acid-free paper

This Springer imprint is published by Springer Nature
The registered company is Springer International Publishing AG
The registered company address is: Gewerbestrasse 11, 6330 Cham, Switzerland

Preface

It is a privilege to introduce "Advances in Applied Strategic Mine Planning", a collection of technical papers addressing core aspects of the sustainable, responsible and optimal development and utilization of Earth's mineral resources. In a world of uncertain markets, mismatches between demand and reserve base growth (supply), emerging technologies, and new technical challenges and solutions, this book aims to support knowledge dissemination and mobilization of new concerns, concepts, methods and technologies. These support step changes in the broader area of strategic mine planning while stressing technical risk management. Arguably, strategic mine planning is the most intricate, demanding and fundamentally important technical aspect of mining ventures, the industry and our profession. Strategic planning has a profound impact on the value of mines and metals produced, as well as shaping the technical plan to be followed from mine and mineral value chain development to closure. It is important to stress that education underpins the transfer of new technologies to both the current and, notably, the next generation of mining professionals and is the reason for this book.

This volume is unique in many ways starting with the contribution of papers from international experts, several of them from the younger generation of professionals in the field, who show great promise in enhancing and further developing the field. It also showcases the extraordinary contribution, support and involvement of the global mining industry, which is an indispensable part of progress in the field. Lastly, it recognizes the exceptional and continued collaboration of the major national mining institutes towards enriching professional excellence in the field: The Australasian Institute of Mining and Metallurgy (AusIMM), Canadian Institute of Mining Metallurgy and Petroleum (CIM), Society for Mining, Metallurgy and Exploration (SME), and the Southern African Institute of Mining and Metallurgy (SAIMM).

This volume comprises 45 papers under the following key themes:

- ***Early Concerns and Innovative Responses***
  The volume opens with a discussion on the limits of conventional optimization for strategic planning and the issues faced in a real and uncertain world. It continues with global optimization of mining complexes which aim to capitalize on synergies between the components of a mining complex, mining optimization and management of multiple objectives. This is followed by a review of the major limitations imposed by the conventional approaches to modelling mineral deposits and their properties of interest. The section concludes by stressing the paradigm shift to stochastic mine planning optimization and technical risk management.
- ***Increasing Value and Technical Risk Management***
  This section presents early work that explores various aspects of optimization developments from additional drilling that add value through mine planning optimization, followed by several aspects of and approaches to geological risk management. Interestedly, the stochastic mine planning approaches summarized here show the resulting counter-intuitive aspect of related mine production schedules where economic value is higher for lower risk in meeting the forecasted production targets, when compared to schedules generated with conventional approaches. The section ends with papers addressing issues of flexibility in mine planning and design.
- ***Simultaneous Optimization of Multiple Operations and Processes***
  This section emphasizes new developments for and approaches to strategic mine planning and mine production scheduling where different components of a mining complex or mineral value chain are optimized simultaneously and within the framework of mineral reserves to market products. The approaches presented here also lay the ground for the evolution of concepts and methods presented in subsequent sections.
- ***Stochastic Simulation for Strategic Mine Planning***
  This section is concerned with the detrimental effect of the representation/modelling of mineral deposits on strategic planning and optimization. The series of papers included focus on several aspects and applications of stochastic or geostatistical simulations that stress both the quantification of geological uncertainty and practical aspects such as the ability to model the local variability of materials mined and their pertinent properties. They document, along with several papers from previous sections, a major contribution to technical risk management within mine planning optimization approaches.
- ***Other Aspects of Open Pit Mine Planning***
  This section presents a collection of critical and pertinent topics related to optimizing mine production and performance, including geological, geometallurgical and geotechnical modelling applications, all complementing the topics presented in other parts of this volume.

- ***Optimization of Underground Mine Planning***
  The rapid growth in the application of optimization approaches in various aspect of underground mining, from sublevel stope mine optimization and related grade risk analysis quantification to strategic mine access design and ventilation, as well as mining methods for deep orebodies is presented here.
- ***Advances and Applications in Mine Optimization***
  The application of new technological advances and innovative concepts is the focus of this section. This includes the elaborate applications of stochastic mine planning and the solution of relatively large stochastic optimization formulations, to multistage approaches and excavating operations, equipment utilization and aspects of waste dump management.
- ***Contributions to Strategic Innovation***
  The concluding section addresses the changing world. It stresses major new concepts, future directions, frameworks and applications. It starts with the simultaneous stochastic optimization of mineral value chains and continues with sensor-based real-time mining for production control. Then, new contributions in the spatial simulation of geometallurgical properties of mineral deposits and the new high-order stochastic simulation framework needed for strategic mine planning are presented. The section concludes with a paper on the optimization of a mineral supply chain under supply (geological) and demand (market) uncertainty.

This book is thanks to the long-standing combined efforts of several colleagues over numerous years. I would particularly like to thank our colleagues and international experts: Gavin Yeates, Jean-Michel Rendu, Wynand Kleingeld, Jeff Whittle, Brian Baird, Vaughan Chamberlain, Edson Ribeiro, Peter Stone, Ian Douglas, Larry Allen, David Whittle, Malcolm Thurston, Rick Allan, Richard Peattie, Olivier Tavchandjian, Jean-Yves Cloutier, Brett King, Peter Ravenscroft, Allen Cockle, Peter Monkhouse, Martin Whitham, Salih Ramazan, Snehamoy Chatterjee, Kadri Dagdelen, Erkan Topal, Jorg Benndorf, Waqar Asad, Marcelo Godoy, Peter Dowd, Andre Journel and our colleagues involved with the COSMO—Stochastic Mine Planning Laboratory.

The invaluable, long-standing support and collaboration of AngloGold Ashanti, Barrick Gold, BHP, De Beers, Kinross Gold, Newmont Gold and Vale is thankfully acknowledged. Special thanks to AusIMM, for the papers in this book originate from the international symposium "Orebody Modelling and Strategic Mine Planning" organized by AusIMM since 2004, as well as the long-standing support, contribution and involvement of its staff that has been widely appreciated by all of us.

Montreal, Canada

Roussos Dimitrakopoulos
COSMO—Stochastic Mine
Planning Laboratory
http://cosmo.mcgill.ca/

Contents

Part I Early Concerns and Innovative Responses

Beyond Naïve Optimisation 3
P. H. L. Monkhouse and G. A. Yeates

Optimal Mining Principles 19
Brett King

The Global Optimiser Works—What Next? 31
J. Whittle

Blasor—Blended Iron Ore Mine Planning Optimisation at Yandi, Western Australia 39
P. Stone, G. Froyland, M. Menabde, B. Law, R. Pasyar and P. H. L. Monkhouse

Roadblocks to the Evaluation of Ore Reserves—The Simulation Overpass and Putting More Geology into Numerical Models of Deposits 47
A. G. Journel

Quantification of Risk Using Simulation of the Chain of Mining—Case Study at Escondida Copper, Chile 57
S. Khosrowshahi, W. J. Shaw and G. A. Yeates

A Risk Analysis Based Framework for Strategic Mine Planning and Design—Method and Application 75
M. Godoy

Mining Schedule Optimisation for Conditionally Simulated Orebodies 91
M. Menabde, G. Froyland, P. Stone and G. A. Yeates

Stochastic Mine Planning—Methods, Examples and Value in an Uncertain World 101
R. Dimitrakopoulos

Part II Increasing Value and Technical Risk Management

The Value of Additional Drilling to Open Pit Mining Projects 119
G. Froyland, M. Menabde, P. Stone and D. Hodson

Stochastic Optimisation of Long-Term Production Scheduling for Open Pit Mines with a New Integer Programming Formulation 139
S. Ramazan and R. Dimitrakopoulos

Stochastic Long-Term Production Scheduling of Iron Ore Deposits: Integrating Joint Multi-element Geological Uncertainty and Ore Quality Control 155
J. Benndorf and R. Dimitrakopoulos

Stochastic Mine Planning—Example and Value from Integrating Long- and Short-Term Mine Planning Through Simulated Grade Control, Sunrise Dam, Western Australia 173
A. Jewbali and R. Dimitrakopoulos

A New Methodology for Flexible Mine Design 191
B. Groeneveld, E. Topal and B. Leenders

Direct Net Present Value Open Pit Optimisation with Probabilistic Models 217
A. Richmond

Part III Simultaneous Optimisation of Multiple Operations and Processes

Simultaneously Optimizing Open-Pit and Underground Mining Operations Under Geological Uncertainty 231
L. Montiel, R. Dimitrakopoulos and K. Kawahata

Combining Optimisation and Simulation to Model a Supply Chain from Pit to Port 251
P. Bodon, C. Fricke, T. Sandeman and C. Stanford

Network Linear Programming Optimisation of an Integrated Mining and Metallurgical Complex 269
E. K. Chanda

Open Pit Transition Depth Determination Through Global Analysis of Open Pit and Underground Mine Production Scheduling 287
K. Dagdelen and I. Traore

Consideration for Multi-objective Metaheuristic Optimisation of Large Iron Ore and Coal Supply Chains, from Resource to Market . . . 297
J. Balzary and A. Mohais

Part IV Stochastic Simulation for Strategic Mine Planning

Application of Conditional Simulations to Capital Decisions for Ni-Sulfide and Ni-Laterite Deposits 319
O. Tavchandjian, A. Proulx and M. Anderson

Simulation of Orebody Geology with Multiple-Point Geostatistics—Application at Yandi Channel Iron Ore Deposit, WA, and Implications for Resource Uncertainty 335
V. Osterholt and R. Dimitrakopoulos

New Efficient Methods for Conditional Simulations of Large Orebodies 353
J. Benndorf and R. Dimitrakopoulos

Transformation Methods for Multivariate Geostatistical Simulation—Minimum/Maximum Autocorrelation Factors and Alternating Columns Diagonal Centres 371
E. M. Bandarian, U. A. Mueller, J. Fereira and S. Richardson

Strategies for Mine Planning and Design 395
P. A. Dowd, C. Xu and S. Coward

Part V Other Aspects of Open Pit Mine Planning

Planning, Designing and Optimising Production Using Geostatistical Simulation 421
P. A. Dowd and P. C. Dare-Bryan

Geometallurgical Modelling and Ore Tracking at Kittilä Mine 451
D. La Rosa, L. Rajavuori, J. Korteniemi and M. Wortley

Predicting Mill Ore Feed Variability Using Integrated Geotechnical/Geometallurgical Models 465
J. Jackson, J. Gaunt and M. Astorga

Using Grade Uncertainty to Quantify Risk in the Ultimate Pit Design for the Sadiola Deep Sulfide Prefeasibility Project, Mali, West Africa 487
S. P. Robins

Applicability of Categorical Simulation Methods for Assessment of Mine Plan Risk 513
A. Jewbali, R. Perry, L. Allen and R. Inglis

Part VI Optimisation of Underground Mine Planning

Cut-off Grade Based Sublevel Stope Mine Optimisation 537
M. T. Bootsma, C. Alford, J. Benndorf and M. W. N. Buxton

Classification of Mining Methods for Deep Orebodies 559
V. Oparin, A. Tapsiev and A. Freidin

Grade Uncertainty in Stope Design—Improving the Optimisation Process 573
N. Grieco and R. Dimitrakopoulos

Strategic Optimisation of a Vertical Hoisting Shaft in the Callie Underground Mine 591
M. G. Volz, M. Brazil and D. A. Thomas

Strategic Underground Mine Access Design to Maximise the Net Present Value 607
K. G. Sirinanda, M. Brazil, P. A. Grossman, J. H. Rubinstein and D. A. Thomas

Part VII Advances and Applications in Mine Optimisation

Production Schedule Optimisation—Meeting Targets by Hedging Against Geological Risk While Addressing Environmental and Equipment Concerns 627
M. Spleit

A Stochastic Optimization Formulation for the Transition from Open-Pit to Underground Mining Within the Context of a Mining Complex 643
J. MacNeil and R. Dimitrakopoulos

An Open-Pit Multi-Stage Mine Production Scheduling Model for Drilling, Blasting and Excavating Operations 655
E. Kozan and S. Q. Liu

Optimising the Long Term Mine Landform Progression and Truck Hour Schedule in a Large Scale Open Pit Mine Using Mixed Integer Programming 669
Y. Li, E. Topal and S. Ramazan

Solving a Large SIP Model for Production Scheduling at a Gold Mine with Multiple Processing Streams and Uncertain Geology 687
M. de Freitas Silva

Part VIII Contributions to Strategic Innovation

Stochastic Optimisation of Mineral Value Chains—Developments and Applications for the Simultaneous Optimisation of Mining Complexes with Uncertainty 707
R. Goodfellow and R. Dimitrakopoulos

Sensor Based Real-Time Resource Model Reconciliation for Improved Mine Production Control—A Conceptual Framework 725
J. Benndorf, M. Buxton and M. S. Shishvan

On the Joint Multi Point Simulation of Discrete and Continuous Geometallurgical Parameters 745
K. G. van den Boogaart, R. Tolosana-Delgado, M. Lehmann and U. Mueller

Geologically Enhanced Simulation of Complex Mineral Deposits Through High-Order Spatial Cumulants 767
H. Mustapha and R. Dimitrakopoulos

Optimising a Mineral Supply Chain Under Uncertainty with Long-Term Sales Contracts 787
J. Zhang and R. Dimitrakopoulos

Part I
Early Concerns and Innovative Responses

Beyond Naïve Optimisation

P. H. L. Monkhouse and G. A. Yeates

Abstract Most practitioners would regard the maximising of the net present value (NPV) of a mine by changing mining schedules, push-backs, cut-off grades, ultimate pit shells and stockpile rules and procedures as encompassing current best practice in mine planning. This optimisation is typically carried out for a single set of assumptions about:

- orebody tonnes and grade,
- processing methods and costs,
- maximum sales volumes in the case of bulk commodities,
- commodity prices, and
- discount rates.

About the only thing we can be sure of is that the assumptions on all these factors will be wrong, yet we continue to naïvely optimise our mine plan. This paper argues that this approach is inherently flawed. Recognising that our assumptions will be wrong, and that our actions can alter over time as new information is made available, means that the mine plan that is 'optimal' under a single set of assumptions may well be suboptimal in the real and uncertain world.

P. H. L. Monkhouse (✉)
Business Strategy for Carbon Steel Materials, BHP Billiton Limited,
PO Box 86A, Melbourne, VIC 3001, Australia
e-mail: peter.hl.monkhouse@bhpbilliton.com

G. A. Yeates
Mineral Resource Development, Business Excellence,
BHP Billiton Limited, PO Box 86A, Melbourne, VIC 3001, Australia
e-mail: gavin.yeates@bhpbilliton.com

R. Dimitrakopoulos (ed.), *Advances in Applied Strategic Mine Planning*,
https://doi.org/10.1007/978-3-319-69320-0_1

Introduction

Best practice is a fuzzy term; when applied to mine planning it can mean many things. Current best practice in mine planning, as viewed by most practitioners, encompasses the maximising of the net present value (NPV) of a mine by changing mining schedules, push-backs, cut-off grades, ultimate pit shells and stockpile rules and procedures. This analysis is typically performed for a single set of assumptions, which we can almost guarantee will be wrong. Assumptions typically cover: orebody tonnes and grade; processing methods and costs; maximum sales volumes in the case of bulk commodities; commodity prices; and discount rates.

Planning for a single set of assumptions that turn out to be incorrect will result in a suboptimal, or naïve, mine plan. There are two possible responses to this. The first is to try harder to correctly estimate (forecast) the future. The second response is to recognise that the future is in many respects unknowable, and to subsequently develop mine plans that have the flexibility to respond to changes to assumptions in the future. This flexible—or robust—mine plan will continue to give high mine values over a wide range of input assumptions (both optimistic and pessimistic), rather than a plan that only gives optimal results over a very small range of assumptions.

The key to addressing these issues is understanding uncertainty and risk, and developing methods to incorporate them into the mine planning process. This allows us to value flexibility and the benefit derived from robust mine plans. Whilst acknowledging that this is difficult, we propose that solutions can be found by combining the research from two broad but quite different areas, those of mine planning and real options. Even if robust or flexible plans are developed, the organisational challenge is to act effectively. For example, how many copper mines changed their mine plans when the copper price doubled over a relatively short period of time? How many of these operations are still working to the cut-off, the schedule and ultimate pit that were in place when the copper price was half what it is today? A mine with flexibility, with exposed ore and with surplus stripping capacity would be able to respond by raising the cut-off, raising the head grade and thereby producing more copper during periods of higher prices and hence capturing value during the price spike. How much value is being destroyed by not changing our current operating plans in light of new information?

In this paper, current industry practice in regard to mine planning is briefly reviewed and the generic assumptions that strongly influence the final mine plan are then discussed. Two key sources of uncertainty—orebody uncertainty and price uncertainty—are then reviewed in some detail. A discussion follows regarding current practices within BHP Billiton before concluding with some suggestions for future developments in this area.

Current Industry Practice

The current practice in industry is to take a single estimate (model) of the orebody, using a single set of mining assumptions, along with a single set of deterministic external economic assumptions, to come up with an 'optimal' ultimate pit design, extraction sequence, and schedule. The term 'optimal' usually means the maximising of a single variable, usually NPV or its proxy, for a given set of assumptions. The optimised model typically defers stripping, brings forward revenue (high grade) and often extends mine life by dynamically changing cut-off grade over time. Sometimes additional effort is applied to look for the potential of additional value in the stockpiling of low-grade material.

The first step in a mine optimisation typically involves coming up with final pit limits. The tool commonly used is the Whittle pit optimisation, the nested pit version of the Lerchs-Grossmann algorithm (Lerchs and Grossmann 1965; Whittle 1988; Muir 2007). The mine planner's dilemma in using these techniques is that they focus on the final limits. Given that the decision about the final limit is usually far into the future and heavily reliant on external economic assumptions, such as the price at the time the final pushback will be mined, the decision is fraught with difficulty. While this decision is likely to be refined during mine life, key investment decisions are often made on the basis of this information. The next steps in mine optimisation are encapsulated in the seminal book in this area, *The Economic Definition of Ore* (Lane 1988) with the general approach being considered as established practice in the industry.

Unfortunately, the big picture is often lost and the mine planning process blindly followed in the beliefs that the assumptions are right and that the resultant plan is optimal in reality. The key concept regarding all of these factors is that they are only optimal for a given set of assumptions (inputs)—today's optimised mine plans have no flexibility to respond to changed circumstances. This is usually due to the stripping being deferred, all exposed ore being minimised, all stockpiles cut to near zero by the accounting drive to minimise working capital, and material movement matched to the fleet capacity thereby eliminating sprint capacity. Further, if we consider current practice in use at most of our mining operations, the mine plan is often not revised, even when we have significant changes to external assumptions.

Sources of Uncertainty or Key Assumptions

The key sources of uncertainty that affect the final mine plan are as follows:

Orebody uncertainty: The three-dimensional distribution of grade over the orebody is estimated by relatively limited drill hole data coupled with a geological interpretation, which may or may not be correct. This uncertainty, however, is often ignored in the mine planning process. This issue is discussed in more detail in a subsequent section.

Processing uncertainty: Just as methods for modelling grade now exist, so do advances in the modelling of what is now called 'geometallurgical' performance. It is now possible to deterministically model variables such as ore hardness, flotation or leach recovery, concentrate grade, and ultimately dollars per hour through the mill (e.g. Wooller 1999). Ultimately, these variables can also be simulated to describe the range of possible outcomes that may be encountered in the future operation. This is essentially modelling the current performance through a given process plant (Flores 2005).

Uncertainty in changing technologies: Another significant uncertainty far more difficult to model is a major technology change; these step changes could well have major impacts on future mine plans. Examples include atmospheric leaching of nickel ores, leaching of chalcopyrite ores, and the use of high phosphorous iron ore in steel plants. The key uncertainties for these particular changes are threefold: Will the breakthrough occur? If so, when will it occur? If it occurs what will be the size of the step change in cost, recovery and therefore reserve definition?

Volume uncertainty: London Metals Exchange (LME) commodities effectively exhibit no volume uncertainty, as product can always be sold and delivered to LME warehouses. However, non-LME commodities, such as coal and iron ore, can only be sold to traders or customers, thereby introducing volume or sales uncertainty. The ability to sell the material is also influenced by its quality.

Price uncertainty: The price forecast we enter into our computer models is problematic, especially when the only certainty is that the price forecast we use will be wrong. This will be discussed in more detail later.

Discount rate uncertainty: The issue of interest rate uncertainty is more subtle, but no less important, in that it affects what discount rate we use. It affects the trade-off decision between future benefits versus current benefits. Again, the only thing we know about our forecast of interest rates, and hence discount rates, is that they will change over time. Political risk, often allowed for in the discount rate, further complicates this issue. Should we allow for a country risk premium on our annual discount rate that declines with time, as we learn to operate in a country? Or does country risk keep growing exponentially, as is implied in a constant per period discount rate?

Orebody Uncertainty

The traditional approach has been to provide mine planners with a single 'best' interpretation of the orebody. This single geological interpretation is then treated as fact. This approach gives no indication of the uncertainty in the interpretation, nor does it communicate the risk that the interpretation could be wrong or the likely range of possible outcomes. Geologists are dealing with imperfect knowledge, they know that the data on which the interpretation is based is incomplete, imprecise and inaccurate. They also know that there are multiple possible interpretations, each of which is valid. Some may have greater probability than others, but each is valid if it

can explain the available data. It is now possible to quantify and model some aspects of the geological uncertainty. The use of simulation techniques is well-developed for modelling the grade uncertainty, but also well known is the critical nature of geological interpretation that controls the grade. There are limited examples of quantifying the range of geological interpretations and hence the grade (e.g. Jackson et al 2003; Khosrowshahi, Shaw and Yeates 2017, this volume; Osterholt and Dimitrakopoulos 2017, this volume).

Dimitrakopoulos, Farrelly and Godoy (2002) illustrate a case where, for a range of equally probable geological outcomes, the mine plan developed on a single estimate of the orebody is excessively optimistic. This is partly driven by any misestimation of grades—resulting in a loss of value either by ore being classified as waste and an opportunity loss suffered—or waste being classified as ore and additional processing costs incurred. This resulting 'bias' is what makes many deterministic plans optimistic. It should be noted, however, that the opposite may also occur unpredictably, to stress the limits of the current modelling and optimisation technologies. This finding has been confirmed by internal research at BHP Billiton Technology (Menabde et al 2017, this volume). Further, and more importantly, this work shows consistently that a mine plan can be developed considering the uncertainty in the geological input assumptions, and this mine plan will have a higher NPV on average (i.e. over a wide range of inputs), a finding independently observed in Godoy and Dimitrakopoulos (2004); and Ramazan and Dimitrakopoulos (2017, this volume).

Price Uncertainty

To illustrate the problems with current best practice, the following hypothetical mine development is used.

A Simplified Example

Consider a mining company that requires an optimal mine plan for a copper orebody shown (simplistically) in Fig. 1.

Waste

For the high-grade block, assume:

1. A grade of 1.25% copper and containing 20 million pounds of copper. At a copper price of US$1/lb this block will produce US$20 M revenue.

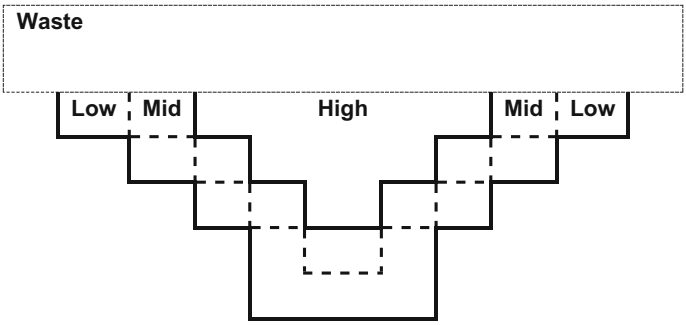

Fig. 1 A simplistic hypothetical copper orebody

2. The total cost of mining and processing for this high-grade block is US$12 M, split US$6 M for the waste removal and US$6 M for the mining and treatment of the ore. Mining and processing should occur in year 1.

For the mid-grade block, assume:

1. A grade of 1% copper and containing 12 million pounds copper. At a copper price of US$1/lb it will produce US$12 M revenue.
2. The total incremental cost is US$12 M, split between additional waste removal (US$2 M) and mining and processing mid-grade. If mining were to be undertaken, the mining and processing should occur in year 2.

For the low-grade block, assume:

1. The low-grade block is not drilled because the Promoter wants the orebody open at depth, but George the Geologist is convinced it has a grade of 0.65 Cu, containing 12 M pounds copper, for revenue of US$12 M.
2. The incremental cost of removing the low-grade block is estimated at US$14 M, split US$2 M for additional waste removal and US$12 M for mining and processing the ore. If undertaken, the mining and processing of this low-grade block should occur in year 3.

Furthermore, assume that all the waste must be extracted in year 0, and that once this decision is made it is very expensive to go back, in either cost and/or time, and re-strip the additional waste.

The Problem Facing the Company

The problem for the mining company is that a decision needs to be made today on what to mine. If the company forecasts the copper price to be US$1/lb:

- Should the company only mine the high-grade block?
- Should it mine the mid-grade block?
- Should it trust George the Geologist and plan to mine the low-grade block?

If our assumption was that the forecast copper price was US$1/lb then we would apply the approach outlined by Lane (1988). Primarily because of the effects of discounting—with cost of waste removal being incurred in year 0 and revenue in years 1, 2 and 3—we would only extract the high-grade block. An alternate approach may be to use a break-even cut-off (and ignore the effects of discounting), where at US$1/lb copper and for the costs outlined previously, a break-even cut-off grade for the high-grade block is 0.75% copper, the mid-grade block is 1% copper, and the low-grade block is some 0.76% copper. Accordingly, using this approach the company would have mined the high- and mid-grade blocks.

Under what circumstances would the company plan on mining all the blocks? How would the company develop a robust (or flexible) mine plan that allows them to respond to changing circumstances? To highlight the impact of price uncertainty, discount rate uncertainty and geological uncertainty, how would the decision change if:

- Analysis of the futures market indicated there was a 50% chance the copper price would exceed US$1.50 in three years' time?
- The deposit was located in a country with a corrupt dictator that may expropriate the operation at any time?
- An independent review of George the Geologist's work indicated there is a 95% chance he is right.

Intuitively, all these assumptions should change the optimal mine plan, yet current best practice would struggle to include these assumptions. It is suggested that the 'best' mine plan should be one that maximises value over a 'reasonable' range of input assumptions.

Framing the Questions in the Language of Real Options

To determine what we mean by 'best' and a 'reasonable' range of assumptions, the previous example will be re-stated.

For the high-grade block, assume:

1. A grade of 1.25% copper containing 20 million pounds of copper. At a copper price of US$1/lb this will produce US$20 M revenue.
2. Total cost of mining and processing the high-grade block is US$12 M, split US $6 M for waste removal and US$6 M for mining and treating the ore. The waste removal will occur in year 0 with mining and processing to occur in year 1.

For the mid-grade block, assume:

1. A grade of 1% copper containing 12 million pounds copper. At a copper price of US$1/lb it will produce US$12 M revenue.
2. For the cost of additional stripping in year 0 of some US$2 M, we have the option to mine and process the mid-grade block in year 2 at a cost of some US $10 M.

For the low-grade block, assume:

1. The low-grade block is not drilled because the Promoter wants the orebody open at depth. George the Geologist is convinced the grade is at least 0.65% copper, and contains 12 million pounds of copper, which would produce revenue of US $12 M if he is correct.
2. For the cost of additional stripping in year 0 of another US$2 M, we have the compound option to mine and process the low-grade block in year 3 at a cost of some US$12 M. It is a compound option because it is conditional on us mining the mid-grade block in year 2. In this example, the low-grade block is only mined if the mid-grade block is already mined. Compound options are highly non-linear and the effects are complex. In general, the second option (on the low-grade block) has the effect of increasing the value of the first option (on the mid-grade block). However, compound options are not that difficult to value.

Considering this scenario, does the company now mine the high grade block? Does the company now buy the (real) option for US$2 M to mine and process the mid-grade block in two years hence? Does the company buy the (real) option over the low-grade block costing a further US$2 M? Unless the options (or flexibility) can be valued, or the benefits of a robust mine plan can be valued, it is unlikely that mine planning will be successful in moving forward. The keys are properly modelling uncertainty and risk, and understanding the value of preserving options and flexibility.

In our example the two key questions are: What options should be purchased? When, if at all, should options be exercised? To answer the first question the company must know the cost of purchasing the option—in the above example this is US$2 M to undertake the additional stripping. The harder question is: What is the value of acquiring this option, or flexibility? If the option is worth more than it costs, then the company will want to purchase it, and develop a flexible, or robust mine plan. Yet there are limits to the amount of flexibility that should be acquired. To answer the second question about when to exercise the options, the company needs to know the value of keeping the option alive, and the value of exercising the option. Again, we will exercise the option, or mine the mid- and possibly the low-grade blocks if the value of exercising the option is greater than the value of keeping the option alive. The harder issue is valuing the option, not the value of exercising it (developing the mine).

Valuing the Real Options for Price Uncertainty

Price uncertainty can be modelled in a real options framework by building a price tree. To simplify the mathematics in this example, it is assumed that the prices will be constant for one year, and then may vary. It is further assumed that the price distribution is log-normal[1] and that the volatility of the copper price is 20% per annum. It is also assumed that this price tree is a risk-neutral price tree, as obtained from futures data. It is **not** the price tree of expected copper price movements. This distinction is very important to ensure price risk is handled properly. With these assumptions, the up price factor is 1.2214 and the down price factor is the reciprocal, or 0.8187. Assuming a 5% per annum risk-free rate (continuously compounded) and these up and down factors it follows that the risk-neutral probability of an up price movement is 0.5775 and the risk-neutral probability of a down price movement is 0.4225.

Copper Price Tree

Given the above assumptions, and assuming the current copper price is US$1/lb, the copper price tree is shown in Table 1.

Value of High-Grade Block

Given there are 20 M pounds of copper and the mining and processing costs are US $6 M, the cash flows from mining the high-grade block (assuming the waste removal has already occurred in year 0) is shown in Table 2.

Table 1 Copper price tree with and copper price at US $1/lb

Now	Year 1	Year 2	Year 3
			1.82
		1.49	
	1.22		1.22
1.00		1.00	
	0.82		0.82
		0.67	
			0.55

[1]This assumption is discussed in detail in corporate finance textbooks (eg., Brealey and Myers 2003, Chap. 21; Hull 2000, Chap. 9).

Table 2 Cash flows from mining the high-grade block (assuming the waste removal has already occurred in year 0)

Now	Year 1	Year 2	Year 3
	18.43[a]		
	10.37		

[a]Calculated as (1.2214 * 20)−6.0

Assuming the risk-free interest rate is 5% per annum (continuously compounded) and that the waste removal has already occurred, the value tree is shown in Table 3.

After spending US$6 M on waste removal we should have a value of US $14.29 M. Thus, before we even start the project it has a value of some US$8.29 M and indicates that the high-grade block should be mined.

Value of Mid-Grade Block

Using the same price tree as above and given there are 12 M pounds of copper and the mining and processing costs are US$10 M, the cash flows from mining the mid-grade block (assuming the waste removal has already occurred in year 0) are shown in Table 4.

Assuming the risk-free interest rate is 5% per annum (continuously compounded) and that the waste removal has already occurred, the value tree is shown in Table 5.

Table 3 Value tree, assuming the risk-free interest rate is 5% per annum (continuously compounded) and that the waste removal has already occurred

Now	Year 1	Year 2	Year 3
	18.43		
14.29[a]			
	10.37		

[a]Calculated as (18.43 * 0.5775 + 10.37 * 0.4225)/exp(0.05). The exponential term is because the interest rate is expressed on a continuously compounded basis

Table 4 Cash flows from mining the mid-grade block (assuming the waste removal has already occurred in year 0)

Now	Year 1	Year 2	Year 3
		7.90	
		2.00	
		−1.96	

Table 5 Value tree, assuming the risk-free interest rate is 5% per annum (continuously compounded), and that the waste removal has already occurred

Now	Year 1	Year 2	Year 3
		7.90	
	5.14		
3.27		2.00	
	1.10		
		0.00	

Spending US$2 M on additional waste removal should give us a value of US $3.27 M. Thus the project, before we start, has a value of some US$1.27 M and means the company should at least undertake the prestrip for the mid grade block. However, we will only mine the mid-grade zone if the copper price is US$1/lb or above. We will not mine the mid-grade zone if the copper price is the low price in year 2 of US$0.67/lb. Ultimately, it is the ability to defer this mining decision that is creating the value, and thus facilitating the mining of the mid-grade zone in some circumstances.

A possible counterintuitive result is also evident from this example. Consider the case where the copper price remains at US$1/lb through the mine life. In this case the company will end up mining the mid-grade block because:

- the option analysis commits the company to undertake the prestrip, as the copper price might rise; however
- when the company gets to make the mining decision it decides to mine even if the copper price is only US$1/lb because the **prestripping is now a sunk cost** and is excluded from the analysis.

More of the deposit is mined if the copper price turns out to be a constant US$1/lb under the robust mine planning framework compared to a current 'best practice' framework. This is despite the fact that if we had perfect foresight we would not have committed to this prestripping and the mining of the mid-grade block. This is of obvious benefit to the host country.

Value of Low-Grade Block

Now let us repeat this procedure for the low-grade block. The price tree is the same as in the previous example. Given that there are 12 M pounds of copper and the mining and processing costs are US$12 M, the cash flows from mining the low-grade block (assuming the waste removal has already occurred in year 0) are shown in Table 6.

Assuming the risk-free interest rate is 5% per annum (continuously compounded), and that the waste removal has already occurred, the value tree is shown in Table 7.

Spending US$2 M on additional waste removal should give us a value of US $2.60 M. The project, before we start, therefore has a value of some US$0.60 M. This means the company should do the prestrip for the low-grade block as well, but

Table 6 Cash flows from mining the low-grade block (assuming the waste removal has already occurred in year 0)

Now	Year 1	Year 2	Year 3
			9.87
			2.66
			−2.18
			−5.41

Table 7 Value tree, assuming the risk-free interest rate is 5% per annum (continuously compounded) and that the waste removal has already occurred

Now	Year 1	Year 2	Year 3
			9.87
		6.49	
	4.15		2.66
2.60		1.46	
	0.80		0.00
		0.00	
			0.00

will only mine the low-grade zone if the copper price is above US$1.22/lb. The low-grade zone will not be mined if the copper price is only US$0.82/lb or less. At the risk of labouring the point, it is the ability to defer this mining decision that is creating the value, and thus facilitating the mining of the low-grade zone in some circumstances.

Note that more of the deposit is mined under the robust planning framework than under the current 'best practice' framework. The expected amount of material mined at the start of the mining operation is greater under the robust mine planning framework than any other framework, with significant benefits to the company, shareholders and the host country.

Introducing Additional Sources of Uncertainty in the Analysis

The simplified example shown previously introduced an additional source of uncertainty. Should the company trust George the Geologist's intuition and plan to mine the low-grade block? What about the risk that George is wrong? Should this risk be allowed for in the analysis? Before discussing this in more detail we need to introduce another concept from corporate finance, namely diversifiable risk and non-diversifiable risk. The key issue is that some (non-diversifiable) risks are priced (investors will pay to avoid them, e.g. commodity price risk, interest rate risk), and other (diversifiable) risks are unpriced (investors are indifferent about bearing them, e.g. geological uncertainty). This concept forms the bedrock of the Capital Asset Pricing Model or CAPM (Brealey and Myers 2003, Chaps. 7 and 8).

If George's estimate of the grade is truly a central estimate then because geological risk is, at least to a first order approximation, unpriced, we should not introduce any additional value reduction because of the 'risk', even if the distribution of possible outcomes is incredibly wide. The key issue is whether George's estimate is a central estimate because, unlike copper price, the risk of the possible outcomes does not enter the valuation.

More General Comments on Uncertainty and Risk

The latter example has introduced two key corporate finance concepts: namely real options,[2] and diversifiable and non-diversifiable risk, but this paper cannot do justice to these concepts.[3] Together these two concepts allow for the classification of risks into priced and non-priced risks, and where they are priced an analytical tool to evaluate them is provided. It allows the valuation of mine plans (and risk) from the perspective of shareholders and allows the company to then compare the cost of acquiring flexibility, versus the value of having flexible mine plans.

Failure to adequately address risk (such as using expected spot prices instead of risk-neutral prices) means that we get the garbage-in-garbage-out problem, a very large problem. Properly valuing the risk introduced by real options is complex. We can quickly end up in the world of stochastic differential equations, or large-scale numerical methods. Yet failing to properly value risk means we are wasting our time. The authors believe that we are better off relying on our intuition than doing some pseudo-maths that does not properly allow for risk.

Possible Criticisms of the Proposed Approach

In these examples, a flexible or robust mine plan means removing all the waste in year 0, which goes beyond standard practice in the industry. One possible criticism of this approach is that the decision to prestrip is made up-front and is artificial. In practice you could go back and prestrip for the mid- and the low-grade blocks if the price spiked. While this is to some extent correct, it can be argued that:

1. going back and undertaking additional prestripping will contribute to cost and time penalties, although these can be modelled if considered appropriate;
2. in a real-world approach you need to model mean reversion in the commodity prices, which means that any time delays suffered could well cause a significant value loss; and
3. in any mining operation, the time taken to do any additional stripping is measured in years.

In any event, the mere fact that we are thinking how we will respond to changed economic circumstances is the whole point of this paper. The aim, in real options

[2]The Nobel Prize in Economics in 1997 was awarded to Scholes and Merton for adequately handling risk in (financial) option valuations. The earlier tool of the Capital Asset Pricing Model—while important and underpinning all NPV analysis – does not allow risk to be accurately valued when we have option-type pay-offs. The seminal option paper by Black and Scholes (1973) effectively provided a numerically quantifiable way of handling non-diversifiable (or priced) risk in option-type pay-offs. This concept has since been extended to real options.

[3]The application of real options is discussed in Copeland and Tufano (2004). The application of real options to a mining example is discussed in McCarthy and Monkhouse (2003).

talk, is to acquire flexibility for less than its inherent value—if that can be done by alternative and lower cost means then so much the better. It could be argued that all this is too hard and that sensitivity analysis will get us most of the way there, but at a fraction of the complexity. To the extent that sensitivity analysis builds intuition, then that is a great outcome. But of itself, sensitivity analysis will have limited benefit in generating a robust or flexible mine plan as it will be unable to justify the cost of investing in flexibility. This can only be achieved by implementing real options analysis as described previously.

State of Play in Bhp Billiton

Within BHP Billiton it is well-recognised that there are limitations to optimising a mine plan for a given set of assumptions that will inevitably turn out to be incorrect. Further, it is accepted that this approach will lead to suboptimal outcomes, for both our shareholders and the host country. Overcoming this deficiency is crucial; it requires the development of new mine planning techniques, and—just as importantly—it requires the development of management systems to facilitate changes to the mining operations in response to changing economic conditions. At BHP Billiton we are developing robust and flexible mine plans, and we have adjusted budgets and incentives to reflect changed economic circumstances. We believe we already have a competitive edge in this area, but we are the first to admit that there is a lot more work to be done.

Concluding Remarks

This paper has discussed current best practice in mine planning and has identified a key shortcoming. The fact that the key assumptions underpinning our mine plans will inevitably prove to be incorrect means that our mine plans are no longer optimal over a reasonable range of real world outcomes. Possible sources of uncertainty were highlighted and discussed. The paper then focused on two key sources of uncertainty: price uncertainty and geological uncertainty. By using a simplified example it was shown that mine plans will change if price uncertainty is explicitly recognised. The issue of geological uncertainty was also introduced in the simplified example and it was indicated that plans will likely change to extract more ore. Perhaps counterintuitively, it was argued that the risk of geological uncertainty did not affect the mine plan and was of a fundamentally different character to that of commodity price risk. Possible criticisms of the proposed approach were also discussed.

What needs to be remembered is that every day mine planners are making decisions about:

- What is waste and what is ore?
- How much exposed ore should we carry?
- When should we run down our levels of exposed ore?
- What sequence of push-backs should we use?
- What stockpiles should we carry?
- How much 'excess' mining capacity we should carry?

We cannot stop the mining operations to perform the analysis. We have uncertainty regarding geology, processing, new technologies, market, prices and discount rates; the opportunity cost of suboptimal mine plans is large. At BHP Billiton we are mindful of the limitations of conventional optimisation techniques, and are developing methods and tools to assist us in valuing flexibility and ultimately developing robust mine plans.

References

Black F, Scholes M (1973) The pricing of options and corporate liabilities. J Political Econom 81:637–659

Brealey RA, Myers SC (2003) Principles of corporate finance, 7th edn. New York, McGraw Hill Irwin

Copeland, T, Tufano, P (2004) A real-world way to manage real options. Harvard Business Rev, March, 90:9

Dimitrakopoulos R, Farrelly CT, Godoy M (2002) Moving forward from traditional optimization: grade uncertainty and risk effects in open-pit design. Trans Inst Min Metall, Section A, Mining Technology 111:A82–A88

Flores L (2005) Hardness model and reconciliation of throughput models to plant results at Minera, Escondida Ltda, Chile In: Proceedings 37th canadian mineral processors conference, Ottawa, 18–20 January

Godoy MC, Dimitrakopoulos R (2004) Managing risk and waste mining in long-term production scheduling. SME Trans 316:43–50

Hull J C (2000) Options, futures and other derivatives, 4th edn (Prentice Hall)

Jackson S, Frederickson D, Stewart M, Vann J, Burke A, Dugdale J, Bertoli O (2003) Geological and grade risk and the golden gift and magdala gold deposits Stawell, Victoria, Australia. In: Proceedings fifth international mining geology conference, pp 207–213 (The Australasian Institute of Mining and Metallurgy: Melbourne)

Khosrowshahi S, Shaw WJ, Yeates GA (2017) Quantification of risk using simulation of the chain of mining—a case study at Escondida Copper, Chile, in this volume

Lane K (1988) The economic definition of ore. Mining Journal Books, London

Lerchs H, Grossmann L (1965) Optimum design of open-pit mines. Trans CIM, LXVII, pp 17–24

McCarthy J, Monkhouse PHL (2003) To open or not to open—or what to do with a closed copper mine. J Appl Corporate Finan, Winter, 63–73

Menabde M, Froyland G, Stone P, Yeates GA (2017) Mining schedule optimisation for conditionally simulated orebodies, in this volume

Muir DCW (2007) Pseudoflow, new life for Lerchs-Grossmann pit optimisation. In: Orebody modelling and strategic mine planning, second edn (ed: R Dimitrakopoulos), pp 113–120 (The Australasian Institute of Mining and Metallurgy: Melbourne)

Osterholt V, Dimitrakopoulos R (2017) Simulation of orebody geology with multiple-point geostatistics—application at Yandi channel iron ore deposit, WA and implications for resource uncertainty, in this volume

Ramazan S, Dimitrakopoulos R (2017) Stochastic optimisation of long-term production scheduling for open pit mines with a new integer programming formulation, in this volume

Whittle J (1988) Beyond optimisation in open pit design. In: Proceedings Canadian conference on computer applications in the mineral industries, Rotterdam, pp 331–337

Wooller R (1999) Cut-off grades beyond the mine—optimising mill throughput. In: Strategic mine planning conference, pp 217–229 (Whittle Programming Pty Ltd: Melbourne)

Optimal Mining Principles

Brett King

Abstract Picture yourself responsible for the exploitation of a world class deposit, creating staggering quantities of products for global consumption over decades, employing thousands of people, about to spend billions of dollars on infrastructure and you are going to design this project. Should it be surface or underground (or both), how big should the processing plants be, what technology should be utilised, what happens if more resources are found or the price forecast changes? This paper aims to help guide engineers faced with the prospect of determining optimal mining policies for large projects. It draws on experiences at some of the largest mining projects and mining companies in the world, including the Bingham Canyon Mine (USA), Freeport (Irian Jaya), Escondida (Chile), Chuquicamata (Chile), Hamersley Iron (Australia), Ekati Diamond Mine (Canada) and several Hunter Valley coal mines (Australia). The paper outlines some important areas to put in place before starting, principles to guide the planning process and suggestions for finding additional value.

Introduction

Terminology

One of the first sources of confusion in strategic planning arises due to the definition of terms (or lack thereof). The terms used in this paper are based on Ken Lane's cut-off grade optimisation work (Lane 1964, 1988), which was based on Richard Bellman foundational dynamic programming methodology (Bellman 1957). Over the last ten years of working with major mining projects and feasibility studies, I have found these definitions useful and applicable in mining and other industries. Mining projects have many choices and therefore many decisions to make. A specific

B. King (✉)
AusIMM, COMET Strategy Pty Ltd, 4163 Suit 16/141 Shore Street West, Cleveland, Qld, Australia
e-mail: Brett.King@COMETstrategy.com

R. Dimitrakopoulos (ed.), *Advances in Applied Strategic Mine Planning*,
https://doi.org/10.1007/978-3-319-69320-0_2

decision that is made in every period is grouped and called a *policy*. For example, an open pit copper mine may have a decision on mill cut-off grade to be made in every period. When the same decision is made at every time period, the result is a *constant policy*. Typically, different decisions are made over time, in which case a *variable policy* is formed. Other operating policies that may change over time would normally include how much material is moved from a certain area, SAG mill grind size and flotation residence time; each needs to be made in every period.

Mining studies must typically determine many different policies during the project life. A group of policies is referred to as a *strategy*. For example, mining policies for a number of pushbacks could be described as a mining strategy. By combining a number of mining and processing policies, we can arrive at the strategy for the project, or a strategic plan. A decision, policy or strategy does not imply any optimisation criteria have been used to define them—it simply defines a number of decisions. Sadly, in real projects, many 'strategic' plans also have very little optimisation applied. In order to 'optimise' a decision (or policy or strategy), we need to have an *objective* or *objective function*. The objective will be discussed later in this paper, but for now, let's assume it is some definition of shareholder value. An optimisation process is a way of making decisions to achieve the project objective. For example, a cut-off grade optimisation process will optimise the cut-off grade policy so that the Net Present Value (objective function) is maximised.

There is a subtle distinction between optimising and maximising. *Decisions, policies and strategies are optimised* (not maximised), Net Present Value (NPV), cash flow or value is maximised (not optimised). If one were to maximise the cut-off grade (to an extreme), then no ore would be sent to the mill and the maximum NPV is unlikely to be achieved. On occasion, maximising a policy may also maximise the objective—it is better to use the right terminology and sound like an expert!

The focus of this paper will be to utilise optimised strategies to create optimised strategic plans. Given that all strategies discussed in this paper will refer to optimal mining plans, a *Strategic Plan* in this paper is defined as the process of making a number of operating decisions over the project life, to achieve the project objective. There is clearly a need in the industry to standardise our terminology and develop an optimal mining practice for the community. Ideally, this will be a collaborative effort between mining companies and the service companies that support them. These groups need to span the industry, to help reduce the misunderstanding that often leads to poor exploitation of the earth's finite resources (King 2008). The paper demonstrates these principles using open pit metalliferous projects, although these are actually generic principles that are appropriately applied to coal, iron ore, diamonds, bauxite, gold and also many non-mining projects.

Objectives

The first issue that needs to be clarified at the start of a planning exercise is the work objective. Although there would appear to be a clear and simple answer to the

objective, the reality is often blurred by conflicting instructions. Maximising shareholder value is normally the objective of large and small mining companies (and non-mining companies). This objective is clarified by the major mining houses as maximising the NPV, subject to a number of constraints such as safety and good stewardship of the environment:

- NPV is a sound basis for evaluating companies outside of the mining world. For example, stock market analysts will often value the share price for a company (in any industry) by calculating the NPV of all of the company assets, then dividing it by the number of shares issued (Brealey and Myers 2000). NPV includes a balanced valuation of short- term value (which receives very little discounting) and long- term value (which receives greater discounting), making it an appropriate instrument for the commercial valuation of most businesses. The main difficulties reported with valuing a project based on NPV include uncertain information and Net Present Value versus present value.
- With regards to uncertain information, typically there is substantial uncertainty in key drivers of the NPV including prices, costs, reserves and productivities. For example, price is normally a huge driver of value, and financial analysts recognise that price is related to supply and demand. Theoretically, as different strategies are evaluated with different quantities of metal produced, the prices could change for each case. The complexity does not stop here—the price is dependent on the supply from competitors, which would require an analysis of what they are doing as well. If this is not complex enough, the price is also dependent on the demand for end products. This means that a comprehensive estimate of price also requires analysis of what competitors and customers are planning. A risk/reward analysis would normally indicate that a comprehensive competitor/customer analysis is not valuable. Although specific aspects of risk are often incorporated using sensitivity studies of targeted issues, there is a still substantial development required to turn this analysis into useful decision making tools for the mining industry. Option value, and the ability to use variability to add value and control risk, is regularly missing from project valuation analysis. Advances in mathematical formulation and simulation methodologies can reveal a more complete understanding of project value. Incorporation of uncertainty and risk needs to become common place in the industry for fair valuation between investment alternatives.

The effort required to truly calculate a ‘Net’ Present Value means that often important components are ignored and a present value is used instead. Key aspects such as period costs, expansion capital, sustaining capital and closure costs are not able to be incorporated in some optimisation algorithms. Ignoring such issues or modelling them inadequately means that the results are crude, and value destroying decisions can be made.

While both of these difficulties appear to limit the suitability of using NPV to value a project or different scenarios within a project, NPV still remains at the heart of project valuations and is normally superior to the other financial instruments such

as internal rate of return, payback period and simple cash flows. Care should be taken when using other measurements to approximate the value of a project. People not aware of NPVs balancing of short- and long-term cash flows may be presented with some of the following alternatives for the planning objectives:

- product quantity—especially in the budgeting period (e.g. gold or copper produced in the first three to five years,
- mineral resources or reserves (especially stated to the stock market),
- smooth production schedules (e.g. constant material movement and constant grades for processing),
- minimising costs or maximising short-term cash flow, and
- maximising employment.

Using the above alternatives for the objective will normally result in a different plan than the one created by maximising NPV and so will have a lower NPV. Take the objective of maximising cash flow as an example. Waste stripping incurs substantial costs that reduce the cash flow. If waste stripping is suspended, cash flow for the first few years may be improved. Eventually, there will be no ore available to process, the mill capacity will not be utilised, and the cash flows (and NPV) rapidly fall. The NPV can be used to balance the early costs of waste stripping with the benefit of having the mill capacity continuously utilised. All aspects of mining and downstream processing that involve costs or revenue are captured directly in the objective function (NPV). The better our estimates of these costs and revenues, the better our estimates of NPV, which will in turn help bring value to shareholders.

Constraints

If an aspect of the project does not have a cost or revenue it will not directly be added to the project NPV, hence the inevitable constraints that must be considered. There are many issues to be considered in strategic planning that are not captured directly in the objective function. Safety and environmental care are two priorities of modern responsible mining that have important issues that are not always evident in cost or revenue. These and many more issues are captured in the optimisation process as constraints to bound the schedules that are considered valid, and are known as the *feasible solutions*. Many processes have a combination of costs, revenue and constraints. The safe operation of a mine or processing plant will involve additional cost components and constraints on how the activities can be undertaken. Typically the constraints will involve restrictions in productivity rates. Good environmental stewardship may involve continual ground rehabilitation and water treatment costs—it may also require some constraints such as tailings dam or waste dump footprints. Some care is needed to make sure a cost is not mistakenly implemented as a constraint.

Creating 'unconstrained' schedules may be of some temporary benefit to understand the value drivers for a project, but be wary of releasing such plans to a wider audience as it may generate unrealistic expectations. For example, when considering the size of a process plant expansion, the mining rates may initially be left unconstrained. This unconstrained case may be used to get the maximum size of the truck and shovel fleets. However, the best process plant capacity, when unconstrained, may not be the best process plant capacity when constrained. The unconstrained cases would tend to over-expand the mill capacity since it does not consider the purchase costs for the mining equipment. These 'unconstrained' schedules and their 'imaginary' values are not achievable and so would only be used for finding the boundaries for analysis.

Plan the Planning

There could well be only one chance to determine the best value of a project, then acquisition, disposal or operation. Time, staff, consultants, computing power and budgets are all limited resources that need to be used wisely. Much like the optimisation process we apply to a project, we need to identify the resources needed for some analysis and make sure that key people and support is available during the study. Experience suggests that very few people have been exposed to this field of the business, and so the need for training before the study is necessary, as well as support for when things do not simply fall into place. One of the problems with using inexperienced people is that they often do not know when additional value is possible from a project. The new planner can make assumptions that are not easily seen in the resulting schedules and so may not be picked up by management or peer review.

The unrealised value 'left on the table' by inexperienced analysis can easily be several percentage points of the NPV, and for large multi-billion dollar projects these are substantial values. It is therefore essential to have the best people working on these projects and have them reviewed by strategic planning specialists (internal and/or consultants). Real world strategic planning is normally constrained by time. The time spent designing a model, collecting and validating inputs, building the model, running cases, analysing the cases and then presenting the results, these activities consume precious and finite time resources. Experience would suggest that gathering and validating inputs often increases as input data is collected and checked. Using available information such as budget costs might initially appear to rapidly provide optimisation inputs, but they may need to be substantially re-categorised into fixed and variable components for strategic planning purposes. A planned work program will have a contingency for some unforseen data collection issues and changes in direction due to initial analysis. Typically, a *Strategic Planning Work Program* would have the components in Table 1.

For new greenfield or acquisition projects, approximately half the available time is typically used to collect appropriate data, validate it and get it into the appropriate

Table 1 Summary of typical strategic planning effort

Tasks	New model (%)	Existing model (%)
Scoping and understanding the existing project	10	10
Gathering, validating and transforming data	50	20
Model building	10	10
Running scenarios and analysing the results	20	50
Reporting on results	10	10

format for use by the planning software. Once a model is validated, a new expansion study, or the incorporation of additional reserves, requires much less data validation and the emphasis shifts to the analysis of results. Several of the tasks in Table 1 are done in parallel due to the iterative nature of the planning process. Note that Table 1 does not include the training time to ensure people understand what to do in each of the phases.

Given how long data validation and analysis takes, it is critical to plan a realistic scope. *'Dry run' strategic planning exercises* can help identify training requirements, holes in data requirements, streamline data acquisition and align scope expectations. There are typically too many options to evaluate and not enough time, so the planned activity should *focus on identifying the highest value controllable drivers*. For example, although blasthole initiation systems may be expensive and have room for reduction, they may not be as important to consider as shovel productivity as a driver of project value. Some value drivers may not be controllable, such as taxation, statutory compliance fees, award wages, cost of power and possibly even the commodity price. Although these uncontrollable drivers are fixed in the analysis, they should be considered in the NPV calculations, since they may influence decisions.

Simplifying Assumptions

Large mineral resources may take many years or even decades to fully exploit and have more decisions to make than there are electrons in the universe (approximately 10^{79}). The currently available algorithms for mine design, scheduling and processing require simplifying assumptions to find a solution and substantial computational power to do any sort of partial optimisation. For example, the Lerchs-Grossman (LG) algorithm, used in finding ultimate pit limits (Lerchs and Grossmann 1965)—fundamentally, this algorithm uses the assumption that we know the value of every block in a model. This is somewhat difficult when we do not know when the block is to be mined, what the price will be at that time, what other blocks are being mined with this one, what processes are available or whether the ideal process will have capacity for the block. This is a simplification in order to estimate the shape of the mine when completely mined.

If the value is dependent on time or capacity-related issues, then this casts doubts as to just how 'optimal' the LG results are. This is not to say that the algorithms cannot be used to guide the best location of the ultimate pit limits, it must however be taken into account when interpreting the results. Phrases with 'optimise' and 'plans' should be regarded with a healthy scepticism—we should also realise that we can rarely claim to have the optimum plan, rather something closer to the highest value plan we could deliver in the time allowed. The algorithms underlying all currently available software tools have limitations due to their assumptions—skilled engineers are able to use them appropriately in spite of these limitations. Some other simplifications typically made in strategic planning include:

- mineral resource estimates accurately reflecting what mining and processing will deliver;
- annual equipment productivity, utilisation and availability estimates;
- predictable costs and prices over the life of the project; and
- pretax and post-tax optimisation leading to the same decisions.

For annual plans that cover the entire life of a major mineral resource, we will not typically model individual salaries, weekly maintenance schedules, shovel loading configurations or the extra day that occurs in leap years. We must draw the distinction between different planning time frames (real time, shift, weekly, monthly, quarterly and annual) and the appropriate level of detail for the analysis.

As a general procedure, it is advisable to *start off with a simple model of the entire project, then add complexity if required*. Once you have a simple model it can be used and its results analysed. When a component of the cash flow calculation is found to be poorly approximating the real value, it can be modelled in greater detail. For example, an initial model of a mine may start with the simple mining cost per mass of material moved. This model then may be broken down into components and their drivers, such as drilling ($/t), blasting ($/t), loading ($/m3) and hauling ($/truck_operating_hour). The haulage component may require further detail by modelling the source elevation, destination of the material and the height of the dumps and so on. The objective is to arrive at a good estimate of the NPV for several different alternatives. If a simple model provides a good estimate, then there is no need to pursue a complex model. Another advantage of this approach is that some analysis can be done quickly into the project—this may enable the project scope to be tailored to the value drivers as they are better quantified. It is often surprising how simple models can estimate value so accurately and drive the decision process appropriately.

Knowledge and Understanding—Keys for Discovering Value

This section of the paper aims to point people in directions to find more value for their projects. It appears that no one person or company has exclusive access to value creating ideas. It is my conviction that many high value ideas will flow

through people who intimately understand a project, not just through the industry expert who comes in for a three day review. A sound knowledge of the project, value drivers and optimisation assumptions are all important to unlocking greater value from a mining project. The variety of geological resources, mining methods and philosophies employed at major projects around the globe mean that value discovered in one project may not be found in another. The following suggestions are general areas that are regularly neglected and so may be sources of additional value.

Project Optimisation

Of all the optimisation analysis that is undertaken in geology, mining, processing and marketing, it seems that very little analysis spans all of these disciplines. Although the same detail cannot be applied for global project analysis as can be applied to detailed component analysis, we need to start with the big picture to make most effective use of our finite resources (such as time, people and budgets). The project analysis allows for determination of where the most important value drivers are, allowing prioritising of analysis effort. The project optimisation can also provide context and scope for a more detailed analysis.

Working Out of Your Discipline

Concentrated and isolated analysis within geology, mining, processing, environmental, marketing and financial can easily develop silos of knowledge and understanding. While this may start at university and a natural affinity with one's discipline, it is essential for project optimisation that some people come to understand the whole project. Many fields are interrelated—for example, problems in the processing plant could well stem from fundamentally different geological ore genesis. The cut-off grade of material mined has substantial implications on processing and marketing parameters.

Multidisciplinary Teams

Major mining projects are well beyond the technical skills of any one individual. Creating teams to look for value has often led to unrealised value. The quantity of information to be absorbed and translated often works well with a multidisciplinary team. Teams would normally include geology, mining, processing, environ- mental and financial members and it is essential that some of the team members should also have a strong optimisation capability. Well-run teams can encourage innovation and building on each other's ideas—they are also often able to quickly discard options unlikely to add value.

Removing Constraints

Because constraints place substantial limits on the value of a project, what is the value of removing these constraints? The concept of de-bottlenecking or using constraints theory may be used, as long as it is in conjunction with value analysis and not just for gaining additional capacity. If the primary crusher is a major bottleneck, would the value obtained by adding capacity cover the new capacity?

Constraints or Targets

The direction of a project can easily take on the preconceived ideas of an influential manager. Creating smooth ore-grade profiles has a cost to the mine—what is the value implication if the processing plant accepted more variability? Marketing 'constraints' may be little more than market predictions; are these creating ceilings on increasing the value of a project? Many of these issues are quickly identified by multidisciplinary teams.

Full Value Focus

Focus on the corporate objective of what adds value, even if that does not suit some parties. Utilise the whole of the resource rather than just the first 20 to 30 years (it will help demonstrate the value of expansions). Making an open pit bigger should be considered in the light of the alternate underground options. How can the project realise the greatest value from one of these options? Don't just use average quantities—know the value of:

- a truck of ore,
- a hole of explosives,
- a conveyor belt,
- SAG steel balls, and
- acid and wheel motors.

The more people understand the value, the more they are likely to make appropriate value based decisions. Break-even cut-off grade costs calculations for reclaiming stockpiles are presented in an appendix of this paper to illustrate the need and value of understanding optimisation assumptions.

Conclusions

This paper has provided guidance to help strategic planning engineers to fully and profitably exploit the resources in their care. Shareholder value within a constraint framework is normally the objective for optimal mine plans—the key is to not get

so distracted by details that focus is lost on what really adds value. These are finite resources that we normally only get one chance to exploit—let's make the most of them while achieving the best value for shareholders.

Appendix—Applying Break-Even Cut-off Grades

The following example has been presented to show how care must be exercised when determining what costs should be included in calculating operational cut-off grades. This example highlights a number of scenarios involving reclaim from stockpiles and which costs should be included in each case. Consider the costs that are used to calculate a mill cut-off grade—should the mining (drill, blast, load and haul) and G&A (General & Administration, $/year) type costs be included for material going to or coming from a stockpile?

First, take the example of a project that is 'mine constrained'—the project is struggling to use the processing capacity due to mining capacity restrictions (truck or shovel capacity, sinking rates, etc.). This will typically occur at the beginning of a project when the high value material is only located at depth. It also may occur after mining one high grade area before the next high grade area is available. Even when using all the mining equipment, there may not be sufficient high grade ore to fill the mill capacity.

What is the minimum grade that can be sent for processing? The question can easily be answered by considering the two options possible for a region of ground:

1. What is the value of sending the material to the mill?
2. What is the value of sending the material to waste (Waste value will be a negative number since all components are negative value costs)?

Since the material is being mined, when the value of sending the material to the mill is greater than sending it to the waste dumps, it should be processed. Using variable definitions as used by Lane (1988) where possible, such as the period cost (f, $/year), processing cost (h, $/t ore), mining cost (m, $/t rock), selling cost (k, $/t metal), price (p, $/t metal), recovery (y, recovered metal/in situ metal), mining capacity (M, t rock/year), mass above cut-off grade (x, t ore/t rock) and grade (g, in situ metal/t rock), the following relationships are clear:

$$V_{ORE} = (p - k).y.g.x - f/M - h.x - m_{ORE}$$
$$V_{WASTE} = -f/M - m_{WASTE}$$

The mining cost of processing material as ore (m_{ORE}) could be different to that when the same material is processed as waste (mWASTE). For example, some operations will blast the material more coarsely if it is being sent to waste, and the haulage costs are often different between ore and waste. The mine constrained

cut-off grade for material mined from the pit (g_{MP}) is determined when $V_{ORE} = V_{WASTE}$ as follows:

$$g_M = \frac{h + m_{ORE} - m_{WASTE}}{(p - k).y}$$

Apparent from the derivations and the formula for g_M above, the period costs do not have to be covered in this situation. This observation makes sense when one considers that the period costs will be incurred irrespective of the destination of the material. When the ore and waste mining costs are identical, they also drop out of the calculation and it becomes the same equation that Ken Lane formulated (1988, page 28). This shows that material mined in a pit will incur mining costs regardless of its final destination. The decision can simply be made depending on whether the project makes more money from processing the rock than sending it to the waste dump. Where a stockpile exists during the same mine constrained period, the following equation to calculate the mine constrained stockpile break-even cut-off grade (g_{MS}) simplifies to:

$$g_{MS} = \frac{h + m_{ORE}}{(p - k).y}$$

The m_{ORE} cost for a stockpile normally only includes the reclaim loading and haulage costs, since drilling and blasting costs are not necessary. Notice that here the waste mining cost does not incur any costs since the material can simply be left on the stockpile. The stockpile re-handling costs must be covered by the processing revenue in this case. This means that higher grade material would need to be reclaimed from the stockpile than what could be sent directly from fresh material mined in the pit. Ore ranking grades need to be updated (such as the cash flow grades, King 1999) to take this into account as material is moved from the pit into a stockpile.

A subtle assumption in the above cut-off grade derivations is that the material will be processed. Let's consider a stockpile at the end of the project life. If the material is not processed, it is left on the ground and the project abandoned (ignoring closure costs and reclamation for the moment). It is also assumed that the environment is no longer mine constrained, but rather we are processing constrained (H, t ore/year), and all the material mined from the stockpile is ore (x = 1). In this case we consider the following equations:

$$V_{ORE} = (p - k).y.g - f/M - h - m_{ORE}$$
$$V_{WASTE} = 0$$

The stockpile cut-off grade (g_s) at the end of the project life is again determined when $V_{ORE} = V_{WASTE}$ as follows:

$$g_S = \frac{h + m_{ORE} + \frac{f}{H}}{(p-k).y}$$

This is an interesting result because now the break-even cut-off grade for processing the last material from the mine stockpile must include the mining costs and also the period costs. If material is added to a stockpile using mine constrained cut-off grades, then there could be substantial uneconomic material mixed in with the economic material and it is likely impossible to separate. The situation has more issues to be considered when the material mined is not at the end of the project life and an opportunity cost exists. There is an opportunity cost to reflect which material is required to fill the limited processing capacity, and the timing to access the remaining material. For a processing constrained stockpile, a formulation of the opportunity cost defines an economic cut-off grade (g_E) as:

$$g_E = \frac{h + m_{ORE} + \frac{f+F}{H}}{(p-k).y}$$

In practice, this formulation is very simplistic since it needs to take into account multiple sequences, several processes, interaction between several ore processing constraints, revenue from multiple elements and time varying issues. It does show that there is not one simply universal answer for the inclusion of period and mining costs in determining what material should be mined from, or deposited to, a stockpile. By taking the time to understand the project situation and algorithm assumptions, appropriate material can be sent to stockpiles and reclaimed. Although opportunity costs or remaining value estimates are implemented in modern cut-off grade optimisation software tools like Comet (Wooller 2007), they may not find the additional value without a model constructed to look for this value.

References

Bellman R (1957) Dynamic programming. Princeton University Press, New Jersey

Brealey RA, Myers SC (2000) Principles of Corporate Finance, 3rd edn. Irwin McGraw-Hill

King B (1999) Cash flow grades—scheduling rocks with different throughput characteristics. In: Proceedings whittle strategic mine planning conference. Whittle Programming, Melbourne, pp 103–109

King B (2008) Optimal mining—Building the practice of optimisation in the mining industry [online]. Available from http://www.optimalmining.org/optimalmining/

Lane KF (1964) Choosing the optimum cut-off grade. Q Col Sch Mines 59(4):811–829

Lane KF (1988) The economic definition of ore—cut-off grades in theory and practice. Mining Journal Books, London

Lerchs H, Grossman IF (1965) Optimum design of open-pit mines. Trans Can Inst Min 68:17–24

Wooller R (2007) Optimising multiple operating policies for exploiting complex resources—An overview of the COMET scheduler. In: Dimitrakopoulos R (ed) Orebody modelling and strategic mine planning, 2nd edn. The Australasian Institute of Mining and Metallurgy, Melbourne, pp 309–316

The Global Optimiser Works—What Next?

J. Whittle

Abstract The Global Optimiser used by Whittle Consulting has gone through three major versions to date. The first was based on the Milawa optimisation algorithm; it worked, but had many shortcomings. The second, known internally as ProberA, had a different approach to optimisation in that it used a series of random starting points and found the nearest local NPV maximum to each. It did this a sufficient number of times to give us some confidence that the best result found was close to optimal. ProberB was an enhanced version of ProberA, with the ability to handle a wider range of constraints, particularly with regard to limits on the differences in depth between adjacent areas of a pit. ProberB has been used successfully for some time now. It has produced excellent Life of Project schedules for a wide range of very large mining complexes. However, like any piece of software, it has its limitations. For example, it only copes directly with three steps—mining, processing, and blending.

It is possible to 'fool' the program into handling other steps, but only by using mental and mathematical gymnastics. This paper reviews the mechanisms behind the Prober series and describes the plans for the next version—ProberC.

Keywords Global optimisation · Long-term scheduling · Net Present Value

Introduction

For some years now a global optimiser has been used to produce long-term mining and processing schedules which maximise the Net Present Value (NPV) of the whole project, taking account of all cash flows including capital expenditure. There have been three versions of this optimiser, known internally as Z3, ProberA and ProberB. Further details can be found in Whittle and Whittle (2007) and in Whittle

J. Whittle (✉)
Whittle Consulting Pty Ltd, 42 Yeneda Street, Balwyn North Vic 3104, Australia
e-mail: jeff@whittle.name

R. Dimitrakopoulos (ed.), *Advances in Applied Strategic Mine Planning*,
https://doi.org/10.1007/978-3-319-69320-0_3

(2007). This paper explains the methods used in Prober and describes the plans for the development of a new optimiser—ProberC.

Modelling

In order to use a computer to optimise any system it is necessary to create a mathematical model of the system. This model must represent the system as accurately as possible, but must also be amenable to optimisation. In theory any mathematical model can be optimised by throwing enough computer power at it. However, as the size of models increases, some types can get rapidly out of hand. There are mathematical problems which are quite easy to describe but could not be fully optimised by using all the computers in the world for a million years. However, it is sometimes possible to find very good near-optimal solutions to problems that defy full optimisation. Occasionally this can be done by simplifying the model, or by using approximate optimisation methods. The Prober approach uses both these techniques to obtain good, long-term schedules for large mining complexes. Keep in mind that all models are wrong but some are useful (Box 1979).

A large mining complex with 20 or more pits with associated processing plants and infrastructure would defy Life of Project NPV optimisation if modelled in day-to-day detail. It is therefore necessary to simplify the model to some degree. The main simplification is to concentrate on long-term scheduling. If a large expense is delayed by five years, this could have a significant effect on the NPV. If the same expense is delayed by a week, the effect will be small. Long-term scheduling decides what will be mined, processed, blended and sold in each year of the life of the complex. Expenses are delayed and revenues are brought forward, while meeting all the required constraints. In short-term scheduling, practicality and convenience are more important than the timing of cash flows. There is also the consideration that the data required for short-term scheduling differs from that for long-term scheduling. For long-term scheduling what matters is the total volume of dirt a truck can move in a year; however, there is no need to consider its detailed movements.

For Prober, the resource is modelled as a number of ‘sequences’ of ‘panels’, and the rule is that mining of a panel can’t start until the panel before it in the sequence has been completely mined. These panels usually represent benches in a push-back, but can also represent parts of an underground mine that must be accessed in a particular order. A panel consists of one or more ‘parcels’ of material, each of which will typically have a material type, a tonnage and a number of grades. If Prober mines only a fraction of a panel in a particular year, it uses the mathematical fiction that the same fraction of every parcel in the panel will be mined in that year. Of course, this is not what will happen in the day-to-day scheduling, but the necessary adjustments should have little effect on the NPV.

The main data input to Prober consists of a ‘resource tree’ showing all possible things that can happen to material after it has been mined. For each parcel, it gives the alternative processing paths that can be taken (e.g. mill or heap leach). For each processing path, it gives the products that the outputs from processing can be blended into, etc. The remainder of the data details cost and price factors which apply to the whole complex, together with the various operational constraints. When modelling the constraints on the operation of the complex, it is not necessary to simplify much at all. Limits can be set on mining and processing throughputs, which can depend not only on tonnage but on grades or other characteristics (e.g. how much power or acid is required to process material). Upper and lower limits can be set for the average grades input to processing and in products, as well as on the depth separation between sequences.

The Problem of Local Maxima

The aim is to find the mining and processing schedule which gives the highest NPV. Consider just one sequence and one year with no blending. This might result in the situation illustrated in Fig. 1. Sequence A has some panels, some of which are ore and others are waste. As mining proceeds through the ore, the value goes up; as it proceeds through waste, it goes down. The result in this case is that there are two peaks. Figure 2 illustrates the same idea for another sequence. Each peak is a maximum in its own part of the graph, but it is a local maximum. Only one is the global maximum. Figure 3 shows what happens if the complexity is increased to two sequences, but still only over one year. Now there are four local maxima. In practice, with a few dozen pits, blending constraints and many years, there can be thousands of local maxima. This can be equated to the search for the highest point in the Himalayas rather than the highest point of Mount Fuji. Merely going uphill from a random start point will get you to a ‘nearest’ local maximum. It is unlikely to be the highest point, that is, the global maximum. Because of the multiplicity of

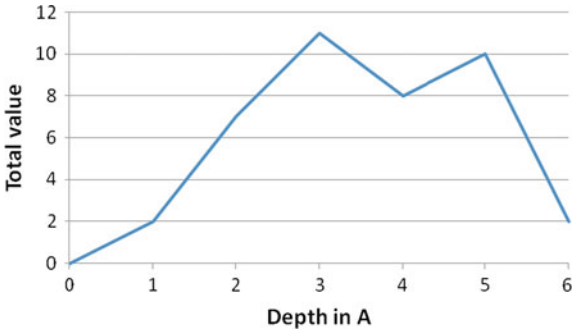

Fig. 1 The total value of material mined from sequence A plotted against depth mined, where some benches are ore and some are waste. The two peaks are local maxima; the left peak is the global maximum

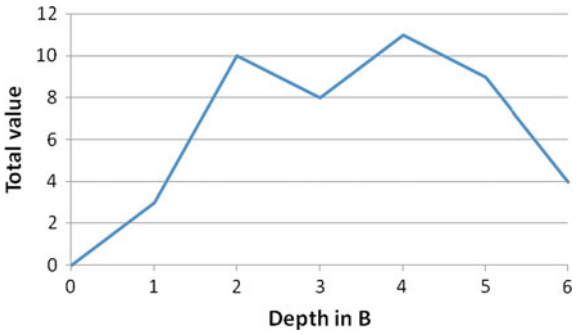

Fig. 2 The total value of material mined from Sequence B plotted against depth mined, where some benches are ore and some are waste. The two peaks are local maxima; the right peak is the global maximum

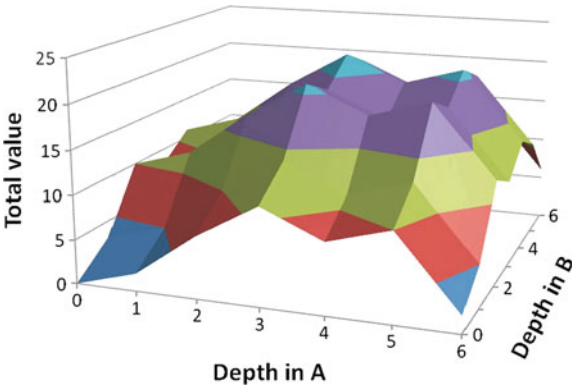

Fig. 3 The total value of material mined when both sequence A and Sequence B are mined to various depths. There are four peaks. Only the rear left peak is the global maximum. This shows just two sequences and one year. In real cases with many sequences and many years, there can be thousands of local maxima

local maxima, this is not a linear problem in the sense of linear optimisation—it is a 'mixed integer' problem.

Although linear optimisation methods are very fast for large problems, the introduction of integers—which is necessary to deal with the multiple local maxima—slows the process down by several orders of magnitude. Indeed, schedules for very large mining complexes are effectively unobtainable using mixed integer software.

How the Prober Series of Programs Work

The Prober series of programs break the problem down into a number of smaller problems which can each be solved quickly using linear optimisation software. Prober first produces a random feasible *mining* schedule consisting of a year-end depth in each sequence for each year in the life of the project. Thus, for 20 sequences and 15 years, there would be 300 depths. This schedule is produced by using pseudo-random numbers to calculate the depths while taking account of all the constraints on *mining* throughput and on depth separation. This fixes the

material available for processing in each year. There is no optimisation in this step, and this is not necessarily a good schedule. Indeed, it is usually very poor, but it is feasible from a mining point of view, so it gives us a starting point. You can think of this schedule as a random point on the ground somewhere in the Himalayas. Given the material made available in each year, it is a straightforward matter to use standard linear optimisation to determine what to process, blend and sell so as to maximise the NPV obtainable by processing the material subject to the throughput constraints.

As explained earlier, the assumption is made, so far as the model is concerned, that parcels within a panel are all mined in the same proportion. This means that changes in mining depth within a panel have linear effects on the quantities of material available for processing and so on. Consequently, in addition to having the linear optimisation package control what to process, blend and sell, it is possible to let it control the depths mined, providing that those depths are constrained to stay within the panel that they started in. The result is the best mining and processing schedule for a given set of year-end panels. Having obtained such a result, the depth details suggest changes to the year-end panels. For example, if the year-end panel for a particular sequence and period is set to three, but the optimisation does not mine any of Panel 3, the program will change the year-end panel to two and try again. If the NPV improves, the process is repeated. The program is effectively going uphill in the NPV landscape, and this process is repeated until a maximum is reached. This is the nearest local maximum to the initial random feasible schedule. One of the peaks in the Himalayas has been found.

The Prober series of programs works by repeatedly creating a random feasible solution and then finding the nearest local maximum. The various NPVs that the program finds are kept track of, and the run is usually stopped when the top ten values lie within 0.1% of each other. This does not guarantee optimality, but it does give confidence that the best results are pretty close. Most projects that we worked on had a distribution of local maximum NPVs that is pretty flat near the highest

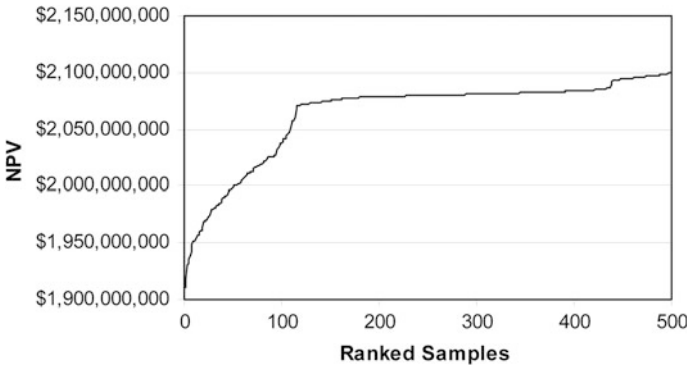

Fig. 4 500 NPVs obtained by moving from 500 random schedules to the nearest local maximum have been sorted into ascending order of value. The curve is relatively flat at the high end and 11 of the local maxima have NPVs that are within 0.1% of the best

values as illustrated in Fig. 4, which is from a real case. That is, many different schedules are found that have NPVs which are very similar to the best. In this case, 11 of the 500 local maxima found are in the top 0.1% and over 200 are in the top 1%. This can be an advantage because it gives managers the opportunity to choose the schedule that best suits less measurable considerations such as social, political, environmental and project risk effects. To date, many projects have been successfully completed with the current version of Prober (ProberB) and very significant NPV gains have been made totalling billions of dollars.

ProberC

ProberC uses the same optimisation system but operates on a greatly enhanced data structure. It can be regarded as a generalisation of ProberB. Grades are expressed as quantities, so that a grade of 1.2 grams/tonne of gold in a 2000 tonne portion of material would be expressed as 2400 grams. Thus, a portion of material, be it run-of-mine or the output from processing, is described by the quantities associated with it. Any of these quantities can be involved in throughput limits, costs, revenues, etc. In ProberC, everything that is done to material is done by a 'procedure'. Mining, processing, smelting, blending, etc. are all procedures. There can be as many procedures as required and any procedure can provide input to another procedure, with the restriction that material cannot 'loop' through the system and thus provide input to the procedure that produced it. Thus, there is an arbitrary tree structure of procedures, starting with a mining procedure and going through as many steps as required to the point(s) of sale or to waste. This contrasts with ProberB, which handles only mining, processing and blending for sale. Delivery of material from a procedure to stockpile, sale, discard or another procedure is much more explicit in ProberC than ProberB and has its own cost structure. For example, long distance delivery costs can be handled explicitly rather than having to be included in the processing cost as in ProberB.

All costs and revenues are calculated as the sum of one or more of three components, multiplied by a scaling factor. The components are:

1. a cost or revenue proportional to one or more of the quantities, which describe the portion of material involved;
2. a cost or revenue proportional to the difference between a grade (ratio between two quantities) and a base grade multiplied by a third quantity; and
3. a constant attached to each portion of material in the resource tree each time it can be processed or delivered.

All the factors and base grades in components 1 and 2 can vary independently with the year. Any number of components of types 1 and 2 can apply. Type 3 components are attached to each portion of material operated on and can be calculated to suit that portion, but are fixed in time. The scaling factor by which the

sum of these components is multiplied can vary with the year. This system allows almost any cost or revenue structure to be modelled. Setting up such costs and revenues might appear somewhat daunting, but it is important to remember that the data is always set up by a specialist consultant, not the end user. Costs and throughput limits can be applied to both the inputs and the outputs of procedures. Despite the great increase in complexity of the processing and cost structures that can be modelled, the problem steps can each still be handled by a standard linear optimisation package as in ProberB. ProberC is currently under development and it is expected to be completed in 2009.

Conclusions

ProberB has established itself as a powerful and flexible tool. ProberC will have the same power as ProberB, but will handle a much wider range of project and costing complexity.

References

Box GEP (1979) Robustness in the strategy of scientific model building. In: Robustness in statistics (eds: R L Launer and G N Wilkinson), p 202 (Academic Press, New York)

Whittle G (2007) Global asset optimisation. In: Orebody modelling and strategic mine planning, 2nd edn (ed: R Dimitrakopoulos), pp 331–336 (Melbourne, The Australasian Institute of Mining and Metallurgy)

Whittle J, Whittle G (2007) Global long-term optimisation of very large mining complexes. In: Proceedings APCOM 2007—33rd international symposium on application of computers and operations research in the mineral industry, Santiago, pp 253–260

Blasor—Blended Iron Ore Mine Planning Optimisation at Yandi, Western Australia

P. Stone, G. Froyland, M. Menabde, B. Law, R. Pasyar and P. H. L. Monkhouse

Abstract A new mine planning optimisation software tool called Blasor has been developed and implemented at BHP Billiton's Yandi Joint Venture operation in the Pilbara. Blasor is specifically configured for designing and optimising the long-term pit development plan for the multi-pit blended-ore operation at Yandi. It is used for optimal design of the ultimate pits and the mining phases contained within those pits. In designing the mining phases, Blasor ensures that all market tonnage, grade and impurity constraints are observed whilst maximising the nett discounted cash flow (DCF) of the joint venture operation.

Introduction

In undertaking a life-of-mine development plan for multi-pit blended-ore mining operations, the mine planner is faced with difficult decisions regarding both the extent of ultimate pits and the design and precedence of the mining phases in each pit. Various commercially available optimisation tools are capable of determining optimal extraction sequences for existing blended-ore pit phase designs—for example NPV

P. Stone · M. Menabde
BHP Billiton Technology, PO Box 86A, Melbourne Vic 3001, Australia

G. Froyland (✉)
School of Mathematics, The University of New South Wales,
Sydney, NSW 2052, Australia
e-mail: froyland@maths.unsw.edu.au

B. Law
BHP Billiton Project Development Services, PO Box 86A,
Melbourne Vic 3001, Australia

R. Pasyar
MAusIMM, BHP Billiton Iron Ore, PO Box 7122, Perth, WA 6850, Australia
e-mail: Reza.Pasyar@bhpbilliton.com

P. H. L.Monkhouse
BHP Billiton Limited, PO Box 86A, Melbourne Vic 3001, Australia

R. Dimitrakopoulos (ed.), *Advances in Applied Strategic Mine Planning*,
https://doi.org/10.1007/978-3-319-69320-0_4

Scheduler, Minemax, ECS Maximiser and Whittle Consulting—but planners are usually forced to rely on a mixture of common sense heuristics and personal experience to design the ultimate pit boundary and the mining phase polygons, e.g. Dincer and Peters (2001) and Noronha and Gripp (2001). A typical pit and mining phase design procedure will require the planner to make arbitrary judgments on in-ground block value—an assumed cut-off grade decision—and then apply a Lerchs-Grossmann algorithm to obtain approximate pit and phase boundaries. These types of approaches become far less tractable when dealing with large multi-pit operations.

The result is that the design of mining phases in blended-ore operations depends largely upon the expertise and experience of the particular mine planner rather than being an objective and repeatable procedure. Once the ultimate pits and mining phases are put in place the flexibility and value attributable to a mining operation over its lifetime is in many ways constrained—no matter what sophistication is applied in optimising panel extraction sequences, the consequences of suboptimal mining phase design can never be overcome.

The mine planning optimisation group within BHP Billiton Technology has developed a mine planning optimisation software tool called Blasor. The concept of Blasor is to use an optimal extraction sequence to design the ultimate pits and mining phases, not the other way around as is the typical approach.

Blasor is specifically designed to optimise the life-of-mine pit development plan for the eleven pits constituting the Yandi Joint Venture operation. It provides Yandi mine planners with a strategic planning tool that can be used throughout the mine life to reconfigure pit development plans as market conditions change. It also enables the operation to rapidly, accurately and optimally value different future market scenarios and/or expansion options using forward pit development plans that are sympathetic to those scenarios and options.

In this paper, we describe the concept and structure of Blasor. The structure of the optimisation problem and the types of constraints applied are outlined before the major design steps are discussed in more detail.

Blasor Implementation

Blasor has been developed as a PC based (Windows 2000 or XP) integrated stand-alone software package that has the following input/output features:

- Block models are supplied as flat ASCII files.
- Optimisation parameters are entered by the planner through a purpose-built graphical user interface.
- Intermediate data, including all block attributes calculated or assigned by Blasor, can be rapidly viewed in a dedicated 3D visualisation tool.
- Schedule output data, including full tonnage movement and financials, is reported via a number of specialised databases automatically generated by Blasor. A 2D graphical display tool is also provided within the Blasor interface for rapid display of the schedule data on an area and pit-wise basis.

Optimisation Parameters and Setup

Blasor's ultimate objectives are to determine the boundaries of the ultimate pits and the best phase designs for those pits so as to maximise the DCF over the life of the operation. In doing so, Blasor uses the commercially available CPLEX mixed-integer linear programming (MILP) optimisation engine from ILOG Inc to determine the optimal extraction sequence contingent upon a number of constraints being strictly observed.

The parameters Blasor uses to constrain the optimisation of the multi-pit development plans are:

- the constraints imposed by practical mining—respecting maximum slopes and mining rates;
- capacity of the downstream supply chain infrastructure; and
- market tonnage, blended ore quality and grade constraints.

A complete list of the constraints applied in the optimisation is given in Table 1. Other limits to the optimisation model of the real operation are:

- Initial stockpiles are allowed (one for each area). No strategic stockpiling capability is allowed throughout the mine life. Blasor attempts to find an extraction sequence that avoids stockpiling between years.
- No material in the pits is designated as waste a priori—the optimiser makes the decision as to how to best blend the material extracted from the pits to make marketable ore. Only blended ore that meets all market grade and quality constraints can have a positive revenue attributed to its extraction.

Table 1 Constraints applied in optimisation

Constraint class	Constraint
Mining	Maximum slope angles enforced at the selective mining unit block size level
	Maximum mining rate for the operation, each mining area and each pit (variable per annum)
	Earliest start year for pits
	Smooth mining constraint—large jumps in operation mining rate can only occur after a prescribed duration of near constant mining rate
	Maximum sinking rate (benches/year)
Transport	Maximum conveying rate for multiple transport paths (variable per annum)
Crushing and screening	Maximum crusher capacity for mining areas and pits (variable per annum)
Market	Target tonnages for fines and lump product individually (variable per annum)
	Maximum and minimum per cent Fe for fines and lump product (variable per annum)
	Maximum and minimum % SiO2, % Al2O3, % P, % Mn and % S for fines and lump product (variable per annum)

- Mining and transport costs are attributed to each block—according to their position in the pit different blocks will have different mining and transport costs.
- All material in the pits is allocated a bin number. Material may be assigned to bins on the basis of any combination of grade and impurity dimensions.
- Within each bin of an AGG (an 'AGG' is an aggregation of blocks), the material is assumed to be of homogeneous quality. The optimiser may extract any proportion of an AGG in any year, contingent on other constraints being obeyed.
- The extraction precedence of each AGG is determined by the extraction precedence of its constituent blocks. No part of any AGG may be extracted before all its precedent AGGs have been totally extracted. The rules of precedence are simply that if a block lies above another block (precisely if its centroid lies within the 'cone' transcribed by the maximum slope line for the underlying block), then the overlying block must be extracted before the underlying block.
- Prices for both fines and lump material may be specified to change from year to year.
- All net cash flows are discounted at an appropriate rate.
- The optimisation objective is to find an extraction sequence that obeys all constraints explicitly and results in a maximum nett discounted cash flow.
- The optimisation is global, over the full life-of-mine.

Blasor Optimisation Procedure

The Blasor optimisation procedure is summarised in Fig. 1, illustrating the major steps:

- aggregation of blocks including binning,
- calculation of optimal extraction sequence and ultimate pit limits,
- mining phase design, and
- valuation of the optimal panel extraction sequence.

In the following section, we describe each step of this procedure in more detail.

Aggregation

For the large block models encountered at Yandi (containing >100 000 blocks), it is necessary to aggregate blocks before they can be tractably scheduled using any linear programming approach. To provide the optimiser with valuable selectivity, binning is used to allow blocks of similar quality to be extracted together by the optimiser. A common method used to aggregate blocks is to re-block the model into a larger block size—this is not the method used in Blasor. The aggregation method used is a proprietary fuzzy clustering algorithm that has the following characteristics, where the term 'AGG' is used to refer to an individual aggregation:

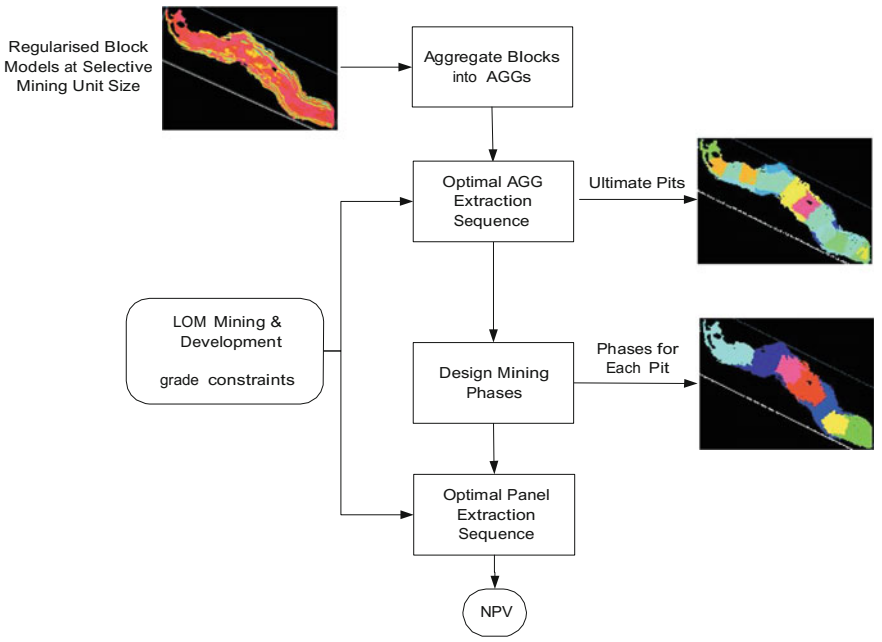

Fig. 1 Blasor pit development optimisation procedure

- blocks that are spatially connected and with similar properties are predisposed to belong to the same AGG, and
- the AGG boundaries respect the maximum slope constraints encoded in the selective mining unit block models.

The user may choose to present Blasor with block models that are already cut back to some nominal 'ultimate pit' surface or to allow Blasor to aggregate a larger volume. Each AGG in the larger volume would be presented to the optimiser as a candidate for extraction over the life-of-mine.

After this step, each pit is described by a set of AGGs. Each AGG contains material which is classified in bins. Each bin is allowed to be extracted independently of other bins in the same AGG. A set of AGG precedence rules is also created. These rules, represented as a set of arcs, force the optimiser to extract material in a valid order.

AGG Extraction Optimisation

This is the vital step in the Blasor design process whereby an optimal AGG extraction sequence is calculated and the blocks in each pit are assigned a period of extraction. The scheduled entities are bins within each AGG and the final AGG extraction sequence will obey all mining, slope precedence, processing and market constraints. The typical size of this optimisation problem for Yandi is:

- 1000 AGGs in total from 11 pits, each AGG containing five bins; and
- 20 time periods over the life-of-mine.

A problem of this size will take between six and ten hours to converge within a 0.5% bound of optimality using the CPLEX MILP engine running on a powerful laptop computer. This optimisation also provides an estimate of the AGG extraction sequence life-of-mine discounted cash flow, which can be used as a benchmark for the DCF of the panel extraction schedule (see below) in assessing the practical optimality of the mining phase design step.

Mining Phase Design

The mining phase design is performed individually on each pit in the operation. The design procedure uses a proprietary algorithm, which uses the 'period of extraction' block attribute to prioritise the phases within each pit. Some user input is required to assist the algorithm in designing mineable phases—so-called 'rat-holing' can be controlled or overcome through the judicious selection of phase design parameters. Because this step cannot be completely automated, a tool is provided which allows the planner to make practical modifications to the automatically generated mining phases. The interface that allows manual modification of phase designs in Blasor is shown in Fig. 2.

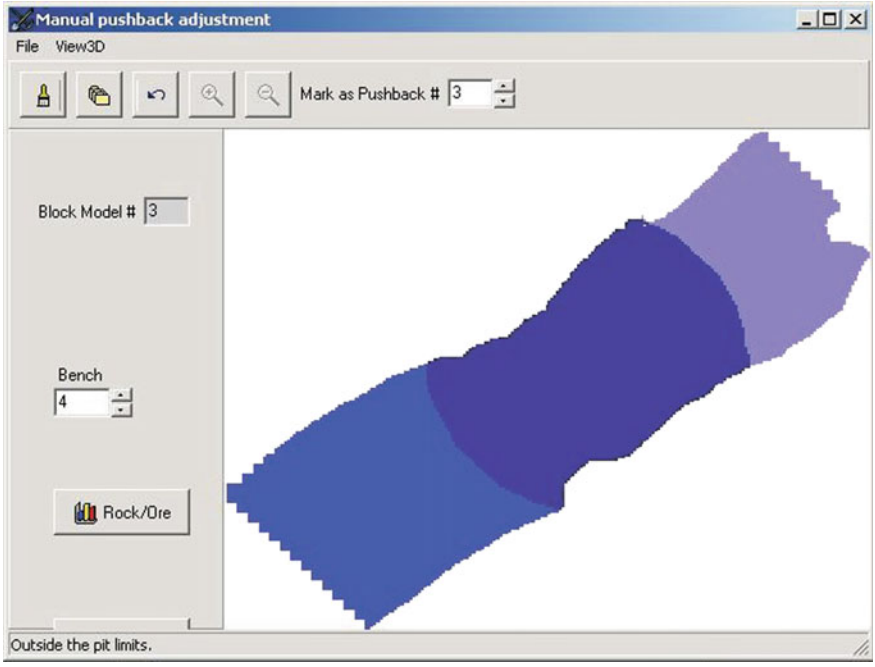

Fig. 2 Interface for the manual phase adjustment tool in blasor

Panel Extraction Optimisation

Having designed the mining phases for each pit, the planner then uses Blasor to generate the panel attributes (where a 'panel' is the intersection of a mining phase and a bench). Panels are represented in the same way as AGGs—via tonnes of all attributes in each bin. The optimal panel extraction sequence is calculated in the same way as for the AGG extraction sequence and uses the same mining, processing and marketing constraints. The final optimal sequence provides the user with a direct estimate of the DCF over the life-of-mine. For the Yandi operation, the optimal panel extraction sequence DCF is usually very close to the optimal AGG extraction sequence DCF, showing that the Blasor phase design process is efficient at preserving the value of the mining operation despite the inevitable compromises that must be made in constructing mineable phases.

The panel extraction optimisation process requires a similar processing time as the AGG extraction sequence optimisation, the final result being an attribution of period of extraction for each block in each pit. An example of the block extraction sequence, illustrated as a colour-coded period of extraction section through the centre line of a single pit, is shown in Fig. 3.

Conclusion

Blasor provides an efficient and integrated long-term pit development planning and evaluation tool for the Yandi Joint Venture operation. It enables mine planners to design ultimate pits and mining phases that are based upon a globally optimal multi-pit life-of-mine extraction sequence and then to generate an optimal panel extraction sequence from which the practically realisible maximum DCF for the operation can be reliably estimated.

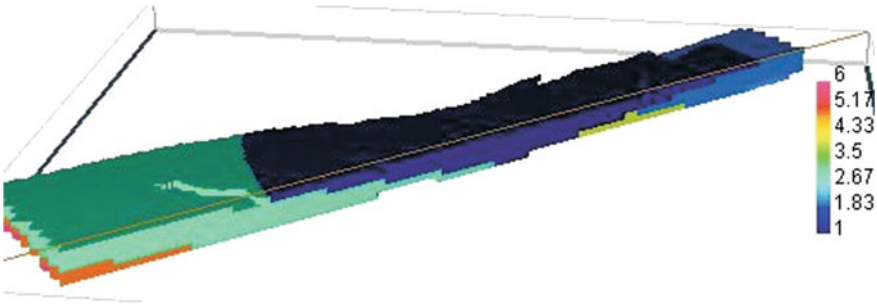

Fig. 3 Optimal period of extraction according to blasor panel schedule

References

Dincer T, Peters B (2001) Blending optimum pit mining sequences. In: Proceedings fourth biennial conference: strategic mine planning 2001, pp 43–53 (Melbourne, The Australasian Institute of Mining and Metallurgy)

Noronha RA, Gripp, AH (2001) Ultimate pit selection and design in iron ore. In: Proceedings fourth biennial conference: strategic mine planning 2001, pp 133–136 (Melbourne, The Australasian Institute of Mining and Metallurgy)

Roadblocks to the Evaluation of Ore Reserves—The Simulation Overpass and Putting More Geology into Numerical Models of Deposits

A. G. Journel

Abstract Many factors including data scarcity, volume support effects, information effect, accessibility and pervasive uncertainty, make the early prediction of recoverable reserves a challenge that cannot be addressed by mere estimation or interpolation algorithms. There is the illusion that as long as one uses the 'best' estimation algorithm based on quality data and sound geological interpretation, one would provide the best possible evaluation.

Introduction

Many factors including data scarcity, volume support effects, information effect, accessibility and pervasive uncertainty, make the early prediction of recoverable reserves a challenge that cannot be addressed by mere estimation or interpolation algorithms. There is the illusion that as long as one uses the 'best' estimation algorithm based on quality data and sound geological interpretation, one would provide the best possible evaluation. Unfortunately, a set of locally accurate ('as best as they can be') estimated values does not generally make for a good, or even an unbiased base on which to assess future recoverable reserves. The dichotomy between local accuracy and global representation is at the source of many arguments and severe prediction errors. A discussion on the various factors affecting the reliability of reserves prediction may help in focusing efforts on what matters, marking common pitfalls, then stress what must be done, such as building into the deposit numerical models geological interpretation beyond mere variogram models. It is suggested that the essential components of a mining operation could be simulated from such numerical models, like the performance of the wings of a future plane is simulated in a wind tunnel.

A. G. Journel (✉)
Department of Energy Resources Engineering Department,
Stanford University, Stanford, CA 94305, USA
e-mail: journel@stanford.edu

R. Dimitrakopoulos (ed.), *Advances in Applied Strategic Mine Planning*,
https://doi.org/10.1007/978-3-319-69320-0_5

Local Versus Global Accuracy

The illusion that a sound estimation algorithm suffices for ore reserves evaluation comes from the lack of understanding of the trade-offs involved when defining the goodness criterion of any estimator. No estimation algorithm, unless trivially based on exhaustive accurate data, can be good for all purposes. Most estimation algorithms, and kriging is no exception, aim at local accuracy, that is providing an estimate $z^*(\mathbf{u}_i)$ as close as possible to the true and unknown value $z(\mathbf{u}_i)$, irrespective of its relation with any other estimated value $z^*(\mathbf{u}_j)$, $j \neq i$. The attribute z could be any variable, say the mineral content of a given volume centred at a location of coordinates vector **u**i. Local accuracy would suffice if the estimation was so good as to allow the approximation: $z^*(\mathbf{u}_i) \approx z(\mathbf{u}_i)$ and $z^*(\mathbf{u}_j) \approx z(\mathbf{u}_j)$, in which case the pair of estimated values $\{z^*(\mathbf{u}_i), z^*(\mathbf{u}_j)\}$ would reflect the continuity in space of the true values $\{z(\mathbf{u}_i), z(\mathbf{u}_j)\}$. Or, more generally, the estimated map would reflect accurately the true patterns of spatial continuity. Unfortunately, the data available at the time of mine planning and reserves prediction are never sufficient to assume that the map of estimated values accurately reflects the spatial variance of the true values. This is the well known smoothing effect of estimation, a smoothing effect made worse by being non-stationary. This effect is minimal next to the data locations, maximal away from the data and may create patterns that are artefacts of the drill hole locations. An example of a potentially misleading effect on mine planning of otherwise locally accurate orebody models is shown in Dimitrakopoulos et al. (2002).

What makes a mine feasible is not only the tonnage of potential payable ore but also how that potential is distributed in space, allowing economical recovery. Hence, a correct assessment of the actual spatial distribution of grades and relevant morphological properties of the deposit is critical, more critical than local accuracy. Local accuracy is critical only at the time of selection, when the mine is already operating. In addition, that selection is typically performed from different data not available at the time of reserves prediction. Thus, for recoverable reserves estimation, one should trade, or at least balance, the local accuracy criterion for a criterion ensuring accurate depiction of the patterns of heterogeneities prevailing over the actual study area, whether that area is the entire deposit, a bench or a mining panel, within which selective mining will take place. In geostatistics, the traditional measure of spatial variability is the variogram model $\gamma(\mathbf{u}_i - \mathbf{u}_j)$. Thus, we should require that the estimated values reproduce that model; the qualifier 'simulated' is then used instead of 'estimated'. In advanced geostatistics, we aim at reproducing patterns of heterogeneities involving multiple locations at a time, as opposed to reproducing a mere variogram, the latter being but a two-point $(\mathbf{u}_i, \mathbf{u}_j)$ statistic. The name multiple-point (mp) geostatistics is therefore given to that advance, see Appendix and Strebelle (2002).

Stochastic simulation trades poorer local accuracy for a better global or 'structural' accuracy as defined by a prior model of spatial variability, whether that model is limited to a histogram plus a variogram as in traditional geostatistics, or that

model is given as a training image as in mp geostatistics. In the presence of limited data, it is suggested to forfeit any attempt at locating precisely each ore block or Selective Mining Unit (SMU). Instead, one should aim at providing a spatial representation of the grades distribution that mimics the spatial patterns of the true grades, those patterns that may affect the mine plan and recovery. Since stochastic simulation trades off local accuracy, any one of the simulated patterns is likely, though probably not at its true location. Hence simulation should provide many alternative representations or realisations of that spatial distribution, all consistent with the few local data available. No result taken from any single simulated realisation should be used as a local estimate. By definition, results should be collected from multiple simulated realisations, that is, a distribution of results should be provided. *A single simulated realisation should not be used,* in lieu of say a kriging map, for any local decision; yet a set of simulated realisations could replace that kriging map for such a local decision, which then leads to a probabilistic decision (Srivastava 1987).

Although it is unreasonable, from sparse data, to try locating and hence estimating any single recoverable SMU, estimation of large panels or homogeneous zones can be attempted because one could capitalise on the averaging of errors over large volumes. However, within-panel or within-zone recovery should be approached through simulation of the spatial patterns of grades distribution within each panel or zone. No localisation of the within-panel recovery is yet possible, nor is such detail needed for mine planning.

Data Scarcity

In a simulation approach data are needed for two purposes:

1. delineation of homogeneous mineralisaton zones, each defined such that its grade distribution could be characterised by a stationary model, typically limited to a histogram and variogram, or better by a training image that includes the two previous statistics; and
2. rough localisation of ore patches within the previous zones.

The data required for the first purpose does not need to all come from drilling; they can be structural and interpretative in nature. The delineation of homogeneous zones is typically guided from geological interpretation, possibly borrowing structural information from outcrops or similar formations mined elsewhere. In modern geostatistics, multiple-point statistics can include information beyond the variogram by borrowing from geological drawings (training images), the patterns of grade variability deemed to prevail in the actual deposit. In the presence of uncertainty about the style of variability, alternative training images can be considered, each leading to a possibly different recovery of the same global tonnage. This is tantamount to varying the variogram model.

Each simulated realisation is then anchored to whatever local data are available. However, here a shortage of data is less consequential because no local accuracy is required, nor should any single simulated result be used as a local estimate.

The Volume Support Effect

Future mining selection will operate on selective mining units whose geometry and volume support may vary considerably. The volumes are typically beyond the resolution of the data available at the time of mine planning and reserves estimation. Within each large homogeneous zone, a histogram of SMU grades is needed to evaluate the proportion of such SMUs that could be recovered as ore. However, that histogram cannot be built from estimated SMU grades because of the smoothing effect of estimation. The solution is not to attempt an awkward analytical correction of the histogram of estimated values, but to simulate the grade distribution at the quasi-point support volume of the data composite used. These simulated point values can then be averaged into simulated grades for SMUs of possibly different sizes, then the selection process can be simulated on the spatial distribution and histogram of the simulated SMU grades. Sensitivity of ore recovery to SMU size and more generally to the mine selection process can then be easily performed. The utilisation of a common quasi-point support realisation ensures consistency of all results, no matter which SMU size is chosen.

The Information Effect

Possibly the most important contribution of the simulation approach is the assessment of the impact of misclassification on recovery. No present estimation-based geostatistical approach, whether by indicator kriging or uniform conditioning, offers that flexibility. Selective mining calls for small SMUs of varying support volumes, far below the resolution of the data available at the time of mine planning. Indeed, SMUs will be sorted on their ultimate estimated values based on future data not yet available, but it is the corresponding true grades that are sent to the mill and contribute to actual recovery. Misclassification is an unavoidable and often critical aspect of any selective mining; its rigorous evaluation cannot be ducked.

One can simulate the future selection data, for example blasthole data, together with the SMU grades $z_v^{(s)}$ from the point-support simulated grade realization $z^{(s)}$, The simulated blasthole date are then combined into "simulated future" SMU estimated values $z_v^{(s)*}$, The superscript (s) stands for simulated, a star * is added for estimated, and subscript v represents the SMU support volume. Availability of the

simulated pairs $\{z_v^{(s)}(\mathbf{u}), z_v^{(s)*}(\mathbf{u})\}$, true SMU grade and selection estimate, at any location **u**, allows an assessment of the impact of misclassification. Again, sensitivity analysis to various aspects of that information effect can be easily performed, say the type and density of the future data available for ore/waste selection, the geometry of the mine dig lines, etc. Consistency of the various results is ensured by the common quasi-point support of any one of the simulated base realisations.

A lot of heat in the debate about the cause and remediation for 'conditional bias' would be reduced if the information effect was better understood. Any set of estimates, kriging being no exception, is conditionally biased if used to predict a recovery that is performed on another set of estimates. What is needed is the joint distribution of the actual selection estimates versus the true values, these are yet unknown but can be simulated and were previously denoted as $\{z^{(s)}(\mathbf{u}), z^{(s)*}(\mathbf{u})\}$. Improving the kriging procedure, say by culling some data or increasing the search neighbourhood, or designing yet another estimator, say through indicator or disjunctive kriging, would not solve the problem.

Accessibility

There is rarely, if ever, free selection: the economic worth of a block in situ depends not only on its metal content but also on the cost of accessing it and then mining it, the total cost involved being shared with other neighbouring blocks. The decision to mine a block as ore or waste depends on the mine plan, which itself depends on the estimated grades at the time of selection. Estimation of recoverable reserves and mine planning are closely related endeavours that call for a difficult optimisation problem.

Unfortunately, with some notable exceptions (Godoy and Dimitrakopoulos 2004), that optimisation is rarely fully addressed. Instead, and too often, mine plan and design are based on rough, large-scale estimates of grade distributions, with little or no account for the impact of the smoothing effect and future misclassification. Fortunately, such large-scale estimates are not significantly affected by the smoothing effect if based on sound prior geological zoning. As for the impact of future misclassification, it usually is dealt with through dilution factors.

I suggest that simulated realisations of both the distributions of mineral zones and their mineral grades could provide the data bases necessary for testing and fine-tuning alternative mining scenarios, accounting for the all-important support and information effect. There will come a time when mine planning will reach the level of rigour and scientific repeatability of the design of a new aircraft. At that time, simulated numerical models of the distribution of grades and rock properties will be needed, and once again global or structural accuracy of the model will prevail over its local accuracy; that is, stochastic simulation will prevail over estimation.

Uncertainty Assessment

Evaluation of recovered reserves from early development data, not the data used for actual selection, is an extremely challenging task fraught with uncertainty at each step. Not only should it be ensured that all known biases are avoided, but a final assessment of uncertainty about the reserves figures should be provided. It is clear that such uncertainty assessment is beyond any estimation or combined kriging variance, because:

1. Kriging variances are independent of the data values; they are no different whether the SMU is selected as ore or sent to the waste.
2. A variance does not suffice to characterise a distribution unless an arbitrary, and here inappropriate, Gaussian-related distribution is assumed. Simulation approaches can, however, provide this uncertainty assessment.

Conclusion

There is no practical alternative to a simulation approach if critical biases are to be avoided and if the uncertainty about global reserves figures is to be assessed. The paradigm is simple, but its application is difficult. One generates alternative data sets, called simulated realisations, on which the process of imperfect selection is simulated. Provided that the simulated realisations mimic reasonably those traits of the actual grade distribution that most affect the recovery of reserves, and provided that the simulation of the future selection process and its related misclassification is possible, a probabilistic distribution (histogram) for the simulated recovery numbers can be obtained, thus providing a model of uncertainty and confidence intervals. Note that for both simulation processes (geology and mining) various scenarios can and should be considered. Given an early and sparse data set, there can be alternative geological scenarios/interpretations and many alternative options for the mining plan.

All previous provisos render the simulation approach extremely demanding, but correspondingly rewarding, an endeavour that befits the critical importance of reserves assessment.

Acknowledgements This paper borrows from a recent book co-authored by this author, Journel and Kyriakidis (2004). Thanks to Roussos Dimitrakopoulos who has been persistent in calling me back to my mining geostatistics roots.

Appendix: Putting More Geology into Numerical Models of Deposits

Most reserves evaluation and mine planning start with a numerical model of the spatial distribution of the deposit mineral zones. Yet no model is better than the algorithm from which it is built, the algorithm that relates the data to the unknowns. Should the estimation or simulation process include explicitly additional structural information indicated but not included in the data? We suggest that it is that additional information, beyond the actual drill hole data, which determines the quality of a mine model, and hence of its reserves forecasts. Local data, particularly when sparse in an early development stage, are less consequential than the structural/geological information used to tie them to the unsampled locations.

Research in mineral deposit modelling should focus on developing algorithms capable of including more geology in the numerical models. Ignoring prior geological interpretation on grounds that it is uncertain or too subjective is not only counterproductive, it is also conceptually wrong. Better an inaccurate geology than an automatic interpolation algorithm, whether geostatistical or not, that replaces all geology by its own canned universal structure, one that is most often maximum entropy forbidding geological organisation. Accordingly, the major source of uncertainty is the geological interpretation.

Recent developments on multiple-point geostatistics have adopted that route (Strebelle 2002; Remy 2004), replacing the two-point variogram by pattern statistics lifted directly from prior training images proposed by geologists to represent their prior concept about facies or rock type geometry and spatial distribution.

These conceptual geometrical patterns are morphed and anchored to the actual local data. Only when the architecture of the deposit has been built on sound geological considerations can grade interpolation or simulation be performed using the traditional variogram-based algorithms.

An eye opener example

Figure 1 gives images of three different binary facies distributions, say the dark grey facies represent the high-grade mineralisation. The three images are conditioned to the same 30 sample data shown at the left of the figure. Although the three facies distributions are clearly different leading possibly to different mining dilution hence recovery, their exhaustive (indicator) variograms in both EW and NS directions are about the same. Had those variograms been calculated from the 30 sample data they would be all identical! The point made is that a variogram, and more generally two-point statistics, does not suffice to characterise complex spatial patterns.

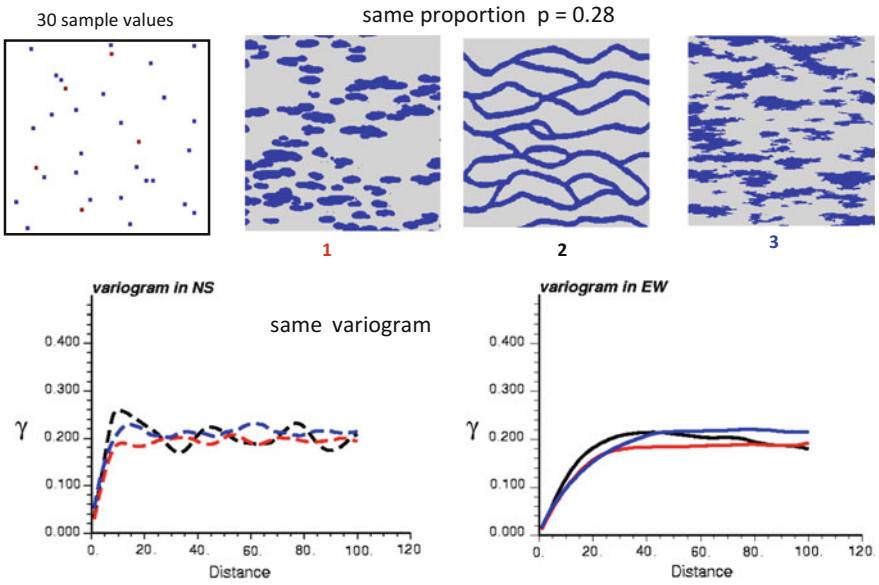

Fig. 1 Widely different patterns, same statistics up to order two

These three images are now used as training images for conditional simulation with an algorithm based on multiple-point (mp) statistics; conditioning is to the same 30 samples. The results are shown at the top of Fig. 2: mp simulation has succeeded to distinguish the three types of spatial patterns; as for variogram reproduction (bottom of Fig. 2) it is as good as, or better than, what would be provided by any traditional variogram-based simulation algorithm. In mp geostatistics, the variogram structural function is replaced by multiple-point spatial patterns lifted from a training image and anchored to the hard conditioning data. The challenge for the geologist is to provide such training images corresponding to their geological interpretation of the data available; alternative geological scenarios could and should be considered. This challenge is no different from that of inferring a variogram model.

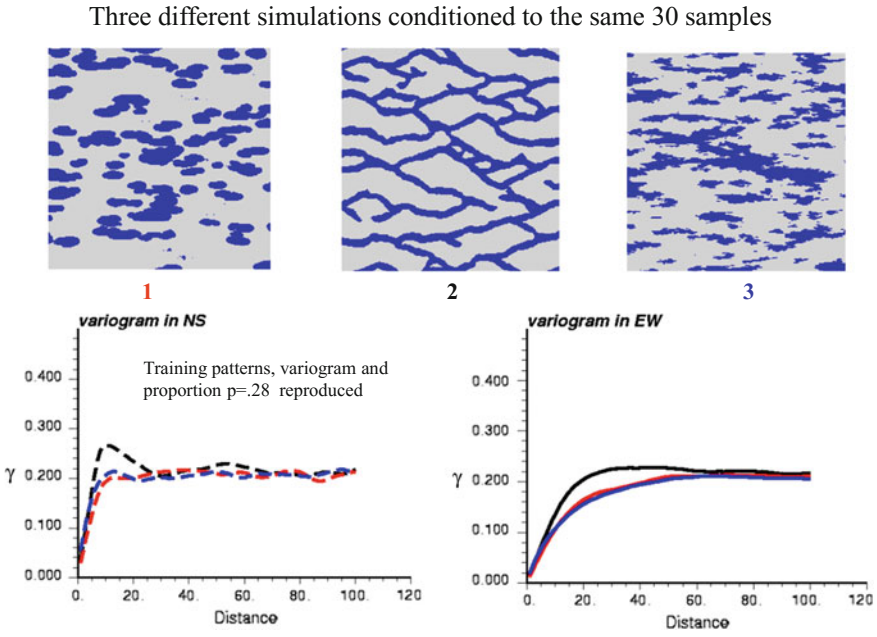

Fig. 2 Simulated realizations using for training images the patterns of Fig. 1

References

Dimitrakopoulos R, Farrelly CT, Godoy M (2002) Moving forward from traditional optimization: grade uncertainty and risk effects in open-pit design. Trans Inst Min Metall, Section A, Mining Technol 111:A82–A88

Godoy MC, Dimitrakopoulos R (2004) Managing risk and waste mining in long-term production scheduling. SME Trans 316:43–50

Journel AG, Kyriakidis PC (2004) Evaluation of mineral reserves: a simulation approach, p 216 (New York, Oxford Press)

Remy N (2004) S-GeMS—Geostatistical earth modeling software: user's manual, Stanford University, p 87 [online]. Available from: http://sgems.sourceforge.net [Accessed: 7 May 2007]

Srivastava RM (1987) Minimum variance or maximum profitability. CIM Bull 80(901):63–68

Strebelle S (2002) Conditional simulation of complex geological structures using multiple-point statistics. Math Geol 34(1):1–22

Quantification of Risk Using Simulation of the Chain of Mining—Case Study at Escondida Copper, Chile

S. Khosrowshahi, W. J. Shaw and G. A. Yeates

Abstract Quantification of risk is important to the management team of any rapidly expanding mining operation. Examples of areas of concern are the likelihood of not achieving project targets, the impact of a planned drilling program on uncertainty and the change in the risk profile due to a change in the mining sequence. Recent advances in conditional simulation and the practical use of such models have provided the opportunity to more fully characterise mineral deposits and to develop empirical estimates of the recoverable resources and ore reserves. This allows meaningful quantification of risk (and upside potential) associated with various components of a mining project. This paper presents an approach referred to herein as 'simulation of the chain of mining' to model the grade control and mining process. Future grade control sampling, mining selectivity and other issues that impact on the final recoverable tonnes and grades are incorporated. The application of this approach to Escondida, a large-scale open pit copper mining operation in Chile, provided a definitive way to assess the expected risk of a number of alternative development strategies on operational performance of the project. This approach is gaining acceptance as one of the most important steps in developing short-term mining models. The concepts developed here also have implications for assessing the ore that will be recovered from ore reserves during mining.

S. Khosrowshahi (✉)
MAusIMM(CP), Golder Associates, Level 2, 1 Havelock Street,
West Perth, WA 6005, Australia
e-mail: sia@golder.com.au

W. J. Shaw
FAusIMM(CP), Ore Control, Perth, WA, Australia
e-mail: bill.shaw@orecontrol.com

G. A. Yeates
FAusIMM(CP)— BHP Limited, 86A, 3001 Melbourne, Vic, Australia
e-mail: gavin.yeates@bhpbilliton.com

R. Dimitrakopoulos (ed.), *Advances in Applied Strategic Mine Planning*,
https://doi.org/10.1007/978-3-319-69320-0_6

Introduction

The Escondida open pit copper mine is located 140 km south east of Antofagasta, Chile. The mine started production in the late 1990s and by 2004 the annual production reached 82.4 Mton of sulfide ore; generating 1,005,200 ton of copper concentrate, 152,300 ton of cathode copper, 179,800 oz of gold and 4.5 Moz of silver. The orebody is a porphyry copper formed by two major stages of sulfide and one stage of oxide mineralisation. The supergene enrichment blanket of the deposit is defined by chalcocite and minor covellite with remnant chalcopyrite and pyrite that reaches a thickness of several hundred metres in places. The largest contributor of mineralised tonnage in the deposit is an Oligocene porphyritic intrusive hosted by andesites, combined with less significant hydrothermal and igneous breccias occurring throughout the deposit.

This study was conducted to assess the risk associated with the use of the Escondida resource model as a basis for developing mine schedules, forecasts and budgets of mineable ore. In addition, it was used to define the impact of risk for the first five years of the Phase IV Expansion and identify the alternative mine schedules that present less risk. The study was based on the construction of a large conditional simulation model, covering a significant part of the Escondida copper mine and the analysis of this model through a 'transfer function' or mining process termed the Chain of Mining (CoM).

More specifically, a geostatistical conditional simulation (CS) model was developed for a large part of the Escondida sulfide resource that contained five years of scheduled mining from the start of year one to the end of year five. The CS model consisted of 50 realisations that independently defined the lithology (andesite or non-andesite), the mineralisation zones (High Enrichment, Low Enrichment and Primary) and the grade (per cent copper as total copper and soluble copper) dependent on the previous two geological variables. A Chain of Mining approach was then used to model the errors impacting upon the translation of the in situ resource to a recoverable ore reserve. A number of CoM models were developed and analysed to determine the parameters that would match actual mining performance at Escondida. The impact of various contributing errors was modelled using parameters for blasting movement, sampling and assaying precision, sampling and assaying bias, and mining selectivity. The CoM models were examined in relation to all available reconciliation results. From available production data it was evident that the Escondida resource model available at that time significantly over-predicted the tonnage that was realised during mining. A base case Chain of Mining model was selected that appeared to best capture the real performance indicated by the production data. This case was used to predict the performance of the current mining practice within the volume defined by the planned next five years of mining. The analysis was done on a quarterly basis and a pushback basis for two alternative (north and east) mining options.

The approach presented herein is based on sequential conditional simulation (e.g. Journel and Huijbregts 1978; Goovaerts 1997; Benndorf and Dimitrakopoulos

2017, this volume; Nowak and Verly 2007, this volume) and the concept of 'future' grade control data for recoverable reserve estimation detailed in Journel and Kyriakidis (2004). Related aspects are discussed in the next sections, which start with the description of available data and conditional simulation modelling at Escondida, followed by the CoM approach (Shaw and Khosrowshahi 2002), a calibration of the resulting models and a comparison with production. Conclusions and comments follow.

Data and Data Analysis

Data sets used for analysis were based on 15 m bench composites for exploration data and grade control data. Subsequent analysis was based on the High Enrichment (HE), Low Enrichment (LE) and Primary (PR) zones. The lithology was considered as two domains, Non-Andesite porphyry/breccia and Andesite. Thus, there were six modelling domains for preliminary analysis, including univariate statistics of exploration and grade control data for total copper (CuT) and soluble copper (CuS).

To assess continuity trends for the characterisation of anisotropies in the data prior to variography, maps of grade and grade indicators were constructed. The interpolated maps were not constrained by the lithology or mineralogical zones and, therefore, reflect an isotropic interpolation of the data in 3D. The maps were used for the preliminary identification of grade continuity trends in order to further the definition of domains and for variographic analysis. The plan view maps indicated different grade continuity trends on either side of the north–south line at 16,300 E. On the eastern side, grade continuity has a NE orientation. This differs from the western side, which shows a NW continuity. An indicator defining the samples coded as andesite or non-andesite was also mapped in the same way.

Variography of the exploration and grade control data sets for total copper and for the ratio of soluble copper to total copper (ratio) was carried out for each of the HE, LE and PR mineralogical zones with subdivision by lithology (andesite and non-andesite, i.e. porphyry) that was separated into east and west at 16,300 E. Preliminary variograms of exploration data did not provide a good definition of short-scale structures. This is mainly due to the exploration data density, which does not allow accurate and detailed variogram definition over small distances. The exploration variograms generally characterised large-scale structures, but these are not as critical to risk assessment as the characterisation of short-scale continuity. It was found that variograms of grade control data generally showed less continuous behaviour, and a far clearer definition of short-scale variability. Accordingly, it was decided to model variograms of grade control data for all domains containing sufficient data to characterise this short-scale variability for simulation purposes. Exploration variograms were also modelled to determine the sensitivity of the study to this approach. For the Primary zone, grade control data was scarce and the variograms were based on exploration data, although this generally produced poorly defined variograms for the west domains.

The enrichment surfaces were based on the HE, LE and PR codes in the exploration and grade control data (Fig. 1). For this analysis, it was considered necessary to use a combined grade control and exploration hole surface data set for each of HE, LE and PR for variographic purposes to ensure that maximum coverage was provided of the spatial data.

Generation of the Conditional Simulation Models

First, the enrichment surfaces were simulated using sequential Gaussian simulation, followed by the simulation of the two lithologies, andesite and non-andesite, using sequential indicator simulation. These models were merged resulting in simulated models, each with its own lithology and enrichment surface. Next, these models were populated with simulated CuT and CuS grades.

Simulation of the Enrichment Surfaces

An example of the final simulated enrichment surfaces are provided in Fig. 2. The influence of the conditioning data is evident when comparing the simulated images of the HE, LE and PR surfaces. The lower number of conditioning data points for the PR surface leads to greater variability in the simulated surface. Variography was carried out for the mineralogical contacts described by the geological interpretation (enrichment surfaces). Variography of the surfaces was performed in 2D (Fig. 3) with the variable analysed being the RL coordinate.

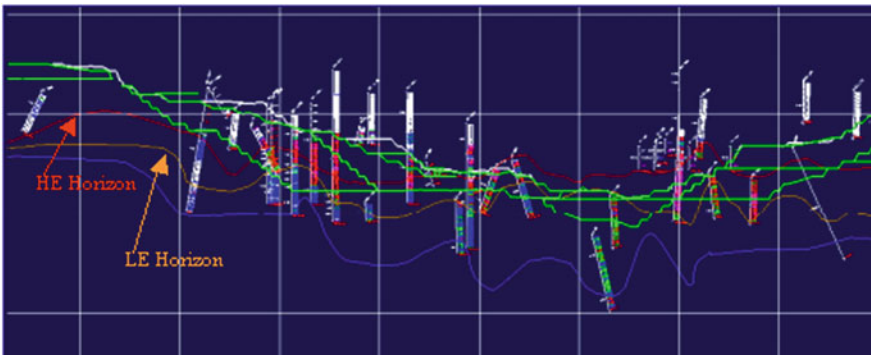

Fig. 1 Typical cross-section at escondida copper

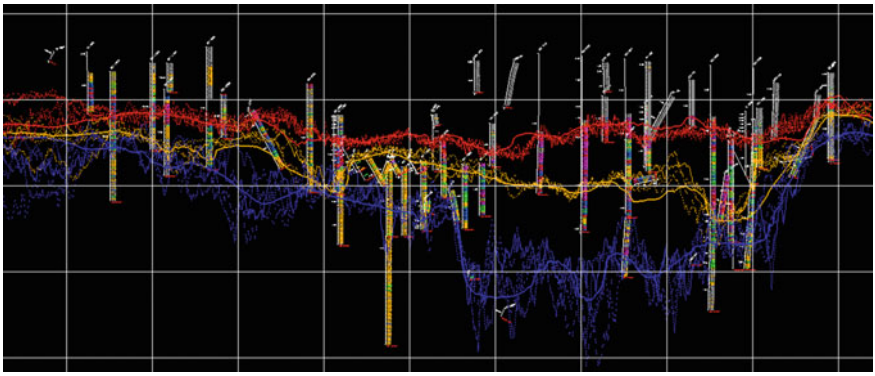

Fig. 2 Example of simulated image of the enrichment profiles

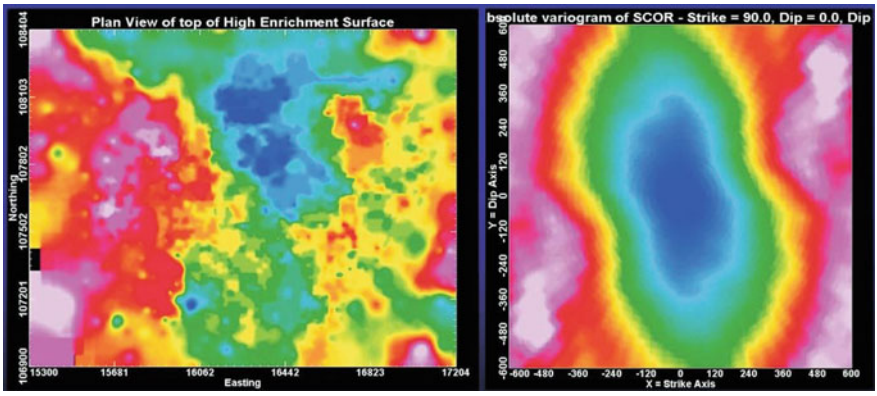

Fig. 3 Example of high enrichment elevation contour and associated variogram map

Simulation of Lithological Data

The dominant rock type for the Escondida deposit is porphyry. Grades in the andesite west of the 16,300 coordinate line are generally recognised to be lower than those in the porphyry lithologies and metallurgical recoveries are lower. The data was examined and it was decided, for the purpose of this study, to define two lithologies, namely andesite and non-andesite (or porphyry), which is used for porphyry/breccia and all other non-andesite lithologies. The lithology variography was based on indicators for andesite (and porphyry) for all data below the top of the HE zone. The indicators were defined from the drill log codes in the grade control and exploration data sets. As for the grade variography, the lithology variography was carried out for separate populations east and west of 16,300 E.

The lithological data was simulated as a categorical variable (Fig. 4). The presence of andesite was defined in the drill hole data using an indicator value of 1

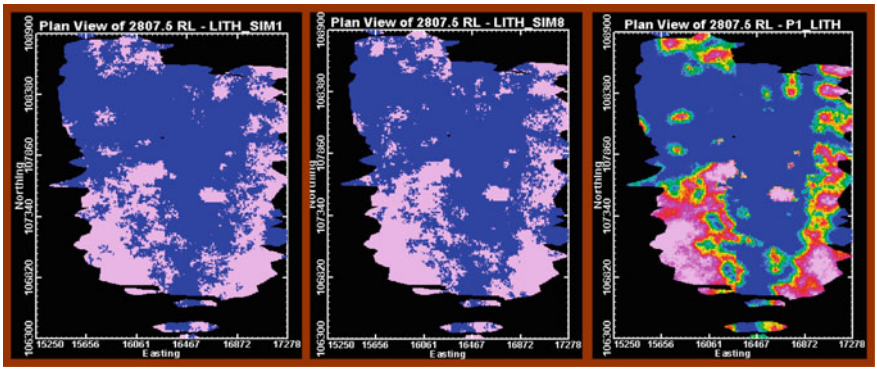

Fig. 4 Various simulated lithological data with associated probability map

with the absence of andesite (i.e. the presence of porphyry) assigned an indicator value of 0. The conditioning data set used for simulation of this categorical variable was the 15 m composited exploration data combined with the grade control 15 m blasthole data. The coded lithology data and the indicator variogram parameters were used to generate a sequential indicator simulation 3D model of the lithology as defined by the distribution of the andesite indicator.

Generation of the Geological Conditional Simulation Model

The 50 two-dimensional simulated realisations of each of the three enrichment surfaces and the 50 three-dimensional simulated realisations of andesites in two separate domains (east and west) were then merged into a single geology conditional simulation model comprising all simulated outcomes. Thus, there were 50 simulations each with a different lithology and Minzone outcome (Fig. 5).

Simulation of Grades for CuT and CuS

Twelve separate domains were considered for simulation of the percentage of copper as CuT and CuS grades. The conditioning data for each domain was the 15 m exploration composite data set. For each domain, appropriate data belonging to that domain was extracted. The sequential Gaussian simulation approach was used to simulate grades (Fig. 6) and simulated realisations for each domain were validated by checking the reproducibility of the weighted histogram of the exploration data, and the normal score variogram model from the grade control data.

It is impossible to produce a perfect representation of any deposit as a resource model since the geological knowledge, the sampled data, and the assumptions made

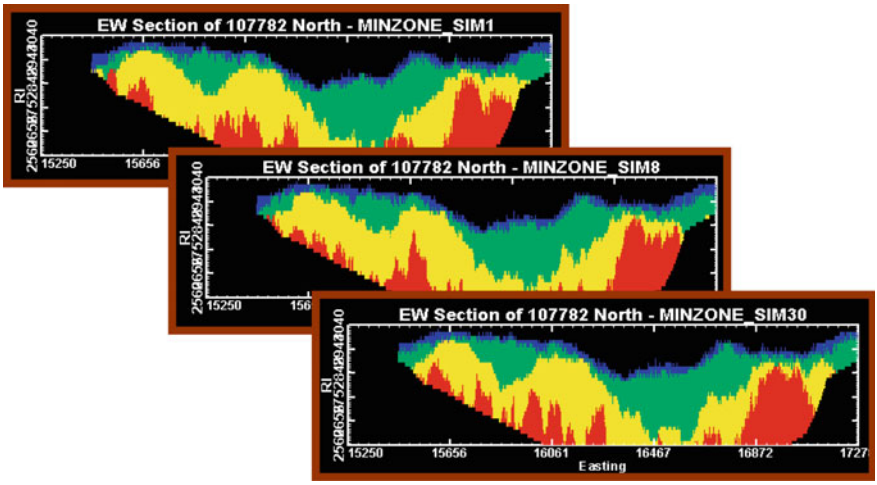

Fig. 5 Example of combined simulated geological data

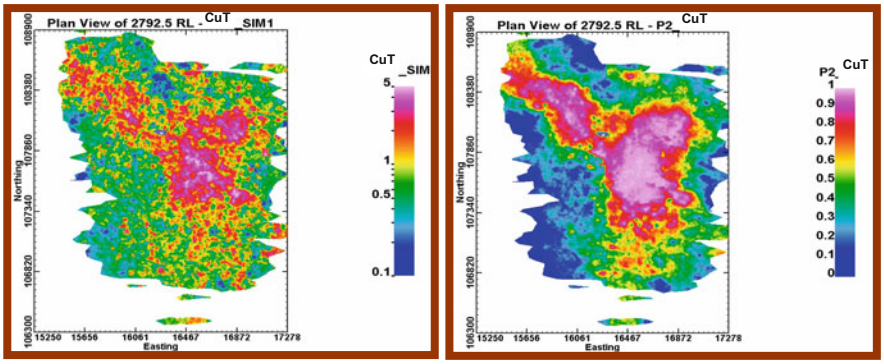

Fig. 6 Typical simulated image for CuT and associated probability map

during estimation are all imperfect. If a model was perfect it could be used as the basis for mining without any requirement for further mapping or sampling. Collectively, these imperfections are termed the *information effect* and can never be overcome completely. During mining, decisions are made based on similar imperfect data. Geological mapping, sampling and assaying are used to provide a basis on which the ore boundaries are defined and mined. Estimates of grades within the ore blocks must be made from the best available data. The impact of such estimates causes dilution (material below the cut-off grade being sent to the mill) and ore loss (ore incorrectly being sent to low grade stockpiles or waste dumps). Imperfect knowledge of the deposit again plays a part, but to this is now added imperfect mining practices. Even if the cut-off grade boundary could be defined perfectly it could not be mined perfectly every time at a practical mining scale.

To differentiate between the impact on resource modelling and the impact on mining, these imperfections are collectively termed the *grade control effect* and, again, can never be overcome completely.

The Chain of Mining Approach

For any measurable value, the term error can be used to indicate the difference between an estimate and the true value. During the process of defining an ore block for mining, a number of measured values are used, such as the location of the ore in 3D space, the representativity of the sample, the quality of the sample, the grade of the sample, and the cut-off boundary of the ore block boundary to be mined. For each of these attributes a 'true' value and an 'estimated' value can be defined.

Mining decisions are in all cases based on the estimated value. However, the results of mining are in all cases determined by the true value. For example, the placement of an ore block boundary and the predicted grade of that ore block might be defined solely by the sampled grades in and around that block. Errors in the sampling process (which leads to imperfect delineation of boundaries) and during mining (which leads to imperfect mining of the planned boundaries) both result in dilution and ore loss such that the grade of the ore delivered to the mill is invariably lower than that predicted by the estimated values. This is because the application of a cut-off grade alters the impact of the distribution of errors. Waste incorrectly sent to ore is by definition always of lower grade than ore incorrectly sent to waste.

There are various approaches that can be taken to solving this nexus between 'predicted' and 'actual' mining performance. For the present study, a series of parameters that model the differences between the predicted and actual mining performance were measured. To define these parameters, the various stages where errors can occur in measured values were considered. The mining process as a whole was considered to be a chain of events with the consequences of each event impacting on the next measurement in sequence. The term Chain of Mining is used to underscore the dependence of the eventual mining result on each link in the process (Shaw and Khosrowshahi 2002; Shaw et al. 2002; Khosrowshahi and Shaw 1997). Figure 7 provides a schematic of the process to characterise the generation of recoverable resource estimates.

Sources of Error During Mining

It was apparent that there were four possible sources of error that contributed to the grade control effect and which could be modelled, namely, sampling and assaying errors of precision, sampling and assaying errors of bias, movement due to blasting as lateral displacement or heave, and mining selectivity. It was recognised that it would be impractical to attempt to define parameters in detail for every possible

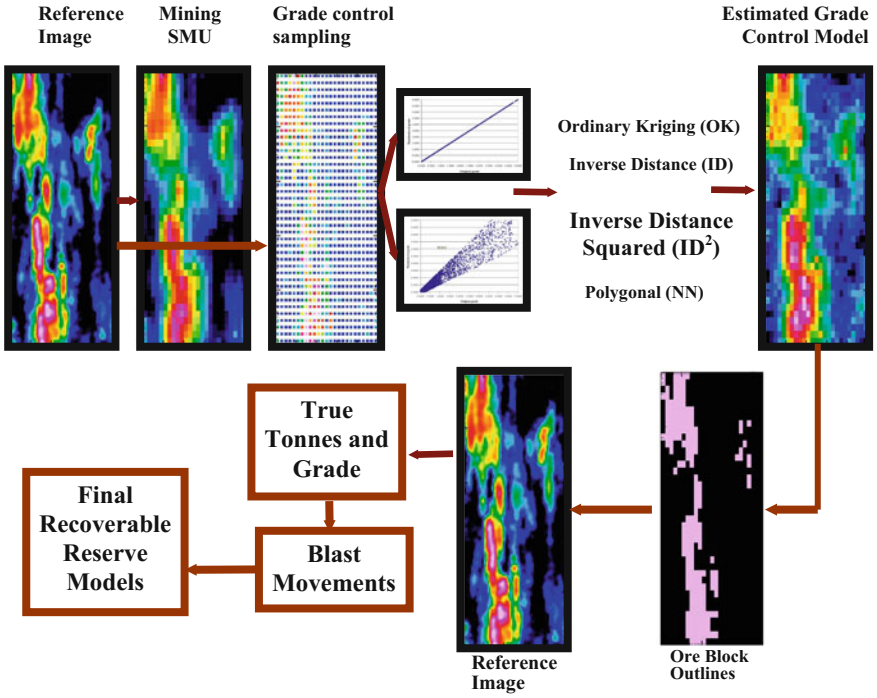

Fig. 7 Using the chain of mining process on a simulation model to characterise recoverable reserve estimates

source of error at Escondida. In addition, due to the large and very complex nature of such a mining operation, there is always the possibility that one or more practices will change in time. Instead, an empirical approach was taken. Error models were developed where observation on site indicated that this would be appropriate and these various error models were tested to determine their impact.

Error Due to Sampling and Assaying Precision

The grade control sampling at Escondida is done using vertical blastholes. The ore is blasted and dug on 15 m high benches. The blastholes are drilled with large rotary air blast equipment, drilled to a depth of 15 m (one mining bench) plus subdrill of approximately 2.5 m. Sampling errors that will lead to a difference between the actual grade of the material in the cone of blasthole cuttings and the true grade of the ore in the ore block are not quantifiable (since they are frequently not repeatable). Nevertheless, these errors exist and include both the sample delimitation error due to subdrill material remaining in the cuttings cone, and sample extraction error due to contamination and loss during the open hole rotary drilling, and due to dust loss.

The subsampling of the spoil cone is done manually after drilling using a tube sampler and eight increments are collected. The sample is then further crushed and subsampled in the MEL site laboratory. The errors that impact on the predicted grade include:

1. the grouping and segregation error that is due to splitting of the spoil cone (in this case due to the tube splitter); and
2. error due to the relationship between particle size and grade, known as the Fundamental Sampling Error (Gy 1979) that results from the process of splitting, crushing and pulverising to reduce the 2 t sample spoil cone to a 200 g pulped sample submitted for assay.

The first type of error is not quantifiable, and every subsampling system incurs the second type of error. The total impact of all these errors was modelled in two scenarios:

Low Sampling Error

A relative sampling precision of ±20% was assumed as the base case. This incorporates the measured precision of ±10% demonstrated by repeat sampling and assaying of blasthole cones (Fig. 8). An allowance for additional error was made due to the drill sampling method. This scenario assumes high quality grade control sampling is available.

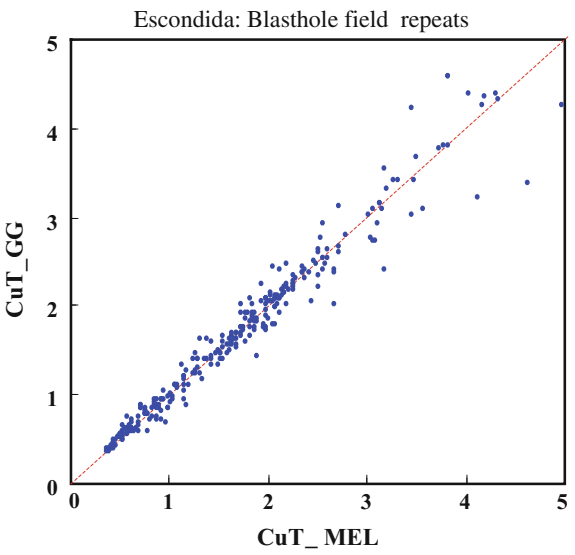

Fig. 8 Field duplicates of escondida blasthole cone sampling from which a relative precision of ±10% was obtained

High Sampling Error

A relative sampling precision of ±60% was assumed as the high error case to indicate the typical level of sampling repeatability that occurs in twinned blasthole drill sampling. No data for this estimate was available. The nearest such data was paired blasthole and resource hole estimates where a precision of ±40% was obtained. The high error case was adopted to allow for the impact of the blasthole subdrill and accounts for the local variability typically seen in blasthole sampling.

Error Due to Blasting

Ore movement can result in the predicted ore being displaced so that the material eventually mined is different from that which was planned. The degree of dilution and ore loss that this causes is dependent on the lateral displacement of the ore block boundaries, and the vertical heave resulting in mixing across horizontal mining levels. Heave is not an issue at Escondida since the ore is blasted and mined on a single mining bench. It was decided to model two scenarios, one where the lateral blast movement was negligible and one where the movement was 3 m in both the east-west and north-south directions, this being the movements observed on site for a number of blasts.

Mining Selectivity

Perfect mining of any orebody is always impossible due to two factors; the availability (and quality) of data to define boundaries, and the ability of the equipment to dig a defined boundary, which decreases with the production scale of the operation. The effective minimum mineable block size can be expected to relate in some way to these factors and, consequently, in a resource model the point estimates of grade, interpolated from drill hole (quasi-point) data, may be aggregated to a mineable block size.

The degree of mining selectivity represented by a resource block model is defined as the selective mining unit (SMU). This SMU block size may be regarded as the minimum viable size of a mining block, although of course, the average size of the mined blocks may be much bigger. The degree of misclassification that generally occurs along any block boundary during mining is directly related to the production rate and size of the mining equipment. The concept of the SMU block size can assist in understanding the impact of the mining method on the orebody and how well this can be represented by the resource model.

Calibration of the Chain of Mining Models and Comparison with Production

The conditional simulation model developed for the Escondida deposit was used to test the impact of various mining selection parameters and the impact of the various expected errors. A series of ten cases was developed using the parameters defined in Table 1 to address misclassification errors likely to arise during mining. These CoM models were then tested against production records and compared to the Escondida resource model.

Analysis of the results for the different scenarios indicated that Case 6 (presented in bold in Table 1) was the closest to the Production data total of 100,294 Mt at 2.11% CuT. The selected case used no blasting movement, a high sampling error consistent with blasthole samples, and an 8 × 8 m SMU block area. The smaller SMU size provided better selectivity at the cut-off grade, producing a lower tonnage and higher grade than that predicted by the resource model. Case 6 was regarded as the base case. Various models were intersected with each wire-frame defining the mine plan, and the results were aggregated by both quarterly period and major pushback increment. For the Chain of Mining cases, each of the 50 simulations was separately intersected with each wire-frame to provide a risk profile of the chance of not achieving the scheduled tonnes and grade for the period that the wire-frames represented. The tonnages and grades within each simulation realisation were determined for the quarterly and pushback increments for the base case (8 × 8 m SMU with high sampling error). The results are presented in graphical form in Figs. 8, 9, 10, 11 and 12. In assessing the relative risk using this graphical data, occurrences below the horizontal line indicate where the expectation of tonnes or grade was not reached, i.e. periods when the resource model is at risk under the assumed mining scenario.

Table 1 Parameters used in the chain of mining (CoM) analysis for the various CoM models examined, with results for the reconciliation period

Case	Blasting movement	Sampling error	SMU (15 m high)	Mt	Grade % CuT	Comment
1	0	Low	16 × 16	109.4	1.875	
2	0	Low	8 × 16	107.5	1.893	
3	0	Low	8 × 8	103.3	1.929	
4	0	High	16 × 16	108.0	1.885	
5	0	High	8 × 16	105.3	1.907	
6	**0**	**High**	**8 × 8**	**99.0**	**1.953**	**closest to mine production data**
7	3	Low	16 × 16	109.4	1.861	
8	3	Low	8 × 16	107.5	1.873	
9	3	High	8 × 16	105.3	1.887	
10	3	High	8 × 8	99.0	1.921	

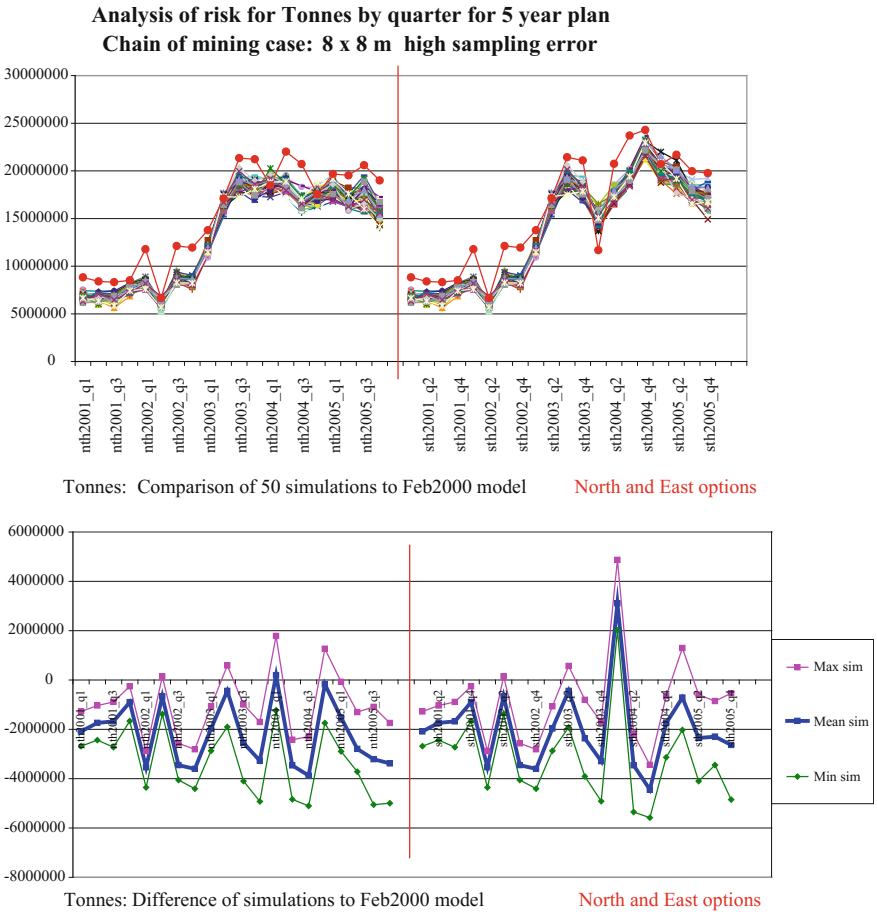

Fig. 9 Risk associated with tonnes in the five year plan by quarters

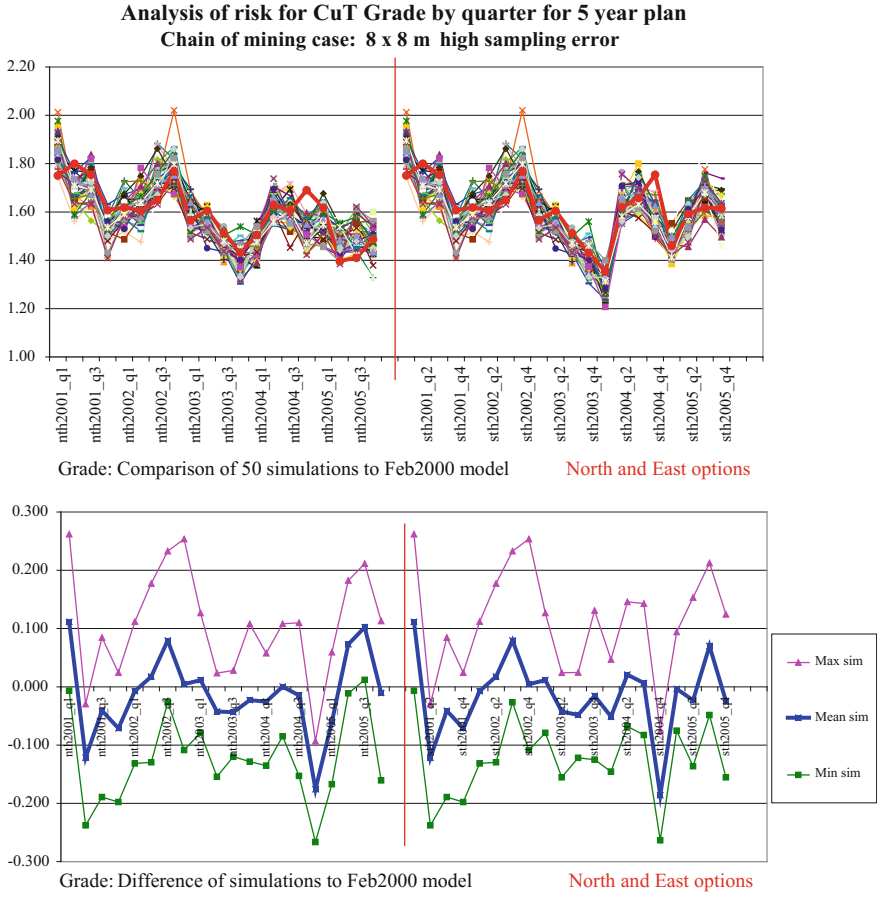

Fig. 10 Risk associated with grade in the five year plan by quarters

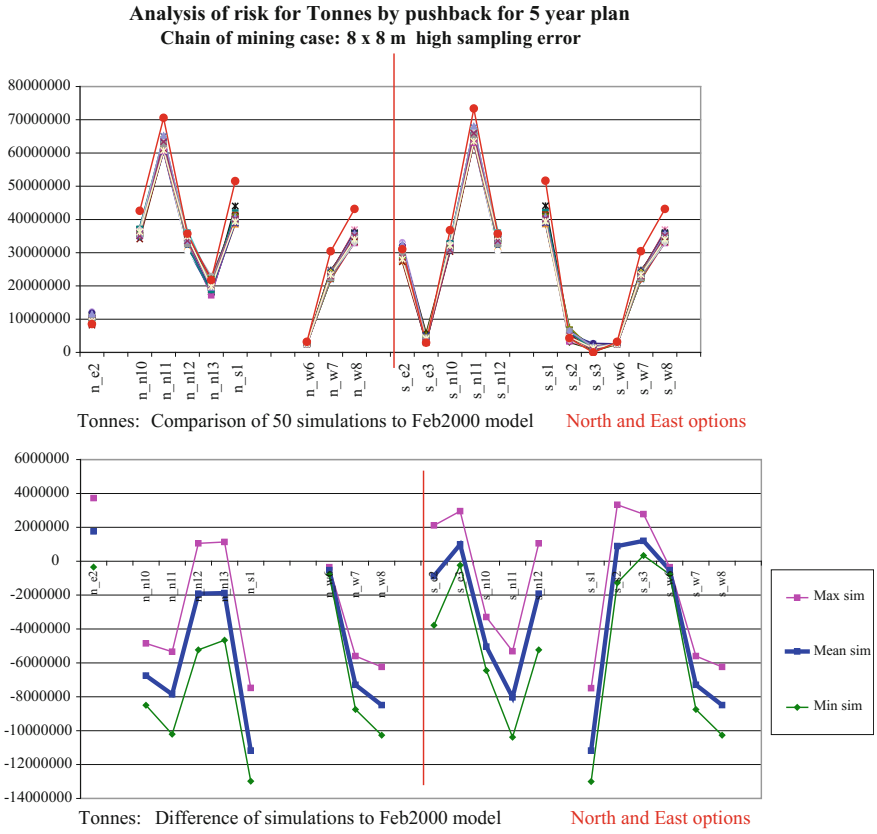

Fig. 11 Risk associated with tonnes in the five year plan by pushback

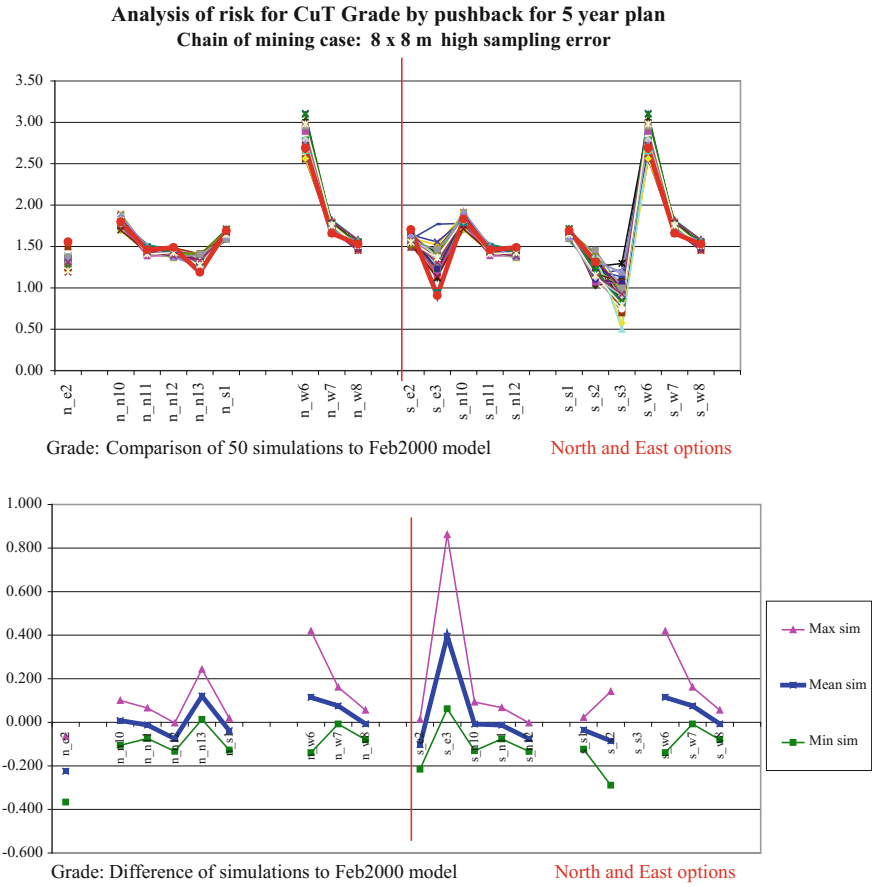

Fig. 12 Risk associated with grade in the five year plan by pushback

Conclusions

The five-year schedule options adequately fit with the in situ resource. However, the Chain of Mining case (8 × 8 m SMU, high error) selected to best emulate the production data indicates a significant expected shortfall in tonnes. What had not been evident until this study, and could only be demonstrated using the exhaustive data set provided by a conditional simulation study, is that there was considerable risk of a shortfall in tonnes. This was because the selectivity evident in the actual mining strategy differed significantly from that inherently assumed in the resource model. High quality grade control practices on site were effectively providing higher selectivity than that assumed in the resource model. This lead to a scenario of 'vanishing tonnes' (David 1977), a concept demonstrated in this study that is familiar to many large mines. This problem can be related to attempts to improve the head-grade to unrealistic targets applied on a short-term (sometimes daily) basis. Visual grade control and other decisions to remove small parcels of contaminating material in order to maintain a high mill head grade may lead to an artificially small effective mining selectivity that is not related to the SMU block size assumed in the resource modelling.

The quantification of risk using simulation of the Chain of Mining is a technique that can be used to identify a potential shortfall in tonnes or grade for a given mining scenario. Alternative plans can then be developed and tested before the shortfall impacts production. An approach such as the one demonstrated here for Escondida can determine if a plan is realistic and the predicted results will be obtained. Hence, the risk inherent in a given plan can be quantified. Testing alternate mining scenarios, operating practices and policies to determine if they will indeed deliver as intended, therefore, provides considerable advantages to both mine planners and operators.

Acknowledgements The authors would like to acknowledge the input of site personnel into this study. Minera Escondida Limitada and BHP Billiton granted permission to publish the results of this study once its direct commercial relevance was superseded by other ore reserve and mine planning studies.

References

Benndorf J, Dimitrakopoulos R (2017) New efficient methods for conditional simulation of large orebodies, in this volume

David M (1977) Geostatistical ore reserve estimation, 364 p. Amsterdam, Elsevier

Goovaerts P (1997) Geostatistics for natural resources evaluation, 483 p. Oxford University Press, New York

Gy P (1979) The sampling of particulate materials—theory and practice, 431 p. Amsterdam, Elsevier

Journel AG, Huijbregts CJ (1978) Mining geostatistics, 600 p. Academic Press, London

Journel AG, Kyriakidis PC (2004) Evaluation of mineral reserves: a simulation approach. Oxford University Press, New York

Khosrowshahi S, Shaw WJ (1997) Conditional simulation for resource characterisation and grade control—principles and practice. Proceedings world gold '97. The Australasian Institute of Mining and Metallurgy, Melbourne, pp 275–282

Nowak M, Verly G (2007) A practical process for geostatistical simulation with emphasis on Gaussian methods. In: Dimitrakopoulos R (ed) Orebody modelling and strategic mine planning, 2nd edn. The Australasian Institute of Mining and Metallurgy: Melbourne, pp 69–77

Shaw WJ, Khosrowshahi S (2002) The use of the chain of mining method, based on conditional simulation models, to quantify mining risk—a reality check for resource estimates. In: Proceedings symposium on quantifying risk and error. Geostatistical Association of Australasia, pp 111–118

Shaw WJ, Khosrowshahi S, Bertinshaw RG, Weeks A, Church P (2002) Beyond grade control: broken links in the Chain of Value. In: Proceedings value tracking symposium. The Australasian Institute of Mining and Metallurgy, Melbourne, pp 85–89

A Risk Analysis Based Framework for Strategic Mine Planning and Design—Method and Application

M. Godoy

Abstract Assessment and management of orebody uncertainty is critical to strategic mine planning. This paper presents an approach that consists of a series of procedures for risk assessment in pit optimisation and design. Multiple block grade simulations are processed in Whittle Software to produce a distribution of possible outcomes in terms of net present value. Examples from an open pit mine are used to illustrate the practical application of the methodology.

Introduction

Traditionally, determination of the spatial distribution of grades in an orebody model is based on geostatistical estimation. The main drawback of estimation techniques, be they geostatistical or not, is that they are unable to reproduce the in situ spatial variability as inferred from the available data. Ignoring such a consequential source of risk and uncertainty may lead to unrealistic production plans (e.g. Dimitrakopoulos et al. 2002). In dealing with uncertainty on the spatial distribution of attributes of a mineral deposit, several models of the deposit can be generated based on and conditional to the same available data and their statistical characteristics. These models are all constrained to:

- reproduce all available information and their statistics, and
- represent equally probable models of the actual spatial distribution of grades.

The availability of multiple equally probable models of a mine deposit enables mine planners to assess the sensitivity of pit design and long-term production scheduling to geological uncertainty. This approach has been proposed by many authors over the last 20 years (David 1988; Journel 1992; Ravenscroft 1992; Dimitrakopoulos 1998; Godoy 2002; Dimitrakopoulos et al. 2007; Kent et al. 2007;

M. Godoy (✉)
MAusIMM, Expert Mining Engineer/Geostatistician, Golder Associates, Av 11 de Septiembre 2353, Piso 2, Proviendencia, Santiago, Chile
e-mail: mgodoy@golder.cl

R. Dimitrakopoulos (ed.), *Advances in Applied Strategic Mine Planning*,
https://doi.org/10.1007/978-3-319-69320-0_7

and others). Figure 1 illustrates the difference between the traditional process used to convert a mineral resource into an ore reserve and the risk based approach based on the technique of conditional simulation.

The goal of this paper is to provide mining planning engineers a series of procedures that can be used to consider the effects of grade uncertainty in mine planning studies. Four cases have been selected to illustrate different types of applications:

1. uncertainty analysis of an ultimate pit shell—Net Value (NV), costs, tonnage, grade and metal;
2. identification of areas of upside potential and downside risk;
3. trade-off analysis for cut-back depletion strategies; and
4. assessment of uncertainty related to ore blocks driving the increment between the successive pit shells.

In the following sections, each application is developed separately and includes a step-by-step description of the procedure and a discussion of the results obtained in a real case application.

Uncertainty Analysis for an Ultimate Pit Shell

The objective of this analysis is to evaluate the sensitivity of key pit optimisation results to grade uncertainty. The process known as pit optimisation is traditionally carried out based on the estimated resource model and using the nested pit

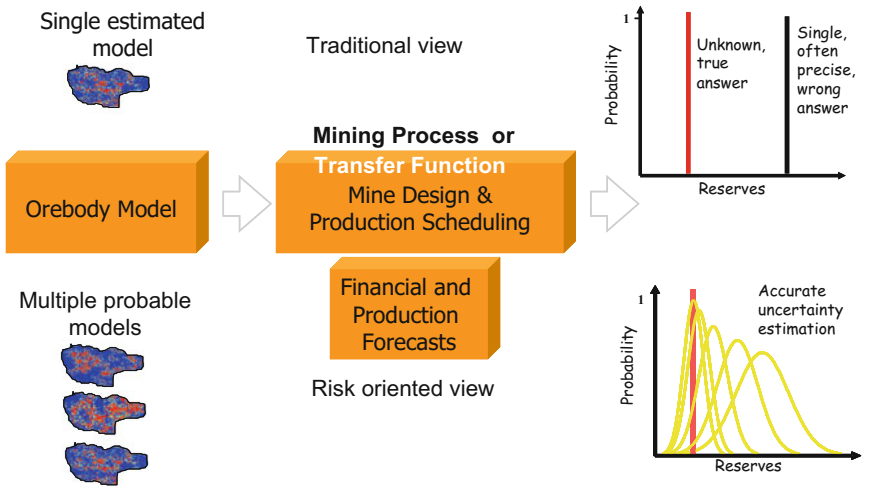

Fig. 1 Conversion of a mineral resource into an ore reserve, traditional and risk oriented views

implementation of the Lerchs-Grossmann algorithm of the Whittle Software (Lerchs and Grossmann 1965; Whittle 1999). The result of the optimisation process is a series of incremental pit shells. Different criteria can be used to select the ultimate pit shell including net pit value and the net present value based on a referential mining sequence. This ultimate pit shell is then used as the basis for pit design and planning. Using conditionally simulated models as input, Whittle's analysis program (FDAN) may be used allowing the quantitative assessment of risk due to uncertainty on the real, but unknown, distribution of grades. In the procedure proposed below an ultimate pit shell produced in Whittle is evaluated against a series of simulated models of the orebody.

To assess uncertainty on the main parameters driving the selection of the ultimate pit shell the following procedure is proposed:

- From the Whittle result file produced by the pit optimisation process, generate a Whittle pit list file containing information about the smallest numbered pit that each block is part of.
- Apply the pit list file produced in Step 1 to each one of the simulated orebody models.
- Run the analysis program configured to generate the same information, previously generated by analysis on the original pit optimisation. The analysis must be carried out for each one of the available simulated models.

The above procedure generates a range of alternative outcomes for the original optimisation process. This allows the planner to evaluate the likely range of contained ore, metal and a series of key economic indicators. Figure 2 shows the predicted ore tonnage produced by risk analysis. Up until pit 27, the cloud of cumulative tonnages derived from the simulated models present an average decrease of approximately 9.76% in relation to the tonnage predicted by the estimated model. At pit 27 the estimated model indicates approximately 180.3 Mt against an expected value of 164.6 Mt derived from the simulations. The expected outcomes of contained ore go from 163.3 to 166.1 Mt, which corresponds to a range of −0.83 to +0.92% in relation to the expected value derived from the simulations. The same type of analysis carried out on the average mill feed grade (Fig. 3) shows a decreasing overestimation in grades of the estimated model in relation to the simulated models. At pit shell number 1, the estimated model predicts an average mill feed grade of 2.6 g/t, while the simulations indicate an expected grade of 2.2 g/t. At pit 27 the estimated model indicates approximately 1.98 g/t against an expected value of 1.95 g/t derived from the simulations. The risk profile on mill feed grade goes from 1.93 to 1.98 g/t, which corresponds to a range of −1.24% to +1.32% in relation to the expected value. Figure 4 shows the predicted recovered metal produced by the analysis. Up until pit 27, the cloud of cumulative recovered ounces derived from the simulated models present an average decrease of approximately 17.41% in relation to the ounces predicted by the estimated model. This result indicates that the estimated model is potentially overestimating grades as an effect of excessive smoothing. At pit 27 the estimated model indicates 9.84 Moz

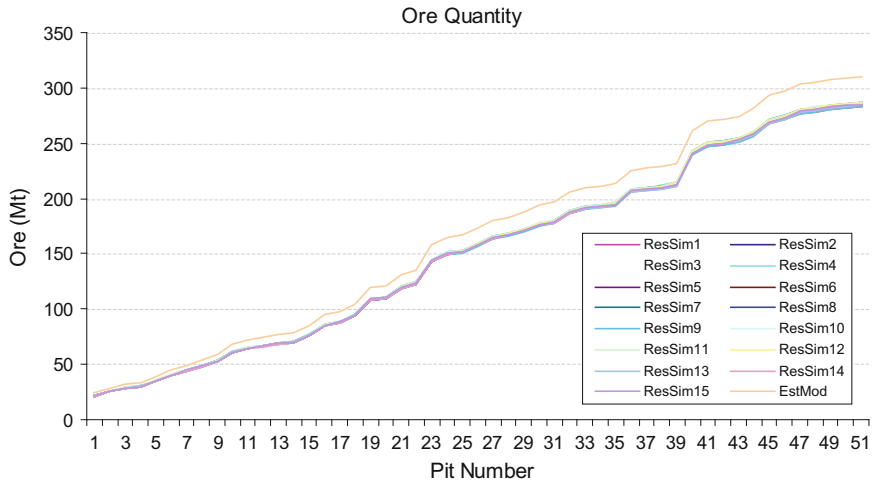

Fig. 2 Uncertainty in ore tonnes for incremental pit shells

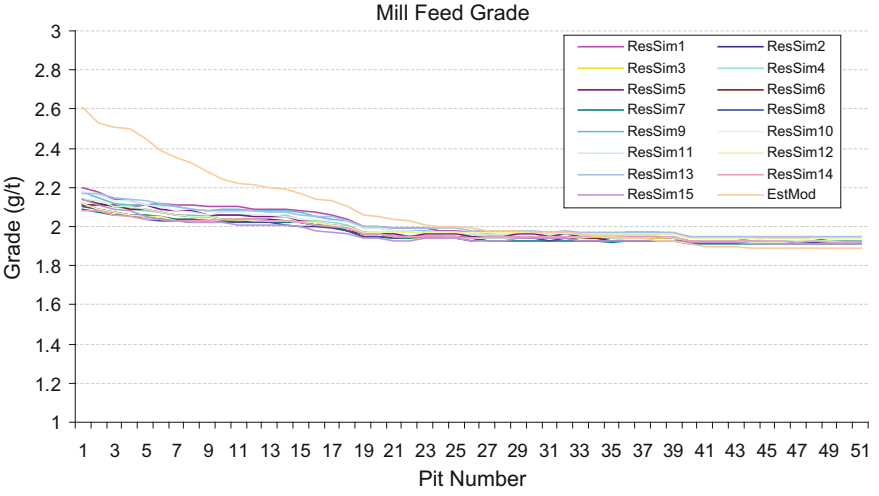

Fig. 3 Uncertainty in mill feed grade for incremental pit shells

against an expected value of 8.85 Moz derived from the simulations. The risk profile on recovered ounces goes from 8.72 to 8.98 Moz, which corresponds to a range of −1.4 to +1.58% in relation to the expected value.

The combination of the overestimation in ore tonnage and mill feed grade has a direct impact on the performance of the pit by pit Net Value. Figure 5 presents the results obtained for the pit Net Value.

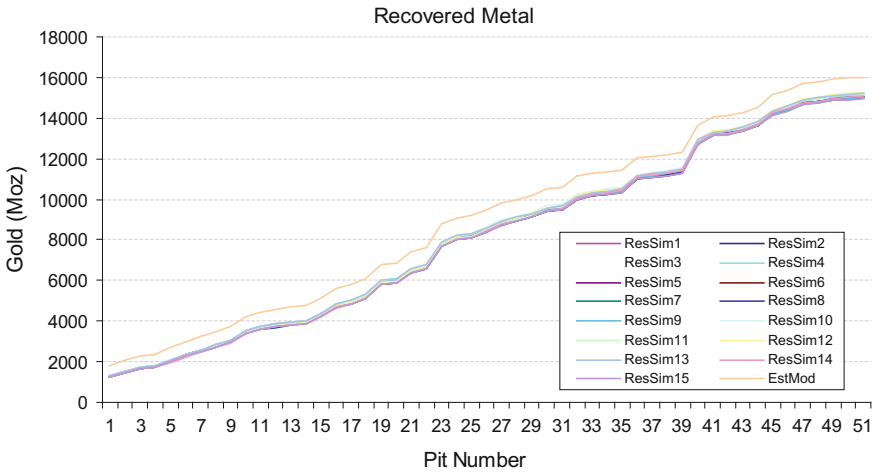

Fig. 4 Uncertainty in recovered ounces for incremental pit shells

It suggests that the estimated model overestimates the pit value over all optimised pit shells. Up until pit 27, the cloud of cumulative Net Value derived from the simulated models present an average decrease of approximately 33.39% in relation to the Net Value predicted by the estimated model. It also indicates a downside potential for pit 27 with expected NV equivalent to $951.6 M or a 26.12% decrease in relation to the $1288 M obtained for the analysis on the estimated block model. It is interesting to note that if Net Value was to be used as the criterion for the selection of the ultimate pit shell the simulations would agree with the estimated model by indicating pit 27. The range of expected Net Values goes from $890 to $1013 M, which corresponds to −6.47 to +6.41% in relation to the expected value.

Identification of Upside and Downside Potential

The goal of this analysis is to explore the possible downside/upside potential of the selected ultimate pit shell regarding the available grade uncertainty models. To achieve this independent pit optimisation runs are carried out on each simulated model. The analysis is divided into two parts:

1. First, each optimisation output is evaluated in terms of contained ore, grade, metal and pit value. This provides a quantification of the project potential given realistic scenarios of the spatial distribution of grades.
2. The second part looks into the spatial extends of a specific pit shell as produced for each independent optimisation. The comparison of this ‘cloud’ of pit shells against a given pit design provides an assessment of areas with upside/downside

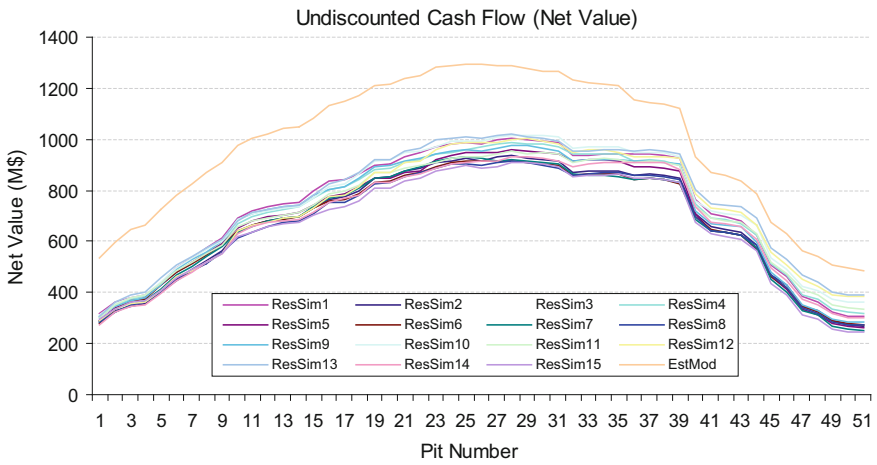

Fig. 5 Uncertainty in Net Value for incremental pit shells

potential and can be used to define targets for additional drilling. It also provides an indication on the robustness of a given pit design in relation to grade uncertainty.

The procedure proposed for the development of this analysis is the following:

- Create a new project in Whittle and import each one of the simulated models. Next, set the optimisation parameters for the optimisation run.
- Apply the same parameters to each model and run the optimisation. The process will generate a series of Whittle result files, one for each simulated model. This step usually requires a large amount of disk space.
- Run analysis program configured to generate the relevant summary information. The analysis must be carried out for each one of the available simulated models.
- Produce cross-sections for a selected pit number over all optimised models.

Contrary to developing a risk analysis on a given ultimate pit shells, as carried out in the previous section, the above procedure generates alternative sets of incremental shells, one set for each simulated model. Figure 6 shows the total rock contained on each incremental shell as produced by each independent optimisation.

The thick orange line corresponds to the results obtained from the analysis on the incremental shells optimised on the estimated model, hereafter termed estimated pit. The thin lines correspond to the results obtained from the analysis on the incremental shells optimised on each one of the simulated models, hereafter termed simulated pits. The figure shows that up to pit shell 24 the estimated and simulated pits present an equivalent quantity of contained rock, that is, they have approximately the same volume. From around pit shell 25, there is a clear separation with the simulated pits showing a progressive increase in comparison to the estimated pit. This scenario remains the same until pit shell 39, when the estimated pit starts to

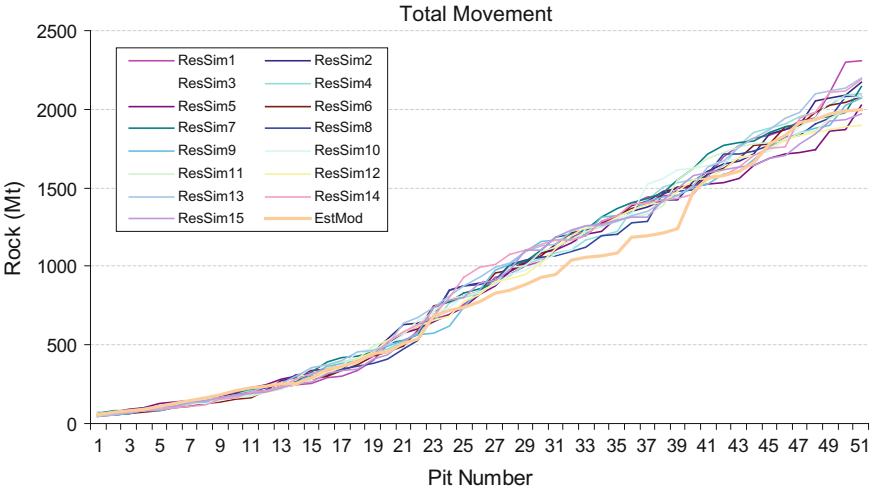

Fig. 6 Total rock tonnage contained on incremental pit shells. Estimated pit is depicted by the thick orange line and the remaining coloured thin lines correspond to simulated pits

converge to the cloud of simulated pits. Pit shell 27 is of particular interest as it corresponds to the pit selected as a basis for pit design. For pit shell 27, the average contained rock over the simulated pits is 925 Mt against 828 Mt in the estimated pit, which corresponds to an increase of approximately 11.7%. Figure 7 presents the results obtained for the total contained ore. In this case, estimated and simulated pits show similar behaviour as the total rock, only that the magnitude of the differences is smaller. For pit shell 27, the average contained ore over the simulated pits is 183.9 Mt against 180.3 Mt in the estimated pit, which corresponds to an increase of approximately two per cent. The risk profile on the contained ore goes from 174 to 195 Mt, which corresponds to a range of −5.92 to +6.06% in relation to the expected value. In terms of mill feed grade, the estimated pit starts with 2.61 g/t against an average 2.43 g/t over the simulated pits. This difference decreases with incremental pit shells and become equivalent at pit shell 27 (Fig. 8).

The risk profile on mill feed grade goes from 1.95 to 2.02 g/t, which corresponds to a range of −1.61 to +1.92% in relation to the expected value. Figures 9 and 10 present the results obtained for recovered metal and total pit value.

As expected, the recovered metal for estimated and simulated pits follow the same trends seen on the ore tonnage graphs. For pit shell 27, the recovered gold over simulated pits is 10.03 Moz against 9.84 MOz in the estimated pit, which is an increase of approximately 0.9%. This combination of slightly higher metal with considerable more rock tonnage in the simulated pits translates into a reduced net pit value when compared to the estimated pit. The estimated pit presents a consistently higher Net Value until pit shell 39 when the total rock tonnage becomes equivalent to that shown on the simulated pits. For pit shell 27 the average Net Value over simulated pits is 1159 million dollars against 1288 million in the

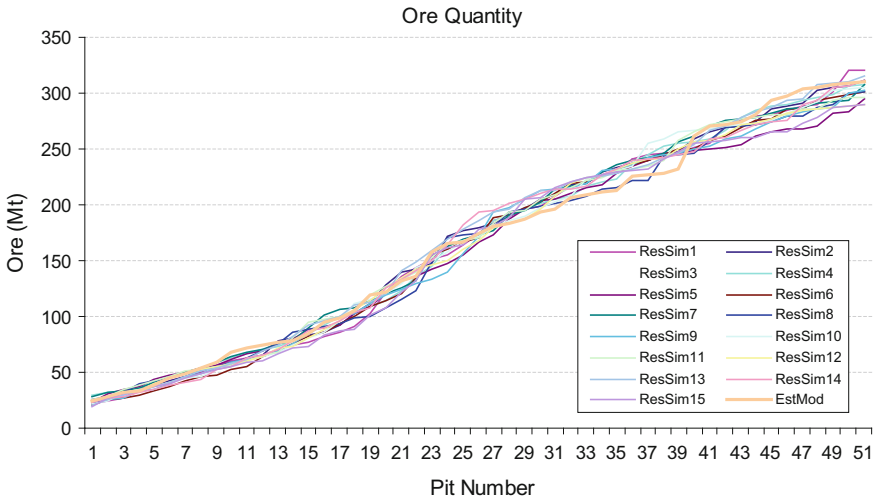

Fig. 7 Total ore tonnage contained on incremental pit shells. Estimated pit is depicted by the thick orange line and the remaining coloured thin lines correspond to simulated pits

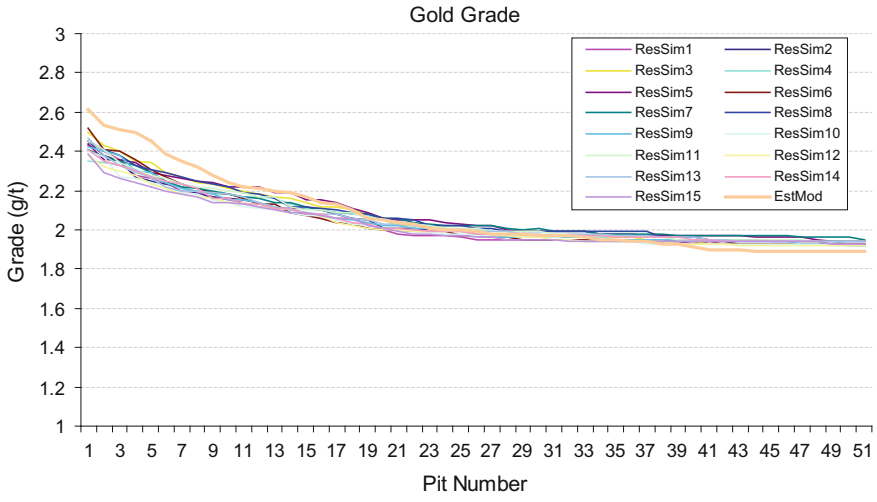

Fig. 8 Average grade contained on incremental pit shells. Estimated pit is depicted by the thick orange line and the remaining coloured thin lines correspond to simulated pits

estimated pit (approximately 10% less). The risk profile on Net Value goes from \$1068 to \$1292 M, which corresponds to a range of −7.86 to +6% in relation to the expected value. It is interesting to note that as for the estimated model the maximum Net Value over all simulated pit corresponds to pit shell number 26. This shows that pit shell 26 is quite robust with regards to grade uncertainty. Another conclusion

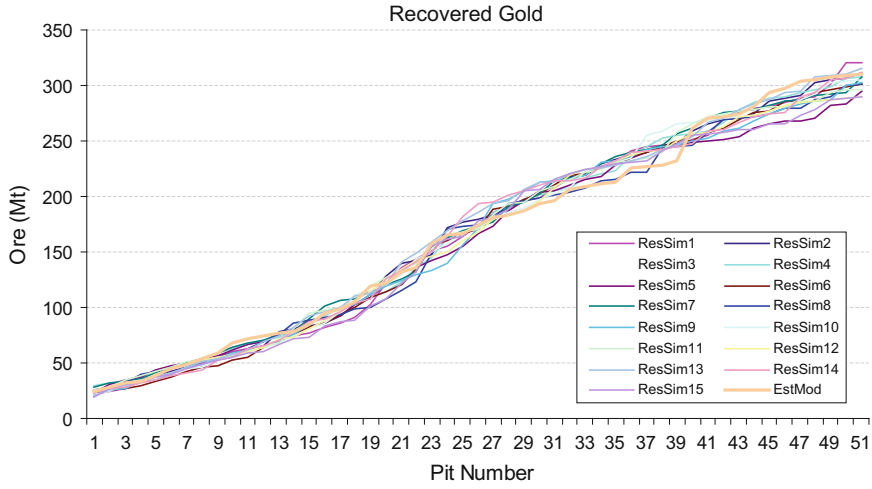

Fig. 9 Total recovered metal contained on incremental pit shells. Estimated pit is depicted by the thick orange line and the remaining coloured thin lines correspond to simulated pits

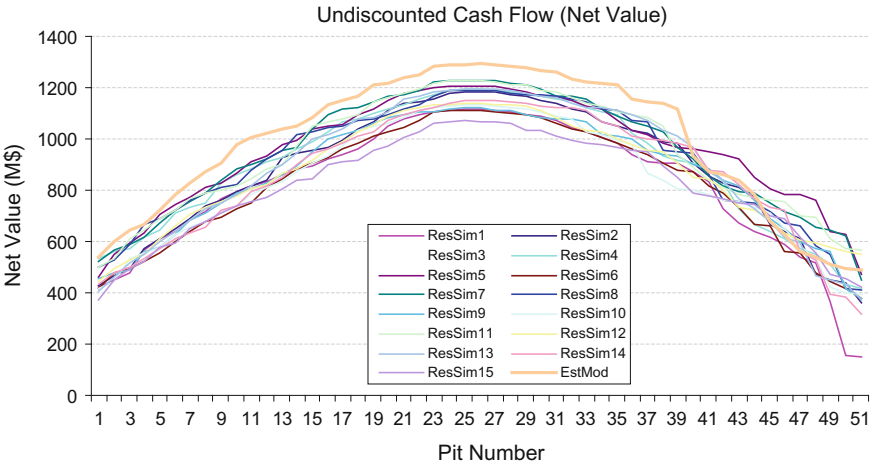

Fig. 10 Total pit value of incremental pit shells. Estimated pit is depicted by the thick orange line and the remaining coloured thin lines correspond to simulated pits

that can be drawn from these results, which is coherent with the results obtained in the analysis presented in the previous section, is that there is a global overestimation of grades and ore tonnage by the estimated model as compared to the simulated models.

A series of cross-sections were produced for pit shell 27 over all optimised models and for a pit design. These cross-sections were overlaid and are presented in Fig. 11. The main conclusions drawn from the analysis of these cross-sections are

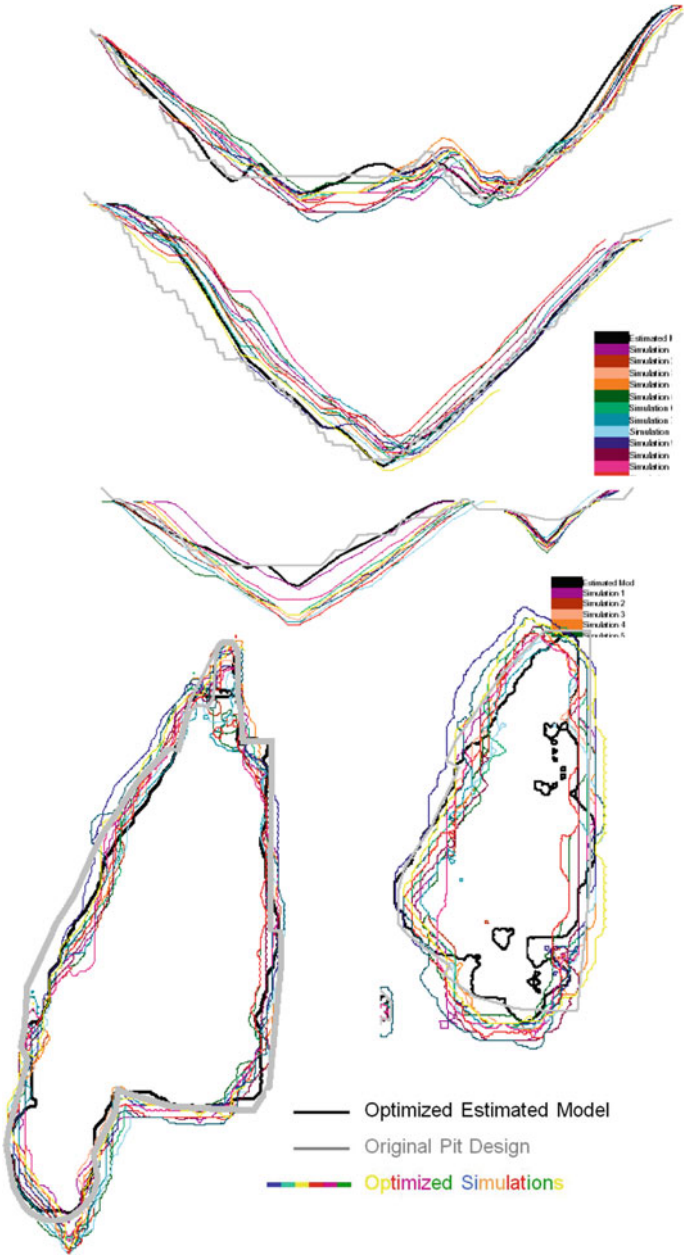

Fig. 11 Cross-sections produced for pit shell 27 over all optimised models overlaid with actual pit design

the following. The simulated pits closely honour the eastern wall of the current pit design, showing that the eastern slope is stable with relation to grade uncertainty. In general, there is a more pronounced fluctuation in the western wall which indicates higher levels of grade uncertainty. The current design has an extension of the western wall, which is not included in the optimisations of both estimated and simulated pits. This extension represents a major downside potential zone and goes from the actual pit surface to the lowest levels of the pit. The simulated pits indicate an upside potential region at the southwest zone of the pit where the simulated pits reach levels that are deeper than the current pit design. The spread of cloud of simulated pits is shown to be low from the surface down to level-350. Bellow that the spread increases considerably. This reflects the increasing uncertainty on the distribution of grades at depth and is directed related to the lack of drilling.

Trade-off Analysis

The goal of this analysis is to quantify the impact of grade uncertainty to tonnage, grades, metal and Net Value of two different mining strategies. Scenario 'A' considers the depletion of a cut back as a single stage, while scenario 'B' defines two separate stages. The analysis consists on the quantification of uncertainty on key mining physicals and economic parameters for the two mining scenarios considered. The objective is to evaluate if one of the scenarios is any better in terms of the compromise between Net Value and risk exposure. The procedure proposed to develop the analysis is the following:

1. generate a wireframe describing the cut-back,
2. filter the block model against the wireframe and retain the blocks lying inside the cut-back as new block model,
3. export the block model produced above into a Whittle Model File,
4. repeat steps 2 and 3 for each one of the simulated models,
5. for each model produced in the previous steps calculate the relevant summary information, and
6. repeat steps 1 to 6 for stages 1 and 2 that correspond to another mining scenario.

The procedure was carried out for a total of 16 models, corresponding to 15 grade simulations plus the estimated model. Figure 12 presents a 3D view of the cut-back showing its position in relation to the current pit design. Figure 13 shows the results in terms of contained ore for each mining scenario:

- the first profile corresponds to the scenario 'A', which corresponds to the cut-back depletions as a single stage; and
- the other profiles correspond to the first and second stages of scenario 'B'.

The expected combined ore tonnage of scenario 'B' is 2.3% higher than scenario 'A' (28.2 Mt against 27.6 Mt). The risk profile for scenario 'A' shows a range of

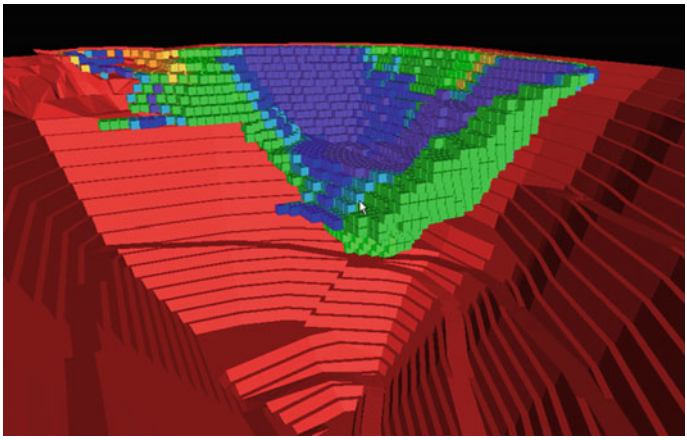

Fig. 12 View of the cut-back aganst the pit design. The colours indicate different incremental pit shells

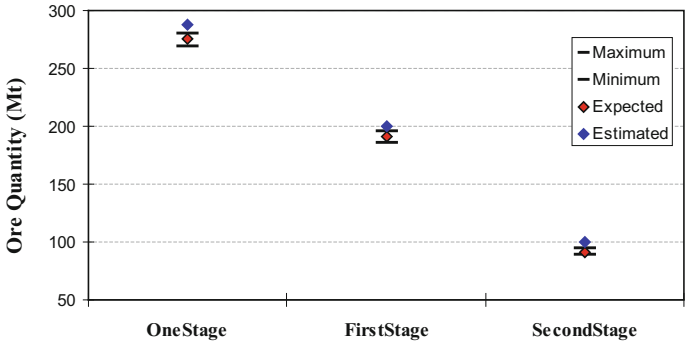

Fig. 13 Risk profiles on contained ore of two mining scenarios

variation that corresponds to 5.2% of the expected ore tonnage. For the two stages of scenario 'B', these ranges correspond to 5.19% and 6.51% respectively. For scenario 'A', the contained ore predicted by the estimated model is 4.16% higher than the expected tonnage derived from the simulations. For the first and second stages, this difference corresponds to 4.63% and 9.89% respectively. Figure 14 shows the results in terms of recovered gold.

The expected recovered metal of scenario 'B' is approximately 1.7% higher than in scenario 'A' (1.63 Moz against 1.60 Mt). The risk profile for scenario 'A' shows a range of variation that corresponds to 7.1% of the expected tonnage. For scenario 'B' this ranges correspond to 8.5% and 12.3%. For scenario 'A' the recovered gold predicted by the estimated model is 10.43% higher than the expected tonnage derived from the simulations. For the first and second stages of scenario 'B', this

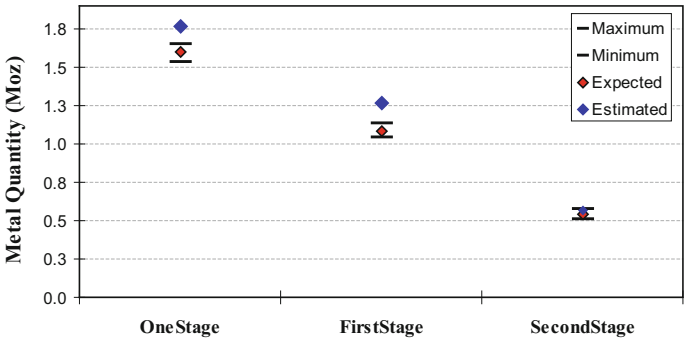

Fig. 14 Risk profiles on recovered metal of two mining scenarios

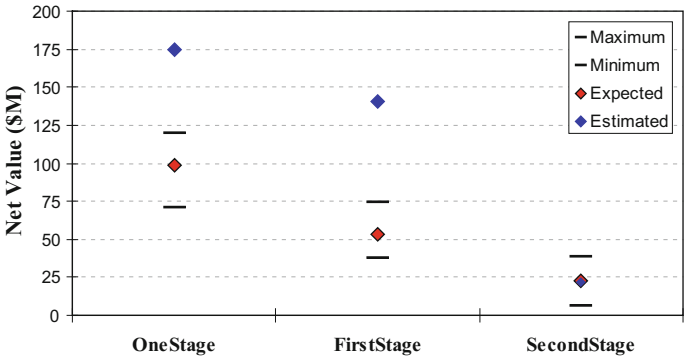

Fig. 15 Risk profiles on pit value of two mining scenarios

difference corresponds to 16.70% and 3.61% respectively. Figure 15 summarises the results in terms of Net Value.

The expected Net Value of scenario 'B' is approximately 22.3% lower than in scenario 'A' ($76.5 M against $98.4 M). The risk profile for scenario 'A' shows a range of variation that corresponds to 50% of the expected Net Value. For scenario 'B' the ranges correspond to 68.61% and 141.2% for the first and second stages respectively. The combined expected range of variation for scenario 'B' corresponds to 67.4%. For scenario 'A' the Net Value predicted by the analysis on the estimated model is 76.85% higher than the expected tonnage derived from the simulations. For the first and second stages this difference corresponds to 162.47% and −2.48% respectively. The results obtained in terms of the risk profiles indicate that both scenarios present high risk of not achieving predicted Net Value. In addition, it was clearly identified that the volume related to stage 1 of the scenario 'B' is the one with all the risk.

It is important to note that this analysis is rather simplistic in the sense that the time effect of money is not included. Ideally, a mining schedule should be

developed in order to account for the mine sequencing. However, the second scenario roughly accounts for the sequencing by developing the depletion in two stages. The analysis indicated that the risk of missing the target when mining the volume related to the first stage of the second scenario is extremely high. This warrants a detailed review of the estimated grades in this volume.

Risk Analysis on Ore Blocks Driving a Pit Increment

The aim of this analysis is the quantification of uncertainty on the ore blocks driving the increment between two successive Whittle pit shells. To assess uncertainty on the main parameters driving increment between two successive pit shells, the follow procedure is proposed:

1. From the Whittle result file produced by the pit optimisation process generate a Whittle pit list file containing information about the smallest numbered pit that each block is part of.
2. Use the re-blocking program—apply the pit list file produced in step 1 to each one of the simulated block models. This will create a set of results files.
3. Produce cross-sections for the incremental pit shells.
4. Generate the summary pit information for the two pits. The analysis must be carried out for each one of the available simulated models. Derive the information referent to the incremental volume by subtracting the cumulative mining physicals (ore and metal quantities) and economic values (Net Value, processing cost and mining cost) between the two successive pit shells.

The above procedure is similar to the procedure used in the first section of this paper. The difference is that here the analysis is limited to two specific pit shells. The increment from pit 26 to pit 27 contains approximately 53 Mt of rock and is located in the southern end of the pit. Table 1 presents the results obtained by the analysis of the pit increment.

The risk profile on the contained ore shows a range between 5.7 and 6.2 Mt, with an expected tonnage of approximately 5.9 Mt. Low ranges of variation are also

Table 1 Risk profile for mining physicals and economic parameters for the increment between pits 26 and 27

	Expected	Minimum	Maximum	Range
Ore (×1000t)	5925	5706	6222	516
Metal (oz)	341,739	309,451	362,982	53,531
Grade (g/t)	1.95	1.93	1.98	0.05
Mcost (×1000$)	−103,594	−103,716	−103,521	195
Pcost (×1000$)	−70,783	−74,285	−68,238	6047
Net value (×1000$)	7381	−8164	17,685	25,849

shown for the risk profiles on grade, metal content and costs. The main issue here is in relation to the Net Value, which has a chance of being negative. Its risk profile goes from approximately $-8.2 M to $17.7 M. The reason for the increase in the risk profile the mining cost associated to a high stripping ratio (~ 9), which makes the Net Value oversensitive to possible variations on the recovered gold. It is important to notice that the risk profile indicates an expected Net Value for this increment of $7.4 M. In fact, only one out of 15 simulated models presented a negative value for the Net Value. The results indicate a relatively low uncertainty in tonnages and grades contained between pits 26 and 27. However, this relatively low uncertainty becomes a critical issue due the high stripping ratio which makes the increment's Net Value very sensitive to grade uncertainty as well as gold price.

Several cross-sections have been generated to show the pit region relative to the increment between pits 26 and 27. These sections show the incremental shells, the current pit design and ore blocks contained inside the increment. The main conclusions drawn from the analysis of these cross-sections have four components. First, the major difference between the incremental Whittle pit shells $550/oz and $560/oz corresponds to a region located at the southern end of the pit. Most of the incremental ore blocks have an expected value inside the range of 1.5–2.5 g/t. Moreover, most of the incremental ore blocks have more than 60% chance of being above the cut-off. The increment contains a high quantity of waste and the pit design has considerably more waste than pit shell 27.

Conclusions

The goal of this work was to illustrate different applications of risk analysis on the effects of grade uncertainty to various aspects of pit optimisation and design. Four cases have been carried out to illustrate different types of applications:

1. The first case consisted of an uncertainty analysis on pit optimisation results—Net Value, tonnage, grade and metal. The procedure consisted in applying a set of incremental pit shells, as produced by the pit optimisation process, to a set of simulated resource models. The subsequent analysis on each model produced a set of equally probably outcomes for the mining physicals and economic forecasts given the initial set of incremental pit shells.
2. The second case identified areas were grade uncertainty has major impact to the definition of the ultimate pit limits (upside/downside potential). Rather than developing a risk analysis on a given set of incremental pit shells, this procedure consisted in the generation of alternative sets of incremental shells, one set for each simulated model.
3. The third case aimed at quantifying the impact of grade uncertainty to tonnage, grades, metal and Net Value of two different mining scenarios for a given cut-back. The main objective was to evaluate if one of the scenarios was any better in terms of the compromise between Net Value and risk exposure.

4. The fourth case consisted of a risk analysis related to pit increments. The objective of this analysis is the quantification of uncertainty on the ore blocks driving the increment between two successive Whittle pit shells.

The results were presented in two steps:

1. first, each optimisation output was evaluated in terms of contained ore, grade, metal and pit value; and
2. the second step of the analysis consisted on the generation of a series of cross-sections.

These cross-sections were taken over all optimised models and included the actual pit design. Several conclusions have been drawn from these graphs indicating areas of upside and downside potential.

This paper presented a set of procedures that enable mine planning engineers to carry out a series of analysis, which can be used to evaluate the sensitivity of incremental pit shells and pit designs to grade uncertainty. The results obtained from the analysis have shown to provide valuable information, which can be used to develop mining strategies that are risk resilient in relation to grade uncertainty.

References

David M (1988) Handbook of applied advanced geostatistical ore reserve estimation. Elsevier Science Publishers, Amsterdam, p 216

Dimitrakopoulos R (1998) Conditional simulation algorithms for modelling orebody uncertainty in open pit optimisation. Int J Surf Min Reclam Environ 12:173–179

Dimitrakopoulos R, Farrelly CT, Godoy M (2002) Moving forward from traditional optimisation: grade uncertainty and risk effects in open-pit design. Trans Institutions of Min Metall Min Technol 111:A82–A88

Dimitrakopoulos R, Martinez L, Ramazan S (2007) A maximum upside/minimum downside approach to the traditional optimization of open pit mine design. J Min Sci 43:73–82

Godoy MC (2002) The effective management of geological risk in long-term production scheduling of open pit mines, Ph.D. thesis, The University of Queensland, Brisbane, p 256

Journel AG (1992) Computer imaging in the minerals industry—beyond mere aesthetics. In Proceedings 23rd APCOM (International symposium on application of computers and operations research in the mineral industry), Society for Mining, Metallurgy and Exploration, Littleton, pp 3–13

Kent M, Peattie R, Chamberlain V (2007) Incorporating grade uncertainty in the decision to expand the main pit at the Navachab gold mine, Namibia, through the use of stochastic simulation. In: Dimitrakopoulos R (ed) Orebody modelling and strategic mine planning, 2nd edn. The Australasian Institute of Mining and Metallurgy, Melbourne, pp 207–216

Lerchs H, Grossmann IF (1965) Optimum design of open pit mines, CIM Bulletin, Canadian Institute of Mining and Metallurgy, vol 58, January

Ravenscroft PJ (1992) Risk analysis for mine scheduling by conditional simulation. Trans Institutions of Min Metall Min Technol 101:A101–A108

Whittle J (1999) A decade of open pit mine planning and optimisation—The craft of turning algorithms into packages. In: Proceedings APCOM '99 International symposium on application of computers and operations research in the mineral industry, Colorado School of Mines, Colorado, pp 15–24

Mining Schedule Optimisation for Conditionally Simulated Orebodies

M. Menabde, G. Froyland, P. Stone and G. A. Yeates

Abstract Traditionally the process of mine development, pit design and long-term scheduling is based on a single deterministic orebody model built by the interpolation of drill hole data using some form of spatial interpolation procedure, e.g. kriging. Typical steps in mine design would include the determination of the ultimate pit, the development of a number of mining phases (pushbacks) and then the development of a life-of-mine schedule. All of these steps would have the aim of maximising the mine's net present value (NPV), along with meeting numerous other business and physical constraints. There are a number of software packages commercially available and widely used in the mining industry that deal with some or all of these issues. The methods employed by all of these packages treat the process described above in a strictly deterministic way. In reality, given the sparse drill hole data, there is usually significant and variable uncertainty associated with a single or unique deterministic block model. This uncertainty is not captured or used in the planning process. This paper describes work undertaken by the Exploration and Mining Technology Group within BHP Billiton to develop a new mathematical algorithm for mine optimisation under orebody uncertainty. This uncertainty is expressed as a number of conditionally simulated orebody models. This optimisation algorithm is implemented in a new software package. The software uses a number of proprietary algorithms along with the commercially available mixed integer-programming package ILOG CPLEX. The development targets all phases of mine optimisation, including the NPV optimal block extraction sequence, pushback design, and simultaneous cut-off grade and mining schedule optimisation.

M. Menabde · P. Stone
BHP Billiton, GPO Box 86A, Melbourne, VIC 3001, Australia

G. Froyland (✉)
School of Mathematics, The University of New South Wales, Sydney, NSW 2052, Australia
e-mail: froyland@maths.unsw.edu.au

G. A. Yeates
Mineral Resource Development, Business Excellence, BHP Billiton Limited, PO Box 86A, Melbourne, Vic 3001, Australia
e-mail: gavin.yeates@bhpbilliton.com

R. Dimitrakopoulos (ed.), *Advances in Applied Strategic Mine Planning*,
https://doi.org/10.1007/978-3-319-69320-0_8

Introduction

This paper describes the development and implementation of a new software package for open pit mine development and scheduling optimisation under conditions of orebody uncertainty and is based on the mixed integer programming method. The approach uses multiple conditionally simulated realisations of the orebody as input to characterise the orebody along with the uncertainty in the estimate.

Traditionally open pit mine planning, pit design and long-term scheduling is based on a block model of the orebody built by interpolation techniques such as kriging from the drill hole sample data. This single model is assumed to be a fair representation of reality and is used for mine design and optimisation. The design process consists of four main steps:

1. Determining the ultimate pit shell to define the scheduling universe.
2. Finding the block extraction sequence which produces the best net present value (NPV) whilst satisfying the geotechnical slope constraints.
3. Designing the practically minable mine phases (pushbacks) which are roughly based on the optimal block sequence.
4. Optimising the mining schedule and cut-off grades (COG) within a set of business and operational constraints. The NPV of this 'optimal' schedule is considered as a main criterion of the economical viability of the project.

In reality, there are many uncertainties in the models and parameters used in optimisation. Thus, the adoption of a single economic criterion for a project can be very questionable. One of the most important sources of uncertainty is the block model itself. The drill hole data for a mining project is typically sparse, particularly at the scale of the selective mining unit and could support a range of possible outcomes for the orebody. A unique deterministic block model will often be a good representation of the global resource, but will not be representative of the potential local variability or the uncertainty in the estimate. An approach that quantifies both the local variability and the potential uncertainty is to use multiple conditional simulation realisation to represent the orebody (see Dimitrakopoulos 1998). This approach allows the generation of a number of equally probable realisations of the block model, at the selective mining unit (SMU) scale, with all of them honouring the drill hole data along with the first and second order statistics of the orebody represented, respectively, by the probability distribution and variogram (e.g. Isaaks and Srivastava 1989).

The simplest and most straightforward use of this set of orebody realisations is to estimate the variability in the project NPV associated with the orebody uncertainty by valuing the 'optimal' schedule obtained from the kriged deterministic model through each of the conditionally simulated realisations.

The more interesting question is whether it is possible to use the set of conditionally simulated realisations to produce a better mine design and production schedule. By 'better' we mean here a higher expected NPV (which becomes a

random variable in case of multiple realisations of the orebody model) and/or less variability from one realisation to other (i.e. lower variance of NPV). A new promising approach to this problem is presented in Ramazan and Dimitrakopoulos (2007, this volume); Jewbali (2006).

In this paper we address one particular aspect of the optimisation under uncertainty, namely the simultaneous optimisation of the extraction sequence and COG. The use and importance of optimal (variable) COG to mining projects has been known for a long time (e.g. Lane 1988). It will be demonstrated here that the use of variable COG optimised under uncertainty, using the set of equi-probable realisations of the orebody can provide a substantial improvement in terms of expected NPV. The approach based on mixed integer programming techniques can provide a truly optimal schedule, as opposed to various heuristic methods used in most of the commercially available mining optimisation software packages.

Mining Schedule Optimisation as a Mixed Integer Programming Model

Typically, the orebody block model contains between 50,000 and 5,000,000 blocks, which must be scheduled over a period of say 5–25 years. The objective of any scheduling procedure is to find the block extraction sequence, which produces the maximum possible net present value (NPV) and obeys a number of constraints. The latter include:

1. geotechnical slope constraints, which are modelled by a set of precedence arcs between individual blocks;
2. mining constraints, i.e. total maximum amount of rock which can be mined in one time period (usually one year);
3. processing constraints, i.e. maximum amount of ore which can be processed through a given processing plant in one time period; and
4. the market constraints, i.e. the maximum amount of metal that can be sold in one time period.

The mathematical formulation of the scheduling procedure in terms of binary decision variables describing in which period the particular block is extracted and what its destination is (either processing plant, stockpile or waste dump), is quite straightforward. The size of the problem is, however, prohibitively large. Apart from the computational difficulties, the hypothetical optimal block extraction sequence may be completely impractical due to the requirements for the mining equipment access and relocation.

Because of these problems the mine scheduling is done using much bigger elementary units that are typically aggregations of hundreds or even thousands of blocks. The aggregation of blocks is a nontrivial problem. For example, simply combining rectangular blocks into a larger rectangular block with dimensions multiples of that of individual blocks can effectively reduce the size of the problem

but will provide a very poor approximation for the geotechnical slopes. An interesting approach to block aggregation based on the concept of 'fundamental trees' has been recently developed by Ramazan (2007, this volume). In this method the aggregations of blocks—fundamental trees—obey the slope constraints and can substantially reduce the number of integer variables required for the scheduling model. However, the number of these aggregations is not user controllable and in many cases the problem can be still too big to be solved by a direct application of the mixed integer programming techniques.

We have recently developed a new algorithm for block aggregation, which preserves the slope constraints, and is very flexible allowing the user to fully control the size and shape of these aggregations. The details of this algorithm will not be discussed here. The optimisation procedure, however, can be applied to any aggregation of blocks with a set of precedence arcs, prescribing which blocks should be extracted before the given one. As an example we consider here the scheduling of mining phases.

In practice, the open pit mine is divided into a number of mining phases, which are mined bench by bench, each bench represented by a horizontal layer of blocks within the given mining phase and having the same elevation. A bench within a mining phase is sometimes referred to as a "panel". The mining phases can be mined one by one from top to bottom, however this kind of schedule is usually suboptimal. Mining several phases simultaneously and applying variable COG can produce much better results in terms of NPV. There are several commercially available packages, which use proprietary (and undisclosed) heuristics to optimise the schedule and COG. It is difficult to estimate their effectiveness, as the upper theoretical limit on NPV remains unknown. Moreover, these methods can only be used on a single orebody representation and cannot be directly used on a set of conditionally simulated orebody realisations.

The standard optimsation technique widely used in many industrial applications is the leanear and integer programming (e.g. industrial applications is the linear and integer programming (e.g. Padberg 1995). The main difficulty in its application to mining scheduling is that the optimsation with variable COG in its direct formulation leads to a non-linear problem, which is much harder to solve. Our approach provides an effective linearsation of this problem, making it possible to use a mixed integer programming (MIP) formulation for a simultaneous optimization of the extraction sequence and COG for a number of conditionally simulated orebody models. The MIP formulation we use here is similar to the one used by Caccetta and Hill (2003) but is generalised to include the multiple realisations of conditional simulations and variable cut-off grades. This approach also allows one to estimate the gap between the obtained solution and the upper theoretical limit.

We consider the simplest case when we have one rock type containing one metal type, which can be processed through one processing plant. Generalisation to the case of multiple rock types, metals and processing streams is cumbersome but straightforward. For simplicity we consider here only the case of a discrete set of COGs, though it is possible to generalise the results to the continuous COG case. We use the following notations:

T is the number of scheduling periods
N is the number of simulations
P is the total number of panels
G is the number of all possible cut-off grades
R_i^n is the total rock in the panel i in simulations n
Q_{ij}^n is the total ore in the panel i, simulation n, when mined with the COG j
V_{ij}^n is the value of the panel i, simulation n, when mined and processed with the COG j
R_t^0 is the maximum mining capacity in period t
Q_t^0 is the maximum processing rate in period t
Si is the set of panels that must be removed before starting the panel i
d^t is the time discount factor
$Xijt$ is the fraction of the panel i is extracted with the COG j in period t
Yit is a binary variable equal to 1 if the extraction of the panel I has started in periods 1 to t, and equal to 0 otherwise;
δjt is a binary variable controlling the selection of the COG applied in period t

The MIP formulation is:

$$Maximise\left(\frac{1}{N}\sum_{n=1}^{N}\sum_{i=1}^{P}\sum_{j=1}^{G}\sum_{t=1}^{T}V_{ij}^{n}x_{ijt}d^{t}\right) \tag{1}$$

Subject to the following constraints:

$$\frac{1}{N}\sum_{n=1}^{N}\sum_{i=1}^{P}\sum_{j-1}^{G}R_i^n x_{ijt} \le R_{t,}^0 \quad for\,all\,t \tag{2}$$

$$\frac{1}{N}\sum_{n=1}^{N}\sum_{i=1}^{P}\sum_{j=1}^{G}Q_{ij}^n x_{ijt} \le Q_{t,}^0 \quad for\,all\,t \tag{3}$$

$$y_{i,\quad t-1} \le y_{it,} \quad for\,all\,i\,and\,t \tag{4}$$

$$\sum_{\tau=1}^{t}\sum_{j=1}^{G}x_{ij\tau} \le y_{it,} \quad for\,all \tag{5}$$

$$y_{it} \le \sum_{j=1}^{G}\sum_{\tau=1}^{T}x_{kj\tau,} \quad for\,all\,i, \quad t\,and\,k \subset S_i \tag{6}$$

$$\sum_{j=1}^{G}\delta_{jt=1,} \quad for\,all\,t \tag{7}$$

$$x_{ijt} \leq \delta_{jt}, \quad \text{for all } i, j \text{ and } t \tag{8}$$

The objective function (1) represents the discounted cash flow. Constraints (2) and (3) enforce the mining and processing limits on average. Constraints (4)–(6) enforce the panel extraction precedence constraints, and constraints (7) and (8) ensure that the same COG is applied to all panels extracted in any given time period.

This MIP formulation is solved by the commercially available software package CPLEX version 9.0, by ILOG Inc.

Case Study

To test the algorithm we have chosen ten conditional simulations of a block model containing one type of metal and using one processing plant. Because of confidentiality requirements, all the economic parameters were rescaled and do not represent reality. All of the relative characteristics which demonstrate the potential of this new method are not affected by this rescaling. The ultimate pit for the design is chosen by applying the Lersch-Grossmann algorithm (Lersch and Grossmann 1965) in a procedure similar to that used in Whittle Four-X software. The ultimate pit contains 191 million tonnes of rock and 62.9 ± 2.7 million tonne of ore (above the marginal COG = 0.6%). The undiscounted value in the ultimate pit (if processed with the marginal COG) is $(1316 ± 99) million. It was divided into six mining phases and scheduled over 12 years. The mining rate was set to 30 Mtpa and the processing rate to 5 Mtpa. The initial capital investment was assumed to be $300 million, and the discount rate 10%. The base case optimisation was done using the marginal COG applied individually to all conditional simulation. The NPV for this case was $(404 ± 31) million. The mining schedule is shown in Fig. 1. The second optimisation was done using the variable COG, but was based on the mean grade block model, i.e. it was similar to an optimisation generated by using a single deterministic model. This schedule was evaluated against all ten realisations of orebody model and produced the NPV = $(485 ± 40) million, an increase of 20% over the base case. This mining schedule is shown in Fig. 2. The third optimisation was done using the algorithm described in earlier, using all orebody realisations as input to the optimisation and produced the NPV = $(505 ± 43) million, a further increase of 4.1% over the case of mean grade based optimisation. This mining schedule is shown in Fig. 3. The relative variability of NPV in all cases was roughly the same, about 8%. The cumulative NPV graphs for the three different schedules are shown in Fig. 4, and the comparison between expected NPVs and their variability is shown in Fig. 5. Another important result of the variable COG policy is that the pay-back period (defined here as the time when the cumulative NPV becomes equal to zero) is decreased from five to three years (see Fig. 4).

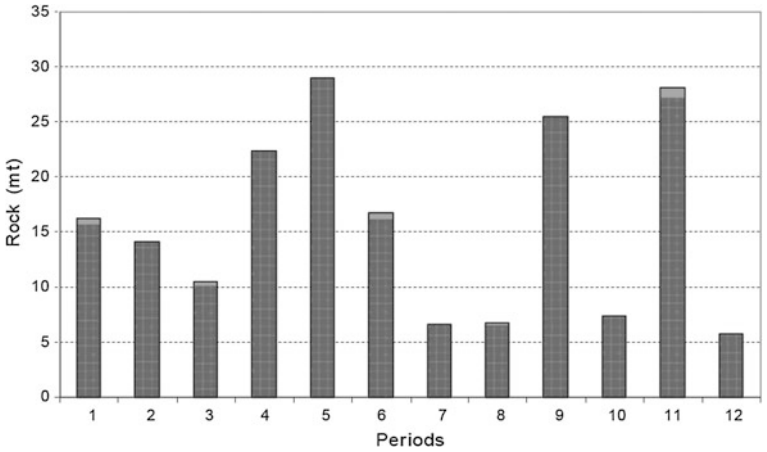

Fig. 1 Mining schedule optimised with the marginal COG

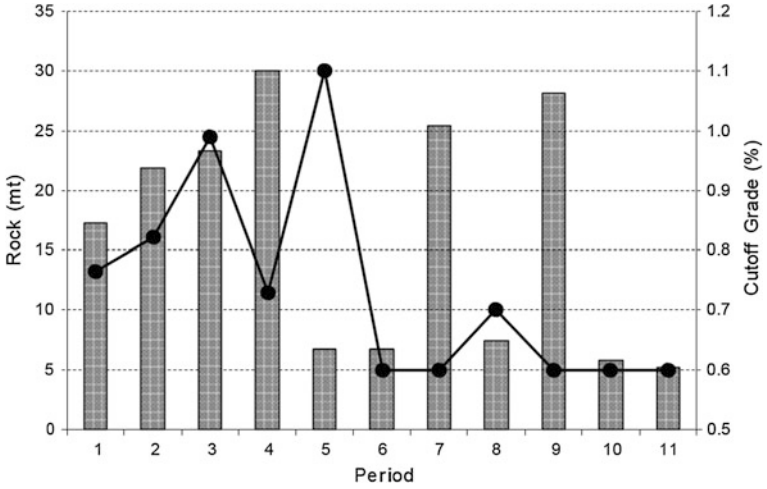

Fig. 2 Mining schedule optimised with the mean grade model

The increase of 4.1% in NPV may be not seen as a very substantial, but it should be mentioned that the block model considered does not have a high variability. The relative variance in the undiscounted value of the ultimate pit is only 7.6%. There are many deposits that have variability of the order of 20–30%. For these kind of deposits the potential improvement in the expected NPV may be substantially higher.

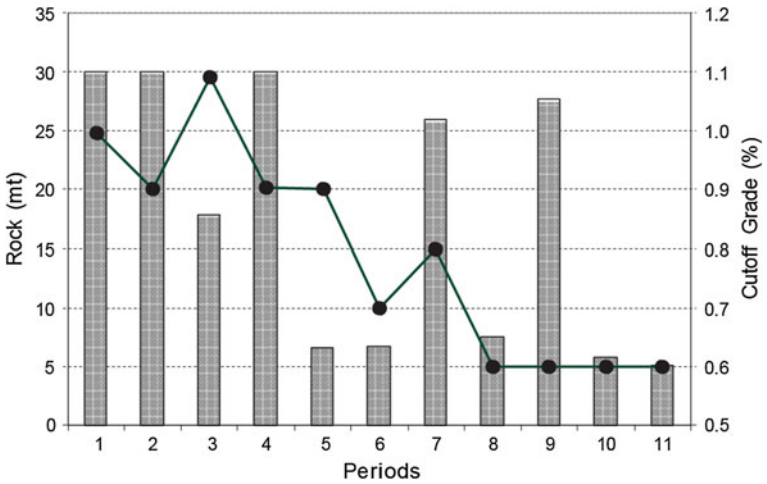

Fig. 3 Mining schedule optimised with the set of conditional simulations

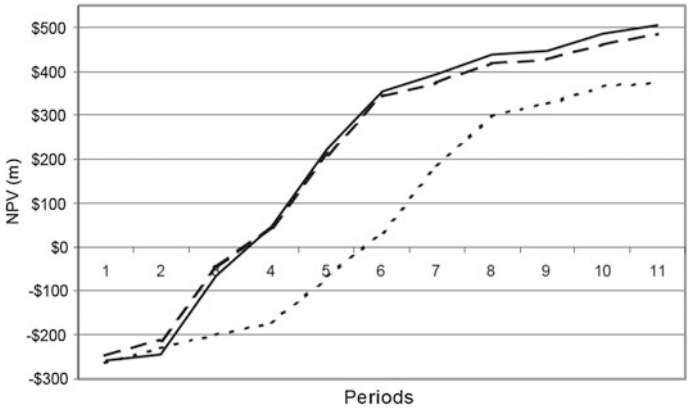

Fig. 4 Cumulative NPV for different missing schedules (solid line-variable COG on conditional simulations; dashed line-variable-COG on the mean grade model; dotted line-marginal COG)

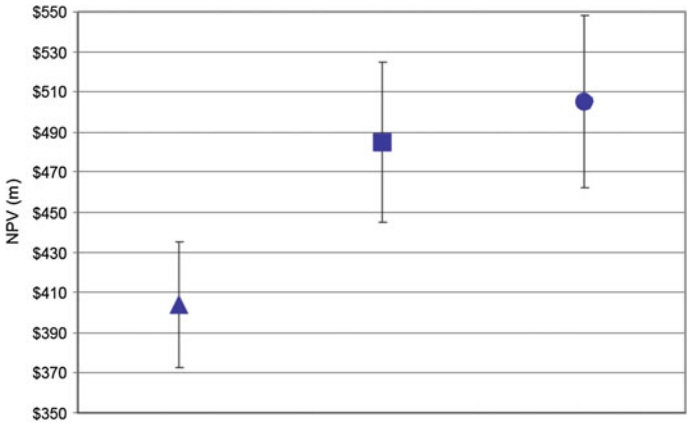

Fig. 5 Comparison of expected NPVs and their variability for different mining schedules (circle-variable COG on the conditional simulations; square-variable COG on the mean grade model; traingle-marginal COG)

Conclusions

A new method for simultaneous optimisation of the extraction sequence and cut-off grade policy for a set of conditionally simulated orebody realisations has been developed and demonstrated. This method is based on the mixed integer programming model and uses the commercially available software package CPLEX by ILOG Inc. The goal of the optimisation is to find the extraction sequence and cut-off grade policy, which, when evaluated through the whole set of conditionally simulated orebodies (representing the range of possible outcomes), will produce the best possible expected NPV. The degree of accuracy of this optimised schedule can be estimated precisely, in contrast to a number of heuristic routines used in current commercially available mining optimisation software packages. A fully functional software prototype that uses the new optimisation method has been developed.

In this study, we were using the expected NPV as the objective function and the mining and processing constraints were applied to the mean rock and ore tonnages. Some of the possible extensions of this method may include some kind of penalty functions in the objective function in order to find a schedule with a reduced variability in NPV, defining hard constraints bounding the NPV from below, or defining a lower bound on the annual cash flows. Another very interesting generalisation may include a stochastic price model for metals and adjustable cut-off grade policy.

References

Caccetta L, Hill SP (2003) An application of branch and cut to open pit mine scheduling. J Global Optim 27(2–3):349–365

Dimitrakopoulos R (1998) Conditional simulation algorithms for modeling orebody uncertainty in open pit optimization. Int J Surf Min 12(4):173–179

Isaaks EH, Srivastava RM (1989) Applied geostatistics. Oxford University Press, New York, p 561

Jewbali A (2006) Modelling geological uncertainty for stochastic short-term production scheduling in open pit metal mines. Ph.D. thesis, The University of Queensland, Australia, p 280

Lane KF (1988) The economic definition of ore. Mining Journal Books Ltd., London, p 147

Lerchs H, Grossmann L (1965) Optimum design of open-pit mines. Trans CIM, LXVII, pp 17–24

Padberg MW (1995) Linear optimization and extensions. New York, Springer, p 449

Ramazan S (2007) Large-scale production scheduling with the fundamental tree algorithm—model, case study and comparisons. In: Dimitrakopoulos R (ed) Orebody modelling and strategic mine planning, 2nd edn. The Australasian Institute of Mining and Metallurgy, Melbourne, pp 121–127

Ramazan S, Dimitrakopoulos R (2018) Stochastic optimisation of long-term production scheduling for open pit mines with a new integer programming formulation. (in this volume)

Stochastic Mine Planning—Methods, Examples and Value in an Uncertain World

R. Dimitrakopoulos

Abstract Conventional approaches to estimating reserves, optimising mine planning and production forecasting result in single, often biased, forecasts. This is largely due to the non-linear propagation of errors in understanding orebodies throughout the chain of mining. A new mine planning paradigm is considered herein, integrating two elements: stochastic simulation and stochastic optimisation. These elements provide an extended mathematical framework that allows modelling and direct integration of orebody uncertainty to mine design, production planning, and valuation of mining projects and operations. This stochastic framework increases the value of production schedules by 25%. Case studies also show that stochastic optimal pit limits:

- can be about 15% larger in terms of total tonnage when compared to the conventional optimal pit limits, while
- adding about 10% of net present value (NPV) to that reported above for stochastic production scheduling within the conventionally optimal pit limits.

Results suggest a potential new contribution to the sustainable utilisation of natural resources.

Introduction

Optimisation is a key aspect of mine design and production scheduling for both open pit and underground mines. It deals with the forecasting, maximisation, and management of cash flows from a mining operation and is the key to the financial aspects of mining ventures. A starting point for optimisation in the above context is the representation of a mineral deposit in three-dimensional space through an orebody model and the mining blocks representing it; this is used to optimise

R. Dimitrakopoulos (✉)
COSMO—Stochastic Mine Planning Laboratory, Department of Mining and Materials Engineering, McGill University, Montreal, QC H3A 2A7, Canada
e-mail: roussos.dimitrakopoulos@mcgill.ca

R. Dimitrakopoulos (ed.), *Advances in Applied Strategic Mine Planning*,
https://doi.org/10.1007/978-3-319-69320-0_9

designs and production schedules (e.g. Whittle 1999). Geostatistical estimation methods have long been used to model the spatial distribution of grades and other attributes of interest within the mining blocks representing a deposit (David 1988). The main drawback of estimation techniques, be they geostatistical or not, is that they are unable to reproduce the in situ variability of the deposit grades, as inferred from the available data. Ignoring such a consequential source of risk and uncertainty may lead to unrealistic production expectations (e.g. Dimitrakopoulos et al. 2002). Figure 1 shows an example of unrealistic expectations in a relatively small gold deposit. In this example (Dimitrakopoulos et al. 2002), the smoothing effect of estimation methods generates unrealistic expectations of net present value in the mine's design, along with ore production performance, pit limits, and so on. The figure shows that if the conventionally constructed open pit design is tested against equally probable simulated scenarios of the orebody, its performance will probably not meet expectations. The conventionally expected NPV of the mine has a 2–4% chance to materialise, while it is expected to be about 25% less than forecasted. Note that in a different example, the opposite could be the case.

For over a decade now, a traditional framework has been used when dealing with uncertainty in the spatial distribution of attributes of a mineral deposit, as well as its implications to downstream studies, planning, valuation, and decision-making. Now, a different framework than the traditional has been suggested and is outlined in Fig. 2. Instead of a single orebody model as an input to optimisation for mine design and a 'correct' assessment of individual key project indicators, a set of models of the deposit can be used. These models are conditional to the same available data and their statistical characteristics, and all are constrained to reproduce all available information and represent equally probable models of the actual spatial distribution of grades (Journel 1994). The availability of multiple equally

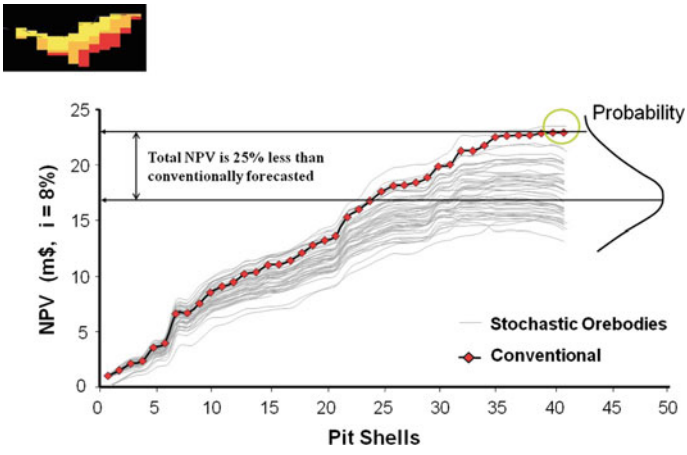

Fig. 1 Optimisation of mine design in an open pit gold mine, NPV versus 'pit shells' and risk profile of the conventionally optimal design

probable models of a deposit enables mine planners to assess the sensitivity of pit design and long-term production scheduling to geological uncertainty (e.g. Kent et al. 2007; Godoy 2010, in this volume) and, more importantly, empower mine planners to produce mine designs and production schedules with substantially higher NPV assessments through stochastic optimisation. Figure 3 shows an example from a major gold mine presented in Godoy and Dimitrakopoulos (2004), where a stochastic approach leads to a marked improvement of 28% in NPV over the life of the mine, compared to the standard best practices employed at the mine; note that the pit limits used are the same in both cases and are conventionally derived through commercial optimisers (Whittle 1999). The same study also shows that the stochastic approach leads to substantially lower potential deviation from production targets, that is, reduced risk. A key contributor to substantial differences is that the stochastic or risk-integrating approach can distinguish between the 'upside potential' of the metal content, and thus economic value of a mining block, from its 'downside risk', and then treat them accordingly, as further discussed herein.

Figure 2 represents an extended mine planning framework that is stochastic (that is, integrates uncertainty) and encompasses the spatial stochastic model of geostatistics with that of stochastic optimisation for mine design and production scheduling. Simply put, in a stochastic mathematical programming model developed for mine optimisation, the related coefficients are correlated random variables that represent the economic value of each block being mined in a deposit, which are in turn generated from considering different realisations of metal content. Note that

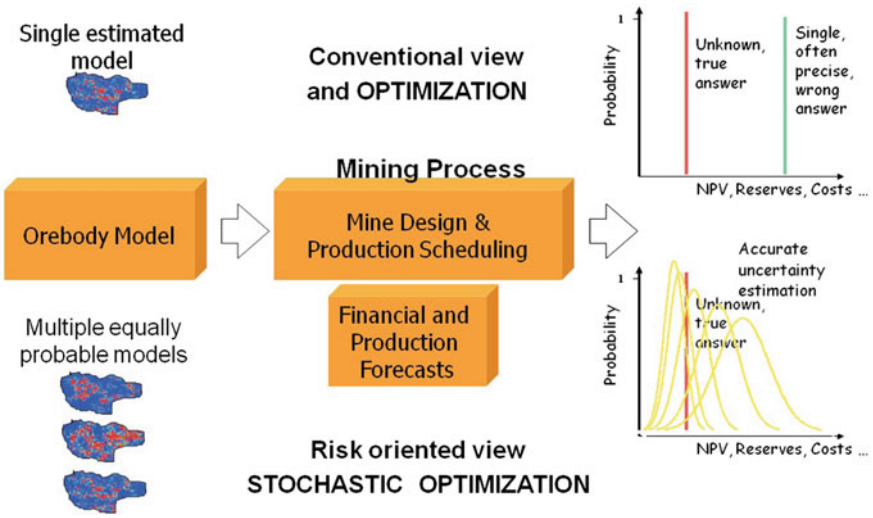

Fig. 2 Traditional (deterministic or single model) view and practice versus risk-integrating (or stochastic) approach to mine modelling, from reserves to production planning and life-of-mine scheduling, and assessment of key project indicators

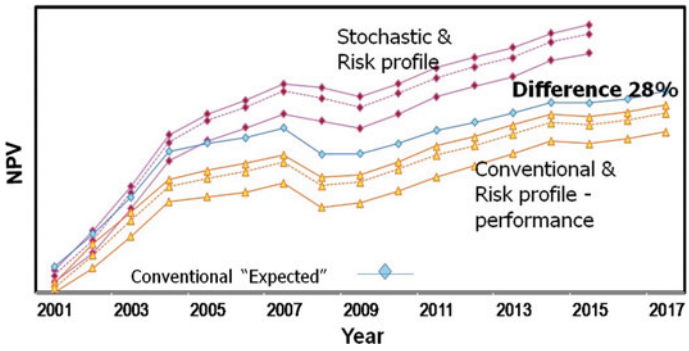

Fig. 3 The stochastic life-of-mine schedule in this large gold mine has a 28% higher value than the best conventional (deterministic) one. All schedules are feasible

the second key element of the risk-integrating approaches is stochastic simulation; the reader is referred to Mustapha and Dimitrakopoulos (2010, in this volume) for the description of a new general method for high-order simulation of complex geological phenomena. The further integration of market uncertainties in terms of commodity prices and exchange rates is discussed elsewhere (Abdel et al. 2011; Meagher et al. 2010).

The key idea in production scheduling that accounts for grade uncertainty is relatively simple. A conventional optimiser (any one of them) is deterministic by construction and evaluates a cluster of blocks, such as that in Fig. 4a, so as to decide when to stop mining, which blocks to extract when, and so on, assuming that the economic values of the mining blocks considered (inputs to the optimiser) are the actual/real values. A stochastic optimiser, also by construction, evaluates a cluster of blocks, but as in Fig. 4b, by simultaneously using all possible combinations of economic values of the mining blocks in the cluster being considered. As a result, substantially more local information on joint local uncertainty is utilised, leading to much more robust schedules that also can maximise the upside potential of the deposit (e.g. higher NPV and metal production) and at the same time minimise downsides (e.g. not meeting production targets and related losses).

To elaborate on the above, the next sections examine a key element in the risk-integrating framework shown in Fig. 2, that of stochastic optimisation. The latter optimisation is presented in two approaches, one based on the technique of simulated annealing, and a second based on stochastic integer programming. Examples follow that demonstrate the practical aspects of stochastic mine modelling, including the monetary benefits.

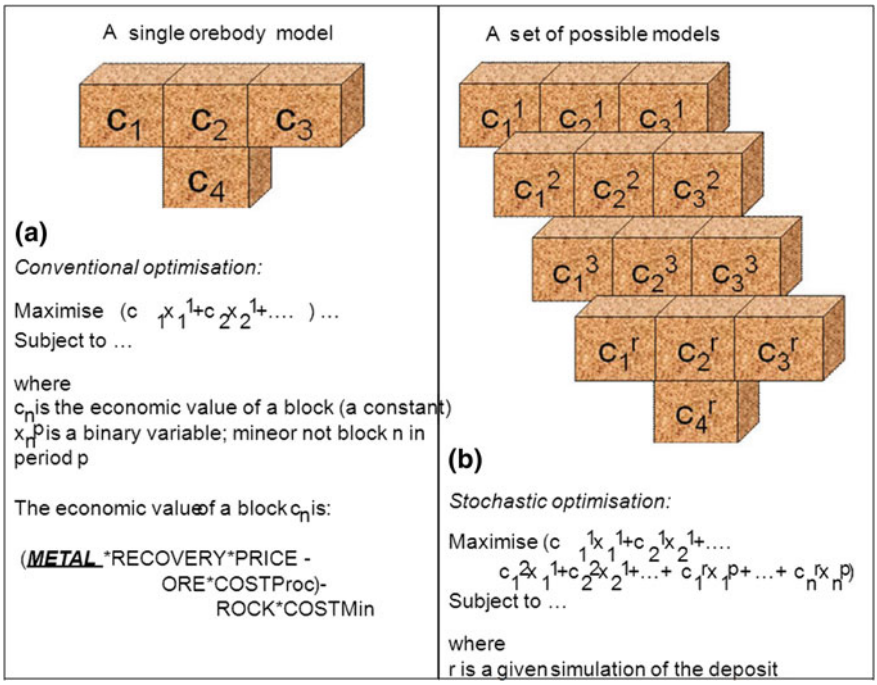

Fig. 4 Production scheduling optimisation with conventional versus stochastic optimisers. **a** Single representation of a cluster of mining blocks in a mineral deposit as considered for scheduling by a conventional optimiser; **b** a set of models of the same cluster of blocks with multiple possible values considered simultaneously for scheduling by a stochastic optimiser

Stochastic Optimisation in Mine Design and Production Scheduling

Mine design and production scheduling for open pit mines is an intricate, complex, and difficult problem to address due to its large-scale and uncertainty in the key parameters involved. The objective of the related optimisation process is to maximise the total net present value of the mine plan. One of the most significant parameters affecting the optimisation is the uncertainty in the mineralised materials (resources) available in the ground, which constitutes an uncertain supply for mine production scheduling. A set of simulated orebodies provides a quantified description of the uncertain supply. Two stochastic optimisation methods are summarised in this section. The first is based on simulated annealing (Godoy and Dimitrakopoulos 2004; Leite and Dimitrakopoulos 2007; Albor et al. 2009); and the second on stochastic integer programming (Ramazan and Dimitrakopoulos, in this volume, 2013; Menabde et al. 2017, in this volume); Leite and Dimitrakopoulos 2014; Montiel et al. 2016; Goodfellow and Dimitrakopoulos 2017a, b).

Production Scheduling with Simulated Annealing

Simulated annealing is a heuristic optimisation method that integrates the iterative improvement philosophy of the so-called Metropolis algorithm with an adaptive 'divide and conquer' strategy for problem solving (Geman and Geman 1984). When several mine production schedules are under study, there is always a set of blocks that are assigned to the same production period throughout all production schedules; these are referred to as the certain or 100% probability blocks. To handle the uncertainty in the blocks that do not have 100% probability, simulated annealing swaps these blocks between candidate production periods so as to minimise the average deviation from the production targets for N mining periods, and for a series of S simulated orebody models, that is:

$$MinO = \sum_{n=1}^{N} \left(\sum_{s=1}^{s} \left| \theta_n^*(s) - \theta_n(s) \right| + \sum_{s=1}^{s} \left| \omega_n^*(s) - \omega_n(s) \right| \right), \tag{1}$$

where $\theta_n(s)$ and $\omega_n(s)$ are the ore and waste production targets, respectively, $\theta_n(s)$ and $\omega_n(s)$ represent the actual ore and waste production of the perturbed mining sequence. Each swap of a block is referred to as a perturbation.

The probability of acceptance or rejection of a perturbation is given by:

$$prob\{accept\} = \begin{cases} 1, if\ 0_{new} \leq 0_{old} \\ e^{\frac{0_{old} - 0_{new}}{T}}, otherwise \end{cases}$$

This implies all favourable perturbations ($Onew \leq Oold$) are accepted with probability 1 and unfavourable perturbations are accepted based on an exponential probability distribution, where T represents the annealing temperature.

The steps of this approach, as depicted in Fig. 5 are as follows:

1. define ore and waste mining rates;
2. define a set of nested pits as per the Whittle implementation (Whittle 1999) of the Lerchs-Grossmann (1965) algorithm, or any pit parameterisation;
3. use a commercial scheduler to schedule a number of where: simulated realisations of the orebody given 1 and 2;
4. employ simulated annealing as in Eq. 1 using the results from 3 and a set of simulated orebodies; and
5. quantify the risk in the resulting schedule and key project indicators using simulations of the related orebody.

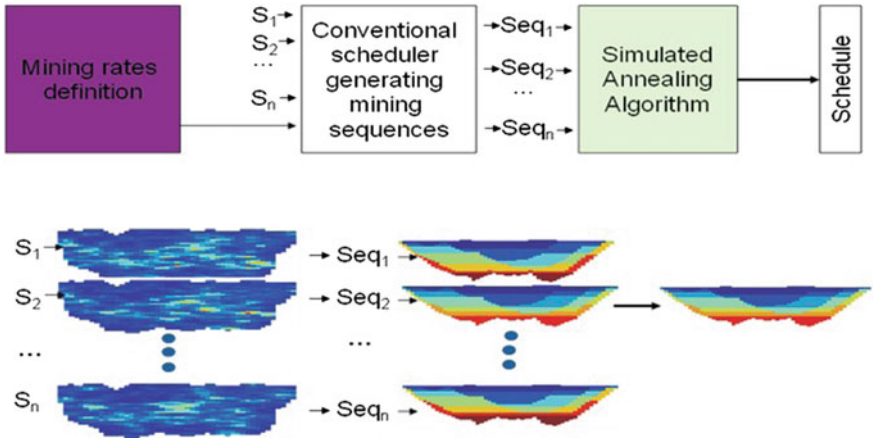

Fig. 5 Steps needed for the stochastic production scheduling with simulated annealing; S_1 … S_n are realizations of the orebody grade through a sequential simulation algorithm; Seq_1 … Seq_n are the mining sequences for each of S_1 … S_n. Mining rates are input to the process

Stochastic Integer Programming for Mine Production Scheduling

Stochastic integer programming (SIP) provides a framework for optimising mine production scheduling considering uncertainty (Dimitrakopoulos and Ramazan 2008). A specific SIP formulation is briefly shown here that generates the optimal production schedule using equally probable simulated orebody models as input, without averaging the related grades. The optimal production schedule is then the schedule that can produce the maximum achievable discounted total value from the project, given the available orebody uncertainty described through a set of stochastically simulated orebody models. The proposed SIP model allows the management of geological risk in terms of not meeting planned targets during actual operation. This is unlike the traditional scheduling methods that use a single orebody model, and where risk is randomly distributed between production periods while there is no control over the magnitude of the risks on the schedule.

The general form of the objective function is expressed as:

$$Max \sum_{t=1}^{p} \left[\sum_{i=1}^{n} E\{(NPV)_i^t\} b_i^t - \sum_{s=1}^{m} (c_u^{to} d_{su}^{to} + c_1^{to} d_{s1}^{to} + c_u^{tg} d_{su}^{tg} + c_1^{tg} d_{s1}^{tg}) \right], \quad (2)$$

where:

p is the total production periods
n is the number of blocks
b_i^t is the decision variable for when to mine block i (if mined in period t, b_t^i is 1 and otherwise b_t^i is 0)

The c variables are the unit costs of deviation (represented by the d variables) from production targets for grades and ore tonnes. The subscripts u and l correspond to the deviations and costs from excess production (upper bound) and shortage in production (lower bound), respectively, while s is the simulated orebody model number, and g and o are grade and ore production targets. Figure 6 graphically shows the second term in Eq. 2.

Note that the cost parameters in Eq. 2 are discounted by time using the geological risk discount factor developed in Dimitrakopoulos and Ramazan (2004). The geological risk discount rate (GRD) allows the management of risk to be distributed between periods. If a very high GRD is used, the lowest risk areas in terms of meeting production targets will be mined earlier and the most risky parts will be left for later periods. If a very small GRD or a GRD of zero is used, the risk will be distributed at a more balanced rate among production periods depending on the distribution of uncertainty within the mineralised deposit. The 'c' variables in the objective function (Eq. 2) are used to define a risk profile for the production, and NPV produced is the optimum for the defined risk profile. It is considered that if the expected deviations from the planned amount of ore tonnage having planned grade and quality in a schedule are high in actual mining operations, it is unlikely to achieve the resultant NPV of the planned schedule. Therefore, the SIP model contains the minimisation of the deviations together with the NPV maximisation to generate practical and feasible schedules and achievable cash flows. For details,

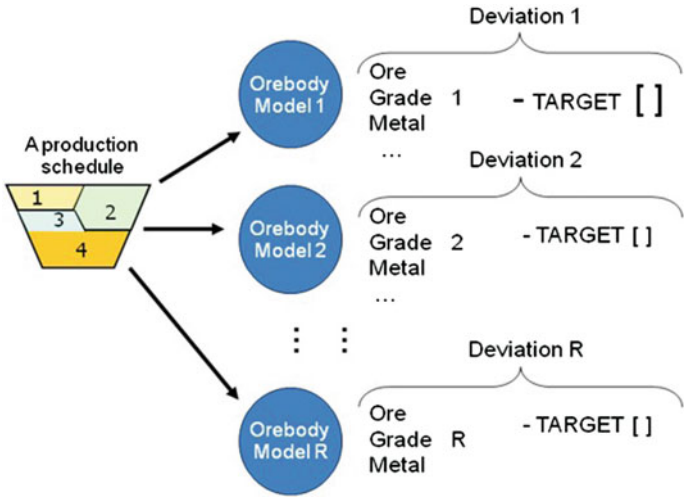

Fig. 6 Graphic representation of the way the second component of the objective function in Eq. 2 minimizes the deviations from production targets while optimizing scheduling. This leads to schedules where the potential deviations from production targets are minimized, leading to schedules that seek to mine first not only for high grade mining blocks, but also with high probability to be ore

please see Ramazan and Dimitrakopoulos (2008) and Dimitrakopoulos and Ramazan (2008).

Examples and Value of the Stochastic Framework

The example discussed herein shows long-range production scheduling with both the simulating annealing approach in Sect. "Simulated annealing and production schedules" and SIP model in Sect. "Stochastic integer programming and production schedules". Section "Stochastically optimal pit limits" focuses on the topic of stochastically optimal pit limits. The application used is at a copper deposit comprising 14,480 mining blocks. The scheduling considers an ore capacity of 7.5 M tonnes per year and a maximum mining capacity of 28 M tonnes. All results are compared to the industry's 'best practice': a conventional schedule using a single estimated orebody model and Whittle's approach (Whittle 1999).

Simulated Annealing and Production Schedules

The results for simulated annealing and the method in Eq. 1 are summarised in Figs. 7, 8, 9 and 10. The risk profiles for NPV, ore tonnages, and waste production are respectively shown in Figs. 7, 8, and 9. Figure 10 compares with the equivalent best conventional practice and reports a difference of 25% in terms of higher NPV for the stochastic approach.

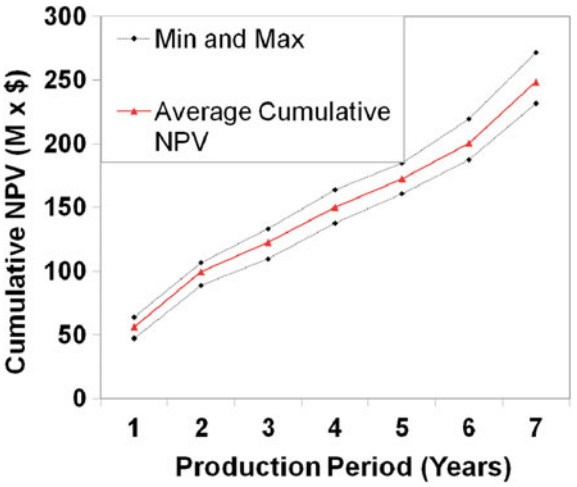

Fig. 7 Risk based LOM production schedule (cumulative NPV risk profile)

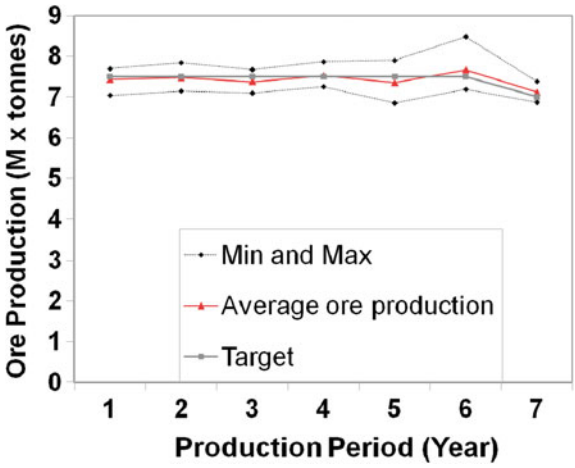

Fig. 8 Risk based LOM production schedule (ore risk profile)

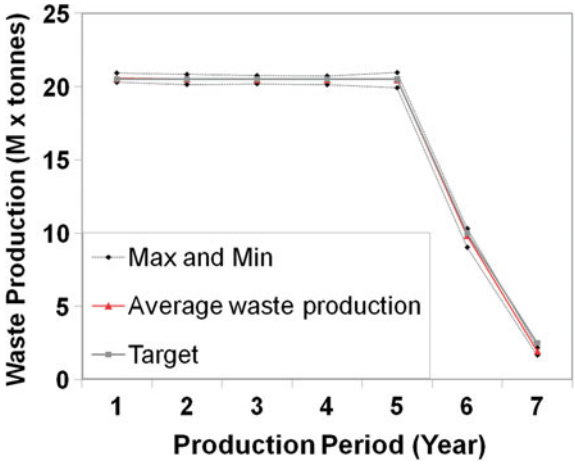

Fig. 9 Risk based LOM production schedule (waste risk profile)

Stochastic Integer Programming and Production Schedules

The application of the SIP model in Eq. 2, using pit limits derived from the conventional optimisation approach, forecasts an expected NPV at about $238 M. When compared to the equivalent traditional approach and related forecast, the value of the stochastic framework is $60 M, or a contribution of about 25% additional NPV to the project. Note that unlike simulated annealing, the scheduler decides the optimal waste removal strategy, which is the same as the one used in the conventional optimisation with which we compare.

Figure 11 shows a cross-section of the two schedules from the copper deposit: one obtained using the SIP model (bottom) and the other generated by a traditional method (top) using a single estimated orebody model. Both schedules

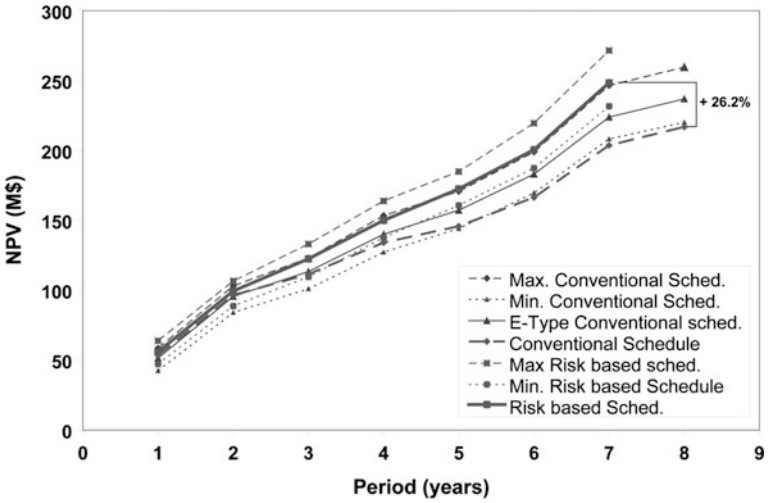

Fig. 10 NPV of conventional and stochastic (risk based) schedules and corresponding risk profiles

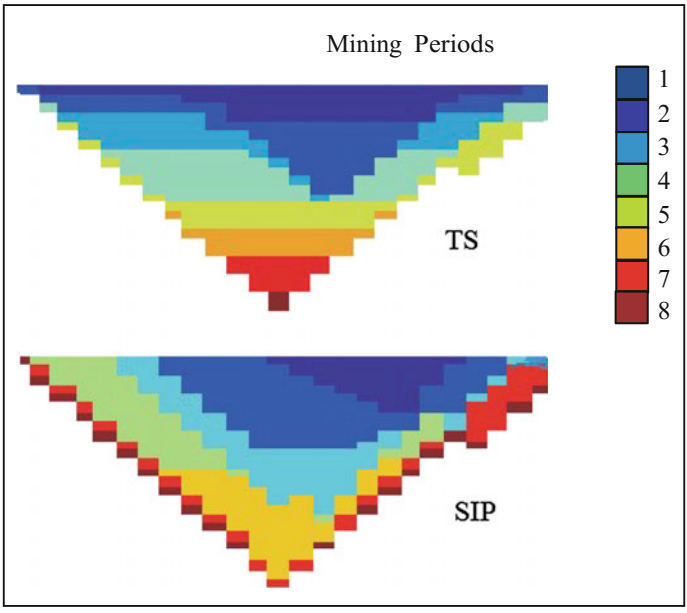

Fig. 11 Cross-sectional views of the SIP (bottom) and traditional schedule (TS—top) for a copper deposit

shown are the raw outputs and need to be smoothed to become practical. It is important to note that:

- the results in the second case study are similar in a percentage improvement when compared to other stochastic approaches such as simulated annealing; and
- although the schedules compared in the studies herein are not smoothed out, other existing SIP applications show that the effect of generating smooth and practical schedules has marginal impact on the forecasted performance of the related schedules, thus the order of improvements in SIP schedules reported here remains.

Stochastically Optimal Pit Limits

The previous comparisons were based on the same pit limits deemed optimal using best industry practice (Whittle 1999). This section focuses on the value of the proposed approaches with respect to stochastically optimal pit limits. Both methods described above consider larger pit limits and stop when discounted cash flows are no longer positive. Figures 12 and 13 show some of the results. The stochastically generated optimal pit limits contain an additional 15% of tonnage when compared to the traditional (deterministic) 'optimal' pit limits, add about 10% in NPV to the NPV reported above from stochastic production scheduling within the conventionally optimal pit limits, and extend the life-of-mine. These are substantial differences for a mine of a relatively small size and short life-of-mine. Further work

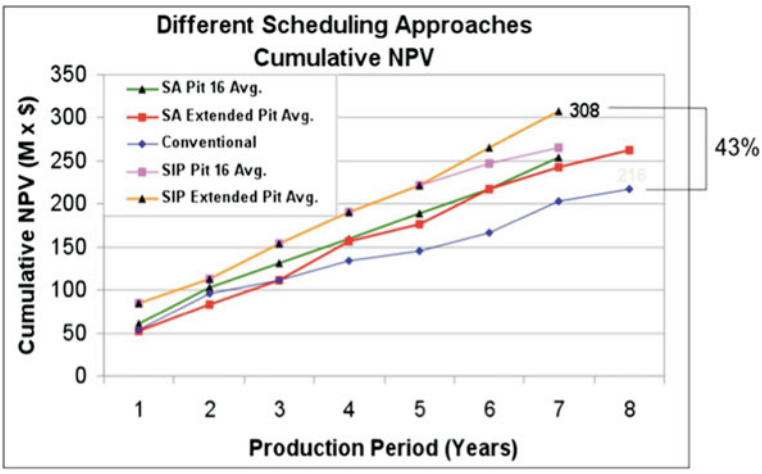

Fig. 12 LOM cumulative cash flows for the conventional approach, simulated annealing and SIP, and is compared to results from conventionally derived optimal pit limits

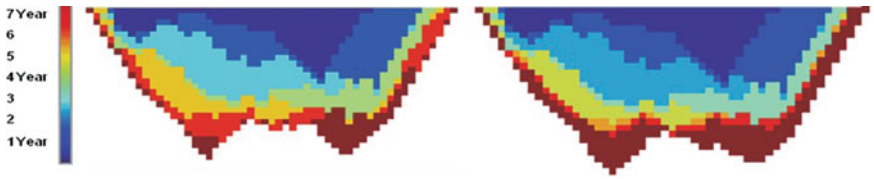

Fig. 13 Stochastic pit limits are larger than the conventional ones; physical scheduling differences are expected when bigger pits are generated

shows that there are additional improvements on all aspects when a stochastic framework is used for mine design and production scheduling.

The new approach yielded an increment of ~30% in the NPV when compared to the conventional approach. The differences reported are due to the different scheduling patterns, the waste mining rate, and an extension of the pit limits which yielded an additional ~5.5 thousand tonnes of metal.

Conclusions

Starting from the limits of the current orebody modelling and life-of-mine planning optimisation paradigm, an integrated risk-based framework has been presented. This framework extends the common approaches in order to integrate both stochastic modelling of orebodies and stochastic optimisation in a complementary manner. The main drawback of estimation techniques and traditional approaches to planning is that they are unable to account for the in situ spatial variability of the deposit grades; in fact, conventional optimisers assume perfect knowledge of the orebody being considered. Ignoring this key source of risk and uncertainty can lead to unrealistic production expectations as well as suboptimal mine designs.

The work presented herein shows that the stochastic framework adds higher value in production schedules in the order of 25%, and will be achieved regardless of which method from the two presented is used. Furthermore, stochastic optimal pit limits are shown to be about 15% larger in terms of total tonnage, compared to the traditional (deterministic) optimal pit limits. This difference extends the life-of-mine and adds approximately 10% of net present value (NPV) to the NPV reported above from stochastic production scheduling within the conventionally optimal pit limits.

Acknowledgements Thanks are in order to the International Association of Mathematical Geosciences for the opportunity to present this work as their distinguished lecturer. The support of the COSMO Laboratory and its industry members AngloGold Ashanti, Barrick, BHP Billiton, De Beers, Newmont, Vale and Vale Inco, as well as NSERC, the Canada Research Chairs Program and CFI is gratefully acknowledged. Thanks to R Goodfellow for editorial assistance.

References

Abdel Sabour SA, Dimitrakopoulos R (2011) Accounting for joint ore supply, metal price and exchange rate uncertainties in mine design. J Mining Science 86(2):191–201 (The Australasian Institute of Mining and Metallurgy: Melbourne)

Albor Consquega F, Dimitrakopoulos R (2009) Stochastic mine design optimization based on simulated annealing: pit limits, production schedules, multiple orebody scenarios and sensitivity analysis. Trans Inst Min Metall Min Technol 118(2):A80–A91

David M (1988) Handbook of applied advanced geostatistical ore reserve estimation. Amsterdam, Elsevier Science, p 216

Dimitrakopoulos R, Ramazan S (2004) Uncertainty based production scheduling in open pit mining. SME Trans 316:106–112

Dimitrakopoulos R, Ramazan S (2008) Stochastic integer programming for optimizing long term production schedules of open pit mines: methods, application and value of stochastic solutions. Trans Inst Min Metall Min Technol 117(4):A155–A167

Dimitrakopoulos R, Farrelly CT, Godoy M (2002) Moving forward from traditional optimization: grade uncertainty and risk effects in open-pit design. Trans Inst Min Metall Min Technol 111: A82–A88

Geman S, Geman D (1984) Stochastic relaxation, Gibbs distribution, and the Bayesian restoration of images. IEEE Trans Pattern Anal Mach Intell PAMI 6(6):721–741

Godoy M (2017) A risk analysis based framework for strategic mine planning and design—Method and application. (in this volume)

Godoy MC, Dimitrakopoulos R (2004) Managing risk and waste mining in long-term production scheduling. SME Trans 316:43–50

Goodfellow R, Dimitrakopoulos R (2017a) Simultaneous stochastic optimization of mining complexes and mineral value chains. Math Geosci. doi:10.1007/s11004-017-9680-3

Goodfellow R, Dimitrakopoulos R (2017b) Simultaneous stochastic optimization of mining complexes and mineral value chains. Math Geosci. doi:10.1007/s11004-017-9680-3

Journel AG (1994) Modelling uncertainty: some conceptual thoughts. In: Dimitrakopoulos R (ed) Geostatistics for the next century. Kluwer Academic, Dordrecht

Kent M, Peattie R Chamberlain V (2007) Incorporating grade uncertainty in the decision to expand the main pit at the Navachab gold mine, Namibia, through the use of stochastic simulation. In: Dimitrakopoulos R (ed) Orebody modelling and strategic mine planning, 2nd edn. The Australasian Institute of Mining and Metallurgy, Melbourne, pp 207–216

Leite A, Dimitrakopoulos R (2007) A stochastic optimization model for open pit mine planning: Application and risk analysis at a copper deposit. Trans Inst Min Metall Min Technol 116(3): A109–A118

Leite A, Dimitrakopoulos R (2014) Mine scheduling with stochastic programming in a copper deposit: Application and value of the stochastic solution. Min Sci Technol 24(6):55–72

Lerchs H, Grossmann IF (1965) Optimum design of open-pit mines. Trans Canadian Inst Min Metall LXVII:47–54

Meagher C, Abdel Sabour SA, Dimitrakopoulos R (2010) Pushback design of open pit mines under geological and market uncertainties. In Dimitrakopoulos R (ed) Advances in orebody modelling and strategic mine planning I. The Australasian Institute of Mining and Metallurgy, Melbourne, pp 291–298

Menabde M, Froyland G, Stone P, Yeates G (2017) Mining schedule optimisation for conditionally simulated orebodies. (in this volume)

Montiel L, Dimitrakopoulos R, Kawahata K (2016) Globally optimising open-pit and underground mining operations under geological uncertainty. Min Technol 125(1):2–14

Mustapha H, Dimitrakopoulos R (2010) High-order stochastic simulations for complex non-Gaussian and non-linear geological patterns. Math Geosci 42(5):455–473

Ramazan S, Dimitrakopoulos R (2013) Production scheduling with uncertain supply: a new solution to the open pit mining problem. Optimi Eng 14:361–380

Ramazan S, Dimitrakopoulos R (2018) Stochastic optimisation of long-term production scheduling for open pit mines with a new integer programming formulation. (in this volume)
Whittle J (1999) A decade of open pit mine planning and optimisation—The craft of turning algorithms into packages, in Proceedings APCOM'99, Computer Applications in the Minerals Industries: 28 International Symposium. Golden, Colorado School of Mines, pp 15–24

Part II
Increasing Value and Technical Risk Management

The Value of Additional Drilling to Open Pit Mining Projects

G. Froyland, M. Menabde, P. Stone and D. Hodson

Abstract The value of a mining project is based upon a quantitative model of material of value in the ground, a block model of the deposit, and a schedule for extracting this material including relevant revenues and costs. The schedule usually attempts to maximise the net present value (NPV) of the project over the life of the mine. Frequently, a block model is the result of a smooth interpolation, such as kriging, of data collected from holes drilled throughout the orebody. More drill holes will lead to greater certainty in the contents of block models and from these 'more accurate' block models, schedules of greater ultimate value may be realised. We discuss how conditional simulations can assist with rigorously valuing the trade-off between the cost of extra drilling and the schedules of greater value that may be constructed from the resultant block models of greater accuracy.

Introduction

In today's competitive world the push to extract ever more value from mining projects continues to increase. Initiatives to decrease costs and increase revenue are being pursued. One of the most attractive options is the application of optimisation tools to schedule the mining operation with the explicit objective of maximising the

G. Froyland (✉)
School of Mathematics, The University of New South Wales,
Sydney, NSW 2052, Australia
e-mail: froyland@maths.unsw.edu.au

M. Menabde · P. Stone
BHP Billiton Technology, 86A, Melbourne, Vic 3001, Australia
e-mail: merab.menabde@bhpbilliton.com

P. Stone
e-mail: peter.m.stone@bhpbilliton.com

D. Hodson
BHP Billiton Project Development Services, 86A, Melbourne, Vic 3001, Australia
e-mail: dave.hodson@bhpbilliton.com

R. Dimitrakopoulos (ed.), *Advances in Applied Strategic Mine Planning*,
https://doi.org/10.1007/978-3-319-69320-0_10

net present value (NPV) over the life of the operation. At present such tools are applied on a short-term basis to cut costs of daily operations through efficiencies, and on a long-term or life of mine basis to maximise NPV. In the latter case, NPV is increased through:

1. Delaying or eliminating waste stripping.
2. More efficient routing of ore through the network of trucks, crushers, conveyors and beneficiation plants.
3. More efficient resource use through better blending and cut-off grade decisions. The promise is that the resulting plan will deliver pure value increases for little or no cost.

The value of all of this number crunching depends upon the reliability of the input data. The valuation of a mine project depends critically upon the accuracy of the geological block model. On the one hand, we will never know precisely what material is deep in the ground until we have excavated that material. On the other hand, we must make plans for the future with the best information available to us at the present time. While realising that information is not perfect, having a plan is better than having no plan; this much is generally accepted as reasonable.

However, what if a planner were given the option of obtaining more information with which to construct his or her plan? In this paper, additional information will take the form of block models with increased accuracy, but the same principles may be applied to other forms of information. Intuition suggests that if one's block model were more accurate, then one could construct a mine plan of greater value by exploiting this additional knowledge (via a different mining sequence or cut-off grade policy, for example). But how much would one be prepared to pay for this additional knowledge? Clearly, the cost of the additional data should be less than the expected increment in value that can be obtained with this new data, otherwise the planner would construct a mine plan with the data already available. This is common sense—the real problem is how to quantify, and value in a rigorous way, the increment in project value that a mine planner can expect from this additional information. If we can do this, then we will have valued the option of obtaining additional information and have put ourselves in a position of making a decision on quantifiable grounds.

We begin with some background on the numerical construction of block models from drill hole data and the process of kriging. We then formalise what is meant by optimising NPV using a kriged block model as the geological input. For optimisation and valuation purposes the mining schedule is modelled as a mixed integer linear program (MILP); see Johnson (1968), Caccetta and Hill (2003) and Ramazan and Dimitrakopoulos (2004) for prior related work and surveys. We introduce the option of undertaking an additional drilling program and briefly explain why this may or may not increase NPV. Conditional simulations are introduced as a way of quantifying uncertainty and we discuss how to optimise with multiple conditional simulations. We detail a formalism that clarifies the notion of additional knowledge and describe a method of determining the maximum value that one should pay for

any additional drilling program. All of the introduced concepts and numerical calculations are illustrated throughout via an example of a simple open pit mine.

Estimated Geological Block Models and Kriging

The information in a block model is gathered from a series of drill holes. Typically, many long, narrow holes are drilled into the ground in the vicinity of the orebody, and their cores are extracted and analysed for mineral concentrations. For simplicity, in the sequel we will assume that the only relevant information contained in the block model is the total tonnage of each block, and the concentration in per cent of mass of a single metal element. Thus, one knows precisely[1] the density of the rock in the drill hole core and the concentration of the element (the grade) along the core. The drill hole cores provide a sparse set of data from which we must construct a full three-dimensional model of rock tonnage and percentage by mass of the metal element in each block. This construction is commonly performed using a process known as kriging. The kriged estimate of the block model is derived as a local linear interpolation of the measured drill hole grades. If one assumes that the linear correlation of the grades of pairs of blocks depends only on the distance between the blocks and the direction in 3D from one block to the other, then the kriged estimate of blocks grades is the best linear estimator of the block grades ('best' in the sense of minimum variance); see Cressie (1991) for further details.

Long-Term Production Scheduling with Estimated (Kriged) Block Models

We now describe how one creates an NPV optimal life-of-mine schedule using a single estimated block model as input data. To simplify the notion of the value of an open pit mine, we shall make several assumptions.

Assumptions for Scheduling Process

1. The infrastructure is fixed throughout the life of the mine. For example, process plant capacities and mining capacities are fixed.[2] By using additional binary variables to encode a small finite number of possibilities, it is relatively

[1]To within error bounds typical of lab analyses.

[2]Truck fleet sizes are varied to maintain a constant mining capacity allowing for changes in haul distance with depth. The cost of these truck fleet size variations are not considered.

straightforward to include the variation of infrastructure in an optimisation. For example, what size process plant is optimal; when should the plant be expanded or shut down; when should truck fleet sizes be altered to change mining capacity? For clarity we do not include these additional variables in the problem formulation.

2. The selling price of the product is known perfectly into the future. The price and market volume limits (if relevant) may fluctuate over time, but in a completely predictable manner. This is of course not reality; more realistic considerations of price and volume are additional complications that should be modelled properly and subjected to a rigorous analysis that is beyond the scope of this paper.
3. Grade control is assumed to be perfect. That is, once a block has been blasted, its contents are precisely known. This means that a block with concentration below a cut-off grade will never be sent to product and a block with concentration above a cut-off grade will never be sent to the waste dump. This is not realistic; errors in grade control do occur and may be significant. These errors should be modelled as best they can with the available data and incorporated into the valuation model. For simplicity, we do not consider this issue here.

The Objective

Our objective is to maximise the net present value (NPV) of the project. Suppose that a project has annual cash flows c1, c2, …, cT. The NPV of the project is:

$$NPV = \sum_{t=1}^{T} \frac{C_t}{(1 + r/100)^t},$$

where:

r is the discount rate

Our mining project will receive a cash flow from every block that is excavated. We assume that at any given time each block can take on one of two values:

$$Value = \begin{cases} -Mining\ Cost, & if\ the\ blocks\ is\ waste, \\ -Mining\ Cost - Processing\ Cost & if\ the\ blocks\ is\ Processed. \\ +Sales\ Price\ X\ Metal\ Tonnes, & \end{cases}$$

We assume that there are N blocks under consideration in our block model. Thus there are N possible cash flows denoted *vi* for $i = 1, \ldots, N$. We will apply our discount rate on an annual basis, so all blocks taken in the same year receive the same discount rate. Using the formula above, we arrive at:

$$NPV = \sum_{t=1}^{T} \frac{\sum_{i=1}^{N} \chi_{i,t} v_i}{(1 + r/100)^t}, \tag{1}$$

where:

$\chi_{i,t}$ is a 0,1 variable which takes the value 1 if block i is excavated in period t and 0 otherwise

The binary numbers $\chi_{i,t}$ encode the order in which blocks are taken over the life of the mine. We call this collection of binary variables a mining schedule.

Mining and Processing Limits

An operation can generally only mine and process certain tonnages each year, depending on the capital invested in the mining and processing capacities. Let M denote the maximum amount that can be mined in one year in tonnes and let P denote the maximum amount that can be processed in one year in tonnes. If r_i and o_i denote the amount of rock (ore and waste) and ore (feed tonnes to a process plant) contained in block *i*, then we can set upper limits on mining and processing rates as follows:

$$\sum_{i=1}^{N} \chi_{i,t} r_i \leq M, \quad \textit{for all } t = 1, \ldots, T \tag{2}$$

$$\sum_{i=1}^{N} \chi_{i,t} o_i \leq P, \quad \textit{for all } t = 1, \ldots, T \tag{3}$$

Wall Slope Considerations

The blocks should be removed in such a way that at the end of each year, the slopes formed by the blocks remaining in the pit are lower than safe upper limits prescribed by geotechnical studies. In reality, these pit slope limits are observed every day; however, as we only track which blocks are taken in which year, and not when a block is taken within a particular year, we only consider slopes at the end of each year. This tracking is accomplished by:

$$\chi_{i,t} \leq \sum_{s=1}^{t} \chi_{j,s}, \quad t = 1, \ldots, T. \tag{4}$$

whenever slope conditions insist that block j must be removed prior to the removal of block i.

Optimising NPV

Our formulation of this deterministic optimisation problem is not new; see, for example, Caccetta and Hill (2003). The objective and constraints on mining and processing limits are all linear, so that in principle we may employ a mixed integer linear program engine to solve our problem. In practice, there are usually too many blocks and periods for such a formulation to be solved in a reasonable amount of time. The results that we will describe in this paper have been constructed using aggregations of blocks as units to be scheduled. It is standard practice in these sorts of problems that blocks be aggregated into larger units; see Ramazan (2007) for example. These aggregations are built in such a way as to attempt to minimise the effect of the loss of resolution. The algorithm used is proprietary information and cannot be elaborated upon in this forum. Certainly, there is no loss in accuracy of slopes with the aggregations that we use. We have used the optimiser CPLEX9.0 to perform the optimisations.

An Example Pit

We will illustrate the concepts in this paper with a single product base metal mine. Our input data is in the form of a kriged block model and 25 conditionally simulated block models. The realdiscount rate used is r = 10%. A metal price is given (assumed known and fixed), and fixed mining and processing rates are given (30 million tonnes/annum and 5 million tonnes/annum respectively). A cut-off grade has been preselected and applied to the block models to generate a value for each block. It is possible, and desirable, to perform the current analysis with variable optimised cut-off grades and variable optimised mining and processing rates, incorporating capital costs, but for simplicity we have not included such considerations. The block models have around 30,000 blocks; for the optimisation process, the blocks were aggregated into larger units in a way that preserves slopes and minimises errors in accuracy. Figure 1 displays a representation of block value for a vertical slice through our example pit. The blocks are grey shaded so that light grey represents the lowest value and dark grey represents the highest value. Figure 1 shows block values for the kriged block model.

Fig. 1 Kriged block values for a vertical slice through our example pit

Realising Optimised NPV and Perfect Block Models

The previous section makes things sound as though the problem of producing a long-term schedule to maximise project NPV is all sewn up, apart from a few approximations with aggregating blocks. In fact, a major assumption is that the block model actually reflects reality in the ground. If the block model contains errors (and it most certainly will) then what have we optimised? We've produced a schedule that maximises project NPV for an incorrect block model. Wherever reality deviates from our block model, our computed NPV will differ from the NPV that will ultimately be realised from the project. It is clear that the closer the block model is to reality, the closer the optimised NPV will be to a value that can be realised. It also seems intuitive that the realised NPV will be greater if one has a more accurate block model to base one's optimisations on. Obtaining a more accurate block model usually involves further drilling to create drill hole data with a finer resolution. Extra drilling costs money, and how can one balance this additional cost against this vague idea that realised NPV increases with more accurate block models? We now embark upon proving and quantifying this intuition that extra knowledge has a real value.

Conditional Simulations and Block Model Uncertainty

We will use the notion of conditional simulations to model the uncertainty in our block model. A conditional simulation (e.g. Goovaerts 1997; Dimitrakopoulos in press) is a stochastically generated block model that is consistent with the drill hole data and their spatial continuity. Consistency with the drill hole data primarily means two things:

1. Each conditional simulation's block attributes (mass, grade, etc.) for blocks wholly contained in the drill hole cores are identical to those block attributes measured in the drill hole cores.
2. Each conditional simulation is generated so that its block model would generate a variogram identical to one constructed from the drill hole data. The construction process guarantees that the first order and second order statistics of each conditional simulation agrees with the first and second order statistics of the drill hole data (e.g. The grade-tonnage curves of each conditional simulation are identical to the grade-tonnage curves of the drill hole data).

Existing computer software (Deutsch and Journel 1997; Remy 2004) and newer specialised algorithms (Godoy 2002; Boucher and Dimitrakopoulos 2012) can produce as many conditional simulations possible; that is, different equally probable block models of a deposit, all consistent with the drill hole data. Why should this be done? Our intention is to think of each of these conditional simulations as an 'alternate reality'. We recognise that our drill hole data will always be incomplete and there will always be uncertainty about the contents of blocks that have not been drilled. By creating multiple random block models we build up a probability distribution on the space of block models. For example, if we generated 25 conditional simulations then block i would have 25 different grades assigned to it (one for each simulation), and 25 different net values $v_{i,k}$, $k = 1, \ldots, 25$. If block i lay along a drill hole core, then the $v_{i,k}$, $k = 1, \ldots, 25$ would all equal the net value computed from the measured grade in the core sample. However, if block i lay away from a drill hole, then the $v_{i,k}$, $k = 1, \ldots, 25$ could all take on different values.

Figure 2 displays a representation of block values for a vertical slice through our example pit. As in Fig. 1 the blocks are grey shaded so that light grey represents the lowest value and dark grey represents the highest value. Figure 2 shows the values constructed from one of the 25 conditional simulations that we produced. Notice

Fig. 2 Conditional simulation block values for a vertical slice through our example pit

that the kriged block model in Fig. 1 has a very smooth value or grade distribution, while the conditionally simulated block model in Fig. 2 has a much more heterogeneous distribution of value (and therefore grade).

Project Valuation with Conditional Simulations

The underlying idea that each conditional simulation represents an alternate equally likely reality of what is actually in the ground rests upon two assumptions. These are that the drill hole data and the derived variogram are:

1. completely true (reality will always agree with the drill hole data and obey the derived variogram), and
2. represent complete information (there is no further information available right now beyond the derived variogram that may help to focus our random sampling further).

If one accepts this idea of alternate realities, which reality should one optimise, if any? Our goal is to determine a schedule

$$S = \{x_{i,t}\} \begin{matrix} t = 1, \ldots, T \\ i = 1, \ldots, N \end{matrix}$$

that performs will on all onnr most possible realities. We argue that if one is interested only in maximizing NPV (without trying to control risk or uncertainty) then the appropriate thing to do is to find a schedule that achieves the greatest expected NPV. To be precise, let NPV(k, s) denote the NPV obtained when the block values in the kth conditional simulation is used to evaluate using the schedule s. Formally

$$NPV(k,s) = \sum_{t=1}^{T} \frac{\sum_{i=1}^{N} x_{i,t} v_{i,k}}{(1 + r/100)^t} \tag{5}$$

Define the expected NPV for a schedule s as:

$$E(NPV(s)) := \frac{1}{k} \sum_{k=1}^{k} NPV(k,s). \tag{6}$$

We propose that one should aim to find the schedule s* such that:

$$\mathrm{E(NPV(s^*))} \ > \mathrm{E(NPV(s)\ for\ all\ feasible\ schedules}\ s \tag{7}$$

The schedule s^* will be known as the schedule that maximizes expected NPV. IF one had the opportunity to run the mining project K times, each time using the same schedule but calculating the NPVs on the K different realities (different conditional simulations), then the expected NPV is the natural quantity to maximize. In real life, one only gets tone chance to dig up the mine, and the expected NPV will never be realized. What will be realized in NPV (k^*, s^*) where k^* represents the real block model, which is probably different to any of the conditional simulations computed. Nevertheless, we maintain that expected NPV is the best quantity to maximise. To emphasise the fact that this expected NPV is computed using only information available at the present time, we denote E(NPV(s^*)) by $\mathrm{NPV}_{present\ knowledge}$.

Optimising Expected NPV

Since E(NPV(s)) is a linear combination of the linear functions NPV(k,s), E(NPV(s)) is also a linear function of

$$S = \{x_{i,t}\} \begin{matrix} t = 1, \ldots, T \\ i = 1, \ldots, N \end{matrix}$$

and so we might try to use a mixed integer linear programming engine to maximize expected NPV. Our objective is:

$$\begin{aligned} E(NPV(s)) &= \frac{1}{k}\sum_{k=1}^{k}\sum_{t=1}^{T}\frac{\sum_{i=1}^{N} x_{i,t}v_{i,k}}{(1+r/100)^t} \\ &= \sum_{t=1}^{T}\frac{\sum_{i=1}^{N} x_{i,t}\left(\frac{1}{k}\sum_{k=1}^{k} v_{i,k}\right)}{(1+r/100)^t} = \sum_{t=1}^{T}\frac{\sum_{i=1}^{N} x_{i,t}v_i}{(1+r/100)^t} \end{aligned} \tag{8}$$

The term on the far right-hand side indicates that the expected NPV may be calculated using the mean values of each black V_i computed as

$$v_i = (1/k)\sum v_{i,k}$$

This seems natural as we are taking an average. Note that we are averaging the dollar value of blocks, and not the grade of blocks. It is important that one uses the individual block grades $g_{i,\,k}$ (for block i in conditional simulation k) to compute the block values $v_{i,k}$ and then averages the $v_{i,k}$ (do not average the $v_{i,k}$ and then copute and 'average' value).

Equation 8 takes the place of Eq. 1 when maximizing expected NPV. We now need to find constraints to replace Eqs. 2–4. Equation 4 may remain the same as all conditional simulations have the same slope conditions. Equations 2 and 3 are problematic as the rock ri and ore oi will vary from simulation to simulation. In the

optimisation results reported in this paper, we replace the rock and ore tonnages ri and oi in Eqs. 2 and 3 with their mean values calculated as

$$r_i = (1/K) \sum r_{i,k}$$

and

$$o_i = (1/K) \sum o_{i,k}$$

This is an approximation that may result in some schedules being infeasible in terms of mining or processing rate for some individual conditional simulations. We believe that the numerical results reported in this paper are relatively insensitive to this approximation.

The schedule obtained by optimising expected NPV is shown in Fig. 3. The expected NPV obtained was \$761.8 M; a value that is guaranteed to be within 0.2% of the true optimum by our mixed integer linear programming engine CPLEX. Figure 3 is a plan view of our example pit with blocks grey shaded according to their year of excavation; those blocks coloured light grey are

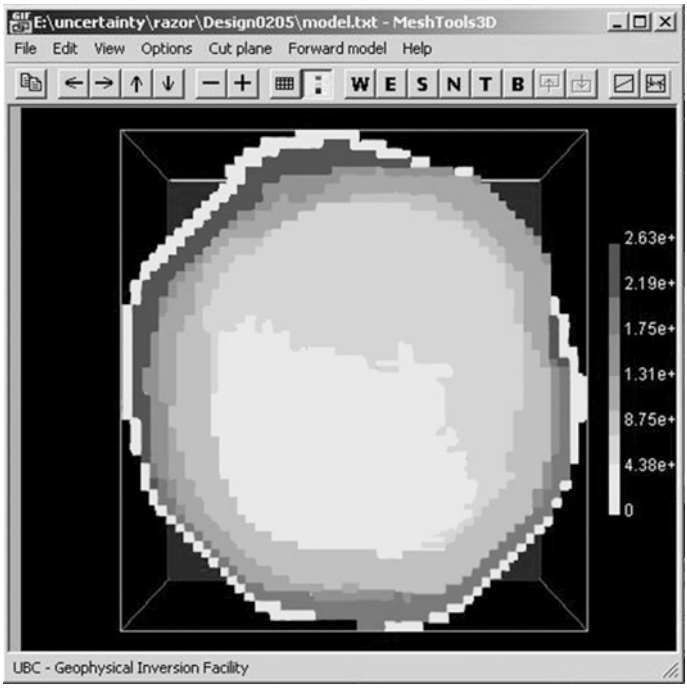

Fig. 3 Plan view of our example pit with blocks coloured according to the schedule obtained by optimising expected NPV

excavated first, while those coloured dark grey are excavated last. The white blocks around the edge of the pit are never excavated.

Project Valuation with Perfect Geological Knowledge

So far we have been able to compute a schedule s* that maximises the expected NPV of our mining project based on our current knowledge of the orebody. We will now compute the best expected NPV we could achieve if we had complete knowledge of the orebody. Complete knowledge of the orebody is the extreme situation where we drill so much that we know exactly what is in the ground in every block.

Because we know the block model exactly before excavation begins, we can tailor our schedule to that block model. At this stage, we only have the K conditional simulations as possible realities. Complete drilling to resolve exactly what is in the ground is equivalent to knowing exactly which conditional simulation is reality (drawing from our limited selection of K alternate realities). If it turns out that simulation k is reality, we can produce schedule s(k) with the property that:

$$NPV(k, s(k)) \geq NPV(k, s) \text{ for all schedules s} \tag{9}$$

Let's look at these schedules *s(k)* for our example pit. Figures 4 and 5 show vertical slices through 2 of the 25 conditional simulations; their simulation numbers are 20 and 8, respectively. The two chosen are the simulations with the highest total block value (#20, Fig. 4) and lowest total block value (#8, Fig. 5). As before, light grey represents low-value blocks and dark grey represents high-value blocks. Each

Fig. 4 Conditional simulation block values for a vertical slice through our example pit. This simulation has the highest total block value

Fig. 5 Conditional simulation block values for a vertical slice through our example pit. This simulation has the lowest total block value

of these two block models was individually optimised to produce schedules $s(20)$ and $s(8)$ each satisfying property (9). These schedules are displayed in Figs. 6 and 7, whereas before, light grey represents those blocks taken early in the mine life and dark grey represents those blocks taken latest in the mine life. In this example, there are subtle differences between the schedules, but no dramatic difference in how one should excavate the two orebodies.

Returning to our discussion, one must bear in mind that we cannot control which simulation is reality, we only know which one it is. We therefore still need to perform an average. If we know before excavation begins which simulation is reality, then on average we can achieve an NPV of:

$$NPV_{Perfect\ Knowledge} = (1/K)\sum_{k=1}^{K} NPV(k, s(K)) \tag{10}$$

where each *s(k)* has the property (9) for k = 1, …, K.

$NPV_{perfect\ knowledge}$ denotes the expected value of the project if we are able to 'wait-and-see' which conditional simulation is reality before making our schedule (our schedule is based on 'perfect' geological information). For each simulation, we tailor our schedule to that block model, and can have different schedules for different simulations, because we know beforehand which block model is reality. Contrast this to Eq. 7 where we had to choose a single schedule upfront. For our example pit, we performed 25 separate optimisations to find the 25 individually optimal schedules $s(k)$. Using Eq. 10, we computed that $NPV_{perfect\ knowledge}$ = \$769.36 M.

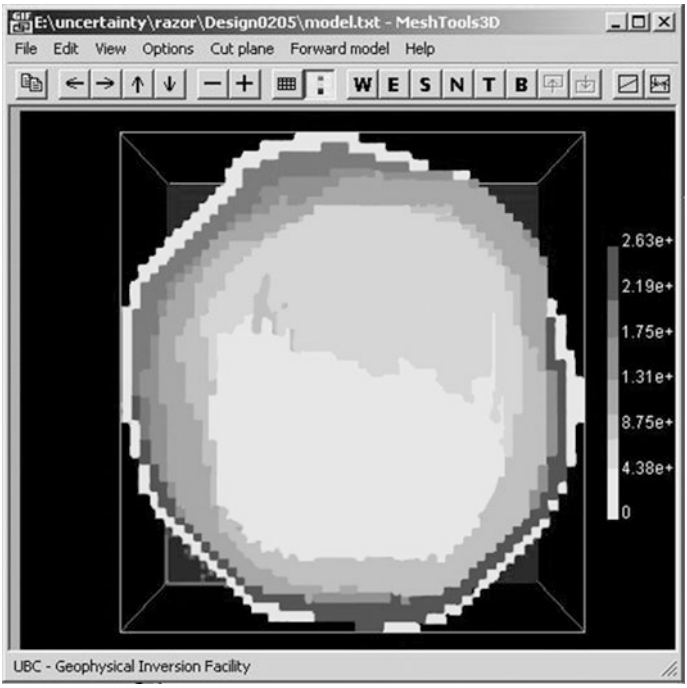

Fig. 6 Plan view of our example pit with blocks coloured according to the schedule obtained by individually optimising the conditional simulation shown in Fig. 4

The Value of Infill Drilling Information

We now have two NPVs; one representing the best expected NPV achievable with no extra drilling and our present state of knowledge, and the other representing the best expected NPV achievable assuming perfect knowledge of the orebody prior to producing a schedule. These values are $\text{NPV}_{\text{present knowledge}} = \$761.8$ M and $\text{NPV}_{\text{perfect knowledge}} = \$769.36$ M respectively. Thus the value of having perfect orebody knowledge prior to scheduling is:

$$\text{VOIDI: } = \text{NPV}_{\text{perfect knowledge}} - \text{NPV}_{\text{perfect knowledge}} \tag{11}$$

where VOIDI stands for 'Value of Infill Drilling Information'. We will show that VOIDI represents an upper bound for the NPV increment (not including drilling costs) achievable through additional drilling.

It is relatively straightforward to see that VOIDI is always non-negative:

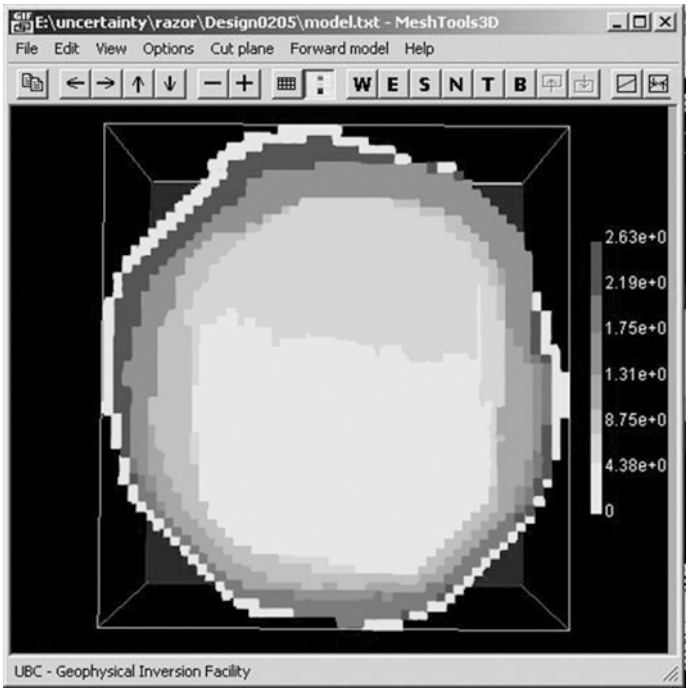

Fig. 7 Plan view of our example pit with blocks coloured according to the schedule obtained by individually optimising the conditional simulation shown in Fig. 5

$$
\begin{aligned}
NPV_{perfect\ knowledge} &= (1/K)\sum_{k=1}^{K} NPV(k, s(k)) \\
&\geq (1/K)\sum_{k=1}^{K} NPV(k, s^{*}) \; by\, property \quad (9) \\
&= NPV_{perfect\ knowledge}
\end{aligned}
$$

How is VOIDI related to the cost of future drilling programs? Any additional drilling will result in the conditional simulations being updated. The spread of block values will generally lessen between simulations because we have more drill holes and we are more certain about the block values. Every extra hole drilled has the potential to add value to the project because we might be able to use that extra information to change our schedule and create greater project NPV. The option to embark on additional drilling can be valued as:

$$\text{Value of Additional Drilling} = (\text{NPV}_{\text{additional drilling}} - \text{NPV}_{\text{present knowledge}}) - \text{Drilling Cost}$$

At present we can value $\text{NPV}_{\text{present knowledge}}$ and Drilling Cost, but we cannot value $\text{NPV}_{\text{additional drilling}}$. What we do know is that

$\text{NPV}_{\text{additional drilling}} \leq \text{NPV}_{\text{perfect knowledge}}$. This is because we can never achieve perfect knowledge through additional drilling, and we will never actually realise $\text{NPV}_{\text{perfect knowledge}}$. Thus:

$$\text{Value of Additional Drilling} \leq (\text{NPV}_{\text{additional drilling}} - \text{NPV}_{\text{present knowledge}}) - \text{Drilling Cost} = \text{VOIDI} - \text{Drilling Cost}.$$

The conclusion that one can draw from this is that one would never embark on an additional drilling program if the drilling costs exceed VOIDI.

Voidi for Our Example Pit

In the case of our example pit, VOIDI = 769.36-761.8 = $7.56 M. As a fraction of total project value, VOIDI is around one per cent; a very low figure. This indicates that it is probably not worthwhile performing any further drilling on our example resource.[3] While we will show in Fig. 8 that there is a significant variation in block values between different conditional simulations, and therefore, significant uncertainty in our block model, the NPV-optimal schedules that are tailored to each conditional simulation are not very different. Thus, knowing which block model is reality does not change your decision about how to excavate the pit, and therefore does not generate any additional value for the project. *Additional information only creates value if value-creating decisions are changed in light of the new information.*

Let us review the results of our optimisations in greater detail. Let NPV(k, $s(m)$) denote the optimal schedule for simulation m evaluated using simulation k, where m = 1, …, 25, and k = 1, …, 25. The grey shaded lines in Fig. 8 plot the 25 × 25 = 625 NPVs corresponding to NPV(k, $s(m)$), where the y-axis is NPV(k, $s(m)$), and the x-axis is k. Thus each vertical column corresponds to a single simulation k. It is clear from Fig. 8 that *the dominant value differences arise from different simulations, not different schedules*. In fact, relative to variations between simulations, the values are insensitive to schedule differences.

The highlighted red (dark grey) dots are the 25 values of NPV(k,$s(k)$), namely, an optimal schedule for simulation k evaluated with its corresponding simulation. Thus the dark grey dots should appear at the top of the vertical spread of points. The value of NPVperfect knowledge is the mean value of the dark grey dots.

The highlighted light grey dots are the 25 values of NPV(k,s*), k = 1, …, 25. The value NPVpresent knowledge is the mean value of the light grey dots. The value of VOIDI is therefore the average difference in value between corresponding light grey and dark grey dots. As the spread for each simulation is relatively small,

[3]Bear in mind that VOIDI has been calculated under specified conditions of mining rate, processing rate and cut-off grade and is dependent on these parameters.

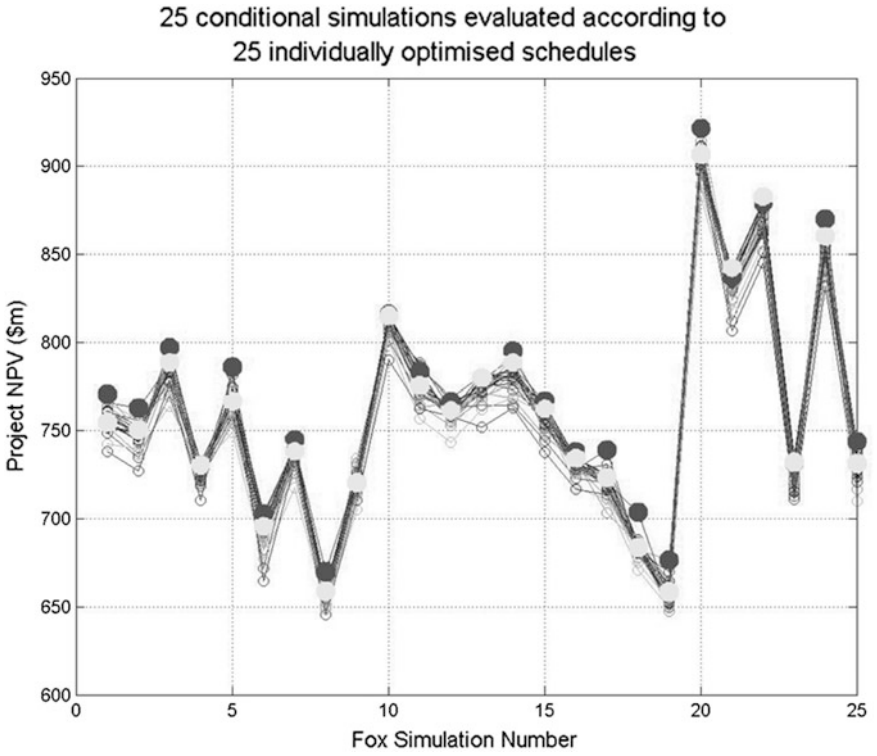

Fig. 8 Valuations of schedules: (i) individually optimised, (ii) optimising expected NPV

and the light grey dots are mostly at the upper side of this small spread, the difference between dark grey and light grey is small (the average difference is $7.56 M).

Conclusions

We have described a rigorous computational method of determining the largest amount that should be paid for a program of additional infill drilling on an existing resource. This method required the construction of K conditional simulations, each of which was consistent with the existing drill hole data. These K conditional simulations were used to produce K individually optimised schedules $s(k)$. A single maximum expected NPV schedule s^* was also generated via a single optimisation. These K + 1 NPVs were then combined to produce VOIDI: = NPVperfect knowledge –NPVpresent knowledge. In the case of our example pit, VOIDI clearly demonstrated that it was highly unlikely that any additional drilling would create further project value, saving the company money on extra drilling. The lesson to be

learnt here is that high block variability in conditional simulations does not always imply that there is value in further drilling to decrease this variability.

The notion of VOIDI is an extremely useful quantification tool that formalises thinking on the matters of risk and uncertainty, and knowledge and information. Without such formal quantities, one's thinking can become very fuzzy. Of course, this analysis is only as good as the conditional simulations are at representing the true uncertainty in our current state of knowledge. If the conditional simulations do not capture the full uncertainty and provide an accurate sample of the full allowable variation of block values, then VOIDI will appear smaller than it really is.

Some Final Observations

1. An infill drilling program may delay the starting of mining.This will mean that NPV perfect knowledge may be lowered due to this delay. We have not taken this delay into account in our analysis, although any effect will be to reduce the value of NPVperfect knowledge, and therefore lower the value of VOIDI.
2. One should bear in mind that VOIDI is a function of parameters such as:
    i. mining rate;
    ii. processing rate; and
    iii. cut-off grade, and that under different conditions, the potential value of a drilling program may be more or less valuable.
        a. For example, a doubling of mining and/or processing rates will increase NPV through a more rapid mine exploitation. VOIDI will increase in proportion to the NPV increase; that is, both expected NPV and VOIDI will increase by a roughly equal percentage.
        b. The effect of changing cut-off grade may have a non-trivial impact on VOIDI.
3. We have assumed that the resource is contained within the boundary of outer drill holes. Clearly we cannot say anything about further value to be gained on extra drilling of resources which are not well contained within the existing drill hole boundary.
4. The conditional simulations we used were based on prescribed geological regions in the block model. Within each of these distinct geological regions a different variogram was used and the block grades were simulated independently of block grades in other regions. The regions arose from a single geological interpretation of the drill hole data. In order to capture the full variability, we require a rigorous method of computing multiple randomly generated volumes and boundaries for each geological region. Within each of these volumes we should conditionally simulate grade values as before. To our knowledge, the problem of properly performing conditional simulation of volumes has not been solved.

5. Our optimisation process produces a block schedule while in practice, blocks are removed as benches in phases or pushbacks. The block schedules that we have evaluated in this paper are valid in the sense that all slope precedence constraints are enforced; however, it is unlikely that our block schedules would be mineable in practice. A full analysis would require constructing phases or pushbacks from our K + 1 optimised block sequences and then optimising a panel or bench schedule for each of the K + 1 pushback designs.
6. In practice, one would not drill the entirety of the orebody to fully achieve the NPV increment promised by VOIDI. Rather, one wishes to target those blocks that if drilled, would lead to the greatest increment in NPV. Ideally, one would like to balance the drilling cost against the NPV increment and arrive at an optimal drilling program that is different to 'drill everywhere'. There are some rules of thumb about which blocks you might choose to selectively drill (e.g. those blocks with high grade variability and a mean grade around the cut-off grade,[4] or those blocks that are extracted in different periods when the different conditional simulations are individually optimised). To formulate the problem rigorously as an optimisation problem is difficult. One could for example:

   (i) select blocks to be drilled based on the above rules of thumb;
   (ii) turn to each of the K conditional simulations and fix the grades of those blocks;
   (iii) for each of the K conditional simulations, produce another K simulations using variograms constructed from the additional hypothetical drill holes, leading to K2 simulations in all; and
   (iv) calculate VOIDI in an analogous way to that described earlier.

This procedure would value a putative additional drilling program. To identify rigorously optimal locations for future drill holes is a far more difficult problem. In this paper we have presented a rigorous valuation method that gives an idea of the 'size of the prize' if additional drilling were undertaken. Our method is a decision-making aid. On the basis of VOIDI, the decision of whether to drill further may become very simple.

Acknowledgments Clearly the project value also depends critically upon fundamental inputs such as the product sales price and the market volume. We do not treat these dimensions in this paper, but they may be considered and quantified in an analogous way.

[4]Rendu (1970) used the mining block kriging variance to estimate the likelihood of a block being re-allocated to ore or waste in light of further drilling information. His work showed that there is little point in drilling a regular drill pattern for areas of 'known' waste or 'known' high-grade ore.

References

Boucher A, Dimitrakopoulos R (2012) Multivariate block-support simulation of the Yandi iron ore deposit. West Aust Math Geosci 44(4):449–468

Caccetta L, Hill SP (2003) An application of branch and cut to open pit mine scheduling. J Glob Optimisation 27:349–365

Cressie N (1991) Statistics for Spatial Data. New York, Wiley

Deutsch CV, Journel AG (1997) GSLIB: geostatistical softwarelibrary and user's guide. Oxford University Press

Dimitrakopoulos R (in press) Applied risk analysis for ore reserves and strategic mine planning: stochastic simulation and optimisation. Springer, SME, Dordrecht

Godoy MC (2002) The efficient management of geological risk in long-term production scheduling of open pit mines. Ph.D. thesis, The University of Queensland, Brisbane, Qld

Goovaerts P (1997) Geostatistics for natural resources evaluation. Oxford University Press

Johnson TB (1968) Optimum open pit mine production scheduling. Ph.D. thesis, University of California, Berkeley, CA

Ramazan S (2007) Large-scale production scheduling with the fundamental tree algorithm—Model, case study and comparisons. In: Dimitrakopoulos R (ed) Orebody modelling and strategic mine planning, 2nd edn. The Australasian Institute of Mining and Metallurgy, Melbourne, pp 121–127

Ramazan S, Dimitrakopoulos R (2004) Recent applications of operations research in open pit mining. SME Trans 316:73–78

Remy N (2004) S-GeMS—Geostatistical earth modeling software: user's manual. Stanford University, p 87 [online]. Available from: http://sgems.sourceforge.net

Rendu JM (1970) Some applications of geostatistics to decision making in exploration. In: Proceedings APCOM 1970, pp 175–184

Stochastic Optimisation of Long-Term Production Scheduling for Open Pit Mines with a New Integer Programming Formulation

S. Ramazan and R. Dimitrakopoulos

Abstract Conventional approaches to optimising open pit mine design and production scheduling are based on a single estimated orebody model, which does not account for geological variability. Conditional simulation can be employed to quantitatively address the resulting grade uncertainty. Multiple simulated orebody models provide a suitable input for stochastic integer programming (SIP), a type of mathematical programming that generates the optimal result for a defined set of objectives under uncertainty. In the case of production scheduling, the objectives are to maximise the total net present value (NPV) and to minimise unsatisfied demand for processed ore. Using a set of multiple simulated orebody models as input into an SIP model allows for the integration of in situ deposit variability and uncertainty directly into the production scheduling optimisation process.

Introduction

Stochastic integer programming (SIP) is a type of mathematical programming and modelling that considers multiple equally probable scenarios and generates the optimal result for a set of defined objectives within the feasible solution space bounded by a set of constraints. SIP is defined as an extension of mixed integer programming (MIP) with uncertainty in one or more of the related coefficients (Escudero 1993). This tends to increase problem size and complexity when compared with scheduling formulations based on MIP (Ramazan 2001). Different approaches in SIP formulations are discussed in (Birge and Louveaux 1997);

S. Ramazan (✉)
MAusIMM, Rio Tinto, GPO Box A42, Perth, WA 6000, Australia
e-mail: salih.ramazan@riotinto.com

R. Dimitrakopoulos
MAusIMM COSMO Laboratory, Department of Mining
Metals and Materials Engineering, McGill University, Frank Dawson Adams
Building Room 107, 3450 University Street, Montreal, QC H3A 2A7, Canada
e-mail: roussos.dimitrakopoulos@mcgill.ca

R. Dimitrakopoulos (ed.), *Advances in Applied Strategic Mine Planning*,
https://doi.org/10.1007/978-3-319-69320-0_11

however, the existing developments in the technical literature are not directly applicable to mining problems.

The effects of orebody uncertainty and in situ geological variability on approaches to optimising open pit mine design have been shown in recent studies. Dimitrakopoulos et al. (2002) show the substantial conceptual and economic differences of risk-based frameworks. Dowd (1997) proposes a framework for risk integration in surface mining projects. Ravenscroft (1992) discusses risk analysis in mine production scheduling, where the use of stochastically simulated orebodies shows the impact of grade uncertainty on production scheduling, and states that conventional mathematical programming models cannot accommodate quantified risk. The need for optimisation methods that can integrate uncertainty raises the need for efficient simulation methods, as discussed in Boucher and Dimitrakopoulos (2007), this volume, Godoy (2003) and Dimitrakopoulos and Luo (2004). Pursuing this line of thought, Ramazan and Dimitrakopolous (2004a) developed efficient MIP formulations to generate feasible mining patterns of optimised probabilistic production schedules.

Although all these studies represent substantial developments in the field, they do not directly integrate uncertainty in the optimisation process. Dimitrakopoulos and Ramazan (2004) propose a probabilistic long-term scheduling optimisation method based on linear programming to deal with uncertainty. The proposed method accounts for risk through probabilities of being above or below a cut-off; however, it still does not directly and explicitly account for orebody uncertainty. Godoy and Dimitrakopoulos (2004) developed a new risk-inclusive long-term production scheduling approach based on simulated annealing and achieved significant improvement in the total NPV of a large gold mine project. Their model does not consider the issues of grade blending and controlling the risk distributions for production targets; although it does minimise the risk of not meeting periodical ore production targets.

This paper presents an efficient new SIP mathematical model that generates optimum long-term production schedules for open pit mines for a defined objective function, considering the operational requirements at the mine. The SIP model takes multiple simulated orebody models, without averaging the grades, and maximises the total NPV when considering geological uncertainty caused by grade variability. The geologic risk discounting concept Dimitrakopoulos and Ramazan (2004; Dimitrakopoulos, in press) is incorporated within the SIP model to control the risk distribution between production periods. The penalty parameters for deviations from targets are implemented to control the geological risk distribution in terms of magnitude and variability. This SIP model has been developed as part of an ARC-Linkage project, initially reported by Ramazan and Dimitrakopoulos (2003).

Stochastic Integer Programming Model

The SIP model developed herein accounts for uncertain inputs by considering simulated grade realisations in the optimisation process. It can thereby minimise the risk of a mine not meeting production targets as a result of geological uncertainty.

The model contains an objective function and a set of constraints representing the operational requirements of the mine. Within these constraints, the model performs the necessary calculations to reach the objective. The objective function is defined as the maximisation of the total NPV of the project minus the cost of deviations between the planned amount of ore tonnage, grade and quality and the amount of those produced from the actual operation. The NPV values of individual blocks in the objective function are calculated from the average of the undiscounted economic values in the simulated orebody models (Godoy and Dimitrakopoulos 2004), not from the average of the grade. The parameters that are included in the objective function to account for deviations are assigned for each simulated orebody model and for each time period for each type of production target, such as maximum periodical grade of ore, minimum grade of ore, maximum ore processing capacity and minimum ore tonnage that has to be processed. These deviation factors are calculated in the related constraint formulations that consider individual simulated orebody models for each of the production periods.

Definition of Symbols and Terms

Two basic concepts for the set-up of the SIP program and model are:

- *'Variable'* is a factor whose value will be determined by solving the mathematical model. The solver CPLEX is used to solve SIP/MIP/LP type mathematical models in this study.
- *'Constant'* is a factor whose value has to be provided to the mathematical model by the user.

The variable and constant factors used in the SIP model are defined below:

P	is the total number of production periods, or mine life; *constant*
N	is the number of blocks considered in modelling; *constant*
b_i^t	is a variable representing the percentage of block i mined in period t; if a b_i^t variable is defined as binary (0 or 1), it is assigned 1 if block i is mined in period t and assigned 0 otherwise; *variable*
M	is the total number of simulated orebody models; *constant*
d_{su}^{to}	is the excess amount of ore tonnage produced below a desired tonnage, or lower limit, in period t if the deposit has the same characteristics defined by the orebody model s variable. Note that g instead of o in this term refers to grade and q to metal quantity.
c_u^{to}	is the unit cost of d_{su}^{to} for the objective function; constant. Note that g instead of o in this term refers to grade and q to metal quantity

d_{sl}^{to} is the deficient amount of ore tonnage produced below a desired tonnage, or lower limit, in period t if the deposit has the same characteristics defined by the orebody model s; *variable*. Note that g instead of o in this term refers to grade and q to metal quantity

c_l^{to} is unit cost of d_{sl}^{to} for the objective function; *constant*. Note that g instead of o in this term refers to grade and q to metal quantity

fl is the orebody risk discounting rate used to calculate c_l^{to} and c_l^{tg} values; *constant*

fu is the orebody risk discounting rate used to calculate c_{11}^{to} and c_u^{tg} values; *constant*

f is used in this project as the orebody risk discounting rate: $f = fl = fu$; *constant*

R is the periodical economic discount rate, which is set to 10% in this case; *constant*

$E\{(EV)_i^0\}$ is the expected economic value to be generated in the future time t if block i is mined in period t; *constant*. The expected value of block i is calculated as follows:

$$E\{(EV)_i^0\} = \left((EV_i)_1^0 + (EV_i)_2^0 + \cdots + (EV_i)_M^0\right)/M$$

$E\{(NPV)_i^t\}$ is the expected discounted value to be generated if block i is mined in period t; *constant.* It is calculated as follows:

$$E\{(NPV)_i^t\} = E\{(EV)_i^o\}/(1+R)^t.$$

V_i^t is a representation of $E\{(NPV)_1^t\}$; *constant*

G_{si} is the grade of block i in orebody model s; *constant*

O_{si} is the ore tonnage inside block i in orebody model s; *constant*

G_{min} and G_{max} are the targeted minimum and maximum average grade of the ore material to be processed in a period; *constant*

m_{sl}^{to} is the dummy variable used to balance the equality constraints when the ore tonnage produced is more than the minimum required amount for the orebody model s; *variable*. Note that g instead of o in this term refers to grade and q to metal quantity

m_{su}^{to} is the dummy variable used to balance the equality constraints when the ore tonnage produced is less than the maximum amount for the orebody model s; *variable*. Note that g instead of o in this term refers to grade and q to metal quantity

Y_i number of blocks overlying ore block i considered for setting the slope constraints; *constant*.

The Objective Function

The objective function of the SIP model is constructed as the 'maximisation of a profit function'. The profit function is defined as the total expected NPV minus the cost of deviations from planned production targets. It is expressed as follows:

$$Max \sum_{t=1}^{P} \left[\underbrace{\sum_{i=1}^{N} V_i^t b_i^t}_{Part1} - \underbrace{\sum_{s=1}^{M} \left(c_u^{to} d_{su}^{to} + c_1^{to} d_{sl}^{to} + c_u^{tg} d_{su}^{tg} + c_l^{tg} d_{sl}^{tg} + c_u^{tq} d_{su}^{tq} + c_l^{tq} d_{sl}^{tq} \right)}_{Part2} \right] \quad (1)$$

Part 1 of the objective function is used for maximising the total discounted economic value while Part 2 is used for managing the risk of not meeting production targets using conditionally simulated orebody models. Traditionally, one orebody model, a smooth image of the deposit, is used for maximising NPV. However, when the expected deviations from the planned amount of ore tonnage having a planned grade and quality in a schedule are high in actual mining operations, the traditional model is unlikely to achieve the resultant NPV of the planned schedule. So, the NPV to be generated from actual mining can be far from optimal even if the schedule is optimised using a traditional true optimiser, MIP model (Ramazan2001; Ramazan and Dimitrakopoulos 2004a, b). Therefore, the SIP model is developed to consider the minimum of the deviations together with maximisation of NPV to generate achievable NPV.

For constructing the objective function, initially, a constant value is assigned for each of the cost parameters representing the cost at time *0* (*base cost*). Then, the risk discounting parameter (*f*) is introduced to determine the cost at different time periods by discounting the *base cost* using *f* (Dimitrakopoulos and Ramazan 2004). The risk-discounting concept is then incorporated into the SIP model (Ramazan and Dimitrakopoulos 2003; Dimitrakopoulos, in press).

If *f* is set to *0*, the deviations in production targets can be expected to result in more or less the same level between different production periods because the cost of a unit deviation will be the same in all periods. However, the distribution of deviations will also depend on how the variability in grade and ore tonnage is distributed over the deposit and on how the relative magnitude of the costs for the deviations used in the SIP model compare with the economic values of the blocks.

The Model Constraints

The deviation parameters are calculated within the SIP model by using the related constraints that consider each of the simulated orebody models. In this paper, equality-type constraints that use simulated multiple orebody realisations are called

'stochastic constraints' or, more specifically, 'soft stochastic constraints' because they are feasible for any value of the decision variables (b_t^i).

Stochastic constraints related to grade blending are used to satisfy not only the grade requirement at the mill but also the requirements for quality parameters, for example, the combination of elements like aluminium and magnesium in nickel mines, or silica in iron ore mines. This type of constraint can be expressed by:

$$\sum_{i=1}^{N} (G_{si} - G_{min}) O_{si} b_i^t + d_{sl}^{tg} - m_{sl}^{tg} = 0 \quad \text{Lower Bound} \tag{2a}$$

$$\sum_{i=1}^{N} (G_{si} - G_{max}) O_{si} b_i^t + d_{su}^{tg} - m_{su}^{tg} = 0 \quad \text{Upper Bound} \tag{2b}$$

These constraints are written for each of the M—equally probable orebody models (s = 1, 2,…, M) and P—time periods (t = 1, 2,…, P). The stochastic constraints for ore tonnage and metal can also be written in a similar way as grade constraits (Ramazan and Dimitrakopoulos 2003). Other operational constraints (Ramazan and Dimitrakopoulos 2004a) are also included in the model although not discussed in this paper.

Tests on a Hypothetical Two-Dimensional Data Set

This section presents applications of the SIP scheduling model using different cost parameters for the deviation factors on a hypothetical two-dimensional single-element gold deposit. The deposit considered herein is a subvertical orebody model that requires mining with a 45° slope angle. The model contains 200 square blocks, 20 and 10 along the horizontal and vertical axes, respectively. The gold deposit is simulated by generating 50 orebody models that represent the deposit with equal probabilities (Ramazan et al. 2004). The grades in these simulated orebody models are then averaged, generating an orebody model referred to herein as the 'e-type' orebody model. This orebody model is the equivalent of an estimated model that is a smoothed image of the deposit, which is often used as input in traditional optimisation methods. The grade distribution of three simulated orebody models and the e-type model are shown in Fig. 1. The figure shows that, although there are some similarities in the general characteristics of the grade distribution, there are local differences between the simulated equi-probable orebody models. All the simulated models have the same histogram and spatial continuity.

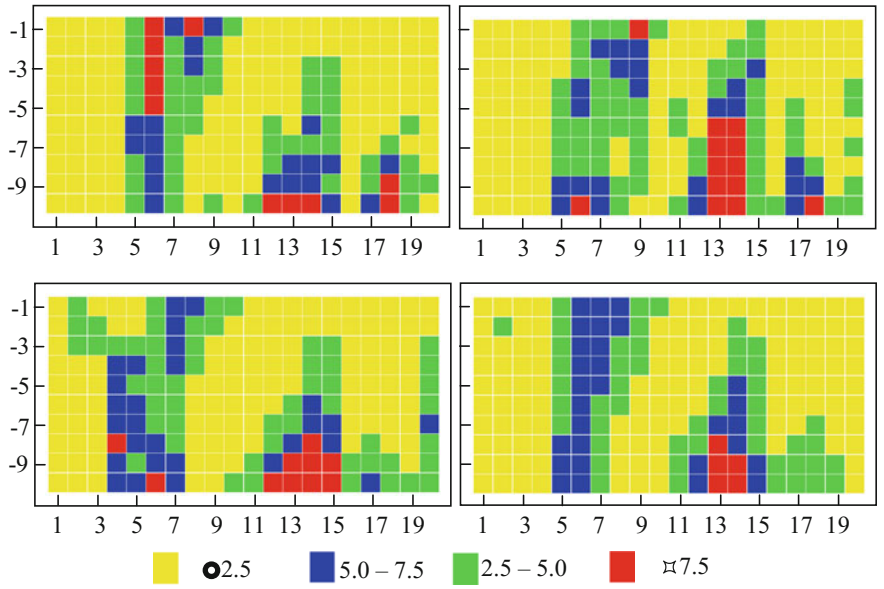

Fig. 1 Grade distributions of the hypothetical 2D deposit in three simulated realisations of the orebody and the e-type orebody model generated from the averaging of 50 simulated realisations (at bottom right)

Implementation of the SIP Model

The artificial deposit is scheduled to be mined for three years of production using the SIP model. During the tests performed, two different cost parameters are used: one aims to penalize the deviations in ore production (c^{to}) in period t and the other aims to penalise the deviations in the average grade of the ore produced (c^{tg}) in period t. In this study, the excess ore production (d^{to}_{su}) and grade (d^{to}_{sl}), and shortage in ore production (d^{to}_{sl}) and grade (d^{tg}_{sl}) are penalized equally ($c^{to} = c^{to}_{l} = c^{to}_{u}$ and $c^{tg} = c^{tg}_{l} = c^{tg}_{u}$). The orebody risk discount rate (f) of 8% is used to distinguish the cost of the deviations over the production periods. All the blocks in the deposit model are considered for the scheduling. Even the blocks at the edges are assumed to be mineable for the purpose of illustrating the new SIP concept, although they would not be feasibly mined in actual operation.

The average grade of the ore tonnage mined in each period is constrained to be between 4.7 and 5.2, and the minimum and maximum periodical ore tonnage production is limited to be between 260 and 290 tonnes.

Generating Multiple Schedules with Different Risk Distributions

Table 1 shows the values calculated from the e-type orebody model corresponding to the summary information of the schedules obtained assigning different values for the c^{0o} and c^{0g} parameters. The first column, S, shows the schedule number, which corresponds to a schedule generated by using the cost parameters given in the table. The values for cost parameters are selected by trial and error. Initially, zero is assigned as the cost of deviations from both ore production and grade targets. Then, the values are randomly increased to generate different risk profiles. In some cases,

Table 1 Summary of the six different SIP schedules generated with different cost parameters. Schedule S7 is the traditional schedule

S	c_{0o}	c_{0g}	Period	Value	NPV	Grade	Ore	Waste	Sum
1	0.00	0.00	1	354.6	328	4.592	340	270	610
	20.0	0.0	2	193.2	166	5.269	310	460	770
			3	−14	−11	4.946	180	370	550
			Sum/Mean	**533.8**	**483**	**4.921**	**830**	**1100**	**1930**
2	0.0	0.5	1	−550	−509	0.000	0	550	550
			2	333.8	286	4.949	310	280	590
			3	750	595	4.905	520	270	790
			Sum/Mean	**533.8**	**372**	**4.921**	**830**	**1100**	**1930**
3	20.0	0.1	1	63.9	59	4.688	290	480	770
	20.0	0.2	2	187.1	160	5.066	270	360	630
	20.0	0.3	3	272.8	217	5.028	270	270	540
	20.0	0.4	**Sum/Mean**	**523.8**	**436**	**4.921**	**830**	**1110**	**1940**
4	20.0	0.5	1	53.8	50	4.773	290	500	790
			2	291.4	250	5.192	280	290	570
			3	188.6	150	4.795	260	310	570
			Sum/Mean	**533.8**	**449**	**4.921**	**830**	**1100**	**1930**
5	25.0	0.0	1	87.07	81	4.647	300	470	770
	30.0	0.0	2	234.6	201	5.237	260	310	570
			3	211.5	168	4.923	270	320	590
			Sum/Mean	**533.8**	**450**	**4.921**	**830**	**1100**	**1930**
6	10.0	0.5	1	77.4	72	4.804	290	480	770
	2.0	0.1	2	267.8	230	5.160	280	310	590
			3	188.6	150	4.795	260	310	570
			Sum/Mean	**533.8**	**451**	**4.921**	**830**	**1100**	**1930**
7	–	–	1	388.4	360	4.718	280	140	420
			2	52.0	44	4.930	280	500	780
			3	173.4	138	5.125	270	380	650
			Sum/Mean	**613.8**	**542**	**4.921**	**830**	**1020**	**1850**

such as models 1, 3, 5 and 6, the same scheduling result is generated by using different cost parameters for ore and grade deviations in the objective function. Although it is possible to calculate the actual cost of not producing a certain amount of metal in this case, it is not the best way of using the SIP model proposed. The purpose of the SIP model is to generate scheduleswith optimal NPV and control the risk distribution. This is because of the fact that different mines may have different preferences of risk distribution, and management should be able to decide the most suitable risk distribution for the specific mine. For example, if there is budget for more exploration drilling after a few years, it may be preferable to mine the risky part of the deposit later; if the mine's overall profit is not very high, it may be best to keep the risk as low as possible, but if the mine's profit looks reasonably high, it may be better to tolerate some risk if it has a significant potential in generating higher NPV. Therefore, there is no method available to determine optimal values for the cost of deviations for any mine. The important issue is to generate a schedule that will produce the optimal NPV for a desired risk distribution rather than the optimality of the costs for deviations.

In this paper, Schedule S7 is generated by applying a general form of MIP formulations with the NPV maximisation objective in a single estimated orebody model that is considered as traditional scheduling.

The first schedule S1 is generated by assigning 0 to both of the cost parameters ($c^{0o} = 0$ and $c^{0g} = 0$), which makes the ore tonnage and grade constraints inactive. Schedule S1 violates ore processing capacity constraints in all the periods by large amounts, and grade constraints significantly. The resultant NPV from the mathematical model cannot be achieved through the actual operation due to the high deviations. This scheduling model is considered to be infeasible and unrealistic due to the resulting high deviations.

The schedule S2 is also not realistic due to the fact that it produces no ore in the first period for two main reasons. The first reason is that the cost of grade deviations, c^{0g}, is too high, dominating and destroying the effect of the NPV parameter in the objective function. The second reason is that assigning zero *base cost* for deviations in ore tonnage disables the processing capacity constraints. Schedules S1 and S2 show that cost parameters are crucial, and assigning wrong values to them may generate infeasible schedules.

The scheduling periods of the schedules S3, S4, S5, S6 and S7 are depicted in Fig. 2. The figure shows that the traditional schedule (S7) mines fewer blocks than the other schedules. This occurs because, in the SIP models, a block is classified as ore if it is considered to be ore in more than 40% of the simulated orebody models, and this has resulted in the classification of more blocks as ore than are so classified in the e-type model in this case.

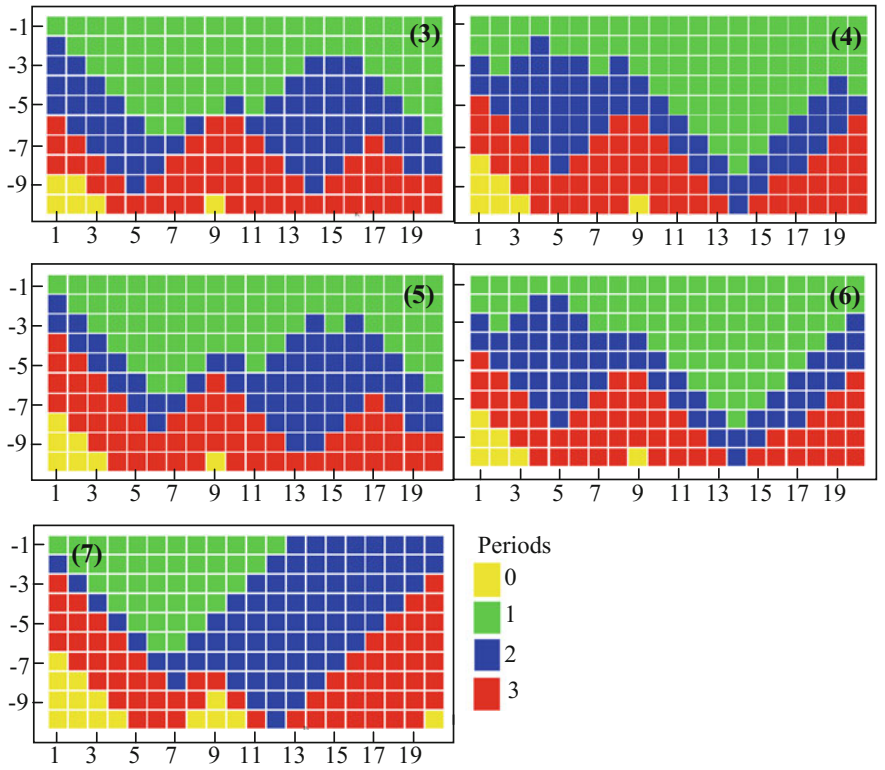

Fig. 2 Cross-sectional view of the schedules at 45° slope constraint

Quantification of Uncertainty Within Schedules

In a schedule, average deviations, average of non-zero deviations and probability to deviate from the production targets according to the simulated orebody models are considered as the uncertainty measurement parameters in this study. Table 2 shows the percentage of deviations for each of the schedules. The third column 'Deviations (per cent) e-type' is the per cent deviations with respect to the e-type orebody model.

The values reported in the fourth column are determined with respect to simulated models as follows:

1. Assuming the values in the actual deposit are exactly the same as the simulated orebody model 1, calculate the resultant ore tonnage (R_o) and the resultant average grade of that ore tonnage (R_g) within each production period.
2. Calculate the percent deviations D_o for ore tonnage and D_g for grade per period:
3. Repeat Step 2 for all the remaining simulated orebody models.

Table 2 Deviations in ore production in scheduled periods and average grade

S	Period	Deviations (%) e-type		Average deviations (%)		Average of non-zero deviations (%)		Probability to deviate	
		Ore	Grade	Ore	Grade	Ore	Grade	Ore	Grade
1	1	18.22	−1.7	13	8	26	16	86	82
	2	7.3	2.11	20	3	35	11	86	58
	3	29.1	0.0	16	6	37	17	86	64
2	1	94.5	−95.0	79	26	79	46	100	88
	2	7.3	0.0	13	3	25	12	76	48
	3	83.6	0.0	80	4	80	13	100	54
3	1	0.0	0.0	10	8	28	17	66	80
	2	0.0	0.0	5	4	22	15	50	48
	3	0.0	0.0	9	2	23	10	76	52
4	1	0.0	0.0	10	5	25	16	78	64
	2	0.0	0.5	7	4	21	10	60	68
	3	0.0	0.0	8	4	24	11	66	58
5	1	3.6	−0.6	11	8	28	17	64	82
	2	0.0	1.4	4	4	17	14	46	22
	3	0.0	0.0	9	3	23	11	76	60
6	1	0.0	0.0	8	5	23	17	76	62
	2	0.0	0.0	7	3	22	11	62	68
	3	0.0	0.0	8	4	24	11	66	58
7	1	0.0	0.0	8	8	23	20	60	80
	2	0.0	0.0	14	4	27	14	86	58
	3	0.0	0.0	9	3	27	13	64	46

4. Find the average of the calculated D_o and D_g values for each period and report under ore and grade columns in the table, respectively.

The third column 'deviations (per cent) e-type' in Table 2 is calculated by determining the R_o and the R_g values for e-type orebody model and using the equations in Step 2.

The fifth column 'Average of non-zero deviations (per cent)' is generated as follows:

1. Perform the above Steps 1 through 3.
2. Count the number of simulated orebody models that deviations are greater than 0, for ore (N_o) and grade (N_g) for each period.
3. Sum up the deviations, D_o and D_g values, and report sum(D_o)/N_o and sum(D_g)/N_g under ore and grade columns.

This fifth column 'average of non-zero deviations (per cent)' provides a quantity in terms of actual magnitudes of the deviations by not including the orebody models with 0 deviations in the averaging process.

The last column 'probability to deviate' shows the probability of each schedule to deviate in each production period. Since there are 50 simulated orebody models used here, the values of ore (P_o) and grade (P_g) in the table are calculated as follows:

$P_o = 100\ N_o/50$, $P_g = 100\ N_g/50$

The SIP scheduling model is designed in such a way that it does not take ore production and average grade constraints in the last period into consideration, because this doesn't affect the optimality of the schedule (Ramazan and Dimitrakopoulos 2004b). Therefore, the schedules are compared and analysed on the basis of the first and the second periods only, which leads to the infeasible schedules S1 and S2 being excluded from further discussion.

Analysis of the Results

Table 2 shows that traditional schedule S7 has the highest total deviations in ore production, 22%, for the first and the second periods among the schedules considered. The total average deviations in ore production in SIP schedules S3, S5 and S6 are about 15, and 17% in schedule S4. Total average of the non-zero deviations in ore production are 45% in schedules S5 and S6, and 46% in S4, which are slightly less than the 50% in the stochastic schedule S3 and traditional schedule S7. Traditional schedule S7 also has the highest total non-zero grade deviations, 34%. The average probability of having the deviations in ore tonnages and grades is highest in the traditional schedule, at 73 and 69% respectively on average for the first two periods. Stochastic schedules S5 and S3 have lower average probability to deviate in ore production at 55 and 58% respectively, while schedules S4 and S6 have 69% average probability during the two periods. These results illustrate that the traditional schedule, which uses a single estimated input orebody model, performs poorly compared with the stochastic scheduling models. The poor performance of the traditional model is the result of its lack of ability to incorporate grade uncertainty in the optimisation process and of a single input orebody model not being able to represent the grade variability.

Schedule 5 seems to perform better than other schedules in terms of meeting the grade and ore production targets as shown in Table 2. Table 1 shows that schedule S5 is assigned higher cost for deviating from the ore production targets than the other SIP schedules. Although zero cost is assigned for the deviations in average grade, the grade deviations are similar to the deviations in the other schedules, and the probability to deviate in grade as an average of the first two periods is lower than in the other methods. This may be due to the fact that this schedule produced more balanced ore tonnage between periods with the blocks that have higher

probability for being ore. In this specific case study, producing ore tonnage with the risk-robust ore blocks may have resulted in low-grade variations.

Figure 3 presents the production of ore tonnes from simulated orebody models, the average of these ore tonne, and the minimum (LO) and maximum (UO) limits of ore production constraining each of the schedules being considered for the first and the second periods. It is shown that the average of the expected ore tonnes using the traditional scheduling method is less than the lower limit, indicating a higher risk in falling short in the first period. Since stockpiling is not considered in these schedules, producing more ore tonnage than the maximum processing capacity, as is the case in schedules S3 and S5 in the first period, should also be considered as undesirable and costly. Schedules S4 and S6 can be considered better than the others from the analysis of ore production in the first period. The variations in the possible ore production of schedules S4, S6 and S7 are slightly less than those of schedules S3 and S5 in the first period. However, schedule S7 should be considered undesirable due to its higher possibility of not producing sufficient ore to feed the mill.

The variations in the ore tonnage production during the second period indicate that schedules S3 and S5 have relatively less risk of producing less than the lower limit, or more than the upper limits of ore. The variability is not particularly large among the stochastic schedules, but it is very large in the traditional schedule. The traditional schedule also has a high probability of exceeding the maximum mill capacity during the second period. Figure 3 indicates that the traditional schedule S7 has the highest risk of deviating from the planned ore production.

There is not a significant difference in the total NPV of the project among the simulated orebody models. The difference is that since the traditional model is not likely to produce the planned amount of metal, the NPV may not be realised, but the proposed method is likely to achieve the planned NPV.

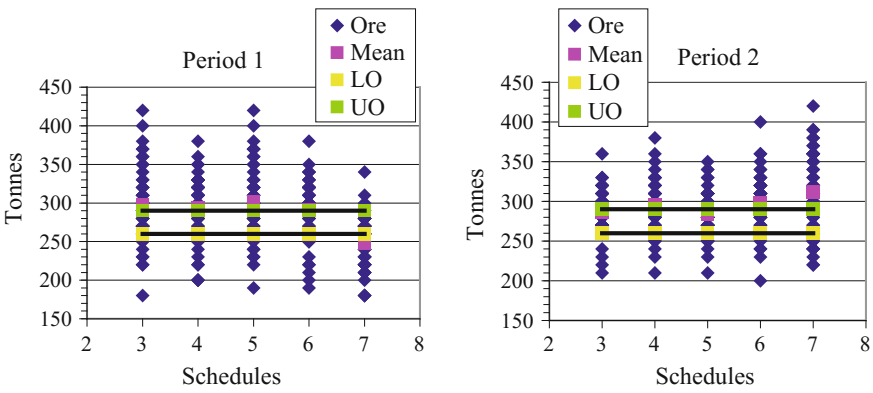

Fig. 3 Possible outcomes of ore tonnages generated by the schedules S3, S4, S5, S6 and traditional schedule S7. LO and UO shown in the two horizontal lines represent lower and upper bounds of ore production per period and are 260 and 290 tonnes, respectively

Conclusions and Further Work

This paper has presented a new and efficient SIP model formulation that can consider multiple simulated orebody models to optimise long-term production scheduling. The objective function in this model is constructed as maximising NPV of the mining operation, with a managed risk of not meeting production targets in terms of ore tonnes, grade and quality. The scheduling method developed here allows the decision-maker to define a risk profile based on the existing uncertainty quantified by simulated orebody models. The decision-maker has the option of minimising the risk in each of the production periods, or tolerating some risk in certain periods, or all periods. In the traditional scheduling model, geological risk is randomly distributed over the periods and can be significantly large. The new SIP model allows the selection of the best mine design based on the resultant NPV and the risk profile defined. The SIP method contains substantially less binary variables than traditional MIP mine scheduling models and the SIP model is efficient in terms of solution time. Although a hypothetical data set has been used to illustrate the strength of the new SIP model in this paper, the model is applicable to large open pit mines.

SIP models are proven to have significant economic benefits compared with traditional models that use deterministic inputs (Birge and Louveaux 1997; Ramazan and Dimitrakopoulos 2003; Ramazan et al. 2004; Dimitrakopoulos in press). A recent example from applications with substantial monetary benefits from the use of the stochastic models presented in this paper are available in (Jewbali 2006). The stochastic programming and modelling concept is useful not only for optimising the production scheduling process, but also for investigating various stages of the whole mining process, such as finding the value of an additional drilling campaign as discussed in (Froyland et al. 2007, this volume).

Acknowledgements The work in this paper is part of ARC Grant # LP0211446 to R Dimitrakopoulos and was also funded by AngloGold Ashanti, BHP Billiton, Rio Tinto and Xstrata.

References

Birge JR, Louveaux F (1997) Introduction to stochastic programming. New York, Springer, p 421

Boucher A, Dimitrakopoulos R (2007) A new efficient joint simulation framework and application in a multivariable deposit. In: Dimitrakopoulos R (ed) Orebody modelling and strategic mine planning, 2nd ed. The Australasian Institute of Mining and Metallurgy, Melbourne pp 345–354

Dimitrakopoulos R (in press) Applied risk analysis for ore reserves and strategic mine planning: stochastic simulation and optimisation. Springer–SME, Dordrecht, p 350

Dimitrakopoulos R, Luo X (2004) Generalized sequential Gaussian simulation on group size v and screen-effect approximations for large field simulations. Mathematical Geology 36(5):567–591

Dimitrakopoulos R, Ramazan S (2004) Uncertainty based production scheduling in open pit mining. SME Transactions 316:106–112

Dimitrakopoulos R, Farrelly CT, Godoy M (2002) Moving forward from traditional optimisation: grade uncertainty and risk effects in open-pit design. Trans Inst Min Metall, Section A, Mining Technology 111:A82–A88

Dowd PA (1997) Risk in minerals projects: analysis, perception and management. Trans Inst Min Metall Section A Min Technol 106:A9–A18

Escudero LF (1993) Production planning via scenario modelling. Ann Oper Res 43:311–335

Froyland G, Menabde M, Stone P, Hodson D (2007) The value of additional drilling to open pit mining projects. In: Dimitrakopoulos R (ed) Orebody modelling andstrategic mine planning, 2nd edn. The Australasian Institute of Mining and Metallurgy, Melbourne pp 245–252

Godoy MC (2003) The efficient management of geological risk in long-term production scheduling of open pit mines. Ph.D. thesis, University of Queensland, Brisbane, p 256

Godoy MC, Dimitrakopoulos R (2004) Managing risk and waste mining in long-term production scheduling. SME Trans 316:43–50

Jewbali A (2006) Modelling geological uncertainty for short-term production scheduling in open pit mines. Ph.D. thesis, University of Queensland, p 280

Ramazan S (2001) Open pit mine scheduling based on fundamental tree algorithm. Ph.D. thesis, Colorado School of Mines, Golden

Ramazan S, Dimitrakopoulos R (2003) Stochastic integer programming based modelling for long-term production scheduling of open pit mines, ARC-Linkage Report N-6002-1. University of Queensland, Brisbane

Ramazan S, Dimitrakopoulos R (2004a) Traditional and new MIP models for production scheduling with in-situ grade variability. Int J Surf Min Reclam Environ 18(2):85–98

Ramazan S, Dimitrakopoulos R (2004b) Recent applications of operations research in open pit mining. SME Trans 316:73–78

Ramazan S, Dimitrakopoulos R, Benndorf J, Archambault L (2004) Extension of SIP modelling for long term production scheduling with stochastically designed stockpiles and multiple ore processors, ARC-Linkage Report N-6003-1. University of Queensland, Brisbane

Ravenscroft PJ (1992) Risk analysis for mine scheduling by conditional simulation. Trans Inst Min Metall Section A Min Technol 101:A104–A108

Stochastic Long-Term Production Scheduling of Iron Ore Deposits: Integrating Joint Multi-element Geological Uncertainty and Ore Quality Control

J. Benndorf and R. Dimitrakopoulos

Abstract Meeting production targets in terms of ore quantity and quality is critical for a successful mining operation. In situ grade variability and uncertainty about the spatial distribution of ore and quality parameter cause both deviations from production targets and general financial deficits. A stochastic integer programming formulation (SIP) is developed herein to integrate geological uncertainty described by sets of equally possible scenarios of the unknown orebody. The SIP formulation accounts not only for discounted cashflows and deviations from production targets, discounts geological risk, while accounting for practical mining. Application at an iron ore deposit in Western Australia shows the ability of the approach to control risk of deviating from production targets over time. Comparison shows that the stochastically generated mine plan exhibits less risk in deviating from quality targets that the traditional mine planning approach based on a single interpolated orebody model.

Keywords Stochastic integer programming · Mine scheduling
Joint-simulation · Iron ore

Introduction

Long-term mine planning and production scheduling aim to define the "best" mine plan subject to the constraints imposed by physical and geological conditions, policies and the operational mining approach. The term "best" is defined by management objectives. These typically include maximising the monetary value of the mining project as well as meeting customer expectations and guaranteeing a safe operation. The expectations of customers are defined largely in terms of ore

J. Benndorf (✉)
MIBRAG MBH, Zeitz, Germany
e-mail: JoergBenndorf@gmx.de

R. Dimitrakopoulos
COSMO—Stochastic Mine Planning Laboratory, McGill University,
Montreal, QC, Canada

R. Dimitrakopoulos (ed.), *Advances in Applied Strategic Mine Planning*,
https://doi.org/10.1007/978-3-319-69320-0_12

tonnage and ore quality characteristics to be delivered. In the case of multi-element deposits, ore quality characteristics are defined by multiple inter-correlated elements. For example, in iron ore deposits, the elements iron (Fe), phosphorus (P), silica (SiO_2), alumina (Al_2O_3) and loss of ignition (LOI) are critical for ore quality. Additionally, in many cases ore is produced out of multiple pits with different ore characteristics. The goal of any global, long-term mine planning approach is to send the most homogeneous ore blend out of multiple pits, meeting customer specifications, while guaranteeing optimal pit development and maximizing the utilization of available mineral resources. In practice, however, when implementing a mine plan, differences frequently occur between the produced ore quantity and quality characteristics. It is well recognized that uncertainty in the description of the spatial distribution of grades of various pertinent elements in the orebody as well as their in situ variability are major contributors to these differences.

Traditional approaches to mine planning optimization are based on a single estimated model of the orebody that is unable to account for in situ variability and uncertainty associated with the description of the orebody (David 1977, 1988). Contrary to estimation techniques, a different set of techniques provide a tool to address shortcomings of estimation methods, termed conditional simulation (Goovaerts 1997; Chiles and Delfiner 1999; Dimitrakopoulos 2007). Based on drill-hole data and their statistical properties, conditional simulations generate several equally probable models (or scenarios) of a deposit, each reproducing available data and information, statistics and spatial continuity, that is, the in situ variability of the data. The difference between the equally probably scenarios are a quantitative measure/description of uncertainty. The subsequent integration of this grade uncertainty and local variability into mine planning optimization allows for the understanding and control of geological risk. This in turn aims to decrease project risk and increase profitability.

The detrimental effects to mine planning optimization from ignoring in situ grade variability and uncertainty in the description of orebodies are well documented (Ravenscroft 1992; Dowd 1997; Dimitrakopoulos et al. 2002, and others). For example, Dimitrakopoulos et al. (2002) show the danger of relying on estimated (average type) orebody models when optimizing. In their example, net present value (NPV) assessment of the conventionally generated life-of-mine schedule using simulated scenarios of the orebody shows the most likely NPV to be materialized standing at 25% lower than forecasted. The substantially positive contribution of accounting for grade uncertainty through multiple simulated scenarios and new stochastic optimization approaches is also well documented. Godoy and Dimitrakopoulos (2004) show a long-term production scheduling approach based on simulated annealing applied to a gold mine to result in a 28% increase of project value compared to the conventional approach. Leite and Dimitrakopoulos (2007) show the same order of improvement using this approach at a copper deposit. A more general and flexible long-term production scheduling method that allows the control of geological risk between production periods in terms of magnitude and variability is based on stochastic integer programming or SIP (Birge and Louveaux 1997), and it is documented in Ramazan and Dimitrakopoulos (2013).

An application of the SIP formulation to the long-term production scheduling of a single-element deposit demonstrates its effectiveness and advantages in terms of additional project value and associated risk management even for a relatively short life of mine.

This paper contributes a mine planning optimization approach that addresses joint multi-element grade uncertainty, as common in many mineral deposits, such as iron ore. More specifically, the stochastic integer programming approach of Ramazan and Dimitrakopoulos (2018, this volume) is expanded to (a) multi-element deposits, and (b) includes new mineability constraints to facilitate accessibility and equipment size constraints. In addition, the formulation developed herein is exhaustively tested in an application at an open pit iron ore mine in Western Australia, and within the context of multi-pit production planning. Testing includes the ability of the SIP to control the risk of deviating from production targets in terms of ore quality characteristics. In the next sections, the stochastic mathematical programming formulation is first presented. The application and testing of the formulation are presented, along with a comparison between the SIP and a traditional approach based on one estimated orebody model. Discussion and conclusions follow.

Stochastic Production Scheduling

Global optimization of long-term production scheduling addresses issues of optimal sequencing considering multiple pits, multiple elements, blending issues, stockpiling options and alternative processing or product options (Whittle 2007). The task of long-term production scheduling in a multi-pit operation can be divided into two stages. The first stage is a multi-pit scheduling approach, which defines ultimate pit outlines as well as proportions and element qualities, where each pit and period contribute to the global target in order to optimize the global asset. In the second stage the physical extraction sequence of blocks in each single pit is defined as constraints to production rates and targeted element grades implied by the multi-pit scheduling approach. This contribution concentrates on the long-term scheduling of a single pit; multi-pit scheduling approaches have already been successfully implemented, e.g. BLASOR, developed in BHP Billiton's Technology group (Stone et al. 2007).

The goal of long-term production scheduling under grade uncertainty of single pits is to define a physical extraction sequence of blocks over periods so as to meet multiple goals. These goals include (a) best mine development and best use of available mineral resources for a maximization of the monetary value of the asset, (b) control of risk of deviating from production targets, and (c) guarantees of a safe operation. In this context, controlling the risk of deviating from production targets is a major contribution and involves controlling probabilities and magnitudes of deviations from production targets, as well as fluctuation of produced grades over periods. The underlying geological uncertainty is captured by a set of conditionally

simulated orebody models. Generally, production targets may be in terms of produced ore and waste tonnes and grades of different elements. Constraints are in terms of practicality of the schedule guaranteeing equipment accessibility, mining capacity, processing capacity, geotechnical aspects as well as blending requirements.

Stochastic Formulation for Long-Term Production Scheduling

A general formulation for long-term production scheduling under geological uncertainty for multi-element deposits based on SIP is presented next. It is based on the single element formulation in Ramazan and Dimitrakopoulos (2008). The objective function and relevant constraints are explained in detail.

Objective Function

The SIP objective function, presented here for scheduling multi-element single deposits, combines several goals. It aims to generate a production schedule that optimizes the economic pit development considering constraints imposed by the global multi-pit approach, while minimising deviations from production targets in terms of tonnages and ore-quality as well as minimising costs of non-smooth mining. Equation (1) presents the three parts of the objective function,

$$\begin{aligned} \text{Maximise} \quad & \sum_{t=1}^{P}\sum_{i=1}^{N} c_i^t \cdot x_i^t \\ & - \sum_{s=1}^{S}\sum_{t=1}^{P}\sum_{r=1}^{R} \left({}^{s}qu_r^t \cdot yu_r^t + {}^{s}ql_r^t \cdot yl_r^t \right) \\ & - \sum_{t=1}^{P}\sum_{j=1}^{K} \left(c_{SM} \cdot Y1_j^t \right) \end{aligned} \tag{1}$$

where P is the number of periods, N denotes the total number of blocks to schedule, S represents the number of simulated orebody models used to capture geological uncertainty, R is the number of targets including grade targets for different elements and ore tonnage targets; c_i^t represents the economic contribution of block number i when mined in period t and is a representation of the expected economic value over all values of block i at time t derived from each realisation s $E\{(\text{NPV})_i^t\}$; x_i^t is a variable representing the percentage of block i mined in period t; if an x_i^t variable is defined as binary (0 or 1), it is assigned 1 if block i is mined in period t and assigned 0 if not; ${}^{s}qu_r^t$ is the upper deviation from production target r at time t considering orebody model s, yu_r^t is the unit cost of ${}^{s}qu_r^t$ to penalise excess production; ${}^{s}ql_r^t$ is the lower deviation from production target r at time t considering orebody model s, yl_r^t

is the unit cost of ${}^{s}ql_r^t$ to penalise a deficit in production. $Y1_j^t$ is the number of surrounding blocks, which are not mined in the period t or earlier when mining block j. Surrounding blocks are those, which are no more than 3 blocks apart in each direction (Fig. 1). The costs c_{SM} are penalties associated with $Y1_j^t$. Note that this penalty only applies to a subset K of all blocks N. To avoid overlapping, only every third block in each direction is considered to be the central block j.

The first part of the objective function is used for maximising the discounted economic value in the context of the global optimization. Note the global multi-pit approach accounts for interactions between different pits and aims to maximise usage of resources and global value. The first part in Eq. (1) maximises the local NPV of the single pit under consideration aiming to define an optimal mine development constricted by the global plan. It accounts for profit-defining aspects, such as stripping ratio. The discounted economic block value is calculated as expected value from each realisation. The second part of the objective function handles the deviations from production targets imposed by the multi-pit scheduling approach for each simulated orebody model s including grades of all elements and ore tonnage. By optimising over S possible scenarios, captured through multiple equally probable orebody models, this part of the objective function aims to control uncertainty and variability of the produced grades and ore tonnage. The magnitude of grade variability in the generated schedule is controlled for each element e considered and time period t by penalties associated with deviations ${}^{s}ql_r^t$ and ${}^{s}qu_r^t$. Note that deviations for each target and period yu_r^t and yl_r^t are calculated by the corresponding constraints, which are the grade constraint and the ore tonnage constraint. Part three of the objective function controls smooth mining by penalising not mining adjacent blocks in same period, the central block j is scheduled, or earlier (Fig. 1). $Y1_j^t$ represents hereby the percentage of the 8 directly adjacent blocks and the 25 blocks that are two block-widths distant, which have not been mined in the same period as block j. Deviations of smooth mining for each considered block j and period t $Y1_j^t$ are calculated in the smooth mining constraint. The priorities of the three competing parts in the objective function are controlled by the magnitude of corresponding cost parameters for each part relative to each other.

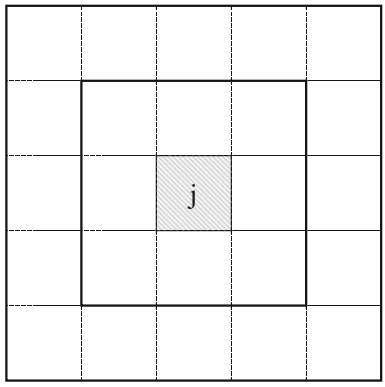

Fig. 1 Inner and outer window around block j in smooth mining constraint (after Dimitrakopoulos and Ramazan 2004)

The mine planner has to adjust these parameters so to define the best schedule that compromises his objectives, for example the level of risk the planner is willing to accept.

Constraints

The reserve constraint ensures that each block i is only being mined once over all periods P and is given by

$$\sum_{t=1}^{p} x_i^t = 1 \tag{2}$$

By setting the sum of binary variables of one block over all periods equal to one, the block must be mined during the life of the mine.

All overlaying blocks m_i must be mined before mining a given block i. This can be implemented using cone templates representing the required wall slopes. One possible formulation is given through

$$m_i \cdot x_i^t - \sum_{l=1}^{m_i} \sum_{r=1}^{t} x_l^r \leq 0 \tag{3}$$

where l is the counter for the m_i overlaying blocks.

Grade deviations ${}^s qu_r^t$ from the upper bound and ${}^s ql_r^t$ from the lower bound for each element, period t and simulated orebody model s are defined by grade constraints given in Eqs. (4a) and (4b).

$$\sum_{i=1}^{n} (g_{si}^e - G_{max}^e) \cdot O_i \cdot x_i^t - {}^s qu_r^t = 0 \tag{4a}$$

$$\sum_{i=1}^{n} (g_{si}^e - G_{min}^e) \cdot O_i \cdot x_i^t + {}^s ql_r^t = 0 \tag{4b}$$

where g_{si}^e is the grade for element e of block i considering orebody model s, G_{min}^e and G_{max}^e are the targeted minimum and maximum average grades of element e of the ore material to be processed in a period t, O_i is the ore tonnage inside block i.

Ore tonnage deviations ${}^s qu_r^t$ from the upper bound and ${}^s ql_r^t$ from the lower bound of the target at each period t are defined by

$$\sum_{i=1}^{n} (O_i \cdot x_i^t) - qu_r^t = PC_{max} \tag{5a}$$

$$\sum_{i=1}^{n} (O_i \cdot x_i^t) + ql_r^t = PC_{min} \tag{5b}$$

where PC_{min} and PC_{max} are the targeted minimum and maximum ore tonnage to be mined limited by the processing capacity.

The absolute tonnage of handled material, ore and waste, at period t is modelled through constraint

$$\sum_{i=1}^{n} (O_i + W_i) \cdot x_i^t \leq MC_{max} \tag{6}$$

where W_i is the waste tonnage inside block i and MC_{max} denotes the maximum mining capacity.

A practical mining requirement is equipment access and mobility realised through smooth mining patterns, which determine a feasible mining sequence. The percentage deviations related to smooth mining as introduced in the objective function ($Y1_j^t$) are calculated through a smooth mining constraint,

$$-\sum_{k=1}^{nb1} 2 \cdot x_k^t - \sum_{k=1}^{nb2} 1 \cdot x_k^t + (nb1 \cdot 2 + nb2 \cdot 1) \cdot x_j^t - Y1_j^t \leq 0 \tag{7}$$

Here, nb1 is the number of blocks directly adjacent (inner window) to block j to mine and nb2 is the number of blocks which are two block-width distant to block j (outer window) as illustrated in Fig. 1. Note that blocks in the inner window are penalised twice as much as blocks in the outer window. This setup indicates that it is more desirable to mine blocks in the inner window together with block j than blocks in the outer window. If possible, blocks in the outer window are mined together with block j; however, the solver has enough flexibility to mine those blocks in other periods.

Controlling Risk Over Time for Different Objectives

As presented in the previous section, penalties associated with deviating from production targets introduced in the objective function aim to control risk of deviation for each element. These penalties can be defined in different magnitudes for each element and period. This enables the mine planner to control the risk for each element over time. The ability to control the risk over time is a concept introduced by Dimitrakopoulos and Ramazan (2004) using a geological risk discount rate. This discount rate is directly applied to penalties and thus controls the risk distribution between periods. A high geological discount rate indicates that the SIP formulation herein is emphasised to generate a schedule that is less risky in early periods than in later periods. This may be useful when the operation aims to

mine less risky parts of the deposits in early periods and more uncertain parts in later periods. As mining progresses, more information about those uncertain parts will become available in form of operational exploration. A geological discount rate of 0% generates schedules that are expected to exhibit a similar level of risk in all periods. The difference between penalties applied to upper deviations and lower deviations defines the priority of upper and lower deviations from targets. For example, it may be more important in an operation to keep the deficit in production as low as possible while excess production may not be of importance.

Production Scheduling Under Uncertainty: An Application at Yandi Central 1 Iron Ore Deposit, WA

Next, mine production scheduling under multi-element grade uncertainty is applied to the Yandi Central 1 iron ore deposit in Western Australia. The first part describes the Yandi Central 1 deposit focusing on geology, mining operation and current production scheduling practice. The problem specification and description of input data are discussed subsequently, in particular the process of incorporating the stochastic production scheduling approach of a single deposit into the global multi-pit scheduling problem. The input in terms of simulated ore body models is presented as well as the operational, economical and risk controlling parameters. Following, the practical approach of scheduling Yandi Central 1 is detailed, including the practical implementation of the scheduling formulation and the manual mine design to convert results to a practical schedule. A comparison between schedules generated using a stochastic formulation to those using a deterministic formulation considering one estimated ore body model is found at the end of this section and demonstrates the benefit of the stochastic approach.

Yandi Operation and Current Production Scheduling Practice

The Yandi Central 1 deposit is part of the larger Yandi channel iron deposits (CID), which occurs alongside the Marillana–Yandicoognica Creek system about 120 km northwest of Newman, Western Australia. This deposit is part of the Yandi joint venture operation, which includes multiple pits. The fundamental objective of this complex operation is the achievement of customer defined on-grade shipments at lowest costs by optimally blending from different pits with a diverse range of resource grades. Critical geochemical parameters when evaluating the deposit are iron content (Fe), silica content (SiO_2), alumina content (Al_2O_3), phosphorus content (P) and the water and organic content measured as loss on ignition (LOI), as they influence the physical and chemical properties of the product and the performance of the beneficiation process.

For the global multi-pit optimization of the Yandi joint venture operation, BHP Billiton's Technology group developed a scheduling-algorithm, termed BLASOR (Stone et al. 2004). Among other details BLASOR assigns targets in terms of produced ore tonnes and grades for each period to each pit as contributing to the global target. Although BLASOR, as used here, accounts for multiple elements, the approach is based on a single estimated orebody model and does not incorporate local uncertainty and in situ variability.

Problem Specifications and Input for Scheduling

The in situ variability and the incomplete knowledge of the spatial distribution of the elements in the orebody are most critical for meeting customer specifications. In order to incorporate in situ variability and uncertainty of geochemical parameters in mine production scheduling, techniques for optimization under uncertainty can be employed. The application of stochastic mine production scheduling to Yandi Central 1 is based on stochastically simulated orebody models generated using the computationally joint direct block simulation approach (Boucher and Dimitrakopoulos 2009). Operational, economic and risk defining parameters are explained in subsequent sections in more detail.

Stochastic Orebody Models at Yandi Central 1

The basis for mine production scheduling under geological uncertainty is a series of simulated orebody models of the deposit. For this case study, 20 simulated orebody models of the main ore zone (MOZ) are used, generated by Boucher (2003). This joint-simulation of the five considered elements Fe, P, SiO_2, Al_2O_3 and LOI guarantees the local reproduction of cross-correlation between the elements. Note that Fe is strongly correlated with the elements SiO_2 and Al_2O_3. Each of the resulting orebody models contains 3049 blocks in total. Block dimensions are 25 m by 25 m by 12 m, representing typical mining units. Each block contains the attributes total tonnage, ore tonnage as well as total content of each element Fe, P, SiO_2, Al_2O_3 and LOI. As an example, a map of the spatial distribution of Fe grades in the orebody model is presented in Fig. 2 for the case of simulated realisation number five.

Operational Parameters

Operational parameters, including ore production and required qualities are defined by the global multi-pit scheduling approach undertaken by BLASOR. BHP Billiton

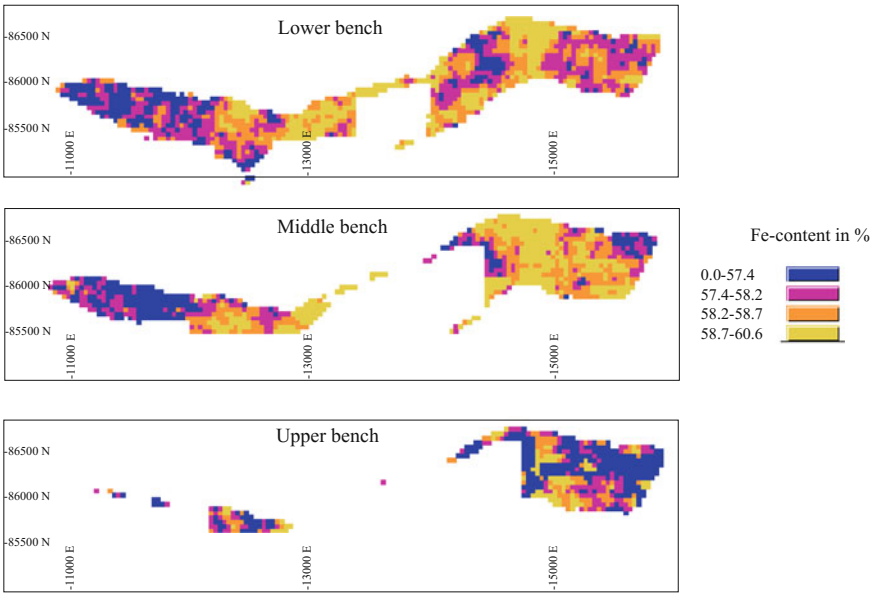

Fig. 2 Spatial distribution of Fe-grades in realisation number five for the lower, middle and upper bench

Table 1 Ore tonnage and grade constraints for scheduling Yandi Central 1

BLASOR scheduling results of Yandi Central 1 for first periods						
Period No	Ore tonnage (wt)	Fe (%)	P (%)	SiO2 (%)	Al_2O_3 (%)	LOI (%)
1	14,000,000	57.1–59.4	0.032–0.038	4.6–5.2	0.90–1.05	9.5–11.0
2	10,000,000	57.1–59.4	0.032–0.038	4.6–5.2	0.90–1.05	9.5–11.0
3	10,000,000	57.1–59.4	0.032–0.038	4.6–5.2	0.90–1.05	9.5–11.0
4	9,000,000	57.1–59.4	0.032–0.038	4.6–5.2	0.90–1.05	9.5–11.0
5	7,200,000	57.1–59.4	0.032–0.038	4.6–5.2	0.90–1.05	9.5–11.0

Note Ore/Waste cut-off grade is Fe $\geq$ 56%

Iron Ore provided scheduling results defining the contribution of Yandi Central 1 to the global target for the following five years referred to as periods. For confidentiality reasons, BLASOR results are scaled (Table 1).

Ideally, shipping grades are to be delivered with nearly zero variability. Since this is unlikely, the industry sets target bands limited by an upper and lower bound. Grades should not fall outside this band. Table 1 summarises initial ore tonnage and

Table 2 Economical parameters for long-term production scheduling of the Yandi Central 1 iron ore operation

Parameter	Costs/Price
Price per ton recovered metal	$30
Mining costs per ton	$5
Processing costs per ton	$5
Economical discount rate	10%
Geological discount rate	10%

grade limits. The differentiation between ore and waste prior to the optimization is realised through an Fe grade cut-off of 0.56%. Further, it is assumed that the operation is flexible enough to account for different ore and waste production rates between periods. For this reason, the maximum mining capacity, including ore and waste production, was set to 20,000,000 t, which is about 5,000,000 t more than the maximum rate. Due to the flat geometry of the deposit, one slope region is sufficient to characterise the geotechnical constraints. The general slope angle is set at 45°.

Economical and Risk-Controlling Parameters

Table 2 presents the economic parameters, including price, mining and processing costs and discount rates. Mining costs include blasting, extraction and transportation costs; processing costs account for crushing, conveying and stockpiling. Two discount rates are identified, the economical discount rate and the geological discount rate. The economical discount rate discounts cash flows over periods, while the geological discount rate controls the risk of producing grades that fall outside the limits over the periods. Recovery is 100%.

The stochastic scheduling approach applied in this case study is concerned with the risk of not meeting production targets of produced element-grades. Penalties for deviating from production targets are set initially to 1$/unit of deviation.

The Practical Scheduling Approach

Initial Run and Practical Mine Design

The upper part of Fig. 3 shows results of an initial run using above specified parameters. The extraction sequence appears smooth and feasible, however there are few blocks scheduled surrounded by blocks scheduled in different periods. To generate a practical mining schedule that guarantees minimum mining width and equipment accessibility, results of the stochastic formulation are refined using manual mine design and haul road construction. These standard tools are available

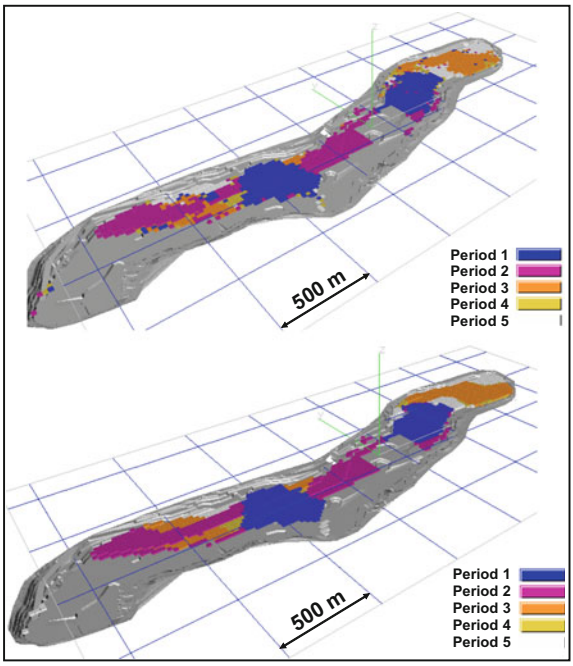

Fig. 3 Stochastic schedule in ultimate pit—before (upper part) and after (lower part) smoothing using manual design

in commonly used mine scheduling software packages. In this study open pit design from Earthworks Datamine is used (Datamine manual 2002). The schedule generated by the formulation can be used as a guideline to construct polygons for each period and bench. These polygons, in combination with haul roads and ramps, define the pit design for each period and provide a mineable production schedule. Parameters used in this designing process are a 12 m bench height, 45° slope angle and a 5 m berm between two toe and crest string, a road width of 25 m and a 8% ramp incline. The lower part of Fig. 3 shows a south-east isometric view of the resulting smooth schedule. Benndorf (2005) demonstrated that this type of smoothing has no significant impact on the results, which means that the smoothed schedule is still near to optimal.

Evaluating Results

In addition to produced ore and waste tonnage, results are evaluated in terms of risk profiles of produced grades per period, in particular for Fe, SiO_2, Al_2O_3, P and LOI (Fig. 4). For each period the grades are shown considering each simulated orebody realisation, which represent possible scenarios based on information available. The spread of the different realisations provide an indication about uncertainty in

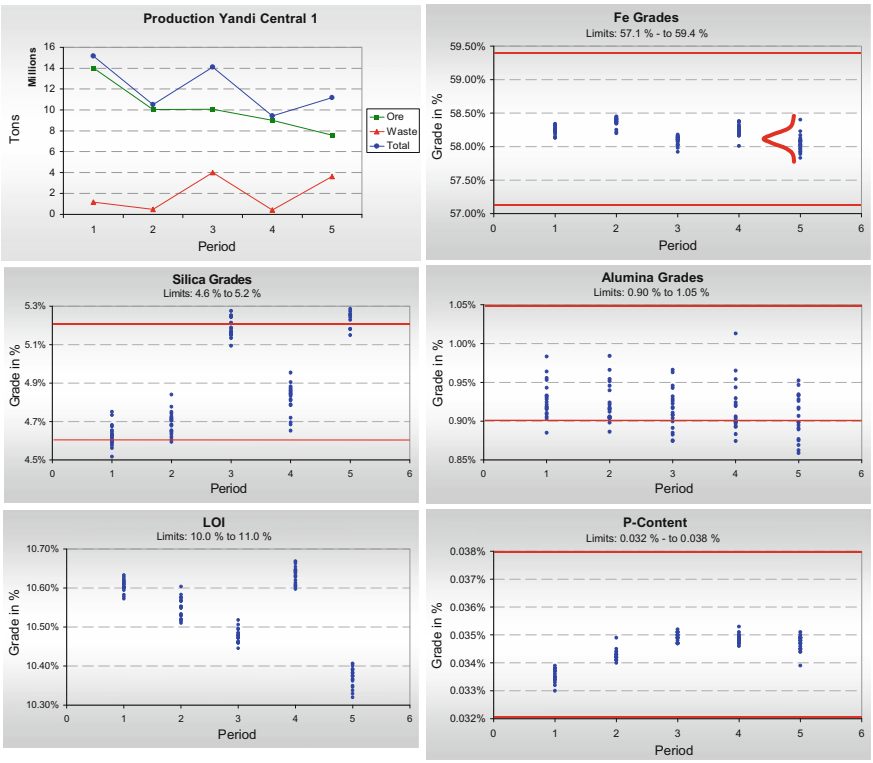

Fig. 4 Results of stochastic scheduling in terms of ore and waste tonnages and risk profiles for Fe, SiO_2, Al_2O_3, P and LOI

produced grades per period when extracting the deposit according to the generated schedule. Analyzing the risk profiles of Fe, P and LOI results concludes that there is no risk of deviating from production targets. SiO_2 and Al_2O_3 appear to be more critical in meeting production targets. For example, four out of twenty simulated orebody models for SiO_2 indicate a deviation from the lower target in period one. Thus, there exists a 20% chance of not meeting production targets for SiO_2 in period one.

The Ability to Control Risk

A major contribution of the presented scheduling formulation is the ability to control risk of deviating from production targets considering different quality parameters. As experienced in the initial run, SiO_2 and Al_2O_3 appear most critical in meeting targets. To investigate the ability to decrease risk, three different schedules were generated applying different penalties to both critical elements. The three

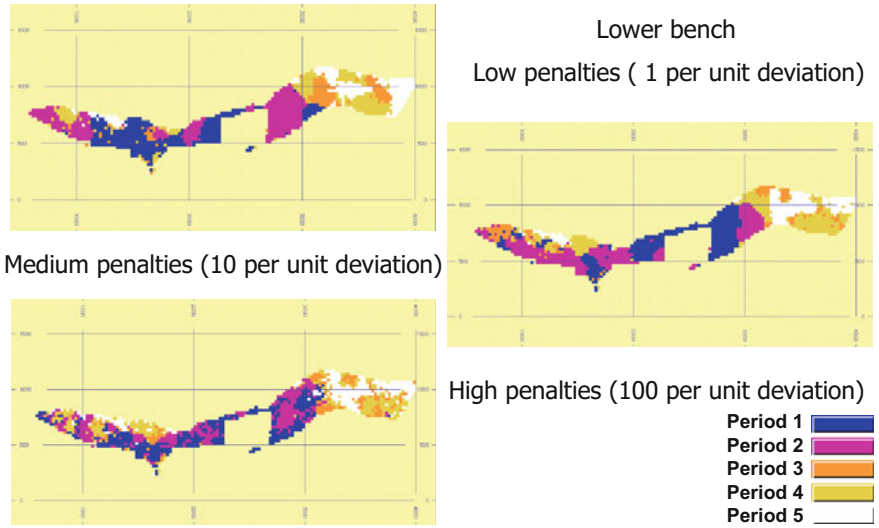

Fig. 5 Different extraction schedules depending on the magnitude of penalties for the lower bench

schedules were generated using low (1$ per unit deviation per ton), medium (10$ per unit deviation per ton) and high penalties (100$ per unit deviation).

Figure 5 shows the extraction sequence of the lower bench for each schedule. In the case of each schedule, the deposit would be extracted in a different sequence. The dispersion of the schedules increases with the magnitude of the penalties. In the case of low penalties, the extraction sequence is smooth. Although medium penalties generate a more dispersed schedule, it is still smooth enough to be converted to a feasible schedule using manual mine design. High penalties generate a very dispersed schedule, which could hardly be efficiently realised. The dispersion is an expression of a higher selectivity, necessary in order to produce a homogeneous product in a tight quality band. Figure 6 shows the risk profiles for SiO_2 and Al_2O_3 for the three generated schedules. In case of SiO_2, the effect of increasing penalties already becomes obvious in the case of medium value penalties. Compared to the low penalty case, the fluctuation of grades between periods decreases significantly and there exists only a slight probability of deviating from targets in period 2, 3 and 4. Higher penalties improve the result only marginally. In the case of Al_2O_3, a decrease in probability of deviating from targets is recognizable with higher penalties, however, there still exists a certain amount of risk. This is an expression of a high in situ variability and uncertainty of the element, which cannot be avoided by blending in the pit. A solution here, to decrease the risk, could be to blend the ore with ore from different mines, where Al_2O_3 is less variable and uncertain.

Generally, this evaluation of the scheduling formulation demonstrates that less risk of deviation comes with a cost of higher selectivity, which is caused by the two

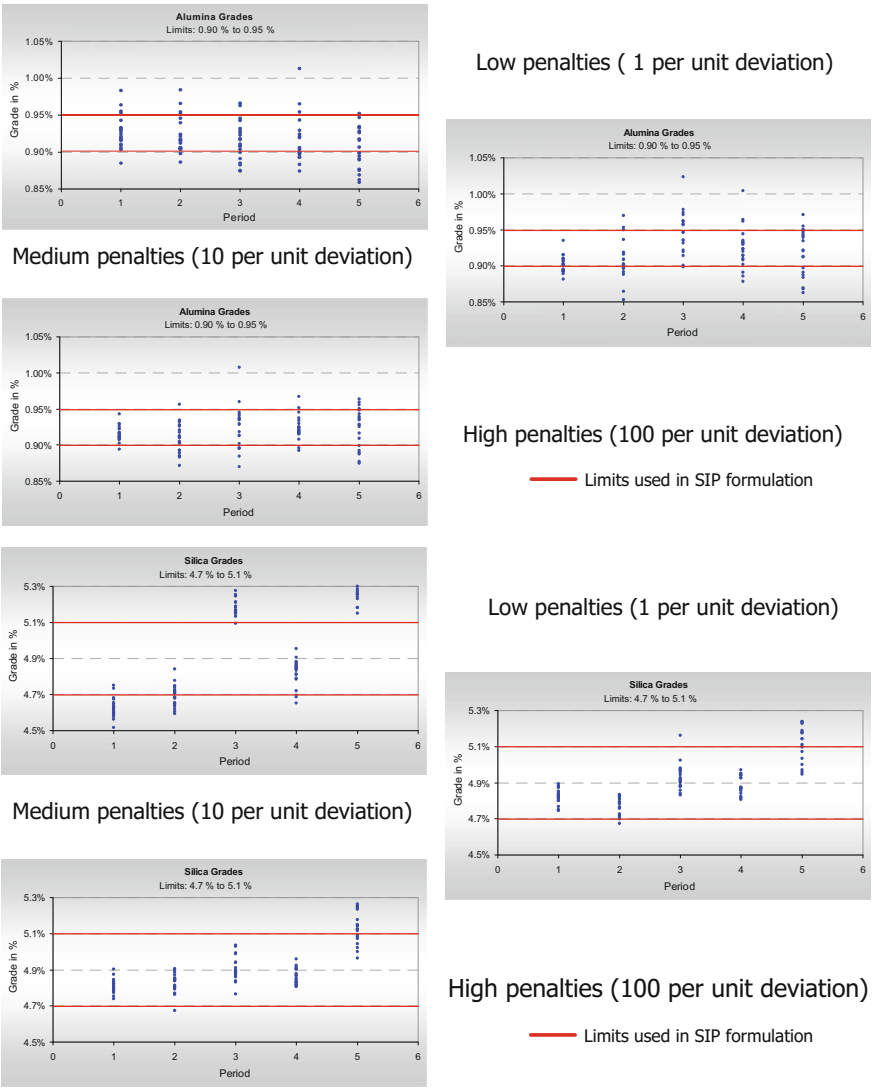

Fig. 6 Risk profiles for produced grades (alumina and silica) depending on penalties

competing objectives in the objective function: minimize risk of deviating from production targets and generate a smooth schedule.

Comparison to Traditional Production Scheduling Approaches

To demonstrate the benefit, stochastic modelling generates compared to an average-type based scheduling formulation, two production schedules are compared; one generated using 20 simulated orebody models referred to as the stochastic schedule and the second schedule is generated using a single average-type orebody model referred to as E-type model. The E-type orebody model is calculated by averaging block values of the 20 simulated orebodies for each element. The same scheduling formulation with parameters comparable to the

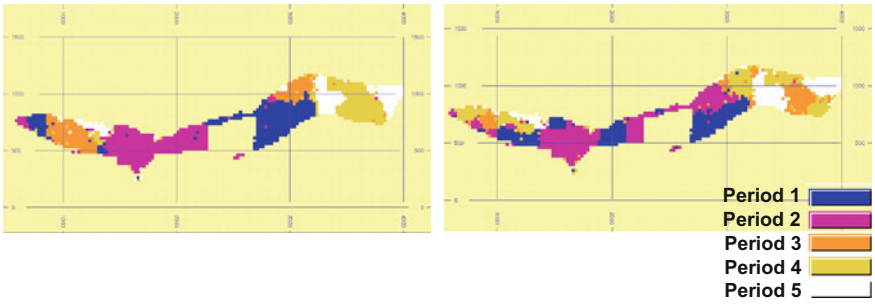

Fig. 7 Extraction sequence for the stochastic schedule (left) and the E-type based schedule (right)

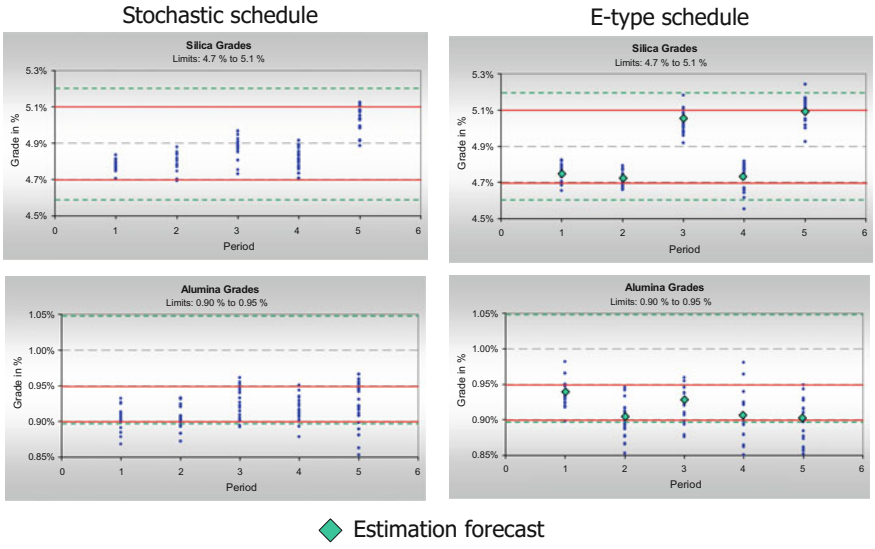

Fig. 8 Risk profiles for produced grades (silica and alumina) for the stochastic schedule (left) and the E-type based schedule (right)

stochastic approach generates the E-type schedule. Figure 7 shows the extraction sequence for the stochastic schedule and the E-type schedule for the lower bench. Both schedules show a relatively smooth sequence, which can be practically realised after manual open pit mine design. Figure 8 presents risk profiles for the critical elements SiO_2 or Al_2O_3 of both schedules. From the risk profiles presented in Fig. 8, it is evident that the E-type based schedule is not able to account for geological uncertainty. Although the mean values of the element grades produced in a period are inside the production targets, considerable deviations from upper and lower production limits for SiO_2 or Al_2O_3 are visible. In the stochastic schedule SiO_2 deviates only slightly in periods two and five with a probability of 5 and 20% respectively. The E-type schedule shows SiO_2 deviations from targets in each period with an average probability of 30%. The probabilities of deviating from upper and lower limits are almost twice as high for the E-type schedule compared to the stochastic based schedule, especially for Al_2O_3.

Conclusions

A new stochastic integer programming based mine production scheduling approach, which considers jointly multi-element geological uncertainty, is presented and successfully applied to production scheduling at the Yandi Central 1 deposit, WA. It is demonstrated that the SIP formulation presented, can be implemented as part of a multi-pit scheduling approach. In this application, results from BLASOR, a multi-pit scheduling optimization approach, are used to define the contribution of the Yandi Central 1 deposit, Western Australia, to the global target per period in terms of desired grades of elements and ore tonnages.

Results demonstrate the ability of the stochastic approach to control risk of deviating from production targets for critical quality defining elements. A comparison between the stochastically generated production schedule and a schedule generated using one estimated orebody model illustrated the benefit, stochastic models can generate. The stochastic schedule shows a higher probability in meeting production targets, which decreases overall project risk and can increase project value.

References

Benndorf J (2005) Efficient sequential simulation methods with implications on long-term production scheduling. Unpublished M.Phil thesis, The University of Queensland, Brisbane, p 225

Birge JR, Louveaux F (1997) Introduction to stochastic programming. Springer, New York, p 421

Boucher A (2003) Conditional joint simulation of random fields on block support. Unpublished M. Phil thesis, University of Queensland, Brisbane, p 168

Boucher A, Dimitrakopoulos R (2009) Block-support simulation of multiple correlated variables. Mathematical Geosciences 41(2):215–237

Chiles JP, Delfiner P (1999) Geostatistics, modeling spatial uncertainty. Wiley, New York, p 695

Datamine Manual (2002) Datamine-guide graphical mining software reference manual

David M (1977) Geostatistical ore reserve estimation. Elsevier, Amsterdam, p 364

David M (1988) Handbook of applied advanced geostatistical ore reserve estimation. Elsevier, Amsterdam, p 216

Dimitrakopoulos R (2007) Risk analysis in ore reserves and mine planning: conditional simulation concepts and applications for the mining industry. AusIMM-McGill 2007 Professional Development Seminar Series, p 385

Dimitrakopoulos R, Farrelly C, Godoy M (2002) Moving forward from traditional optimization: grade uncertainty and risk effects in open pit design. Trans Inst Min Metall Sect A 111:A82–A87

Dimitrakopoulos R, Ramazan S (2004) Uncertainty based production scheduling in open pit mining. SME Trans 316:106–112

Dowd PA (1997) Risk in minerals projects: analysis, perception and management. Trans Inst Min Metall Sect A 106:A9–A18

Godoy MC, Dimitrakopoulos R (2004) Managing risk and waste mining in long-term production scheduling. SME Trans 316:43–50

Goovaerts P (1997) Geostatistics for natural resources evaluation. Oxford University Press, New York, p 483

Leite A, Dimitrakopoulos R (2007) A stochastic optimization model for open pit mine planning: application and risk analysis at a copper deposit. IMM Trans Min Technol 116(3):109–118

Ramazan S, Dimitrakopoulos R (2004) Recent applications of operations research in open pit mining. SME Trans 316:73–78

Ramazan S, Dimitrakopoulos R (2013) Production scheduling with uncertain supply: a new solution to the open pit mining problem. Optim Eng 14(2):361–380

Ramazan S, Dimitrakopoulos R (2018) Stochastic optimisation of long-term production scheduling for open pit mines with a new integer programming formulation, in this volume

Ravenscroft PJ (1992) Risk analysis for mine scheduling by conditional simulation. Trans Inst Min Metall Sect A 101:A104–A108

Stone P, Froyland G, Menabde M, Law B, Pasyar R, Monkhouse P (2007) Blasor-blended iron ore mine planning optimization at Yandi. In: Orebody modelling and strategic mine planning: uncertainty and risk management models. The Australian Institute of Mining and Metallurgy, Spectrum Series 14, 2nd edn. pp 133–136

Whittle G (2007) Global asset optimization. In: Orebody modelling and strategic mine planning: uncertainty and risk management models. The Australian Institute of Mining and Metallurgy, Spectrum Series 14, 2nd edn, pp 331–336

Stochastic Mine Planning—Example and Value from Integrating Long- and Short-Term Mine Planning Through Simulated Grade Control, Sunrise Dam, Western Australia

A. Jewbali and R. Dimitrakopoulos

Abstract A new multistage stochastic mine production scheduling approach is developed and tested in a large operating gold mine. The proposed approach takes short-scale orebody information in the form of grade control data into account. As simulated orebodies used in stochastic long-term mine planning are based on sparse exploration data and while grade control data are unavailable at the time of production scheduling, the short-scale information is first simulated stochastically and then serves as input to the optimisation process. Stage 1 of the approach generates high density future grade control data for incorporation into the production scheduling process based on sequential co-simulation and pseudo cross-variograms between exploration data and grade control in previously mined out parts of a deposit. In Stage 2, the technique of conditional simulation by successive residuals enables pre-existing simulated orebody models to be updated using the simulated future grade control information. Stage is based on a stochastic programming mine scheduling formulation that handles multiple simulated orebody models from Stage 2 and accommodates both maximising Net Present Value (NPV) and minimising deviations from production targets. Stage 4 includes quantification of risk in the produced schedules generated, comparison of schedules and reporting. The application at a large operating gold mine demonstrates that the proposed approach is practical and adds value to the operation. The approach is shown to deliver additional ore (3.6 Mt more) and metal (2.6 million grams) which matches the mined reconciliations and results in a cumulative NPV which is on average A$7.7 M higher than that of a stochastic schedule without the simulated grade control data and substantially higher (about 30%) compared to the NPV from the actual schedule of the mine.

A. Jewbali (✉)
Rio Tinto, 152-158 St. Georges Terrace, Perth, WA 6000, Australia
e-mail: Arja.Jewbali@riotinto.com

R. Dimitrakopoulos
COSMO—Stochastic Mine Planning Laboratory, Department of Mining and Materials Engineering, McGill University, Montreal, QC H3A 2A7, Canada
e-mail: roussos.dimitrakopoulos@mcgill.ca

R. Dimitrakopoulos (ed.), *Advances in Applied Strategic Mine Planning*,
https://doi.org/10.1007/978-3-319-69320-0_13

Introduction

Stochastic mine planning is a relatively recent development aimed at addressing uncertainty in ore supply from an orebody, commodity prices and metal demand, as well as expanding to other issues of uncertainty in mine planning. The existing work focuses largely on open pit mine design and production scheduling with uncertain grades/metal content and geological conditions. It includes life-of-mine (LOM) production scheduling based on optimal mining rates and simulated annealing (Godoy and Dimitrakopoulos 2004), simulated annealing with constant mining rates (Leite and Dimitrakopoulos 2007), stochastic integer programming formulations including a stochastic stock pile (Ramazan and Dimitrakopoulos 2013), further tests of this last approach (Leite and Dimitrakopoulos 2007, 2014, in this volume), expansion for multiple elements (Benndorf and Dimitrakopoulos 2018, in this volume) and others. The two key aspects of all the above mentioned approaches and related example case studies are that the derived long-term production schedules:

1. Have substantially higher present value than the traditionally used approaches with differences between 20 and 30%, and
2. Minimise the potential deviations from production targets set given the available drilling and orebody models.

Recent work further considers integrating market uncertainty in choosing from different mine designs which also consider geologic uncertainty and show further monetary benefits of quantifying and integrating uncertainty (Dimitrakopoulos and Abdel Sabour 2007). Meagher et al. (2010) explore the effects of optimising pits in a new approach that assesses the combined effect of metal and price uncertainties using a network flow approach; their study shows once again the value of stochastic approaches and the integration of key uncertainties to mine planning.

The work above is all based on two elements, in addition to new stochastic mine design and scheduling methods. Firstly, the ability to simulate sets of equally possible representations of the orebody being assessed. This set of orebodies is the input to the above mentioned stochastic optimisers and represents the geological uncertainty and local grade variability of the orebody, as understood from the available drill hole data—this drastically differs from the conventional single estimated (smoothed out or average type) input to conventional mine design and optimisation methods and is the major reason for improved results from the stochastic scheduling methods discussed. Secondly, the ability to assess cash flows using evaluation methods based on multiple simulated realisations of the related commodity price, rather than single average and typically constant, over the LOM and metal price forecasts. Both this second element and the use of uncertainty in metal content leads to improvements in the last two studies above.

A limit of both stochastic and conventional long-term planning and optimisation of production planning is that short-term schedules may frequently deviate from the expectations of long-term ones. While long-term production scheduling is used to

maximise the Net Present Value (NPV) of a project, short-term production scheduling focuses on meeting short-term production demand within the long-term plan, given the processing capacity of the mill and managing the quality of ore being processed. Both short- and long-term scheduling are usually based on exploration-scale orebody models, whereas the actual short-term production performance is controlled by local, blasthole-scale data used for grade control and ore/waste selection, usually not available at the time of scheduling. As a result, short-term production sequences deviate from the long-term plans and are adjusted to meet mill demand or the production performance may substantially deviate from forecasts. In short, discrepancies occur between what is forecasted and what is actually mined.

A solution to the above is to consider production scheduling approaches that are capable of reflecting short-scale behavior of the orebody beforehand, that is, at the planning stage and through grade information available before the actual grade control drilling. High density grade control information offers tighter controls on geology and mineralisation characteristics and predicts qualities and quantities closer to what is actually being mined. Although not available prior to blasthole drilling, grade control data can be simulated in different ways. Simple random sampling errors added to simulated realisations from exploration data, have been used to assess production schedules reported in a feasibility study (Guardiano et al. 1995) and a conceptually similar more sophisticated approach is considered for assessing mineral resources by Journel and Kyriakidis (2004). In operating mines, errors from field duplicates or from nearest paired grade control holes and drill holes have been used to simulate realisations of future grade control data and assess short-term production schedules at Escondida copper mine, Chile (Khosrowshahi et al. 2017). Multiple simulations of correlated sampling errors using data from previously mined parts of the deposit have been used at Morila gold deposit, Mali (Peatie and Dimitrakopoulos 2013) with excellent results in reconciliations. With the exception of the last one, past approaches are relatively simplistic. All existing work in this area assesses potential risks in production schedules or potential reserves—however, it does not address the major question: How to improve or reduce deviations of forecasts from actual production at the time of planning while maximising the present value of an asset. This can be effectively addressed only by technically integrating short-scale orebody variability and grade control with, short- and long-term LOM production planning into one approach.

Short-scale information is the core element in the above-mentioned integration. As this information is unavailable and needs to be stochastically simulated at the time of LOM planning, the way to utilise a range of possible scenarios is through the stochastic optimisation formulations used in stochastic mine planning as reviewed above. This paper contributes a new multistage approach to production scheduling that incorporates, short-scale deposit information and related grade uncertainty into the scheduling process. The approach allows for the realistic integration of short- and long-term mine production schedules, as well as the generation of more reliable mine production forecasts. A case study at an operating gold deposit demonstrates the approach, provides comparisons between the

traditional schedules of the mine, accounts for stochastic schedules before and after simulated dense grade control information and quantifies the expected monetary value of the method. In the next sections, the proposed approach is first outlined, the case study presented, results are analysed and conclusions follow.

A New Multistage Approach to Production Scheduling

The multistage approach to production scheduling proposed here is as sequence of steps employing separate techniques for each stage. The approach differs conceptually from the traditional approaches in many aspects. A major difference is that it requires multiple, equally probable representations of the orebody, which are generated from spatial Monte Carlo simulation methods and at two different levels. The first level is that of exploration-type data sets and information; the second level is that of grade control data. This simulation-based framework assists in quantifying and generating risk managing schedules as well as accommodates the interaction of information at different scales, both in space and time. Different scales in space refer to the:

- Local variability of the deposit and local classification of materials selected as ore and waste through a grade control process, and
- Physical parts of the orebody that are mined over long periods of time as individual pit units (cut-backs) and parts of individual pit units that correspond to the parts of cut-backs mined over short periods of time from the same mining front.

Different scales in time refer to the:

- Yearly time units on which the long-term plans are reported, and
- Relatively shorter time periods in short-term planning (weekly, monthly or quarterly).

As a result of the ability to link information at different scales in space and time, short scale variability, short- and long-term schedules are integrated. The proposed approach or process has four stages shown in Fig. 1, which also shows how this compares to the four steps followed in the existing stochastic LOM planning:

1. *Stage 1*: Generate high density future grade control data for incorporation into the production scheduling process. This data is not yet available at the time of planning and is simulated.
2. *Stage 2*: Update pre-existing simulated orebody models using the simulated future grade control information and a suitable stochastic simulation technique.
3. *Stage 3*: Generate production schedules using a stochastic optimisation method handling multiple simulated orebody models from Stage 2, which accommodates both maximising net present value and minimising deviations from production targets.

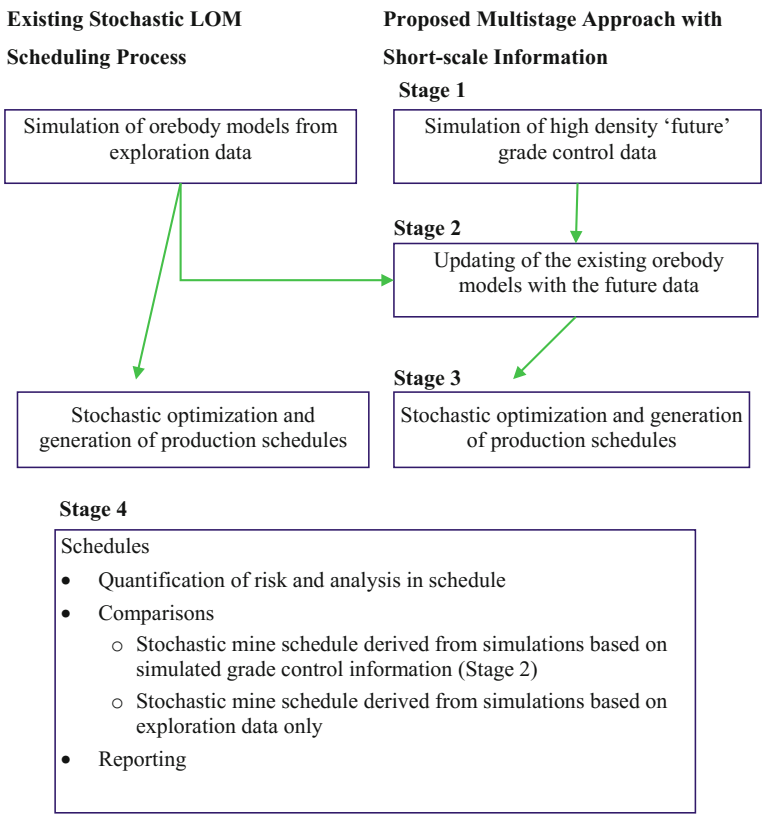

Fig. 1 Schematic presentation of the proposed multistage mine scheduling approach

4. *Stage 4*: Quantify grade risk in the produced schedules, compare schedules with and without simulated short scale orebody information, and report mine schedules as needed.

These four stages are discussed next in greater detail.

Stage 1—Simulation of Future Grade Control Drilling Data

High density future grade control data can be simulated using several approaches, such as those reviewed in the introduction. A more elaborate and effective method is outlined here and is used in the case study that follows. The method, schematically shown in Fig. 2, assumes that there are mined out parts of an orebody with grade control information of comparable quality and characteristics to the remainder (as yet un-mined) of the orebody being studied.

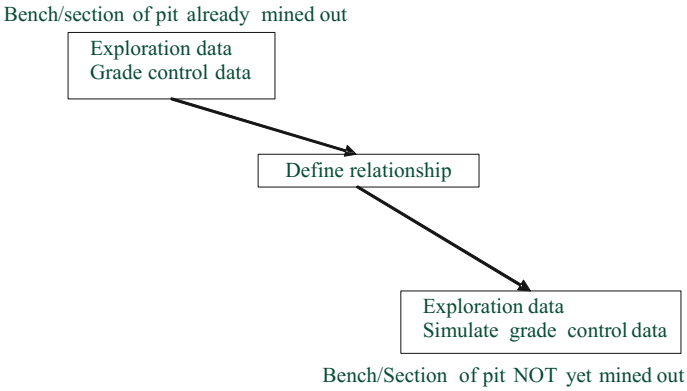

Fig. 2 Simulating future grade control data

Exploration drilling and grade control data from a mined out section or bench of a deposit is used to quantify the spatial relationship between the two types of data. As it is not physically possible to have exploration and grade control information available at the same location, their spatial cross-correlation (relationship) is quantified through the so-called pseudo cross-variogram (Myers 1991). Having quantified this spatial relationship, a method such as the sequential Gaussian co-simulation of two variables (Goovaerts 1997) can be used to generate the future grade control data in un-mined sections of an open pit. The co-simulation approach ensures that the simulated future grade control data have the same distribution as past grade control information and the same auto- and cross-correlation (with exploration data).

Stage 2—Updating of Existing Simulations with Future Grade Control Data

The second stage of the production scheduling approach presented herein involves the updating of pre-existing simulated orebody models. This is because orebodies under study have frequently already been simulated for other purposes, or because there can be more than one scenario of possible sets of future data to consider, and so on. Generally the ability to update pre-existing realisations of an orebody is useful in improving the efficiency of the process. The only known simulation technique that is capable of providing updating capabilities to accommodate the updating of pre-existing simulations with new data such as grade control is the technique of conditional simulation by successive residuals or CSSR (Vargas-Guzman and Dimitrakopoulos 2002). The end result of the use of CSSR is

a set of simulated orebody models that are conditioned on both the known exploration data and the simulated future grade control data. Note that new information for updating may also be additional data from near mine exploration drilling, or in fill drilling.

Stage 3—Stochastic Integer Programming Formulation

To generate production schedules, a stochastic optimisation formulation based on Stochastic Integer Programming (SIP) is used, and it is a simpler version of the one developed in Ramazan and Dimitrakopoulos (2013, 2017) as well as discussed in Leite and Dimitrakopoulos (2014). The objective function of this formulation maximises the expected discounted cash flows while minimising the cost of deviating from the set production targets and it is:

$$Max \sum_{t=1}^{p} \sum_{i=1}^{N} E(NPV)_i^t X_i^t - \sum_{s=1}^{S} \sum_{t=1}^{P} \sum_{r=1}^{R} \left({}^{s}Cu_r^t Yu_r^t + {}^{s}C1_r^t Y1_r^t \right) \quad (1)$$

where:

P	is the number of periods to schedule
N	is the total number of blocks to schedule
S	refers to the number of simulated orebody models
R	is the number of targets
X_i	is a binary variable indicating block i mined in period t (1 = mined/0 = not mined)
$E(NPV)_i$	is the expected NPV to be generated if block i is mined in period t
Yu_r^t	is the excess amount produced compared to the target (grade/tonnage) r in period t for orebody model s
${}^{s}Cu_r^t$	is the unit cost to penalise Yu_r^t in period t
$Y1_r^t$	is the deficient amount produced in relation to target (grade/tonnage) r in period t for orebody model s
${}^{s}Cu_r^t$	is the unit cost to penalise $Y1_r^t$ in period t

The first component in Eq. 1 maximises the total discounted cash flow and the expected Net Present Value (NPV) is determined by calculating economic values for each simulated model, then averaging them. This component reflects the conventional goal of optimising total discounted cash flow over the LOM. The second component minimises the deviations between expected productions as these are described by simulated orebody models used as input and a set of mine production targets and minimises the risk of not meeting targets due to grade uncertainty. The deviations are calculated over the set of simulated orebody models and are penalised with costs. This second component reflects the goal of short-term production

scheduling, and its use together with the first component provides the means to integrate long- and short-term planning, in the context of the approach proposed herein. It should be noted that a novelty of this formulation is that the costs can be discounted for each subsequent period using a geological discount rate. As a result, the cost related to not meeting mill requirements can be set higher in the first period than in subsequent periods, allowing the risk distribution between production periods to be managed.

Stage 4—Quantification of Uncertainty

Stage 4 aims to quantify grade risk in the produced schedules that have been generated. Any schedule can be assessed against possible scenarios of orebodies, be they constructed from exploration datasets only or in combination with future grade control data. This allows comparisons and assessments, including an evaluation of effects from potential short-scale orebody variability.

Case Study at a Gold Mine

The Gold Deposit and Mine

The gold deposit in this case study lies along a shear zone and the general trend of the gold mineralisation is parallel to this zone. Gold mineralisation can be both secondary and primary. Secondary mineralisation is related to iron oxidation fronts and water tables and to aggregation within paleochannels, while primary mineralisation can roughly be related to high strain shear zones by low strain stockwork-vein zones. Based on the deposit geology, 17 domains are inside the open pit (sections of which are shown in Fig. 3). Mining is done using four excavators which load into 25 rear dump trucks. Since opening, the mine has produced more than two million ounces of gold. The pit is about 2.1 km long and 1.1 km wide with a final depth of 450 m to be reached at end of its life. The total amount of waste mined in 2004 was about 43 Mt, which drops to about 26 Mt in 2005 and again to 11 Mt in 2007. This will necessitate a resizing of the equipment fleet sometime in mid-2005. Figure 3 depicts the long-term (yearly) production schedule in use at the mine. The mine's schedule proceeds one layer at a time and indicates that the pit will be exhausted by the end of the fifth year. At this mine, blasting occurs on 7.5 m benches and grade control is done using reverse circulation drilling on 5 m $\times$ 7 m spacing. The plant capacity is 3.6 Mt/a and the mill circuit consists of crushing and grinding after which the gold is recovered through a Carbon in Leach (CIL) circuit.

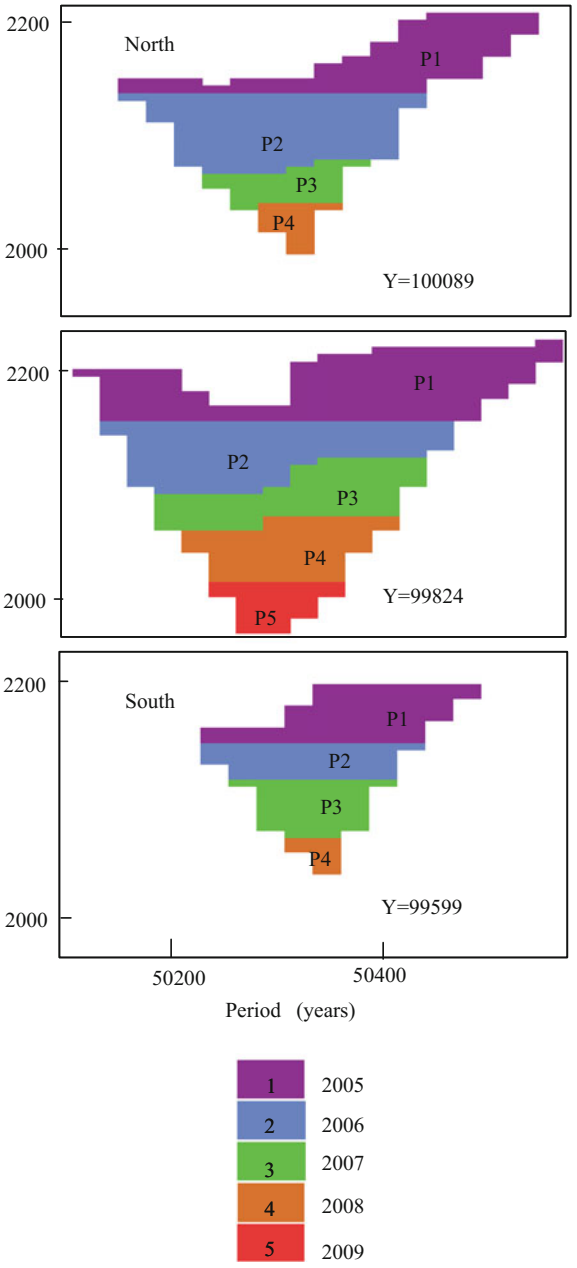

Fig. 3 East–West sections of the yearly schedule in a gold mine

Generation of Future Grade Control Data

Within the mined out section of the pit, 75,789 grade control drill holes were available. These were separated based on the geological domain they belonged to. In addition, 3934 exploration diamond and reverse circulation holes were available within the same section of the pit. These were also divided based on geological domains. For each geological domain these two sets of information were used to derive the relationship between exploration and grade control data. This relationship can than be extended to unmined sections of the pit where only exploration data is available. For the purposes of this study, twenty future grade control data simulations were generated, using the sequential cosimulation method discussed earlier, on 5 m $\times$ 7 m $\times$ 2.5 m spacing in the unmined sections of the pit (the volume displayed in Fig. 3).

Updating Existing Simulations with Future Grade Control Data

Stage 2 of the production scheduling approach involves using conditional simulation by successive residuals to update pre-existing orebody models. The 20 available simulations (on 2 m $\times$ 2 m $\times$ 2.5 m spacing) conditioned on exploration data were updated with the 20 simulated future grade control data generating a set of 400 simulations that are conditioned on both the known exploration data and the simulated future grade control data scenarios. Twenty updated simulations are chosen at random for further study. For reasons of comparison and processing, the simulations are reblocked to 15 $\times$ 30 $\times$ 7.5 m^3 blocks, which is the block size used at the mine. Grade tonnage curves are shown in Fig. 4. It is apparent from the figure that for the model based on exploration data, the average grade above cutoff is higher at all cutoffs. The amount of tonnes above cutoff is lower compared to the updated models.

Figure 5 displays the ore tonnes and metal recovered when mining is done according to the mine's yearly schedule (as shown in Fig. 3) when short scale deposit information is taken into account. The risk profiles were generated by running the 20 updated models through the mine's yearly schedule. During this process the tonnes of ore/metal produced and NPV generated by each updated model was recorded and plotted on Fig. 6. The updated models indicated that the amount of ore tonnes produced is not enough to fill the plant to capacity (3.6 Mt/a) for all the years from 2005 to 2009. They also indicate a 50% chance of negative NPV in 2005 when insufficient metal is produced.

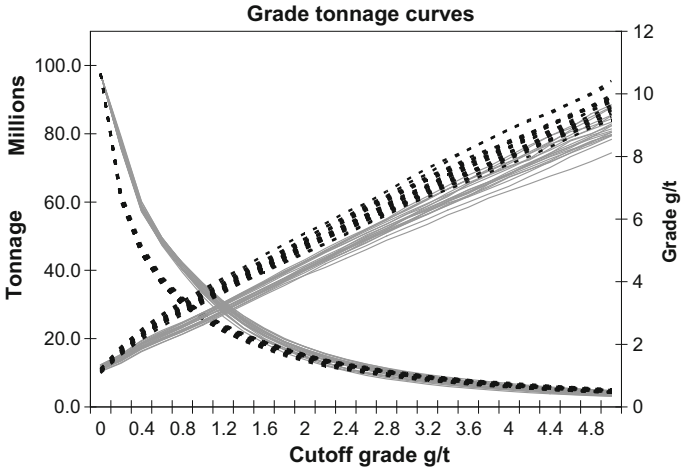

Fig. 4 Grade tonnage curves for the models based on exploration data (dotted lines) and the models updated with simulated future grade control data (solid lines)

Deriving Production Schedules using the SIP Formulation

The following section describes the process, as given in Fig. 1, used to derive the production schedules. First the 20 simulated orebody models conditioned on exploration data are put through the SIP formulation in Eq. 1. Next, the 20 updated orebody models are then run through the SIP formulation and a production schedule accounting for short-scale orebody information is derived. This methodology allows for a comparison of the schedules derived using orebody models based on two sets of information. As a result, it provides a look at the consequences of not taking closer spaced grade control information into account when performing production scheduling.

The production schedules were generated for four month periods (short-term schedules). The production capacity for each four month period was set at 1.2 MT and the targeted grade constraints between 2 and 7 g/t. To make the schedules practical for equipment mobility and space, the schedules were smoothed. After smoothing, the simulated orebody models are run through their respective schedules to generate risk profiles for ore, metal and NPV. Each short-term schedule was regrouped to generate the yearly LOM schedule of the mine. The risk profiles of the production schedule derived from the 20 exploration based models for ore, metal and NPV are shown in Fig. 6. As the figure shows, the yearly production target of 3.6 Mt/a is met for 2005–2007. Note that this schedule predicts that the pit will be exhausted by 2008. Figure 7 describes the schedule derived from the updated models. This schedule extends the life of mine by another year to 2009. As the figure shows, the short-term schedule has no problem delivering 3.6 Mt/a of ore in all years except in 2009, when the last of the ore will be mined.

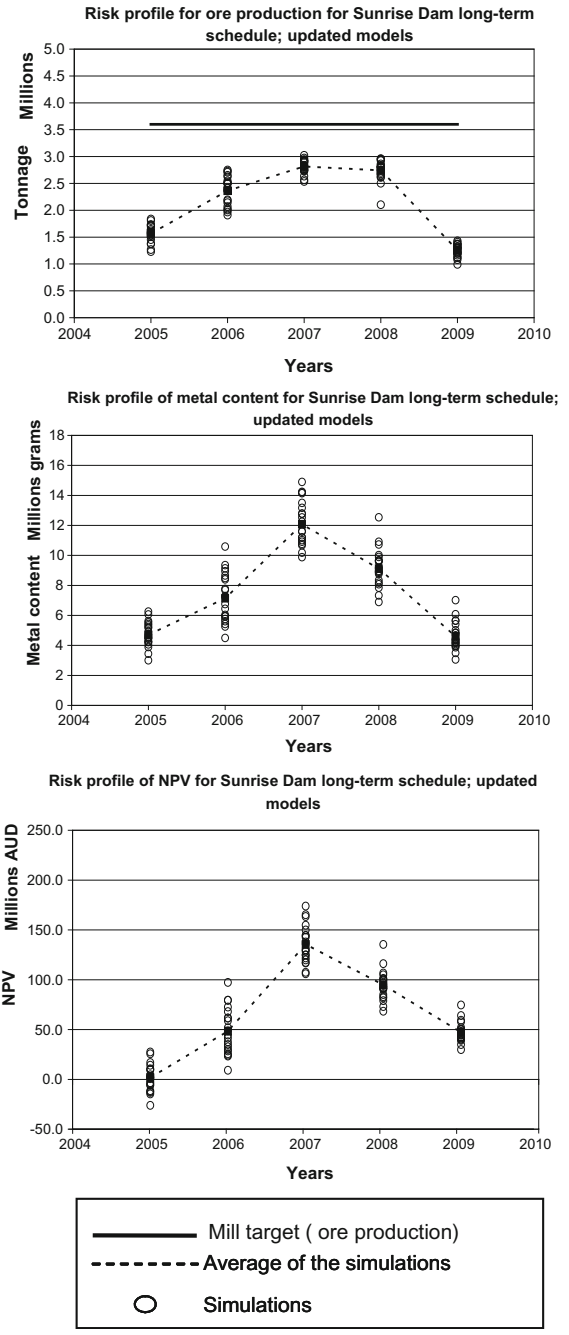

Fig. 5 Performance of the mine's yearly schedule when local orebody information is taken into account

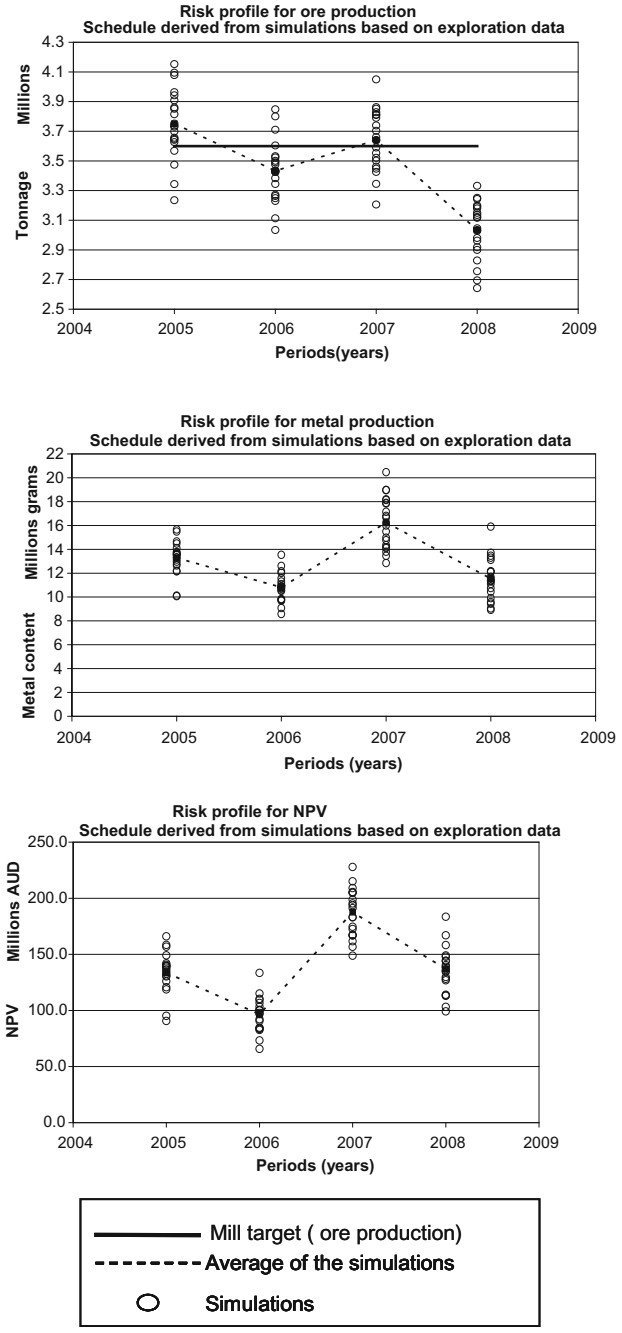

Fig. 6 Risk profile of ore, metal and NPV for the production schedules derived from orebody models based on exploration data

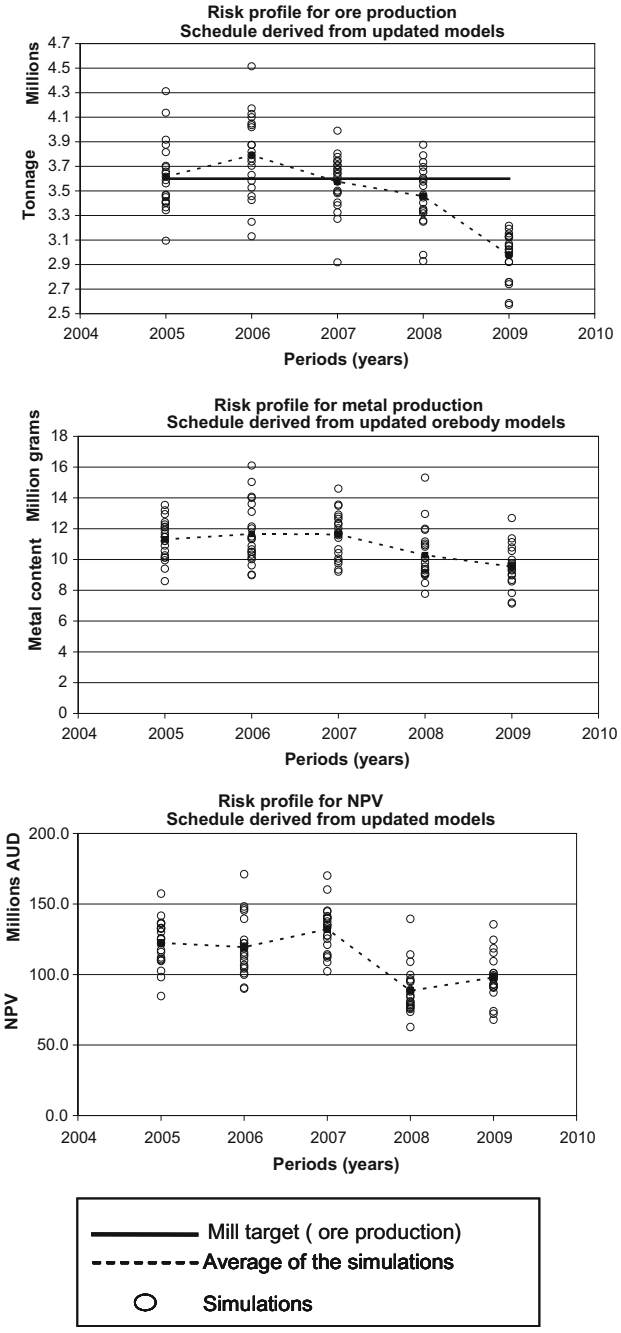

Fig. 7 Risk profiles of ore, metal and NPV for the production schedule derived from orebody models displaying grade control characteristics

The schedules based on updated models produce 3.6 Mt more ore and as a consequence 2.6 million grams more metal, which results in a cumulative NPV that is A$7.7 M higher. The production schedules based on orebody models derived from exploration data (that do not account for local orebody knowledge and characteristics) underestimate the actual tonnes of ore mined from the orebody. The derived exploration based schedules are a conservative option. Taking local grade control information into account indicates that there is probably sufficient ore to extend the life of mine to 2009 compared to 2008 when only exploration data is used. Figure 8 displays the production schedules for the exploration based simulations and the updated simulations. As Fig. 8 shows, the two schedules are different in that different sections of the pit are mined out in different time periods. However, when compared to Fig. 3, both of the SIP derived schedules mine the pit out in a series of successive cones, while the mine's yearly schedule proceeds in layers (Table 1).

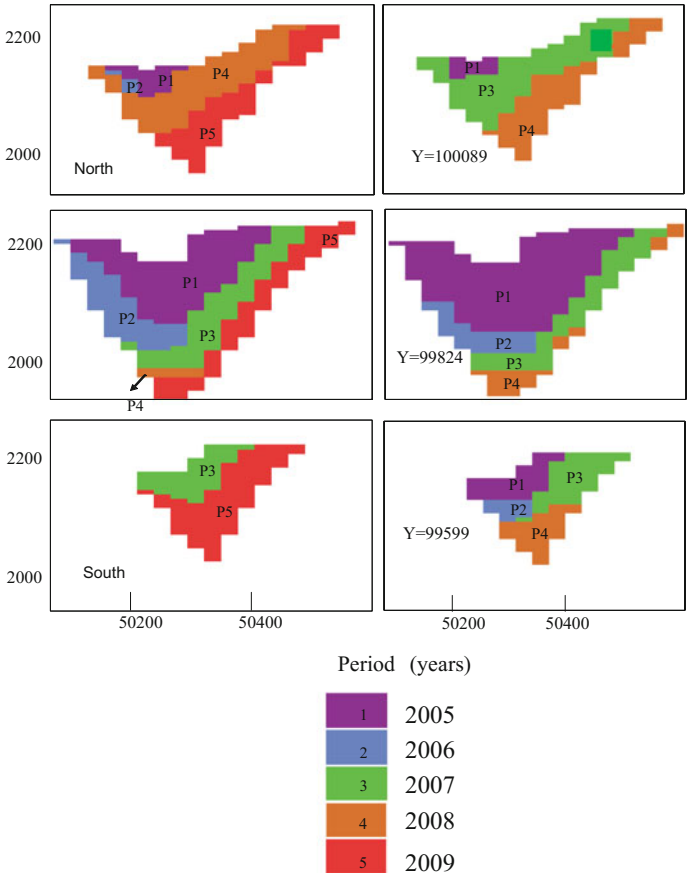

Fig. 8 West–East sections of the sunrise pit displaying production schedules derived from simulation based on exploration data (right) and updated models (left)

Table 1 Cumulative averages for ore tonnes, metal and NPV over all simulated orebody models (both exploration data based and updated models)

	SIP and simulations with exploration data	SIP and updated simulations with 'future' data	Mines schedule performance with updated simulations
Ore tonnes (million grams)	14	18	10
Metal tonnes (million grams)	52	55	38
NPV (million AUD)	552	560	330

Conclusions

A new multistage stochastic mine production scheduling approach presented herein includes four stages:

1. *Stage 1*: generates high density future grade control data for incorporation into the production scheduling process. It is based on sequential Gaussian co-simulation of exploration and grade control data from previously mined out parts of a deposit.
2. *Stage 2*: employs conditional simulation by successive residuals to update pre-existing simulated orebody models with the simulated future grade control information from Stage 1.
3. *Stage 3*: uses a stochastic integer programming mine scheduling formulation and balances both maximising net present value and minimising deviations from production targets.
4. *Stage 4*: includes quantification of risk in the produced schedules generated and reporting.

The application at a large operating gold mine demonstrates that the proposed approach is practical and adds value to the operation. The approach is shown to deliver 3.6 Mt of additional ore and 2.6 million grams more metal—which matches better with the mine's reconciliations. The approach also results in a cumulative NPV which is on average $7.7 M higher that that of a comparable stochastic schedule without the simulated grade control data and substantially higher when compared to the NPV from the actual schedule of the mine.

Acknowledgements The authors are grateful to AngloGold Ashanti for funding and multifaceted support, Rio Tinto for funding, as well as additional support from NSERC grants and McGill's COSMO Stochastic Mine Planning Laboratory.

References

Benndorf J, Dimitrakopoulos R (2018) Stochastic long-term production scheduling of iron ore deposits—integrating joint multi-element geological uncertainty, in this volume

Dimitrakopoulos R, Abdel Sabour SA (2007) Evaluating mine plans under uncertainty: can the real options make a difference? Resour Policy 32:116–125

Godoy M, Dimitrakopoulos R (2004) Managing risk and waste mining in long-term production scheduling of open pit mines. Trans Soc Min Metall Explor 316:43–50

Goovaerts P (1997) Geostatistics for natural resources evaluation, Oxford University Press, New York, p 483

Guardiano E, Parker HM, Isaaks EH (1995) Prediction of recoverable reserves using conditional simulation: a case study for the Fort Knox gold project, Alaska, Unpublished report, Mineral Resources Development Inc, Foster City

Journel AG, Kyriakidis PC (2004) Evaluation of mineral reserves: a simulation approach. Oxford University Press, New York, p 216

Khosrowshahi S, Shaw WJ, Yeates GA (2018) Quantification of risk using simulation of the chain of mining—a case study on Escondida Copper, in this volume

Leite A, Dimitrakopoulos R (2007) A stochastic optimisation model for open pit mine planning: application and risk analysis at a copper deposit. Trans Inst Min Metall Min Technol 116: A109–A118

Leite A, Dimitrakopoulos R (2014) Mine scheduling with stochastic programming in a copper deposit: application and value of the stochastic solution. Min Sci Technol 24(6):755–726

Meagher C, Abdel Sabour SA, Dimitrakopoulos R (2010) Pushback design of open pit mines under geological and market uncertainties. In: Dimitrakopoulos R (ed) Advances in orebody modelling and strategic mine planning I. The Australasian Institute of Mining and Metallurgy, Melbourne, pp 291–298

Myers D (1991) Pseudo cross-variograms, positive definitness and cokriging. Math Geol 14:805–816

Peatie R, Dimitrakopoulos R (2013) Forecasting recoverable ore reserves and their uncertainty at morila gold deposit, Mali: an efficient simulation approach and future grade control drilling. Math Geosci 45(8):1005–1022

Ramazan S, Dimitrakopoulos R (2013) Production scheduling with uncertain supply: a new solution to the open pit mining problem. Optim Eng 14:361–380

Ramazan S, Dimitrakopoulos R (2018) Stochastic optimisation of long-term production scheduling for open pit mines with a new integer programming formulation, in this volume

Vargas-Guzman JA, Dimitrakopoulos R (2002) Conditional simulation of random fields by successive residuals. Math Geol 34:507–611

A New Methodology for Flexible Mine Design

B. Groeneveld, E. Topal and B. Leenders

Abstract Uncertainty and risk are invariably embedded in every mining project. Mining companies endeavouring to maximise their return for shareholders make important strategic decisions which take years or even decades to 'play out'. Therefore, developing a model that analyses the potential payoff of a decision based on current fixed assumptions is severely flawed. A model that incorporates uncertainty and is able to adapt, almost certainly will help deliver a design with a better risk-return profile. In this paper, a new approach is developed in order to have a design that is flexible and able to adapt with change. This is achieved by developing a mixed integer programming model that determines the optimal design for simulated stochastic parameters. This research has incorporated optionality (flexibility) in relation to mining, stockpiling, processing plant and port capacity. The results are promising and are helping decision makers to think in terms of value, risk and frequency of execution.

B. Groeneveld (✉) · E. Topal
Mining Engineering Department, Western Australian School of Mines,
Curtin University of Technology, GPO Box U1987, Perth, WA 6845, Australia
e-mail: benjamin.groeneveld@gmail.com

E. Topal
e-mail: e.topal@curtin.edu.au

B. Groeneveld
Oyu Tolgoi Underground Mine Planning and Technical,
Rio Tinto, 123 Albert Street, Brisbane 4000 QLD, Australia

B. Leenders
Expansion Projects, Resource Development Division, Rio Tinto Iron Ore,
Perth, WA 6000, Australia
e-mail: bob.leenders@riotinto.com

R. Dimitrakopoulos (ed.), *Advances in Applied Strategic Mine Planning*,
https://doi.org/10.1007/978-3-319-69320-0_14

Introduction

Mining projects are characterised as being highly uncertain and variable mainly due to the volatile nature of commodity prices and uncertainty around geological conditions encountered in ore bodies. Uncertainty can arise from many different sources including; market prices, grade distribution, ground conditions, equipment reliability, recovery of ore, human capital and legislative change (Topal 2008). The mining industry will be more sustainable if projects are developed in a manner that increases flexibility to respond to uncertainties the business cycle. For example, the global minerals industry has seen an unprecedented demand for its products in recent years, however the industry has struggled to change its level of supply in response to price movements. Being able to design an operation that has flexibility to respond to this change quickly will deliver better returns to stakeholders.

Geological uncertainty and risk have been incorporated in optimum mine planning and design by a few studies to date. Ramazan and Dimitrakopoulos (2004) develop a stochastic based mixed integer programming (MIP) model for multiple element that uses several simulated orebodies in order to minimise the grade uncertainty in the life of the mine schedule. The model also takes into account risk quantification, equipment access and mobility and other operational requirement such as blending, mill capacity and mine production capacity. Godoy and Dimitrakopolus (2004) develop a new set of way to generate a mine production schedule under geological uncertainty. The first stage of the method generates a stable solution domain which shows the possible ore and waste extraction rates for a given open pit. The second stage generates optimum ore production and waste removal under uncertainty. The third stage generates a series of physical schedules which obey slope constraints, maximise the equipment utilisation and meet mill requirements while matching the mining rates previously derived by the optimisation. The last stage generates a single mining sequence from alternative sequences produced in the third stage by using a new algorithm based on the simulated annealing method. Leite and Dimitrakopoulos (2007) develop a stochastic based optimisation model for open pit mines and apply it to a copper deposit for risk analysis. The study shows the stochastic approach generates 26% higher NPV than the conventional schedule. Also, the study suggests that life of mine schedules which incorporate geological uncertainty lead to more informed investment decisions and improved mining practice.

A developing decision making tool aimed at increasing the flexibility of an engineering system is Real Options 'in' projects. Significant research into this method has been undertaken by Wang and de Neufville (2005, 2006) and his colleagues with applications in various industries. This method is located midway between financial Real Options analysis (which does not deal with system flexibility) and traditional engineering approaches (which does not to deal with financial flexibility). A popular example used to explore the concept of Real Options 'in' projects is that of a multi-story car park. Flexibility in this situation is in the design of the footing and columns of the building so that additional levels can be added at a later date. This flexibility comes at a cost, and the designer must determine if this is

warranted. An example of the opportunity this technique poses is applied by Cardin et al. (2008) in conjunction with Codelco, to a Chilean mine in the 'Cluster Toki' region. In this example, a staged development of the Real Option 'in' projects methodology is used where different operating plans are designed to respond to changing prices. Truck fleet capacity and crusher size were altered in the different operating plans. The application of this method resulted in approximately 30–50% more accurate project value than current estimates. This approach provides a strong basis on which to grow Real Options 'in' projects theory for mining. However, there are several deficiencies in the current model. First, the initial scenario construction used in the model, limits the flexibility up front in the model and prevents the optimal design being chosen. Therefore, how useful is this technique for valuing flexibility? Secondly, the model fails to deal with variations in grade and recovery in a transparent manner; one of the key drivers. Finally, the model does not incorporate options at all stages of a typical mine value chain (de Neufville et al. 2005; Wang and de Neufville 2005, 2006; Cardin 2007; Cardin et al. 2008). This paper outlines a new methodology to evaluate the flexibility of strategic mine design under uncertainty, using Mixed Integer Programming (MIP) and Monte Carlo Simulation (MCS). An application of this methodology to a hypothetical case study will be undertaken in order to show the power of the model to handle complex strategic decisions.

Methodology

In order to evaluate the flexibility in strategic mine design, this research employs MIP and MCS. In particular, MIP allows for 'go' or 'no go' decisions to be modelled for the optimal execution under a set of uncertainties. Uncertainties (or stochastic parameters) can be simulated using MCS. In this way, each model (or trial) represents a single path of a lattice tree (or binomial tree).

Description of Model Components

The model consists of three main components which feed the MIP model; resource model, design options and stochastic parameters (Fig. 1). Running the model multiple times generates a database of optimal designs for a given 'state-of-the-world'. This dataset then provides a pathway to determine the flexibilities that provide the best risk-return profile.

Overview of Resource Model

Resource characteristics are a driving force in mine design. The MIP model uses a resource model to provide a representation of material that is available for

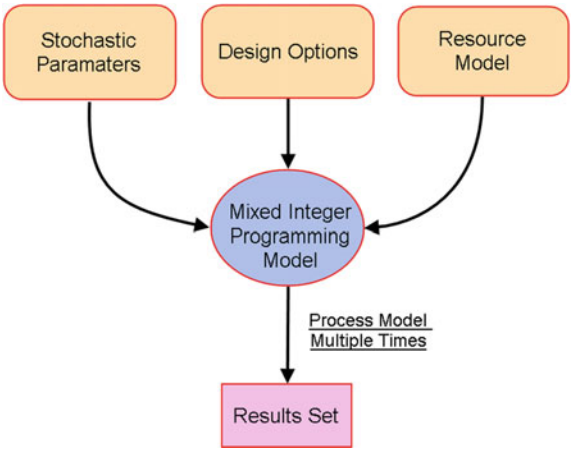

Fig. 1 Conceptual diagram of how the various model components feed the Mixed Integer Programming model and the result set

processing through the life of mine (both ore and waste is considered). The representation of the resource is carried out by parcels of material. A parcel of material can be defined as a quantity of material with an average grade determined by the weighted average of the grade bins contained within the parcel. A parcel may be made up of one or more grade bins. A grade bin represents a quantity of material at a specified grade. This is incorporated to provide a higher level of detail to the model which will alter the decisions on how material is processed, whilst minimising the number of integer variables. These parcels are designed to represent a physical constraint on the resource. The most common physical constraint is the vertical mining constraint which is included in the model through parcel dependency. Mining of the grade bins within a parcel can occur in any order as long as the average parcel grade (within a nominal deviation) is extracted each period. This forces the model to take waste and ore in the same proportion.

Overview of the Design Options

Flexibility is included through various design options in the MIP model. Solving the MIP models will determine which options are executed and when. A full set of design option are dynamically incorporated in the model which determine if and when these options should be executed. These options are broken into four categories; mine, pre-processing stockpiling, processing plants and port capacity. More than one option type can be executed in each period, hence these are not mutually exclusive decisions. An illustration of the material flow and points where design options may occur is shown in Fig. 2. Some assumptions have been made to simplify the model at this early stage of development. These assumptions can be removed with further refinement to the model; one type of circuit exists in each plant with one set of beneficiation characteristics; port stockpiles are not available in the model. This means the model must ship material as soon as it is processed.

Available Mine Options in the Model

Mine options are incorporated in the model to reflect mining capacity constraints that exist in an operation. It is not feasible to have unlimited mining capacity, due to the high capital cost associated with additional capacity and/or technical pit constraints (geotechnical and equipment interaction). Mine options can be modelled to reflect truck capacity or shovel capacity. This type of decision is repeatable many times in each period (i.e. you can purchase more then one truck of the same type), thus mine options are represented as integers. This allows for one or more trucks of the same type to be purchased in each period.

Available Stockpile Options in the Model

Stockpiling is used in mine operations for many reasons including; blending of material, storage of excess mine production and storage of low grade ore for future production. Long-term stockpiling is included in the model allowing material to be stored on a stockpile in time (t) and removed in subsequent periods ($t + 1 \ldots t + N$). A further ability of the stockpile option is its ability to represent long-term waste dumps. This functionality allows the model to consider waste movement and dynamically changes the cut-off grade. Waste dumps are developed by entering an option that is similar to a stockpile but has no plants for the material to flow too, forcing it to remain on the waste dump.

Available Plant Options in the Model

Plant flexibility is incorporated to model the options managers have around processing of mined ore through varying plant designs. A plant option is characterised by its capacity, capital cost, fixed operating cost, recovery characteristics and grade limits. A processing plant is the link between the mine and the port in the flow of

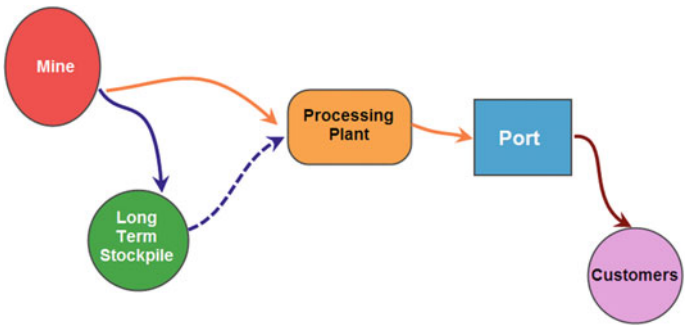

Fig. 2 Material flow in the model and the location of the design options

material in the model. Plant options can also be dependent on other plant options being built, allowing the idea of modular plant capacity to be modelled. That is where a high initial capital cost is incurred to allow for expansion at a later date with a smaller capital cost.

Available Port Options in the Model

Port options allow the sale of material to customers in the model. Enough port capacity must exist in a period in order for any plant production to occur in that period. For example, if we have two million tonnes of plant capacity and no port capacity in the first period then the production from the plant is forced to be zero.

Overview of how Mine Scheduling work in the Model

Resource characteristics are a driving force in mine design. The MIP model uses a resource model to provide a representation of material that is available for processing through the life of mine (both ore and waste is considered).

The representation of the resource is carried out by parcels of material. A parcel of material can be defined as a quantity of material with an average grade determined by the weighted average of the grade bins contained within the parcel. A parcel may be made up of one or more grade bins. A grade bin represents a quantity of material at a specified grade. This is incorporated to provide a higher level of detail to the model which will alter the decisions on how material is processed, whilst minimising the number of integer variables. These parcels are designed to represent a physical constraint on the resource. The most common physical constraint is the vertical mining constraint which is included in the model through parcel dependency.

Mining of the grade bins within a parcel can occur in any order as long as the average parcel grade (within a nominal deviation) is extracted each period. This forces the model to take waste and ore in the same proportion.

Options in the Model to test best Plant or Stockpile location through varying Mining Costs

The optimal location for a processing plant varies with time as the resource is mined in different regions. Therefore, determining the best location for a plant or a stockpile is not a simple case and must consider these multiple uncertainties as it will most likely change over the life of the project. Different plant locations and stockpile locations can be tested by developing a mining cost which varies by parcel and destination in the model.

Overview of what Stochastic Parameters Are Included

Uncertainty in the mining process is incorporated through the market price, cost (capital and operating), utilisation of equipment, plant recovery and time to build an option. Values for these various inputs are simulated through a MCS process.

Model Formulation

The developed MIP model optimises the available mine, stockpile, plant and port flexibility for a simulated scenario. These various design options dictate how the system is configured and consequently the amount of production that can occur. They also dictate the financial viability of the operation and drive both revenue and operating costs. An outline of the mathematical formulation is provided below.

Objective Function

The objective function seeks to maximise before tax net present value (NPV):

$$\sum_{\mathrm{t}=1}^{\mathrm{T}} \frac{1}{(1+\mathrm{r}^*)^{\mathrm{t}}} \Bigg[S_t \sum_{l=1}^{L} M_{l,t} - \sum_{m=1}^{M} C_m I_{m,t} - \sum_{s=1}^{S} C_s Y_{s,t} - \sum_{l=1}^{L} C_l Y_{l,t} - \sum_{o=1}^{O} C_o Y_{o,t} - \sum_{m=1}^{M} D_m ID_{l,t} - \sum_{l=1}^{L} D_l ID_{l,t} - \sum_{o=1}^{O} D_o ID_{o,t} - \sum_{m=1}^{M} V_{m,t} X_{m,t} - \sum_{l=1}^{L} V_{l,t} X_{l,t} - \sum_{s=1}^{S} V_{s,t} X_{s,t} - \sum_{o=1}^{O} V_{o,t} X_{o,t} - \sum_{m=1}^{M} F_{m,t} I_{m,t} - \sum_{l=1}^{L} F_{l,t} Y_{l,t} - \sum_{o=1}^{O} F_{o,t} Y_{o,t} - \sum_{m=1}^{M} FR_{m,t} ID_{m,t} - \sum_{l=1}^{L} FR_{l,t} ID_{l,t} - \sum_{o=1}^{O} FR_{o,t} ID_{o,t} - \sum_{l=1}^{L} L_l - \sum_{\mathrm{p}=1,\mathrm{b}=1}^{\mathrm{P,B}} X_{p,b,l,t} - \sum_{s=1}^{S} L_s \sum_{\mathrm{p}=1,\mathrm{b}=1,\mathrm{l}=1|l\in s}^{\mathrm{P,B,L}} XI_{p,b,s,l,t} \Bigg]$$

Where;

r^*	is the rate of return on the project
S_t	is sale price in time period t (in \$/metal unit)
$M_{l,t}$	is the metal units exiting plant l in time t

C_m, C_s, C_l, C_o is the capital cost of mine m or stockpile s or plant l or port o
$I_{m,t}$ is the execution integer on mine option m in time t.
0 is no execution of option;
otherwise, is the number of times the option is executed in time t.

$Y_{s,t}, Y_{l,t}, Y_{o,t}$ is the execution binary on stockpile s or plant l or port o.
0 is no execution of option;
otherwise, the option is executed in time t.

D_m, D_s, D_l, D_o is the disposal cost of mine m or stockpile s or plant l or port o
$ID_{m,t}$ is the disposal integer on mine option m in time t.
0 is no disposal occurs in time t;
otherwise, is the number of options disposed of in time t.

$ID_{l,t}, ID_{o,t}$ is the disposal integer on plant l or port o.
0 is no disposal occurs in time t;
otherwise, is option is disposed in time t.

$V_{m,t}, V_{s,t}, V_{l,t}, V_{o,t}$ is the variable cost of mining a tonne of ore from mine m or stockpile s or plant l or port o in time t
$X_{m,t}, X_{s,t}, X_{l,t}, X_{o,t}$ is the tonnage processed through mine m or stockpile s or plant l or port o in time t
$F_{m,t}, F_{l,t}, F_{o,t}$ is the fixed cost of mining from mine m or plant l or port o in time t
$FR_{m,t}, FR_{l,t}, FR_{o,t}$ is the reduction in fixed cost of disposing of an option in time t
L_l is the cost of mining a tonne of ore to plant l
L_s is the cost of mining a tonne of ore to stockpile s
$X_{p,b,l,t}$ is the tonnage mined from parcel p bin b to plant l in time t
$XI_{p,b,s,l,t}$ is the tonnage mined from parcel p bin b to stockpile s at plant l in time t

The objective function represents the following:

> The revenue from the sale of the ore less the capital cost of building an option less the disposal cost of reducing capacity less the variable cost of processing ore less the fixed cost of maintaining an option; all multiplied by the relevant discount factor for the cash flow in time t. The model seeks to maximise this relationship.

The constraints in the model can be divided into five categories: production, mining, stockpiling, processing plant and port constraints.

Production Constraints

Resource Constraint

This constraint makes sure the total amount of material extracted from a mining pit has an upper bound based on the resource. This constraint is applied at a parcel and bin level in the model:

$$\sum_{t=1}^{T} X_{p,b,t} - R_{p,b} \leq 0 \quad \forall p, b$$

Where;

$X_{p,b,t}$ is the tonnage mined from parcel p bin b in time t
$R_{p,b}$ is the resource of parcel p bin b

Sequencing Constraint 1

This constraint in conjunction with the next constraint forces the binary value to be one in the period the parcel is fully mined. This then allows the model to mine any successor parcels of ore:

$$\sum_{b=1,tt=1}^{B,t} X_{p,b,tt} \geq R_p \ * \ Y_{p,t} \quad \forall p, t$$

Where;

R_p is the resource of parcel p

Sequencing Constraint 2

This constraint ensures that a parcel's predecessor is mined before the successor is mined:

$$\sum_{b=1,tt=1}^{B,t} X_{p+1,b,tt} \leq R_{p+1} \ * \ \sum_{tt=1}^{t} Y_{p,tt} \quad \forall p, t$$

Where;

R_{p+1} is the resource of the successor parcel p + 1
$X_{p+1,b,tt}$ is the tonnage mined from the successor parcel p + 1 bin b in time tt

Sequencing Constraint 3

This constraint is a set packing constraint that forces a parcel to only be fully mined once:

$$\sum_{t=1}^{T} Y_{p,t} \leq 1 \qquad \forall p$$

Equal Mining of a Parcel

This constraint forces the model to take high grade ore, waste and low grade ore in equal proportions. This prevents the model taking high grade in the first period, followed by low grade in the second period and waste in the following period. A minimal deviation (γ) of 2% was allowed to prevent an infeasible solution:

$$\sum_{b=1}^{B} X_{p,b,t} G_{p,b} \geq \left[\sum_{b=1}^{B} X_{p,b,t}\right] G_p * (1 - \gamma\%) \qquad \forall p, t$$

$$\sum_{b=1}^{B} X_{p,b,t} G_{p,b} \leq \left[\sum_{b=1}^{B} X_{p,b,t}\right] G_p * (1 + \gamma\%) \qquad \forall p, t$$

Where;

$G_{p,b}$ is the grade of parcel p and bin b
G_p is the grade of parcel p

Flow Balance Constraint

This constraint links the flow paths in the model and ensures that the material available to the processing plant and stockpiling options originates from the resource:

$$X_{p,b,t} = \sum_{l=1}^{L} X_{p,b,l,t} + \sum_{s=1,k=1,l=1}^{S,K,L} XI_{p,b,s,k,l,t} \qquad \forall p, b, t$$

Mining Constraints

Mining Requirements

The constraint makes sure that mining includes all movement to plant options, stockpile options and movement off stockpiles:

$$\sum_{m=1}^{M} X_{m,t} = \sum_{p=1,b=1}^{P,B} X_{p,b,t} + \sum_{s=1,l=1}^{S,L} XO_{s,l,t} \qquad \forall t$$

Where;

$XO_{s,l,t}$ is the tonnage sent from stockpile s at location l in time t

Mining Capacity Limit

This constraint ensures that mining only occurs if there is sufficient capacity in a period to handle the movement. Capacity is determined dynamically based on when mining options are executed:

$$\sum_{u=1}^{t} A_{m,u,t} I_{m,u} - \sum_{u=2}^{t} A_{m,u,t} ID_{m,u} \leq X_{m,t} \qquad \forall m, t$$

Where;

$A_{m,u,t}$ is the capacity of mine option m that was executed in period u in time t

Mine Option Disposal Constraint

This constraint ensures disposal of an option can only occur if the option has been built. For example, if a mine option is built in period one and in period five there is no more material to mine, then the model can dispose of this capacity in order to reduce the fixed cost incurred:

$$ID_{m,t} \leq \sum_{tt=2}^{t} I_{m,tt-1} \qquad \forall m, t$$

$$\sum_{tt=2}^{t} ID_{m,tt} \leq \sum_{tt=2}^{t} I_{m,tt-1} \qquad \forall m, t$$

Maximum Execution

Since the mine option can be modelled as an integer variable, limits on how many times it can be applied in the model may be included. This is an optional constraint which can be turned on or off when running the model.

Period Constraint

This constraint restricts the number of mine options built in a period to the period constraint maximum:

$$I_{m,t} \leq PC_m \qquad \forall m, t$$

Overall Constraint

This constraint restricts the total number of mine options built over the life of a mine:

$$\sum_{t=1}^{T} I_{m,t} \leq OC_m \qquad \forall m$$

Where;

PC is the period constraint limit or the maximum number of times an option can be executed in any period;
OC is the overall constraint which is the maximum number of times an option can be executed over the life of the project.

Stockpiling Constraints

Total Inflow Constraint

This constraint makes the total amount of material that is entering a stockpile equal the material entering each stockpile bin:

$$XI_{s,l,t} = \sum_{k=1}^{K} XI_{s,k,l,t} \qquad \forall s, l, t$$

Where;

$XI_{s,l,t}$ is the total tonnage sent into stockpile s at plant l in time t

Flow Balance Constraint

This constraint restricts the total amount of material coming into each bin in the stockpile to be equal to the material sent from the each parcel to the bin:

$$XI_{s,k,l,t} = \sum_{p=1,b=1}^{P,B} XI_{p,b,s,k,l,t} \qquad \forall s,k,l,t$$

Where;

$XI_{s,k,l,t}$ is the tonnage sent into stockpile s grade bin k at plant l in time t
$XI_{p,b,s,k,l,t}$ is the tonnage from parcel p bin b sent into stockpile s grade bin k at plant l in time t

Stockpile Capacity Constraint

This constraint makes sure the tonnage of material stockpiled across all plant locations does not exceed the stockpile capacity:

$$\sum_{l=1,tt=1}^{L,t} XI_{s,l,tt} - \sum_{l=1,tt=2}^{L,t} XO_{s,l,tt} \leq \sum_{tt=1}^{t} A_s Y_{s,tt} \qquad \forall s,t$$

Where;

$XO_{s,l,t}$ is the total tonnage sent from stockpile s to plant l in time t
A_s is the total capacity of stockpile s

Stockpile Grade Constraint on Bins

This constraint applies the grade limits of the stockpile bins to material entering each stockpile bin:

$$\sum_{tt=1}^{t} G_{p,b} XI_{p,b,s,k,l,tt} \leq \sum_{tt=1}^{t} GU_{s,k} XI_{p,b,s,k,l,tt} \qquad \forall p,b,s,l,t$$

$$\sum_{tt=1}^{t} G_{p,b} XI_{p,b,s,k,l,tt} \geq \sum_{tt=1}^{t} GL_{s,k} XI_{p,b,s,k,l,tt} \qquad \forall p, b, s, l, t$$

Where;

$GU_{s,k}$ is the upper grade limit of stockpile s bin k
$GL_{s,k}$ is the lower grade limit of stockpile s bin k

Bin Removal Constraint

The constraint ensures material moved from the stockpile has been added to the stockpile at least one period ago and that material removed from the stockpile is not removed again:

$$XO_{s,k,l,t} \leq \sum_{tt=1}^{t} XI_{s,k,l,tt} + \sum_{tt=2}^{t} XO_{s,k,l,tt-1} \qquad \forall s, k, l, t$$

Where;

$XO_{s,k,l,t}$ is the tonnage removed from stockpile s bin k to plant l in time t

Bin Extraction

This constraint makes the total tonnage of material that is extracted from each stockpile bin equal the overall extraction from the stockpile:

$$\sum_{k=1}^{K} XO_{s,k,l,t} = XO_{s,l,t} \qquad \forall s, l, t$$

Metal Extraction

This constraint ensures the total amount of metal units extracted from a stockpile equals the metal units extracted from the individual grade bins:

$$MO_{s,l,t} = \sum_{k=1}^{K} GA_{s,k} XO_{s,k,l,t} \qquad \forall s, l, t$$

Where;

$MO_{s,l,t}$ is the metal units removed from stockpile s at location l in time t
$GA_{s,k}$ is the average grade of stockpile s grade bin k

Opening Limit

This constraint ensures that a stockpile can only be opened once:

$$\sum_{t=1}^{T} Y_{s,t} \leq 1 \qquad \forall s$$

Processing Plant Constraints

Grade Limits (Upper and Lower)

This constraint applies the grade limits on a given plant in each time period. This ensures every plant processes material it can handle:

$$\sum_{s=1|\delta\varepsilon l}^{S} MO_{s,l,t} + \sum_{p=1,b=1}^{P,B} G_{p,b} X_{p,b,l,t} \leq GU_l \sum_{s=1}^{S} XO_{s,l,t} + GU_l \sum_{p=1,b=1}^{P,B} X_{p,b,l,t} \qquad \forall l,t$$

$$\sum_{s=1|\delta\varepsilon l}^{S} MO_{s,l,t} + \sum_{p=1,b=1}^{P,B} G_{p,b} X_{p,b,l,t} \geq GL_l \sum_{s=1}^{S} XO_{s,l,t} + GL_l \sum_{p=1,b=1}^{P,B} X_{p,b,l,t} \qquad \forall l,t$$

Where;

GL_l is the lower grade limit of plant l
GU_l is the upper grade limit of plant l

Plant Capacity Constraint

The constraint ensures that the total tonnage of material processed in a period shall is less than the capacity of plant options built and disposed:

$$\sum_{s=1}^{S} XO_{s,l,t} + \sum_{p=1,b=1}^{P,B} X_{p,b,l,t} \leq \sum_{u=1}^{T} A_{l,u,t} Y_{l,u} - \sum_{u=2}^{T} A_{l,u,t} ID_{l,u} \qquad \forall l,t$$

Where;

$A_{l,u,t}$ is the capacity of plant option l built in u in time t

Plant Disposal Constraint

This constraint ensures that a plant option is only disposed if the plant has been built in a previous period. This will result in a fixed cost saving, however an additional disposal cost will be incurred in the objective function:

$$YD_{l,t} - \sum_{t=1}^{t} Y_{l,t} \leq 0 \qquad \forall l, t$$

$$\sum_{t=1}^{t} YD_{l,tt} - \sum_{tt=1}^{t} Y_{l,tt} \leq 0 \qquad \forall l, t$$

Tonnage Produced

This constraint restricts the tonnage exiting the plant to be equal to the material entering the plant multiplied by the plant recovery:

$$X_{l,t} = \sum_{p=1,b=1}^{P,B} E_{l,t} X_{p,b,l,t} + \sum_{s=1,t=2|s\in l}^{S,T} E_{l,t} XO_{s,l,t} \qquad \forall l, t$$

Where;

$E_{l,t}$ is the recovery of plant l in time t

Metal Units Produced

This constraint calculates the metal production of a plant option by multiplying the metal units into the plant by the recovery and grade multiples for the plant. This is used to calculate the revenue of the mine:

$$M_{l,t} = \sum_{p=1,b=1}^{P,B} E_{l,t} GM_{l,t} X_{p,b,l,t} + \sum_{s=1,t=2|s\in l}^{S,T} E_{l,t} GM_{l,t} MO_{s,l,t} \qquad \forall l, t$$

Where;

$GM_{l,t}$ is the grade multiple of plant option l in time t

Plant Option Dependency

Plant option dependency dictates the relationships that occur between options. Two types of relationships are available; one-for-one and one-for-many.

One for One Relationship

This constraint makes sure a successor option is built prior to the predecessor option being built in an equal ratio. For example, this can be used to model a modular plant design where an initial investment can be made in plant capacity that has the ability to be expanded easily for a lower capital than if the initial investment was not made (this later expansion is optional):

$$\sum_{tt=1}^{t} Y_{l,tt} \leq \sum_{tt=1}^{t-DT} Y_{c,tt} \qquad \forall l, c, t | c \in l$$

One for Many Relationships

This constraint allows a successor option to be built if its predecessor option has been built at least once. This can be used to model a rail link to a plant location where an initial capital investment is required. However, once this has been built numerous plants can be built at the same location:

$$Y_{l,t} \leq \sum_{t=1}^{T-DT} Y_{c,t} \qquad \forall l, c | c \in l$$

Where;

C is the predecessor plant option of plant option l
DT is the lead time on the relationship
$Y_{c,tt}$ is the execution variable of the predecessor plant c of plant l in time tt.

Port Constraints

Port Production Constraint

The constraint ensures the total tonnage of material processed through all plant options is less than or equal to the total port capacity:

$$\sum_{l=1}^{L} X_{l,t} \leq \sum_{o=1}^{O} X_{o,t} \qquad \forall t$$

Capacity Constraint

The constraint requires the total tonnage of material shipped in a period to be less then the port capacity:

$$X_{o,t} \leq \sum_{u=1}^{t} A_{o,u,t} Y_{o,u} - \sum_{u=2}^{t} A_{o,u,t} ID_{o,u} \qquad \forall o, t$$

Where;

$A_{o,u,t}$ is the capacity of port option o built in u time t

Disposal Constraint 1

Disposal of a port option may only occur if the option has previously been built:

$$ID_{o,t} \leq \sum_{tt=1}^{t} Y_{o,tt} \qquad \forall o, t$$

$$\sum_{tt=1}^{t} ID_{o,t} \leq \sum_{tt=1}^{t} Y_{o,tt} \qquad \forall o, t$$

Port Option Dependency

Port option dependency may occur in one for one or one for many relationships.

One for One Relationship

This constraint makes sure a successor option is built prior to the predecessor option being built in an equal ratio:

$$\sum_{tt=1}^{t} Y_{o,tt} \leq \sum_{tt=1}^{t-DT} Y_{c,tt} \qquad \forall o, t | c \in o$$

One for Many Relationships

This constraint allows a successor option to be built if its predecessor option has been built at least once. This relationship can be used to model a rail link that must be built before any port can be built:

$$Y_{o,t} \leq \sum_{tt=1}^{t-DT} Y_{c,tt} \qquad \forall o, t | c \in o$$

Where;

DT is the lead time on the relationship
$Y_{c,tt}$ is the execution variable of the predecessor port c of port o in time tt.

Non-negativity, Binary and Integer Restrictions

Non-negativity

The following variables are restricted to taking on positive values as a negative would represent an infeasible situation:

$$X_{p,b,t}, XI_{p,b,s,k,l,t} \geq 0 \qquad \forall p, b, s, k, l, t$$

$$X_{m,t}, X_{l,t}, X_{o,t} \geq 0 \qquad \forall m, l, o, t$$

$$XO_{s,l,t}, XO_{s,k,l,t}, XI_{s,k,l,t} XI_{s,l,t} \geq 0 \qquad \forall s, k, l, t$$

Integers

The following variables must take on integer values in the model:

$$I_{m,t}, ID_{o,t}, ID_{m,t}, ID_{l,t} \qquad \forall m, l, o, t$$

Binaries

The following variables must take on binary values; integers with an upper bound of one and lower bound of zero:

$$Y_{c,tt}, Y_{p,t}, Y_{o,t}, Y_{l,t}, Y_{s,t} \qquad \forall p, o, l, s, t, c, tt$$

Case Study: Open Pit Mine

An application of the methodology was implemented to a hypothetical mining scenario. The problem is similar in nature to an iron ore mine, although it could be applied to any open cut mine. A single mine site is used in this example.

The Problem

The operation consists of three mining pits (two high grade and one low grade), two plant locations with associated rail infrastructure, stockpiling and waste storage capabilities at each location and two port options with associated rail requirements (Fig. 3). In this diagram, the rectangular boxes represent different plant locations (note that location A has the shortest haul for pit 1 and location B has the shortest haul for pit 3 whilst pit 2 has an equivalent haul to either location). In order to process material through a plant at location A, a rail link of 35 km with a capital of $65 M needs to be built. Likewise, at location B a rail link of 10 km needs to be built for a capital of $30 M. Finally, in order to process any material through the port, a rail link from the junction of A and B to the coast needs to be built for a capital of $20 M. The analysis will look at the system configuration over five periods.

The Model Inputs

Multiple options were included in the model of this problem as summarised in Table 1. A full list of the fixed costs, variable costs and grade constraints is not provided for simplicity purposes. In order to simulate the different processing plant locations available to the model, a differential mining cost was used based on the destination of material. A summary of the different costs associated with each location is outlined in Table 2.

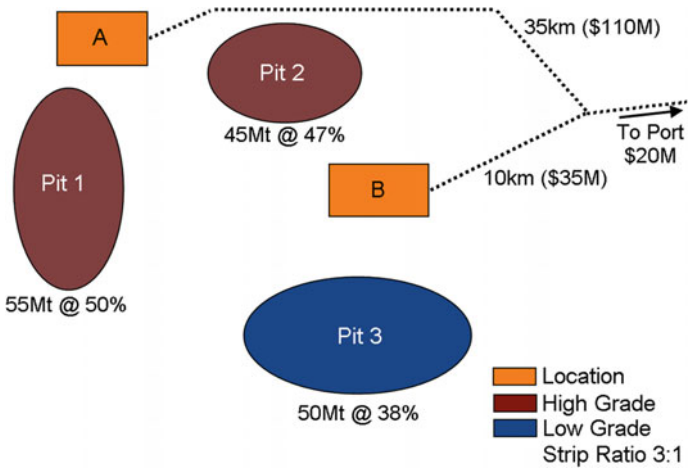

Fig. 3 Conceptual layout of hypothetical mine

Table 1 Options available in hypothetical example

Type	Cost ($M)
Mine options	
1 Mt/a unit	3
2 Mt/a unit	4.5
Stockpile options	
Waste stockpile (500 Mt capacity)	0
Low-grade (30 Mt capacity)	0
Plant options	
5 Mt/a fixed (lead 0.5 yr)	50
10 Mt/a fixed (lead 1.5 yr)	92
5 Mt/a flexible (modular, lead 0.5 yr)	75
Additional 5 Mt/a flexible (modular, lead 0.5 yr)	30
Port capacity	
10 Mt/a (lead 0.75 yr)	100
20 Mt/a (lead 1.5 yr)	175

The Stochastic Variables

In this problem, it was determined that seven stochastic parameters would be included. These were price, recovery, capital cost, operating cost and utilisation for mine, plant and port options.

Choice of underlying distributions was done through discussions with professionals. No detailed analysis of the underlying nature of the stochastic variables has

Table 2 Differential mining costs to handle different locations in the model

Cost ($/t)	Pit 1	Pit 2	Pit 3
Plant location A	0.2	0.6	1.8
Plant location B	2.2	0.6	0.4
Waste location A	0.1	0.3	0.9
Waste location B	1.1	0.3	0.2

been carried out, as detailed research in other papers is available which was not the primary purpose of this paper (Dimitrakopoulos and Abdel Sabour 2007; Godoy and Dimitrakopoulos 2004; Lima and Suslick 2006; Morley et al. 1999; Topal 2008).

A summary of the values used for each distribution is as follows:

- Price follows a lognormal distribution with a mean of $85, standard deviation of $25 and a correlation of 0.30 between periods;
- Recovery follows a triangular distribution with a maximum value of 90%, likely value of 80%, minimum value of 70% and a correlation of 0.05 between periods;
- Capital cost multiple follows a normal distribution with a mean of 1.08, standard deviation of 0.20 and a correlation of 0.40 between periods;
- Operating cost multiple follows a normal distribution with a mean of 1.03, standard deviation of 0.10 and a correlation of 0.10 between periods;
- Mine equipment utilisation follows a triangular distribution with a maximum value of 95%, likely value of 75%, minimum value of 60% and a correlation of 0.22 between periods;
- Plant utilisation follows a triangular distribution with a maximum value of 95%, likely value of 80%, minimum value of 65% and a correlation of 0.21 between periods; and
- Port utilisation follows a triangular distribution with a maximum value of 95%, likely value of 80%, minimum value of 65% and a correlation of 0.34 between periods.

Results Analysis

Based on the input parameters 200 trials were run, with CPLEX™ used to solve the MIP model. In total it took 3 h to process the model, which was deemed a good solution time for this model size. The raw data from the results exceeds four gigabytes. A results analysis process has been developed which summarises this data. After processing of the model, the frequency of execution for each options was analysed (Table 3). Frequency of execution is calculated by dividing the count of the number of times an option is executed by the maximum number of times it could be executed. Some categories of options (plant, port, mine) sum to more than 100% because multiple expansions of that type can occur in the same time period as the options are not mutually exclusive.

Table 3 Frequency of execution for all options in the model

	Period 1 (%)	Period 2 (%)	Period 3 (%)	Period 4 (%)	Period 5 (%)	All periods (%)
Mine 1 Ml/a	18	4	5	0	0	5
Mine 2 Mt/a	98	32	9	3	1	29
Rail link to A	94	0	0	0	0	19
Rail link to B	45	1	0	0	0	9
Plant 5 Mt/a (A)	69	26	14	6	2	23
Plant 10 Ml/a (A)	66	14	5	1	0	17
Plant 5 Mt/a modular (A)	90	41	13	2	0	29
Additional 5 Mt/a modular (A)	0	82	35	16	1	27
Plant 5 Mt/a (B)	19	4	1	1	0	5
Plant 10 Mt/a (B)	44	19	6	2	0	14
Plant 5 Mt/a modular (B)	41	15	4	2	0	12
Additional 5 Mt/a modular (B)	0	35	14	3	2	11
Port 10 Mt/a	98	1	0	0	0	20
Port 20 Mt/a	91	84	53	28	8	53

From examining Table 3 several conclusions can be developed. First, it is evident that larger port capacity options should be investigated as the execution frequency is over 50% for the 20 Mtpa port option (the largest in the model) for three periods. Second, the mine option with 1 Mtpa capacity and the plant with 5 Mtpa at location B are not valuable options as there execution is lower than 20%. Finally, location A is preferred over location B as the rail link options which dictate which locations can be used are executed 94% and 45% for A and B respectively.

A value at risk graph (VARG) shows the risk to return relationship. Figure 4 displays the VARG for this example with the base case representing a fixed mine design with no optionality. The design chosen for the base case was based on the 50th percentile design when the model with optionality was run. This design was then fixed in the MIP model and reprocessed with the same uncertainties. This shows the outcome of management not changing the operating policy of the mine. The mean NPV of the base case was $702 M and for the case with options was $1298 M, an 85% increase.

Further to these analysis methods, experimentation is currently underway with using various data mining techniques. An open source software package called Rapid Miner is currently being used. An example (from a different problem set) of the output generated is shown in Fig. 5. This example shows a decision tree with the associated percentages of times the decision paid off highlighted in the Yes/No boxes at the bottom of the nodes.

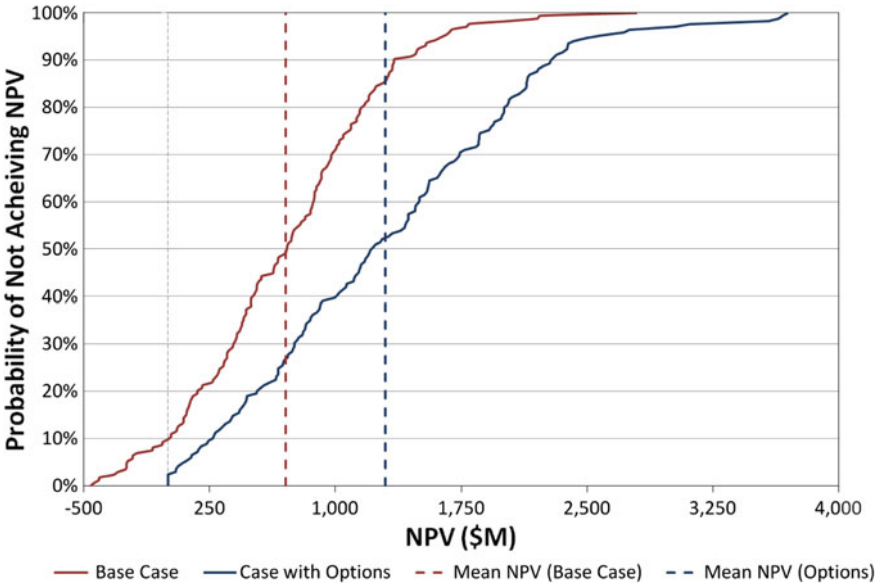

Fig. 4 Value at risk for hypothetical example

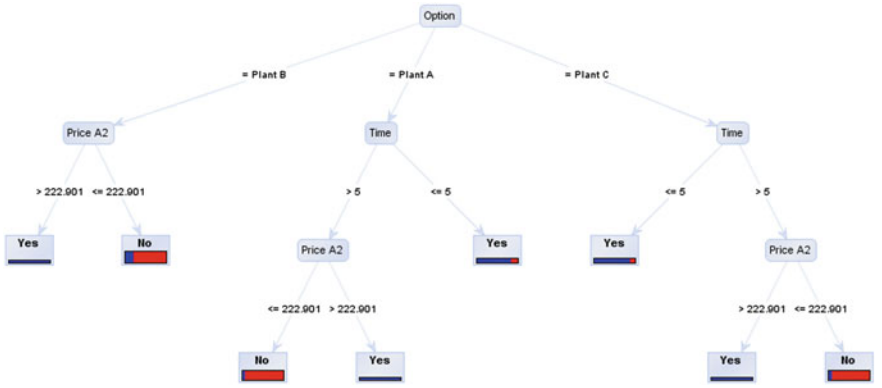

Fig. 5 Sample of Decision Tree output from Data Mining

Conclusions

In conclusion, this paper has developed a methodology to evaluate the strategic mine design flexibility under stochastic environment. The proposed methodology is a unique approach that allows flexible mine designs to be justified. The decision maker is supported in their choice of and refinement mine design. Increasing flexibility in mine designs would be advantageous for responding to changing business conditions across the full economic cycle.

For the sake of comparison, the proposed methodology has been implemented to a hypothetical mining scenario. The results demonstrated that the value of expected NPV increases by 85% with flexible mine design compared to without flexibility. The paper illustrates how to incorporate design options (flexibility) into a strategic mine plan in a manner that proactively manages inevitable uncertainties. It is hoped this research will help in justifying more flexible mine designs and further the sustainability of the industry.

Recommendations

Whilst the model handles a simple case, currently further research and model improvements continue in the following areas:

- More detailed modelling which considers multiple process options and multi product options;
- Handling of grade variability through the use of conditional simulation methods will greatly improve the power of the model (Dimitrakopoulos and Ramazan 2004);
- Further investigation into appropriate results analysis techniques is required to fully understand how the primary question of flexibility is answered;
- MIP performance improvement algorithms need to be investigated, these methods may include reducing the feasible region with additional constraints and/or developing a node selection routine for the branch and bound algorithm that exploits some of the nuances in the model; and
- Application of this technique to underground mining is needed to fully capture the options available to mine management. In particular, incorporating the process to optimise the open cut and underground transition point would be highly beneficial. This would assist in strategic planning for the entire orebody.

Acknowledgements The authors wish to thank Rio Tinto Iron Ore for their support of this project.

References

Cardin MA (2007) Facing reality: design and management of flexible engineering systems, masters (unpublished), Engineering System Divisions, Massachusetts Institute of Technology, MA

Cardin MA, de Neufville R, Kazakidis V (2008) A process to improve expected value of mining operations. Min Technol Trans Inst Mater Miner Min 117(2):65–70

de Neufville R, Scholtes S, Wang T (2005) Real options by spreadsheet: parking garage case example. J Infrastruct Sys 12(2):107–111

Dimitrakopoulos R, Ramazan S (2004) Uncertainty-based production scheduling in open pit mining. SME Trans 316:106–112

Dimitrakopoulos RG, Abdel Sabour SA (2007) Evaluating mine plans under uncertainty: can the real options make a difference? Resour Policy 32(3):116–125

Godoy M, Dimitrakopoulos R (2004) Managing risk and waste mining in long-term production scheduling. SME Trans 316:43–50

Leite A, Dimitrakopoulos R (2007) A stochastic optimization model for open pit mine planning: application and risk analysis at a copper deposit. Min Technol Trans Inst Mater Miner Min 116(3):109–118

Lima GAC, Suslick SB (2006) Estimating the volatility of mining projects considering price and operating cost uncertainties. Resour Policy 3:86–94

Morley C, Snowden V, Day D (1999) Financial impact of resource/reserve uncertainty. J S Afr Inst Min Metall 6:293–302

Ramazan S, Dimitrakopoulos R (2004) Traditional and new MIP models for production scheduling with in-situ grade variability. International Journal of Mining, Reclamation and Environment 18(2):85–98

Topal E (2008) Evaluation of a mining project using discounted cash flow analysis, decision tree analysis, monte carlo simulation and real options using an example. Int J Min Miner Eng 1(1):62–76

Wang T, de Neufville R (2005) Real Options 'in' projects. Paper presented at 9th Real Options Annual International Conference Paris, France

Wang T, de Neufville R (2006) Identification of real options 'in' projects. Paper presented at 16th. Annual International Symposium of the International Council on Systems Engineering (INCOSE), Orlando, US

Direct Net Present Value Open Pit Optimisation with Probabilistic Models

A. Richmond

Abstract Traditional implementations of open pit optimisation algorithms are designed simply to find a set of nested open pit limits that maximise the undiscounted financial pay-off for a series of commodity prices using a single 'estimated' orebody model. Then, the maximum Net Present Value (NPV) open pit limit is derived by considering alternate (usually only best and worst-case) mining schedules for each open pit limit. Divorcing the open pit limit delineation from the NPV calculation in this two-step approach does not guarantee that an optimal NPV open pit solution will be found. A new open pit optimisation algorithm that considers the mining schedule is proposed. As a consequence, it can also account explicitly for commodity price cycles and uncertainty that can be modelled by stochastic simulation techniques. This state-of-the-art algorithm integrates Monte Carlo-based simulation and heuristic optimisation techniques into a global system that directly provides NPV optimal pit outlines. This new approach to open pit optimisation is demonstrated for a large copper deposit using multiple orebody models.

Introduction

Several open pit optimisation techniques such the Lerchs–Grossman algorithm (Lerchs and Grossman 1965; Whittle 1999), network flow (Johnson 1968), pseudoflow network models (Hochbaum and Chan 2000) and others, involve a 3D grid of regular blocks that is converted *a priori* into a pay-off matrix by considering a 3D block model of mineral grades and economic and mining parameters. These algorithms rely on the block pay-offs averaging linearly, as is the case when undiscounted block pay-offs are considered. However, the Net Present Value (NPV) of the block pay-offs is a non-linear function of the undiscounted block pay-offs that depends explicitly on the discount to be applied to the individual blocks, which in turn depends on the block mining schedule. To overcome the issue of discounting

A. Richmond (✉)
Martlet Consultants, 20 Warrawong Street, Chapel hill, QLD 4069, Australia
e-mail: arichmond@martlet.com.au

R. Dimitrakopoulos (ed.), *Advances in Applied Strategic Mine Planning*,
https://doi.org/10.1007/978-3-319-69320-0_15

block pay-offs, traditional implementations of open pit optimisation algorithms are designed simply to find a set of nested open pit limits that maximise the undiscounted financial pay-off for a series of constant commodity prices using a single 'estimated' orebody model. Then, the maximum NPV open pit limit is derived by considering alternate (usually only best and worst-case) mining schedules for each open pit limit. This two-step approach to finding the maximum NPV open pit limit raises three significant issues:

1. Divorcing the open pit limit delineation from the NPV calculation does not guarantee that an optimal (maximum) NPV open pit solution will be found;
2. NPV calculations are based on a constant commodity price that fails to consider its time-dependant and uncertain nature; and
3. The single 'estimated' orebody model is invariably smoothed, thus it fails to consider short-scale grade variations.

Consequently, the block model does not accurately reflect the grade and tonnage of ore that will be extracted and processed during mining.

To overcome the inadequacy of undiscounted pay-offs in commonly used algorithms for open pit optimisation, it is proposed to embed a scheduling heuristic within an open pit optimisation algorithm. This may be seen as an alternative avenue to that taken by mixed integer programming approaches (eg. Caccetta and Hill 2003; Ramazan 2007; Stone et al. 2018; Menabde et al. 2007) that may become numerically demanding in the case of large deposits. As a consequence, uncertain and time-dependent variables such as commodity prices can also be incorporated stochastically into the optimisation process. This permits strategic options for project timing and staging to be assessed as discrete optimisation problems and compared quantitatively and is more advanced than other recent approaches (Monkhouse and Yeates 2018 in this volume; Dimitrakopoulos and Abdel Sabour 2007). It is also proposed to consider multiple conditional simulations in the optimisation process such that the mining and financial implications related to small-scale grade variations are honoured (Menabde et al. 2018 in this volume; Ramazan and Dimitrakopoulos 2013, 2017 in this volume; Leite and Dimitrakopoulos 2007; Godoy and Dimitrakopoulos 2004; Ravenscroft 1992). By considering discounted block pay-offs, stochastic models of commodity prices and short-scale grade variations a more accurate discounted pay-off matrix (revenue block model) is generated, which in turn will yield an open pit limit that will be closer to the true optimum.

NPV Calculations with Uncertain Variables

Calculation of the NPV for a given open pit limit relies on estimates of numerous parameters, including (but not restricted to) the mineral grades, extraction sequence and timing, mineral recovery, prevailing commodity price and capital and operating

costs. All of these parameters are uncertain and should be modelled stochastically. For example, mineral grade values by geostatistical simulations, operating costs with growth functions and commodity prices using long-term mean reverting models that account for periodicity. Consequently, the cumulative distribution of total financial pay-offs for an open pit limit can be derived from the combination of a series of stochastic models of mineral grades, costs, prices, recoveries, etc.

Given L potential NPV outcomes for a block (related to L realisations of grade values, commodity prices, etc), we can calculate the NPV for any realisation l:

$$NPV_l = \sum_{j=1}^{B} d^l(b_j) i_j \tag{1}$$

and the expected NPV for L realisations:

$$NPV_L = \frac{1}{L}\left\{\sum_{l=1}^{L} NPV_l\right\} \tag{2}$$

where:

B is the number of blocks under consideration
$d^l(b_j)$ is the discounted value for block b_j for the lth realisation
$i_j = 1$ if b_j falls within the open pit limit and 0 otherwise

The idea being to find the open pit limit that maximises NPV_L. Additional financial goals, for example minimising downside risk (Richmond 2004a) could also be considered, but are outside the scope of this paper.

Accounting for Multiple Orebody Models

Pit optimisation algorithms found in the literature invariably consider an orebody block model with a single grade value for each block (or parcel). In such an approach, a simple decision rule is used where block b_j is processed using option k if $g_k \leq z^*(b_j) < g_{k+1}$, where:

g_k is the cut-off grade for processing option k (by convention $g_1 = 0$ and $k = 1$ indicates waste)

z^* is the estimated grade value

To account for grade uncertainty in open pit optimisation, Richmond (2004a) proposed incorporating L grade values for each block. In this approach, multiple grade values $z^l(b_j)$, l=1,…,L were generated by conditional simulation and a processing option $k^l(b_j)$ was determined for each realisation. Alternatively, conditional simulation provides short-scale grade variations that permit local ore loss and mining dilution to be readily accounted for in open pit optimisation by (Richmond 2004a):

- Generating geometrically irregular dig-lines (that separate ore and waste) based on small-scale grade simulations with a floating circle algorithm, and
- Assimilating the dig-lines into large-scale geometrically regular blocks by a novel re-blocking method.

This two-step approach accounts for short-scale grade variation, but also provides 'recoverable' grade and tonnage information for large regular blocks suitable for open pit optimisation. In other words, the simulated grade models are compressed without loss of accuracy so that optimisation is computationally tractable.

An NPV Open Pit Optimisation Algorithm

For the vast majority of open pit optimisation techniques a directed graph is superimposed onto the pay-off matrix to identify the blocks that constitute an optimal open pit limit. To paraphrase Dowd and Onur (1993)—each block in the grid, represented by a vertex, is assigned a mass equal to its net expected revenue. The vertices are connected by arcs in such a way that the connections leading from a particular vertex to the surface define the set of vertices (blocks) that must be removed if that vertex (block) is to be mined. A simple 2D example is shown in Fig. 1. Blocks connected by an arc pointing away from the vertex of a block are termed successors of that block, ie. b_i is a successor of b_i if there exists an arc directed from b_i to b_i. In this paper, the set of all successors of b_j will be denoted as Γ_j. For example, in Fig. 1, $\Gamma_8 = \{2, 3, 4\}$. A closure of a directed graph, which consists of a set of blocks B, is a set of blocks $B_p \subset B$ such that if $b_j \in B_p$ then $\Gamma_j \in B_p$. For example, in Fig. 1, $B_p = \{1–5, 7–9, 13\}$ is a closure of the directed graph. The value of a closure is the sum of the pay-offs of the vertices in the closure. As each closure defines a possible open pit limit, the closure with the maximum value defines the optimal open pit limit.

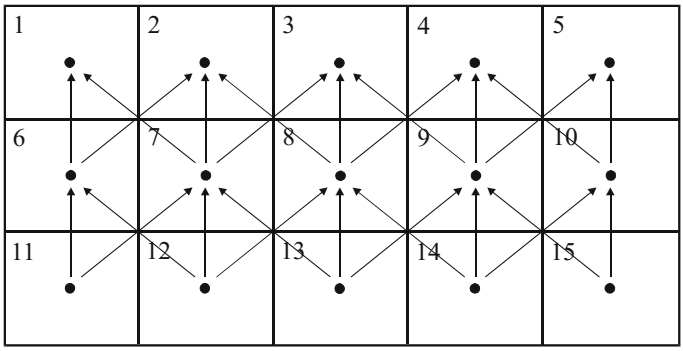

Fig. 1 Directed graph representing 2D vertical orebody model

For simplicity of notation, the algorithm proposed in this paper is described for a single orebody model. The undiscounted pay-off matrix $\{w(b), b \in B\}$ typically used for open pit optimisation is calculated as:

$$w(b) = ton_b(vz(b)r_k - c_k) \tag{3}$$

where:

ton_b represents the tonnage of block b
v is the commodity (attribute z) value per concentration unit
r_k is the proportion of the mineral recovered using processing option k
c_k is the mining and processing cost for k (\$/ton)

In practice, r_k and c_k commonly vary spatially and v and c_k temporally. The discounted pay-off matrix $\{d(b|S), b \in B\}$, conditional to a mining schedule S, that is required for NPV open pit optimisation is calculated as:

$$d(b|S) = [ton_b(v_t z(b)r_k - c_{k,t})]/(1 + \mathrm{DR})^t \tag{4}$$

where:

t is the time period in which block b is scheduled for extraction and processing
v_t $c_{k,t}$ are the prevailing commodity price and operating cost at time t
DR is the discount rate

In Eq. 4, discounted pay-offs are conditional to the mining schedule as alternate schedules can be derived for the same open pit closure. It is also important to note that, cut-off grades and consequently the processing option k, may change in response to commodity price and operating cost fluctuations over time. Does not imply that the discounted value for is positive.

The traditional floating cone algorithm decomposes the full directed graph problem into a series of independent evaluations of individual Γ_j and if the sum of the pay-offs associated with Γ_j is positive, then b_j is added to B_p. However, a positive undiscounted value for Γ_j. does not imply that the discounted value for Γ_j is positive. In other words, negatively-valued successors b_j or block b_j that may be mined significantly earlier in the mining schedule and receive substantially less discounting may not be carried by a more heavily discounted positively-valued b_j. Furthermore, the modified schedule may have shifted more profitable b_j into later periods and additional wasted blocks into earlier periods, reducing the discounted value of the pit. As traditional independent evaluation of locally decomposed Γ_j.

To allow for discounting, it is proposed that a Direct NPV Floating Cone algorithm (DFC) proceeds as follows:

1. Select the time for initial investment (start of construction) t_1;
2. Define a cone that satisfies the physical constraints of the desired open pit slope angles;

3. Define an ordered sequence of visiting blocks [1,2,…#<B] with positive $w(b)$, by ordering the blocks b_i firstly on decreasing elevation, and then for blocks with identical elevations on decreasing value in $w(b_i)$;
4. Set the open pit closure counter $n = 0$, the initial open pit closure B_p^n to a null set of blocks, and the Net Present Value of initial open pit closure $NPV^n = 0$;
5. Set $j = 0$;
6. Set $j = j + 1$;
7. Float the cone to b_j to create a new closure $B_p^{n+1} = B_p^n + \Gamma_j$ (excluding from Γ_j any block that currently belongs to B_p^n);
8. Determine the schedule S for the new closure B_p^{n+1};
9. Calculate the discounted pay-off matrix $\{d(b|S), b \in B_p^{n+1}\}$ using Eq. 4 and the Net Present Value of the new closure using Eq. 1;
10. Accept the new closure if $NPV^{n+1} - NPV^n > 0$, whereupon the current closure is updated into a new optimal closure, ie. $n = n + 1$ and go to step 5; and
11. if $j <$ #, the number of blocks with positive pay-offs $w(b)$, then go to step 6.

The deterministic floating cone algorithm presented above is heuristic in nature and not be optimal. Alternate B_p can be generated by varying the initial investment timing (step 1), the ordered path (step 3) and/or the mining schedule (step 8).

Investment timing to satisfy corporate constraints or to take advantage of cyclical commodity prices can be investigated as mutually exclusive opportunities by varying t_I, which modifies implicitly the mining schedule in step 8 above. For example, given a schedule S commencing at $t = 0$, the modified schedule $t' = t + t_I$. For delayed investment, the NPV for many potential production assets will typically be reduced unless maximum production/grade happens to coincide with the peak in cyclical commodity prices. However, for a risk averse and capital constrained company, the shift of the capital cost into future years may be strategically advantageous when considered in conjunction with other mining assets. Re-initiating the test sequence from the top of the mineral deposit each time a positively-valued cone is found and added to the closure is generally regarded to estimate the heuristic maximum undiscounted pay-off solution (Lemieux 1979). Computational experimentation on the ordering of blocks in step 3 above suggested that this also holds true for the discounted case when t_I is fixed. Note that, due to re-initiation of the test sequence it is p common for $B_p^{n+1} = B_p^n$ in step 7 above. For such instances, steps 8–10 above are ignored.

It is well known that the floating cone algorithm may not return the maximum undiscounted pay-off solution. However, it is used in the algorithm presented above to generate physically feasible solutions. The author has not investigated whether the Lerchs–Grossman and network flow algorithms could be substituted for the floating cone algorithm, but the non-linearity of the proposed objective function may present some difficulty. The computational efficiency of the proposed algorithm is enhanced significantly when a simple scheduling algorithm in step 8 above is employed. However, more complex risk-based scheduling algorithms to account

for multiple orebody models and production goals (eg. Godoy 2002; Richmond and Beasley 2004) could be considered.

Application to a Copper Deposit

This section demonstrates the proposed concepts for a large subvertical copper deposit. The geometry and contained copper per level are variable, but there is no strong trend. The options considered in this study were:

- Two processing options (ore and waste), ie. $K = 2$;
- 60 Mt/year mill constraint;
- 25 realisations of copper grades by Sequential Gaussian Simulation (SGS);
- 25 stochastic simulations of future copper prices with a two factor Pilipovic model that was modified to account for periodicity and cap and collar aversion (Fig. 2);
- 25 stochastic simulations of operating costs with a growth model (Fig. 3);
- Monthly copper recoveries randomly drawn from normal distribution with mean of 80% and a standard deviation of 1%;
- A fixed annual discount rate of 10%; and
- Initial investment timings at discrete yearly intervals for five years.

Figure 2 shows 25 stochastic simulations of future copper prices. The assumptions in this study were:

- A long-term copper price of $1.30/lb,

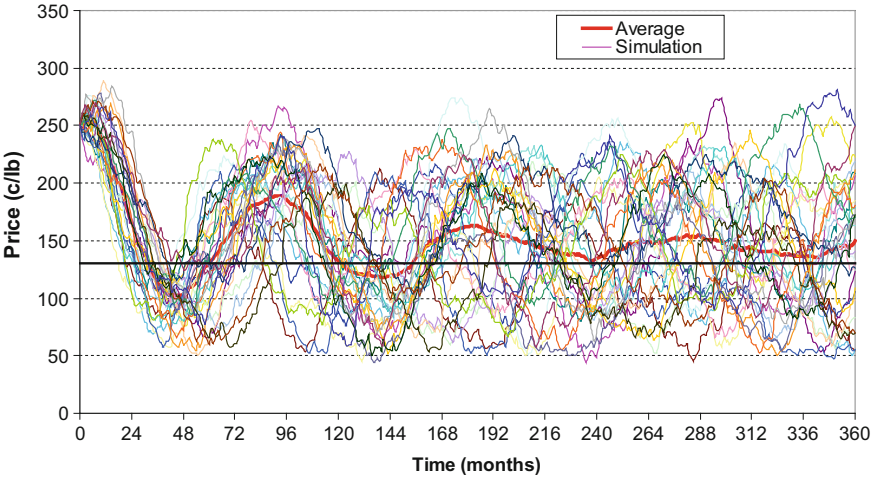

Fig. 2 Thirty year future copper price simulations with mean reversion and collar and cap aversion

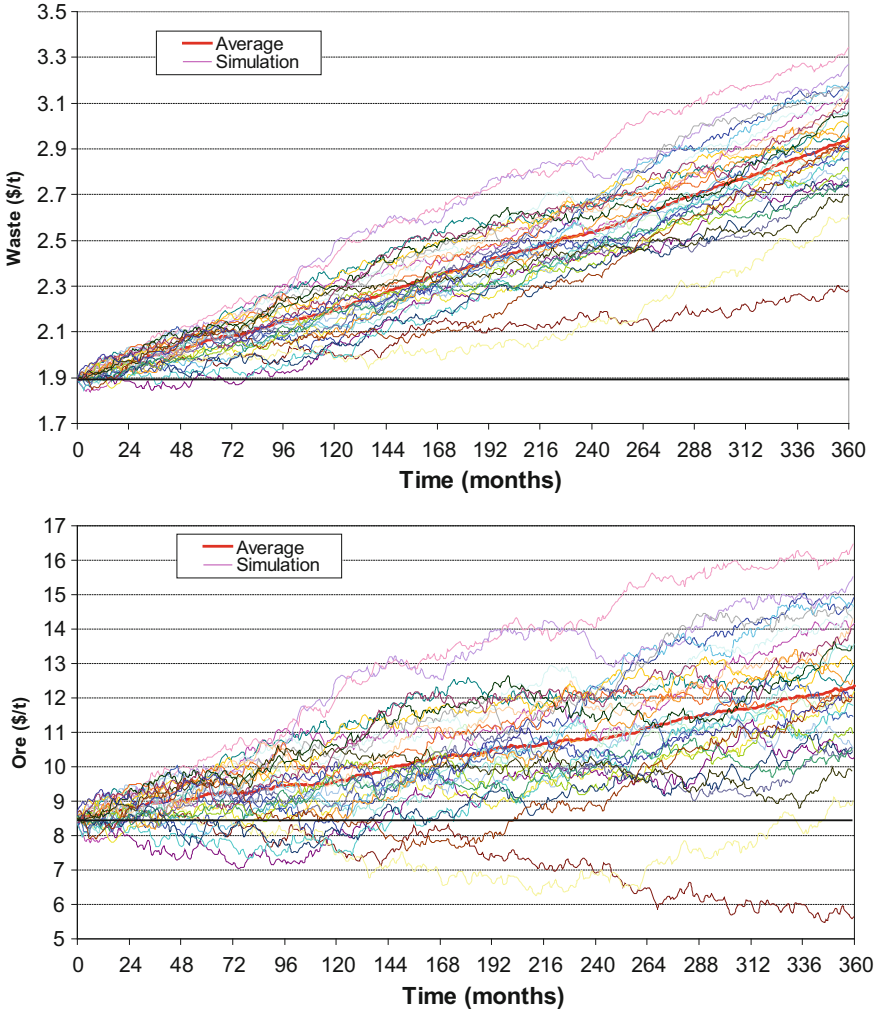

Fig. 3 Thirty year wate and ore processing cost simulations

- The present time ($2.50/lb) was near the peak of the price cycle,
- An average eight year copper price cycle, and
- $0.50/lb and $3.00/lb lower and upper aversion values.

Note that, as time increases uncertainty in the simulated copper price increases and the deviation of the average simulated value to the long-term price decreases. The average copper price does not fluctuate symmetrically around the long-term copper price due to the asymmetrical aversion limits. Figure 3 shows 25 stochastic simulations of waste and ore processing costs.

To assess the potential improvement in NPV against the traditional two-stage pit optimisation approach a base case scenario ($1.30/lb—80% recovery, $1.90/t waste cost and $8.50/t milling cost) was run to generate a series of nested pits using a FCA. The E-type (or average) of the 25 SGS realisations was adopted as the single grade model as it is known to be smoothed. The NPV for this series of pits using the base case assumptions are shown in Fig. 4 as crosses. The maximum NPV under the base case scenario is associated with a pit closure of 26,402 blocks. Note that, the capital cost, which could also be modelled stochastically, was not included in this study.

The NPV for the FCA nested pits were also calculated using the simulated grades, metal prices, costs and recoveries for the six annual investment timings, shown in Fig. 4. Note that:

- These curves vary substantially from the base case.
- In all instances the maximum NPV pit is significantly larger (49,239–85,093 blocks) than the base case and the maximum NPV is higher than for the base case.
- Delaying the investment from Year 3 to Year 5 results in a higher NPV ($3.02 billion versus $2.88 billion). At first this relationship appears counter-intuitive as costs are greater and discounting greater. However it is related to higher Cu prices in key production periods.

The NPV of the proposed DFC approach for the six annual investment timings are also shown in Fig. 4. Note that, considering the mining schedule explicitly in the optimisation process was successful in finding the maximum NPV pit in a single run. Whilst the improvement over the maximum NPV pit from the two-step

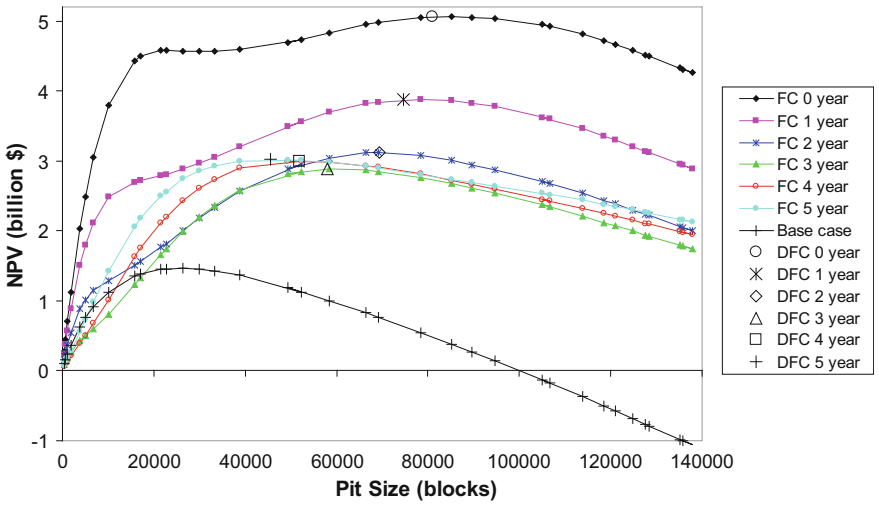

Fig. 4 Pit size versus NPV (FCA = floating cone algorithm; DFC = proposed direct NPV FCA)

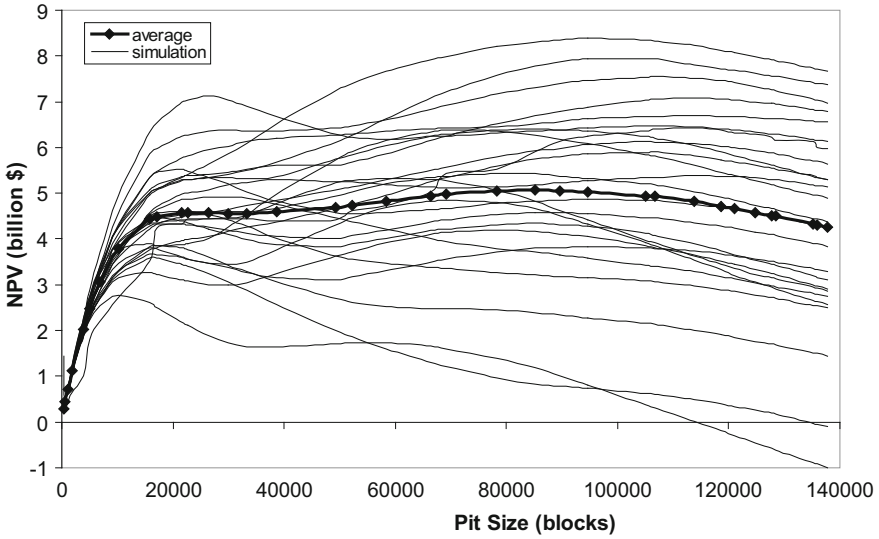

Fig. 5 Pit size versus NPV distirbution

approach that considered the stochastic inputs was limited (usually <0.5% in NPV), there was often some difference in the pit dimension. It is likely that these differences would be reduced further if additional pit closures had been generated for evaluation in the two-step approach. Computationally, it was more efficient to post process a finite series of pit closures than embed the scheduler in the pit optimisation process. In the example shown, the DFC approach that generated a single pit required around the same computational time as that required in generating 36 nested pits by a simple FC approach.

Figure 5 shows the distribution of potential NPVs for the set of nested FCA pits without any investment delay. As expected, the uncertainty increases with pit size with some possibility of negative NPVs for large pit closures. If minimising downside financial risk is of greater importance than maximising the NPV then the financially efficient set (frontier) of open pit limits could be determined under a stochastic framework (Richmond 2004a).

Conclusions

A novel method for working with discounted pay-off matrices during open pit optimisation was proposed. The approach used in this study embedded a simple ore scheduler in a floating cone-based heuritic algorithm. It was a trivial exercise to further consider multiple orebody models, local ore loss and mining dilution, time-dependent commodity prices and costs and variable metal recoveries during

optimisation. As a consequence, alternate project development timings could be strategically assessed. Traditional evaluation of a set of nested pit shells with constant metal prices and operating costs failed to determine the maximum NPV pit under uncertain conditions. However, provided that sufficient pit shells were generated and evaluated with the same stochastic price and cost input as for the proposed algorithm there was little difference in the maximum NPV shell derived. Further experimentation should be undertaken to determine whether this observation holds for more complex mining schedule algorithms and geometrically irregular orebodies, as well as when a smoothed block model other than the E-type of the stochastic grade model is used to generate a series of nested closures.

This study demonstrated that uncertainty in future metal prices and operating costs cannot be adequately captured in open pit optimisation by simply post-processing a series of nested pit closures with constant values. Stochastic modelling of mineral grades, mineral recovery, commodity prices and capital and operating costs provide an ideal platform to:

- Generate an optimal pit to maximise the overall project NPV considering geological and market uncertainty,
- Determine the optimum investment and project start up timing, and
- Quantify the multiple aspects of uncertainty in a mine plan.

The example studied in this paper indicates periods of potential financial weakness that could benefit from management focus (eg. forward selling strategies and placing the mine on care and maintenance) prior to difficulties arising.

References

Caccetta L, Hill SP (2003) An application of branch and cut to open pit mine scheduling. J Glob Optimisation 27:349–365

Dimitrakopoulos R, Abdel Sabour SA (2007) Evaluating mine plans under uncertainty: can the real options make a difference? Resour Policy 32:116–125

Dowd PA, Onur AH (1993) Open pit optimisation—part 1: optimal open-pit design. Trans Inst Min Metall Min Technol 102:A95–A104

Godoy M (2002) The effective management of geological risk in long-term production scheduling of open pit mines. Ph.D. thesis, University of Queensland, Brisbane

Godoy MC, Dimitrakopoulos R (2004) Managing risk and waste mining in long-term production scheduling. SME Trans 316:43–50

Hochbaum DS, Chan A (2000) Performance analysis and best implementations of old and new algorithms for the open-pit mining problem. Oper Res 48:894–914

Johnson TB (1968) Optimum open pit mine production scheduling. Ph.D. thesis, University of California, Berkeley, p 120

Korobov S (1974) Method for determining ultimate open pit limits, department of mineral engineering. Ecole Polytechnique, Montreal

Leite A, Dimitrakopoulos R (2007) A stochastic optimisation model for open pit mine planning: application and risk analysis at a copper deposit. Trans Inst Min Metall Min Technol 116: A109–A118

Lemieux M (1979) Moving cone optimising algorithm. In: Computer methods for the 80s, SME of AIMMPE, New York, pp 329–345

Lerchs H, Grossman IF (1965) Optimum design of open pit mines. Bull Can Inst Min 58:47–54

Menabde M, Froyland G, Stone P, Yeates, GA (2017) Mining schedule optimisation for conditionally simulated orebodies, in this volume

Menabde M, Stone P, Law B, Baird B, (2007) Blasor—a generalised strategic mine planning optimisation tool, 2007 SME Annual Meeting and Exhibit

Monkhouse PHL, Yeates G (2018) Beyond naive optimisation, in this volume

Ramazan S (2007) The new fundamental tree algorithm for production scheduling of open pit mines. Eur J Oper Res 177:1153–1166

Ramazan S, Dimitrakopoulos R (2013) Production scheduling with uncertain supply: a new solution to the open pit mining problem. Optim Eng 14:361–380

Ramazan S, Dimitrakopoulos R (2017) Stochastic optimisation of long-term production scheduling for open pit mines with a new integer programming formulation, in this volume

Ravenscroft PJ (1992) Risk analysis for mine scheduling by conditional simulation. Trans Inst Min Metall Min Tech, 101:A101–108

Richmond AJ (2004a) Integrating multiple simulations and mining dilution in open pit optimisation algorithms. In: Dimitrakopoulos R (ed) Orebody modelling and strategic mine planning, spectrum series, vol 14. The Australasian Institute of Mining and Metallurgy, Melbourne, pp 317–322

Richmond AJ (2004b) Financially efficient mining decisions incorporating grade uncertainty. Ph.D. thesis, Imperial College, London, p 208

Richmond AJ, Beasley JE (2004) An iterative construction heuristic for the ore selection problem. J Heuristics 10(2):153–167

Stone P, Froyland G, Menabde M, Law B, Pasyar R, Monkhouse P (2018) Blended iron-ore mine planning optimisation at Yandi Western Australia, in this volume

Whittle J (1999) A decade of open pit mine planning and optimisation—the craft of turning algorithms into packages. In: Proceedings APCOM' 99 computer applications in the minerals industries 28th international symposium, Colorado School of Mines, Golden, pp 15–24

Part III
Simultaneous Optimisation of Multiple Operations and Processes

Simultaneously Optimizing Open-Pit and Underground Mining Operations Under Geological Uncertainty

L. Montiel, R. Dimitrakopoulos and K. Kawahata

Abstract A method that optimizes mining complexes which are comprised of multiple processing destinations, open pits and underground operations is presented. Mining, blending, processing and transportation decision variables are simultaneously optimized while accounting for geological uncertainty. The method uses a simulated annealing algorithm at different decision levels in order to generate a stochastic-based extraction sequence and processing policies. A case study shows its ability to generate a higher NPV while facing a reduced amount of risk when compared to traditional optimization methods.

Introduction

A mining complex is a value chain with multiple components: deposits, stockpiles, processing destinations and transportation systems. Optimizing a mining complex demands the simultaneous optimization of all its components, a problem known in the mining literature as global optimization of mining (Whittle 2007, 2018). Several methods have been developed to incorporate multiple components of the value chain during the optimization. Hoerger et al. (1999) formulate the problem of optimizing the simultaneous mining of multiple pits and the delivery of ore to multiple plants as a mixed integer program. The model groups blocks into increments and accounts for multiple stockpiles. The authors implement the model at Newmont's Nevada operations where 50 sources, 60 destinations and 8 stockpiles

L. Montiel (✉) · R. Dimitrakopoulos
COSMO—Stochastic Mine Planning Laboratory,
McGill University, Montreal, QC H3A 0E8, Canada
e-mail: luis.montiel@mail.mcgill.ca

R. Dimitrakopoulos
e-mail: roussos.dimitrakopoulos@mcgill.ca

K. Kawahata
Newmont USA Limited, Golconda, NV 89414-0069, USA
e-mail: kazuhiro.kawahata@newmont.com

R. Dimitrakopoulos (ed.), *Advances in Applied Strategic Mine Planning*,
https://doi.org/10.1007/978-3-319-69320-0_16

are present, and leads to an increase of profitability by taking advantage of the synergies. Stone et al. (2018, this volume) present the Blasor optimization tool developed by the mine planning optimization group within BHP Billiton technology. Blasor formulates the problem of determining the optimal extraction sequence of multiple pits as a mixed integer linear program and solves it using ILOG CPLEX (Ilog 2011). Blasor aggregates spatially connected blocks that have similar properties and generates nearly-optimal solutions in practical times in large-scale operations: Yandi (1000 aggregates, 11 pits, 20 periods) and Illawarra Coal mine (8 domains) (Rocchi et al. 2011). Zuckerberg et al. (2007) present Blasor-InPitDumping (Blasor IPD) that is an extension of Blasor that accounts for waste handling; that is, it incorporates refilling mined-out areas with waste. Zuckerberg et al. (2011) introduce Bodor to optimize the sequence of extraction of bauxite 'pods' at Boddington bauxite mine, south-western Australia. Pods are distinct bodies of modest-sized ore that are lying close to the surface. Chanda (2018, this volume) formulates the delivery of material from different deposits to a metallurgical complex as a network linear programming optimization problem. The model attempts to minimize the costs through the network that encompasses mines, concentrators, smelters, refineries and market regions. Wooller (2007) describes COMET, software used to optimize mill throughput/recovery and cut-off grade. COMET uses an iterative algorithm to define operating policies and process routes; e.g., heap leach versus concentration. Whittle (2007) introduces the global asset optimization tool incorporated in Whittle software. The tool is designed to optimize the sequence of extraction of multiple deposits considering complex processing and blending operations.

The methods described above ignore the uncertainty associated with different parameters. Groeneveld et al. (2018, this volume) incorporate uncertainty in market price, costs, utilization of equipment, plant recovery and time for building options (infrastructure) while simultaneously optimizing mining, stockpiling, processing and port policies. Bodon et al. (2017, this volume) models the problem of supplying exports in a coal chain as a discrete event simulation model (DES). The model is able to asses various operating practices, including maintenance options and capital expenditure to determine the best infrastructure for a given system. In both methods, geological uncertainty is discarded, which is the major contributor of not meeting production targets and NPV forecasts. Although efficient and able to incorporate several components of the value chain, the methods available in the technical literature have at least one of the following limitations when globally optimizing mining complexes: some decisions are fixed when they should be dynamic (operating modes, destinations of mining blocks, etc.); component-based objectives are imposed, which may not coincide with global objectives; many parameters are assumed to be known when they are uncertain (Whittle 2007).

Several methods have been used to incorporate geological uncertainty for the open pit production scheduling problem (Ravenscroft 1992; Dowd 1994; Godoy 2002; Dimitrakopoulos and Ramazan 2004; Albor and Dimitrakopoulos 2009, 2010; Ramazan and Dimitrakopoulos 2013, 2018 in this volume; Lamghari and Dimitrakopoulos 2012; Menabde et al 2018 this volume; Lamghari et al. 2013);

however, little work has been done regarding the production scheduling of underground mines. Grieco and Dimitrakopoulos (2018, this volume) implement probabilistic programming in stope design optimization. The authors evaluate the probabilities of the different rings of being above specified cut-offs. However, the probabilistic programming formulation discards the compound relationship between rings whereas stochastic formulations make full use of joint local uncertainty. Bootsma et al. (2018, this volume) present sublevel stope mine optimisation based on simulated mineral deposits.

Global (simultaneous) stochastic optimization formulations for mining complexes is a new development (Montiel and Dimitrakopoulos 2015; Goodfellow and Dimitrakopoulos 2016, 2018 this volume) and is explored herein. This paper describes a method for the simultaneous stochastic optimization of different components of a mining complex comprised of open pits and underground operations. The method is described in the next section, its implementation at a gold complex is then displayed and finally conclusions are presented.

Optimizing the Components of the Value Chain

Preliminaries

The components of a mining complex are strongly interrelated (Fig. 1). Any decision taken in a particular component affects the decisions taken at the others. To optimize a mining complex the different components must be optimized simultaneously. Mineral deposits are the sources of material. Different types of ore are extracted via open pits or underground mining methods. Open pits are discretised into mining blocks whereas underground mines are comprised of development, preparation and production activities. Different underground mining methods have different activities; however, regardless of the mining method, the mine design can be discretised in activities and dependencies; that is, each activity has a set of successor and predecessor activities, similar to slope constraints in an open pit.

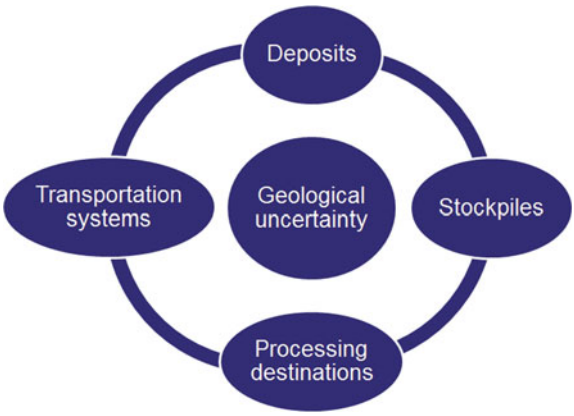

Fig. 1 Components of a mining complex

Mining blocks in open pits and activities in underground mines are named as 'units' in this article. Each unit can be sent to a particular processing destination or a stockpile. There may be as many stockpiles as metallurgical ore types available from the deposits. Stockpiles contain potential ore, contribute to the blending operation and serve as a backup supply of material. Each processing destination may have operating modes that determine the operating costs, metallurgical recoveries, operational blending limits for the metallurgical properties and throughputs. For example, the capacity, operating cost and recovery of a milling plant change if it operates to generate fine material (80 μm) or coarse material (120 μm). The choice of operating mode at a processing destination should be made by accounting for the decisions taken at the other components of the value chain. In some cases, the quality of the material extracted from different deposits does not meet the specific blending requirements at a given processing destination. To meet the quality targets, external blending materials are added to specific destinations (Fig. 2). These materials come from external sources and have very specific qualities. For example, in an autoclave, external material with high sulphide and low carbonate may be added to meet the SS/CO_3 ratio if the ore extracted from the deposits have low sulphide.

The output material from the processing destinations is transported to final stocks or ports using available transportation systems (Fig. 3). It is important to account for transportation systems when optimizing a mining complex given that they can limit the overall throughput of the system (bottleneck). Each transportation system has its associated cost and capacity.

Mathematical Model

The goal is to maximize expected NPV while minimizing deviations from targets associated with the different components of the value chain. The objective function

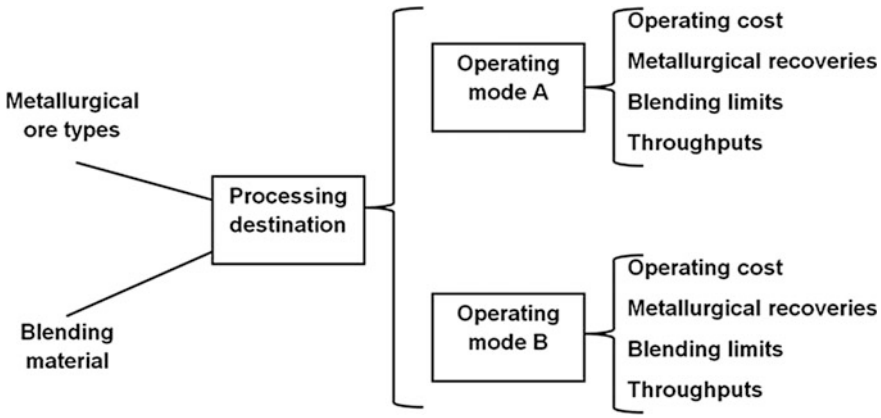

Fig. 2 Processing destination

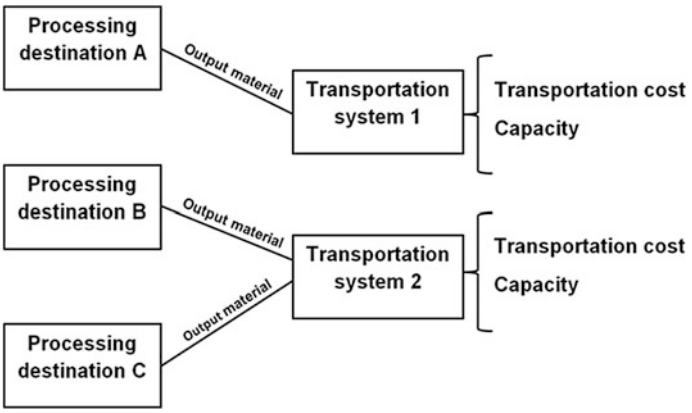

Fig. 3 Transportation systems

(Eq. 1) has two terms: *discprofit(s, t)* is the discounted profit in period t under scenario s; *penalty(s, t)* is a term that accounts for the penalized deviations from the targets at different components in period t under scenario s. Each scenario is a combination of orebody simulations of the deposits.

$$maximize\, O = \sum_{s=1}^{S} \sum_{t=1}^{T} (discprofit(s,t) - penalty(s,t)) \tag{1}$$

The discounted profit at each period and scenario is calculated by accounting for the revenue obtained by selling the different products, the cost of mining at all deposits, the cost of processing the material at all destinations, the cost of stockpiling the material, the cost of sending material from the stockpiles to the available processing destinations and the transportation costs.

$$\begin{aligned} discprofit(s,t) = {} & revenue(s,t) - minecost(s,t) - procost(s,t) - stockcost(s,t) \\ & - rehandlecost(s,t) - transcost(s,t) \end{aligned} \tag{2}$$

The second term of the objective function, $penalty(s,t)$, accounts for the penalized deviations, and is evaluated as.

$$penalty(s,t) = penalmine(s,t) + penaltrans(s,t) + penalpro(s,t) + penalmetal(s,t) \tag{3}$$

where *penalmine(s, t)* are the penalized deviations from the capacities of the different mines, *penaltrans(s, t)* are the penalized deviations from the capacities of the different transportation systems, *penalpro(s, t)* are the penalized deviations from the

capacities at the different processing destinations and *penalmetal(s, t)* are the penalized deviations from the operational ranges of some operational properties.

Three sets of decision variables are used to evaluate revenues, costs, production and deviations at the different components of the value chain. X_{itd} is a binary variable that represents whether or not a particular unit i is mined in period t and sent to processing destination d. Y_{tdo} is a binary variable that represents whether or not an operating mode o is used in destination d during period t. Z_{tdr} represents the proportion of output material from destination d transported using transportation system r during period t. The following equations show the evaluation of tonnages at different components using the decision variables described above.

$$mineproduction(s,t) = \sum_{i=1}^{I} \sum_{d=0}^{D} X_{itd} \cdot m_{is} \tag{4}$$

$$tonneoutprocess(s,t,d) = \sum_{o=1}^{O(d)} (tonneprocess(s,t,d) \cdot Y_{tdo} \cdot P_{do}) \tag{5}$$

$$tonnetransport(s,t,r) = \sum_{d=1}^{D} (tonneoutprocess(s,t,d) \cdot Z_{tdr}) \tag{6}$$

The amount of material extracted from the deposits can be evaluated using Eq. 4, the output material from a given destination can be evaluated using Eq. 5 and the amount of material transported using a particular transportation system using Eq. 6. The set of all units from the deposits is represented by I, D is the set of processing destinations, m_{is} is the tonnage of unit i under scenario s, $O(d)$ is the set of operating modes available at destination d, *tonneprocess(s, t, d)* is the tonnage sent to destination d from the deposits and the stockpiles in period t under scenario s and P_{do} is the proportion output/input tonnage in destination d using operating mode o.

A mining complex may contain a large number of units which leads to a complex optimisation model that is hard to solve. Hence, it is necessary to find solution methods that overcome this limitation.

Solution

Any solution of the optimization model must answer the questions associated with the three main sets of decision variables: (i) which units are going to be extracted in each period and where are they going to be sent? (X_{itd} variables); (ii) which operating modes are going to be used at the different processing destinations? (Y_{tdo} variables); (iii) which transportation systems are going to be used? (Z_{tdr} variables).

Given a particular solution, it is possible to modify the objective value by generating perturbations at the three different decision levels. These perturbations should be done towards improvements in the objective value. Given the monetary value associated with time due to discounting, profitable units should be pushed to be extracted in early periods and non-profitable ones should be pushed to later periods. Operating and transportation decisions should minimize processing and transportation costs and deviations.

The Perturbation Mechanism

For each unit u, it is possible to calculate the cumulative profit of u in every destination by accumulating the economic value in each scenario (Fig. 4). The cumulative profit provides a guidance of the most profitable destinations for a particular unit and controls the iterating process when swapping periods and destinations of a mining unit (Fig. 5). If the greatest cumulative profit of a unit is positive, extracting that unit in an earlier period will be favoured; otherwise, the iterating process will favour extracting the unit in a later period. The candidate destinations include the destinations with positive cumulative profit if the unit is profitable, or the less unprofitable destination in the opposite case.

The iteration process over the candidate periods and destinations of a mining unit is designed to increase the expected NPV given the time value of money. However, the objective value of the perturbed solution is also affected by the

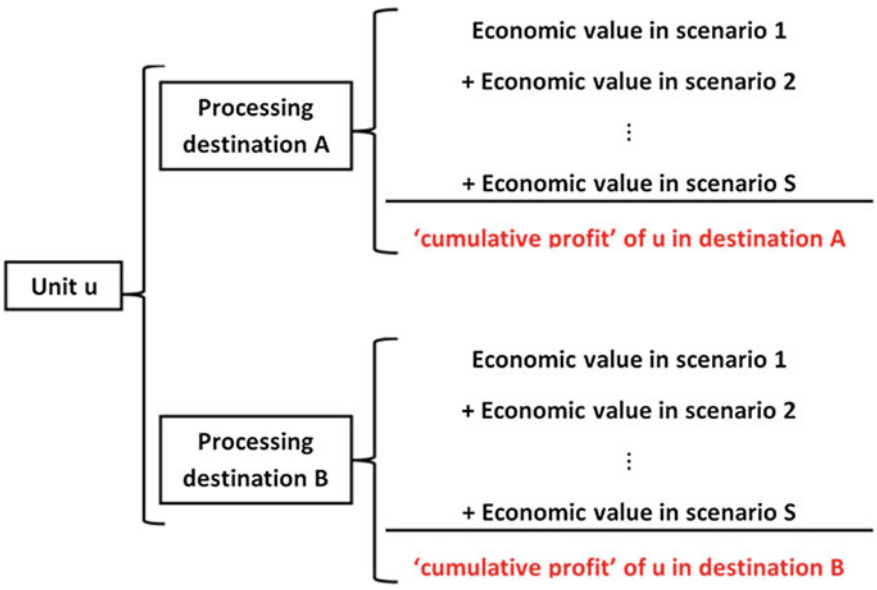

Fig. 4 Cumulative profit of a unit

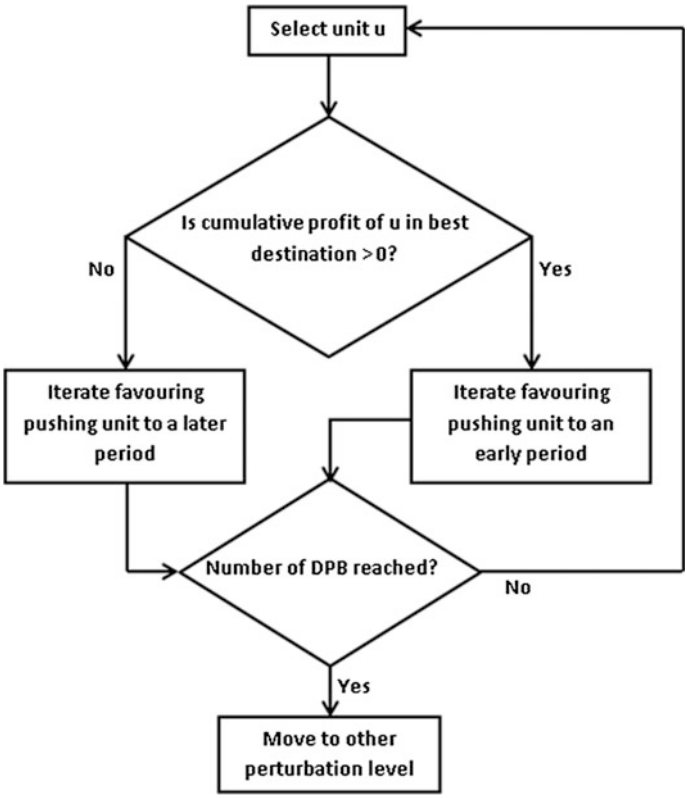

Fig. 5 Perturbation of units

penalized deviations, therefore, there might be cases when pushing a profitable unit to a later period or an unprofitable one to an earlier period increases the objective value given the lower deviations in the new solution. In these cases, the objective function can be seen as trade-off between maximizing the expected NPV and minimizing the penalized deviations.

The perturbations at an operating decision level consist in swapping operating modes at different processing destinations towards improvements in the objective value. The perturbations at the transportation decision level consist in modifying the transportation proportions of the output material from the different processing destinations; for example, changing the transportation of the output material from a mill from 50% trucks/50% pipeline to 70% trucks/30% pipeline. The transportation perturbation mechanism seeks for minimizing transportation costs and deviations. At any level, perturbations are accepted or rejected using Eq. 7 from the Metropolis algorithm (Metropolis et al. 1953; Kirkpatrick et al. 1983).

$$P(\Delta O) = P(O_{new} - O_{current}) = \begin{cases} 1 & if\, \Delta O \geq 0 \\ e^{\frac{-\Delta O}{T}} & otherwise \end{cases} \quad (7)$$

where T is the annealing temperature. The probability of accepting an unfavourable perturbation is greater at higher temperatures. As the optimization proceeds, the temperature is gradually lowered by a reduction factor. When the temperature approaches to zero, the probability of accepting an unfavourable swap tends to zero. This allows the algorithm to converge to a final solution.

The Method

The method proposed to optimize a mining complex has three stages (Fig. 6). The first stage consists in assigning periods and destinations to the mining units from an initial solution. In the second stage the method evaluates the profits, productions and deviations at the different scenarios. It also evaluates the cumulative profit of the mining units at the different destinations. The last stage is the perturbation mechanism at the three different decision levels. The algorithm stops when it reaches a user-specified number of iterations or poor improvement is presented in the objective value after a certain number of perturbations (Fig. 6).

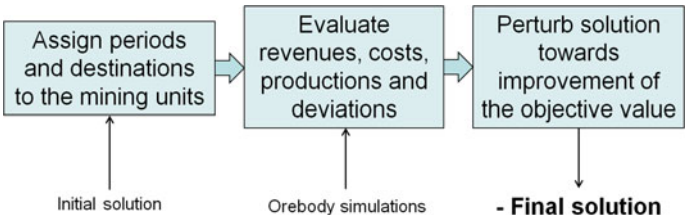

Fig. 6 Method

Fig. 7 Gold mining complex

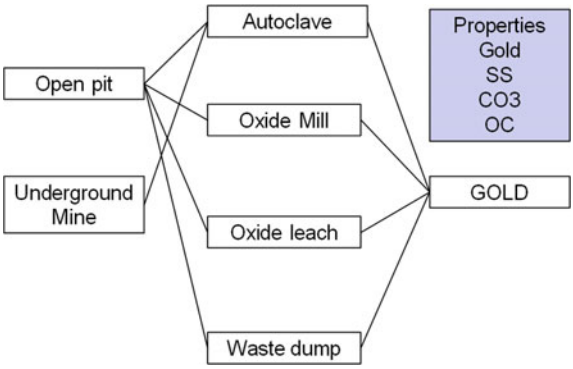

Case Study: A Gold Operation

The method is implemented at a gold mining complex comprised of one open-pit and one underground mine (Kawahata et al. 2013). Higher-grade oxide ore is processed at a mill, lower-grade is treated on heap leach pads. Refractory ore is processed at one autoclave. The open pit provides both oxide and refractory ore whereas the underground mine just provides refractory ore for the autoclave. Twenty orebody simulations for gold, sulphide sulphur, CO_3 and organic carbon are provided for the open-pit, generated using the direct block simulation method for correlated variables (Godoy 2002; Boucher and Dimitrakopoulos 2009). The higher concentrations of gold are located in the north-east part of the deposit where the current mining phases are located (Fig. 8). The gold and sulphide sulphur grades are controlled by the mineralized domains whereas the carbonate and organic carbon are spread in all the area of the deposit.

The underground mine uses underhand-cut-and-fill due to the relatively low rock quality in the ore zones. Intensity of gold mineralization is related to structural complexity and the location of rocks chemically receptive to mineralization. The production zones are located in the high grade areas (Fig. 9). Twenty orebody simulations are generated for the underground deposit using direct block simulation by considering the drillhole data within the mineralized domain (Godoy 2002; Benndorf and Dimitrakopoulos 2017 in this volume). Figure 10 shows the validation of the orebody simulations generated. It can be observed that the simulations respect the statistics of the drillhole data as they reproduce its histograms and variograms at the main directions of anisotropy. The simulated values at each unit are calculated by averaging the simulated points that fall inside; that is, given the different shapes and sizes of the underground mining units, there is no single support size as in the open pits where the mining blocks have the same size. Figure 11 shows three different orebody simulations and the production zones of the mine.

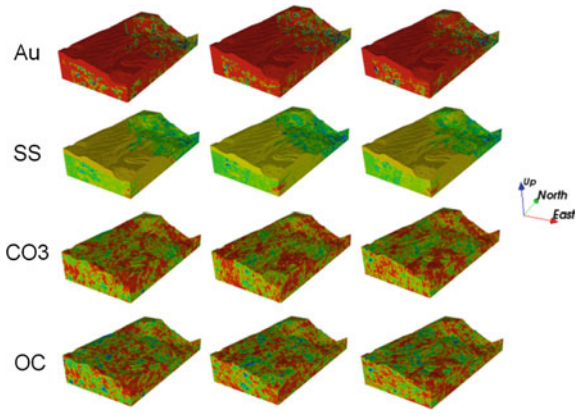

Fig. 8 Three orebody simulations of the open pit

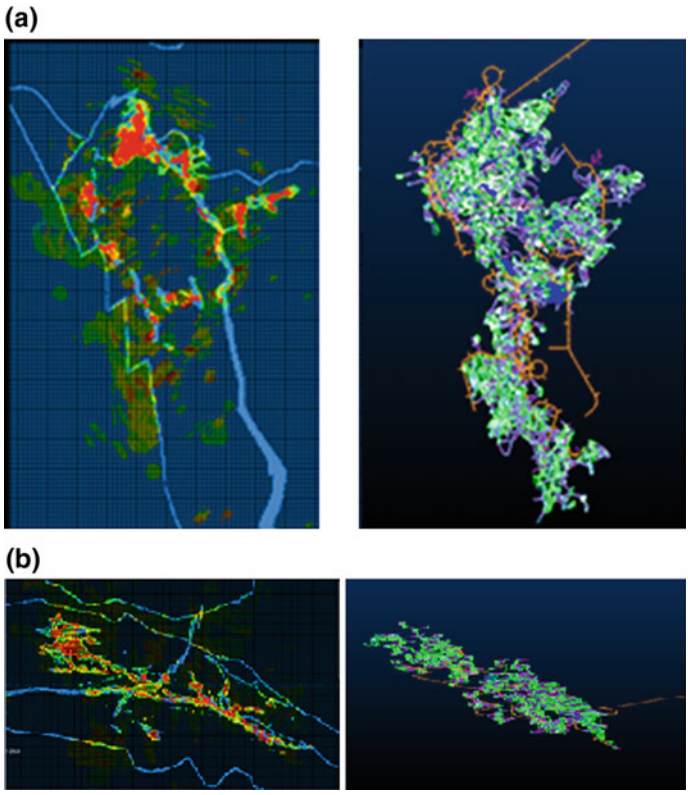

Fig. 9 Gold grades (left) and production zones (right) in the underground mine: **a** Plan view; **b** Cross section

The autoclave has tight operating ranges for SS/CO_3, SS, CO_3 and organic carbon. To help metallurgical blending, concentrates from other plants are added to the process (Fig. 12). In the three processing destinations the metallurgical recovery of gold follows non-linear curves. In the autoclave the recovery curve is a function of the gold grades and the organic carbon whereas in the oxide mill and the heap leaching plant the recovery is a function of gold grades only.

Initial Solution

An initial solution for the optimization of the gold complex was generated by: (i) Considering the current mining plan in the underground mine that was developed by the mine planners using Enhanced Production Scheduler (EPS) software; (ii) using Milawa scheduler in Whittle software for the open-pit using the e-type of

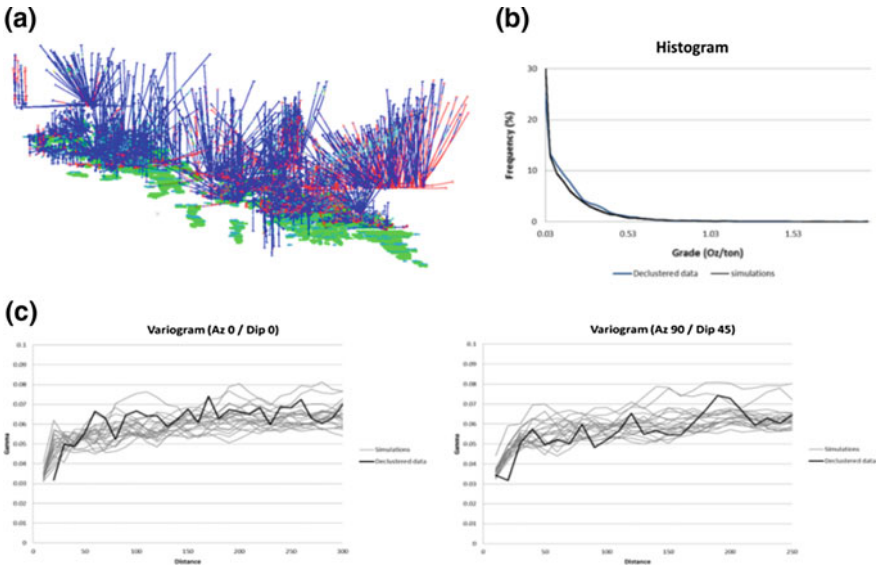

Fig. 10 Validation of the simulations in the underground mine: **a** Drillhole data; **b** Histogram reproduction; **c** Variogram reproduction

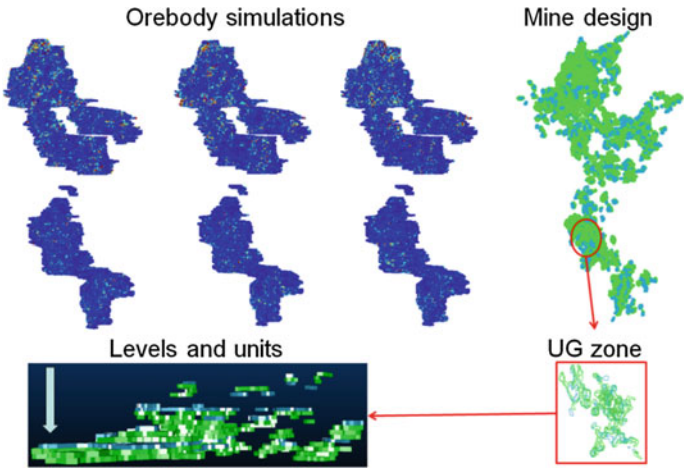

Fig. 11 Orebody simulations and production zones of underground mine

the orebody simulations; that is, the average grades of the mining blocks at the different realizations.

The amount of external blending material used in the autoclave is considered when evaluating the results of the implementation of the initial solution over the different scenarios (combinations of orebody simulations of both deposits).

Fig. 12 Sage autoclave

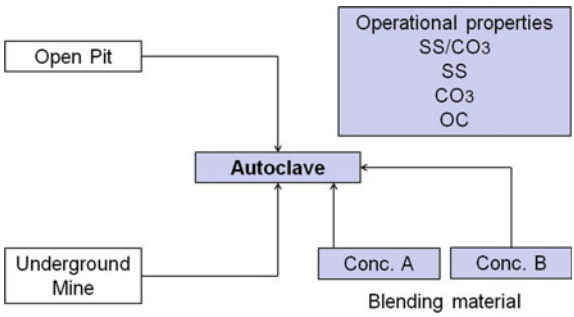

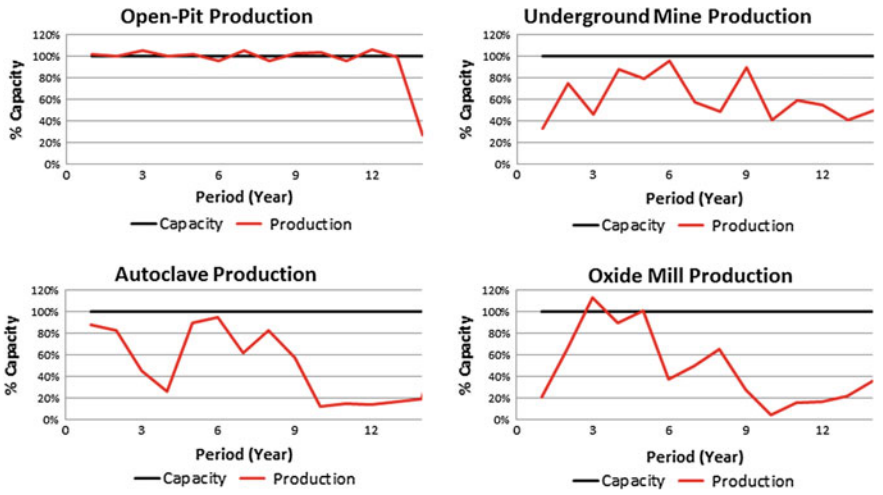

Fig. 13 Productions with the initial solution

The productions of the two mines, the autoclave and the oxide mill are shown in Fig. 13. It can be observed that the underground mine operates below the capacity whereas the open-pit operates very close to its capacity until the depletion of the reserves. Although external blending material is added to the autoclave, given the tight blending constraints imposed to this processing destination, the conventional scheduler can only find blended material to fill the capacity in three periods of the life of the mine (LOM). There is a big shortfall in production in the autoclave in year 4, and after year 9 the tonnage sent to this processing destination is very marginal. Regarding the oxide mill, the production is going to be close to the capacity in years 2–4 but deficient production is observed in the rest of the periods of the LOM. However, most of the oxide ore filled to this processing destination comes from another pit that is not considered in this study.

The *SS* is below the operational ranges in most of the years whereas the SS/CO_3 ratio falls below the operational ranges in the last years (Fig. 14). The CO_3 increases with time and falls inside the operational ranges in most of the years.

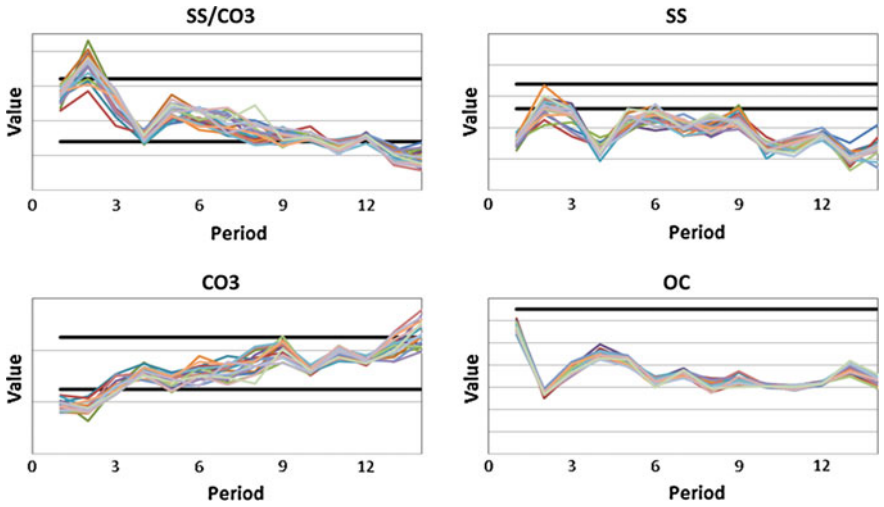

Fig. 14 Operational properties with the initial solution

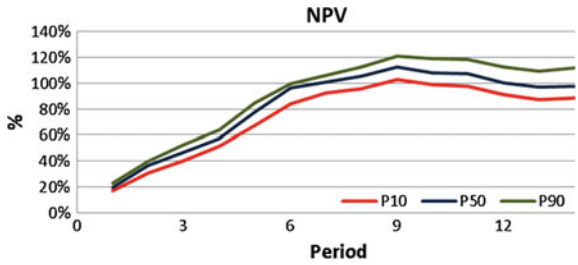

Fig. 15 NPV with the initial solution

The organic carbon is well controlled in all the different scenarios. The risk profile of the NPV is displayed in Fig. 15. It is observed that after year 9 the cumulative NPV starts to decrease given the marginal tonnage sent to the autoclave. It will be more profitable to stop the operation after year 9. However, there is another pit that is not considered in this study, which can add more years of profitable operation.

Optimisation Parameters

Different tests are performed to define the optimization parameters that lead to the largest improvement of the objective value. Different initial temperatures, reducing factors and number of perturbations were evaluated. Figure 16 shows the evolution of the objective value with the number of perturbations for six different initial temperatures. The largest improvement in the objective value is obtained with an initial temperature of the order of 1 million.

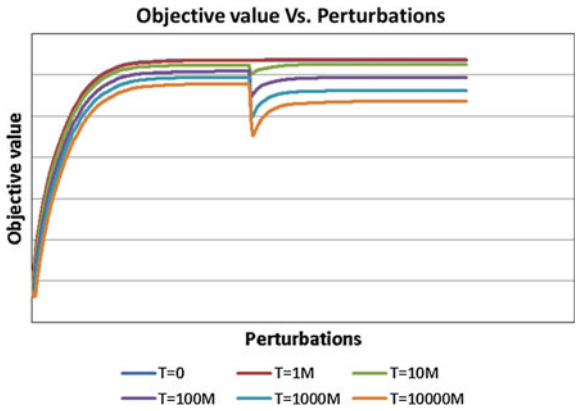

Fig. 16 Evolution of the objective value with different temperatures

Other important parameters to define are the per-unit penalty values associated with the targets at the different components. The magnitude of the penalties must be defined so as to balance the two terms of the objective function. Too high penalty values will improve the reproduction of the targets ignoring the first term of the objective function generating poor improvement of expected NPV. Conversely, too small penalty values will generate impractical solutions with large and non-realistic NPV forecasts given the large violations of the targets.

Stochastic Solution

The method is next implemented after setting up the optimization parameters. It is possible to observe from Fig. 17 that the solution asks for operating the underground mine very close to its target except in year 12 where there is a big shortfall. However, the productions at the autoclave and the oxide mill are below their capacities in all the periods of the LOM. Regarding the blending properties, a similar behaviour is observed when compared with the deterministic initial solution (Fig. 18). Given the low sulphide sulphur presented in the simulations, the method is not able to accommodate the sulphide sulphur inside the operational ranges. The expected NPV is 14% greater than the one obtained with the deterministic initial solution (Fig. 19).

The method is implemented considering different amounts of external blending material input to the autoclave. In particular, the amount concentrate A fed to the autoclave is increased five times given its high sulphide sulphur. The productions at the underground mine and the autoclave and the sulphide sulphur with the new stochastic solutions are displayed in Fig. 20. It can be observed that by increasing the amount of concentrate A the method is able to find more material to blend in order to increase the production in the autoclave. Furthermore, the sulphide sulphur approaches the operational ranges by increasing the external blending material given its large sulphide sulphur content compared to the material extracted from the

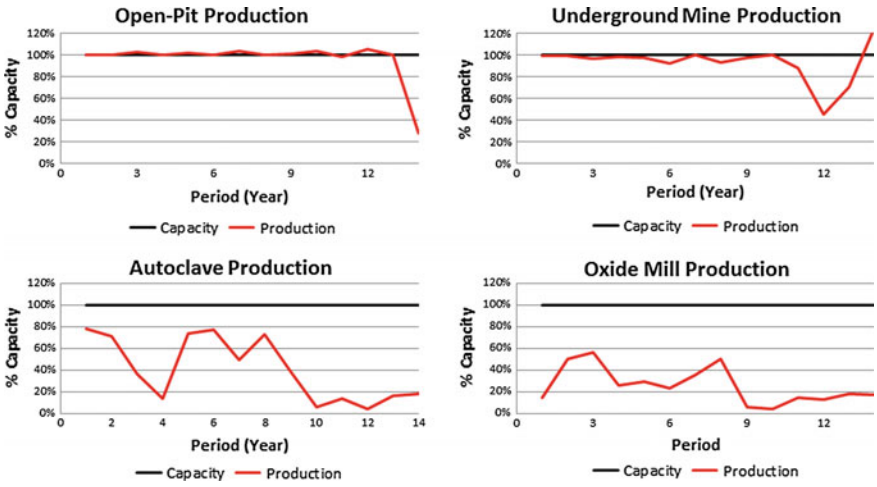

Fig. 17 Productions with the stochastic solution

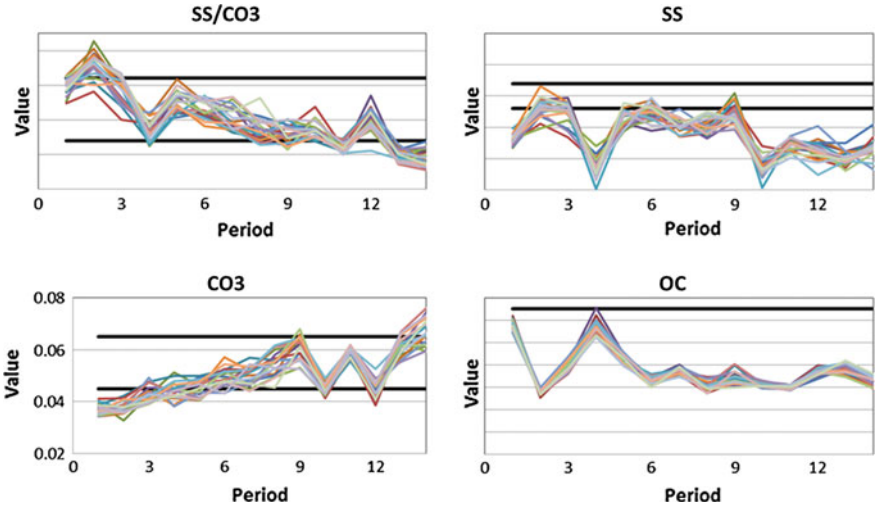

Fig. 18 Metallurgical properties with the stochastic solution

Fig. 19 NPV with the stochastic solution

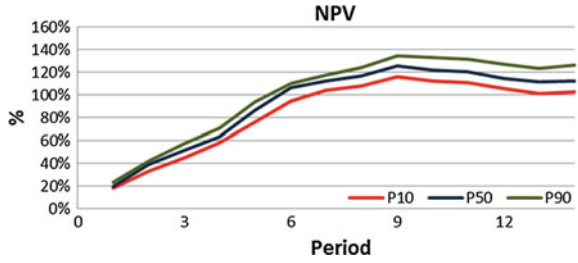

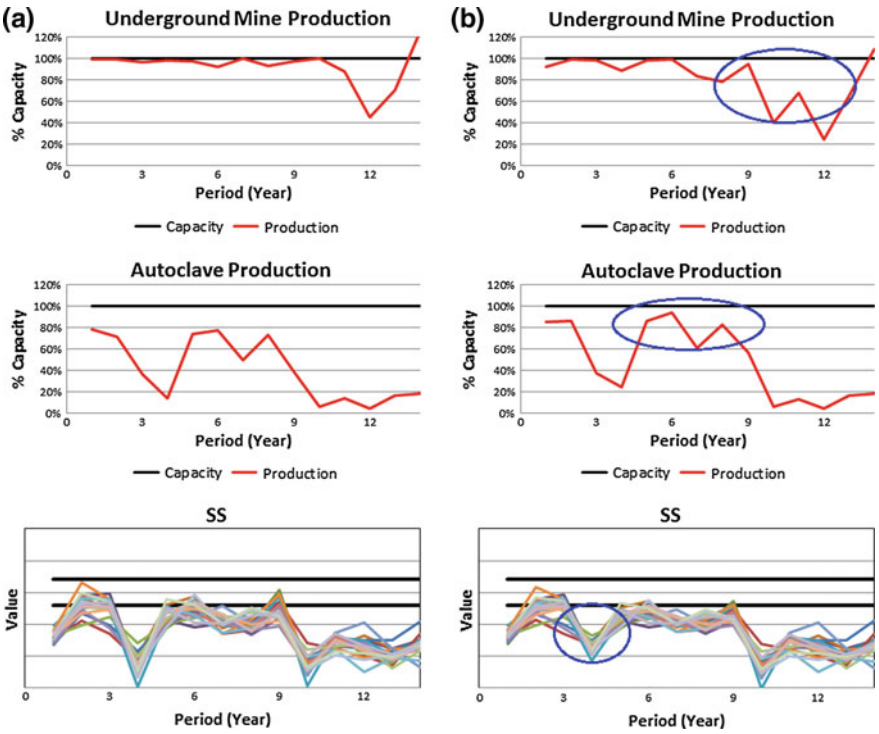

Fig. 20 Productions with the new stochastic solution: **a** Concentrate A; **b** Concentrate A × 5

deposits. However, the content of sulphide sulphur is still below the operational ranges given the low grade in the orebody simulations.

The expected NPVs of both stochastic solutions are very similar (Fig. 21). However, the availability of concentrate A is a strong assumption. The shortfall in production in the autoclave in year 4 in both stochastic solutions suggests that the method got trapped in a local optimum. To overcome this situation, a diversification strategy in the perturbations at the unit decision level is desired. A better control of the operational ranges and the capacity of the autoclave are obtained with the stochastic approach when considering a set of initial stockpiles. These results are displayed in Appendix 1.

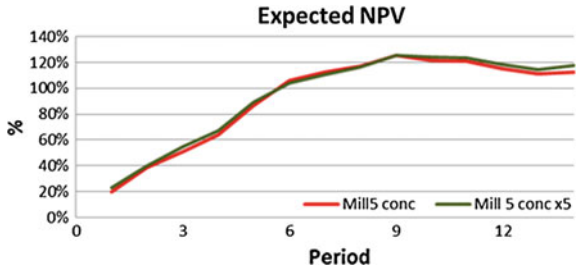

Fig. 21 Expected NPVs of stochastic solutions

Conclusions

This paper presents a method to simultaneously optimize different components of mining complexes comprised of open pits and underground operations. The method can be easily adapted to different underground mining methods. At the different processing destinations, the method accounts for operating modes and external sources of material used for blending purposes. The implementation of the method at a gold mining complex shows substantial improvement in expected NPV and in meeting operational targets for the autoclave. The perturbations at operating and transportation decision levels act as a diversification strategy for the unit-based perturbations. However, as in the case study, no operating modes and transportation systems are considered, a stand-alone diversification strategy for the unit-based perturbations must be included to explore better the solution domain.

Future extensions of the method may consider stochastic stockpiles, geotechnical and environmental aspects of the underground activities and the optimal consumption rate of external blending material.

Acknowledgements We would like to thank the organizations and companies who funded this research: Canada Research Chairs (Tier I) in Sustainable Mineral Resource Development and Optimization under Uncertainty, and NSERC Collaborative Research and Development Grant CRDPJ 411270-10, entitled Developing new global stochastic optimization and high-order stochastic models for optimizing mining complexes with uncertainty; industry collaborators: AngloGold Ashanti, Barrick Gold, BHP Billiton, De Beers, Newmont Mining and Vale, and NSERC Discovery Grant 239019. Particular thanks to Mern Vatcha from Barrick for his generous contribution.

Appendix 1—Stochastic Solution with Initial Stockpiles

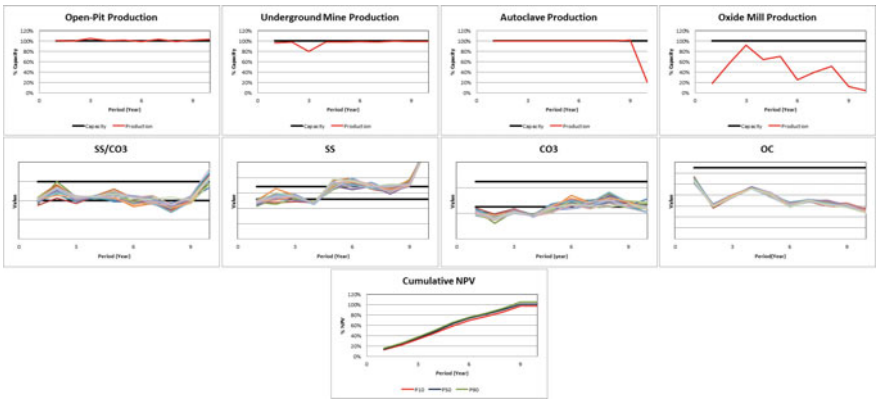

References

Albor F, Dimitrakopoulos R (2009) Stochastic mine design optimization based on simulated annealing: pit limits, production schedules, multiple orebody scenarios and sensitivity analysis. IMM Trans Min Technol 118(2):80–91

Albor F, Dimitrakopoulos R (2010) Algorithmic approach to pushback design based on stochastic programming: method, application and comparisons. IMM Trans Min Technol 119(2):88–101

Benndorf J, Dimitrakopoulos R (2018) New efficient methods for conditional simulations of large orebodies, in this volume

Bodon P, Fricke C, Sandeman T, Stanford C (2018) Combining optimisation and simulation to model a supply chain from pit to port, in this volume

Bootsma MT, Alford C, Benndorf J, Buxton MWN (2018) Cut-off grade-based sublevel stope mine optimisation—Introduction and evaluation of an optimisation approach and method for grade risk quantification, in this volume

Boucher A, Dimitrakopoulos R (2009) Block-support simulation of multiple correlated variables. Math Geosci 41(2):215–237

Chanda E (2018) Network linear programming optimisation of an integrated mining and metallurgical complex, in this volume

Dimitrakopoulos R, Ramazan S (2004) Uncertainty based production scheduling in open pit mining. SME Trans 316:106–112

Dowd P (1994) Risk assessment in reserve estimation and open-pit planning. Trans Inst Min Metall Sect A Min Ind 103:A148–A154

Godoy M (2002) The effective management of geological risk in long-term production scheduling of open pit mines. Ph.D. Thesis, School of Engineering, University of Queensland, Brisbane, Qld, Australia

Goodfellow R, Dimitrakopoulos R (2016) Global optimization of open pit mining complexes with uncertainty. Appl Soft Comput 40:292–304

Goodfellow R, Dimitrakopoulos R (2018) Simultaneous stochastic optimisation of mineral value chains: developments and applications with technical risk management, in this volume

Grieco N, Dimitrakopoulos R (2007) Managing grade risk in stope design optimisation: probabilistic mathematical programming model and application in sublevel stoping. IMM Trans Min Technol 116(2):49–57

Grieco N, Dimitrakopoulos R (2018) Grade uncertainty in stope design—improving the optimisation process, in this volume

Groeneveld B, Topal E, Leenders B (2018) A new methodology for flexible mine design, in this volume

Hoerger S, Seymour F, Hoffman L (1999) Mine planning at Newmont's Nevada operations. Min Eng 51:26–30

IBM corp. (2011) IBM ILOG CPLEX optimization studio. CPLEX User's Manual 12. IBM Corporation, USA, pp 1–468

Infomine Website (2014). http://www.infomine.com/minesite/minesite.asp?site=turquoise

Kawahata K, Schumacher P, Hufford R (2013) Mine production scheduling optimization at Newmont's twin creeks mine. Min Eng 65(6):49–54

Kirkpatrick S, Gelatt CD, Vecchi MP (1983) Optimization by simulated annealing. Science 220:671–680

Lamghari A, Dimitrakopoulos R (2012) A diversified Tabu search approach for the open-pit mine production scheduling problem with metal uncertainty. Eur J Oper Res 222(3):642–652

Lamghari A, Dimitrakopoulos R, Ferland JA (2013) A variable neighbourhood descent algorithm for the open-pit mine production scheduling problem with metal uncertainty. J Oper Res Soc: 1–10

Menabde M, Froyland G, Stone P, Yeates G (2018) Mining schedule optimisation for conditionally simulated orebodies, in this volume

Metropolis N, Rosenbluth A, Rosenbluth N, Teller A, Teller E (1953) Equation of state calculations by fast computing machines. J Chem Phys 21:1087–1092

Montiel L, Dimitrakopoulos R (2015) Optimizing mining complexes with multiple processing and transportation alternatives: an uncertainty-based approach. Eur J Oper Res 247:166–178
Ramazan S, Dimitrakopoulos R (2018) Stochastic optimisation of long-term production scheduling for open pit mines with a new integer programming formulation, in this volume
Ramazan S, Dimitrakopoulos R (2013) Production scheduling with uncertain supply: A new solution to the open pit mining problem. Optim Eng 14:361–380
Ravenscroft PJ (1992) Risk analysis for mine scheduling by conditional simulation. Trans Inst Min Metall Sect A Min Technol 101:104–108
Rocchi L, Carter P, Stone P (2011) Sequence optimization in longwall coal mining. J Min Sci 47(2):151–157
Stone P, Froyland G, Menabde M, Law B, Pasyar R, Monkhouse P (2018) Blasor—Blended iron ore mine planning optimisation at Yandi, Western Australia, in this volume
Whittle G (2007) Global asset optimization. In: Proceedings, orebody modeling and strategic mine planning, AusIMM, Spectrum Series 14, pp 331–336
Whittle J (2018) The global optimizer works—what next?, in this volume
Wooller R (2007) Optimising multiple operating policies for exploiting complex resources—an overview of the COMET scheduler. In: Proceedings, orebody modeling and strategic mine planning, AusIMM, Spectrum Series 14, pp 309–316
Zuckerberg M, Stone P, Pasyar R, Mader E (2007) Joint ore extraction and in-pit dumping optimisation. In: Proceedings, orebody modeling and strategic mine planning, AusIMM, Spectrum Series 14, pp 137–140
Zuckerberg M, Van der Riet J, Malajczuk W, Stone P (2011) Optimal life-of-mine scheduling for a bauxite mine. J Min Sci 47(2):158–165

Combining Optimisation and Simulation to Model a Supply Chain from Pit to Port

P. Bodon, C. Fricke, T. Sandeman and C. Stanford

Abstract An export supply chain, beginning with the extraction of ore from a pit and ending with the loading of this ore onto vessels at a port, is a key component of many mining operations. These supply chains are comprised of a number of complex subsystems such as mining, ore processing, transportation, stockyard management and vessel loading. Typically, the operation and performance of each of these subsystems is analysed in isolation, with little consideration of their interaction with upstream and downstream subsystems. In reality, stochastic and dynamic influences that affect one of these subsystems will have flow on effects for all other subsystems in the supply chain. Hence, evaluation of the performance of the total integrated system needs to capture the interaction of these subsystems. Discrete Event Simulation (DES) has proved to be a powerful tool in modelling supply chains, capturing the system dynamics and interactions, and evaluating the overall performance of the integrated system. The primary objective of mining export supply chains is typically to maximise production capacity, i.e. tonnes of ore loaded onto vessels at the port. In some mining operations, the extracted ore is blended into a variety of products with differing characteristics before being exported. This can be the case for ores such as coal, iron and manganese. In these operations, an additional objective, in the form of achieving a predetermined quality of material on the vessels, is equally important as a measure of system performance

P. Bodon (✉) · T. Sandeman
TSG Consulting, Level 11, 350 Collins Street, Melbourne, VIC 3000, Australia
e-mail: peter@tsgconsulting.com.au

T. Sandeman
e-mail: tom@tsgconsulting.com.au

C. Fricke
AAusIMM, TSG Consulting, Level 11, 350 Collins Street,
Melbourne, VIC 3000, Australia
e-mail: chrisf@tsgconsulting.com.au

C. Stanford
Coal Technology, PT Kaltim Prima Coal, Sangatta,
Kutai Timur, Kalimantan Timur 75611, Indonesia
e-mail: Chris.Stanford@kpc.co.id

R. Dimitrakopoulos (ed.), *Advances in Applied Strategic Mine Planning*,
https://doi.org/10.1007/978-3-319-69320-0_17

as production capacity. The objective of delivering a certain quality of product often conflicts directly with the objective of maximising production capacity, resulting in an increased level of complexity within the supply chain. In these supply chains, the decision-making process of planning the movement and blending of ore through the system is paramount to the overall system performance. Capturing this complex planning process in a DES modelling language is possible, but proves to be a very difficult and time-consuming task. Since planning problems are often modelled and solved using an optimisation framework, an alternative approach is to decouple the decision-making process from the simulation model, develop a stand alone optimisation model for it, and then integrate the two to create a holistic model of the supply chain. This paper describes the approach taken and presents a case study of a successful implementation on the export supply chain of PT Kaltim Prima Coal (KPC) in Indonesia.

Discrete Event Simulation and Optimisation

Discrete event simulation (DES) modelling is the process of emulating real world operations in a controlled environment on a computer. This DES provides a rational and quantitative process for increasing understanding of the potential consequences of alternate proposals. This may range from a change in operational philosophies through to the commissioning of new infrastructure. Hence DES modelling is a useful tool for both long-term strategic decision-making and short-term planning and operational decisions.

Zeigler et al. (2000) describe a method for simulating a system using a discrete event system specification. These models are constructed by considering each physical item (train, car dumper, reclaimer, ship, etc.) as a discrete entity, with its own uniquely defined set of properties or attributes (speed, material type, reliability, carrying capacity, etc.). These entities act out the operational activities that make up the processes being modelled. They consume discrete periods of time for each activity, and incur delays that can be logically induced (e.g. bin empty, no rake, etc.). They also use stochastic methods to generate randomly induced delays (e.g. breakdown, failures, etc.), all of which are dependent on the data and operational rules that are defined for that particular process or piece of equipment. This combination of logical and random events is designed to reflect the most likely operational environment. Each system within a DES model has individual operating rules and parameters which need to be accurately defined. In the context of a mining operation, an export supply chain involves the movement of ore from pit to port, via any number of subsystems. In many mining supply chains, the operational rules regarding the movement of ore are simply defined (e.g. lump material goes to a lump stockpile, fines material goes to a fines stockpile). The lack of product

diversification in these instances means that there are little or no blending requirements throughout the supply chain. These simple operational rules are able to be incorporated into DES models of the mining supply chain relatively easily, allowing the DES model to provide a realistic representation of the export supply chain as a whole. However, in some mining supply chains, the process of moving ore from pit to port is significantly more complicated. This is particularly the case when the ore is blended into a variety of products with differing characteristics before being exported, which can be the case for ores such as coal, iron and manganese. For operations such as these, day-to-day movements of ore are typically planned and executed by groups of experienced individuals, who match current mining stocks and stockpile levels with a shipping plan. The decision process by which they do so is complex, and cannot be described using a simple set of rules. This limits the ability of a DES modelling language to precisely replicate the decision-making process that is used in practice, and hence provide an accurate representation of the export supply chain.

Optimisation modelling is ideally suited for analysing complex decision-making processes, where any number of (possibly conflicting) objectives have been identified as being desirable, though subject to constraints such as system capacity, operational limitations and time. One of the most powerful features of an optimisation model is its ability to consider hundreds of thousands of possibilities and determine the optimal decision in a very short period of time. In the mining industry, optimisation modelling has been widely applied in long-term mine planning, particularly production scheduling problems and ultimate pit design. It is also possible to apply optimisation modelling to the problem of planning the movement and blending of ore through a complex export supply chain, such as those described above. This optimisation component can then be integrated into a DES model of the entire supply chain, enabling a holistic model of the system to be developed. There are a number of advantages to modelling a complex export supply chain in this manner. Automating the process of generating the plans and carrying them out in the simulation reduces the need for human input, and aids in the process of knowledge capture and retention. In addition, a stand-alone optimisation model provides the ability to easily modify and test alternative planning strategies in isolation. Optimisation models also have the ability to evaluate multiple criteria (e.g. product quality, demurrage, amount of ROM rehandling), as well as explore the effect of changing priorities on each of these objectives.

Recently, the authors developed an automated optimisation planning engine (APE) for use in DES models of complex export supply chains. The APE plans the movement and blending of ore through the system and interacts with the DES model, which attempts to enact this plan under realistic conditions, hence providing an accurate representation of the system dynamics of the export supply chain. The design of the APE is described below.

Development and Implementation of the Automated Optimisation Planning Engine

Generally, a DES model of a supply chain will consider the performance of the system over a one year time period, using a mine plan and shipping plan for one year as inputs. The APE is used to plan material movements on a more frequent basis, such as fortnightly, weekly, or a number of days in advance. The time horizon used for the planning process is an important factor in determining the complexity of the planning problem, hence the computation time required to solve a problem instance with the APE. Once a short-term plan is produced, it has to be translated into 'tasks' to be carried out by the simulation. The DES model then attempts to carry out these tasks as close as possible to the plan, subject to real life conditions and variability. A small amount of intelligence is required within the simulation for dealing with unexpected occurrences such as bad weather shutting down pits, or pieces of equipment failing. At the end of the planning period, control is passed back to the optimisation model with an updated set of inputs for the next planning period. This process is then repeated. A diagrammatic representation of the interaction between the simulation and optimisation models is presented in Fig. 1.

The aim of the APE is to plan movements of ore from pit to ship via intermediate subsystems such as processing plants, transportation systems (rail networks or

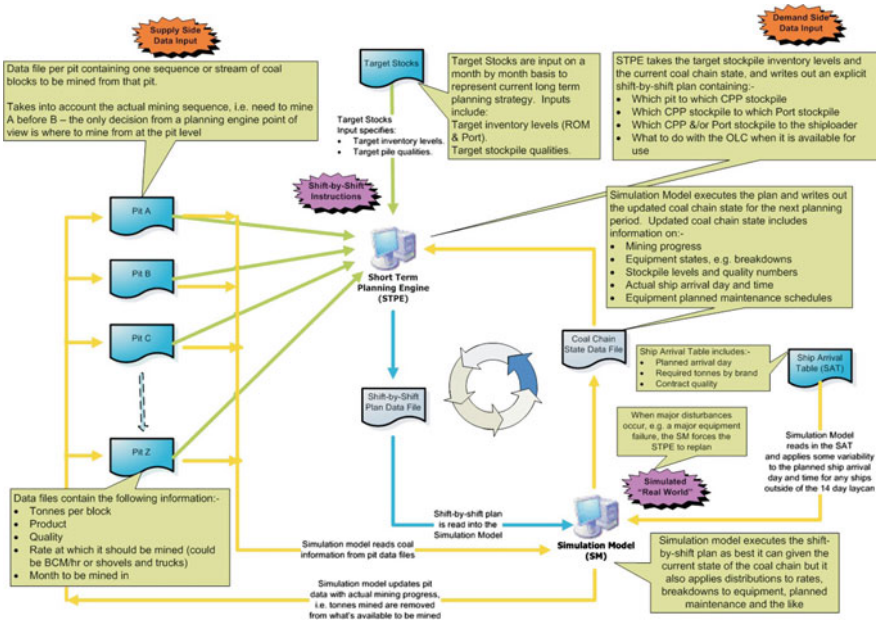

Fig. 1 Process of interaction between the simulation and optimisation models

conveying systems) and stockyards. A feature of export supply chains in the mining industry is the inclusion of buffers (stockpiles and queues) between these subsystems to mitigate the impact of subsystem performance variability on overall system performance. In the case of a multi-pit, multi-product blended ore mining operation, intermediate stockpiles are used for blending the ore into products to be shipped, as well as for buffering purposes. It follows that inputs to the APE are short-term mine and shipping plans and the current levels in the intermediate stockpiles. The APE will then determine the manner in which material is to be moved through the system via the intermediate buffer stockpiles to attempt to satisfy the shipping plan. The objective is to maximise the throughput of material while keeping shipped quality as close to target as possible, subject to equipment availability constraints. It is formulated as a mixed integer linear program involving multiple time periods. Specific complicating concepts related to the formulation used in the APE are discussed below.

Non-linear Constraints

A direct formulation of a planning problem involving blending will typically feature a number of non-linear constraints. This was the case in the original formulation proposed for use in the APE. A period of experimentation in the use of non-linear solvers was undertaken with little success, as solution times tended to be unwieldy. To overcome this issue, a small number of simplifying assumptions are made to enable the formulation to be linearised, so that the solution time of the APE is reduced considerably without losing significant detail in the plans produced.

Variation in Stockpile Quality Over Time

The major complicating factor in this area is the variation in stockpile quality over time. The quality of material extracted from a stockpile in any time period is dependent on the quality and quantity of material added to that stockpile in the preceding time periods. This relationship is inherently non-linear in nature. Assuming a fixed quality in each stockpile throughout the planning period under consideration enables this relationship to be modelled linearly. In addition, this assumption leads to the possibility of a further level of planning which is more tactical than operational, i.e. setting the target stockpile qualities for each time period.

Through Loading

Many port operations in mining export supply chains allow for through loading of material onto vessels. Through loading occurs when material arrives at the port and

is loaded onto a vessel berthed at the port immediately, effectively bypassing the buffer stockpiles in the stockyard. From a modelling perspective, this is achieved by including a splitter at the port, which allows a variable amount of feed to be directed to stockpiles in the yard, and the remainder to be sent directly to the ship loading operation. Initial modelling of the decision of the quantity of material to send to each respective destination resulted in non-linear constraints. This non-linearity was overcome by assuming that through loading is always carried out when a vessel is at berth, and that when this occurs, a fixed proportion of the feed is split between the through loading operation and the yard stockpiles.

Building Stockpiles to Completion Before Being Turned Over

Ideally, each port stockpile is built to completion before being turned over and reclaimed from to load vessels. This constraint is included in the APE by applying a penalty for turning over a stockpile before it is full. An integer variable is included in the formulation to represent the state of each stockpile (stacking or reclaiming), and a fixed penalty is applied when a stockpile is turned over before it is in a reclaim state.

Solution Time

Even the most sophisticated optimisation engines generally require a significant amount of time to determine the optimal solution to a complex mixed integer linear programming problem with a large number of decision variables and constraints. One of the drawbacks of the techniques used to linearise the formulation used in the APE is that additional decision variables and constraints are added to the formulation. The purpose of the APE is to improve the decision-making processes within a DES model and facilitate the generation of realistic outputs by the DES model. Since it is used to solve many instances of the planning problem throughout a single simulation run, it is imperative that the solution time for the APE is not excessive. One approach explored in an attempt to reduce solution times was to split the planning problem in two (planning from mine to an intermediate buffer, then taking this solution and planning from the intermediate buffer to the vessels). While this resulted in a small decrease in overall solution time, the loss of the ability to effectively plan for ships earlier in the supply chain operation resulted in a decrease in the quality of products loaded to vessels. Therefore, this approach to the planning problem was abandoned.

Case Study—PT Kaltim Prima Coal Supply Chain

PT Kaltim Prima Coal (KPC) operates a coal mine near Sangatta in East Kalimantan, Indonesia. Coal is mined at various grades and blended through a series of intermediate stockpiles that are linked by a 13 km overland conveyor (OLC) before being loaded as multiple products onto a ship. To determine the potential consequences of increased production and alternative production scenarios, KPC required an understanding of the interaction between throughput and quality, and how these are impacted by any changes in infrastructure and/or operating policy. The nature of planning the KPC operation to achieve contracted coal qualities involves multiple objectives including throughput, blending and on time delivery onto ships. An APE was constructed that incorporated these multiple objectives, as well as the ability to interact with the DES model. The optimisation replicates the planning activity that is regularly performed on site to enable the DES model to operate for an extended duration (anywhere from one week to several years). The integration of the optimisation within the simulation allowed KPC to link the effects of real life uncertainties to the strategic plans being developed. The addition and integration of the APE within the simulation model was a complex task. In isolation, the three key elements of this model (quantity model, quality model and planning) are well established, however the incremental addition of each of these elements into an integrated DES and optimisation model exponentially increases the model complexity. The insights gained from this complex modelling system hold the potential to revolutionise the way the KPC operation is planned and operated.

Overall Benefit

The integrated DES model has helped KPC in making strategic long term decisions, short-term planning decisions and also provides the possibility of aiding the operational decisions of creating and evaluating weekly plans.

Strategic Decision-Making

The primary purpose of building the integrated DES model was to help KPC understand the likely impacts of increased production, identify bottlenecks in the system and evaluate the effect and feasibility of various potential future expansions of the operation. The ability to easily change the inputs of the model enables KPC to quickly understand the effect of upgrades to equipment, such as increasing crusher capacity, improving conveyor rates and reliability, and increasing ship loading capacity. In addition, the integrated DES model provides the flexibility to test different stockpiling configurations and examine the effect of reducing the amount of through loading.

Short-term Planning

The ability to take a short-term marketing plan in terms of shipping demand for tonnes and quality, and evaluate the potential of the operation to supply these tonnes given a mine plan, has been of great benefit to KPC. The DES allows KPC to see which plans are harder to achieve, as well as indicating the potential bottlenecks and areas which are causing problems.

Operational Decision-Making

The optimisation component of the integrated DES model is able to operate in stand-alone mode. This provides the ability to easily modify and test alternative planning strategies in isolation. In addition, further detailed modelling of the planning process that occurs on a day-to-day or even hour-to-hour basis could be included in this stand-alone model. This could provide sufficient detail to enable the optimisation component to be used in the weekly planning sessions that are held on site, where the daily movements of ore for the next week are determined.

The Integrated DES Model

The KPC Coal Chain Integrated DES model is a large, complex model that incorporates many features to enable it to accurately replicate the real operation. The inputs for this model include the: key plant and equipment capability/capacity, equipment configuration, equipment reliability (planned and unplanned downtime), mine plan, and shipping plan (forecast). Equipment capacity and reliability is determined through analysis of the existing operation. Equipment configuration is based on the current operation and may be manipulated to simulate different operating conditions. Mine and shipping plans are supplied by KPC in the form of mine log files and the current shipping program spreadsheet. Scenarios are arranged by manipulating these key input parameters to test the system under different configurations. To enable the estimation of maximum system capacity and to identify and quantify system bottlenecks, it is necessary to scale the demand and supply components to ensure that the model is tested to its capacity. The supply (mine plan) is scaled by simply scaling the coal quantity of each block in the mine plan, while the demand (shipping plan) is scaled by adding ships to, or removing them from the plan. The primary aim of the APE used within the integrated DES model is to determine a sequence of tasks to deliver the required coal to the waiting vessels. The DES model then follows the list of tasks developed by the APE until such time that the tasks are completed or replanning is required. The following is an outline of the functionality of the APE used in the integrated model of the KPC Coal Chain.

Planning Horizon

The planning horizon used by the APE is able to be varied. Following a testing phase it was established that a planning horizon of 21 shifts (seven days), with plans updated every nine shifts (three days), provided realistic results and did not require significant solution times. This configuration enabled the APE to provide planning based on a seven day look ahead to ensure that both near term and longer term (seven day) objectives could be optimised, but also meant that the DES model was unlikely to become significantly out of synchronisation with the plan.

Optimisation Formulation

The optimisation is a general linear program as described by Winston (1987). As such, it has an objective function which in this case is a maximisation, subject to a number of constraints, of the general form:

$$\text{Maximise} \sum X_i$$

$$\text{Subject to} \sum a_i.x_i <= b_i$$

The model is formulated in Lingo using a combination of the techniques described by Schrage (2003).

Objective Function

The following is a list of objectives that the APE has to optimise against, given the constraints listed below. The importance of each of these objectives is controlled by weighting multipliers in the solver:

- Maximise throughput. Primarily this means to maximise the tonnage down the OLC, however it is extended to also maximise tonnes mined and tonnes shipped.
- Minimise deviation of both crushed ore and port stockpiles from their assigned lower and upper bounds. Quality deviance is calculated by creating a variable which is the difference between the desired and actual quality, then including this variable in the objective with a negative value to penalise this deviance.
- Minimise deviation from each vessels' target quality.
- Minimise deviation of each vessels' loading time from its arrival time.

Constraints

The following are the list of constraints that the APE must operate within when finding a solution that optimises the objective function.

Pits

- *Only mine blocks that are available*: blocks must be mined in sequence. This is achieved by limiting the number of blocks that are available to be planned, based on the provided mine plan sequence. For example, blocks nominated to be mined in the month of September cannot be mined in August unless all of August's blocks have been mined. Changing the bucket size for the blocks affects how closely the model tracks the provided mine plan. Whilst in the short-term the order that the blocks are mined is critical, as the model moves further into the future, so the need for strict adherence diminishes due to uncertainties in the orebody mapping. The ore blocks are 'binned' by month—finer resolution would require more accurate mine plans extending possibly for a number of years.
- The APE is allowed to mine blocks that are assigned to a following time period in the input mine plan, but a penalty is incurred. Essentially, blocks assigned to an upcoming period would only be mined to deal with a quality issue.
- Precedence constraints between blocks are not explicitly modelled. It is assumed that precedence requirements have been handled in the mine plan, and excursion from the mine plan is allowed only on a quality issue.
- Do not exceed shovel capacity in any pit and across all pits in any shift.
- Do not mine more than the tonnage of any given block.

Crusher Stockpiles

- Do not exceed crusher rates.
- Physical configuration constraints regarding which crusher feeds to which crusher stockpile.
- Do not exceed each crushed ore stockpiles' capacity.
- Do not exceed each crushed ore stockpiles' maximum reclaim rate.
- Aim to have each stockpiles' quality within its nominated quality range at all times.

Overland Conveyor

- Do not exceed the maximum OLC rate.

Port Stockpiles

- Do not exceed each port stockpiles' capacity.
- Aim to have each stockpiles' quality within its nominated quality range at all times.
- Do not exceed total port capacity.

Vessels

- Load vessels to their stated tonnage.
- Do not load vessels prior to their arrival time.
- Do not exceed the rated capacity of the ship loader.
- Aim to have each vessel within its nominated quality range.

Outputs

The following data is output from the APE to the DES model. The DES model then uses these outputs to control (direct) the flow of coal.

- *Tonnes to crusher stockpiles*: number of tonnes from each block in the mine plan to be sent to each crusher stockpile in each planning period. There is the potential that a block may be split across more than one crusher stockpile.
- *Crusher stockpile to port stockpile*: number of tonnes to be sent from each crusher stockpile to each port stockpile via the OLC in each planning period. It is possible to have more than one crusher stockpile feeding a port stockpile and more than one port stockpile being fed from the same crusher stockpile.
- *Port stockpile to vessel*: number of tonnes to be sent from each port stockpile and loaded onto each vessel in each planning period. The APE also determines which planning period the vessels in the queue will be loaded in.

Example of Scenario Analysis

DES modelling is a complex process that has the ability to generate a significant quantity of output results. The interpretation of these results requires an in depth knowledge of the model and its outputs. To best describe the performance of the operation under varying operating scenarios requires a statistical comparison of results and an understanding of statistics in general. To simplify this process, a reduced number of key performance indicators (KPIs) have been identified that

enable a simplified and more manageable understanding of the outputs. Just as the real system has variability associated with its performance (due to varying equipment reliability, varying times to perform tasks and variances in the quality of ore), so too does the DES model. For this reason, no two actual or simulated years will ever be the same. To cope with this fact, it is necessary to run the DES model for the same simulated period a number of times and then calculate the mean and standard deviation of the results for this period. Calculating the standard deviation quantifies the effect of variability on the process, and enables the range of results that could be expected to be produced by the operation under similar circumstances to be gauged. System performance is a combination of the KPIs that describe the performance of the system in terms of its ability to load coal onto ships in the correct quantity and quality within reasonable time frames. Hence system performance cannot be described alone by any one performance indicator, but rather is a combination of KPIs. Furthermore, testing the system at a single throughput is not sufficient to enable the successful identification of system bottlenecks and inefficiencies. To enable a complete under-standing of the system performance, the combination of the following two KPIs is the focus of the integrated DES model of the KPC Coal Chain:

1. *Quantity*: tonnes moved from mine to ship and the utilisation of the intermediate stockpiles.
2. *Quality*: the match between the customers' contracted shipments and the coal that is actually loaded onto their vessels. Quality is measured by the gross calorific value (GCV) of the coal.

Quantity

DES modelling allows the user to quantify the amount of extra production from a proposed capital expansion, as well as providing valuable insight into the auxiliary effects from any actions. This is particularly valuable in systems that contain many interacting components, such as the KPC Coal Chain. Testing the sensitivity of the system performance to varying equipment rates allows the potential benefit of changing the operating philosophies used in this area of the supply chain to be determined, and also provides a means of evaluating whether each piece of equipment is, or could potentially be, a restriction or bottleneck on the overall system. The following is an example of the analysis that is able to be undertaken using the integrated DES model of the KPC Coal Chain. In this case, the aim is to examine the effect of modifying the ship loading rate, both in isolation and in conjunction with the option of increasing the OLC rate.

To establish system performance sensitivity, the model is run at a number of throughput levels, i.e. using shipping plans and mine plans with different levels of demand for, and supply of, tonnes of coal. This establishes a response curve for the system. The response curve describes the system performance as the demands on it are increased, and provides a visual quantification of the benefit of differing system

configurations at varying levels of throughput, as shown in Fig. 2. As can be seen, increasing ship plan tonnes will increase the quantity moved through the system, however beyond a certain tonnage, it becomes harder to meet quality targets. This causes increased penalty payments, meaning profit eventually suffers. Figure 3 shows that increasing ship loading rate in isolation yields very little increase in the number of tonnes shipped at the lower throughput levels. This indicates that the ship loading configuration is sufficiently capable of meeting the shipping plan at these lower throughput levels. As the throughput is increased, it becomes clear that increasing the ship loading rate on its own yields no significant increase in shipped tonnes. When the increased ship loading rate is combined with an increased OLC rate, the higher throughput levels show measurable increases over the base case configuration, although it would appear that the majority of the gain is provided by the increase in OLC rate.

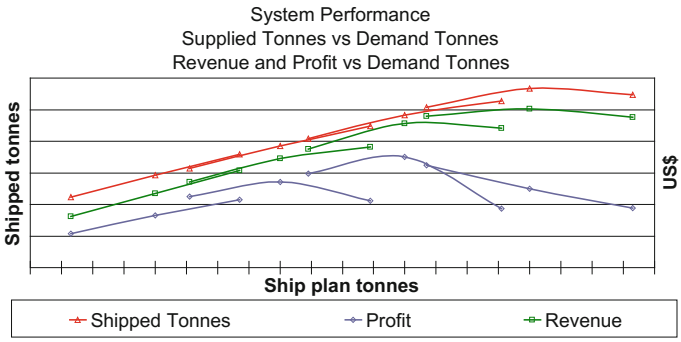

Fig. 2 System response to increasing demand

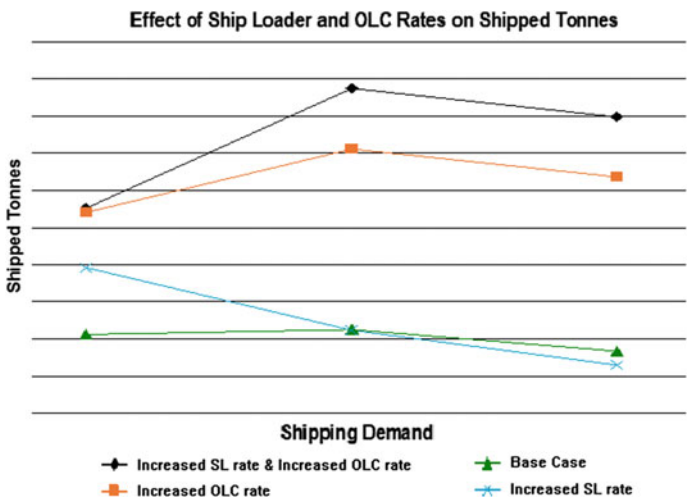

Fig. 3 Effect of ship loader and overland conveyor rates on shipped tonnes

Inspection of the stockpile levels (CPP = crusher stockpiles, TBCT = port stockpiles) with the increased ship loading rate in Fig. 4 reveals that the port stockyard is running empty, particularly towards the end of the year. The results from increasing ship loader rates indicate that the system is unable to supply sufficient coal to maintain adequate inventories in the port stockpiles. This is evidenced by inspection of the scenario with OLC rate increased only (Fig. 5). This chart shows that the system was far more capable of maintaining adequate port inventory levels, and thus able to ship more tonnes and more easily match quality targets.

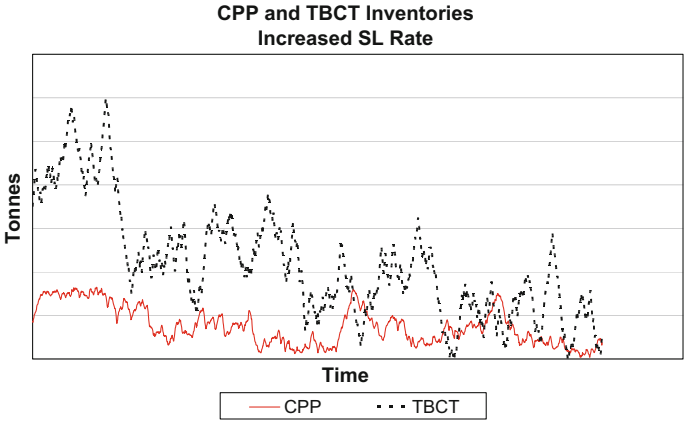

Fig. 4 Effect of increasing ship loader rate on stockpile levels

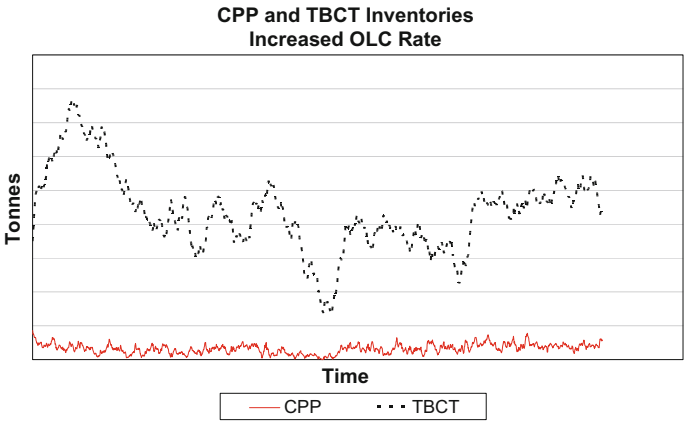

Fig. 5 Effect of increasing overland conveyor rate on stockpile levels

Quality

The two critical elements of the KPC Coal Chain are its ability to deliver the correct quantity and quality of coal onto ships. In the KPC Coal Chain operation, quality of coal is measured by gross calorific value (GCV). The integrated DES model incorporates the tracking of coal quality through the system and so has the ability to measure the quality of coal loaded onto ships. To quantify the effectiveness of the operation under various scenarios, it is necessary to compare the contracted consignment quality of coal with the loaded quality. Each dot in Fig. 6 represents a ship. The y axis indicates the error in the quality of the material that was loaded onto each ship. Therefore a positive value indicates the model has shipped too much of a given quality.

Continuing with the previous example of increasing the ship loading rates, Fig. 7 shows the shipped qualities from the increased ship loading rate scenario. As a result of the low levels of port stockpiles, it has become difficult to provide each ship with the quality of material requested. This mismatch of quality has a direct impact on profits, either from loss of potential revenue when providing higher quality than required, or penalties from customers when providing lower quality than requested. As can be seen from this small example, there are a large number of outputs that can be produced by a DES model, describing each aspect of the simulated process.

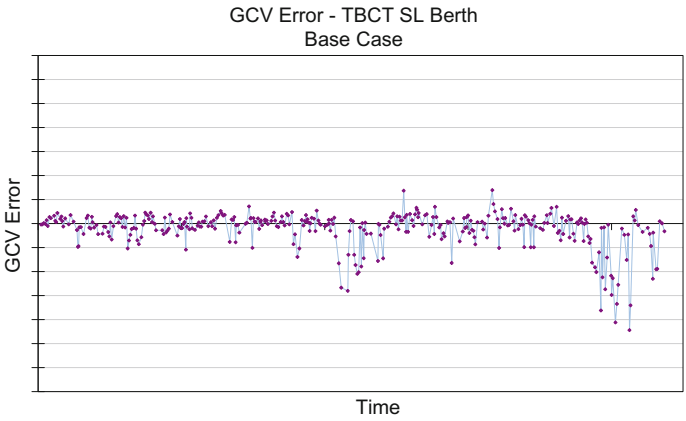

Fig. 6 Difference between quality of coal shipped and quality of coal demanded over a one year time period

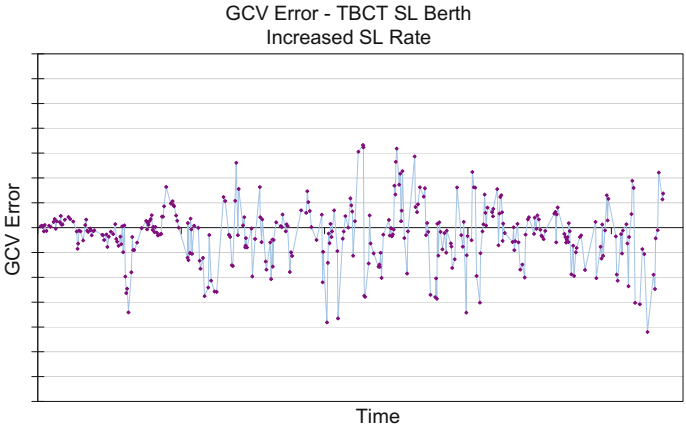

Fig. 7 Effect of increasing ship loader rate on quality of coal shipped

Conclusions

The application of a properly developed DES model provides a range of significant benefits in assessing an integrated export supply chain. These benefits include the ability to assess various operating practices, including maintenance options, through quantification of performance. In addition to operating practices, various capital expenditures can be compared to determine the best infrastructure for a given system. By analysing all of these options, the optimal capacity of the supply chain can be determined along with the robustness of this capacity under uncertainty. The ability of DES to investigate outcomes over many situations makes it ideal for risk analysis. Finally, quantification removes the 'gut feel' approach and replaces it with 'what if' fact based analysis.

In the case of operations that have multiple, conflicting objectives, such as delivering a certain quality of product while also maximising production capacity, an increased level of complexity is added to the export supply chain. In a mining context, examples of ores for which this may be the case include coal, iron and manganese. The decision-making process of planning the movement and blending of ore through the supply chain is paramount to the overall system performance for operations such as these. Capturing this complex planning process in a DES modelling language is possible, but proves to be a very difficult and time-consuming task. Since planning problems are often modelled and solved using an optimisation framework, an alternative approach is to decouple the decision-making process from the simulation model, develop a stand-alone optimisation model for it, then integrate the two to create a holistic model of the supply chain.

The case study of a successful implementation on the export supply chain of PT Kaltim Prima Coal in Indonesia shows the benefits of taking this approach to modelling for project evaluation and strategic mine planning purposes.

References

Schrage L (2003) Optimisation modelling with Lingo. pp 197–320
Winston WL (1987) Operations research: applications and algorithms. Duxbury Press, Boston
Zeigler BP, Praehofer H, Tag Gon K (2000) Theory of modelling and simulation, 2nd edn. Academic Press, pp 176–180

Network Linear Programming Optimisation of an Integrated Mining and Metallurgical Complex

E. K. Chanda

Abstract Mining companies seek to mine, route and process ore to make the most efficient use of capital equipment during the life of the mine. The situation analysed in this paper relates to optimisation of medium-term production strategy for a group of mines and metallurgical plants. Typical operations under this scenario involve mining of crude ore from shafts and/or open pits; transportation of ore to the milling plants, run-of-mine stockpiles and leach-pads. The concentrate from the mill(s) is sent to the smelters and refineries, from where the finished metal is sent to the markets. If one assumes that the grade of run-of-mine ore varies according to source and that the milling plants are designed to handle different types of ore, plus the fact that mines and plants may separate by considerable distances, optimisation of the production plan becomes imperative. Most of the publications dealing with the subject of mine production planning are limited to mine scheduling optimisation and do not include metallurgical plants. However, the nature of the problem requires the application of a model that incorporates all the elements of the mineral production system. The methodology outlined in this paper is based on a Network Linear Programming formulation of the production-planning problem for a mining and metallurgical complex. Network LP models are particularly useful in analysing production-distribution type systems such as the one involving a group of mines and metallurgical plants. The problem is formulated using the theory of dual-primal relationships in linear programming. The solution algorithm finds the minimum cost of production and distribution, hence the optimal production and material routing plan for a group of mines and metallurgical plants. The graphs of optimality conditions for each arc in the network could be exploited as a tool for strategic mine planning. The advantages of this formulation are outlined and its application is demonstrated using a hypothetical situation involving an integrated mining and metallurgical complex, specifically six mines, five concentrators, three smelter and two copper refineries. A computer program called Linear Integer Discrete Optimiser (LINDO) is used to solve the network linear programming model. This program

E. K. Chanda (✉)
Mining Engineering, WA School of Mines, Curtin University of Technology,
Locked Bag 22, Kalgoorlie, WA 6433, Australia
e-mail: chandae@wasm.curtin.edu.au

R. Dimitrakopoulos (ed.), *Advances in Applied Strategic Mine Planning*,
https://doi.org/10.1007/978-3-319-69320-0_18

allows the user to quickly input an LP formulation, solve it and perform 'what if' type analyses.

Introduction

The practical mine planning problem analysed in this paper relates to the optimisation of a medium-term production strategy for a group of mines and metallurgical plants (concentrators, smelters and refineries). Most of the publications dealing with the subject of production planning focus on mine scheduling optimisation and do not include metallurgical plants (Thomas 2001). However, the nature of the problem requires a model that incorporates all the elements of the production system. Hoerger et al. (1999) have described a mixed integer/linear programming model for long-term scheduling that includes material tonnage flows between mines, stockpiles and process plants. The resulting Linear Programming (LP) model is very large in terms of the number of variables. The methodology outlined in this paper is based on a network linear programming formulation of the problem of production planning optimisation for a mining and metallurgical complex. Models called network LPs are particularly useful in analysing production-distribution type systems such as the one discussed in this paper.

The section entitled 'Linear programming and network techniques' introduces the structure of network LPs, primal-dual relationships and complementary slackness conditions. This review of relevant principles sets the scene for their application to the problem of production planning for a mining and metallurgical complex, presented in the section entitled: 'Network LP formulation of mining and metallurgical production planning problem'. Finally, the section entitled 'A hypothetical mining and metallurgical complex', presents results of LINDO optimisation of the production planning for a typical mining and metallurgical complex.

Linear Programming and Network Techniques

Linear Programming (LP) is a mathematical procedure for determining optimal allocation of scarce resources. LP has been used to solve a variety of practical planning problems in the industry including agricultural, banking, government services, manufacturing and transport problems. Application of this technique in mining dates back over 40 years. Linear programming is the most widely applied operations research technique in the mining industry. Linear programming principles have successfully been used for production scheduling in open pit and underground mining environments, each with their own specific needs (Ricciardone and Chanda 2001; King 2001; Chanda 1990; Saul 1990; Dagdelen et al. 2000; Scheepers and Wellbeloved 1992; Graham-Taylor 1992; Ramazan 2001; Ramazan and Dimitrakopoulos 2004). The approach adopted in this paper is to combine the

concepts of duality in linear programming and network flow to model the production-planning problem as discussed in the introduction. Network LPs are particularly useful in analysing production-distribution type systems. These models have the following advantages:

- they are describable using simple graphical figures (networks),
- they have integer answers and one may find a network LP a useful device for describing and analysing mine-mill production and material routing strategies, and
- they are frequently easier to solve than general linear programs.

In this section, a brief overview of duality in linear programming and the formulation of equivalent network flow (minimal cost) is provided. Though there are a number of techniques for finding the optimal flow through a network, the algorithm in LINDO (Schrage 1999) is employed because of its simplicity and use as a strategic tool in production planning. This is demonstrated in the section entitled: 'Network formulation of mine production planning problem'. For more details on the theory of network LPs the reader is referred to Ahuja et al. (1993) and Bazaraa et al. (1990).

Theoretical Background

Each linear programming problem called the primal has a closely related associated linear programming problem called the dual problem (Fulkerson 1961). The following example illustrates how linear programming duality can be used to analyse production-planning problems in the minerals industry. Consider a copper/cobalt mining operation with six sources of ore (shafts).

Table 1 presents the mine planning data for this operation. It is desired to optimise the mining plan for the month using linear programming. It is assumed that shaft capacities are sufficient to handle the planned mine production. The budget targets production of 20,000 and 200 tonnes of finished copper and cobalt respectively during the period.

Table 1 Mine planning data for a copper/cobalt mining operation

Parameter	Ore source (shaft)					
	1	2	3	4	5	6
Copper grade (%)	2.70	5.00	3.50	4.50	0.90	3.90
Cobalt grade (%)	0.40	0.70	0.07	0.08	0.60	0.20
Unit cost ($/tonne ore)	7.00	5.00	6.00	8.00	4.00	6.50

The Primal Problem

The LP formulation of this problem is presented as follows:

Let:

x_i = unknown tonnes of ore to be produced from shaft j

The objective is to minimise the total cost of mining. This optimisation criterion will ensure that the mining contribution to profit over the quarter will be maximised. Thus, the objective function is:

$$\text{Minimise } Z = 7x_1 + 5x_2 + 6x_3 + 8x_4 + 4x_5 + 6.5x_6$$

Metal production targets are formulated as constraints:

(i) $0.027x_1 + 0.050x_2 + 0.035x_3 + 0.045x_4 + 0.009x_5 + 0.039x_6 \geq 20{,}000$
(ii) $0.004x_1 + 0.007x_2 + 0.0007x_3 + 0.0008x_4 + 0.006x_5 + 0.002x_6 \geq 200$

Non-negativity constraint ensures that production from each shaft is positive:

$$x_j \geq 0 \quad \forall j$$

The Dual Problem

The dual problem to the above primal problem is formulated as follows:

Let:

y_1 = price of copper on the world market ($/tonne)
y_2 = price of cobalt on the world market ($/tonne)

The objective function is to maximise metal sales value in dollars:

Maximise $\upsilon = 20{,}000\ y_1 + 200\ y_2$

The objective function is subject to the following constraints:

(i) $0.027\ y_1 + 0.004\ y_2 \leq 7.0$
(ii) $0.050\ y_1 + 0.007\ y_2 \leq 5.0$
(iii) $0.035\ y_1 + 0.0007\ y_3 \leq 6.0$
(iv) $0.045\ y_1 + 0.0008\ y_2 \leq 8.0$
(v) $0.009\ y_1 + 0.006\ y_2 \leq 4.0$
(vi) $0.039\ y_1 + 0.002\ y_2 \leq 6.5$

Non-negativity constraints:

$$y_j \geq 0 \quad \forall j$$

Complementary Slackness Optimality Conditions

The necessary and sufficient conditions for a feasible solution of primal and dual to be optimum is they satisfy:

(1) $Y(AX - B) = 0$
(2) $X(C - YA) = 0$

where:

X decision variables in the primal problem (vector)
Y decision variables in the dual problem (vector)
C coefficients of the objective function in the primal problem (vector)
B coefficients of the objective function in the dual problem (vector).

Network LP Formulation of the Mining and Metallurgical Production Planning Problem

The above concepts can be applied to production planning for a mining and metallurgical complex. To illustrate the practical application of complementary slackness conditions, the following problem is presented. Consider a simple mining-processing-marketing system as shown in Fig. 1. Formulation of an LP model to optimise the production strategy for the system follows.

The following notation is used for the labels in Fig. 1 [e.g. (1, 5/4)]:

$$(l_{ij}, u_{ij}/c_{ij})$$

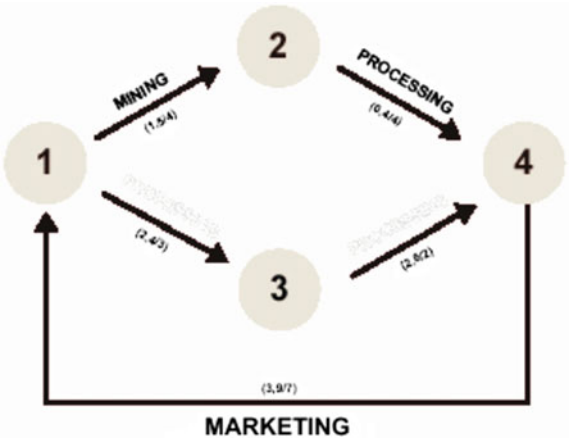

Fig. 1 Mining-processing-marketing business system

where:

l_{ij} lower bound of material flow through arc (i, j)
u_{ij} upper bound of material flow through arc (i, j)
c_{ij} cost per unit flow of material through arc (i, j)

Figure 1 is in fact a network representation of movement of ore from the mine (node one) to the plants (nodes two and three) and marketable product to the market. In certain network formulations, the principle of conservation of flow has to be maintained at all nodes. Closing the circuit from node four to node one with a negative unit cost does this. The objective here is to optimise flow through the network, i.e. minimise the total cost of the production-distribution system. The out-of-kilter formulation of the primal-dual minimal cost network flow problem for the system is presented as follows.

Let:

X_{ij} = amount of material processed in process (i, j) of the system

The objective function is to minimise total cost of flow through the network.

$$Minimise\, Z = \sum_{i,j} c_{i,j}\, x_{i,j} \tag{1a}$$

There are three types of constraints in this LP system:

1. Conservation of flow through each node:

$$\sum_{i} x_{i,j} - \sum_{j} x_{j,i} = 0 \quad \forall i, j \tag{1b}$$

2. Lower bound flow through the arcs:

$$x_{i,j} \geq l_{i,j} \quad \forall i \tag{1c}$$

3. Upper bound on flow through the arcs:

$$-x_{i,j} \geq -u_{i,j} \quad \forall j \tag{1d}$$

The above formulation is equivalent to the minimal cost flow problem. Equations 1a–1d are taken over existing arcs only. It is assumed that c_{ij}, 1_{ij} and u_{ij} are integral, although this is not a requirement in practice.

For the dual problem, the following dual variables are defined:

π dual variable for the conservation of flow at each node (node potential)
ϕ dual variable for the lower bound on flow constraint
ψ dual variable for the upper bound on flow constraint

For a given set of node potential π, the reduced cost of an arc is defined as:

$$c_{ij}^{\pi} = c_{ij} - \pi_i + \pi_j \tag{2a}$$

The objective function for the dual problem is:

$$Maximise\upsilon = \sum_{i,j} \phi_{i,j} l_{ij} - \sum_{i,j} \psi_{i,j} u_{i,j} \tag{2b}$$

The general equation for the dual constraints is as follows:

$$\pi_i - \pi_j + \phi_{i,j} - \psi_{i,j} = c_{i,j} \tag{2c}$$

Non-negativity:

$$\phi_{i,j} \geq 0;\ \psi_{i,j} \geq 0 \tag{2d}$$

The complementary slackness conditions for optimality of the OKA formulation are the following:

$$\pi_i \left[\sum_{i,j} x_{i,j} - \sum_{j,i} x_{j,i} \right] = 0 \tag{3a}$$

$$\phi(x_i - l) = 0 \tag{3b}$$

$$\psi\left(u_{i,j} - x_{i,j}\right) = 0 \tag{3c}$$

$$\left[c_{i,j} - \left(\pi_i - \pi_j + \phi_{i,j} - \psi_{i,j}\right)\right] x_{i,j} = 0 \tag{3d}$$

As mentioned earlier, any conservation of flow that satisfies the above equations will be optimal. The problem, then, is to search over value of π_i, and conserving $x_{i,j}$ until these conditions are satisfied. The complimentary slackness optimality conditions can be stated simply as follows (Ahuja et al. 1993):

$$If x_{ij} = l_{ij,} \quad then \quad c_{ij}^{\pi} \geq 0 \tag{4a}$$

$$If l_{ij} < x_{ij} < u_{ij}, \quad then \quad c_{ij}^{\pi} = 0 \tag{4b}$$

$$If x_{ij} = u_{ij}, \quad then \quad c_{ij}^{\pi} \leq 0 \tag{4c}$$

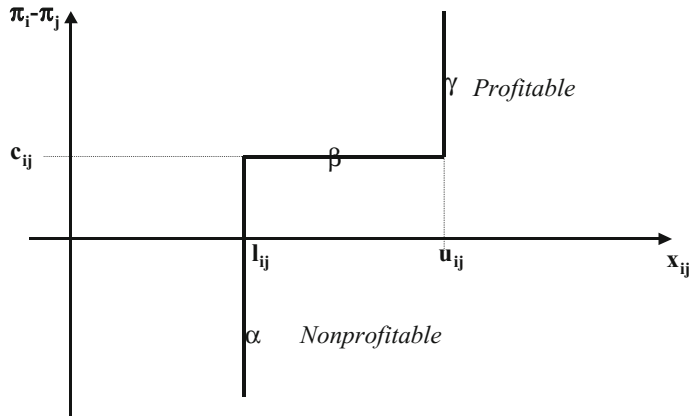

Fig. 2 Graph of optimality conditions for arc (i, j)

This is the basis for the solution procedure called the out-of-kilter algorithm. The name out-of-kilter reflects the fact that arcs in the network either satisfy the complimentary slackness optimality conditions (are in kilter) or do not (are out-of-kilter). The so-called 'kilter diagram' is a convenient way to represent these conditions (Ahuja et al. 1993). As shown in Fig. 2, the kilter diagram of an arc (i, j) is the collection of all points $(x_{ij}, c_{ij}\pi)$ in the two dimension plan that satisfy optimality conditions. For every arc (i, j), the flow x_{ij} and reduced cost $c_{ij}\pi$ define a point (x_{ij}, $c_{ij}\pi$) in the two-dimensional plane. If the point lies on the thick lines in Fig. 2, it is in-kilter, otherwise out-of-kilter. One can define a kilter number k_{ij} of each arc (i, j) as the magnitude of the change in x_{ij} required making the arc an in-kilter arc while keeping $c_{ij}\pi$ fixed. As expected, the kilter number of any in-kilter arc equals zero. The three-kilter states marked by α (non-profitable), β and γ (profitable) in Fig. 2 correspond to arc states satisfying the complimentary optimality conditions (Eqs. 4a, 4b and 4c). Any arc (processing path) (i, j) for which (x_{ij}, c_{ij}) lies on γ, is a profitable arc and is therefore, appropriately at its upper bound, and any arc (i, j) for which (x_{ij}, c_{ij}) lies on α is a non-profitable arc (and is therefore appropriately at its lower bound. From a mining economics point of view, it is preferable for all processing paths to be profitable. This concept is not investigated further here.

A Hypothetical Mining and Metallurgical Complex

Model Development

Suppose that a mining company has a number of ore sources (open pits, underground mines and stockpiles) producing copper ore for delivery to a number of concentrators for downstream processing. The following assumptions are made for the hypothetical copper mining and metallurgical complex (number of facilities):

- underground mines (UG) = 5
- open pits (OPT) = 1
- concentrators (CT) = 5
- smelters (SM) = 3
- refineries (RF) = 2

Each mine has a concentrator located in the vicinity of the mine. The copper concentrate is transported to smelters located in the vicinity of the mine(s). Some of the concentrate is transported to smelters located beyond a radius of more than 50 km from the concentrators. The copper anodes from the smelters are transported to the two refineries for electrowinning of copper. Copper cathodes are shipped to various markets from the refineries. The basic business structure is shown in Fig. 3, while Fig. 4 shows the network model of the system. The model shown in Fig. 4 has the following types of nodes:

1. Mine nodes, representing various ore sources.
2. Plant nodes representing concentrators, smelters and refineries.
3. Intermediate nodes corresponding to each material type processed at a plant. In this application, it is assumed that there is no differentiation in material (ore) types.
4. Market nodes corresponding to each market region. There are two types of arcs in the model:

- Production arcs—they connect a mine or plant node to an intermediate node. The cost of this arc is the cost of ore mining ($/tonne ore). Production control may place upper and lower bounds on these arcs.
- Transportation arcs—connect intermediate nodes to plant nodes in accordance with the copper production process. The cost of such an arc corresponds to the cost of transporting the process product from one plant to the other.

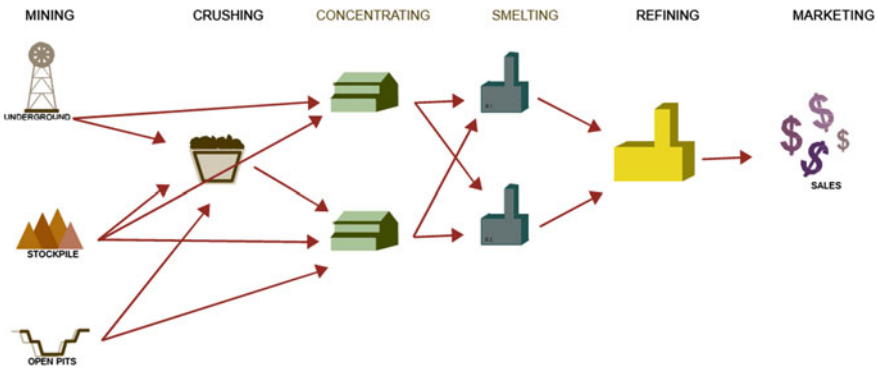

Fig. 3 Basic mining and metallurgical business complex

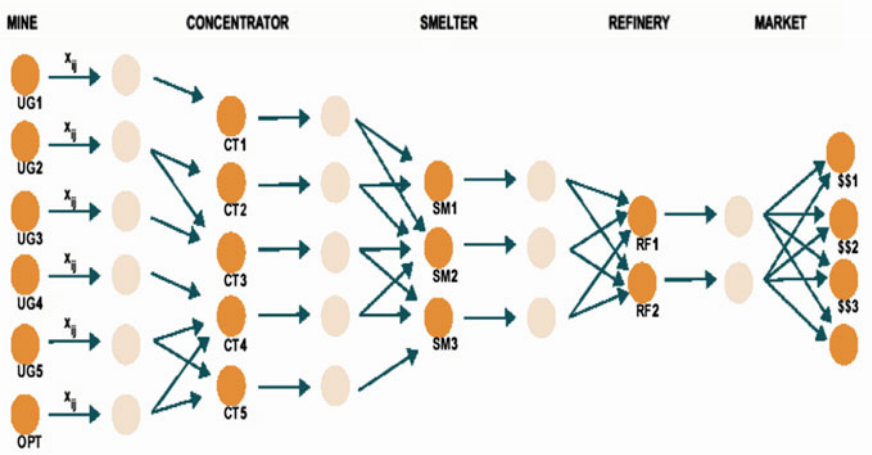

Fig. 4 Network model of the hypothetical mining and metallurgical complex

The problem is to generate a medium-term (quarterly) production plan for the mining and metallurgical complex with the objective of minimising the total unit cost of production and transportation.

Looking at Fig. 4, it is quite clear that there are several combinations of routes along which the material can flow. Each of the routes has a different cost structure, and therefore an opportunity to generate revenue. Clearly, the production and transport plans for the mining and metallurgical complex correspond in a one-to-one fashion with the feasible flows in this network model. Consequently, a minimum cost flow would yield an optimal production and shipping plan.

Let X_{ij} represent the equivalent tonnage of ore that flows along route (i, j). For each arc in the network the lower bound on material tonnage is l_{ij} and the upper bound is u_{ij}. The unit cost of production/transportation is c_{ij} ($/tonne ore). Unless otherwise stated, the lower bound on the flow through an arc is assumed zero and the upper bound infinity. The unit costs are made of the following:

- production cost at source i,
- production cost at destination j, and
- transport cost from source i to destination j.

Considering the hypothetical mining and metallurgical complex the following costs in $/tonne of ore apply:

- mining cost at each ore source,
- ore transport cost from mine to mill,
- milling cost at the concentrator,
- transport for concentrates from the concentrator to the smelter,
- smelting cost,
- transport cost for copper anodes from smelter to refinery,

- refining cost, and
- shipping cost for wire-bars from the refinery to markets.

Table 2 presents the mine production planning criteria for the hypothetical mining and metallurgical complex. Tables 3 and 4 list the cost elements for the production facilities and different routes respectively. For consistence, all costs are expressed in $/tonne ore equivalent.

Modelling in LINDO

Schrage (1999) describes the application of LINDO (Linear INteractive Discrete Optimiser) software in solving Network Linear Programming models. This software was chosen for this analysis because it is easy to use and is easily understandable to an average mine planner. The essential condition on an LP for it to be a network problem is that it is representable as a network. In this example, there are four levels of nodes and several arcs between nodes.

The following simplifying assumptions are made:

- mining capacity is a major consideration;
- milling capacity is not very critical, as the plants are running at 70% capacity;
- only one type of ore (oxides) is considered, hence simplifying the network;
- unless otherwise specified the lower and upper bound on the arcs equal to zero and infinity respectively;
- two market destinations for finished copper; demand as indicated in the model; and
- material flow as shown in Fig. 4, except for the market destinations.

Table 2 Production planning criteria

Mining	**UG1**	**UG2**	**UG3**	**UG4**	**UG5**	**OPT**
Run-of-mine grade (% Cu)	3.6	4.2	3.0	3.3	3.8	5.2
Contained copper (kg Cu/t ore)	36.0	42.0	30.0	33.0	38.0	52.0
Mining capacity (ore tonnes/quarter)	750,000	500,000	1,000,000	575,000	624,000	375,000
Milling	**CT1**	**CT2**	**CT3**	**CT4**	**CT5**	
Mill feed grade (% Cu)	3.6	3.6	3.6	3.6	3.6	
Mill recovery (%)	85.0	87.0	85.0	87.0	84.0	
Copper recovered in mill (kg/t ore)	30.6	31.3	30.6	31.3	30.2	
Smelting	**SM1**	**SM2**	**SM3**			
Smelting loss (kg Cu/t ore)	0.10	0.15	0.20			
Refining	**RF1**	**RF2**				
Refining loss (kg Cu/t ore)	0.09	0.09				

Table 3 Production cost for the hypothetical mining-metallurgical complex

Facility (mine/plant)	UG1	UG2	UG3	UG4	UG5	OPT	CT1	CT2	CT3	CT4	CT5	SM1	SM2	SM3	RF1	RF2
Unit cost ($/t ore)	2.5	5.0	3.0	2.5	4.5	2.0	25	30	16	22	33	12	15	10	5	7

Table 4 Transport cost ($/t ore) matrix for the hypothetical mining-metallurgical complex

	UG1	UG2	UG3	UG4	UG5	OPT	CT1	CT2	CT3	CT4	CT5	SM1	SM2	SM3	RF1	RF2
UG1	–	–	–	–	–	–	0.4	0.7	1.00	1.3	1.5					
UG2	–	–	–	–	–	–	1.5	0.5	1.5	1.1	1.2					
UG3	–	–	–	–	–	–	1.5	1.0	0.4	0.8	0.9					
UG4	–	–	–	–	–	–	1.2	1.4	1.6	0.3	0.9					
UG5	–	–	–	–	–	–	1.3	1.4	1.2	1.3	0.2					
OPT	–	–	–	–	–	–	1.0	1.0	1.0	1.1	0.3					
CT1							–	–	–	–	–	0.07	0.04	0.30		
CT2							–	–	–	–	–	0.01	0.05	0.04		
CT3							–	–	–	–	–	0.04	0.01	0.05		
CT4							–	–	–	–	–	0.03	0.06	0.01		
CT5							–	–	–	–	–	0.04	0.05	0.10		
SM1												–	–	–	0.1	0.4
SM2												–	–	–	0.3	0.1
SM3												–	–	–	0.5	0.6
RF1															–	–
RF2															–	–

Defining variables in an obvious way, the general LP describing this problem is:

```
! Group Mine/Plant Production Plan—Linear Programming System
! 2nd Quarter 2004
! Analyst: Senior Mining Engineer
! Run: 15/6/04
! Note: coefficients of each variable in the objective function equals
! the sum of production and transport costs
! Objective Function
MIN
2.9XUG1CT1+5.5XUG2CT2+6.1XUG2CT3+3.9XUG3CT3+2.
8XUG4CT4+5.8XUG5CT4+4.7XUG5CT5+3.1XOPTCT4+2.3X OPTCT5
+25.07XCT1SM1+25.04XCT1SM2+30.07XCT2SM1+30.05XCT2SM2
+16.01XCT3SM2+16.05XCT3SM3+22.06XCT4SM2+22.01XC T4SM3
+23.1XCT5SM3+12.1XSM1RF1+12.04XSM1RF2+15.3XSM2RF1
+15.1XSM2RF2+10.5XSM3RF1+10.5XSM3RF2+5. 09XRF1$$1+5.05XRF1$$2
+7.9XRF2$$1+7.05XRF2$$2
SUBJECT TO
! Constraints
! Mining Capacity
2) XUG1CT1=750000
3) XUG2CT2+XUG2CT3=500000
4) XUG3CT3=1000000
5) XUG4CT4=575000
6) XUG5CT4+XUG5CT5=624000
7) XOPTCT4+XOPTCT5=375000
! Flow balance Constraints
! Concentrators
8) -XUG1CT1+XCT1SM1+XCT1SM2=0
9) -XUG2CT2+XCT2SM1+XCT2SM2=0
10) -XUG2CT3-XUG3CT3+XCT3SM2+XCT3SM3=0
11) -XUG4CT4-XUG5CT4-XOPTCT4+XCT4SM2+XCT4SM3=0
12) -XUG5CT5-XOPTCT5+XCT5SM3=0
! Smelters
13) -XCT1SM1-XCT2SM1+XSM1RF1+XSM1RF2=0
14) -XCT1SM2-XCT2SM2-XCT3SM2-XCT4SM2+XSM2RF1+ XSM2RF2=0
15) -XCT3SM3-XCT4SM3-XCT5SM3+XSM3RF1+XSM3RF2=0
! Refineries
16) -XSM1RF1-XSM2RF1-XSM3RF1+XRF1$$1+XRF1$$2=0
17) -XSM1RF2-XSM2RF2-XSM3RF2-XSM3RF2+XRF2$$1+X RF2$$2=0
! Market demand
18) -XRF1$$1-XRF2$$2=-1000000
19) -XRF1$$2-XRF2$$2=-2000000
END
```

There is one constraint for each node that is of the 'sources = uses' form. For example, constraint number three states that the amount transported out, minus the amount transported in, must equal zero.

Table 5 presents the base case optimal production plan. Note that the optimal solution is in terms of equivalent ore tonnes flowing through the network. For example, the mine should haul 750,000 from UG1 to CT1. The minimised cost of production and transport is $156,375,700. For arcs connecting the concentrators and smelters, the amount of concentrate flowing through can easily be calculated from the concentration ratio, which is a function of run of mine and concentrate grades. Similar calculations can be carried out to determine the equivalent tonnes of copper anodes and cathodes flowing through the arcs connecting the smelters and refineries.

Table 5 Optimum computer solution

Variable	Value	Reduced cost
XUG1CT1	750,000	0
XUG2CT2	0	0
XUG2CT3	500,000	0
XUG3CT3	1,000,000	0
XUG4CT4	575,000	0
XUG5CT4	0	0
XUG5CT5	624,000	0
XOPTCT4	375,000	0
XOPTCT5	0	0.29
XCT1SM1	750,000	0
XCT1SM2	0	3.0
XCT2SM1	0	10.4
XCT2SM2	0	13.44
XCT3SM2	74,000	0
XCT3SM3	1,426,000	0
XCT4SM2	0	0.09
XCT4SM3	950,000	0
XCT5SM3	624,000	0
XSM1RF1	0	4.62
XSM1RF2	750,000	0.000000
XSM2RF1	0	4.76
XSM2RF2	74,000	0.0
XSM3RF1	3,000,000	0.0
XSM3RF2	0	3.34
XRF1$$1	1,000,000	0
XRF1$$2	2,000,000	0
XRF2$$1	824,000	0
XRF2$$2	0	13.93

Analysis of Results and Sensitivity Analysis

Sensitivity analysis involves the study of the responsiveness of the conclusions of an analysis to changes or errors in input values used to generate a particular solution to the LP network. This is equivalent to answering 'what if' type of questions by interrogating the model. As an example, the impact of reducing the number of refineries to one is considered, i.e. remove refinery RF2 from the model. This action results in an optimal solution of $139,696,240 (being the minimum cost of production and transport). Of course, the flow of material through the network changes, but the single refinery produces enough copper to satisfy the market. Such types of analysis can be easily performed on any business decision that the company makes, in order to evaluate the impact of the decision on the business.

Conclusions

The Network LP formulation of the problem of optimising the production planning for a mining and metallurgical complex results in a solution procedure that is easier to solve compared to the general Linear Programming model. There are three types of data required for the Network LP model:

1. for each node (facility) the amount of material available or its capacity;
2. for each arc or route, the cost per unit of material transported along that route; and
3. the lower and upper bound for the quantity of material along that route.

For the hypothetical mining-metallurgical complex presented here, the base case optimum production plan costs $156,375,700, which is the absolute minimum under the given set of economic and technical data. The material flows through the network of mines and metallurgical plants are thus optimised and satisfy all the capacity, demand and flow constraints.

Computerised modelling and optimisation allows one to investigate various business decisions prior to actual implementation. For example, shutting down refinery RF2 would result in the total cost of production and transportation reducing to $139,696,240 for the quarter, a saving of $16 million compared to operating the two refineries.

References

Ahuja RK, Thomas LM, Orlin JB (1993) Network flows—theory, algorithms and applications, Prentice-Hall, 846 p

Bazaraa MS, Jarvis JJ, Sherari HD (1990) Linear programming and network flows, 2nd edn. Wiley, 565 p

Chanda EK (1990) An application of integer programming and simulation to production planning for a stratiform orebody. Min Sci Technol 11:165–172

Dagdelen K, Topal E, Kuchta M (2000) Linear programming applied to scheduling of iron ore production, at the Kiruna Mine, Sweden. In: Panagiotou GN, Mikhalakopoulos, TN (eds) Proceedings ninth international symposium on mine planning and equipment selection, Balkema, Rotterdam, pp 187–192

Fulkerson DR (1961) An out-of-kilter method for minimal cost flow problems. SIAM J Appl Math 9:18–27

Graham-Taylor T (1992) Production scheduling using linear and integer programming. In: Proceedings 1992 AusIMM annual conference, The Australasian Institute of Mining and Metallurgy, Melbourne, pp 159–162

Hoerger S, Bachmann J, Criss K, Shortridge E (1999) Long term mine and process scheduling at Newmont's Nevada operations. In: Dagdelen K (ed) Proceedings 28th international symposium on computer applications in the minerals industries, Society for Mining, Metallurgy, and Exploration, Littleton, pp 740–748

King B (2001) Optimal mine scheduling. In: Edwards AC (ed) Mineral resource and ore reserve estimation—the AusIMM guide to good practice, The Australasian Institute of Mining and Metallurgy, Melbourne, pp 451–458

Ramazan S (2001) Open pit mine scheduling based on fundamental tree algorithm. Ph.D. thesis, Colorado School of Mines, Mining Engineering Department

Ramazan S, Dimitrakopoulos R (2004) Recent applications of operations research and efficient MIP formulations in open pit mining. SME Trans 316:73–77

Ricciardone J, Chanda EK (2001) Optimising life of mine production schedules in multiple open pit mining operations: a study of effects of production constraints on NPV. Min Resour Eng 10(3):301–314

Saul B (1990) Optimisation of waste haulage with linear programming. In: Singhal RK (ed) Proceedings Mine Planning and Equipment Selection, Balkema, Rotterdam, pp 455–461

Scheepers L, Wellbeloved D (1992) Optimisation of integrated mining and metallurgical complexes by means of linear programming and case study. In: Survival strategies for the metallurgical industry, South African Institute of Mining and Metallurgy, Johannesburg

Schrage L (1999) Optimisation modelling with LINGO, LINDO Systems Inc, 530 p

Thomas GS (2001) Optimisation of mine production scheduling—the state-of-the-art. In: Edwards AC (ed) Mineral resource and ore reserve estimation—the AusIMM guide to good practice, The Australasian Institute of Mining and Metallurgy, Melbourne, pp 441–450

Open Pit Transition Depth Determination Through Global Analysis of Open Pit and Underground Mine Production Scheduling

K. Dagdelen and I. Traore

Abstract This paper presents an iterative Net Present Value (NPV) maximization method to determine the optimum surface to underground transition depth for an ore body to be mined by multiple open pits and an underground mine. The determination of transition depth from open pit to underground mining is based on global production scheduling optimization of open pit and underground mines using Mixed Integer Linear Programing (MILP). The method is applied to a case study coming from a gold mining complex with six open pits and a large underground mine using long hole open stoping. The results indicate potential improvements of the NPV of global operations when compared to the traditional techniques based on independently optimized open pit first, followed by the underground mining.

Introduction

In recent years, a certain number of open pit mines have transitioned to underground. The open pit to underground transition problem is one of the important topics in the mining industry that has not been mathematically solved yet. Currently there is no mathematical algorithm that can successfully optimize the transition depth by considering the life of the mine schedule of both open pit and underground combined. Due to the complexity of the problem and its size, often the transition depth is defined by considering the open pit and the underground separately. Usually the transition depth is defined by comparing the cost of mining using open pit vs underground methods. As the pit gets deeper the stripping ratio increases and the transition depth is defined when the cost of mining the open pit is equal to the

K. Dagdelen (✉) · I. Traore
Mining Engineering Department, Colorado School of Mines,
Golden, CO 80401, USA
e-mail: kdagdelen@mines.edu

I. Traore
e-mail: traoreismail@yahoo.fr

R. Dimitrakopoulos (ed.), *Advances in Applied Strategic Mine Planning*,
https://doi.org/10.1007/978-3-319-69320-0_19

underground mining cost. Defining the transition depth by comparing the costs of these two mining methods, the underground development work and the value of the underground mine are not appropriately considered therefore the economics of the mining project may not be optimized in terms of the net present value of the overall project.

The transition depth when correctly defined can significantly improve the discounted net present value of the project. In this paper, the transition depth from open pit to underground is determined by an iterative process of optimizing the life of the mine production schedules of both the open pit and underground mines using Mixed Integer Programing (MILP). Using Whitlle software from GEMCOM, a series of pits are generated by constraining the Lerchs and Grossmann pits to a given pit bottom elevation. The underground mining lodes and stopes are sequenced using Studio 5D and EPS software from CAE. For each pit depth scenario, a permanent crown pillar of 30 m is left between the open pit bottom and the underground workings, the reserves are updated, and both the open pit and the underground mine are rescheduled by maximizing Net Present Value (NPV) using OptiMine® software developed at Colorado School of Mines. The combined values of both open pit and underground production schedules are evaluated using discounted cash flow analysis. The optimum transition depth is determined by comparing the life of mine NPV of each scenario.

Gold Mine Case Study

The case study gold mine is a complex mining operation that includes six open pits, namely: Main (the biggest pit), Pak1, MH2, Pam3, Kom4 and Ses5 and one underground mine below Main open pit (see Fig. 1).

There are 3 phases in the initial base case Main pit, 3 phases in the Pak1 pit and the other pits consist of one phase. The material mined from the pits can be sent to different destinations such as waste dumps, stockpiles, and the processing plant. There are three different material types in the open pits named oxide, transition and fresh. The case study gold operation is modeled as a large scale, multi-mine, multi-time period scheduling problem with multiple material types, multiple grade intervals, and mining capacities.

Main Deposit

The Main deposit is the biggest deposit and is mined using a combination of open pits and underground mining methods. As shown in Fig. 2, for accessing the underground ore zones, twin declines of about 1400 m and a vertical shaft of 750 m are driven. Some ore material will be transported by truck via the twin declines to the surface. The transportation of ore from the ore passes to the crusher is done

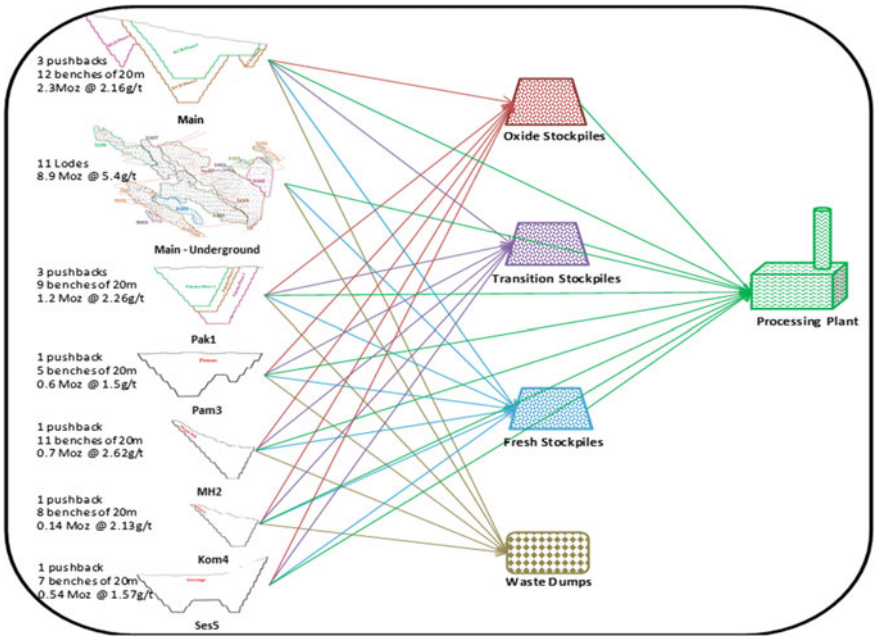

Fig. 1 Case study—gold mine overview

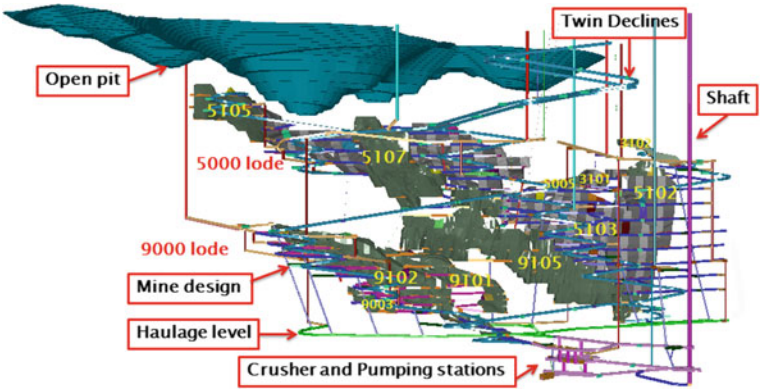

Fig. 2 Main underground mine

through the transportation level. The ore is loaded from an ore pass and the material is dumped through a grizzly into the crusher. The crushed material is transported by conveyor into the skips and hoisted to the surface for processing.

The underground mine consists of 11 lodes, namely 5103, 9101, 5102, 9105, 5105, 9102, 3102, 5107, 5005, 3101, and 9003 (Fig. 3). Transverse longhole stoping is used for mining part of the orebody that is approximately flat (less than 50) and with a thickness greater than 20 m and will take place in lodes 5103, 5102,

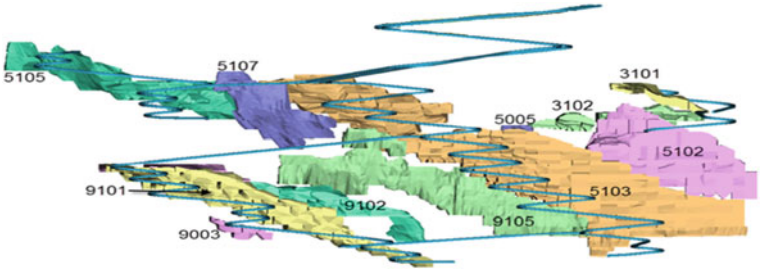

Fig. 3 Underground mining lodes

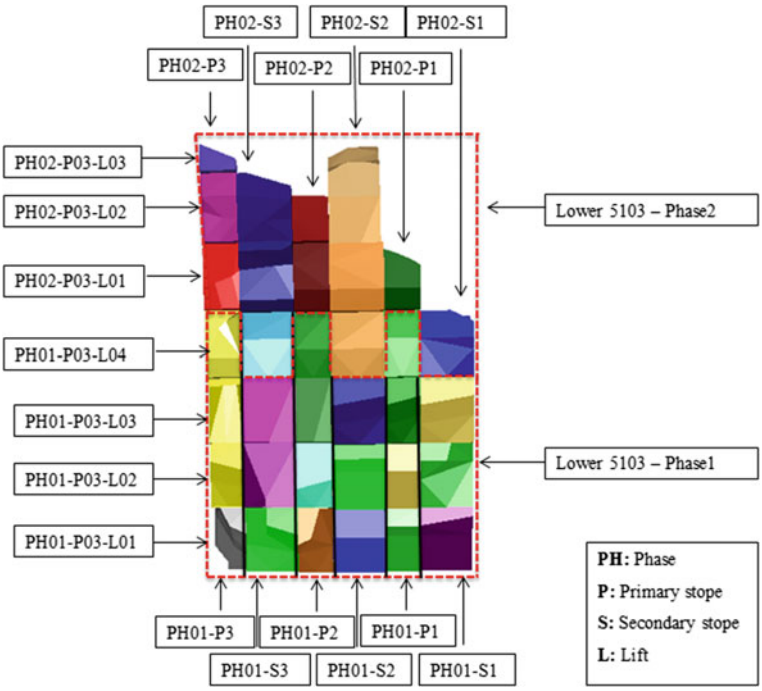

Fig. 4 Lower 5103—transversal (long view)

5105, 9101, 9102, and 9003 (Fig. 4). Longitudinal longhole stoping method is used where the dip of the orebody is approximately steep (greater than 50°) and the thickness is less than 20 m and takes place on 5103 lower zone, 5102 upper zone, 5105, 5107, 9101 lower, 9102 lower and 9105 (Fig. 5). Advance transverse face will take place in 9101 and 9102 upper part (Fig. 6).

Transversals stopes are organized by phase, stope type and lift. For example, the Lower 5103 is divided into two phases. Phase1 consists of stopes located in the lower part and phase2 consists of stopes in the upper part. Each mining phase consists of primary and secondary stopes and there are a certain number of lifts within each stope (see Fig. 4).

The sequence is as follows:

- Phase1 has to be mined and backfilled before mining of Phase2 can start.
- In a given mining phase, Primary stopes have to be mined before secondary stopes.
- In a given stope, lift1 has to be mined before lift2 and lift2 before lift3, etc.
- In a given phase, primary and secondary stopes can be mined independently.
- Primary stope height cannot exceed 4 levels and secondary stopes cannot exceed 3 levels due to geotechnical constraints.

For longitudinal stope the sequencing is as follows:

- Stope1 is to be completed before stope2 and stope2 before stope3.
- In each stope, lift1 has to be mined before lift2 and lift2 before lift3, etc.

The Upper 9101 and the Upper 9102 are mined using advance transverse long hole stoping.

The sequence is as follows:

- All of phase1 has to be completed before phase2 and phase2 before phase3, etc.
- Stopes located in different raw in a given phase can be independently mined
- In each stope, lift1 has to be mined before lift2 and lift2 before lift3, etc. For the long term sequencing purposes lifts located in the same stopes are merged.

Transition Depth Determination Through Life of Mine Production Scheduling Optimization of Open Pits with the Underground Mine

For defining the transition depth through life of mine production scheduling optimisation, the Mixed Integer Linear Programming (MILP) based optimization software OptiMine® is used. The Optimine® software is a multi mine, multi time period production schedule optimizer that maximizes NPV of cash flows coming from the open pit and underground operations subject to operational constraints. The OptiMine® program needs the pit reserves information organized by pit phase, bench, material type and grade intervals for each pit. The underground reserve information needs to be organized by the lode, section and stope for each underground lode and must then be entered into the program. The special sequencing requirements between open pits and the phases of open pits needs to be identified and entered into the program. The special sequencing requirements between the lodes, between the sections of a given lode and between primary and secondary stopes also needs to be identified and entered into the program. The program takes into account all the material sources available from open pit phases and underground lodes and determines the open pit and underground yearly mine production schedules for life of Mine (LOM) by maximizing net present value of cash flows

considering all the revenues, mining and processing capacities, and the related costs associated with mining, stockpiling and processing during the life of the project. The OptiMine® program provides results that not only optimizes LOM production schedules in terms of yearly mined sequences from the open pits and underground but also results that optimizes cutoff grades for the material coming from these sequences to be directed to waste dumps, stockpiles, and the processing plant by period (Fig. 1).

Approach for Determining the Optimum Transition Depth

The methodology used for defining the best transition depth is an iterative process that consists of two parts. The general steps for the first part are as follows:

1. Perform the base case ultimate pit limit analysis of the effected pit by constraining Lerch-Grossman pits to base case pit bottom depth using Whittle software from GEMCOM.
2. Design the underground mine using Studio 5D and EPS from CAE by locating the crown pillar at this depth.
3. Choose the mining and processing capacities and determine open pit and underground mining costs and the discount rate.
4. Optimize the life of mine production schedules for combined open pit and underground operations using OptiMine® software and determine the yearly cash flow and resulting net present value.

In the second part of the analysis, the optimum transition depth that achieves the maximum net present value is determined. The steps can be written as follows:

1. Strategically increase the constraining open pit depth and perform the ultimate pit limit analysis by using Whittle software.
2. Adjust the underground mine reserves by excluding the material that will now be mined by open pit and for the areas that will be left in the crown pillar.

Fig. 5 Lower 9105—longitudinal stope (long view)

3. Strategically increase the open pit mining rate and adjust the underground mining rate
4. Optimize the combined life of mine production schedules for both open pit and underground using Optimine® software and determine the cash flow and resulting net present value.
5. If the net present value is more than the previous one, GO TO step 0.
6. If the net present value is less than the previous one, the best transition depth is reached. END the iteration.

Main Pit Bottom Depth and Crown Pillar Elevations

Before analyzing any scenario, a baseline schedule was developed using OptiMine®. This was done so that the Net Present Value (NPV) for different scenarios would be comparable to the initial plan developed. The base case pit bottom is chosen to be at 5685 m elevation (Fig. 7).

Fixing three different crown pillar locations between Main pit and the underground mine created three different scenarios. The 5620 m elevation scenario, the 5585 m elevation scenario, and the 5545 m elevation scenario were developed respectively by lowering the Main open pit depth from base case elevation to elevation 5620 m (about 65 m deeper than the base case), to elevation 5585 m (about 100 m deeper than the base case), and to elevation 5545 m (about 140 m

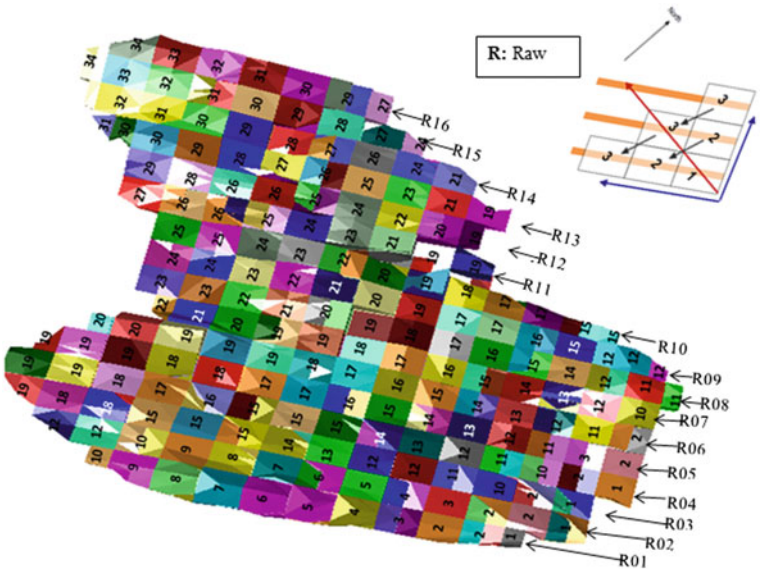

Fig. 6 Lode 9101—Transverse advance facing (plan view)

deeper than the base case) and optimizing the production schedule of the life of mine open pit and underground plans. During that process, the open pit mining rate was increased, the underground mine was adjusted by excluding those stopes that will be included in the open pit and left in the crown pillar, and the NPV was generated. During these studies, the major underground development design, such as declines, vent raises, ore passes and shafts (as shown in Fig. 2) was kept intact since they were assumed not to be affected by the open pit depth scenario analyzed. However, the access drifts and cross cuts of impacted lode stopes were excluded. For determining the best transition depth from Main open pit to underground, different scenarios are investigated through life of mine production scheduling and cutoff grade optimization including: the base case scenario, 5620 case scenario, 5585 case scenario, 5545 case scenario. The Main pit transition depth case scenarios investigated are presented in Fig. 7.

Impact of the Transition Depth on Open Pit and Underground Reserves

Deepening the Main open pit affects both the open pit and the underground reserves. The open pit reserve will increase and the underground reserve will decrease. Some underground stopes will be mined by open pit and others will be left in the crown pillar. During this study a permanent crown pillar of 30 m between the open pit and the underground mine was assumed.

Prior to deciding the transition depth, the location of the crown pillar must be very closely analyzed.

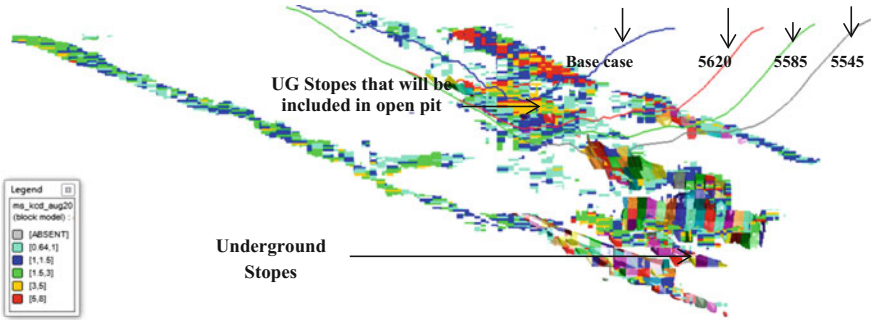

Fig. 7 Main grade model with base case, 5620, 5585, 5545 case scenarios (cross section)

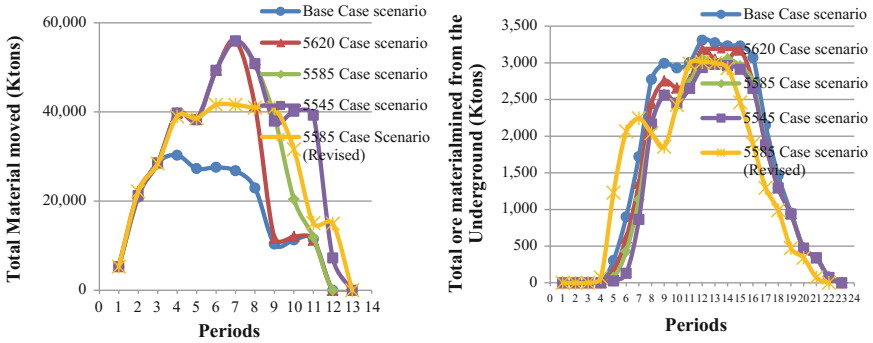

Fig. 8 Ore and waste tonnes mined from the open pit and ore material mined from the underground of different scenario

Comparative Study of Different Case Scenarios

As shown in Fig. 8, the yearly ore produced in the base case appears to achieve the highest ore production, followed by: 5620 case scenario, 5585 case scenario and 5585 revised case scenario, and 5545 case scenario, respectively. The lower ore production in each of the those cases (5620 case scenario, 5585 case scenario and 5585 revised case scenario and 5545 case scenario) is explained by the impact of deepening the Main pit. By increasing the open pit depth through relocation of the crown pillar, the open pit reserve increases and the underground reserve decreases.

Economic Comparison of Different Case Study Scenarios

Using a US$1200 gold price and a discount rate of 10%, the before tax net present value of each case is shown in Fig. 9. The costs used includes all the open pit mining costs, transportation costs, stockpiling costs, re-handling costs, processing cost and the underground capital and operating costs (as shown in Fig. 8). The maximum net present value is reached in the Main 5585 case revised scenario.

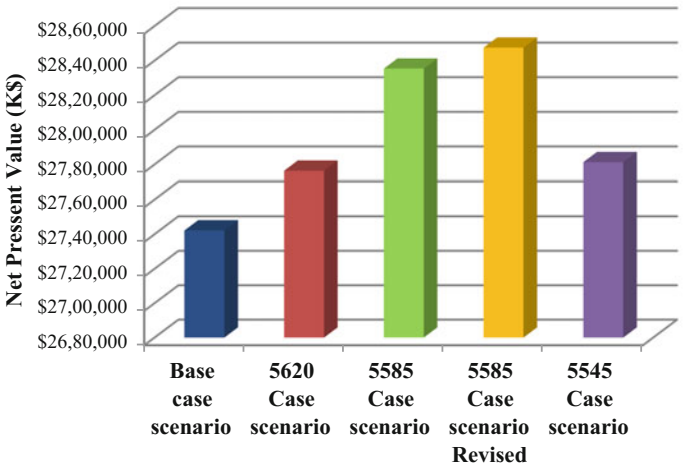

Fig. 9 Comparative study of the before tax net present value of different scenario

Conclusion

The determination of open pit to underground optimum transition depth requires the consideration of many parameters such as the deposit geology, reserves, the location of the pit bottom and the crown pillar, the open pit and underground mine sequencing, the costs of mining for open pit and underground, cost of processing, the mining and process rates and the discount rate and revenues. These parameters interact with one another in a complex process, defining the financial outcome of the project. This paper provides an iterative method to determine open pit to underground optimum transition depth by incorporating all the interactions between critical geologic, mining and economic parameters in a combined production scheduling optimization model using Mixed Integer Linear Programing (MILP).

Consideration for Multi-objective Metaheuristic Optimisation of Large Iron Ore and Coal Supply Chains, from Resource to Market

J. Balzary and A. Mohais

Abstract Dynamic market and operating conditions coupled with an environment in which multiple objectives and trade-offs are common, pose major challenges for planners and schedulers working in any mining entity. Many mining companies recognise the need to shift from a siloed mining-focused push model to an integrated value chain, demand-driven approach but there are still fundamental barriers in business process and the supporting technology preventing a consideration of end-to-end optimality. This paper presents some elements of experiences working with companies to adopt such advanced approaches. In addition to algorithmic elements, an approach to phased and gradual deployment of progressively more sophisticated optimisation models is described. From a practical software adoption perspective, it is believed that this last concern is also of primary importance. Next generation approaches to the optimisation of complex bulk commodity demand chains; namely iron ore and coal are presented, with case studies in the world's largest integrated operations in Western Australia and Queensland from the raw material mined through to market. Utilising accurate simulation models supported by metaheuristic optimisation techniques, a range of ways to engineer a dynamic decision support framework that can adapt and change with the inevitable changes in commodity markets is explored. Objectives such as total revenue, margin, cost, NPV, throughput, asset utilisation, contractual penalties and bonuses, and energy consumption can be managed simultaneously across the mine, plant, logistics network, port operation, shipping and sales domains.

J. Balzary (✉) · A. Mohais
Supply and Demand Optimisation, Schneider Electric, Level 1,
99 Frome Street, Adelaide 5000, Australia
e-mail: james.balzary@schneider-electric.com

A. Mohais
e-mail: arvind.mohais@schneider-electric.com

R. Dimitrakopoulos (ed.), *Advances in Applied Strategic Mine Planning*,
https://doi.org/10.1007/978-3-319-69320-0_20

Introduction

The Resource-to-Market mining supply or demand chain can be represented most broadly from the pre-extracted, in situ resource through to the point at which an organisation can invoice upon sale. Much effort is placed on systems facilitating mathematical and computational improvements in decision making at various points in this value chain. Technologies exist to assist in optimal mining operations sequencing, and also in subsequent material handling and logistics processes down the chain. According to current mathematical knowledge, for the class of problem represented by the full Resource-to-Market supply chain and all of its complexities, there is no known method of solution that would give an absolute and irrefutable optimal planning or scheduling outcome. Whilst this is a mathematical reality that businesses must come to terms with, from an opportunistic point-of-view, it presents stakeholders with the ever-present possibility that they can continually improve decision support and modelling technologies and do better.

With this opportunity as a motivator and using of practical and real-world learnings as atomic components, this paper presents a next-generation optimisation framework that would deliver further benefit and profit to mining organisations globally. Included is a brief overview of the nature of bulk mining supply chains, conceptualised from a software point of view—from available raw material, through beneficiation, transport, storage and onto vessels. Within this supply chain, we will identify a number of important component segments that can be treated as silos, or preferentially, should be treated as integrated parts of a larger global operation. Standardised key performance indicators are described, with targets set for each as reward-based fitness measures. Methodologies for the utilisation of advanced science solutions involving modern heuristic optimisers and metaheuristic algorithms are described guiding the search efforts of the lower-level searches.

Supply Chain Objectives

Companies seeking to optimise the planning and scheduling of their Resource-to-Market supply chains express their view of an optimal solution in terms of certain objectives that they would like to achieve. These objectives are often either to maximise or minimise a particular measure of performance in the supply chain, or sometimes to keep a measure confined to a targeted band of values. Although we can identify typical objectives that are common across mining entities, different companies often would attribute different degrees of importance to these objectives, in effect weighting their contribution to the overall evaluation of a plan or schedule. Typical objectives encountered in the mining industry are:

1. Increase margin
2. Maximise cash inflow
3. Minimise cash outflow
4. Maximisation of asset utilisation, fixed and mobile plant
5. Maximisation of sequenced activities—e.g. vessels berthed per tide
6. Maximisation of efficiency—e.g. direct train to vessel loading
7. Minimisation of variability—e.g. quality through processing
8. Minimisation of penalty—e.g. demurrage
9. Achieve target tonnage value e.g. rail and shipped.

Conflicting Objectives

Typically in mining supply chains, and in fact every business, objectives conflict with each other. These conflicts involve the interrelationships of complex business rules, processes, constraints and performance measures. Take for example the desire to maximise fixed asset utilisation in a port operation. Maximising asset utilisation is in direct conflict with a common objective to maximise direct train to vessel loading. A model of these activities seeking to keep car dumpers, stackers and reclaimers in continual use would like come up with a sequence that schedules and dumps trains as soon as there is an available time slot on any of these pieces of equipment. The alternate view is to delay arrival of a train so that it coincides with the berthing of a vessel therefore allowing for direct loading, but possibly at the cost of keeping the aforementioned pieces of equipment idle.

There are many other such examples of conflicting objectives. It is inherent in any company's expression of their optimisation wishes.

Handling Multiple Objectives

In the literature a common theoretical construct that is proffered for managing situations with multiple conflicting objectives is to use the notion of Pareto fronts (citation), but limited application of this exists in decision support in production environments (citation). Under this approach, instead of seeking a single optimised solution, a collection of solutions is retained, forming a so-called Pareto front of non-dominated solutions. Any solution in this set has the characteristic of being better than all the others on at least one of the objectives.

The philosophy behind this approach is that the value of the work done by the optimisation software should be retained in the form of the Pareto front, and then this set of high-quality solutions should then be passed to a human expert for final analysis and evaluation, and the human expert would make the final decision on which should be selected. In some situations, this approach is feasible. However,

we believe that in the Resource-to-Market context, the number of possible conflicts is reasonably high, and the presentation of a Pareto front to a human expert by the software would be of limited value because of the number of potential solutions that would be expected in such a set, and the work required to make a final decision would not at all be straightforward.

Another factor that currently weighs against purely multi-objective algorithms in the Resource-to-Market space is that when the magnitude of the supply chain, coupled with the number of data elements and the time horizon are taken into consideration, the potential running time of such an algorithm is infeasible for the decision making timeframe. A more appropriate methodology given these considerations is the relative weighting of each objective, and their combination into a single unified evaluation measure. A downside to this approach is the fact that the scales on which different objectives are measured could vary dramatically Therefore trying to combine them using appropriate weights would often require re-tuning to get the right values. A possible approach to eliminate this variability is to allow an authorised end-user to state their weighting preferences using a unit-free normalised scale, and to let the science and software experts to devise and tune appropriate multiplicative factors to compensate for the inherent scale differences of the different objectives.

Objective Function

Although each mining operation would have idiosyncrasies necessitating modifications to the objective function used by an optimisation algorithm, it is still possible to provide in closed mathematical form, an expression of that function, using typical and common terms. This is illustrated below for the case of a scheduling problem:

Let X be an element of the unconstrained solution space. Then X can be expressed as a collection of scheduled activities, across train loading, railing, car dumping, stacking, reclaiming, conveyance, ship loading and berthing. Hence X can be expressed as the union of disjoint subsets of activities in each of these areas as follows:

$$X = X_{TLO} \cup X_R \cup X_{CD} \cup X_S \cup X_{RE} \cup X_C \cup X_{SL} \cup X_B$$

where X_{TLO} is a set of train loading activities, X_R is a set of railing activities, X_{CD} is a set of car dumping activities, X_S is a set of stacking activities, X_{RE} is a set of reclaiming activities, X_C is a set of conveyance activities, X_{SL} is a set of ship loading activities, and X_B is a set of berthing activities. These discrete activities are the required steps move excavated material from the pit onto a ship at berth at the port.

The elements contributing to the objective function would be:

Revenue	$\$R = \sum_{x \in X_{SL}} saleprice(x)$
Costs	$\$C = \sum_{x \in X} cost(x)$
Resource utilisation (fraction)	$RU = \sum_{Y \in \{X_{TLO}, X_R, X_{CD}, X_S, X_{RE}, X_C, X_{SL}, X_B\}} \frac{constrained\ capacity - \sum_{x \in Y} duration(x)}{constrained\ capacity}$
Demurrage costs	$\$D = \sum_{x \in X_B} demurrage\_penalty(x)$
Silo constraint violations	$CV = \sum_{Y \in \{X_{TLO}, X_R, X_{CD}, X_S, X_{RE}, X_C, X_{SL}, X_B\}} \sum_{x \in Y} constraint\_violation\_severity(x)$
Target shipped tonnes penalty	$TSTP = shipped\ tonnage\ target - \sum_{x \in X_{SL}} tonnage(x)$
Target railed tonnes penalty	$TRTP = railed\ tonnage\ target - \sum_{x \in X_R} tonnage(x)$

Using these contributing elements as representative, the objective function can then be expressed as:

$$f(X) = w_1\$R - (w_2\$C + w_3\$D) - (w_4RU + w_5CV + w_6TSTP + w_7TRTP)$$

The coefficients $w_1, \ldots, w_7$ are weights that are configurable by users with the right access privileges. The first three terms of the function are intuitive dollar values which are readily justified. The last four terms are penalties due to violations of constrains and operating rules, or for un-achieved targets. To justify the a simply numeric difference with the dollar values requires human input into the weightings so that their relative importance is correctly judged in relation to the hard dollar values.

Literature Survey

Although Supply Chain Modelling and Supply Chain Management are heavily researched areas, the published literature addressing resource-to-market optimisation in the mining context is relatively small. Bodon et al. (2017, in this volume), describe the challenges of using a discrete event simulation language to model the complexities of a pit to port coal supply chain, and propose a de-coupling of the simulation aspect of the model from optimisation aspects. They used a general linear program as an optimiser, and couple this with discrete event simulation, and presented their results on scenarios from a real-world coal mining operation in Indonesia. Further related work is available in Bodon et al. (2011). Peng et al. (2009) provide an analysis of an integrated coal supply chain, and apply the model to the Xuzhou coal mine in China. They present results showing that not only optimal profit is obtained, but that a level of customer satisfaction is achieved. Their results enabled recommendations to be made for the mine operations, and assisted in decision making.

Montiel and Dimitrakopoulos (2013) look at a coper mining supply chain, with emphasis on global optimisation from the point of view of taking into account the output of multiples mines and products in a given mining complex. Their work also focuses on the variability of orebody models, and deals with their stochastic nature by producing stochastic mine production schedules. Montiel and Dimitrakopoulos' work was based on using Simulated Annealing, a metaheuristic approach, for producing mine schedules. Their results showed that a stochastic schedule produced expected deviations from mill and waste production targets smaller than 5%, versus that of conventionally generated schedules which was 20%. Although their work did not focus on the Resource-to-Market supply chain as it has been outlined in this paper, their model nevertheless considers a large subset of the mining supply chain, particularly around the details of excavation, waste haulage, milling, and further value-adding preparation and handling of the product.

Singh et al. (2012) provide a detailed elaboration of a mathematical model constructed to represent the operations of the Hunter Valley coal chain in eastern Australia. Their goal was to create a model that could find a supply chain schedule/plan that would meet a given demand profile, whilst concurrently suggesting any capacity increases or new equipment that would be required to support that solution. Singh et al's model was not built into an end-user enterprise application, and their results potentially could take up to several hours to compute, which would make it challenging for the kind of software implementations that Schneider Electric's SDO is interested in. However, their work is remarkable to us because of the level of detail that was built into the model in certain places, and because of the hybrid nature and multi-phase approach to their solution.

Their model was developed around assumptions for a demand-driven, cargo-assembly type operation. Historical demand profiles were used to drive the model and optimisation process. The main goal of the optimisation model was to minimise the cost of running the terminal for that demand profile. The cargo-assembly approach required that all products required for loading a vessel be delivered and already stacked at the port before loading begins. Hence, direct loading was not considered in their model. Rail was modelled around the key factors of a limited number of consists (potential trains) per day, and a limited number of paths through rail junctions at the mine and at the port.

They explored using Genetic Algorithms, and Squeaky Wheel heuristics to generate individuals with representation components involving job sequences, and capacity/equipment increments. The solutions produced by these algorithms are then passed to a CPLEX algorithm to generate a final solution. Singh et al. concluded that it was a challenging problem that could not be easily solved by then-currently available MILP (mixed integer linear programming) commercial software or straight application of general metaheuristics like genetic algorithms. Some of their other approaches (squeaky wheel and another called large neighbourhood search) produced somewhat better results, but they acknowledged room for improvement, possibly by exploring alternative or more closely coupled hybridisations between the MILP approach and heuristic search methods.

Live Software Implementation Experience with Mining Companies

Enterprise level software solutions in the Resource-to-Market domain for iron ore and coal mining have been deployed into live use for major Australian mining companies over the last three years. Some experiences, modelling and algorithmic details from these implementations are provided utilising two scenario sections of the paper. In each case, a future extension of the approach is described, which seeks to apply meta-level optimisation in an effort to further improve on the results that have been previously achieved in practice.

Two scenarios are presented to illustrate different time horizons, one of which necessitates a finer-grained "scheduling" approach, and the other a more coarse-grained "planning" approach. There are substantive differences between the approaches, and the algorithms used must be tailored accordingly. As an added benefit, the cases described were chosen so as to reflect both iron ore mining and coal mining.

Scenario #1—Scheduling System for Iron Ore

Fortescue Metals Group (FMG) is Australia's third largest iron ore producer operating 3 mines, a dedicated rail line and port in Western Australia. In this scenario the model manages several silos from post-beneficiation to vessel. Focus is placed on important elemental aspects of the algorithms used in the software with an outline of a future-state meta-level algorithm proposed. This progression in algorithmic complexity follows a prescribed staged approach where initial deployment of optimisation technology is managed in a step by step fashion, beginning with simplified acceptable techniques and migrating to more advanced, automated decision support paradigms.

The deployed decision support model focuses on the modelling of trains and the rail network between the various train load-out (TLOs) and the port. The system is configured with a fixed number of rakes or consists (a collection of wagons assembled to carry an iron ore product) that need to be scheduled in order to meet demand at the port. Queuing of rakes at the TLOs is an important factor in the local scheduling decisions considered when looking at the rail silo. For the iron ore scheduling problem, two elements of the deployed algorithm that are particularly important include (i) the demand-driven nature of the algorithm, and (ii) the technique of disruption propagation. These are both used as baseline elements of the current and future version of the algorithm.

Components of a Scheduling Solution

In the scheduling (versus planning) domain, the emphasis is on very detailed and comprehensively-specified activities scheduled with a start and an end time. Many details of each activity in question, such as the equipment utilised and inventory produced must be modelled and calculated. The computational effort is often prohibitive and the respective granularity and accuracy of data diminishes over a long time horizon, making long term decisions on highly detailed models infeasible. The need to manage the level of detail and the importance of these finite elements in the scheduling horizon naturally focuses attention in the short-term (hours, shift, days).

In a typical mining Resource-to-Market requirement for a scheduling purpose, the following activities are specified (as examples):

Train (rake/consist) service	
• Rake/Consist ID • Train destination (mine) • Port depot departure time • Selected loader at mine (TLO) • Product to be loaded (type, tonnage, quality)	• Queuing time at mine • Loading duration • Journey time • Queuing time at port • Selected unloader at port • Optional periodic maintenance at port
Train loading activity	
• TLO ID • Product type • Product tonnage	• Product quality • Loading start time • Loading end time
Car dumping activity	
• Car Dumper ID • Rake ID • Product type • Product tonnage • Product quality • Conveyor route ID	• Stockpile destination ID (if applicable for stacking) • Shiploader ID (if applicable for direct loading) • Dumping start time • Dumping end time
Stacking activity	
• Car Dumper ID • Stacker ID • Stockpile ID • Conveyor route ID • Product ID	• Product tonnage • Product quality • Stacking start time • Stacking end time
Reclaiming activity	
• Reclaimer ID • Stockpile ID • Shiploader ID • Conveyor route ID • Product ID	• Product tonnage • Product quality • Reclaiming start time • Reclaiming end time

(continued)

(continued)

Ship berthing/de-berthing activity	
• Vessel ID • Berth ID • "Pilot on board" (POB) time • "First line" time	• "All fast" time • "Ready to load" time • Depart berth time
Ship loading activity	
• Shiploader ID • Berth ID • Conveyor route ID • Product ID	• Product tonnage • Product quality • Loading start time • Loading end time

Demand-Driven Solution Generation

This iron ore case study uses a demand-centric perspective to drive the optimised solution generation with primary demand based on vessel nominations and the associated attributes for contractual fulfilment.

The market factor is very important in this model, as it is the primary determinant in the schedule produced. The client organisation provides data on future sales for the time horizon under consideration. This consists of firm orders, which are ones which have already been confirmed by the end buyers, as well as tentative orders, which are indications of intention to buy. This data is provided to the scheduling software by means of direct data integration. The scheduling software has a data exchange interface with other software systems used by the client organisation, and the latest variations are always available for use in generating new and updated schedules. The data is provided in the form of Vessel Nominations, which are contracts for the sale of iron ore commodities to be loaded at a designated port by a particular vessel. The data contains the Estimated Time of Arrival (ETA) of the vessel at the anchor point associated with a port. This date and time is used by the scheduling algorithm to determine possible choices for a time of berthing for that vessel.

During simulation, when a particular instant in time is being considered, a vessel that has been tentatively selected for berthing at that time is examined to see what its nomination is, i.e. which products, their respective volume and quality are required for loading once it is berthed at the port. This demand triggers a backward-looking analysis agent that retraces the steps along the supply chain that are needed for the required amount of the right products to be available at the port at the time of the vessel's arrival. This then creates precursor demands within upstream silos in the supply chain, which must be optimised concurrently with other scheduled activities in those silos.

Disruption Propagation

When a certain magnitude of change occurs to a scheduled activity, for example the berthing of a vessel an hour earlier than planned, it is possible to locally propagate the effect of those changes and quickly get the overall schedule back into a correct feasible state without having to undergo a computationally expensive re-building of the entire schedule. An understanding of the implications of this propagation without optimisation is managed via constraint handling which references the available capacity and buffer between each related activity and determines if violations have occurred that are infeasible.

Assuming stockpiles that were intended to be used to load the vessel were already at their required inventory levels several hours before, the fact that the vessel is early does not cause any problem with loading. Alternatively, it may be that a sequence of trains that were scheduled to arrive throughout the duration of the vessel being at berth are now out of sync with this shift in time, and the problem could be fixed by shifting the train schedules all by one hour earlier. We would have to check how this triggers knock-on effect higher up the supply chain, and also potentially look at effects like congestion or conflict on the rail network, if the supply chain is being modelled to that extent.

The key thing to note is that it is possible for small disruptions in one silo to be relatively easily absorbed by adjacent silos in the supply chain, and it is a wise tactic to attempt to use this propagation opportunity to quickly absorb these changes as opposed to attempting brute force re-optimisation.

Realities of Global Optimisation

It is important to note that within the confines of the decision making timeframe, it would be impractical to create a problem representation that encompasses the entire supply chain, and then use a population-based algorithm that simply treats the individuals as candidate solutions to this massive problem. In practice the computational power required to process that magnitude of scope and complexity would be infeasible, and so would the required computing time under current hardware constraints. Furthermore it would be naïve to expect that simple operators (such as intra-silo mutations, or crossovers across silos, or even across the global representation) working on a massive representation would be able to effectively or efficiently find the truly high-quality solutions that human experts are seeking.

It is important to recognise that although the global context must be considered, and the desired solution would have less-than-optimal sub-solutions within silos, we should nevertheless respect the local logic and intelligence that exists within the silos (human or modelled). It is through judicious use of this intelligence that we can arrive at a solution that can be considered globally optimised.

Hybrid Global Optimisation

We propose that a hybrid approach is needed, which acknowledges the fact that a truly optimised solution must take into account the global, multi-silo nature of the problem, but which also intelligently operates on the representation so that infeasible solutions are avoided, and also that natural heuristic corrections to adjacent silos are carried out in response to an evolutionary disruption in a target silo.

Consider for example a change in the vessel-loading activities at the port, wherein a particular ship loader requires more material than is currently scheduled, and thus draws upon a stockpile to an extent surpassing its current stock. (This is not possible in physical reality, but can certainly be considered as part of an individual representation). This shortfall in inventory at that stockpile is a natural impetus for the adjacent rail module to undergo an amount of re-optimisation, whether it be a small or a large change remains to be determined). This principle gives rise to a multi-silo algorithm which can be called "Disruption Dampening and Transmission". Changes in one silo may cause nudging on an adjacent silo, which may be accommodated by slight movement, i.e. a dampening of the disruption, or it may be necessary to completely re-adjust the neighbour to try to align its endpoints with the disruption, i.e. a full transmission of the disruption.

Figure 1 illustrates the concept of disruption dampening and transmission, using the analogy of sitting on a bench. To get a better understanding of how this proposed algorithm would be implemented, Fig. 2 provides a pseudo-code outline. The key idea of this algorithm is to choose a most influential silo (or weight them in importance and choose probabilistically), and run a full optimisation routine on it, but after each iteration, as individuals are modified, the effect of their modifications either get dampened by virtue of adjacent silos being able to absorb the impact of the change with small-scale modifications, or get transmitted with a more disruptive effect into the adjacent silo, triggering a full re-optimisation of the current state within that neighbouring silo.

If this approach is contrasted with a more straightforward approach to global optimisation, one could imagine that a change in a silo would be followed immediately by an evaluation of the overall individual. The resulting individual is likely to contain multiple constraint violations and task misalignments. These could be handled by penalty components in the fitness evaluation of the individual, but the likelihood of this being able to successfully guide the algorithm is very low.

The above proposed approach could be likened somewhat to repair algorithms from evolutionary computation. What is substantially different however, is the

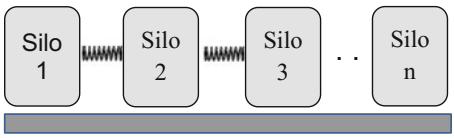

Fig. 1 Disruption dampening and transmission between silos

```
heuristically initialise N candidate solutions

while (termination condition not satisfied)
{
  probabilistically select silo for disruption initiation
  heuristically effect local beneficial change in selected silo
  initialize disruption-queue with adjacent silos
  while (disruption-queue is not empty)
  {
   remove and process silo at front of queue
    {
      run local propagation algorithm to repair silo

      if (repair successful){
        for each adjacent silo no longer aligned, add silo to disruption
        queue
      }
      else
      {
        run heavy-weight full optimisation on silo
      }
    }
  }
}
```

Fig. 2 Disruption dampening and transmission algorithm outline

possibility of complete local re-optimisation of certain silos, and also phased propagation of the disruption of a change throughout the supply chain.

Case Study #2—Planning System for Coal

Glencore (previously Xstrata) Coal is a major global energy materials producer. This example includes a multi-mine operation centred on raw coal management, coal handling and preparation through the plant, rail logistics to vessel loading using two berths at the Abbott Point Coal Terminal in Queensland, Australia.

In this model, attention was paid to the maximisation of the potential total revenue by not only relying on the supplied data on contracts for Month 1–3 years, but also considering the more detailed addition of place-holder vessels in order to make enable recommendations to the Sales department, highlighting where additional product is available to be sold. The importance of shipping data for capacity assessment is elaborated by Boland et al. (2011).

The fact that the Australian coal industry often fails to meet demand due to inadequate planning, infrastructure deficiencies and other reasons is outlined by Bayer et al. (2009) and represents a primary driver for organisations to look at exploiting latent value associated through improved planning and optimisation. Previous work in optimising an Australia coal supply chain with respect maintenance activities presented in Boland et al. (2011). As before with the iron ore case study, the coal case study is described from an abstract point of view, all the way to a vision of future algorithmic approach. For the coal planning problem, a few elements of the current production-implemented model and associated optimisation algorithm that are

particularly important include (i) a stock accumulation-based representation for vessel loading, (ii) quality up-building and down-building heuristics, and (iii) upstream heuristic plan completion based on the vessel-loading driver. These elements form the baseline optimisation improvements upon which enhanced future state optimisation is considered. The main realisations that are used when proposing the future-state algorithm is that heuristic construction of seed individuals is important for a modern heuristic algorithm, therefore a simplified heuristic approach as a foundation element to optimised plan generation is a feasible. There is a careful balance that is needed between those kinds of individuals and more randomly generated ones in order to find an appropriate balance between biased and free range exploration of the search space. A meta-level algorithm is part of the proposal to find this appropriate balance.

Solution Representation for a Planning Context

In contrast to the level of model complexity in scheduling (minutes, hours, shifts, days), planning systems (days, weeks, months) are orientated towards a higher-level summary view of what can be achieved, and safely planned for, in a long-term time horizon—for example 1 month to several years. Similar to heavily constrained activity scheduling relationships, the planning requirement must take into consideration numerous parameters and hard and soft constraints, in order to ensure that the results are valid. Whereas a schedule would consist of a number of discrete activities assigned to different resources, planning models are generally defined around summarised aggregated activities or capacities within a fairly large time bucket, in this case monthly. Plans are created starting at month 3 (from the current time), out to 3.5 years. The initial period of 3 months is not covered because this is considered to be within the scheduling period, not planning. For each month of the planning horizon, the following information must be generated:

Haulage Plan:

- Aggregated tonne-hours for movement between ROM and stockyards, inter-stockyard, and stockyard to CHPP. Individual journeys are not modelled.

Field Stockyards Plan:

- The total tonnes of each product type on field stockpiles for that month.

ROM Stockyard Plan:

- The total tonnes of each product type on a ROM stockpiles for that month.

CHPP Operation Plan:

- Tonnes of each coal type sent to each CHPP module, and bypass.
- Output tonnes for each coal type for each CHPP module, as well as new ash %, and reject tonnes.

CHPP Clean Coal Plan:

- Tonnes of each clean coal product added to each stockpile.
- Stockpile tonnes and % capacity.
- Quality attributes of each blended stockpile.

Rail Plan:

- Train-hours—Tonnes of each coal type transported by train from each mine

Port Stockyard Plan:

- Tonnes of each Brand
- Quality attributes for coal assigned to a Brand

Shipping Plan:

a. The number of satisfied 'TBC' (to be confirmed) shipments, including tonnage and product quality attributes. TBC shipments are derived using a typical vessel size and accounting for customer contracts (i.e. tonnage and quality requirements)
b. Number of non-contracted proposed shipments of coal brands, including tonnage and product quality attributes. This is coal that is not linked to a contract. This provides a view of how much additional coal product is produced by the mines and needs to be sold by Marketing.

Optimisation Algorithm

Part of the local optimisation heuristic for a vessel stock accumulation plan is the tuning of the selected components for blending to achieve a shippable product type, i.e., one which is within the target quality specification bandwidths. The representation of an individual in this algorithm consists of a set of ordered pairs, where each pair consists of a viable stockpile id, and a desired tonnage to be reclaimed from that stockpile (Fig. 3).

Low-Grade Up-Build Blending Sub-algorithm

The approach of the Low-Grade Up-Build blending algorithm is to initialise an individual in a deficient sub-space of the coal blending selection space. Such individuals would be of a low grade, and a search algorithm would need to be structured so that overarching directional vectors of the search tend towards sub-spaces that are richer in terms of coal quality. It is important to control the velocity of movement so that there is an increased likelihood of discovering suitable blends within the required quality tolerances at an early stage within the search process, without exploring too deeply within the high quality areas of the search space.

High-Grade Down-Build Blending Sub-algorithm

The High-Grade Down-Build blending algorithm uses a converse approach, which is to initialise an individual in an adequate or rich sub-space of the coal blending space. Such individuals would be of a high grade, and a search algorithm would need to be structured so that the direction of the search moves at low velocity towards lower quality regions. The objective being to have a high likelihood of settling in a region that maximises the use of lower grades, whilst still remaining within the required quality tolerances.

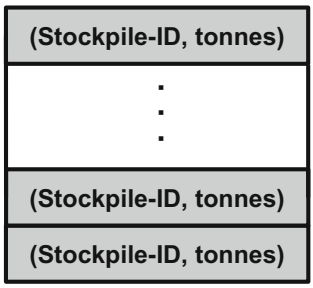

Fig. 3 Individual representation for stock accumulation

For both blending algorithms, evolutionary operators are used to gradually bring an individual to within tolerance, the main operator being a swap of a small tonnage of ore, exchanging low with high grade, or vice versa.

Upstream Scheduling Building Based on Ship Loading Profile

Once a candidate vessel berthing sequence has been determined, a heuristically-built individual representing a schedule for the entire supply chain can be constructed by working backwards, upstream in the supply chain, to create nominal activities to match the requirements of the vessel at berth within a given period of time. This gives rise to a so-called heuristically built individual that contains elements of a good-quality solution, but has not yet been optimised.

The Evolution to Metaheuristic Optimisation

Evolutionary algorithms often can be made to produce excellent results on problems in a particular domain, but one of the issues that arises is that there are often several algorithmic parameters involved, and these parameters need to be correctly tuned in order to achieve positive results. In certain situations, it is the case that a meta-algorithm, or metaheuristic, can be engineered to run at a higher level and perform the tuning of the lower-level evolutionary algorithm. Thus, any human manual intervention in the finding of high-quality solutions is minimised, and the work can be relegated mostly to the computational machinery and software.

Since we are considering primarily Population-Based Modern Heuristic (PBMH) optimisation algorithms as the key tools for optimising the supply chain, we will describe the concept of a metaheuristic optimiser in this context. For the Coal Planning problem under consideration, in order for the PBMH to operate effectively, it is critical that it be seeded with candidate solutions that have already been placed into reasonably feasible sub-spaces of the search space (Fig. 4). This is accomplished by using a percentage of the seeded individuals that are passed through a local optimisation routine to achieve some moderate level of fitness before entering into the PBMH algorithm. Furthermore, there is another percentage (typically quite small) of individuals that are heuristically built, but which have not been subjected to the local optimisation. There are also introduced into the seed population for the purpose of maintaining genetic diversity.

Details of how the Initial Seeding component of the algorithm would work are illustrated in Fig. 5. The V1 and V2 local searches referenced in that diagram refer to the Low-Grade Up-Build and High-Grade Down-Build heuristics defined earlier. The initial population of the main population-based modern heuristic (PBMH)

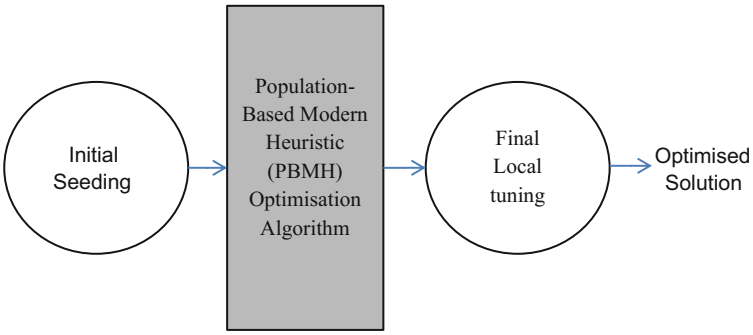

Fig. 4 Pre and post processing needed for a population-based modern heuristic optimisation algorithm

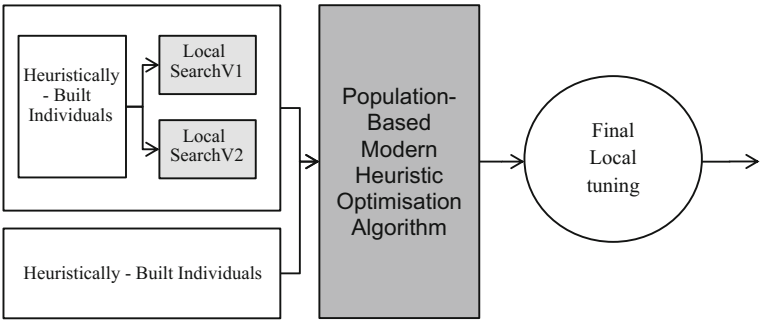

Fig. 5 Use of local search algorithm for coal blending, pre PBMH

optimisation algorithm is divided into 3 parts: (i) individuals that have gone through V1 local optimisation, (ii) individuals that have gone through V2 local optimisation and (iii) individuals that have not gone through any local optimisation. Each part can be thought of as being of a particular percentage.

For the PBMH operating at a meta-level, the goal is to find an optimised combination of these percentages (two would suffice), such that when used to seed the lower-level PBMH, the best possible planning solution results (Fig. 6). To get a better understanding of how this proposed algorithm would be implemented, Fig. 7 provides a pseudo-code outline.

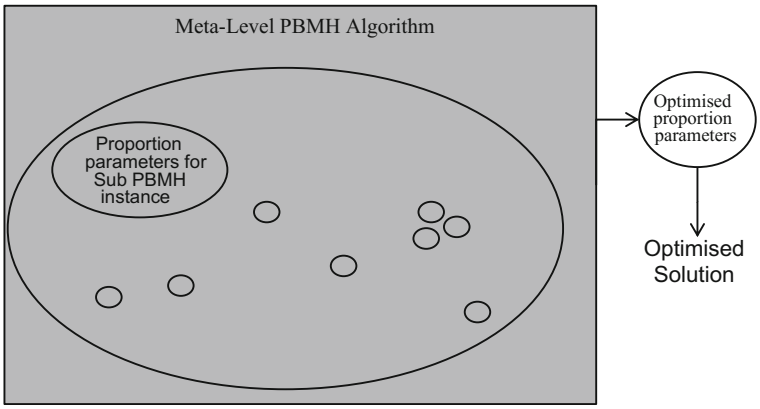

Fig. 6 Each individual of the meta-level algorithm is a set of parameters for a base-level PBMH

```
heuristically initialise  N candidate solutions consisting of
 1.  Percentage of locally optimised seed candidates using V1 algorithm.
 2.  Percentage of locally optimised seed candidates using V2 algorithm.

while (termination condition not satisfied)
{
  evaluate all candidate solutions by running lower-level PBMH
  optimisation

  prune population to standard size N

  probabilistically select individuals for percentage-shift mutation
  probabilistically select individuals for vector midpoint sampling

  run percentage-shift mutation
  run vector midpoint sampling
}
```

Fig. 7 Meta-level PBMH algorithm for parameter tuning

Conclusions

Any mining value chain scheduling problem involves the assignment of a high number of variable activities to a set of resources. From a computational complexity perspective, this problem is known to be NP-Complete, effectively indicating the Resource-to-Market scheduling problem is currently amongst the most challenging problems known. Furthermore, many of the constraints that exist within that domain are non-linear in nature. Due to these complexity characteristics it is expected that population-based modern heuristic methods are highly appropriate for finding high-quality solutions, as opposed to methods premised on linear constraints and linear models as they can inherently manage more complex business rules and non-linear constraints.

The planning problem appears to be less complex in nature than detailed scheduling since jobs are not being assigned to resources, but rather aggregated capacity is being consumed against those resources in less-granular time buckets. Nevertheless, this apparent reduction in complexity is usually offset by the practice of considering much longer time horizons—many months or years into the future.

The Resource-to-Market problem is currently managed in the real world production environment by predominantly talented human experts who, together with various rudimentary tools, for example spreadsheet models, and very limited-scope and narrowly-focused software applications such as discreet event simulators, are coping with the task of keeping businesses running by finding suitable, though arguably sub-optimal solutions to the problem. The mining business community has a strong appetite for advanced software solutions using novel and innovative mathematics, science and technology to improve in this area.

Considerable care must be taken when embarking upon the journey of making major changes to how scheduling and planning tasks are carried out by all mining organisations. The deployment of software that instantaneously and dramatically shifts the scheduling/planning paradigm in place, even if this does hold the potential for much higher-quality results, more often than not is a sure recipe for immediate reticence, incomprehension, doubt, overall inertia, and eventual rejection of the new system. Despite the potential of advanced scientific software solutions, it is important to recognise and respect that the process of adoption of such systems is in no small part a human activity. It is important to carry out such an endeavour as a staged process, using a roadmap of checkpoints that guides the organisation and its experts in an incremental fashion. At each step, clearly-understood solutions must be produced by the software in a manner that the human expert would feel comfortable signing-off on. Especially in the early stages of the roadmap, it is critical that the actions of the software be explainable and comprehendible.

Modern heuristic algorithms have been discussed and applied at length in the research community for more than 30 years. In the last ten years however, there has been a noticeable emergence of commercial-grade enterprise level software that incorporates these kinds of algorithms though arguably their uptake has been limited in production environments.

Currently implemented elements in existing clients for Schneider Electric are presented as components of a framework for meta-level optimisation. These baseline elements are designed to be expanded, scaled and enhanced as the understanding and acceptance of their output is trusted. The benefit that would be achieved from any optimisation technique needs to be carefully weighed against the increase in runtime that would ensue. The continual increase in power and capability of computer hardware, including the ability to leverage parallel computation diminishes the impact of this downside.

It is expected that these approaches will yield higher quality solutions than the perceived state-of-the-art production models in use today, whilst remaining amenable to implementation in enterprise software designed for mining supply chain experts who are not necessarily mathematical modelling and optimisation specialists.

References

Bayer A, Rademacher M, Rutherford A (2009) Development and perspectives of the Australian coal supply chain and implications for the export market. Zeitschrift fur EnergiewirtschaftI 33(3):255–267 (Springer)

Bodon P, Fricke C, Sandeman T, Stanford C (2011) Modelling the mining supply chain from mine to port: a combined optimization and simulation approach. J Min Sci 47(2):202–211 (SP MAIK Nauka/Interperiodica)

Bodon P, Fricke C, Sandeman T, Stanford C (2017) Combining optimisation and simulation to model a supply chain from pit to port

Boland N, Engineer F, Reisi M, Savelsbergh M, Waterer H (2011) Data generation in the Hunter Valley coal chain: a case study in capacity assessment. In: Proceedings of the 35th Application of Computers and Operations Research in the Minerals Industry Symposium. The Australasian Institute of Mining and Metallurgy, Wollongong, NSW, Australia, pp 795–806

Bolan N, McGowan B, Mendes A, Rigterink F (2013) Modelling the capacity of the Hunter Valley coal chain to support capacity alignment of maintenance activities. In: 20th International Congress on Modelling and Simulation. Adelaide, Australia, pp 3302–3308

Montiel L, Dimitrakopoulos R (2013) Stochastic mine production scheduling with multiple processes: application at Escondida Norte, Chile. J Min Sci 49(4):583–597 (Pleiades Publishing)

Peng H, Zhou M, Liu M, Zhang Y, Huang Y (2009) A dynamic optimization model of an integrated coal supply chain system and its application. Min Sci Technol (China) 19(6): 842–846 (Elsevier)

Singh G, Sier D, Ernst A, Gavriliouk O, Oyston R, Giles T, Welgama P (2012) A mixed integer programming model for long term capacity expansion planning: a case study from the Hunter Valley coal chain. Eur J Oper Res 220(1):210–224 (Elsevier)

Part IV
Stochastic Simulation for Strategic Mine Planning

Application of Conditional Simulations to Capital Decisions for Ni-Sulfide and Ni-Laterite Deposits

O. Tavchandjian, A. Proulx and M. Anderson

Abstract Prior to the acquisition of data from production drilling and grade control sampling, the spatial density of data is usually insufficient to properly address issues related to short-scale variability. Grade interpolation, whether conducted through ordinary kriging or other linear or non-linear regression techniques, usually suffers from significant over-smoothing or conditional bias. Four examples presented in this paper show that conditional simulations provide a viable and powerful alternative in assessing the sensitivity of key variables that are critical to the decisions made prior to moving forward with significant capital expenditures. These variables include the selection of the most appropriate mining method and mining equipment, the optimum cut-off strategy and the short-term variability constraints on process plant feed. The results also demonstrate that conditional simulations can be used to assess the risk associated with many of the technical aspects of the project and its financial performance.

Introduction

Traditional approaches to mineral deposit appraisal use non-geostatistical and/or geostatistical estimation methods to provide optimal local block grade estimates. When the drilling density is too sparse for the level of detail required for mine

O. Tavchandjian (✉)
CVRD Inco, 2060 Flavelle Boulevard, Sheridan Park, L5K 1Z9
Mississauga, ON, Canada
e-mail: tavchandjiano@inco.com

A. Proulx
CVRD Inco, 5000, R8N 1P3 Thompson, MB, Canada
e-mail: aproulx@inco.com

M. Anderson
Voisey's Bay Nickel Company, Suite 700, Baine Johnston Centre,
10 Fort William Place, A1C 1K4 St John's, NL, Canada
e-mail: manderson@inco.com

R. Dimitrakopoulos (ed.), *Advances in Applied Strategic Mine Planning*,
https://doi.org/10.1007/978-3-319-69320-0_21

planning, these methods fail to properly represent the spatial variability of the estimated grade. Mining decisions made using the resulting smooth estimates may lead to false assumptions about the mineral deposit. Alternative interpolation strategies aimed at reducing the smoothing effect, such as using fewer samples in the search ellipsoid or interpreting geology in a deterministic model, usually result in a grade distribution with significant conditional bias (Krige 1996).

As with many other metal deposits, the success or failure of a Ni-sulfide or a Ni-laterite mining project is highly dependent on a few key variables, all ultimately related to metal price and metal grade. A proper characterisation of the spatial variability in the grade distribution can lead to more realistic mining and/or processing assumptions and reduced project risk. Project evaluations, which can demonstrate to the company management and investors that the risk is recognised and quantified, and that the implementation plan includes a strategy to manage that risk, have a better chance of advancing to the construction and production stages.

Conditional simulation ('CS') methods aim at reproducing the in situ grade variability as opposed to obtaining optimal local estimates. The end results are models of equal probable realisations, which reproduce the input sample data histogram and variogram and are conditioned to local sample point values. A proper characterisation of the spatial variability of the grade provides mining engineers and metallurgists with realistic models for mine planning and the information required to address processing issues related to short-term variability in the feed grade to the processing plant (e.g. Abzalov and Mazzoni 2007; Audet and Ross 2007).

This paper presents four examples of practical applications of CS in both Ni-sulfide and Ni-laterite deposits conducted by Inco over the past seven years. These examples cover a wide range of projects from the optimisation of open pit and underground mining plans to the risk assessment on the variability of the daily feed grade to both mineral beneficiation and chemical processing facilities. The successful deepening of the Birchtree mine in Northern Manitoba, was dependent on the selection of optimum mining cut-off and production rate together and on a flexible mining schedule. A reliable model was also required to properly assess the risk-weighted benefits of raising the cut-off in an orebody with significant short-scale variability. Similar challenges were faced in the deepening of the Thompson 1D orebody in the same mining camp. In this case, CS were also used early in the evaluation process to compare the economic performance of bulk and selective mining methods. During the feasibility study of an open pit operation at Voisey's Bay in Northern Labrador, the short-scale variability of the feed to the concentrator was identified as an area of risk for the project. In particular, significant variations in the Cu to Ni ratio on a daily, weekly or monthly basis could result in processing recovery losses. The optimisation of the number of concurrent mining faces, the size of stockpiles and the mining sequence was investigated based on CS results in order to minimise the impact of feed variability on milling recovery.

At the Goro Project in New Caledonia, the Ni ore mined from the laterite profile will be processed by a high-pressure acid leaching technology (HPAL).

The performance of the HPAL technology is dependent on the chemistry of the feed including Ni and Co content as the two minerals of economic interest but also other major elements such as Mg, Fe and Al oxides because of their impact on acid consumption and Ni-Co recovery. Since the chemistry is highly variable between the various layers of the alteration profile and even within some layers between various size fractions, a proper characterisation of the short-scale variability in both layer geometry and layer composition was recognised as a key factor for a successful feasibility study of this project.

Conditional Simulation Methodology

Geostatistical CS were developed over 30 years ago in order to perform sensitivity and risk analysis. In a conditional simulation, reproducing certain statistical characteristics of the global population takes precedence over local accuracy. In addition to respecting the histogram, a geostatistical simulation model reproduces the variogram (i.e. reproduction of spatial correlation) and honours the actual existing data (i.e. conditioning).

In addition to the original turning bands method (Journel and Huijbregts 1983), there are now several established methods of carrying out geostatistical simulations including the Sequential methods (Gaussian and Indicator), the LU decomposition algorithm, (Goovaerts 1997; Armstrong and Dowd 1993; Chiles and Delfiner 1999), and more recently, generalised sequential simulation (Dimitrakopoulos and Luo 2004; Benndorf and Dimitrakopoulos 2007, this volume). It is not the intent of this report to detail the pros and cons of each technique. Comparisons can be found in a number of publications. Gotway and Rutherford (1993) make a comparison of six different simulation methods performed on a variety of datasets. This study revealed the sensitivity of results to particular simulation algorithms and demonstrated some advantages of the conditional Gaussian based algorithms (i.e. turning bands and Sequential Gaussian) over the other methods. The turning bands approach was selected for this study. Some authors (Deutsch and Journel 1992; Ravenscroft 1993) have qualified the method as being computer intensive with built-in limitations, i.e. number and orientation of bands, number of discretisation points along the bands, rotation of anisotropy axis. Gotway and Rutherford (1993) indicate that most of these problems are related to the improper algorithms used and not to the turning band method itself. The algorithm used in this study is slightly modified from Lantuejoul (1993). The program used for the four projects presented in this paper is not affected by any of the above listed limitations.

The turning band algorithm involves a series of steps including the recognition of different geological domains, the selection of the variables to be simulated, the gaussian transformation of these variables, the non-conditional simulation of these gaussian variables and their linear combination, the conditioning to the actual data by Simple Kriging and their post-processing to reconstitute the original variables. In addition, the simulations presented in this paper benefit from the application of an

unfolding algorithm (Datamine 1997) in order to better simulate the geological controls on grade distribution. At each step, a series of checks is performed and to successfully validate the model.

Calibration and Validation of Conditional Simulations

In order to validate the conditional simulations, a calibration exercise is undertaken wherever production data are available either in a mined out portion of the same deposit, or in an analogue deposit. The areas selected for these back analyses are usually well drilled and benefit from extensive mapping of underground openings. The record of the mill-credited production may also be used if available. The methodology applied is as follows:

- create an exploration-based data set by removing all infill production drilling;
- perform polygonal, kriging and CS modelling from the exploration data set and assess recoverable resource at various cut-off grades;
- perform polygonal, kriging and CS modelling from the production data set and assess recoverable resource at various cut-off grades;
- compare historical credited production, polygonal, kriging and CS results based on both the exploration dataset and the production dataset; and
- compare actual detailed mapping in the mine openings to spatial patterns produced by all models.

The DATAMINE^{TM} Floating Stope Optimiser (FSO) is used at Inco operations to quickly assess the recoverable resource from all orebody and simulated models at various cut-off grades. The FSO is analogous to the floating cone algorithm used in open pit situations. The FSO does not provide a final mining plan but rather a 'close to finished' product, which requires refinement but provides an effective tool for comparing alternative mining scenarios in a conceptual planning exercise. In order to validate the parameters used in the FSO, a manual exercise of mine planning is performed on one of the simulations. Comparing the FSO runs to manual planning verifies the FSO parameters. All subsequent FSO runs on the simulation models and estimation models use these same parameters.

Examples of successful results indicating the benefit of conditional simulation over traditional interpolation techniques and polygonal method are shown on Figs. 1 and 2 for two Ni sulfide deposits. When an exploration dataset is used, the spatial patterns created by CS are more realistic and better represent the anticipated internal dilution. The results show that when little information is available for estimation, the spatial continuity of both the high-grade and low-grade mineralisation is overstated in the polygonal and MIK models. This results in an overestimation in recoverable grade and in an underestimation in recoverable tonnage.

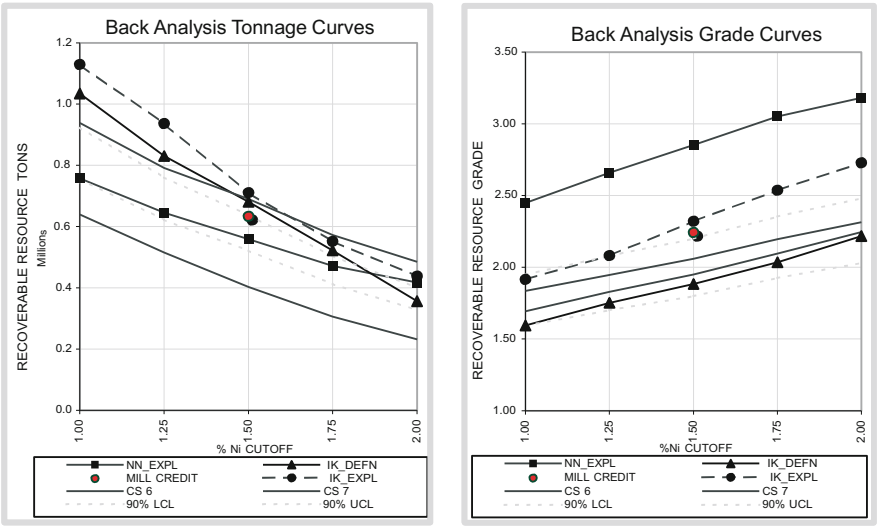

Fig. 1 Comparison of tonnage and grade curves obtained with the various methods with mill credit in the calibration zone. CS 6 and 7 represent the range of 90% of simulated outcomes, while the 90% control limits represent a ±10% difference from the median simulation

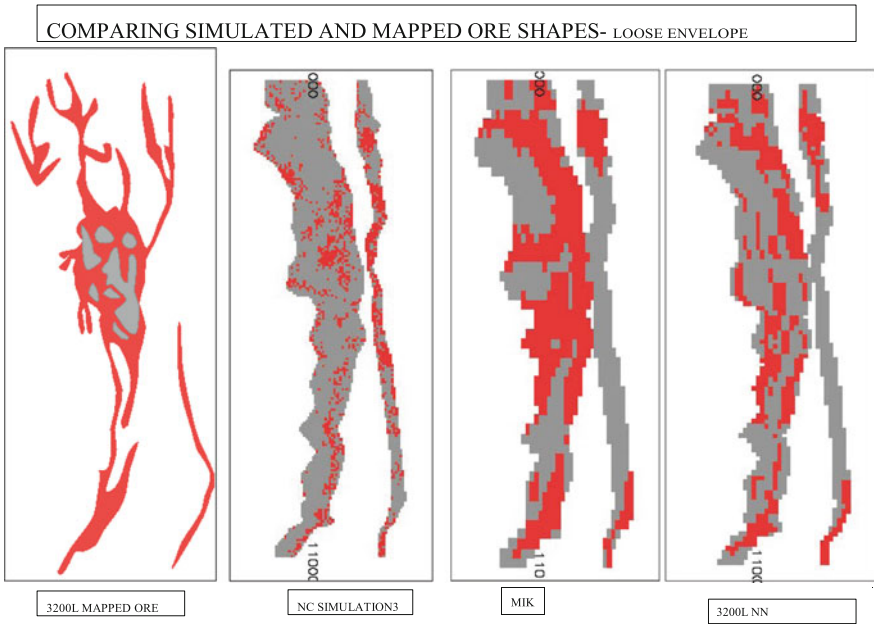

Fig. 2 Compared assessment of actual ore mapping, polygonal (NN), MIK and CS in the calibration zone

Application of CS to the Selection of the Optimum Mining Method for Underground Ni-Sulfide Deposits

The first application of CS to Ni sulfide deposits is related to prefeasibility studies conducted at two Inco mines in Northern Manitoba, Canada. In both cases, the studies aim at assessing the economic viability of mining deeper in existing deposits and assessing different mine plans and production schedules in the deposit extension based on advanced exploration drilling only. The Birchtree Mine 83 orebody and the Thompson Mine 1D orebody are located in the Thompson Nickel Belt. Orebodies in this belt consist of nickel sulfides with varying amounts of ultra mafic inclusions hosted in Proterozoic-aged metasedimentary units.

Only per cent Ni is simulated in these two cases since it is the only metal of economic significance. Domains of mineralisation are identified using conceptual geological ore genesis models with lithology and structure as the most important features controlling the final emplacement of the mineralisation.

Comparison of Mining Methods in the 1D Lower Orebody

Figure 3 summarises the results of a comparative study performed on the lower portion of the 1D deposit between a bulk and a selective mining method. For reference, the results obtained with the polygonal and Multiple Indicator Kriging (MIK) models are also plotted on these graphs.

The series of grade and tonnage curves shown on Fig. 3 are obtained by performing a FSO analysis of each simulation and interpolation model with a consistent set of parameters including the minimum stope dimensions, the stope increments, the minimum pillar waste dimensions, the target headgrade and the maximum internal waste allowances. These parameters have been calibrated on a selection of sections and plans against manual interpretation done by experienced mine engineers.

The MIK model provides globally a similar estimate to the CS for the bulk-mining scenario but a significant different estimate for the selective mining scenario. As expected, applying the FSO to a polygonal model also yields significantly different results. The differences obtained from the various methods are related to their different handling of short-scale variability and therefore of internal dilution between mineralised zones. While polygonal techniques clearly overstate the continuity of the high grade mineralisation as expected, the MIK model also underestimate internal dilution when the drill spacing is too large for the level of details required for mine planning as it is the case in the assessment of selective mining. These results imply that making a development decision based on a MIK model only would present a significant risk of incorrectly selecting the most beneficial mining method for the project.

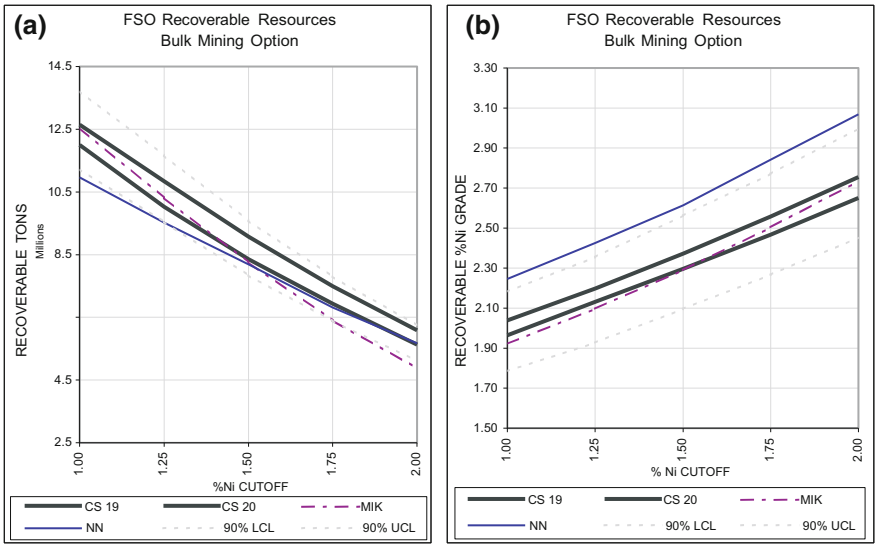

Fig. 3 **a** Comparison of bulk-mining grade-tonnage curves obtained with the various assessment methods. CS 19 and 20 represent the range of 90% of simulated outcomes, while the 90% control limits represent a ±10% difference from the median simulation. **b** Comparison of cut and fill mining grade-tonnage curves obtained with the various assessment methods. CS 19 and 20 represent the range of 90% of simulated outcomes, while the 90% control limits represent a ±10% difference from the median simulation

Based on the CS results, mechanised cut and fill mining was selected as the best suited mining method for the deepening for the 1D orebody. A set of sections and plans from selected simulations were further investigated by a team of experienced geologist and mine engineers with production experience in this orebody to perform some sensitivity studies and to optimise the proposed mine plan including ore and rock handling systems, ventilation, etc. The economic and technical parameters were then used as inputs in discounted cash flow analysis. Based on the CS results, a range of ROR and NPV were calculated in order to quantify the risk associated with the base case assumptions together with potential downsides and upsides.

Comparison of Production Profiles in the Birchtree 83 Orebody

For the deepening of the Birchtree 83 deposit, the comparison of mining methods provided similar results to the 1D Lower deposit but the high-grading potential was not deemed sufficient and the risk too high to justify a selective mining approach. In this prefeasibility study, the benefit of CS was realised by revisiting the production profile. Due to the large drill hole spacing at depth, the MIK and polygonal models

suffer from significant conditional bias. As a result, large areas of high-grade mineralisation are artificially created. A production plan based on these models aim at mining these deep high-grade zones first. The CS produce a radically different model of the deposit showing a much more consistent grade distribution from top to bottom (Fig. 4). Based on the CS results, the production profile was modified to both increase the production rate and to mine the orebody both bottom-up and top-down. This orebody has now been in production for two years and operating results have confirmed the validity of the CS results and the bias in the MIK and polygonal estimates.

As in the case of the 1D deposit, mine planners were able to complete a pre-feasibility study including estimates on capital costs, mining rate, mining sequence and production profile based on the CS results. These estimates do not suffer from an under-estimation of the spatial variability in the metal grade distribution and therefore provide more realistic estimates than previous estimates based on polygonal and MIK models.

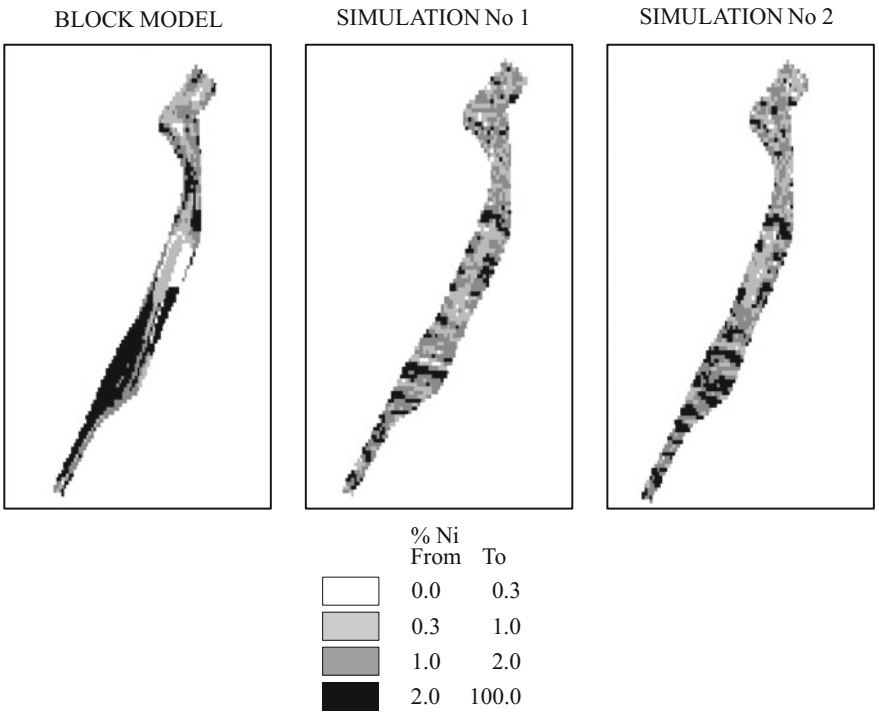

Fig. 4 Comparison of MIK and CS models in the deepening of the Birchtree 83 orebody

Application of CS to the Modelling of Short-Term Variability in a Sulfide Concentrator Feed

The second application of CS in Ni sulfide deposits is an investigation into the optimisation of the mining sequence and the validation of the concentrator design at the Inco Voisey's Bay project in Northern Labrador. The objective is to validate the mining sequence in order to ensure the short-term variability in the composition of the concentrator feed remains within an acceptable range.

Mineral Domains and Simulation Process

The Voisey's Bay concentrator will be supplied for the first 16 years of operation by open pit production from the Ovoid deposit. This deposit is hosted by a troctolite intrusive complex, which is divided into three different domains with variable ratios of massive and disseminated sulfides. In each domain, the massive and disseminated zones were simulated separately. The turning band approach is constrained by a model of linear coregionalisation (Wackernagel 1998) to maintain the spatial correlations observed in the input data between per cent Ni, per cent Cu, per cent Co, per cent S and per cent Fe.

Short-Term Variability in the Concentrator Feed

In order to maximise Ni recovery in the concentrator, it is typically desirable to homogenise the chemistry of the feed on a short-range basis. In particular, the Cu to Ni ratio variability will influence the recovery of the two metals in their respective concentrate. Twenty CS realisations were generated over the three domains of the Ovoid deposit and were used to simulate the daily, weekly and monthly variability in the chemistry of the concentrator feed based on the initial mine plan and production profile (Fig. 5).

The preliminary results obtained were used to validate and to modify the initial mine plan, including the mining sequence and the number of operating faces in the disseminated and massive sulfides. These simulations also demonstrated the validity of the design of the concentrator and its ability to cope with the anticipated daily variability in mine production. The use of CS also provided a range in the production rate, metal grade and processing recoveries required to conduct Monte-Carlo simulations on the discounted cash flow analysis of the project.

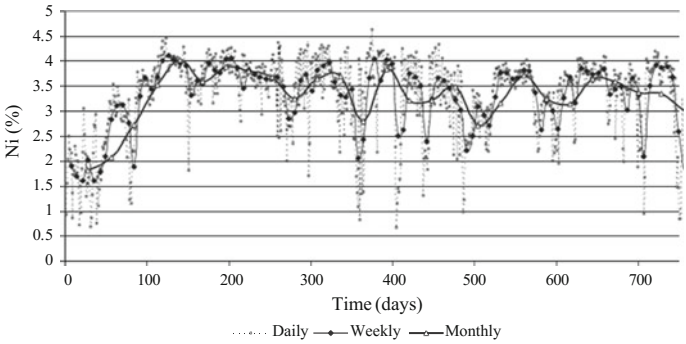

Fig. 5 Short-scale variability in concentrator feed composition at VBN

Application of CS to the Optimisation of the Life of Mine Plan for a Ni-Laterite Project

Conditional simulations were extensively used for the Goro Ni-Laterite Project located on the French island of New Caledonia in order to optimise and validate several aspects of the life of mine plan. These aspects included the estimation of bottom ore recovery, grade control as well as the short-term variability in the process plant feed chemistry.

Geological Setting and Simulation Process

The Goro laterite deposit hosts three geological layers of significant economic interest. During the mine planning process, it was recognised that the transition and saprolite layers, when screened at an appropriate size fraction, were entirely representing ore-grading mineralisation. Due to the reduced thickness of these layers, they would likely be mined with one bench. As a result, only 2D simulations were conducted for these two layers. Due to its greater thickness and the presence of a variable portion of the top of the layer grading below the selected cut-off, 3D simulations were required in the yellow laterite layer.

The simulation methodology used for the Goro deposit can be summarised as follows:

1. 2D simulation of the five layers in the profile;
2. 2D simulation of the average chemistry for the yellow laterite, transition and saprolite layers, i.e. per cent Ni, per cent Co, per cent Fe, per cent SiO_2, per cent MgO, per cent Al_2O_3, per cent Cr_2O_3 and per cent MnO;

3. linear regression of the vertical drift in chemistry based on 2D simulation and unfolded position of node within the simulated yellow laterite layer; and
4. 3D conditional simulation of residuals to the linear regression done in the previous step and creation of a full 3D simulation of chemistry for the yellow laterite layer.

The use of the unfolding process was critical to produce a realistic laterite profile and vertical grade distribution, however, added complexity to the simulation process, since each 2D simulation of the layer profile originated from a new reference system.

Models of linear coregionalisation were used both for the 2D simulations, to maintain the spatial correlation between the physical and chemical properties of the various layers, and for the 3D simulations in the yellow laterite layer to maintain the vertical correlation between the different chemical elements.

Application to Mine Planning

An initial application to mine planning was to use the 2D simulations to target the areas with the highest probability of combining high-grade nickel, with high mining recovery and large thickness of saprolite. The most favourable area would be preferentially selected as the start up zone for the open pit. The combination of results obtained from layer thickness, saprolite recovery and grade simulations clearly indicated that the southwest extremity of the deposit presents the best economic mineralisation for the first years of production.

The 40 simulations completed for the Goro deposit were rank by increasing variance of bedrock topography, i.e. bottom of the saprolite layer. Figure 6 shows a cross-section of the interpreted profile for various drill spacing (i.e. 2 m, 12 m, 24 m and 100 m, respectively) for simulation number 29, selected as the median case for the variance criteria.

A dramatic decrease in the variability of the layer geometry is observed as the drilling density decreases. This variability would impact the recovery and the dilution of the three mineralised layers and also the risk of misclassification of limonitic and saprolitic mineralisation for the purpose of stockpiling. Since the resource model is based on 100 m spaced drill holes, it will suffer from a high level of over-smoothing for layer geometry.

These preliminary findings indicate the value conditional simulations provide in the conceptual mine planning of the deposit (‘desktop mining’) to assess the impact and the applicability of cut-off grades, bench heights, size of equipment and limonite/saprolite sorting for stockpiling and measure the mining dilution and ore loss factors. Two east-west cross-sections and two north-south cross-sections sliced through these simulations were provided to mine engineers to be used as a basis for planning. These four sections were reproduced using the second worst, the median and the second best simulations ranked according to the variance criteria.

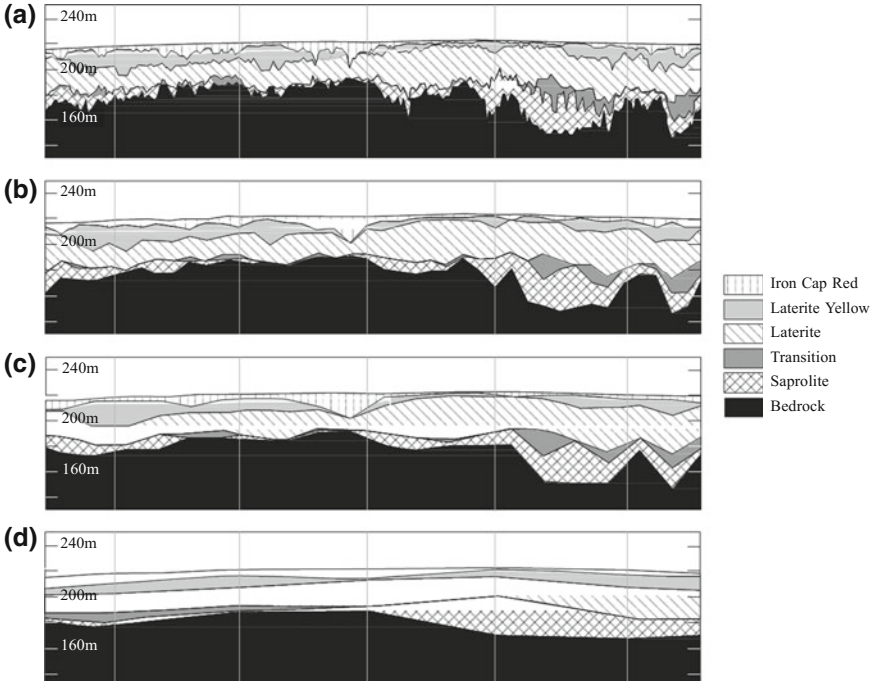

Fig. 6 **a** Examples of S-N cross-section for 2 m drill hole spacing; **b** examples of S-N cross-section for 12 m drill hole spacing, **c** examples of S-N cross-section for 24 m drill hole spacing; **d** examples of S-N cross-section for 100 m drill hole spacing

Application to Grade Control

In the yellow laterite layer, a variable Ni cut-off had initially been proposed in order to maintain a consistent limonite/saprolite ratio for the process plant feed on an annual basis. The proposed cut-off ranged between 1.15 Ni and 1.45% Ni. The method suggested in the initial mine plan to define the top of the ore was applied to the simulations assuming a 25 m grade control grid. From simulated drill holes the top of the ore was defined by the first intersection down the hole of two consecutive metres grading above the proposed cut-off. The volume and average grade recovered between the top of the ore and the bottom of the layer were compared in each case with the average of all the simulated nodes, i.e. assumed reality.

Figure 7 shows the results obtained for Ni cut-off ranging from 1.15 to 1.50%. This figure clearly shows that applying a cut-off grade higher than 1.3% Ni would result in an unrealistic estimation of the production headgrade, and produce in a significant reduction of the recoverable volume. Although this approach can be used to increase the combined production headgrade of limonite and saprolite by lowering the limonite/saprolite ratio, it also results in the significant loss of ore grading material. This ore-grading limonite would be treated as overburden and

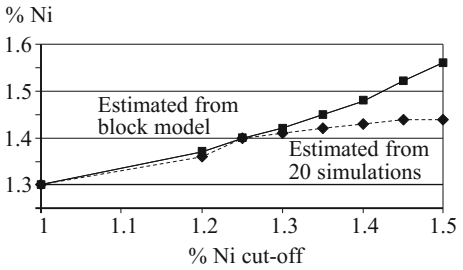

Fig. 7 Comparison of estimated Ni headgrade for various per cent Ni cut-off from block model and simulations

used as backfill. Alternatives should consider stockpiling to use this mineralisation as incremental ore. Based on these results, a new grade control strategy was adopted to use a cut-off grade no higher than 1.3% Ni in defining the top of the ore in the yellow laterite layer.

Application to Predicting and Managing the Autoclave Feed Variability

Another important application of the 2D simulations at Goro was to estimate the process plant feed variability. In order to meet the planned production, availability of the saprolite mineralisation with the proper chemistry profile is key. Conditional simulations provide a tool to assess the variability in the plant feed at any given scale (e.g. weekly, monthly, annually). With the proposed mining pushback and 20 simulation realisations, the variability of recoverable metal sent to the preparation plant for each year is assessed.

As expected, the average of the 20 simulations indicate similar results to those obtained from the kriged model for the entire simulated domain. On shorter production periods however, the results presented on Fig. 8 indicated that without stockpiling, a potential shortfall in saprolite would exceed ten per cent for 25% of the simulations. The choice of the period to evaluate feed availability is critical as this potential shortfall becomes even more important for a two-month period. The only way to mitigate this potential problem is through stockpiling, blending and through careful scheduling of saprolite production at the mining face. It is critical for mining projects to identify these potential issues at the planning stage rather than having to fix them in an ongoing operation.

The 2D and 3D CS of the entire profile were also used to generate combined simulation of the mine production on a daily basis using three different scenarios based on four concurrent mining faces on a test area representing approximately one year of production. The test area was selected as being representative of the first eight years of production according to the most current mine plan. The daily feed was used to simulate stockpiles and daily autoclave feed. Results were used to validate the production plan with respect to acid requirements and Ni production targets.

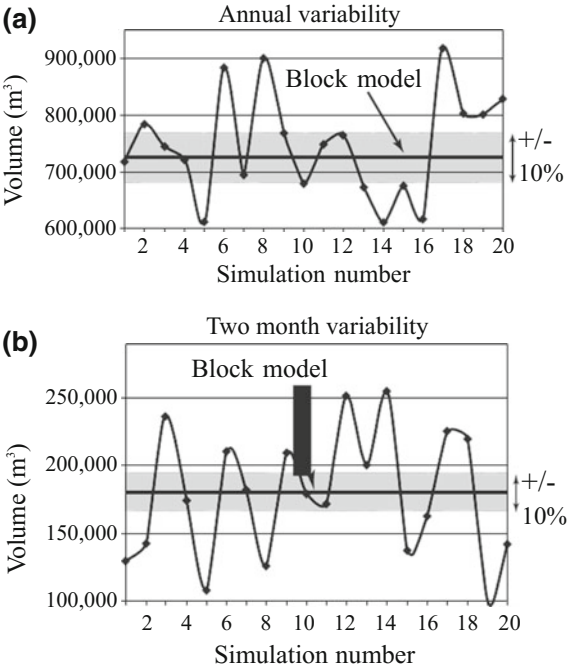

Fig. 8 Availability of saprolite volume from 20 independent simulations for **a** a one year period and **b** a two-month period

Conclusions

In the four applications presented in this paper, emphasis is put on demonstrating how the use of conditional simulations has led to the ability to make better business and technical decisions than those from models based on traditional interpolation methods. A proper life-of-mine plan relies on having a good understanding of the grade variability, CS allow the spatial grade variability to be properly characterised.

CS allows practitioners to quantify risk and to perform meaningful sensitivity analyses on project financials. CS used as an additional tool in mineral project assessments enable senior management to better assess the risk associated with mining projects.

In order to gain confidence in the simulation results, seven years of applications of CS at Inco Limited operations have highlighted two fundamental keys to success:

1. to recognise that conditional simulations are only models and to constantly challenge the stationarity and other model assumptions; and
2. whenever possible, to conduct calibration studies based on back analysis of orebodies with production history.

Acknowledgements The authors would like to acknowledge the contribution and support of key Inco personnel to the successful application of conditional simulations to these projects: Alan Aubut, Scott Bishop, Jean-Yves Cloutier, John Kelly, Andre Lauzon and Brian Plamondon. We would also like to thank Lawrence Cochrane for his help in the final edition of this paper.

References

Abzalov M, Mazzoni P (2007) The use of conditional simulation to assess process risk associated with grade variability at the corridor sands detrital ilmenite deposit, Mozambique. In: Dimitrakopoulos R (ed) Orebody modelling and strategic mine planning, 2nd edn. The Australasian Institute of Mining and Metallurgy, Melbourne, pp 95–102

Armstrong M, Dowd PA (eds) (1993) Geostatistical simulations. Kluwer Academic Publishers, p 255

Audet M, Ross AF (2007) Koniambo lateritic Ni-Co deposits, New Caledonia—A case study from geological modelling to mineral resource classification. In: Dimitrakopoulos R (ed) Orebody modelling and strategic mine planning, 2nd edn. The Australasian Institute of Mining and Metallurgy, Melbourne, pp 235–244

Benndorf J Dimitrakopoulos R (2007) New efficient methods for conditional simulations of large orebodies. In: Dimitrakopoulos R (ed) Orebody modelling and strategic mine planning, 2nd edn. The Australasian Institute of Mining and Metallurgy, Melbourne, pp 61–67

Chiles JP Delfiner P (1999) Geostatistics: modelling spatial uncertainty, Wiley, 695 p

DATAMINE ™ Ltd (1997) User manual for unfolding module. In: Deutsch CV, Journel AG (eds) GSLIB: Geostatistical Software Library and User's Guide. Oxford University Press, New York, 134 p (1992)

Deutsch CV, Journel AG (1992) GSLIB: Geostatistical Software Library and User's Guide. Oxford University Press, New York

Dimitrakopoulos R, Luo X (2004) Generalised sequential Gaussian simulation on group size n and screen—effect approximations for large field simulations. Math Geol 36(5):567–591

Goovaerts P (1997) Geostatistics for natural resources evaluation. Oxford University Press, New York, p 483

Gotway CA, Rutherford BM (1993) Stochastic simulation for imaging spatial uncertainty: comparison and evaluation of available algorithms. In: Armstrong and Dowd (eds) Proceedings geostatistical simulation workshop. Kluwer Academic Publishers, pp 1–22

Journel AG, Hjuibregts CJ (1983) Mining geostatistics. Academic Press, San Diego, CA, p 600

Krige DG (1996) A practical analysis of the effects of spatial structure and of data available and accessed, on conditional biases in ordinary kriging. In: Baafi E, Schofield N (eds) Proceedings geostatistics Wollongong '96. Kluwer Academic Publishers, pp 799–810

Lantuejoul C (1993) Non conditional simulation of stationary isotropic multigaussian random functions. In: Armstrong and Dowd (eds) Proceedings geostatistical simulations. Kluwer Academic Publishers, pp 147–177

Ravenscroft PJ (1993) Conditional simulation for mining: practical implementation in industrial environment. In: Armstrong, Dowd (eds) Proceedings geostatistical simulation workshop. Kluwer Academic Publishers, pp 79–88

Wackernagel H (1998) Multivariate geostatistics, second edition edn. Springer, Berlin Heidelberg, p 291

Simulation of Orebody Geology with Multiple-Point Geostatistics—Application at Yandi Channel Iron Ore Deposit, WA, and Implications for Resource Uncertainty

V. Osterholt and R. Dimitrakopoulos

Abstract Development of mineral resources is based on a spatial model of the orebody that is only partly known from exploration drilling and associated geological interpretations. As a result, orebody models generated from the available information are uncertain and may require the use of stochastic or geostatistical simulation techniques. Multiple-point methods have been developed for petroleum reservoir modelling enabling reproduction of complex geological geometries for ore bodies. This paper considers a multiple-point approach to capture the uncertainty of the lithological model at the Yandi channel iron ore deposit, Western Australia. Performance characteristics of the method for the application are discussed. It is shown that the lithological model uncertainty translates into considerable grade-tonnage uncertainty and variability that is now quantitatively expressed.

Introduction

Geological controls of physical-chemical properties of ore deposits are important, thus, understanding and modelling the spatial distribution of deposit geology is critical to grade estimation, as well as the modelling of any pertinent attributes of orebodies (e.g., Sinclair and Blackwell 2002; King et al. 1986). In iron ore deposits, for example, geological domains typically include lithology, weathering, ore and contaminant envelopes. Domains for other physical properties such as density, hardness and lump-fines yield may be required. The traditional approach to model geological domains is the drawing of outlines of the geological units by the geologist, resulting in an over-smoothed subjective interpretation. Automatic interpre-

V. Osterholt (✉)
BHP Billiton Iron Ore, Melbourne, Victoria, Australia

R. Dimitrakopoulos
Deptartment of Mining, Metals and Materials Engineering,
McGill University, Quebec, Canada

R. Dimitrakopoulos (ed.), *Advances in Applied Strategic Mine Planning*,
https://doi.org/10.1007/978-3-319-69320-0_22

tations are rare and include solids models that are, however, also inherently smooth. Furthermore, such single "best-guess" interpretations do not account for uncertainty about the location of boundaries and corresponding volumes, leading to inconsistencies between mine planning and production.

Stochastic simulation techniques address the above type of challenges in modelling the geology of, or the uncertainty about, a deposit. Unlike in the petroleum industry, stochastic simulation of geological units of mineral deposits has been limited in the mining industry due to the above-mentioned traditional practices, despite early efforts (David 1988). The principle behind stochastic simulation is interpreting the occurrence of a geological unit at a location as the outcome of a discrete random variable. This probabilistic approach honours the fact that the geology at any location cannot be known precisely from drilling data. All available information including data, data statistics/geostatistics, and geological interpretations are included in such an approach to yield the most realistic models. Stochastic simulation methods have been developed and tested on geological models of mineral deposits. Methods mainly consist of sequential indicator simulation or SIS (Goovaerts 1997) type approaches and the truncated pluri-Gaussian simulation approach or PGS (Le Loc'h and Galli 1997; Langlais and Doyle 1993). Various implementations and applications include the modelling of mineralized envelopes with a predecessor to SIS approach (David 1988), simulating geologic units with nested indicators (Dimitrakopoulos and Dagbert 1993), generation of ore textures with "growth" (Richmond and Dimitrakopoulos 2000), simulation of oxidisation fronts with PGS (Betzhold and Roth 2000), ore lenses in an underground mine (Srivastava 2005), uranium roll-fronts (Fontaine and Beucher 2006) and kimberlite pipes (Deraisme and Field 2006). Alternative approaches include methods based on Markov transition probabilities (Carle and Fogg 1996; Li 2007) and object based methods (e.g., Seifert and Jensen 2000).

The main drawback of the above methods is their inability to capture non-linear geological complexities, and it becomes obvious when curvilinear features such as faults, multiple superimposed geological phases, fluvial channels, or irregular magmatic bodies are simulated. The reason for this limit is that conventional methods represent geological complexity in terms of second order (two-point) statistics. Variograms describe the variability of point-pairs separated by a given distance and, although they capture substantial geological information (David 1988), there is a limit to the information they can convey (Journel 2018, in this volume). Figure 1 illustrates the limits of variograms in fully characterizing geological patterns. Figure 1 shows three geological patterns with different spatial characteristics where the variograms of the three patterns cannot differentiate between the three geological patterns.

In advancing from the above limits, substantial efforts have been made to develop new techniques that account for the so-called high-order spatial statistics. These include the most well established multiple-point (multi-point or MP) approach (Strebelle 2002; Zhang et al 2006), as well as Markov random field based, high-order statistical approaches (Daly 2004; Tjelmeland and Eidsvik 2004) or computer graphic methods that reproduce multiple-point patterns (Arpat and Caers 2007). These

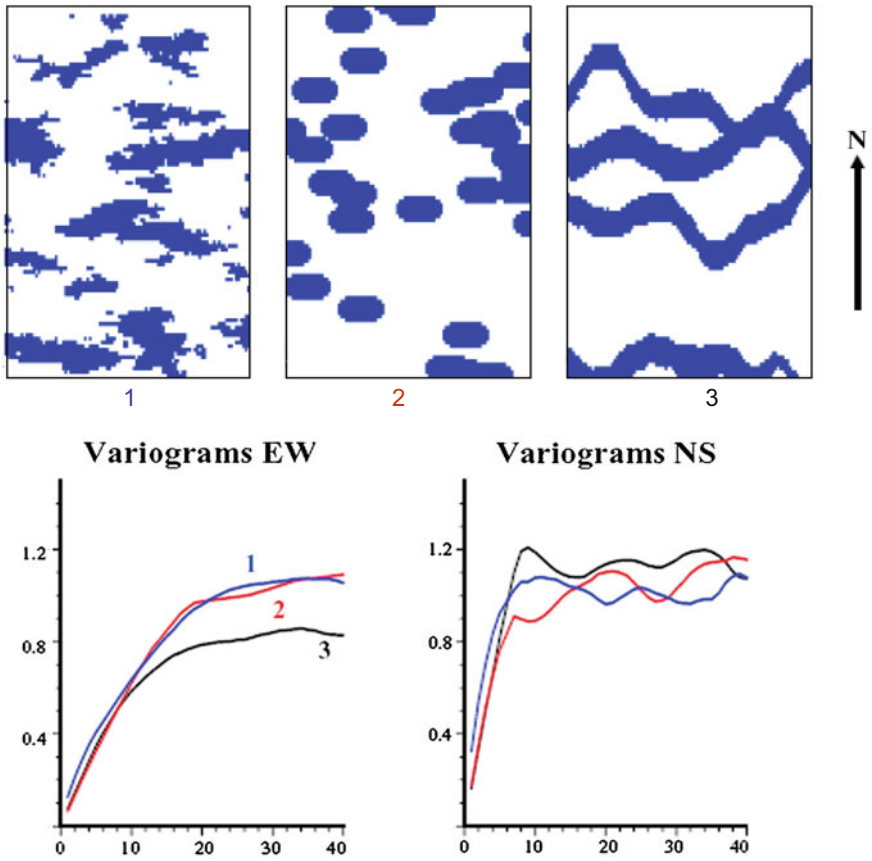

Fig. 1 Vastly different patterns show same variogram (modified from Journel 2017, in this volume)

efforts replace the two-point variogram with a training image (or analogue) so as to account for higher order dependencies in geological processes. The training image is a geological analogue of a deposit that describes geometric aspects of rock patterns assumed to be present in the attributes being modelled and reflects the prior geological understanding of a deposit considered.

The multiple-point or MP simulation approach examined herein and adopted for the modelling of the geological units of an iron ore deposit is based on the MP extension of SIS (Guardiano and Srivastava 1993; Strebelle 2002; Liu and Journel 2004), where MP statistics are inferred by scanning a training image (TI). The TI is regarded as a geological analogue, forms part of the geological input, and it should contain the relevant geometric features of the units being simulated. Until recently, the MP simulation approach has mainly been used for modelling of fluvial petroleum reservoirs. It is logical to extend its application to modelling mineral deposits,

where the TI can be derived from geological interpretations of the relatively dense exploration or grade control drill hole data, and/or face mappings.

This paper revisits multiple-point simulation as an algorithm for the simulation of the geology for mineral deposits. In the next sections, the MP method is first reviewed and outlined. Subsequently, an application at the Yandi channel iron ore deposit is detailed. Implementation issues, the characteristics of the resulting simulated realisations and the resource uncertainty profile are also discussed. Finally, conclusions from this study are presented.

Simulation with Multiple-Point Statistics Revisited

Definitions

Multiple-point or MP statistics consider the *joint* neighbourhood of any number n of points. As indicated above, the variogram can be seen as a MP statistic consisting of only 2 points; hence, it can not capture very complex patterns. Using MP statistics sequentially on difference scales, large and complex patterns can be reproduced with a relatively small neighbourhood size n of about 20 to 30. MP statistics can be formulated using the multiple-point data event D with the central value A. The geometric configuration of D is called the template τ_n of size n. Figure 2shows an example of a data event on a template with $n = 4$.

The size n of the template and its shape can be adjusted to capture any data events informing central value A. As MP statistics characterise spatial relations of closely spaced data, they may not always be calculated directly from drilling data. The method used for this study defines MP statistics on a regular grid, and are inferred from the TI, a regular cell model that serves as a 3D representation of the geological features concerned. The geometries contained in the TI should be consistent with the geological concept and interpretation of the deposit. In practice, this can always be confirmed by a geologist familiar with the deposit.

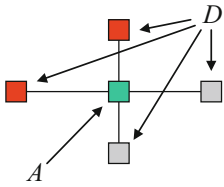

Fig. 2 Naming conventions to define MP statistics

A Stochastic Simulation Algorithm

Consider an attribute S taking K possible discrete states $\{s_k,\ k = 1, \ldots, K\}$, which may code lithological types, metallurgical ore types, grindability units, and so on. Let d_n be a multiple-point data event of n points centred at location $\mathbf{x}$. d_n is associated with the data geometry (the data *template* τ_n) defined by the set of n vectors $\{\mathbf{h}_\alpha,\ \alpha = 1, \ldots, n\}$ and consists of the n data values $s(\mathbf{x}+\mathbf{h}_\alpha) = s(\mathbf{x}_\alpha),\ \alpha = 1, \ldots, n$. While traditional variogram-based simulation methods estimate the corresponding conditional distribution function (*ccdf*) by somehow solving a kriging system consisting on the two-point covariances, the MP *ccdf* is conditioned to single joint MP data events d_n

$$f(\mathbf{x}; s_k|d_n) = E\{I(\mathbf{x}; s_k)|d_n\} = \Pr\{S(\mathbf{x}) = s_k|d_n\}, \quad k = 1, \ldots, K \tag{1}$$

Let A_k denote the binary random variable indicating the occurrence of category s_k at location $\mathbf{x}$:

$$A_k = \begin{cases} 1\ , & \text{if } S(\mathbf{x}) = s_k \\ 0\ , & \text{otherwise} \end{cases} \tag{2}$$

Similarly, let D be a binary random variable indicating the occurrence of data event d_n. Then, the conditional probability of node $\mathbf{x}$ belonging to state s_k is given by the simple indicator kriging (SIK) expression

$$f(\mathbf{x}; s_k|d_n) = \Pr\{A_k = 1|D = 1\} = E\{A_k\} + \lambda[1 - E\{D\}] \tag{3}$$

where, $E\{D\} = \Pr\{D = 1\}$ is the probability of the conditioning data event d_n occurring, and $E\{A_k\} = \Pr\{S(\mathbf{x}) = s_k\}$ is the prior probability for the state at $\mathbf{x}$ to be s_k. Solving the simple kriging system for the single weight λ leads to the solution of Eq. 3

$$f(\mathbf{x}; s_k|d_n) = E\{A_k\} + \frac{E\{A_k D\} - E\{A_k\}E\{D\}}{E\{D\}} = \frac{\Pr\{A_k = 1, D = 1\}}{\Pr\{D = 1\}} \tag{4}$$

Therefore, given a single global conditioning data event, this solution is identical to Bayes' definition of the conditional probability. However, one might consider decomposing the global event D_J into more simple components whose frequencies are easier to infer. From its definition, it is obvious that D_J can be any one of the 2^J joint outcomes of the J binary data events $A_\alpha = A(\mathbf{x}+\mathbf{h}_\alpha),\ \alpha = 1, \ldots, J$ with $A_\alpha \in \{0, 1\}$. Equivalent to the common SIK estimate, the conditional probability of the event $A_0 = 1$ can be written in a more general form as a function of the J conditioning data (Guardiano and Srivastava 1993).

$$\begin{aligned}&\Pr\{A_0 = 1 | A_\alpha = s_i \,;\, \alpha = 1, \ldots, J \,;\, i \in \{1, \ldots, K\}\} \\ &= E\{A_0\} + \sum_{\alpha 1=1}^{J} \lambda_{\alpha 1}^{(1)} [A_{\alpha 1} - E\{A_0\}] + \sum_{\alpha 1=1}^{J} \sum_{\alpha 2 > \alpha 1}^{J} \lambda_{\alpha 1 \alpha 2}^{(2)} [A_{\alpha 1} A_{\alpha 2} - E\{A_0\}] \\ &+ \sum_{\alpha 1=1}^{J} \sum_{\alpha 2 > \alpha 1}^{J} \sum_{\alpha 3 > \alpha 2}^{J} \lambda_{\alpha 1 \alpha 2 \alpha 3}^{(3)} [A_{\alpha 1} A_{\alpha 2} A_{\alpha 3} - E\{A_0\}] + \cdots + \lambda^{(J)} \left[\prod_{\alpha=1}^{J} A_\alpha - E\left\{ \prod_{\alpha=1}^{J} A_\alpha \right\} \right]\end{aligned} \tag{1}$$

The $2^J - 1$ weights $\lambda_{\alpha j}^{(i)}$ call for an extended system of normal equations similar to a simple kriging system that takes into account the multiple-point covariances between all the possible subsets $D'_J = \prod_{\beta \in J'} A_\beta$, $J' \subseteq \{1, \ldots, J\}$ of the global event D_J. These multiple-point covariances are inferred by scanning the training image for each specific configuration. For the case when all J values a_α are equal to 1, Eq. 4 is identical to Bayes' relation for conditional probability. The decomposition of the global event D_J illustrates that the traditionally used two-point statistics loose their exclusive status in an extended simple kriging system.

The numerator and denominator of Eq. 4 are inferred by scanning a training image and counting both the number of replicates of the conditioning data event $c(d_n)$, and the number of replicates $c_k(d_n)$, among the c previous ones, with the central value $S(\mathbf{x}) = s_k$. In the Single Normal Equation Simulation or SNESIM algorithm (Strebelle 2002), these frequencies are stored in a search tree enabling fast retrieval. The required conditional probability is then approximated by

$$f(\mathbf{x};\, s_k | d_n) = \Pr\{A_k = 1 | D = 1\} \approx \frac{c_k(d_n)}{c(d_n)} \tag{6}$$

To simulate an unknown location $\mathbf{x}$, the available conditioning data forming the data event d_n is retained. The proportions for building the *ccdf* (Eq. 6) are retrieved from the search tree by searching the retained data event and reading the related frequencies.

The SESIM algorithm and the options provided in the implementation have been covered elsewhere (Strebelle 2002; Remy 2004; Liu 2006) and will not be repeated here in detail. An overview of the general steps of the simulation is given below:

1. Scan the training image and store occurrences of all data events D. This may be seen as building a database of jigsaw puzzle pieces of different shapes (D) and their central values (A) from the TI.
2. Define a random path and visit nodes one by one.
3. Simulate each node by

   (a) Retrieving all data events (jigsaw puzzle pieces) fitting the surrounding data and previously simulated nodes.

(b) Derive the local probability distribution from stored frequencies of central values; the probability of finding a certain lithology at the node given the surrounding data event D is given by Bayes relation for conditional probability.
(c) Pick randomly from the distribution and add simulated node to the grid.

4. Start again at (1) for the next realisation, as may be needed.

Case Study

Geology of the Yandi Channel Iron Ore Deposit

A number of operations in the Pilbara region of Western Australia produce iron ore from clastic channel iron ore deposits (CID) formed in the Tertiary. These deposits contribute a significant portion of the overall production from the region. Their formation in a fluvial environment with variable sources and deposition of the material as well as post-depositional alteration resulted in very large high quality but complex iron orebodies. The CID consists of an incised fluvial channel filled with detrital pisolite ore that is affected by variable clay content. Ore qualities depend on lithological domains that are modelled using sectional interpretations and grade cut-offs. Defining and modelling boundaries to low-grade over-burden and to internal high-aluminous areas cause problems in the current resource estimation, assessment and modelling practices.

Figure 3 shows a schematic cross-section through the CID showing the various lithologies: ALL—Alluvium, ECC—Eastern Clay Conglomerate, WCH—Weathered Channel, GVU—Goethite-Vitreous Upper, GVL—Goethite-Vitreous Lower, LGC—Limonite-Goethite Channel, BCC—Basal Clay Conglomerate, WW—Weeli Wolli Formation. The erosional surface of the incised channel is covered by the BCC. From bottom to top, LGC, GVL, GVU, WCH and ECC sequentially fill the channel. ALL covers the whole channel sequence including the surrounding WW bedrock. The GVU and the GVL are the only units that currently fall within economic mining parameters. The WCH is a high SiO_2 waste unit with a gradational uncertain boundary to the GVU below. These two ore bearing lithologies and the transitional WCH are encapsulated by high Al_2O_3 waste (WAS), which consists

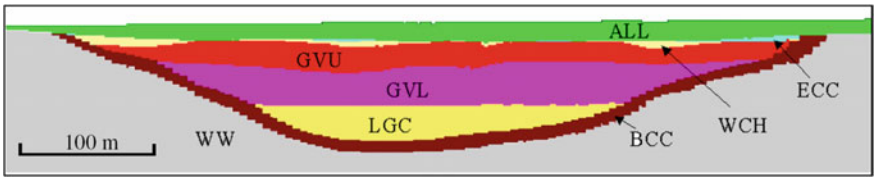

Fig. 3 Schematic cross-section through CID showing the various lithologies

of various clay-rich low-grade strata in both the hanging wall and the foot wall (ALL, ECC, LGC, BCC and WW).

The study area is located at Junction Central deposit of the Yandi CID (Fig. 4) and consists of the so-called Hairpin model area. The existing Hairpin resource orebody model is rotated by 45°. To accommodate for this rotation, this case study was performed in a local grid with North oriented to 285°. All results are presented in this rotated grid.

The study area has been drilled out in various campaigns to nominal spacing of 100 m by 50 m. This data and the knowledge of absence of CID outside the drilled area are used to interpret the deposit. To introduce the knowledge about un-drilled areas into the simulations, the areas around the drilled CID was 'infilled' using 50 m by 50 m spaced data points with WAS code assigned (Fig. 5).

Deriving a Training Image

The training image (TI) has to contain the relevant geological patterns of the simulation domain. In the context of the Yandi CID, this means that the TI has to characterise the shape of the channel and of the internal boundaries within the study area. The geological model of the mined out initial mining area (IMA) is the best available source for this information:

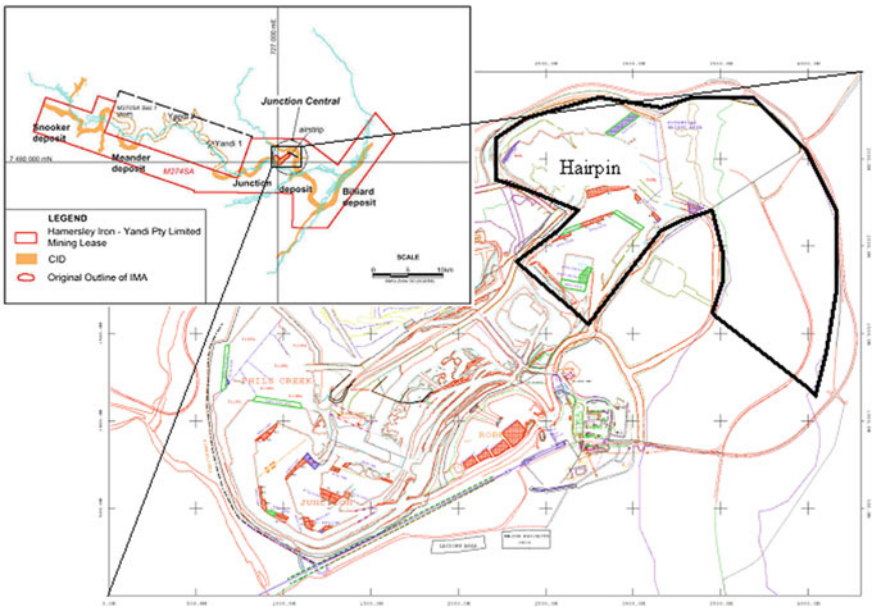

Fig. 4 Location map of the study area

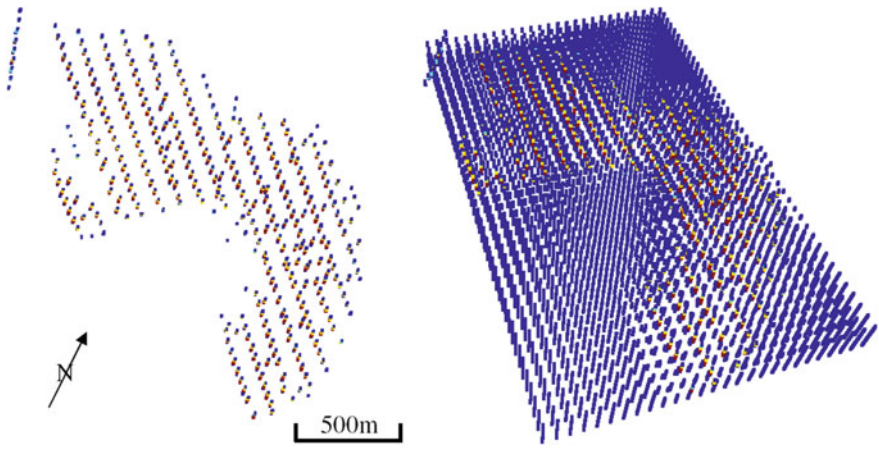

Fig. 5 Drill hole data set (left) and infilled grid data (right)

1. The model is based on relatively dense exploration drilling on a 50 m × 50 m grid.
2. It consists of a straight section of the CID thus having a constant channel axis azimuth.

The TI was generated as a regular geological block model of the IMA prospect into 10 m × 10 m × 1.25 m blocks. This resulted in 80 × 80 × 125 or 800,000 blocks in total. Four slices of the training image are depicted in Fig. 6and show the main direction of the channel (EW) and the slight undulation of the channel axis. The boundaries between the various units are smooth, reflecting the wireframe model upon which the TI was based.

As such, ensuring that the training image is consistent with the available data within the simulation domain is a measure needed to assess the validity and limits of the TI. Here, the variograms and cross-variograms of the geological categories are used for this validation. Two data sets will be compared with the TI:

1. The data at IMA that was used for constructing the geological model; this shows the differences of two-point statistics occurring between exhaustive 3D data and sparse drillhole data.
2. The data available in the simulation domain (HPIN) then serves the validation of the TI for use within that domain.

Note that this procedure checks the change of the two-point statistics between the data in the TI-domain (IMA) and the simulation domain (HPIN). The statistics of the TI help to evaluate this change: If the differences between the TI-statistics and the HPIN-statistics are grossly larger than those between the TI and the IMA statistics, one will have to consider the reasons for and consequences of these differences.

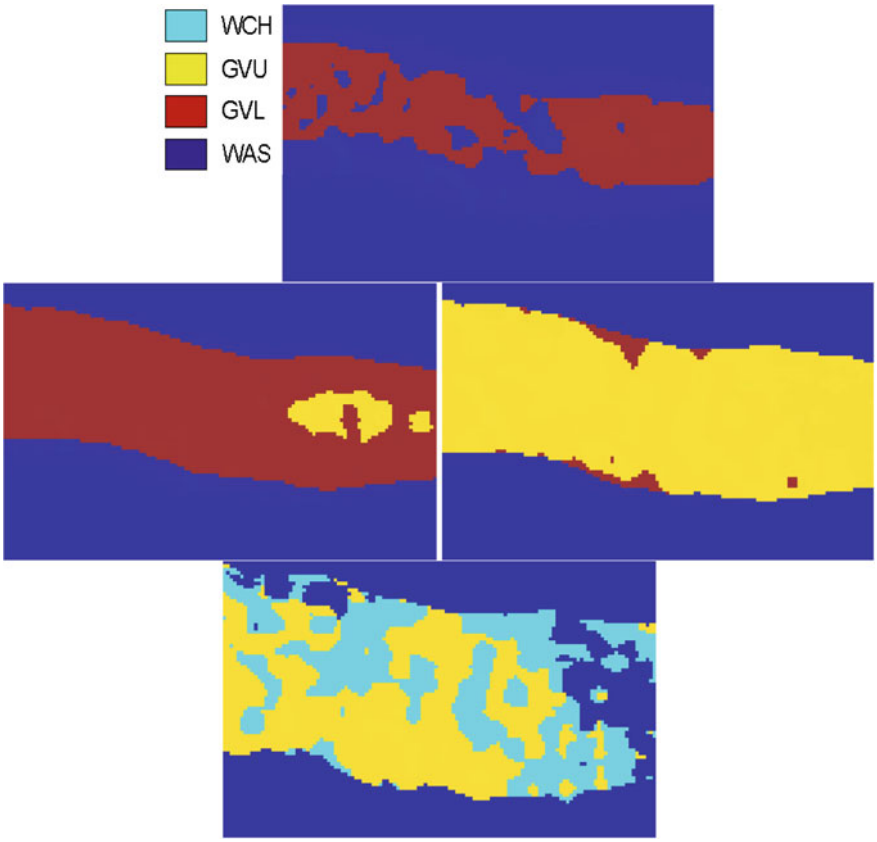

Fig. 6 Bench sections (channel bottom to the top) of the lithological interpretation at Yandi IMA used as training image

Overall, the variograms of the four categories perform well in this validation (Fig. 7). For unit WAS (please refer to the geological unit abbreviations in the previous section), the HPIN variogram coincides more closely with the TI than the IMA. The WCH variogram of the HPIN data shows larger values at lags up to 350 m than both IMA data variograms and TI. However, these differences are relatively small. The GVU variograms follow a very similar structure; only at short lags do the HPIN variograms have slightly larger values. For the GVL, both data variograms have almost the same values but they are smaller than the TI variogram, suggesting stronger continuity.

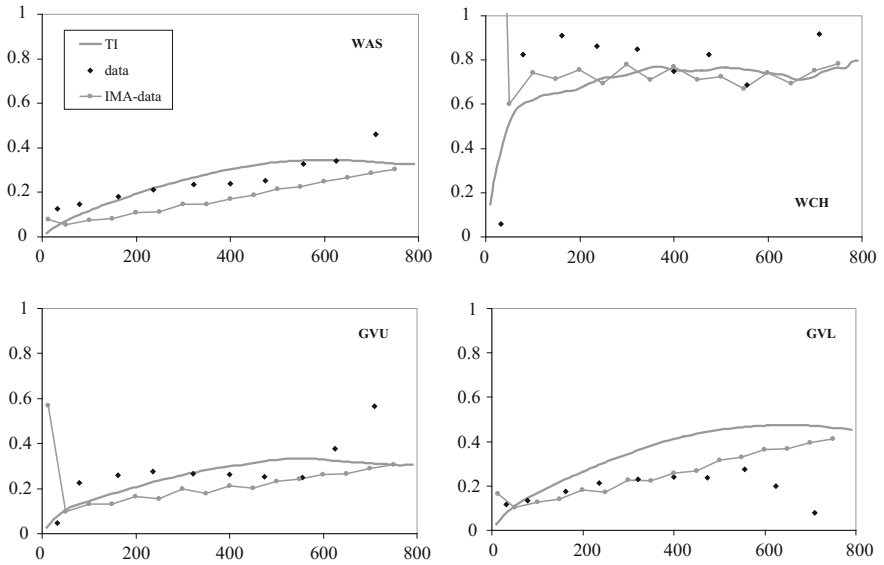

Fig. 7 Variograms of the four categories parallel to the channel axis for the TI, the data (at HPIN) and the data at the IMA, i.e., the area of the TI. The x-axis shows the lag in m, the gamma values are given on the ordinate

Simulation Results

To assess the geological uncertainty 20 realisations were generated. Each realisation of the 3.6 m nodes took 7.5 min on a 2.4 GHz personal computer, making the process very practical in terms of computational requirements.

Figures 8 and 9 show bench 490RL and a cross-section of the channel, respectively; each figure includes two realisations along with the interpreted deterministic model (wireframe). The bench view shows that the overall shape of the channel has been well reproduced. The incised shape of the channel was generated on a large scale and the stratigraphic sequence has been reproduced. The continuation of the tributary in the North-East was not generated due to very widely spaced drilling in the area. The proportion of GVL in this bench is higher in the simulations than in the interpreted model however, globally, proportions were reproduced. Boundaries in the simulations are less smoothed for both the GVL-GVU and the GVL-WAS contacts. In some areas, channel material was generated in small pods outside the continuous channel. The cross-section view supports these observations. However, on the channel margins, holes and saw-tooth shaped contacts are inconsistent with the depositional environment of the deposit.

Bench 490RL (Fig. 8) crosscuts the boundary of GVL and GVU. The boundary is undulating and shows an increased irregularity in comparison with the geological model WIREFRAME MODEL. Furthermore, the overall proportion of GVU in

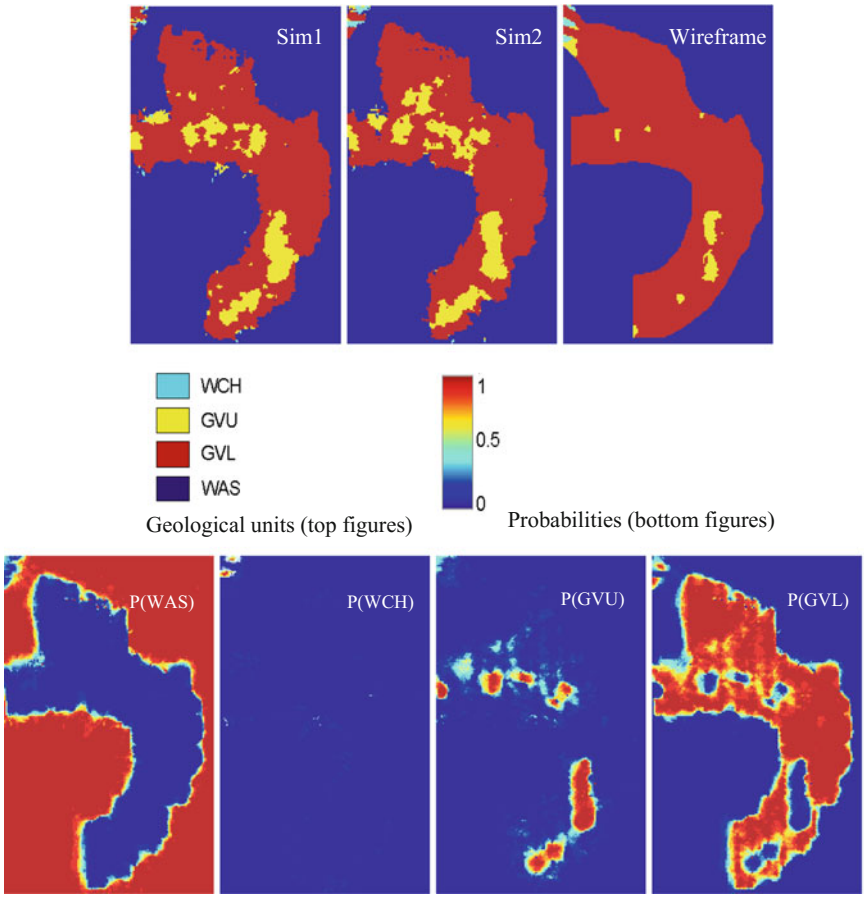

Fig. 8 Two simulations and wireframe interpretation (top); probability maps (bottom) for bench 490 mRL—units WAS, WCH, GVU, and GVL

bench 490RL is larger in the realisations than in the HIY model. On average probability for unit GVU (P(GVU)), the locations of the lowermost parts of the GVU are related to the wireframe model. However, there are areas in the northern part of the channel where the realisations contain GVU, while the wireframe model consists mainly of GVL. At the southern end of the channel, the GVU patches in the realisations have an increased extension compared to the wireframe model. The outline of the GVU to the surrounding WAS in the realisations is very fuzzy, overall, compared with the wireframe model. This higher disorder occurs on two scales:

1. On a very fine scale of a few blocks, the outline is strongly undulating;
2. On a larger scale of about 15–25 blocks, the undulations are less extreme. However, they are still present and not consistent with the TI.

In the cross-section in Fig. 9, the shapes of the channel margins are not well reproduced. Instead of an expected rather smooth outline as in wireframe model, the appearance is sharply stepped (left margin of Sim1 and Sim2). The top part of the channel is very fringy. All the sections depicted in Fig. 9show saw-tooth shaped features at the channel margins, indicating slight problems of the algorithm to reproduce the patterns of the channel margins.

Reproduction of Two Point Statistics

The validation takes the major direction of continuity, EW or along the channel axis, into account: Fig. 10 shows the experimental variograms of the data (black diamonds), of the TI (dark grey line), and of the 20 simulations (bright grey lines). The consistency of the data and the TI was described earlier. Two interesting aspects are compared here: (a) simulations versus TI; and (b) simulations versus data.

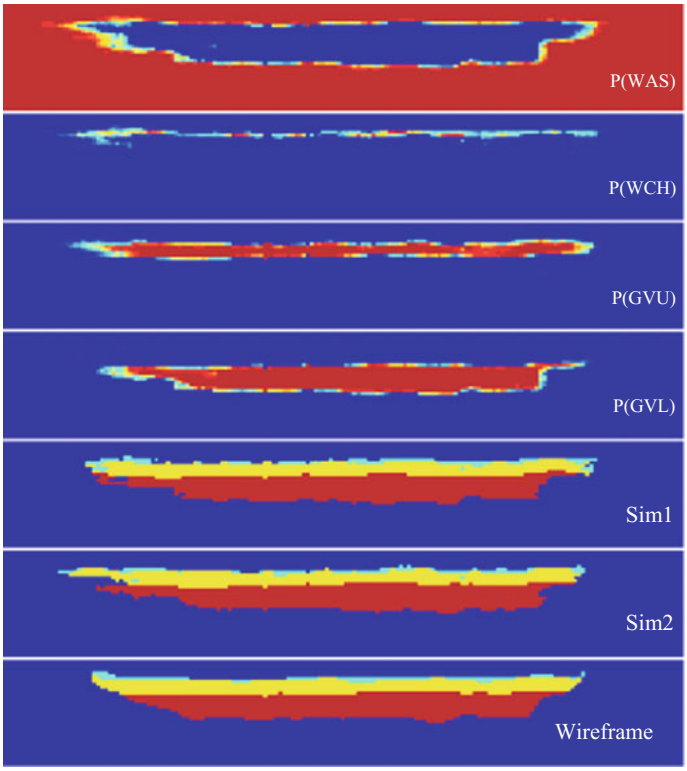

Fig. 9 Two simulations and interpretation and indicator probability for an E-W cross section (please see Fig. 8 for color coding)

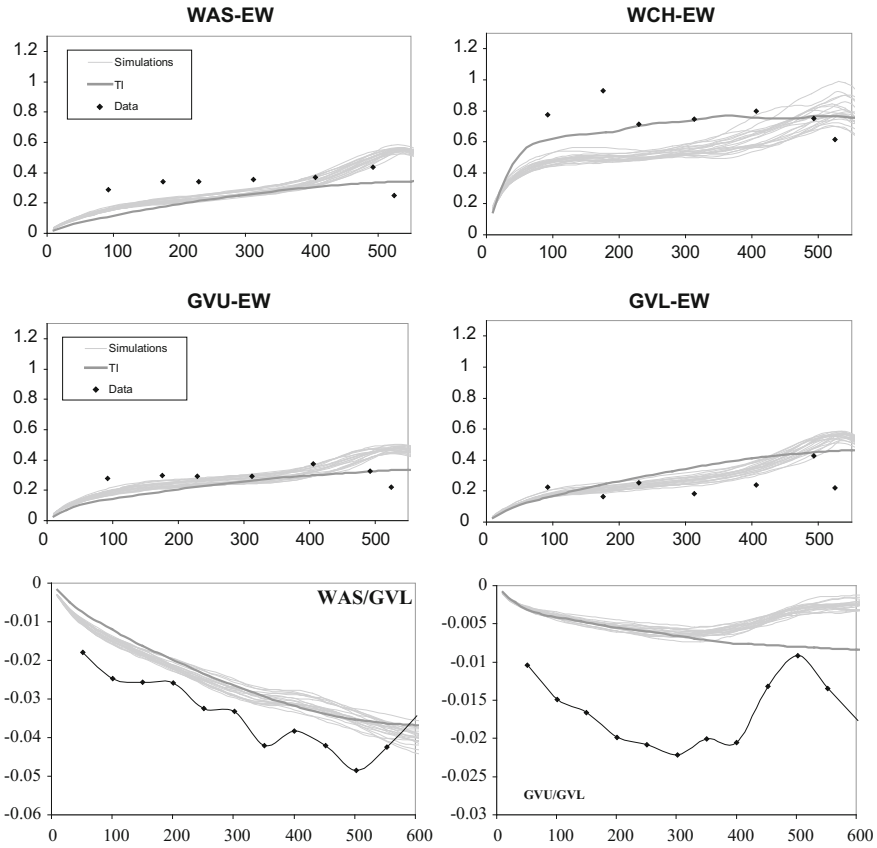

Fig. 10 Variogram and cross-variogram reproduction of simulations versus TI and data for various units

The WAS variograms are well reproduced in the main direction (EW), but the experimental data variograms suggest less continuity of lags up to 350 m, although this difference is not excessive. For WCH, the variogram reproduction is mediocre and suggests more continuity of the simulations compared to the data. The simulations deviate for lags larger than 50 m and reach the sill of the TI-variogram only at a lag of about 450 m. GVU and GVL variograms are well reproduced and correspond to the experimental data variograms. Cross-variogram reproduction for WAS/GVL and GVU/GVL is good regarding the TI however the is inconsistency with the data.

Volumetric Differences with Deterministic Wireframes and Uncertainty in Grade Tonnage Curves

The intersection of stochastic realisations and estimated grades allows an assessment of uncertainty due to uncertain geological boundaries. For example, Al_2O_3 is chosen here to show the differences between simulated geology and conventional wireframing, because Al_2O_3 is not a well understood variable in the resource model of the deposit. Grade-tonnage curves below Al_2O_3 cut-offs are generated to reflect ore cut-offs. Blocks were selected only within the limits of the ultimate pit as optimised for the deposit at Harpin and below the WCH/GVU boundary that serves as the hanging-wall ore limit. The grades used in the comparisons are estimated conventionally (ordinary kriging) and within each of the 20 simulated lithology models.

A 2% Al_2O_3 cut-off was applied to the Yandi Hairpin block grades to generate a product of about 1.35% Al_2O_3. Figure 11 shows the grade—tonnage curve of Al_2O_3 for the resource within the ultimate pit limits and the uncertainty profile for Al_2O_3 grade and resource tonnage. The two figures compare results based on the simulated lithology models (solid lines) and the deterministic (wireframe) lithology model (dashed line). The grade uncertainty appears relatively small. However, the resource tonnage indicated by simulations is on average 12 Mt (9%), smaller than the tonnage indicated by the best-guess wireframe model. The simulations allow for estimating a tonnage confidence interval. With 70% confidence, the final pit at the Hairpin deposit contains 95-97 Mt of ore within Al_2O_3 specifications. This shows that the contribution of the geological uncertainty to the overall grade uncertainty is considerable.

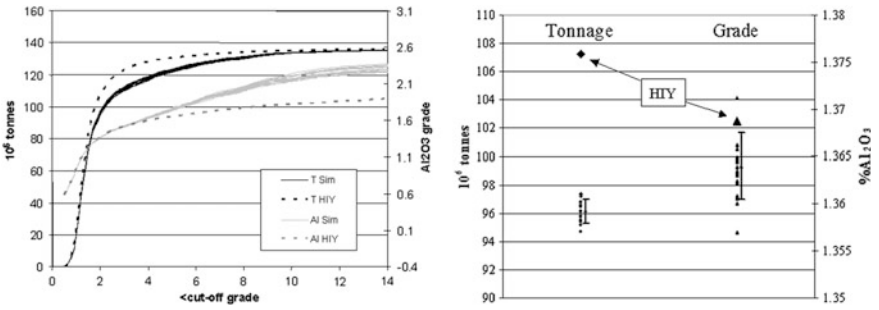

Fig. 11 Al2O3 Grade-tonnage curves between WCH and the ultimate pit limits (left) and uncertainty profile @2% Al_2O_3 (right) where bars depict the mean of the simulation $\pm 1\sigma$. Note that the grade variability (<1%) is not significant. (T—tonnage, Al—Al_2O_3, Sim—simulations; HIY—wireframe)

Conclusions

Multiple-point simulation provides a practical and powerful option to assess uncertainty in the geologic units of mineral deposits. The application of the MP method at Yandi utilises geometric information from a mined-out area. The generated realisations are easily comparable to the existing geological model and reproduce general channel shapes and the rotation of the channel axis. Geometries borrowed from the mined-out area are, in general, well reproduced. The position of boundaries in between drillholes changes from realisation to realisation, thus reflecting the uncertainty about the boundaries' exact shape. On the margins of the channel, the generated patterns are not always geologically meaningful. The MP method can incorporate information from dense drillhole data as available in typical mining applications.

The visual validation showed inconsistencies of the algorithm, reproducing patterns at the margins of the channel. In bench views, the outline of the GVL, the GVU, and the WCH undulates on a scale of 15–25 blocks. Additionally, the simulations show a strong, short-scale fuzziness for the GVU and the WCH. This visual impression is underpinned by the larger perimeter-to-volume ratio of the realisations compared to the TI. In the cross-sections, the major critical observation is that the erosional contact to the Weeli-Wolli formation is not consistent with observations in the pit nor with geological knowledge originating from modern geomorphologic analogues. Two sources for these issues with pattern reproduction have to be considered, i.e., the TI and the algorithm.

It was shown that the TI and the data in the simulation domain are not fully consistent with respect to two-point statistics. The extent to which this influences the quality of reproduced patterns is difficult to assess. Using a set of different training images can provide further insight.

Resource grade and tonnage uncertainty due to uncertain lithological boundaries was assessed by combining probabilistic realisations of the geology with a standard grade estimation technique. At an alumina cut-off of 2.0%, the ore tonnage based on the simulated geology ranges from 94.5 to 97.5 Mt (wireframe model: 107 Mt) with bulk alumina grades below the cut-off ranging insignificantly between 1.357 and 1.37% (interpreted model: 1.37%). Using grade simulation instead of grade estimation techniques would add realistic grade variability to this model and allow the assessment of total grade tonnage uncertainty.

Potential areas of application are in areas of little geological understanding or definition of boundaries by drilling. At Yandi, internal clayey high-aluminous waste that cannot be defined with the 50–100 m spaced resource evaluation drilling and simulation could create value by better defining grade tonnage curve with regard to contaminants. Training images could be constructed from geological interpretation and data gained in previously mined areas of the deposit.

Acknowledgements Special thanks to Micheal Wlasenko and Jim Farquhar from Rio Tinto Iron Ore for their support of the case study at Yandi.

References

Arpat GB, Caers J (2007) Conditional simulation with patterns. Math Geol 39(2)

Betzhold J, Roth C (2000) Characterising the mineral variability of a Chilean copper deposit using plurigaussian simulations. J SAIMM 100(2):111–120, March/April 2000

Carle SF, Fogg GE (1996) Transition probability-based indicator geostatistics. Math Geol, v 28 (4):5453–5476

Daly C (2004) High order models using entropy, Markov random fields and sequential simulation. In: Leuangthong O, Deutsch C (eds) Geostatistics Banff 2004, vol 2. Springer, Dordrecht, p 215–224

David M (1988) Handbook of applied geostatistical ore reserve estimation. Elsevier, The Netherlands

Deraisme J, Field M (2006) Geostatistical simulations of kimberlite orebodies and application to sampling optimisation. In: Proceedings 6th international mining geology conference. Darwin, NT, 21–23 August 2006

Dimitrakopoulos R, Dagbert M (1993) Sequential modeling of relative indicator variables: dealing with multiple lithological types. In: Soares A (ed) Geostatistics Troia '92, Kluwer Academic Publishers, vol 2, pp 413–424

Fontaine L, Beucher H (2006) Simulation of the Muyumkum uranium roll front deposit by using truncated plurigaussian method. In: Proceedings 6th international mining geology conference. Darwin, NT, 21–23 August 2006

Goovaerts P (1997) Geostatistics for natural resource evaluation. Oxford, New York

Guardiano F, Srivastava RM (1993) Multivariate geostatistics: beyond bivariate moments. In: Soares A (ed) Geostatistics Troia'92, vol 1, p. 133–144. Kluwer Academic Publishers, Dordrecht

Journel AG (2018) Roadblocks to the evaluation of ore reserves—the simulation overpass and putting more geology into numerical models of deposits, in this volume

King HF, McMahon DW, Bujtor GJ, Scott AK (1986) Geology in the understanding of ore reserve estimation: an Australian viewpoint. In: Ranta DE (ed) Ore reserve estimation, applied mining geology, vol 3, p. 55–68. SME, Littleton, Colorado

Langlais V, Doyle J (1993) Comparison of several methods of lithofacies simulation on the fluvial gypsy sandstone of Oklahoma. In: Soares A (ed) Geostatistics Troia'92, vol 1, p 299–310. Kluwer Academic Publishers, Dordrecht

Le Loc'h G, Galli A (1997) Truncated Plurigaussian method: theoretical and practical points of view. In: Baafi EY, Schofield NA (eds) Geostatistics Wollongong'96, vol 1, p 211–222., Kluwer Academic Publishers, Dordrecht

Li W (2007) A fixed-path Markov algorithm for conditional simulation of discrete spatial variables. Math Geol 39(2)

Liu Y (2006) Using the Snesim program for multiple-point statistical simulation. Comput Geosci 32(10):1544–1563

Liu Y, Journel A (2004) Improving sequential simulation with a structured path guided by information content. Math Geol 36(8):945–964

Remy N (2004) S-GEMS—stanford geostatistical earth modeling software: user's manual. Stanford University, http://sgems.sourceforge.net/doc/sgems_manual.pdf (13 March 2006)

Richmond AJ, Dimitrakopoulos R (2000) Evolution of a simulation: implications for implementation. In: Kleingeld WJ, Krige DG (eds) Geostatistics Cape Town 2000, vol 1, p 135–144. Geostatistical Association of South Africa

Seifert D, Jensen JL (2000) Object and pixel-based reservoir modelling of a braded and fluvial reservoir. Math Geol 32:581–603

Sinclair AJ, Blackwell GH (2002) Applied mineral inventory estimation, p 381. Cambridge University Press, Cambridge

Srivastava RM (2005) Probabilistic modeling of ore lens geometry: an alternative to deterministic wireframes. Math Geol 37(5):513–544

Strebelle S (2002) Conditional simulation of complex geological structures using multiple-point statistics. Math Geol 34(1):1–21

Tjelmeland H, Eidsvik J (2004) Directional metropolis: hastings updates for posteriors with non linear likelihood. In: Leuangthong O, Deutsch C (eds) Geostatistics Banff 2004, vol 1 p 95–104. Springer, Dordrecht

Zhang T, Switzer P, Journel A (2006) Filter-based classification of training image patterns for spatial simulation. Math Geol 38:63–80

New Efficient Methods for Conditional Simulations of Large Orebodies

J. Benndorf and R. Dimitrakopoulos

Abstract The application of conditional simulation techniques for modelling orebodies requires efficient algorithms, particularly due to the large number of grid nodes required, often in order of tens of millions. In this paper, two new efficient conditional simulation methods are reviewed: the generalised sequential Gaussian simulation (GSGS) and the direct block simulation (DBSIM). Both methods gain computational efficiency by simulating groups of nodes simultaneously, using a local neighbourhood as the conditioning data set. The relationship between the group and local neighbourhood sizes used is found to be important to both the accuracy of results and processing efficiency, and it is assessed numerically through a measure of the loss of accuracy.

Practical aspects of the GSGS are demonstrated and assessed in a case study at a porphyry copper deposit. Computational efficiency is demonstrated in the case study involving orebody models with up to 14,000,000 grid nodes, where the method is up to 20 times faster than the well-established sequential Gaussian simulation. At the same time, GSGS maintains a high level of accuracy. The practical aspects of DBSIM are demonstrated in simulating the same copper deposit in a comparable way to GSGS. In the case study, the computational efficiency of DBSIM is marginally better than GSGS; however, there are two major improvements. First, the application of DBSIM results in a substantial reduction of storage requirements and leads to improved data management. Second, the validation of the reproduction of variogram models is performed at the block support scale, which leads to a substantially more efficient variogram validation process than at the point support scale. Both methods, GSGS and DBSIM, provide efficient and reliable tools for practitioners to assess geological uncertainty in large mining applications.

J. Benndorf (✉)
MIBRAG MBH, Zeitz, Germany
e-mail: JoergBenndorf@gmx.de

R. Dimitrakopoulos
COSMO—Stochastic Mine Planning Laboratory, McGill University, Montreal, QC, Canada

R. Dimitrakopoulos (ed.), *Advances in Applied Strategic Mine Planning*,
https://doi.org/10.1007/978-3-319-69320-0_23

Introduction

Conditional simulation techniques are being applied more often in the mining industry, realising the value of information these techniques can generate along the chain of mining (Dimitrakopoulos 2004). However, applications in mining present their own challenges, including the size of simulations, computational efficiency and data management in a range of applications from resource/reserve classification to mine design, production scheduling and production reconciliations, and financial analysis. Large orebody models, frequently discretised by up to 10^8 grid nodes, need to be generated (e.g. Omre et al. 1993; Godoy 2002; Kent et al. 2007). Using conventional conditional simulation techniques, such as sequential Gaussian simulation (Isaaks 1990), the simulation process can be substantially time demanding. In addition, data management becomes an issue when large size simulated realisations are needed. The application of conditional simulation would be enhanced if practical and computationally efficient methods were available, as already noted in the technical literature (e.g., Ravenscroft 1994; Godoy 2002).

There are several conditional simulation methods available (e.g. Goovaerts 1997; Chiles and Delfiner 1999). A frequently used method is the sequential simulation (Scheuer and Stoller 1962; Journel 1994), which is based on the decomposition of the multivariate probability density function of a stationary random function, $Z(\mathbf{x})$, $\mathbf{x} \in R^d$, into a product of univariate conditional probability density functions (Rosenblatt 1952). When $Z(\mathbf{x})$ is Gaussian, the method is termed sequential Gaussian simulation or SGS (Isaaks 1990), which is a frequently used method due to its relative computational efficiency. Dimitrakopoulos and Luo (2004) suggest the generalisation of this method, termed generalised sequential Gaussian simulation or GSGS, to enhance computational efficiency. The generalisation is founded upon the observation that adjacent nodes share a common neighbourhood (Fig. 1), and therefore the GSGS simulates groups of clustered nodes simultaneously instead of node-by-node. The use of groups of nodes amounts to the decomposition of the multivariate probability density function of $Z(\mathbf{x})$ into groups of products of univariate conditional probability density functions. This group decomposition is general and includes as "end member" cases the SGS, where each group has one node only, and the LU simulation method (Davis 1987), where all nodes to be simulated are in one group. A major extension of the GSGS is the direct block simulation, or DBSIM, presented by Godoy (2002, 2017 in this volume). DBSIM generates realisations directly on a block support to substantially reduce storage requirements. The method is based on averaging internal nodes of one group during the simulation process. The latter process represents a joint point-block LU-type approach. Both GSGS and DBSIM can be extended to the efficient joint simulation of multi-element orebodies using minimum/maximum autocorrelation factors (Desbarats and Dimitrakopoulos 2000; Dimitrakopoulos and Fonseca 2003). Further discussion of multivariable joint simulation is presented in this volume by Boucher and Dimitrakopoulos (2009).

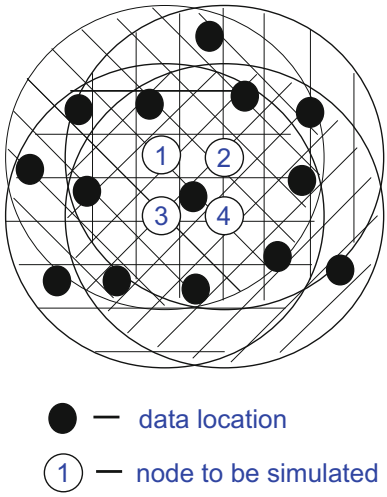

Fig. 1 Shared neighbourhood of group-nodes (from Dimitrakopoulos and Luo 2004)

This paper first reviews the theoretical background of GSGS and DBSIM. Then, using GSGS as an example, practical aspects of efficient conditional simulation methods are linked to accuracy in terms of the neighbourhood sizes used and how they are assessed. Subsequently, computational efficiency is demonstrated in an application of the method to a porphyry copper deposit. The application of DBSIM at the same deposit and a comparison with GSGS conclude the paper.

Efficient Generation of Conditional Simulation

Following the geostatistical terminology, a geological attribute under consideration is conceptualised as a random function $Z(\mathbf{x_i})$. Consider the stationary random function $Z(\mathbf{x_i})$, $\mathbf{x_i} \in R^d$, indexed on a discrete grid D_N of N grid nodes at location $\mathbf{x}_i$, i = 1,…,N, and a set of conditioning data $\mathbf{d}_n = \{d(\mathbf{x}_\alpha), \alpha = 1, \ldots n\}$ representing exploration data. In addition, consider the set including conditioning data and previously simulated nodes Λ_i for each location $\mathbf{x}_i$ such that, $\Lambda_0 = \{\mathbf{d}_n\}$ and $\Lambda_i = \{\Lambda_{i-1} \cup Z(\mathbf{x}_i)\}$, for example $\Lambda_1 = \{\mathbf{d}_n, Z(\mathbf{x}_1)\}$. Following this notation, the conditional simulation on D_N is based on sampling from the N-variate distribution conditioned on the data set Λ_0

$$F(\mathbf{x}_1, \ldots, \mathbf{x}_N; z_1, \ldots, z_N | \Lambda_0) = P(Z(\mathbf{x}_1) \leq z_1, \ldots, Z(\mathbf{x}_N) \leq z_N | \Lambda_0) \quad (1)$$

The sequential conditional simulation is based on the decomposition of the multivariate probability density function into a product of univariate conditional distribution functions (Rosenblatt 1952; Scheuer and Stoller 1962; Journel 1994).

$$f(\mathbf{x}_1,\ldots,\mathbf{x}_N;z_1,\ldots z_N|\Lambda_0)=f(\mathbf{x}_1;z_1|\Lambda_0)\cdot f(\mathbf{x}_2;z_2|\Lambda_1)\ldots f(\mathbf{x}_N;z_N|\Lambda_{N-1}) \quad (2)$$

The decomposition, described in Eq. (2), is general and well established in the general field of simulation (e.g. Law and Kelton 1999).

Generalised Sequential Gaussian Simulation

As mentioned in the introduction, grids D_N that are to be simulated have, in practice, overlapping neighbourhoods between adjacent grid nodes. It is therefore reasonable to consider the use of groups of nodes simultaneously instead of node-by-node as in the common simulation process. This sequential Gaussian conditional simulation of groups of nodes is described in Dimitrakopoulos and Luo (2004) and briefly outlined here.

The simulation starts with the partitioning of the simulation grid D_N into k groups of v_j, j = 1,…, k clustered nodes and define N_j as number of nodes in the first j groups $N_j=\sum_{i=1}^{j} v_i$; j = 1,…, k; N = N_k. Then, the decomposition of the conditional density in Eq. (2) into conditional densities for k groups becomes

$$f(\mathbf{x}_1,\ldots,\mathbf{x}_N;z_1,\ldots z_N|\Lambda_0)=\prod_{i=1}^{N_1} f(\mathbf{x}_i;z_i|\Lambda_{i-1})\ldots\prod_{i=N_{k-1}+1}^{N_k} f(\mathbf{x}_i;z_i|\Lambda_{i-1}) \quad (3)$$

In the implementation of Eq. (3) the exhaustive neighbourhood Λ_{i-1} is replaced by a local neighbourhood λ_{i-1}, resulting in Eq. (4)

$$f(\mathbf{x}_1,\ldots,\mathbf{x}_N;z_1,\ldots z_N|\Lambda_0)\approx\prod_{i=1}^{N_1} f(\mathbf{x}_i;z_i|\lambda_{i-1})\ldots\prod_{i=N_{k-1}+1}^{N_k} f(\mathbf{x}_i;z_i|\lambda_{i-1}) \quad (4)$$

where λ_{i-1} denotes the local conditioning data set, including sample data and previously simulated nodes. The nodes of group j are generated using Cholesky decomposition (Davis 1987) of the conditional covariance matrix of one group into an upper **U** and lower triangular **L** matrix, and are computed by the following operation

$$Z\left(\mathbf{x}_i^{Nj}|\lambda_{i-1}\right)=\mathbf{m}_j+\mathbf{C}_{j\lambda_{j-1}}\mathbf{C}^{-1}_{\lambda_{j-1}\lambda_{j-1}}(\mathbf{Z}_{\lambda_{j-1}}-\mathbf{m}_{\lambda_{j-1}})+\mathbf{L}\mathbf{w}_j \quad (5)$$

where $\mathbf{m}_j$ and $\mathbf{m}_{\lambda j-1}$ are the vectors of prior means of group $Z(\mathbf{x}_i^{Nj})$ and the set of data in λ_{j-1}, $\mathbf{C}^{-1}_{\lambda j-1\lambda j-1}$ denotes the inverse of the prior covariance matrix of conditioning data, $\mathbf{Z}_{\lambda j-1}$ denotes the vector of the conditioning data set λ_{j-1}, $\mathbf{C}_{j\lambda j-1}$ is

the prior covariance between $Z(\mathbf{x}_i^{Nj})$ and λ_{j-1}, $\mathbf{w}_j$ is a vector of identically and independently distributed N(0,1) random numbers. It is obvious that, if the number of nodes in one group v is equal to one, the algorithm is identical to SGS. And if the number of nodes in one group is equal to the whole grid size, the algorithm is identical to LU-decomposition. The implementation of the algorithm includes the following major steps:

1. Define a path visiting each group j of the grid and a path visiting each node in a group.
2. Define the local neighbourhood of the current group.
3. Calculate the conditional mean vector and conditional covariance matrix.
4. Generate the simulated values of one group using Eq. (5).
5. Add the simulated data values of the current group to the conditioning data set.
6. Loop through steps 2–5 until all groups are simulated.

Direct Block Simulation

A natural extension of the GSGS algorithm is the direct block simulation detailed in Godoy (2002) and briefly reviewed here. When simulating large grids, values simulated need to be retained as conditioning information. This generates increased memory requirements, issues of data management and, in general, leads in practice to performance decline. A new simulation algorithm is developed to simulate directly at the block support scale based on GSGS, whereby the group of nodes discretises a block.

Consider a normal score transformation of the random function $Y(\mathbf{x}_i)$ to $Z(\mathbf{x}_i)$. The regularised random function over a block support $Z_v(\mathbf{x}_j)$ with $x_j \in R^d$, can be expressed as a linear average of $Z(\cdot)$ over the volume V, centred at the block centre $\mathbf{x}_j$, and approximated by averaging the v internal nodes from a group: $Z_v(\mathbf{x}_j) = \frac{1}{\nabla} \int_{\mathbf{x} \in v} Z(\mathbf{u}) d\mathbf{u} \approx \frac{1}{v} \sum_{i=1}^{v} Z(\mathbf{x}_i)$. Since the objective is to simulate block values $y_v(\mathbf{x}_j)$ in data space and not Gaussian space $z_v(\mathbf{x}_j)$, after simulation a back-transformation from the Gaussian space into the data space needs to be performed. However, since the normal score transformation was done using point values, there is no back transformation for blocks of type $y_v(\mathbf{x}_j) = \Phi_v^{-1}(z_v(\mathbf{x}_j))$ available, unless restricting distribution assumptions are made. A solution to this problem is given by the approximation $y_v(\mathbf{x}_j) \approx \frac{1}{v} \sum_{i=1}^{v} \Phi^{-1}(z(\mathbf{x}_i|\lambda_{j-1}))$, which is an averaging of all back-transformed internal nodes $y(\mathbf{x}_i|\ \lambda_{j-1})$ for i = 1, …, v of one group. To derive these values, the group $Z(\mathbf{x}_i^{Nj}) = (Z(\mathbf{x}_i), i = 1, \ldots, v)$ is first simulated, which corresponds to simulating the v internal nodes discretising the block.

After simulation of the internal nodes of a group and back-transforming these, the simulated block value is calculated as the average of the point values in Gaussian space and in data space, and subsequently point values are discarded. The simulated Gaussian block value is then added to the conditioning data set, and the block value in data space is added to the results.

Conditioning data come in two types: point values Λ_i and block values included in the new subset Λ_i^V With this definition, and considering the screen effect approximation, the GSGS formulation in Eq. (4) can be rewritten in terms of point and block conditioning

$$f(\mathbf{x}_1,\ldots,\mathbf{x}_N;z_1,\ldots z_N|\Lambda_0) \approx \prod_{i=1}^{N_1} f(\mathbf{x}_i;z_i|\lambda_{i-1}) \cdot \prod_{i=N_1+1}^{N_2} f(\mathbf{x}_i;z_i|\lambda_{i-1}\cup\lambda_1^V)\ldots \prod_{i=N_{k-1}+1}^{N_k} f(\mathbf{x}_i;z_i|\lambda_{i-1}\cup\lambda_{k-1}^V) \tag{6}$$

To integrate the block support conditioning data, the algorithm is developed in terms of a joint-simulation. The second variable relates to the block value sequentially derived throughout the simulation process. The parameters of the successive conditional Gaussian distributions are obtained by solving a joint simulation system (Myers 1989), identical to joint LU-simulation. The simulation of the internal nodes of each block is similar to GSGS. The only difference is the inclusion of conditioning data of different support scale, namely point values and block values. The implementation of the direct block simulation algorithm proceeds as follows:

1. Define a random path visiting each of the blocks to be simulated.
2. Normalise data.
3. For each block, generate the simulated values in Gaussian space of the internal nodes discretising the block.
4. Derive the simulated block value by averaging values of simulated nodes in one group in Gaussian space and calculate the block value in data space.
5. Discard values of internal nodes and add the simulated block value in Gaussian space to the conditioning data set; keep the block value in data space as the result.
6. Loop through steps 3–5 until all blocks are simulated.

A major practical advantage of the algorithm above is the decrease in memory allocation due to the discarding of the internal points. Furthermore, the method takes advantage of the GSGS formalism and is thus a fast algorithm. Note that the method does not call for a block transformation function, which is often based on a global change-of-support model. Note also that the variogram validation at a block support scale is substantially more efficient than at point support.

Practical Aspects of GSGS

Computational costs of GSGS, implemented according to Eq. (5), may be assessed in terms of the number of floating point operations (flops) required. Dimitakopoulos and Luo (2004) show computational costs of GSGS to be

$$O\left(\frac{N}{v}\left(v_{max}^3 + v^3\right)\right) \tag{7}$$

where O denotes the number of flops ("in the order of"), N is the number of grid nodes, v is number of nodes in one group and v_{max} is the maximum size of the local neighbourhood, including sample data and previously simulated nodes. The grid size has a linear influence on the runtime behaviour of the algorithm. Critical parameters in terms of efficiency are group size and local neighbourhood size, as they influence the runtime behaviour to the power of three. Considering a grid of N = 1,000,000 nodes, the number of flops required as a function of the group size v and local neighbourhood size v_{max}, is shown in Fig. 2. For a fixed local neighbourhood size v_{max}, minimum computational costs occur when $v \approx 0.8\ v_{max}$. Considering a fixed group size v, increasing the size of the neighbourhood drastically increases the runtime (number of flops). On the other hand, a smaller neighbourhood size causes a larger difference between the simulated value conditioned to the local neighbourhood and the "ideal" value conditioned to all available information. This difference is the loss of accuracy due to the use of a finite neighbourhood (screen effect approximation) and can be quantified using the measure "relative screen effect approximation loss" (Dimitrakopoulos and Luo 2004), which is discussed in the next section.

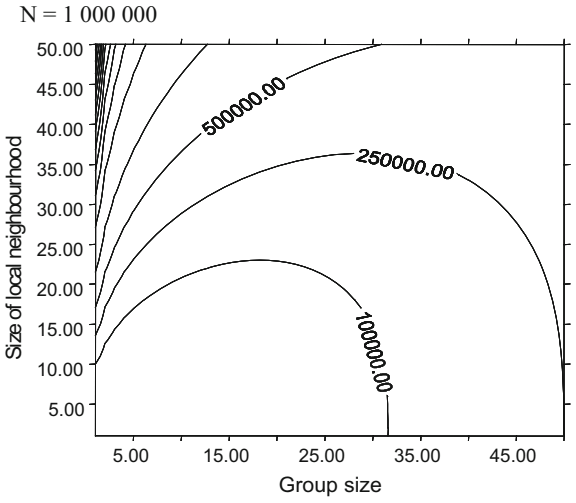

Fig. 2 Theoretical runtime behaviour of the GSGS algorithm as a function of the local neighbourhood size and the group size, for a grid size N of 1,000,000 nodes

Successful application of GSGS requires an understanding of the interaction between group size v and local neighbourhood size v_{max} and their effect on accuracy and computational efficiency. As a convention in the following paragraphs, GSGS with group size v will be denoted as group configuration GSGS i × j × k, where i denotes the number of nodes in X direction, and j and k in Y and Z directions respectively.

Group Size, Neighbourhood Size and Accuracy: Theory and Practice

To assess the effects of group size and neighbourhood size, the relative screen effect approximation loss (RSEAL) may be defined by the half of the expected value of the squared difference between simulated values $Z(\mathbf{x}_i)$ conditioned on a local neighbourhood λ_{i-1} and conditioned on all values Λ_{i-1}, standardised by the mean. That is

$$\rho_R(Z(\mathbf{x}_i|\lambda_{i-1}\Lambda_{i-1}) = \frac{[E\{\ Z(\mathbf{x}_i|\lambda_{i-1}) - Z(\mathbf{x}_i|\Lambda_{i-1})\}^{\ 2}]}{2 \cdot E\{Z(\mathbf{x}_i)|\Lambda_{i-1}\}} \tag{8}$$

The RSEAL depends on the local neighbourhood size v_{max} and on the group size v. To understand the interaction between those two parameters and the accuracy of the result, a relatively simple study can be carried out, as described here. This experimental determination of the RSEAL is based on Eq. (8) and includes the following two steps. (i) For the given dataset a base-case simulation is generated using an exhaustive neighbourhood Λ_{i-1}, resulting in a grid containing values $Z(\mathbf{x}_i|\Lambda_{i-1})$. (ii) Simulations are subsequently generated, using an incrementally decreased local neighbourhood of size λ_{i-1} and the same random seed, resulting in a grid containing the values $Z(\mathbf{x}_i|\lambda_{i-1})$. A node-by-node comparison of the generated simulation with the base case, in combination with the application of Eq. (8), gives the RSEAL.

For illustration purposes, a test data set containing 100 data is used. The study field represents the southwest area of the Walker-Lake data set (Isaaks and Srivastava 1989). Simulations are performed on a 2D grid of 7,600 nodes, using the inferred covariance structure of the data. Group configurations under investigation are 2 × 2, 4 × 4, 8 × 8 and 16 × 16. Figure 3 summarises the results.

Results show a higher loss of accuracy for larger group sizes than for smaller groups, when considering a fixed local neighbourhood size. A larger local neighbourhood size has to be chosen for larger groups to maintain a certain level of accuracy. By drawing a horizontal line at an acceptable loss of accuracy, e.g. 5%, the appropriate local neighbourhood size can be obtained, as shown in Fig. 3. Generally, when only a small local neighbourhood is used, internal nodes for large groups no longer share a common neighbourhood. As well, adjacent groups only

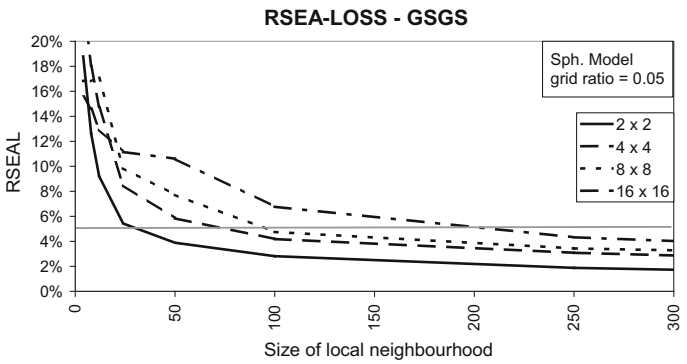

Fig. 3 Relative screen effect approximation loss (RSEAL) considering different GSGS group configurations

have a few neighbourhood data in common, which can cause non-continuous transitions between adjacent groups, experienced as artefacts.

An approach as described above provides a general and relatively simple way to obtain an understanding of the effects of neighbourhood sizes on accuracy.

Group Size, Neighbourhood Size and Computational Efficiency: Theory and Practice

To understand the relationship between group size, neighbourhood size and computational efficiency, the theoretical runtime behaviour of the GSGS algorithm will be analysed in more detail, and practical aspects will be stressed.

Recall that Fig. 2 plots contour lines of the computational costs of GSGS as a function of group size and local neighbourhood size, as in Eq. (7). The plot is characterised by very dense contour lines at a group size of one. Thus, considering a fixed local neighbourhood size, an increasing group size substantially decreases computational costs up to a certain point. Following the contour lines, it can be seen that, even if the neighbourhood size has to be increased by a few data when increasing the group size, there is still a reduction of computational costs. The theoretical runtime analysis of an algorithm considers the most expensive computations to be simulated, in the case of GSGS the solution of Eq. (5), which has a linear relationship with the grid size N. The theoretical analysis does not consider that there are more operations in the algorithm that are linear with problem size, including handling of the irregular shape of the orebody or the neighbourhood search. Larger group sizes will drastically reduce search time, since it is done simultaneously for all nodes in a group. Then, the algorithm may in practice perform much faster (and does as demonstrated next) than Eq. (7) indicates, while still maintaining a high level of accuracy.

Table 1 Orebody model definitions

Orebody model name	Model size	X-spacing (m)	Y-spacing (m)	Z-spacing (m)
Model 1	72,900	10	10	5
Model 2	291,600	5	5	5
Model 3	1,821,500	2	2	5
Model 4	3,590,300	2	1	5
Model 5	7,100,600	1	1	5
Model 6	14,201,000	1	0.5	5

An application of GSGS to a porphyry copper deposit aims to demonstrate the practical aspects of the technique. Key questions under investigation, in addition to reproduction of data, statistics and variogram, are the computational costs and performance using different group sizes. The deposit accounts for 185 drill holes in total, and 1407 composites of 5 m length are taken from these drill holes. After inferring declustered sample statistics and variography, simulated orebody models are generated. To study the effect of different group sizes as a function of grid size, the deposit is discretized by different density grids, as specified in Table 1. The six resulting orebody model sizes range from 72,900 to 14,201,000 nodes.

Figure 4 shows exemplarily a plan view of orebody realisations for different group sizes applied to orebody model three (discretisation: 2 m by 2 m by 5 m). A visual inspection suggests that the algorithm performs well for all group sizes, and no artefacts can be detected in the realisations. Figure 5 shows the excellent reproduction of histogram and variogram models in normal space using GSGS $2 \times 2 \times 2$. All other group configurations performed equally well on all considered orebody models.

To compare the runtime of GSGS for different group sizes, one realisation was generated for all orebody models, as specified in Table 1, using GSGS with group configurations $1 \times 1 \times 1$, $2 \times 2 \times 1$, $2 \times 2 \times 2$, $3 \times 3 \times 2$ and $4 \times 4 \times 2$. Suitable neighbourhoods were used for different GSGS group sizes, based on the accuracy of results derived in the previous section. Table 2 summarises the neighbourhoods used. Figure 6 and Table 3 shows the computing times for each considered orebody model size. To make the comparison general, in Fig. 6 runtimes are standardised to GSGS $1 \times 1 \times 1$ applied to model six. Figure 6 concludes that when simulating small orebody models, say less than one million nodes, there is limited benefit of using GSGS considering any of the group sizes. In this case, the runtime of the algorithm can be reduced, by up to about 30% compared with SGS, using small groups. When simulating large orebody models containing several millions of nodes, the runtime can be reduced substantially, up to 20 times in the case of GSGS $3 \times 3 \times 2$. Results demonstrate that GSGS can substantially reduce the computational costs, especially when simulating relatively large orebody models. Experiments with GSGS show that small groups, such as $2 \times 2 \times 2$ to $3 \times 3 \times 2$ nodes, perform best and balance accuracy with efficiency.

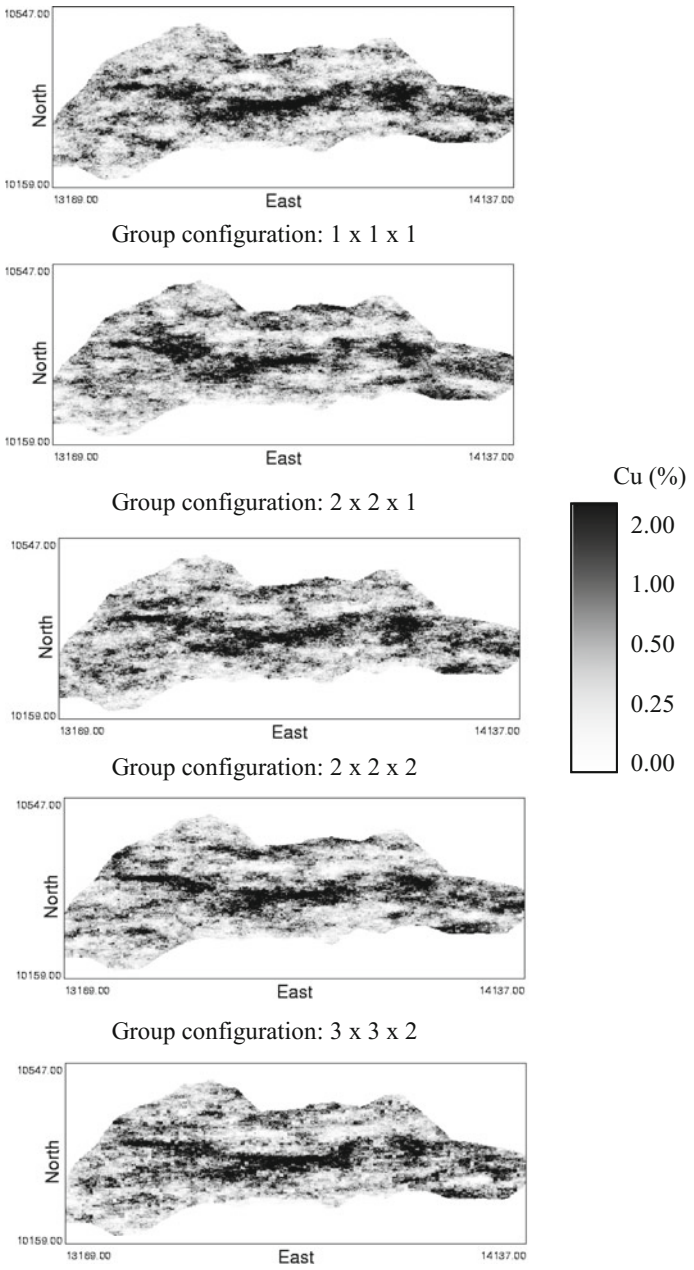

Fig. 4 Plan view of realisations of GSGS using different group sizes applied to model three

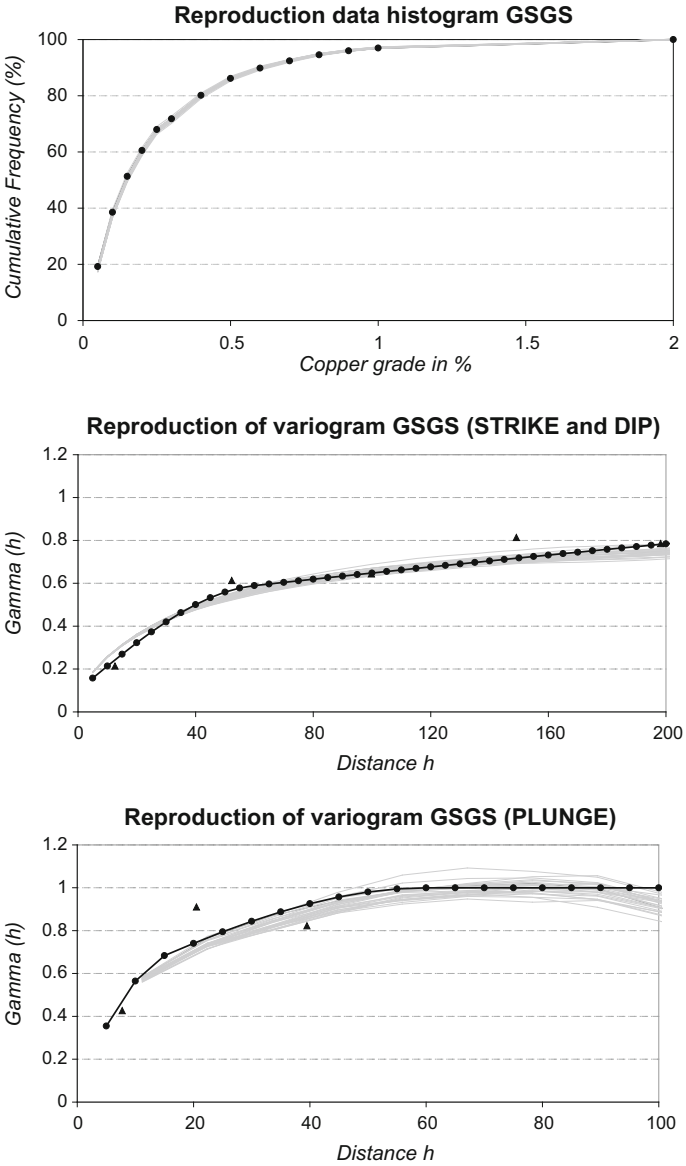

Fig. 5 Reproduction of data histogram, variogram model and reproduction of experimental variogram in normal space for the directions of anisotropy

Table 2 Neighbourhood sizes used for different GSGS group configurations

	GSGS 1 × 1 × 1	GSGS 2 × 2 × 1	GSGS 2 × 2 × 2	GSGS 3 × 3 × 2	GSGS 4 × 4 × 2
Number of data and previously simulated nodes	20	30	45	60	90

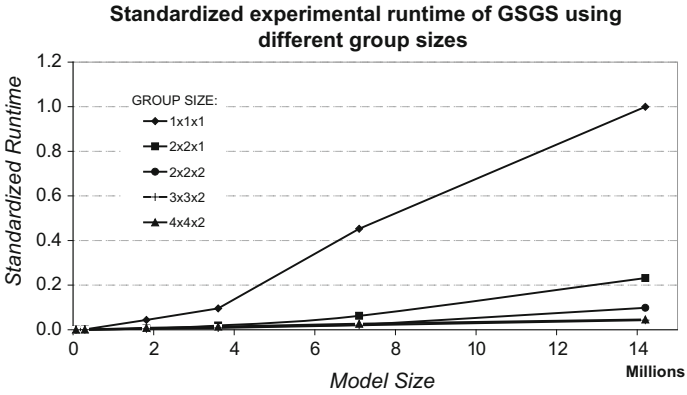

Fig. 6 Standardised experimental runtime of GSGS using different group sizes applied to different large orebody models

Table 3 Runtime of GSGS using different group sizes relative to SGS applied to different large orebody models

Model	Group size				
	1 × 1 × 1	2 × 2 × 1	2 × 2 × 2	3 × 3 × 2	4 × 4 × 2
	Runtime of GSGS relative to SGS				
Orebody model 1 %	100.0	53.5	64.8	71.8	142.3
Orebody model 2 %	100.0	33.1	39.2	42.1	73.9
Orebody model 3 %	100.0	12.8	10.8	9.6	20.1
Orebody model 4 %	100.0	19.8	12.1	8.3	14.7
Orebody model 5 %	100.0	13.8	4.8	4.5	6.0
Orebody model 6 %	100.0	23.2	9.8	4.3	4.6

Aspects of DBSIM and Comparison

To demonstrate practical aspects of the direct block simulation algorithm, the data from the porphyry copper deposit described in the previous section is used to generate ten realisations of the orebody. Block dimensions are chosen to be 10 m by 10 m by 5 m and are discretised by 10 × 10 × 1 internal nodes. The neighbourhood used includes six previously simulated blocks and 12 sample data. Figure 7 represents the reproduction of point-histogram and regularised variogram for DBSIM. Both aspects indicate a good reproduction of data statistics.

To compare DBSIM with GSGS, for instance, in terms of reproduction of sample statistics and the benefit in terms of storage requirements when simulating direct block values, the following is performed. Ten realisations were generated using GSGS 2 × 2 × 2 on a grid using a discretisation of 1 m by 1 m by 5 m. The GSGS neighbourhood was chosen according to Table 2. Realisations were

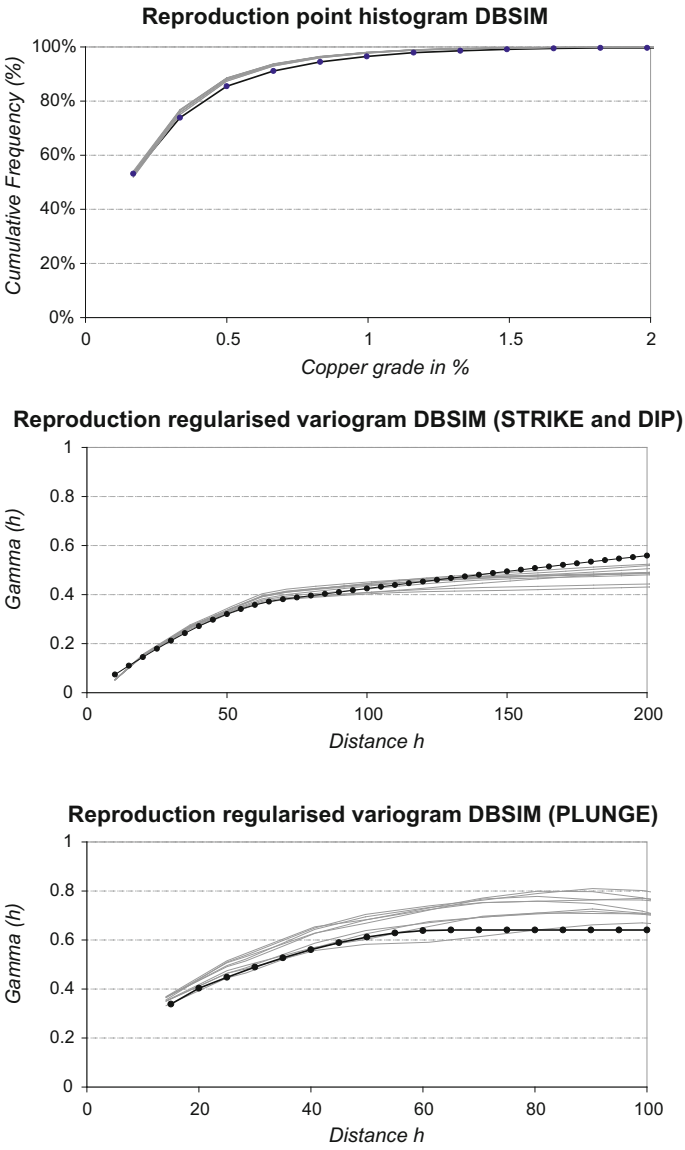

Fig. 7 Reproduction of point histogram and regularised variogram model for DBSIM applied to a copper deposit

re-blocked to a block size 10 m by 10 m by 5 m, to comply with the block size used for the DBSIM generated realisations. Figure 8 compares realisation number one of Cu % in the deposit for both methods. The results are indistinguishable and both methods are "artefact free".

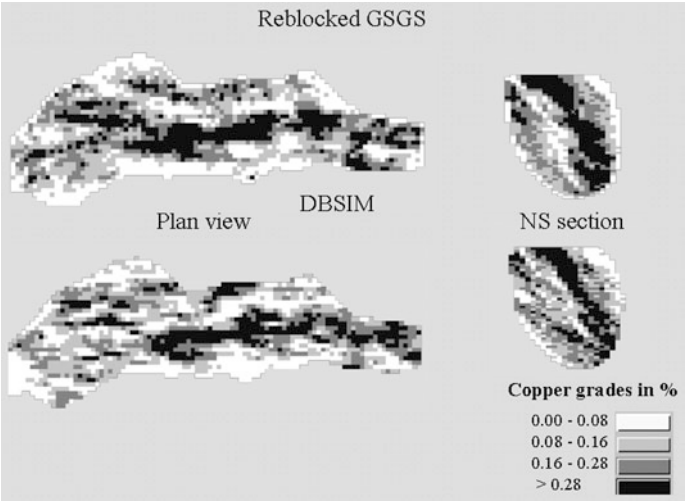

Fig. 8 Plan view and NS section of realisations generated by DBSIM and reblocked GSGS

The computing time for DBSIM was 20 h and 10 min compared with 21 h and 40 min in case of GSGS without reblocking (Pentium 4, 2 GHz processor). The difference can be explained by differences in implementation details and the faster neighbourhood search in the case of DBSIM, since only a few blocks need to be considered instead of a number of point data. The difference in the storage requirements of result files is substantial: 36 Mbytes in case of DBSIM and 3.65 Gbytes in case of GSGS, reflecting the block discretisation. In addition, the validation of the variogram on block support requires, on average, 33,000 pairs to be calculated, on a point support about 3,300,000.

The above results demonstrate that a simulation done directly at block support scale, as realised through DBSIM, meets industrial requirements for the above-discussed reasons. It is more computationally efficient than point-by-point methods and delivers reliable results. Note that issues on DBSIM neighbourhoods are different from GSGS, and generally DBSIM is insensitive to the size used. Experience shows that a neighbourhood with about six blocks and about twice as much sample data is sufficient for excellent simulation results (Godoy 2002). An application of the method is also shown in Godoy (2017, this volume)

Conclusions

The application of stochastic simulation techniques in mining generally requires efficient algorithms for large size applications. In this paper, two new efficient and practical methods for large applications are reviewed: the generalised sequential Gaussian simulation, and the direct block simulation.

Using GSGS as an example, practical issues pertinent to computational efficiency and accuracy were studied. Accuracy of results is predominantly affected by the size of the local neighbourhood. The relative screen effect approximation (RSEAL) is a measure that quantifies this accuracy and assists the selection of suitable neighbourhood sizes for different group sizes. The results presented herein on the size relationships are reasonably general. Results suggest that, when using larger group sizes, larger neighbourhoods sizes need to be considered to maintain the desired level of accuracy. The application of GSGS to a porphyry copper deposit demonstrated the efficiency of the method. While maintaining a given level of accuracy, GSGS can improve computational efficiency substantially, being up to 20 times faster.

A comparison of GSGS and DBSIM using the same deposit shows that both algorithms are fast, due to the fact that both are based on the group decomposition of the multi-variate probability density function. The application of DBSIM results in a substantial reduction of storage requirements and leads to improved data management. Both GSGS and DBSIM provide efficient and reliable tools for practitioners to assess geological uncertainty in large mining applications.

References

Boucher A, Dimitrakopoulos R (2009) Block-support simulation of multiple correlated variables. Math Geosci 41(2):215–237

Chiles JP, Delfiner P (1999) Geostatistics, modelling spatial uncertainty, 695 p. Wiley, New York

Davis MD (1987) Production of conditional simulations via the LU triangular decomposition of the covariance matrix. Math Geol 19(2):91–98

Desbarats AJ, Dimitrakopoulos R (2000) Geostatisical simulation of regionalized pore-size distributions using min/max autocorrelation factors. Math Geol 32(8):919–942

Dimitrakopoulos R, Fonseca MB (2003) Assessing risk in grade-tonnage curves in a complex copper deposit, northern Brazil, based on an efficient joint simulation of multiple correlated variables. In: APCOM 2003, 31st international symposium on the application of computers and operations research in the minerals industries, May 14–16, 2003, Cape Town

Dimitrakopoulos R, Luo X (2004) Generalized sequential Gaussian simulation on group size ν and screen—effect approximations for large field simulations. Math Geol 36(5):567–591

Godoy M (2002) The effective management of geological risk in long-term production scheduling of open pit mines. Ph.D. Thesis, School of Engineering, University of Queensland, Brisbane, Qld, Australia

Godoy M (2018) A risk analysis based framework for strategic mine planning and design—method and application, in this volume

Goovaerts P (1997) Geostatistics for natural resources evaluation, 483 p. Oxford University Press, New York

Isaaks EH (1990) The application of Monte Carlo methods to the analysis of spatially correlated data: unpublished. Ph.D. thesis, department of applied earth sciences, Stanford University, Stanford, California, 213 p

Isaaks EH, Srivastava RM (1989) An introduction to applied geostatistics, 561 p. Oxford University Press, New York

Journel AG (1994) Modelling uncertainty: some conceptual thoughts. In: Dimitrakopoulos R (ed) Geostatistics for the next century, Kluwer Academic Publishers, Dordtrecht, pp 30–43

Kent M, Peattie R, Chamberlain V, Sanhueza R (2007) Incorporating geological uncertainty in the decision to expand the main pit at the Navachab Gold Mine through use of stochastic simulation. Orebody modelling and strategic mine planning, Spectrum Series 14. The Australian Institute of Mining and Metallurgy, Melbourne, pp 207–216

Law AM, Kelton WD (1999) Simulation modelling and analysis, 760 p. McGraw-Hill Higher Education, Singapore

Myers DE (1989) Vector conditional simulation. In: Armstrong M (ed), Proceedings of the third international geostatistical congress, D Reidel Publishing Company, Avignon, pp 283–293

Omre H, Sølna K, Tjemeland H (1993) Simulation of random functions on large lattices. In: Soares A (ed) Geostatistics Troia'92, Kluwer Academic Publishers, Dordrecht, pp: 179–199

Ravenscroft PJ (1994) Conditional simulation for mining. In: Amstrong M, Dowd PA (eds) Geostatistical Simulations. Kluwer Academic Publishers, Dordtrecht, pp 79–87

Rosenblatt M (1952) Remarks on multivariate transformation. Ann Math Stat 23:470–472

Scheuer EM, Stoller DS (1962) On the generation of normal random vectors. Technotronics 4:278–281

Transformation Methods for Multivariate Geostatistical Simulation—Minimum/ Maximum Autocorrelation Factors and Alternating Columns Diagonal Centres

E. M. Bandarian, U. A. Mueller, J. Fereira and S. Richardson

Abstract To speed up multivariate geostatistical simulation it is common to transform the set of attributes into spatially uncorrelated factors that can be simulated independently. The main method in recent years has been minimum/maximum autocorrelation factors, either based on the coefficient matrices of a two structure linear model of coregionalisation (LMC) or on a pair of experimental covariance matrices. In both cases there is an underlying assumption that the covariance structure of the data set can be adequately modelled using a two structure LMC. We consider an extension that removes the restriction imposed by this assumption by using the experimental matrices for a larger set of lags. The method relies on an iterative algorithm that approximately diagonalises a set of symmetric matrices, and is referred to as the Alternating Columns-Diagonal Centres method. We use the Jura data set to evaluate the extent to which factors obtained from each method are spatially decorrelated and to assess the effect of the transformation method on the simulated attributes.

E. M. Bandarian (✉)
Cyril Jackson Senior Campus, 53 Reid Street,
Bassendean, WA 6054, Australia
e-mail: ebandari@cyriljackson.wa.edu.au

U. A. Mueller · J. Fereira · S. Richardson
School of Engineering, Edith Cowan University,
270 Joondalup Drive, Joondalup, WA 6027, Australia
e-mail: u.mueller@ecu.edu.au

J. Fereira
e-mail: jferrer0@ecu.edu.au

S. Richardson
e-mail: s.richardson@ecu.edu.au

R. Dimitrakopoulos (ed.), *Advances in Applied Strategic Mine Planning*,
https://doi.org/10.1007/978-3-319-69320-0_24

Introduction

The simulation of one or more attributes in a multivariate data set is enhanced through the exploitation of the relationships between them. However, multivariate modelling and simulation can be time consuming and computationally inefficient. Some of the shortcomings of multivariate methods can be avoided by transforming the spatially correlated set of attributes into a set of spatially uncorrelated factors. These factors can then be modelled and simulated independently using univariate geostatistical methods. The oldest method for obtaining uncorrelated factors is principal component analysis (Wackernagel 2003). While this technique is easy to implement, the factors are uncorrelated for all distances other than zero only in the case of intrinsic correlation. In recent years the method of minimum/maximum autocorrelation factors (MAF) has received much attention as the factors are derived so that they are approximately spatially uncorrelated for all distances (Desbarats and Dimitrakopoulos 2000; Boucher and Dimitrakopoulos 2012). This method assumes that the data to be modelled are multivariate normal and so in most cases the first step is to normalise the data. While the method of direct minimum/maximum autocorrelation factors (DMAF) (Bandarian et al. 2008) removes the requirement of normality of the data and so simplifies the MAF procedure, one still requires the assumption of a two structure linear model of coregionalisation (2SLMC) in order to determine the transformation coefficients. Extensions of MAF to more than two structures are not possible (Vargas-Guzman and Dimitrakopoulos 2003), unless the model can be described as a nugget model together with an intrinsic spatial component (Tran et al. 2006). The use of a 2SLMC to derive the transformation matrix is largely of theoretical interest and while there are versions of MAF that work directly with the model (Bandarian 2008), in most implementations it is common to work with experimental matrices directly as proposed by Desbarats and Dimitrakopoulos (2000), thus cutting down on the effort spent in finding a reasonably well fitting 2SLMC. As a trade-off however time needs to be invested in choosing the lag spacing at which to calculate the experimental semi-variogram matrix. Whichever approach is chosen, be it theoretical or experimental, the factors calculated from the input data are only approximately spatially orthogonal.

Because of the restrictions in the MAF-method, a more general approach such as joint approximate diagonalisation (JAD) can be considered. JAD consists of finding a transformation matrix that will approximately diagonalize a set of matrices. These techniques have been developed for image-filtering and blind noise separation (see for example Yeredor (2002) and references therein). JAD algorithms for approximate diagonalisation of symmetric matrices can be broadly split into two categories: those that derive an orthogonal diagonalising matrix like that proposed by Manton (2005) and those that weaken the orthogonality constraint to non-singularity of the diagonaliser. The algorithm we will consider is of the latter type and is referred to as the Alternating Columns Diagonal Centres (ACDC) method (Yeredor 2000, 2002). For geostatistical applications the set to be jointly approximately diagonalised

consists of experimental semi-variogram matrices. The transformation matrix derived from this method will approximately spatially decorrelate the given attributes, in the sense that the cross correlations between distinct attributes are approximately equal to zero.

In the standard implementation, MAF is applied to normal scores data and the resultant factors are subsequently simulated. There is no theoretical requirement to apply MAF to standard normal data (Bandarian 2008) and we will be taking the approach to calculating the required transformation matrices from standardised raw data instead. The reason for this approach is partly the observation that the application of MAF to normal scores can result in transformed data that are no longer normally distributed, thus resulting in the need for a further normal scores transform if a Gaussian simulation algorithm is to be used.

In what follows, we present a brief review of the MAF and ACDC methods and illustrate them using a subset of the Jura data set (Goovaerts 1997). The transformations are calculated from the correlation matrix and semi-variogram matrices of standardised data. The factors resulting from each of the methods are transformed to normal scores in order to implement sequential Gaussian simulation (SGS). The normal scores simulations are back-transformed to factors, then to the original data space. The resultant simulations are assessed for reproduction of the spatial and statistical characteristics of the sample.

Problem Data

A four variable subset of the Jura data set (Goovaerts 1997) consisting of Cd, Co, Cr and Ni is used to illustrate each transformation method and the resultant simulations. Location maps (see Fig. 1) for the sample data show no obvious trends in the spatial distribution of the data. The sample data have quite disparate means and variances (see Table 1) and of the four metals, only Chromium is approximately normally distributed (Bandarian 2008). The sample correlation coefficients indicate varying strengths of linear relationships, with those between Cd–Cr, Co–Ni and Cr–Ni having the stronger correlations (Table 2). For stability of implementation the data are first standardised by subtracting the sample mean from each value then dividing by the sample standard deviation.

Multivariate Transformation Methods and Simulation

Let $\mathbf{Z}(\mathbf{u}) = [Z_1(\mathbf{u}), Z_2(\mathbf{u}), \ldots Z_K(\mathbf{u})]^T$ be a vector of K second-order stationary random functions over a study region A, let $z(u) = \left[z_1(\mathbf{u}_\alpha), z_2(\mathbf{u}_\alpha), \ldots z_K(\mathbf{u}_\alpha)\right]^T$, $\alpha = 1, \ldots n,$. be the corresponding isotopic sample vectors and let $\mathbf{B}$ denote the correlation matrix of the random function.

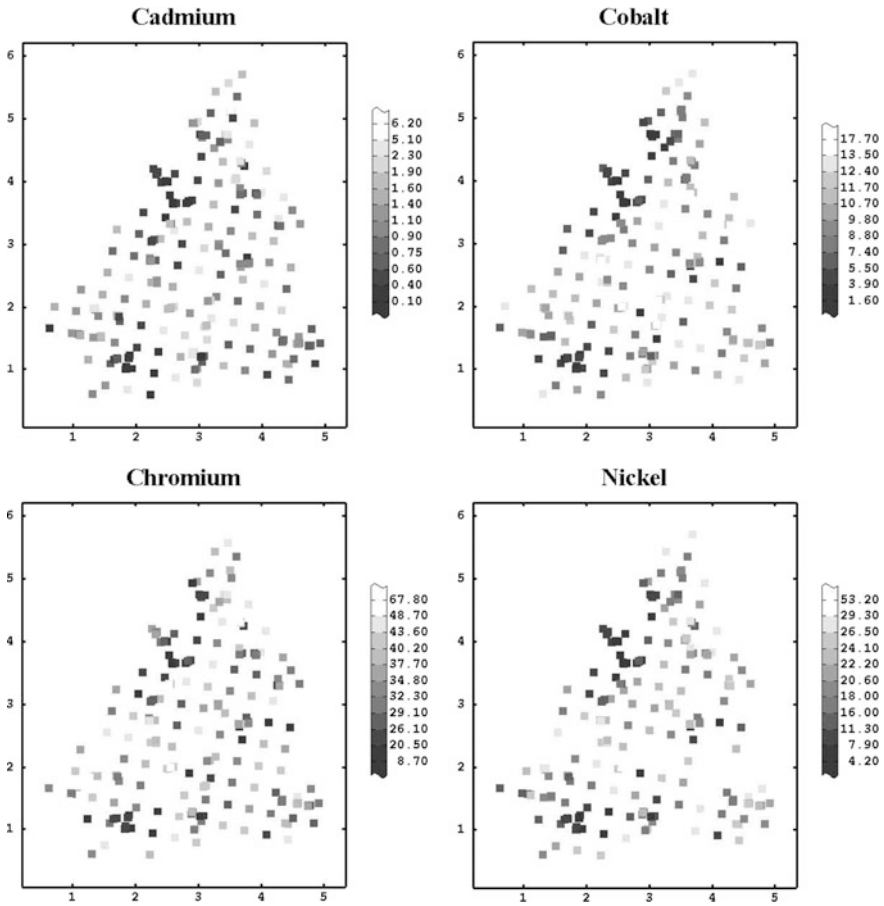

Fig. 1 Location maps for cadmium, cobalt, chromium and nickel. The colour scales are based on the deciles of the respective sample data

Table 1 Summary statistics for the input data, for each attribute there are 259 values

Variable	Mean	Variance	Skewness	Minimum	LQ	Median	UQ	Maximum
Cd	1.31	0.84	1.50	0.14	0.63	1.07	1.72	5.13
Co	9.30	12.79	−0.18	1.55	6.52	9.76	12.00	17.72
Cr	35.07	120.07	0.29	8.72	27.44	34.84	42.32	67.60
Ni	19.73	67.78	0.16	4.20	13.72	20.56	25.44	53.20

Table 2 Correlation matrix for sample data

Variable	Cd	Co	Cr	Ni
Cd	1.00	0.25	0.61	0.49
Co	0.25	1.00	0.45	0.75
Cr	0.61	0.45	1.00	0.69
Ni	0.49	0.75	0.69	1.00

The general procedure for applying transformation methods for multivariate simulation is:

Step 1 transform the data to approximately decorrelated factors,
Step 2 independently model and simulate factors, and
Step 3 back transform simulated factors to simulated attributes.

Step 1 includes the calculation of the transformation matrix from the data, in the case of MAF this requires in the first instance a decision what lag spacing to choose for the calculation of the experimental semi-variogram matrix, for ACDC a decision needs to be made as to how many semi-variogram matrices are to be included in the computation. In addition in step 1 an assessment needs to be made whether or not the resultant factors are sufficiently well decorrelated. Assuming the spatial decorrelation is satisfactory, then step 2 is only concerned with the univariate simulation of the factors. Either a direct simulation algorithm, such as the sequential simulation proposed by Soares (2001) or a standard Gaussian algorithm, such as Sequential Gaussian Simulation can be used. In the latter case a Gaussian anamorphosis will need to be carried out to compute normal scores for the factors. For both methods, Step 3 consists merely of the back transformation of the simulated factors via matrix multiplication. The resultant realisations are still standardised and so shifting and scaling to restore the appropriate mean and variance respectively concludes the workflow.

Minimum/Maximum Autocorrelation Factors

For MAF it is assumed that the semi-variogram function $\Gamma(\mathbf{h})$, of the multivariate random function $\mathbf{Z}(\mathbf{u})$ can be modelled by a two structure linear model of coregionalisation $\Gamma(\mathbf{h}) = \mathbf{B_1}g_1(\mathbf{h}) + \mathbf{B_2}g_2(\mathbf{h})$, where the symmetric coregionalisation matrices $\mathbf{B_1}$ and $\mathbf{B_2}$ contain the sills of the permissible semi-variogram models $g_1(\mathbf{h})$ and $g_2(\mathbf{h})$, and $\mathbf{B} = \mathbf{B}_1 + \mathbf{B}_2$ is the correlation matrix. Since $\mathbf{B}_1$ and $\mathbf{B}_2$ are symmetric (therefore diagonalisable) and $\mathbf{B}_2$ is *positive definite* (has positive eigenvalues), then $\mathbf{B_1}$ and $\mathbf{B}_2 = \mathbf{B}-\mathbf{B}_1$ may be diagonalised simultaneously by congruence (that is, there exists a non-singular matrix $\mathbf{X}$, not necessarily orthogonal, such that $\mathbf{S} = \mathbf{X^T A X}$) and the diagonalising matrix is the solution to the *symmetric definite generalised eigenvalue problem* (Datta 1995):

$$\mathbf{B}_1\mathbf{X} = (\mathbf{B} - \mathbf{B}_1)\mathbf{X}\boldsymbol{\Lambda}$$

The diagonal matrix Λ in the equation above is the matrix of *generalised eigenvalues* and the matrix $\mathbf{X}$ is the matrix of *generalised eigenvectors*. The equation may be rewritten as:

$$\mathrm{B}_1\mathbf{X} = \mathbf{B}\mathbf{X}\,\Lambda_1$$

where: $\Lambda_1 = \Lambda(\mathbf{I} + \Lambda)^{-1}$

The generalised eigenvalue problem may be converted into a standard eigenvalue problem with a symmetric matrix on the left hand side of the equation using the Cholesky factorisation of the matrix $\mathbf{B}$ where $\mathbf{B} = \mathbf{L}\mathbf{L}^T$ and $\mathbf{L}$ is a non-singular lower triangular matrix. If we put $\mathbf{G} = \mathbf{L}-1\mathbf{B}_1(\mathbf{L}^T)^{-1}$ and $\mathbf{Y} = \mathbf{L}^T\mathbf{X}$, then $\mathbf{GY} = \mathbf{Y}\Lambda_1$.

The matrix $\mathbf{G}$ is symmetric by construction and so orthogonally diagonalisable. The matrix $\mathbf{X}$ obeys $\mathbf{X}^T\mathbf{B}\mathbf{X} = \mathbf{Y}^T\mathbf{L}^{-1}\mathbf{B}(\mathbf{L}^T)^{-1}\mathbf{Y} = \mathbf{Y}^T\mathbf{L}^{-1}\mathbf{L}\mathbf{L}^T(\mathbf{L}^T)^{-1}\mathbf{Y} = \mathbf{Y}^T\mathbf{Y} = \mathbf{I}$ and the column vectors in $\mathbf{X}$ are $\mathbf{B}$-orthonormal, that is $\mathbf{X}^T\mathbf{B}\mathbf{X} = \mathbf{I}$. Furthermore, $\mathbf{X}^T\mathbf{B}_1\mathbf{X} = \mathbf{Y}^T\mathbf{L}^{-1}\mathbf{B}_1(\mathbf{L}^T)^{-1}\mathbf{Y} = \mathbf{Y}^T\mathbf{G}\mathbf{Y} = \Lambda_1$

Thus the non-singular matrix $\mathbf{X}$, whose columns are the generalised eigenvectors $\mathbf{x}_k$,k = 1, … K, simultaneously diagonalises the matrices $\mathbf{B_1}$ and $\mathbf{B}$ by congruence (Bandarian and Mueller 2008).

The MAF factors are derived by putting $\mathbf{F}_{MAF}(\mathbf{u}) = \mathbf{X}^T\mathbf{Z}(\mathbf{u})$.

Since the matrix $\mathbf{X}$ is $\mathbf{B}$-orthogonal the factor variances are equal to one and the transformation ensures that the factors $\mathbf{F}(\mathbf{u})$ are uncorrelated for all $|\mathbf{h}| \geq 0$ because:

$$\begin{aligned}\Gamma_F(\mathbf{h}) &= \mathbf{X}^T\Gamma(\mathbf{h})\mathbf{X} \\ &= \mathbf{X}_T\mathbf{B}_1\mathbf{X}g_1(\mathbf{h}) + \mathbf{X}^T(\mathbf{B}-\mathbf{B}_1)\mathbf{X}g_2(\mathbf{h}) \\ &= \Lambda_1 g_1(\mathbf{h}) + (\mathbf{I}-\Lambda_1)g_2(\mathbf{h})\end{aligned}$$

Hence $\Gamma_F(\mathbf{h})$ is diagonal for all $\mathbf{h}$.

The MAF transformation thus diagonalises the semi-variogram model of the attributes exactly. However, the associated experimental semi-variogr ams of the MAF-factors are only approximately diagonalised.

Where the theoretical LMC is not known the experimental semi-variogram matrices $\hat{\Gamma}(\cdot)$ are used to calculate the MAF transformation coefficients. Assuming that the semi-variogram function of $\mathbf{Z}(\mathbf{u})$ is fully characterised by a 2SLMC, an experimental semi-variogram $\hat{\Gamma}(h_1)$ matrix calculated at lag spacing $\mathbf{h}_1$ can be used to approximate $\Gamma(\mathbf{h})$ at $\mathbf{h}_1$. In this care the MAF transformation matrix is derived from the generalised eigenvalue problem reformulated in terms of the correlation matrix $\mathbf{B}$ and the experimental semi-variogram matrix $\hat{\Gamma}(h_1)$ at lag h_1 where $|\mathbf{h}_1| < a$ (a is the maximum range of the semi-variogram). Regardless of the suitability of the 2SLMC the transformation matrix X simultaneously diagonalises $\hat{\Gamma}(h_1)$ and $\mathbf{B}$ yielding factors which are orthogonal at lag spacings zero and $|\mathbf{h}_1|$ only.

A crucial assumption in the construction of the MAF factors is the requirement that the covariance structure of the underlying random function is fully characterised by a 2SLMC. This assumption is restrictive in practice and extensions to more general models have been discussed in the literature (see for example the discussion in Vargas-Guzman and Dimitrakopoulos (2003). However, in general, for three covariance structures or more there exists a matrix $\mathbf{X}$ that diagonalises the variogram only when all but (at most) one of the coefficient matrices in the LMC are proportional to one another (Tran et al. 2006; Bandarian 2008).

Alternating Columns Diagonal Centres

The Alternating Columns Diagonal Centres (ACDC) method (Yeredor 2002, 2004) iteratively determines a matrix $\mathbf{X}$ that diagonalises a set of J symmetric $K \times$ K matrices $\{\mathbf{B}_1,\mathbf{B}_2, \ldots, \mathbf{B}_J\}$

By minimising:

$$\Psi(\mathbf{X}\mathbf{D}_1, \mathbf{D}_2, \ldots, \mathbf{D}_J) = \sum_{j=1}^{J} W_j \left\| B_j - \mathbf{X}\mathbf{D}_j\mathbf{X}^T \right\|_F^2,$$

where $\| \cdot \|_F$·denotes the Frobenius norm, $w_j > 0$, $j = 1, \ldots J$ are (optional) weights and $\{\mathbf{D}_1,\mathbf{D}_2, \ldots, \mathbf{D}_J\}$ is a set of diagonal matrices. The algorithm consists of alternating phases, the AC phase, where the objective function is minimised with respect to the columns of $\mathbf{X}$ while the set $\{\mathbf{D}_1,\mathbf{D}_2, \ldots, \mathbf{D}_J\}$ is kept fixed and the DC phase, where the objective is minimised with respect to $\{\mathbf{D}_1,\mathbf{D}_2, \ldots, \mathbf{D}_J\}$ while $\mathbf{X}$ is kept fixed.

Given $\{\mathbf{B}_1,\mathbf{B}_2, \ldots, \mathbf{B}_J\}$ the algorithm is initialised by specifying either an initial set of diagonal matrices $\{\mathbf{D}_1,\mathbf{D}_2, \ldots, \mathbf{D}_J\}$ or an estimate of the diagonalising matrix $\mathbf{X}$. The initial phase in the iteration is dependent on the specification made: if an initial guess for the diagonalising matrix is made, then the algorithm starts with a DC phase, otherwise the starting point is an AC phase. In the absence of either specification the diagonalising matrix is set to the identity matrix and the algorithm is initialised with a DC phase. Thus the standard iterations are as follows:

given $\{\mathbf{B}_1,\mathbf{B}_2, \ldots, \mathbf{B}_J\}$,

put $\hat{\mathbf{X}} = \mathbf{I}$.

DC Phase

1. Set $\mathbf{G} = \left[\hat{\mathbf{X}}^{\mathrm{T}}\mathbf{X} \otimes \hat{\mathbf{X}}^{\mathrm{T}}\mathbf{X}\right]^{-1}$
2. For $j = 1,\ldots J$

   Set $\hat{\mathbf{D}}_j = diag\left(\mathbf{G}\, diag\left(\hat{\mathbf{X}}^T\mathbf{B}_\mathbf{j}\hat{\mathbf{X}}\right)\right)$.

AC Phase

For $k = 1,\ldots K$

1. $Set\ P = \sum_{j=1}^{J} W_j \hat{\lambda}_k^{[j]} \left[\boldsymbol{B}_j - \sum_{\substack{n=1 \\ n \neq k}}^{k} \hat{\lambda}_n^{[k]} \hat{\mathbf{X}}_n \hat{\mathbf{X}}_n^T \right]$
2. Find the largest eigenvalue μ of P and an associated eigenvector of unit norm.
3. If $\mu < 0$ set $\hat{\mathbf{x}}_k = 0$ otherwise put $\hat{\mathbf{x}}_k = \frac{a\sqrt{\mu}}{\sqrt{\sum_{j=1}^{J} W_j \left(\hat{\lambda}_k^{[j]}\right)^2}} \kappa$.

The algorithm alternates between the two phases and halts once a prespecified tolerance has been reached. The algorithm is applied to a sequence of semi-variogram matrices, calculated at increasing distance from the origin. There are no requirements other than real symmetry of the matrices. If X denotes the matrix that approximately diagonalises the given semi-variogram matrices then the ACDC factors are derived putting $\boldsymbol{F}_{ACDC}(\mathbf{u}) = \mathbf{X}^{-1}\mathbf{Z}_{(\mathbf{u})}$. Thus for both methods the factors are derived using a linear transformation, however neither of thematrices is orthogonal, as would be the case for PCA. The transformations are both local transformations, in that they act on the attributes at each location, but the matrix coefficients are constant across the entire study region. Provided the factor scores are sufficiently spatially orthogonal the factors may be independently modelled and simulated. In this paper, a standard Gaussian algorithm will be used for the factors. As a first step the factors are transformed to normal scores (Gaussian anamorphosis), then they are independently modelled and simulated using Sequential Gaussian Simulation (100 realisations). The simulated attribute scores are retrieved via Gaussian anamorphosis from normal scores to factor scores, then from factor scores to standardised scores using the inverse MAF and ACDC transformation matrices. Finally the sample means and standard deviations are reincorporated.

Performance

Spatial Decorrelation

The quality of the spatial decorrelation of the factors will be assessed both graphically and numerically. For a graphical assessment the cross semi-variogram for each factor pair will be graphed in order to detect any remaining spatial correlation. Quantitative measures (Tercan 1999) used to assess spatial decorrelation are the absolute deviation from diagonality $\zeta(\mathbf{h})$, the relative deviation from diagonality $\tau(\mathbf{h})$, and the spatial diagonalisation $K(\mathbf{h})$.

The absolute deviation from diagonality, $\zeta(\mathbf{h})$ at lag $\mathbf{h}$ is define dto be the sum of squares of the off-diagonal elements of the factor experimental semi-variogam matrix at lag $\mathbf{h}$:

$$\zeta(\mathbf{h}) = \sum_{k=1}^{K} \sum_{j \neq k}^{K} \left(\hat{\Upsilon}_F(\mathbf{h}; k, j)\right)^2 |\mathbf{h}| > 0$$

where $\hat{\gamma}_F$ (., k, j) denotes the experimental cross-semi-variogram for the factors *Fj* and *F*κ.

The function $\tau(\mathbf{h})$ compares the absolute sum of off-diagonal elements of the factor experimental semi-variogram matrix $\hat{\Gamma}_F(\mathbf{h})$ with the sum of the absolute values of the diagonal elements calculated at each lag **h**:

$$\tau(\mathbf{h}) = \frac{\sum_{k=1}^{K} \sum_{j \neq k}^{K} \left| \hat{\Upsilon}_F(\mathbf{h}; k, j) \right|}{\sum_{k=2}^{K} \left| \hat{\Upsilon}_F(\mathbf{h}; k, k) \right|}, |\mathbf{h}| > 0$$

Finally, the function $K(\mathbf{h})$ compares the sum of squares of the off diagonal elements of the factor experimental semi-variogram matrix $\hat{\Gamma}_F(\mathbf{h})$ at a lag **h** to the sum of squares of the off diagonal elements of the sample experimental semi-variogram matrix $\hat{\Gamma}_z(\mathbf{h})$:

$$k(\mathbf{h}) = 1 \frac{\sum_{k=1}^{K} \sum_{j \neq k}^{K} \hat{\Upsilon}_F(\mathbf{h}; k, j))^2}{\sum_{k=1}^{K} \sum_{j \neq k}^{K} (\hat{\Upsilon}_2(\mathbf{h}; k, j))^2}, |\mathbf{h}| > 0$$

Perfect spatial decorrelation occurs when $\zeta(\mathbf{h}) = r(\mathbf{h}) = 0$ and $\kappa\ \mathbf{h}) = 1$ for all lag vectors **h**. A set of factor semi-variogram matrices may be considered to be nearly in diagonal form if $\kappa(\mathbf{h}) \geq 0.9$ for all **h** lags (Xie et al. 1995).

Global measures for the spatial decorrelation are the averages $\bar{\zeta}, \bar{\tau}$ and $\bar{K}$ calculated over *J* lag spacings:

$$\bar{\zeta} = \frac{1}{J} \sum_{j=1}^{J} \zeta(\mathbf{h}_j), \bar{\tau} = \frac{1}{J} \sum_{j=1}^{J} \tau(\mathbf{h}_j) \text{ and } \bar{K} = \frac{1}{J} \sum_{j=1}^{J} k(\mathbf{h}_j)$$

Simulations and Reproduction of Sample Characteristics

For each attribute, the suite of realisations is assessed for reproduction of the attribute (target) histogram, semi-variogram, mean, variance and correlation coefficients. Qualitative analysis consists of visual inspection of the histogram and semi-variogram swarms of the realisations and boxplots of the realisation means, variances and correlation coefficients about the target statistic.

Quantitative measures for the reproduction of the target statistics are the semi-variogram and histogram mean square deviation (VMSD and HMSD respectively) which are calculated for each realisation. The HMSD is given by:

$$HMSD = \sqrt{\frac{1}{P}\sum_{p=1}^{P}(Z_p - Z_p^1)^2}$$

where:

Z_p is the pth percentile of the target cumulative distribution function (cdf)
Z_p^l is the pth percentile of the lth simulated cdf
P denotes the total number of percentiles calculated

The VMSD is given by:

$$VMSD = \sqrt{\frac{1}{J}\sum_{j=1}^{J}(\hat{\Upsilon}_j - \hat{\Upsilon}_j^1)^2}$$

where $\hat{\Upsilon}_j$ *and* $\hat{\Upsilon}_j^1$ and are the target and the simulated experimental semi-variogram values respectively calculated at the jth lag spacing and J is the total number of lags.

Results and Analysis

Transformations

For ACDC, the set of target matrices consists of thirteen experimental semi-variogram matrices calculated at a lag spacing of 0.2 km with a lag tolerance of 50%. The weight vector was set to be $\mathbf{w} = [10\ 10\ 1\ \ldots\ 1]^T$. The transformation matrix is:

$$\mathbf{X}_{ACDC}^{-1} = \begin{bmatrix} 0.841 & -0.048 & -0.289 & -0.152 \\ 0.049 & 0.782 & 0.525 & -0.811 \\ -0.382 & -1.045 & 1.247 & 0.457 \\ 0.132 & 0.121 & -0.966 & 1.939 \end{bmatrix}$$

The MAF transformation matrix, shown is obtained using the sample correlation matrix **B** and an experimental semi-variogram

matrix $\hat{\Gamma}(\mathbf{h})_1$, calculated at $|\mathbf{h}|_1 = 0.220$ km:

$$\mathrm{X}_{MAF}^{T} = \begin{bmatrix} -1.082 & 0.215 & -0.036 & 0.288 \\ -0.663 & -0.934 & 1.005 & 0.695 \\ -0.114 & 1.062 & 1.062 & -1.493 \\ -0.152 & -0.305 & 0.485 & -0.955 \end{bmatrix}$$

This spacing was chosen from a set of separation distances as it provided the best overall decorrelation for the MAF (Bandarian 2008).

The cross semi-variograms for each factor set are displayed in Fig. 2. For ACDC the spatial decorrelation is excellent with the majority of cross semi-variogram values satisfying $-0.15 \leq \Upsilon_{ik}(\mathbf{h}) \leq 0.15$. For this method there are only three instances where the factor pairs still show some correlations. For MAF, as expected, the spatial decorrelation is perfect at $|\mathbf{h}_1| = 0.220$ km, while for other lag spacings the semi-variogram values are typically $-0.2 \leq \Upsilon_{ik}(\mathbf{h}) \leq 0.2$ (with the exception of factors 2 and 4 at $|\mathbf{h}_1| = 1.199$ km). These results are summarised in Table 3.

Plots of the measures of spatial decorrelation $(\zeta(\mathbf{h}), \tau(\mathbf{h})\ and\ \kappa(\mathbf{h}))$ are displayed in Fig. 3 and the corresponding averages of these measures for all lags (0.037 to 2.407 km inclusive) and for the lower lags (0.037 to 1.199 km inclusive) are shown in Table 4.

The plots of $(\zeta(\mathbf{h}), \tau(\mathbf{h})\ and\ \kappa(\mathbf{h}))$ reflect the excellent spatial decorrelation achieved by ACDC, which outperforms MAF for all lag spacings other than 0.220 km. The average diagonalisation efficiency for ACDC is 0.975 for all lags

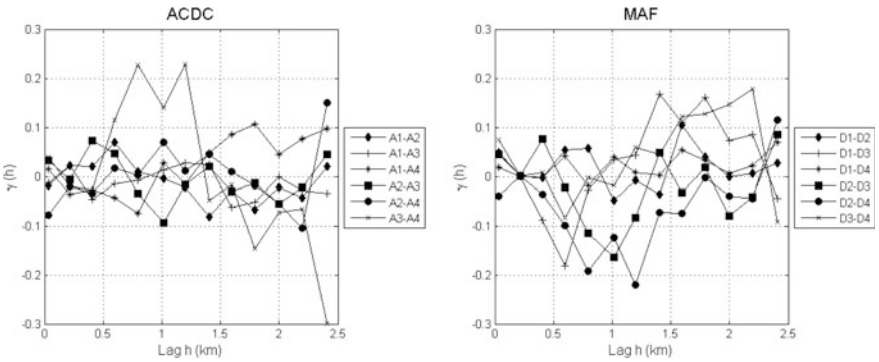

Fig. 2 Experimental cross semi-variograms of factors

Table 3 Summary of factor pairs with remaining spatial correlation

Method	Factor pairs	Lag spacing (km)	γ_{ik}
AC-DCAC-DC	A_3 –A_4	0.797	0.227
		1.199	0.228
		2.407	−0.300
MAF	D_1–D_3	0.595	−0.182
		1.405	0.168
		1.795	0.160
	D_2–D_3	1.012	−0.163
	D_2–D_4	0.797	−0.182
		1.199	−0.221
	D_3–D_4	2.196	0.178

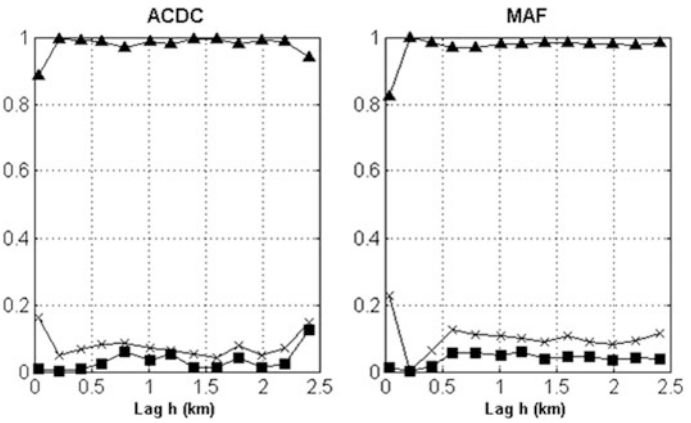

Fig. 3 Plots of spatial decorrelation (ζ(h): ▬ ,τ(h): * and κ(h): ▲)

Table 4 Average ξ(***h***),τ(***h***) and κ(***h***) for all lags and lower lags (0.037 km to 1.199 km inclusive)

	All			Lower		
	ξ(**h**)	τ(h)	κ(h)	ξ(h)	τ(h)	κ(h)
ACDC	0.065	0.157	0.975	0.055	0.166	0.970
MAF	0.076	0.202	0.968	0.071	0.201	0.957

and 0.97 for the lower lags, which is slightly higher than that achieved by MAF where the values are 0.97 for all lags and 0.96 for the lower lags.

The factor scores from each method are transformed to normal scores using a Gaussian anamorphosis with 50 Hermite polynomials to approximate the factor histograms, independently modelled then simulated using SGS. In order to avoid spurious correlations resulting from the use of the same random paths for each factor, the random number seeds were changed, so that corresponding factors for the two methods used the same seed, but within the simulation of the factors the seeds were distinct. The simulated attribute scores are retrieved via back transformation from normal scores to factor scores, then from factor scores to standardised scores using the inverse ACDC and MAF transformation matrices:

$$\mathbf{X}_{ACDC} = \begin{bmatrix} 1.258 & 0.416 & 0.277 & 0.207 \\ -0.189 & 1.024 & -0.131 & 0.4445 \\ 0.215 & 0.862 & 0.660 & 0.222 \\ 0.033 & 0.337 & 0.318 & 0.585 \end{bmatrix}$$

$$\left(\mathbf{X}_{MAF}^{T}\right) = \begin{bmatrix} -0.926 & -0.247 & -0.094 & -0.271 \\ 0.030 & 0.009 & -0.471 & -0.882 \\ -0.382 & -0.592 & -0.691 & -0.164 \\ -0.121 & -0.621 & -0.229 & -0.740 \end{bmatrix}$$

Finally the sample means and standard deviations are reincorporated.

Simulations

Mosaic maps for one of the realisations (picked at random) generated for each metal are shown in Fig. 4. The mosaic maps are broadly similar. The spatial variability of the sample data has been reproduced in the simulation.

Reproduction of the Target Statistics

The realisation cdf swarms overlaid with the corresponding sample cdf for each attribute and transformation method indicate that the attribute distributions have generally been reproduced (see Fig. 5). The most notable deviation from the target cdf occurs for Co. For both methods the Co target cdf is poorly reproduced on the interval from approximately 4–6 ppm with the realisation swarms being consistently lower than the target cdf. This is more pronounced for ACDC than for MAF.

Boxplots of the HMSDs for each set of attribute realisations (Fig. 6) reflect the overall reproduction of the target cdfs. For Cd and Co the HMSDs from MAF are slightly lower than those for ACDC, for Ni and Cr, the situation is reversed. For Cd the HMSDs are higher for ACDC than those for MAF, with the former having 75% of values less than 0.209 while the latter has 75% of values less than 0.160. The distribution of HMSDs for Co is similar for both methods although those for MAF are generally slightly lower than for ACDC. For Cr the HMSDs for ACDC are typically lower than those for MAF with the former having 75% of values less than

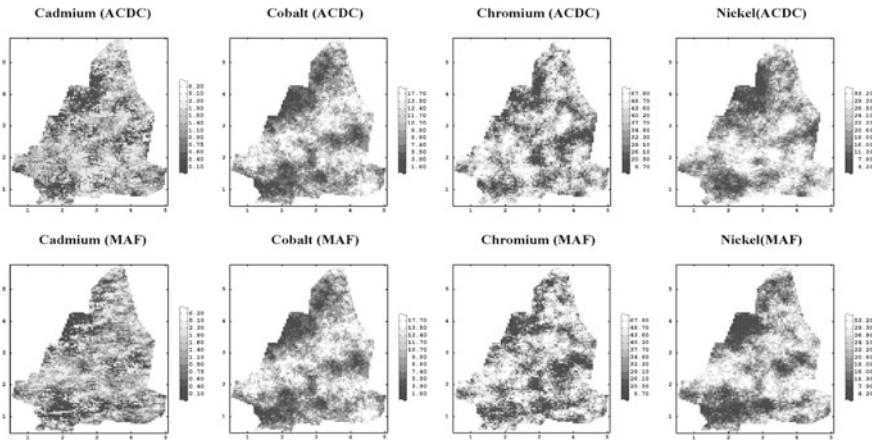

Fig. 4 Mosaic maps of realisation 25 for Cd, Co, Cr and Ni

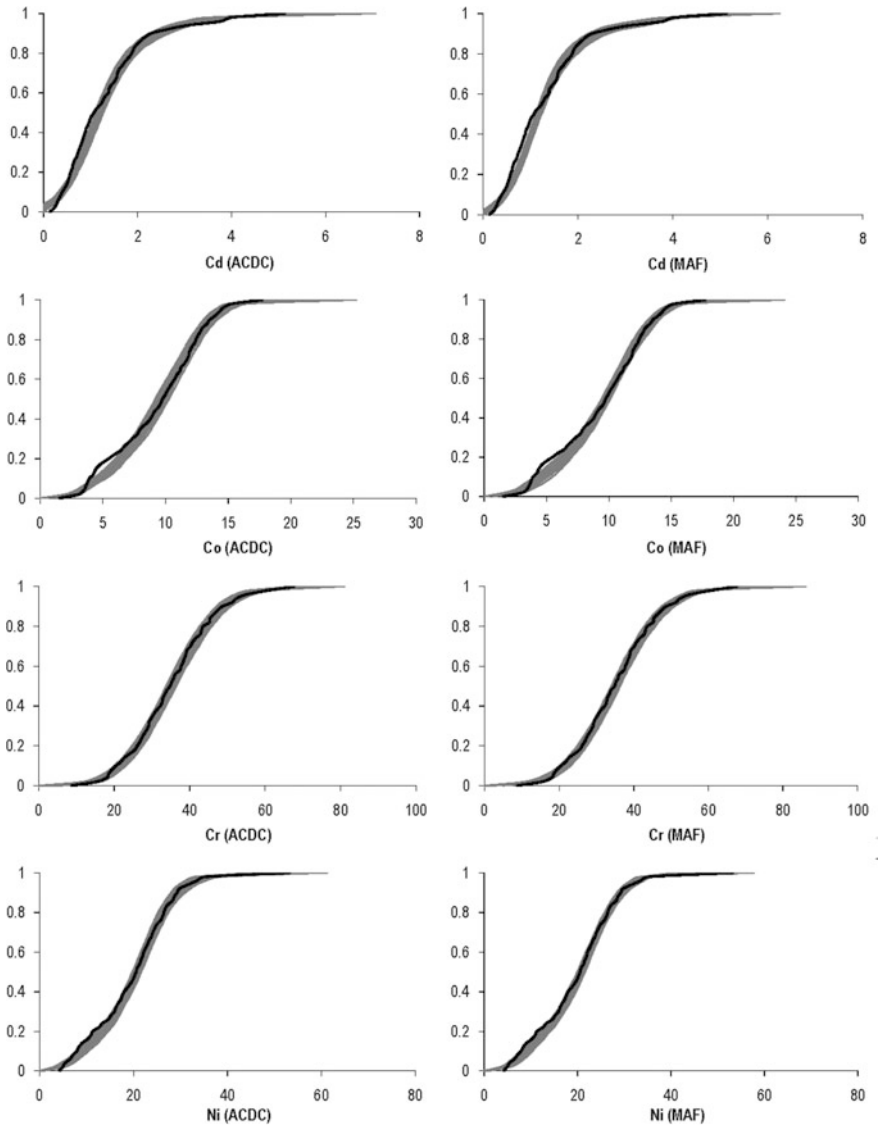

Fig. 5 Histogram swarms

2.007 while the latter has 75% of values less than 2.238. Similarly for Ni where ACDC has 75% of values less than 1.385 while MAF has 75% of values greater than 1.507.

Figure 7 displays the boxplots of the realisation summary statistics. For both methods and all attributes the target means have been reproduced with the majority of realisation means being within ±5% of the target. For Cd, ACDC and MAF 80

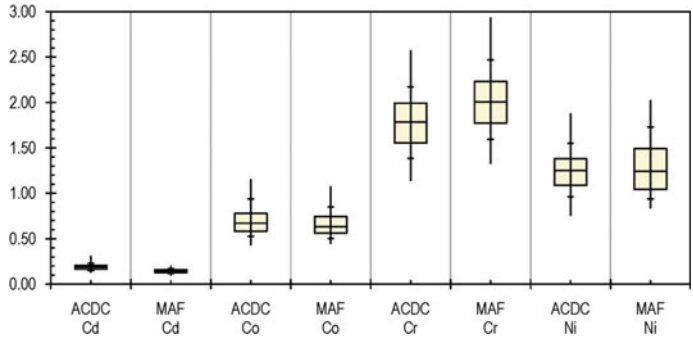

Fig. 6 Boxplots of histogram mean square deviation

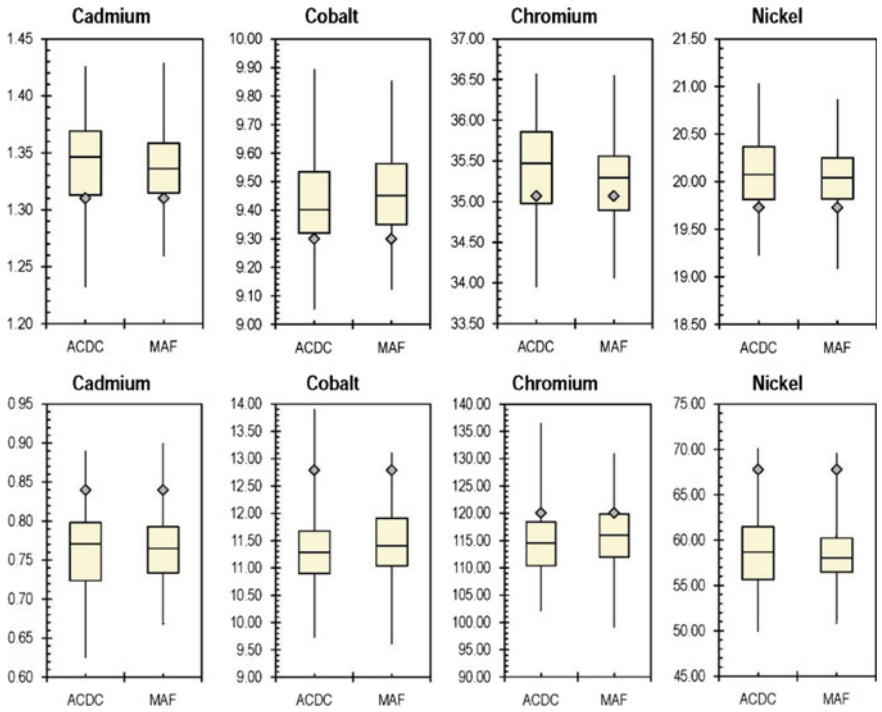

Fig. 7 Boxplots of realisation means and variances

and 84% of realisation means respectively lie within ±5% of the target. For Co this increases to 98 and 97% respectively while for Ni the percentages are 96 and 97% respectively. For Cr the realisation means are within ±5% of the target for both methods. The MSD of the means for each attribute (Table 5) are generally lower for MAF, with the exception of Co where ACDC is lower.

Table 5 Mean squarev deviation of realisation means and variances

MSD		Cd	Co	Cr	Ni
Means	AC–DC	0.051	0.198	0.673	0.527
	MAF	0.045	0.223	0.515	0.462
Variances	AC–DC	0.091	1.635	8.198	9.827
	MAF	0.088	1.485	7.439	9.974

Reproduction of the target variances is similar for both methods. In general the realisation variances are lower than the corresponding targets, however the majority of realisation variances are within ±15% of the target for both methods. For ACDC Cd, Co, Cr and Ni have 84, 78, 100 and 62% of realisation variances within ±15% of the target respectively. For MAF these percentages are 86, 84, 98 and 58% respectively. The MSD of the variances for each attribute (Table 5) are generally lower for MAF, with the exception of Ni where ACDC is lower.

Reproduction of the target correlation coefficients (see Fig. 8) between attributes is similar for both methods. With the exception of Cd–Co the targets have been reproduced with the majority of realisation correlations being within ±10% of the target. For Cd–Cr, Co–Ni and Cr–Ni in excess of 96% of realisation correlations are within ±10% of the target for both methods. For Cd–Ni the percentages are 78 and 75% for ACDC and MAF respectively, while for Co–Cr they are 84 and 69% respectively. For Cd–Co the target correlation coefficient has not been reproduced by either method, although to a lesser extent for ACDC than for MAF. ACDC yields 27% of realisation correlations within ±10% of the target while for MAF

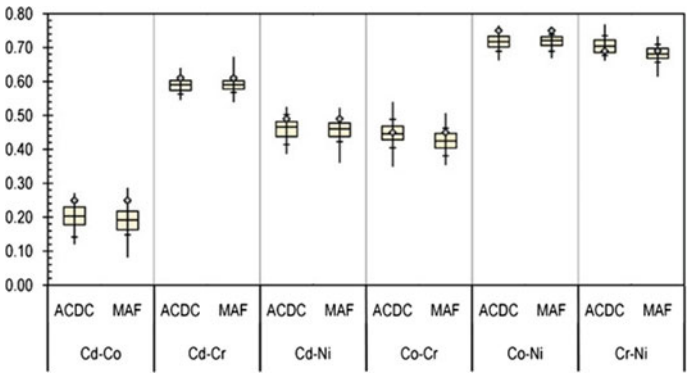

Fig. 8 Boxplots of realisation correlation coefficients

Table 6 Mean square deviation of correlation coefficients

MSD		Cd–Co	Cd–Cr	Cd–Ni	Co–Cr	Co–Ni	Cr–Ni
Correlations	AC–DC	0.065	0.029	0.040	0.035	0.040	0.026
	MAF	0.072	0.028	0.041	0.043	0.038	0.024

this percentage is only 19%. The MSD of the correlations for each attribute pair (Table 6) are similar for both methods, with ACDC being slightly lower for Cd–Co, Cd–Ni and Co–Cr while for the remaining attribute pairs MAF is slightly lower.

Reproduction of the Target Variograms

Experimental semi-variograms for the MAF and ACDC simulations in Fig. 9 indicate that both approaches have resulted in adequate reproduction of the experimental sample semi-variograms. The variograms swarms are similar for both transformation methods for each attribute and attribute pair.

In general the direct semi-variograms have been reproduced with the overall shapes, ranges, nuggets and sills of the simulations being similar to those of the target variograms. The most notable exception to this is the nugget for Cd (both transformations) where the target is somewhat lower than those of the simulations.

For the cross semi-variogram swarms, the simulations obtained from both transformation methods are again similar. In general, the target cross semi-variograms have been reproduced (Fig. 10) with respect to the overall shapes, nuggets and sills (except Cd–Co where the target sill is underestimated in both cases). With the exception of Cd–Cr the target ranges have been overestimated. For Co–Ni, the cross semi-variogram swarm from ACDC reproduces the target cross semi-variogram slightly better than the swarm resulting from MAF, in particular for lag distances between 1 and 1.5 km. However, for both methods the cross semi-variograms have lower sills than the experimental data. This is also featured in the correlation coefficients for this attribute pair, for Co and Ni the correlation at lag 0 is lower than that of the target.

The overall reproduction of the direct and cross semi- variograms is reflected by the low values of the VMSDs for all attributes and attribute pairs for both transformation methods (Table 7 and 8). The majority of VMSDs are less than 0.15, with the exception of those for Co–Ni where the majority of VMSDs are less than 0.2. The distribution of VMSD values is generally similar for each transformation method, with results for ACDC slightly better than for MAF.

For both ACDC and MAF, the transforms are constructed from omnidirectional semi-variogram matrices. Of the data under consideration Ni and Co exhibit anisotropy with direction of greatest continuity approximately E–W for Ni and SW–NE for Co. A comparison of the average experimental semi-variograms of the simulations and the standardised Co data indicates that both methods capture the anisotropy and that there is almost no difference in the average directional variograms calculated from the realisations (Fig. 11). Similarly for Ni, the average experimental semi-variograms reproduce the E–W anisotropy (Fig. 12). For Cr and Cd, the average semi-variograms show the realisations to be isotropic. Thus at the univariate level, the spatial features of the raw data are broadly reproduced, even though the spatial decorrelation methods were based on omnidirectional semi-variogram matrices.

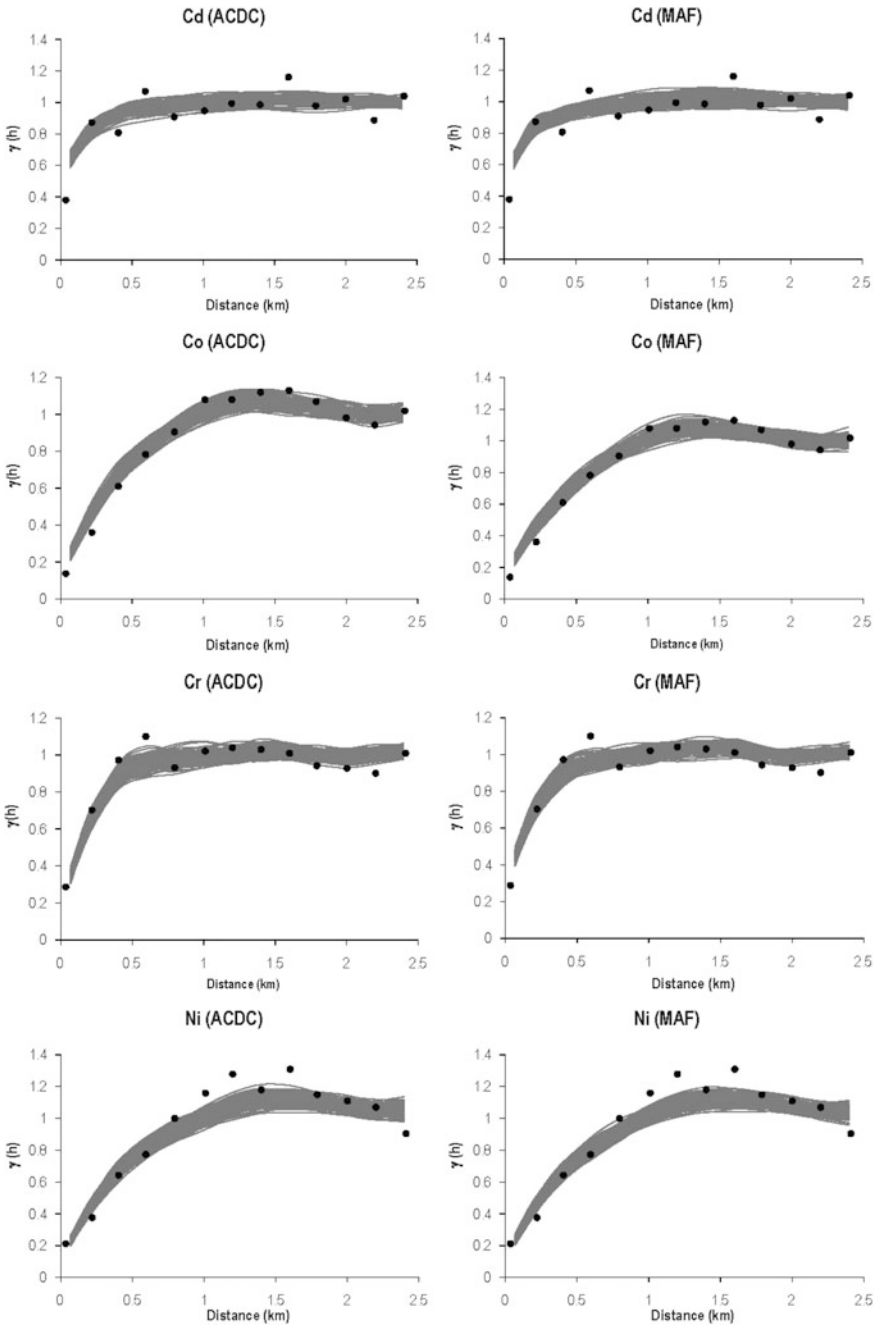

Fig. 9 Experimental semi-variogram swarms (grey lines) and corresponding targets (•)

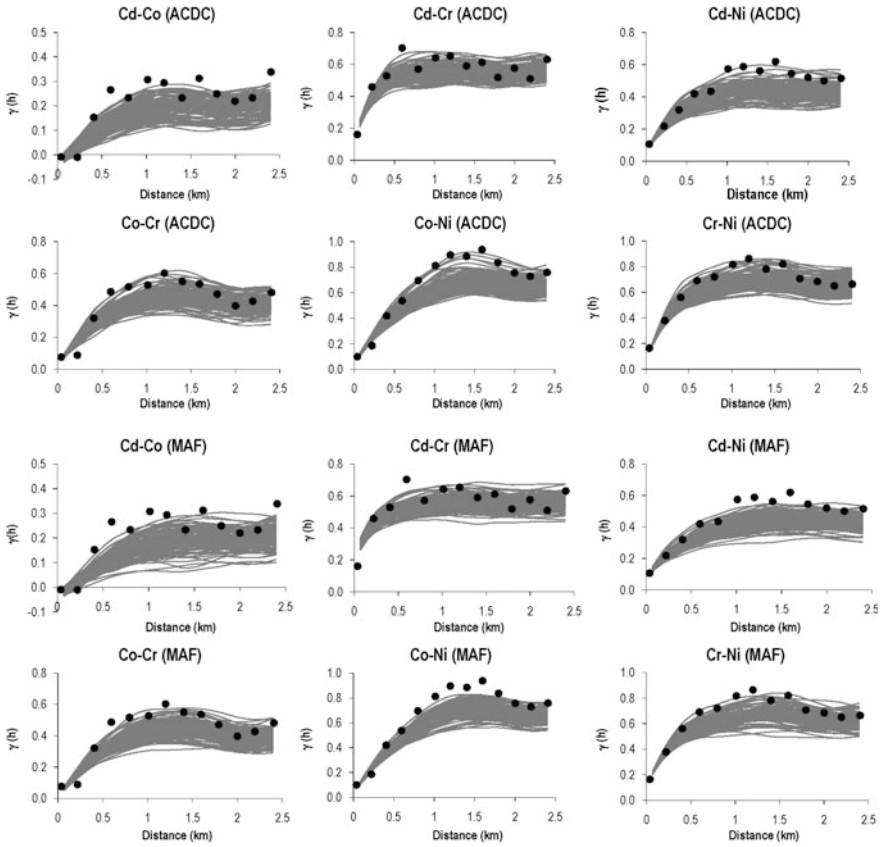

Fig. 10 Experimental cross semi-variogram swarms (grey lines) and corresponding targets (•)

Table 7 Mean square deviation of semi-variogram values

	ACDC				MAF			
	Cd	Co	Cr	Ni	Cd	Co	Cr	Ni
Min	0.098	0.043	0.049	0.064	0.096	0.04	0.061	0.071
Lq	0.104	0.055	0.06	0.097	0.101	0.049	0.072	0.096
Med	0.108	0.062	0.066	0.109	0.104	0.056	0.076	0.106
Uq	0.111	0.07	0.073	0.122	0.108	0.064	0.08	0.117
Max	0.118	0.09	0.095	0.15	0.115	0.087	0.091	0.149
Mean	0.108	0.063	0.068	0.109	0.105	0.057	0.076	0.106
Variance	0	0	0	0	0	0	0	0

Table 8 Mean square deviation of cross-semi-variogram values

	Cd-Co (ACDC)	Cd-Co (MAF)	Cd-Cr (ACDC)	Cd-Cr (MAF)	Cd-Ni (ACDC)	Cd-Ni (MAF)	Co-Cr (ACDC)	Co-Cr (MAF)	Co-Ni (ACDC)	Co-Ni (MAF)	Cr-Ni (ACDC)	Cr-Ni (MAF)
Min	0.039	0.043	0.054	0.062	0.033	0.039	0.044	0.041	0.041	0.062	0.041	0.045
Lq	0.069	0.074	0.067	0.072	0.079	0.08	0.068	0.075	0.121	0.112	0.077	0.091
Med	0.083	0.088	0.08	0.081	0.101	0.102	0.085	0.093	0.141	0.137	0.098	0.108
Uq	0.111	0.108	0.094	0.099	0.128	0.12	0.101	0.111	0.171	0.164	0.12	0.126
Max	0.146	0.175	0.137	0.158	0.182	0.205	0.17	0.184	0.226	0.238	0.179	0.216
Mean	0.088	0.093	0.083	0.086	0.104	0.103	0.088	0.097	0.143	0.138	0.098	0.109
Variance	0.001	0.001	0	0	0.001	0.001	0.001	0.001	0.002	0.001	0.001	0.001

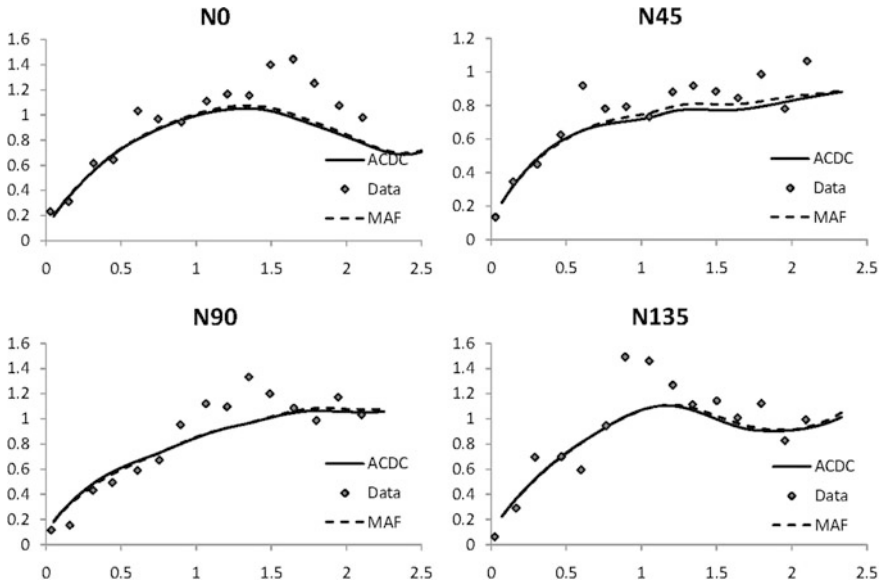

Fig. 11 Directional experimental semi-variograms for standardised cobalt compared to mean directional semi-variograms for Alternating Columns Diagonal Centres simulations and minimum/maximum autocorrelation factors simulations

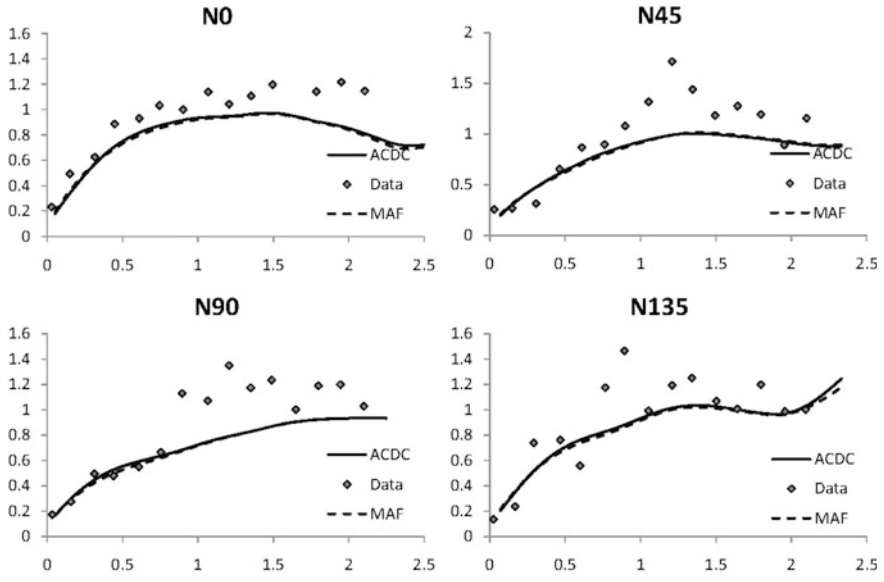

Fig. 12 Directional experimental semi-variograms for standardised nickel compared to mean directional semi-variograms for Alternating Columns Diagonal Centres simulations and minimum/maximum autocorrelation factors simulations

Similarly, an inspection of the directional cross-semivario-grams for Co and Ni and the corresponding realisations reinforces the observations from the omnidirectional cross-semivariogram swams. There is good coincidence between the average experimental cross variograms for both sets of realisations and the corresponding data cross-variograms for shorter separation distances, while for distances between 1 and 1.5 km the sills in directions SW–NE and E–W do not reach the data sills, in direction SE–NW the averages fit well.

Conclusion

In this study, we have presented two approaches to the simulation of a multivariate data set which rely on successful spatial decorrelation of the raw data, standardised to unit variance and mean zero, prior to simulation. The approach differs from the standard approach in that the data were not transformed to normal scores prior to the application of the decorrelation algorithms. However, in contrast to the implementation in Bandarian (2008), rather than using a direct sequential simulation algorithm, the factors were simulated using sequential Gaussian simulation. Thus, it was necessary to the convert each factor to normal scores and back-transform after completion of the simulations, the latter operation being automatic in sequential Gaussian simulation. The choice of a standard algorithm was largely prompted by its ready availability in commercial software, even though the need to use a non-linear transformation may well be regarded as a disadvantage.

The data used for our study were a subset of the Jura data set and the variables chosen are linearly correlated, an aspect which is important as it is known that MAF does not cope well with non-linear relationships between the data (see for example Rondon and Tran 2008). The four variables in our subset provided a mix of isotropic and anisotropic data, making the use of an algorithm such as sequential Gaussian co-simulation unattractive as a parsimonious model of coregionalisation would have had to be chosen for the simulation. For both methods the anisotropy in the data is broadly reproduced, both at the univariate and the bivariate level, even though omnidirectional semi-variogram matrices were used for the derivation of the factor transformations.

The results show that both decorrelation methods are viable for the simulation of the Jura data set. The results indicate that ACDC performs at least as well as MAF for this set. Both decorrelation methods considered use approximate diagonalisation via a congruence transformation. The main difference lies in the assumption that a 2SLMC describes the LMC for the data in the case of MAF, which is not needed for ACDC. The ACDC method thus gives the user greater flexibility and is as easy to use as the MAF decorrelation method. Given the performance for the Jura data, the ACDC method for decorrelation has the potential to be used successfully with data sets whose LMC is not fully characterised by two structures.

References

Bandarian EM (2008) Linear transformation methods for multivariate geostatistical simulation. Ph. D. thesis (unpublished), Edith Cowan University, Perth

Bandarian EM, Bloom LM, Mueller UA (2008) Direct minimum/maximum autocorrelation factors for multivariate simulation. Comput Geosci 34:190–200

Bandarian EM, Mueller UA (2008) Reformulation of MAF as a generalised eigenvalue problem. In: Ortiz J, Emery X (eds) Proceeding of the eighth international geostatistics congress, pp 1173–1178

Boucher A, Dimitrakopoulos R (2012) Multivariate block-support simulation of the Yandi iron ore deposit, Western Australia. Math Geosci 44(4):449–468

Datta BN (1995) Numerical linear algebra and applications. Brookes/Cole Publishing Company, Pacific Grove

Desbarats JA, Dimitrakopoulos R (2000) Geostatistical simulation of regionalized pore-size distributions using min/max autocorrelation factors. Math Geol 32(8):919–942

Goovaerts P (1997) Geostatistics for natural resources evaluation. Oxford University Press, New York, p 483

Manton JH (2005) A centroid (Karcher mean) approach to the joint approximate diagonalisation problem: the real symmetric case. Digit Signal Process 16(5):465–478

Rondon O, Tran TT (2008) Multivariate simulation using min/max autocorrelation factors: practical aspect and case studies in the mining industry. In: Ortiz J, Emery X (eds) Proceedings of the eighth international geostatistics congress, pp 269–278

Soares A (2001) Direct sequential simulation and cosimulation. Math Geol 31(2):155–173

Tercan AE (1999) Importance of orthogonalization algorithm in modelling conditional distributions by orthogonal transformed indicator methods. Math Geol 31(2):155–174

Tran TT, Murphy, M, Glacken I (2006) Semivariogram structures used in multivariate conditional simulation via minimum/maximum autocorrelation factors In: Proceedings XI international congress, IAMG, Liege

Vargas-Guzman JA, Dimitrakopoulos R (2003) Computational properties of min/max autocorrelation factors. Comput Geosci 29:715–723

Wackernagel H (2003) Multivariate geostatistics, 3rd revised edn. Springer, Berlin, 387 pp

Yeredor A (2000) Approximate joint diagonalization using non-orthogonal matrices. In: Proceedings international workshop on independent component analysis and blind source separation (ICA2000), pp 33–38

Yeredor A (2002) Non orthogonal joint diagonalization in the least square sense with application in blind source separation. IEEE Signal Process 50(7):645–648

Yeredor A (2004) ACDC: Approximate joint diagonalisation (in the direct Least-Squares sense) of a set of Hermitian matrices, using the iterative ACDC algorithm [MATLAB code]. Available from: www.eng.tau.ac.il/∼arie/. Accessed: 3 May 2009

Xie T, Myers DE, Long AE (1995) Fitting matrix-valued variogram models by simultaneous diagonalization (Part II: Application). Math Geol 27:877–888

Strategies for Mine Planning and Design

P. A. Dowd, C. Xu and S. Coward

Abstract This paper provides an assessment of the current challenges in strategic mine planning and design and suggested approaches for addressing them. The specific challenges covered are:

(1) Realistic quantification of downstream processes applied to orebody models to provide an integrated approach to mine design and optimisation.
(2) Modelling, estimation and simulation of geometallurgical variables and their integration into resource and reserve estimation and mine planning.
(3) Modelling, estimation and simulation of new variables for new forms of mining —deep mining, particularly block caving, and solution mining.
(4) Flexibility in planning and design to manage risk and minimise its impact.
(5) IT infrastructure and platforms for rapid on-line data collection, storage, access and processing.

Most of these challenges require new types of data, variables, modelling and estimation methods. Foremost among the new types of variables and data are geometallurgical and dynamic rock mass characterisation variables. New types of data and data collection include rapid generation of very large amounts of on-line sensor data and the consequent need for rapid processing and modelling of these data. This paper outlines the challenges and strategies in each of these areas and uses examples of models and outputs to illustrate approaches and potential solutions.

Introduction

The five challenges outlined in the Abstract are not all independent and a solution to any one of them may require the simultaneous solution of part or all of another.

P. A. Dowd (✉) · C. Xu
The University of Adelaide, Adelaide, Australia
e-mail: peter.dowd@adelaide.edu.au

S. Coward
Principal Consultant, Interlaced, 6 Cliff St, Fremantle, WA, Australia

R. Dimitrakopoulos (ed.), *Advances in Applied Strategic Mine Planning*,
https://doi.org/10.1007/978-3-319-69320-0_25

Challenge (1) requires modelling specific processes (e.g., selection, loading, blending, physical and chemical processing), integrating them with orebody models and estimating the impacts of the processes at each stage of the mining operation.

Challenge (2) covers a wide range of new variables to be included in resource and reserve modelling and estimation and requires integration with downstream processes as in (1). Many of these variables are non-additive and, in some cases, are measured indirectly by sensing and/or by proxy variables.

The fundamental requirement in (3) is a stochastic model of in situ fractures together with a fracture propagation model and, for solution mining, a flow model. The stability of excavations is also important requirement.

Challenge (4) requires an integrated orebody/extraction model that maximises flexibility in design across a range of alternative optima for changes in prices, costs and technical variables.

Whilst the infrastructure requirement in (5) is an IT and industry/government investment problem, the adaptation of current resource and reserve estimation and optimal production methods to massive volumes of continuously sensed proxy data is highly relevant to the theme of the conference.

Two of the most significant issues for mining operations are cost reduction (especially energy reduction) and geometallurgy (much of which is related to energy reduction). An example of both is optimal fragmentation of rock in blasting to minimise down-stream rock breakage costs, optimise packing in trucks, optimise ore selection and reduce processing costs. Processing and breakage require geometallurgical variables and modelling.

Another major area is the increasing focus on deep mining and, in particular, large-scale block and panel caving. The deep mining focus is accompanied by developments in deep exploration, such as those being led by the Australian Co-operative Research Centre (CRC) for Deep Drilling Technologies. Both deep exploration and deep mining require new approaches to resource/reserve modelling, estimation and simulation and to process modelling.

Geometallurgy brings new challenges: non-additive variables often with very little data; difficulty in correlating geometallurgical variables with the variable of primary interest (usually grade); and the compositional nature of many variables. Many of the deep mining resources are low-grade complex ores, which require the spatial modelling and integration of complex geometallurgical relationships.

Integrating Orebody Models with Down-Stream Processes

In our view the largest gap in current approaches to quantitative strategic mine planning, design and optimisation is the need for realistic models of downstream processes to be applied to orebody models. In other application areas these processes are often termed transfer functions to emphasise that there is an input (e.g., orebody model) to the process (e.g., a blast) and an output (e.g., blast profile of fragmented ore and waste). The integration of the sequence of inputs to, and outputs

from, staged processes is critical for mine optimisation and for optimising the processes themselves. Orebody modelling, estimation and simulation are now well developed, tested and widely used. But their integration into mining processes is less developed. Where orebody models are integrated with mining processes it is done, more often than not, in an over-simplified manner. For example, the usual approach to estimating recoverability at different scales of selection is to assume perfect selection of one well-defined geometrical shape from a larger, equally well-defined, geometrical shape.

Here, for the sake of example, we demonstrate realistic quantification of ore selection processes during mining. This requires modelling and estimation of spatial rock breakage characteristics and spatial ore location indicators. In addition to providing more accurate estimates of recovery, integrating the orebody model with the selection process provides a means of optimising recovery, optimising blasting and loading strategies and optimising fragmentation to reduce energy costs at subsequent stages of the mining process (e.g., haulage, mineral processing). Analogous quantitative approaches can be devised for other processes and incorporated into models for each stage of the mining process.

The method (Dowd and Dare-Bryan 2017 in this volume) comprises:

- generation of an in situ model of the orebody comprising the grade, geology, geomechanical properties and grade control variables within sufficiently small volumes determined by the smallest selectable volume within a blast profile;
- definition of a blast volume comprising a large number of the in situ model volumes, and subjecting it to a blast simulator, which effectively moves each of the component model volumes to its final resting place in the blast muck pile; and
- application of selective loading processes to the simulated muck pile to determine the degree of selectivity that can be achieved by various sizes of loader and types of loading and to quantify ore dilution and ore loss.

The in situ model, representing perfect knowledge at all relevant scales, is obtained by geostatistical simulation. An in situ model that represents the reality of knowing only the data and information that are available from specific grade control drilling and sampling grids can be obtained by sampling the geostatistically simulated model on a specified grid. The volumes comprising the in situ model are then populated by estimates based only on the data corresponding to the specified grade control drilling and blast-hole sampling grids. Different drilling and sampling grids can be used to generate different models, each reflecting the levels of data and information available. Selectivity can then be assessed as a function of the drilling and sampling grids as well as the size and type of loader. Performance is assessed against the ideal selectivity achieved on the perfect knowledge model, comprising simulated values of each component volume. Applying costs, prices and financial criteria enables optimal selection of the grade control drilling grid, size of loader, type of loading and blast design.

An example is given in Fig. 1. Figure 1a and b show simulated copper grades ('reality') for a mining bench of dimensions 80 m × 40 m × 10 m. The simulated bench is then sampled on a specified scale, in this case 8 m × 6 m blast holes and the blast hole sample grades are used to estimate the grades in the bench. The simulated ('reality') and the estimated grade volumes are then subjected to a blast simulator that generates the 'actual' blast profile in Fig. 1c and the predicted blast profile in Fig. 1d. Selection and loading would be informed and guided by the profile in 1d, which would deliver a significantly different recovery than applying selection and loading to the profile in 1c; ore in 1c is much more dispersed through the profile than in 1d. The difference between selecting and loading from 1c and d quantifies the ore loss and ore dilution for the amount and location of sample data.

To illustrate further the consequences of using the over-simplified geometrical shape approach to predicting recoverability, consider the two blast profiles (from a different bench in the same orebody) in Fig. 2. Figure 2a is the actual blast profile and Fig. 2b is the predicted blast profile based on grades estimated from samples from a 8 m × 6 m blast-hole pattern. Figure 2c and d are the result of applying a cut-off grade to define contiguous parcels of ore.

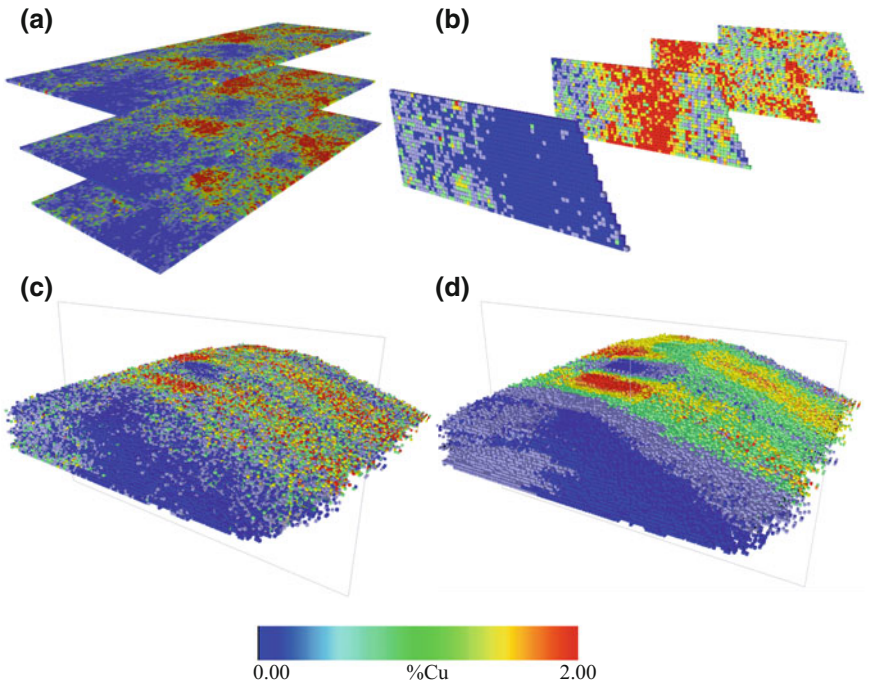

Fig. 1 **a** Simulated copper grades in bench: three horizontal sections; **b** simulated copper grades in same bench: four vertical sections; **c** blast profile resulting from simulated blast applied to simulated grades; **d** predicted composition of blast profile from simulated blast applied to in situ grades estimated from samples taken from blast-holes on 8 m spacing

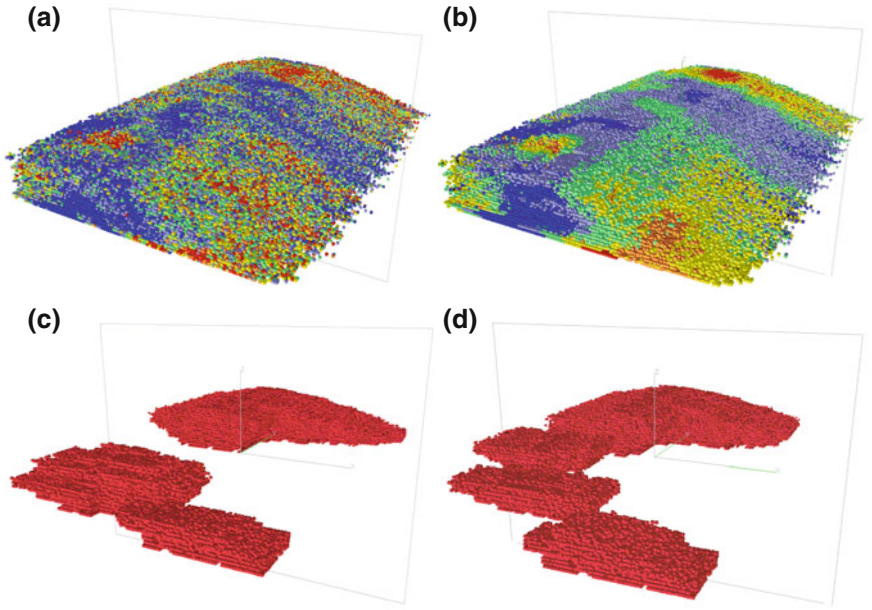

Fig. 2 **a** Simulated ('actual') blast profile; **b** predicted blast profile; **c** ore zones in simulated ('actual') profile; **d** ore zones in predicted blast profile

Once the selection and recovery processes are quantified and integrated with the orebody model they can be used to plan, design and optimise the processes. For example, to determine a blast design that will optimise fragmentation and recovery for a specified budget.

Geometallurgy

Geometallurgy originally referred to the incorporation of metallurgical variables into spatial geological models of orebodies to provide an integrated predictive basis for mine and mineral processing design and optimisation. The definition has evolved over time to recognise the uncertainty of variables and to extend the concept beyond the strict definition of metallurgy; for example, "the integration of geological, mining, metallurgical, environmental and economic information to maximize the Net Present Value of an orebody while minimizing technical and operational risk" (SGS 2014). Geometallurgy may be viewed as a specific example of the integration of down-stream processing as covered in the previous section. However, the fundamental difference is that geometallurgical variables are spatial variables that must be integrated in the block model whereas the processes covered in the previous section are physical processes applied to the block model (including geometallurgical variables).

Ignoring the effects of geometallurgical variables in mine planning (and operation) disregards a critical section of the value chain and, in many cases, leads to sub-optimal mine plans and operations. The authors take a systems approach to mine planning and operation by, for example, optimising processing routes for blocks of ore based on their mineralogical composition and processing characteristics. The approach is to optimise the system as a whole, rather than independently optimising components of the system such as, for example, optimally scheduling a block-grade model.

Coward and Dowd (2014) summarise the current general approach to geometallurgical modelling as:

- identify the variables required to understand critical process responses;
- find ways to sample and measure these variables; and
- develop techniques to estimate and simulate these characteristics spatially at the correct scale and incorporate the values into block models.

The missing components are the equivalent of the integrated transfer functions or processes illustrated in the previous section, namely to integrate the spatial geometallurgical model into a complete mine systems model to quantify the impact of variable and uncertain rock properties on all stages of process performance, mine design and optimisation. This aspect, with the addition of mining, environmental and economic variables and processes, provides the basis for an integrated systems approach to complex mining systems problems.

As an example, we provide some results from a geometallurgical study of a polymetallic sulphide mineralisation in which surface alteration reduces progressively with depth (Coward and Dowd 2014, 2015). The minerals of economic interest are silver, lead, zinc, gold and copper. The oxidation state, determined from core samples, is classified in six levels from fresh to extremely weathered. It is planned to leach weathered material and float fresh material. The spatial block model comprises the five grade variables and one geometallurgy variable in the form of a weathering index. The weathering index is used to determine the processing route for each block: direct leach; flotation followed by leaching tails; waste. Figure 3 shows a process flow chart with the four possible routes, two of which have two or more sub-routes. Experimental values were used to establish recovery curves for each metal for each process. An estimated block model was created by kriging the values of the variables for each block. Values of the variables were also simulated at the block scale 100 times to provide 100 realisations of the orebody. In addition, a second estimated block model was created by averaging the 100 simulations for each block. The expected recovery from each process was calculated from the multivariate grades and recovery curves for each metal.

For each of the 102 models, the net smelter return (NSR) was calculated for each route for each block. Any combination of block and route that returns a positive NSR deems the block to be ore for that route; otherwise the block is deemed to be waste. Each block was then assigned its optimal route together with the ranked remaining positive routes. An optimal pit was generated for each of the 102 models

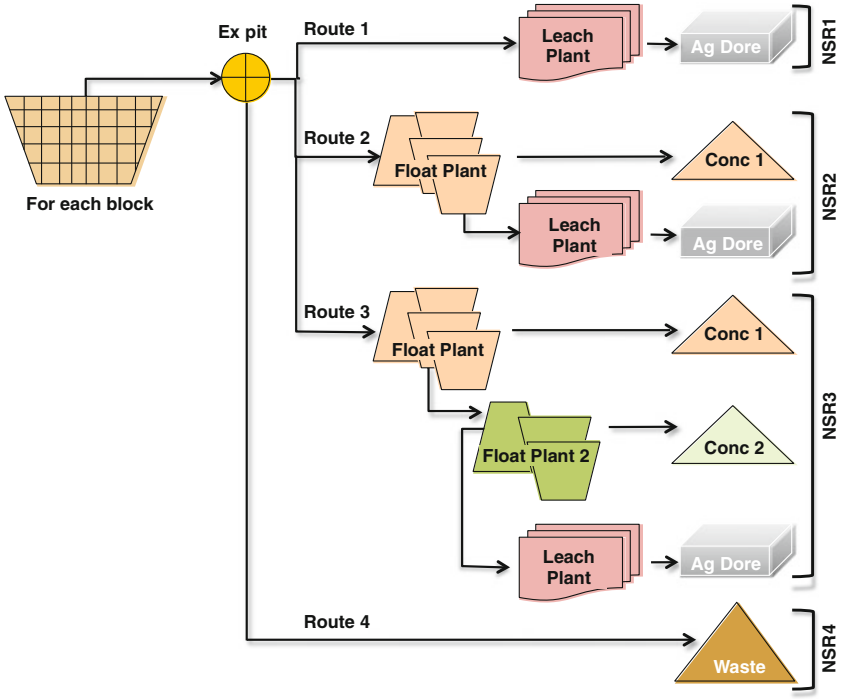

Fig. 3 Processing routes for a polymetallic sulphide deposit (Coward and Dowd 2015)

and the blocks within each of these pits were scheduled by year for the mine-life of the orebody. To simulate the operation, each individual block is processed in sequence and, depending on the status of each processing route, the block may or may not be sent through its optimal route. In cases where the optimal route is unavailable (either due to being over fed or to full downstream product stockpiles), the block is either stockpiled for later processing (incurring a re-handling cost) or sent through an alternative route if its contribution is positive and less than the re-handling cost. The process model thus reflects the actual decision-making that would occur during mine operation. Schedules were generated in MineSight using the expected NSR value and the qisk model was used to explore how dynamic constraints might result in blocks not being treated through their optimal processing route, at times that may differ from the mine plan.

Figure 4 shows the resulting optimal tonnes of combined metal in concentrate for each year of the mine life for each of the 102 models and assuming no uncertainty in the process recoveries. The variability in the 102 sets of plotted values is a measure of resource uncertainty. To provide an indication of process uncertainty, normal distributions of errors were assumed and 25 alternative recovery values were simulated for each process and applied to the kriged block model (i.e. certainty assumed for the block model and uncertainty for the process

models). The resulting combined metal in concentrate curves are also shown in Figure 4.

From the plots in Fig. 4 it can be seen that in early years of operation the process and resource uncertainties overlap and there is very little difference in the two sets of curves. Beyond year 13 the two sets of curves begin to deviate significantly. The resource uncertainty curves beyond year 27 indicate that higher grades will have been mined and processed in the earlier years and production outputs become more variable.

This brief summary of an extended case study (Coward and Dowd 2014) is presented here as an example of the integrated systems approach to complete geometallurgical modelling. In the full case study three different economic scenarios (different prices and costs) were also included. A more realistic approach would be to include any interactions among the various uncertainties: in situ variables, processes and economic variables (and also any environmental variables). In the example summarised in Fig. 4 this would have entailed simulating the process recoveries for each of the simulated block models. In the general case, for in situ geological and geometallurgical variables, process models, economic variables and environmental variables the number of combinations and outcomes rapidly increases. Further significant increases in outcomes are incurred if other process models, such as blasting, stockpiling and blending are also included. The associated computational issues are examples of the fifth challenge and are visited again in the section on IT Infrastructure and platforms.

The remaining issues for geometallurgical modelling are identification and collection of sufficient data for metallurgical variables that are currently either not spatially sampled or are grossly under sampled; spatial modelling of these variables and of their spatial relationships with primary variables such as grade; and, where

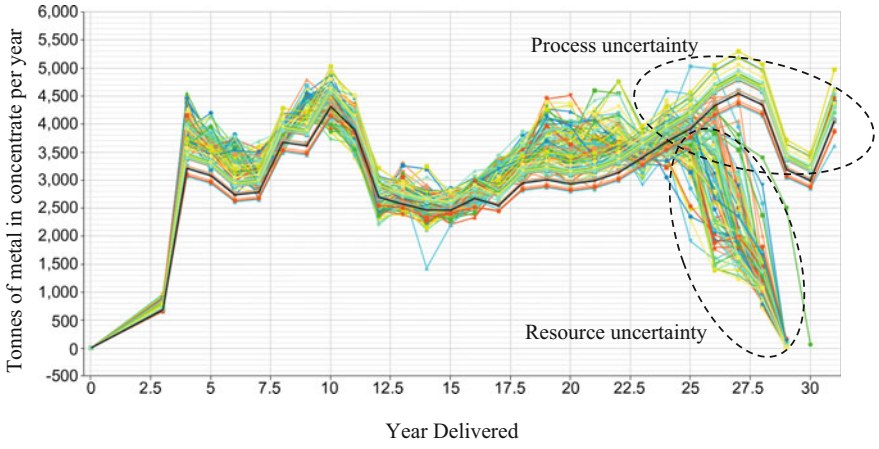

Fig. 4 Tonnes of metal in concentrate by year for simulated and estimated block models and simulated process recoveries

relevant, adequate accounting for non-additivity and compositional constraints. The most commonly quoted impediment in collecting and analysing geometallurgical variables is cost. However, applications such as the case study quoted here clearly demonstrate the added value that an integrated geometallurgical approach brings to mine design, mine planning, scheduling and to optimising total system measures (such as NSR).

Other Types of Variables

Many variables are not uniquely geological, geomechanical, or metallurgical in nature. For example, in an orebody in which gold occurrence is associated with small quartz veins and rock fractures, 90% of the ore in any mining block may be contained in less than 25% of the rock mass, which may not be a single contiguous volume and there may be insufficient data to identify the locations of veins and fractures. This has important consequences for grade prediction, blast design, rock fragmentation, selection, loading, crushing, grinding and processing—and each of these processes cannot be considered independently of the others.

Figure 5 shows a schematic north-south cross-section through a low-grade, east-west striking gold orebody in an open-pit operation (Dowd 1995). Due to the low grade of the orebody most samples are from percussion drilling and record gold in g/t and quartz in %; fracture and vein information are lost in the percussion chips. A statistical analysis shows insignificant correlation between gold and quartz assays; it is more likely that the correlation is between gold occurrence and the numbers of quartz-granodiorite contacts, i.e. the numbers of veins and/or fractures,

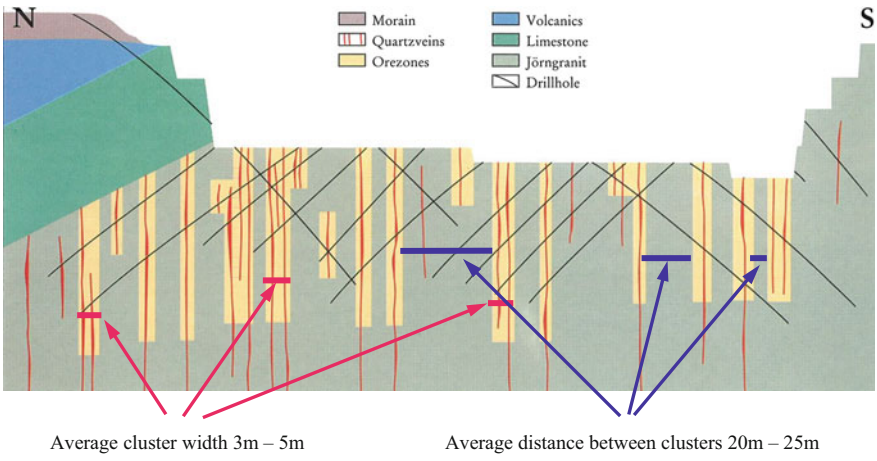

Fig. 5 Schematic cross-section of gold orebody with concepts of fracture and vein controlled mineralisation and associated ore zones

which cannot be determined from the samples. A geostatistical analysis yields a north-south horizontal (i.e. perpendicular to strike and dip) gold variogram with a nugget variance and two ranges: 4 and 20 m; and a quartz variogram with a nugget variance and a single range of 3 m. There is no difference in the spatial variability of gold from samples that contain gold and quartz and those that contain only gold. Standard geostatistical analyses do not reveal any discernible spatial co-variation between gold and quartz even though the latter is the best available ore location indicator. A simple analysis of the samples in each drill-hole shows that 90% of all significant gold assays are either directly associated with quartz or are within 4 m of a quartz occurrence in the same hole; a down-hole distance of 4 m corresponds to a horizontal distance of approximately 3 m. The variogram models are consistent with the schematic model indicated in Fig. 5: veins and fractures occur in clusters of 3–5 m with an average spacing of 20–25 m between the clusters; the smaller range gold variability is associated with the small range quartz variability. Similar models and interpretations (with different ranges) were found in the other principal geological directions; the complete analysis and resulting variogram models can be found in Dowd (1995).

This study enabled optimal blasting and selection strategies and maximised quartz occurrence as a proxy ore location indicator. A specifically geometallurgical extension would be to link crushing and grinding characteristics of major rock types to the quartz indicator variable.

New Models for New Mining Methods

The process models (or transfer functions) for traditional mining methods are well known and, in many cases, the modelling methods (e.g., blast simulation) are readily available. However, as the industry transitions to different forms of mining there is a critical need to develop new models that adequately characterise the physical processes and their associated or inherent uncertainties. The most significant examples of new (either because of the scale and depth or the basic technology) mining methods are deep mining, particularly large-scale block caving, and solution mining (or in situ recovery). Deeper mining and in situ recovery will increase as current mineral resources are depleted.

Block Caving

There is an accelerating transition from surface mining to underground mining. The transition is being driven by cost as well as access to deeper resources. According to Moss (2012) block caving operating costs range from $US5 to $US7 per tonne versus large open-pit operating costs of $US1.00 to $US1.20 per tonne. However,

for the former each tonne is a tonne of ore whereas for the latter each tonne is a tonne of material moved.

As an indication of the rate of transition from surface to underground mining, Rio Tinto expects 43% of its copper production and 25% of the entire world's copper production to come from underground operations by 2021 (Moss 2012).

There is a significant increase in risk with large-scale caving not least because around 70% of the capital cost is incurred before any revenue is generated (Moss 2012). McCarthy (2002) identifies two additional increased areas of risk associated with deep mining. Firstly, the increased geological risk due to sparse data and secondly, the increased technical risk in areas such as ground control, materials handling and safety. To these could be added the additional types of data required to characterise the rock mass for planning, designing and managing large caves and the difficulty in obtaining direct measurements of the relevant variables. Brown (2012) provides a comprehensive overview of the geotechnical risks associated with caving.

The fundamental scientific and technical challenge is to quantify and manage the rock mass behaviour under in situ, pre-conditioning (hydraulic fracturing or blasting) and caving conditions. In each of these phases, there are many uncertainties to be quantified and included in quantitative process models. There is also a need to quantify and manage geomechanical risk—departure from optimum performance of the cave as well as ground control risk.

The basis for a quantitative model is a realistic fracture network and a fracture propagation model. For orebodies for which large block sizes are likely to result from caving it may be necessary to precondition by hydraulic fracturing. In designing fracture stimulation programmes it is essential to be able to predict fracture propagation with some level of confidence. Ideally, the fracture stimulation processes should be designed to optimise pre-conditioning outcomes; the more difficult challenge is to design them to maximise the ability to control the cave or at least to predict the cave with an acceptable level of reliability.

Solution Mining

Solution mining, or in situ leaching or in situ recovery, in which leaching solution is injected into stimulated fracture networks and the dissolved mineral content is pumped to the surface, will become a more widely used mining method as existing deposits are depleted and deeper and/or lower grade deposits, for which conventional mining methods are neither technically nor economically feasible, are exploited. In 2011, 45% of world uranium production was from in situ leaching operations (World Nuclear Association 2014), an increase from 16% in 2000.

Solution mining requires a low-permeability reservoir to be stimulated to create a connected fracture network to enable fluid flow. The fundamental problem is to induce flow through the stimulated fracture network to achieve effective, efficient recovery at minimum cost and acceptably low environmental risk. Current models

of flow through stimulated fracture-based reservoirs are inadequate. The critical requirement is to develop a modelling technique that can solve large-scale problems efficiently without compromising on sufficient fracture detail and fracture network connectivity. There are many complex unresolved issues impeding a solution to this problem and one of the most critical is the lack of a clear understanding of system behaviour, output and performance. This is the direct consequence of the inability of standard models to describe, effectively, realistically and efficiently, the fluid flow in a fracture-based reservoir on multiple scales.

In situ leaching has significant potential due to its low cost, low surface footprint and 'greener' operation. However, retrieval of solutions post-mining will almost certainly become an environmental protection requirement. Again, adequate fracture and flow models will be critical to the ability to comply with such requirements.

Other

An additional area of application is in the conventional mining of deep deposits, in which ground water invasion into the mine and the environmental impact of mining on local aquifers will become critical. This requires tools for assessing leaching fluid and ground water movement as well as chemical reactions within the leaching field.

Stochastic Fracture Models and Fracture Propagation Modelling

The characterisation of rock fracture networks is a very difficult problem not least because accurate field measurement of a single fracture is difficult and measurement of all fractures is impossible. Thus, in practice, the whole fracture system is not observable on any meaningful scale and the only realistic approach is via a stochastic model informed by sparse data and/or by analogues. In block caving and solution mining applications, a realistic solution is even more difficult as the only reference data related to the fracture system are from limited drill core samples, geophysical borehole logs or sparse seismic events detected during hydraulic fracture stimulation. For these reasons most of the standard models of fracture systems for these applications are oversimplified representations of reality.

Recently, however, there have been some significant advances in the stochastic modelling of fracture networks and fracture propagation for hot dry rock geothermal reservoirs. These developments are transferable, with minimal adaptation, to block caving and solution mining.

The immediate problem in any application is the requirement for sufficient data. Fracture networks in caving and solution mining systems are essentially the product of hydraulic fracture stimulations that, together with ground conditions and the local stress regime, determine how fractures are formed and propagated. Thus the data requirements are measurements of in situ stress and fracture propagation.

The most obvious ways of collecting sufficient amounts of fracture data are from geophysical sensing, measuring fracture proxies and/or fracture propagation: acoustic impedance surveys, and recording of micro-seismic events triggered by fracture stimulation during pre-conditioning tests, full-scale pre-conditioning and/or production monitoring.

The recent advances in fracture network modelling and propagation, using micro-seismic events triggered by fracture stimulation, can be broadly classified as stochastic optimisation—optimal fitting of fracture shapes to clouds of seismic points. The methods developed include Markov Chain Monte Carlo optimisation (Mardia et al. 2007; Xu et al. 2013), spatial clustering (Seifollahi et al. 2013), the Random Sampling Consensus (RANSAC) algorithm (Fadakar et al. 2013) and the Point and Surface Association Consensus PANSAC) algorithm (Xu and Dowd 2014). All of these methods are available in a public domain software package (Xu and Dowd 2010). The methods can be further classified into those that consider only the locations of the seismic points and those that consider location and time sequence of the events. The latter group provides the basis of fracture propagation models.

By way of example, we present here a short overview of the PANSAC model together with outcomes from applying it to the fracture stimulation of the Geodynamics' Habanero geothermal reservoir in the Cooper Basin. Full details of the modelling methods and the specific application can be found in Xu and Dowd (2014).

The fundamental assumption of the algorithm is that at least one fracture passes through the location of any seismic event detected. This is a reasonable assumption as seismic events occurring in the fracture stimulation process result from slips of existing fractures, creation of new fractures or propagation of existing fractures. Fitting surfaces through to a point cloud set is mathematically and computationally difficult (Bercovier et al. 2002), particularly when the fracture surface profiles are unknown and the data points are sparse. A further widely used simplification is to assume that, as a first-order approximation, planar polygons can be used to represent actual tortuous fracture surfaces. The RANSAC approach fits random fracture planes through the point cloud by minimising a cost function. The resulting fracture model consists of a sequence of fracture planes with a number of associated points arranged in descending order, implying the increasing uncertainty of fractures fitted at later stages. RANSAC, and the earlier MCMC approach, ignore the time sequence of the seismic events. Fracture stimulation begins near the stimulation source and moves further away from the source as the stimulation intensifies. In other words, different parts of the rock masses are stimulated at different times. As fracture creation or propagation is highly dependent on any existing fracture network (Kear et al. 2013), it is important to consider the sequence of fractures

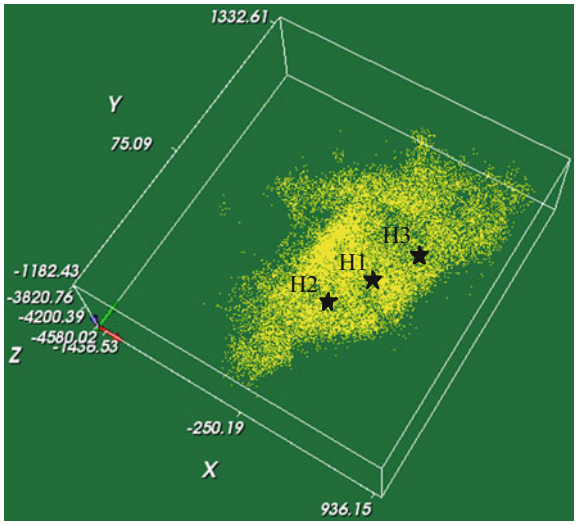

Fig. 6 Absolute hypocentre locations of the seismic events

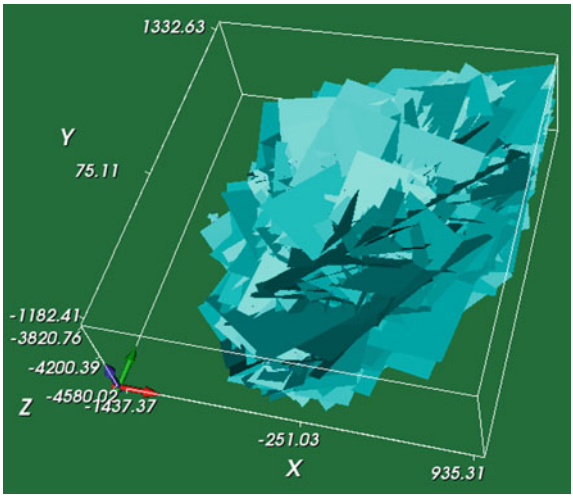

Fig. 7 Final PANSAC fracture model for the Habanero reservoir

simulated at earlier stages when fitting fracture models to a set of seismic points. Failure to do so could potentially produce a misleading fracture network model (Xu and Dowd 2014). The PANSAC approach addresses this issue by taking every individual seismic event in turn and optimising the association between the point and the previously fitted fracture surfaces, taking into account the existing fracture network, possible routes (connections) back to the stimulation source and preferential fracture propagation paths. The parameters used in the fitting process are optimised using the fundamental principle that the most likely fracture propagation

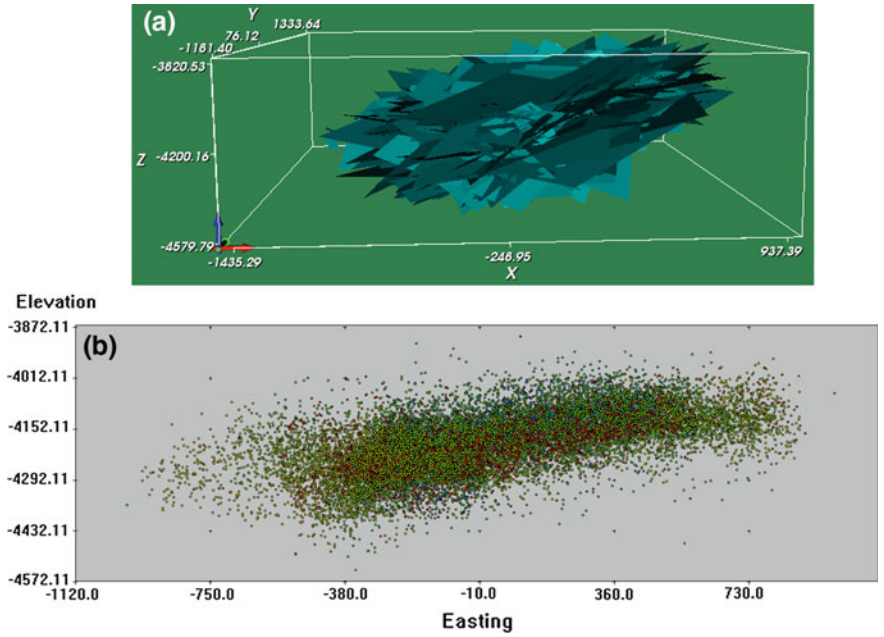

Fig. 8 Dipping feature of the fractures in the east–west direction. **a** Three-dimensional view; **b** north–south projection

path is the one that requires the least amount of energy. The final fracture network fitted by PANSAC consists a sequence of fractures following closely the fracture stimulation process from the stimulation source to the boundary of the stimulation.

Figures 6, 7, 8 and 9 illustrate the application of PANSAC to Geodynamics' Habanero geothermal reservoir in Cooper Basin of South Australia. The targeted hot granite is about 4 km below the surface with a temperature close to 250 °C. Figure 6 shows the locations of 23,232 seismic events detected during the fracture stimulation in 2003 using Habanero 1 (H1) as the stimulation well. Eight geophones deployed in wells surrounding H1 at depths of 100–2300 m were used to record the seismic signals generated by the stimulation process. Note that wells H2 and H3 shown in Fig. 6 were drilled later and did not contribute to the events shown in the figure. The final fracture model generated by PANSAC is shown in Fig. 7.

Figure 8a is a view of the fractures in Fig. 7 looking north and Fig. 8b shows the propagation sequence of the seismic points projected onto an east-west vertical cross-section. Both figures clearly show that a significant number of fractures dip gently to the west, that is the propagation of fractures trends upward as they propagate towards the eastern part of the reservoir. The PANSAC model captures correctly this feature.

Figure 9 shows a sequence from the fracture propagation model at different times in the stimulation process. The time t is in units of days after 12:51 pm, 30 Oct. 2003, Central Australian time. Note that t from 12 to 18 corresponds to the first

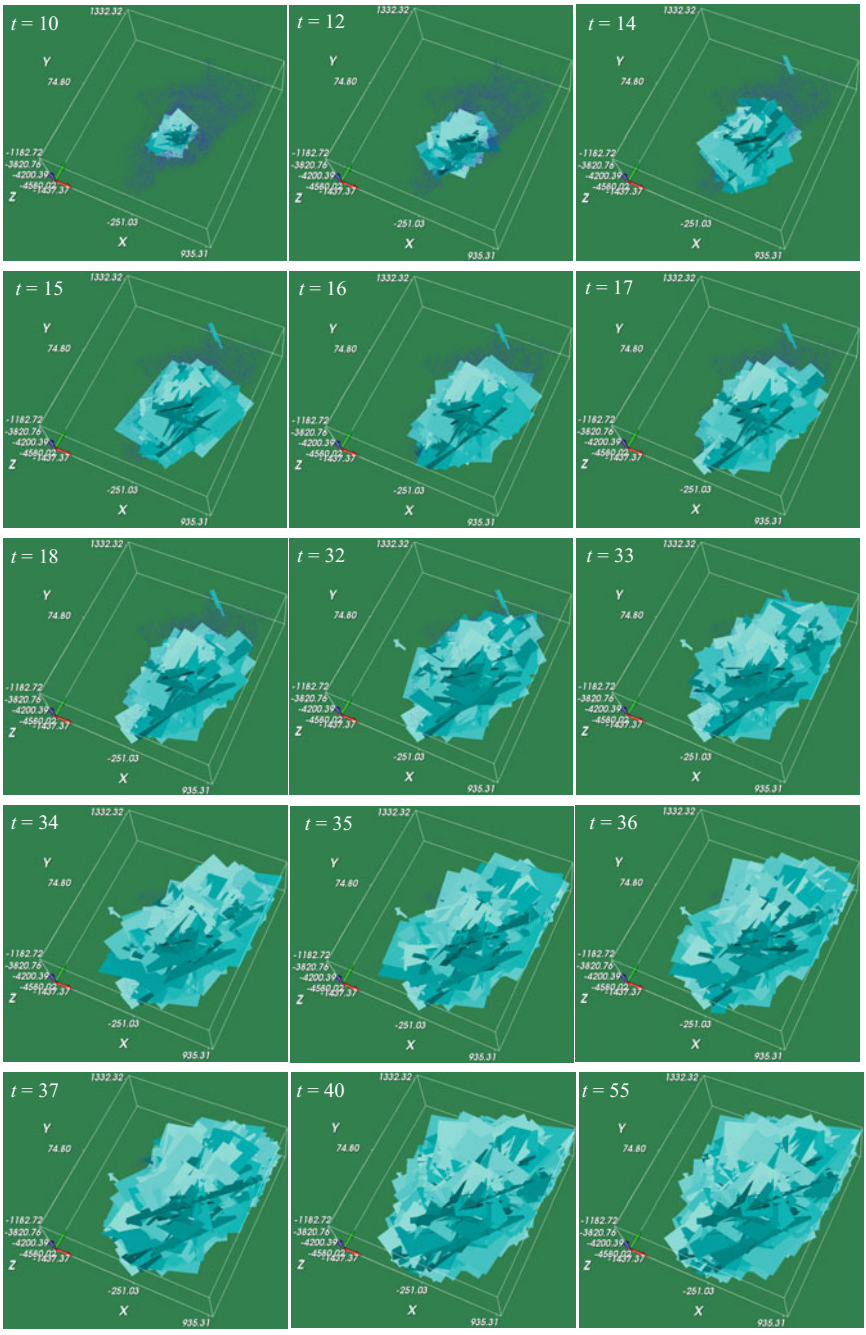

Fig. 9 Fracture propagation model generated by PANSAC

major fracture propagation stage and t from 32 to 40 corresponds to the second major fracture propagation stage. The fitted fracture propagation model correctly captures these fracture propagation stages.

This example clearly shows the potential for the application of these models to characterising fracture networks and modelling fracture propagation for block caving and solution mining. With the help of seismic monitoring during the pre-conditioning for block caving or ground stimulation for solution mining, these models can be used to assess the effectiveness of the stimulation process, the degree and the adequacy of ground fracturing for the intended operations and to help optimise the stimulation process to minimise the associated costs.

Flow Modelling for Solution Mining

The additional component for solution mining is to model the flow through the reservoir. Flow characteristics of a stimulated fracture network depend mainly on the connectivity of the fractures in the network. This connectivity can be represented by channels (connection pathways) connecting the injection and recovery wells through the fracture network. However, finding these channels is by no means simple, especially for large size fracture networks. In our work we search for all potential pathways and select on the basis of the shortest connection paths but even so there are still significant numbers of potential flow pathways even for a moderate size fracture network. Figure 10 shows an example of the identified flow channels through the fracture network between the H1 and H3 wells for the MCMC model described in Xu et al. (2015). There are 27,293 channels in this case and most of these connection paths pass through more than 100 fracture planes. Clearly, Habanero 1 is well connected to the surrounding rock through the fracture model, which is expected because it is the source of the fracture stimulation. Habanero 3 has only a small number of connections to the reservoir, which is also expected, as Habanero 3 plays no part in the fracture stimulation process.

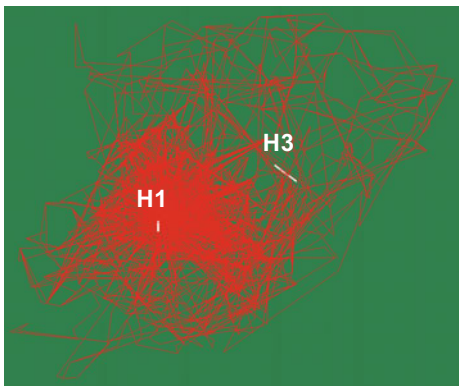

Fig. 10 Connection channels between Habanero 1 and 3

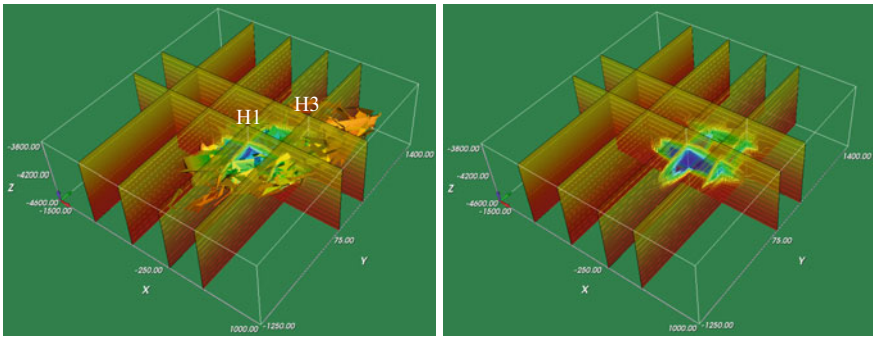

Fig. 11 Reservoir temperature distribution after 20 years production

For geothermal applications, once the detailed structure of the reservoir is modelled, further analysis in terms of fluid flow and heat extraction is needed. For a large-scale reservoir such as Habanero (approximately $2.0 \times 2.0 \times 0.5$ km^3) and with detailed reservoir structures on the scale of metres, it is not possible to use conventional numerical tools due to the computation cost (Bodin et al. 2007). We have developed a simplified flow and heat extraction analysis tool, based on an equivalent pipe network, which significantly improves the computational efficiency and makes the reservoir scale analysis possible (Xu et al. 2015). Figure 11 shows the temperature distribution of the Habanero reservoir after 20 years of heat extraction based on H1–H3 doublet and 35 L.s^{-1} extraction rate. The temperature drawdown and power produced can also be calculated accordingly.

The technique described here is readily applicable to solution mining where the mine scale is, in general, significant and both flow and heat will play important roles in the minerals impregnation and transport processes. The additional component that has to be considered in this application is the chemical reaction, which is relatively easier to model once the flow and temperature models are established.

Flexibility in Planning and Design

The ability to adapt mining operations to increasingly volatile external environments (e.g., prices, markets) and changing internal circumstances (e.g., geomechanical conditions, grades) is difficult but, nevertheless, critical for many projects. It requires sufficient flexibility in models to enable plans to be adapted and to manage risk and minimise its impact. Models that attribute value to system flexibility (at strategic, mid-term and tactical levels) will lead to plans and designs that can be adapted to deal with emergent risks and minimise their impact on the operation.

The integrated model approaches advocated here provide a basis on which flexibility can be valued. The integrated systems modelling of variables, processes and

their associated uncertainties allows options to be assessed, the system to be re-optimised on the basis of changed circumstances, and risk to be quantified and managed. In particular, the output for the polymetallic sulphide case study given earlier in this paper is not only a fully flexible plan in terms of optimal processing routes but also a fully flexible operational schedule that allows operators to choose the best available route when the optimal route is not available, i.e. the plan includes all relevant processing decision-making that would occur during actual operations.

The inclusion of quantified uncertainty in the modelling of variables and processes during planning and design provides a sound basis on which to identify, prioritise and manage risk and minimise its impact. As acknowledged by other authors, (see, for example, Dimitrakoploulos et al. 2002), the quantification of uncertainty and risk provides greater flexibility in mine planning and design and can add significant value to projects.

The real options framework has been widely used to accommodate uncertainty and flexibility in optimising mine planning see, for example, Dimitrakopoulos et al. (2002), Dimitrakopoulos and Abdel Sabour (2007), Abdel Sabour et al. (2008), Botin et al. (2012) and, in a broader context, Armstrong et al. (2004). Other authors have used more traditional methods such as Monte Carlo simulation of scenarios (prices, costs, recoveries, etc.) together with optimisation methods (see, for example, Groeneveld and Topal 2011). Armstrong et al. (2013) also used real options to reduce the number of scenarios in project valuation, which is a significant issue when using large numbers of simulations.

Another area of flexibility is in the physical design of mining operations. This work is best exemplified for underground 11 mine design by the output of Brazil et al. (2003, 2004, 2009).

The case study presented in this paper together with the somewhat limited overview of other work in this field is intended to give an indication of the approaches that have been successfully applied to real mining operations. A question that arises is the extent to which these approaches have been adopted and meaningfully used in the mining industry. The question is particularly pertinent to the current economic conditions for most mined commodities – a situation for which the incorporation of uncertainty and flexibility in mine planning and design is specifically intended.

IT Infrastructure and Platforms

There is a growing need for mining industry IT infrastructure and platforms for rapid on-line data collection, storage, access and processing and to support the increasing amount of automation in many stages of the mining process. The increasing generation and use of large sets of remotely sensed data at mine and exploration sites requires new platforms and infrastructure to realise the potential of the data in short-term decision-making and longer term strategic planning. These data range from down-hole sensing of mineralisation indicators and rock properties

in deep exploration drilling to online sensing of blast-hole cuttings and blast profiles to online sensing of truck performance. The effective use of these data requires immediate, and often remote, access to very large data sets and rapid processing of data to optimise processes such as drilling directions, blast design, selective loading and choice of mineral processing routes.

Whilst the largest companies have established their own facilities, it makes sense for others to come to collaborative arrangements for joint provision with appropriate protocols to ensure security of commercial data and information. Given the key economic role that mining plays in many economies, governments may take the view that this is essential infrastructure and provide support in establishing it.

The Collaborative Remote Operations Centre project funded by the South Australian State Government's Mining and Petroleum Services Centre of Excellence (DMITRE 2014) is a good example of an industry/government/university collaboration to provide an IT platform to support automation, remote analysis, data storage and on-line access, and the testing of software and hardware for remote mining operations. The Collaborative qualifier refers to the shared nature of the Centre.

Collaborative centres such as this require ICT architectures that provide rigorously secure access to the IT systems of members so as to allow data integration and analysis on the platform without compromising the security of a member's data. The University of South Australia, in collaboration with mining company OZ Minerals Ltd, has led the development of a 'test and trial' Collaborative Remote Operations Centre, that is intended to provide a future innovation hub for the mining industry with longer term access for students, researchers and ICT companies for research, teaching and testing of new products and services (Sriram et al. 2014).

New real-time logging while drilling (LWD) technologies are being developed in the Deep Exploration Technologies Co-operative Research Centre (DETCRC 2015). Almost all mine design and planning are based on analyses of core samples and hence the modelling and optimisation methods used to deliver designs, plans and schedules are, of necessity, largely limited to grades and tonnages. However, cores limit the types of data that can be collected and they reduce productivity because of time lost in transporting them to laboratories and analysing them. In addition, cores limit the type of drilling technologies, which is one of the focus areas of DETCRC. The potential of LWD for mine planning and design is real-time information on geological controls on mineralisation, delineation of ore zones, geotechnical characteristics and, possibly, geometallurgical characteristics particularly those related to rock breakage. One of the key objectives of programme 2 of DETCRC is to develop technologies to invert LWD sensed petrophysical data for rapid updating of three-dimensional geological models. In the deep exploration context, these very large LWD data sets are already available and similar types of data are being generated in operating mines. In the context of strategic mine planning, the challenge is to adapt modelling, design, estimation, simulation and optimisation algorithms to real-time processing of these types of

rapidly acquired, and very large, data sets so as to improve the speed and quality of decision-making.

Conclusions

Most of the challenges outlined here do not require new models or new approaches, they require adapting existing techniques to new applications (as in fracture modelling for caving and fracture network and fluid flow modelling for in situ leaching) and a systems approach to integrating resource/reserve models with mine processes (as in geometallurgy and the more general mining response or transfer functions). There is a need for more work on adequate spatial modelling of geometallurgical variables, particularly in dealing with non-additive and compositional variables, and in providing tested and validated response functions. There is also a need for the computational speed of modelling, simulation and estimation algorithms to be commensurate with the speed with which sensed data are collected and decisions on them need to be made.

In the context of the integrated systems approach and the need for flexibility in models and outcomes proposed here it may be more important to ensure that outcomes are robust and resilient rather than strictly "optimal" for a rigidly specified set of geological, geometallurgical, operational and economic criteria.

References

Abdel Sabour SA, Dimitrakopoulos R, Kumral M (2008) Mine design selection under uncertainty, transactions of the institution of mining and metallurgy, Section A. Mining Tech 117(2):53–64

Armstrong A, Galli A, Couët B (2004) Incorporating technical uncertainty in real option valuation of oil projects. J Pet Sci Eng 44(1–2):67–82

Armstrong M, Ndiaye A, Razanatsimba R, Galli A (2013) Scenario reduction applied to geostatistical simulations. Math Geosci 45(2):165–182

Bercovier M, Luzon M, Pavlov E (2002) Detecting planar patches in an unorganized set of points in space. Adv Comput Math 17:153–166

Bodin J, Porel G, Delay F, Ubertosi F, Bernard S, de Dreuzy J-R (2007) Simulation and analysis of solute transport in 2D fracture/pipe networks: the SOLFRAC program. J Contam Hydrol 89:1–28

Botin JA, Dell Castillo MF, Guzmán RR, Smith L (2012) Real options: a tool for managing technical risk in a mine plan. In: SME Annual Meeting. Seattle, USA, SME, Pre-print 12–121, 7

Brazil M, Lee DH, Van Leuven M, Rubinstein JH, Thomas DA, Wormald NC (2003) Optimising declines in underground mines, transactions of the institution of mining and metallurgy, section A. Mining Tech 112:164–170

Brazil M, Lee D, Rubinstein JH, Thomas DA, Weng JF, Wormald NC (2004) Optimisation in the design of underground mine access. In: Orebody modelling and strategic mine planning, spectrum series, vol 14. Australasian Institute of Mining and Metallurgy, Melbourne, Australia, pp 121–124

Brazil M, Grossman PA, Lee D, Rubinstein JH, Thomas DA, Wormald NC (2009) Access optimisation tools in underground mine design. In: International symposium on orebody modelling and strategic mine planning: old and new dimensions in a changing world. Melbourne, Australasian Institute of Mining and Metallurgy, pp. 237–241

Brown ET (2012) Progress and challenges in some areas of deep mining. Deep Mining 2012. Australian Centre for Geomechanics, Perth, Australia

Coward S, Dowd PA, Vann J (2013) Value chain modelling to evaluate geometallurgical recovery factors. In: Proceedings of the 36th APCOM Conference. Brazil, pub. Fundação Luiz Englert, pp 288–289

Coward S, Dowd PA (2014) Geometallurgical models and the quantification of uncertainty in mining project value chains. Presentation at Geometallurgy 2014, London, Institute of Materials, Minerals and Mining; 9–10 June 2014

Coward S, Dowd PA (2015) Geometallurgical models for the quantification of uncertainty in mining project value chains. In: Proceedings of the 37th APCOM Conference. Publication of Society for Mining, Metallurgy and Exploration (SME), pp 360–369

DETCRC (2015) Available at: http://detcrc.com.au

Dimitrakopoulos RG, Abdel Sabour SA (2007) Evaluating mine plans under uncertainty: can real options make a difference? Resour Policy 32:116–125

Dimitrakopoulos R, Farrelly CT, Godoy M (2002) Moving forward from traditional optimization: grade uncertainty and risk effects in open-pit design, transactions of the institution of mining and metallurgy, Section A. Mining Tech 111(1):82–88

DMITRE (Department for Manufacturing, Innovation, Trade, Resources and Energy) (2014) http://www.dmitre.sa.gov.au/manufacturing_works/programs_and_initiatives/mining_industry_participation_office_mipo/mining_and_petroleum_services_centre_of_excellence

Dowd PA (1995) Björkdal gold-mining project, northern Sweden. Trans Instn Min Metall, Sect A: Min Ind 104:A149–A163

Dowd PA, Dare-Bryan PC (2017) Planning, designing and optimising using geostatistical simulation. In this volume

Fadakar AY, Dowd PA, Xu C (2013) The RANSAC method for generating fracture networks from micro-seismic event data. Math Geosci 45:207–224

Groeneveld B, Topal E (2011) Flexible open-pit mine design under uncertainty. J Mining Sci 47 (2):212–226

Kear J, White J, Bunger AP, Jeffrey R, Hessami MA (2013) Three dimensional forms of closely-spaced hydraulic fractures. In: Proceedings of International Conference for Effective and Sustainable Hydraulic Fracturing 2013, Brisbane, May 2013

Mardia KV, Nyirongo VB, Walder AN, Xu C, Dowd PA, Fowell RJ, Kent JT (2007) Markov Chain Monte Carlo implementation of rock fracture modelling. Math Geol 39:355–381

McCarthy P (2002) Flexible studies and economic models for deep mines. In: Proceeding of First Internat. Seminar on deep and high stress mining. Australian Centre for Geomechanics, Perth

Moss A (2012) Keynote address at MassMin 2012. Canada (unpublished), Sudbury

Seifollahi S, Dowd PA, Xu C, Fadakar-Alghalandis Y (2013) A spatial clustering approach for stochastic fracture network modelling. Rock Mech Rock Eng 47(4):1225–1235

SGS (2014) http://www.sgs.com. Accessed 12 June 2014

Sriram V, Kearney D, Andrews S (2014) Collaborative remote operations centre report. Department of State Development, Government of South Australia, Available at: http://www.statedevelopment.sa.gov.au/upload/manufacturing/1446_collaborative_remote_centre_operations_report.pdf

World Nuclear Foundation (2014) http://www.world-nuclear.org/info/Nuclear-Fuel-Cycle/Mining-of-Uranium/In-Situ-Leach-Mining-of-Uranium/. Accessed 28 May 2014

Xu C, Dowd PA (2010) A new computer code for discrete fracture network modelling. Comput Geosci 36:292–301

Xu C, Dowd PA, Fidelibus C (2014) Realistic pipe models for flow modelling in discrete fracture Networks. In: Proceedings of the first international discrete fracture network engineering conference. Vancouver, Canada

Xu C, Dowd PA, Wyborn D (2013) Optimisation of a stochastic rock fracture model using Markov Chain Monte Carlo simulation. Min Technol 122(3):153–158

Xu C, Dowd PA (2014) Stochastic fracture propagation modelling for enhanced geothermal systems. Math Geosci 46(6):665–690

Xu C, Dowd PA, Tian ZF (2015) A simplified coupled hydrothermal model for enhanced geothermal systems. Appl Energy 140:135–145

Part V
Other Aspects of Open Pit Mine Planning

Planning, Designing and Optimising Production Using Geostatistical Simulation

P. A. Dowd and P. C. Dare-Bryan

Abstract The full potential of geostatistical simulation as a tool for planning, designing and optimising production is only realised when it is integrated within the entire design and production cycle. In the planning and design stages this involves the simulation of components of the production cycle that depend on (simulated) grades and geology. In the production stage it involves integration with the mining method and the type and use of equipment. This paper explores the general concepts of integrated geostatistical simulation and illustrates them with particular reference to blast design, equipment selection and the associated quantification of ore loss, ore dilution and the ability to select ore on various scales. The critical component of most metalliferous open pit mining operations is ore selection, i.e. the minimisation of ore loss and ore dilution during extraction. In general, extraction comprises drilling, blasting and loading, all of which are planned and designed on the basis of uncertain models of geology and grade. The application describes the integration of geostatistically simulated grade, geological and geomechanical models with blast modelling to provide a link between the estimated in situ characteristics of the orebody and the locations of the same (displaced) characteristics following the blast. This approach provides a means of evaluating different types of selection and thereby enables planners to optimise the selection process in terms of blast design, type and size of loading equipment, maximisation of ore recovery and minimisation of ore loss and dilution. This conversion of the in situ/block model resource to a realistically recoverable reserve may, in many instances, be the most significant source of uncertainty in reserve estimation.

P. A. Dowd (✉)
Faculty of Engineering, Computer and Mathematical Sciences,
The University of Adelaide, Adelaide, SA 5005, Australia
e-mail: peter.dowd@adelaide.edu.au

P. C. Dare-Bryan
Orica Australia Pty Ltd, 188-189 Churchill Avenue, Subiaco, WA 6008, Australia

R. Dimitrakopoulos (ed.), *Advances in Applied Strategic Mine Planning*,
https://doi.org/10.1007/978-3-319-69320-0_26

Simulation

Geostatistical simulation is rarely an exercise in its own right and is usually undertaken to provide a model for further studies. In the simplest applications the purpose may be to estimate ore reserves; or to assess the uncertainty associated with mine planning based on specified drilling densities; or to assess the effect on recoverability of various sizes of selective mining units. In more complex applications a simulated orebody model may be used to assess the effects of sequences of downstream activities. All of these applications, in one way or another, are assessing uncertainty and its operational consequence—risk.

An effective evaluation of risk must include adequate quantifications of all sources of uncertainty. Too often in these applications the quantification of uncertainty is limited to in situ grade and geological variables, with little attention to the uncertainties that arise from the technical processes that are applied to extract ore from the in situ material. The usual assessment of recoverable reserves, for example, is limited to a simple volumetric exercise in which ore recovery is assessed as a function of applying a range of selection volumes to a simulated orebody. This simplistic approach ignores the practicalities of the actual mining, selection and loading processes—blast design, behaviour and performance; equipment type, size and operation; ore displacement during blasting and loading; and ability to identify ore zones within a blast muck pile. In many applications, the uncertainties introduced by these technical processes are at least as significant as those that derive from the in situ spatial characteristics of grades and geology.

In mining applications, the full effectiveness of geostatistical simulation can only be realised by integrating it with adequate and realistic simulations of the technical processes. The authors demonstrate this argument with an application to selection and recovery of ore in open pit mining. The in situ simulation of geology and grades can be achieved by any of the standard algorithms. Ore, however, is not selected and recovered from this in situ mass, but from the broken and displaced components of the mass that results from the blasting process. The integration of the simulation of blasting, selecting and loading with the simulation of in situ grade, geology and geomechanical characteristics provides a realistic means of evaluating selection and recoverability, as well as an effective basis for mine planning and equipment selection.

The Method

The method comprises:

- generation of an in situ model of the orebody comprising the grade, geology, geomechanical properties and grade control variables within sufficiently small volumes determined by the smallest selectable volume within a blast muck pile;

- definition of a blast volume comprising a large number of the in situ model volumes, and subjecting it to a blast simulator, which effectively moves each of the component model volumes to its final resting place in the blast muck pile; and
- application of selective loading processes to the simulated muck pile to determine the degree of selectivity that can be achieved by various sizes of loader and types of loading and to quantify ore dilution and ore loss.

The in situ model, representing perfect knowledge at all relevant scales, is obtained by geostatistical simulation. An in situ model that represents the reality of knowing only the data and information that are available from specific grade control drilling and sampling grids can be obtained by sampling the geostatistically simulated model on a specified grid. The volumes comprising the in situ model are then populated by estimates based only on the data corresponding to the specified grade control drilling and sampling grids. Different drilling and sampling grids can be used to generate different models, each reflecting the levels of data and information available. Selectivity can then be assessed as a function of the drilling and sampling grids as well as the size and type of loader. Performance is assessed against the ideal selectivity that can be achieved on the perfect knowledge model, comprising the simulated values of each component volume. Applying costs, prices and financial criteria enables an optimal selection of the grade control drilling grid, size of loader, type of loading and even blast design.

Blast Simulation

A discrete block modelling approach was used in the work reported here. The discrete block model is based on the SCRAMBLE code (Sophisticated CRA Model of Blasting with Explosives) developed by CRA (now Rio Tinto PLC) Advanced Technical Development from the ICI SABREX code (Scientific Approach to Blasting Rock with Explosives) (Harries and Hengst 1977; Jorgenson and Chung 1987; Kirby et al. 1987; Chung and Tidman 1988; Mohanty et al. 1988). The code has been revised to include, inter alia, a fragmentation model based on the Bond Work Index. Details of the basis of the blast simulation are given in Appendix A.

A standard regular block model is input to the blast simulator, which then moves each block to its final position within the muck pile. Although the block effectively remains intact in the muck pile, it is assigned an estimated degree of fragmentation. Movement and final position are determined from models of the behaviour of explosive gases, energy release, heave mechanics, fragmentation, throw and velocity of movement as functions of, inter alia, bench height, burden, hole spacing, hole diameter, rock density and rock fracture density.

This approach becomes more realistic as the block size becomes smaller and approaches the average size of particles in the muck pile. In principle, the block size can be made as small as desired but in practice the size is limited by computing constraints.

Simulating the Loading Process

The Floating Stope Optimiser (FSO) routine in the Datamine mine planning software was used to simulate an optimised selective loading process on the muck pile block model generated from a blast design. The FSO procedure is similar to the 'floating cone' method of open pit optimisation and provides a flexible means of locating optimal envelopes of block model grades (Randall and Wheeler 1998a, b).

To apply the FSO to a selective mining operation, the envelope size is defined as the selective mining unit for the excavation of the muck pile. The subcell size, which defines the grid spacing at which the envelope is successively positioned throughout the block model, is determined by the minimum digging width of the excavator used.

As an excavator works through a muck pile the broken rock continually recovers the natural angle of repose. Thus, to recover a pocket of ore near the bottom of a muck pile a 'cone' of material, projected up from the ore pocket, must be removed with it. To incorporate this in the selection process a slope of 45° is applied to the four vertical sides of the cube envelope from its base in the XY plane, generating the envelope shape shown in Fig. 1.

The output from the FSO flags all blocks as ore or waste. These are then processed to generate total tonnes mined, tonnes excavated as ore and waste, head grade of ore and tonnes of metal in ore. Multiple runs are taken for each muck pile over a range of cut-off grades to find the optimum.

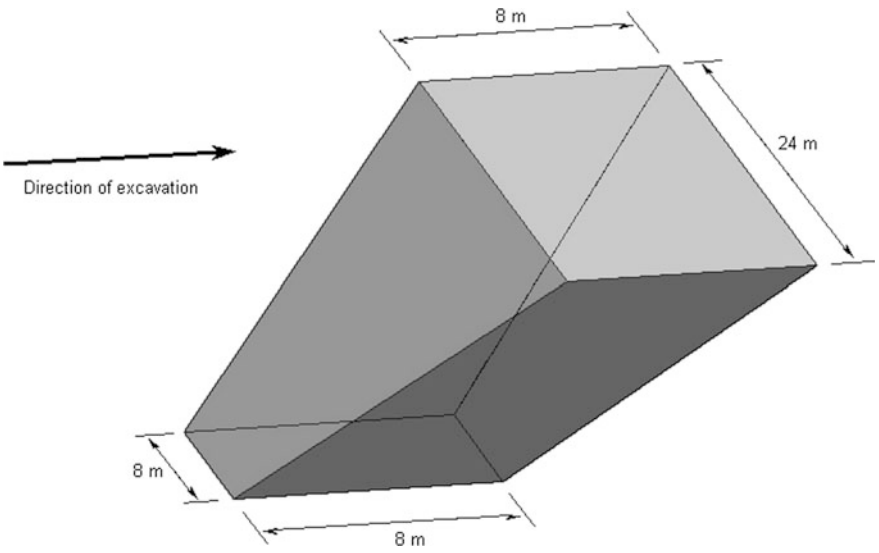

Fig. 1 Envelope shape for floating stope optimiser

Optimisation Procedure

A blast design is applied to the complete geostatistically simulated blast volume (the 'reality') and to the estimated block models for the blast design. Once the block models have been heaved to generate the corresponding muck piles, the muck pile block models, with associated block grade values, are entered into the FSO to evaluate the ore/waste excavation boundaries to give the optimum head grade based on a selected cut-off grade and selective mining unit size. The region of the bench that is to be excavated as ore is evaluated on the basis of the total tonnes of metal/mineral within that region minus the portion of metal/mineral expected to be lost in the processing operation.

The 80% passing size of the resulting muck pile (cf Appendix A) is then used to adjust the standard cost per tonne values for the downstream processes of loading, hauling and primary crushing. The total mining cost for the bench comprises the drilling and blasting costs derived from the blast design, the revised loading and hauling costs and the mining services costs, all as a cost per tonne blasted (cf Appendix B). The total processing cost comprises the adjusted primary crushing costs and the remaining processing operations costs, which are expressed as a cost per tonne processed.

The value of the bench is thus the value of the concentrate output from the processing plant less the mining and processing costs.

Case Study

The case study is based on the Minas de Rio Tinto SAL (MRT) open pit copper mine at Rio Tinto, southern Spain, which is typical of a low-grade operation in the later stages of its life. The application described here is to the low-grade Cerro Colorado mineralisation. Ore/waste delineation for selective mining is particularly difficult because the head grades are near the economic cut-off grade and there are no clear geological controls on the mineralisation.

At the time of this study, the mine had been temporarily closed pending an increase in the copper price. During operation the mine produced concentrate with an average grade of 24% copper. The mine re-opened, under new management, in 2014.

Geological Setting

The Rio Tinto deposit lies in the eastern Iberian Pyrite Belt. Submarine volcanic activity created an anticline structure, the edges of which formed pyroclastic rocks, where the massive sulphide mineralisations are located. The volcanic mass is buried under carboniferous slates, but subsequent folding has exposed the volcanic

sequence locally in the eastern half of the anticline to form the Cerro Colorado deposit (Pryor et al. 1972).

The Cerro Colorado mineralisation is a stockwork of sulphide accumulations, fed by several near-vertical brecciated feeder pipes. The predominant sulphides are pyrite and chalcopyrite, with galena, sphalerite, tetrahedrite, arsenopyrite and cassiterite present in much smaller quantities.

Mining Method

The operation at MRT used traditional drilling and blasting on 10 and 12 m benches that were drilled with two Buycrus Eyre 45R rigs and one 60R rig drilling 250 mm holes to a depth of 11.2 m or 13.7 m depending on the bench height. A square blast pattern was employed with burden and spacing dimensions ranging from 5.5 m 6.5 m to 6.6 m × 8.0 m. The holes were charged with heavy ANFO because of water problems in the lower benches. P&H 2100 BL electric face shovels and Caterpillar 994 wheel loaders were used for loading and Caterpillar 789 dump trucks used for hauling. Two blasts, B4053 and B4056, were selected for this study.

Generating Block Models

Experimental semi-variograms were calculated from the blasthole data using a conical search. As no significant directional anisotropies were detected within the two blast volumes, all directional semi-variograms for each blast were combined into a single omni-directional semi-variogram for modelling purposes. For both blast volumes a two-structure, spherical semi-variogram model was fitted to the experimental semi-variograms as shown in Fig. 2.

Sequential Gaussian simulation (Journel and Alabert 1989, 1990), with the blasthole grades as conditioning data, was used to generate a realisation of each entire bench on a block grid of 0.5 m × 0.5 m × 0.5 m, the grid determined on the basis of blast and selection criteria. The histograms of simulated values and conditioning data are shown in Fig. 3a and b; corresponding statistics are given in Table 1. There were no significant differences between the input variogram models shown in Fig. 2 and those fitted to the simulation outputs for the two blasts.

The simulations for both benches used ordinary kriging and an octant search strategy with an isotropic search radius of 60 m. A minimum of two and a maximum of ten conditioning values (original data plus previously simulated values) were specified for each octant with a minimum of three informed octants. The maximum proportion of previously simulated values in each set of conditioning values was set to 70% and the coordinates of the original data were retained, i.e. data was not assigned to simulation grid nodes. Linear extrapolation was used in the upper and lower tails for back transformation of the Gaussian simulated values.

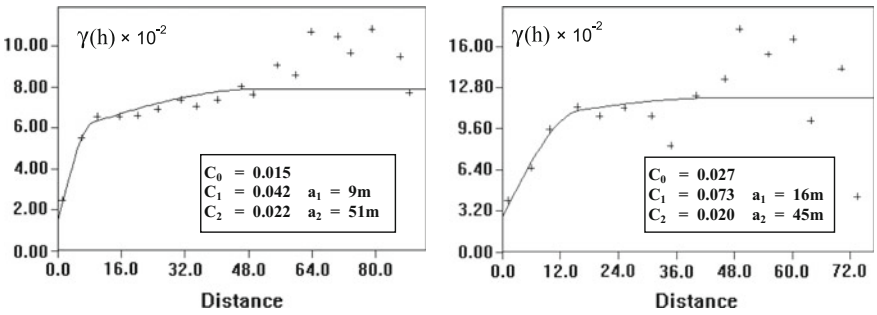

Fig. 2 Experimental semi-variograms and two-structure spherical models for B4053 (left) and B4056 (right) blasthole data

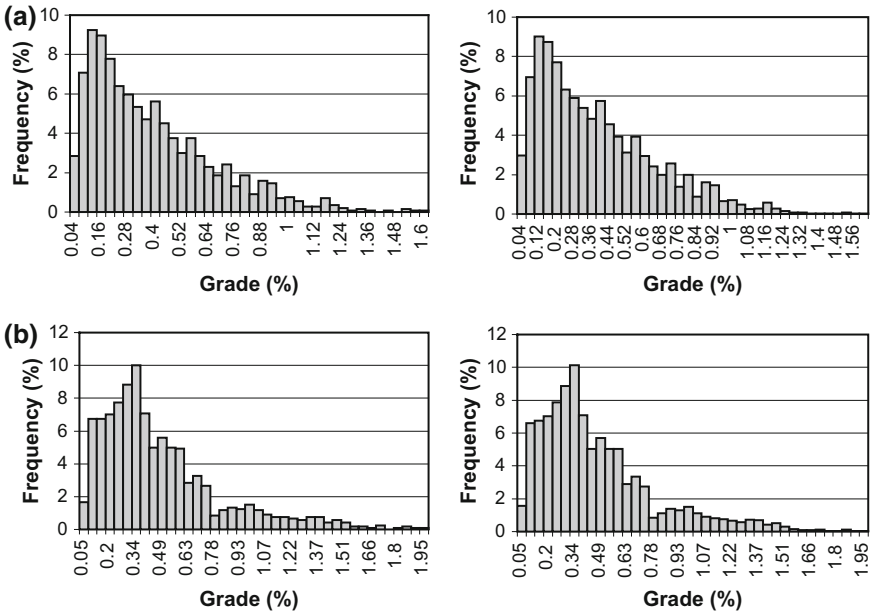

Fig. 3 **a**—Histograms of blasthole grades for blast B4053; data (left) and simulated values (right), **b**—Histograms of blasthole grades for blast B4056; data (left) and simulated values (right)

Table 1 Statistics of conditioning data and simulated values

	Blast B4053		Blast B4056	
	Conditioning data	Simulated values	Conditioning data	Simulated values
Mean	0.403%	0.401%	0.494%	0.489%
Variance	$0.075\%^2$	$0.072\%^2$	$0.113\%^2$	$0.105\%^2$
No of values	1440	288 000	1200	240 000

The simulation provides a realisation of the grade distribution throughout the bench on the scale required for the blast simulation. For each specified blast design, new 'sample hole data' is taken from the simulation block model of the bench. This sample data is then used to generate ordinary kriging estimates of the block grades to produce an estimated block grade model of the bench. The semi-variogram used for kriging is the model fitted to the experimental semi-variogram of the sample 'data' taken from the simulation block model.

Blast Modelling Parameters

The simulated heaving action and muck pile generation were adapted to replicate the muck piles generated by the actual blasts, based on the data available for throw and the overall shape of the muck pile profile.

The blast pattern specifications for the two blasts used in this study are shown in Table 2 and the geomechanical data used is summarised in Table 3. The modelling was calibrated against the original blast designs for B4053 and B4056 using the input data in Tables 2 and 3 and the muck pile profiles from field data.

Selection of Ore/Waste Boundaries in Muck Piles

For the excavators used at MRT, with a bucket size of 13 m^3, an FSO envelope of 8 m × 8 m × 8 m was selected with a subcell size of 2.7 m. More selective loading was also assessed using a 6 m × 6 m × 6 m envelope.

Costs of the Blasting and Selection Processes

For a given blast design it is relatively straightforward to calculate the costs associated with drilling and blasting, by summing the constituent costs. However, the composition of the muck pile produced by the blast directly affects the downstream processes of loading, hauling and primary crushing, and the overall

Table 2 Blast pattern specifications used in case study

Burden	6.5 m	Main explosive charge	540 kg ANFO
Spacing	8.0 m	Initiation sequence	S1
Bench height	12 m	Inter-hole delay	50 ms
Vertical blasthole length	13.7 m	Inter-row delay	100 ms
Hole diameter	250 mm		

Table 3 Geomechanical data used in case study

Young's modulus	750 kbars
Poisson's ratio	0.25
Uniaxial compressive strength	1.2 kbars
Rock density	2.75 g.cm^{-3}

cost evaluation of a blast must include the costs of these processes. It is not possible to quantify directly the effect of different quality blasts on the downstream processes, and the best common variable for comparisons is the degree of fragmentation achieved by the blast. It is generally recognised that the costs of the downstream processes, including operation and maintenance, decrease as fragmentation improves (MacKenzie 1966). A common practice is to use a functional relationship, formulated through in-pit operational assessment, to adjust the cost per unit weight worked as a function of the degree of fragmentation. A summary of the cost functions and their derivation is given in Appendix B.

Optimisation Procedure

The flow diagram in Fig. 4 shows the procedure applied to each bench. The chosen blast design is applied to the standard geostatistical simulation and estimated block models for that blast design.

Once the block models are heaved to generate the corresponding muck piles, the muck pile block models, with their associated block grade values, are entered into Datamine. Within Datamine, the FSO is applied to the block models to evaluate the ore/waste excavation boundaries to give the optimum head grade based on a selected cut-off grade and selective mining unit. The region of the bench that is to be excavated as ore is evaluated on the basis of the total tonnes of copper within that region, minus the portion of copper expected to be lost during processing.

The flow chart in Fig. 4 is an example of what might be termed a transfer function that transforms the idealised/in situ/simulated, and/or estimated, block grades into realistically recoverable grades and tonnages. These transfer functions are not generally linear and in most cases their effects cannot be approximated by simple dilution factors.

Ore reserve statements, or resource statements expressed in terms of production units, that are derived by selecting blocks directly from in situ/block models ignore some of the most significant sources of uncertainty. There may be other highly non-linear transfer functions (e.g. some types of mineral processing operations) that have significant effects on recoverability, but generally the extraction and loading processes are the most significant.

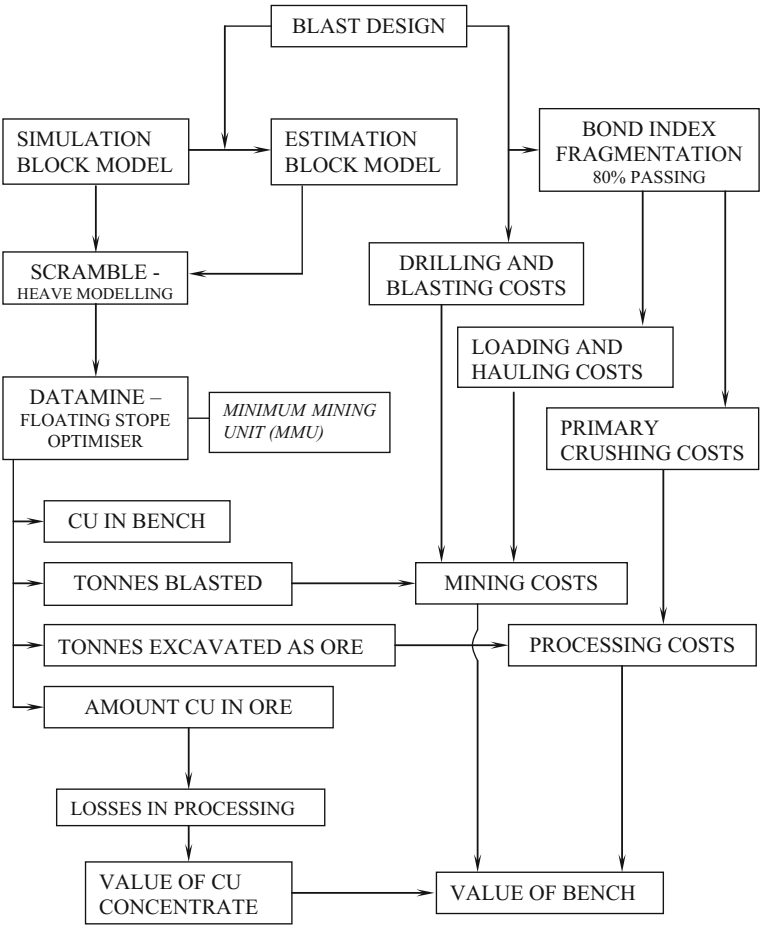

Fig. 4 Flow chart for optimisation procedure

Results

By way of example, Fig. 5 shows colour-coded simulated grades of sections of the 0.5 m × 0.5 m × 0.5 m blocks that comprise bench B4056 and Fig. 6a shows the muck pile generated by applying the blast modelling process to this bench.

Figure 6b shows the muck pile that results from applying the blast modelling to the same bench but with the component block grades kriged from the simulated grades on the 6.5 m × 8 m drilling grid. The smoothing effect of kriging is clearly evident when comparing Fig. 6a and b. Figure 6a represents the muck pile given complete information, whereas Fig. 6b is the interpretation of the composition of the muck pile on the basis of the data. Selection is planned and implemented on the

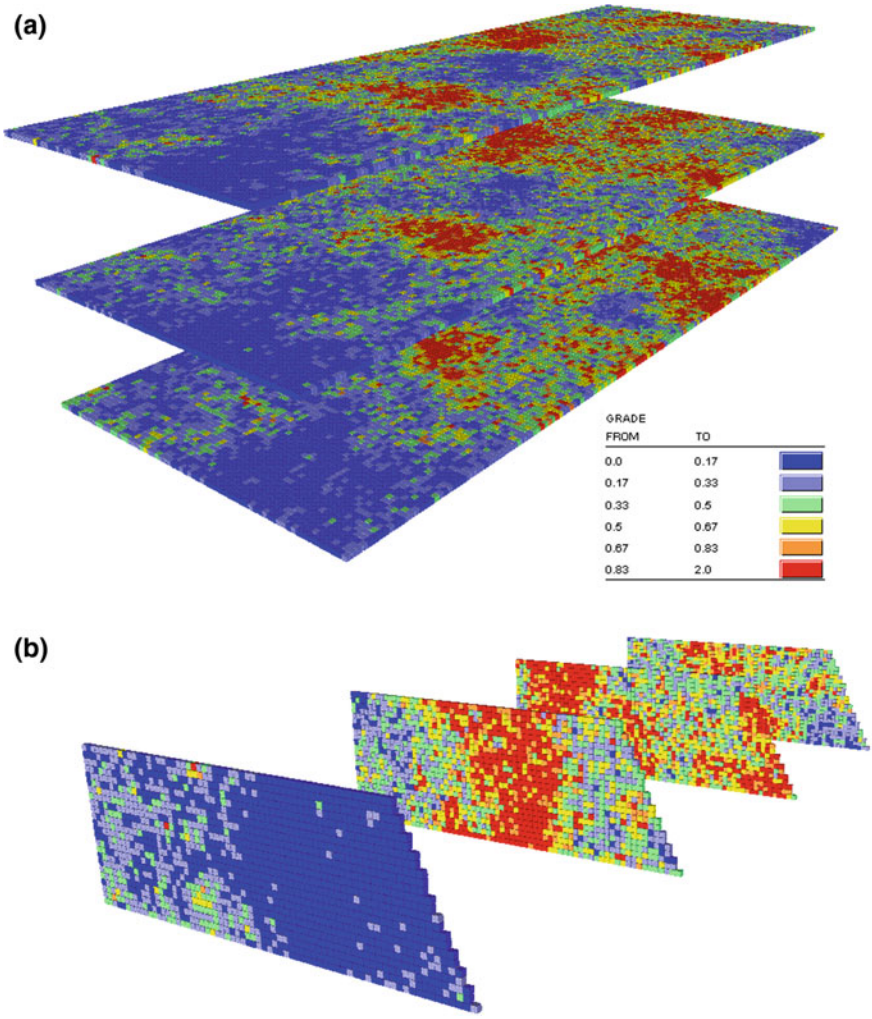

Fig. 5 Representations of the simulated in situ bench grades for 84,056 showing colour-coded grade ranges on **a** horizontal planes and **b** cross-sectional planes. Horizontal planes are top and bottom of t 2 m bench and 6 m mid-plane. Vertical planes are extremities (0 and 80 m) and intermediate planes at 26 m intervals

basis of Fig. 6b but the volume selected will have the grade and tonnage of the equivalent volume in Fig. 6a.

Figure 7 shows the corresponding muck piles generated from simulated and estimated block grade models for B4053. Figures 6 and 7 clearly show the significantly different spatial distribution of grades in the two muck piles with consequent implications for selection.

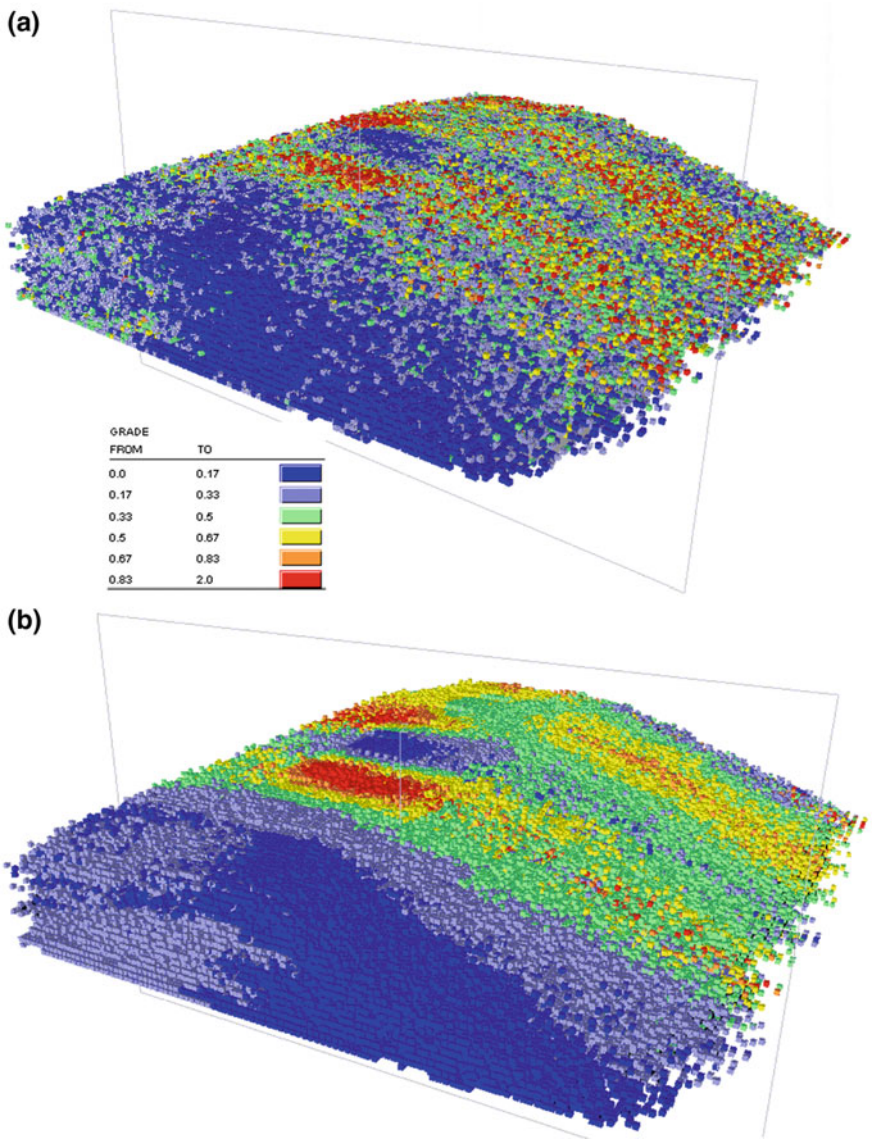

Fig. 6 84056: Muck piles generated by blast design number one from (a) simulated bench grades and (b) from kriged bench grades

By way of example, when selection is applied via the FSO to the two muck piles shown in Fig. 7, the volumes selected are those shown in Figs. 8 and 9.

For each bench there are nine block models: the simulated block grades, taken as 'reality', and eight models of estimated block grades kriged from simulated values on various drilling grids, together with variations in other blast design parameters as summarised in Table 4.

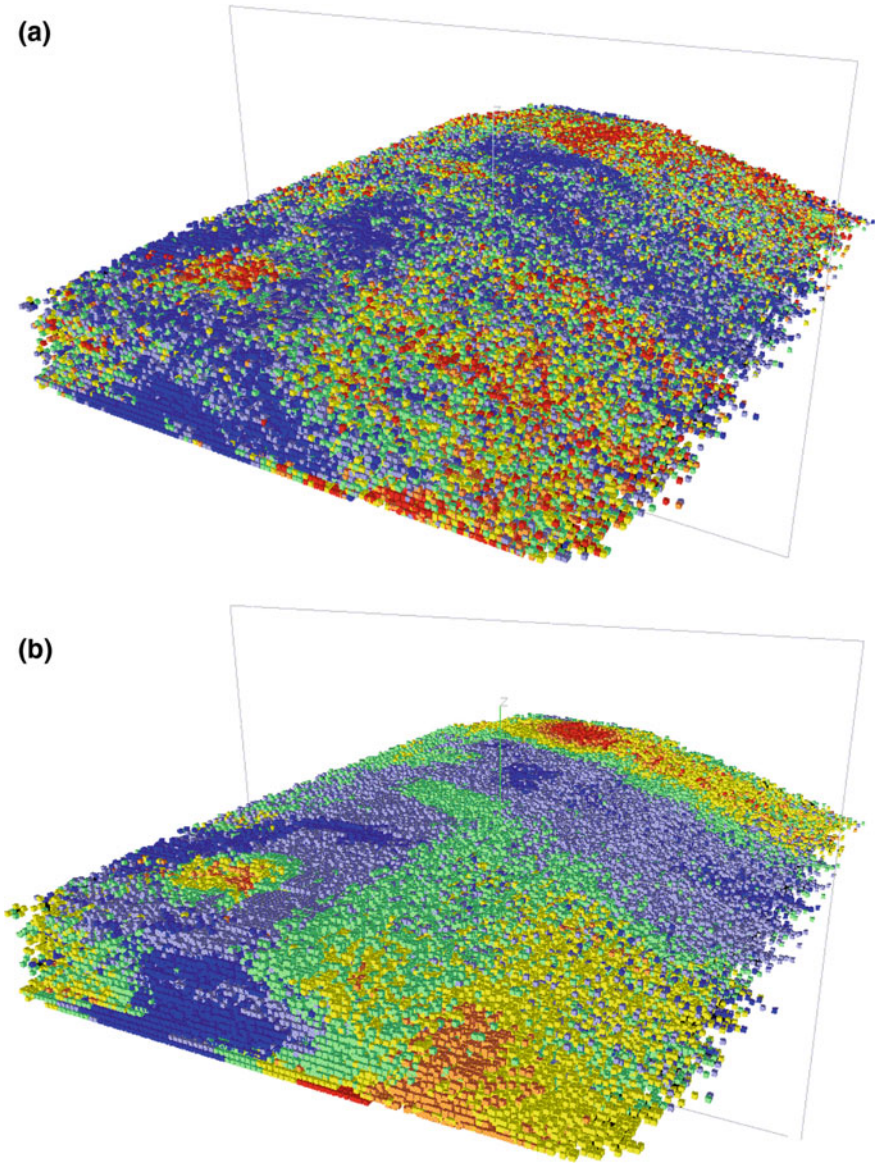

Fig. 7 B4053: Muck piles generated by blast design number one from **a** simulated bench grades and **b** from kriged bench grades

The grades of the blocks that comprise the two benches are similar in terms of histograms (cf Fig. 3) but they differ significantly in their spatial distributions within the respective benches. It is the latter that has the major effect on the spatial distribution of the grades in the muck pile and consequently on the ability to load selectively.

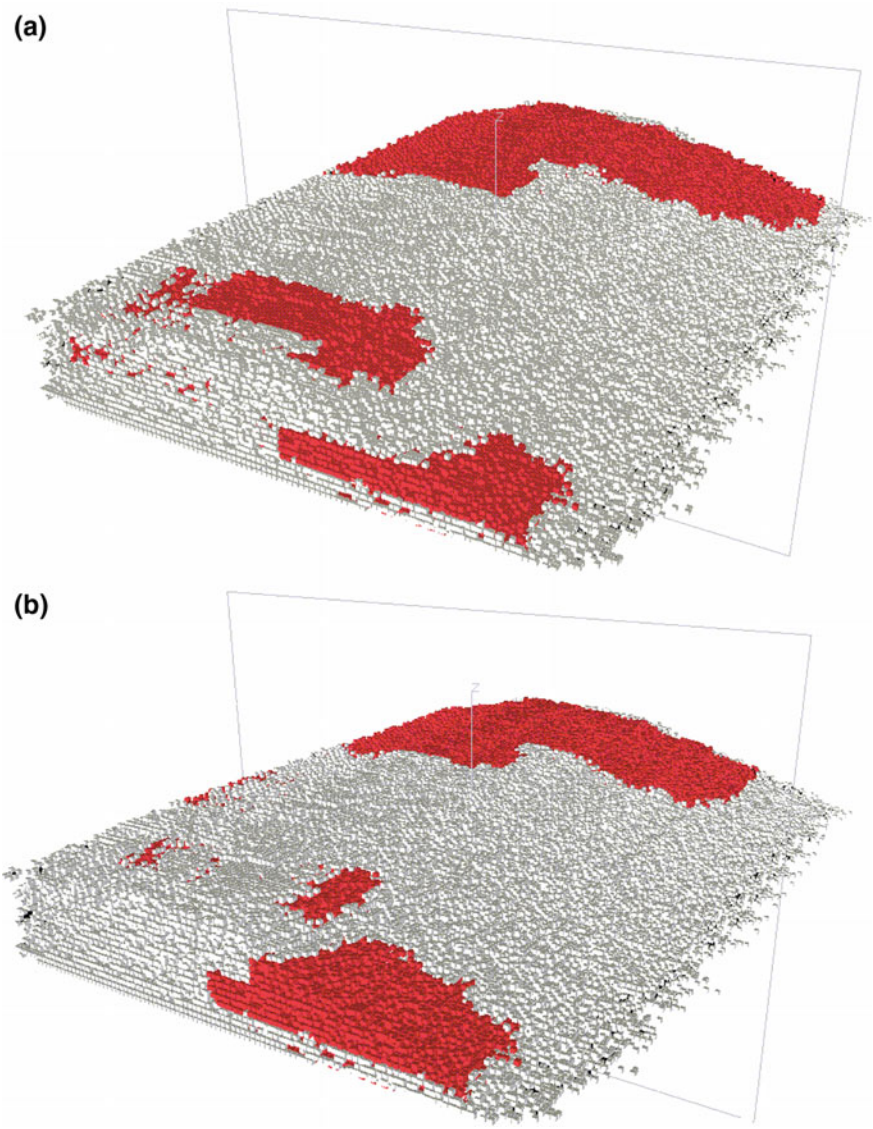

Fig. 8 Muck piles for B4053. **a** Muck pile generated from simulated block grades (reality). **b** Muck pile generated from estimated block grades using blast design one. The darker shade indicates exposed selected ore and the lighter shade is non-selected broken rock

Bench B4053 is subeconomic for some blast designs but must still be blasted to allow continuing mine development. Having blasted this bench, any losses are minimised by processing the ore in the muck pile. Bench B4056 is economic for all blast designs and is mined and processed in the normal manner.

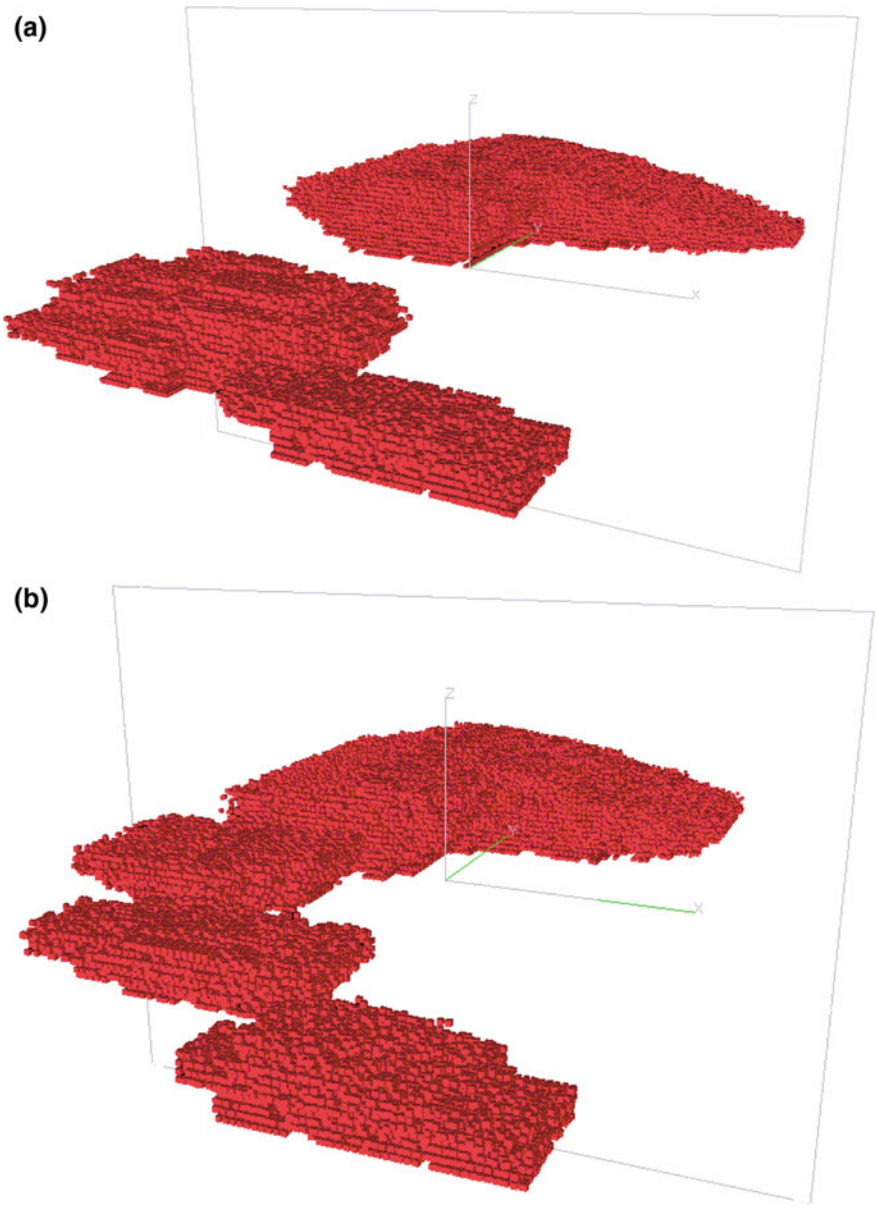

Fig. 9 Volumes of ore selected from muck pile for blast design 1, generated from **a** simulated block grades and **b** from estimated block grades

The financial performances of each blast design against the 'reality' of the simulated block model are summarised in Fig. 10 for B4053 and in Fig. 11 for B4056. These figures show the ideal or maximum bench values corresponding to

Table 4 Blast designs used in study for estimated block grades

Blast design	Design changes	Burden (m)	Spacing (m)	Powder factor (kg tonne^{-1})	Hole diameter (m)
1	Control	6.5	8	0.31	0.25
2	Changing hole diameter	6	7.5	0.31	0.23
3		7	9	0.31	0.27
4		8	9.5	0.31	0.30
5	Increasing powder factor	6	7.5	0.37	0.25
6		5.5	7	0.43	0.25
7	Decreasing powder factor	7.5	9	0.25	0.25
8		8.50	10.5	0.19	0.25

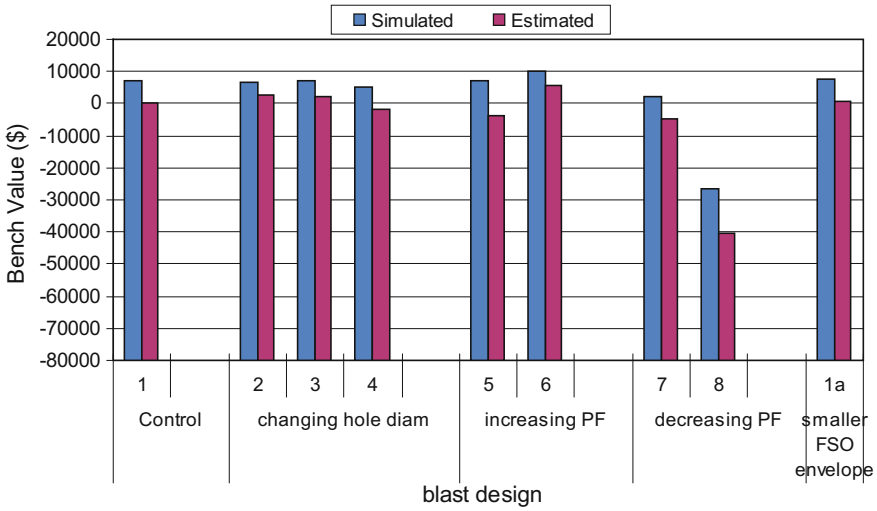

Fig. 10 B4053 optimised bench values for blast designs

the simulated block grades, together with the actual bench values achieved by selecting from the muck piles generated from the estimated block grades for the various blast designs.

Figures 12 and 13 show the tonnages of copper within the ore selected from the muck pile generated from the simulated block grades, together with the actual tonnages recovered from the muck piles generated from the estimated block grades for the various blast designs.

Numbers on the horizontal axes of Figs. 10, 11, 12 and 13 denote the blast designs given in Table 1. Blast 1a (smaller FSO envelope) is a smaller selection envelope applied to blast one, in which the envelope corresponds to smaller-scale selection (6 m × 6 m × 6 m) using a wheel loader.

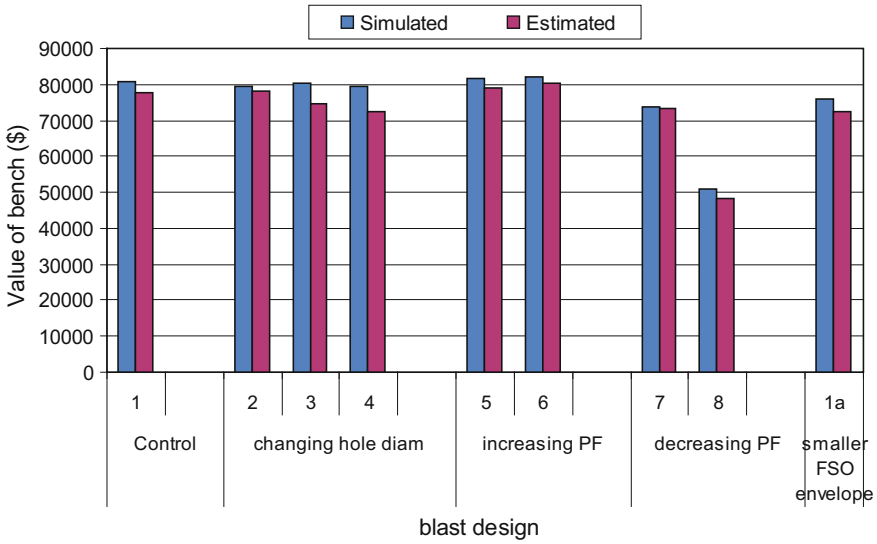

Fig. 11 B4056 optimised bench values for blast designs

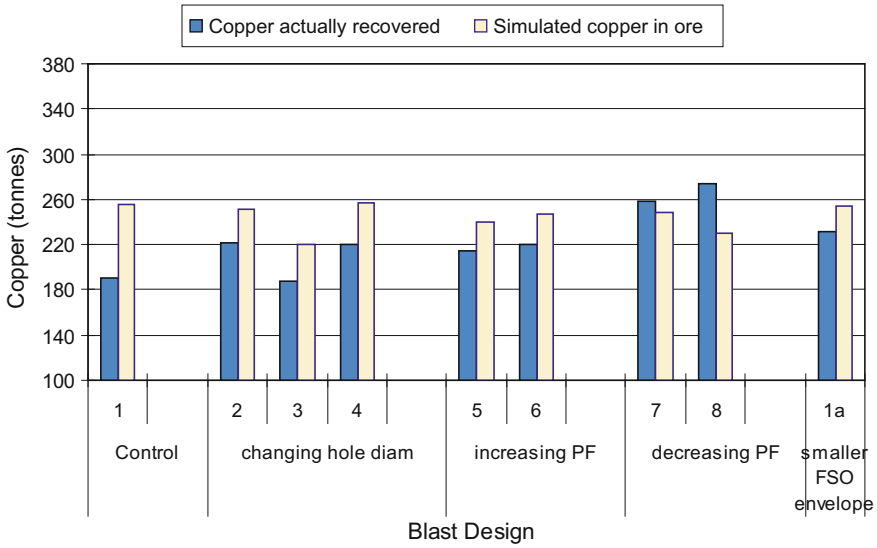

Fig. 12 B4053: simulated ('actual') copper in ore selected from muck pile and amounts recovered on the basis of estimations from Design

Note that in some cases, more copper is recovered from the muck pile generated from the estimated block grades than from the muck pile generated from the simulated block grades (e.g. blast designs seven and eight in Fig. 12). This is,

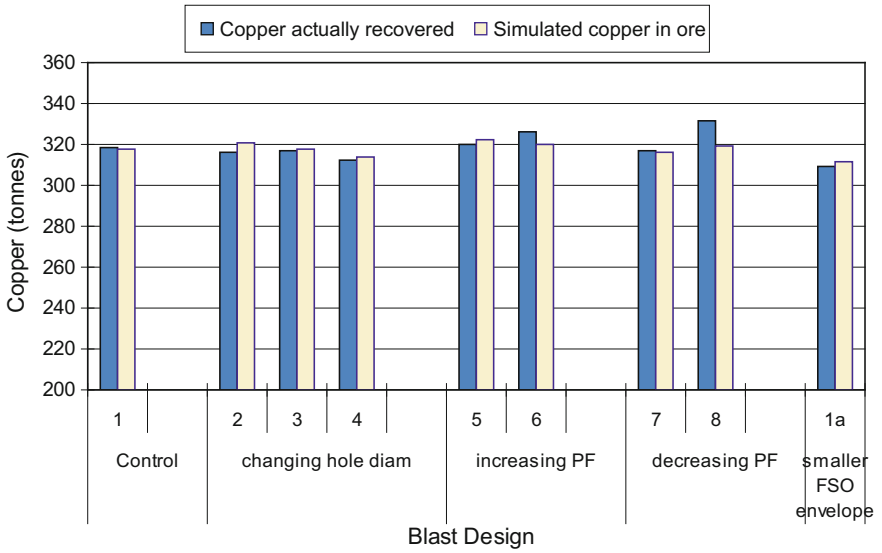

Fig. 13 B4056: simulated ('actual') copper in ore selected from muck pile and amounts recovered on the basis of estimations from various blast designs

however, at the expense of diluting the ore with additional waste, which reduces profit (e.g. as indicated by the bench values for blasts seven and eight in Fig. 10).

The differences between ideal selection and selection based on estimated block grades are more significant for B4053 because the economic grades are more widely dispersed through the bench and the muck piles than they are for B4056. The differences are large and critical for B4053, as planning on the basis of the estimated block grades leads, more often than not, to financial loss.

The real effects on the operation can be quantified by comparing the expected performance against the actual performance. Figures 14 and 15 show, for each blast design and for selection based on the estimated block grade models, the difference between the estimated copper content and the actual copper content of the selected ore regions, together with the difference between the estimated and actual financial values of the selected ore regions. It is these differences between planned and actual performances that have the greatest impact on the viability of the operation.

The results summarised in Figs. 14 and 15 are functions of the complex relationships among block grade values, heave mechanics of the blasting process, the spatial distribution of ore and waste blocks in the muck pile and the method of selecting from the muck pile. The absolute values of the bars shown in Figs. 14 and 15 are the deviations from planned outcomes and are measures of the ability to plan the operation to acceptable levels of accuracy and of the consequences of not being able to do so. The larger differences for B4056 (Fig. 15) are a function of the more distinct ore/waste boundaries in the resulting muck pile, which in turn provide a greater propensity for ore loss and ore dilution with small changes in the selection

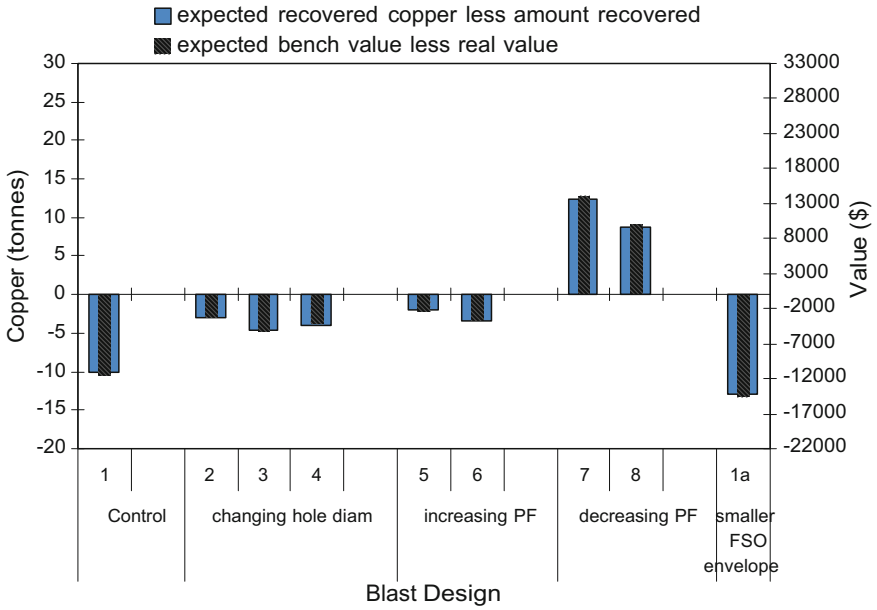

Fig. 14 Differences between planned and actual performance for B4053

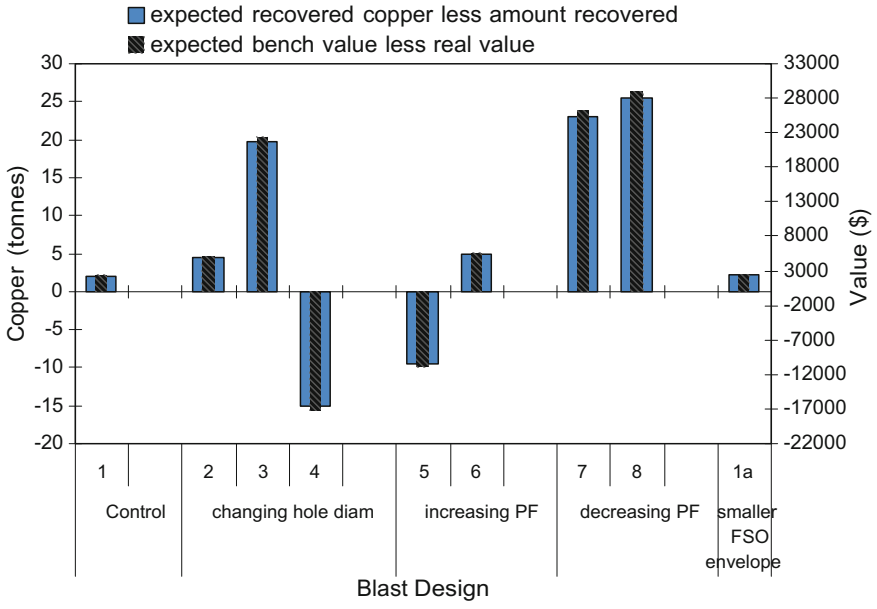

Fig. 15 Differences between planned and actual performance for B4056

volumes. By contrast, the greater dispersion of the ore throughout the muck pile generated from B4053 offers less scope for selectivity and less adverse consequences arising from changes in the selection volumes.

Summary and Conclusions

This study demonstrates the potential of geostatistical simulation in the optimisation of blasting and loading in selective mining processes. In particular, it provides a means of quantifying the effects of grade distribution smoothing on blast design and the selection of ore regions within the resulting muck pile. It also provides a means of assessing the financial consequences of ore loss and dilution arising from planning and implementing specific blasting and loading practices on the basis of various drilling grids.

Although a very specific blast modelling process has been used in this study, it could readily be replaced by any other type of modelling, either to provide a more realistic simulation of heave mechanics and fragmentation or to simulate other types of blasting and selection. Similarly, other types of geostatistical simulation could be used and multiple variables, including qualitative geological variables, could be simulated and incorporated into the selection procedure, for example by selecting gold-bearing ore on the basis of observable quartz veins and fracture networks in the muck pile (Dowd 1995). The methods and approach used in this study do not limit the generality and practical potential of the application.

A real-time, virtual reality version of the approach described here could also be used to guide loader operators in making optimal selections from muck piles. Real-time applications would require very rapid capture of accurate survey and locational data, which could readily be provided by GPS.

More generally, the application described here demonstrates that the full effectiveness of geostatistical simulation can only be realised in mining applications by integrating it with adequate simulations of the technical processes that turn the simulated in situ characteristics into mined products. This is an important issue in determining and reporting reserves.

Appendix A: Blast Modelling

The adapted version of the SCRAMBLE/SABREX blast modelling code used in this study is an energy-based approach comprising two separate models: heave mechanics and fragmentation. The heave mechanics are based on the energy released from the adiabatic expansion of the explosive gases following detonation. Fragmentation is based on the powder factor (ratio of charge weight in kilograms to mass in tonnes of rock broken by the charge) converted to an energy equivalent via the Bond Index.

The velocity of detonation for each blasthole is taken as infinite and the wall is allowed to expand until it reaches a state of equilibrium determined by the isotropic expansion characteristics of the quasi-static gas pressure and the elastic resistance of the rock. The expanded blasthole sets up hoop stresses in the surrounding rock, creating a system of radial cracks that, because of tensile failure, spread away from the hole. The radial fractures, together with any pre-existing geological discontinuities, define the damage created in the rock mass by the blast.

The gaseous detonation products flow into the fractured rock mass at the local speed of sound until the gas vents through a free face; at this stage a rarefaction wave travels back toward each blasthole decompressing the cracks. As the rarefaction wave travels through the rock, the pressurised crack system imparts an impulse, which heaves the broken rock mass out from the bench.

In generating the muck pile, empirical routines are used to limit the angle of repose whilst producing a smooth surface and adding swell factors.

Equation of State for Explosive Gases

The equation of state for the gaseous products of detonation is:

$$p = \frac{\alpha E \rho (1 + \beta\rho)^3}{100(1 + 2\beta\rho)} \tag{A1}$$

where:

p	is the gas pressure in kbars
ρ	is the gas density in g.cm^{-3}
E	is the available energy in J.g^{-1}
α and β	are dimensionless constants.

The available energy E is the work done by the explosive gases in expanding adiabatically from the density ρ to ambient conditions, and is obtained from:

$$\ln\left(\frac{E}{E_0}\right) = \alpha\left(\frac{(\beta\rho)^2 + 5\beta\rho}{4} - \frac{(\beta\rho_0)^2 + 5\beta\rho_0}{4} + \frac{1}{8}\ln\left[\frac{\rho(1 + 2\beta\rho_0}{\rho_0(1 + 2\beta\rho)}\right]\right) \tag{A2}$$

where:

ρ_0	is the initial gas density after detonation (equal to the explosive density)
E_0	is the initial available energy

The values for E_0, α and β can be obtained from an ideal or non-ideal detonation model. An ideal detonation model is adequate for the large diameter holes used in this study; more accurate data could be obtained from non-ideal models such as CpeX (Leiper and Plessis 1987).

Equation A1 reduces to the ideal gas law for small gas densities and, together with Eq. A2, allows available energy and pressure to be generated as a function of their density during the expansion process.

Heave Mechanics

All regions within the gas envelope have a common gas density and pressure. The leading edge of the envelope is regarded as the gas front, which is assumed to move at the local speed of sound (m.s^{-1}) given by:

$$c = \left(\frac{100000\gamma p}{\rho}\right)^{\frac{1}{2}} \tag{A3}$$

where γ is the adiabatic exponent for the gases at pressure p (*kbar*) and the density ρ(g.cm^{-3}), γ is given by:

$$\gamma = \left(\frac{1+\alpha(1+\beta\rho)^3}{1+2\beta\rho}\right) + \left(\frac{3\beta\rho}{1+\beta\rho}\right) \tag{A4}$$

and is derived from the equation of state given in Eq. A1.

To calculate the necessary density and pressure of the gas within the envelope the volume of rock within the envelope is assumed to be in a state of hydrostatic compression at pressure p. The resultant reduction in the volume of rock is given by:

$$\Delta V + \frac{Vp}{G} \tag{A5}$$

V is the initial volume (m^3)
G is the bulk modulus
ΔV is the volume increase in the envelope contributing to the reduction in gas density and pressure.

Another small increase in volume is associated with the gas pressure compressing the rock below and behind the blasthole.

As the gas expands with the moving gas front, the local speed of sound in Eq. A3 falls and a time-stepping loop is used to track the expansion of the gas. The time steps used are defined by:

$$\Delta t = \frac{b + \Delta b}{c} \tag{A6}$$

where:radius $b + \Delta b$ is the equilibrium radius blasthole.

Equation A6 shows that, although the time steps can vary, the corresponding spatial steps are constant and equal to the equilibrium borehole radius.

The time-stepping procedure is:

1. calculate the initial local speed of sound from Eqs. A3 and A4 prior to the expansion of gas into the rock mass;
2. calculate the appropriate time step from Eq. A6 and generate the appropriate gas front profile;
3. calculate the increase in volume from Eq. A5 and then calculate the new gas pressure and density using Eqs. A1 and A2;
4. recalculate the local speed of sound using Eqs. A3 and A4; and
5. repeat the steps while keeping track of the total elapsed time.

Venting of the explosive gas begins when the gas front meets a free face. At that time the gas fronts retrace their original paths and, during this period of contraction, the gas density, pressure and speed of sound are assumed to be constant within the volume of the gas envelope. The respective constant values are those that were calculated at the time of venting, while the pressure beyond the gas fronts is assumed to be insignificant.

At the time of venting, the rock mass is assumed free to move, reacting to a momentum impulse that is imparted on the rock mass. The calculated impulse is based on the assumption that the rock mass does not start to move until the gas fronts have (kg.ms^{-1}) is given by:

$$10^8 \int_{t_v}^{t_0} p(t_v)A(t)dt - M.v \tag{A7}$$

where:

t_v is the time (s) at which gas venting takes place
t_0 is the time (s) at which the contracting gas fronts reach their blastholes
$p(t_v)$ is the gas pressure (kbar) in the gas envelope
$A(t)$ is the area (m^2) over which the pressure is applied
M is the mass (kg) associated with each blasthole
v is the velocity (ms^{-1}) with which the rock mass is heaved
t is the time (s).

To derive heave velocities from Eq. A7 an expression for M can be applied for a vertical free face to calculate the mass of rock associated with each blasthole using:

$$M = B.S.H\rho_R.1000 \tag{A8}$$

where:

B is the burden (m)
S is the hole spacing (m)
H is the bench height (m)
ρ_R is the rock density (g.cm^{-3}).

In practical situations the highwall of a bench is not vertical and the program has an input variable for face angle to calculate the true mass of rock associated with the first row of holes.

The momentum impulse for each blasthole is resolved into the vertical and horizontal directions on the basis of the areas defined by the gas envelope. For the vertical impulse the area at the base of the envelope is used in Eq. A7. However, due to the angled highwall, the front row has an inconsistent burden and the area is taken as an average of the areas at the top and bottom of the explosive column length.

Two impulses are computed in the horizontal direction. The first is the section of rock between the toe of the bench and the top of the explosive column, and the second impulse is the region at the top of the bench where the blasthole is filled with stemming material.

A similar averaging process is used to account for the effect of the front row of holes in the calculation of the horizontal impulse, which results in three horizontal heave velocities defining the heave velocity profile. On subsequent rows the effective free face is assumed to be vertical.

For the heave action, the blocks comprising the block model are treated sequentially within a time-stepping loop using a raster pattern starting at the toe of the bench with priority given in order to z, x and then y. For each run through the time-stepping loop all block positions and velocities are recalculated from ballistic trajectory equations and the revised values are stored in three-dimensional arrays; in-flight interactions with other blocks are not modelled. Each block remains in the time-stepping loop until it travels to a point in space at which, ahead or below it, another three-dimensional array describing the mine floor has a positive value, defining that volume of space as containing a block.

When a block drops out of the time-stepping loop to form part of the muck pile it immediately comes to rest on the ground and becomes part of the array that defines the floor and the developing muck pile. The input value for maximum angle of repose ensures that if the defined angle is exceeded in the generation of the muck pile then the block is moved down the surface of the muck pile until it reaches a point of stability.

When all blocks have come to rest, swell is applied to the muck pile by raising each block by a pre-defined factor proportional to the change in vertical height the block underwent in moving from the bench to the muck pile.

Fragmentation

The Bond Index equation from comminution theory is used to assess the effect of different blasting practices on the degree of fragmentation resulting from a blast (Van Zeggeren and Chung 1975; Nielsen 1983). The equation relating energy input to degree of comminution is:

$$W = K_B\left[\frac{1}{P^{1/2}} - \frac{1}{F^{1/2}}\right] \tag{A9}$$

where:

W is the energy input to a machine reducing particle size (kWh.t^{-1})
F is the feed size, measured in microns (10^{-6} m), and defined as the mesh size of a screen that allows 80% of the material to pass
P is the product size in microns also at 80% passing
K_B is a constant determined for a specific feed material

The constant K_B is determined by rearranging Eq. A10 to give:

$$K_B = W\left[\frac{P^{1/2}F^{1/2}}{F^{1/2} - P^{1/2}}\right] \tag{A10}$$

and the amount of energy required to reduce a known feed size to a given product size is measured. For MRT the amount of energy needed to reduce the secondary crushed product from −19 mm to a final product size of −210 microns was, on average over a two-month period, 16.10 kWh.tonne^{-1}. As the Bond Index works on 80% passing size, the feed and product sizes are taken as 16,300 microns (16.3 mm) and 180 microns respectively. Substituting these values into Eq. A10 gives:

$$K_B = 16.10 \times \left[\frac{180^{1/2} \times 16300^{1/2}}{16300^{1/2} - 180^{1/2}}\right] = 241.4kWh - micron^{1/2}.tonne^{-1}$$

Equation A9 can also be rearranged to calculate the energy required to reduce an infinite feed size ($F = \infty$) down to any product size P. This is referred to as the total energy (W_t) and is given by:

$$W_t = K_B\left[\frac{1}{P^{1/2}} - \frac{1}{\infty^{1/2}}\right] = \frac{K_B}{P^{1/2}} \tag{A11}$$

Based on Eq. A11, the Bond Work Index (W_i) is the amount of energy required to reduce an infinite feed size down to an 80% passing size of 100 microns. This is used as a common basis of comparison across different materials and processes and is given by:

$$W_i = K_B\left[\frac{1}{100^{1/2}} - \frac{1}{\infty^{1/2}}\right] = \frac{K_B}{100^{1/2}} \tag{A12}$$

Substituting the calculated K_B in Eq. A12 gives:

$$W_i = \frac{241.4}{100^{1/2}} = 24.1 kWh.tonne^{-1}$$

From Eqs. A11 and A12 it is possible to calculate the energy required to reduce material from an infinite size down to the desired 80% passing size as:

$$W_t = W_i \left[\frac{100}{P}\right]^{1/2} \tag{A13}$$

If it is assumed that the only factor that influences the degree of fragmentation in blasting is the amount of energy imparted to the rock mass, and that the energy distribution and initiation variables can be ignored, then Eq. A13 should give a good representation of the energy input from the explosive in a blast, based on the resulting fragmentation.

For the 6.5 m × 8 m MRT blast designs, the material in the resulting muck piles had an 80% passing size of approximately 0.5 m. From Eq. A13 the energy imparted by the explosive is:

$$W_t = \left[\frac{100}{5 \times 10^5}\right]^{1/2} = 0.34\, kWh.tonne^{-1} = 1.23\, MJtonne^{-1}$$

The energy supplied by the explosive acting on the rock mass can be derived from the known powder factor (PF) at 0.31 kg.tonne^{-1} for the blasts and the energy contained in the explosive used. The energy for the heavy ANFO used, with specific density 1.2 g.cm^{-3}, is 4.5 MJ.kg^{-1}. The explosive energy per tonne is therefore:

$$\text{PF} \times \text{Explosive Energy} = 0.31 \times 4.5 = 1.40 \text{ MJ.tonne}^{-1}$$

This value of 1.40 MJ.tonne^{-1} compares favourably with the value of 1.23 MJ.tonne^{-1} derived using the Bond Index for comminution (Hustrulid 1999). If it is assumed that the difference in values is due to slight differences in the efficiencies of the two processes then it is reasonable to reconcile the two values by applying a factor (α) that is appropriate over a range of energies.

By rearranging Eq. A13 and applying the correction factor α (Van Zeggeren and Chung 1975) the equation for product size from the powder factor used in the blast design is:

$$P = \left(\left[\frac{W_i}{W_t}\right] \times \alpha\right)^2 \tag{A14}$$

where:

W_t is the energy equivalent of the powder factor.

Appendix B: Costing the Blasting and Selection Processes

To simplify calculations, all process costs are calculated as cost per tonne worked.

Drilling Costs

Drilling costs are expressed as a cost per metre drilled (DC_m) for the 250 mm hole diameter used in this study. The tonnage of rock associated with each blasthole, taken as a standard for a specific hole pattern, is given by Eq. A8, divided by 1000 to give tonnes. Cost per tonne (DC_t) is then:

$$DC_t = \frac{DC_m \times HL}{M} \tag{B1}$$

where:

HL is the hole length (m), including subdrill.

Blasting Costs

The initial costs are calculated for a single hole and are divided into fixed costs per hole—booster, detonator, surface connection and manpower costs—and the variable cost of the main charge placed in the hole. The main charge costs (EX_m) in dollars are calculated using:

$$EX_m = EX \times (A_h \times EC_l) \times \rho_e \tag{B2}$$

where:

EX is the cost of the explosive ($\$.kg^{-1}$)
A_h is the cross-sectional area of the hole (m^2)
EC_l is the charge length of the explosive in the hole (m)
ρ_e is the density of the explosive used ($g.cm^{-3}$).

Loading Costs

The loading costs for the original blast design are taken as \$0.14/tonne for a muck pile with 80% passing size of 0.5 m. Within reasonable limits, as passing size decreases loading costs decrease, due mainly to an increase in the ease of digging, which leads to faster loading rates and reduced maintenance costs. MacKenzie (1966) reports a linear relationship between cost per unit loading and degree of fragmentation for Quebec Cartier's 16-D iron ore mine. Van Zeggeren and Chung (1975) found that their data followed a square root relationship and Nielsen (1983) used a variable exponent selected by the user. For this application, with too few operational data to derive an appropriate relationship, the linear equation is:

$$C_l = (D80 \times \alpha) + (SC_l - \beta) \tag{B3}$$

where:

Cl is the adjusted loading cost ($.tonne^{-1})
$D80$ is the calculated 80% passing size (m) using Eq. A14
SC_l is the standard loading cost (0.14 $.tonne^{-1})
α, β are constants.

The incorporation of the standard loading cost (SC_l) in Eq. B3 allows the loading cost relationship to be adjusted for different loaders with different attributes.

Haulage Costs

Haulage costs also decrease with muck pile particle size because the truck is more completely filled, providing the ore density allows it. The relationship used for haulage costs, (Ch), in $/tonne is:

$$C_h = \chi.e^{D80} \tag{B4}$$

where:

χ is a constant.

Primary Crushing Costs

Because variations in feed size to the primary crusher affect power costs much more than general maintenance and plate replacement costs, the Bond Index Eq. A9 was used to calculate crushing costs:

$$C_{cr} = \delta \times 241.4 \times \left(\frac{1}{16300^{1/2}} - \frac{1}{D80^{1/2}} \right) \tag{B5}$$

where:

C_{cr} is the adjusted crushing cost ($.tonne^{-1})
δ is a constant.

Costs Unaffected by Blasting Practices

Costs incurred in producing a saleable product that are not affected by blasting practices include mining services and the entire mineral processing operation downstream of the primary crushing. These values, also expressed as $/tonne, are assumed to remain constant.

References

Chung SH, Tidman JP (1988) Effective modelling for cast blasting. In: Singhal RK (ed) Proceedings international symposium for mine planning and equipment selection. A A Balkema, Rotterdam, pp 357–360

Dowd PA (1995) Björkdal gold mining project, northern Sweden. Trans Inst Min Metall Sect A Min Technol 104:A149–A163

Harries G, Hengst B (1977) Use of a computer to describe blasting. In: Proceedings 15th APCOM symposium. Melbourne, The Australasian Institute of Mining and Metallurgy, pp 317–324

Hustrulid W (1999) Blasting principles for open pit mining. General Design Concepts, vol 1. A A Balkema, Rotterdam

Jorgenson GK, Chung SH (1987) Blast simulation surface and underground with the SABREX model. CIM Bull 80:37–41

Journel AG, Alabert F (1989) Non-gaussian data expansion in the earth sciences. Terra Nova 1:123–134

Journel AG, Alabert F (1990) New method for reservoir mapping. J Petrol Technol 42(2):212–218

Kirby IJ, Harries G, Tidman JP (1987) ICI's computer blasting model SABREX—the basic principles and capabilities. In: Boddorff RD (ed) Proceedings 13th conference on explosives and blasting technique. Society of Explosives Engineers, pp 184–198

Leiper GA, Plessis MP (1987) Describing explosives in blasting models. In: Fourney WL, Dick RD (eds) Proceedings second international symposium on rock fragmentation by blasting. Society for Experimental Mathematics, pp 462–474

MacKenzie AS (1966) Cost of explosives—do you evaluate it properly? Min Congr J 32–41

Mohanty B, Tidman JP, Jorgenson GK (1988) Advanced computer simulations—the key to effective blast designs in open pit and underground mines. In: Fytas K, Collins JL, Singhal RK (eds) Computer applications in the mineral industry. Rotterdam, pp 41–48

Nielsen K (1983) Optimisation of open pit bench blasting. In: Proceedings first international symposium on rock fragmentation by blasting, vol 2. Society for Experimental Mechanics, pp 653–664

Pryor RN, Rhoden HN, Villalon M (1972) Sampling of Cerro Colorado, Rio Tinto, Spain. Trans Inst Min Metall Sect A Min Technol 81:A143–A159

Randall M, Wheeler A (1998a) Balancing the books. Mining Magazine 337–342

Randall M, Wheeler A (1998b) Where did it go? Mining Magazine 245–249

Van Zeggeren F, Chung SH (1975) A model for the prediction of fragmentation, patterns and costs in rock blasting. In: Hoskins ER (ed) Proceedings 15th symposium on rock mechanics. The American Society of Civil Engineers, Reston, pp 557–569

Geometallurgical Modelling and Ore Tracking at Kittilä Mine

D. La Rosa, L. Rajavuori, J. Korteniemi and M. Wortley

Abstract Geometallurgical modelling of an orebody provides benefits to a mine by gaining a better understanding of the ore characteristics and how these affect the performance of the concentrator. With this knowledge, plant operating conditions can be adjusted to optimise throughput and recovery in advance of the arrival of particular ore types. Therefore it is extremely important that the origin of the ore being processed is known as accurately as possible. Depending on the homogeneity of the ore characteristics, reliance on assumptions about stockpile residence times, scheduling and material handling can render the best geometallurgical models useless. The solution adopted at Kittilä was to utilise Metso SmartTags™ and in-house expertise to develop a system that continuously and accurately links geotechnical and lab data from the mine to the performance of the plant. This application presented several unique opportunities and challenges. For example, this was the first installation of a SmartTag™ system for geometallurgical modelling in an underground mine. Challenges included the fact that the system installation is routinely subjected to temperatures below −20 °C. The system was installed and commissioned in early 2013 and has been operating continuously since. Kittilä has begun to see the benefits of the system with an increased understanding of how different ores are processed in the concentrator. Other advantages include the ability to alert operators about the arrival of difficult ores and

D. La Rosa (✉) · M. Wortley
Metso Process Technology and Innovation, Queensland Centre for Advanced Technology, 1 Technology Court, Pullenvale 4069, Australia
e-mail: David.La.Rosa@metso.com

M. Wortley
e-mail: Michael.Wortley@metso.com

L. Rajavuori · J. Korteniemi
Agnico Eagle Kittilä Mine Agnico Eagle Finland Oy, Kittilä Mine, Pokantie 541, 99250 Kiistala, Finland
e-mail: Leena.Rajavuori@agnicoeagle.com

J. Korteniemi
e-mail: jyrki.korteniemi@agnicoeagle.com

R. Dimitrakopoulos (ed.), *Advances in Applied Strategic Mine Planning*,
https://doi.org/10.1007/978-3-319-69320-0_27

a better understanding of their ore handling systems. This paper describes the installation and use of the system at Kittilä, and details some of the geometallurgical relationships that have been developed using the data collected so far.

Introduction

Geometallurgical modelling of an orebody provides benefits to a mine by allowing a better understanding of how different ore types—as defined by their strength, structure and grade—respond to crushing, grinding and flotation processes. Advance knowledge of how each part of the circuit will perform when a particular ore type is treated allows overall plant performance to be optimised by adjusting equipment parameters proactively. One issue that can arise in geometallurgy is the uncertainty that surrounds linking the instantaneous properties of the circuit feed measured in the mine with the performance of the plant. Assumptions in residence times, scheduling and material handling can cause ambiguity in the actual mill feed at any given time. Agnico Eagle's Kittilä mine has overcome some of these issues by using Metso Process Technology and Innovation's (2013) SmartTag™ ore tracking system. This paper describes how Kittilä utilise the SmartTag™ system and details some of the benefits they have derived from it.

Background

Issues with Metallurgical Reconciliation

Two persistent issues reduce the effectiveness of even the best attempts at quality metallurgical accounting, reconciliation and optimisation. Firstly ore must be reliably tracked from its source to its destination or product, and secondly variable process holdups inherent to most mining processes (e.g. stockpiles, feed bins, ROM pads, muckpiles and ore silos) must be taken into account. Ore tracking is an important aspect of reconciliation as it allows the quantity and quality of a particular type of ore entering a processing plant to be determined at any given time. This allows both plant operation optimisation and account of the material processed and metal produced (Jansen et al. 2009).

Due to the inherent pseudo continuous nature of mining operations, highly variable time delays may often exist in the flow of run of mine ore. In order to determine the process inventory at a particular time and location these need to be estimated as accurately as possible. Process holdups provide additional uncertainty, not only through additional variable source to product time, but also due to the potential for mixing or size and density classification in the material. In the coarse holdups prior to grinding, segregation can occur based on size and density. This is

difficult to quantify, making process performance difficult to predict, even when testing in situ ore properties. Furthermore, whilst blending of ores may smooth out production differences, it adds further complexity to reconciliation calculations (Jansen et al. 2009).

The SmartTag™ system allows spatial ore characteristic data of a parcel of ore to be linked with time based plant performance data, such as particle size distribution, specific energy and throughput. This can be used to update block models in real time with these temporal characteristics. Due to the increased accuracy in predicting ore delivery characteristics, the plant will be advised in advance of the ore entering the processing plant, and the number of routine ore characterisation tests required to adjust processing strategy may be reduced due to the increased knowledge of the feed at any given time (Lynch-Watson et al. 2013).

Issues with Tracing Ore Assays

Ore grade is generally determined by the assay of valuable components, in the case of Kittilä, by gold content. The industry standard for obtaining gold and platinum group element content of high grade ores is the lead collector fire assay. Lead collection is the most definitive method for gold analysis in all samples including drill core, soil and chip samples. However, this process is highly technical and time consuming, requiring several preparation steps. As such, the turnaround time for grade determinations can be lengthy.

The fire assay process is as follows. The ore to be assayed is sampled and sub-sampled, pulverised, weighed and mixed with fluxing agents. These help the sample to melt and fuse at lower temperatures, and promote gangue separation. Lead is added as a collector and the material is placed in a crucible inside a furnace preheated to 1000 °C for between 20 min to 1 h to fuse (SGS Mineral Services 2013; Juvonen et al. 2004). The lead and valuable materials separate into a button at the base of the crucible. When cooled, this can be hammered from the gangue layer that forms on top. The button then undergoes a process called cuppelation, whereby the lead is oxidised at 960 °C and is absorbed into a ‘cupel’ (a porous container used for assaying). This leaves a bead of the valuable material behind called a ‘prill’ (SGS Mineral Services 2013). The cuppelation process takes in excess of 20 min (Austin 1907).

The gold content may then be determined through gravimetric weighing or dissolution of the prill in acid for solution analysis. Dissolution may be conducted in nitric or hydrochloric acid, with the prill usually hammered flat to speed the process. Solution analysis techniques include flame atomic absorption, inductively coupled plasma mass spectrometry and instrumental neutron activation analysis (SGS Mineral Services 2013).

High sulphide concentrate in samples interferes with the fusion process, requiring the prior roasting of samples. Furthermore, significant nickel, copper or

cobalt content require removal between the fusion and cuppelation stages, as they are unable to be removed before concentration or in the final material. A process called scorification is utilised for the removal of these elements, and essentially comprises a further re-fusion stage with added lead and flux (Juvonen et al. 2004). The time for scorification is in the region of 30 min (Austin 1907).

From an overview of the process it can be seen that a gold fire assay can take in excess of several hours to process, and whilst samples are likely be processed concurrently, the time requirement is certainly high. Due to the time and resource requirements of the fire assay procedure, it is not only lengthy but also costly. Furthermore, due to the small sample size utilised for assay determination of each sample, it is difficult to obtain representative information without a multitude of samples. Using ore tracking to provide more accurate data regarding the ore reporting to the plant, the number of samples required for certainty of grade and value may be reduced, reducing overall turnaround time and cost while increasing accuracy.

Previous Uses of the SmartTag™ System

The SmartTag™ system comprises tags, detection antennas, data collectors and a central database. The tags themselves are built around robust passive radio frequency transponders (RFID tags), and are available in a number of sizes. The tags can survive the blasting, excavation and crushing processes, and do not utilise an internal power source, meaning that they can remain in stockpiles and ROM pads for extended periods of time (La Rosa et al. 2007).

Each tag is encoded with a unique ID which is scanned by a handheld computer, which can be assigned to a specific location within the mine, for example, in the stemming column of a blast hole or on a muck pile. The tag then flows with the blasted ore as it travels through the process—from the muckpile, through the primary crusher and then into the grinding circuit. Antennas that detect the tags are located at critical points in the process—for example at the primary crusher discharge, and at the primary grinding circuit stockpile reclaim. An individual tag may be detected several times at different antennas, providing valuable information regarding material movement, particularly making it possible to link process data to the ore properties (Lynch-Watson et al. 2013).

When a tag is detected the data logger assigns the detection time and location to the event and sends this information to the database. This aggregates process historian data such as throughput and recovery. This information is utilised to update the mine block model. The process is illustrated in Fig. 1.

The SmartTag™ system has been utilised globally in a variety of commodities, in permanent, temporary and trial installations.

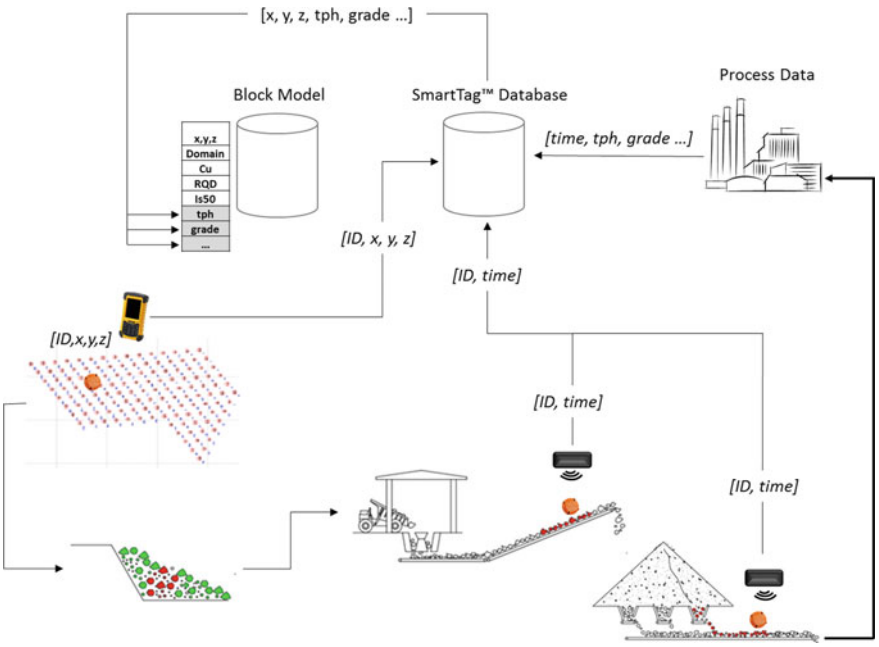

Fig. 1 SmartTag™ system data flow

Overview of the Smarttag™ System at Kittilä

Agnico Eagle's Kittilä operations are located in Lapland in Northern Finland. Kittilä mines and processes approximately 3000 t of material per day. In 2013 Kittilä produced 146,421 oz. of gold, and at the time of writing this paper, mine life will extend to 2034. As of November 2012 Kittilä is an entirely underground operation and consists of three main ore bodies—the Rimpi zone, Roura zone and Suuri zone. The ore body at Kittilä is complex and this was one of the major motivations for installing the SmartTag™ system. Ore type can vary between each loader bucket which makes reconciliation and scheduling very difficult.

The mining method used is open stoping followed by delayed back filling. Ore is brought to the surface using haulage trucks via approximately 3 km of access ramps. Figure 2 shows a simplified view of the mine.

Kittilä's processing plant consists of a grinding circuit, flotation, pressure oxidisation and then leaching. Figure 3 shows the flow sheet of the Kittilä processing plant.

Metso originally provided Kittilä with a temporary SmartTag system for a 3 month trial. After this proved successful, the system was purchased outright and a second unit, for the expanded processing plant, was also purchased. The units are installed on the primary crushed product conveyor belts before the surge bins and SAG Mill. As the environmental conditions at Kittilä can be extreme with the

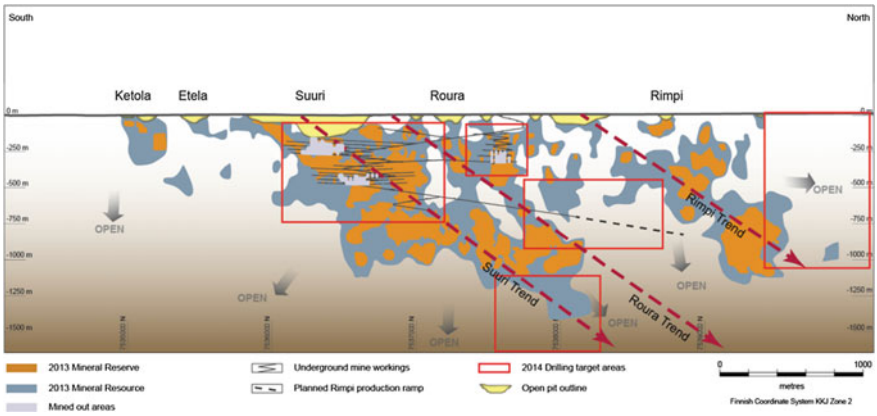

Fig. 2 Simplified mine diagram (after Agnico Eagle 2014)

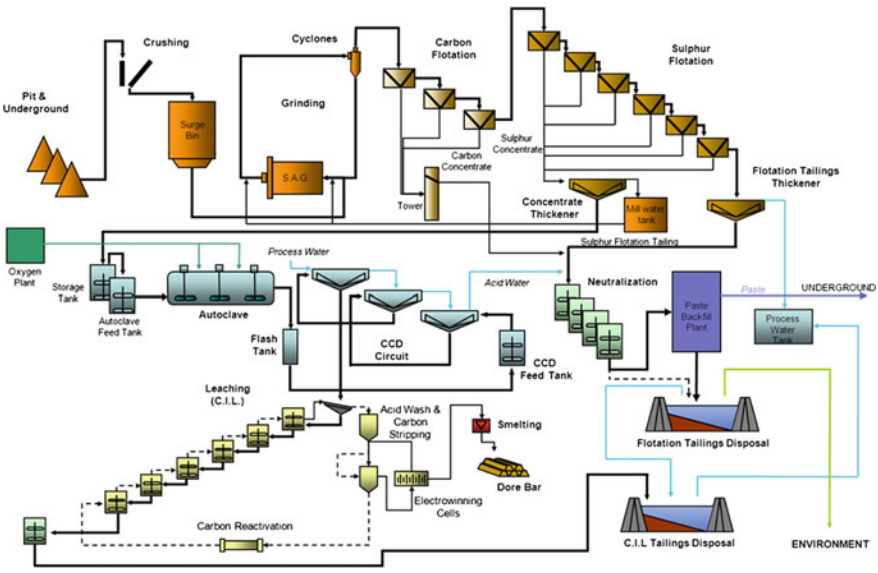

Fig. 3 Processing plant flow sheet (after Agnico Eagle 2014)

lowest recorded temperature in Finland, −51.5 °C, recorded not far from the mine, Metso supplied the system with low temperature enclosures and tested the tags and antennas down to −20 °C to ensure that the materials retained their strength.

The data loggers in the field enclosures communicate to the central SmartTag™ server via the Kittilä network. The server retrieves data from the field units and inserts it into a SQL Server database. This is linked to the site's lab network so underground assays can be automatically linked to individual tags.

Smarttag™ Methodology

Inserting the Tags

Kittilä experimented with different methods of inserting the tags into their run of mine ore. The final solution involved the following procedure:

1. Geotechnicians prepare labelled underground ore sample bags and link these to SmartTag IDs.
2. Underground loader operators take a muck sample from the scoop approximately every 100 t, resulting in a material sampling rate of 1 sample per 100t of material
3. At every 3rd muck sample, the operator also adds a SmartTag™. The sampling frequency for the SmartTags™ is therefore one for every 300 t of material.

Each sample is then taken to the laboratory where the quality of the sample is checked and paperwork completed. The samples are then analysed for gold, sulphur, and arsenic and the results entered into Kittilä's laboratory information management system (LIMS). The best case turnaround time, from sampling to results reported, is 24 h.

The tags take a different path. Once they have been inserted into the bucket of the underground loader they are loaded onto the trucks, hauled to the surface, stockpiled, crushed and detected on the crusher product conveyor before flowing through the surge bins, and ultimately into the SAG mill where they are consumed. Tags can also be placed on surface stockpiles, as illustrated in Fig. 4.

Fig. 4 Surface tag placement

Incorporating SmartTag Data into a Lab Database System

Each sample is assigned a unique ID when it is entered into Kittilä's LIMS. This unique ID is associated with the SmartTag ID (this is also globally unique) using the hand held scanner. Once the tag information is loaded into the SmartTag™ database, Kittilä have developed in-house software to link the sample ID to underground production information (e.g. stope location, tonnage etc.). The same software then links this data to the SmartTag ID in the SmartTag database using the sample ID. The combined data then resides in the SmartTag™ SQL Server database.

Data Utilisation

There are three main uses for the data obtained using the SmartTag™ system:

Mill Grade Prediction

Once a tag is detected at the plant, the characteristics of the ore associated with it are retrieved. This is compared to the ore that the plant is expecting, and if there is a difference, changes can be made to the plant's operating strategy in order to maintain throughput and/or recovery. This type of feed forward or 'heads-up' control is very valuable to sites that have complex, heterogeneous ore bodies. Without the advantage of physically tracking the ore from the mine, it is often only when the plant starts performing poorly that the operators become aware that the ore type has changed.

Figure 4 shows mill grade (Au ppm) predictions as estimated by tag arrivals compared with mill feed daily samples. The process noise in the muck sample daily average is due to the fact that muck samples are composed of individual rock samples with very little blending or homogenisation that would be present in the mill feed. The process noise can be reduced by the addition of a moving average of course, but increasing the SmartTag addition rate from 1 tag per 1000 t to 1 tag per 700 t reduced the fundamental sampling error. This reduced the average absolute error (in ppm) by about 50%. Further increases in tag addition rate to 1 tag per 300 t should further decrease the prediction errors in mill grade.

Reconciliation

As discussed earlier, accurate reconciliation is often an issue on mine sites. The differences between what is being reported as being sent from the mine, and what is being received at the plant can be quite significant. At Kittilä these arguments have

been reduced as they can use the SmartTags as proof of delivery. This is extremely powerful, as it eliminates handling errors as a reason for poor reconciliation. In turn, this allows the operation to look for other causes of incorrect ore delivery and to then rectify them.

Geometallurgical Modelling

When the plant struggles to meet throughput and recovery targets, and the source of those issues can be traced back to the ore type, this provides the basis for a geometallurgical model of the ore body. In effect, each detected SmartTag™ is linking the physical characteristics of the ore with its performance in the plant. Once troublesome ore types are identified, plant feed with similar properties in the block model or from physical sampling at the underground muckpiles can be flagged as having the potential to negatively affect plant performance and remedial actions taken prior to its arrival at the concentrator. In effect, by identifying troublesome ores and adjusting the operating strategy of the plant, Kittilä are implementing a geometallurgical model and continually improving their understanding of the ore body.

Results

To date, statistics show that around 85% of tags dropped underground are detected on the surface, with tags sometimes surviving for several years on surface stockpiles, through the extreme cold of winter in Kittilä.

When tags are detected the geology team analysis the data and informs the plant if the feed is a problematic ore. As the tag detectors are located before the mill silos there is enough time for the analysis to be done and the information relayed. An example of how this improves processing is that the plant can increase throughput when low sulphur ore types are detected. This is due to the fact that sulphur content determines how much ore the autoclave can process.

Estimations of mill feed based on SmartTag™ detections and their associated sample characteristics match the actual analysed mill feed well (as determined by the combination of daily samples). This gives confidence that the tags flow with the ore and that no segregation takes place. Tags and analysis results are used on a daily basis to evaluate and adjust mill feed (based on gold and sulphur grades).

At the end of each month SmartTags™ are used to reconcile the amount of mill feed from each stope. Figure 4 shows the cumulative tonnage of extracted and processed ore from a particular stope over about a one month period. As each tag has a grade associated with it, this can be converted into a monetary value by Kittilä. The variable time lag between when ore was excavated and processed is also apparent in this figure.

Potential Extensions to the Smarttag™ System

The SmartTag™ system allows ore to be tracked from the spatial domain in the mine, to the temporal (time-based) domain in the plant. Figure 5 shows tags inserted into blast holes in the spatial domain of an open cut operation, with the geotechnical block model overlain. This could equally apply to a stope or a block cave in an underground mine.

Once the tags are allocated to a blast hole or three dimensional coordinate (blast hole, muck pile, loaded truck etc.), the SmartTag™ software assigns the nearest ore block to it and all its associated characteristics (e.g. strength, structure and grade). When the tag is then subsequently detected at the crusher or concentrator, time based characteristics such as throughput and recovery can then be assigned back to the ore block. This is illustrated in Fig. 6.

The physical tracking of ore from the mine, from both underground or open-pit, gives a unique opportunity to correlate plant performance with the characteristics of the ore as defined in the mine's block model or from grab samples. Some examples are mill throughput vs. hardness or structure rockmass parameters, recovery versus grade or simply dilution, where tags associated with waste blocks appear in the process stream (Figs. 7 and 8).

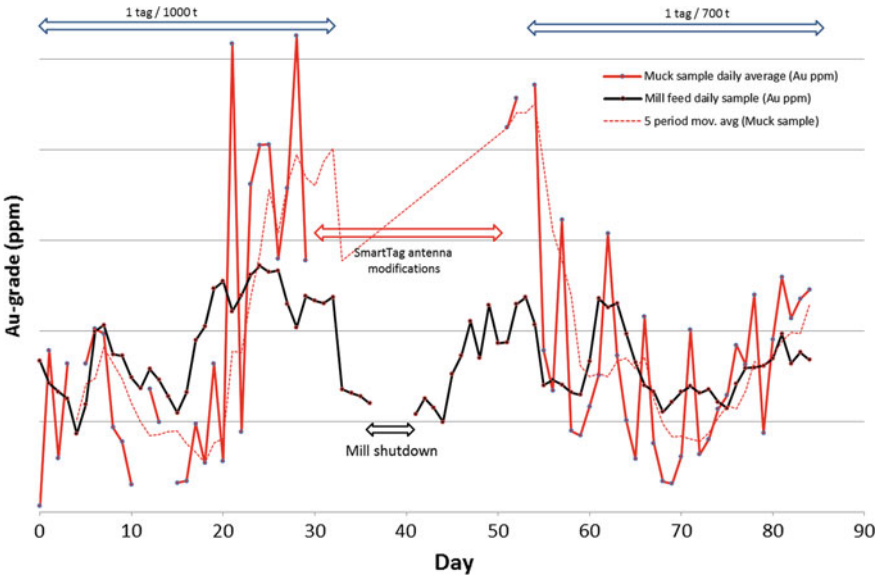

Fig. 5 Mill grade prediction

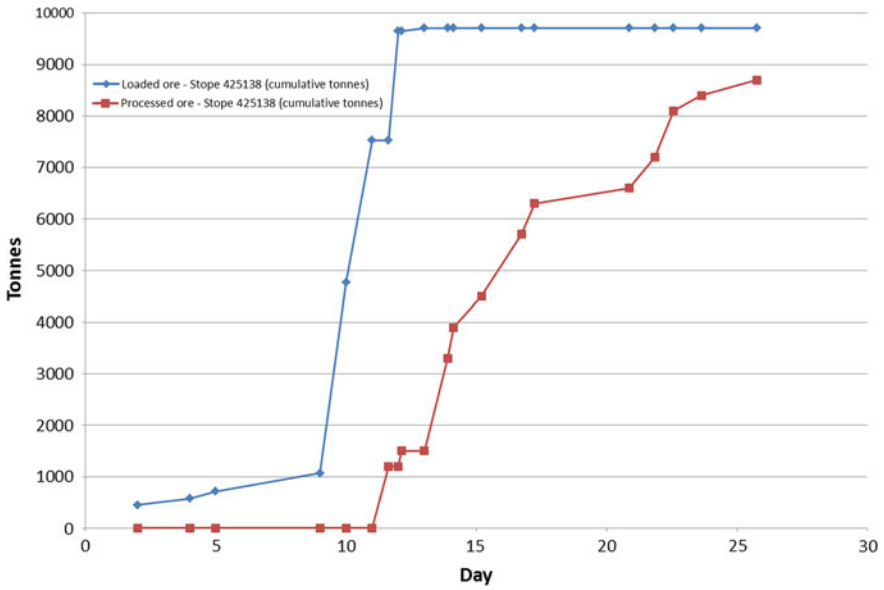

Fig. 6 Loading and processing rates for Stope 425138

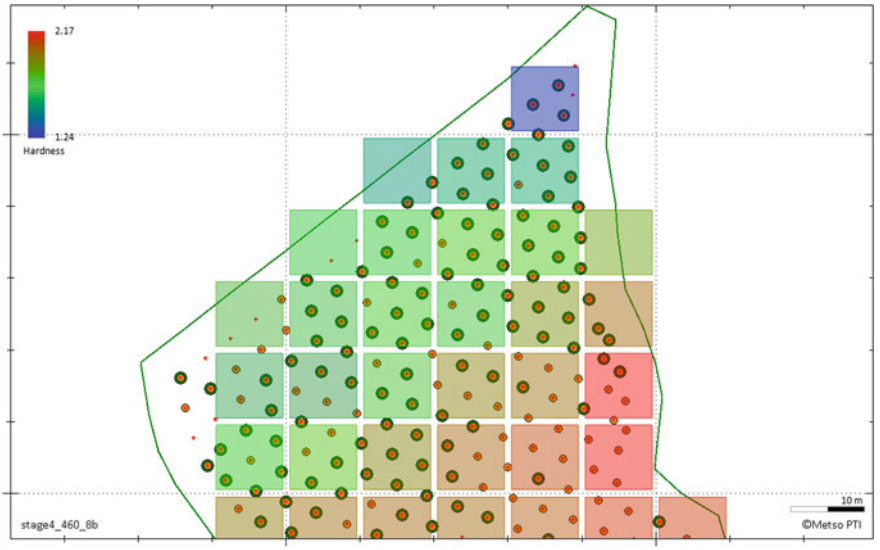

Fig. 7 SmartTags overlain with geotechnical block model

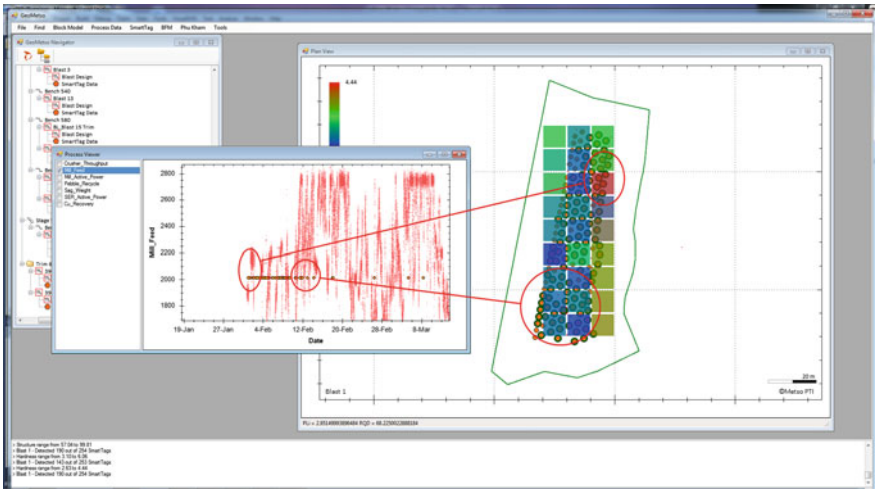

Fig. 8 Correlations between mill throughput and ore source

Next Steps and Conclusions

In conclusion, the SmartTag system has been successfully implement at Kittilä and provides ongoing benefits to the operation. The system has led to improvements in Kittilä's reconciliation and metallurgical accounting and is now providing a method to predict head grades, in real time, without the need to wait for plant assay results. The system also allows the Geologists to warn the plant about problematic ore types before they cause processing issues.

Extending these last two benefits are now a priority at Kittilä as so far only geologists have direct access to the information acquired from the SmartTag™ system. It is planned for metallurgists and mill supervisors to also have online access to the information generated by the system to better utilise it. This will increase the benefits of the system as the site will not have to rely on busy geologists to warn the metallurgists that problematic ore is about to be delivered to the plant. Presentation of the data is also being improved, with graphs, trends, rolling averages etc. to be added.

References

Agnico Eagle Mines Limited 2014 (Agnico Eagle 2014), Kittilä, www.agnicoeagle.com, 8 July 2014, Website, viewed 8 July 2014, http://www.agnicoeagle.com/en/Operations/Our-Operations/Kittila/Pages/Mining-and-Processing.aspx?PagePreview=true&isDlg=1

Austin L (1907) The fire assay of gold, silver, and lead in ores and metallurgical products, 1st edn. University of California, Mining and Scientific Press, San Francisco

Jansen W, Morrison R, Wortley M, Rivett T (2009) Tracer-based mine-mill ore tracking via process hold-ups at northparkes mine, tenth mill operators' Conference, Adelaide, South Australia

Juvonen M, Bartha A, Lakomaa T, Soikkeli L, Bertalan E, Kallio E, Ballok M (2004) Comparison of recoveries by lead fire assay and nickel sulfide fire assay in the determination of gold, platinum, palladium and rhenium in sulfide ore samples. Geostand Geoanal Res 28(1):123–130

La Rosa D, Valery W, Wortley M, Ozkocak T (2007) The use of radio frequency ID tags to track ore in mining operations, Proceedings of the 31st international symposium on computer applications in the mineral industries (APCOM), Santiago, Chile, 23–25 April 2007

Lynch-Watson S, Valle R, Duffy K, La Rosa D, Valery W (2013) GeoMetso™: a site-specific methodology to optimize production and efficiency over the Life-of-Mine, Procemin 2013, Santiago, Chile

Metso Process Technology & Innovation (2013) Capability Statement, Brisbane, Australia

SGS Minerals Services (2013) Fire assay gold, SGS Group Management, SA

Predicting Mill Ore Feed Variability Using Integrated Geotechnical/Geometallurgical Models

J. Jackson, J. Gaunt and M. Astorga

Abstract The Ban Houayxai Mine (BHX) is a relatively low grade, low cost, open pit gold-silver deposit in Laos operated by Phu Bia Mining, a subsidiary of PanAust. Ore production rate is 4.5Mt pa with direct tipping to a SAB mill with a carbon in leach process plant. Approximately 100,000 oz of gold is produced per annum. The operation is located in mountainous terrain with minimal ROM stockpiling are which results is limited capacity for blending from stockpile with the mill instead reliant upon direct feed ex-pit. Since commissioning in 2012, the plant has seen significant variation in milling rates due to variability in the feed properties of the oxide, transition and primary ores. As part of an ongoing continuous improvement program, an integrated approach was initiated focussing on maintaining and enhancing production in the future as the proportion of harder primary ore increases with focus on direct blending from the loading face using the ore properties and blast fragmentation to maintain mill throughput. This approach was based on the concept of physical assets management, commencing with improving information and knowledge of the condition of the ore body through modelling the characteristics, variability and performance of the feed for processes relevant to throughput. These models are used to support both mine and process plant production planning. The key ore feed characteristics and parameters modelled for the life of mine are blastability index (BI), powder factor, crushability or impact resistance (A*b) and grindability (BWi). These predictive spatial models were based on the data from diamond drill holes used in resource definition and geotechnical drilling programs by integrating geotechnical, geological, geochemical

J. Jackson (✉)
JKTech Pty Ltd, 40 Isles Rd, Indooroopilly, Australia
e-mail: j.jackson@jktech.com.au

J. Jackson
JKMRC, 40 Isles Rd, Indooroopilly, Australia

J. Gaunt
Ban Houaxyai Operation, Phu Bia Mining, 23 Singha Rd, Saysetha, Laos

M. Astorga
JK Tech, Riverleigh Dr, Hope Island 3163, Australia

R. Dimitrakopoulos (ed.), *Advances in Applied Strategic Mine Planning*,
https://doi.org/10.1007/978-3-319-69320-0_28

and metallurgical data. Although, at the early stages of implementation, the models are being utilised for ore blending decisions, to provide guidance and support for budgeting, long term mine planning, blast design for mill feed and providing the mill with an expectation of performance.

Introduction

Pan Aust's Ban Houayxai Mine (BHX) is located in Laos approximately 100 km north of the capital, Vientiane and 25 km from Phu Kham copper mine (Fig. 1). The mine is an open pit operation with an SAB-CIL processing circuit, which commenced production in May 2012. The mine is producing approximately 100,000 oz of gold and 600,000 oz of silver per annum.

Since commissioning the plant has seen significant variation in milling rates due to variability in the feed properties of the oxide, transitional and result primary ores. There is limited opportunity for short term stockpiling and blending to create a feed with constant hardness over any significant timeframe. Impacts of this variability may include inefficiencies in milling and mining, variation in mill throughput rates, risk damaging SAG mill liners and lead to reactive mining and milling. As mining progresses the proportion of primary ore will increase and a proactive management program was initiated to focus on maintaining and enhancing production in the future.

One aspect of this program focussed on throughput by applying a scaled down concept of physical asset management through four components—predicting the ore's characteristics and performance; analysis and assessment of engineering solution options; reacting to unexpected issues; monitoring review and feedback.

The goal of this paper is to outline the approach and the development, results and initial implementation of the predictive spatial modelling of key parameters related to throughput, for the life of mine (LOM). These key parameters are the feed size and mill hardness in terms of crushing and grinding.

The predictive models are based on the data from diamond drill holes used in resource definition and geotechnical drilling programs by integrating geotechnical, geological, geochemical and metallurgical data types together with the associated lithological model. The key parameters modelled are:

- blastability index (BI), index of the ease to blast the rock mass, and the required powder factor (pF) for a constant mean fragmentation size using empirical engineering models;
- crushability or resistance to impact breakage (A*b) through a relationship between the geotechnical rock mass rating (RMR), the intensity of weathering/oxidation and A*b from metallurgical SMC Tests.
- grindability, the bond ball mill work index (BWi), through relationships between lithology, geochemistry, intensity of weathering/oxidation and bond ball work index metallurgical tests.

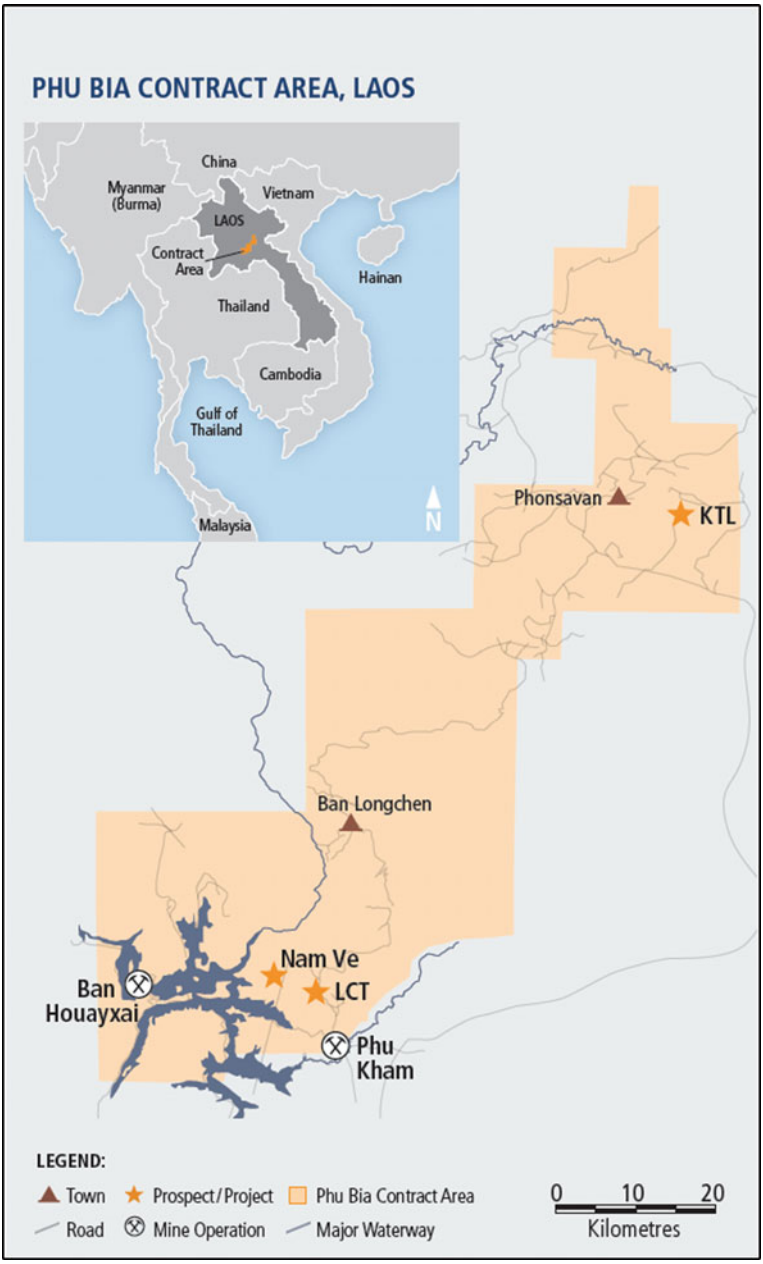

Fig. 1 Location of Ban Houayxai gold mine in Laos

Due to the data types and sampling density, the models of these parameters are a combination of differing levels of granularity and resolution. They are not considered a precise reflection of reality but show likely spatial and performance variability allowing options and controls to be considered in maintaining or enhancing production in a proactive manner.

Although, at the early stages of implementation, the models are being utilised to provide guidance and support for budgeting, long term mine planning, blast design for mill feed and providing the mill with an expectation of performance.

Physical Asset Management

The standard definition of asset management is 'the systematic and coordinated activities and practices through which an organisation optimally and sustainably manages its assets, their associated performance, risks and expenditures over their lifecycle to achieve the strategic plan (BSI 2008; Woodhouse 2011). Although historically the management of physical assets is strongly associated with equipment maintenance, this concept can and has been extended to other physical assets such as oil reservoirs or mineral deposits. Some companies within the oil and gas industry, particularly BP and Shell, adopted this approach during the mid to late 1990s resulting in large improvements in project value such as 17% increased output at 50% lower operating costs, rather than the business as usual case of chasing efficiency gains through doing the same thing quicker and cheaper (Woodhouse 2010). Elements which enable successful asset management include: clear direction and leadership, cross functional coordination, staff awareness, competency and commitment and importantly adequate information and knowledge of asset condition, performance, risks and costs and the interrelationship between these.

The approach adopted at BHX is a scaled down concept of the asset management system which focusses on the enabling elements mentioned above in relation to throughput mine production forecasts and the associated mine life cycle plan only. The concept can be divided into four components of predict, control, react and monitor as shown in Fig. 2.

The first component, prediction, develops models of the expected conditions and performance of the orebody including spatial variability. This includes the rock properties and process attributes associated with the key process such as blasting, crushing and grinding within the block model. The prediction of performance is developed under constrained conditions for each block, is not treated as a deterministic outcome but as aid in the next component.

The second component, control, is where engineering solutions to manage or optimise the predicted performance are developed together with management plans.

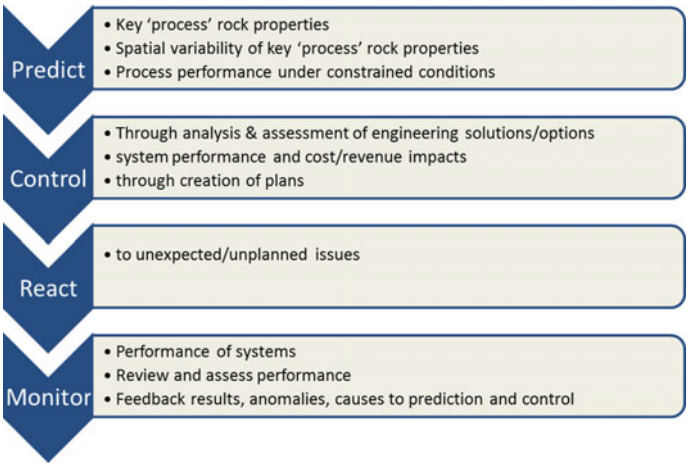

Fig. 2 Schematic of the proactive management system for BHX

This may include solutions such as blending, scheduling, alternative blast designs, processing conditions, or simply nothing.

As all of the predictive models are estimates with uncertainty, there will still be a need for reacting to unplanned/unexpected issues that could not be predicted. But rather than dominating the operation, the focus switches to proactive prediction and control with monitoring and review as a feedback loop.

Modelling and Use of the Models

There are many perspectives of models in the literature (Giere 2010; Knuuttila 2011). The standard view is that a model directly represents an object, however here we take the more pragmatic perspective in that an agent intends to use the model to represent part of the world for some purpose, so it is the agent that specifies which similarities are intended and for what purpose (Giere 2010; Cunningham 2005). Thus the success of a model depends not only on the direct accuracy of representation to the real world, particularly given limitations on spatial resolution, input data and process descriptions, but on the purpose for which the model is employed. In this case the model needs to satisfy a distinct purpose—an improvement of current method in spatially and temporally predicting the key rock properties and the associated performance under constrained conditions for use by many agents—mine planners, metallurgists, blasting engineers and geologists.

BHX Geology and Operations

The Ban Houayxai is a structurally controlled epithermal gold-silver deposit hosted within an early Permian volcano-sedimentary sequence of the Trong Son Fold belt in the south western extremity of the Phu Bia Contract Area (Manaka et al. 2014). The deposit is located on a steep narrow north-south oriented ridge that protrudes into the Nam Ngum 2 Reservoir, a recently filled hydro electric scheme. As at the end of 2013, the published Mineral Resource at Ban Houayxai stood at 64Mt @ 0.90 g/t Au and 7.1 g/t Ag for a total of 1.8Moz Au with Ore Reserves at 36Mt @ 0.81 g/t Au and 8.0 g/t Ag (Aust 2014).

Gold and silver mineralisation occurs as structurally controlled narrow veins and disseminations and within the volcano-sedimentary sequence. The most commonly mineralised veins are quartz-pyrite+/-carbonate+/-electrum+/-native silver veins with wall rock alteration of sericite, chlorite and adularia hosted (Manaka et al. 2014; Brost 2011). The disseminated mineralisation predominately is associated with silicification of the feldspathic sandstone with higher grades in breccias. At least three phases of deformation have been imposed on the deposit resulting in a significant structural complexity in shearing, faulting, fracturing and jointing.

The life of mine plan comprises of 3 pits—north, central and south, with a LOM stripping ratio of 1.5:1. Due to the topography, space is at a premium hence the operation is a direct tip operation into the primary crusher with only a very small stockpile capacity. The process plant consists of a 26 ft 6.5 MW SAG-Ball mill circuit feeding a conventional carbon in leach (CIL) circuit.

Three ore types have been defined at Ban Houayxai based on the weathering profile—oxide, transitional and primary. Average throughputs were assigned to these ore types, based on test work within the feasibility study and during construction/commissioning, and are a critical component of planning, scheduling and forecasting. However since commissioning, the variability in throughput has been high, both in terms of amplitude and period not only due to the mix of the oretypes but also due to variability within the ore types.

Predictive Modelling Approach

The approach to the predictive modelling initially consists of decisions as to:

- Which key parameters to be predicted;
- What methodology is to be applied to predict key parameters and potential performance;
- what input variables are suitable and relevant;
- the domaining methodology for each of the variables;
- the spatial modelling methodology for each variable and parameter

based on (a) the type, quantity and quality of available data and (b) the purpose of the models to improve and support mine and process plant production planning. These decisions are often interrelated, developed iteratively.
Methods for the prediction of the key parameters include:

- direct tests including small scale tests;
- empirical 'engineering' models;
- empirical 'proxy' models—where a relationship is established between variables or proxies and parameters from a limited set of direct tests.

In an ideal world, the most relevant, direct tests and measurements of the key parameters would be undertaken at a sample density relevant to their spatial variability and spatially modelled. For geotechnical and geometallurgical parameters this rarely the case as direct measures of a parameter are often problematic plus the logistics, cost and time of obtaining and processing the relevant data is significant. Hence the empirical engineering and proxy models are the more common. These models require the input of many disparate data types at varying sample intervals and density with varying sensitivities and thus the final outputs are multi layered consisting of a mix of levels of model granularity and resolution. It is our preferred approach to spatially model the primary input variables with the appropriate methodologies, where possible, and then apply the empirical models to predict the parameters (response) rather than vice versa. This approach better matches the spatially modelling methodology to the data (Coward et al. 2009).

Domaining is a first order decision that partitions the dataset into spatially coherent, geological and statistically acceptable 'domains' (Coombes 2009; Vann 2008). Some apriori knowledge of the key parameters is required to identify the geological drivers of the parameter's variability and performance that can be related back to the drill hole. However this isn't always possible and thus other domaining options should be considered. Domaining methods include:

- value or grade based—the domains are based on selected cut off values;
- population based—the domains are defined on down hole zones that are statically similar;
- generic geological based—domains are based on geological units or model e.g.: lithology/alteration
- process/variable geological driver based—domains based on the differing casual geological drivers of the parameter's performance.

For practical purposes the predictive models are required to have spatial representation within a block model. For this initial model, a number of the input variables were spatially modelling using relatively simple linear estimation approaches. Although the block model implies a certain level of granularity this not always the case and an understanding of the underlying data and model limitations is required.

Key Parameters

The key ore related parameters relevant to throughput for the BHX circuit are the size distribution of the feed to the mill and the comminution or mill hardness.

The feed size is a function of the fragmentation from blasting and primary crushing. Rather than predicting the feed size, the approach taken is to predict the ease of which the rock breaks due to blasting (Blastability Index or BI) and the required energy or powder factor to achieve a constant mean fragmentation to the mill using empirical rock mass and fragmentation 'engineering' models.

The parameters relating to mill hardness consist of and grindability. As the milling circuit at Ban Houayxai is an SAB circuit, the key comminution parameters are crushability using the JK A*b derived from SMC tests and grindability using the bond ball work index (BWi) derived from the bond ball mill test (Napier-Munn et al. 1996; Morrell 2004). The approach to predicting these is via an empirical proxy model for the BWi and a combination of empirical 'engineering' and proxy models for the A*b as will be discussed later.

Dataset

The dataset used for the predictive models included the 330 diamond resource definition drill holes with a nominal drill spacing of 50 × 25 m and 49 geotechnical drill holes. A number of data types were available as potential inputs into the models including geological logging and models; geotechnical logging and testing; geochemistry and metallurgical testing. The main data types associated with these drill holes are shown in Table 1. Other data types used included:

Table 1 Main data types within the drilling database

Data Table	Key data types
Collars	East, north, RL, length
Survey	Depth, azimuth, dip
Lithology	Lithology, weathering, texture & deformation
Alteration	Supergene type/mode/intensity, alteration type/mode/intensity
Assays	Au, Ag, Zn with selected intervals assayed for a wide range of multi elements
Point Load	Coresize, caliper, $IS_{(50)}$MPA, failure on new or preexisting structure, fracturetype, estimatedUCS
Geotech	Rock quality designator (RQD%), # of sets, strength, fracture frequency (FF)
Structure	Structural type, orientation and roughness
Veining	Type and intensity
Mineralisation	Oxide and sulphide minerals and quantity

- 3D geology and grade models
- Pit design stages
- Geotechnical reports—including uni-axial compressive strength (UCS) tests
- Comminution test results—including SMC Tests for A*b, Bond Ball Work Index, mineralogy and point load tests.

Blastability Index and Powder Factor Models

The approach adopted for the modelling of the powder factor (pF) is based on Cunningham's empirical Kuz-Ram fragmentation model (Cunningham 1986, 2005). This estimate the mean fragmentation (X) that would result from a known energy factor used in specific rock mass conditions. Reworking of the model results in the estimation of the required energy or powder factor (pF) to achieve a mean fragmentation (X) as shown in Eq. 1. For BHX, analysis of mill and comminution test results data indicated that a mean fragmentation of 150 mm was appropriate for ore.

$$\text{Required Powder Factor } \left(\text{kg/m}^3\right) \mathbf{pF} = \left(\mathbf{X}/\left(\left(\mathbf{A} * \mathbf{Q}^{0.167}\right) * \left(\left(\frac{\mathbf{RWS}}{115}\right)^{-0.633}\right)\right)\right)^{-1.25} \quad (1)$$

The inputs into the Kuz-Ram model are:

- X = mean fragmentation diameter
- Q = mass of explosive per blast hole
- RWS = relative weight strength of the explosive
- A = rock factor-specific rock mass conditions.

The rock factor, A, is used to take into account variations in rock mass conditions. This can be related to the Lilly's blastability index (BI) through a simple multiplication factor of 0.12 (Lilly 1986, 1992; Widzyk-Capehart and Lilly 2001). The blastability index model is shown in Eq. 2.

$$\mathbf{BI} = 0.5 * (\mathbf{JPS} + \mathbf{RMD} + \mathbf{JPO} + \mathbf{RDI} + \mathbf{S}) \quad (2)$$

The inputs into the BI are:

- JPS = Joint Plane Spacing Rating
- RMD = Rock Mass Description Rating
- JPO = Joint Plane Orientation Rating
- RDI = Rock Density Influence
- S = Rock Strength

The JPS and RMD ratings are derived from the fracture frequency data with the JPO rating derived from the orientation of structures in relation to the final pit design. RDI expresses the influence the density of the rock while S is a function of the uni-axial compressive strength (UCS) which was estimated from point load data. An overview of the data quantity and quality of the input variables of fracture frequency, structure, density and point load for the relevant inputs into the BI are outlined below.

The blastability and powder factor estimates were calibrated for BHX through blasting studies that were in progress as the model was developing.

Inputs

JPS and RMD

The level of fracturing within the resource development holes was recorded as the number of fractures per drill run which was converted to fractures per metre. Analysis indicated that the distribution of fracture frequency was very similar for all lithologies indicating that lithology is not a control on fracturing, nor could the existing structural model explain the fracture distribution. Hence the domaining method selected was population based utilising the CuSum statistical method for zoning the data based on changes in the data using a 5 m composite length down the drill hole (Keeney and Walters 2011). The zones were then clustered into groups based on the mean and standard deviation for each of the zones, to create five spatially coherent FF domains. For the initial model, the FF was interpolated into the block model using inverse distance weighting (IDW) methodology from which the JPS and RMD rating was derived.

JPO

The structural database is dominated by data for veining which accounts for some 53% of the data followed by foliation and joints at 18% respectively. The structural analysis of joints and faults/shears indicated that both have similar orientations and are lithology independent. However there is a significant difference in orientation between the northern and central pit areas. The northern pit is dominated by those dipping steeply to the WNW-NW, whereas the majority in the central pit dip steeply to the ENE-NE.

A total of 12 structural regions were defined based on the analysis of the structural orientation against the slope and orientation of the final pit design. Within the spatial model, each block within these regions were assigned a JPO rating based on the dominant orientation in relation to the pit wall design using Lilly's rating system.

S

As part of the geotechnical studies, a limited number (2–5) UCS tests had been conducted on each of the main 6 lithologies. This data indicates a large variation and overlap in UCS for the lithologies with ranges from 30-160MPA.

The database also contained single break point load data on drill core corrected to 50 mm drill core($Is_{(50)}$). Point load tests are commonly used as an indirect test to predict UCS (ASTM_International 2008). Although there were some 20,000 point load results in the database, each was a single point break and over 50% were recorded as failing on a pre-existing defect and of the remaining, only 1180 did not record an associated defect. Thus in order to obtain an representative indication of in situ rock strength, a more detailed analysis was undertaken by only considering the data where the point load tests had not failed on a pre-existing structure, were diametral tests, the fracture frequency (FF/m) was less than 2 and rock was fresh/primary. This resulted in a significantly reduced dataset where individual lithology's were grouped based on their distribution of point load estimated UCS.

A total of 7 lithological based rock strength groups resulted in three groups of volcanic lithologies with an average estimated UCS of 75, 80 and 175MPA and four groups of sedimentary lithologies with average estimated UCS of 50, 80, 125 and 175MPA. Similar investigations based on a combination of alteration with and without lithology did not identify distinct populations of rock strength suggesting that lithology was a key geological driver. Due to the limited data and the simplified 3D lithological model rock strength was assigned to the block based on the average estimated UCS for that lithology. The conversion factor from estimated UCS to the S rating was increased to improve the calibration between the predicted BI and pF to the site blasting studies. The estimates of UCS do not take into account any anisotropy or rock strength at scales larger than drill core (Pierce et al. 2009).

RDI

As some 66,000 bulk density measurements were obtained from the drilling dataset using the caliper method, there was sufficient data for interpolation of the densities into the block model. The domaining of this data was based on lithology with interpolation by IDW followed by the conversion to the RDI using the standard BI rating system.

Q and RWS

The inputs for the mass of explosive per blasthole (Q) and the relative weight strength of the explosive (RWS) were kept constant at 165 kg/hole and 95 respectively. These were based on assumptions of the blast engineering design with respect to drill hole diameter, stemming height, explosive characteristics for a 10 m bench height.

Results

The application of Eq. 1 and Eq. 2 to the inputs at block level resulted in the estimated BI and pF. Over the life of mine 65% of the ore is estimated to need powder factors between 1.3 and 1.9 kg/m^3 to achieve an X50 fragmentation of 150 mm (Fig. 3). The results for the primary ore suggest that 53% of the ore requires powder factor greater than 1.6 kg/m^3.

On a yearly basis from the current mine plan, 2015 and 2018 are expected to require the most blasting energy with the model predicting that 10% of ore requires a pF less than 1.3 kg/m^3 and 25% greater than 1.9 kg/m^3 whereas for 2017 and 2020 the estimates are 40% and 10% respectively.

An example of the spatial variability of the BI and pF for the North and Centre pits at the 570 m level is shown in Fig. 4. The BI is shown for both ore and waste within the pit design due its application either, whereas the pF X150 mm is shown for ore blocks only. The relatively short range and large amplitude variability in both Bi and pF can be observed in the Northern pit suggested that achieving a constant size distribution will be difficult. The Centre pit appears to have less spatial variability with larger more consistent zones however it is likely that blast areas will straddle some of these boundaries.

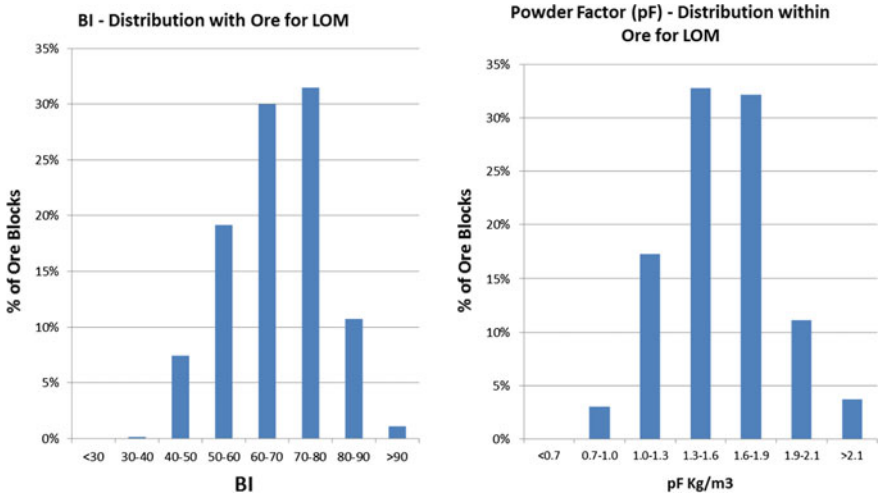

Fig. 3 Histograms of Blastability Index (BI) and powder factor (pF) for ore over life of mine

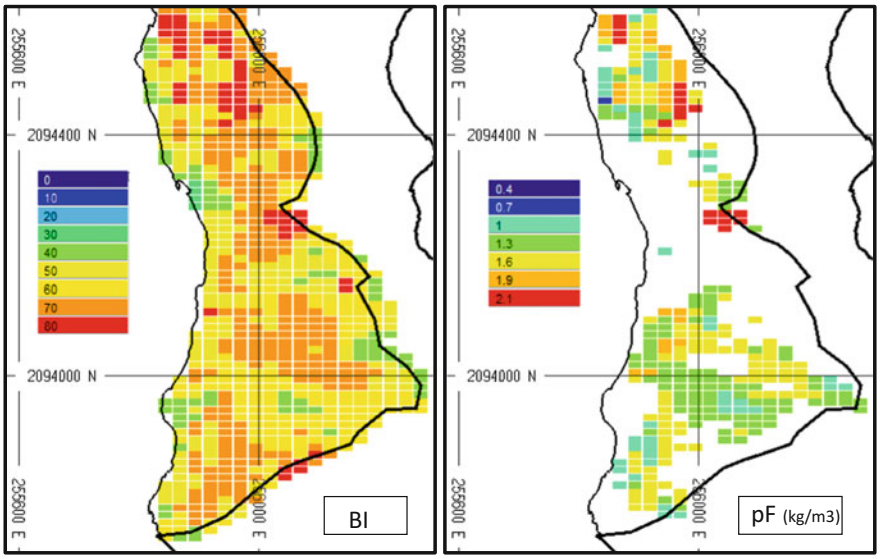

Fig. 4 Plan view of predicted BI and pF for an X50 of 150 mm within ore at the 570 mRL

Comminution Models

The approach to predict the common measures of crushability and grindability, A*b and BWi respectively, is through empirical proxy models. Relationships are identified and developed between A*b and BWi from 'training' datasets and commonly logged or measured aspects of drill core such as geological logging, and assays. Thus analysis of the training dataset is required with aim of identifying geological drivers and related variability to the A*b and BWi parameters.

Analysis of Comminution Dataset

The initial comminution test work consisted of 32 drill core composites ranging in intervals from 4 to17 m, that represented material from within the yearly production periods 2013–2015, and were tested by SMC and bond ball mill tests. The results from a further 25 samples were added to the dataset later in the project to represent material from production periods 2015 to +2020. The data shows a wide range in both impact resistance and grindability as shown in Fig. 5. The impact resistance as indicated by A*b ranges from a very hard 25 to soft 118 although the majority are between 30 and 55. Similarly, grindability as indicated by the bond ball mill work index BWi ranges from 10 to 35 kWh/t with the majority between 15 and 27 kWh/t.

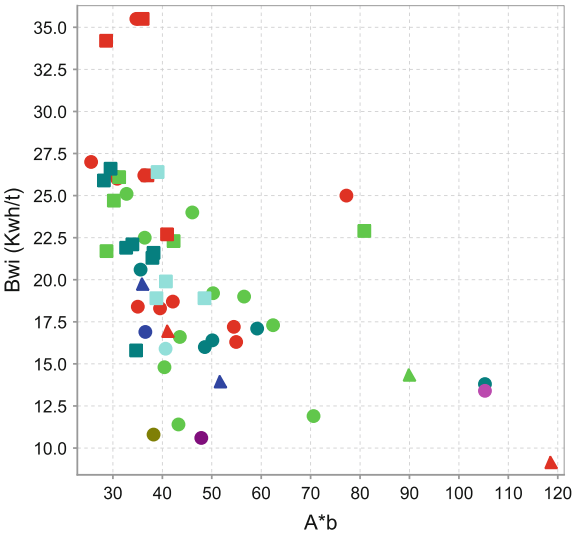

Fig. 5 Summary of results from comminution test work. The colour indicates lithology and shape oretype—oxide as triangles, transition as circles and primary as squares

No clear relationships in terms of distribution of A*b and/or BWi can be identified with geological aspects logged from the drill core such as weathering, lithology, alteration, alteration intensity, veining or combinations of these. The best correlation was between A*b and BWi themselves together with density.

The point load data was not considered as (a) the point load from the drill core was very poorly correlated with the comminution parameters due to the low representivity of the point load measurements from the drill core relative to the composite length of the comminution samples and (b) the issues around the quality of the point load data as outlined in the previous section.

In an attempt to understand the geological drivers, whole rock XRF and QXRD mineralogy was obtained for the comminution dataset. In terms of A*b, the XRF geochemistry shows poor correlations with no element >0.2. From the QXRD data, mica correlated best with A*b at 0.4. The better correlations to BWi from the QRDX data were again mica (−0.43) followed by chlinochlore, chlorite/kaolin and calcite (0.1–0.2) and from the XRF dataset, Ba, K and Na at only 0.2.

The correlations improved when the dataset was partitioned by the logged supergene type (oxidation) with correlation coefficients increasing to up to 0.75 in the case of Mn and Mg for Supergene Type SLE and OSM. The variables with correlations >0.3 (either positive or negative) are outlined in Table 2. This suggests that oxidation and mineralogy (relating to subtle hydrothermal alteration) have an influence on the comminution parameters.

Table 2 Summary of correlations of BWi and A*b with XRF whole rock geochemistry and QXRD mineralogy

	SuperGene type			
	SLE	OSM	SEC	PRI
BW*i*	Mg, Mn, P, K	Mn, Mg, Fe, Si	Ba, K	Mn, Si
	Clays, mica	Amphibole, clays, quartz	Mica	Mica, quartz, pyrite
	Density	Density	Density, FF	
	Zn, Ag, S	Zn, S		Ag, Zn, S
A*b	K, Mn, Mg	P, Mn	Fe, K, S, P (0.35)	Fe
	Mica, clays, serpentine	Quartz, serpentine, clays	Mica, quartz, pyrite	Mica
	Density	Density	FF	FF, density
	Zn	Zn, S	S	

SLE = completely oxidised, OSM = partially oxidised, mixed oxides after sulphides, SEC = transition zone with consistent presence of sulphides with iron oxides, PRI = primary with no oxidiation

*A*b*

As the standard geological drivers of A*b parameters could not be determined modeling using the geological based variables such as lithology or assays was not possible. Hence an alternative approach was sought.

The crushability of a sample is a function of the physical properties of the rock which includes the rock strength, the quantity and quality of any fractures or discontinuities. This together with the correlations with FF and density for A*b pointed towards the possibility of rock mass aspects having a significant influence the parameter. A standard method of rating rock mass is through Bieniawski's empirical rock mass rating scheme or RMR (Bieniawski 1976, 1989; Karzulovic and Read 2009). The parameters and calculation of the RMR is:

$$\text{RMR} = \text{SIR Rating} + \text{RQD Rating} + \text{DS Rating} + \text{CD Rating} + \text{GW Rating} \quad (3)$$

Where

SIR = Strength of Intact Rock
RQD = Rock Quality Designation
DS = Spacing of Discontinuities
CD = Conditions of Discontinuities
GW = Groundwater

The approach firstly calculates the RMR for the dataset at block level followed by an adjustment factor based on supergene unit to create the comminution rock mass rating or CRMR. The CRMR is then related to A*b from the SMC tests via regression to create a predicted A*b. The model was created using a subset of the A*b data from the comminution dataset.

Inputs

The SIR is a rating based on the estimated UCS with the DS rating based on FF. Both of these are inputs in the BI as discussed earlier, the only difference being that the RMR rating system was applied as compared to the BI rating system.

The RQD rating is based on the RQD measurements and similarly to the FF, a population based approach using the CuSum method and manual clustering into five domains based on the mean and standard deviation of the zones. For this initial model, the FF was interpolated into the block model using the IDW methodology to which the RMR rating system was applied.

CD is a function of the roughness of structures which is derived from core logging using the International Society of Rock Mechanics Suggested Methods and the Australian Standard AS 1726—1993 with the roughness classified by Stepped, Undulating and Planar together with Rough, Smooth or Slickensides resulting in nine categories (Phi-Bia-Mining 2010). The distribution of these roughness categories varies according to lithology. Hence the roughness rating was based on lithology a where lithologies with a significant proportion of planar structures with smooth or slickenslide structures received a lower rating compared to those dominated by stepped rough structures.

GW rating related to the groundwater condition of the rock mass which for open pit mines is assumed to be constant and damp with its associated RMR rating.

The predicted A*b verses measured A*b from all of the SMC dataset and not just those used in the development dataset is shown in Fig. 6. The methodology provides a prediction that is practical given that the purpose of the model is to highlight regions of significant variability in A*b.

BWi

The analysis of the BWi data with respect to geological, geochemical and geotechnical variables indicated that if domained by the oxidation/supergene then density and FF together with Zn and Ag are the most correlated of the variables that were consistently measured across the deposit. Thus the BWi was predicted using linear regression of combinations of these variables for each supergene type. The very high BWi's >30 Kwh/t are excluded from the proxy models.

Due to the small number of samples in the SLE and OSM zones, the number of variables within the regression was limited to a maximum of two. The regression performed well for all supergene units in terms of R^2 (>70), however the SEC had the largest residuals which requires further investigation and refinement. As an example, the prediction for the primary supergene zones is shown in Fig. 7.

The spatial modelling of two of the variables used in the proxy modeling of BWi, density and FF, were discussed earlier as part of the BI. Silver and zinc, were imported from the existing BHX resource model which has been estimated using ordinary kriging. The regression was once again applied at block level resulting in a predicted BWi.

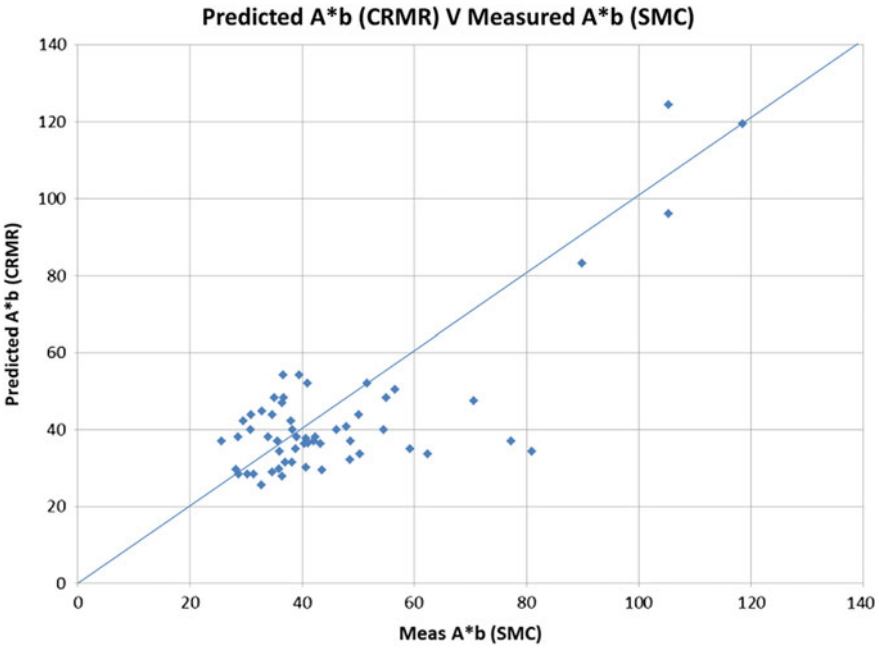

Fig. 6 Predicted A*b via the CRMR verses measured A*b from SMC tests using drill core samples

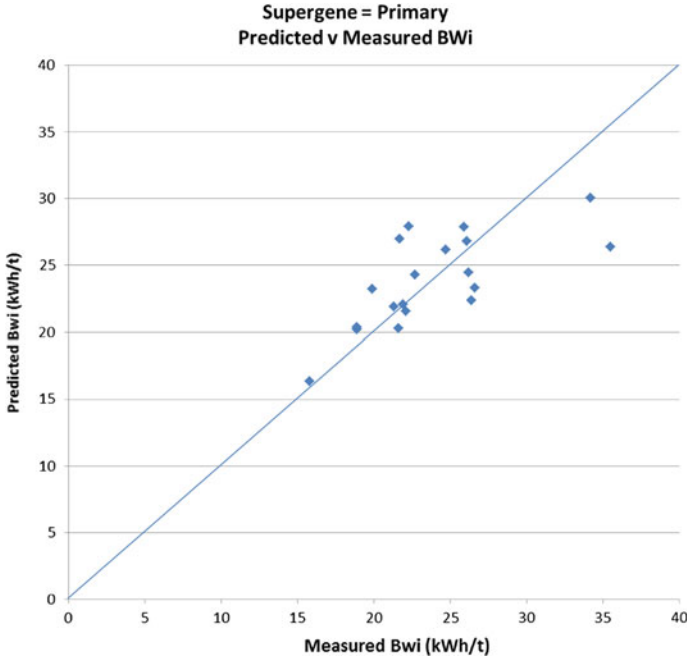

Fig. 7 Predicted BWi verses measured BWi for the primary supergene zone

Results

The predictive models of A*b and BWi for each supergene zone were applied to the inputs at block scale resulting in estimates of A*b and BWi for each block that contained the relevant data. Analysis of the results indicate that for supergene zones SLE and SEC, the range of the input variables within the block model were greater than those used in the development of the regression models resulting in anomalous values. These were set to null to avoid any misinterpretation by users. Of all the parameter models, the BWi has the least confidence due to the limited development dataset and variables sampled across the deposit.

The results of the predicted A*b and BWi within ore over the life of mine indicates:

- that 60% of the ore has an A*b of 28–45 which is considered hard to moderately hard material with only a small proportion in the very hard category (Fig. 8).
- Approximately 55% of the ore has a BWi greater than 20 kWh/t.
- That 50% of the ore is estimated to have an A*b of < 45 and BWi > 20 kWh/t with 14% having an A*b < 35 and a BWi > 25 kWh/t.
- Approximately 50% of the primary ore is predicted to have an A*b less than 35.
- On a yearly basis from the current mine plan, 2018 consists of the hardest milling ore with 65% predicted to have an A*b < 35 (hard ore) and 5% > 55 (moderately soft—very soft).
- Conversely, the softest ore milling conditions are expected in 2016 when only 15% of the ore is predicted to have an A*b < 35 (hard ore) and 40% > 55 (moderately soft—very soft).

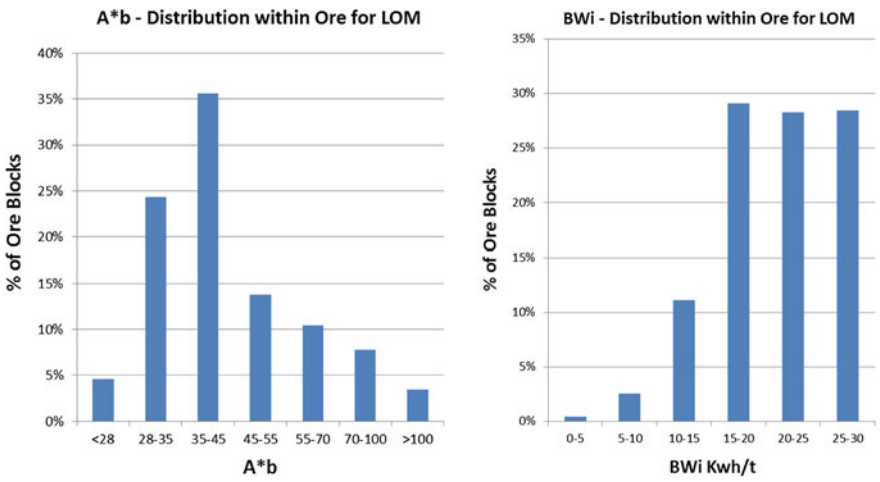

Fig. 8 Histograms of A*b and BWi for ore over life of mine

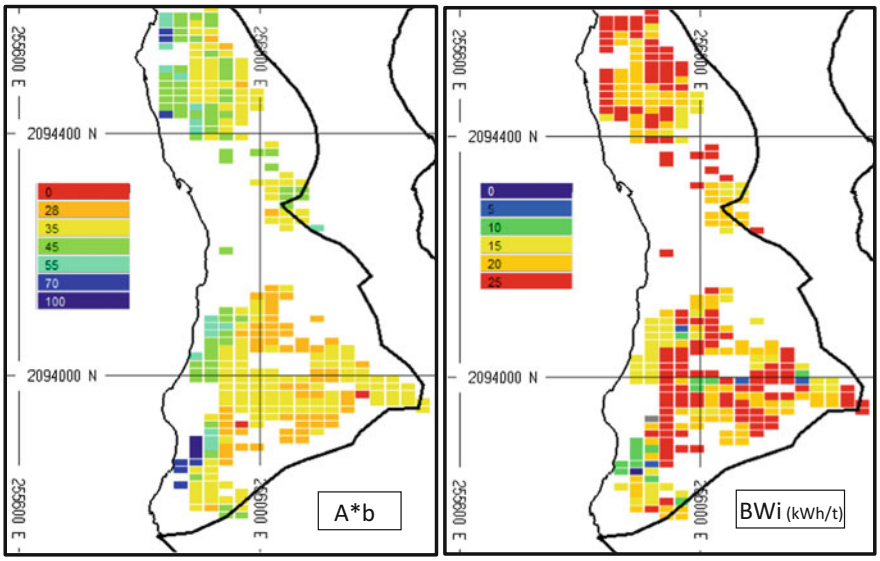

Fig. 9 Plan View of the predicted A*b and BWi within ore at the 570mRL

An example of the spatial variability of the A*b and BWi for the North and Centre pits at the 570 m level is shown in Fig. 9.

Initial verification of A*b indicates that the model compares favourably with material from belt cuts over a number of days. An indicative A*b was measured with a modified RBT methodology (Shi et al. 2009).

Implementation of the Models

Although at the early stages of implementation, the model are being utilised in the operation by mine planning, blasting and mill personnel.

As the models are for life of mine, their main function is supporting the life of mine and medium term planning and budgeting. This not only includes mine planning per se but also analysis of the likely impact of potential capital and operational improvements in the mine and mill.

However, the models are also being utilised guidance in tactical operational planning. The blasting related models, including fracture frequency, blastability index and powder factor, are providing guidance:

- as to areas at risk of producing coarse fragmentation and hence impacting on throughput;
- in the identification of areas where and how the planned blast design may be modified to achieve an optimal fragmentation;

- in the identification of at risk areas for interim and final walls and providing guidance for the trim blast design.

The comminution parameters are currently used to provide an indication of expected SAG and ball mill hardness and variability. Even at this relatively coarse resolution, the information allows a more proactive control in terms of throughput management within the operation.

Summary and Conclusions

The integration of geological, geotechnical and metallurgical data has enabled the development of an integrated model of key geotechnical/geometallurgical parameters. The key parameters modelled were those that relate to the rock characteristics relevant to estimating throughput for a SAB milling circuit - blast fragmentation for feed size distribution, A*b and BWi. This has allowed the numeric and spatial variability of those rock characteristics to be mapped. Although in the early stages of implementation the models are being used to support mine and production planning through:

- assessing the long term mine plan and identifying potential improvement opportunities;
- to provide guidance and support for budgeting;
- blast design for mill feed;
- ore blending decisions.

The empirical 'engineering' models for blast fragmentation at present are predicting the mean fragmentation under a set of assumptions and do not attempt to predict the full size distribution. Thus blast optimisation is required to increase the proportion of the fines within the blast which improves throughput.

In any modelling, the model is constrained by the available data and in order to overcome limitations in relating traditional data such as lithology/alteration/geochemistry to A*b, a predictive model was developed based on the geotechnical rating of rock mass, RMR. The RMR is an empirical based model to quantify rock properties relevant to geotechnical engineering applications and considers properties such intensity and condition of fracturing, rock quality and rock strength. These properties are also relevant to the 'crushability' of a rock and thus the RMR, together with the intensity of oxidation/weathering of the rock, was used to create a predictive model of A*b.

Further enhancements could include: the acquisition of data in under sampled areas; improving the quality of key variables; the inclusion of a confidence or uncertainty level; understanding the impact of upscaling point related data to blocks (support); the conversion of the key parameters to processing performance and further validation/calibration against field data.

To facilitate further improvements in maintaining and enhancing production of throughput, such as direct blending from the loading face using the ore properties and blast fragmentation, a similar model is being developed with a higher granularity and spatial resolution based on grade control drilling and pit mapping.

The life of mine models of mill ore feed variability are an improvement in spatially and temporally predicting the key rock properties and the associated performance at BHX and are being utilised by the by mine planners, metallurgists, blasting engineers and geologists.

Acknowledgements The authors would like to acknowledge Phu Bia Mining for permission to publish this work and to the reviewers for their contributions in improving the paper.

References

ASTM_International (2008) D5731-08: Standard test method for determination of the point load strength index of rocks and applications to rock strength classifications. ASTM International, Pennsylvania

Aust P (2014) Annual review 2013

Bieniawski ZT (1976) Rock mass classification in rock engineering. Explor Rock Eng, 97–106

Bieniawski ZT (1989) Engineering rock mass classifications—a complete manuel for engineers and geologists in mining, civil and petroleum engineering. Wiley, New Jersey

Brost D (2011) Exploring and developing mineral deposits in Northern Laos-the Ban Houayxai gold-silver deposit. SMEDG

BSI (2008) PAS 55-1:2008 Asset Management-Part 1: Specification for the optimised management of physical assets. Institute of Asset Management

Coombes J (2009) Validation of resource models—myths, materiality and modern approaches. Project evaluation. AUSIMM, Melbourne, Australia

Coward S, Vann J, Dunham S, Stewart M (2009) The primary-response framework for geometallurgical variables. 7th international mining geology conference, Perth, Australia. AUSIMM, pp 109–113

Cunningham CVB (1986) The Kuz-Ram model for prediction of fragmentation from blasting. Proceedings of the 1st international symposium on rock fragmentation by blasting, Lulea, Sweden pp 439–542

Cunningham CVB (2005) The Kuz Ram fragmentation model -20 years on. In: Holmber R (ed) 3rd EFEE World conf on explosives and blasting, Brighton, UK

Giere RN (2010) An agent-based conception of models and scientificrepresentation. Synthese 172:269–281

Karzulovic A, Read J (2009) Rock mass model. In: Read J (ed) Guidelines for open pit slope design. CSIRO Publishing, Clayton

Keeney L, Walters SG (2011) A methodology for geometallurgical mapping and orebody modelling. First AUSIMM international geometallurgy conference. The AUSIMM, Brisbane, Australia

Knuuttila T (2011) Modelling and representing: an artefactual approach to model-based representation. Stud Hist Philos Sci, Part A, 42:262–271

Lilly PA (1986) An empirical method of assessing rock mass blastability. In: Davidson JR (ed) AUSIMM large open pit mining conference, Newman, WA. AUSIMM/IE Combined Newman Group, pp 89–92

Lilly PA (1992) The use of the Blastability Index in the design of blasts for open pit mines. In: Szwedzicki T, GRBATNL (ed) Proceedings Western Australian Conference on Mining

Geomechanics, Kalgoorlie, WA. Western Australian School of Mines, Curtin University of Technology, 421–426

Manaka T, Zaw K, Meffre S, Vasconcelos PM, Golding SD (2014) The Ban Houayxai epithermal Au–Ag deposit in the Northern Lao PDR: Mineralization related to the Early Permian arcmagmatism of the Truong Son Fold Belt. Gondwana Res 26:185–197

Morrell S (2004) Predicting the Specific energy of autogenous and semi autogenous mills from small diameter drill core samples. Mining Engineering 17:447–451

Napier-Munn TJ, Morrell S, Morrison RD, Kojovic T (1996) Mineral comminution circuits: Their operation and optimization, 1st edition Julius Kruttschnitt Mineral Research Centre, Brisbane, Qed, 413p

PHI-BIA-MINING (2010) Phu Bia mining technical field procedure manual—logging and data capture

Pierce M, Gaida M, Degange D (2009) Estimation of rock block strength. In: Diederichs M, Grasselli G (eds) Rock Eng09: 3rd CANUS Rock mechanics symposium, 2009 Toronto

Shi F, Kojovic T, Labri-Bram S, Manlapig E (2009) Development of a rapid particle breakage characterisation device—The JKRBT. Miner Eng 27:602–612

Vann J (2008) Applied geostatistics for geologists and mining engineers—Course Notes. Quantitative Group

Widzyk-Capehart E, Lilly P (2001) A review of general considerations for assessing rock mass blastability and fragmentation. EXPLO 2001. Hunter Valley, NSW

Woodhouse J (2010) Asset management in the oil and gas, process and manufacturing sectors. In: Lloyd C (ed) Asset management—whole-life management of physical assets. ICE Publishing, Westminister, London

Woodhouse J (2011) Physical Asset Management. In: Darling P (ed) SME Mining Engineering Handbook, 3rd edn. Society for Mining, Metallurgy and Exploration Inc (SME), Englewood

Using Grade Uncertainty to Quantify Risk in the Ultimate Pit Design for the Sadiola Deep Sulfide Prefeasibility Project, Mali, West Africa

S. P. Robins

Abstract In order to quantify the uncertainty in the grade estimate for the Sadiola deep sulfide prefeasibility project, a conditional simulation model was generated using the direct block simulation methodology. Compared to conventional sequential Gaussian simulation, the direct block simulation algorithm produced a reliable model in significantly less time, lending its application to a production environment. Through application of a mining transfer function, risk pits were generated for comparison with the deep sulfide prefeasibility pit. The results of this study revealed that the prefeasibility pit is optimal at the applied gold price and cost parameters, and that the risk of not achieving the project grade profile is low. Should the gold price increase, or the operating costs of the project decrease significantly, the deep sulfide reserve tonnage would realise significant upside potential. Probability and uncertainty analysis revealed that the greatest risk to the project is the confidence in the footwall grade estimate. At a drill spacing of 50 m × 50 m and a sample interval of 1 m, the probability of the footwall grade exceeding the economic cut-off of 2.0 g/t is low, while the uncertainty in the grade estimate is high. Although significantly lower in grade than the main zone, which is the primary economic driver of the project, the footwall mineralisation is important in terms of reducing stripping ratio and delivering ore tonnes to optimise the treatment schedule. This zone is therefore a focus area for further drilling.

Introduction

Sadiola Hill Gold Mine is located at latitude 13°56′N, longitude 11°40′W, and altitude 125 m above mean sea level, which places it approximately 500 km north west of Bamako, the capital of Mali in West Africa (Fig. 1). The mine is operated by the Societe d'Exploration des Mines d'Or de Sadiola SA (SEMOS SA), which comprises a joint venture partnership between AngloGold Ashanti (38%),

S. P. Robins (✉)
AngloGold Ashanti, 76 Rahimamoosa Street, Newtown, Johannesburg, South Africa
e-mail: srobins@anglogoldashanti.com

R. Dimitrakopoulos (ed.), *Advances in Applied Strategic Mine Planning*,
https://doi.org/10.1007/978-3-319-69320-0_29

IAMGOLD (38%), the Malian Government (18%) and the IFC (six per cent). Construction of the Sadiola plant began in March 1995 and was completed in June 1997. Gold production began in mid 1997 from the saprolite oxide orebody and more recently from saprolite sulfide ore as mining has progressed through the weathered profile towards the hard/soft boundary. The Sadiola orebody extends substantially below the weathered horizons into the underlying hard sulfide lithologies. However, the current Life of Mine plan (LOM) does not exploit this material because the plant is unable to treat more than ten per cent hard material. In 2005, Sadiola treated approximately 5.3 Mt of ore at 2.83 g/t, accounting for a gold production of 483 koz (Van der Westhuizen 2005). The Sadiola plant was designed to treat this material, comprised almost entirely of saprolite and laterite. At a cut-off grade of 1.42 g/t, the remaining Sadiola Main Pit Reserve (at the end of 2005) was 21 Mt at 3.35 g/t, accounting for 2.3 Moz. This reserve would accommodate mining to the end of 2009.

The hard sulfide portion of the Sadiola main pit mineral resource at the end of 2005 was 48.5 Mt at 2.25 g/t, accounting for 3.5 Moz (at 0.70 g/t cut-off grade), providing large upside potential for the mine. Should Sadiola be able to treat hard sulfide material, mining could continue to the end of 2015 and the LOM extended to 2024. SEMOS SA therefore initiated the deep sulfide prefeasibility project to

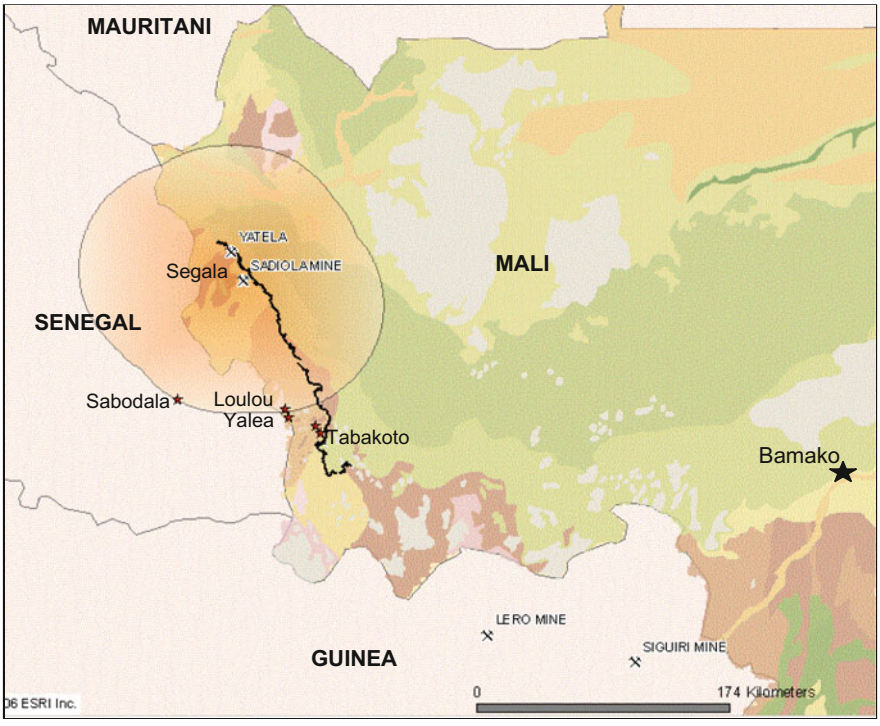

Fig. 1 Locality map for Sadiola mine, Mali, West Africa

optimise the exploitation of the hard sulfide component of its mineral resource. The prefeasibility project focused on the pit expansion potential of the deposit, as well as the options available to upgrade the current gold treatment plant to process the hard sulfide material. As of June 2006, cost estimates indicated that a capital outlay of approximately USD$145 million would be required to upgrade the treatment plant to efficiently process hard sulfide material.

Given the large capital outlay required to commence with the deep sulfide Project, it was necessary to quantify the technical risk of exploiting the Sadiola hard sulfide resource. Quantification of the grade uncertainty was vital to providing focus areas that required additional drilling before a reliable feasibility study grade model could be obtained. The Sadiola mineral resource model used for the prefeasibility study was comprised of a grade estimate, into 30 m × 30 m × 10 m blocks, using ordinary kriging. This was followed by a change of support calculation, using uniform conditioning, to an SMU support size of 10 m × 10 m × 5 m. The sample information on which this model was built was comprised predominantly of NQ (53 mm diameter) half diamond core, with 4.5 inch RC precollars through the soft material. The final model comprised 13 independent estimation domains to honour the stationarity requirements for kriging.

This model effectively generated a single grade outcome for planning purposes. Questions remained as to how accurate this grade estimate was, and if there was a practical method for determining the uncertainty in the grade estimate. Conditional simulation was utilised to answer these questions. Conditional simulation, a Monte Carlo-type simulation approach, generates multiple and equally probable realisations that provide a model of the spatial uncertainty of the grade in the in situ orebody (Dimitrakopoulos et al. 2002). The resultant realisations are not only conditioned to the available sample data, and therefore all reasonably match the same sample statistics, but also reasonably duplicate the histogram and semi-variogram model of the sample data (Goovaerts 1997). Spatial features are deemed ‘certain’ if they are present in most of the simulated maps and ‘uncertain’ if seen on a few simulated maps.

According to Goovaerts (1997), generating alternative realisations of the spatial distribution of an attribute is rarely the goal. Rather these alternative realisations serve as the input to other transfer functions, which in the open pit mining environment would comprise a mining process such as a pit optimisation algorithm. In assessing the uncertainty in the grade estimate for the Sadiola mineral resource model, the goal was to generate a number of different grade realisations and run each of these realisations through a pit optimisation algorithm in order to determine where the prefeasibility design pit ranked. The challenge lay in selecting a simulation method that was practical to use in an operating mine environment. Sequential Gaussian simulation (or SGS) (Goovaerts 1997), the industry norm at the time, proved impractical because of the computing time involved in generating the 50 realisations required per estimation zone. The relatively new method of direct block simulation was therefore selected.

Dimitrakopoulos et al. (2002), proposed the direct block simulation (DBSIM) method as a viable alternative to conventional simulation methods that considerably

reduces computational time. DBSIM detailed in Godoy (2003) and also outlined in Boucher and Dimitrakopoulos (2009), Peattie (2005) simulates the internal points of each block, and when the simulated block is calculated, the point values are discarded. The simulated block value is then added to the conditioning dataset. To integrate the block support conditioning data, the algorithm has been developed in terms of a joint simulation, where the second variable relates to the block values sequentially derived through the simulation process. The algorithm simulates several hundreds of blocks per second and is considerably faster than any point conditional simulation combined with reblocking. Furthermore, Godoy (2003), Benndorf and Dimitrakopoulos (2007) and others show that in addition to being substantially faster and more efficient in terms of computing requirements, the DBSIM method is reliable in terms of reproduction of the sample statistics.

General Geology

The Sadiola deposit is located within the Malian portion of the Kenieba-Kedougou window, a major Early Proterozoic—Birimian outlier along the NE margin of the Kenema—Man shield (Fig. 2). The Birimian of the window can be interpreted as a collage of at least two NS trending terrains of different nature. To the west, an older (±2.2 Ga) tholeitic mafic volcanic unit with island arc type volcanics, intruded by a major calc-alkaline batholith, belongs to the Saboussire Formation. It is separated from the dominantly sedimentary sequence of the Kofi Formation by a major north-to-northeast trending shear zone. This sedimentary domain is significantly younger and is intruded by calc-alkaline batholiths dated at 2.0–2.05 Ga. Within this domain metamorphic grade is greenschist facies, with formation of metamorphic biotite and locally amphibolite grade near major intrusions. The Kofi Formation is obliquely cut by the approximately N–S to N10° trending Senegalo-Malian shear zone (SM), which is punctuated by several gold deposits along its splays (Loulo, Yalea, Sadiola, Yatela), (Robins et al. 2005).

The Sadiola deposit is located in the north of the window and is hosted by sediments of the Kofi Formation, which have been intruded by numerous felsic intrusives. The dominant sediments consist of fine-grained greywacke and impure carbonates with minor tuffs and acid volcanics. At Sadiola, the intensely folded impure carbonate packages comprise an alternation of limestone beds, a few millimetres to several decimetres thick, with thinner, more detritic beds. The Sadiola deposit occurs along the N10° striking Sadiola Fracture Zone (SFZ), which is thought to be a brittle-ductile splay off the SM Shear at a sinistral releasing bend. The SFZ follows the steeply westerly dipping contact between greywacke to the west and impure carbonate to the east. Along the SFZ, both the greywacke and impure carbonate are transposed. The SFZ and its wall-rock are injected by discontinuous diorite dikes. Silicified quartz-feldspar-porphyry (QFP) dikes often intrude along later steep west dipping, N20° striking structures. The QFPs cross-cut

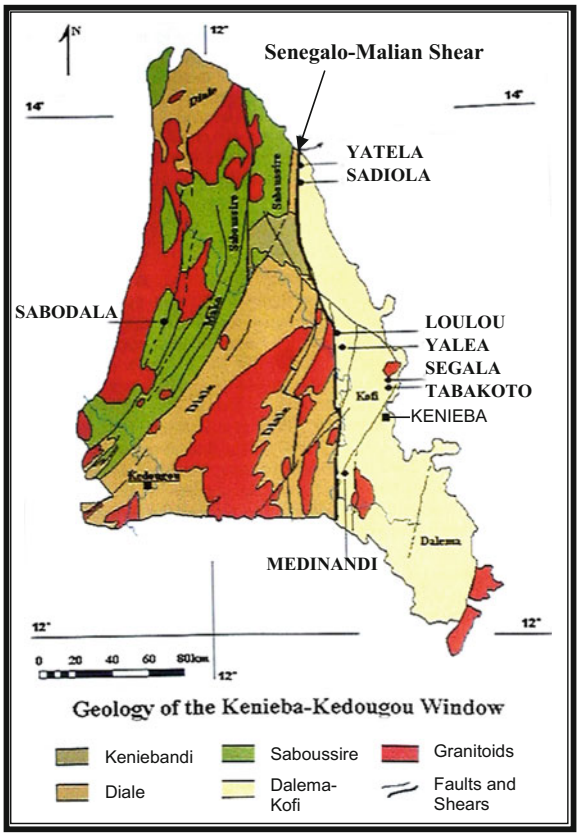

Fig. 2 Geology of the Kenieba-Kedougou window

the diorites and may show brittle fracturing. Post mineralisation deformation has complicated structural relationships in the deposit.

Gold mineralisation at Sadiola occurs along the SFZ over a drilled strike length of approximately 2500 m, and remains open to the north and south. N20° trending fault splays off the SFZ are also well mineralised. The mine geological and grade block model indicates the presence of 20°–25° south dipping ore shoots within the plane of the SFZ. Mineralisation occurs in all of the four major rock types (marble, greywacke, diorite, and quartz-feldspar porphyry) and is spatially associated with a complex alteration pattern. Drilling of the (unweathered) primary mineralisation has allowed detailed investigation of major and minor hydrothermal alteration processes that were active during the formation of the deposit. Alteration assemblages identified to date include calc-silicate, potassic, chlorite-calcite, carbonate and silicification, and have allowed the deposit to be classified as a mesothermal-shear-zone hosted deposit. Gold is associated with both arsenic and antimony dominated sulfide assemblages including arsenopyrite, pyrrhotite, pyrite, stibnite and gudmuntite (Robins et al. 2005). Deposits of this type world-wide exhibit good continuity of mineralisation along the strike and extending to great depth.

Structurally controlled, high grade pay shoots' typically occur within a more pervasive lower grade halo. At Sadiola, the location and geometry of high grade mineralisation appears to be controlled by the confluence of the SFZ with the N20° splays, resulting in steeply to vertically plunging zones within the plan of the SFZ. The geometry of the extensive soft 'saprolitic' oxide deposit at Sadiola relates almost exclusively to the supergene weathering history of the primary mineralisation. The permeability of the rock formation, controlled mainly by faulting, shearing and porosity, allows deep penetration of ground water, causing oxidation of primary sulfides. Oxidation of pyrite (and other sulfide species) results in the formation of sulfuric acid, further promoting the downward argillisation of the bedrock to form the clay rich assemblages present in the saprolite. The irregular, 'karst like' soft rock/hard rock contacts can be related to the extent of faulting and the original sulfide content of the overlying profile. The intense weathering has resulted in a tropical climate forming a series of decarbonated- argillised troughs of variable depth (up to 180 m depth) along the SFZ. This is the rich oxide orebody currently being mined (Fig. 3).

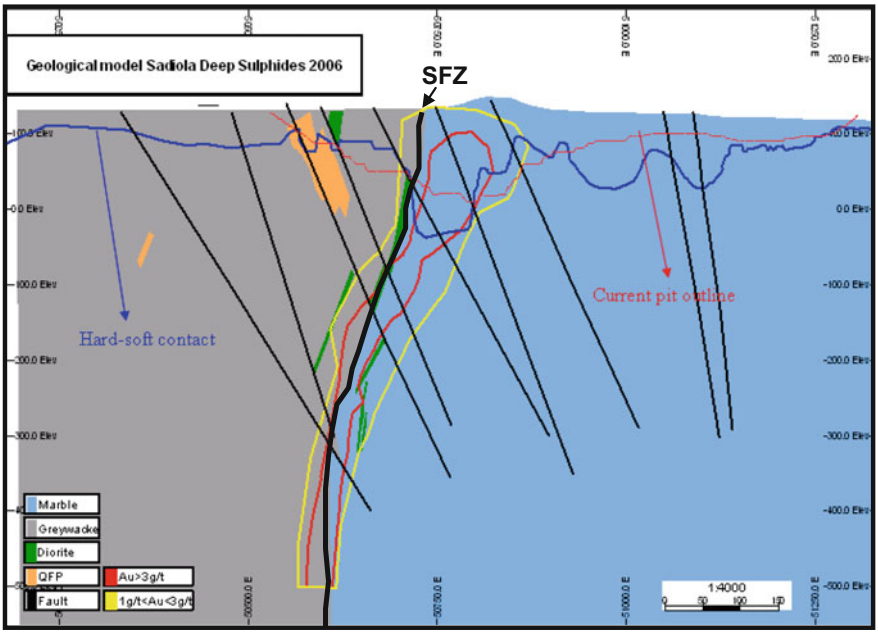

Fig. 3 Section 5600 N through Sadiola orebody. Mineralisation sits along the greywacke-marble contact (Sadiola Fracture Zone). N20° faults are indicated in black. Section compiled by Dr. A Smeesters, 2006

Creation of the Simulation Model

Simulation Methodology

Although the deep sulfide project has focused specifically on the hard sulfide component of the Sadiola resource, a significant amount of mineralised saprolite material occurs between the hard/soft boundary and the current LOM pit design. Since this material would contribute towards the economics of the project, it was necessary to account for it in the simulation model. The laterite material only occurs close to the original ground surface, and would have limited influence on the project economics since most of the ore within this zone has already been mined. To speed up the simulation process, the laterite estimation domains were excluded from the study. All other estimation domains used in the Sadiola recoverable resource model were honoured. Furthermore, the same densities as per the recoverable resource block model were retained in the simulation model (Table 1). The determination of the various estimation domains in the recoverable resource model was based on trend analyses and sample statistics. This process is outlined in Robins et al. (2005).

Sample Data

Almost all the deep sulfide sample data comprised NQ diamond core at 1 m sample intervals. However, since a significant amount of saprolite material—which was drilled with 125 mm RC method and at 2 m sample intervals—would be included in the Deep Sulfide Project, all conditioning (sample) data was composited to 2 m sample intervals. To test for clustering, data was declustered using a moving window method. It was found that there was no significant spatial clustering present in the data and therefore declustering was unnecessary. This was likely a result of domaining the data and therefore achieving a relatively regular sample grid per domain. A sample input file was supplied with the conditioning data zoned according to the estimation domains (ZONECODE), outlined in Table 2. The input data comprised raw grade information that was converted to normal space by the

Table 1 Table of rock types and their associated densities

Rocktype code	Description	Density (g/cm^3)
1	Laterite and clay	1.97 (average)
2	Saprolite	1.80 (average)
3	Silicified oxide	2.57 (average)
4	Saprolite sulfide	2.00 (average)
5	Hard sulfide	1.55 to 3.03 (kriged)
6	Blast oxide	2.10 (average)
7	Blast sulfide	2.10 (average)

DBSIM program during the simulation runs. During this process, DBSIM declustered the data, and output 'equal weighted' statistics for the conditioning data, simulated nodes and blocks.

Normal Score Semi-variogram Models

Double structured, normal score spherical semi-variogram models were calculated per ZONECODE (Table 3). The search distances are those used for simulation in the x, y, and z orientations. The general characteristics of the normal score variograms can be summarised as follows:

- The northern and southern mineralisation is separated by a WNW trending fault that appears to have rotated the strike of the mineralisation so that to the north, the mineralisation trends 030, and to the south, it trends 000.
- Most of the hard sulfide mineralisation (zones 5000, 6000 and 7000) is situated in the south of the orebody and therefore their variogram structures resemble that of the South Saprolite ore (zone 4000), for which the relatively low nugget is attributable to supergene enrichment of the grade. The main ore high- and low-grade variograms (zones 5000 and 6000 respectively) are similar in all respects.
- The Far North (zone 1000) and North Saprolite (zone 3000) ore zones have similar structure and orientation trending 030, in line with the change in strike of the mineralisation. The Far North saprolite has significantly more continuity in the y direction, though it was necessary to reduce the search distance in this direction to minimise negative kriging weights.

The North Hard Ore (zone 8000) predominantly underlies the North Saprolite, and has the same structure, though not the same orientation. This is most likely a result of insufficient sample data to define a trend.

Table 2 Table of rock types and their associated densities

Zonecode	Description	Project
1000	Far north saprolite ore	Main pit—oxide
2000	Saprolite waste	Main pit—oxide
3000	North saprolite ore	Main pit—oxide
4000	South saprolite ore	Main pit—oxide
5000	Main ore—high grade	Deep (hard) sulfide
6000	Main ore—low grade	Deep (hard) sulfide
7000	Footwall/hangingwall ore	Deep (hard) sulfide
8000	North hard ore	Deep (hard) sulfide
9000	Waste	Deep (hard) sulfide

Table 3 Normal score semi-variogram models by ZONECODE

ZONECODE	C0	C1	C2	Range 1			Range 2			Search distance			Azimuth/dip
				X A2	Y A1	Z A3	X A5	Y A4	Z A6	X	Y	Z	
1000	0.190	0.510	0.300	14	35	15	50	130	30	30	30	20	030/00
2000	0.258	0.450	0.284	42	30	28	170	270	55	30	30	10	170/00
3000	0.200	0.400	0.398	10	10	12	40	50	30	25	40	15	030/00
4000	0.150	0.370	0.478	9	9	9	65	65	45	33	45	16	000/00
5000	0.300	0.370	0.328	11	11	11	35	35	23	65	65	30	000/00
6000	0.380	0.370	0.248	11	11	10	43	43	30	65	65	35	000/00
7000	0.350	0.270	0.479	9	9	8	33	33	25	120	120	60	000/00
8000	0.200	0.400	0.399	8	8	8	26	26	18	120	120	60	000/00
9000	0.231	0.301	0.467	13	13	13	132	132	105	60	60	30	000/00

- All the hard sulfide variograms have isotropic horizontal structures, attributable to the absence of close spaced grade control data necessary to define the structures causing anisotropy.
- The waste variograms for the saprolite (zone 2000) and hard sulfide (zone 9000) are similar because of a relative lack of grade variability between sample locations. This is to be expected, considering that most of the mineralisation had been included in the mineralised envelope.

Representative Number of Realisations

To determine the number of realisations that would be required to obtain a reliable uncertainty model, the number of realisations were plotted against the progressive mean and progressive Coefficient of Variation (COV) for each simulated domain. The number of simulated blocks for each domain was greater than 95% of the total number of available blocks. For the first few realisations, the mean and COV values in the plots 'bounced around', but as the progressive values included more realisations, they stabilised, and where they levelled sufficient realisations, they were considered to have been used to model the variability. In this study, the grade for five out of the nine simulation domains could have been considered sufficiently simulated with up to 25 realisations, however, the remaining four domains required additional realisations. Since it was easier to deal with 50 realisations than 25 realisations in the probability calculations, and most of the Deep Sulfide 'ore' zones required more than 25 realisations, it was decided to use 50 realisations for all the mineralised domains, and 25 realisations for the 'waste' domains. Thus the 25 realisations for ZONECODE 2000 and 9000 were repeated for the second 25 (26 to 50) mineralised domain realisations. In this way, the simulation time was reduced by not performing unnecessary simulations on the 'waste' domains, while simultaneously achieving sufficient variability in the 'ore' domains, which were relatively quick to simulate.

Initial Validations on Point Data

The internal nodes were estimated on 2.0 m $\times$ 2.0 m $\times$ 1.25 m centres for each simulation, totalling 100 nodes per regularised (SMU) block. These were only output for the first ten simulations in order to check that the results honoured the conditioning data, the histogram of the normal score and raw data, and the variograms of the normal score and raw data. For the remaining simulations, only the block values were retained. Raw grade values were input into the program. The DBSIM algorithm transformed them to normal score values for simulation, and then back-transformed the resultant normal score values to raw grade values. Both

the raw and normal score data sets were output, though because they show the same trends, only the raw data is presented below.

Statistical Validation

The base statistics for the raw grade data are summarised in Table 4.

From Table 4, the base statistics indicated that the mean grades and variances for the saprolite material (ZONECODES 1000–4000) were generally slightly under-estimated with the conditioning data, exhibiting values slightly higher than the simulated values. Though the mean grades for the Saprolite waste (ZONECODE 2000) and North Saprolite ore (ZONECODE 3000) were only marginally lower, both the mean grade and variance for the South Saprolite ore (ZONECODE 4000) were significantly lower than the corresponding conditional data values. This was initially a cause for concern for the pit optimisation phase of the project because the South Saprolite ore comprises the majority of the saprolite material below the current LOM pit. However, the total saprolite ore only comprises 16 per cent of the total ore tonnes between the current LOM and Deep Sulfide pit designs. The far north Saprolite (ZONECODE 1000) is relatively insignificant regarding its ore tonnage contribution towards the Deep Sulfide Project.

From the base statistics, the simulation mean and variance for the main ore high grade and low grade (ZONECODEs 5000 and 6000 respectively)—the primary drivers for the Deep Sulfide Project—though marginally high, are reasonably close to the mean and variance of the conditioning data, which fall within the range of values of the ten realisations. Similarly for the Hangingwall and Footwall mineralisation (ZONECODE 7000), the conditioning data mean and variance are within acceptable limits of the corresponding ten realisation values. The simulated mean and variance values for the North Hard ore (ZONECODE 8000) are significantly

Table 4 Summary base statistics for raw grade point data

ZONECODE	Conditioning data		Simulation range in mean value		Simulation range in variance	
	Mean	Variance	Minimum	Maximum	Minimum	Maximum
1000	1.65	7.27	1.44	1.62	4.87	6.55
2000	0.36	1.69	0.31	0.33	0.72	1.21
3000	2.03	25.74	1.86	2.02	17.01	23.36
4000	2.93	32.18	2.62	2.71	19.99	25.13
5000	2.84	8.73	2.82	3.03	8.84	16.43
6000	1.36	6.26	1.35	1.44	5.68	7.27
7000	1.14	6.94	1.17	1.33	6.24	10.65
8000	2.09	28.49	2.16	2.54	19.30	47.66
9000	0.26	0.54	0.50	0.54	0.54	0.73

higher than the corresponding conditioning data. A poor result, however, is to be expected since this domain has been insufficiently sampled. Furthermore, the North Hard ore comprises a relatively insignificant proportion of the total Deep Sulfide ore and therefore is not expected to have significant influence on the pit optimisation runs. For the Hard Sulfide waste zone (ZONECODE 9000), the simulated mean grade (0.50 g/t to 0.54 g/t) was significantly higher than the mean of the conditioning data (0.26 g/t), though the variance is similar. This zone was expected to remain largely subeconomic and was therefore unlikely to impact significantly on the pit optimisation runs.

Histogram Validation

Histograms were generated for the first ten realisations of both the raw grade and normal score simulation nodes. Since the two data sets are similar, only the raw data is discussed. The raw grade histograms for the saprolite material (ZONECODES 1000 to 4000) indicated that, except for the North Saprolite ore (ZONECODE 3000), the simulated grade for the saprolite material has been understated. The Saprolite material (ZONECODES 1000 and 4000) was only marginally so, but the grade for the Saprolite waste (ZONECODE 2000) has been significantly understated. Since this is a 'waste' domain, with only five per cent of the conditioning data above an economic cut-off grade to begin with, this grade understatement is not expected to have a significant impact on the pit optimisation runs. For the primary drivers of the Deep Sulfide Project, the Main Ore High Grade and Low Grade (ZONECODES 5000 and 6000 respectively), the raw grade histograms show good correlation between the ten realisations and the conditioning data. Figure 4 illustrates this deduction for the main high-grade mineralisation (ZONECODE 5000).

For the Hard Sulfide Hangingwall and Footwall mineralisation (ZONECODE 7000), the simulated grade appears to be marginally overstated between 3 g/t and 5 g/t. The same is evident for the North Hard ore (ZONECODE 8000) between 5 g/t and 7 g/t. Both of these domains require additional drilling to ensure they are representatively sampled. The histograms for the Hard Sulfide 'waste' domain (ZONECODE 9000) show that the grade is significantly overstated up to about 2.5 g/t, however 94% of the conditioning data is below the lower marginal cut-off grade of 1.20 g/t. The overstatement of grade is therefore unlikely to have a significant impact on the pit optimisations. From a statistical perspective, the Sadiola simulation model can be considered to be representative of the conditioning data.

Variogram Validation

The final test to determine the validity of the simulation model was to test the reproduction of the spatial correlation between the simulated results and the

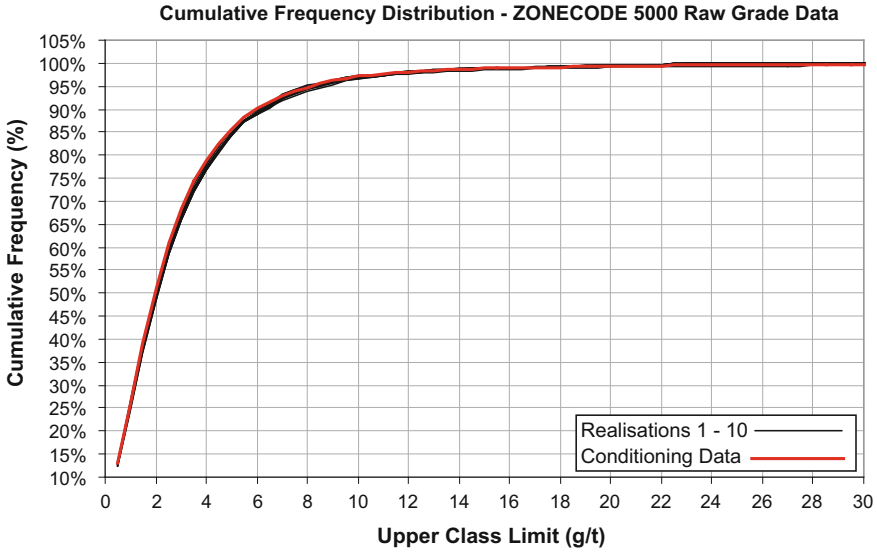

Fig. 4 Cumulative frequency distribution for ZONECODE 5000 raw grade data

conditioning data. Experimental variograms were calculated for the first ten realisations and plotted against the semi-variogram model that was input into the simulation process. To facilitate this process, the DBSIM program converted the input semi-variogram models to block support and output the results. The resultant normal score variogram model for the Main High-Grade mineralisation (zone 5000) is presented in Fig. 5.

Although not an exact match, the normal score simulated experimental data compares well with the regularised variogram model for the Main High-Grade mineralisation (ZONECODE 5000). This was generally the case for the other zones, particularly the Hard Sulfide mineralised domains (ZONECODES 5000–8000).

Post Simulation Processes

After the simulation process, the base statistics per block for all the realisations were calculated. The following statistics were calculated for each block:

$$mean, \mathbf{m} = \frac{\sum AU_{(1\,to\,n)}}{n}$$

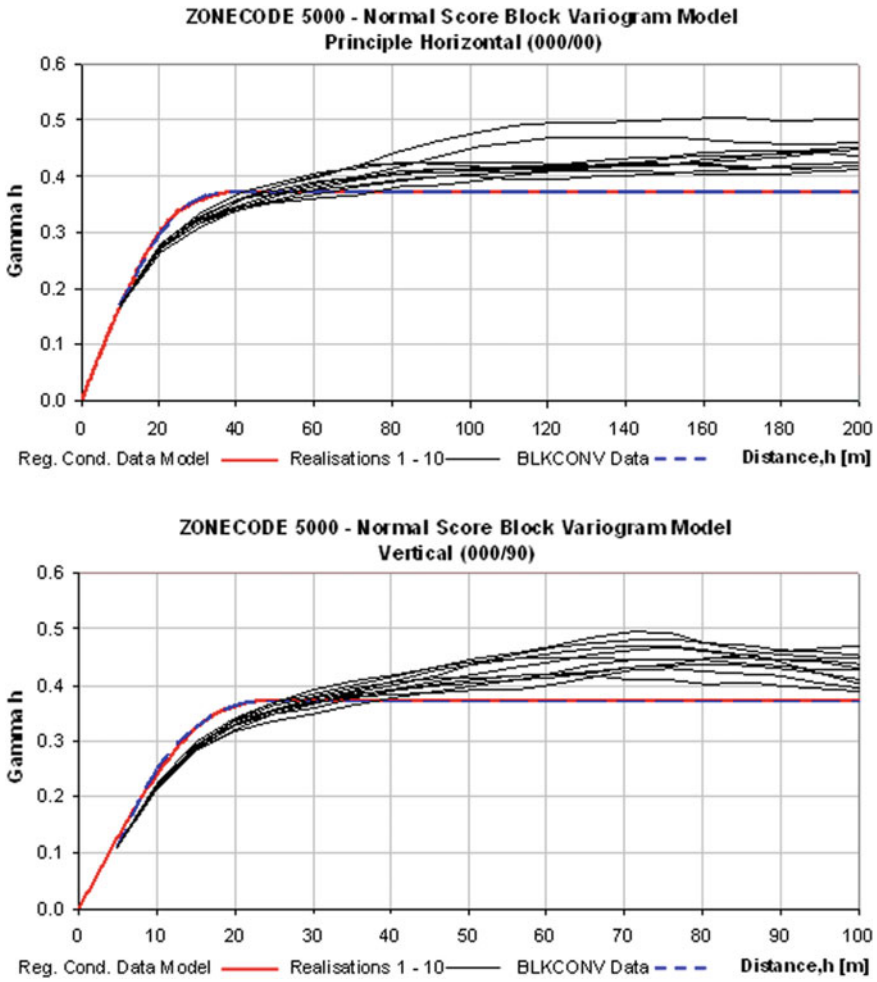

Fig. 5 Normal score variogram model for ZONECODE 5000

where:
n is the number of realisations

$$\text{variance}, \mathbf{s}^2 = \frac{\sum (AU - m)^2}{(n-1)}$$

standard deviation, $s = \sqrt{s^2}$coefficient of variation, $\mathbf{COV} = \frac{s}{m}$

Similarly, the probability of each block grade being above 2.0 g/t was calculated.

$$\text{probability}, \mathbf{P}_{(\mathbf{AU} > \mathbf{2.0\,g/t})} = \frac{\text{No of realisations} > 2.0\text{g/t}}{\text{Total no of realisations}(\mathbf{n})}$$

Next, for pit optimisation purposes, the laterite domains were added to the simulation model, with each realisation adopting the estimated grade for the laterite model blocks. The final simulation model was depleted by the saprolite life of mine volume.

The final simulation model contained primary fields for 50 grade realisations, coefficient of variation (providing an indication of uncertainty in the grade value), and probability that the grade would be greater than 2.0 g/t. Secondary fields were the remaining base statistics, the initial classification and rock type fields, and the ZONECODE field. A representative section (EW-5550) is presented to illustrate the primary fields of the final simulation block model (Figs. 6, 7 and 8). The $475/oz prefeasibility pit shell is shown in white, and the models have been depleted to the current 'oxide' LOM design.

From Figs. 6 and 7 it is evident that although realisation one shows significant material within the prefeasibility pit shell above 2.0 g/t, the probability of the actual grade being above 2.0 g/t is low. For this reason, one shouldn't place too much emphasis on the grade of a single realisation, but rather consider a number of realisations simultaneously. The use of probability calculations provides a good overview of the results of all the realisations simultaneously.

Figure 8 illustrates how the coefficient of variation calculation provides an indication of uncertainty in the simulated block grade. The diagonal white lines are

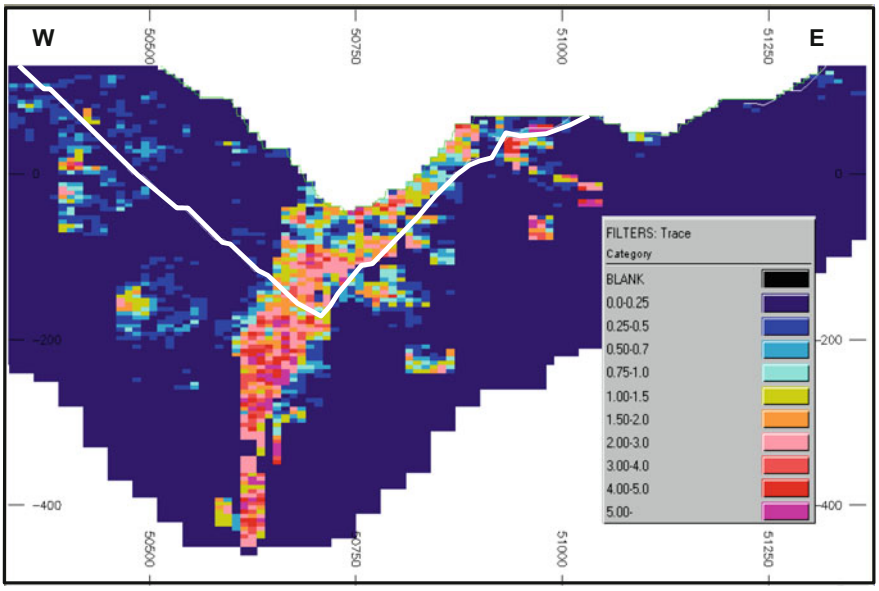

Fig. 6 Simulated block grade for realisation 1 on Section EW-5550

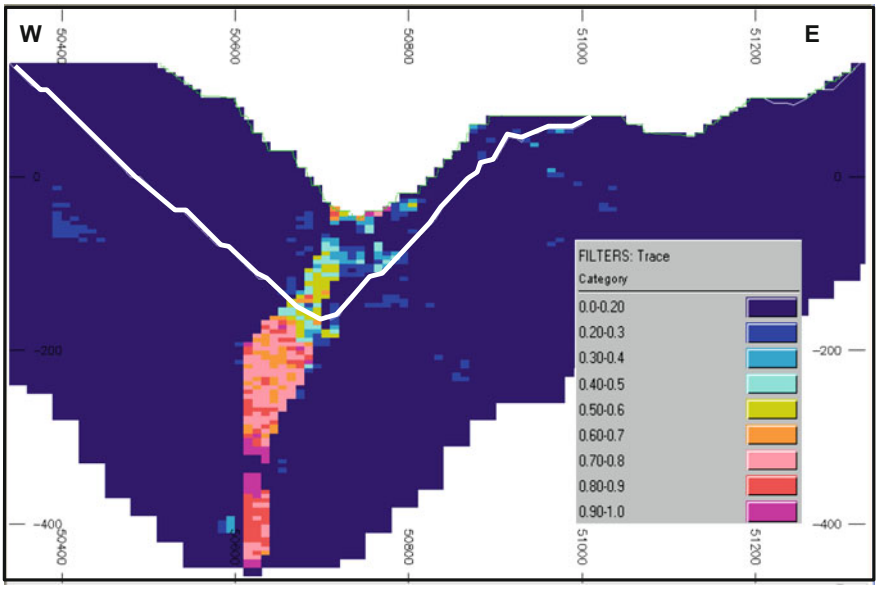

Fig. 7 Probability of grade greater than 2.0 g/t on Section EW-5550

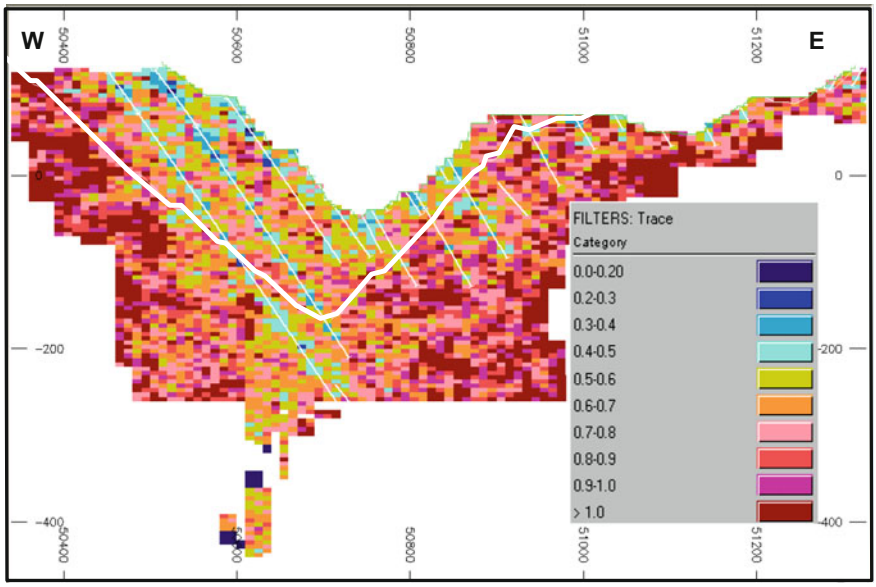

Fig. 8 Block coefficient of variation on Section EW-5550

borehole traces, and it is evident that zones of high confidence (low uncertainty) correspond well with the borehole traces, while zones of high uncertainty correspond with zones that have been insufficiently sampled. Since the coefficient of variation provides a reliable indication of uncertainty in the simulated grade, it can also be used as a tool for confirming, or even improving, the classification of the Deep Sulfide mineralisation. Furthermore it has potential to direct drilling programs in zones that require additional sample information, for example, the Footwall zone to the east.

Pit Optimisations and Data Processing

For each simulated orebody model, an ultimate pit shell, or maximum cash flow pit, was derived using the Lerch-Grossman algorithm (Lerchs and Grossmann 1965). The algorithm essentially begins at the model surface and 'mines down' into the model making two basic decisions for each block:

1. Should the block be mined?
2. Does the material go to the treatment plant or the waste dump?

These two decisions are essentially based on the revenue generated by the block at a defined gold price, which is offset against the cost of mining the block and the cost of processing the material. Although valued individually, the decision to mine a block or not is determined by considering the surrounding blocks in conjunction with the block in question. For example, mining a high grade block below waste blocks may in fact pay for the cost of mining the waste blocks and still generate a profit. The ultimate pit is thus generated from all the blocks that the optimiser decides to mine. The pit optimisation parameters were used to optimise the simulation realisations (Tables 5 and 6).

The 50 NPV results for the various realisation ultimate pits were plotted with the NPV for the recoverable resource model (Fig. 9). From Fig. 9 it is evident that the NPVs for all the simulation realisations are greater than the NPV for the recoverable resource model and that most of them are significantly greater. This indicates that significant upside potential exists for the Deep Sulfide Project. Although this is indicative of upside potential, it would be more useful to take this information a step further and calculate probability or risk pits from the individual realisation pits.

Calculation of Probability/Risk Pits

The probability of mining each block was determined from the number of times it was mined in each of the 50 ultimate pits. Each block was then flagged in the simulation model, based on its probability of being mined, and risk pit shells were generated at five per cent probability intervals from five per cent to 95% (Figs. 10 and 11).

Table 5 Pit optimisation parameters

Gold price	$475	(6% royalty + 1% management fee)		
Selling cost	7%			
Annual throughput	5.2 Mt			
Rock type	Mining	Processing		
	Mining unit cost	Mining CAF	Processing unit cost	Recovery
	US$/t		US$/t	
Laterite (ox)	1.70	1.02	17.05	0.93
Saprolite oxide—soft	1.67	1.00	16.30	0.93
Siliceous oxide—hard	1.58	0.94	22.67	0.93
Saprolite sulfide—soft	1.50	0.90	21.01	0.8
Hard sulfides—hard	1.32	0.79	20.29	0.8
Intermediate oxide	1.59	0.95	17.05	0.93
Intermediate sulfide	1.59	0.95	21.76	0.8
Mixed oxide	1.59	0.95	22.67	0.93
Mixed sulfide	1.59	0.95	21.52	0.75
	$/tonne/bench (10 m)	Applicable to 160 level		
Adjustments	0.0159			

Table 6 Slope parameters for the pit optimisation

North/south division	Slope angle	Domain	Slope
0 to 180	35	1	East oxides
180 to 359	40	1	West oxides
0 to 180	52	2	East sulfides
180 to 359	48	2	West sulfides

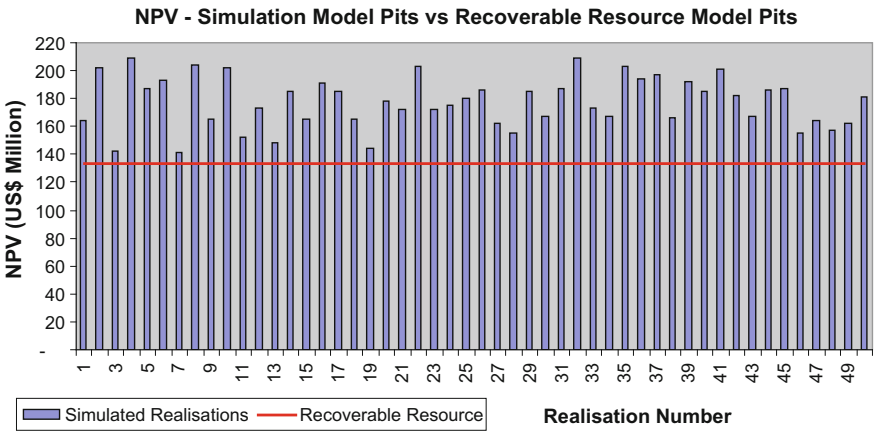

Fig. 9 NPV for simulation realisations and recoverable resource model

The $475/oz prefeasibility pit shell is shown as a white line in Figs. 10 and 11. It is evident in both figures that the prefeasibility pit does not fetch a significant amount of high probability/low risk material, and that in the east (Fig. 10), it mines low probability/high risk Footwall material. The Footwall is known to be under-drilled and is the target for the Phase 8 Deep Sulfide drilling program.

Generation of Grade Tonnage Curves

For each of the 50 realisations, and the recoverable resource (SMU) model, grade tonnage curves were generated for the P05, P50, P80, P95, and prefeasibility probability pit shells. Less variability than expected was achieved in each of the grade tonnage curves:

- *P05*: At the approximate economic cut-off grade of 2.0 g/t, the SMU model grade was 3.70 g/t, while the simulated realisation grades varied between 3.65 g/t and 3.87 g/t. The realisations indicated significant upside potential for both grade and tonnage above cut-off.
- *P50*: At 2.0 g/t cut-off, the SMU grade of 3.76 g/t falls in the middle of the realisation grade distribution (3.65 g/t to 3.93 g/t), though the tonnes above cut-off show significant upside potential.

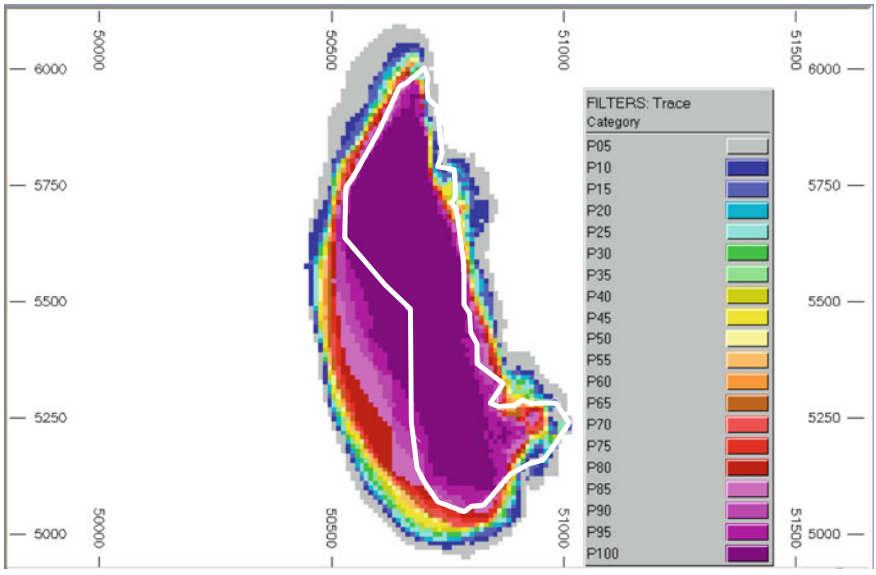

Fig. 10 Plan view (elevation −90 m) showing the probability of mining

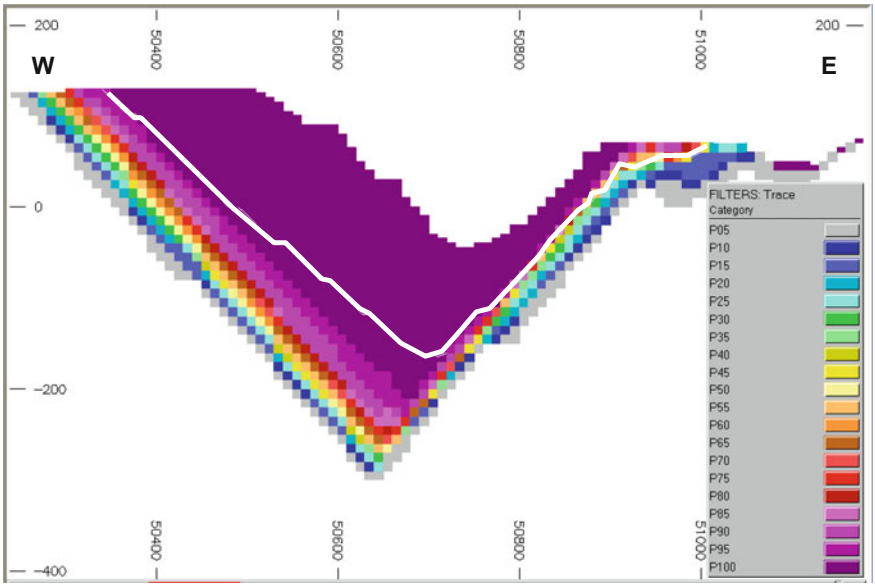

Fig. 11 Section EW-5550 showing probability of mining

- *P80*: The grade tonnage curve is similar to that of P50 at 2.0 g/t cut-off, with the SMU grade of 3.79 g/t falling in the middle of the realisation grade distribution of 3.67 g/t to 3.93 g/t. Upside tonnage potential is indicated above cut-off.
- *P95*: Similarly indicates significant upside potential to the tonnage above 2.0 g/t, with the SMU grade of 3.83 g/t midway between the realisation grade limits of 3.74 g/t and 4.0 g/t.

Except for P05—for which the average grade above 2.0 g/t cut-off is marginally low—the above probability pit shells indicate that the SMU grade has been estimated with reasonable accuracy, even though within all the shells, the tonnes above cut-off have been understated in the SMU model. The tonnage and grade results are not too dissimilar despite the different techniques. Within the prefeasibility pit shell, a comparison of the simulation and SMU model grade tonnage curves indicates that at 2.0 g/t cut-off, both the SMU grade and tonnage curves lay within the range of the realisation distribution. This is illustrated in Fig. 12, where the tonnage curve has been re-scaled to a maximum of 70 million tonnes. Although one may argue that the SMU model is marginally too selective, Fig. 12 indicates that this selectivity is acceptable. Above 2.0 g/t cut-off grade, the average grade above cut-off for the SMU model is 3.82 g/t, while the realisation grade ranges from 3.75 g/t to 3.99 g/t. At the same cut-off grade, the SMU tonnage of 19.5 Mt falls within the realisation distribution range of 19.0–21.0 Mt.

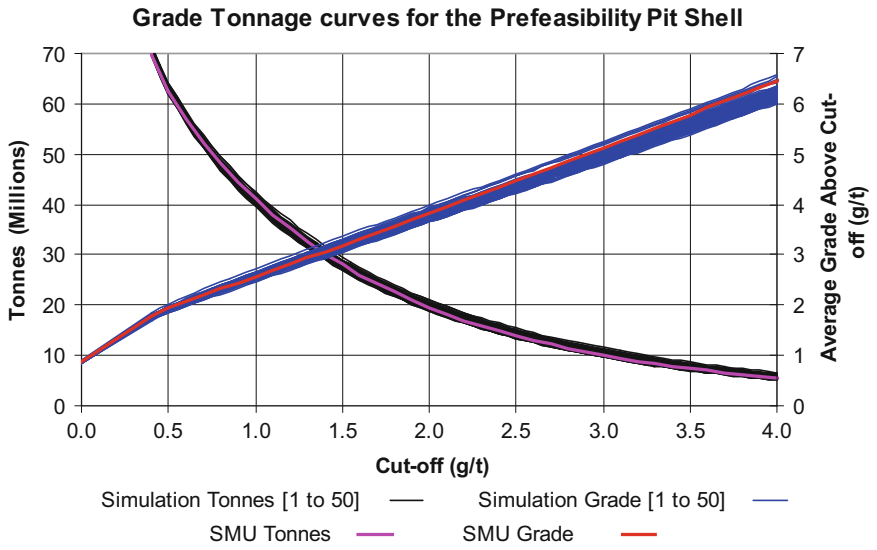

Fig. 12 Grade tonnage curves within the prefeasibility pit shell

Valuation of the Pit Shells

A pit value was calculated for each of the probability pits (P05 to P95 at 0.5 intervals) using the recoverable resource model. Since the extraction of the resource within these shells was not scheduled, it was not possible to calculate an NPV for each pit, but an open pit value was obtained for each scenario, based on the cost of mining ore and waste, the cost of treating the different material types, and the revenue generated at a gold price of $475/oz. The 2006 grade control cut-off grades were used to define ore and waste material for the various rock types (Table 7), with material above the cut-off categorised as ore.

The cut-off grades correspond with 'break-even' marginal grade material. The various parameters of recovery, cost, and revenue that were used in the pit valuation calculations are presented in Table 8. The cost values are those calculated by the Sadiola long-term mine planner in February 2006. The rehabilitation (rehab) costs had been included in the variable process costs and were therefore set to zero.

The calculated open pit values using the recoverable resource model for each of the probability pits (P05 to P95 at 0.5 intervals) are presented below in Fig. 13. As expected, an inverse relationship exists between the pit value and stripping ratio with increasing mining volume. There is an interesting kink in both curves for probability pit P80, which leads to its inclusion in further pit value analyses. These additional analyses involved comparing the values for each of the simulation model realisations with the SMU model value within selected probability pits. Open pit values were calculated for selected probability/risk pits (P05, P50, P80, P95) and the $475/oz prefeasibility pit using all 50 simulated realisations and the recoverable

Table 7 Ore/waste cut-off grades

Rock type	Cut-off (g/t)	Rock type	Cut-off (g/t)
Laterite	1.10	Hard sulfide	1.90
Saprolite	1.00	Intermediate oxide	1.10
Siliceous oxide	1.50	Intermediate sulfide	1.60
Saprolite sulfide	1.60		

Table 8 Cost parameters applied during pit valuation

Item	Material type	Value
Mine call factor		100%
Recovery saprolite oxide		93%
Recovery saprolite sulfide		80%
Recovery hard sulfide		80%
Fixed mining ($/tonne treated)		2.40
Fixed process costs ($/tonne)		1.07
Variable process costs ($/tonne)	Laterite (oxide)	9.84
	Saprolite oxide—soft	9.09
	Siliceous oxide—hard	15.46
	Saprolite sulfide—soft	13.80
	Hard sulfide—hard	15.58
	Intermediate oxide	9.84
	Intermediate sulfide	14.56
Admin costs ($/tonne)		3.59
Capital replacement ($/tonne)		0.46
Rehab costs ($/tonne)		0.00
Variable ore ($/tonne)	Laterite (oxide)	2.089
	Saprolite oxide—soft	2.058
	Siliceous oxide—hard	1.938
	Saprolite sulfide—soft	1.852
	Hard sulfide—hard	1.825
	Intermediate oxide	1.960
	Intermediate sulfide	1.960
Variable Waste ($/tonne)	Laterite (oxide)	2.083
	Saprolite oxide—soft	2.051
	Siliceous oxide—hard	1.933
	Saprolite sulfide—soft	1.846
	Hard sulfide—hard	1.820
	Intermediate oxide	1.954
	Intermediate sulfide	1.954
Gold price ($/oz)		475

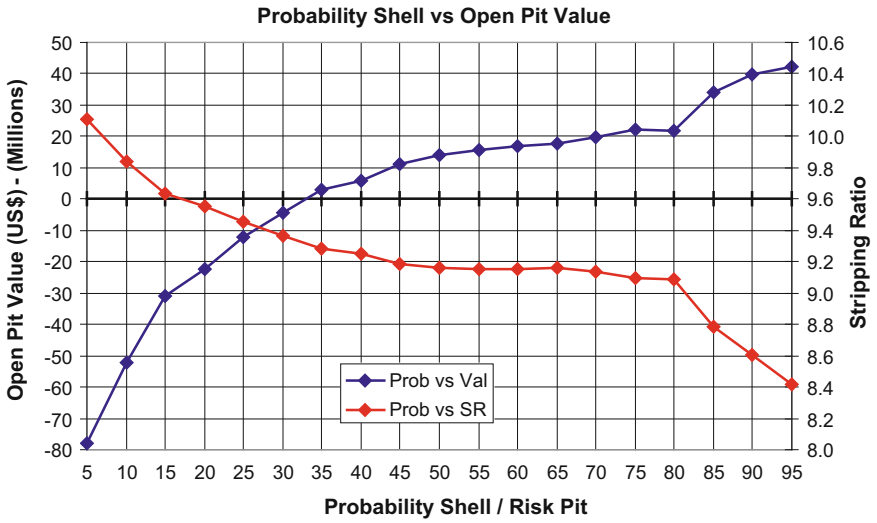

Fig. 13 Open pit values for the probability pits

resource (SMU) model. Table 9 summarises the pit value base statistics for the 50 realisations and SMU model per pit shell, and Fig. 14 illustrates the distribution of the realisation pit values.

From Fig. 14 and Table 9 it is evident that the $475/oz prefeasibility pit offers the greatest profit margin but not the least risk. Probability pit P95, not surprisingly, has the tightest distribution about the mean and would therefore offer the least risk to achieving the indicated profit. However, considering the respective mean profit values for the prefeasibility and P95 pits, the value offered by P95 is significantly lower than that of the prefeasibility pit. Given the relatively minor additional risk, the prefeasibility pit may be the preferred pit option. Figure 15 confirms that the prefeasibility pit is the optimal pit for the Deep Sulfide project, given the $475/oz gold price and cost parameters. The SMU model produces a profit of $112 million and falls in the middle of the distribution of the simulated realisations. The risk does exist that a profit of only $64 million may be realised, however a profit of $179 million is also possible, with the most likely profit ranging between $87 million and

Table 9 Base statistics for the realisation pit values per pit shell

Pit	SMU profit ($ million)	Mean profit ($ million)	Std dev ($ million)	Max profit ($ million)	Min profit ($ million)
P05	−78.010	−2.621	34.782	86.379	−67.288
P50	14.011	85.385	31.119	160.421	30.655
P80	21.745	82.204	24.921	139.124	37.691
P95	42.085	89.025	21.389	136.528	47.883
P-PF	112.889	108.036	24.400	179.400	60.870

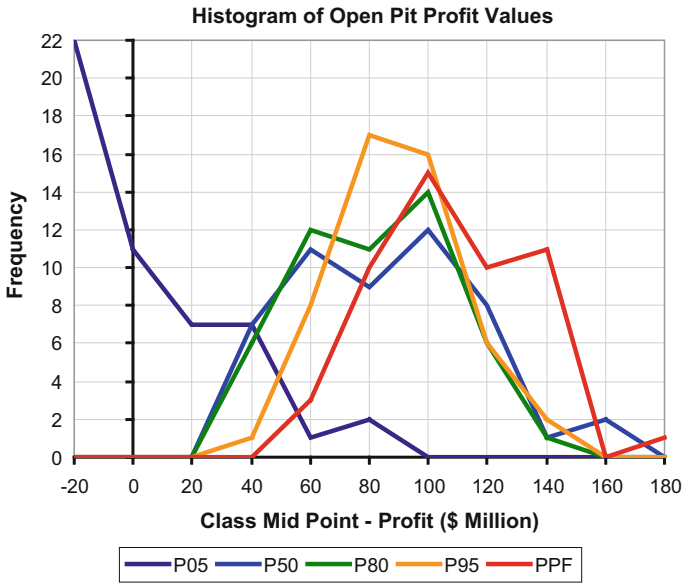

Fig. 14 Histogram of the open pit values for the 50 realisations

$148 million. It is evident from Fig. 15 that the profit curves flatten off significantly from the P50 to the P95 risk pit, and that there is no insignificant difference in their mean profit (Table 9). Though a marginal decision at a gold price of $475/oz, mining an equivalent of the P80 or P50 pits could dramatically improve the Deep Sulfide reserve ounces, and the P50 pit would most probably become a real option should the gold price increase significantly.

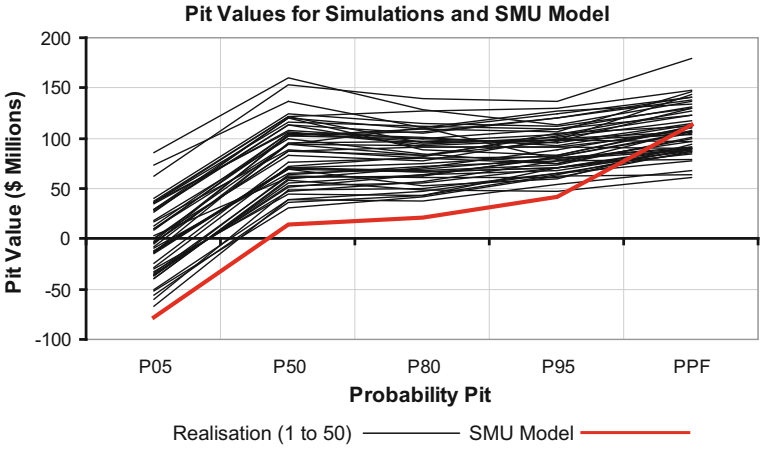

Fig. 15 Pit value per probability pit for the simulation and SMU models

Conclusion

The final risk pits generated from the simulation model indicated that the prefeasibility pit is generally conservative, corresponding with the 100 per cent probability shell. There is however a certain amount of risk involved with mining the Footwall mineralisation, where the prefeasibility pit digs on high-risk/low-probability material. This is confirmed by the COV values in this zone, which indicate high uncertainty in the grade estimate. Based on these results, an infill drilling program has been planned to mitigate this risk. At the current economic cut-off grade of 2.0 g/t, grade tonnage curves generated for selected risk pits have shown that although upside tonnage potential exists for the Deep Sulfide Project, the recoverable resource (SMU) model grade estimate is reliable. With the current cost information, and a gold price of $475/oz, the prefeasibility pit is optimal. The calculation of economic pit values for the realisations within the same selected risk pits indicated that the P50 to P95 pits and the prefeasibility pit are not significantly different. Therefore, there is potential to add reserve ounces to the project without significantly decreasing its value. An increase in gold price, or a decrease in operating costs, would make this additional material available to the project. At a gold price of $475/oz, and with current cost parameters, the prefeasibility pit shows maximum value for the project with no significant additional risk.

This study has highlighted the potential to use the COV values as a reliable classification method. It is recommended that the classification is re-run using the simulation COV information, as proposed by Dohm (2005). This exercise would eliminate unnecessary drilling and potentially save drilling costs. The gold price used for this project was $475/oz (the recommended Anglogold Ashanti resource reporting gold price for 2005). Anglogold Ashanti has since increased their resource reporting gold price to $1000/oz, and at $720/oz, their reserve reporting gold price is significantly greater than the gold price used for this project. Since the current gold price provides significant upside potential for the Deep Sulfide Project, it is recommended that the pit shell work is rerun using a suggested gold price of $700/oz and the latest mining and processing costs derived from the prefeasibility project.

References

Benndorf J, Dimitrakopoulos R (2007) New efficient methods for conditional simulation of large orebodies. In: Dimitrakopoulos R (ed) Orebody modelling and strategic mine planning, 2nd edn, The Australasian Institute of Mining and Metallurgy, Melbourne, pp 103–110

Boucher A, Dimitrakopoulos R (2009) Block-support simulation of multiple correlated variables. Math Geosci 41(2):215–237

Dimitrakopoulos R, Farelly CT, Godoy M (2002) Moving forward from traditional optimisation: grade uncertainty and risk effects in open-pit design. Trans Inst Min Metall Min Technol 111: A82–A88

Dohm C (2005) Mineral resource classification from innocence to excellence and beyond, presentation made to the Anglo American mine geology conference 2005, MinRED, 24 p
Godoy M (2003) The effective management of geological risk in long-term production scheduling of open pit mines, Ph.D. thesis (unpublished), University of Queensland, Brisbane
Goovaerts P (1997) Geostatistics for natural resources evaluation, pp 370–382. Oxford University Press, New York
Lerchs H, Grossmann L (1965) Optimum design of open-pit mines, Trans CIM, LXVII:17–24
Peattie R (2005) DBSIM—direct block simulation algorithm user's manual (Draft 1), unpublished document. AngloGold Ashanti, South Africa, p 18
Robins SP, Nicholls CE, Fouche F, De Hert G (2005) Sadiola—Identified Mineral Resource Statement 2005—Part Two A—Sadiola Main Pit and Hard Sulfides, unpublished company report. SEMOS, SA, Mali, pp 38–39
Van der Westhuizen R (2005) Sadiola reserve report December 2005, unpublished company report. SEMOS, SA, Mali

Applicability of Categorical Simulation Methods for Assessment of Mine Plan Risk

A. Jewbali, R. Perry, L. Allen and R. Inglis

Abstract The use of conditional simulation to characterize mine plan uncertainty is gaining more use for assessment of risk in mining projects. While the development of grade uncertainty profiles is relatively straightforward and can be validated using standard geostatistical techniques, the addition of geological uncertainty to evaluate total risk remains problematic. Some of the problems associated with geological uncertainty methods include the clustering of data in favourable geologic units, difficulty in training image definition, and the inability to address change of support issues for categorical variables. Despite these obstacles the importance of geological uncertainty as a contributor to total uncertainty has prompted Newmont to explore and evaluate the use of various techniques (and combinations of techniques) on different deposit types. Two orogenic deposits of different geological complexity were selected for the study: Subika, a shear zone hosted deposit and Merian, a deposit containing gold mineralisation associated with quartz vein zones and stockwork within which are found higher-grade quartz breccia zones. Newmont trialed various categorical simulation approaches to determine the applicability of these methods for each deposit type and the effect of parameter choice on the width of the uncertainty interval. Some of the techniques that were trialed include Multiple Point Statistics (MPS) methods, Sequential Indicator Simulation using local probabilities (SIS-lvm) as well as variations of these methodologies. Goals of this study included: (1) an understanding of which techniques may work best in which deposit types, (2) an understanding of the intricacies of each method, (3) and

A. Jewbali (✉) · R. Perry · L. Allen · R. Inglis
MAusMM, Newmont Mining Corporation, 6363 S. Fiddlers Green Circle, Greenwood Village, CO 80111, USA
e-mail: arja.jewbali@newmont.com

R. Perry
e-mail: robert.perry@newmont.com

L. Allen
e-mail: lawrence.allen@newmont.com

R. Inglis
e-mail: richard.inglis@newmont.com

R. Dimitrakopoulos (ed.), *Advances in Applied Strategic Mine Planning*,
https://doi.org/10.1007/978-3-319-69320-0_30

an understanding of the effect each method used has on total uncertainty analysis. This paper presents a comparison of the various techniques and makes recommendations for their use in uncertainty analysis.

Introduction

The use of conditional simulation to characterize mine plan uncertainty is gaining popularity for assessment of risk in mining projects. While the development of grade uncertainty profiles is relatively straightforward and can be validated using standard geostatistical techniques, the addition of geological uncertainty to evaluate total risk remains problematic. In general there is a lack of understanding of how the different simulation methods affect the uncertainty profile. How geological uncertainty is modeled also depends on the amount of geological knowledge available. If very little is known about the deposit, modeling geological uncertainty should include modeling the deposit with different geological concepts that all honor the available drillhole data. For projects with good geological knowledge and a large amount of data, modeling geological uncertainty considers uncertainty of contacts between, and proportions of, the different geological units. This paper deals primarily with the second case. Some of the problems associated with modeling geological uncertainty for ore deposits are:

- **The nature of the data collection process.** Mining companies tend to collect more information in mineralised geological domains. It is not uncommon for non-mineralised geological domains to have no or very limited data. Data in mineralised geological domains are usually clustered. While declustering techniques can be used to derive declustered proportions of the different geological units, this only addresses part of the problem as declustering is not applicable if no data has been collected.
- **Requirement of a training image for use of multiple point methods**. A training image is necessary to derive multiple point statistics. Developing training images for a class of ore deposits is difficult because most ore deposits tend to have unique characteristics and the resource model is typically used as the training image. This is problematic because orebody models are seldom stationary and may not contain repetitive features.
- **Change of support issues.** Generally geological information collected from drillholes is on a different support compared to the resource model. Most methods treat these two sets of information as if they are on the same support.
- **The weighting given to the existing geological model**. Most geological simulation algorithms require the target proportions of the different geological units. These proportions are unknown but are usually derived from the existing geological model. Is this a reasonable assumption to make or should modeling geological uncertainty include modeling the uncertainty in target proportions as well?

This paper presents two case studies involving deposits of different geological complexity which were selected for modeling of geological uncertainty: Subika, a shear zone hosted orogenic deposit and Merian, containing gold mineralisation associated with quartz vein zones and stockwork within which are found higher-grade quartz breccia zones. Newmont trialed various categorical simulation techniques and variations of these techniques to determine the applicability of these methods for each deposit type and the effect of parameter choice of the width of the uncertainty interval. A description of the techniques trialed is provided below.

Methods

Sequential Indicator Simulation with Local Varying Mean (SIS-lvm)

To determine uncertainty related to the geological interpretation, a Sequential Indicator Simulation (SIS) approach was used. In SIS, each mutually exclusive rocktype (category) is expressed as an indicator variable. These indicators are simulated and for every location, a category is drawn according to the local conditional distribution function determined through simple kriging. Drawbacks of the SIS approach include the unstructured appearance of the simulations, the inability to impose structural control over the simulations and its inability to handle the non-stationary nature of rock type proportions. To partially account for these drawbacks, a deterministic categorical variable model (usually the resource model) is filtered to calculate local varying probabilities near the boundaries of the different categories i.e. the contacts are uncertain (Deutsch 2006). The size of the filter determines the width of the uncertainty region adjacent to the contact. Next, simple kriging is used to derive the local conditional distribution.

$$I^*_{LVM}(u;\ k) - p_k(u) = \sum_{\alpha=1}^{n} \mu^{sk}_{\alpha}(u_{\alpha};\ k)[i(u_{\alpha};\ k) - p_k(u_{\alpha})]$$

where,

$I^*_{LVM}(u;k)$	is the simple kriged estimate at location u for category k.
$p_k(u)$	is the probability of category k at location u.
$\mu^{sk}_{\alpha}(u_{\alpha};k)$	are the simple kriging weights for data at location u_{α} for category k.
$i(u_{\alpha};k)$	are the indicators for category k at data location u_{α}.
$p_k(u_{\alpha})$	are the local probabilities for category k at location u_{α}.

The estimates for each category are performed independently which can lead to order relations deviations. Due to the noisy nature of the simulations a post-processing step is usually applied to clean the simulations up (Deutsch 2006).

CatSim

CatSim (Hardtke 2014) is a variation on the SIS method that incorporates the use of a preferred orientation of continuity between different data values. During simulation a weight is assigned to every existing data point (both original and simulated) within the search area. The weight is very large when the point is on the preferred orientation and decreases to a value of 1.0 when it is normal to that direction. The user specifies a maximum number of points to be used for simulation so the points with the largest total weight (weight divided by distance) are selected. The final value for a node can be determined by either a random draw or a simple weighted majority. There is no limit to the number of categorical values that are simulated. Orientation is assigned for every node and different areas of the deposit can be simulated using different preferred orientations. Depending on the degree of anisotropy, a weighting factor is applied as an exponent to the total weight.

The original drillhole data are moved to nodes on the grid and the method does not distinguish between original and simulated nodes. The simulations are typically better when searches are not very long and the maximum number of samples is small, as the method assumes that the most likely value for a node is the value of the nearest data point along the preferred orientation. The search distance appears to be more important when the random draw is used because if the search is too long, a value may be selected that does not occur in the local area around the node being simulated.

Multiple Point Simulation (MPS)

A shortcoming of SIS is that it fails to reproduce complex non-linear geological features as seen in mineral deposits. This is due to its reliance on the variogram, which can only characterize the linear relationship between data points. Multiple Point Simulation (MPS) (Strebelle 2002; Remy et al. 2009) is a technique which characterizes the relationship between points with higher order statistics. In doing so it is able to reproduce complex patterns and domain interactions (Strebelle 2002). MPS requires the use of a stationary Training Image (TI) to extract the higher order statistics at various scales. However storing and deriving the multiple point statistics from the training image requires additional RAM and CPU time. For this study SNESIM (Strebelle 2002) is used to generate multiple realizations of the different mineralised domains.

Self-Healing Sequential Indicator Simulation

In order to generate more realistic simulations of geology, Self-healing Sequential Indicator Simulation integrates the geological interpretation into SIS (Richmond and Godoy 2006). The approach allows for a local correction of the indicator

kriging estimate with the aid of a variable indicative of the confidence in the geological interpretation such as, for example, the kriging variance which is indicative of data density:

$$I(u;k)^c = (1 - \lambda(u))I(u;k) + \lambda(u)I(u;k)^g$$

where,

$I(u;k)$	is the indicator kriged estimate at location u for category k.
$\lambda(u)$	is the confidence in the geological interpretation at location u $(0 \leq (\lambda(u) \leq 1)$
$I(u;k)^g = 1$	is the geological interpretation at location u.

Leapfrog® Models

To further analyse uncertainty an indicator approach utilising Radial Basis Function (RBF) was used to produce a range of results. The inputs to the RBF interpolant are the categorical data in the form of a numerical indicator, the variogram and a structural trend which is similar to locally varying anisotropy. The approach allows for locally varying directions of continuity. Volumes were created at desired values to represent probability shells. Leapfrog® software was used for this approach.

The RBF interpolant is similar to the general expression of dual kriging (Stewart et al. 2014)

$$s(x) = \sum_i \omega_i \varphi(|x - x_i|) + \sum_k^K c_k q_k(x)$$

where,

x_i	are the data locations over which the interpolation is to be constrained.
ω_i	are RBF coefficients (weights).
$\varphi_k(x)$	is a spatial distance function (the RBF—from which the method takes its name).

The term on the right refers to the set of K drift functions $(q_k(x))$ each having a coefficient (c_k) applied globally across all data.

Case Studies

Two deposits were used to develop case studies for testing and evaluating the various geological uncertainty methodologies: (1) the Merian deposit in Suriname, and (2) the Subika deposit at Newmont's Ahafo mine in Ghana. While both

deposits are orogenic in genesis, each has different types of controls on mineralisation from which to assess uncertainty.

Merian

The Merian deposit lies within Lower Proterozoic aged rocks of the Guiana Shield in north-east Suriname, South America, approximately 100 km east of the capital Paramaribo (Fig. 1). In Suriname the Guiana Shield is composed of distinct, east west trending belts of low-grade metamorphic rocks which are separated by large areas of granitic rocks and gneisses. Gold mineralisation within the Merian deposit occurs as a vein type Proterozoic lode gold deposit; gold is found within and immediately adjacent to quartz veins, quartz stockworks and irregular quartz breccia bodies. Host rocks are composed of highly folded sandstones and siltstones. Gold mineralisation at Merian occurs over a strike length of approximately 3.5 km, elongate in a northwest-southeast direction and over a width of 200–600 m. Two distinct structural styles of mineralisation exist:

- Gold mineralisation associated with northwest striking, shallow to moderately northeast dipping sheeted and or tabular quartz vein zones and quartz stockworks.
- Gold mineralisation associated with higher angle, northeast dipping veins and irregular quartz breccia bodies.

Fig. 1 Location of the Merian deposit

The Merian geologic model was constructed using the following attributes collected from drill core logging:

- Stratigraphy, faults and folds
- Oxidation states (Saprolite, Fresh rock etc.)
- Quartz vein density
- Quartz breccia.

Simulation Methodology

Percent quartz vein content and quartz breccias have long been recognized to be a primary control on the geometry and grade of gold mineralisation. These were used to create a mineralised envelope for the Merian deposit. Figure 2 displays three cross-sections of the Merian mineral envelope as coded in the Merian resource model. It clearly illustrates the spatial continuity features of the the mineralisation. In tightly drilled areas the drillhole spacing is approximately 25 m across and 25 m along sections.

In order to assess the volumetric uncertainty of the mineralised envelope categorical simulations were generated using various methods:

1. 50 simulations using the CatSim approach. This approach only takes the conditioning data as input (and geological directions of continuity).
2. 50 multiple point simulations using Snesim, where the resource model in Fig. 2 was used as the training image (servo system factor of 0.5).

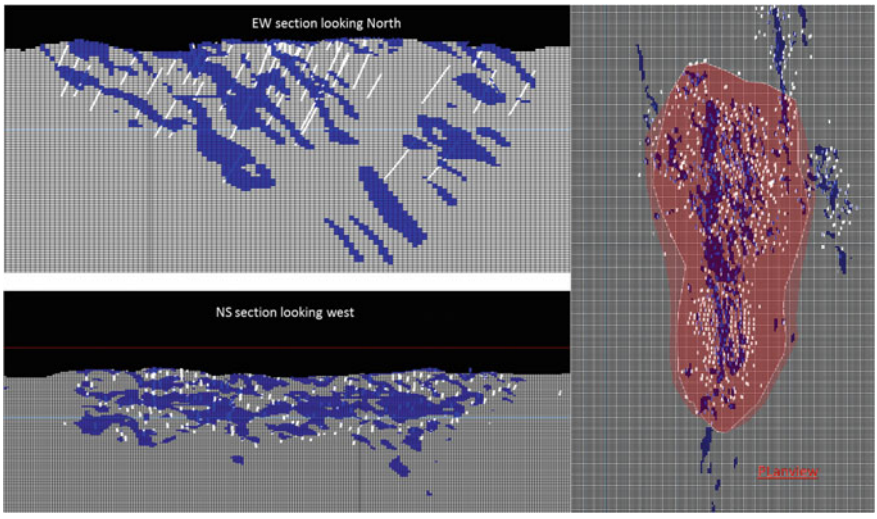

Fig. 2 Mineralised envelope for the Merian deposit with drillhole data. The area outlined in red is used for the study

3. 50 simulations using the self-healing SIS approach. Here the kriging variance (Fig. 3) was used as an indicator of the confidence in the geological interpretation.
4. 50 simulations using the SIS-lvm approach where local varying probabilities were calculated using the geological interpretation and moving window sizes of 12 × 12 m (0.5 times the tightest drillhole spacing), 25 × 25 m (the tightest drillhole spacing), 50 × 50 m (twice the tightest drillhole spacing) and 75 × 75 m (three times the tightest drillhole spacing) (Fig. 4). It is expected that larger filter distances will yield larger bands of uncertainty.
5. Leapfrog® models: in addition to the simulations three volumes were produced using RBF indicator probability shells. Volumes were analysed based on selecting volumes contoured from a range of interpolated values (P30 to P50), Indicator statistics were analysed to determine the Balanced Shell (P38) which is the volume that includes as many indicator data misclassified inside the shell as it excludes indicator data misclassified outside the shell and to determine the Russian Doll Shell (P30) where the next larger volume incrementally includes data where the indicator mean is less than the probability of the shell. In order to produce a range of results an arbitrary smaller volume was selected at P46 (Inglis 2013) (Fig. 5).

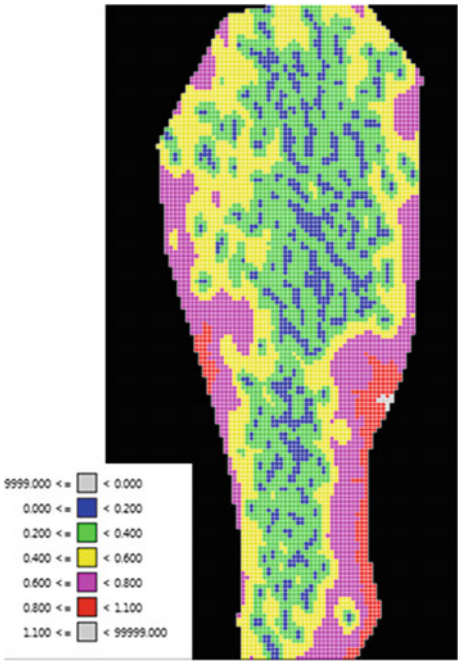

Fig. 3 Kriging variance as input into the SIS self-healing approach

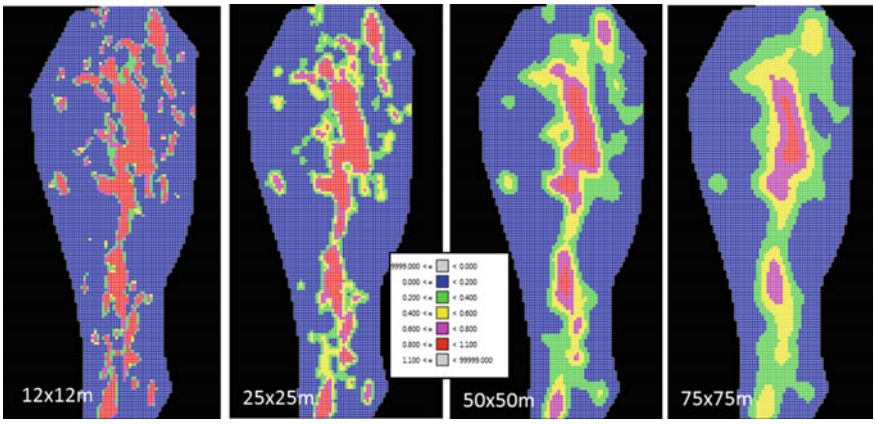

Fig. 4 Local varying probabilities to be inside the mineralised domain derived from the resource model

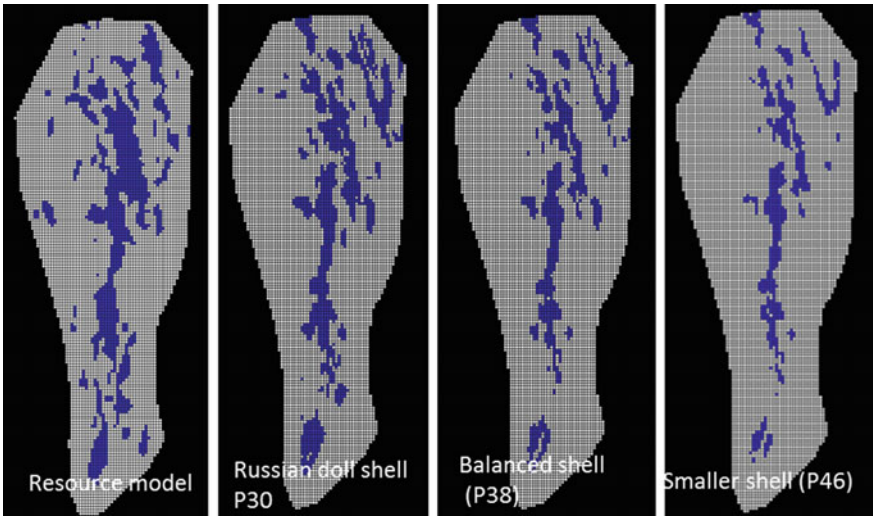

Fig. 5 Models build using Leapfrog®

Uncertainty in the Volume of the Mineralised Envelope

Views of the generated simulations for the various methods are shown in Figs. 6 and 7. Out of all the methods tested, only CatSim and Leapfrog® are based on conditioning data, they do not consider the existing resource model in any shape or form. Both the Sequential Indicator Simulation (SIS-lvm) based models and Snesim take the existing interpretation into account through local probabilities, proportions or the use of a training image. The figures show that the simulations generated by

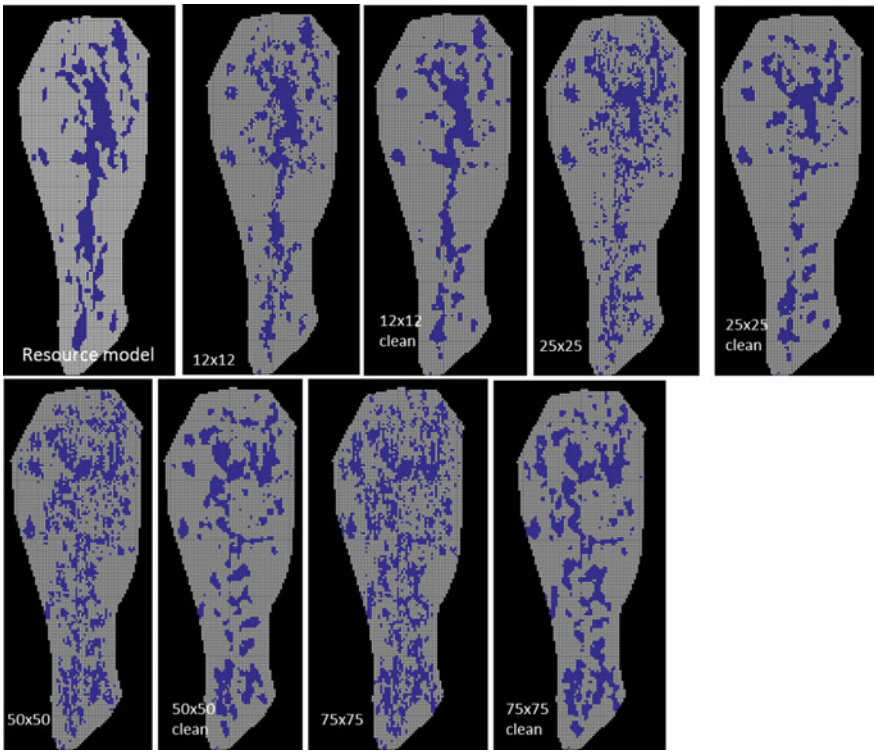

Fig. 6 Simulation results for SIS-lvm-plan view

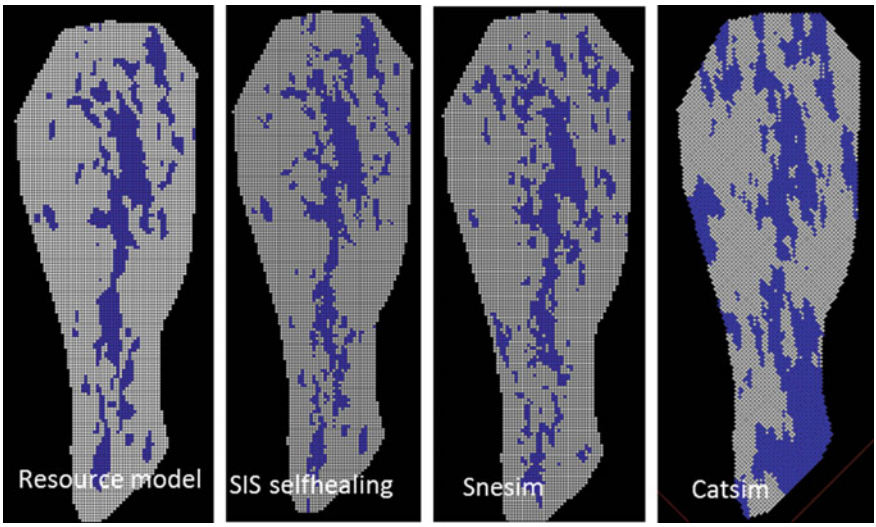

Fig. 7 Simulation results for SIS with self-healing, Snesim and CatSim-plan view

SIS-lvm are noisier compared to the model. This is especially so, when a large window is used to generate local probabilities. As shown in Fig. 4, this creates lower probabilities in areas where the probability to be inside the mineralised shape was previously high. This causes the simulations to have a dispersed appearance. After clean-up, the simulations for the 25 × 25, 50 × 50 and 75 × 75 still do not display the same level of continuity in the north-south direction seen in the resource model. The Snesim and SIS-lvm simulations look very similar compared to the resource models. The CatSim approach is based on the existing data and in areas of limited information; blowouts can occur (southern point).

Figure 8 displays the uncertainty profile for the mineralised volume. It shows the smallest, largest and average (over all 50 simulations) volume. Figure 9 shows the width of the uncertainty interval (difference between the smallest and largest volume). In general from these figures the following can be derived:

1. For most of the methods, the volumes fluctuate above or below the volume defined by the resource model. Only three methods (SIS-lvm 75 × 75 m with post-processing clean, Leapfrog® and self-healing SIS) contain the volume defined by the resource model in their uncertainty interval. Whether simulation volumes are above or below that defined by the resource model, appears entirely arbitrary and depends on the chosen parameters.
2. As expected, for the SIS-lvm, the wider the uncertainty window used to generate the local probabilities, the wider the uncertainty interval. The width of the uncertainty interval for SIS-lvm (75 × 75 m) is wider compared to that of SI-lvm (50 × 50 m). For this approach there appears to be a bias related to the size of the window used to create the local probabilities. For larger windows the simulations tend to generate more mineralised volume (that is also more dispersed).

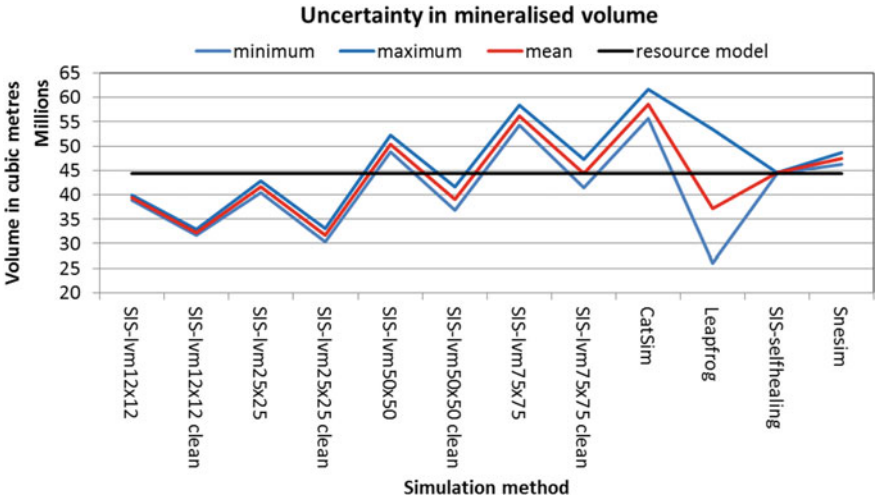

Fig. 8 Uncertainty profile for mineralised volume

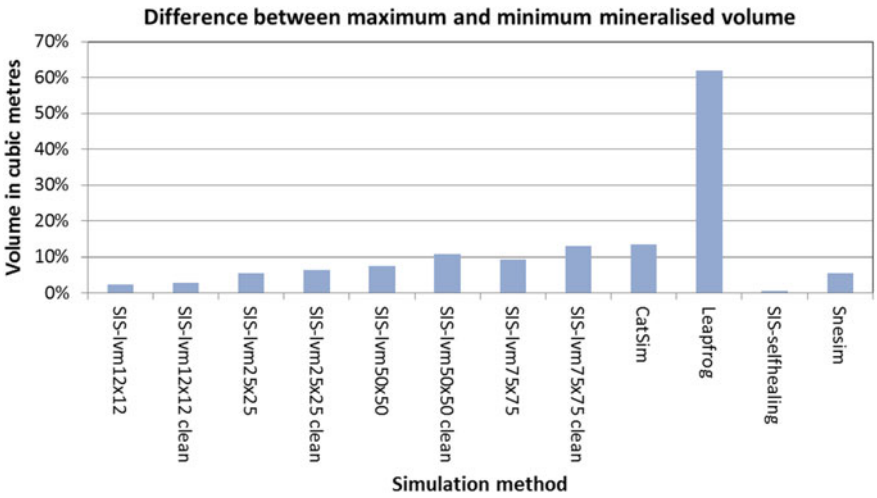

Fig. 9 Width of the uncertainty profile for mineralised volume

3. SIS with self-healing has the tightest uncertainty interval. Its uncertainty interval is approximately 25–30% of the smallest uncertainty interval for SIS-lvm 12 × 12 m.
4. For Snesim the width of the uncertainty interval is approximately similar to SIS-lvm 25 × 25 m.
5. The Leapfrog® approach delivers the widest uncertainty interval which none of the other methods are able to match.

In general at Newmont, the approach has been to combine the simulations of geology with simulations of grade to derive the uncertainty interval for tonnes of metal, tonnes of ore and average grade for annual/quarterly production volumes. If for example the SIS-lvm 12 × 12 m was chosen for the geological simulation, one would tend to think that the resource model was too optimistic. The opposite can be said for the use of SIS-lvm 50 × 50 m, i.e. the model is too pessimistic. If SIS with self-healing was chosen for the geology simulations, one would possibly conclude that the resource model is reasonable in terms of contained volume. Generation of these simulations of geology is non-trivial and the end results very much depend on the parameters and method chosen. It is therefore imperative that one understands the impact the choice of method and parameters will have on the uncertainty profile. Most of these methods (except for CatSim and Leapfrog®) are based on information derived from the existing resource model whether through probabilities, proportions or resource model as training image. By doing this there is an implicit assumption that there is some level of confidence in the resource model. For pre-feasibility or feasibility stage projects where there is a lot more data available this assumption might be justified, however for early stage projects with far less data, these methods might not be applicable.

Subika

The Subika deposit is the southernmost of the known Ahafo deposits (Fig. 10) and is hosted entirely within the granitoid package in the hanging wall of the Kenyase Thrust. High-grade gold mineralization is focused in a dilatant fracture zone, locally referred to as the Magic Fracture Zone (MFZ). This zone ranges from 1 to 60 m wide with a halo of lower grade mineralization extending out to 30 m. A number of higher grade ore shoots, which appear to be controlled by dilatant left lateral jogs in the MFZ are recognized and plunge steeply to the southeast.

Quartz-Sericite-Pyrite and Iron-Carbonate (QSP-Fe) is the dominant alteration associated with high grade mineralization. Alteration fluids appear to have accessed the MFZ via a network of shallow angle, brittle fractures within an overall steeply dipping shear zone. QSP alteration intensities are logged as 1, 2, or 3. The combined QSP 2/3 alteration forms the basis of the higher grade population, while QSP 1 alteration correlates well with a lower grade population. These two alteration categories have been used to define the geologic framework used in the resource estimates, and are the main focus of this study.

Simulation Methodology

Four methods were used for this case study, SIS-lvm, self-healing SIS, Snesim and Leapfrog®. All the methods except for Leapfrog® used the interpreted geologic model as input (Fig. 11), and attempted to reproduce the target input proportions. For these three methods, the simulated volumes fluctuated slightly above the volume of the geologic model, with the exception of one MPS case.

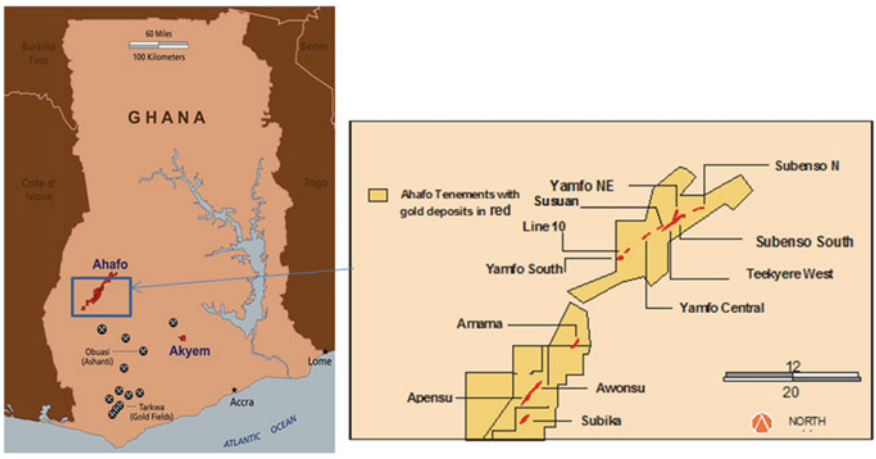

Fig. 10 Location of the Subika deposit

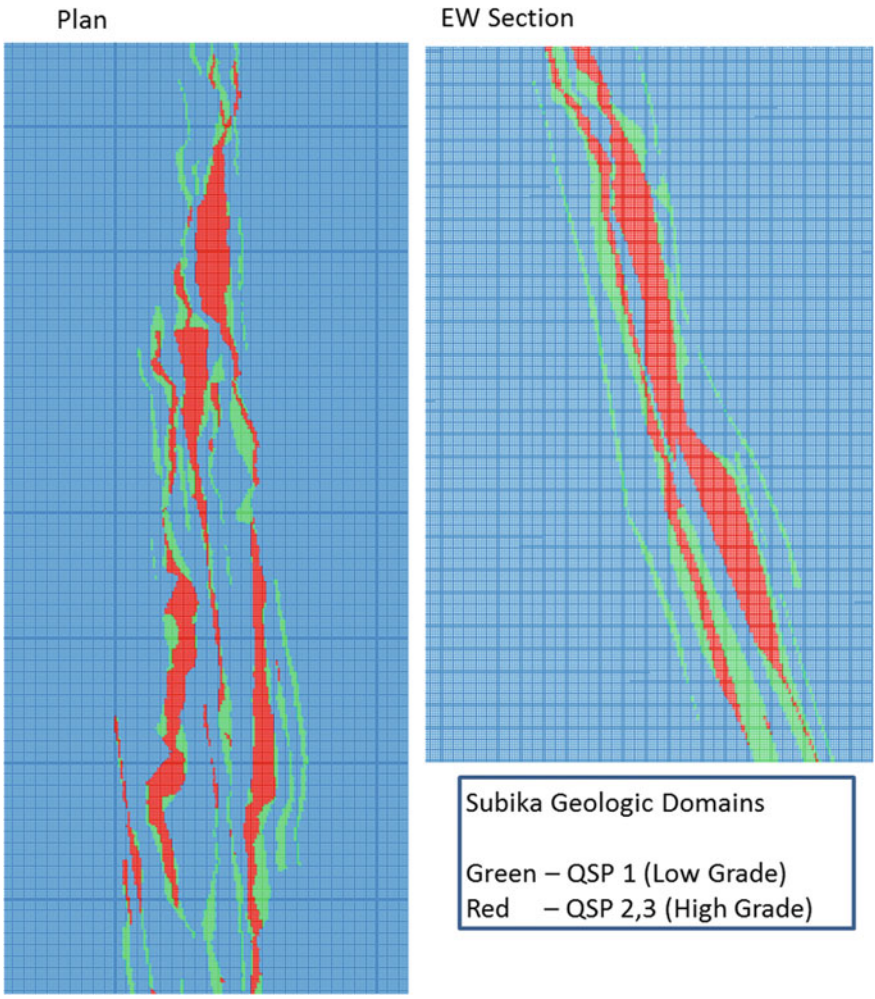

Fig. 11 Subika geologic framework

The SIS-lvm case was constructed using 2 × 2 × 2 m nodes and the window of influence applied to the lvm was based on the average drill spacing (approximately 35 m) within the simulated area (Fig. 12). This parameter being based on drill spacing allows block probabilities to be calculated within ranges equivalent to the spacing of hard information, and will result in bands of uncertainty around geologic features at a scale similar to the drill spacing. Large filter distances associated with wide spaced drilling will yield large bands of uncertainty around interpreted geologic features, while small filter distances associated with close spaced drilling will yield tight bands of uncertainty around the same features. This coincides with the idea that uncertainty should decrease as drilling density increases. In addition,

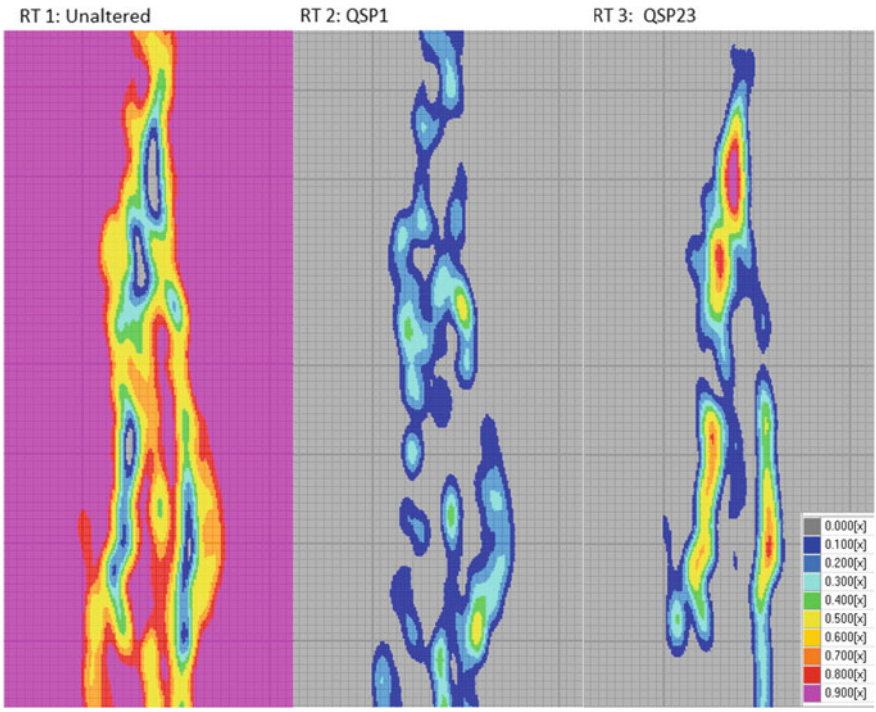

Fig. 12 Block probabilities for alteration type (unaltered, QSP2 and QSP23)

anisotropy derived from the variogram model was applied to the calculation of the lvm in order to preserve the preferred orientation of the structure and mineralisation. The resulting SIS with the lvm used as control is shown in Fig. 13.

The self-healing SIS case was constructed on the same 2 × 2 × 2 m grid and geologic interpretation as the above SIS-lvm case (Fig. 14). It has the tightest range of uncertainty of all the methods tested. The Leapfrog® model on the other hand delivers the widest range of uncertainty.

The MPS case was developed on 6 × 12 × 6 m blocks, using the interpreted geologic model as the training image (Fig. 15). Three different scenarios were developed, where the servosystem factor was modified in each run (0.1, 0.5 and 0.9). This parameter controls how Snesim reproduces the target input proportions from the TI. The higher the factor, the better the reproduction of the input target proportions. The selection of this value is somewhat subjective, and should be chosen with the quality of the geologic model in mind. There are other parameters that have an impact on the result, but they were not tested during this exercise.

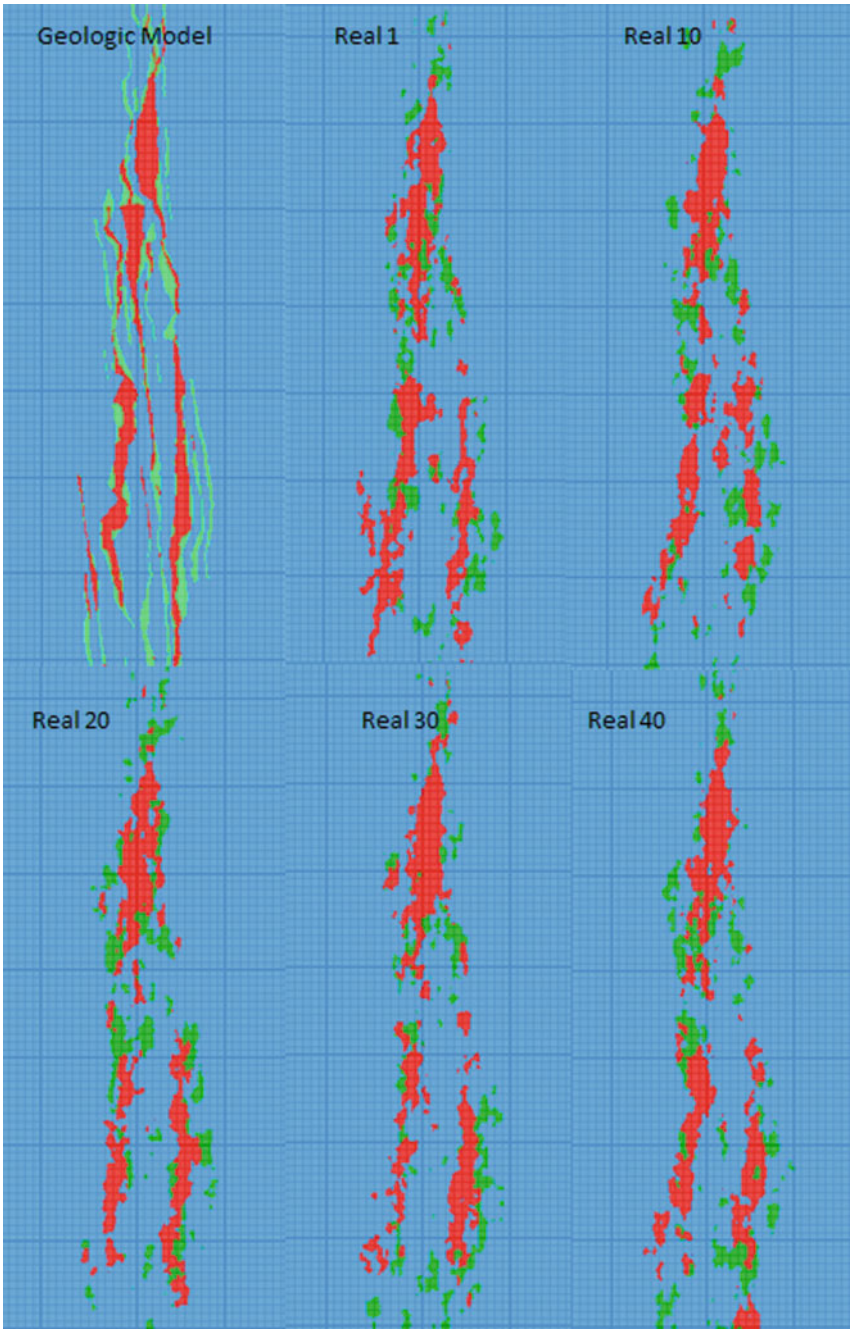

Fig. 13 Geologic model and BlockSIS results (Cleaning set to 1, Mild)

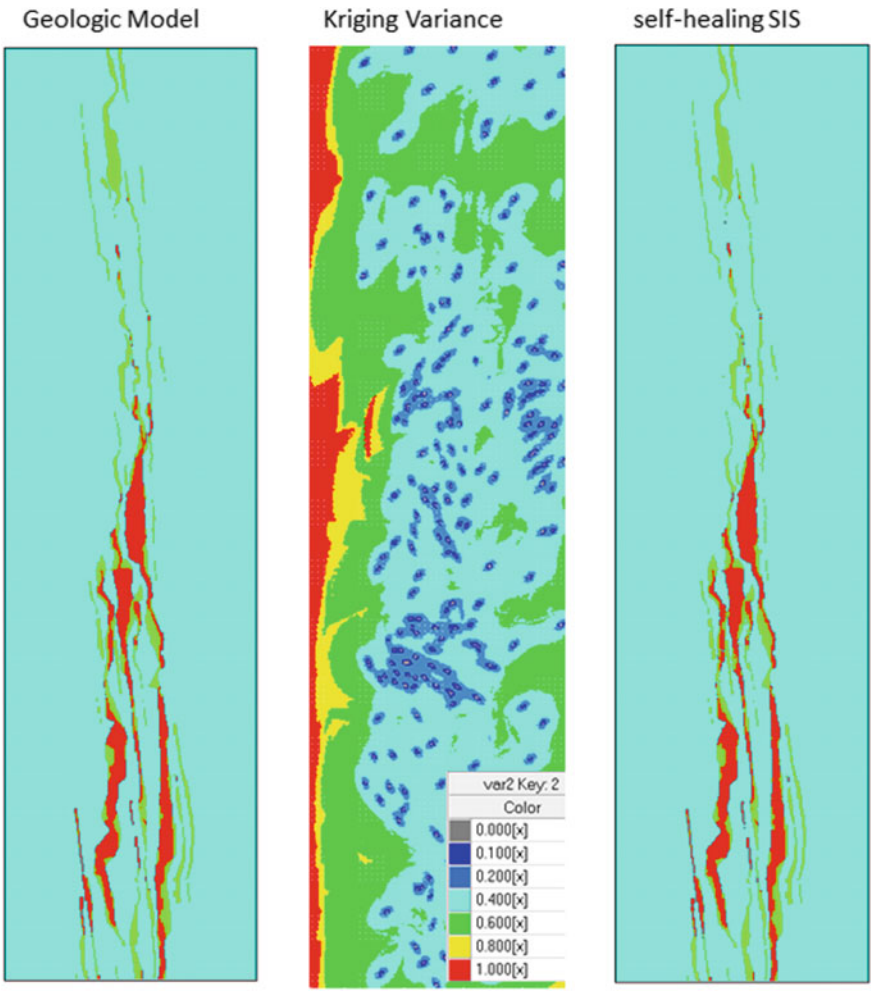

Fig. 14 Geologic model and self-healing SIS results

Uncertainty in the Volume of the Geologic Domains (QSP1/QSP23)

Using the results from the above techniques uncertainty around the modelled volumes within QSP1 and QSP23 were quantified. 50 realizations were generated using both techniques and the results were compared to the input volumes from the geologic model, as well as to each other.

The uncertainty profiles for QSP1 and QSP23 are shown in Figs. 16 and 17. Note that the SIS-lvm and MPS 0.5 show similar results, while MPS 0.1 results in a wider range of uncertainty and more volume than any of the other techniques. MPS 0.9 on the other hand has a much smaller range of uncertainty and appears to be biased low on volume. It is understandable that the range of uncertainty would

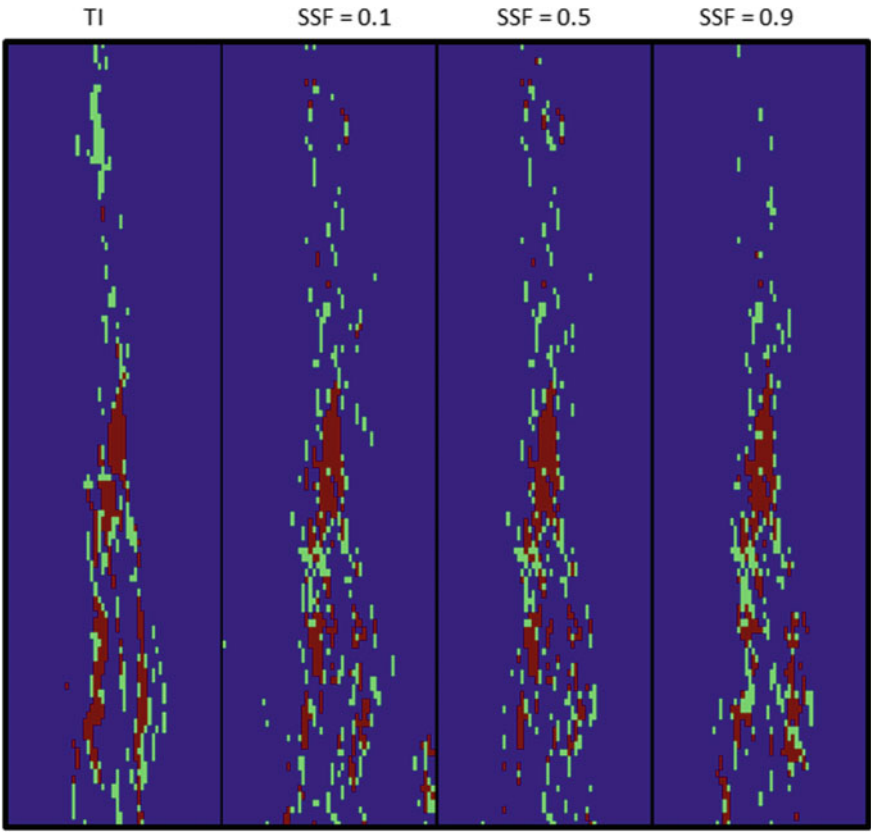

Fig. 15 Geologic model and Snesim (servosystem factors (SSF) = 0.1, 0.5 and 0.9)

diminish with an increasing servosystem factor, because we are more strictly enforcing reproduction of the input target proportions, but the reduction in volume is not so easily explained. The results from self-healing SIS indicate that there is very little uncertainty around the geologic interpretation. The controls for this technique need to be investigated further to determine the parameters that most influence the outcomes. Figures 18 and 19 illustrate the differences between the minimum and maximum volumes of each technique. This shows the variability of ranges of uncertainty depending on technique and parameter selection.

All the techniques yield promising results, and given that it is reasonable to put a fairly high level of confidence on the geologic interpretation, it seems acceptable to try to achieve ranges of uncertainty that fluctuate around the interpretation. In earlier stages of the Subika project this would not have been the case. Over time tonnages at Subika have shown large fluctuations caused by the wide spaced drilling and overall complexity of the geologic framework. With drill spacing at $\sim$35 m and a significant amount of thought and effort placed on the geologic interpretation, Newmont is to the point of applying these results to the risk associated with the mine plan.

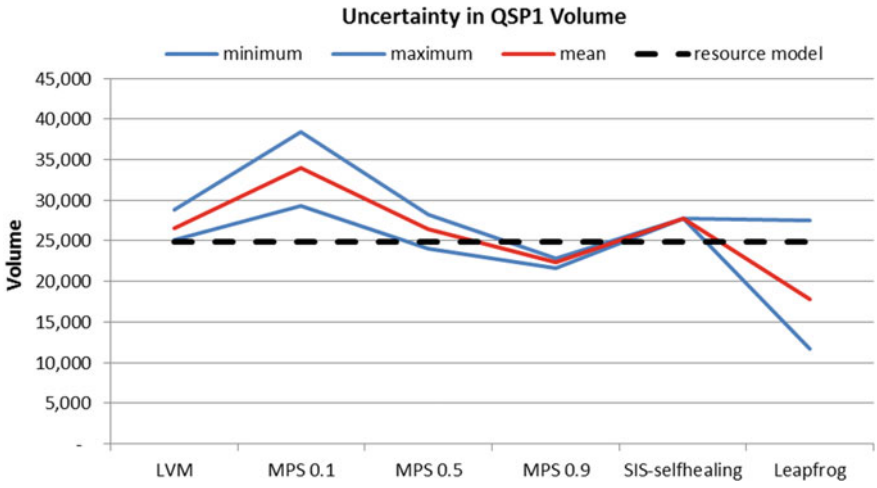

Fig. 16 Uncertainty profile for QSP1

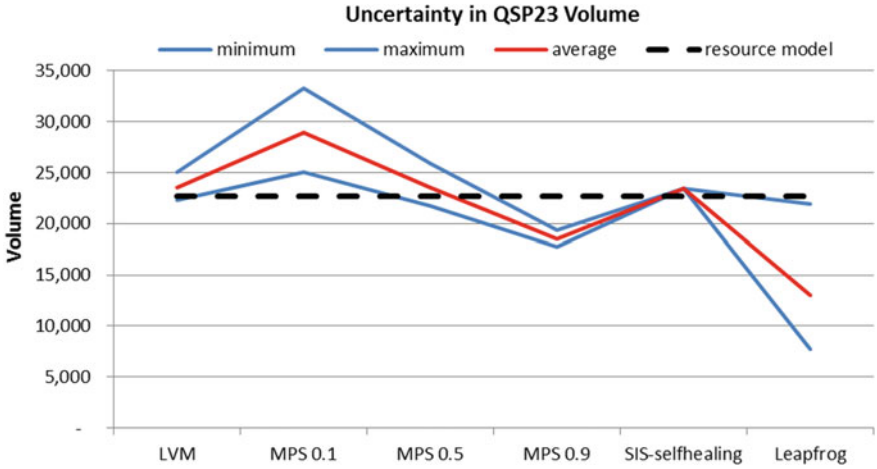

Fig. 17 Uncertainty profile for QSP23

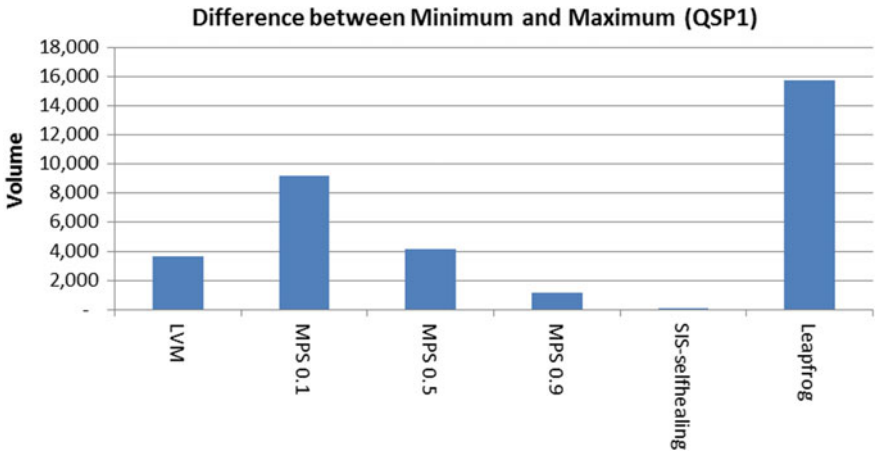

Fig. 18 Width of Uncertainty profile for QSP1

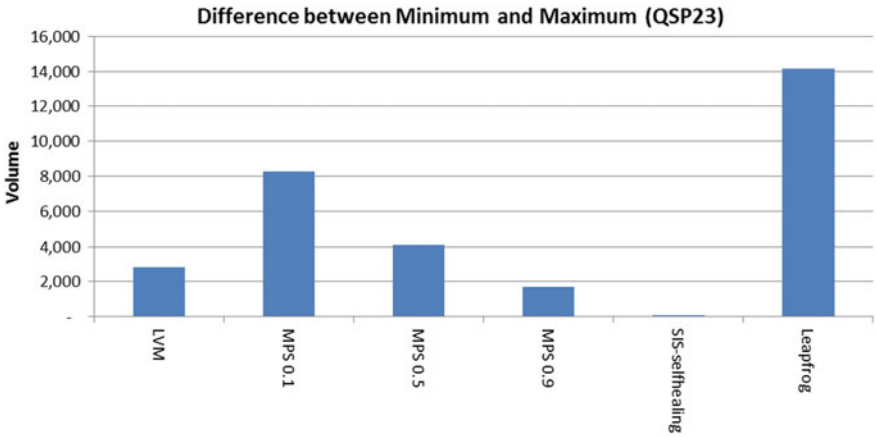

Fig. 19 Width of Uncertainty profile for QSP23

Conclusions

The two case studies have shown that simulating uncertainty in geological units is non-trivial, the width and center of the uncertainty profiles are very dependent on the method and the parameters selected. For the SIS-lvm approach, the size of the uncertainty window has an impact on the width of the uncertainty profile, with wider profiles resulting in wider uncertainty windows (not necessarily centred on the input resource model) and more dispersed simulations. For MPS the servo system factor also appears to control the width of the uncertainty interval with servo

system factors closer to one delivering narrower uncertainty intervals (not always centred on the target proportions). Out of all the methods, the SIS-self-healing approach delivers the narrowest uncertainty intervals with proportions centred on the input resource model. Most of the methods (except for CatSim and Leapfrog®) require the existing interpretation as input through local probabilities, proportions or the use of a training image.

Leapfrog appears to be a better tool at early stages because it allows for a more complete testing of different geological concepts with a wider band of uncertainty. In later stage projects where there is a fairly high level of confidence (due to the amount of data collected) on the geologic interpretation, other methods that achieve ranges of uncertainty around the interpretation likely provide a more realistic assessment of uncertainty. The case studies have also shown that in order to get ranges of uncertainty that fluctuate around the interpretation, the parameters for the various methods need to be selected carefully.

References

Deutsch C (2006) A sequential indicator simulation program for categorical variables with point and block data: BlockSIS. Comput Geosci 32:1669–1681

Inglis R (2013) How to select a grade domain—a gold mine case study in exploration, resource and mining geology conference, Cardiff, UK, Oct 21–22

Hardtke W (2014) CatSim description. Newmont internal memorandum

Richmond A, Godoy M (2006) Local self-healing: a method to incorporate geological interpretations into sequential indicator simulation. In: Ortiz J (ed) MININ 2006 2nd international conference on mining innovation. University of Chile, pp 349–355

Stewart M, de Lacey J, Hodkiewicz PF, Lane R (2014) Grade estimation from radial basis functions—how does it compare with conventional geostatisitcal estimation. In: ninth International Mining Geology Conference 2014. The Australian Institute of Mining and Metallurgy, pp 129–139

Strebelle S (2002) Conditional simulation of complex geological structures using multiple-point statistics. Math Geol 34:1–21

Remy N, Boucher A, Wu J (2009) Applied geostatistics with SGeMS: a user's guide, 263p. Cambridge University Press, Cambridge, UK

Part VI
Optimisation of Underground Mine Planning

Cut-off Grade Based Sublevel Stope Mine Optimisation

Introduction and Evaluation of an Optimisation Approach and Method for Grade Risk Quantification

M. T. Bootsma, C. Alford, J. Benndorf and M. W. N. Buxton

Abstract Research in the field of cut-off grade optimisation has shown a relationship between cut-off grade, project life and Net Present Value. Lane's theory demonstrates that cut-off grades can be optimised in order to maximise project profitability. Although the theory forms the basis for many open pit mining projects, application of the theory in underground mining remains limited to-date. The main reason for this is the complex interaction between all processes in underground mine planning which makes it difficult to apply Lane's mathematical optimisation approach. Recently a new Stope Optimiser product was released. The AMS Stope Optimiser automates the design of underground stopes at user defined cut-off grades and allows for rapid evaluation of mine designs at different cut-off grades. Using this software, an optimisation approach was developed and validated on an underground gold deposit in northern Sweden. Potential project NPV increased by approximately 30% when using this new approach. Spatial grade uncertainty in mineral resources was identified to be a major risk in underground stope design. The optimisation approach was further extended to account for grade risk using estimated and stochastic simulated resource models. The resulting optimisation process accounts for grade risk early in the design process and reduces the risk of a stope not meeting the cut-off grade with subsequent financial loss.

M. T. Bootsma (✉) · J. Benndorf · M. W. N. Buxton
TU Delft, Stevinweg 1, 2628 CN Delft, The Netherlands
e-mail: Bootsma.matthijs@gmail.com

J. Benndorf
e-mail: J.Benndorf@tudelft.nl

M. W. N. Buxton
e-mail: M.W.N.Buxton@tudelft.nl

C. Alford
Alford Mining Systems, Suite 5, 1153-1157 Burke Road,
Kew, VIC 3101, Australia
e-mail: Chris@alfordminingsystems.com

R. Dimitrakopoulos (ed.), *Advances in Applied Strategic Mine Planning*,
https://doi.org/10.1007/978-3-319-69320-0_31

Introduction

It has long been realised that mining simply every part of an orebody with a grade higher than 0 is not economical and will not lead to a successful mining operation. By selecting a cut-off grade it is decided what part of the orebody is economical to extract and what material is to be considered as waste. In its most basic form the cut-off grade is defined as a break-even grade which makes sure that each block of ore pays for its own mining, processing and refining costs resulting in zero gains and losses for a block of ore containing this grade (zero profit). It is the ambition of mining companies to maximise the Net Present Value (NPV) of mining projects. Simply using the break-even grade is in most cases not enough to accomplish this goal and hence time and effort should be spent to determine the optimum cut-off grade(s).

Lane (1988) described a relationship between cut-off grade, project life and Net Present Value. The theory demonstrates that a cut-off grade (often higher than the break-even grade) can be found that maximises Net Present Value. The work by Lane forms the basis for the optimisation of many open pit mining projects within the industry today but application of the theory in underground mine optimisation remains limited to research projects to-date (Poniewierski et al. 2003; Gu et al. 2010; Elkington et al. 2010). This is caused by the complexity of underground mining compared to open pit mining, which makes it more difficult to apply Lane's mathematical approach and to develop optimisation software.

This paper presents the findings of a nine-month research project (Bootsma 2013) carried out for Boliden Mineral AB, a Swedish mining company. The paper analyses Lane's theory and uses the theory to introduce a practical underground mine optimisation method for sublevel open stope mines using automated stope optimisation software. The method can be used to rapidly evaluate multiple project scenarios in order to determine the optimum project strategy that maximises the profitability of a mining project. Finally a method for risk-based stope design is introduced to expand the optimisation method.

Cut-off Grade and Net Present Value

Lane's methodology is based on maximising Net Present Value. The NPV takes into account the time value of money based on the principle that money today is worth more than the same amount of money tomorrow. The NPV presents the net difference of all future cash inflows and all cash outflows in present value terms.

In the mining industry, investments in new mining projects are often large before mining can actually start and the return on these investments takes place over long periods of time. This means that the future returns (cash inflow) on the capital investment of today (cash outflow) have to be discounted in order to calculate the profitability of the project.

The Net Present Value is the sum of the present value of all future cash flows and is defined as:

$$NPV = \sum_{n=0}^{N} \frac{F_n}{(1+i)^n}$$

in which;

N *Life of project*
F_n *Cash flow in period n*
i *Discount rate*

Lane developed the theory that a relationship exists between cut-off grade and NPV. According to the theory there is a cut-off grade (that may vary over the life of the mine) for which the Net Present Value is optimised. Lane's theory is clarified by the function defining F_n, the cash flow in period n.

The cash flow function for a period n is defined as:

$$F_n = M_n[(s-r)\cdot \bar{g}_n y - m - p - o]$$

in which;

M_n *Amount of material mined in period n* (*t*)
s *Selling price per unit of product* (*USD/unit*)
r *All smelting and Refining costs* (*USD/unit*)
$\bar{g}_n$ *Average grade of ore in period n* (*g/t*)
y *Yield or recovery* (%)
m *Mining Cost* (*USD/t*)
p *Processing Cost* (*USD/t*)
o *Overhead Cost* (*USD/t*)

By substituting the cash flow function F_n into the NPV equation, the NPV equation is rearranged into:

$$NPV = \sum_{n=0}^{N} \frac{M_n[(s-r)\cdot \overline{g}_n y - m - p - o]}{(1+i)^n}$$

Lane defined the average grade and size of the mineable reserve using the grade-tonnage curve of the deposit. The grade-tonnage curve provides the average grade and size of the mineable reserve based on a chosen cut-off grade. If the production rate is assumed constant (regardless of the chosen cut-off grade and resulting size of the reserve) then the life of mine (N in the NPV equation) is defined as:

$$N = \frac{Q_m}{M}$$

in which;

Q_m *size of the mineable reserve (t)*
M *Mine production rate (t/a)*

Lane showed that a combination of cut-off grade and life of mine exists for which the project NPV is maximised (Fig. 1).

However, in order to apply Lane's theory to underground mining operations much more complex algorithms are required. The main difficulty is the fact that the whole mine plan for an underground operation depends on the reserves (stope shapes) generated for a particular cut-off grade. Based on these stope shapes development designs and mine schedules are evaluated to determine the optimum mine plan for the particular cut-off grade. Because each mine plan only applies to a particular cut-off grade, separate mine plans have to be developed for each cut-off grade under consideration before the optimum can be determined.

It is because of the complex interaction between all processes in underground mine planning that cut-off grade optimisation to maximise project NPV has not progressed much since Lane introduced his theory. Many operations are designed based on a break-even grade which is defined as the minimum grade that a tonne of ore should have in order to pay for its own mining processing and refining (Rendu 2008). However, by using the break-even grade as the cut-off grade it is questionable whether the NPV is optimised (Alford and Hall 2009; Hall 2007; Hall and Steward 2004; Hall and de Vries 2003). Lane has shown that the optimal NPV is based on a combination of cut-off grade and the life-of-mine (as a function of production rate) due to the implementation of a discount rate. In other words, using the break-even grade as the cut-off grade is too simplistic and does not take into account the complex relationships involved in underground mining.

Based on the cut-off grade theory by Lane, a practical underground mine optimisation method was developed that allows for the rapid evaluation of mining project scenarios in order to find the optimum strategy that maximises project NPV. The proposed optimisation method considers the underground mining constraints that are not accounted for in Lane's equations and is expanded to allow for risk-based optimisation.

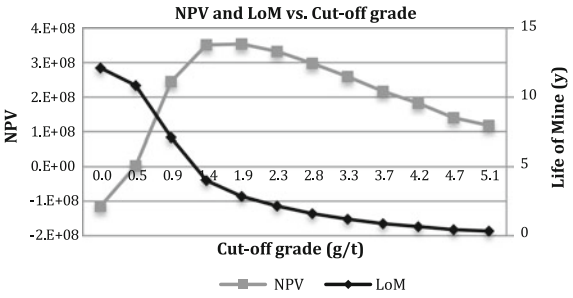

Fig. 1 NPV and LoM versus Cut-off grade

Underground Mine Optimisation—General Concept

The underground mine planning approach as shown in Fig. 2 (after Poniewierski et al. 2003) is centred around a mineral resource block model and forms the basis of the underground optimisation process.

The process starts with the application of a cut-off grade to the mineral resource model. Often the break-even grade is used here to define the economic part of the mineral resource. The chosen cut-off grade does not only separate ore and waste but also determines the geometry of the mineral reserve. Based on the obtained orebody shape, orientation and geology together with geotechnical conditions appropriate production areas (comprised of multiple stopes) are designed. A feasible mine design is created by connecting the production areas to the surface with basic access development (shafts, declines, level development, ore drives). The mine design is loaded into a scheduling package to produce a life-of-mine schedule for the operation. Feasible mining sequences, development and production rates are evaluated and the resulting production schedule is fed into a spread sheet based Cash Flow Model. The Cash Flow Model uses the production data to calculate all costs and revenues related to the mining operation on a monthly basis. It also includes all other costs (e.g. capital expenditures) related to the mining operation. The resulting cash flow can be discounted to obtain the project NPV for a selected cut-off grade and production schedule.

Underground mine optimisation can be described as repeating the mine planning process for a range of cut-off grades and production schedules in order to find the best mine strategy. In other words, the more scenarios are evaluated, the more likely it is that an optimum strategy is found. A helpful method to determine the optimum

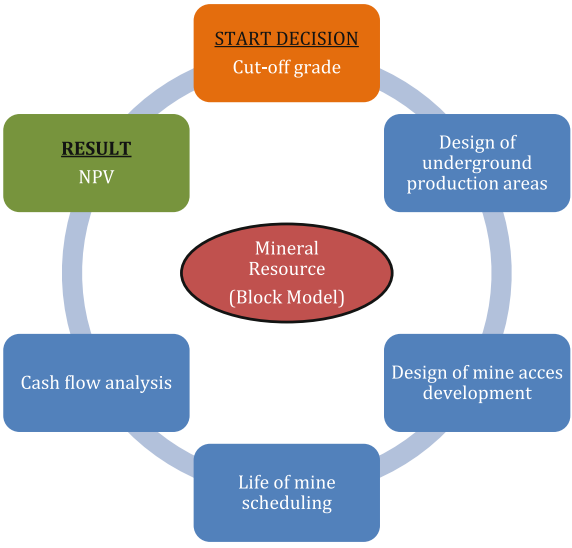

Fig. 2 A typical approach to underground mine planning

strategy is to plot all the evaluated scenarios in a Hill of Value graph (Fig. 3). The optimum strategy is found at the 'top of the hill'.

Due to a lack of automated optimisation tools, the underground mine optimisation process has been largely a manual and time-consuming process. Especially the design of underground stopes and associated development can take a significant amount of time when multiple cut-off grades are evaluated. As a result, underground mine optimisation has in many cases been carried out with inadequate data, potentially resulting in sub-optimal project performance and loss of potential profit.

Semi-automated Stope Optimisation

New techniques for stope optimisation have been advanced by Alford Mining Systems (AMS) through two industry funded research projects, AMIRA P884 "Planning and Rapid Integrated Mine Optimisation" (2007–2010) and AMIRA P1037 "Optimisation of Stope Design and Stope Layouts" (2011–2014). The software has been commercialised by three mining software supplier sponsors of these projects—CAE, Maptek and Deswik. While earlier work in 1995 led to the concept of the 'Floating Stope' heuristics, the newer techniques produce rapid, optimal and repeatable design shapes suitable for strategic and tactical mine planning.

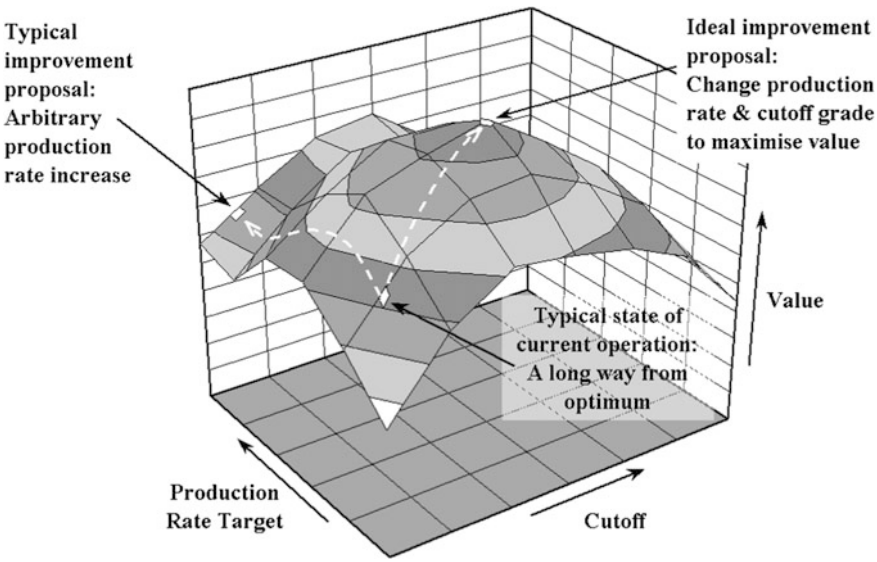

Fig. 3 Hill of value graph showing NPV as a function of cut-off grade and production rate (Alford and Hall 2009)

The AMS Stope Optimiser is a tool that assists in automating the design of underground stopes. It optimises both the location and shape of the stope to *maximise the total value or metal above a set cut-off* within the stope boundaries. The output of the automated stope design process is a set of wireframes that can be used for further mine design and scheduling. To control the optimisation process and to ensure that the stope designs are technically viable, factors that control the maximum allowable stope shape can be altered. These can be geotechnical stress field conditions, faults and fractures, orebody characteristics and/or production limitations (e.g. maximum production drill-hole lengths). The controlling factors together result in constraints to the maximum stope dimensions and orientation that are supplied to the optimisation software.

The stope optimisation process is block model driven and does not consider geological wireframes whilst designing stopes. The quality of the optimisation is therefore depending on the accuracy of the block model.

The approach taken in the stope optimisation process incorporates three stages; slice evaluation, seed generation and stope shape annealing.

During the slice evaluation stage, the mineralisation is sampled on a regular grid to identify the economic zone. Slices are placed within a regular optimisation framework (depicting a sublevel of stopes) and represent the smallest mining unit (the smallest volume that can be selectively mined). The optimisation algorithm will then progress through the resource model in a direction perpendicular to the optimisation framework whilst evaluation slices against the user supplied cut-off grade.

The seed generation algorithm finds the best combination of slices whilst respecting user-supplied constraints such as stope and pillar sizes, hanging and footwall dips and the maximum internal waste percentage. The resulting seed shape represents the approximate size and location of stopes that meet the both the cut-off and design constraints. An annealing algorithm then explores adjustments to the seed shapes to maximise the final value while continuing to satisfy the design constraints.

The stope optimisation is solely economic, generating optimal stopes shapes that would satisfy the cutoff grade, without immediate consideration for the mining practicality and technical feasibility for the inventory of stopes and the final stope layout required for access and sequencing.

Mineral Resource Models

Both estimated and simulated resource models can be used as an input to the AMS Stope Optimiser. The required techniques to create such models are well described in literature such as Goovaerts (1997). Both types of models and their differences are briefly introduced, as the resource model determines the stope optimisation method(s) that can be used.

Estimated Models

Estimated resource models are created by use of estimation algorithms such as Kriging. The Kriging algorithm minimises the error variance at each interpolated location and ensures local accuracy of the interpolated grades.

A side effect in Kriging estimation is the smoothing effect. Typically, low grades are overestimated whereas high grades are underestimated (David 1977, 1988). As a result of this effect, spatial variability is not properly reproduced and the estimated block model may not be the best representation of the grade distribution within the orebody.

Conditional Simulated Models

The smoothing effect as present in Kriging estimation algorithms does not occur when conditional simulation is used to model grades in a resource model. Whereas Kriging estimation aims to minimise the local error variance, conditional simulation reproduces available data, sample statistics and spatial variability (Goovaerts 1997). The model resulting from conditional simulation therefore guarantees global accuracy. By simulating multiple equi-probable realisations of the resource model global grade uncertainty can be quantified and used in the stope optimisation process.

Numerous conditional simulation algorithms are available of which sequential Gaussian simulation is often used to simulate resource models. The method requires a regular simulation grid and follows the following steps (after Goovaerts 1997):

Composited drill hole data is transformed into a Gaussian Random Field by means of normal score transformation and placed onto the simulation grid at the respective measured location. This assures that hard data is considered during simulation (conditional) and measured values are reproduced in the final simulated model. Next, a random path is defined visiting each node on the simulation grid exactly once. At the first node, Simple Kriging is used to estimate the local mean and variance. A conditional cumulative distribution function is created and the Monte Carlo algorithm draws a random value between 0 and 1 to determine the associated grade. This is the grade for the first node and is placed onto the grid. Each successive node along the random path is subsequently visited and the estimation process is repeated with inclusion of the previously simulated nodes as data values in the Kriging process. Once all nodes along the random path are visited, the simulated normal scores are transformed backwards into simulated values for the original variable (the grade).

By repeating the simulation process using different random paths, a series of equi-probable realisations of the mineral resource can be created. These equi-probable realisations of the orebody provide a valuable insight of grade uncertainty present within the mineral resource model and can be used in the stope optimisation process.

Stope Optimisation Methods

Depending on the available block model type the AMS Stope Optimiser can apply one of two types of stope optimisation methods; Conventional and Risk-based.

Conventional stope optimisation is carried out using the estimated resource model only. The stope optimisation software optimises both the location and shape of the stopes (Fig. 4) for a user supplied cut-off grade.

Risk based stope optimisation using conditional simulated resource models is a relatively new concept. A previous study was conducted by Grieco and Dimitrakopoulos (2007) and uses multiple simulated models to optimise stopes above a certain cut-off grades for a range of certainty levels.

A similar method was introduced to AMS Stope Optimiser as part of the AMIRA P1037 project. The optimisation process is carried out using the estimated resource model and all simulated resource models simultaneously. By the application of a target confidence level to the desired cut-off grade, the underground stopes are designed to meet the cut-off grade in the estimated model, as well as a percentage of the simulated models.

As an example, optimising stopes at a cut-off grade of 2.0 g/t and a minimum confidence level of 80% (based on 25 simulations) will result in stope shapes at or above this cut-off grade in the estimated model as well as at least 20 of the 25

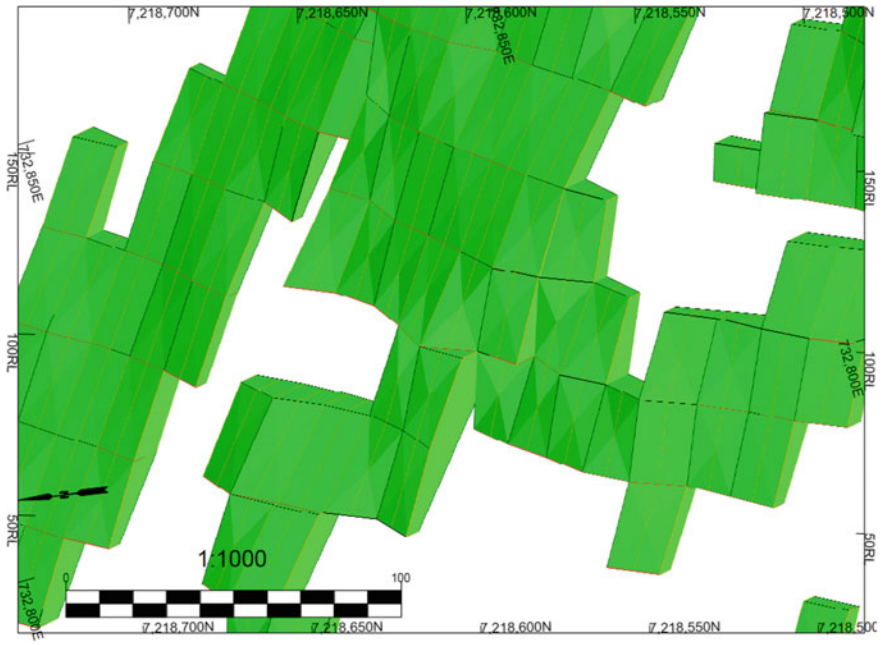

Fig. 4 Example AMS stope optimiser stope solids output in Deswik.CAD

simulations. By increasing the minimum confidence level, the risk of under-performance of the optimised stopes decreases, as the stopes must meet the cut-off criterion for an increased number of simulations.

Another approach to reducing risk would be the option to increase the minimum desired head-grade, but this was not explored in the current case study.

As a trade-off for increased confidence, the number of stopes and stope tonnages are likely to reduce with increasing minimum confidence levels. The reduction of the stopes and tonnages is a quantification of the spatial grade uncertainty in the resource model. A confidence level of 100% requires all simulations to meet the cut-off grade in each stope shape. This confidence level can never be achieved in practice, as a degree of uncertainty will always remain in the sample collection, variography and geostatistical modelling, and the number of simulations that might be necessary. The analysis is a result of the spacing between drill-holes and number of samples taken from drill-holes. As such, a 100% confidence level at the mine production stage would require an infinite number of drill-holes, which is unrealistic. The acceptable confidence level should be a trade-off between exploration costs and the cost of uncertainty (i.e. the range of possible project profit).

Case Studies

Two case studies were carried out to evaluate the principles of underground mine optimisation using conventional and risk-based optimised stopes. As the aim of these case studies was to illustrate the introduced principles rather than to conduct a full mine optimisation, a limited number of cut-offs, production and development rates were evaluated.

The Boliden Mineral AB owned Älgträsk gold deposit in Northern Sweden was selected for the experiments. Originally considered for open pit mining, the potential for a small-scale sublevel stoping operation to mine the high-grade zones of the deposit was recently investigated.

The Älgträsk intrusive gold mineralisation consists of several ore lenses dipping at an angle of circa 63 degrees in a north-westerly direction. The mineralisation is both disseminated and in veins, hosted within a coarse-grained granodiorite (Bejgarn 2009).

Case Study I—Conventional Optimisation

The goal of this case study was to prove the basic concept of underground mine optimisation using the AMS Stope Optimisation software to generate input data and was carried out using a Kriging estimated resource model.

Cut-off Grade Based Mine Design

Basic costs and revenues related to the mining, processing and refining of the ore coming from the Älgträsk deposit were determined based on company data and similar mining operations within the area. Using these basic revenues and costs, a break-even grade was estimated at 1.6 g/t Au. This grade was used as a starting point for optimisation. Based on the break-even grade estimate, six cut-off grades (1.5–1.6–1.7–1.8–1.9–2.0) were evaluated for the deposit.

The Modified Stability Graph method (Mathews 1980; Potvin 1988) together with rock mechanical data as supplied by the Boliden geotechnical department was used to determine a feasible and stable stope size and these parameters were used as constraints in the stope optimisation process.

The AMS Stope Optimiser was used to design stopes at all user-defined cut-off grades and the resulting stope shape solids were loaded into the Deswik.CAD environment for further mine design. Basic infrastructure was designed to connect and access the stopes whilst respecting geotechnical, economical and practical constraints.

The design of infrastructure is still a manual process and the resulting design is therefore not guaranteed to be optimal. Due to the relatively short stope lengths, longitudinal stoping was selected as opposed to transverse stoping reducing the overall development costs. A decline centralised between the three ore lenses further reduced development costs.

An example of a resulting basic mine design is shown in Fig. 5.

Life of Mine Scheduling

The basic mine design was imported into a scheduling package. Interactive Scheduler by Deswik was selected for life-of-mine scheduling as it is fully integrated within the Deswik.CAD software package. The first step in scheduling is to subdivide the development works in multiple tunnel sections (task solids) and to assign an activity type to each task solid (i.e. decline-, level-, ore-development). A similar approach was used for the stopes to which activity types for production drilling, stoping and backfilling were assigned.

With the mine design broken down into many smaller individual task solids, dependencies were created between these tasks. Dependencies are links between two task solids that prevent the next task from starting before the previous task is finished. In case of the development tasks this means that a level development task cannot start before the decline has reached the specific level. Also, an ore drive task cannot be started before the level development has reached the respective ore drive starting point. In similar fashion dependencies exist for the stopes. Once the ore drive for a specific mining area is finished, the stope production process can start with drilling & blasting followed by the actual stoping (ore production). Finally the stope is backfilled and left to cure for a certain period of time. During this curing

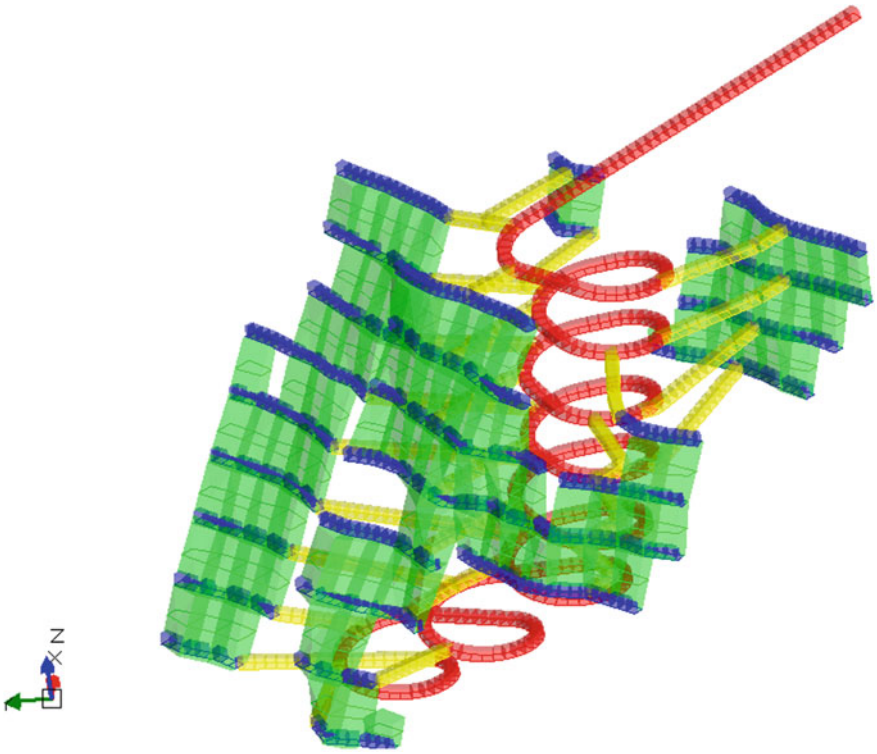

Fig. 5 Example optimised stopes and basic mine infrastructure in Deswik.CAD

period, production in adjacent stopes (laterally and vertically) within specified distances cannot start.

To offset development costs and initial capital expenditures, an overall downward mining progression was chosen using a longitudinal retreat type stoping sequence. Dependencies were created between all tasks and visually checked by animating the resulting sequence. Once a feasible development and production sequence was determined, different development and production rates were evaluated. Task rates (i.e. development rate and production rate) were assigned to each individual development or mining task as well as a resource (a piece of mining equipment) to complete the task.

For each cut-off grade based mine design, two possible development rates and two production rates were evaluated. The goal was to match development and production rate as much as possible to retain a relatively constant production rate over the life-of-mine whilst aiming to maximise resource utilisation. The resulting production schedules indicated a life-of-mine ranging from circa five to three years depending on chosen cut-off grade and task rates.

Cash Flow Analysis

Using the life-of-mine production schedules, four processing routes were evaluated within a spread sheet based cash flow model, resulting in a total of 96 evaluated scenarios. The resulting NPVs of these scenarios were systematically plotted in a Hill of Value graph from which the optimum strategy was determined.

Optimisation Results

Figure 6 presents the net present values for processing route 3 (Gravity and Flotation of Low Arsenic ore and Gravity and Leaching of High Arsenic ore).

The graph clearly shows that the optimal project strategy is a combination of cut-off grade and life-of-mine (as a function of production and development rate). This is in line with the cut-off grade theory by Lane. For the limited number of cases evaluated, the optimum cut-off grade was found to be 1.8 g/t of gold at a production rate of 1500 tonnes of ore per day and development task rate of 60 metres per tunnel face per month. For this production and development rate the NPV of the optimal mining project increased by circa 30% compared to the break-even mining scenario of 1.6 g/t.

A dip in the NPV curve is observed at a cut-off grade of 1.7 g/t which is caused by an unfavourable production schedule resulting in a slightly delayed revenue

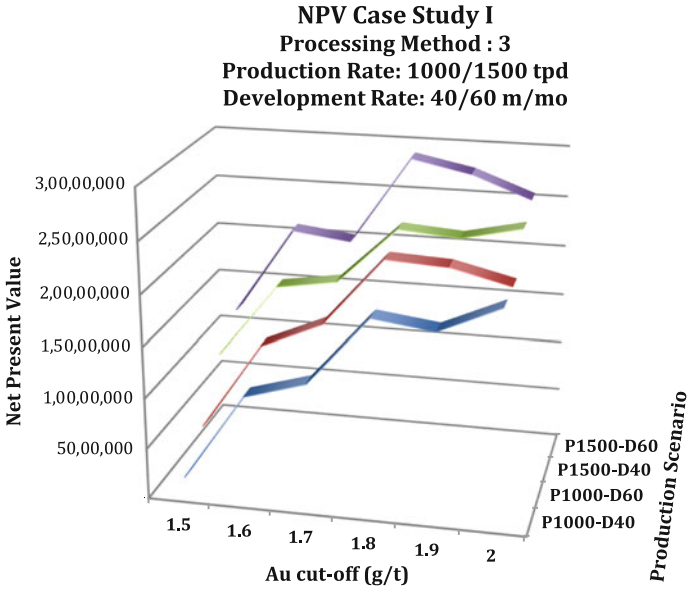

Fig. 6 Optimisation results for evaluated production and development rates—Älgträsk case study I

stream and increased refining penalty due to unfavourable Arsenic contamination of the ore concentrate. The Älgträsk underground project proved to be marginally profitable with a high risk. The project requires large investments compared to the potential profit and payback period (payback period equals life-of-mine). Marginally profitable projects require solid knowledge of the mineral resource to reduce the risk of project failure. In other words, there should be a high level of certainty about tonnage and grade of the ore that will be produced once the project is taken into production.

Case Study II—Risk Based Optimisation

This case study consisted of two parts. First the grade uncertainty in the optimised project strategy resulting from case study I was evaluated using conditionally simulated resource models. Subsequently, the use of simulated resource models during the underground mine planning process was investigated.

Grade Uncertainty Evaluation

In order to evaluate and quantify the grade uncertainty present in the optimised mine strategy a series of conditionally simulated resource models were created. The following process was adopted to create these models:

Data Analysis

Raw exploration drill-hole data was cleaned, composited and loaded into the Stanford Geostatistical Modelling Software (Stanford University 2009a, b) for statistical analysis. The grade distribution of the drill-hole data was determined after which the dataset was normalised and variogram modelling was conducted to describe the deposits' directional grade anisotropy.

Block Model Simulation

GSLIB (Stanford University 2009a, b) was used to create 25 simulation based block models. The Geostatistical Software Library is a set of freely available software tools to perform Sequential Gaussian Simulations. A regular block size was selected, as the Sequential Gaussian Simulation algorithm cannot deal with sub-blocking. In order for the block model to resemble the orebody geology as accurately as possible, a small block size of $2.5 \times 2.5 \times 2.5$ was chosen. This small block size ensures that the stope optimisation process (which assumes that the block model represents true geological boundaries) is carried out as accurately as possible. Ore lenses were individually simulated and the results were later combined into one model. By simulating the lenses separately, grade contamination between closely spaced ore lenses was avoided. Finally, the simulated grade data was combined with the estimated grade data to create a model in which each individual block has an estimated and 25 simulated grades assigned to it.

Model Comparison

The grade tonnage curve and grade distribution of block model blocks for the Kriging estimated model and 25 simulated models are shown in Fig. 7. Clearly observable is the smoothing effect present in the Kriging estimate. Tonnages of both low and high-grade material are under-estimated whilst mid-range grade material is over-estimated. The average grade above cut-off is under-estimated for all cut-off grades. The simulated models do not show this smoothing effect and retain the grade distribution as observed in the composite drill-hole data.

When the Kriging model is compared to the simulated resource models (Fig. 8) the smoothing effect is clearly observable in the estimated model. The equi-probable simulated resource models do not show this effect but show a significantly different distribution of high- and low-grade areas in the model. This indicates that grade uncertainty is present in the Kriging model, which may affect the likelihood of the designed stopes meeting the expected head grade when only the estimated model is used for stope optimisation.

Stope Confidence Levels

To quantify the grade uncertainty in the estimation model-based optimised stopes, a confidence level of achieving the estimated head-grade was assigned to each stope. The optimised stope design was interrogated against the conditional simulated resource models to obtain simulation based stope head-grades. These simulation

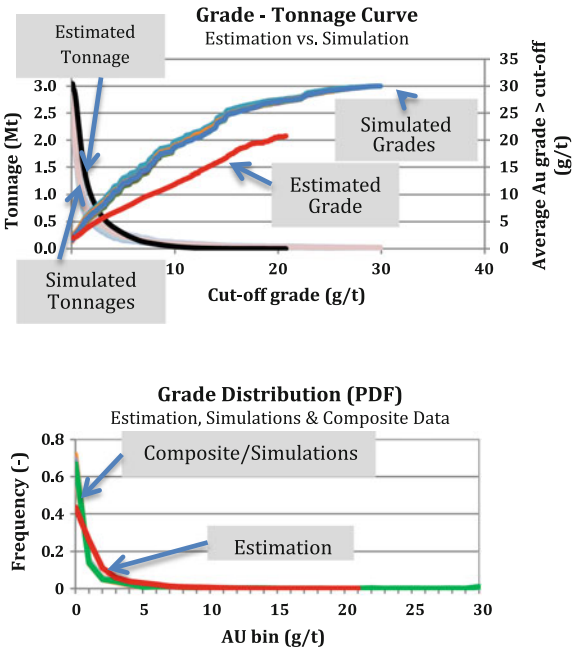

Fig. 7 Estimation/ Simulations grade-tonnage curve and grade distribution

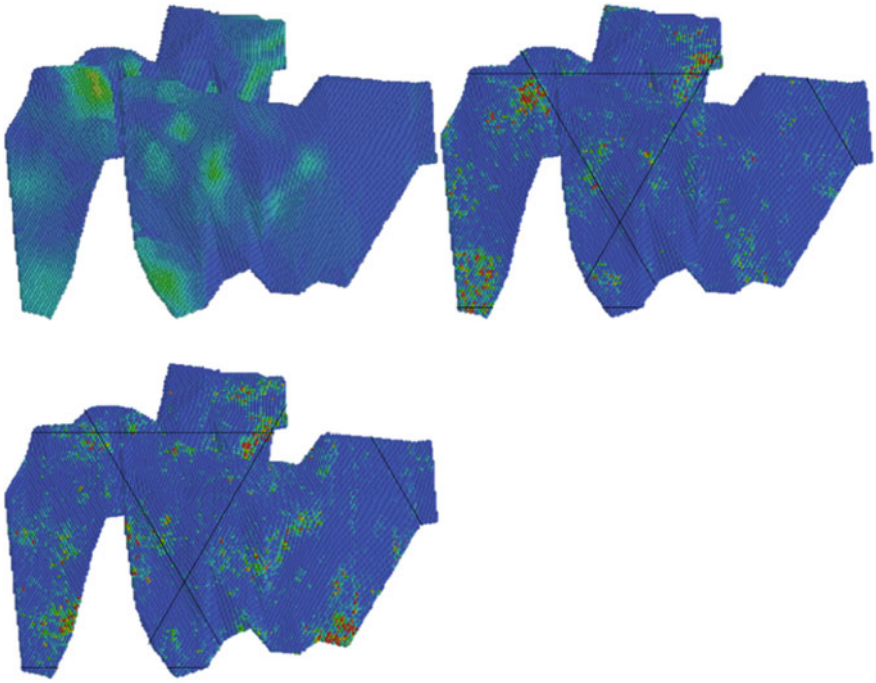

Fig. 8 Kriging Estimated model (top left), Simulation 7 (top right) and Simulation 13 (bottom left). Brighter areas are of higher grade

based stope head-grades were evaluated against the estimation based stope head-grade to determine the stope confidence level by the following equations:

$$C_n = \begin{cases} 1, & S_n \geq Au_{OK} \\ 0, & else \end{cases}$$

$$Confidence\ level = \frac{1}{N}\sum_{n=1}^{N} C_n$$

In which S_n is the nth simulated stope head-grade, C_n is an integer (0 or 1) assigned to a simulated stope grade to define if it is equal to or exceeds the Ordinary Kriging Estimated stope head-grade and N is the total number of simulations considered. The confidence level is expressed as a number between 0 and 1.

Analysing the resulting confidence levels of the estimation based stope designs (Fig. 9) it was found that in general the confidence levels are low. The estimated model based stope designs show confidence levels that are rarely over 50% and the majority of stopes show confidence levels between 0 and 30%.

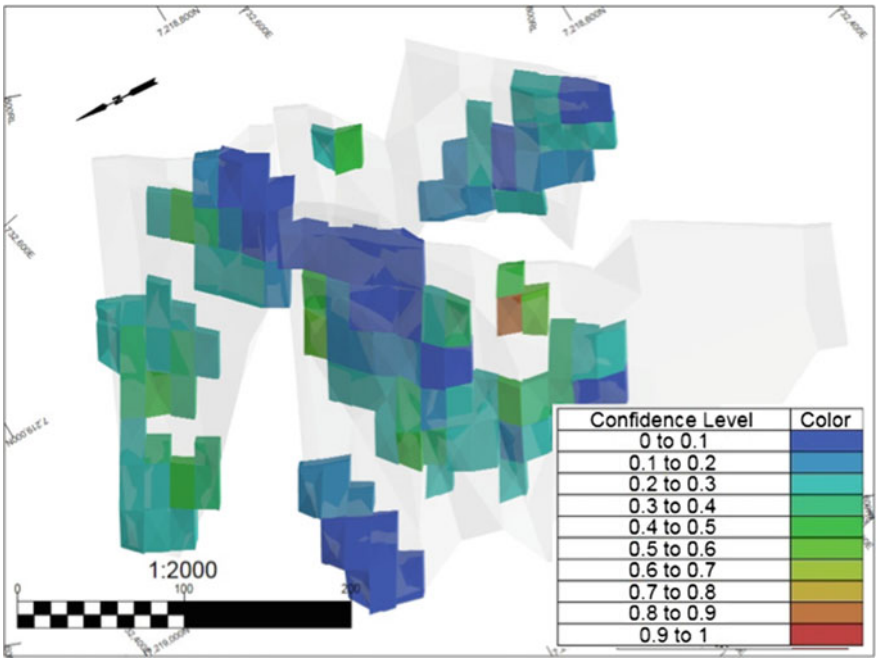

Fig. 9 Stope confidence level evaluation (simulated stope head grade equal to or higher than estimated stope head grade)

This means that the likelihood that the mine will actually produce the ore tonnage and grade as expected based on the estimated resource model is very low. With the project already being only marginally profitable based on the estimated resource model, the likelihood of project failure (economic loss) is very high.

To further analyse the economic consequences of the high grade uncertainty in the estimation model based optimised mining project, the estimated and all simulated grades were used as inputs to the cash flow model (Fig. 10). The undiscounted

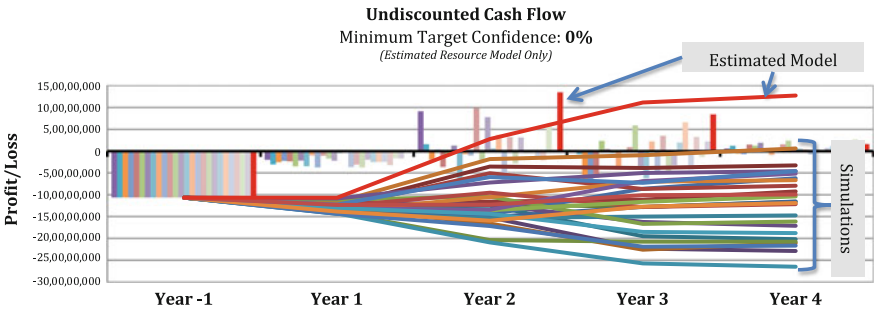

Fig. 10 Cash flow analysis (Estimation model based project optimisation)

cash flow analysis emphasises the project risk involved in the mining project when only the estimated model is used to optimise mine plans. The range in which the profit is to be expected is very large and shifted towards the negative 'loss' side with only one simulation resulting in a profit on an undiscounted basis.

Based on this cash flow analysis, it was concluded that the project when optimised on the estimated block model only, would not be profitable. A large smoothing effect is present in the estimated resource model as a result of limited availability of 'hard' drill-hole data. The underground mine optimisation based on this smoothened model results in an over-estimation of the project profitability, which is confirmed by the simulated cumulative cash flows.

Including Grade Risk in the Optimisation Process

The grade uncertainty evaluation showed that the decision to optimise a mine design on the estimation model only might result in a high-risk project strategy, especially when resource confidence is low as a result of limited exploration. It would be of great benefit if the estimated block model and the simulated block models could be used simultaneously whilst optimising the stope shapes for a given cut-off grade. By assigning a minimum confidence level to the final optimised stope prior to optimisation, the risk of a stope head-grade being below cut-off can be reduced. If the grade uncertainty is minimised, there is increased likelihood that the selected optimum project strategy will be successful once the mine is taken into production.

The AMS Stope Optimiser was used to re-optimise the underground stope designs at a cut-off grade of 1.8 g/t gold (the optimal cut-off grade based on the estimated model optimisation) and multiple minimum target confidence levels. The resulting optimised stope designs at 0, 20, 40, 60 and 80% minimum target confidence are presented in Fig. 11. It is observed that with increased confidence levels, the total number of stopes and therefore stope tonnage reduces rapidly. At a minimum confidence level of 60%, the stope configuration has reduced to a non-mineable situation where development costs are no longer offset by the stope tonnage and grade. To evaluate the potential of risk-based stope optimisation and its impact on project profitability, the 40% confidence level was chosen for further analysis. Although this would still be considered high-risk (stopes are accepted even if there is less than 50% chance for the stope to meet the cut-off grade) it is expected that the economic risk of the project is reduced compared to the optimised project based on the Kriging Estimated Model only.

Development was designed for the new set of optimised stopes in order to develop life-of-mine schedules and perform subsequent cash flow analysis. The resulting undiscounted cash flow analysis is presented in Fig. 12. Compared to conventional project optimisation (based on the estimated model only) the economics of risk-based optimisation are slightly more favourable. The potential project profitability based on the Kriging estimated cash flow reduced as a result of the increased confidence and hence reduced number of stopes and total stope

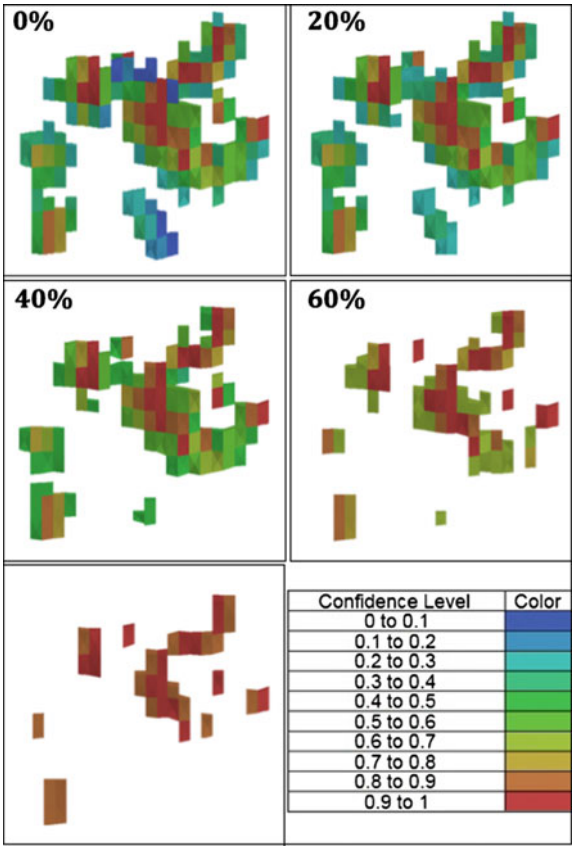

Fig. 11 Optimised stope designs at increased confidence levels (cut-off grade @ 1.8 g/t Au)

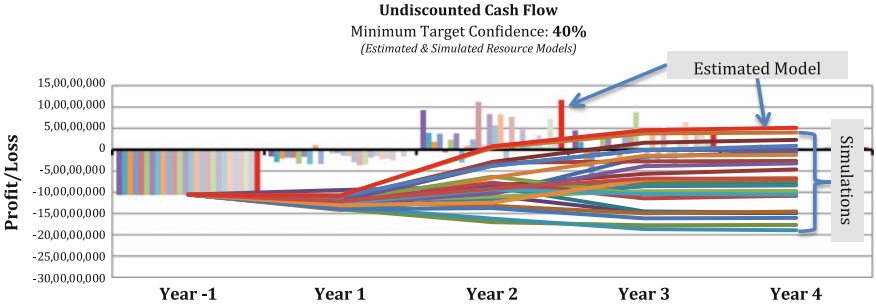

Fig. 12 Cash flow analysis (Risk-based project optimisation)

tonnage. However, the increased grade confidence makes the project more likely to produce up to expectation (therefore reducing economic risk). Besides the positive cumulative cash flow based on the estimated block model, three out of the 25 simulation models also result in an undiscounted project profit. The range in which

the project profit is to be expected has slightly reduced and is shifted more towards the positive 'profit' side. This is an improvement, compared to the project as evaluated in Case Study I (Fig. 10) for which only one simulation resulted in a positive cumulative cash flow.

Conclusion

Based on Lane's theory, a practical cut-off grade based mine optimisation process was developed. The process allows the rapid evaluation of different mine plans based on user-defined cut-off grades, in order to determine the optimum project strategy that maximises profitability. To speed up the design process, the AMS Stope Optimiser was used to automatically design optimised stope shapes based on user-supplied cut-off and design constraints. Further design and scheduling was carried out using Deswik CAD and scheduling software after which a spread sheet package was used for cash flow modelling.

The optimisation process was successfully tested on the Boliden Mineral AB owned Älgträsk gold deposit in Northern Sweden for which it was found that the optimal cut-off grade of 1.8 g/t increased the project NPV by circa 30% compared to the break-even grade of 1.6 g/t when optimising on a Kriging estimated resource model.

Conditional simulations of the Älgträsk gold deposit were created to quantify grade uncertainty (grade-risk) as present in the optimised project. It was found that a high grade uncertainty is present in the optimised project strategy due to limited exploration drilling. The smoothing effect introduced by the Kriging algorithm makes the project seem more profitable than is really the case.

The optimisation process was adapted to account for grade uncertainty by optimising stopes using the estimated and simulated resource models simultaneously. By assigning minimum target confidence levels, it is assured that the optimised stope is at or above a user selected cut-off grade in the estimated resource model as well as a percentage of the simulated resource models. By subsequently increasing the minimum confidence level, a trade-off can be made between potential profit and the risk of under-performance of the optimised stopes.

Further research work is required to extend the results of this work to design underground mines with varying cut-off grades over the life of the mine. This is a fundamental insight in the cut-off grade theory of Lane but was not practically applicable to the small sized Älgträsk deposit.

Acknowledgements The authors wish to thank Boliden Mineral AB for providing the possibility to perform this research project and allowing to publish some of its results.

References

Alford C, Hall B (2009) Stope optimisation tools for selection of optimum cut-off grade in underground mine design. In: Proceedings project evaluation conference, The Australasian Institute of Mining and Metallurgy, Melbourne, pp 137–144, 21–22 April 2009

Bejgarn T (2009) New styles of intrusive related copper-gold deposits in northern Sweden. Licentiate Thesis, Lulea University of Technology, Lulea

Bootsma MT (2013) Cut-off grade based sublevel stope mine optimization. M.Sc. Thesis. Available at: repository.tudelft.nl. Delft University of Technology, Delft

David M (1977) Geostatistical ore reserve estimation. Elsevier, Amsterdam, 364p

David M (1988) Handbook of applied advanced geostatistical ore reserve estimation. Elsevier, Amsterdam, 216p

Elkington T, Durham R, Myers P (2010) Optimising value for an underground project configuration. In: Proceedings advances in orebody modelling and strategic mine planning I, The Australasian Institute of Mining and Metallurgy, Melbourne, pp 241–248

Goovaerts P (1997) Geostatistics for natural resources evaluation, Oxford University Press, Oxford

Grieco N, Dimitrakopoulos R (2007) Managing grade risk in stope design optimisation: robabilistic mathematical programming model and application in sublevel stoping. Trans Inst Min Metall, Sect A: Min Technol 116(2):49–57

Gu X, Wang Q, Chu D, Zhang B (2010) Dynamic optimization of cutoff grade in underground metal mining. J Cent S Univ Technol 17: 492–497 (Central South University Press and Springer-Verlag, Berlin Heidelberg)

Hall BE (2007) Evaluating all the alternatives to select the best project strategy. In: Proceedings project evaluation 2007, The Australasian Institute of Mining and Metallurgy, Melbourne, pp 53–64

Hall BE, de Vries JC (2003) Quantifying the economic risk of suboptimal mine plans and strategies. In: Proceedings mining risk management conference, The Australasian Institute of Mining and Metallurgy, Melbourne, pp 59–69

Hall BE, Stewart CA (2004) Optimising the strategic mine plan—methodologies, findings, successes and failures. In: Proceedings orebody modelling and strategic mine planning conference, The Australasian Institute of Mining and Metallurgy, Melbourne, pp 49–58

Lane K (1988) The economic definition of ore, cut-off grades in theory and practice. Mining Journal Books Limited, London

Mathews KE (1980) Prediction of stable excavation spans for mining at depths below 1000 m in hard rock. Report to Canada Centre for Mining and Energy Technology (CANMET), Department of Energy and Resources

Poniewierski P, MacSporran G, Sheppard I (2003) Optimisation of cut-off grade at Mount Isa Mines Limited's Enterprise Mine. In: Proceedings 12th international symposium on mine planning and equipment selection, The Australasian Institute of Mining and Metallurgy, Melbourne, pp 531–538

Potvin Y (1988) Empirical open stope design in Canada. Ph.D. thesis, University of British Columbia, Vancouver

Rendu JM (2008) An introduction to cut-off grade estimation. Society for Mining, Metallurgy and Exploration, Littleton

Stanford University (2009) GSLIB: geostatistical Software Library [Geostatistical software and guideline]. Available at: www.gslib.com [Accessed 1 Oct 2013]

Stanford University (2009) SGeMS: geostatistical modeling software [Geostatistical software and guideline]. Available at: sgems.sourceforge.net [Accessed 1 Oct 2013]

Classification of Mining Methods for Deep Orebodies

V. Oparin, A. Tapsiev and A. Freidin

Abstract Classifications of mining methods date back to the 1960s and use the following criteria: type and size of a mineral deposit, mined-out space support, state of a working excavation, type of a face, roof support, etc. Since that time mobile mining machinery has appreciably advanced, and some mining methods have lost their importance. Mobile mining equipment is effective in definite mining methods: in open mined-out space, mining with backfill and combined schemes. The transition to deep mining inevitably results in the sharply worsened technical and geomechanical conditions, and some well-established techniques for safe mining at rock burst hazardous deposits can not be considered self-sufficient. This paper puts forward a classification of deep mining methods, considering rock pressure control. The classification involves three classes: mining with backfill, mining with caving of overlying rocks and combined mining with backfill and caving.

Introduction

Many foremost Russian and foreign researchers and mining engineers have been scrutinising methods of grouping existing underground mining methods. More than 60 published classifications have undergone critical analysis in fundamental monographs by Trushkov (1947), Agoshkov (1965), Baikonurov (1969) and Imenitov (1978). Trushkov conceded on inexpediency to try and embrace all coal and ore mining methods in a uniform classification due to 'crockness and inconsistency of these methods, and their not-hands-down use in practice' (Trushkov 1947). Unlike coal formations, orebodies have multiple sizes and shapes, occurrence conditions, physico-mechanical properties, mineral composition and mineral values, which gave rise to a range of 170–200 variants of ore mining schemes applied in underground mines in the 20th century (Trushkov 1947; Agoshkov 1965).

V. Oparin · A. Tapsiev (✉) · A. Freidin
Institute of Mining, Siberian Branch, Russian Academy of Sciences, 54 Krasny Prospect, Novosibirsk, Russia630091
e-mail: atapsiev@misd.nsc.ru

R. Dimitrakopoulos (ed.), *Advances in Applied Strategic Mine Planning*,
https://doi.org/10.1007/978-3-319-69320-0_32

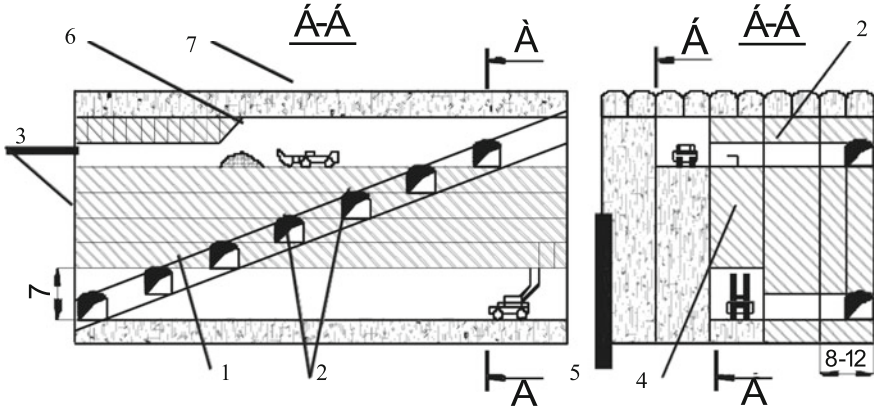

Fig. 1 Class I, Group A, Type 1: 1—inclined shaft; 2—entry; 3—levels; 4—stoping; 5—backfilling; 6—level extraction; 7—roof safety layer (please refer to Table 1)

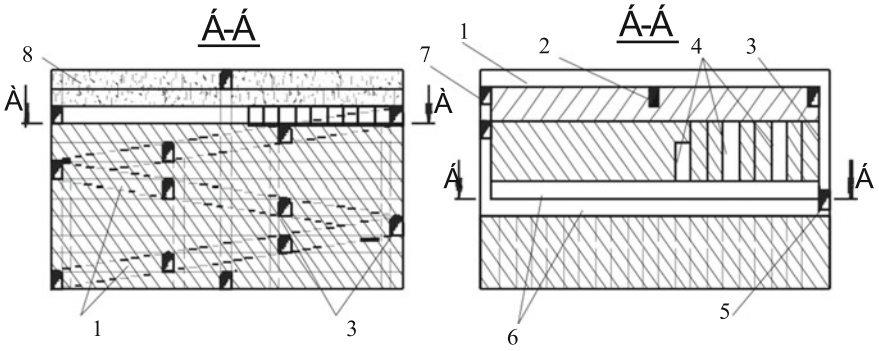

Fig. 2 Class I, Group A, Type 2: 1—inclined shaft; 2—ore chute; 3—cross adit; 4—stopes; 5—air raise; 6—twin stope drifts; 7—air-fill raise; 8—filled levels (please refer to Table 1)

The totality of underground ore mining methods caused difficulties with scientific grouping, however, it also fostered many characteristics for classifying them. Different researchers assumed different classification criteria (please refer to Baikonurov 1969); for example, the type and size of a deposit (Crane, G J Young, I Pokrovsky, G E Bakanov and L I Baron); mined-out space support (F W Sperr, Y H Rayt, E C Mitke and V N Semevsky); working excavation support (J F Clelland, C F Sackson and E D Gardner, USA Mining Bureau's classification, N I Trushkov, N A Starikov, G N Popov and V R Imenitov); working excavation state (M I Agoshkov and R P Kaplunov); mined-out space support during mining and backfill (V T Markelov); type of a face, roof support, block undercutting technique (American Institute of Mining Engineers and Metallurgists); direction of mining advance and backfill method (Baikonurov 1969); mining stages (Steshenko). The above-listed criteria rank and characterise mining methods in varying degrees and

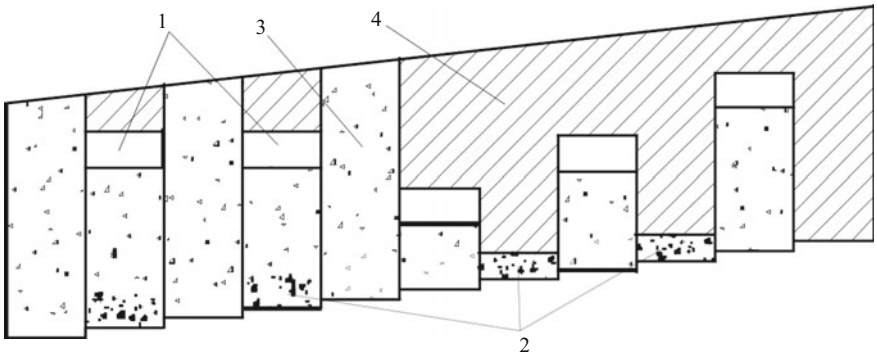

Fig. 3 Class I, Group A, Type 3: 1—stope; 2—soft pillars; 3—backfill; 4—orebody (please refer to Table 1)

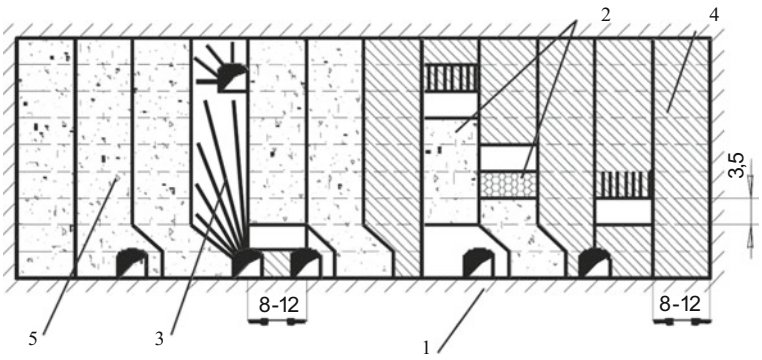

Fig. 4 Class I, Group A, Type 4: 1—entry; 2—extraction levels in a chamber; 3—temporary pillar (secondary chamber); 4—orebody; 5—filling mass (please refer to Table 1)

yet are of little use in actual comparison and selection. In Russia, the classifications by Agoshkov (1965) and Imenitov (1978) have found deserved recognition and wide application in underground mine planning. Agoshkov grouped mining methods by 'the state of the working excavation in the course of actual mining' and Imenitov used the criterion of 'working excavation support method in the course of mining'. We acknowledge the effectiveness and advantages of both classifications, though some comments should be made. First, these classifications appeared in the mid-1960s. Mining methods have been continuously evolving since then, and many of them have dwindled, especially for medium thick and very thick ore deposits. These days, underground mining practice involves lively mobile machinery sets, which has drastically simplified preparatory and development operations as well as stoped excavation, boosted mining works and minimised hand-labour amount due to the overall mechanisation.

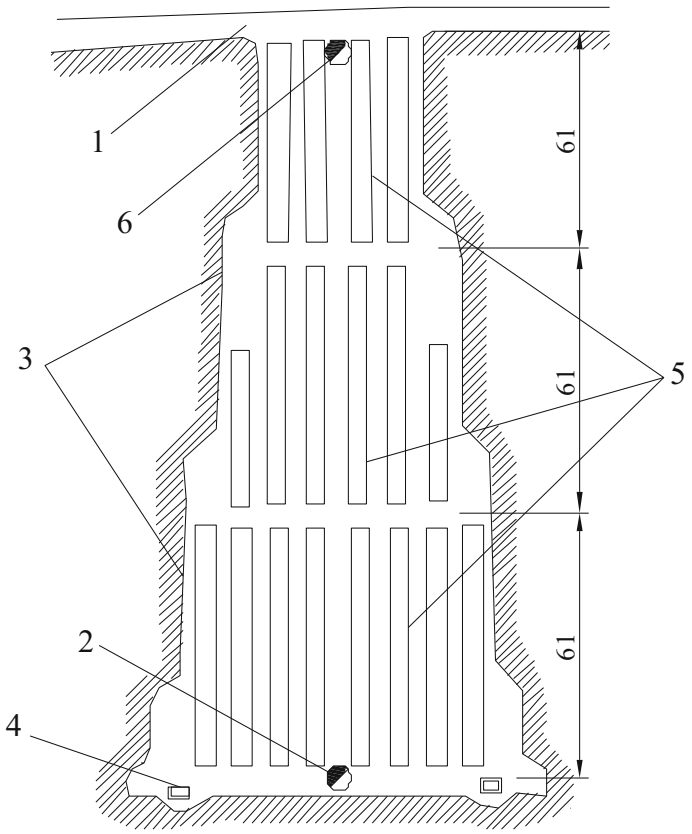

Fig. 5 Class I, Group A, Type 5: 1—gallery; 2—ore chute; 3—langwall; 4—scraper excavator; 5—pack; 6—raise (please refer to Table 1)

Highly laborious mining with portable equipment is now used in the excavation of very thin orebodies with high useful mineral content. This method and equipment may only be applied for actual mining of medium thick and very thick ore deposits if low-paid manpower is in employment, mineral resources are of low value and the total enterprise is of no consequence to be re-constructed or technically modernised. The analysis of the mobile machinery operation shows that they are efficient in a limited number of mining methods, namely:

- mining with backfill (longwall and chamber mining, including the chamber-and-pillar method);
- mining without backfill (chamber-and-pillar and flat-bottom- chamber mining);
- mining with ore and rock caving (block caving and, especially, sublevel caving with frontal and frontal-areal ore drawing); and
- combined mining (with backfill and caving).

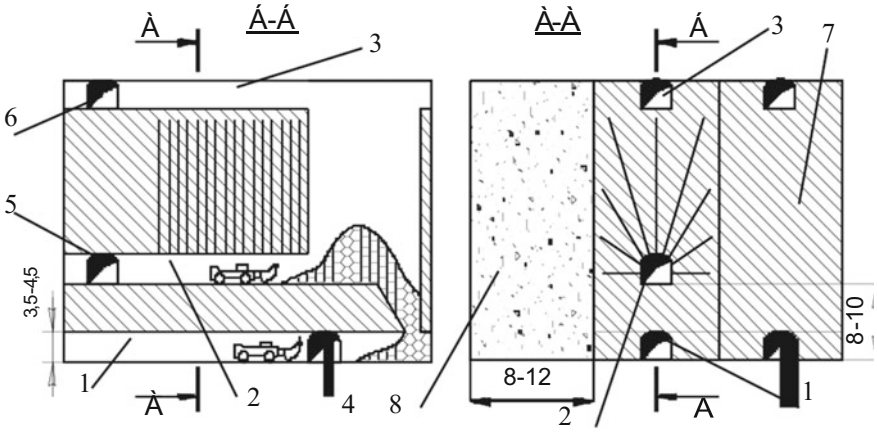

Fig. 6 Class I, Group B, Type 6: 1—haulage heading; 2—drilling and haulage roadway; 3—air ort; 4—ventilation connection; 5 and 6—air drifts; 7—orebody; 8—filling mass (please refer to Table 1)

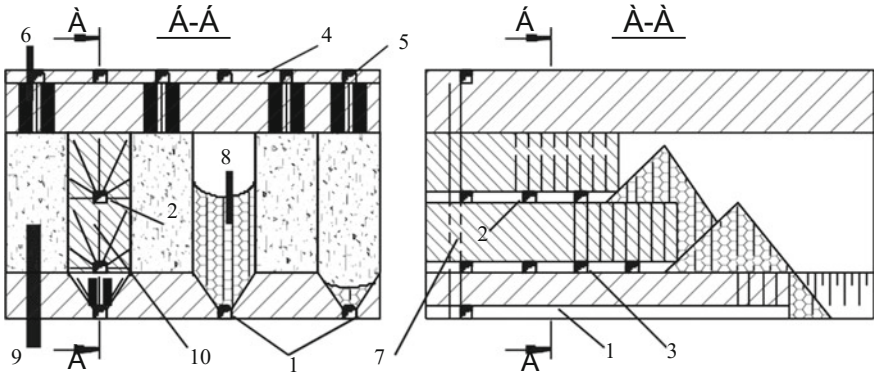

Fig. 7 Class I, Group B, Type 7: 1—haulage heading; 2—drilling roadway; 3—entry; 4—air and backfill cross-drifts; 5—air and backfill ort; 6—filling holes; 7—raise; 8—broken ore; 9—filled primary chamber; 10—secondary chamber (pillar) (please refer to Table 1)

The gained engineering level of underground mining with mobile machinery and successful robotic automation of ore excavation processes at some enterprises (Bronnikov et al. 1982; Oparin et al. 2007) will lead to further universalisation of mining methods. It is also important to consider that underground mining gets deeper by 20–40 m annually, and now reaches nearly a 4 km depth in South Africa and India. More than ten underground mines in USA, Canada and South Africa are below 2.5 km depth. Deep mining conditions are very difficult: rock temperature is higher, the physico-mechanical properties of rocks change, angles of rock mass movement flatten and rock pressure grows and manifests itself dynamically. More

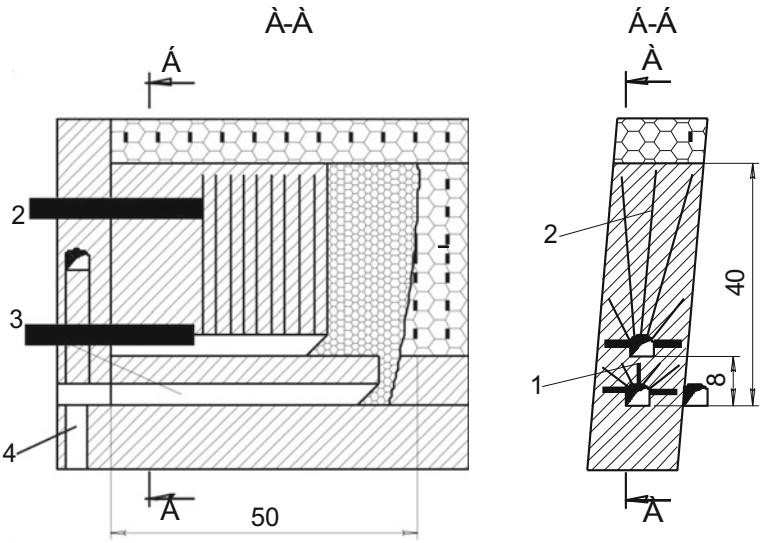

Fig. 8 Class I, Group A, Type 1: 1—fan-patterned holes intended to cave safety shield; 2—main fan-patterned holes; 3—drilling and haulage level; 4—ore chute (please refer to Table 1)

and more deposits acquire the category of rock burst hazardous. Mining theory and practice have elaborated measures for minimising the hazard of rock pressure (Bronnikov et al. 1982) to:

- prepare and develop orebodies in a minimum fractured rock mass so that no stress concentration areas arise (pillars, overhangs) resulting in burst-like rock failure;
- orient development workings and stopes along the maximal effective stresses; and
- to advance stoped excavation as divaricated fronts, or as a single front towards the wing of a level.

These measures collide with many methods of underground mining, for example, with 'ore shrinkage' and 'mining without backfill' by Agoshkov (1965), or 'mining with naturally supported working excavation' by Imenitov (1978).

Different methods of mining with ore shrinkage that are in wide application in thin and steep orebodies, involve ascending stoping towards a diminished pillar. This is not permissible for us in rock burst hazardous rock masses. For instance, at Yuzhny complex deposit (GMK Dalpolimetal Co), where thin and strong ore veins occur in hard host rocks prone to elastic energy accumulation and dynamic failure (Pilenkov et al. 1990), series of rock bursts with severe after-effects took place at a depth of 150–200 m from the surface when mining with ore shrinkage approached the crown pillar. The ground control is extremely limited when mining is carried out without backfill, and the roof is supported with ore pillars and lining. In this case, the growing mined-out space loses its equilibrium, dynamic rock failure conditions

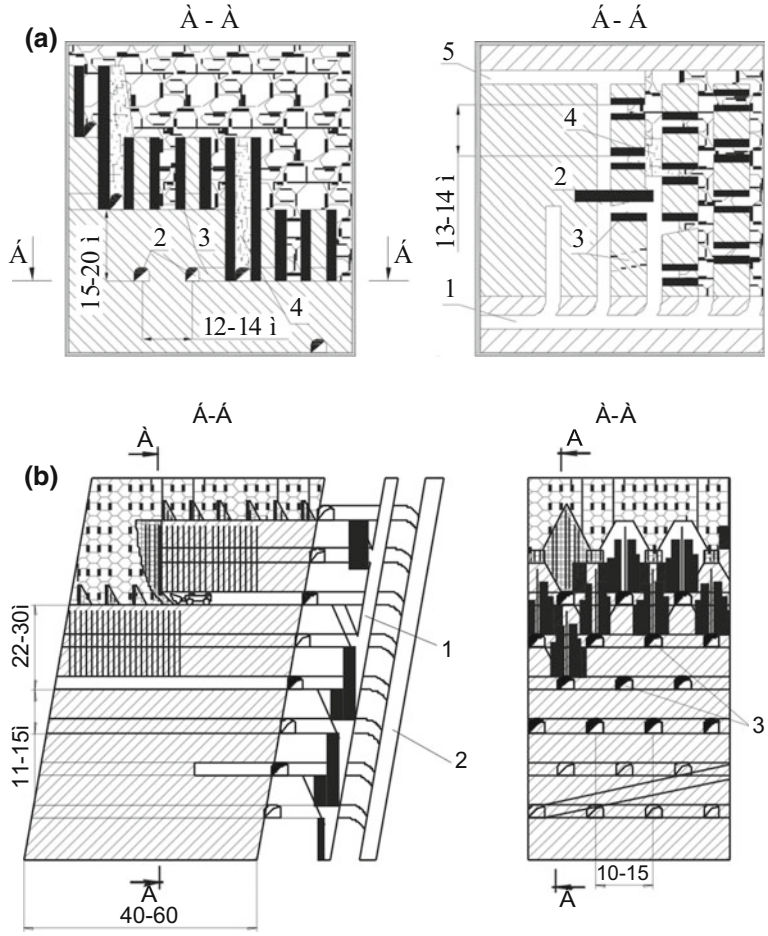

Fig. 9 **a** Class II, Group B, Type 2: sublevel caving with areal-frontal ore drawing: 1—haulage roadway; 2—drilling and haulage cross-drift; 3—loading slopes; 4—broken ore; 5—air drift (please refer to Table 1). **b** Class II, Group B, Type 2: sublevel caving with frontal ore drawing: 1—ore chute; 2—incline shaft; 3—drilling and haulage cross-drift (please refer to Table 1)

originate and large-scale rock fall becomes highly possible. A representative illustration of the above is the underground mines at Zhezkazgan cupriferous sandstone deposit (Yun et al. 1997), where the chamber-and-pillar method involves retaining enlarged inner-chamber and panel pillars (up to 40% and above of a panel area). Nonetheless, starting from a 450 m depth, falls and burst-like failure of pillars occur again and again. The calculations indicate that for chamber-and-pillar mining at a depth of 1000 m, more than half-reserves should be left as pillars for roof support safety (Bronnikov et al. 1982; Zamesov 1979).

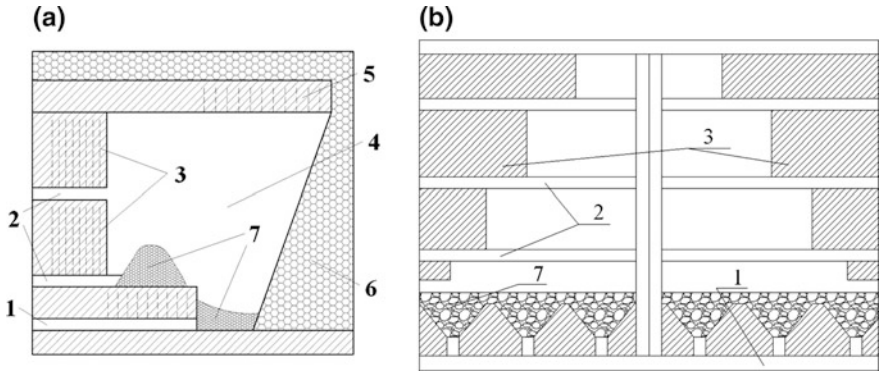

Fig. 10 Class II, Group B, Type 3: (A) mid-thick orebody; (B) thin orebody: 1—haulage heading; 2—subdrift; 3—holes; 4—under cantilever area; 5—crown pillar; 6—caved rock; 7—broken ore (please refer to Table 1)

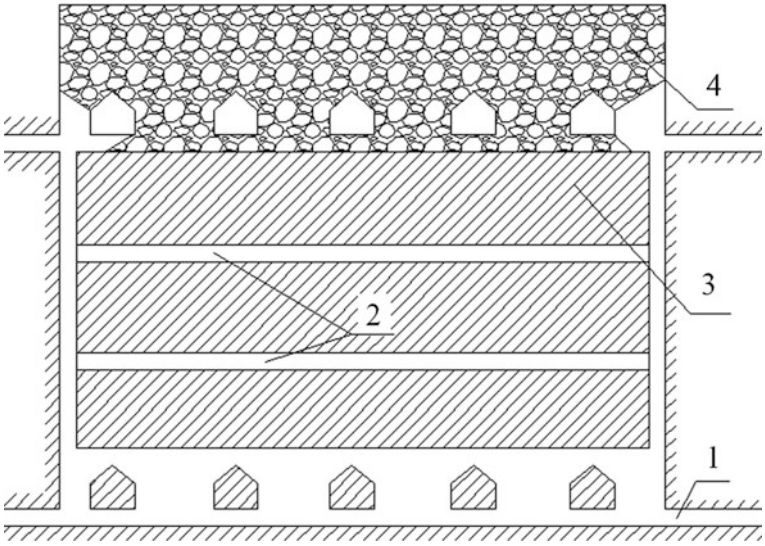

Fig. 11 Class II, Group B, Type 4: 1—haulage heading; 2—inclined shaft; 3—ore chute; 4—haulage cross-drift (please refer to Table 1)

Method of Classification

An important point in Agoshkov (1965) and Imenitov's (1978) mining method classifications is the lack of the systems of chamber mining with backfill. These systems are of use in longwalling and chamber-and-pillar working at 1000 m depth and deeper. The underground chamber-and-pillar mining with backfill is applied

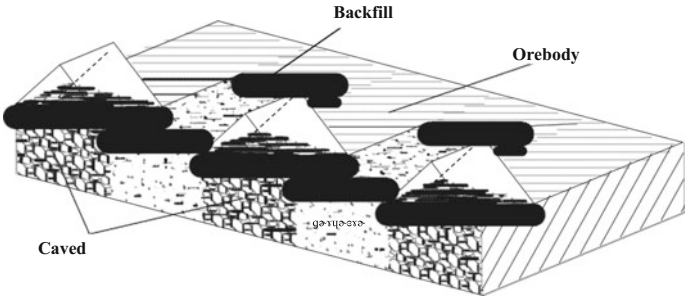

Fig. 12 Combined ground control; caving and backfill (please refer to Table 1)

extensively in Canada (Inco, Geco, Kidd Creek Mines), Finland (Outokumpu) and Australia (Mount Isa) (Khomyakov 1984), as well as in the former USSR countries (Gaisky, Leninogorsky, Zyryanovsky Mines, etc.). Some engineers think these geo-technologies are useful in mining no deeper than 600–800 m, due to the growing bearing pressure after the first chambers are extracted (Bronnikov et al. 1982; Zamesov 1979). Failure of pillars and excavations at ore drawing-off level necessitates introduction of longwall chamber methods that proved themselves in the Norilsk mines. Thus, for rock burst hazardous ore deposits, we think it is possible to characterise the allowable mining systems by:

- the principal ground control method for the mined-out space,
- the stoping excavation advance direction, and
- the ore breaking and drawing method.

The ground control is the governing factor for any deep mining technology. It is always present in the description and in the name of a mining method. We assume it the basic classification criterion.

It is natural that the principal ground control method is contributed to by the known design solutions oriented to enhance strain capacity of a rock mass and to monitor stresses in the near-face area. Such supportive measures include, for example, overworking (undermining) of the orebody, advance boring of larger diameter holes, confined explosions, directional hydro- fracturing, etc. These measures are feasible with any mining method and are not the attributes of a particular recovery mechanism. The second-listed characteristic is often present in the name of a mining method and gives a description of it. For example, the horizontal slicing with backfill may be ascending and descending. Steep rock burst hazardous ore veins are mined with sublevel stoping to the dip or on the strike. The third characteristic in our list details the way of ore drawing, namely, areal (from inclines), frontal or frontal-areal. Pillar mining may involve VCR, parallel or fan-patterned boreholes. So, the second and third criteria can and must serve for the grouping of the mining methods.

We are proposing a variant of classification of the mining methods for rock burst hazardous ore deposits based on the following principles:

Table 1 Classification of mining methods for rock burst hazardous ore deposits

Class	Group	Mining method	Application conditions	Advantages	Disadvantages
1	2	3	4	5	6
I. Ground control with backfill	A. Horizontal slicing with backfill	1. Horizontal slicing and ascending mining	Any geometry of a deposit. Medium and greater thickness. Average stability ores, mid-stable to unstable host rocks. Medium to high-grade ore. Unlimited depth of application	Simple geometry of stoping faces, high extraction index. Mobile machinery use. Sufficient stoping productivity. Possible separation of dirt rocks for backfill	Strict regulation of slicing. In case of high rock pressure, overworking is desirable, which is highly laborious. Organizational difficulties in stoping automation (Fig. 1)
		2. Horizontal slicing and descending mining	Any geometry of a deposit. Medium and greater thickness. Very unstable and heavily dislocated ores and host rocks. High-grade ore. Unlimited depth of application. Open cast and underground mining	The same as in ascending mining. Safe mining in heavily dislocated orebodies	The same as in ascending mining. High labour intensity and cost of backfilling (Fig. 2)
		3. Horizontal slicing with pillars on soft basis	Gently dipping medium thick and very thick orebodies. Mid-stable to unstable ores and host rocks. High-grade ore. Depth of application is to be determined	Ascending and descending mining of main reserves and temporary pillars. Increased mining front and more stopes under development. High extraction index	Driving and backfill of extra mine workings in the bottom of temporary pillars. Stoping in stages (Fig. 3)
		4. Room work and slicing	Mid-thick to very thick deposits. Any dipping. Mid-stable to unstable ores. Mid-stable host rocks. Medium to high-grade ores. Depth of application is to be determined	Higher quality and completeness of pillar extraction	Mining in stages. Higher labour intensity and lower stoping production (Fig. 4)
		5. Longwall mining	Horizontal and gently dipping orebodies. Very thin to 3–4 m thick ores. Any stability ores, mid-stable host rocks. Paste backfill, packs, stony and artificial blocks. High-grade ores. Unlimited depth of application	Selective mining. Elongated stoping front. High extraction index	Arduous working conditions and high labour intensity. Use of portable equipment, limited use of mobile machinery (Fig. 5)
	B. Room work mining	6. Continuous chamber mining	Medium thick to very thick deposits. Any dipping. Medium stable ores and host	High stoping productivity. Automation of	High ore dilution with cement-containing

(continued)

Table 1 (continued)

Class	Group	Mining method	Application conditions	Advantages	Disadvantages
			rocks. Depth of application is to be determined. Medium to high-grade ores	principal operations in stoping	backfill. Limited mining front (Fig. 6)
		7. Chamber-and-pillar mining (areal, frontal and frontal-areal ore drawing)	Medium thick to very thick deposits. Any dipping. Medium stable ores and host rocks. Medium and high-grade ores. Areal, frontal and frontal-areal ore drawing depending on the orebody thickness	High stoping productivity. Automation of principal operations in stoping. Extracted ore quality control	Mining in stages. Higher requirements to ore extraction standards. Probable failure of secondary chambers (pillars) in case of high pressure. High ore dilution (Fig. 7)
II. Ground control with overlying rocks caving	A. Block caving	1. Block caving with slicing and frontal (frontal-areal) ore drawing	Very thick, high dip outcropping or close to surface ores. Limited application in gently dipping and inclined ore deposits with weak and unstable overlying rocks. Hard medium stable and stable, low and medium grade ores. Limited depth of application. Unstable and medium stable host rocks. Ores are non-liable to spontaneous ignition and caking	High stoping productivity. Relatively low mining costs. High automation of stoping and use of mobile machinery. Sufficient extraction index with frontal-areal ore drawing. Ventilation due to mine depression	Probable hanging-up of host rocks with following burst-like destruction of large structural rocks. Forced ventilation of ore drawing-off workings (Fig. 8)
	B. Sublevel caving	2. Sublevel caving with frontal (frontal-areal) ore drawing	Thick and very thick, high dip outcropping or close to surface orebodies. Blind deposits with unstable overlying rocks. Limited application in gently dipping and inclined deposits. Medium hard and hard ores, non-liable to spontaneous ignition and caking. Low and medium grade ores. Depth of application is to be determined	Separation of dirt bands to backfill. High stoping productivity. Mining in with many stoping faces, extracted ore quality control. Automation of stoping. Sufficient extraction index with frontal-areal ore drawing. Ventilation due to mine depression	Probable hanging-up of overlying rocks, displacement and burst-like failure of large structural blocks. Forced ventilation of ore drawing-off workings (Figs. 9a, b)
		3. Strike-line sublevel stoping	Thin and medium thick, high dip orebodies. Mining front divaricates. Medium stable ores,	Use of mobile machinery, high productivity. Automation	High ore losses. High dilution, inclusive of secondary dilution (Fig. 10)

(continued)

Table 1 (continued)

Class	Group	Mining method	Application conditions	Advantages	Disadvantages
			stable host rocks. Low and medium grade ores. Depth of application is to be determined		
		4. Dip-line sublevel stoping	Thin and very thin, high dip orebodies, medium stable ores, stable host rocks. Depth of application is to be determined	Selective mining, without nonmetallic rocks, slot faces. Comparatively high ore extraction index	High labour intensity. Great amount of preparatory driving. Use of portable equipment (Fig. 11)
III. Ground control with backfill and caving	A. Mining with alternating backfill and caving	1. Primary horizontal slicing with ascending (descending) mining and paste backfill and secondary block (sublevel) caving	Thick and very thick, gently dipping and weakly inclined orebodies, unstable and medium stable ores, medium stable overlying rocks. Medium grade ore. Depth of application is to be determined	Overlying rock mass stability. Lower costs as compared with Class I methods	Mining in stages. Higher requirements to ore extraction standards. Lower extraction index as compared with Class I methods (Fig. 12)
		2. Continuous room work with primary mining with backfill and secondary mining with block (sublevel) caving	Thick and very thick, gently dipping and weakly inclined orebodies. Medium stable ores and host rocks. Medium grade ore. Depth of application is to be determined	Overlying rock mass stability. Higher stoping productivity as compared with the previous method	Mining in stages. Higher requirements to ore extraction standards. Lower extraction index as compared with Method 1 in Class II

table includes references to the corresponding figures

- the mining methods should be obligated to meet the stringent standards of operations in the conditions of rock burst hazard;
- the classification is for industrial-scale mining, with only the exclusion of thin ore deposits where portable mining equipment is unavoidable due to space-limited environment;
- the secondary criteria should be disregarded, for example, when strike-line or dip-line mining is governed not by the mining method, but by the parameters of the deposit and its mining-technical and geomechanical conditions;
- the systems with support are withdrawn from the classification as all of the known mining methods involve the support; and
- the basic classification criterion allows entering any new mining method to the classification.

Thus, in accordance with the effective ground control methods, we divide deep mining system into three classes:

1. Class I—mining with backfill,

2. Class II—mining with overlying (host) rock caving, and
3. Class III—combined mining with backfill and caving.

Classes I and II are commonly known from technical literature and the practice of underground mining. We would only note the undesirable large-scale blasting during mining with caving and frontal ore drawing at rock burst hazardous deposits. Large-scale explosions release huge energy, which initiates displacement of large rock blocks, causes dynamic events in the rock mass and failure of the weakened ore drawing-off level. These events are frequent at the Tashtagol iron-ore deposit, where the mining method includes block caving, vibration areal drawing of ore and large-scale block breakage. The Kiruna Mine in Sweden has the same rock mechanics and identical depth of mining, but with sublevel caving, slice breaking and frontal ore drawing. As a result, dynamic pressure manifestations are absent here. Therefore, we include only slice breaking with frontal and frontal-areal ore drawing into our classification (Freidin et al. 2008).

The technologies involved with the combined ground control methods are as follows:

- paste filling costs are expensive, and
- mining of low and mid-grade ores calls for cheaper methods.

In particular, partial backfill is admissible in thick and very thick gentle and weak-inclined deposits, with the purpose of providing the roof support and smooth sagging, limited displacements and strains of the host rocks. In this case, the filled areas alternate with the areas of mining under the caved roof formed as a stable dome. First, mining captures areas with artificial pillars, and secondly, the areas with temporarily retained ore pillars. The smooth sagging of the roof is ensured with the help of the artificial pillars, the sides of which are supported by caved overlying rocks. Parameters of these pillars should limit the rate of the roof sagging to the values of mining with full backfill. The width of the temporary ore pillars is designed with allowance for the stable span. Depending on the stability of ore and host rocks, and orebody thickness, mining with backfill may include horizontal slicing with ascending (or descending) pillar mining, and the temporary pillar mining may involve sublevel caving (for very thick orebodies) or block caving (for thick deposits). The offered classification of the mining methods is presented in Table 1. The information in this table in terms of mining methods is further depicted in a series of related figures.

Conclusions

This classification of mining methods for deep orebodies has been offered for the first time, and is based on the underground mining practice in Russia, in particular, in Norilsk Region. The authors think the classification may successfully be used for selecting and optimising the extraction of rockburst-hazardous ore and rock masses.

References

Agoshkov MI (1965) Calculating and designing ore mining methods and technologies. Nauka, Moscow

Baikonurov OA (1969) Classification and selection of the underground mining methods. Nauka, Alma-Ata

Bronnikov DM, Zamesov NF, Bogdanov GI (1982) Deep ore mining. Nedra, Moscow

Freidin AM, Neverov SA, Neverov AA (2008) Mine stability with application of sublevel caving schemes. J Min Sci 44:82–91

Imenitov VR (1978) Underground mining methods for ore deposits. Nedra, Moscow

Khomyakov VI (1984) Foreign experience of mining with backfill. Nedra, Moscow

Oparin VN, Rusin EP, Tapsiev AP (2007) World experience gained in underground mining automation. SO RAN, Novosibirsk

Pilenkov YY, Freidin AM, Antipov AV (1990) Estimation of natural impact of the origination of rockburst hazard at shallow depths. In: Rock pressure and underground ore mining technology for large depths, IPKON AN SSSR, Moscow

Trushkov NI (1947) Ore mining, volume II: mining methods. Metallurgizdat, Moscow

Yun RB, Gerasimenko VI, Malyshev VN (1997) Dynamic rock pressure manifestations at Zheskazgan deposit. Gorny Zhurnal 3

Zamesov NF (1979) Influence of the ground control on the design of the mining method for gentle ore formations. In: Problems of underground ore mining at large depths, IPKON AN SSSR, Moscow

Grade Uncertainty in Stope Design—Improving the Optimisation Process

N. Grieco and R. Dimitrakopoulos

Abstract Decisions in the mining industry are made in the presence of uncertainty whether it is in the form of technical, financial or environmental risk. In recent years, the main focus of uncertainty has been the mineral resource. Methods for assessing and quantifying grade risk in open pit operations has lead to the ability to forecast problems and improve the design and planning process by integrating this risk. This paper successfully implements these risk-based methods in an underground stoping environment using data from Kidd Creek Mine, Ontario, Canada. Risk is quantified in terms of the uncertainty a conventional stope design has in contained ore tonnes, grade and economic potential. A mathematical formulation optimising the size, location and number of stopes in the presence of uncertainty is introduced and applied. The implementation of different geostatistical simulation methods to the optimisation formulation is discussed briefly and observations made.

Introduction

Risk is present in all facets of mining be it technical, financial or environmental (Rendu 2002). When determining the feasibility of a project the uncertainty associated with all sources must be considered and contingencies made. Geological uncertainty is a major component of technical uncertainty, along with mining, and has been isolated as a primary source of risk affecting the viability of projects. This uncertainty is recognised as the key factor responsible for many mining failures (Baker and Giacomo 1998; Vallee 1999). Hence, the necessity to quantify geo-

N. Grieco (✉)
AMEC Americas Limited, 2020 Winston Park Drive, Oakville, ON L6H 6X7, Canada
e-mail: nikki.grieco@amec.com

R. Dimitrakopoulos
COSMO Laboratory, Department of Mining, Metals and Materials Engineering,
McGill University, Montreal, QC H3A 2A7, Canada
e-mail: roussos.dimitrakopoulos@mcgill.ca

R. Dimitrakopoulos (ed.), *Advances in Applied Strategic Mine Planning*,
https://doi.org/10.1007/978-3-319-69320-0_33

logical risk is well appreciated. Modelling geological uncertainty in a mineral resource can be achieved through conditional simulation technologies. The last few years in open pit mining these technologies have been coupled with mine design optimisation methods to assess risk in conventionally generated mine designs and production schedules. The approach allows planners to anticipate fluctuations in key project parameters that would otherwise be impossible (Ravenscroft 1992; Dowd 1997; Dimitrakopoulos et al. 2002). These studies have also documented that conventional methods may be misleading in their forecasts as they assume certainty. Recent developments in open pit mining show that direct integration and management of inherent grade risk in mine design and planning have begun (Dimitrakopoulos and Ramazan 2004; Ramazan and Dimitrakopoulos 2013, 2017, this volume; Menabde et al. 2017, this volume; Froyland et al. 2017, this volume). The developments provide the opportunity to generate substantially more profitable mine designs; for example, Godoy and Dimitrakopoulos (2004) report a 28% higher NPV from managing geological risk. It is logical to consider how to develop concepts and similar risk-based technologies for underground mining methods.

Optimisation in underground mine design has had less routine application than open pit mines, which is attributed to the diversity of underground mining methods that does not allow the production of general optimisation tools. Related in the technical literature is the work of Ovanic (1998) who considers the economic optimisation of stope geometry, a topic directly linked to the present study; and work on conventional stope optimisers (Thomas and Earl 1999; Ataee-pour and Baafi 1999). None of these approaches consider risk and hence assume the inputs are certain. Limited initial work reported, combines simulated orebodies and grade risk models with conventional optimisers (Myers et al. 2007, this volume); these however, are limited in their assessment as optimisation formulations are, in general, a non-linear process. Geological risk-based approaches to stope optimisation that directly integrate risk have been recently introduced (Grieco 2004) and open the possibility to further develop risk-based underground mine design. Current efforts, however, focus on the issue of grade uncertainty. In the longer run these developments need to be fused with geotechnical issues critical to underground mining (Bawden 2007).

This paper stems from the need to explore the contribution of geological uncertainty quantification and the direct integration to stope optimisation through a new, risk-based approach to stope design. In the following sections a conventional stope design in a part of Kidd Creek base metal mine, Ontario, Canada, is assessed in terms of copper grade risk, to explore uncertainty in terms of upside potential as well as downside risk. Subsequently, a probabilistic mathematical programming optimisation formulation is outlined and applied. The question of the sensitivity to the geostatistical simulation method is briefly visited. Finally, summary and conclusions follow.

Quantifying Grade Risk in Conventional Stope Designs: An Example

Grade risk quantification in a given underground stoping design is similar to that used in the design and production schedule of an open pit mine (Dimitrakopoulos et al. 2002). The quantification process requires two main components:

1. The design of a stoping outline generated using a conventionally estimated orebody model; and
2. A series of simulated realisations of the orebody, quantifying the uncertainty and in situ variability.

By putting each realisation through the stoping outline, as if the realisation is the actual orebody being mined, and accounting for potential production from the design, distributions or risk profiles for the pertinent project indicators are generated, thus allowing the quantification of geological uncertainty and risk assessment for the design being considered.

The Deposit and Study Area

Applying the concepts outlined for quantifying the grade risk in a conventional stope design is presented with a case study involving data from Falconbridge Ltd's Kidd Creek Mine. Kidd Creek is a volcanic massive sulfide deposit located in Ontario, Canada and produces about 7000 tonne per day (Roos 2001) from two major orebodies containing silver, copper, zinc and lead, the main commodities. Production began in 1966 via an open pit mine and has extended into three underground mines reaching depths of over 2000 m and employing various mining methods including sublevel caving, open stoping and sublevel stoping.

The focus of this study is a densely drilled area located in the copper concentrated stringer ore 1400 m below the surface in Phase I of Mine No 3. The drill hole configuration consists of 37 drill holes with 1.5 m copper composites in nine vertical fans that are spaced approximately four metres apart. The resulting samples show a high-grade zone in the central region. Statistics outlining the distribution of declustered copper samples is given in Table 1.

Table 1 Declustered data statistics of copper

Statistic	Declustered data set
Number of samples	2723
Mean	2.43%
Standard deviation	3.17%
Maximum	27.59%
75th percentile	3.00%
Median	1.34%
25th percentile	0.54%
Minimum	0.0%

Mining in this region is via open stoping methods with stope sizes typically 15 m wide by 20 m long by 40 m high. Blast rings are spaced generally every three metres and have a copper cut-off of 3%.

Generating Estimated and Simulated Orebody Models

Estimation methods are by construction smoothing operations. Conditional simulation methods aim at modelling the in situ spatial variability of a given attribute and, unlike the equivalent estimation approaches, reproduce the data histogram and spatial continuity. At Kidd Creek, the study area is first geostatistically estimated, producing 16,236 blocks within the orebody model. Blocks are estimated with a block size of 3.0 m $\times$ 3.0 m $\times$ 4.5 m, spanning 123 m in the east, extending 51 m in the north and reaching 99 m in the vertical direction. A horizontal section of this estimated model is shown in Fig. 1. The same area of the deposit is then geostatistically simulated using the well-established sequential Gaussian simulation method or SGS (Goovaerts 1997). Forty realisations of the deposit are generated on a 1.5 m $\times$ 1.5 m $\times$ 1.5 m grid of 19,880 nodes. Figure 2 shows a simulated realisation of copper grades of the same horizontal section as in Fig. 1. When comparing the estimated and simulated models in Figs. 1 and 2, both reproduce the regions of high-grade mineralisation in the drill hole configuration. The figures also show the typically smooth representation of reality by the estimated model whilst the simulated realisation reflects the likely in situ copper variability.

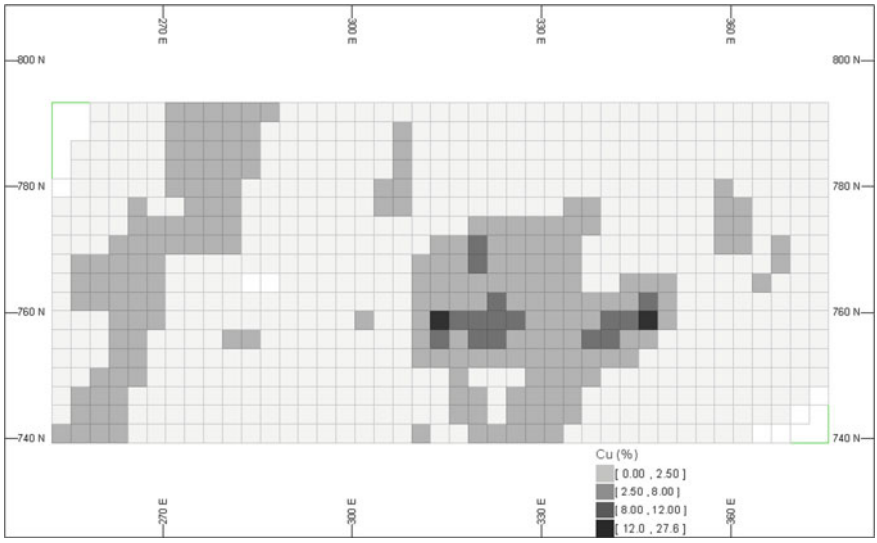

Fig. 1 Horizontal section of the estimated orebody model

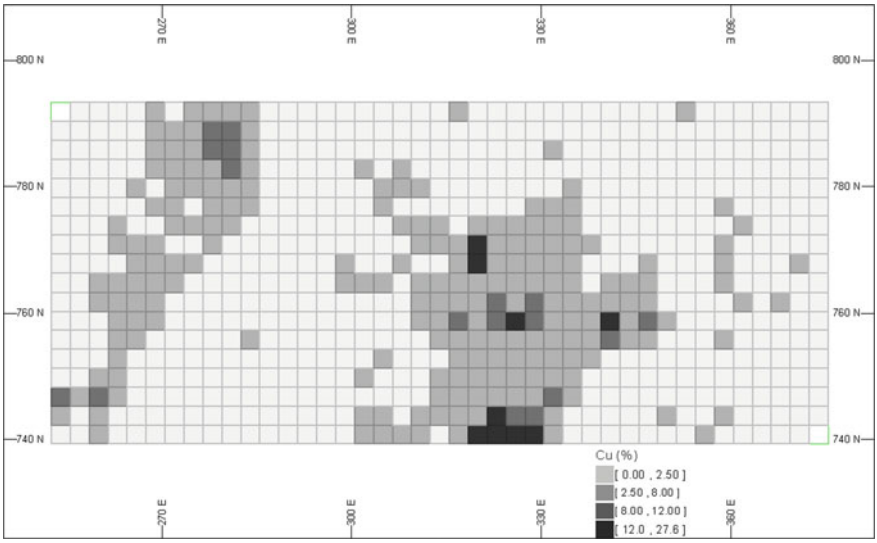

Fig. 2 Horizontal section of a simulated orebody model

Risk Quantification

In establishing a conventional stope design, a conceptual stoping layout recognising potential development and stoping levels must be first determined. Due to the vertical extent of the orebody models, two potential stoping levels are configured accounting for required drilling and hauling levels (Fig. 3). It is assumed that the lower level will be mined and backfilled before the upper level is extracted. Accounting for this stoping layout, a stope outline is produced given the estimated copper grade model using the DATAMINE™ floating stope facility, hence providing a conventional design for which a risk quantification and analysis can be performed. Figure 4 shows a three-dimensional view of the conventional outline generated here incorporating both stoping levels.

For the quantification of copper grade risk in this conventionally generated stope design, first, the simulated copper realisations are re-blocked into mineable rings by averaging the nodes contained within consecutive ring dimensions (15 m × 3 m × 40 m). Then, the conventional design outline is put through each of the orebody realisations and values pertaining to copper grades are recorded. It is subsequently simple to calculate for a set of realisations, such as the 40 here, the ore tonnage, metal, average grade and revenues or any other project indicator, the corresponding histogram of possible outcomes and from that histogram statistics of interest such as the various percentiles and so on. The following discussion refers to the risk profiles of some project indicators.

Figure 5 depicts the risk profiles for the upper and lower stoping outlines providing a means of quantifying copper grade risk in terms of the potential average

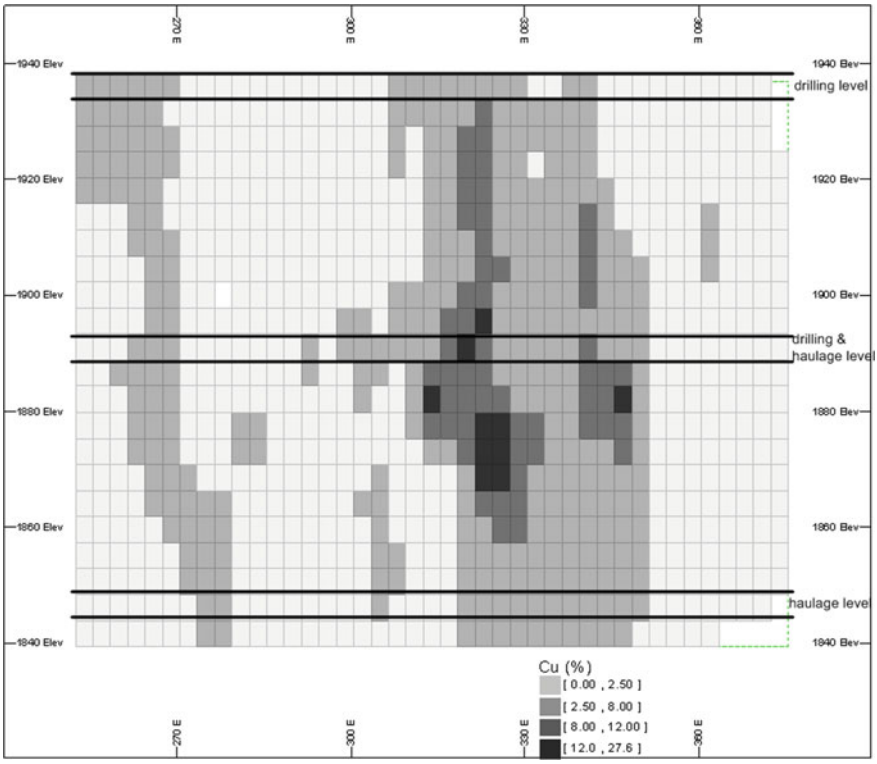

Fig. 3 Stoping layout indicating two stoping levels

copper grade the conventional design could contain. The conventional design and approach tend to underestimate the likely contained grade in the lower stoping level, while in the upper level tends to overestimate copper grade.

For analysis purposes only, the rings within the design outline that are less than 3% copper are removed to uncover how the grade uncertainty within the orebody model effects the amount of ore tonnes, metal and economic potential that could in reality, be realised. Figures 6, 7 and 8 illustrate the resulting risk profiles of these parameters respectively. Figure 6 also highlights the amount of material within the original design outline before any waste rings are removed (black diamonds). This demonstrates a potential for the conventional outline (both levels) to contain up to 32% waste, significantly affecting the tonnes expected to reach the mill. Both Figs. 6 and 7 illustrate a generally small risk the conventional outline presents in the amount of ore and metal tonnes expected from the upper level, as the extreme grade values present a tight distribution in which the expected values fall.

Figure 8 shows the results of an economic evaluation of the stoping levels using values representing the present value before tax. The figure illustrates significant risk in the conventional outline's ability to predict its potential economic value in each level. In addition, the single estimate in the lower level is 17% less than the

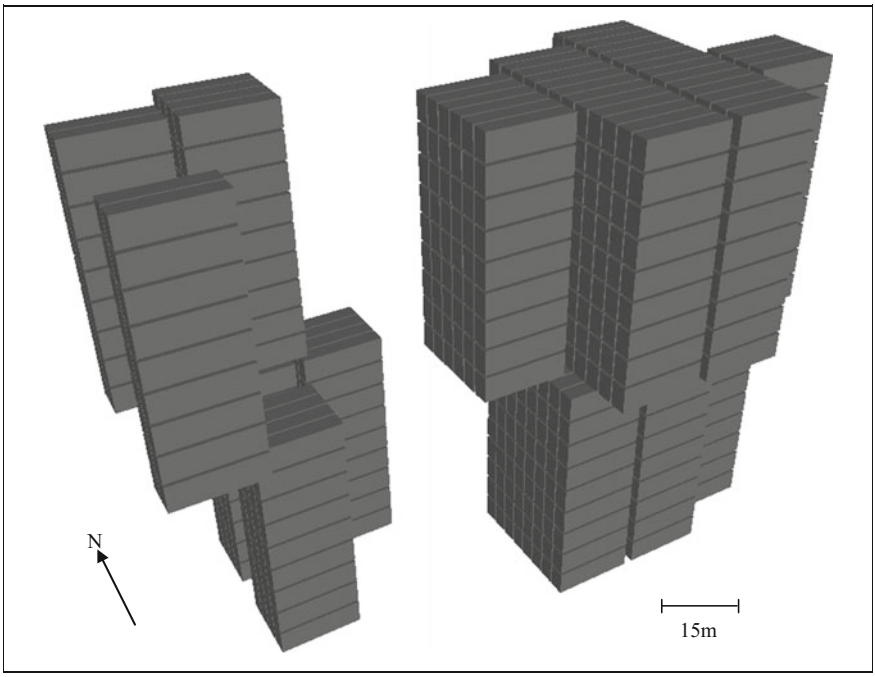

Fig. 4 Conventional stope envelope

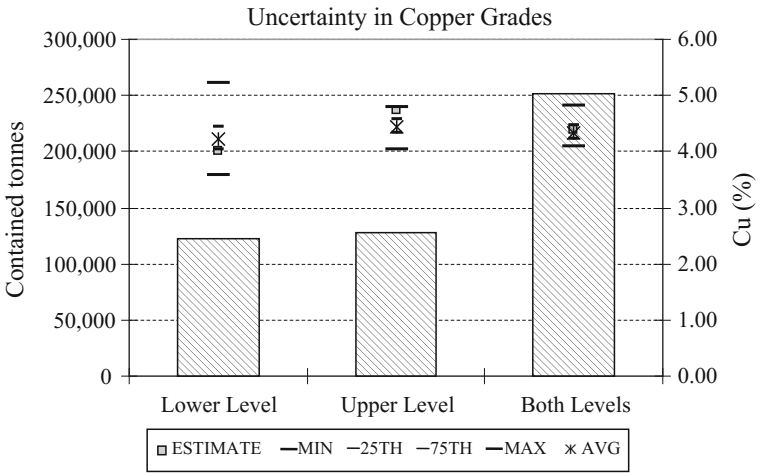

Fig. 5 Quantifying the conventional stope envelope's uncertainty in copper grade

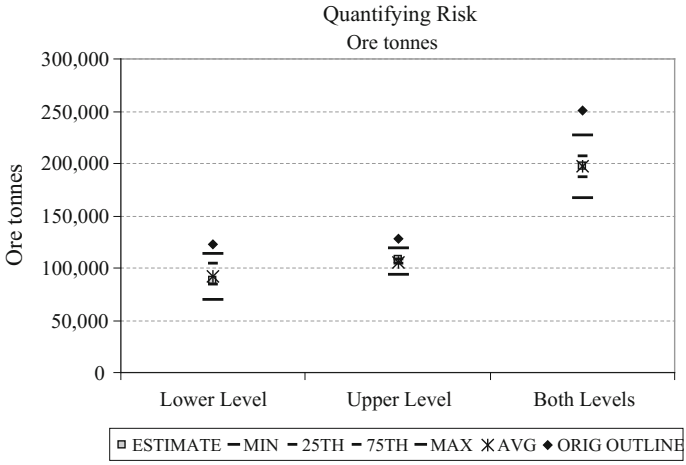

Fig. 6 Quantifying the conventional stope envelope's uncertainty in contained ore tonnes

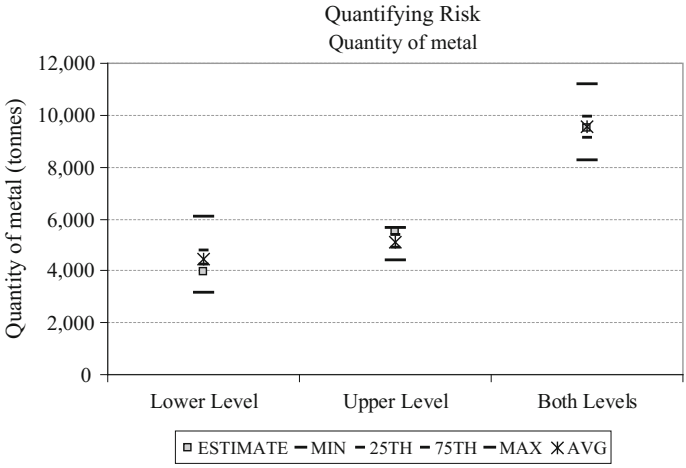

Fig. 7 Quantifying the conventional stope envelope's uncertainty in contained metal

average predicted economic potential expected, while the estimate in the upper level is 33% above this equivalent average value. Since each level will likely be mined in separate periods, the profit made in the upper level cannot compensate for the potential loss (7%) in the lower level. This potential to incur monetary losses on production could, for example, affect monthly profits expected from this part of the mine.

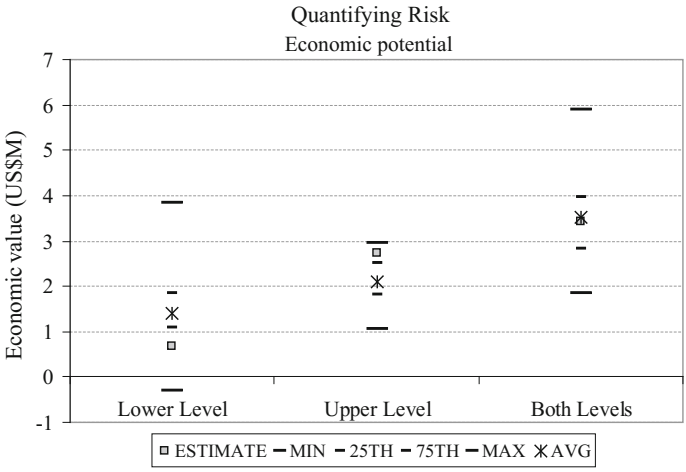

Fig. 8 Quantifying the conventional stope envelope's uncertainty in economic potential

The conventional stoping design in this specific example is generally straightforward and is found to provide a reasonable assessment of the average economic value of the design. However, several points can be made, including the following:

1. The size of the study area is small and at the same time uncommonly well drilled (nearly three times the density of fans normally expected), thus results are not surprising;
2. If the ability to quantify risk was not available, the assessment would not be possible; and most importantly
3. Conventionally, one is unable to foresee the significant upside potential and/or downside risk the conventional design may actually produce (e.g. Table 2).

In the example presented here, quantifying the risk in terms of economic potential recognises the potential to earn 62% more and the risk of earning 38% less than expected. In dollar terms, this conventional design could be worth as little as 1.8 million dollars or as much as 5.9 million dollars. The above lead to considerations such as:

Table 2 Project indicators based on the conventional stope design

Model	Ore (t)	Metal (t)	Cu (%)	Economic potential ($)	Economic potential % difference
Estimate	196,830	9490	4.82	3,412,999	–
Realisation 3	191,909	8769	4.57	2,285,625	−33
Realisation 18	167,306	8228	4.92	1,858,484	−46
Realisation 31	216,513	11,187	5.17	5,905,110	+73
Realisation 35	211,592	10,492	4.96	4,820,407	+41

1. Can grade uncertainty be not only quantified for a design, but also employed during the design process to capture the upside economic potential of the deposit?
2. Can designs be based on a minimum acceptable risk? And generally, can the design process manage grade risk directly and generate benefits?

In the last decades, major improvements have been made to the time-consuming manual approach to stope design. However, these computer-aided tools are limited in their ability to mathematically optimise the location of designs under uncertainty similarly to the optimisation methods in open pit mine design. With a methodology in place for quantifying grade risk in conventional mine design, the limitations of existing computer planning and optimisation tools force the development of a new optimisation approach based on and integrating grade uncertainty directly into the optimisation process, essentially creating a more versatile computer-aided tool.

Generating Risk-Based Designs

Mathematical programming methods provide a means of optimising an objective function subject to a set of constraints through a mathematical formulation. Such methods allow the development of formulations that integrate grade uncertainty directly into the optimisation process, as well as allow the consideration of a user-selected minimum acceptable risk. In this section, a mathematical programming formulation considering the above to optimise the location of stopes in the presence of grade uncertainty is presented and used at Kidd Creek to produce a risk-based design for comparison and analysis.

The Optimisation Formulation

A mixed integer programming (MIP) formulation with the aim of locating an optimal stope layout is presented here. This optimal layout is defined by the size, location and number of stopes within an orebody model. Such a model is described as consisting of a series of layers, each of which is composed of a number of rows referred to as panels, where the panels are made up of a series of rings. With multiple simulated orebodies available, each ring can be identified by a probability to be above any cut-off grade and have an average grade, hence introducing grade risk into the process.

The objective function of the formulation focuses on maximising the grade content within a layout in the presence of grade uncertainty, and is:

$$\text{Maximise} \sum_{j=1}^{m} \sum_{i=1}^{n} g_{ij} p_{ij} B_{ij} \tag{1}$$

where:

m is the number of panels within the orebody model
n is the number of rings within a panel
p_{ij} is the probability of ring ij being above a specified cut-off
g_{ij} is the expected grade of ring ij above the cut-off
B_{ij} is a binary variable representing every ring within the model and identifies whether it has been selected ($B_{ij\ =1}$) or not ($B_{ij} = 0$) in the optimal layout

Further to the above, the presence of simulated orebody models allows risk-based designs to be generated for a given minimum level of acceptable risk specified by the planner or decision-maker. The following constraint restricts the total average probability of selected rings within a panel to be greater than or equal to an assigned value representing the minimum acceptable level of risk (PL).

$$\sum_{i=1}^{n} (p_{ij} - PL) B_{ij} \geq 0 \tag{2}$$

By changing the value of the minimum acceptable level of risk, PL, a number of different risk-based designs can be generated, compared and assessed. Risk profiles can then be generated for the key project indicators by putting each outline through all simulated realisations, in the same procedure that was used to quantify risk in the conventional design of the previous section. A design that best suits the operational requirements can be selected with the risk being quantifiably assessed (Grieco 2004).

The formulation above is also constrained by limitations on the stope size—both minimum and maximum, which are a direct reflection of the geotechnical restrictions and production requirements of the area. These stope size constraints are based on the number of consecutive rings allowed to form a single stope. The size of the pillars between two primary stopes is also considered. This algorithm determines the minimum number of rings to be left un-mined between stopes and is directly related to the size of the stopes surrounding them. The larger a stope, the larger the pillar is.

Application at Kidd Creek

The MIP formulation for optimising a stope as above is applied to the study area at Kidd Creek mine. Geotechnical requirements in the region restrict a given stope to consist of a minimum of two rings and a maximum of seven. Applying a cut-off grade of 3%, each ring within the re-blocked orebody model (same configuration as the one used in simulation) is represented by the probability of being above 3% copper and the average copper grade above this cut-off. A risk-based design with a minimum acceptable level of risk at 80% is generated. Figure 9 illustrates a

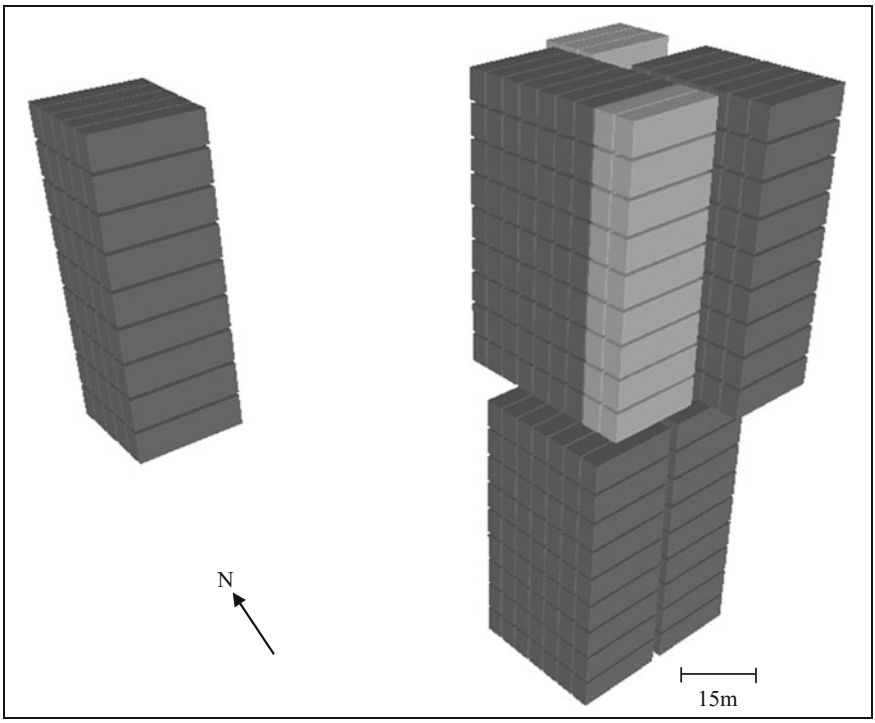

Fig. 9 LP stope design layout based on SGS and 80% acceptable level of risk

three-dimensional aspect of the resulting design layout using the simulated model, with dark grey rings representing primary stopes and light grey rings the recoverable pillars. In comparing the size and shape of the conventional design outline (Fig. 4) with the new, risk-based design, a notable difference in size is recognised. Introducing the minimum acceptable level of risk has limited the amount of waste (tonnes) contained within the new design as it forces the stopes within a given panel to have an average probability above 80%. This approach grants the planner control over the level of risk permissible within a given design.

The formulation constraints require the stopes and pillars to contain a minimum of two rings and a maximum of seven, providing an optimal combination for obtaining the most metal. The conventional approach produces an envelope of rings for which some combination satisfies the minimum grade and size requirements and further development of a mineable stope layout is needed.

The fluctuation in copper grade within the risk-based design can be predicted by putting the outline through all simulated realisations generated with the SGS method, similarly to the conventional design in a previous section. Figure 10 illustrates the amount of contained material within the primary stopes and recoverable pillars, and the potential grade variation within each. Although grade uncertainty has been accounted for within these designs, the simulated realisations

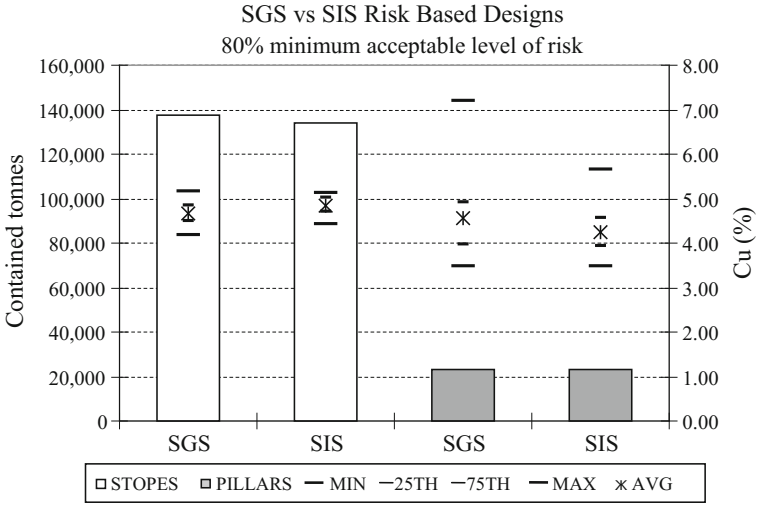

Fig. 10 Primary stoping layout for LP designs based on SGS and SIS orebodies and 80% acceptable level of risk

reflect the variability in grade within this area. Additional information shown in Fig. 10 is discussed in the next section.

Effects of the Simulation Method

Conventional estimation approaches used for orebody modelling differ in their formulations as well as orebody models they generate from the same original dataset. Similarly, different implementations of the same method will result in somewhat different representations of the orebody being modelled. The same is also true for simulation methods and the orebody models generated, including the average ring grades and probabilities above the cut-off considered in the stope optimisation approach used here. Thus, it may be of interest to consider how the stope optimisation results may differ, if the orebody used was simulated independently and with a different simulation method. For this study, an alternative method is the sequential indicator simulation method or SIS (Goovaerts 1997) and was implemented independently from this study at Kidd Creek by Kay (2001). The latter study provides 40 simulated realisations of the same broader domain.

Figure 10 compares the two designs (both with an 80% acceptable level of risk) in terms of the contained tonnage and grade for both the primary stoping and pillar recovery layouts. As expected, these design layouts contain the same amount of tonnes with only slight variations in potential copper grade. The wider risk profile

in the pillar recovery layout is not unexpected due to the limited selection of rings remaining for the second pass of the optimiser. The limited extent of pillar recovery can be explained using the same rationale. From the observations made from Fig. 10, the difference in simulation method cannot be said to affect the stoping optimising process.

Figures 11 and 12 illustrate, on a given section, the location and size of the relative stoping (dark grey) and pillar (light grey) layouts based on the simulated orebody with the two different methods at an 80% probability above cut-off set as the minimum acceptable risk. The figures reflect how the central high-grade zone evident in the drill holes is consistently reproduced by both simulation techniques, as expected, and hence located by the optimisation process at the specified probability constraint. The lower level stoping layouts are almost identical. In the upper level, the SGS-based layout considers a stope in the north-east part of the study area not included in the layout shown in the figure based on SIS at the same 80% probability. However, if the minimum acceptable level of risk governing these designs is lowered to say, 70%, the same part of the study area is highlighted as the location of a possible stope by the optimization based on the SIS models. This stoping layout in the upper level based on the SIS models, recongnises a larger stope in the sixth panel whose extent is not considered by the layout based on the SGS models. These minor differences between designs are normal and not

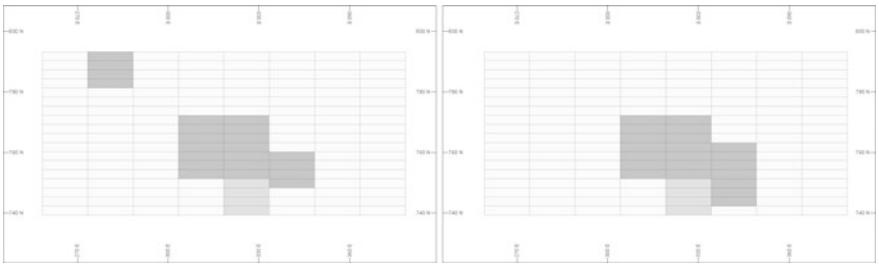

Fig. 11 Horizontal section of the risk-based stope designs in the upper level from the orebodies generated with SGS (left) and SIS (right), for 80% acceptable level of risk

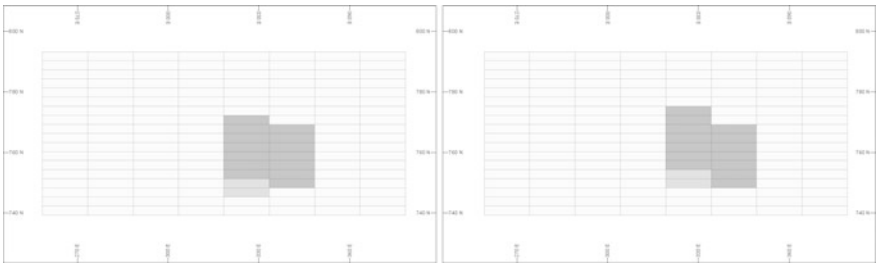

Fig. 12 Horizontal section of the risk-based stope designs in the lower level from the orebodies generated with SGS (left) and SIS (right), for 80% acceptable level of risk

significant. Similarly to the various conventionally used estimation methods for orebody modelling leading to variations in stope designs, different simulation methods will perform somewhat differently from each other, as their specific technical specifications and characteristics dictate. For example, SGS is based on one grade variogram whilst SIS requires multiple variograms, each for a series of grade cut-offs (Goovaerts 1997). The discrepancies arising from different methods are more extensively documented in other areas of application of simulations such as grade control that have long been in practice (Dimitrakopoulos, in press). Independent implementations provide a source of variance for the results, because the detailed specifications of the simulated orebody models and the parameters for their generation are different. These deviations become apparent in the stoping layouts generated.

Summary and Conclusion

This paper extends concepts and technologies used in managing geological risk in open pit mines to underground mining methods. It shows that geostatistical simulation technologies allow grade risk quantification in a stoping design. The example from the Kidd Creek mine, Ontario, Canada illustrates how conventional technologies cannot quantify risk, thus are unable to foresee a significant upside potential and/or downside risk for the conventionally produced designs. The example shows a conventional design could be valued from as little as 1.8 million dollars to as much as 5.9 million dollars. To provide the means of incorporating risk in stope design, geological uncertainty is integrated into the design process through a new mathematical programming formulation that uses risk grades above a cut-off value for rings within a stope, as well as geometric and other traditional constraints. An additional constraint introduced is the minimum acceptable risk allowed in a design. The application shows that the risk-based approach has the ability to generate different designs that meet the pre-specified minimum acceptable risk with a desired risk profile accommodating the selection of designs with preferred upside/downside profiles. Grade uncertainty quantification may be based on different simulation methods. A comparison of orebody models constructed independently with the sequential Gaussian and indicator simulation methods show stope designs with some variation, which is not significant and considered normal when different methods are used.

The work presented here could be further developed. Such developments could include:

1. The formulation of a stope optimisation formulation that replaces the probability of grades above cut-off with the direct use of all available simulated orebodies, and thus integrate more geological information;

2. Consider sequencing and thus accommodate risk management and/or geological risk discounting as part of the stope design process; and
3. Extend to integrate geotechnical uncertainties starting from over-breaking and under-breaking.

Acknowledgements Special thanks to Paul Roos and Arie Moerman from Falconbridge, Kidd Creek mine who supplied the data and provided support. Thanks also to Mark Noppe and Jörg Benndorf for their constructive comments.

References

Ataee-pour M, Baafi EY (1999) Stope optimisation using the maximum value neighborhood (MVN) concept. In: Dagdelen K (ed) Proceedings 28th international symposium on the application of computers and operations research in the mineral industry. Colorado School of Mines, Golden, pp 493–501

Baker CK, Giacomo SM (1998) Resource and reserves: their uses and abuses by the equity markets. Ore reserves and finance. The Australasian Institute of Mining and Metallurgy, Melbourne, pp 65–76

Bawden WF (2007) Risk assessment in strategic and tactical geomechanical underground mine design. In: Dimitrakopoulos R (ed) Orebody modelling and strategic mine planning, 2nd edn. The Australasian Institute of Mining and Metallurgy, Melbourne, pp 263–271

DATAMINE™ (1995) Floating stope optimiser user guide, 1.2 edn. Mineral Industries Computing Limited, p 20

Dimitrakopoulos R, Farrelly CT, Godoy M (2002) Moving forward from traditional optimisation: grade uncertainty and risk effects in open-pit design. Trans Inst Min Metall, Sect A, Min Technol 111:A82–A88

Dimitrakopoulos R, Ramazan S (2004) Uncertainty based production scheduling in open pit mining. SME Trans 316:106–112

Dowd PA (1997) Risk in minerals projects: analysis, perception and management. Trans Inst Min Metall, Sect A, Min Technol 106:A9–A18

Froyland G, Menabde M, Stone P, Hodson D (2018) The value of additional drilling to open pit mining projects, in this volume

Godoy MC, Dimitrakopoulos R (2004) Managing risk and waste mining in long-term production scheduling. SME Trans 316:43–50

Goovaerts P (1997) Geostatistics for natural resources evaluation. Oxford University Press, New York, p 483

Grieco NJ (2004) Risk analysis of optimal stope design: incorporating grade uncertainty, M.Phil. thesis. University of Queensland, Brisbane, p 204

Kay MH (2001) Geostatistical integration of conventional and downhole geophysical data in the metalliferous mine environment, M.Sc. thesis. University of Queensland, Brisbane, p 204

Menabde M, Froyland G, Stone P, Yeates GA (2017) Mining schedule optimisation for conditionally simulated orebodies, in this volume

Myers P, Standing C, Collier P, Noppè M (2007) Assessing underground mining potential at Ernest Henry Mine using conditional simulation and stope optimisation. In: Dimitrakopoulos R (ed) Orebody modelling and strategic mine planning, 2nd edn. The Australasian Institute of Mining and Metallurgy, Melbourne, pp 191–200

Ovanic J (1998) Economic optimization of stope geometry, Ph.D. thesis. Michigan Technological University, Houghton

Ramazan S, Dimitrakopoulos R (2013) Production scheduling with uncertain supply: a new solution to the open pit mining problem. Optim Eng 14:361–380

Ramazan S, Dimitrakopoulos R (2017) Stochastic optimisation of long-term production scheduling for open pit mines with a new integer programming formulation, in this volume

Ravenscroft PJ (1992) Risk analysis for mine scheduling by conditional simulation. Trans Inst Min Metall Sect A Min Tech 101:A104–A108

Rendu J-M (2002) Geostatistical simulations for risk assessment and decision making: the mining industry perspective. Int J Surf Min Reclam Environ 16:122–133

Roos (2001) Underground tour guidebook. Kidd Creek Mine, p 21

Thomas G, Earl A (1999) The application of second-generation stope optimisation tools in underground cut-off grade analysis. Proceedings strategic mine planning. Whittle Programming Pty Ltd, Perth, pp 175–180

Vallee M (1999) Resource/reserve inventories: what are the objectives? CIM Bull 92 (1031):151–155

Strategic Optimisation of a Vertical Hoisting Shaft in the Callie Underground Mine

M. G. Volz, M. Brazil and D. A. Thomas

Abstract The Callie underground mine, located in the Tanami Desert in the Northern Territory, includes two parallel declines accessing a large orebody extending some two kilometres below the surface. One of several ideas considered in strategic mine planning is to incorporate a vertical hoisting shaft and an orepass as an alternative to trucking material to the surface along the declines. In this work, we use network optimisation techniques to investigate the feasibility of the proposed system, and to mathematically determine the optimum positions and geometry of the shaft, orepass and surrounding infrastructure. We propose a modelling procedure taking aspects from a mathematical problem, called the Fermat-Weber problem, which asks for a point minimising the sum of weighted distances to a given set of points. We describe the implementation of the procedure into a computer program for solving the problem iteratively, and present results over a range of infrastructure and haulage costs, decline gradients and life-of-mine (LOM) schedules.

M. G. Volz (✉)
TSG Consulting, Level 11, 350 Collins Street, Melbourne, VIC 3000, Australia
e-mail: marcus.volz@tsgconsulting.com.au

M. Brazil
Department of Electrical and Electronic Engineering,
The University of Melbourne, Parkville, VIC 3010, Australia
e-mail: brazil@unimelb.edu.au

D. A. Thomas
Department of Mechanical and Manufacturing Engineering,
The University of Melbourne, Parkville, VIC 3010, Australia
e-mail: doreen.thomas@unimelb.edu.au

R. Dimitrakopoulos (ed.), *Advances in Applied Strategic Mine Planning*,
https://doi.org/10.1007/978-3-319-69320-0_34

Introduction

Located in the Tanami Desert in the Northern Territory, approximately 550 km north-west of Alice Springs, the Tanami operations comprise a processing facility, several open pit mines, the Tanami Mill and the Callie Underground Mine. Gold was discovered at Tanami in 1900 and modern mining began in 1983 following an agreement with traditional landowners. Initial production came from the open pit mines at the Granites, while current production comes from the high-grade Callie underground mine at Dead Bullock Soak. The Callie underground mine services a large orebody running approximately in an east-west direction, plunging into the ground at an angle of about 45° towards the east (Fig. 1). The orebody is divided into two major veins. At the time of the study, the orebody had been accessed by a single decline, called the Callie decline, with material having been mined to a depth of about 1000 m below the surface (Fig. 2). Rock is extracted from the orebody in primary stopes, which are replaced with fill material to allow adjacent secondary stopes to be subsequently extracted. Once loaded onto trucks, ore is hauled along cross-cuts (horizontal tunnels) to the decline. Levels are at 40 m vertical intervals. In addition to the planned extension of the primary Callie decline, a secondary decline, called the Wilson Drill Decline (WDD), is to branch out from the Callie decline about 950 m below the surface (Fig. 2). Both declines are to have fixed gradients. Levels servicing the WDD are also at 40 m vertical intervals, however they are offset from the Callie levels. The Callie decline services the Wilson shoot, while the WDD is to service a second shoot called the Federation shoot.

One of several ideas considered in strategic mine planning is to incorporate a vertical hoisting shaft and an orepass as an alternative to trucking material to the surface along the declines. Using this system, ore is hauled to a common tipping

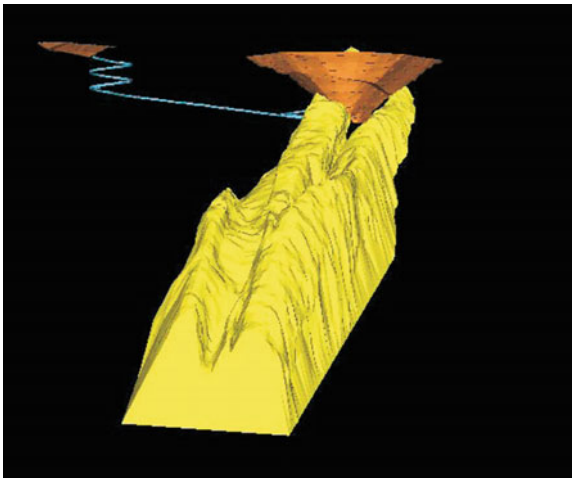

Fig. 1 Typical cross-section through the orebody (looking west)

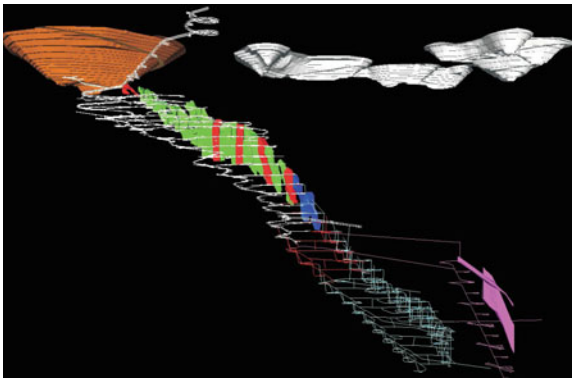

Fig. 2 The Callie underground mine (looking north), including the existing Callie decline (white), its planned extension (red/blue) and the proposed Wilson drill decline (pink)

level, called the haul level, where it is crushed, loaded into a skip and hoisted to the surface via the shaft. This method can provide significant reductions in operating costs, although it requires a large capital cost associated with a hoisting shaft. In addition to the shaft, it was proposed to include an orepass into the mine. An orepass is a near-vertical chute down which ore from upper levels is dropped to the haul level (which is three levels above the shaft base), and transported to the shaft in one of several ways, for example:

- Ore is loaded into a truck by a load-haul-dump vehicle at the bottom of the orepass. It is then trucked from the bottom of the orepass to the shaft.
- A load-haul-dump vehicle trams ore directly from the base of the orepass to the shaft.
- If the horizontal distance between the orepass and the shaft is greater than say 300 m, a loading chute may be installed at the base of the orepass, allowing trucks to be loaded automatically before transporting ore to the shaft. For operational reasons the orepass is assumed to be constrained to the northing 9250 N, which is about halfway between the two declines in plan.

The primary goal of this investigation is to mathematically determine:

- the optimum position (depth and plan coordinates) of the hoisting shaft;
- the optimum position (top, bottom and plan coordinates) of the orepass and identification of the levels which access the orepass; and
- the optimum geometry of the main haulage drive network at the tipping level and shaft haulage level.

The analysis is undertaken over a range of infrastructure and haulage costs, decline gradients and life-of-mine schedules.

Problem Data

The nominal data used for the purposes of this project is summarised here and includes mine costs, decline gradients, access points, life-of-mine schedules and no-go zones. Mine costs are listed in Table 1. A range of values have been provided for some of the items, so that sensitivity analyses could be undertaken to examine the effects of these parameters. All other costs are assumed to be fixed, in the sense that they are invariant to the geometry of the shaft, orepass and surrounding infrastructure. At the time this study was undertaken, the Callie and Wilson Drill declines were designed to about 1400 m below the surface with gradients 1:8 and 1:7 respectively. It is assumed that both declines will continue downwards in the same manner as the current design. An alternative scheme is to have the Callie decline gradient equal to 1:7 and the WDD gradient set at 1:6.

Access points are locations where the nominal cross-cuts intersect the declines. Each access point is designated a nominal level corresponding to its approximate Reduced Level (RL). The surface is at approximately 1400 m RL, and access points on the Callie decline extend from 340 to −660 m RL at 40 m vertical intervals (26 points), while access points on the WDD extend from 390 to 70 m RL, also in 40 m vertical increments (nine points). Hence in total there are 35 access points. Their associated declines, (X, Y and Z) coordinates and nominal levels are not provided in this paper. Three life-of-mine production schedules for the Callie underground mine were proposed. They are base, probable and best. Details of the three schedules are provided in Table 2. The predicted tonnage to be accessed from each of the 35 access points can be determined for the three schedules. To avoid disruption to the shaft over the life of the mine, it must avoid impinging on several

Table 1 Mine costs

Component	Cost
Shaft development	$25000/m, $50000/m or $75000/m
Orepass development	$1210/m
Level and haul drive development	$3265/m
Haulage up decline and across levels	$0.75/(t.km) or $1.05/(t.km)
Haulage down decline	$0.85/(t.km) or $1.20/(t.km)
Orepass fit-out	$1 M

Table 2 Base, probable and best life-of-mine schedules

Name	Callie decline			Wilson drill decline		
	Rate (Mt/a)	Quantity (Mt)	Final year	Rate (Mt/a)	Quantity (Mt)	Final year
Base	2	10	2015	0.35	1.4	2014
Probable	2.5	17.5	2018	0.5	2.5	2015
Best	3.5	30	2019	0.5	3.5	2017

no-go regions. Firstly, the shaft must not be too close to the orebody. The no-go region is modelled as a barrier around the Wilson and Federation orebodies. Polygons digitised around the boundaries of the orebodies were expanded 200 m in any direction. Secondly, the shaft is required to avoid faults by at least 50 m. The main haulage drive is allowed to pass through a fault so long as it does not travel along (parallel) to it for any great length, say, no more than 15 m at a time. Thirdly, the preferred area for the shaft collar is in a region south of the main entrance road.

After a preliminary analysis of the model, it was identified that the faults and surface infrastructure constraints could be relaxed. For the remainder of this paper we assume that the only the orebody standoff constraint is enforced.

Problem Formulation and Solution Procedure

Mathematical Network

Figure 3 shows: (i) a perspective view; and (ii) a plan view of the shaft, orepass and surrounding infrastructure.

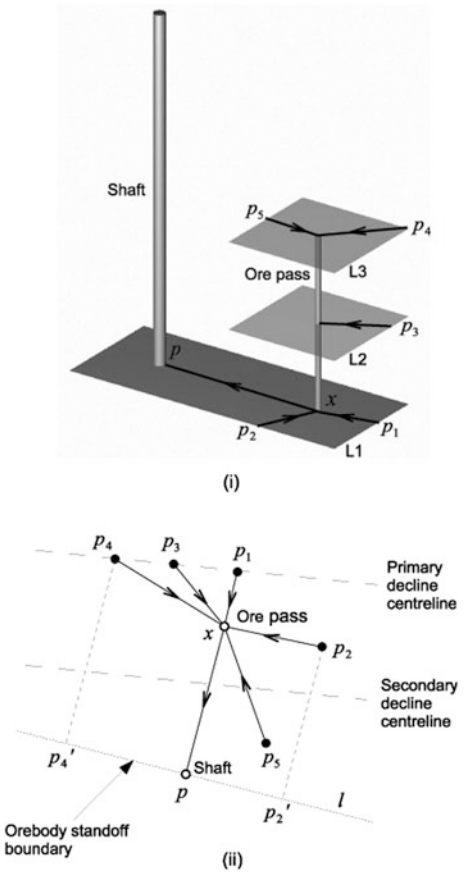

Fig. 3 (i) Perspective view and (ii) plan view of the shaft, orepass and surrounding infrastructure

Under this arrangement, ore from the lower levels is trucked up both declines to a level, L1, from where it is transported to the base of the shaft via a horizontal tunnel. Ore from the upper levels is trucked down both declines to another level, L3, from which it is transported via a horizontal tunnel to the top of the orepass. It is dropped down the orepass to L1 and transported to the shaft base. Ore from levels between L1 and L3 on the secondary decline is either trucked up to L3 or down to L1, whichever is closest. Ore from levels between L1 and L3 on the Callie decline also has the option of being trucked to an intermediate level, L2, which is between the top and bottom of the orepass. It is transported to a second tipping point to the orepass at L2 via a horizontal tunnel, dropped down the orepass to L1 and transported to the shaft base.

Let p_1, p_2 be points on the Callie decline and WDD respectively at L1, p_3 the point on the main decline at L2 and p_4, p_5 points on the two respective declines at L3. If levels L1, L2 and L3 are known, the five points are fixed points corresponding to access points on the two declines. Denote the plan location of the orepass by x and that of the shaft by p. While the orepass is allowed to be positioned anywhere on the northing 9250 N (which runs between the two decline centrelines), the hoisting shaft must avoid the orebody standoff no-go region. The boundary of this orebody standoff zone is modelled by the straight line l. Clearly, the optimal position of p will be on l, rather than behind it, since in the latter case, the length of the tunnel connecting the two points can be reduced by moving p onto l. The system of tunnels can be modelled as a mathematical network T with a star topology, where x is the centre of the star, $p_1,\ldots, p_5$ are fixed and p is free to slide along l.

For a given LOM schedule, the quantities $t_1,\ldots, t_5$ of ore (in tonnes) can be computed for each fixed point $p_1,\ldots, p_5$. For example, the quantity of ore assigned to p_1 is the sum of tonnages from the levels on the Callie decline below L1 and the levels immediately above L1 on the same decline.

Let d denote the cost per unit length of developing a tunnel, and h the cost per unit length of hauling a unit quantity of ore along a level tunnel. Then the sum of development and haulage costs for the tunnel from $p_1,\ldots, p_5$, to x is $(d + ht_i)l_i$, where l_i is the length of the tunnel from p_i to x.

Thus the associated weight is $w_i = d + ht_i$. Similarly, the weight associated with the tunnel from x to p is:

$$w_6 = d + h\sum_{i=1}^{5} t_i,$$

since that tunnel routes all the ore from the orepass base to the shaft base.

The total cost of the mine (ignoring fixed costs) has the following components:

- shaft development, which depends on the shaft depth (determined by L1);
- decline haulage, which depends on the levels L1, L2 and L3; and
- surrounding infrastructure development and haulage, which depend on the levels L1, L2 and L3 and the plan positions of the orepass and shaft.

Hence, the total cost of the mine can be minimised by determining an optimal layout of the shaft, orepass and surrounding infrastructure.

The Fermat-Weber Problem

The problem of minimising the development and haulage costs associated with the horizontal tunnels connecting the declines, orepass and shaft can be solved by projecting everything onto a horizontal plane (Brimberg et al. 2002). Then the problem reduces to positioning x and p so as to minimise the function:

$$f(x,p) = \sum_{i=1}^{6} w_i l_i$$

This is an extension of a well known mathematical problem called the Fermat-Weber problem. The problem asks for a point, called a Fermat-Weber point, minimising the sum of weighted distances to a set of given points in space. In this case the orepass position is the Fermat-Weber point, while the points $p_1,\ldots, p_5$ and p are the fixed points.

An added complexity is that the shaft is not fixed, but is free to slide along the line l. We can immediately state the following result. If $x = x_0$ and $p = p_k$ minimise the cost function $f(x, p)$, then the line segment between x_0 and p_k is perpendicular to l. Thus, the position of p is a function of the position of x. This can be seen by noticing that if x_0p is not perpendicular to l, then the length of x_0p can be reduced by moving p along l until it is. Hence, for given L1, L2 and L3, the optimum network of tunnels interconnecting the declines, orepass and shaft can be obtained by solving an extension of the Fermat-Weber problem. This problem can be solved iteratively using a well known descent algorithm due to Weiszfeld (1937). For this study, the algorithm was generalised to account for the fact that the shaft can lie anywhere on the orebody standoff boundary and is not confined to a fixed point. We do not give details of this amended algorithm in this paper.

Iterative Solution Procedure

Initially, we proposed a simplified procedure for determining the positions, lengths and orientations of the shaft, orepass and main haulage drive. By this procedure, the problem was broken down into two subproblems:

1. The optimum shaft depth was computed based on ‘vertical’ costs—decline haulage, shaft development and orepass development—using a further extension of the Fermat-Weber problem, called the gradient-constrained Fermat-Weber problem (see Brazil et al. 2005).

2. A minimum-cost network interconnecting the declines, orepass and shaft was constructed at the level determined by the first subproblem. The optimum network was computed based on 'horizontal' costs—haul drive development and haulage—using the Fermat-Weber problem described above.

Although the simplified procedure seems to obtain good intuitive solutions, it does not guarantee an optimal solution for a given problem. To see this, suppose the haul level is placed at 100 m RL based on vertical costs. Numerical tests have shown that moving the haul level to 140 m RL can reduce the cost of the network of tunnels. If the reduction in horizontal costs outweighs the increase in vertical costs, then the solution determined by the simplified procedure is not optimal. Hence, we propose a rigorous procedure which guarantees an optimal solution for a given problem. Refer to Fig. 3. Placing the haulage drive L1 at each of the 35 levels (on both declines) from −660 m RL up to 390 m RL, the vertical costs can be computed. If an orepass is used, it is tested at every level above the haulage drive, and if an intermediate tipping point is added to the orepass, it is also tested at every level between the haulage drive and the top of the orepass. For every possible arrangement of L1, L2 and L3, a minimum-cost network interconnecting the declines, orepass and shaft is computed using the amended Fermat-Weber problem. Once the cost for every mine layout has been computed, the arrangement giving the lowest cost is selected as the globally optimal solution.

Results

The mathematical model and algorithm described in the previous section were implemented into a computer program for determining the optimum shaft, orepass and surrounding infra-structure layout for a given set of infrastructure and haulage costs, decline gradients and life-of-mine schedules. Thirty-six tests were undertaken for each of three cases—no orepass, one orepass and one orepass with two tipping points (108 tests in total).

The gradients and cost parameters were varied across the tests. Optimum haul levels and costs for the three orepass configurations are compared in Table 3.

Analysis

In this section we analyse the results of Table 3.

Table 3 Summary of results

Case ID	Schedule	Shaft development	Haulage up	Haulage down	Callie decline gradient	WDD gradient	No orepass		One orepass		Orepass with two tipping points		Best option
							Haul level	Cost ($M)	Haul level	Cost ($M)	Haul level	Cost ($M)	
BA01	Base	25,000	0.75	0.85	1:8	1:7	158	53.4	19	53	−21	52.6	Two tipping points
BA02	Base	25,000	0.75	0.85	1:7	1:6	158	51.4	19	51.8	−21	51.6	No orepass
BA03	Base	25,000	1.05	1.2	1:8	1:7	99	60.8	−21	58.8	−101	57.7	Two tipping points
BA04	Base	25,000	1.05	1.2	1:7	1:6	99	58.3	−21	57.3	−21	56.5	Two tipping points
BA05	Base	50,000	0.75	0.85	1:8	1:7	299	83.1	219	85.3	219	85.2	No orepass
BA06	Base	50,000	0.75	0.85	1:7	1:6	299	80.3	278	82.8	259	82.8	No orepass
BA07	Base	50,000	1.05	1.2	1:8	1:7	219	92.1	99	92.8	99	92.8	No orepass
BA08	Base	50,000	1.05	1.2	1:7	1:6	219	88.9	99	90.6	99	90.6	No orepass
BA09	Base	75,000	0.75	0.85	1:8	1:7	398	109.2	358	112.6	318	113.2	No orepass
BA10	Base	75,000	0.75	0.85	1:7	1:6	398	105.7	358	109.3	318	110.2	No orepass
BA11	Base	75,000	1.05	1.2	1:8	1:7	299	121	278	123.7	259	123.7	No orepass
BA12	Base	75,000	1.05	1.2	1:7	1:6	398	116.9	278	120	259	120.2	No orepass
PR01	Probable	25,000	0.75	0.85	1:8	1:7	59	68.6	−21	64.6	−101	63	Two tipping points
PR02	Probable	25,000	0.75	0.85	1:7	1:6	99	65.4	−21	62.6	−101	61.5	Two tipping points
PR03	Probable	25,000	1.05	1.2	1:8	1:7	59	81.6	−101	74.5	−101	71.6	Two tipping points

(continued)

Table 3 (continued)

Case ID	Schedule	Shaft development	Haulage up	Haulage down	Callie decline gradient	WDD gradient	No orepass		One orepass		Orepass with two tipping points		Best option
							Haul level	Cost ($M)	Haul level	Cost ($M)	Haul level	Cost ($M)	
PR04	Probable	25,000	1.05	1.2	1:7	1:6	59	77.2	−21	71.9	−101	69.6	Two tipping points
PR05	Probable	50,000	0.75	0.85	1:8	1:7	158	100.9	19	99.8	−21	99	Two tipping points
PR06	Probable	50,000	0.75	0.85	1:7	1:6	158	97.3	99	97.3	19	97.1	Two tipping points
PR07	Probable	50,000	1.05	1.2	1:8	1:7	99	114.7	−21	110.3	−21	108.8	Two tipping points
PR08	Probable	50,000	1.05	1.2	1:7	1:6	99	110.1	−21	107.5	−21	106.2	Two tipping points
PR09	Probable	75,000	0.75	0.85	1:8	1:7	219	131.1	99	132.7	99	132.6	No orepass
PR10	Probable	75,000	0.75	0.85	1:7	1:6	219	126.9	179	129.5	158	129.4	No orepass
PR11	Probable	75,000	1.05	1.2	1:8	1:7	158	146.5	59	145.1	−21	144.3	Two tipping points
PR12	Probable	75,000	1.05	1.2	1:7	1:6	158	141.4	99	141.3	99	141.2	Two tipping points
BE01	Best	25,000	0.75	0.85	1:8	1:7	−21	100.6	−221	89.2	−261	85.3	Two tipping points
BE02	Best	25,000	0.75	0.85	1:7	1:6	−21	94.3	−181	85.7	−261	82.6	Two tipping points
BE03	Best	25,000	1.05	1.2	1:8	1:7	−61	125.6	−221	107.1	−341	101	Two tipping points

(continued)

Table 3 (continued)

Case ID	Schedule	Shaft development	Haulage up	Haulage down	Callie decline gradient	WDD gradient	No orepass		One orepass		Orepass with two tipping points		Best option
							Haul level	Cost ($M)	Haul level	Cost ($M)	Haul level	Cost ($M)	
BE04	Best	25,000	1.05	1.2	1:7	1:6	−21	116.8	−221	102.3	−261	97.4	Two tipping points
BE05	Best	50,000	0.75	0.85	1:8	1:7	19	135.7	−141	128.3	−141	126.5	Two tipping points
BE06	Best	50,000	0.75	0.85	1:7	1:6	59	129.1	−101	124.2	−141	122.8	Two tipping points
BE07	Best	50,000	1.05	1.2	1:8	1:7	−21	161.2	−181	147.3	−261	142.8	Two tipping points
BE08	Best	50,000	1.05	1.2	1:7	1:6	19	152.3	−141	141.9	−181	138.9	Two tipping points
BE09	Best	75,000	0.75	0.85	1:8	1:7	77	169.5	−101	166	−61	164.7	Two tipping points
BE10	Best	75,000	0.75	0.85	1:7	1:6	139	162.3	−21	161.1	−21	160.2	Two tipping points
BE11	Best	75,000	1.05	1.2	1:8	1:7	19	195.9	−141	185.9	−181	183.1	Two tipping points
BE12	Best	75,000	1.05	1.2	1:7	1:6	59	186.5	−101	179.9	−141	178.2	Two tipping points

Shaft Depth and Location

The optimum haul level ranges from 390 to −340 m RL (1010 m to 1740 m below the surface). A breakdown of minimum and maximum haul levels is shown in Table 4. The shaft optimally lies on the orebody standoff boundary between points (60097, 9043) and (60667, 8900), over 588 m.

Orepass Versus no Orepass

If an orepass is justified, it is always economical for it to have two tipping points. For the 'base' schedule, an orepass is not justified, except if the shaft development is $25,000/m, in which case it is generally more economical to include an orepass with two tipping points. For the 'probable' schedule, an orepass with two tipping points is justified in all cases except PR08 and PR09. In these latter cases an orepass is not justified. For the 'best' schedule, an orepass with two tipping points is always justified. The orepass optimally lies on 9250 N between 60250 E and 60755 E, over 505 m.

Effects of Parameters

We now discuss the effects of changing various parameters on the output of the model.

Shaft Development

A breakdown of costs, averaged over all 108 tests, was computed. This breakdown showed that shaft development is by far the most significant cost component, followed by decline haulage. This explains why varying the shaft development from $25,000/m to $50,000/m to $75,000/m has such a significant impact on the shaft depth and the total cost of the mine. On average, increasing the shaft development from $25,000/m to $50,000/m causes the optimum haul level to move

Table 4 Optimum haul levels

Schedule	Minimum haul level	Maximum haul level	Range
Base	−60 m RL	390 m RL	450 m
Probable	−220 m RL	350 m RL	570 m
Best	−340 m	310 m RL	650 m

up by three 40 m levels. On average, increasing the shaft development from $50,000/m to $75,000/m causes the optimum haul level to move up by one 40 m level. Thus, increasing the shaft development causes a significant decrease in the shaft depth, because the resulting increase in decline haulage is outweighed by the decrease in shaft development.

Orepass

The following effects of including an orepass in the model were observed:

- on average, including an orepass with one tipping point causes the optimum haul level L1 to move down by three levels;
- on average, including an orepass with two tipping points causes the optimum haul level to move down by seven levels;
- including an orepass provides additional savings by reducing decline haulage; and
- provision of a second tipping point introduces further savings.

Providing an orepass causes the optimum haul level to become lower. This is because decline haulage is fixed for levels serviced by the orepass, i.e. the cost of decline haulage for these levels is independent of the shaft depth and is ignored in the model. Hence the shaft tipping level must be lowered to account for the unbalanced haulage, shaft and orepass components. Including additional tipping points causes the shaft depth to increase further. The more ore is dropped down the orepass, the deeper the shaft will be.

Gradients

The effect of increasing the Callie and WDD gradients from 1:7 and 1:6 to 1:8 and 1:7 respectively is to increase decline haulage costs. If decline haulage costs were very large compared to shaft development, the orepass and shaft tipping levels would tend to space themselves out over the depth of the mine, so as to minimise the average haulage distance. Consequently the shaft depth would increase. In this study, shaft development is very large compared to decline haulage, and the effect of increasing gradients has little or no effect.

The following observations were noted when the model was run with decline gradients set to zero. For the no orepass case, the optimum haul level is 180 m RL. If an orepass with one tipping point is used, the optimum haul level is −460 m RL, the top of the orepass is 180 m RL, upwards haulage is from the level at −180 m RL. If an orepass with two tipping points is used, the optimum haul level is −160 m RL, the top of the orepass is 180 m RL (haul up from −20 m RL), and the second

tipping point is at −180 m RL (haul up from −300 RL). It can be verified that, in all three cases, the haul and orepass levels have positioned themselves so as to minimise the total haulage cost.

Haulage Costs

On average, increasing the decline haulage costs from $0.75/t.km and $0.85/t.km for upwards and downwards haulage to $1.05/t.km and $1.20/t.km respectively has the effect of lowering the optimum haul level by one 40 m level. The reasons are similar to the reasons for the gradient effects.

One Versus Two Tipping Points

The provision of more than two tipping points could potentially result in further savings, although the additional cost of developing tunnels from the declines to the orepass must be considered. Moreover, experiments have indicated that having two orepasses, one for each decline, reduces haulage and development costs associated with the haulage drive which, on average, account for about 12% of the total variable cost of the mine.

Confinement of Orepass to Fixed Northing

Confining the orepass to be fixed on the northing between the two declines has the effect of increasing the main haulage drive development and haulage costs. The increase, however, is not significant.

Conclusions

In this work, we have developed and a network model for the Callie underground mine. An algorithm was developed to mathematically determine an optimum location and depth of a vertical hoisting shaft in the Callie underground mine. The algorithm was implemented into a software product for solving the problem iteratively. Results were analysed over a range of infrastructure and haulage costs, decline gradients and life-of-mine schedules.

Acknowledgements We thank Newmont Australia Limited and the Australian Research Council for their joint sponsorship of this research via an ARC Linkage Grant. In particular, we thank Newmont for suggesting and formulating the Callie shaft location study. A simplified version of study was originally proposed by Steven Harvey and the detailed investigation was proposed and commissioned by Andrew Fox and Ian Suckling. I thank Robert Parr and Nadine Wetzel for their time and effort collecting and preparing data and for their constructive feedback. Further details of this work can be found in the author's Ph.D. thesis (Volz 2008).

References

Brazil M, Rubinstein JH, Volz M (2005) The gradient-constrained Fermat-Weber problem for underground mine design. In: Caccetta L, Rehbock V (eds) Proceedings 18th national ASOR conference and eleventh australian optimisation day, pp 16–23

Brimberg J, Juel H, Schobel A (2002) Linear facility location in three dimensions—models and solution methods. Oper Res 50(6):1050–1057

Volz MG (2008) Gradient-constrained flow-dependent networks for underground mine design, PhD thesis (unpublished), University of Melbourne, Melbourne

Weiszfeld E (1937) Sur le point pour lequel la somme des distances de n points donnes est minimum. Tohoku Math J 43:355–386

Strategic Underground Mine Access Design to Maximise the Net Present Value

K. G. Sirinanda, M. Brazil, P. A. Grossman, J. H. Rubinstein and D. A. Thomas

Abstract To date, the scheduling and access design of an underground mine have only been considered as two separate optimisation problems. First, access to the mine is designed and then the scheduling is completed. One drawback of this approach is that the costs of access construction fail to be reflected in the Net Present Value (NPV) calculation. In this paper, designing the access and scheduling its construction are formulated as a single optimisation problem. The underground mine access construction process can be classified according to the number of faces being developed concurrently. An underground mine with a single decline branching at a junction point into two declines is considered. After construction reaches the junction, the two faces of the decline can be constructed sequentially or concurrently. This paper proposes an efficient algorithm for optimally locating a junction point to maximise the NPV where two faces are being developed concurrently. The NPV is defined by taking the locations of ore bodies and their values, decline construction costs, decline development rate and discount rate into account. The variation of the NPV and the optimal locations of the junction point for one and two concurrent development faces for a range of discount rates are discussed and

K. G. Sirinanda (✉) · P. A. Grossman · D. A. Thomas
Department of Mechanical Engineering, The University of Melbourne, Melbourne, VIC 3010, Australia
e-mail: kash.sirinanda@gmail.com

P. A. Grossman
e-mail: peterag@unimelb.edu.au

D. A. Thomas
e-mail: doreen.thomas@unimelb.edu.au

M. Brazil
Department of Electrical and Electronic Engineering, The University of Melbourne, Melbourne, VIC 3010, Australia
e-mail: brazil@unimelb.edu.au

J. H. Rubinstein
Department of Mathematics and Statistics, The University of Melbourne, Melbourne, VIC 3010, Australia
e-mail: rubin@ms.unimelb.edu.au

R. Dimitrakopoulos (ed.), *Advances in Applied Strategic Mine Planning*,
https://doi.org/10.1007/978-3-319-69320-0_35

compared. The proposed algorithm is applied in a simulated case study based on hypothetical values for an underground mine.

Introduction

Underground mine access design has previously been studied with the objective of minimising the haulage and development costs (Brazil et al. 2004; Brazil and Thomas 2007). However, maximising the Net Present Value (NPV) has not been investigated. Current methods that are available design the underground access first and then complete the scheduling. One weakness with this process is that the costs of access construction are not reflected in the NPV calculation. This paper presents a way of optimising the access design and scheduling its construction simultaneously to improve the NPV.

Lane (1988) applied optimisation techniques for underground mines to maximise the NPV. He formulated the cash flows for the complete underground mining process. Nevertheless, his theory can only be applied to underground mines with a given access geometry. In the past decade, mixed integer programming techniques have been widely used in optimisation processes in (Nehring and Topal 2007; Nehring et al. 2010; Newman and Kuchta 2007). However, in these papers different techniques have been applied for different underground mines and it is always assumed that the underground access is given. A review of this literature has identified an opportunity to develop algorithms to design the underground mine access to maximise NPV. Such algorithms have not been available prior to this research. In this paper, a generic way of optimising the underground access network is presented.

The underground mine access construction process can be classified according to the availability of the mining equipment to develop a number of faces concurrently. The simplest scenario is to complete one development face at a time. If an underground mine is developed with one development face, then only a single decline can be constructed at a time. This type of approach was first discussed in (Sirinanda et al. 2014) in which the underground access network was designed to maximise the NPV. The objective was to optimally locate a junction point when a single development face is being deployed. The junction points are located in the network to maximise the NPV. The authors emphasised that the time value of money has a crucial effect on locating the junction points in the access network for maximum value. The algorithm discussed in (Sirinanda et al. 2014) locates a junction point to access ore bodies most efficiently so as to maximise the NPV. The authors showed that in the maximum NPV network, the paths from the junction point to the surface portal and the first resource point make equal angles with the path from the junction point to the second resource point. The algorithm provides higher NPV compared with the placement of the junction point at the location where minimum development length occurs in the network. However, the present

paper examines the way of locating a junction point where there is enough equipment available to complete two development activities simultaneously.

The main advantage of using two development faces is to reduce the mining equipment idle time because with two development faces two decline links can be constructed at a time. As an example for drill and blast development, a jumbo is typically the rate limiting piece of equipment. The jumbo can be moved to a nearby second face, if it is not needed for e.g. rock bolting, during the sequence, drill, blast, support, muck. In this paper, an underground mine with a single decline branching at a junction point into two declines is considered. After construction reaches the junction, the two faces of the decline can be constructed concurrently and so the mining equipment idle time can be reduced. Machine placement is an important aspect in an underground mine which is discussed in (Topal 2008; Newman and Kuchta 2007) for the Kiruna underground mine in Sweden. However, in the present paper more focus is given to utilising the available mining equipment rather than the machine placement.

The Discounted Junction Point Algorithm (DJPA) proposed in this paper will find the optimal location of a junction point. This algorithm can be applied to an underground mine with declines. Once this point has been located, the access to the mine can be designed by including the links between the junction point and each of the given draw points and the surface portal or breakout point. In general, these links should represent minimum length navigable paths between the end points. However, in order to make the model as simple and general as possible the navigability conditions in this paper are relaxed. The decline links are assumed to be straight line segments. A consequence of this assumption is that the theory and the algorithm outlined in this paper can only be directly applied to underground mines where the terminal points lie in a near-horizontal plane and then gradient constraint would be satisfied. This does match certain industry problems..

This paper consists of five sections. Section "Formulation of the Objective Function" formulates and explains the optimisation problem. Section "Discounted Junction Point Algorithm (DJPA)" introduces the discounted junction point algorithm to solve the problem. Section "A Simulated Case Study—Designing the Optimal Connector Between Two Underground Mines" investigates the performance of the algorithm and applies the DJPA to a case study. The final section contains the conclusions and future research work.

Formulation of the Objective Function

In this section, the objective function is formulated for an underground mine that is being operated with two development faces. The total NPV is expressed as the sum of development and production cash flows. The two development faces allow the

construction of two decline links at a time. The problem is formulated as an optimisation problem and an iterative approach is proposed to solve the problem.

Let $p_0 = (x_0, y_0, z_0), p_1 = (x_1, y_1, z_1), p_2 = (x_2, y_2, z_2)$ be three given terminal points as shown in Fig. 1. The point p_0 is the surface portal or breakout point from existing infrastructure. The points p_1, p_2, represent draw points for resources (ore deposits) with values V_1, V_2 respectively. The aim is to locate a junction point s to maximise the NPV.

The line segments $p_0\mathrm{s}, \mathrm{s}p_1, \mathrm{s}p_2$ are called decline links of the underground mine. First the decline link $p_0\mathrm{s}$ is constructed, then the decline links sp_1, sp_2 are constructed concurrently. The locations of the ore deposits and their values, the development rate D m p.a., the cost rate C \$/m and the discount rate $d\%$ p.a. are assumed to be given. The lengths l_0, l_1, l_2 are construction lengths from p_0, p_1, p_2 to s respectively which are given by Euclidean distances. The parameters $r = 1 + d$, $V_c = CD/\ln r$ are used throughout this paper.

The expression for the discounted cost of constructing a decline link of length l is now formulated. The time taken to construct a portion of the decline link of length x is x/D. Therefore, the discount factor is $(1+d)^{-x/D}$. The discounted cost of developing the decline link can be written as:

$$\begin{aligned}\text{Construction cost of the decline link} &= \int_0^l C(1+d)^{-x/D}dx = \frac{CD}{\ln r}\left(1 - r^{-l/D}\right)\\ &= V_c\left(1 - r^{-l/D}\right)\end{aligned}$$

The construction costs define the total discounted costs involving the development of the decline links $p_0\mathrm{s}, \mathrm{s}p_1, \mathrm{s}p_2$. The discounted cost for constructing each decline link is expressed as above with an appropriate time discount factor.

$$\begin{aligned}\text{Cost of the decline link } p_0s &= V_c\left(1 - r^{-l_0/D}\right)\\ \text{Cost of the decline link } sp_1 &= V_c r^{-l_0/D}\left(1 - r^{-l_1/D}\right)\\ \text{Cost of the decline link } sp_2 &= V_c r^{-l_0/D}\left(1 - r^{-l_2/D}\right)\end{aligned}$$

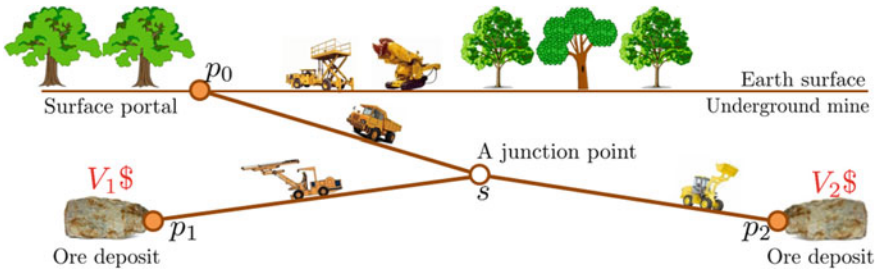

Fig. 1 A schematic representation of a simple underground mine

The cash flows generated from the access construction are the sum of all the negative discounted costs above and are given by NPV_{dev} where,

$$\begin{aligned} NPV_{dev} &= V_c\left[\left(1-r^{-l_0/D}\right)+r^{-l_0/D}\left(1-r^{-l_1/D}\right)+r^{-l_0/D}\left(1-r^{-l_2/D}\right)\right] \\ &= V_c\left(r^{-(l_0+l_1)/D}+r^{-(l_0+l_2)/D}-r^{-l_0/D}-1\right) \end{aligned} \tag{1}$$

The total construction times taken to reach p_1, p_2 are t_0+t_1, t_0+t_2 respectively where $t_0 = l_0/D, t_1 = l_1/D, t_2 = l_2/D$. Therefore, NPV for ore production is written as,

$$NPV_{pro} = V_1 r^{-(t_0+t_1)/D} + V_2 r^{-(t_0+t_2)/D} = V_1 r^{-(l_0+l_1)/D} + V_2 r^{-(l_0+l_2)/D} \tag{2}$$

In this paper variable costs are formulated in terms of the location of the junction point. The discounted variable costs are generated from the access construction process and the ore production. These two discounted costs are formulated in (1), (2). The total NPV is derived as the combination of both discounted fixed and variable costs. The fixed costs include the equipment maintenance costs, environmental management costs and fixed haulage costs, and these costs are assumed to be given.

$$\begin{aligned} NPV &= NPV_{variable} + NPV_{fixed} = NPV_{dev} + NPV_{pro} + NPV_{fixed} \\ &= V_c\left(r^{-(l_0+l_1)/D}+r^{-(l_0+l_2)/D}-r^{-l_0/D}-1\right) + V_1 r^{-(l_0+l_1)/D} + V_2 r^{-(l_0+l_2)/D} + NPV_{fixed} \\ &= (V_1+V_c)r^{-(l_0+l_1)/D} + (V_2+V_c)r^{-(l_0+l_2)/D} - V_c\left(r^{-l_0/D}-1\right) + NPV_{fixed} \end{aligned} \tag{3}$$

Equation (3) is the objective function for the problem of optimally locating the junction point to maximise the NPV. Therefore, this problem can be expressed as the following optimisation problem;

$$\text{Maximise } (V_1+V_c)r^{-(l_0+l_1)/D} + (V_2+V_c)r^{-(l_0+l_2)/D} - V_c\left(r^{-l_0/D}-1\right) + NPV_{fixed}$$
$$\text{such that } l_0, l_1, l_2 \geq 0$$

The objective function is differentiable in the problem domain with respect to x, y, z except at the points p_0, p_1, p_2. The distances l_0, l_1, l_2 are functions of the junction point coordinates x, y, z. A maximum exists as the NPV is bounded above by $V_1 + V_2$. The feasible region is the interior of the triangle including the boundary which is defined by the points p_0, p_1, p_2. Apart from that there are additional constraints on l_1, l_2 which are discussed in the appendix.

Discounted Junction Point Algorithm (DJPA)

The Discounted Junction Point Algorithm (DJPA) is proposed to locate a single junction point given that two faces are being developed at a time in the underground mine. The two discount Eqs. (21), (22) and two geometric Eqs. (23), (24) discussed in the appendix are used in the iterative algorithm, to optimally locate the junction point. Based on many numerical trials, the iterative process always appears to converge rapidly and the results are independent of the initial conditions for θ_1, θ_2.

Algorithm: Discounted Junction Point Algorithm (DJPA)

Input: The locations of the surface portal or breakout point p_0 and the drawpoints p_1, p_2 with values $\$V_1$, $\$V_2$, development rate D m p. a, cost rate C \$/m, discount rate d % p. a.
Output: The optimal location of the junction point and the maximum NPV.

1. Calculate d_0, d_1, d_2, ν, μ, λ from the triangle $p_0p_1p_2$ and φ, ω, ψ using (27), (32), (36) respectively.
2. **if** $\lambda \geq \varphi$, **then**
   The junction point coincides with the draw point p_0 and NPV is given in (28).
3. **else if** $\mu \geq \omega$, **then**
   The junction point coincides with the draw point $p_1$and NPV is given in (33).
4. **else if** $\nu \geq \psi$, **then**
   The junction point coincides with the breakout point p_2 and NPV is given in (37).
5. **else**
   Initialisation $\theta_1(0) = 2\pi/3, \theta_2(0) = 2\pi/3, \epsilon = 10^{-6}$
   $i = 0$
6. **repeat**
   Compute l_1, l_2 :

$$l_2(i+1) = \frac{d_0 d_1 |\sin(\theta_1(i) + \theta_2(i) + \nu)|}{\sqrt{d_0^2 \sin^2\theta_1(i) + d_1^2 \sin^2\theta_2(i) + 2\cos(\theta_1(i) + \theta_2(i) + \nu)\sin\theta_1(i)\sin\theta_2(i) d_0 d_1}}$$

$$\gamma_1(i+1) = \sin^{-1}\left(\frac{l_2(i+1)\sin\theta_1(i)}{d_1}\right)$$

$$l_1(i+1) = \frac{d_1 \sin\big(\theta_1(i) + \gamma_1(i+1)\big)}{\sin\theta_1(i)}$$

   Calculate intermediate parameters A and B:

$$A(i+1) = \left(\frac{V_1 \ln r}{D} + C\right) r^{-l_1(i+1)/D}$$

$$B(i+1) = \left(\frac{V_2 \ln r}{D} + C\right) r^{-l_2(i+1)/D}$$

   Update θ_1, θ_2:

$$\theta_1(i+1) = \cos^{-1}\left(1 + \frac{C\big(C - 2A(i+1) - 2B(i+1)\big)}{2A(i+1)B(i+1)}\right)$$

$$\theta_2(i+1) = \cos^{-1}\left(-1 + \frac{C\big(C - 2A(i+1)\big)}{2B(i+1)\big(C - A(i+1) - B(i+1)\big)}\right)$$

   $i = i + 1$
   until $|\theta_1(i) - \theta_1(i+1)| < \epsilon$ and $|\theta_2(i) - \theta_2(i+1)| < \epsilon$
7. $\theta_1^* = \theta_1(i)$, $\theta_2^* = \theta_2(i)$, $l_1^* = l_1(i)$, $l_2^* = l_2(i)$
8. Calculate l_0^* using (38).
9. The optimal NPV is given in (39).
10. The optimal location of the junction point is calculated using (40), (41), (42).

A Simulated Case Study—Designing the Optimal Connector Between Two Underground Mines

In this section a case study is proposed. An underground mine (Mine A) with a single decline is given as shown in Fig. 2. There is no infrastructure yet built in underground Mine B where there are two draw points. These two draw points connect to two ore bodies with significant values that are worth mining. The aim is to design an underground connector between the Mines A and B so as to maximise the NPV associated with that connector. The connector will break out from the access infrastructure of Mine A and extend to Mine B. A set of potential breakout points on the existing Mine A access, two draw points with values $\$V_1, \$V_2$ in Mine B, the cost rate of constructing tunnels (C \$/m), the rate of tunnel construction (D m p.a.) and the discount rate (d% p.a.) are assumed to be given.

A junction is placed on the connector to allow two development faces which reduces the idle time of the mining equipment. The algorithm developed in this paper can be applied since the resource points and potential breakout point from existing infrastructure lie in a plane that is nearly horizontal and hence the gradient constraint would be satisfied. The DJPA is applied and used to obtain the optimal location of the junction points and the corresponding NPVs for a range of discount rates. Then, the optimal locations of the junction point for single and two faces developed concurrently are compared. Next, several possible breakout points in the Mine A to connect with the Mine B are considered in the optimisation.

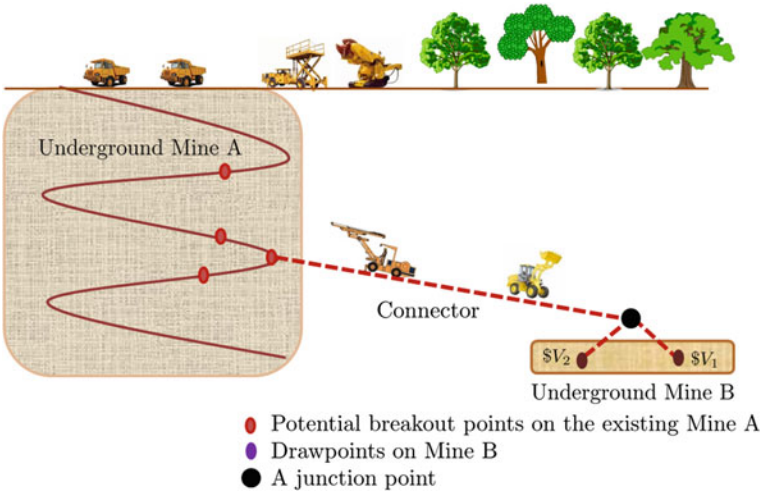

Fig. 2 The connector that connects Mine A and Mine B

The Connector Connects to a Single Breakout Point in Mine A

The optimal locations of the junction points are obtained for a range of discount rates for the data-set below.

$V_1 = \$60\text{M},\ V_2 = \$40\text{M},\ C = \$6000/\text{m},\ D = 1560$ m p.a, $NPV_{fixed} = \$500\text{k}$, $d = 5, 8, 10, 12, 15, 20\%$ p.a.

This range of discount rates is often used in underground mine operations. The coordinates of the location of the breakout point in Mine A and the draw points in Mine B are $(0, 400, 400), (800, 800, 0), (1000, 1000, 0)$ respectively.

Figure 3 illustrates the optimal locations of the junction point for a range of discount rates when the mines are being operated with two development faces. Table 1 shows the location of the junction point for a range of discount rates. When the discount rate increases the construction of the third decline link starts earlier. However, the construction lengths l_1, l_2 increase with the discount rate. The NPV is reduced with increased discount rates.

NPV Comparison for One and Two Development Faces

Figure 4 shows the optimal locations of the junction point for a range of discount rates when the mines are being operated with either a single or two faces developed concurrently. For one development face, the optimal location of the junction is obtained from the algorithm discussed in (Sirinanda et al. 2014). When the mine operates with two development faces the optimal location of the junction point is located closer to the breakout point whereas with one development face, it is closer to the higher value resource. Moreover, in both the cases for higher discount rates,

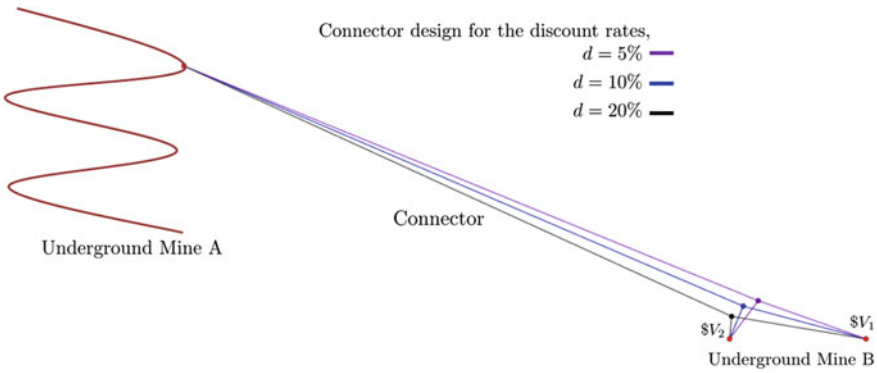

Fig. 3 The optimal design of the connector for a range of discount rates

Table 1 Variation of the NPV for a range of discount rates

Discount rate / % p.a	Optimal location of the junction	Optimal NPV / $M
5	(842, 898, 56)	89.542
8	(827, 879, 52)	87.919
10	(820, 868, 48)	86.872
12	(815, 860, 45)	85.853
15	(809, 849, 40)	84.372
20	(803, 836, 33)	82.030

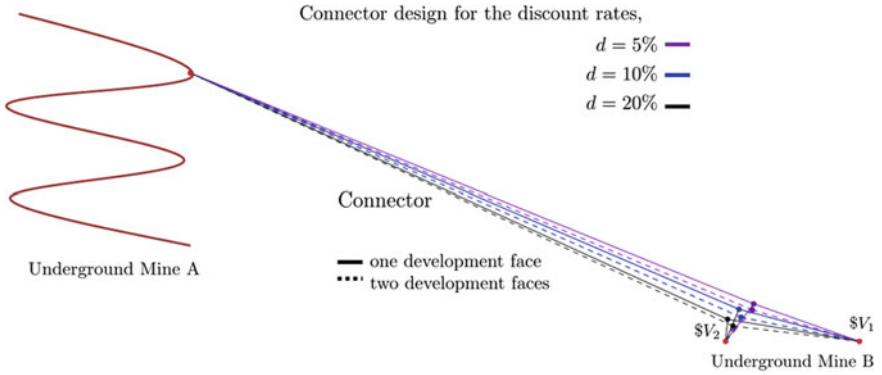

Fig. 4 The optimal design of the connector for one and two development faces

the construction of the third decline link starts earlier. As seen in Fig. 5 two development faces provide better NPV than a single face. The last column of Table 2 shows that improvement of the NPV increases with the discount rate.

The Connector Connects to a Range of Possible Breakout Points in Mine A

In this section, the optimisation is carried out by considering several possible breakout points in Mine A. Figure 6 illustrates the optimal connector design for a fixed discount rate of 10% p.a. and the draw points of Mine B are located at the same places as before.

Table 3 shows the optimal locations of the junction point and the corresponding NPVs. According to this table, NPV is maximised if the breakout point is designed at the coordinates $(0, 200, 200)$. However, this is without considering the haulage costs through the decline of Mine A.

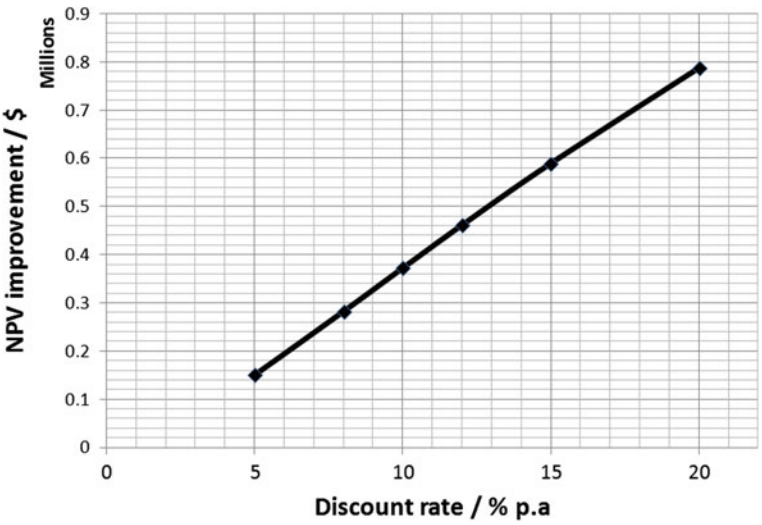

Fig. 5 NPV improvement for two development faces compared with one development face

Table 2 Improvement of the NPV for two development faces compared to one face

Discount rate / % p.a	NPV for two development faces / $M	NPV for one development face / $M	NPV improvement / $
5	89.542	89.391	151000
8	87.919	87.636	283000
10	86.872	86.499	373000
12	85.853	85.391	462000
15	84.372	83.782	590000
20	82.030	81.242	788000

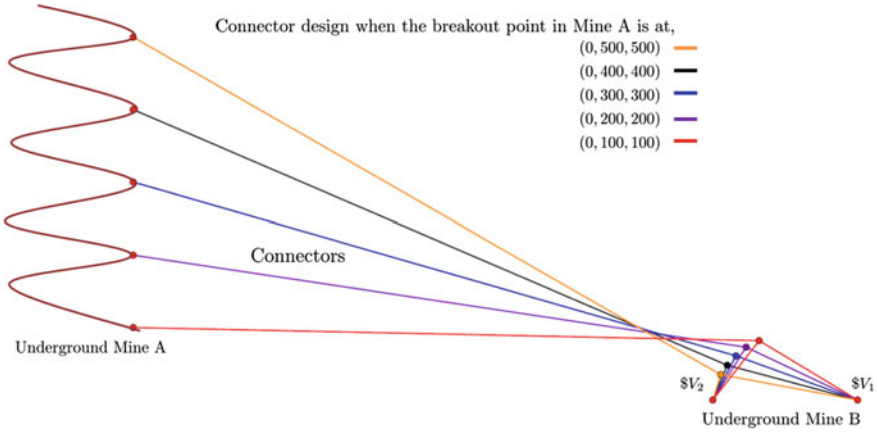

Fig. 6 The optimal design of the connector for a range of breakout points in the Mine A

Table 3 NPV variation of the possible breakout points in Mine A

The coordinates of the possible breakout points in Mine A	The coordinates of the optimal location of the junction point	Optimal NPV / $M
(0, 500, 500)	(811, 846, 35)	86.959
(0, 400, 400)	(820, 868, 48)	87.372
(0, 300, 300)	(832, 893, 61)	87.611
(0, 200, 200)	(846, 919, 73)	87.661
(0, 100, 100)	(864, 946, 82)	87.526

Conclusions

This paper proposes an efficient algorithm to locate a junction point for an underground mine when two faces are being developed concurrently. The proposed optimisation technique is to design the underground mine access and schedule its construction simultaneously to improve the NPV. The discounted junction point algorithm allows the construction of the underground mine access to generate maximum NPV during the life time of the mine. This algorithm locates the junction point to access ore bodies most efficiently so as to maximise the NPV.

The discounted junction point algorithm is applied to a case study. In the proposed case study, the connector that links two underground mines is designed to obtain the maximum NPV. The junction is placed on the connector to allow two development faces which reduces the idle time of the mining equipment. The discounted junction point algorithm improves the NPV compared with the underground mine operation with a single face. Also, the improvement of the NPV increases with the discount rate. In the optimisation several breakout points are considered and then the best location of the breakout point is identified to obtain the maximum NPV.

In future research, a new algorithm will be developed to locate a single junction point with more realistic constraints such as the gradient constraint, variable cost rates, geo-mechanical conditions and potential spatial constraints on the junction points, and then the optimal configurations will be studied. In addition, the discounted junction point algorithm will be extended to locate a number of junction points in a network of declines.

Acknowledgements The authors would like to thank Dr. John Andrews from Rand Mining and Tribune Resources for his valuable comments and sharing his knowledge. This work was also partly funded by a grant from the Australian Research Council.

Appendix

In this section, the equations that are used in the discounted junction point algorithm are derived.

To maximise the NPV, differentiate (3) with respect to x and set equal to 0:

$$\begin{aligned}&-(V_1+V_c)r^{-(l_0+l_1)/D}\frac{\ln r}{D}\left(\frac{\partial l_0}{\partial x}+\frac{\partial l_1}{\partial x}\right)\\&-(V_2+V_c)r^{-(l_0+l_2)/D}\frac{\ln r}{D}\left(\frac{\partial l_0}{\partial x}+\frac{\partial l_2}{\partial x}\right)+Cr^{-l_0/D}\frac{\partial l_0}{\partial x}\\&=0\end{aligned}$$

which can be simplified to,

$$(A+B-C)\frac{\partial l_0}{\partial x}+A\frac{\partial l_1}{\partial x}+B\frac{\partial l_2}{\partial x}=0 \tag{4}$$

where,

$$A=\left(\frac{V_1\ln r}{D}+C\right)r^{-l_1/D} \tag{5}$$

$$B=\left(\frac{V_2\ln r}{D}+C\right)r^{-l_2/D} \tag{6}$$

Similarly, differentiating (3) with respect to y, z and setting equal to 0 yields:

$$(A+B-C)\frac{\partial l_0}{\partial y}+A\frac{\partial l_1}{\partial y}+B\frac{\partial l_2}{\partial y}=0 \tag{7}$$

$$(A+B-C)\frac{\partial l_0}{\partial z}+A\frac{\partial l_1}{\partial z}+B\frac{\partial l_2}{\partial z}=0 \tag{8}$$

Equations (4), (7), (8) can be expressed in terms of gradients,

$$(A+B-C)\nabla l_0+A\nabla l_1+B\nabla l_2=0 \tag{9}$$

If the operating discount rate is zero then the corresponding junction point is mapped to the location which minimises the total length of the network. When $d=0, r=1$ and so,

$$A=\lim_{r\to 1}\left(\frac{V_1\ln r}{D}+C\right)r^{-l_1/D}=C \tag{10}$$

$$B = \lim_{r\to 1}\left(\frac{V_2 \ln r}{D} + C\right) r^{-l_2/D} = C \tag{11}$$

Therefore, $A = B = C$. By substituting this into (9),

$$\nabla l_0 + \nabla l_1 + \nabla l_2 = 0 \tag{12}$$

From Eq. (12), the optimisation problem is reduced to a length minimisation problem when the discount rate is zero. Therefore by standard Steiner tree theory an angle of $2\pi/3$ is generated between the junction point and each pair of adjacent points.

Let $\mathbf{u}_0, \mathbf{u}_1, \mathbf{u}_2$ be the unit vectors directed from the fixed points p_0, p_1, p_2 towards the junction point as shown in Fig. 7. Let $\theta_0, \theta_1, \theta_2$ be the angles between $\mathbf{u}_0$ and $\mathbf{u}_1, \mathbf{u}_1$ and $\mathbf{u}_2, \mathbf{u}_2$ and $\mathbf{u}_0$ respectively. The unit vectors are expressed using the corresponding gradients $\mathbf{u}_0 = \nabla l_0, \mathbf{u}_1 = \nabla l_1, \mathbf{u}_2 = \nabla l_2$. Hence, Eq. (9) becomes,

$$(A + B - C)\mathbf{u}_0 + A\mathbf{u}_1 + B\mathbf{u}_2 = 0 \tag{13}$$

Equation (13) can be rewritten,

$$A(\mathbf{u}_0 + \mathbf{u}_1) + B(\mathbf{u}_0 + \mathbf{u}_2) - C\mathbf{u}_0 = 0 \tag{14}$$

Also note that $\mathbf{u}_0 \cdot \mathbf{u}_1 = \cos\theta_0, \mathbf{u}_1 \cdot \mathbf{u}_2 = \cos\theta_1, \mathbf{u}_2 \cdot \mathbf{u}_0 = \cos\theta_2$ and since this is a planar problem, $\theta_0 + \theta_1 + \theta_2 = 2\pi$ and so $\theta_0 = 2\pi - (\theta_1 + \theta_2)$.

By taking the dot product of (13) with $\mathbf{u}_0$,

$$(\mathrm{A} + \mathrm{B} - \mathrm{C})\mathbf{u}_0.\mathbf{u}_0 + \mathrm{A}\mathbf{u}_1.\mathbf{u}_0 + \mathrm{B}\mathbf{u}_2.\mathbf{u}_0 = 0$$

$$\cos(\theta_1 + \theta_2) = \frac{\mathrm{C} - \mathrm{A} - \mathrm{B} - \mathrm{B}\cos\theta_2}{\mathrm{A}} \tag{15}$$

By taking the dot product of (14) with $\mathbf{u}_0 - \mathbf{u}_1$,

$$A(\mathbf{u}_0 + \mathbf{u}_1) \cdot (\mathbf{u}_0 - \mathbf{u}_1) + B(\mathbf{u}_0 + \mathbf{u}_2) \cdot (\mathbf{u}_0 - \mathbf{u}_1) - C\mathbf{u}_0 \cdot (\mathbf{u}_0 - \mathbf{u}_1) = 0 \tag{16}$$

Note that $(\mathbf{u}_0 + \mathbf{u}_1) \cdot (\mathbf{u}_0 - \mathbf{u}_1) = |\mathbf{u}_0|^2 - |\mathbf{u}_1|^2 = 1 - 1 = 0$.

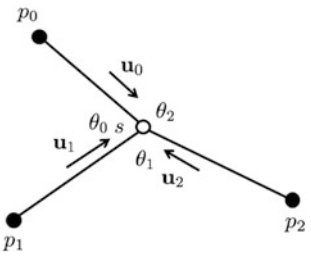

Fig. 7 Vector representation of the problem

By substituting the result above into (16),

$$B(\mathbf{u}_0+\mathbf{u}_2)\cdot(\mathbf{u}_0-\mathbf{u}_1)-C\mathbf{u}_0\cdot(\mathbf{u}_0-\mathbf{u}_1)=0$$

$$(C-B)\cos(\theta_1+\theta_2)+B\cos\theta_2-B\cos\theta_1=C-B \tag{17}$$

By substituting the value of $\cos(\theta_1+\theta_2)$ into (17),

$$B\cos\theta_2(B-C+A)-AB\cos\theta_1=(C-B)(2A+B-C) \tag{18}$$

Similarly, by taking the dot product of (14) with $\mathbf{u}_0-\mathbf{u}_2$ and following the same steps as above,

$$A\cos(\theta_1+\theta_2)-A\cos\theta_1+(C-A)\cos\theta_2=C-A \tag{19}$$

Then, by substituting the value of $\cos(\theta_1+\theta_2)$ into (19),

$$\cos\theta_2(C-A-B)-A\cos\theta_1=B \tag{20}$$

Equation (20) is multiplied by B and subtracted from (18),

$$\cos\theta_2=-1+\frac{C(C-2A)}{2B(C-A-B)} \tag{21}$$

By substituting the value of $\cos\theta_2$ into (21),

$$\cos\theta_1=1+\frac{C(C-2A-2B)}{2AB} \tag{22}$$

Equations (21), (22) can be verified for zero discount rate as follows. For the zero discount rate θ_1,θ_2 should be $2\pi/3$.

If $d=0$, Eqs. (10), (11) imply $A=B=C$ and so,

$$\cos\theta_2=-1+\tfrac{A(A-2A)}{2A(A-A-A)}=-0.5 \quad \theta_2=\tfrac{2\pi}{3}$$
$$\cos\theta_1=1+\tfrac{A(A-2A-2A)}{2AA}=-0.5 \quad \theta_1=\tfrac{2\pi}{3}$$

Hence, Eqs. (21), (22) are correct in this case. Equations (21), (22) are called the *discount equations* since θ_1,θ_2 depend on V_1,V_2 and d. These two discount equations are used in the iterative process in the DJPA.

Let $\gamma_0=\angle sp_0p_2,\gamma_1=\angle sp_1p_2,v=\angle p_0p_1p_2$ as shown in Fig. 8. The distances d_0,d_1 are from p_0 to p_2 and from p_1 to p_2. By applying the Sine rule to triangles p_0sp_2,p_1sp_2,

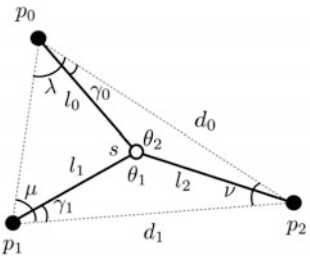

Fig. 8 The geometric parameters

$$\gamma_0 = \sin^{-1}\left(\frac{l_2 \sin\theta_2}{d_0}\right) \quad \gamma_1 = \sin^{-1}\left(\frac{l_2 \sin\theta_1}{d_1}\right)$$

Also, by applying the Sine rule to the triangle $p_1 s p_2$,

$$l_1 = \frac{d_1 \sin(\theta_1 + \gamma_1)}{\sin\theta_1} \tag{23}$$

Setting the sum of the angles in the quadrilateral $p_0 s p_1 p_2$ equal to 2π and substituting the values for γ_0, γ_1 the distance l_2 can be shown to be,

$$l_2 = \frac{d_0 d_1 |\sin(\theta_1 + \theta_2 + v)|}{\sqrt{d_0^2 \sin^2\theta_1 + d_1^2 \sin^2\theta_2 + 2\cos(\theta_1 + \theta_2 + v)\sin\theta_1 \sin\theta_2 d_0 d_1}} \tag{24}$$

Equations (23), (24) are called the *geometric equations* since l_1, l_2 depend on the constants d_0, d_1, v that define the geometry of the network. These two geometric equations are also used in the iterative process in the DJPA.

The Junction Point at One of the Vertices

The *critical angle* is the minimum angle for each vertex for which the junction point coincides with the breakout point p_0 or draw points p_1, p_2. The critical angles associated with the degenerate point are calculated by using (21), (22), (23), (24). The angles v, μ, λ are calculated by applying the cosine rule to the triangle $p_0 p_1 p_2$. The critical angles are given by ψ, ω, φ when the junction point is at the points p_2, p_1, p_0 repectively.

The Junction Point at the Breakout Point or Surface Portal p_0

The conditions that need to be satisfied so that the junction point is at the breakout point p_0 are:

$l_1 = d_2, l_2 = d_0, \theta_1 = \varphi$. By substituting these values into (5), (6), (22)

$$A = \left(\frac{V_1 \ln r}{D} + C\right) r^{-d_2/D} \tag{25}$$

$$B = \left(\frac{V_2 \ln r}{D} + C\right) r^{-d_0/D} \tag{26}$$

$$\cos\varphi = 1 + \frac{C(C - 2A - 2B)}{2AB}$$

By substituting the values of A, B into the equation above, we get:

$$\varphi = \cos^{-1}\left(1 + \frac{CD\big(CD(1 - 2r^{-d_2/D} - 2r^{-d_0/D} - 2(V_1 \ln r + V_2 \ln r)\big)}{2(V_1 \ln r + CD)(V_2 \ln r + CD) r^{-(d_0 + d_2)/D}}\right) \tag{27}$$

The maximum NPV at this point is $NPV_{s=p_0}$ where,

$$NPV_{s=p_0} = (V_1 + V_c) r^{-d_2/D} + (V_2 + V_c) r^{-d_0/D} - V_c + NPV_{fixed} \tag{28}$$

The Junction Point at the Drawpoint p_1

The conditions that need to be satisfied so that the junction point is at the draw point p_1 are:

$l_1 = 0, l_2 = d_1, \theta_2 = \omega$. By substituting these values into (5), (6), (23)

$$A = \left(\frac{V_1 \ln r}{D} + C\right) \tag{29}$$

$$B = \left(\frac{V_2 \ln r}{D} + C\right) r^{-d_1/D} \tag{30}$$

$$\cos\omega = -1 + \frac{C(C - 2A)}{2B(C - A - B)} \tag{31}$$

By substituting the values of A, B into (32),

$$\omega = \cos^{-1}\left(-1 + \frac{CD(CD + 2V_1 \ln r)}{2(V_2 \ln r + CD) r^{-d_1/D}(V_1 \ln r + (V_2 \ln r + CD) r^{-d_1/D})}\right) \tag{32}$$

The maximum NPV at this point is $NPV_{s=p_1}$ where,

$$NPV_{s=p_1} = (V_1 + V_c)r^{-d_2/D} + (V_2 + V_c)r^{-(d_0+d_2)/D} - V_c\left(r^{-d_2/D} + 1\right) + NPV_{fixed} \tag{33}$$

The Junction Point at the Drawpoint p_2

The conditions that need to be satisfied so that the junction point is at the draw point p_2 are:

$l_2 = 0, l_1 = d_1, 2\pi - (\theta_1 + \theta_2) = \psi$. By substituting these values into (5), (6)

$$A = \left(\frac{V_1 \ln r}{D} + C\right) r^{-d_1/D} \tag{34}$$

$$B = \left(\frac{V_2 \ln r}{D} + C\right) \tag{35}$$

First, the value of $\cos(\theta_1 + \theta_2)$ is calculated in terms of A, B, C. By substituting the values of $\cos\theta_1, \cos\theta_2$, into (19),

$$\psi = \cos^{-1}\left(\frac{(C - A - B)(4B(C - A) + C(C - 2A)) + C(C - A)(C - 2A)}{2AB(C - A - B)}\right) \tag{36}$$

where A, B are given in (35), (36) respectively.

The maximum NPV at this point is $NPV_{s=p_2}$ where,

$$\begin{aligned} NPV_{s=p_2} = {} & (V_1 + V_c)r^{-(d_0+d_1)/D} + (V_2 + V_c)r^{-d_0/D} \\ & - V_c\left(r^{-(d_0+d_1)/D} + 1\right) + NPV_{fixed} \end{aligned} \tag{37}$$

Let $l_1^*, l_2^*, \theta_1^*, \theta_2^*$ be the optimal values obtained from the DJPA. The distance l_0^* is calculated by applying the Sine rule to the triangle $p_0 s p_2$.

$$l_0^* = \frac{d_0 \sin(\theta_2 + \gamma_0)}{\sin\theta_2} \tag{38}$$

Therefore, the maximum NPV is calculated using (3) and is given by NPV^* where,

$$NPV^* = (V_1 + V_c)r^{-\left(l_0^* + l_1^*\right)/D} + (V_2 + V_c)r^{-\left(l_0^* + l_2^*\right)/D} - V_c\left(r^{-l_0^*/D} - 1\right) + NPV_{fixed} \tag{39}$$

Since l_0^*, l_1^*, l_2^* are known, the junction point coordinates x, y, z can be calculated by solving three quadratic simultaneous Eqs. (40), (41), (42).

$$l_0^{*2} = (x_0 - x)^2 + (y_0 - y)^2 + (z_0 - z)^2 \tag{40}$$

$$l_1^{*2} = (x - x_1)^2 + (y - y_1)^2 + (z - z_1)^2 \tag{41}$$

$$l_2^{*2} = (x - x_2)^2 + (y - y_2)^2 + (z - z_2)^2 \tag{42}$$

References

Brazil M, Lee D, Rubinstein JH, Thomas DA, Weng JF, Wormald NC (2004) Optimisation in the design of underground mine access In: Orebody modelling and strategic mine planning, pp 121–124

Brazil M, Thomas DA (2007) Network optimisation for the design of underground mines. Networks 49(1):40–50

Lane KF (1988) The economic definition of ore—cutoff grade in theory and practice. Mining Journal Books Limited, London

Nehring M, Topal E (2007) Production schedule optimisation in underground hard rock mining using mixed integer programming In: Project evaluation conference, issue 4, pp 169–175. The Australasian Institute of Mining and Metallurgy, Carlton

Nehring M, Topal E, Little J (2010) A new mathematical programming model for production schedule optimisation in underground mining operations. J S Afr Inst Min Metall 110(8): 437–447

Newman AM, Kuchta M (2007) Using aggregation to optimize long-term production planning at an underground mine. Eur J Oper Res 176(2):1205–1218

Sirinanda KG, Brazil M, Grossman PA, Rubinstein JH, Thomas DA (2014) Optimally locating a junction point for an underground mine to maximise the net present value. ANZIAM J 55: C315–C328

Topal E (2008) Early start and late start algorithms to improve the solution time for long-term underground mine production scheduling. J South Afr Inst Min Metall 108:99–107

Part VII
Advances and Applications in Mine Optimisation

Production Schedule Optimisation—Meeting Targets by Hedging Against Geological Risk While Addressing Environmental and Equipment Concerns

M. Spleit

Abstract A long-term production schedule for the LabMag iron ore deposit in northern Quebec, Canada is derived using stochastic integer programming. The optimization formulation maximizes the schedule's net present value, while simultaneously managing the risk of deviations in production tonnages and qualities by considering stochastic simulations of the orebody instead of a single deterministic model. The formulation also smooths and minimizes haul truck requirements and ensures that as mining progresses, space is created within the mined out pit for the return of waste material.

Introduction

The LabMag iron ore deposit is part of the Millennium Iron Range, a 210 km belt of taconite in northern Québec and Labrador, Canada. Taconite is a sedimentary rock in which the iron minerals are interlayered with quartz, chert, or carbonate and the iron content is commonly present as finely dispersed magnetite between 20 and 35% Fe. LabMag has significant economic potential: it contains 3.7 billion tonnes of measured resources at an average total iron content of 29.8% and a low average silica of 2.1%. However, the capital expenditure needed to build this project is estimated at over 5 billion dollars (SNC-Lavalin 2014), which necessitates careful evaluation of all sources of risk. Resource estimation is one of the main sources of risk in a mining project since knowledge of the orebody is primarily based on drilling, which is often sparse because it is expensive. If the expected ore tonnages and qualities are not obtained when mining, the project cash flows are directly affected. The expected quantities and qualities of ore and waste are defined by the mine production schedule, which specifies the sequence of extraction and is dependent on the resource estimation. The goal of mine production scheduling is

M. Spleit (✉)
Senior Mining Engineer, New Millennium Iron Corp, 1303 Greene Ave., 2nd Floor, H3Z 2A7 Westmount, QC, Canada
e-mail: mspleit@NMLiron.com

R. Dimitrakopoulos (ed.), *Advances in Applied Strategic Mine Planning*,
https://doi.org/10.1007/978-3-319-69320-0_36

thus to maximize the expected profit (while also meeting all production targets and constraints) by creating an extraction schedule that is robust in the face of geological risk and has the highest chance possible of actually being realized.

Conventional mine planning optimization methods are based on a single deterministic orebody model and can yield misleading results because they do not account for the likely deviation from the model in reality (Ravenscroft 1992; Dowd 1997; Dimitrakopoulos et al. 2002; Godoy and Dimitrakopoulos 2004). In order to consider the geological risk of an orebody, a set of different scenarios can be created that are all equally probable representations of the orebody, and which all reproduce the orebody's spatial variability (Goovaerts 1997). Such geostatistical simulations can be used to quantify the various elements of risk associated with a mining project: operating costs, capital costs, royalties, commodity price, taxation, tonnage, and grade (Dowd 1997; Godoy and Dimitrakopoulos 2011). Geological uncertainty can then be managed by directly incorporating stochastic simulations within the mine scheduling framework.

One flexible method for long-term production scheduling is based on stochastic integer programming (SIP) (Birge and Louveaux 1997), a type of mathematical programming and modelling that considers multiple equally probable scenarios and generates the optimal result for a set of defined objectives within the feasible solution space bounded by a set of constraints. SIP for mine scheduling is introduced in Ramazan and Dimitrakopoulos (2013), Dimitrakopoulos and Ramazan (2008), which proposes a formulation that maximizes the NPV while minimizing deviations from production targets using a different penalty for each target. Leite and Dimitrakopoulos (2014) apply the same formulation at a copper deposit and produce a risk-robust NPV 29% higher than that of a conventional schedule. Benndorf and Dimitrakopoulos (2013) applies a SIP formulation at an iron ore deposit with a formulation that integrates joint multi-element geological uncertainty. Additional considerations are easily incorporated into the modelling framework: two other relevant studies use SIP to optimize the NPV while simultaneously optimizing the cut-off grades (Menabde et al. 2018 in this volume) and incorporating simulated future grade control data at a gold deposit (Jewbali 2006). Boland et al. (2008) demonstrate stochastic formulations for mine production scheduling with endogenous uncertainty, in which decisions made in later time periods can depend on observations of the geological properties of the material mined in earlier periods, and most recently they characterize the minimal sufficient constraints for such formulations so that solving them is more efficient (Boland et al. 2014).

In this study, a SIP formulation similar to Benndorf and Dimitrakopoulos (2013) is presented to control the risk profiles of the mine production in terms of four underlying metallurgical properties: the head iron (FeH), Davis Tube weight recovery (DTWR) (Schulz 1964), the concentrate iron (FeC) and silica (SiC) grades. The existing conventional schedule has two classifications of ore, where the lower grade ore is stockpiled. The stochastic optimization seeks to avoid stockpiling and lower costs by deciding dynamically to which of two destinations to send each block (the waste dump or the process plant) while still meeting grade

constraints. Constraints are also included to smooth the annual haul truck fleet requirements in order to avoid purchases that lead to under-utilized equipment. The formulation also seeks to maximize the space available for in-pit tailings disposal (roughly two thirds of the ore to be mined at LabMag) in order to reduce the environmental footprint. LabMag is a stratigraphic deposit and its layers co me to the surface at a low dip of only six degrees, which makes it amenable to this type of tailings management strategy.

In the following sections, a SIP formulation for long-term production scheduling with equipment and tailings management is presented. The case study at LabMag follows, and the scheduling results are compared to conventionally scheduled results. Finally, the results are discussed and conclusions follow.

Sip Formulation

The following objective function is defined as the maximisation of the NPV minus various penalty terms that control the geological risk profile, minimize fleet requirements, and promote mining adjacent blocks in the same period in order to generate a practical schedule.

Notation

The constant and variable factors used in the SIP model are defined below:

P	Number of periods
N	Number of blocks in the orebody model
D	Number of destinations
S	Number of simulations
Q	Number of metallurgical qualities
$V_{i,d,s}$	Value of block i in simulation s going to destination d in time period t
$TH_{d,t}$	Total truck hours in period t for destination d

Small differences in tonnage (and thus truck hours) can be expected due to variations in the lithology and thus the density but are ignored here for simplicity.

C_t^{TH}	Operating Cost ($/hour) for trucking, discounted by period t
$b_{i,d,t}$	Binary variable with a value 1 if block i is mined in period t and sent to destination d; and 0 otherwise.
Pen^{conc}	The penalty per tonne deviation ($/t concentrate) from the target concentrate production in each period; constant
Pen^{q}	The penalty per tonne of quality content ($/t quality q) in each perove or below the associated upper or lower limits respectively; constant

$\overline{dev}_t^{conc}$	Concentrate tonnes in excess of the upper limit
$\underline{dev}_t^{conc}$	Concentrate tonnes less than the lower limit
$\overline{dev}_t^{q}$	Tonnes of metal or mineral q in excess of the upper limit, where $q = 1,\ldots,Q$ considered qualities
$\underline{dev}_t^{q}$	Tonnes of metal or mineral q less than the lower limit
$c_t = \frac{1}{(1+\mathrm{r})^{t-1}}$	A function for discounting profits and costs with the discounting factor r according to the period t when the block is mined
$g_t = \frac{1}{(1+\mathrm{GRD})^{t-1}}$	A function for discounting geological risk with the discounting factor GRD according to the period t when the block is mined

Mining Block Economic Value

The undiscounted value for each block is defined as:

$$V_{i,d,s} = \begin{cases} NR_{i,s} - CONC_{i,s} * \mathrm{PCost} - ROM_{i,s} * \mathrm{OCost} - W_{i,s} * \mathrm{WCost}, d = 1 \\ -\left(ROM_{i,s} + W_{i,s}\right) * \mathrm{WCost} \qquad , d = 0 \end{cases} \quad (1)$$

given that

$$CONC_{i,s} = ROM_{i,s} = *eWR_{i,s} \quad (2)$$

where for block i and simulation s, $NR_{i,s}$. Represents the net revenue, *OCost* and *WCost* the mining cost of ore and waste respectively (excluding truck haulage, which is penalized directly in the objective), *PCost* the processing cost (considers crushing, concentration, filtration, pelletization, transportation, administration, etc.), *ROM* the run-of-mine tonnage from the iron-bearing lithologies, *W*. The tonnage from waste rock, and *eWR* the effective weight recovery (considers ideal Davis Tube Weight Recovery as well as plant efficiency parameters).

Note that by having trucking costs in the objective function as opposed to the block value, it is possible to consider trucking costs for a block that vary depending on the period that block is scheduled to be mined. In future research, if mobile crushers are considered rather than a fixed plant location, the haulage cost could also be dependent on the variable distance to the crusher.

Objective function

The objective function of the SIP model is constructed as the maximization of a profit function, defined as the total expected net present value minus penalties for deviations from planned production targets and penalties for not mining the blocks adjacent to a mined block (Ramazan and Dimitrakopoulos, 2013; Benndorf and Dimitrakopoulos 2013).

$$\text{Maximize Obj} = \sum_{t=1}^{P}\sum_{i=1}^{N}\frac{1}{S}\sum_{d=1}^{D}\sum_{s=1}^{S} c_t V_{i,d,s} b_{i,d,t} \tag{3a}$$

$$-\sum_{t=1}^{P}\sum_{i=1}^{N}\sum_{d}^{D} b_{i,d,t} c_t TH_{d,t} C_t^{TH} \tag{3b}$$

$$-g^t \sum_{t=1}^{P}\sum_{\mathrm{s}=1}^{S}\left[Pen^{\mathrm{conc}}\left(\overline{dev}_{st}^{conc} + \underline{dev}_{st}^{conc}\right) + \sum_{q=1}^{Q} Pen^{q}\left(\overline{dev}_{st}^{q} + \underline{dev}_{st}^{q}\right)\right. \tag{3c}$$

$$-\sum_{\mathrm{t}=1}^{P}\sum_{i=1}^{N} Pen^{\mathrm{smooth}} dev^{smooth} \tag{3d}$$

This objective function includes four distinct terms. The term Eq. (3a) is the imary term and represents the net present value of all blocks mined in the optimization. The term Eq. (3b) represents the trucking operating cost, which is minimized. The term Eq. (3c) acts to penalize deviations from target concentrate tonnes, and the target silica grade and weight recovery (see the next section for more details). The variables for the deviations are determined by the optimization process, based on the corresponding constraints that are set. The term Eq. (3d) is a penalty for not mining adjacent blocks. It is desirable to mine blocks in groups in order to generate a practical schedule. There is a trade-off between the penalty terms, and it is the relative size of the penalties that determine this trade-off.

Constraints

Constraints are applied for ensuring equipment accessibility, processing capacity, geotechnical aspects, and blending requirements, the details of which are described in Benndorf and Dimitrakopoulos (2013). In addition, constraints are included here to control the schedule sequence and the number of haul trucks in each period.

Sequencing constraints

In order to accommodate in-pit tailings disposal, each block is set to be mined only if the block to the south-west (cross-dip, towards where the deposit daylights at surface) is mined in the same or an earlier period.

For each i, where $j \in$ {predecessors blocks of block i}

$$\sum_{d=1}^{D}\left(b_{i,d,t}-\sum_{k=1}^{t}b_{j,d,k}\right)\leq 0 \tag{4}$$

Haulage capacity constraints

To avoid a truck being leased, or purchased and then left unused, a constraint is added to enforce that the number of trucks in each period must be equal to or more than in the previous period. Leeway of half the available working hours of one truck in one period is given.

$$\begin{aligned}&\sum_{i=1}^{N}\sum_{d=1}^{D}H_d b_{i,d,t}-\sum_{i=1}^{N}\sum_{d=1}^{D}H_d b_{i,d,(t-1)}\\ &\geq -\tfrac{1}{2}\,\textit{Total working hours available for one truck in one period}\end{aligned} \tag{5}$$

where $t = 2,\ldots,P$; H_d is the total time (hours) required for transportatn of a block to destination d (the cycle time for one truck is on the order of minutes, but since each block can contain approximately half a million tonnes, many truck cycles are needed).

Application at the Labmag Iron Ore Deposit

The formulation in the previous section is applied at the LabMag taconite iron ore deposit in northern Labrador, Canada in order to create a mine production schedule that considers multi-element grade uncertainty as well as equipment and tailings requirements.

Stochastic Orebody Models at LabMag

Mine production scheduling here considers geological variability by using ten stochastic conditional simulations. Each realization consists of a joint simulation of the seven correlated layer thicknesses as well as the joint simulation of four correlated ore characteristics in each layer. Each model consists of 13,400 blocks (100 m × 100 m × 15 m). Since all ore lithologies are processed in the plant in the same manner, scheduling considers the average qualities of all layers in each block.

The two primary waste-types for the LabMag deposit are overburden (OB) and Menihek Shale (MS). The OB overlies the entire deposit and is minimal (the underlying rock is commonly exposed at surface). The MS layer is present on the north-east side of the deposit, overlying the iron layers and dipping parallel to them at approximately 6° (see Fig. 1).

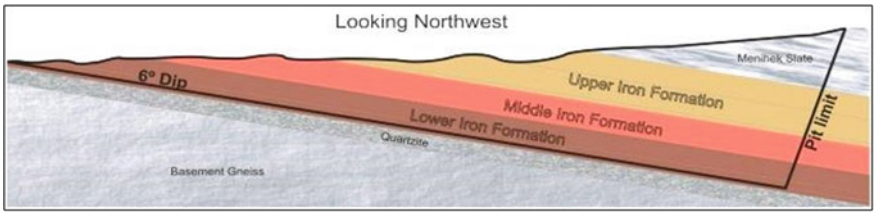

Fig. 1 LabMag typical cross-section

Implementation

The SIP model described above was implemented in Visual C++ using the ILOG CPLEX API. The initial attempts to solve the full orebody model for all 10 periods proved to be unsolvable in a reasonable amount of time (the optimization had made little progress after several days, running on a 64-bit Dell Precision M6500 Intel I7 quad-core @ 1.73 GHz and 16 GB of RAM). The initial 13,400 blocks considered are the blocks contained within the ultimate pit derived using the nested Lerchs-Grossman algorithm. Since only the first ten years are scheduled within the optimization and the LabMag ultimate pit contains more than twenty-five years of ore at the planned capacity, the precise pit limit need not be discussed further here. To reduce the number of blocks, a new pit was designed that takes as many blocks as possible but avoided the MS waste layer. Since the optimization targets the first 10 years and tries to minimize trucking hours as well as unnecessary waste, it was evident that the optimization would avoid the MS region of the deposit anyway. This brought the number of blocks down to 8411. The optimization is broken down into four sub-optimizations (see Fig. 2) each set to stop once there was less than 1% gap between the solution and the optimal solution.

The optimization uses DTWR and SiC bounds and penalizes values outside those bounds. The process plant is designed for 27% DTWR, but an range around this target that the plant can still handle is permitted to allow the optimization to select the most economic material when also considering haul cycle times and the other constraints. Scheduling higher DTWR has a trade-off with haul distance however, because most of the higher grade DTWR material is located in the north end of the deposit, which is further from the crusher. The silica range is selected to be within the plant tolerance levels. The average silica of the single period (10 year) optimization is 2.2%, so this became the new target for subsequent optimizations because a consistent silica blend is desired across all periods.

Deviations from the targets are penalized in the objective function. The highest weight penalty is given to the concentrate tonnage and is determined by increasing a low initial value it until the expected scheduled concentrate tonnages meet the targets. The other quality penalties are then set relative to the concentrate tonnage deviations penalty. As discussed in Benndorf and Dimitrakopoulos (2013), high penalties for tonnage and quality deviations relative to non-smooth mining penalties tend to yield

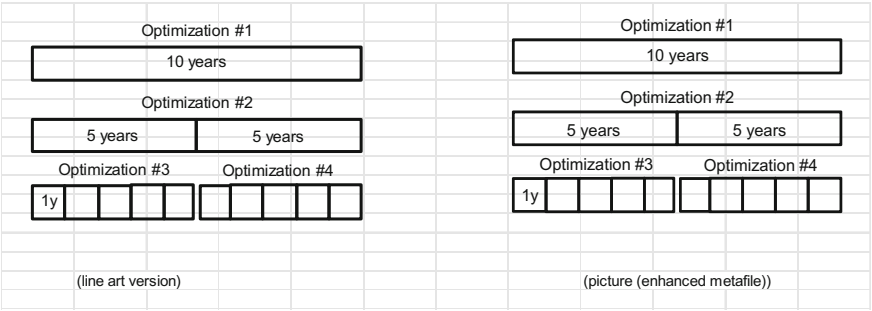

Fig. 2 Schematic representation of four-stage schedule optimization

schedules with more dispersion of the scheduled blocks. The non-smooth mining penalty here are determined by setting it to zero initially, and then slowly increasing it until the number of scattered blocks in each period are few enough that a feasible schedule could be manually designed without too much difficulty.

Results

The results of the optimization provide the optimal period in which to mine each block, and whether to send the block for processing or to the waste dump. An interesting result is that the only blocks sent to the waste dump are located at the surface of the deposit and contain mostly OB, and/or MS waste, which means that all scheduled material within the 7 iron-bearing units is sent to the plant. Had ore blocks with a low DTWR been sent to the dump, this would have promoted the concept of stockpiling ore with a low weight recovery. However, this is not the case so the only reason to stockpile ore would be to restrict the silica levels. In the optimized schedule, the silica levels are managed without the need for such a restriction.

A practical mining schedule was designed based on the block-scale optimization. The optimization considers the first 10 years, and an additional 15 years were scheduled manually to allow for full comparison against an existing conventional schedule. The pit designs use a 15 m bench height, 45° slope angle for the pit sides and hanging wall, and the pit bottom follows the natural inclination of the orebody at approximately 6° (10.5%). Although this slope is not optimal for the haul trucks, various truck manufacturers were consulted and they agreed that it is manageable. Catch berms of 9.5 m with a face angle of 70° were included for additional safety considerations. Since the orebody daylights at surface, the ultimate pit does not require the design of a permanent access ramp to the pit bottom. The benches will be mined flat and the pit access will be developed along the floor as the pit wall advances towards the East.

The evolution of the pit in the stochastic optimization schedule is along the full length of the deposit, progressively deepening perpendicular to the strike. This differs from the conventional design that is based on slots that are mined West to East along the full width of the defined resource and mining at depth already in early periods. The stochastic optimization schedule thus has shorter haul times in earlier periods and less trucks since they can travel at near top-speed (30–35 km/h on a straight-away), whereas the trucks are limited to 15 km/h or less when exiting the deeper areas of the pit due to the incline of 8% with 2–3% rolling resistance. Another advantage of mining along the length of the deposit is that the grades vary primarily along the strike: higher DTWR material is found to the north, but with higher SiC as well. Having open faces along the full length of the deposit allows for more flexibility during operations to achieve the necessary blend.

Figure 3 shows that the truck productivity of the optimized schedule is at its maximum in the earlier periods, and steadily declines with each period as the pit is deepened and the cycle times increase. For the deterministic schedule, the productivity moves up and down as each full-width slot is mined. The optimized schedule ensures higher productivity in earlier periods and thus lower corresponding operating costs.

Risk Management in the Stochastic Schedule

Beyond seeking the maximum NPV, the stochastic optimization schedules material that has a high probability of meeting production targets, both in terms of qualities and tonnages. Conventional scheduling consists of non-probabilistic approaches that can produce misleading results.

In Fig. 4, the annual concentrate tonnages from a previous conventional schedule designed based on a deterministic geological model are shown. The solid

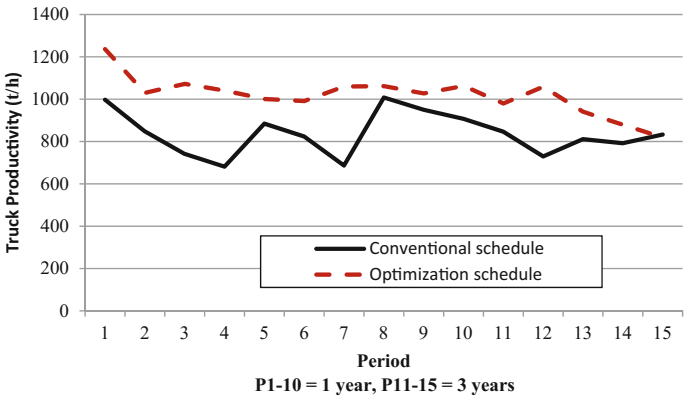

Fig. 3 Truck productivity comparison (conventional and stochastic schedule)

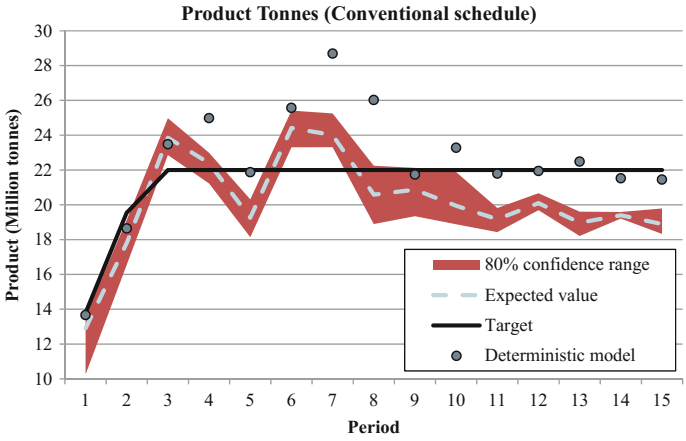

Fig. 4 Product tonnes in conventional schedule

black line shows the target tonnages (22 million tonnes per year with a ramp-up). The grey points show the estimated values when evaluating the schedule using the conventional deterministic orebody model that the schedule was based on. There are a few periods with excess tonnage due to the fact that inferred resources were ignored in designing the original conventional schedule, but they are included in the evaluation here to demonstrate the probability of schedule deviations when the deposit is actually mined. In most periods, the values obtained using the deterministic model are consistent with the targets. However, these single estimated values are misleading. The dashed light blue line shows the expected value for each year, which is the mean of the set of values obtained by evaluating the schedule using each of the simulations. In addition, the uncertainty in these values is shown in red. The range of values obtained by evaluating the schedule with each of the simulations allows for estimating the probabilistic distribution of true values instead of a providing a single estimated value. The probabilistic evaluation shows that the deterministic model systematically over-estimates the quantity of concentrate tonnes. This is due to differences in the head iron (FeH) in the simulations compared to the FeH in the deterministic model. The densities of each lithology are dependent (and calculated using regressions) on the FeH in each layer as determined in a previous density study (Milord 2012). The fact that the deterministic model predicts slightly higher ROM tonnages per period indicates that the averaged FeH values of the deterministic model result in overestimation of the tonnages.

In Fig. 5, the annual concentrate tonnages from the stochastic optimization schedule are shown. The expected tonnages from the stochastic schedule are consistent with the targets and also have a greatly reduced risk profile, which is shown by how tight the 80% confidence range is.

The annual values for the stochastic schedule for the two primary qualities (DTWR and SiC) are shown in Figs. 6 and 7 to demonstrate the effectiveness of the stochastic schedule to control the qualities and their risk profiles. DTWR values

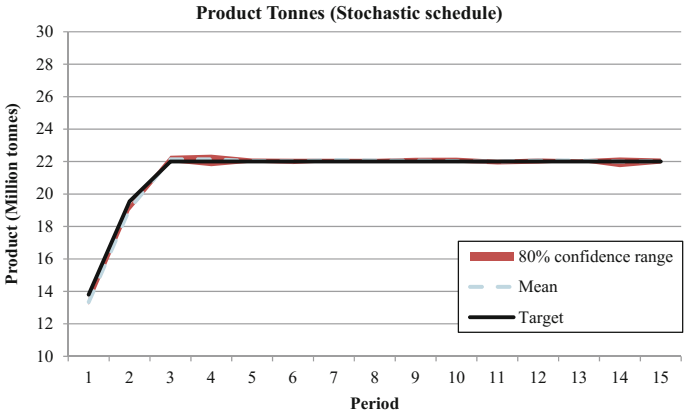

Fig. 5 Product tonnes in stochastic schedule

(Fig. 6) vary by only 0.4% on average. An interesting result was that the DTWR was not higher in earlier periods as expected. This was expected because a greater weight recovery means less ore must be mined to produce the same tonnage of concentrate, which means lower costs. This result can be explained by the benefit of a higher DTWR compared to a higher cost of mining at depth. The optimization seeks the greatest profit, so lower DTWR ore can be mined as long as the benefit of mining nearer to the surface offsets the benefit of any potential material with a higher DTWR. However, this may be an artificial result: processing costs and plant efficiencies are variable with respect to feed material, yet they are assumed as fixed in this study. With the inclusion of more detailed variable processing costs and efficiencies, it is likely that higher DTWR material would be scheduled in earlier periods before the process plant is fully commissioned and operating consistently. The silica (SiC) range for each year in the stochastic schedule (Fig. 7) can be seen

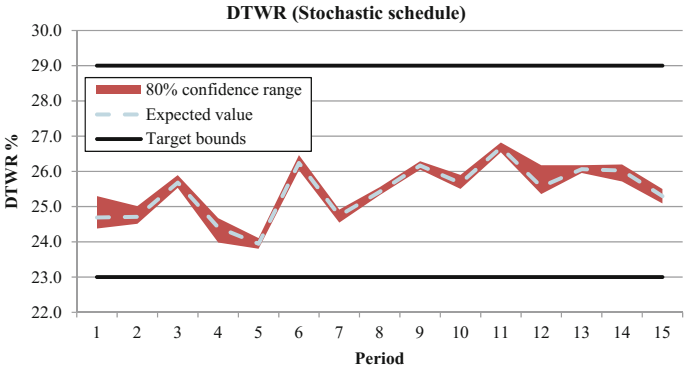

Fig. 6 Annual DTWR of feed ore and risk profile in the stochastic schedule

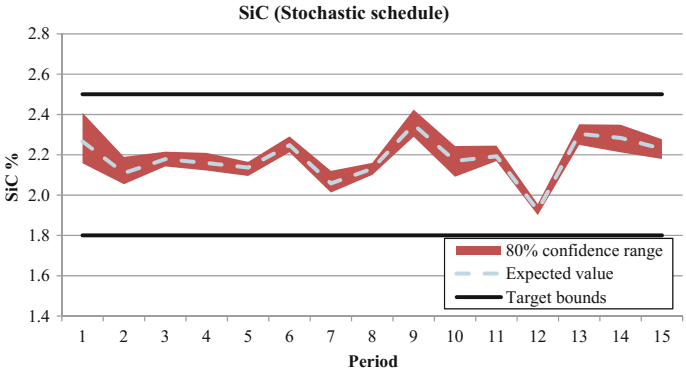

Fig. 7 Annual silica of concentrate and risk profile in the stochastic schedule

to fall within the specified upper and lower limits of 2.5% and 1.8% respectively, hovering around the target of 2.2% and demonstrating the ability of the stochastic modelling to ensure low risk of not meeting targets.

Financial Impact of Stochastic Scheduling

In addition to controlling the qualities and tonnages, the stochastic optimization maximizes the discounted cash flows. This can be accomplished by minimizing waste mining, minimizing haulage cycle times, and by scheduling higher grade material. The stochastic optimization not only maximizes the discounted cash flows, but by controlling the geological uncertainty it also ensures a greater certainty in the financial forecasts.

Compared to the stochastic optimization schedule, there is a significant amount of MS waste mined in the conventional schedule as well as additional ore that is stockpiled instead of being sent to the plant. Mining these two materials requires a significant amount of additional equipment, which translates to higher costs than those for the stochastic schedule. The expected annual waste and stockpile tonnages (based on evaluating the schedule with the simulations) are shown in Fig. 8 for both the conventional and stochastic schedule. Low grade ore is stockpiled in the conventional schedule based on a fixed cut-off in order to ensure the desired ore qualities going to the plant. There is no stockpile in the optimization schedule, which seeks instead to meet the desired ore quality constraints by sending material only to either the process plant or the waste dump. Figure 8 shows that the combined tonnage of waste and stockpiled ore is roughly between 20–50 mtpy for all periods, whereas the stochastic schedule has no stockpiled tonnes and only minimal waste. The stochastic optimization was performed on a pit that purposely avoided the MS, and so there is minimal stripping in all years. The very low amount of waste mining was intended, and is a crucial component to minimizing costs in the first 10 years.

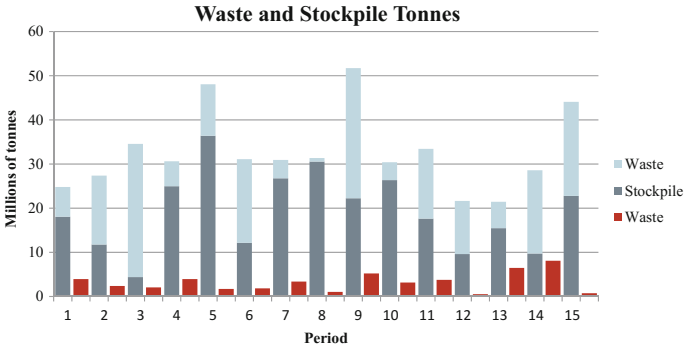

Fig. 8 Expected waste and stockpile tonnes comparison (conventional and stochastic schedule)

Figure 9 shows a comparison between the fleet requirements of the two schedules (conventional and stochastic) for haul trucks and the primary cable shovels. Equipment calculations take into account a variety of factors including mechanical availability, utilization, job efficiency, operating delays, payload, spot times, dump times, load times, and cycle times. The new maximum number of trucks required over the 10 year period is 20 trucks, as opposed to the previous 35 trucks. Less trucks are needed because the haul cycle times are shorter, so the trucks are more productive. In addition, there is less waste mining, which also contributes to the reduced number of equipment. The necessary cable shovels was reduced by one, which is significant because each cable shovel costs almost four times as much as one truck. The change in fleet requirements reduces the capital cost requirements by 23.7% and a corresponding reduction in the operating costs by 26.2%.

The impact of these cost reductions and the reduction of geological variability can be seen together in a comparison of discounted cash flows for both schedules (Fig. 10). The dashed black line shows the estimated results from the conventional schedule when it is evaluated using a single deterministic orebody model. All other

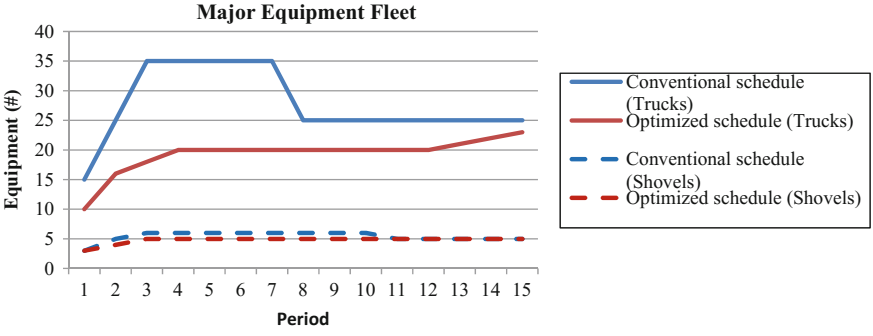

Fig. 9 Major equipment fleet comparison (conventional and stochastic schedule)

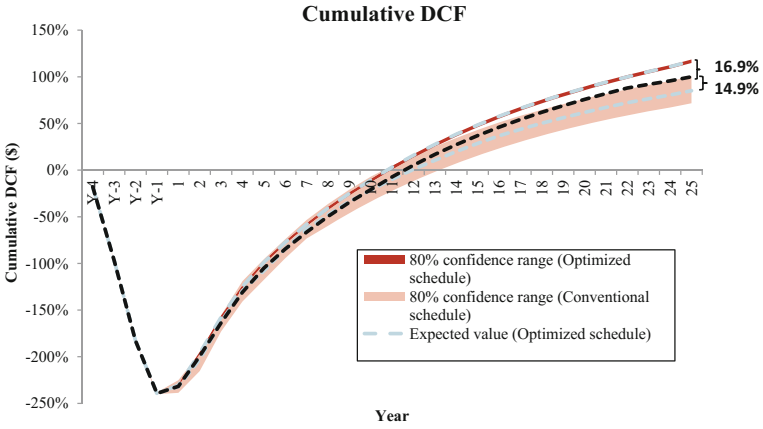

Fig. 10 Cumulative DCF comparison (conventional and stochastic schedule)

results are shown relative to this. The pink zone shows the 80% confidence range of the conventional schedule when it is evaluated with the stochastic simulations. Almost all simulations result in a lower NPV and the expected value of the simulations is 14.9% less than the estimated value. This is directly related to the overestimation of product tonnes by the deterministic orebody model. The 80% confidence range spans 28.9% of reference conventionally estimated NPV, which indicates significant uncertainty in the NPV.

The stochastic optimization schedule, however, has an expected NPV that is 16.9% higher than the reference conventionally estimated NPV. The 80% confidence range is 2.5%, ranging from 15.6% to 18.1% more than the NPV of the deterministic schedule, which represents a significantly reduced risk profile. This indicates that a higher NPV is achieved with the stochastic schedule and that there is a much greater probability of actually achieving this result.

Conclusions

A feasible mining schedule was derived for the LabMag iron ore deposit using a SIP formulation that minimizes the risk of deviation of target concentrate tonnages and product silica grades from their targets. The optimized schedule also yielded an expected NPV 16.9% higher than that of a conventional schedule and has a higher chance of being realized due to the reduced risk in concentrate tonnages. These benefits are obtained because stochastic scheduling uses multiple simulations to assess the risk of different block groupings, which is ignored by conventional scheduling based on a single estimated orebody model. The SIP framework used here also allows for easily balancing multiple goals simultaneously, which is otherwise a challenging task. An even higher NPV could potentially be achieved if

the optimization used a block selectivity closer to that of the equipment selectivity, as there would be greater flexibility in the combinations of blocks for scheduling purposes.

The presented scheduled formulation accounts for haulage distances by minimizing trucking costs while also ensuring a smooth truck fleet with no sudden jumps or drops in requirements. In comparison to the first ten years of the previous life-of-mine schedule, the proposed schedule reduces the required number of trucks by 15 (previous total of 35 trucks) to 20 total trucks and the required number of shovels by 1–5 shovels total. This has a corresponding impact of 23.7% reduction in capital costs, and 26.2% reduction in operating costs over the first 10 years. The proposed schedule mines the orebody in a progressively deepening fashion, maintaining a larger working area at any given time, rather than mining a slot that reaches the full depth of the deposit. This also permits the eventual disposal of dry tailings and waste inside the pit in order to reduce the environmental footprint.

References

Benndorf J, Dimitrakopoulos R (2013) Stochastic long-term production scheduling of iron ore deposits: integrating joint multi-element geological uncertainty. J Min Sci 49(1):68–81

Birge JR, Louveaux F (1997) Introduction to stochastic programming. Springer series in operations research, New York

Boland N, Dumitrescu I, Froyland G (2008) A multistage stochastic programming approach to open pit mine production scheduling with uncertain geology. Optimizaton Online. http://www.optimization-online.org/DB_FILE/2008/10/2123.pdf. Accessed 10 Apr 2014

Boland N, Dumitrescu I, Froyland G, Kalinowski T (2014) Minimum cardinality non-anticipativity constraint sets for multistage stochastic programming with endogenous observation of uncertainty. Univ NSW, Sch Math Stat. http://web.maths.unsw.edu.au/~froyland/Non-anticip_Gen_Matroid_v6.pdf. Accessed 10 Apr 2014)

Dimitrakopoulos R, Ramazan S (2008) Stochastic integer programming for optimizing long term production schedules of open pit mines: methods, application and value of stochastic solutions. Min Technol: Trans Inst pp 155–167

Dimitrakopoulos R, Farrelly C, Godoy MC (2002) Moving forward from traditional optimisation: grade uncertainty and risk effects in open pit mine design. Section A Mining Industry, Transactions of the IMM, pp A82–A89

Dowd PA (1997) Risk in minerals projects: analysis, perception and management. Section A Mining Industry, Transactions of the IMM, pp A9–18

Godoy M, Dimitrakopoulos R (2004) Managing risk and waste mining in long-term production scheduling. SME Trans 316:43–50

Godoy M, Dimitrakopoulos R (2011) A risk quantification framework for strategic risk management in mine design: method and application at a gold mine. J Min Sci 84(2):235–246

Goovaerts P (1997) Geostatistics for natural resources evaluation. Oxford University Press, New York

Jewbali A (2006) Modelling geological uncertainty for stochastic short-term production scheduling in open pit metal mines. PhD Thesis, Queensland: School of Engineering, University of Queensland

Leite A, Dimitrakopoulos R (2014) Production scheduling under metal uncertainty: application of stochastic mathematical programming at an open pit copper mine and comparison to conventional scheduling. J Min Sci Technol 24 (in press)

Menabde M, Froyland G, Stone P, Yeates G (2018) Mining schedule optimization for conditionally simulated orebodies, in this volume

Milord I (2012) Densité relative de LabMag et KéMag. Table jamésienne de concentration minière, Chibougamou

Ramazan S, Dimitrakopoulos R (2013) Production scheduling with uncertain supply: A new solution to the open pit mining problem. Optim Eng 14:361–380

Ravenscroft PJ (1992) Risk analysis for mine scheduling by conditional simulation. Section A (Mining Technology), Transactions of the Institute of Mining and Metallurgy, pp 104–108

Schulz NF (1964) Determination of the magnetic separation characteristics with the Davis Magnetic Tube. SME-AIME Trans 229:211–216

SNC-Lavalin (2014) Technical report on the feasibility study of the LabMag iron ore deposit, Labrador, Canada. Montréal

A Stochastic Optimization Formulation for the Transition from Open-Pit to Underground Mining Within the Context of a Mining Complex

J. MacNeil and R. Dimitrakopoulos

Abstract As open-pit mining of a deposit deepens, the cost of extraction may increase up to a threshold where transitioning to mining through underground methods is more profitable. This paper provides an approach to identify an optimal depth at which a mine should transition from open-pit to underground mining. The value of a set of candidate transition depths is investigated by optimizing the production schedules for each depth's unique open-pit and underground operations. By considering the sum of the open-pit and underground mining portion's value along with the cost of transitioning corresponding to each candidate transition depth, the optimal transition depth can be identified. The optimization model presented is based on a stochastic integer program that integrates geological uncertainty. As an input, the stochastic integer program utilizes a set of several stochastic simulations that represent equally probable scenarios of the mineral resource. This group of simulations describes the uncertainty in the deposit while the optimizer aims to maximize value based on discounted profits of both the open-pit and underground components of the deposit.

Introduction

The transition from open-pit (OP) to underground (UG) methods requires a large capital cost for development and potential delays in production but can provide access to a large supply of reserves and consequently extend a mine's life. Additionally, an operating mine may benefit from a transition because of the opportunity to use existing infrastructure and equipment, particularly when in a remote location. Any optimization approach to the open-pit to underground transition decision (or OP-UG) may be simplified by discretizing the space above and below ground. For surface mining, material is typically discretized into mining

J. MacNeil (✉) · R. Dimitrakopoulos
COSMO Stochastic Mine Planning Laboratory,
McGill University, Montreal, QC H3A 0E8, Canada
e-mail: james.a.l.macneil@gmail.com

R. Dimitrakopoulos (ed.), *Advances in Applied Strategic Mine Planning*,
https://doi.org/10.1007/978-3-319-69320-0_37

blocks, while underground, material is frequently grouped into stopes of varying size depending on the mining method chosen. From there and through production scheduling optimization, the interaction between the OP and UG components can be modeled to realistically value the asset under study.

Historically, optimization research efforts in mine planning have been focused on open-pits as opposed to underground operations. Most commonly, the open-pit planning process begins by determining the ultimate pit limits and industry standard is the nested implementation of the Lerchs–Grossman's (LG) algorithm (Lerchs and Grossman 1965; Whittle 1988, 1999) which utilizes a maximum closure concept to determine optimal pit limits while the nested implementation facilitates discounting. Newer developments allow for the joint optimization of an extraction sequence leading to optimal pit limits based on mathematical programming implementations, such as those in BHP Billiton's BLASOR (e.g. Stone et al. 2007; Zuckerberg et al. 2010). For underground mine planning, optimization techniques are less advanced as when compared to those employed for open-pit, and heavily depend on the mining method used. In practice, underground long-term planning is divided into two phases: design and production sequencing. For stoping methods, the Floating Stope algorithm (Alford 1995) is the oldest computerized design tool available, although not an optimization algorithm. Mine optimization research has developed methods that schedule the extraction of discretized units in underground mines (e.g. Trout 1995; Nehring and Topal 2007) based on mixed integer programming (MIP) approaches. Nehring et al. (2009) and Little and Topal (2011) extend MIP approaches to reduce the solution times. Adaptation of open pit MIP approaches for optimization of underground strategic mine planning are also known (Roberts and Bloss 2014, in this volume).

Some of the world's largest mines are expected to reach their ultimate pit in the next 15 years (Kjetland 2012). Despite the importance of the topic, there is no established algorithm to simultaneously generate an optimal mine plan that outlines the transition from open-pit mining to underground (Fuentes and Caceres 2004). From the early work described in Popov (1971), a movement towards optimization is made by Bakhtavar et al. (2008) who present a heuristic method that compares the economic value of mine blocks when extracted through OP versus their value if extracted by UG techniques. The method iterates progressively downwards through a deposit, concluding that the optimal transition is the depth is reached when the value of a block mined by UG methods exceeds the corresponding OP mining value. Drawback of this method is that it remains an idea applied to a small two-dimensional case study. A main effort is presented in Newman (2013) where the transition depth problem is formulated as a longest-path network flow. This approach determines the optimal transition depth by creating a network that outlines possible mining sequences, their corresponding transition depths along with the associated net present value (NPV). Major limitation of this development is that it amounts to a 2D solution of what is a 3D problem, as the orebody is discretized into horizontal strata for the above and below ground mining components. At the same time worst-case bench-wise mining schedule is adopted for open-pit production

(Whittle 1988; Godoy 2002) and a bottom-up schedule for the underground block caving component of the mine. The last aspects do not adequately value the asset, since the schedule is far from optimal. More realistic selective mining units and an optimized schedule can also provide a more accurate representation of a mine's value, and this is the approach taken by Dagdelen and Traore (2018; in this volume) who further extend this to the context of a mining complex.

All above mentioned attempts to optimize the OP-UG transition depth discussed above fail to consider geological uncertainty, the major source of failure in mining projects (Vallee 2000). Stochastic optimizers integrate and manage geological uncertainty (e.g. grades, material types, metal, rock properties) through the scheduling process. Such scheduling optimizers have been long shown to increase the net present value (NPV) of an operation, while providing a schedule that has a high probability of meeting metal production and cash-flow targets (e.g. Godoy 2002; Ramazan and Dimitrakopoulos 2005, 2013; Jewbali 2006; Albor and Dimitrakopoulos 2010; Whittle 2010; Goodfellow 2014; Montiel 2014; and others).

In this paper, a two-stage stochastic integer programming (SIP) formulation is presented and is based on the one proposed in Ramazan and Dimitrakopoulos (2013) but adopted to find the optimal transition depth by maximizing the value of the operation while considering geological uncertainty. The proposed framework discretizes the material above ground into blocks, and uses a SIP formulation that accounts for uncertain supply to determine the long-term production schedule. For the underground portion of the mine, a stope layout design is assumed and the stope sequence is developed through the SIP proposed, but with added constraints developed in Little et al. (2008). The method presented in the next section advances the previously completed research by jointly deciding the transition depth in three-dimensions as a stochastically optimal ultimate pit limit valuing the open-pit and underground mining components based on optimal extraction sequences while considering geological uncertainty.

Method

The General Set Up: Candidate Transition Depths

The method proposed herein to jointly determine the transition depth from OP to UG mining is based on the discretization of the orebody space in different ways and then assessing jointly the OP and UG mine scheduling optimizations, which follow the discretization of the orebody space selected. More specifically, this leads to several candidate transition depths being assessed in terms of production scheduling and the depth generating the highest total discounted profit is chosen. SIP provides the required optimization framework in dealing with stochastic representations of geological uncertainty in generating the OP and UG long-term production schedules needed.

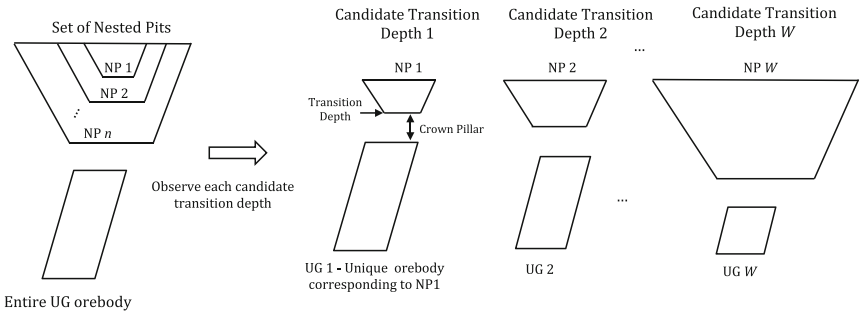

Fig. 1 Generating candidate transition depths

For the potential OP portion of a mine considered, the orebody space can be discretized using the nested LG approach (Whittle 1988), noting that different approaches may be used, to find possible truly three-dimensional transition depths. Selected nested pit shells can then serve as the ultimate pit for a certain candidate transition depth to be tested, which allows to eventually generate the subsequently referred to as the transition pit. Below the transition pit lies the crown pillar, which is a large portion of undisturbed host material serving as the first line of protection between the lowest OP working and the highest UG levels. For each candidate transition pit, the crown pillar location changes, thus also influencing the size and dimension of portion of the orebody that can be accessed by underground mining (Fig. 1). It follows that each candidate transition depth has a corresponding unique OP and UG part of the orebody being considered.

To forecast the value of the mining asset through the interaction between the OP and UG operations these two components viewed as separate but interacting entities. It is possible to consider different scenarios which would require the two portions of the mine to be optimized simultaneously; however, here it is assumed that underground mining will commence after open-pit production has finished. An optimization solution producing a long-term schedule maximizing NPV, the OP and UG operations are optimized separately, and considering each of the candidate transition depths (and ultimate pit) being assessed. Once optimal extraction sequences above and below ground have been derived for each depth, the value of transitioning at a certain depth can be determined by summing the value of the OP and UG components. From here, the combined NPVs at each depth can be compared to easily identify the most favorable transition decision. This process is outlined in Fig. 2.

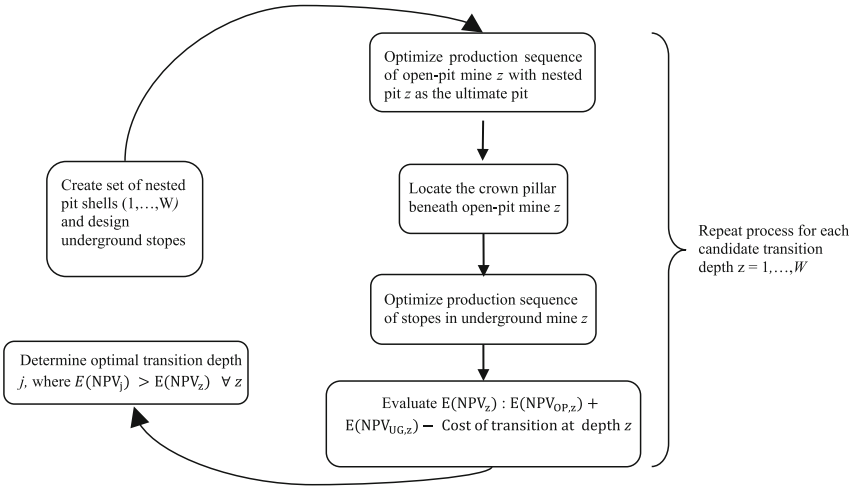

Fig. 2 Schematic representation of the proposed optimization approach

Stochastic Integer Programming: Mine Scheduling Optimization

In general, the optimization procedures for the two portions of an orebody have similar objectives but substantially different intricacies in their details and, importantly, constraints because of their disparate extraction procedures. OP optimization produces a long-term schedule that outlines the optimal extraction sequence for the mining blocks within a specific transition pit. The stochastic integer program aims to maximize discounted cash-flow while producing a sequence that abides by the relevant constraints. Operationally-specific constraints such as processing capacity, mining capacity, blending requirements, as well the standard reserve and precedence relationships are included. A two-stage stochastic programming approach allows for the inclusion of recourse variables which penalize deviations from metal and grade blending targets. The UG optimization adopts the same two-stage stochastic programming approach to underground mining constraints. The description of each of the formulations follow.

Indices:

g and o are target parameters, or type of production targets; g is for the grade targets; o if for the ore production target;
i is the block identifier;
j is the stope identifier
l is the minimum target (lower bound);
s is a simulated orebody model;
t is a scheduling time period;
u is the maximum target (upper bound).

Known Parameters:

COT_z is the cost of transitioning at transition depth z;
C_h is the haulage cost during OP mining;
$c_u^{OP,to}, c_l^{OP,to}, c_u^{OP,tg}, c_l^{OP,tg}$ are unit costs for $d_{su}^{OP,to}, d_{sl}^{OP,to}, d_{su}^{OP,tg}, d_{sl}^{OP,tg}$ respectively in the OP optimization's objective function;
$c_u^{UG,to}, c_l^{UG,to}, c_u^{UG,tg}, c_l^{UG,tg}$ are unit costs for $d_{su}^{UG,to}, d_{sl}^{UG,to}, d_{su}^{UG,tg}, d_{sl}^{UG,tg}$ respectively in the UG optimization's objective function;
e_j is the set of stopes horizontally and vertically adjacent to tope j;
$E\{V_{i/j}\} = \begin{cases} NR_{i/j} - MC_{i/j} - PC_{i/j} & \text{if } NR_{i/j} > PC_{i/j} \\ -MC_{i/j} & \text{if } NR_{i/j} \leq PC_{i/j} \end{cases}$ is the economic value of a block i/stope j;
$E\{(NPV_i^t)\} = \frac{E\{(EV)_i^0\}}{(1+r)^t}$ is the expected NPV to be generated if the block i is produced in period t;
$E\left\{(NPV_j^t)\right\} = \frac{E\{(EV)_j^0\}}{(1+r)^{t+u}}$ is the expected NPV to be generated if the stope j is produced in period t;
G_{tar} is the targeted grade of the ore material to be processed;
$g_{i/j}^s$ grade of block i/stope j in orebody model s;
l_i is the set of predecessor for block i
M is the number of simulated orebody models;
$MCap_{min}^{OP}$ / $MCap_{min}^{UG}$ is the minimum amount of OP/UG material required to be mined in a given period;
$MCap_{max}^{OP}$ / $MCap_{max}^{UG}$ is the maximum amount of OP/UG material that can possibly be mined in a given period;
$MC_i = C_e + C_h$ is the cost of mining block i;
$MC_j = C_{de} + \frac{C_{dr}}{(1+r)^{t_{de}}} + \frac{C_e}{(1+r)^{(t_{de}+t_{dr})}} + \frac{C_b}{(1+r)^{(t_{de}+t_{dr}+t_e)}}$ is the cost of mining stope j;
$NR_{i/j} = T_{i/j} \times G_{i/j} \times Rec \times (\text{Price} - \text{Selling Cost})$ is the net revenue generated by selling all the metal contained in block i/stope j in simulated orebody s;
N is the number of blocks within the OP portion of the mine;
O_{tar} is the targeted amount of ore material to be mined in a given period;
O_{si} is the ore tonnage is block i in the orebody model s;
P is the number of periods to be scheduled;
$PC_{i/j}$ is the processing cost of block i/stope j;
Rec is the mining and processing recovery of the operation;
r is the discount rate;
$T_{i/j}$ is the weight of block i/stope j;
V is the number of stopes within the UG portion of the mine;
W is the number of candidate transition depths considered.

Variables to be determined:

$$b_i^t = \begin{cases} 1 & \text{Block } i \text{ is mined through OP in period } t; \\ 0 & \text{Otherwise} \end{cases}$$

$$a_j^t = \begin{cases} 1 & \text{UG mining activities begin at stope } j \text{ in period } t; \\ 0 & \text{Otherwise} \end{cases}$$

d_{su}^{to}, d_{su}^{tg} are the excessive amounts for the target parameters produced above a desired limit;
d_{sl}^{tg}, d_{sl}^{to} are the deficient amounts for the target parameters produced below a desired limit;
u is the year in which the transition is made from OP to UG mining.

OP Formulation:

Objective function

$$Max: \underbrace{\sum_{t=1}^{P}\sum_{i=1}^{N} E\{(NPV_i^t)b_i^t\}}_{\text{Part 1}} - \underbrace{\sum_{s=1}^{m}\left(c_u^{OP,to}d_{su}^{OP,to} + c_l^{OP,to}d_{sl}^{OP,to} + c_u^{OP,tg}d_{su}^{OP,tg} + c_l^{OP,tg}d_{sl}^{OP,tg}\right)}_{\text{Part 2}} \quad (1)$$

The objective function for the OP SIP model in (1) is designed to maximize discounted cash-flows while minimizing the deviations from targets, and is very similar to the one in Ramazan and Dimitrakopoulos (2013). Part 1 of the objective function represents a summation of profits of each block mined in a given period. These profits are appropriately discounted based on which period they are to be extracted in Part 2, is comprised of geological risk parameters that are used to manage the uncertainty in the ore supply during the optimization. The second-stage recourse (or d) variables are the gap above or below the mine's ore and grade targets. This optimizer discourages deviations from these targets by minimizing the second part of the objective function. It is reasonable to suggest that if a schedule markedly deviates from ore and grade targets, then it is unlikely that the resultant NPV of the planned schedule will be realized. Therefore, including these parameters in the objective function and reducing deviations allows the SIP to produce a practical and feasible schedule along with achievable cash-flow projections.

OP Constraints:

Grade blending constraints for each time period t

$$\sum_{i=1}^{N}(g_{si} - G_{tar})O_{si}b_i^t - d_{su}^{tg} + d_{sl}^{tg} = 0 \quad s = 1, 2, \ldots, M;\ t = 1, 2, \ldots, P \quad (2)$$

Processing constraints

$$\sum_{i=1}^{N} O_{si} b_i^t - d_{su}^{to} + d_{sl}^{to} = O_{tar} \quad s = 1, 2, \ldots, M;\ t = 1, 2, \ldots, P \tag{3}$$

Slope constraints

$$b_i^t - \sum_{k=1}^{t} b_j^k \leq 0 \quad i = 1, 2, \ldots, N;\ t = 1, 2, \ldots, P;\ j \in l_i \tag{4}$$

Reserve constraints

$$\sum_{t=1}^{P} b_i^t = 1 \quad i = 1, 2, \ldots, N \tag{5}$$

Mining capacity constraints

$$MCap_{min}^{OP} \leq \sum_{i=1}^{N} T_i\, b_i^t \leq MCap_{max}^{OP} \quad t = 1, 2, \ldots, P \tag{6}$$

Constraints (2) and (3) are the main stochastic constraints while constraints (3), (4), and (5) are operational constraints designed to model the logistics of the mining process.

UG Formulation:

UG Objective Function:

$$Max: \underbrace{\sum_{t=u}^{P} \sum_{j=1}^{V} (NPV_j^t) a_j^t}_{\text{Part 1}} + \underbrace{\sum_{s=1}^{m} \left(c_u^{UG,to} d_{su}^{UG,to} + c_l^{UG,to} d_{sl}^{UG,to} + c_u^{UG,tg} d_{su}^{UG,tg} + c_l^{UG,tg} d_{sl}^{UG,tg} \right)}_{\text{Part 2}} \tag{7}$$

The UG objective function is similar to the OP objective function, in that the UG objective function's goal is to maximize discounted profits, while minimizing deviations from ore and grade targets. However, the details differ.

Note that the UG mining cost used for Part 1 in (7) displays a method to expense these activities in the period they are executed in. Binary decision variable a_i^t designates the period in which extraction-related activities for each stope i. These activities may be carried out in a predetermined sequence which is constant for all stopes and often spans many periods of the life-of-mine. Tracking these incurred costs in the proper period results in a more realistic NPV for the UG operation. The cost of development, drilling, extraction, and backfilling are represented by the variables C_{de}, C_{dr}, C_e, and C_b respectively shown in the definition of the UG mining cost for a stope MC_j defined ealyer. The time required to execute each activity and the order in which they occur is considered to be constant. The constants t_{de}, t_{dr}, t_e and t_b shown in the definition of MC_j represent the time required to execute the development, drilling, extraction and backfilling required for a single stope. The incurred costs are discounted based on the amount of time the previous activities require.

It is important to also recall that the capital cost required to develop the underground component of the mine considered is contingent on the transition depth, as this will influence the development schemes. The mining costs for each stope can also vary for each transition depth because as the depth varies, so does the size of the pit and the shape of underground orebody to be mined. Having a unique combination of OP and UG components of a mine, aims to result in a different underground development scheme for the UG portion of the mine. For example, a deep transition depth will have a large pit; this will affect the shaft location and likely lengthen the size of the declines which need to be constructed to access ore.

UG Constraints:

Grade blending constraints for each time period t

$$\sum_{j=1}^{V}(g_{sj}-G_{tar})O_j a_j^t - d_{su}^{UG,tg} + d_{sl}^{UG,tg} = 0 \quad s=1,2,\ldots,M;\ t=u,u+1,\ldots,P \tag{8}$$

Processing constraints

$$\sum_{j=1}^{V} O_{sj} a_i^t - d_{su}^{UG,to} + d_{sl}^{UG,to} = O_{tar} \quad s=1,2,\ldots,M;\ t=u,u+1,\ldots,P \tag{9}$$

Mining capacity constraints

$$MCap_{min}^{UG} \leq \sum_{j=1}^{V} T_j a_j^t \leq MCap_{max}^{UG} \quad t = 1, 2, \ldots, P \tag{10}$$

Backfill stability constraints

$$\sum_{k=1}^{P} a_j^k + \sum_{t=k}^{P} a_h^t \leq 2 \quad j = 1, 2, \ldots, V;\ h \in e_i \tag{11}$$

Adjacency constraints

$$a_j^t + a_h^t \leq 1 \quad j = 1, 2, \ldots, V;\ h \in e_i \tag{12}$$

Constraints (11) and (12) are specific to underground stoping methods and are originally presented by Little et al. (2008). The backfill stability constraint limits the number of stopes that can be produced around a backfilled stope in a given time period, since exposing several sides of a backfilled stope can cause stability issues. The adjacency constraint prevents the simultaneous production of two adjacent stopes.

Once the optimization for both the OP and UG components is completed for each candidate transition depth, the optimal transition depth can then be identified as the depth that leads to a maximum value of Eq. (13).

$$NPV_y^{OP} + NPV_y^{UG} - COT_y \tag{13}$$

Conclusions and Future Work

A new method for the determination the optimal OP-UG transition depth was presented. The proposed method improves upon previously developed techniques by taking a true three-dimensional approach to determining the optimal OP-UG transition depth, optimizing extraction sequences for both OP and UG, and considering geological uncertainty. There are many interesting opportunities to build on the proposed model in the future by including: multiple operating mines in the

mining complex, non-linear recovery functions on the processing streams and variable cut-off grades. The current model also only considers a mine that is transitioning from OP to UG. Cases with concurrent OP and UG operations would also be of interest.

Acknowledgements The work in this paper was funded from the Natural Sciences and Engineering Research Council of Canada (NSERC) Discovery Grant xxxxx, and the COSMO Consortium—AngloGold Ashanti, Barrick Gold, BHP Billiton, De Beers, Newmont Mining, Vale.

References

Albor A, Dimitrakopoulos D (2010) Algorithmic approach to pushback design based on stochastic programming: method, application and comparisons. IMM Trans, Mining Technol 199:88–101

Alford C (1995) Optimisation in underground mine design. In: APCOM XXV 1995 conference, Brisbane. http://dx.doi.org:10.1016/0148-9062(96)80055-6

Bakhtavar E, Shahriar K, Oraee K (2008) A model for determining the optimal transition depth over from open-pit to underground mining. In: Proceedings of the fifth international conference & ex-hibition on mass mining, pp 393–400

Dagdelen K, Traore I (2018) Open pit transition depth determination through global analysis of open pit and underground mine production scheduling, in this volume

Fuentes S, Caceres J (2004) Block/panel caving pressing final open pit limit. CIM Bull 97:33–34

Godoy M (2002) The effective management of geological risk in long-term production scheduling of open-pit mines, Ph.D. thesis, (Brisbane, The University of Queensland)

Goodfellow R (2014) Unified modeling and simultaneous optimization of open pit mining complexes with supply uncertainty, Ph.D. thesis, (McGill University)

Kjetland R (2012) Chuquicamata's Life Underground Will Cost a Fortune, but is Likely to Pay Off for Codelco. Copper investing news. Retrieved from: http://copperinvestingnews.com/12788-chuquicamata-underground-mining-codelco-chile-open-pit.html

Lerchs H, Grossmann IF (1965) Optimum design of open pit mines, *CIM Bulletin*, Canadian institute of mining and metallurgy, vol 58, January

Little J, Topal E (2011) Strategies to assist in obtaining an optimal solution for an underground mine planning problem using mixed integer programming. Int J Mining Mineral Eng 3:152–172

Little J, Nehring M, Topal E (2018) A new mixed-integer programming model for mine production scheduling optimisation in sublevel stope mining. In: Proceedings—Australian mining technology conference, Twin Waters. pp 157–172 (Melbourne, The Australasian Institute of Mining and Metallurgy)

Montiel L (2014) Globally optimizing a mining complex under uncertainty: integrating components from deposits to transportation systems, Ph.D. thesis, (McGill University)

Nehring M, Topal E (2007) Production schedule optimisation in underground hard rock mining using mixed integer programming. In: Proceedings—project evaluation. pp 169–175 (Melbourne, The Australasian Institute of Mining and Metallurgy)

Nehring M, Topal E, Little J (2009) A new mathematical programming model for production schedule optimisation in underground mining operations. J Southern Afr Inst Mining Metall 110:437–446

Newman A, Yano C, Rubio E (2013) Mining above and below ground: timing the transition. IIE Transactions 45:862–882

Popov G (1971) The working of mineral deposits [Translated from the Russian by V. Shiffer], Mir Publishers, (Moscow)

Ramazan S, Dimitrakopoulos R (2005) Stochastic optimisation of long-term production scheduling for open pit mines with a new integer programming formulation. In: Orebody modelling and strategic mine planning, Spectrum Series, vol 14, pp 385–391 (Melbourne, The Australasian Institute of Mining and Metallurgy)

Ramazan S, Dimitrakopoulos R (2013) Production scheduling with uncertain supply: a new solution to the open pit mining problem. Optimization Eng 14:361–380

Roberts B, Bloss M (2014) Adaptation of an open pit optimiser for underground strategic planning. In: Orebody modelling and strategic mine planning 2014 (Melbourne, The Australian Institute of Mining and Metallurgy)

Stone P, Froyland G, Menabde M, Law B, Pasyar R, Monkhouse P (2007) Blasor—blended iron ore mine planning optimisation at Yandi. In: Orebody modelling and strategic mine planning, 2nd edn, pp 285–288 (Melbourne, The Australian Institute of Mining and Metallurgy)

Trout P (1995) Underground mine production scheduling using mixed integer programming. In: 25th international APCOM symposium, pp 395–400 (Melbourne, The Australian Institute of Mining and Metallurgy)

Vallee M (2000) Mineral resource + engineering, economic and legal feasibility = ore reserve. Can Mining metallurgy Soc Bull 93:53–61

Whittle J (1988) Beyond optimisation in open pit design. In: Proceedings Canadian conference on computer applications in the mineral industries, Rotterdam, pp 331–337

Whittle J (1999) A decade of open pit mine planning and optimization—the craft of turning algorithms into packages. In: Proc. 28th computer applications in the mineral industries. (APCOM) (pp 15–24). Golden, Co: SME

Whittle G (2010) Enterprise optimisation. In: Proceedings of the 19th international symposium on mine planning and equipment selection, pp 105–17 (Melbourne, Australasian Institute of Mining and Metallurgy)

Zuckerberg M, van der Riet J, Malajczuk W, Stone P (2010) Optimal life-of-mine scheduling for a bauxite mine. In: Orebody modelling and strategic mine planning, 2nd edn, pp 101–105 (Melbourne, The Australian Institute of Mining and Metallurgy)

An Open-Pit Multi-Stage Mine Production Scheduling Model for Drilling, Blasting and Excavating Operations

E. Kozan and S. Q. Liu

Abstract This paper proposes a new multi-resource multi-stage scheduling problem for optimising the open-pit drilling, blasting and excavating operations under equipment capacity constraints. The flow process is analysed based on the real-life data from an Australian iron ore mine site. The objective of the model is to maximise the throughput and minimise the total idle times of equipment at each stage. The following comprehensive mining attributes and constraints have been considered: types of equipment; operating capacities of equipment; ready times of equipment; speeds of equipment; block-sequence-dependent movement times of equipment; equipment-assignment-dependent operation times of blocks; distances between each pair of blocks; due windows of blocks; material properties of blocks; swell factors of blocks; and slope requirements of blocks. It is formulated by mixed integer programming and solved by ILOG-CPLEX optimiser. The proposed model is validated with extensive computational experiments to improve mine production efficiency at the operational level. The model also provides an intelligent decision support tool to account for the availability and usage of equipment units for drilling, blasting and excavating stages.

Introduction

Mining activities have been carried out by humans for millennia. Nowadays, mining activities take place all over the world and become a major source of a country's natural wealth, especially for Australia. Mining methods are mainly divided into two groups: open-pit/surface mining and underground mining. In underground mining, the mineral is able to be accessed and hauled to the surface

E. Kozan (✉) · S. Q. Liu
Decision Science Discipline, Mathematical Sciences School, Queensland University of Technology, 2 George St, GPO Box 2434, Brisbane, QLD 4001, Australia
e-mail: e.kozan@qut.edu.au

S. Q. Liu
e-mail: sq.liu@qut.edu.au

R. Dimitrakopoulos (ed.), *Advances in Applied Strategic Mine Planning*,
https://doi.org/10.1007/978-3-319-69320-0_38

through a network of tunnels. In comparison, open-pit mining method is implemented when deposits of minerals are found near the surface or where mine structure is inappropriate for tunnelling. This paper is concerned with short-term open-pit mine production process including drilling, blasting and excavating stages.

In open-pit mining, the initial optimisation problem, called *mine design planning* (**MDP**), aims to provide the optimal answer for the question at the strategic level, that is, what to be mined or what is the ultimate pit contour that yields the maximum total value based on the estimated geological information. As pioneers, Lerchs and Grossmann (1965) presented to the mining community the methodology known as the Lerchs-Grossmann approach. Caccetta and Giannini (1988) proposed several mathematical theorems in order to improve the Lerchs-Grossmann approach. Underwood and Tolwinski (1998) developed a dual simplex approach to solve the integer-linear-programming (ILP) model of MDP. Hochbaum and Chen (2000) presented a detailed study of the push-relabel network flow algorithm to solve MDP.

After the determination of the ultimate pit contour, the next important optimisation problem is called *mine block sequencing* (**MBS**). The purpose of MBS is to answer the question at the tactical level, that is, which part of orebody will be mined over mid-term periods. In the literature, the following important papers dealt with MBS. Caccetta and Hill (2003) proposed a general mixed-integer-programming (MIP) model and a branch-and-cut algorithm with LP relaxation to solve MBS. Boland et al. (2009) developed a LP-based relaxation approach to solve large-size MBS instances. Bley et al. (2010) relaxed this MIP formulation by adding inequalities derived by combining the precedence and production constraints. Ramazan (2007) proposed a method to aggregate a subset of blocks as branched trees, which are able to reduce number of integer variables and number of constraints required within the MIP formulation. Many researchers indicated that solving the MBS-MIP model is computationally intractable for large-size instances, thus leading to the development of numerous heuristic algorithms. Kumral and Dowd (2005) developed a simulated annealing metaheuristic combined with Lagrangian relaxation. Ferland et al. (2007) modelled the MBS problem as a resource-constrained project scheduling problem, which was solved by a particle swam optimisation algorithm. Myburgh and Deb (2010) reported an application of evolutionary algorithm for solving MBS. Cullenbine et al. (2011) recently developed a sliding-time-window heuristic for MBS. Chicoisne et al. (2012) developed an efficient heuristic algorithm based on decomposition and topological sorting techniques for solving MBS.

After the determination of blocks to be mined over mid-term periods, mining practitioners need to determine how and when mining equipment at various operational stages (e.g., Drills, MPUs and Excavators) should be allocated to perform the detailed operations (e.g., Drilling, Blasting and Excavating) over a short time interval. This **operational-level** question will be answered by the short-term multi-stage mine production scheduling methodology. Using the sequence of blocks over mid-term periods (i.e., due windows of blocks), multi-stage *mine production scheduling* (**MPS**) is prepared. This helps to optimise multi-resource

multi-stage timetable at the operational-level and determine: how and when the mining equipment will be allocated to the selected blocks to perform the mining tasks at various processing stages over a short time interval. According to recent comprehensive literature review (Newman et al. 2010; Kozan and Liu 2011) on the applications of Operations Research approaches to mining industry, multi-resource multi-stage scheduling methodologies have not been applied to mining optimisation yet. In a sense, this paper would initially fill this gap to extend the boundary of the development of more advanced MPS methodology at the operational level.

Mathematical Formulation

The MPS problem is defined according to the flow process of short-term mine production processing stages under a real-life mining project. This flow process is analysed based on observations, historical data and feedbacks from an Australian ore mine site. In the block model at strategic exploration, a *"**block**"* is regarded as the smallest element with 10m in width, 10m in length, and 15m in height. At the operational level, a set of several same-grade blocks on the same bench in the same pit are aggregated to be mined at the same production rate. In this paper, such an aggregation of blocks is defined as a "***mining job***" in our MPS model. Each mining job will be processed through several operational stages such drilling, blasting and excavating. In the drilling stage, the blocks in each mining job are drilled in order to collect the samples for blasting, which will be sent to laboratories for checking ore properties such as ingredients and density. The sampling results will be used to determine blasting patterns for achieving a good fragmentation after blasting. Mobile Processing Units (MPUs) will provide exploding equipment and blasting service. At the excavating stage, blasted blocks will be extracted by excavators (shovels or front-end-loaders).

According to the above analysis a model is formulated to optimise open-pit drilling, blasting and excavating operations for maximising throughput and reducing the idle time of equipment units at each stage.

Indices and Parameters

I number of mining jobs.

i index of a mining job indexed from 1, $i = 1, \ldots, I$; $i = 0$ is a dummy mining job. The dummy job has zero quantity in volume, surface and drilling metres. The purpose of adding a dummy job is to determine the movement distance for the first/last mining job on an equipment unit at a stage in the mathematical formulation model.

K number of operational stages.

k index of an operational stage from 0, $k = 0, \ldots, K - 1$.

L_k number of equipment units used at stage k.

l_k index of an equipment unit at stage k indexed from 0, $l_k = 0, \ldots, L_k - 1$.

r_i ready time of mining job i.

d_i due date of mining job i.
w_i weighting factor associated the tardiness of mining job i.
s_{ikl_k} setup time of mining job i by equipment unit l_k at stage k.
Ω_{ik} workload for mining job i at stage k.
$\theta_{l_k k}$ operating capacity of resource unit l_k at stage k.
$\eta_{i'i}$ distance between mining job i' and mining job i, in which i' should be the immediate predecessor of mining job i.
$v_{i'ikl_k}$ speed of the l_k^{th} equipment unit at stage k from mining job i' to mining job i,, which may be asymmetric due to up-slope or down-slope.
U a constant large value

Decision Variables

C_{ik} completion time of mining job i at stage k; $0 \le C_{ik} \le U,\ i = 0, \ldots, I;\ k = 0, \ldots, K-1$.
x_{ikl_k} assignment variable which equals 1, if the l_k^{th} equipment unit is allocated to mining job i at stage k; 0, otherwise; $x_{ikl_k} \in \{0, 1\},\ i = 0, \ldots, I;\ k = 0, \ldots, K-1;\ l_k = 0, \ldots, L_k - 1$.
$y_{i'ikl_k}$ immediate sequencing variable which equals 1, if mining job i' just precedes mining job i on the l_k^{th} equipment unit at stage k; 0, otherwise; $y_{ii'kl_k} \in \{0, 1\},\ i, i' = 0, \ldots, I | i \neq i';\ k = 0, \ldots, K-1;\ l_k = 0, \ldots, L_k - 1$

MPS Model

Objective:

$$Minimise\left(max_i\, C_{i,K-1} + \sum\nolimits_{i=1}^{I} max\left(0, C_{i,K-1} - d_i\right) w_i\right) \tag{1}$$

Equation (1) defines the objective function of minimising the makespan and the total weighted tardiness of mining jobs.

Subject to:

$$C_{0k} = r_i, \quad k = 0, \ldots, K-1 \tag{2}$$

$$C_{ik} \ge C_{0k} + \sum\nolimits_{l_k=1}^{L_k} x_{ikl_k}\left(s_{ikl_k} + \frac{\Omega_{ik}}{\theta_{l_k k}}\right) \quad i = 1, \ldots, I;\ k = 0; \tag{3}$$

$$C_{ik} \ge C_{i,k-1} + \sum\nolimits_{l_k=1}^{L_k} \frac{y_{i'ikl_k}\eta_{i'i}}{v_{i'ikl_k}} + \sum\nolimits_{l_k=1}^{L_k} x_{ikl_k}\left(s_{ikl_k} + \frac{\Omega_{ik}}{\theta_{l_k k}}\right), \quad i, i' = 1, \ldots, I | i \neq i';\ k = 1, \ldots, K-1; \tag{4}$$

Equations (2–4) satisfy the processing routes of mining jobs.

$$\sum_{l_k=1}^{L_k} x_{ikl_k} = 1, \quad i = 1, \ldots, I;\ k = 0, \ldots, K-1 \tag{5}$$

$$\sum_{l_k=1}^{L_k} y_{0ikl_k} = 1, \quad i = 1, \ldots, I;\ k = 0, \ldots, K-1 \tag{6}$$

$$\sum_{i'=0|i'\neq i}^{I} y_{i'ikl_k} = x_{ikl_k}, \quad i = 0, \ldots, I;\ k = 0, \ldots, K-1;\ l_k = 0, \ldots, L_k - 1 \tag{7}$$

$$\sum_{i'=0|i'\neq i}^{I} y_{ii'kl_k} = x_{ikl_k}, \quad i = 0, \ldots, I;\ k = 0, \ldots, K-1;\ l_k = 0, \ldots, L_k - 1 \tag{8}$$

Equations (5–8) satisfy the exclusive assignment relationship and immediate sequencing relationship between each pair of mining jobs on each equipment unit at each processing stage.

$$C_{ik} + U\left(1 - \sum_{l_k=1}^{L_k} y_{0ikl_k}\right) \geq C_{0k} + \sum_{l_k=1}^{L_k} x_{ikl_k}\left(s_{ikl_k} + \frac{\Omega_{ik}}{\theta_{l_k k}}\right), \quad i = 1, \ldots, I;\ k = 0, \ldots, K-1; \tag{9}$$

$$C_{ik} + U\left(1 - \sum_{l_k=1}^{L_k} y_{i'ikl_k}\right) \geq C_{i'k} + \sum_{l_k=1}^{L_k} \frac{y_{i'ikl_k}\eta_{i'i}}{v_{i'ikl_k}} + \sum_{l_k=1}^{L_k} x_{ikl_k}\left(s_{ikl_k} + \frac{\Omega_{ik}}{\theta_{l_k k}}\right), \quad i, i' = 1, \ldots, I | i \neq i';\ k = 0, \ldots, K-1; \tag{10}$$

Equations (9–10) satisfy the disjunctive relationship between each pair of mining jobs at each processing stage.

Case Study

The model could be exactly solved by commercial MIP optimiser (e.g., ILOG-CPLEX) for small-size instances in a reasonable time. The proposed approach has been applied to a case study based on the data collected from an iron ore mine site in Australian, for the purpose of maximising the productivity of short-term open-pit mine production process through several operational stages.

Due to confidentiality agreement, values are relatively modified and only some parts of the case study data are given in Table 1.

In this case study, 54 mining jobs will be scheduled in an expected 18-week scheduling horizon. Note that a mining job is an aggregated set of blocks each of which has the identical size with 10 m in width, 10 m in length, 15 m in height, about 100 m^2 in surface and about 1500 m^3. If a block is high-grade ore with the density of 3 tons/cubic meters, then this block's tonnage is about 4500 tons. For

Table 1 Input data of 54 mining jobs

Job ID	Tonnes (t)	Volume (m^3)	Surface (m^2)	Drilling (m)	Number of blocks	Job ID	Tonnes (t)	Volume (m^3)	Surface (m^2)	Drilling (m)	Number of blocks
0	97,656	32,552	2170	768	22	27	394,582	131,527	8769	2828	88
1	175,780	58,593	3906	1382	39	28	710,247	236,749	15,783	5091	158
2	117,187	39,062	2604	921	26	29	473,498	157,833	10,522	3394	105
3	259,440	86,480	5765	1994	58	30	369,212	123,071	8205	2603	82
4	466,992	155,664	10,377	3590	104	31	664,581	221,527	14,769	4685	148
5	311,328	103,776	6918	2393	69	32	443,054	147,685	9846	3123	99
6	302,019	100,673	6712	2233	67	33	424,090	141,363	9424	3260	94
7	543,635	181,212	12,081	4019	121	34	763,362	254,454	16,964	5868	170
8	362,423	120,808	8054	2679	81	35	508,908	169,636	11,309	3912	113
9	373,895	124,632	8309	2640	83	36	351,549	117,183	7812	2722	78
10	673,010	224,337	14,956	4752	150	37	632,788	210,929	14,062	4899	141
11	448,673	149,558	9971	3168	100	38	421,859	140,620	9375	3266	94
12	416,945	138,982	9266	3112	93	39	327,072	109,024	7268	2344	73
13	750,501	250,167	16,678	5601	167	40	588,730	196,243	13,083	4219	131
14	500,334	166,778	11,119	3734	111	41	392,486	130,829	8722	2813	87
15	419,868	139,956	9331	3187	94	42	327,072	109,024	7268	2344	73
16	755,762	251,921	16,795	5736	168	43	588,730	196,243	13,083	4219	131
17	503,842	167,947	11,197	3824	112	44	392,486	130,829	8722	2813	87
18	384,422	128,141	8543	3140	86	45	325,535	108,512	7234	2366	73
19	691,960	230,653	15,377	5652	154	46	585,962	195,321	13,021	4258	131
20	461,307	153,769	10,251	3768	103	47	390,642	130,214	8681	2839	87

(continued)

Table 1 (continued)

Job ID	Tonnes (t)	Volume (m^3)	Surface (m^2)	Drilling (m)	Number of blocks	Job ID	Tonnes (t)	Volume (m^3)	Surface (m^2)	Drilling (m)	Number of blocks
21	385,224	128,408	8561	2993	86	48	359,902	119,967	7998	2578	80
22	693,402	231,134	15,409	5387	154	49	647,824	215,941	14,396	4641	144
23	462,268	154,089	10,273	3591	103	50	431,882	143961	9597	3094	96
24	394,582	131,527	8769	2828	88	51	263,993	87,998	5867	1875	59
25	710,247	236,749	15,783	5091	158	52	475,188	158,396	10,560	3375	106
26	473,498	157,833	10,522	3394	105	53	316,792	105,597	7040	2250	71

Volume, surface and drill metres are measured as workloads of each mining job at excavating, blasting and drilling stages

example in Table 1, mining job 1 has 8648 cubic metre, which means that it consists of about three blocks. In total, these 54 mining jobs consist of 380 blocks with 569,936 m^3 in this case study. Each mining job will be processed consecutively through drilling; blasting and excavating stage. The critical equipment type at drilling stage is drill equipment with two units in this case study. The average blast-hole-drilling rate of a drill is 50 m/h at this mine site. At blasting stage, the critical resource type is mobile processing unit (MPU) with two units. Due to the safety requirements for subsequent marking the blasted blocks, this mine site does not allow personnel or equipment on a blast about 12 h. The critical resource type at excavating stage is excavator (shovel or front-end-loaders) with 5 units and the production rate of an excavator unit is 1200 m^3/h on average. Based on the above data, the processing times of each mining job are determined by the size (drilling meter, surface, volume) of each mining job and the operating capacity of an allocated equipment unit at each stage.

The MPS MIP model of this case study is solved by IBM ILOG-CPLEX 12.4 with the time limit of 36,000 s and thus a good feasible mine production timetable that synchronises drilling, blasting and excavating operations of each mining job is obtained and presented in detail in Table 2. IBM ILOG-CPLEX (a commercial MIP optimiser) can indicate whether the proposed MIP model is solved or not. The constraints are satisfied by evaluating the values of key variables in the model, that is, whether only an equipment unit at each stage is assigned only to a mining job at a time; and whether each pair of mining jobs has only one directed immediate sequencing relationship on the assigned equipment unit at each stage. The obtained timetable shown in Table 2 is constructed according to the values of completion times C_{ik}, equipment-assignment variables x_{ikl_k}, sequencing variables $y_{i'ikl_k}$ obtained by ILOG-CPLEX.

Conclusion

This paper is a pioneering work to optimise short-term mine production operations due to the fact that most mining optimisation papers dealt with long-term mine design planning at the strategic level and mid-term mine block sequencing problems at the tactical level. In this sense, it is innovative to model a short-term mine production scheduling process as a multi-resource multi-stage scheduling problem.

In this paper, we define an operational multi-resource multi-stage mine production scheduling problem based on the real-life mining data and mathematically formulate by mixed integer programming that has been solved by ILOG-CPLEX optimiser. A numerical case study is given for illustrating and validating the proposed scheduling methodology with a practical implementation. As a result of the application of the proposed methodology, mining practitioners can maximise the mining productivity and the utilisation of mining equipment through multiple processing stages.

Table 2 Mine production timetable of 54 mining jobs

	Drilling stage (2 Drills)						Blasting stage (2 MPUs)					
Job ID	Drill ID	MTime	ITime	Etime	PTime	CTime	MPU ID	Mtime	ITime	Etime	PTime	CTime
0	1	0.00	3.50	3.50	12.79	16.29	0	0.00	24.00	40.29	7.23	47.53
1	0	0.00	3.00	3.00	27.63	30.63	0	0.00	24.00	71.53	13.02	84.55
2	1	0.14	3.50	19.93	15.35	35.14	1	0.00	48.00	83.14	5.79	88.93
3	1	0.03	3.50	38.67	33.24	71.88	0	0.00	24.00	108.55	19.22	127.76
4	0	0.15	3.00	33.78	71.80	105.43	1	0.00	48.00	153.43	23.06	176.49
5	1	0.10	3.50	75.48	39.89	115.27	0	0.00	24.00	151.76	23.06	174.83
6	0	0.10	3.00	108.53	44.66	153.09	0	0.00	24.00	198.83	22.37	221.20
7	1	0.10	3.50	118.87	66.98	185.75	1	0.00	48.00	233.75	26.85	260.60
8	0	0.10	3.00	156.19	53.59	209.67	0	0.00	24.00	245.20	26.85	272.04
9	1	0.10	3.50	189.35	44.00	233.25	0	0.00	24.00	296.04	27.70	323.74
10	0	0.10	3.00	212.77	95.03	307.70	0	0.00	24.00	347.74	49.85	397.59
11	1	0.10	3.50	236.85	52.80	289.54	1	0.00	48.00	337.54	22.16	359.70
12	1	0.04	3.50	293.08	51.86	344.90	1	0.00	48.00	407.70	20.59	428.29
13	0	0.12	3.00	310.82	112.01	422.72	1	0.00	48.00	476.29	37.06	513.35
14	1	0.07	3.50	348.48	62.23	410.63	0	0.00	24.00	434.63	37.06	471.70
15	1	0.04	3.50	414.17	53.12	467.25	0	0.00	24.00	495.70	31.10	526.80
16	0	0.11	3.00	425.83	114.73	540.45	1	0.00	48.00	588.45	37.32	625.77
17	1	0.07	3.50	470.82	63.74	534.49	0	0.00	24.00	558.49	37.32	595.81
18	1	0.04	3.50	538.02	52.33	590.32	0	0.00	24.00	619.81	28.48	648.28
19	0	0.11	3.00	543.55	113.04	656.48	0	0.00	24.00	680.48	51.26	731.74
20	1	0.07	3.50	593.89	62.80	656.62	1	0.00	48.00	704.62	22.78	727.40
21	1	0.04	3.50	660.15	49.88	710.00	0	0.00	24.00	755.74	28.54	784.27
22	0	0.06	3.00	659.55	107.74	767.22	1	0.00	48.00	815.22	34.24	849.46

(continued)

Table 2 (continued)

	Drilling stage (2 Drills)						Blasting stage (2 MPUs)					
Job ID	Drill ID	MTime	ITime	Etime	PTime	CTime	MPU ID	Mtime	ITime	Etime	PTime	CTime
23	1	0.09	3.50	713.59	59.85	773.35	0	0.00	24.00	808.27	34.24	842.52
24	1	0.02	3.50	776.87	47.14	823.99	0	0.00	24.00	866.52	29.23	895.74
25	0	0.07	3.00	770.29	101.82	872.04	1	0.00	48.00	920.04	35.07	955.11
26	1	0.05	3.50	827.53	56.57	884.05	0	0.00	24.00	919.74	35.07	954.82
27	0	0.05	3.00	875.08	56.57	931.61	0	0.00	24.00	978.82	29.23	1008.05
28	1	0.05	3.50	887.60	84.85	972.40	1	0.00	48.00	1020.41	35.07	1055.48
29	0	0.04	3.00	934.65	67.88	1002.49	0	0.00	24.00	1032.05	35.07	1067.12
30	1	0.06	3.50	975.96	43.38	1019.29	0	0.00	24.00	1091.12	27.35	1118.47
31	0	0.06	3.00	1005.54	93.70	1099.19	0	0.00	24.00	1142.47	49.23	1191.70
32	1	0.11	3.50	1022.90	52.06	1074.84	1	0.00	48.00	1122.84	21.88	1144.72
33	1	0.06	3.50	1078.40	54.34	1132.68	1	0.00	48.00	1192.72	20.94	1213.66
34	0	0.17	3.00	1102.36	117.37	1219.56	1	0.00	48.00	1267.56	37.70	1305.25
35	1	0.11	3.50	1136.29	65.20	1201.38	0	0.00	24.00	1225.38	37.70	1263.08
36	1	0.05	3.50	1204.93	45.36	1250.25	0	0.00	24.00	1287.08	26.04	1313.12
37	0	0.12	3.00	1222.68	97.98	1320.54	1	0.00	48.00	1368.54	31.25	1399.79
38	1	0.10	3.50	1253.85	54.44	1308.18	0	0.00	24.00	1337.12	31.25	1368.37
39	1	0.05	3.50	1311.73	39.07	1350.75	0	0.00	24.00	1392.37	24.23	1416.60
40	0	0.15	3.00	1323.69	84.39	1407.93	0	0.00	24.00	1440.60	43.61	1484.21
41	1	0.06	3.50	1354.31	46.88	1401.13	1	0.00	48.00	1449.13	19.38	1468.51
42	1	0.03	3.50	1404.66	39.07	1443.70	0	0.00	24.00	1508.21	24.23	1532.43
43	0	0.08	3.00	1411.00	84.39	1495.31	0	0.00	24.00	1556.43	43.61	1600.04
44	1	0.05	3.50	1447.25	46.88	1494.08	1	0.00	48.00	1542.08	19.38	1561.46
45	1	0.03	3.50	1497.61	39.43	1537.01	1	0.00	48.00	1609.46	16.08	1625.54

(continued)

Table 2 (continued)

	Drilling stage (2 Drills)						Blasting stage (2 MPUs)					
Job ID	Drill ID	MTime	ITime	Etime	PTime	CTime	MPU ID	Mtime	ITime	Etime	PTime	CTime
46	0	0.08	3.00	1498.39	85.16	1583.48	0	0.00	24.00	1624.04	43.40	1667.45
47	1	0.06	3.50	1540.57	47.31	1587.82	1	0.00	48.00	1673.54	19.29	1692.83
48	1	0.04	3.50	1591.36	42.97	1634.29	0	0.00	24.00	1691.45	26.66	1718.11
49	0	0.11	3.00	1586.58	92.81	1679.29	1	0.00	48.00	1740.83	31.99	1772.82
50	1	0.07	3.50	1637.86	51.56	1689.35	0	0.00	24.00	1742.11	31.99	1774.10
51	0	0.07	3.00	1682.36	37.50	1719.79	0	0.00	24.00	1798.10	19.56	1817.65
52	1	0.07	3.50	1692.93	56.25	1749.11	1	0.00	48.00	1820.82	23.47	1844.29
53	0	0.07	3.00	1722.86	45.00	1767.79	0	0.00	24.00	1841.65	23.47	1865.12

	Excavating stage (Five excavators)					
Job ID	Excavator ID	Mtime	ITime	Etime	PTime	CTime
0	4	0.00	4.50	52.03	32.55	84.58
1	4	0.04	4.50	89.12	58.59	147.67
2	3	0.00	4.00	92.93	43.40	136.33
3	3	0.02	4.00	140.35	96.09	236.42
4	2	0.00	3.50	179.99	194.58	374.57
5	4	0.20	4.50	179.53	103.78	283.10
6	3	0.15	4.00	240.57	111.86	352.28
7	4	0.10	4.50	287.70	181.21	468.81
8	1	0.00	3.00	275.04	172.58	447.63
9	3	0.15	4.00	356.43	138.48	494.76
10	4	0.15	4.50	473.46	224.34	697.65
11	2	0.29	3.50	378.36	186.95	565.02
12	1	0.09	3.00	450.72	198.55	649.17

(continued)

Table 2 (continued)

	Excavating stage (Five excavators)					
Job ID	Excavator ID	Mtime	ITime	Etime	PTime	CTime
13	2	0.06	3.50	568.58	312.71	881.23
14	3	0.21	4.00	498.96	185.31	684.07
15	0	0.00	2.50	529.30	233.26	762.56
16	3	0.07	4.00	688.14	279.91	967.98
17	4	0.26	4.50	702.42	167.95	870.10
18	1	0.11	3.00	652.28	183.06	835.23
19	4	0.07	4.50	874.67	230.65	1105.25
20	0	0.09	2.50	765.15	256.28	1021.34
21	1	0.05	3.00	838.28	183.44	1021.67
22	3	0.16	4.00	972.14	256.82	1228.80
23	2	0.21	3.50	884.94	192.61	1077.34
24	1	0.04	3.00	1024.71	187.90	1212.57
25	2	0.03	3.50	1080.87	295.94	1376.78
26	4	0.07	4.50	1109.82	157.83	1267.58
27	0	0.05	2.50	1023.89	219.21	1243.05
28	3	0.09	4.00	1232.89	263.05	1495.85
29	4	0.04	4.50	1272.13	157.83	1429.92
30	1	0.06	3.00	1215.63	175.82	1391.38
31	4	0.04	4.50	1434.46	221.53	1655.94
32	0	0.05	2.50	1245.60	246.14	1491.69
33	2	0.11	3.50	1380.39	176.70	1556.98
34	3	0.17	4.00	1500.02	282.73	1782.58
35	1	0.14	3.00	1394.52	242.34	1636.72

(continued)

Table 2 (continued)

	Excavating stage (Five excavators)					
Job ID	Excavator ID	Mtime	ITime	Etime	PTime	CTime
36	0	0.09	2.50	1494.28	195.31	1689.50
37	4	0.26	4.50	1660.70	210.93	1871.37
38	2	0.17	3.50	1560.65	175.77	1736.25
39	1	0.10	3.00	1639.82	155.75	1795.47
40	3	0.26	4.00	1786.84	218.05	2004.63
41	2	0.13	3.50	1739.88	163.54	1903.29
42	0	0.15	2.50	1692.15	181.71	1873.70
43	4	0.15	4.50	1876.02	196.24	2072.12
44	1	0.06	3.00	1798.53	186.90	1985.36
45	2	0.06	3.50	1906.85	135.64	2042.43
46	0	0.04	2.50	1876.25	325.53	2201.74
47	3	0.10	4.00	2008.73	144.68	2153.31
48	1	0.06	3.00	1988.43	171.38	2159.75
49	4	0.19	4.50	2076.81	215.94	2292.56
50	2	0.13	3.50	2046.06	179.95	2225.88
51	3	0.14	4.00	2157.45	97.78	2255.08
52	1	0.07	3.00	2162.82	226.28	2389.03
53	2	0.09	3.50	2229.47	132.00	2361.38

MTime: movement time; ITime: installation time; ETime: starting time; PTime: processing time; and CTime: completion time

Acknowledgements The authors would like to acknowledge the support of CRC ORE, established and supported by the Australian Government's Cooperative Research Centres Programme.

References

Boland N, Dumitrescu L, Froyland G, Gleixner AM (2009) LP-based disaggregation approaches to solving the open pit mining production scheduling problem with block processing selectivity. Comput Oper Res 36:1064–1089

Bley A, Boland N, Fricke C, Froyland G (2010) A strengthened formulation and cutting planes for the open pit mine production scheduling problem. Comput Oper Res 37:1641–1647

Caccetta L, Giannini LM (1988) An application of discrete mathematics in the design of an open pit mine. Discrete Appl Math 21:1–19

Caccetta L, Hill SP (2003) An application of branch and cut to open pit mine scheduling. J Global Optimisation 27:349–365

Chicoisne R, Espinoza D, Goycoolea M, Moreno E, Rubio E (2012) A new algorithm for the open-pit mine production scheduling problem. Oper Res 60(3):517–528

Cullenbine C, Wood RK, Newman A (2011) A sliding time window heuristic for open pit mine block sequencing. Optimisation Lett 5(3):365–377

Ferland J, Amaya J, Djuimo MS (2007) Application of a particle swarm algorithm to the capacitated open pit mining problem. Stud Computat Intell 76:127–133

Hochbaum DS, Chen A (2000) Performance analysis and best implementations of old and new algorithms for the open-pit mining problem. Oper Res 48(6):894–914

Kozan E, Liu SQ (2011) Operations research for mining: a classification and literature review. ASOR Bull 30(1):2–23

Kumral M, Dowd PA (2005) A simulated annealing approach to mine production scheduling. J Oper Res Soc 56:922–930

Lerchs H, Grossmann IF (1965) Optimum design of open-pit mines. Transactions on CIM, LXVIII, pp 17–24

Myburgh,C, Deb K (2010) Evolutionary algorithms in large-scale open pit mine scheduling. Paper presented at the GECCO'10, Portland, Oregon, USA

Newman AM, Rubio E, Weintraub RCA (2010) A review of operations research in mine planning. Interfaces 40(3):222–245

Ramazan S (2007) The new fundamental tree algorithm for production scheduling of open pit mines. Eur J Oper Res 177:1153–1166

Underwood R, Tolwinski B (1998) A mathematical programming viewpoint for solving the ultimate pit problem. Eur J Oper Res 107(1):96–107

Optimising the Long Term Mine Landform Progression and Truck Hour Schedule in a Large Scale Open Pit Mine Using Mixed Integer Programming

Y. Li, E. Topal and S. Ramazan

Abstract A mine landform progression plan can provide a clear outlook of the entire mining operation. To produce such an output requires detailed placement schedule of the mined material, including the volume (or tonnage) and the allocated dumping location. However, current practise mainly focuses on the ore production, over-simplifying the waste material scheduling. As a result, a rock dump is often treated as a single point in long term planning, making it difficult to predict the progression pattern over the life of mine. Without such a guidance, it is almost impossible to carry out progressive rehabilitation of the waste rock dumps. The lack of dumping schedule could cause delay in development construction, i.e., tailing storage facility (TSF) and ROM-pad. Other downstream effect due to the over-simplification is inaccurate estimation of required truck hours, which could have huge financial impact on the operation. In this paper, mixed integer programming (MIP) models of different objective functions, i.e., maximise truck productivity by minimising the overall haulage distance, minimise required truck deviation between adjacent years, and a hybrid between the two objectives, are utilised to generate the long term optimum rock placement schedules under the criteria of satisfying site specific conditions. All three MIP models are implemented in a large scale open pit mine. The numerical solutions from the models forms three different rock placement schedules, based on which, the yearly truck requirements are easily calculated and compared. The graphical results show the three corresponding landform progression patterns over the life of mine, providing the optimised long term forecast of the operation.

Y. Li (✉)
Rio Tinto Iron Ore, Perth, Australia
e-mail: luke.yu.li@gmail.com

E. Topal
Western Australia School of Mines, Curtin University, Kalgoorlie, Australia

S. Ramazan
Mining & Technical Group—COO International, AngloGold Ashanti, Johannesburg, South Africa

R. Dimitrakopoulos (ed.), *Advances in Applied Strategic Mine Planning*,
https://doi.org/10.1007/978-3-319-69320-0_39

Introduction

In a large-scale open pit mine, waste stripping and hauling are as important as ore mining and processing, because large quantity of earth moving is involved, hence the material handling cost. However, current practice predominately focuses on scheduling ore recovery, subsequently neglecting the waste scheduling in long term planning.

The waste allocation is often decided by the production engineers based on day to day site condition and personal experience. The rule of thumb is the shortest haul principle, as illustrated in Fig. 1, to minimise the haulage cost (Wang and Butler 2007). The disadvantage of this approach is lacking long term vision, which was challenged by Sommerville and Heyes (2009). It was claimed that shortest haul strategy will incur 8% higher in cost compared to some other dumping schedule when taking rehabilitation into account.

There are other dumping strategies available, such as long-haul then short-haul and centred expansion strategy, as shown in Figs. 2 and 3, respectively. A quantitative analysis is required to compare the three dump progression pattern, which could be very time-consuming; nevertheless, there may be other better sequences available that are more cost effective than the listed three.

An alternative method is to determine the optimum dumping schedule, i.e., the material flow from its source location to the dumping location, according to the requirement of the business. Once it is solved, the detailed landform progression, and the required truck hours can be calculated.

To seek the most cost effective solution, the haulage cost from each waste block to all possible dumping locations must be evaluated, as shown in Fig. 4. The extent of the problem is proportional to the number of mining blocks and the possible dumping locations, which is often too numerous to analyse by manual method.

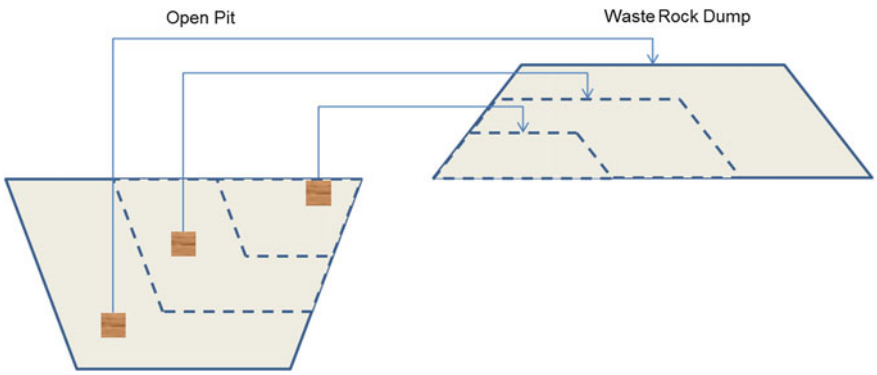

Fig. 1 Waste rock dump progression with a shortest haul strategy

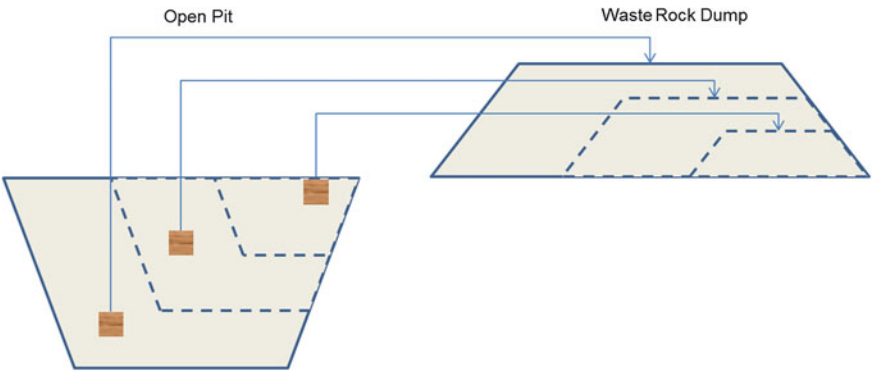

Fig. 2 Waste rock dump progression with a long-haul then short-haul strategy

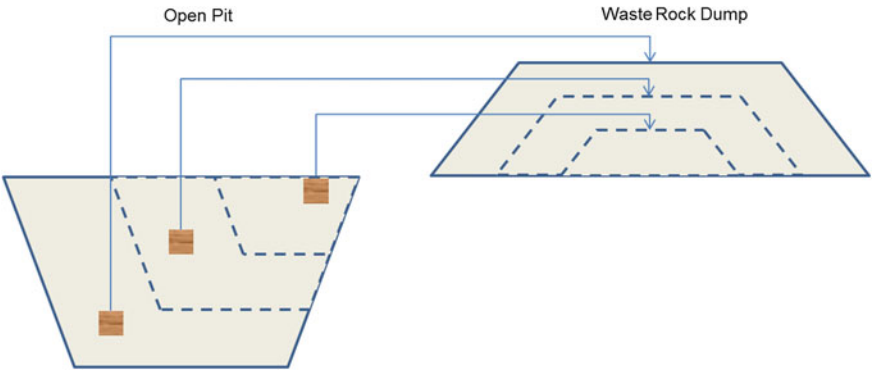

Fig. 3 Waste rock dump progression with a centred expansion strategy

In addition, the time cost for occupying each individual dumping location should also be considered, as shown in Fig. 5. This is because the cost in different time period has different money value.

Furthermore, the entire landform could involve many other structures, such as tailing storage facility (TSF), run of mine (ROM) pad, growth medium (GM) stockpile, and low grade dump. Some structures are required to be built in a certain time frame, while some must be constructed using particular waste material.

In order to seek the optimum solution, which also satisfies multiple criterion, mixed integer programming (MIP) models are proposed to aid the decision making. The main objective of this paper is to demonstrate the use of the MIP models in solving the long term dumping schedule problem in a large scale open pit mine. The expected outcomes include the optimised landform progression and the estimated truck schedule.

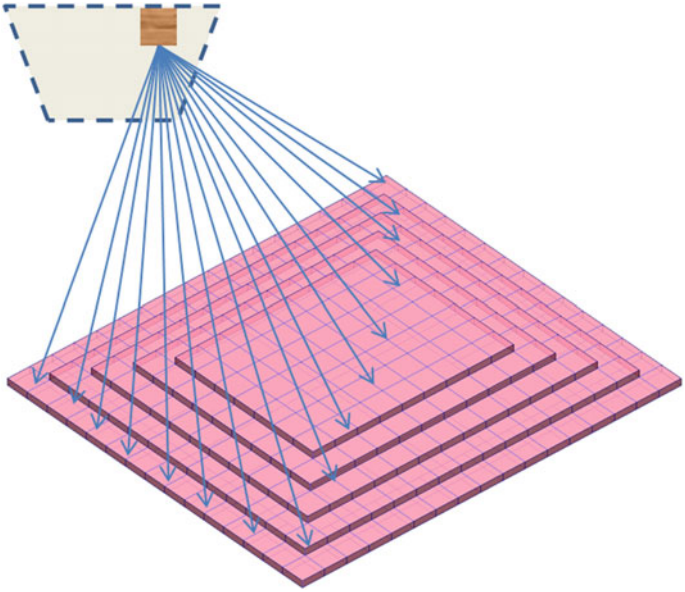

Fig. 4 Selection of dumping location(s) for each mining block

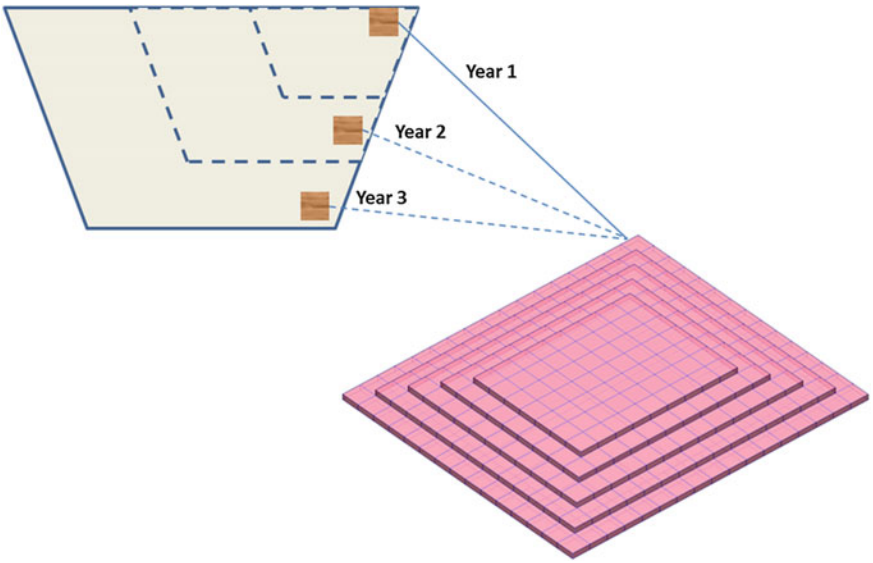

Fig. 5 Evaluating the different time cost to occupy one dumping location

Background Information and Problem Definition

A large scale open pit mine in Western Australia is to commence operation. It has an estimated surface mine life of 10 years, and possible extension for underground mining. The proposed life of mine landform design is illustrated in Fig. 6.

There will be three rock dumps, i.e., LTA, LEA and LWE, which are designed to accommodate the majority of waste rock. The tailing storage facility (TSF) and ROM-pad are to be built by the waste rock in the early stage of mining. In addition, seven growth medium (GM) stockpiles will be used to store GM material for rehabilitation, covering the top of three rock dumps by the end of mine life.

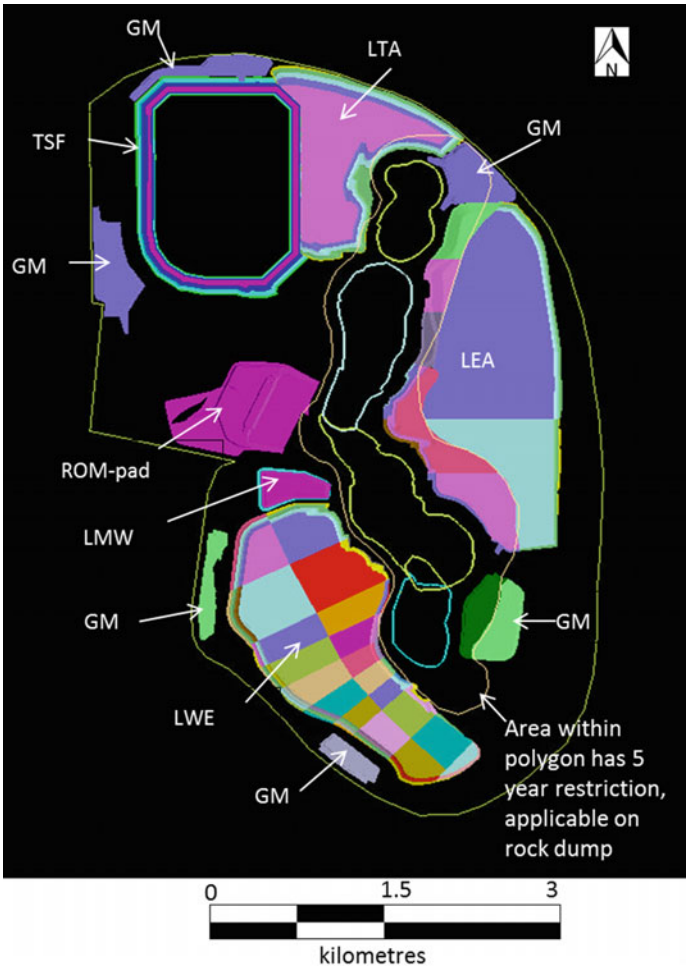

Fig. 6 Mine site layout and overall landform design

According to the given design, the total waste rock (including GM material) storage capacity is approximately 229.9 million loose cubic metre (LCM), which is summarised in Table 1.

Low-grade stockpile (LMW) is also designed to segregate low-grade material (MW) for future processing. Ore is to be stockpiled on the top of the ROM-pad, from where it is transported to a processing plant nearby.

Each structure in the landform design is divided into smaller dump blocks. For example, the rock dumps are first cut into smaller dump divisions by vertical cuts, and then to dump blocks according to the lift height. Each dump block represents a dumping location of certain capacity. The total number of possible dump blocks in the design is 221, as summarised in Table 2.

The annual material movement from the production schedule is presented in Fig. 7. A preliminary check shows that the overall volume to be removed from the open pits is 234.8 million Loose Cubic Metre (LCM), which comprises the following:

- 199.3 million LCM of waste;
- 3.2 million LCM of MW; and
- 32.3 million LCM ore.

Table 1 Landform capacity for waste rock

Dump name	Capacity (million m^3)
LTA	42.7
LEA	78.3
LWE	65.8
TSF	17.0
ROM pad	9.5
GM stockpile	16.6
Grand total	229.9

Table 2 Summary of dump block in given design

Waste dump	Number of division	Number of blocks
LTA	4	24
LEA	12	66
LWE	19	88
TSF	1	32
ROM_Pad	1	1
GM stockpile	7	7
LMW	1	2
Plant	1	1
Total	46	221

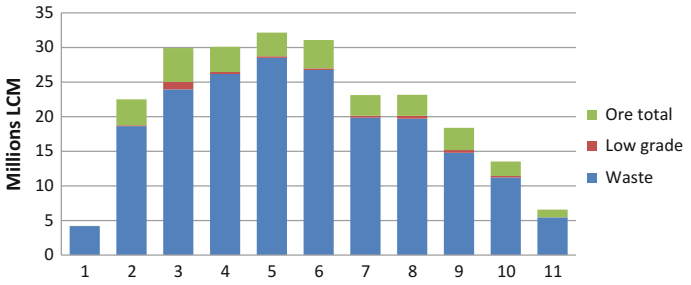

Fig. 7 Material movement schedule from operating pits

Table 3 Simplified schedule of mining blocks

Period	Waste	MW	Ore	Yearly sum
1	14		11	25
2	92	28	248	368
3	105	37	278	420
4	100	45	281	426
5	30	20	109	159
6	46	24	132	202
7	41	21	144	206
8	35	15	97	147
9	26	17	116	159
10	31	24	154	209
11	18	18	97	133
Total blocks	538	249	1667	2454

Since the overall waste material from the pits is less than the designed capacity, it is certain that all waste material from the operation can be fully contained within the proposed landform design.

The production schedule in terms of mining blocks can be seen in Table 3. These blocks are modified by grouping conventional mining blocks, based on their attributes and spatial location, thereby reducing the total number of mining blocks to 2454.

Given the number of dump blocks and mining blocks, it is estimated that 542,334 combinations are possible to schedule the mined material to the dumping locations.

Additionally, the case study involves multiple pits, pit exit points, rock dumps and dump entry points, which further complicates the problem. Take pit exit points for example, the design specifies 20 different exits, as summarised in Table 4 and illustrated in Fig. 8. Some exits are interim, which will disappear as pits expand. These design information must be correctly modelled so that logical pit expansion sequence is correctly reflected in the solution output.

Table 4 Summary of pit exits

Pit(s)	Exit name	Number of exits
BS	J, O	2
TP	P, U, T, G, E, H, D, M	8
HA	L, R, B, I, A, C, Q, S, N, F	10
Total		20

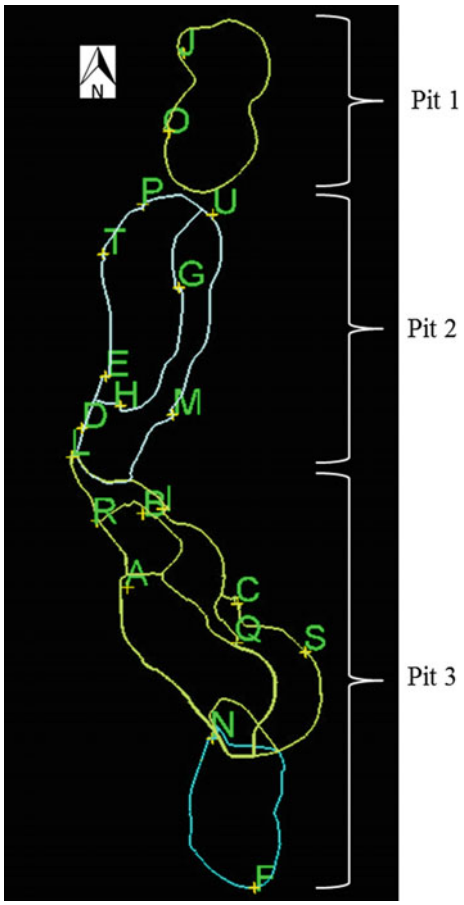

Fig. 8 Temporary and permanent pit exits according to the given design

Problem Modelling and Implementation

MIP Modelling

The problem is modelled in MIP form, which involves a series of variables, parameters, objective functions, and a list of constraints. Then an optimisation engine is used to read the model and the data in order to generate optimum solution.

Main Variables and Parameters

V1 main variable to represent the ex-pit material flow from its source mining block to the dumping location in a time period;
V2 variable to represent GM material re-handled in a time period;
B binary variable to control the sequence in each dump lift, and
D parameter that states the equivalent flat distance from the in-pit mining block location to a dump block.

Objective Function

Three different objectives are set for the models, simply they are:

- Optimum productivity (OP) model to maximise truck productivity (LCM/km), i.e., maximise $\sum (V1/D + V2/D)$;
- Truck balance (TB) model to minimise truck requirement deviation between adjacent years, i.e., minimise $\sum |\Delta(V1 \times D + V2 \times D)$ between each adjacent year|;
- Combo model to achieve a balance between truck productivity and requirement, i.e. minimise $\sum (V1 \times D + V2 \times D) + \sum |\Delta(V1 \times D + V2 \times D)$ between each adjacent year|.

Constraints Modelling

According to the provided information, a framework of material flow for the mine is constructed, as illustrated in Fig. 9. A list of rules are applicable:

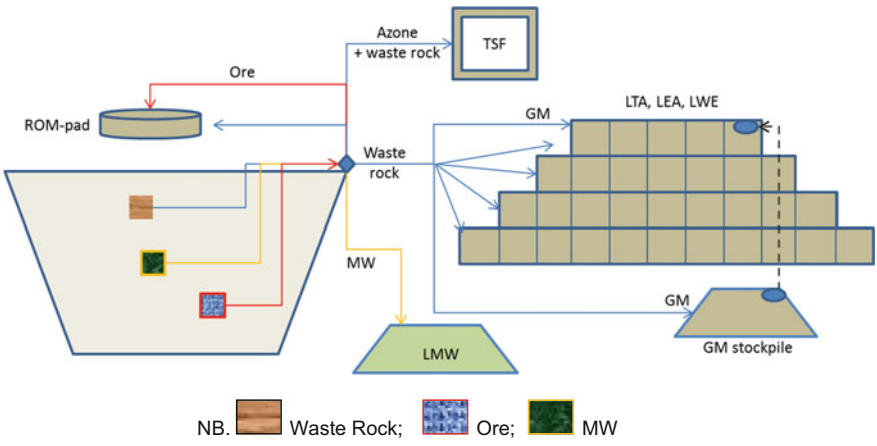

Fig. 9 Modified mining and dumping framework for the open pit project

- Ore is to be stockpiled to the ROM-pad, which is constructed by waste rock.
- Low grade is to be stockpiled to LMW.
- Waste material are further catergorised into Azone material, GM material, and other waste rock.
- Azone material is preferred to be sent to TSF to form an impermeable layer until the completion of TSF by the end of time period 4.
- GM material is only allowed to be transported to the GM stockpile or to the top of the main rock dumps.

The mentioned material flow obeys a series of generic constraint sets. The name and functionality of each constraints are summarized in Table 5, and the further details of the mathematical formulations were described by Li et al. (2013).

Apart from the generic constraints, some site specific constraints are also introduced to model the site specific conditions:

- Waste rock dumping within the 5-year restriction zone, as indicated in Fig. 6 is restricted, until after time period 5;
- Prioritising a two-staged ROM-pad construction, with phase one to be built by the end of time period 2, and then completion in time period 3; and
- Prioritising a two-staged TSF construction, with phase one to be built by the end of time period 2, and then completion in time period 4.

Table 5 Generic constraint sets and functionality

Constraint sets	Functionality
Mining schedule	To ensure a mining block is removed according to the defined mining schedule
Dump block capacity	To monitor the filling of a dump block in each time period
Logical lift sequence	To model the logical lift-by-lift rock dump construction sequence
Non-negative	To set non-negative value for all variable

Table 6 Problem size and solution time

	Number of	OP Model	TB Model	Combo Model
Problem size	Linear variable	643,063	643,085	643,085
	Binary variable	1,719	1,719	1,719
	Constraints	12,537	12,547	12,547
Solving process	Simplex iterations	335,094	51,550,326	8,184,228
	Branch and bound cut	2,316	208	531
Solution time (min)		4.7	3557.4	244.3

Solution Generation

The MIP models were written using a mathematical programming language (AMPL) and the optimisation problems were solved using the optimisation engine CPLEX 12.4, running on a computer of 2.8 GHz CPU and 24 GB RAM. The key statistics of the problems are summarised in Table 6. It can be seen that each problem involves more than 640,000 variables, which is impossible to be solved by any manual methods.

It is noted that OP model required only five minutes to solve this scheduling problem. The most time-consuming problem, generated by TB model, was solved within two and half days.

Landform Footprint and Progression

Upon solving the problems, V1 and V2 are used to determine the dumping sequence, enabling generating the yearly landform progression pattern.

The yearly landform progression, generated by the OP, TB and Combo models, are illustrated in Figs. 10, 11, and 12, respectively.

The differences in the landform progression is resulted from the different objectives in each MIP model.

It is noted that both ROM-pad and TSF are constructed as planned. The 5-year dumping restriction zone is also properly followed. These outcomes indicate that correct site specific constraints are modelled across the three MIP models.

Performance Factor Analysis

Apart from the graphical results, key performance factors for all three dumping schedules, such as overall haulage distance, truck requirement, and truck productivity, are analysed for comparisons.

Haulage Distance Analysis

With an explicity dumping schedule, the haulage distance for completely mining and hauling each block can be calculated. Table 7 summarises the overall return trip haulage distance to be covered by each schedule, including the distance covered for the GM material re-handling. A graphical comparison is presented in Fig. 13. The OP model schedule specifies the least distance to be covered, i.e., 14.06 million

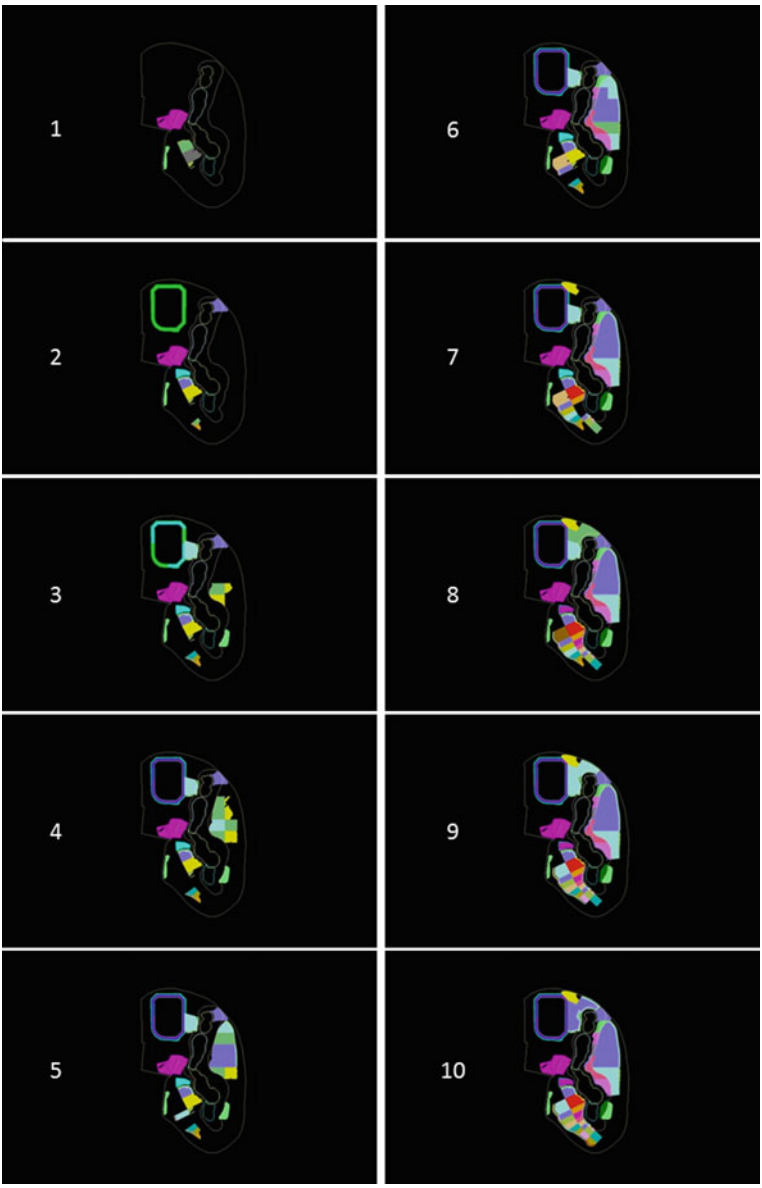

Fig. 10 Landform progression according to OP model dumping schedule

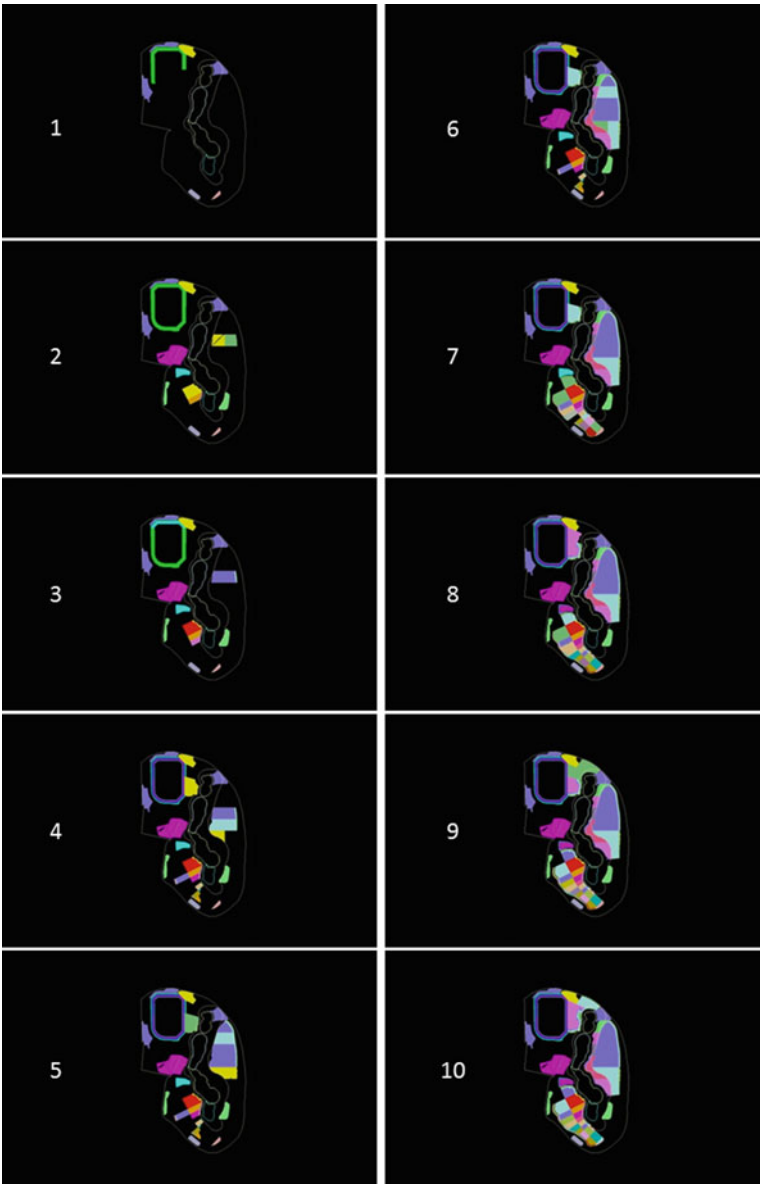

Fig. 11 Landform progression according to TB model dumping schedule

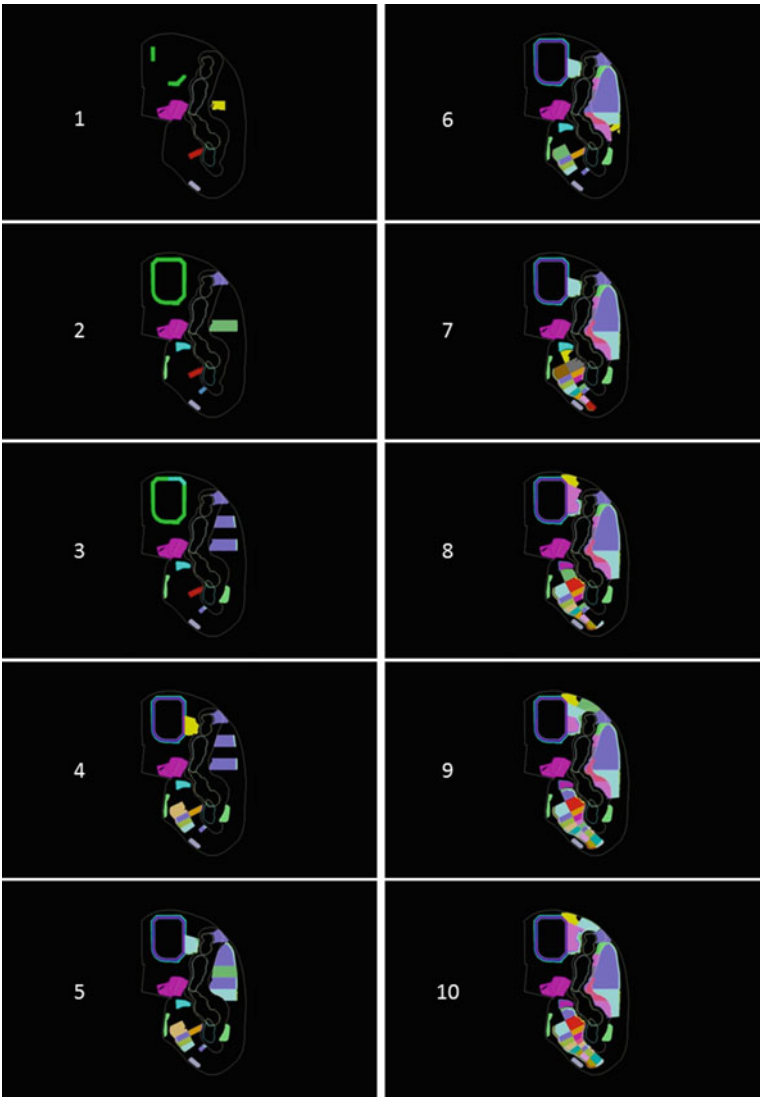

Fig. 12 Landform progression according to Combo model dumping schedule

Table 7 Yearly return trip haulage distance (1000 km)

Period	OP	TB	Combo
1	164.0	444.3	258.4
2	1238.5	1187.9	1371.7
3	1541.5	1620.0	1643.0
4	1663.5	1836.4	1975.8
5	2050.1	1949.6	1914.6
6	1692.9	1675.5	1876.1
7	1368.2	1505.0	1327.2
8	1505.2	1363.0	1418.5
9	1398.1	1293.1	1085.5
10	870.4	874.5	791.5
11	568.6	448.2	520.9
Sum	14,061.2	14,197.6	14,183.1

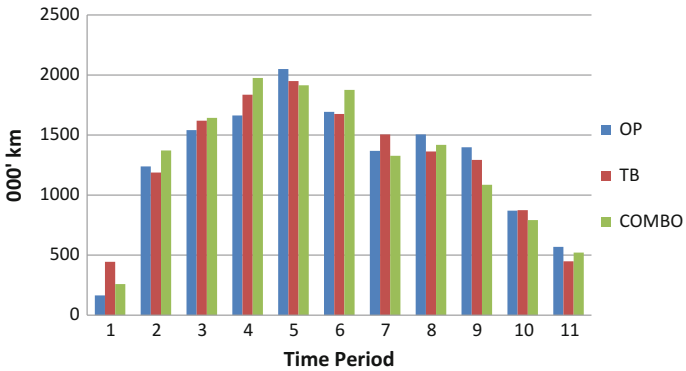

Fig. 13 Overall haulage distance including re-handle by three dumping schedules

km (equivalent flat based distance), which indicates the most efficient dumping schedule of the three.

Estimated Truck Requirement

With known haulage distance, it is possible to estimate the required number of haul trucks in each time period. This result is summarised in Table 8, along with the deviation between adjacent time period. The overall deviation by TB models schedule is the smallest among the three schedules.

It is evident in Fig. 14, that compared to the OP model schedule, the TB and Combo model schedules yield smaller deviations in truck requirement over the

Table 8 Yearly truck hour requirement

Period	OP	ΔOP	TB	ΔTB	Combo	ΔCombo
1	1		3		2	
2	9	8	8	5	10	8
3	11	2	12	4	12	2
4	12	1	13	1	14	2
5	15	3	14	1	14	0
6	12	3	12	2	13	1
7	10	2	11	1	9	4
8	11	1	10	1	10	1
9	10	1	9	1	8	2
10	6	4	6	3	6	2
11	4	2	3	3	4	2
Sum		27		22		24

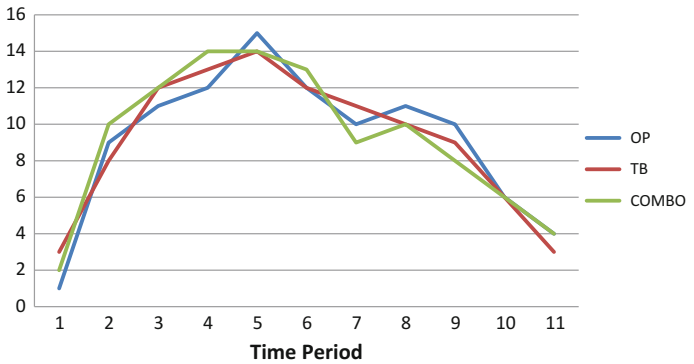

Fig. 14 Yearly truck requirement by three dumping schedules

time. This output aligns with the objectives that the two models additionally consider truck deviation.

Truck Productivity Comparison

The total rock volume handled each year is divided by the total return trip distance to calculate truck productivity, which is measured in LCM/km, or tonnes/km if average density is applied. This indicates the efficiency of the haulage system.

The yearly truck productivity yielded by the three schedules is summarised in Table 9, and is illustrated in Fig. 15. Over the life of mine, the average productivity yielded by the OP, TB and Combo models are 17.9, 16.46 and 17.03 LCM/km, respectively. It suggests that the OP model schedule will be the most efficient.

Table 9 Yearly truck productivity in LCM/km

Period	OP	TB	Combo
1	25.73	9.50	16.34
2	18.17	19.07	16.40
3	19.41	18.54	18.21
4	18.22	16.54	15.41
5	15.76	16.56	16.80
6	18.38	18.80	16.57
7	16.90	15.63	17.42
8	15.61	17.38	16.34
9	14.23	14.57	17.48
10	16.03	16.35	17.09
11	18.49	18.07	19.23
Average	17.90	16.46	17.03

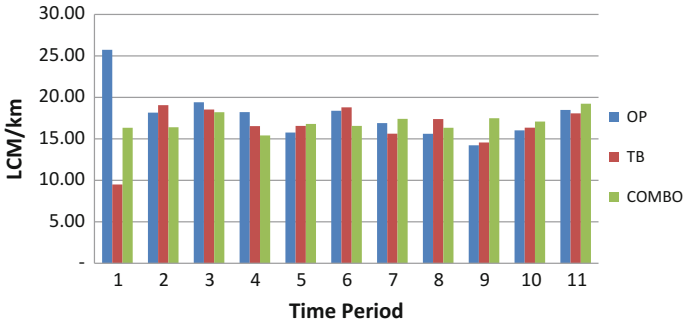

Fig. 15 Yearly LCM/km performance by three options

Conclusions

Three developed MIP models are utilised to solve the dump scheduling problem in a large scale open pit mine. The optimised dumping schedule enables the generation of optimised landform progression, and the estimation of required trucks.

The three landform progression sequences are produced under three different objectives. The graphical results increase the confidence level in planning the waste rock dumps over the life of mine. The two site specific constraints, i.e. ROM-pad and TSF constructed, and the 5-year dumping restriction rule, are properly honored, shows the advantage of using MIP models to reduce deviation from the plan.

The analysis of the dumping schedules proves that the OP model produces the most efficient schedule. It will result in the lowest overall haulage distance, 14.06 million km, and the highest truck productivity, 17.9 LCM/km on average.

However, the truck requirement over the mine life will deviate severely. The dumping schedules produced from TB and Combo models require longer haulage distance to be covered, yet truck deviations over the mine life are smaller than those of by the OP model.

An improvement to the Combo model is to apply impact factors to different objectives, such that the dumping schedules could adjust its focus on either maximising truck productivity or minimising truck deviation.

The scope of the study is limited to optimise the long-term dumping plan, which is a guideline, assuming all required equipments are available. However, the production efficiency on daily basis is still dependant on the availability of the trucks, dig units, and other auxiliary equipments.

References

Li Y, Topal E, Williams D (2013) Waste rock dumping optimisation using mixed integer programming (MIP). Int J Min Reclam Environ 27(6):425–436

Sommerville K, Heyes J (2009) Be open to closure—it can save you money. In: Proceedings iron ore 2009, The Australasian Institute of Mining and Metallurgy, Victoria, Australia, pp 317–322

Wang LZ, Butler GJ (2007) XPAC destination scheduling for waste dumps at BHP Billiton. In: Proceedings iron ore conference 2007, 20–22 Aug, 2007, The Australasian Institute of Mining and Metallurgy, Victoria, Australia, pp 421–425

Solving a Large SIP Model for Production Scheduling at a Gold Mine with Multiple Processing Streams and Uncertain Geology

M. de Freitas Silva

Abstract One of the main steps during the decision-making process of long-term mine planning is the definition of the optimal sequence of extraction, which usually is synonymous of maximizing the discounted cash flow of the project subjected to several constraints arising from aspects of technical, physical, and economic limits. The Open-Pit Mine Production Scheduling (OPMPS) comprises several intricacies related to its size and uncertainty of input parameters. Due to its complexity and prohibitive size, traditional mine planning usually relies on heuristic or meta-heuristic methodologies which are able to provide good solutions in a reasonable amount of time. However, most of the uncertainty that surrounds the mining complex is ignored leading to non-realistic results. In this paper, a new heuristic approach is explored in order to solve a stochastic version of the OPMPS problem accounting for geological uncertainty in terms of metal content, multiple processing streams, and stockpiling option. The methodology involves generating an initial solution by solving a series of sub-problems and this initial solution is improved using a network-flow based algorithm. The algorithm was applied to a relatively large gold deposit with more than 119 thousands blocks. Results have shown that the methodology is promising to deal with large-size mine instances in reasonable time.

Introduction

Open-pit mine production scheduling (OPMPS) generates the optimal sequence of extraction of mining units over the life-of-mine (LOM), given a set of physical and technical constraints. Such a decision process needs to be made under conditions of uncertainty, however, conventional approaches for optimizing OPMPS (e.g., Johnson 1969; Dagdelen and Jonhson 1986; Gershon 1987; Whittle 1988; Tolwinski and Underwood 1996; Cacceta and Hill 2003; Hustrulid and Kuchta

M. de Freitas Silva (✉)
Vale SA, Av. Getúlio Vargas 671, Belo Horizonte, Brazil
e-mail: mario.freitas@vale.com

R. Dimitrakopoulos (ed.), *Advances in Applied Strategic Mine Planning*,
https://doi.org/10.1007/978-3-319-69320-0_40

2006) tend to assume that parameter inputs are fully known, ignoring potential risks and opportunities that might arise from the different sources of uncertainty (Ravenscroft 1992; Dowd 1994, 1997). An example in Dimitrakopoulos et al. (2002) shows that the results in key performance indicators of a conventional mine design are misleading in the presence of geological uncertainty, highlighting the limits of deterministic optimization techniques.

Spatial uncertainty of geological attributes can be modelled through stochastic simulation techniques which are able to provide a series of equally probable scenarios of the orebody (Goovaerts 1997; David 1988). The availability of these models leads to the development of stochastic optimization frameworks that are able to integrate uncertainty into the decision process, minimizing downside risks and maximizing potential upsides. During the last decade, a substantial focus has been given for the development of new models and solution approaches for the stochastic version of the OPMPS. For example, Godoy (2003) introduces a stochastic framework where multiple schedules derived from each geological scenario are firstly joined up. Thereafter, a combinatorial optimization problem is solved by an algorithm based on simulated annealing in order to provide a single schedule with a higher net present value (NPV) (improvements of 28%) and substantially lower deviations from production targets, when compared with the results reported by the conventional schedule. Similar conclusions are drawn in Leite and Dimitrakopoulos (2007) for an application of the framework in a copper deposit. Albor and Dimitrakopoulos (2009) show for a specific case study that the application of this stochastic framework leads to a larger ultimate pit with an NPV 10% larger than the one obtained by constraining the schedule with a conventional pit limit.

Menabde et al. (2018) develop a mathematical formulation to maximize the expected NPV over several scenarios while minimizing deviations from production targets in an average sense. Dimitrakopoulos and Ramazan (2008) bring a stochastic integer programming (SIP) formulation which maximizes the expected net present value (NPV) and incorporates recourse actions to tackle the uncertainty modelled through stochastic simulations, by minimizing possible deviations from production targets over the life-of-mine. Ramazan and Dimitrakopoulos (2013) extend this SIP formulation to introduce a stockpile option, reporting an increase of 10% in the NPV if compared to the economic performance reported by a conventional schedule. In addition, the method provides more realistic schedules that minimize the chance of deviating from production targets, regarding geological uncertainty. These results highlight the ability of stochastic schedules on simultaneously maximising economic returns and driving the mining sequence through zones where the risk of not achieving the target ore production is minimised.

Other variants and applications of SIP have also shown significant improvements over the deterministic OPMPS: Leite and Dimitrakopoulos (2014) show through an application to a porphyry copper deposit that, even for a low grade variability deposit, the NPV can be increased by 29%; Dimitrakopoulos and Jewbali (2013) incorporate in the SIP model simulated future data information, outperforming the NPV of the conventional mine design at a gold mine; Benndorf

and Dimitrakopoulos (2013) extend the model to account for several elements of an iron-ore operation, showing that the capability of the stochastic approach to controlling risks of deviating from production targets for critical quality-defining elements. Boland et al. (2008) incorporate metal uncertainty via a multistage stochastic programming approach in such a way that, decisions made in later time periods might depend on observations of the properties of the material mined in earlier periods.

The stochastic models proposed by Ramazan and Dimitrakopoulos (2004), Menabde et al. (2007) and Boland et al. (2008), are all solved using a mixed integer programming solver such as CPLEX (ILOG 1998), which limits their practical application to instances of relative small sizes, typically accounting for less than 20 thousands blocks (Lamghari and Dimitrakopoulos 2012). As a result, over the past few years, several authors have been seeking the development of new solution approaches, which can efficiently tackle large instances of the stochastic OPMPS. Lamghari and Dimitrakopoulos (2012) introduce a metaheuristic approach based on Tabu search for solving large-scale SIP models within a few minutes up to few hours (while a commercial solver would take days for some instances), with a deviation of less than 4% from optimality for most of their runs. Comparable results are obtained in Lamghari et al. (2013) who use two variants of a variable neighbourhood decent algorithm and average deviations of less than 3% from optimality for several instances.

The present paper focuses on an application of a heuristic approach introduced by Lamghari and Dimitrakopoulos (2013) which incorporates geological uncertainty, multiple processors, stockpiles, and is capable of solving large-size mining schedule problems in a reasonable time. The solution approach can be seen as a very large-scale neighbourhood search method (Ahuja et al. 2002) and it basically involves two stages: (i) the generation of an initial solution and (ii) the application of an improvement algorithm based on network flow. In the following sections, the SIP formulation and the solution approach are revisited, followed by the application at a gold mine employing two processing streams and one ‘grade’ stockpile. Discussions and conclusions follow.

Stochastic Integer Formulation Revisited

The stochastic integer formulation proposed by Lamghari and Dimitrakopoulos (2013) is briefly outlined in this section. The following notation is used:

- N, T, S and P are respectively the total number of blocks, periods, geological simulations and processing facilities.
- $Pred(i)$ is the set of predecessors for a given block i, which means that all blocks in this set must be exploited before i in order to satisfy the slope constraints;
- dr is the economic discount rate over the time basis being considered;

- d_{ips} is a parameter indicating the most profitable destination for a block i under scenario s.
- w_i is the total tonnage of a given block i;
- $E[BEV_i]$ is the expected block economic value (BEV) of a given block i. This value is calculated for each geological scenario, considering the best destination of the block accordingly to the cut-off policy of the project, which is given by the d_{ips}.
- SC_P^t and RC_P^t are both undiscounted costs related to stockpile activities for a given process p during period t. The former cost stands for sending material to the stockpile and the latter for reclaiming material from the stockpile.
- $\tilde{r}_{ps}^t$ is the discounted revenue returned, if a tonne of ore under a given scenario s is reclaimed from the stockpile and sent to process p during production period t.
- W^t and Θ_p^t are the maximum mining and processing capacities (for each processing option p) respectively, for a given period t.
- I_p is the initial amount of material in the stockpile of processor p.
- Binary variables (x_i^t) for each block i and period t. It is considered that x_i^t is equal to one if the block i is already mined by period t, otherwise it assumes the value of zero.
- Linear variables (y_{ps}) related to processing streams. In the model proposed, y_{ps}^{t+} and y_{ps}^{t-} represent the surplus and shortage of material in a given period t, for a process destination p, regarding a specific scenario s. These variables are used to model the stockpile streams related to each process p. In case of surplus under a given scenario, y_{ps}^{t+} is the amount of material that must be stockpiled in order not to violate the processing capacity available. In case of shortage, y_{ps}^{t-} accounts for the amount reclaimed from the stockpile to fulfil the processing capacity. Finally, the variables y_{ps}^t denote the amount of ore in the stockpile at the end of period t.

The mathematical model aims to maximise the discounted cash flow (Eq. (1)) given some physical and technical constraints related to the mining operation (Eqs. (2–10)) as summarised below:

$$max \sum_{t=1}^{T} \frac{1}{(1+dr)^t} \left\{ \sum_{i=1}^{N} E[BEV_i]\left(x_i^t - x_i^{t-1}\right) + \frac{1}{S} \sum_{s=1}^{S} \left[- \sum_{p=1}^{P} \left(\tilde{r}_{ps}^t + SC_P^t\right) y_{ps}^{t+} + \sum_{p=1}^{P} \left(\tilde{r}_{ps}^t - RC_P^t\right) y_{ps}^{t-} \right] \right\} \tag{1}$$

Subject to:

$$x_i^{t-1} \leq x_i^t \quad \forall i, t \tag{2}$$

$$x_i^t \leq x_j^t \quad \forall i, j \in Pred(i), t \tag{3}$$

$$\sum_{i=1}^{N} w_i\left(x_i^t - x_i^{t-1}\right) \leq W^t \quad \forall t \tag{4}$$

$$\sum_{i=1}^{N} d_{ips} w_i\left(x_i^t - x_i^{t-1}\right) - y_{ps}^{t+} + y_{ps}^{t-} \leq \Theta_p^t \quad \forall t, p, s \tag{5}$$

$$y_{ps}^{t-1} + y_{ps}^{t+} - y_{ps}^{t-} = y_{ps}^t \quad \forall t, p, s \tag{6}$$

$$x_i^t = 0 \, or \, 1 \quad \forall i, t \tag{7}$$

$$x_i^0 = 0 \quad \forall i \tag{8}$$

$$y_{ps}^{t+}, y_{ps}^{t-}, y_{ps}^t \geq 0 \quad \forall t, p, s \tag{9}$$

$$y_{ps}^0 = I_p \quad \forall p, s \tag{10}$$

As per Eq. (1), the objective function can be separated in two major terms: the first one refers to the mining decisions, without having access to full information about the material that is underground (scenario independent); the remaining is associated to scenario dependent variables (stockpile actions), because once a block is mined, the operation can take the most suitable decision about where to send a given mined block, leading to different stockpile actions under each scenario. The first part of the stockpiling term refers to the total approximated undiscounted cost related to send exploited material from the mine to the stockpile of processor p in period t under scenario s; and the second part refers to the total approximated undiscounted net revenue after reclaiming material from the stockpile of processor p in period t under scenario s. As one may note, the option of using the stockpile incurs additional costs in the objective function. Thus, in an optimal solution the use of the stockpile is minimised, which means that the risks of overproduction regarding all geological simulations are also minimised.

In order to avoid the non-linearity that arise from the calculation of the parameters $\tilde{r}_{ps}^t$ in the objective function (1), the set of average grades $\tilde{G}_{ps}^t$ needed for the calculation of $\tilde{r}_{ps}^t$ is iteratively approximated and may vary from period to period and scenario to scenario. This iterative approximation is performed in the following way: first, the schedule is solved using an approximated average grade, which might come from the average grade of all blocks in the deposit which are candidates to go to the destination related to the stockpile, or the average grade of materials within the cut-off between its processor and the low-grade processor. After solving the OPMPS with this approximation, the optimiser outputs the amount of material going in and out of the stockpile (respectively given by the linear variables y_{ps}^{t+} and y_{ps}^{t-}), but it does not track which blocks specifically are being stockpiled. Since no blending constraints are considered, it is assumed that in each period, from the set of blocks scheduled to be sent to a given destination, the ones that go to the

stockpile are the ones with the lowest grades, because in an optimal solution, due to the time value of money, the low-value material is stockpiled in order to leave room for the processing of high-value material. By doing such an analysis, it is possible to calculate the "expected" average grade of the stockpile for that given schedule. These average grades by period are then fed as input to the optimiser to generate a new schedule. The same process of approximating the grades and rerunning the solver keeps looping until the difference between the input grade and the "expected" one is less than a threshold ε (e.g., 10%). A similar approach is used by Sarker and Gunn (1997) to solve nonlinear problems, where the authors iteratively solve multiple linear programming problems approximating the quality of the blended material at different locations in terms of sulfur, ash and BTU content. The same authors show that, not only it is a simple and fast way of dealing with nonlinear problems, it is able to provide solutions near optimality after few iterations.

Constraints in Eq. (2) are the *reserve constraints*, which guarantee that each block is mined at most once. Constraints in Eq. (3) are the *slope constraints*, which entails that to access a given block, a set of predecessors must be mined before, assuring the slope angles are predefined. Constraints in Eq. (4) are the *mining constraints* which enforce that the total amount of material mined in a given period t cannot be higher than the mining capacity available for that period. Constraints in Eq. (5) are the *processing constraints*, which imposes an upper bound for the total material sent for a given process, in period t and under scenario s. Constraints in Eq. (6) are the *stockpiling constraints* which balance the mass flows of each stockpile.

It is noteworthy that, although the model does not consider explicitly a lower bound capacity for the processing streams in order to better control the ore feeding, the optimiser always tries to use all the capacity available, mostly in earlier periods as an attempt to increase the NPV of the project. From constraints (5) and (6) one may also note that, in an optimal solution, either stockpiling or reclaiming is active, since both incur costs in the objective function. Thus, in an optimal solution the use of the stockpile is minimised, which means that the risks of overproduction regarding all geological simulations are also minimised. These features are expected to drive the optimiser to maximise value and minimise geological risk throughout the life-of-mine.

A Review of the Solution Approach

For solving the OPMPS model introduced in the previous section, a multistage heuristic algorithm described in Lamghari and Dimitrakopoulos (2013) is used. It comprises two major steps: generation of an initial feasible solution and then its improvement by using a network flow based algorithm which efficiently searches for improving solutions over a large neighbourhood.

Generating an Initial Feasible Solution

Two heuristics methodologies are used to test different initial solutions. Both of them are based on the "divide and conquer" principle, by solving the model period by period, and thus, each period composes a reduced sub-problem. As soon as an earlier period is solved, the mining blocks scheduled to this period are taken out from the model to reduce the problem's size. The later periods are sequentially solved in a similar way. After this sequential process, the solutions found are merged, providing an initial feasible solution.

The differences existing between the two heuristic methods used are basically in the way each one solves the sub-problems. In the first method, the solutions are given by an exact mathematical programming method implemented in CPLEX. The second method is a greedy heuristic procedure (GH) which at each iteration tries to include in the set of mining blocks scheduled for a given production period t, a set of blocks represented by a base block (i) and its predecessors ($Pred(i)$) not mined yet, in such a way as to maximise the objective function of the sub-problem model, respecting the mining capacity constraint and at the same time postponing the extraction of waste and advancing the extraction of ore, thus, deferring costs and advancing profits to earlier periods. This greedy heuristic incorporates a *look ahead* feature, since it looks after blocks with all their unmined predecessors instead of treating blocks separately one by one. In both methods for generating initial feasible solutions, blocks that are not included in the sets of mined blocks in each period until the last one (T) are left behind. To represent these unmined blocks, they are included in a set corresponding to a fictitious period (T + 1).

Improving the Initial Solution with a Network Flow Algorithm

It is well known that sequentially solving the mine production schedule does not lead to an optimal solution of the long-term production schedule (Gershon 1983). Therefore, in a second stage, the goal is to improve the initial solution generated by any of the two heuristic approaches explained above, providing a new schedule with a higher NPV. To achieve this, the improvement algorithm proposed basically tries to postpone the extraction of blocks responsible to decrease the objective function (1) and advance those which improve it.

The algorithm is based on a network-flow structure, where each problem is defined on a graph G = (V, E) (V is the set of nodes and E is the set of arcs). Different graphs are built according to the problem being solved: delaying (*backward pass*) or advancing (*forward pass*) extraction of blocks. Only the construction of the first case is shown henceforth, since the formulation of the *forward structure* is straightforward. Thus, for the *backward structure*, the set of nodes represent blocks which matches the following characteristics:

- the total expected economic value of a given block and all its successors scheduled for the same period t is negative, since NPV increases as the costs are deferred, and;
- the total tonnage of this same group of blocks, summed to the total tonnage already scheduled for the next period $(t + 1)$, minus the total tonnage of a candidate group of blocks scheduled to period $(t + 1)$ which can be postponed to $(t + 2)$, must not exceed the mining capacity W^{t+1}. This condition ensures that the mining capacity is not violated when blocks are moved from one period to another.

Each node of the graph is associated to a block and its predecessors scheduled for the same period, respecting the conditions stated above. To complete the network, an additional node is added to the fictitious period T + 1 which represents the set of blocks that will not be extracted; for each period, one extra node is added for fictitious blocks with neither weight nor costs, representing a path through where no modifications are done to the current schedule. In addition, two extra nodes must be added to the network referring to its source and sink. In this formulated graph, the set of arcs E involves all possible connection between two nodes currently scheduled in consecutive periods t and $t + 1$. In addition, some arcs are added connecting the source to the nodes belonging to the first period and one more arc is connected from the fictitious node in T + 1 to the sink. As a result, each path from the source to the sink, passing through nodes in consecutive periods, represents a new solution to the stochastic mine production schedule, where a given mining block and its successors represented in a node has their extraction delayed to the next period and so on. Blocks at the head of the arc are moved to the following period and the blocks represented by the node at the tail of the arc are mined in their place. Figure 1 shows a simplified illustration of graph G.

Thus, the goal is to find a single feasible path which improves the value of the objective function as in Eq. (1). If no such path is found, the solution given by the algorithm is the path which includes the set of fictitious nodes introduced before, and no block would be moved from one period to the other and the value of the objective function remains the same. To identify the feasible path which increases the value of the objective function the most, each arc is weighted accordingly to the feasibility of the delaying movement and the gain it brings to the objective function. After weighting each arc the model becomes a *longest path problem*, which consists in finding the simple path of maximum length, where the length in this case is represented by the sum of the weighted arcs.

As mentioned earlier, once the graph is built, solutions are generated by solving the *longest path problem*, associating each arc to a binary variable and sending a unitary flow from the source to the sink, which guarantees that the solution provided is always a simple path. It is interesting to note that the constraint matrix (nodes-arcs incidence matrix) of this integer programming problem is unimodular. This property indicates that the integrality constraints can be dropped and only restricts $z_{ij} \in [0, 1] \; \forall \; (i, j) \in E$. Subsequently, the problem can be efficiently solved using linear programming or network-flow techniques.

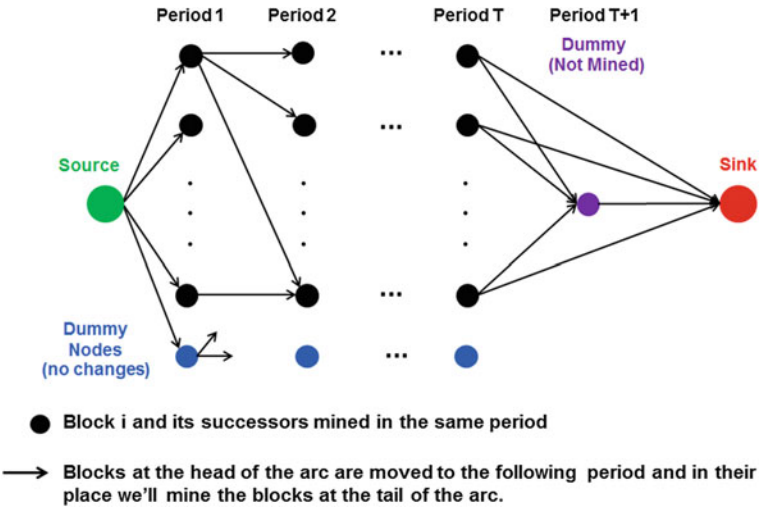

Fig. 1 Ilustration of the graph built for the network-flow improvement algorithm (backward Case)

In summary, the algorithm works in an interactive way such as the following: first, it performs a *backward pass* (initial mode), trying to delay the extraction of blocks. If the solution changes, a new network is built for the new current schedule and another *backward pass* is carried out. Otherwise, if the *longest path* found identifies the set of fictitious nodes, meaning that no improvement can be made, the problem is switched to a *forward pass*, and the algorithm looks for blocks to advance their extraction. In the same way as in the first, several passes are performed until no improvement is achieved, and then the problem switches its mode again. The algorithm stops when it executes two consecutive modes, that is, *backward* and *forward passes* (and vice versa) without any improvement in the value of the objective function.

Case Study at a Gold Mine

To demonstrate the application related aspects of the method previously described, a case study at gold mine is presented here. The deposit being mined consists of an intensely mineralized shear system localised in mainly steeply dipping, NNW to NW striking lodes. Gold lodes can be up to 1800 m (5900 ft) long, have vertical extents of 1200 m (3900 ft) and be up to 10 m (33 ft) wide. The mine feeds two processing streams, a mill and a leaching facility, with the first having an associated stockpile. Fixed stockpiling/reclaiming costs are used throughout the LOM and no material is in stock for the first production period.

A set of 15 stochastic simulations, discretised in about 120 thousand blocks of $20 \times 20 \times 20$ m^3 and generated by direct block simulation (Godoy 2003), are used to model the spatial uncertainty of grades through the deposit. This number of scenarios is used because past works, such as in Leite (2008) and Albor and Dimitrakopoulos (2009), indicate that after about such number of representations of an orebody, the stochastic schedules tend to converge to a stable final schedule and to provide stable forecasts of production performance. Such results are not surprising because, despite the spatial uncertainty modeled over blocks with few cubic meters, a production schedule of a mine represents a grouping of several hundreds to thousands of these blocks in one mining period under different constraints. Thus, with this significant increase of support (from blocks to production in mining periods), the stochastic schedules tend to be less sensitive to additional scenarios after a relatively small number of scenarios.

The general parameters for the stochastic mine production schedules are summarised in Table 1.

The case study is split in two subsections in order to show the differences obtained when using *branch-and-cut* (Wolsey 1998), an exact mathematical programming method implemented in CPLEX (ILOG 2008) or a greedy heuristic to generate the initial solution. The computations are performed in a Intel Xeon 5650 (2.66 GHz) with 24 GB RAM. In both case studies, CPLEX is used to solve the *longest path problem* over the network during the improvement stage of the algorithm.

Stochastic Schedules

Two different schedules are generated, each respectively using CPLEX and the greedy heuristic (GH) to generate the initial feasible solutions. The risk profiles for the ore throughput for the mill and the material stockpiled by the end of each period

Table 1 Technical and economic parameters for OPMPS

Mining cost	$ 1.80/t	Mining capacity	90 Mta
Metal price	$ 730/oz	Selling price	$5.0/oz
Discount rate	8.0%	Slope angle	45°
Mill—high grade			
Recovery	90%	Proc. cost	$ 9.50/t
Stockpiling cost	$ 0.50/t	Reclaiming cost	$ 0.85/t
Proc. capacity	22.0 Mta	Stockpile capacity	20 Mt
Leaching—low grade			
Recovery	50%	Proc. cost	$ 5.00/t
Proc. capacity	1.0 Mta		

are respectively shown in Figs. 2 and 3. In these graphs, the black and gray solid lines refer to the expected ore input to the mill in the schedules generated by respectively using CPLEX and GH as initial solutions. The dashed lines represent the percentiles P10 and P90 for the ore throughput over the different geological scenarios.

The schedule using CPLEX as initial solution considers an additional year to the LOM, shown in black (Fig. 2) and an ultimate pit 1.1% bigger than the schedule using GH as initial solution. As seen in Fig. 2, the range of variability about the expected value of throughput for the mill is quite low, which suggests that this process is likely to operate with low uncertainty for the expected throughput. For the schedule obtained using the initial solution from CPLEX, the mill will potentially work at full capacity (22Mt) during the first sixteen years, while for the OPMPS using the GH as initial solution, this period is shortened to eleven years. During these time spans, the mill potentially works with almost no risks of over/under production. This occurs because during those periods, the tonnage uncertainty is somehow "shifted" to the stockpile, since for each scenario, the overproduction is sent to the stockpile and in case of shortages, material can be reclaimed from the stockpile. During the years for which the mill works below its capacity (Fig. 2), the mine operates at full mine capacity (90Mt) and not enough material is available in the stockpiles under all geological scenarios (Fig. 3). These factors lead the optimiser to work below the mill's maximum capacity, since the mining rate entails in a bottleneck for the operation and no penalties are incurred for underproduction in the SIP formulation presented in a previous section. A way of dealing with this would be to explicitly incorporate penalties for idle capacity (shortage in production) in the formulation, in such a way that they do not compete with the reclaiming variables, or allow a flexibility to the mine to increase its capacity during later periods, through the acquisition of mining equipment.

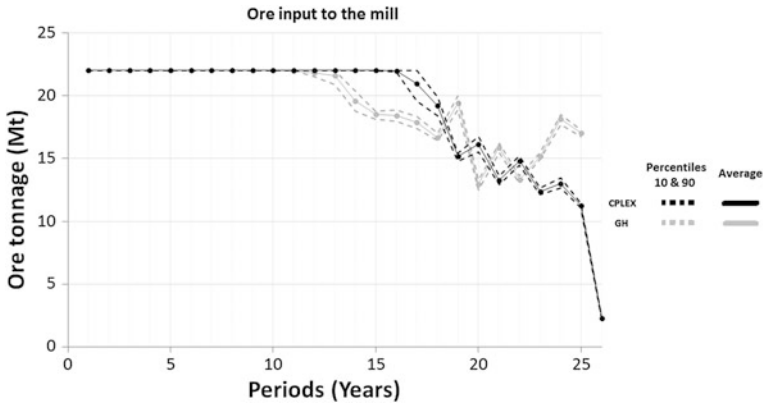

Fig. 2 Expected ore tonnage throughput for the mill and related risk profiles, using CPLEX (black) and GH (gray) to generate initial solutions

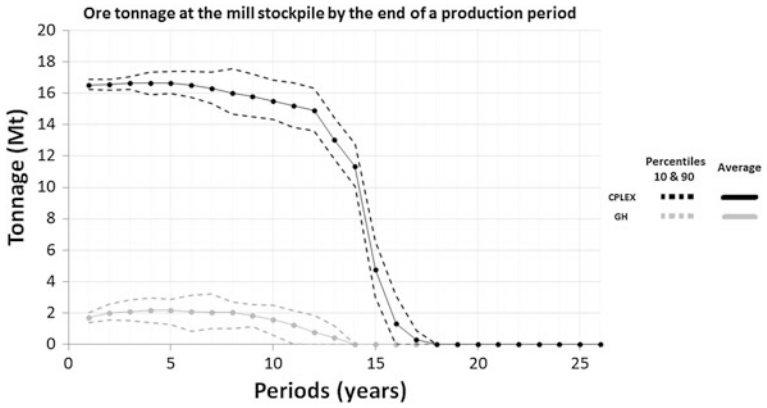

Fig. 3 Expected ore tonnage at the mill stockpile and related risk profiles, using CPLEX (black) and GH (gray) to generate initial solutions

Figure 3 shows that, for both schedules generated, the first period is when most of the material is sent to the stockpile, which allows the mill to advance the metal production, by working with a high grade material as shown in Fig. 4. These results show, as expected, the flexibility added to the project by the use of a stockpile: (i) it allows the operation to reach high grade material earlier during the LOM and (ii) 'buffers' the risks of oversupply of ore and/or having idle processing capacity, with respect to geological uncertainty.

Regarding the differences between the two schedules generated, Fig. 2 shows that the OPMPS using CPLEX to generate the initial solution is able to advance the production of ore (*see* years 13–18) and to reach high grade areas during earlier periods if compared to the solution by using the GH as initial solution. The metal

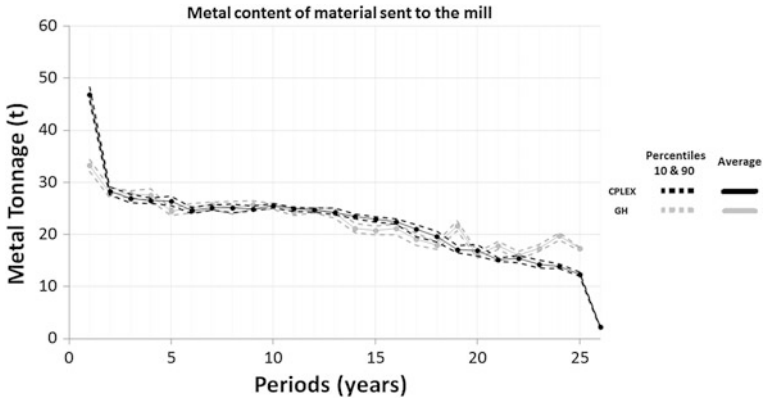

Fig. 4 Expected metal input to the mill and related risk profiles, using CPLEX (black) and GH (gray) to generate initial solutions

content for the ore input to this processor during the first year is about 40% larger in the first production schedule than in the second. Figure 3 shows that these differences are mostly related to the fact that, in the first solution approach the greater use of the stockpile provides a larger flexibility to the operation.

In contrast to the behaviour seen for the mill, Fig. 5 shows that the leaching process will potentially work under its nominal capacity of 1Mt and with a much more variable throughput. Such a result is expected because the SIP formulation used in this paper, controls the geological risks exclusively through the use of a stockpile associated to the mill, which is not the case for leaching. Figure 6 shows the risk profile for the metal production of this same processing destination.

Regarding the economic performance of the project, the risk profiles of the cumulative NPV are shown in Fig. 7. These curves show a very low uncertainty about the expected NPVs for the project (less than 3% of upper/lower deviations regarding the P10 and P90). In addition, Fig. 6 shows that, the OPMPS using the GH as initial solution has an overall NPV of M$215 which is 7.9% lower than the one obtained by using CPLEX as initial solution. In this specific case study, this difference is mostly related to the ability of the latter solution to produce a larger amount of metal during the first period. In this year, its NPV of M$245 is 56% higher than the one achieved by the mine production scheduling obtained by using GH as initial solution.

While CPLEX takes hours to generate an initial solution, the GH takes only seconds. In addition, the final OPMPS using CPLEX as initial solution took a total time of 32 h against the 38 h required for the generation of the final solution by the approach using the GH as initial solution. This excessive time reported by this last approach is related to the size of the neighbourhood found in each iteration when it tries to make a *backward move*. In many of these iterations, the graph built has

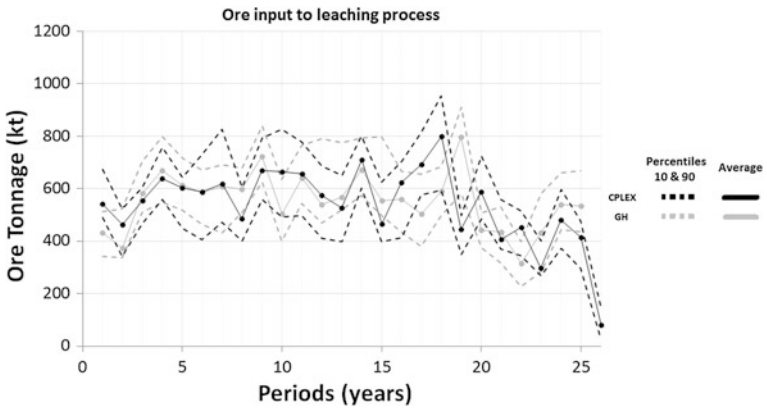

Fig. 5 Expected ore tonnage throughput for the leaching and related risk profiles, using CPLEX (black) and GH (gray) to generate initial solutions

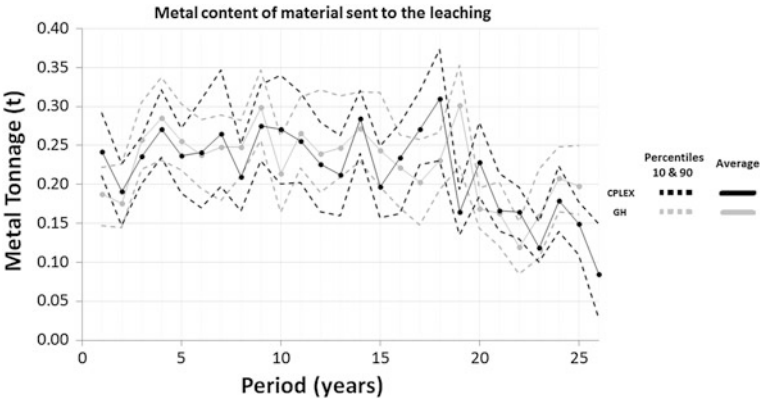

Fig. 6 Expected metal input to the leaching and related risk profiles, using CPLEX (black) and GH (gray) to generate initial solutions

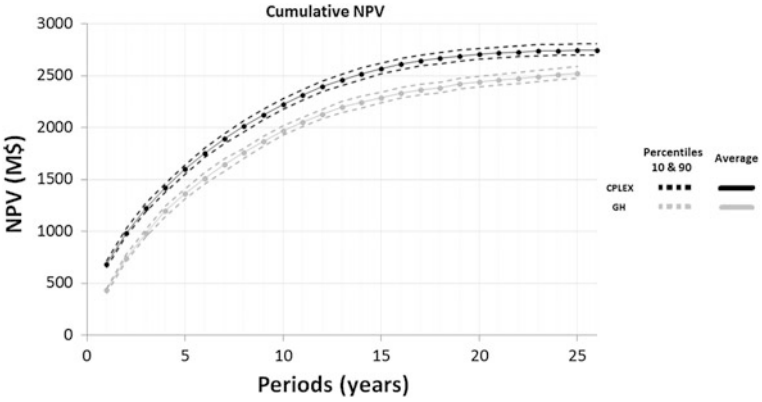

Fig. 7 Expected cumulative NPV and related risk profiles, using CPLEX (black) and GH (gray) to generate initial solutions

contained more than 2.7 thousands of nodes and 22 millions of arcs. This represents a very large linear programming problem, requiring more than 30 min to be solved. Thus, as one may observe, for this case study, besides providing a higher NPV, the final schedule generated using CPLEX's initial solution also demands a smaller computational time than the approach using GH to generate an initial solution.

Figure 8 brings South-North cross sections of the schedules, illustrating the differences in their physical sequence of extraction. Using CPLEX as initial solution produces a less smooth sequencing pattern than the one provided by employing GH as initial solution. For this case study, this latter approach tends to maintain the "clustered" structure intrinsic from its formulation.

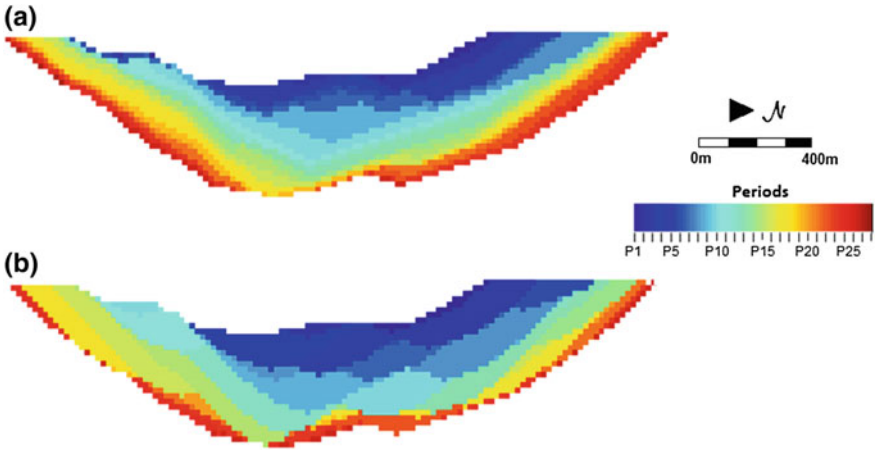

Fig. 8 South-North vertical cross-section of the physical sequences of extraction for the schedules using different initial solutions **a** CPLEX and **b** GH

Conclusions

The present study highlights the practical aspects and performance of a neighborhood search method based on a network flow algorithm, developed to solve a stochastic version of the open-pit mine production scheduling. A case study was performed at a relatively large gold mine comprising about 120 thousand blocks, two processing streams and a stockpile. This consists of a very large mathematical programming model, with about 3 million integer variables. Two different ways of generating initial feasible solutions to be input to the network flow algorithm were tested. The first uses CPLEX and the second a greedy heuristic to sequentially solve the mine production schedule period-by-period. For the specific case study, although the greedy heuristic was able to find the initial solution in a few seconds and the exact method demanded hours for the same task, the improvement stage was much longer when using the greedy heuristic solution. This latter approach took 38 h to generate a final schedule, against 32 h required by the optimiser when the CPLEX initial solution is used. This behavior is different to the common trend observed in previous tests (Lamghari et al. 2013). Note that, when CPLEX was used to produce the linear relaxation of the stochastic integer programming model of this case study, it could not provide an optimal solution after two weeks, highlighting the advantages of looking for computationally efficient solutions, such as the one used in this paper.

In this case study, the production schedules generated showed that by using the initial solution from CPLEX, a better final solution can be achieved in terms of NPV (7.9% higher than starting from the initial solution generated by the GH). All results have shown that the stochastic mine production schedules have controlled deviations in ore production for the processor with a stockpile associated to it, since

the SIP formulation used in this paper, considers that the recourse actions to control the geological risk are incorporated in the stockpiling actions. The overproduction under any scenario is sent to the stockpile and shortages are only controlled if there is material available in the stockpile. These actions imply costs associated to rehandling of material and the opportunity cost of leaving valuable material in the stockpile, and therefore, penalizing deviations related to uncertainty. The shortcoming is that, if in a giving production period, no material is available at the stockpile, shortages are not explicitly penalised.

These observations highlight that the heuristic method tested in this paper is able to tackle large SIP formulations for realistic mine environments, producing mine production schedules with low deviations about expected production rates.

Acknowledgements The work in this paper was funded from the National Science and Engineering Research Council of Canada, Collaborative R&D Grant CRDPJ 411270-10 with AngloGold Ashanti, Barrick Gold, BHP Billiton, De Beers, Newmont Mining, and Vale. A special thanks to McGill's COSMO Stochastic Mine Planning Laboratory and Professor Roussos Dimitrakopoulos for all the support and guidance.

References

Ahuja K, Ergun Ö, Orlin B, Punnen P (2002) A survey of very large-scale neighborhood search techniques. Discrete Appl Math 123(1):75–102

Albor F, Dimitrakopoulos R (2009) Stochastic mine design optimisation based on simulated annealing: pit limits, production schedules, multiple orebody scenarios and sensitivity analysis. Min Technol (Trans Inst Min Metall A) 118(2):A80–A91

Benndorf J, Dimitrakopoulos R (2013) Stochastic long-term production scheduling of iron ore deposits: integrating joint multi-element geological uncertainty. J Min Sci 49(1):68–81

Boland N, Dumitrescu I, Froyland G (2008) A multistage stochastic programming approach to open pitmine production scheduling with uncertain geology. Optim Online. [online]. Available from: www.optimizationonline.org/DBHTML/2008/10/2123.html

Caccetta L, Hill SP (2003) An application of branch and cut to open pit mine scheduling. J Global Optim 27(2–3):349–365

Dagdelen K, Johnson TB (1986) Optimum open pit mine production scheduling by lagrangian parameterization. In: Proceedings 19th APCOM symposium of the society of mining engineers, AIME, New York, pp 127–142

David M (1988) Handbook of applied advanced geostatistical ore reserve estimation. Elsevier, Amsterdam, p 232

Dimitrakopoulos R, Ramazan S (2008) Stochastic integer programming for optimizing long-term production schedules of open pit mines: methods, application and value of stochastic solutions. Min Technol (Trans Inst Min Metall A) 117(4):155–160

Dimitrakopoulos R, Jewbali A (2013) Joint stochastic optimization of short- and long- term mine production planning: method and application in a large operating gold mine. Min Technol (Trans Inst Min Metall A) 122(2):110–123

Dimitrakopoulos R, Farrelly CT, Godoy M (2002) Moving forward from traditional optimization: grade uncertainty and risk effects in open pit design. Min Technol (Trans Inst Min Metall A) 111(1):82–88

Dowd P (1994) Risk assessment in reserve estimation and open pit planning. Min Technol (Trans Inst Min Metall A) 103:148–154
Dowd P (1997) Risk in minerals projects: analysis, perception and management. Min Technol (Trans Inst Min Metall A) 106:9–18
Gershon M (1983) Optimal mine production scheduling: evaluation of large scale mathematical programming approaches. Geotech Geol Eng 1(4):315–329
Gershon M (1987) Heuristic approaches for mine planning and production scheduling. Int J Min Geol Eng 5(1):1–13
Godoy M (2002) The effective management of geological risk in long-term production scheduling of open pit mines, Ph.D. thesis (unpublished), University of Queensland, Brisbane, Australia
Goovaerts P (1997) Geostatistics for natural resources evaluation. Oxford University Press, New York, p 496
Hustrulid WA, Kuchta M (2006) Open pit mine planning & design. Taylor and Francis, London, p 991
ILOG (2008) ILOG CPLEX 11.2 user's manual. IBM, Armonk
Johnson T (1969) Optimum production scheduling. In: Proceedings of the 8th international symposium on computers and operations research, Salt Lake City, pp 539–562
Lamghari A, Dimitrakopoulos R (2012) A diversified tabu search approach for the open-pit mine production scheduling problem with metal uncertainty. Eur J Oper Res 222:642–652
Lamghari A, Dimitrakopoulos R (2013) A network-flow based algorithm for scheduling production in multi-processor open pit mines accounting for metal uncertainty. [online]. Available from: www.gerad.ca/fichiers/cahiers/G-2013-63.pdf [Accessed 1 April 2014]
Lamghari A, Dimitrakopoulos R, Ferland J (2013) A variable neighborhood descent algorithm for the open-pit mine production scheduling problem with metal uncertainty. J Oper Res Soc. doi:10.1057/jors.2013.81
Leite A (2008) Application of stochastic mine design and optimization methods, M Eng Thesis, McGill University, Montreal, Canada
Leite A, Dimitrakopoulos R (2007) Stochastic optimization model for open pit mine planning: application and risk analysis at a copper deposit. Min Technol (Trans Inst Min Metall A) 116 (3):109–118
Leite A, Dimitrakopoulos R (2014) Mine scheduling with stochastic programming in a copper deposit; Application and value of the stochastic solution. J Min Sci Technol 24(6):755–762
Menabde M, Froyland G, Stone P, Yeates G (2018) Mining schedule optimisation for conditionally simulated orebodies, in this Volume
Ramazan S, Dimitrakopoulos R (2004) Traditional and new MIP models for production scheduling with in-situ grade variability. Int J Surf Min Reclam Environ 18(2):85–98
Ramazan S, Dimitrakopoulos R (2013) Production scheduling with uncertain supply: a new solution to the open pit mining problem. Optim Eng 14(2):361–380
Ravenscroft P (1992) Risk analysis for mine scheduling by conditional simulation. Min Technol (Trans Inst Min Metall A) 101:104–108
Sarker RA, Gunn EA (1997) A simple SLP algorithm for solving a class of nonlinear programs. Eur J Oper Res 101(1):140–154
Tolwinski B, Underwood R (1996) A scheduling algorithm for open pit mines. IMA J Math Appl Bus Ind 7:247–270
Whittle J (1988) Beyond optimisation in open pit design. In: Fytas K (ed) Proceedings computer applications in the mineral industries, Balkema, Rotterdam, pp 331–337
Wolsey LA (1998) Integer programming. Wiley, New York, p 288

Part VIII
Contributions to Strategic Innovation

Stochastic Optimisation of Mineral Value Chains—Developments and Applications for the Simultaneous Optimisation of Mining Complexes with Uncertainty

R. Goodfellow and R. Dimitrakopoulos

Abstract One of the primary objectives when optimising a mining complex is to maximise its value for the primary stakeholders. In order to achieve this objective, it is necessary to holistically optimise all aspects of the mining complex, including decisions of when to extract materials from the available sources, how to blend or stockpile these materials, and how to best use the available processing streams to satisfy customer demand. Existing methods for global, or holistic, optimisation ignore the compounded effects that risk has on the performance of a mining complex. Over the past decade, several stochastic optimisation approaches have been proposed to integrate various forms of uncertainty into the open pit mine design and production scheduling. These methods, however, are limited in their ability to simultaneously optimise the production schedules for the portfolio of mines, material destination policies, the use of the available processing streams and the various products that are produced at each location of the mining complex. This paper aims to discuss a new method for the global optimisation of open pit mining complexes with geological uncertainty. The proposed generalised methodology is capable of modelling and holistically optimising mining complexes, including aspects related to production scheduling, blending, stockpiling and non-linear interactions that often occur in practice, but are over-simplified in existing models. Two case studies are discussed to highlight the need for these complex, stochastic optimisers. First, a case study for a nickel laterite blending operation highlights the need to integrate geological uncertainty into the optimisation in order to ensure product quality constraints are respected. Second, a case study for a copper-gold mining complex highlights the added value when simultaneously optimising the production schedule and the stockpiling and treatment of extracted materials.

R. Goodfellow (✉) · R. Dimitrakopoulos
COSMO—Stochastic Mine Planning Laboratory, McGill University, Montreal, QC, Canada
e-mail: ryan.goodfellow@mail.mcgill.ca

R. Dimitrakopoulos (ed.), *Advances in Applied Strategic Mine Planning*,
https://doi.org/10.1007/978-3-319-69320-0_41

Introduction

A mining complex, or a mineral value chain, is an integrated business that extracts materials from open pit or underground mines, treats the extracted materials using a set of processing facilities that are connected via various materials handling methods, and generates a set of products that are sold to customers or on the spot market. The primary objective when optimising a mining complex is to maximise the value of the operation for the business and its stakeholders, while obeying the technical constraints for each operation that limit the quantities of materials or products extracted, treated and sold. Traditionally, this optimisation is performed for each of the various components of the mining complex independently, leading to the sub-optimal use of the mineral resource(s) and financial capital. The global optimisation of mining complexes (Urbaez and Dagdelen 1999; Hoerger et al. 1999; Stone et al. 2017; Whittle 2007, 2017, this volume) aims to simultaneously optimise aspects related to the long-term extraction sequence of materials from the available mines, and the optimal use of the processing streams in order to maximise the utility of the extracted materials while meeting contractual obligations related to the quantity and quality of the products generated. One of the challenges associated with the global optimisation of mining complexes is a result of non-linear optimisation models that arise from integrating stockpiling, blending and non-linear transformations (e.g. grade-recovery curves, throughput-hardness relationships, etc.) that occur in the various processing streams. In order to avert these challenges, optimisation models are simplified in order to obtain a linear formulation. One of the most common examples of these simplifications is the economic value of a block (Lerchs and Grossmann 1965; Johnson 1968; Picard 1976; Dagdelen 1985; Tolwinski and Underwood 1996; Caccetta and Hill 2003; Meagher et al. 2010). Naturally, this definition assumes prior knowledge of the optimal processing method for a block, and values each block independently of other blocks that may be extracted, blended and treated in the same period. A more appropriate approach is to consider the economic value of the products sold, which may be a function of product quality, rather than the value of the materials extracted. A global optimisation approach can avoid such simplifications by permitting the ability to model these non-linear aspects that are commonly seen in practice, and provide efficient optimisation methods and algorithms that can be tailored according to the objectives, needs and constraints for each operation.

As the complexity of the mineral deposits increase, in terms of number of elements and materials, a traditional approach for mine optimisation fails because it only considers a single set of inputs (e.g. orebody models, metal prices and costs), and does not consider the compounded effects that uncertainty may have on the mineral value chain as a whole. The assumption of constant (deterministic) inputs leads to an unrealistic assessment of the mining complex's performance—particularly its ability to meet annual production targets and financial forecasts (Dimitrakopoulos et al. 2002). Recently, stochastic optimisation models have been developed in order to manage various forms of uncertainty, particularly geological

uncertainty, directly into the optimisation of mining operations. Godoy (2002) proposes a sequential optimisation method that first determines the appropriate level of ore and waste production from an orebody, and creates a single production schedule that manages the risk of not being able to meet ore and waste production targets. Ramazan and Dimitrakopoulos (2013) propose a two-stage stochastic integer program (SIP) (Birge and Louveaux 2011) that aims to generate a life-of-mine (LOM) production schedule that maximises the net present value (NPV) of the materials mined and simultaneously reduce the risk of not being able to meeting production targets (e.g. ore production, total material movement and metal production). This risk management is achieved by penalizing deviations from targets using a set of penalty costs. A geological risk discount rate is used, similar to that used in the calculation of the NPV, in order to impose high penalty costs at the beginning of the mine's life, and are relaxed over time. As a result, the optimiser not only attempts to extract material with a high economic value earlier in time, but it also blends levels of risk in order to ensure that production targets are met at the beginning of the mine's life and defers riskier material to later periods when more information is available. This basic SIP model has been expanded upon and tested (Albor and Dimitrakopoulos 2010; Benndorf and Dimitrakopoulos 2013; Dimitrakopoulos and Jewbali 2013; Leite and Dimitrakopoulos 2014), and results consistently demonstrate that stochastic designs are able to not only reduce the risk of not meeting production targets, thus leading to improved reliability in financial forecasting, but also result in designs with a higher NPV.

The aforementioned methods, however, are limited because: (i) they only consider mining operations with a single mine; (ii) they assume an a priori definition of the classification of ore and waste material, hence do not dynamically optimise the destination policies (e.g. cut-off grades) that define where materials are sent post-extraction; and (iii) do optimise the use of stockpiles and the downstream processes. Stochastic optimisation of multi-mine operations is computationally challenging because of the exponential increase in the number of joint scenarios that occur with multiple, independent representations of the geological conditions; for example, a mining complex that is comprised of two mines, each represented using 20 orebody simulations, results in 400 joint scenarios to consider during optimisation. The decisions of where to send material after extraction also increases the size of the model, particularly when considering geological uncertainty. The three main methods to integrate these destination decisions are to: (a) decide where each block is sent for each scenario (Boland et al. 2008); (b) decide where each block is sent, regardless of the scenario (Montiel and Dimitrakopoulos 2013); or (c) define a policy, such as a robust cut-off grade, where blocks with similar grades are sent (Menabde et al. 2017). The first two options are computationally challenging because the number of decision variables increase linearly with the number of blocks in the model. While the second method reduces the number of decision variables because it is scenario-independent, it is likely that the optimiser will choose to send materials to incompatible processing streams (e.g. sending oxide materials to a stream that only treats sulphide materials). The third option (a robust cut-off grade policy) is appealing because it creates a scenario-independent policy

that both reduces the number of decision variables by discretising the continuous grade distribution into a small number of "bins" (decision units), but also avoids the challenges of misclassification. Cut-off grade policies, however, are not always ideal, particularly for multi-element mining complexes that impose product quality or grade blending specifications on secondary elements. Finally, modelling the downstream aspects of a mining complex often results in non-linear blending or pooling (Audet et al. 2004), which are difficult to solve using mathematical programming approaches. Recent work has investigated cutting plane approaches for integrating stockpiles (Bley et al. 2012), however these methods have not been extended for stochastic optimisation models or cases with multiple elements.

This work discusses recent developments and applications in the stochastic global optimisation of open pit mining complexes, which simultaneously optimises multi-mine production schedules, destination policies and the various processing streams (Montiel et al. 2017). First, a generalised modelling approach is proposed that permits a mine planner to model the material flow through a mineral value chain, from the mines through to the final products, including the ability to integrate non-linear transformations. A generalised two-stage SIP formulation is then discussed, which permits a modeller to integrate the unique objectives and constraints for their own operation. These models are optimised using a combination of two metaheuristic algorithms: particle swarm optimisation and simulated annealing. Two applications of the developed methods are then discussed. The first application is for the blending optimisation (ignoring production scheduling) for a nickel laterite operation, which highlights the importance of considering uncertainty when optimising mining complex with stringent blending constraints. The second application for a copper-gold mining complex highlights the global optimiser's ability to not only reduce the risk of meeting production targets, but also increase the NPV. Finally, conclusions and future extensions are presented.

Modelling and Optimizing Mineral Value Chains

A Generic Modelling Approach for Mining Complexes

Given the wide diversity in the types of mineral value chains, which often vary depending on the type of commodity produced, geographical and geological conditions, a generic modelling approach is developed and may be adapted to model the unique intricacies of each operation. A *material* is a term used to describe a product that is extracted from a mine or generated via blending, separation or processing. Often, these materials have unique mineralogical or geometallurgical characteristics that influence the decision of where it can be sent for further blending or treatment in a processing stream. An *attribute* is a term used to describe a property or characteristic of a material that is of interest to the modeller, and may be categorised into two groups:

- Primary attributes ($p \in \mathbb{P}$) are the variables of interest that are sent from one location in the value chain to another (e.g. metal tonnage, total tonnage). The values of primary attributes may be added together directly (i.e. adding total tonnages for material received from two mines).
- Hereditary attributes ($h \in \mathbb{H}$) are the variables of interest at specific locations in the value chain that are of interest to the modeller, but are not necessarily forwarded between locations in the value chain. Some examples include mining, stockpiling and processing costs, revenues from metal sale, throughput rate, energy consumption and revenues from the sale of the product). These attributes are calculated using (non-) linear equations, $f_h(p, i)$, which are defined by the modeller and are evaluated dynamically during optimization.

A mineral value chain, $\mathcal{C}$, may be comprised of sets of mines ($\mathcal{M}$), stockpiles ($\mathcal{S}$) or other destinations ($\mathcal{D}$), i.e. $\mathcal{C} = \mathcal{M} \cup \mathcal{S} \cup \mathcal{D}$, and operates in the set of contiguous time periods, $\mathbb{T}$. In order to simplify the description of the modelling and optimisation methods developed herein, consider the case where each location in the mining complex may receive products from multiple sources, but only generates a single product. The more general case where multiple products are generated is a minor extension. Let $\mathbb{S}$ represent a set of equally probable scenarios that are used to describe the uncertainty in the mining complex. Only geological uncertainty is considered in this work, whereby each block $b \in \mathbb{B}_m$ at mine $m \in \mathcal{M}$ has simulated attributes and material types. The value of a block's attribute ($p \in \mathbb{P}$) for each scenario ($s \in \mathbb{S}$) will herein be denoted by $\beta^p_{b,s}$. The set of locations that send material to a location $i \in \mathcal{S} \cup \mathcal{D}$ is denoted by $\mathcal{I}(i)$. Alternatively, the set of locations that receive materials from $i \in \mathcal{C}$ is denoted by $\mathcal{O}(i)$. The value of a primary or hereditary attribute in any scenario s and period $t \in \mathbb{T}$ at a location $i \in \mathcal{C}$ is given by the state variables $v^p_{i,t,s}$ and $v^h_{i,t,s}$, respectively. Similarly, the recovery of a primary attribute is given by the variable $r^p_{i,t,s}$, which may either by a constant factor or equal to the value of a hereditary attribute, which may, for example, be governed by a grade-recovery curve (i.e. $r^p_{i,t,s} = v^h_{i,t,s} = f_h(p, i)$).

The terms defined above are used to describe the material flow directions, and the (potentially non-linear) transformations that occur at each location. In order to quantify the flows through the mining complex, three types of decision variables are defined:

1. Production scheduling decisions ($x_{b,t} \in [0, 1]$) define whether (1) or not (0) a block b is extracted in period t. It is noted that in order to safely extract a block b, it is necessary to have first extracted its overlying blocks, $\mathbb{O}(b)$.
2. Destination policy decisions ($z_{g,j,t} \in [0, 1]$) define whether (1) or not (0) a subset of materials with similar block attributes (referred to as a *group*), $g \in \mathbb{G}$, is sent to destination $j \in \mathcal{O}(g)$ in period t. The definition of these groups is similar to the *bins* used to define robust cut-off grade policies (Menabde et al. 2017), but consider multivariate distributions of primary attributes (e.g. multiple grades, block density, etc.). See Fig. 1 for an example of the definition of destination policies. These groups may be generated using a pre-processing step with the

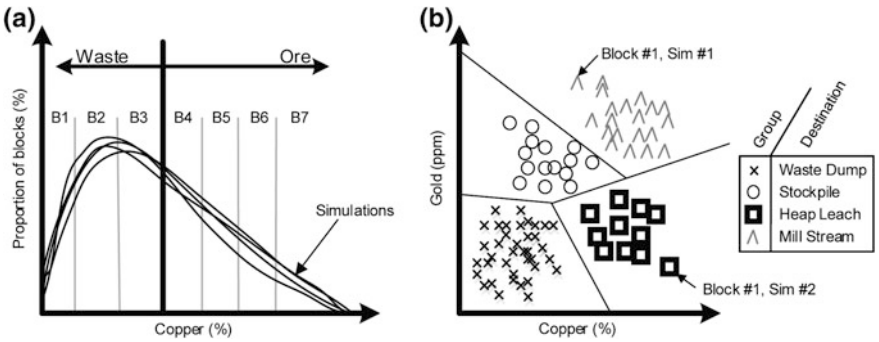

Fig. 1 **a** Robust cut-off grades based on "bins". **b** Extension to create destination policies based on multivariate distributions of primary attributes (e.g. copper and gold grades). Note that a block's destination may change between simulations according to its simulated attributes

k-means++ clustering algorithm (Lloyd 1982; Arthur and Vassilvitskii 2007), whereby the number of groups per material type are defined by the modeller, and the clustering is performed based on the block's primary attributes, $\beta^{p}_{b,s}$. In this pre-processing step, a parameter, $\theta_{b,g,s}$ is generated to define whether (1) or not (0) block b belongs to the group g in scenario s. Given that these destination policies are defined based on (possibly) multivariate distributions, they are more adept for mining complexes with multiple elements and blending constraints.

3. Processing stream decisions ($y_{i,j,t,s} \in [0, 1]$) define the proportion of a product sent from a location $i \in \mathcal{S} \cup \mathcal{D}$ to a destination $j \in \mathcal{O}(i)$. It is noted that, unlike the previous two decision variables, these variables are scenario-dependent decisions, which may, for example, be used to define the quantity of material processed from a stockpile, if there happens to be a shortfall in the quantity of ore material sent directly from the mines.

Two-Stage Stochastic Optimisation Model

A two-stage SIP model (Birge and Louveaux 2011) is used to generate a LOM production schedule, destination policies and the use of the available processing streams. A generalised optimisation model is presented, which may be tailored to accurately model the objectives and constraints that are unique to each operation. Similar to the SIP defined by Ramazan and Dimitrakopoulos (2013), the primary objective is to maximise the net present value, while simultaneously accounting for deviations from production or targets.

Inputs and parameters:

a. Block attributes, $\beta_{p,b,s}$.

b. Block extraction precedence constraints, $\mathbb{O}(b)$, e.g. Khalokakaie et al. (2000).
c. Block sub-group memberships, $\theta_{b,g,s}$.
d. A model of the mining complex, i.e. $\mathcal{O}(i)$ and $\mathcal{I}(i) \forall i \in \mathcal{S} \cup \mathcal{D} \cup \mathbb{G}$.
e. A model of the hereditary attribute transformation functions, $f_h(p, i)$.
f. Time-discounted price (or cost) per unit of attribute, $p_{i,t}^h$. Often, this is only a discount rate, and is used to calculate the net present value.
g. Upper- and lower-bounds for an attribute, $U_{i,t}^h$ and $L_{i,t}^h$, respectively. Often, these will be required for tonnage, metal production and product quality constraints, but may used to identify any potential bottleneck in the mineral value chain.
h. Penalty costs, $c_{i,t}^{h,+}$ and $c_{i,t}^{h,-}$, which are used to penalise deviations from the upper- and lower-bounds. These penalty costs may be time-varied to provide geological risk discounting, i.e. $c_{i,t}^{h,+} = c_i^{h,+} / \left(1 + grd_i^h\right)^t$, where $c_i^{h,+}$ is a base penalty cost and grd_i^h is the geological risk discount rate for the attribute of interest (h). For further discussion of this parameter, see Benndorf and Dimitrakopoulos (2013).

Objective function:

$$\max \frac{1}{|\mathbb{S}|} \underbrace{\sum_{s \in \mathbb{S}} \sum_{t \in \mathbb{T}} \sum_{h \in \mathbb{H}} p_{i,t}^h \cdot v_{i,t,s}^h}_{\text{Discounted costs and revenues}} - \frac{1}{|\mathbb{S}|} \underbrace{\sum_{s \in \mathbb{S}} \sum_{t \in \mathbb{T}} \sum_{h \in \mathbb{H}} \left(c_{i,t}^{h,+} \cdot d_{i,t,s}^{h,+} + c_{i,t}^{h,-} \cdot d_{i,t,s}^{h,-} \right)}_{\text{Penalties for deviations from targets}}$$

Subject to:

I. Mine reserve and slope constraints—enforce slope stability and one-time extraction of blocks.

$$\sum_{t \in \mathbb{T}} x_{b,t} \leq 1 \quad \forall b \in \mathbb{B}_{\mathrm{m}}, \mathrm{m} \in \mathcal{M}$$

$$x_{b,t} \leq \sum_{t'=1}^{t} x_{u,t'} \quad \forall b \in \mathbb{B}_{\mathrm{m}}, \mathrm{m} \in \mathcal{M}, \mathrm{u} \in \mathbb{O}(\mathrm{b}), \mathrm{t} \in \mathbb{T}$$

II. Destination policy constraints—ensure a sub-group of material is only sent to a single destination.

$$\sum_{j \in \mathcal{O}(\mathrm{g})} z_{g,j,t} = 1 \quad \forall g \in \mathbb{G}, \ \mathrm{t} \in \mathbb{T}$$

III. Processing stream constraints—calculate the quantity of primary attributes at each location and ensure mass-balancing.

$$v^p_{j,(t+1),s} = \underbrace{v^p_{j,t,s} \cdot \left(1 - \sum_{k \in \mathcal{O}(j)} y_{j,k,t,s}\right)}_{\text{Material from previous period}} + \underbrace{\sum_{i \in \mathcal{I}(j) \setminus \mathbb{G}} r^p_{i,t,s} \cdot v^p_{i,t,s} \cdot y_{i,j,t,s}}_{\text{Incoming materials from other locations}}$$
$$+ \underbrace{\sum_{g \in \mathcal{I}(j) \cup \mathbb{G}} \left(\sum_{b \in \mathbb{B}_m} \sum_{m \in \mathcal{M}} \theta_{b,g,s} \cdot \beta^p_{b,s} \cdot x_{b,t} \right) \cdot z_{g,j,t}}_{\text{Materials sent directly from mines}} \quad \forall p \in \mathbb{P}, j \in \mathcal{S} \cup \mathcal{D},\ t \in \mathbb{T},\ s \in \mathbb{S}$$

$$\sum_{j \in \mathcal{O}(i)} y_{i,j,t,s} = 1 \quad \forall i \in \mathcal{D}, t \in \mathbb{T}, s \in \mathbb{S}$$

$$\sum_{j \in \mathcal{O}(i)} y_{i,j,t,s} \leq 1 \quad \forall i \in \mathcal{S}, t \in \mathbb{T}, s \in \mathbb{S}$$

IV. Attribute calculations—used to calculate the values of the hereditary attributes based on the values of the primary attributes.

$$v^p_{m,t,s} = \sum_{b \in \mathbb{B}_m} \beta^p_{b,s} \cdot x_{b,t} \quad \forall m \in \mathcal{M},\ p \in \mathbb{P}, t \in \mathbb{T}, s \in \mathbb{S}$$

$$v^h_{i,t,s} = f_h(p, i) \quad \forall h \in \mathbb{H}, i \in \mathcal{S} \cup \mathcal{D} \cup \mathcal{M},\ t \in \mathbb{T},\ s \in \mathbb{S}$$

V. Deviation constraints—calculates the amount of constraint violation from upper- and lower-bounds imposed on hereditary attributes.

$$v^h_{i,t,s} - d^{h,+}_{i,t,s} \leq U^h_{i,t} \quad \forall h \in \mathbb{H},\ t \in \mathbb{T},\ s \in \mathbb{S}$$

$$v^h_{i,t,s} + d^{h,-}_{i,t,s} \geq L^h_{i,t} \quad \forall h \in \mathbb{H},\ t \in \mathbb{T},\ s \in \mathbb{S}$$

VI. Recovery calculations.

$$r^{p}_{i,t,s} = 1 \quad \forall p \in \mathbb{P}, i \in \mathcal{S}, t \in \mathbb{T}, s \in \mathbb{S}$$

$$r^{p}_{i,t,s} = v^{p}_{i,t,s} \quad \forall p \in \mathbb{P}, i \in \mathcal{D},\ t \in \mathbb{T},\ s \in \mathbb{S}$$

VII. End-of-year stockpile quantity calculations (optional).

$$v^{h}_{i,t,s} = v^{h}_{i,t,s} \cdot \left(1 - \sum_{i \in \mathcal{O}(i)} y_{i,j,t,s}\right) \quad \forall h \in \mathbb{H}, i \in \mathcal{S}, t \in \mathbb{T}, s \in \mathbb{S}$$

VIII. Variable definitions.

$$x_{b,t} \in \{0,1\} \quad \forall b \in \mathbb{B}_m, m \in \mathcal{M}, t \in \mathbb{T}$$

$$z_{g,j,t} \in \{0,1\} \quad \forall g \in \mathbb{G},\ j \in \mathcal{O}(g), t \in \mathbb{T}$$

$$y_{i,j,t,s} \in [0,1] \quad \forall i \in \mathcal{S} \cup \mathcal{D}, j \in \mathcal{O}(i), t \in \mathbb{T},\ s \in \mathbb{S}$$

$$v^{p}_{i,t,s} \geq 0 \quad \forall p \in \mathbb{P}, i \in \mathcal{S} \cup \mathcal{D} \cup \mathcal{M},\ t \in \mathbb{T}, s \in \mathbb{S}$$

$$v^{h}_{i,t,s} \in \mathbb{R} \quad \forall h \in \mathbb{H}, i \in \mathcal{S} \cup \mathcal{D} \cup \mathcal{M},\ t \in \mathbb{T}, s \in \mathbb{S}$$

$$r^{p}_{i,t,s} \in [0,1] \quad \forall p \in \mathbb{P},\ i \in \mathcal{S} \cup \mathcal{D}, t \in \mathbb{T}, s \in \mathbb{S}$$

$$d^{h,+}_{i,t,s}, d^{h,-}_{i,t,s} \geq 0 \quad \forall h \in \mathbb{H}, i \in \mathcal{S} \cup \mathcal{D} \cup \mathcal{M}, t \in \mathbb{T}, s \in \mathbb{S}$$

Given the possibility to use stockpiles and incorporate transformation functions (e.g. grade-recovery curves), traditional mathematical optimisers are generable unable to optimise over these non-linear aspects, particularly for large-scale and real-world examples. As a result, a solver has been developed that uses a combination of metaheuristic algorithms to obtain solutions. Metaheuristics are algorithmic optimisers that do not necessarily provide a mathematically optimal solution, but are highlight adaptable for various types of problems, including non-linear optimisation models, and have been successfully used in the past for mine design and production scheduling models (Godoy 2002; Lamghari and Dimitrakopoulos 2012; Goodfellow and Dimitrakopoulos 2013; Lamghari et al. 2015). The proposed approach combines two metaheuristics, simulated annealing (Kirkpatrick et al. 1983; Geman and Geman 1984) and particle swarm optimisation (Kennedy and Eberhart 1995). The simulated annealing algorithm is used to optimise the multi-mine production scheduling and destination policy decision variables. The particle swarm optimisation algorithm is used to optimise the destination

policy and processing stream decision variables. The two algorithms are used alternatingly in order to improve the current solution and, ideally, converge on a globally optimal solution.

Application 1—Blending Policy Optimisation for a Nickel Laterite Mineral Value Chain

The first application that is discussed is for a nickel laterite mining complex. Figure 2 provides an overview of the material flow through the value chain. The purpose of this example is to highlight the importance of integrating geological uncertainty into destination policy optimisation. The optimiser seeks to generate an optimal definition of a multi-element destination policy (based on nickel, iron, silica and magnesia grades, and a dry tonnage density factor), and the use of the stockpiles and homogenization piles. It is noted that production scheduling is not performed; the production schedule used is based off an existing plan. Using the generalised modelling methodology, it is possible to model the flow of the materials from the two mines to the processing plant. Rather than presenting the entire mathematical model, the general goals for the optimiser are listed in order of importance, as follows:

1. Maximise NPV.
2. Satisfy the plant feed's silica-to-magnesia ratio (SiO_2:MgO), which should lie between 1.5 and 1.8.
3. Meet plant production target, which is withheld for confidentiality.
4. Satisfy plant feed iron grade blending constraints, which should lie between 12 and 16%.
5. Satisfy end-of-year stockpile capacity constraints, which are withheld for confidentiality.

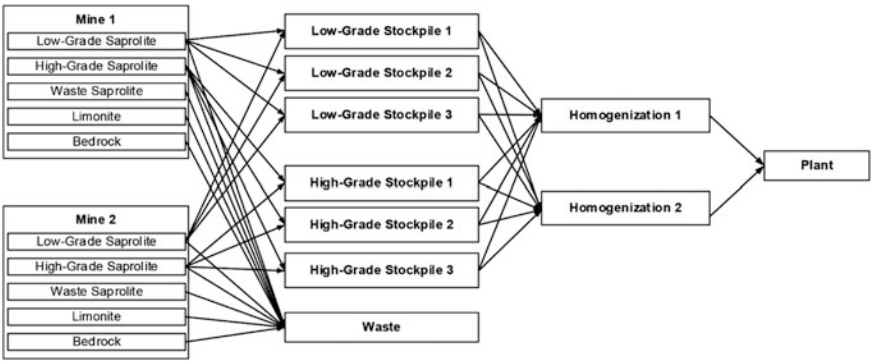

Fig. 2 Material flow diagram for the nickel laterite value chain

Estimated orebody models are provided by the mine and are generated using ordinary kriging. Twenty geological simulations have been generated using the direct block min/max autocorrelation factor simulation method (Boucher and Dimitrakopoulos 2009), which results in 400 scenarios in total. First, the limonite and saprolite layer thicknesses are jointly simulated. The primary attributes (nickel, silica, magnesia, iron and dry tonnage factor) are simulated for the within the saprolite layer for each of the lithological simulations.

Using the estimated orebody model, a deterministic optimisation is performed using the proposed methods. Figure 3 (left) shows a summary of the SiO_2:MgO, tonnage and iron grades for the material received at the processing plant from the homogenization piles. Generally, the optimiser is able to satisfy the key quality constraints on the SiO_2:MgO and the iron grade, and is able to fill the processing plant up to capacity over time. Using the set of orebody simulations, it is possible to perform a sensitivity analysis of the destination policies generated by freezing these decision variables, $z_{g,j,t}$, which were generated using the deterministic-equivalent optimiser, and re-optimising the processing stream (stockpile and homogenization

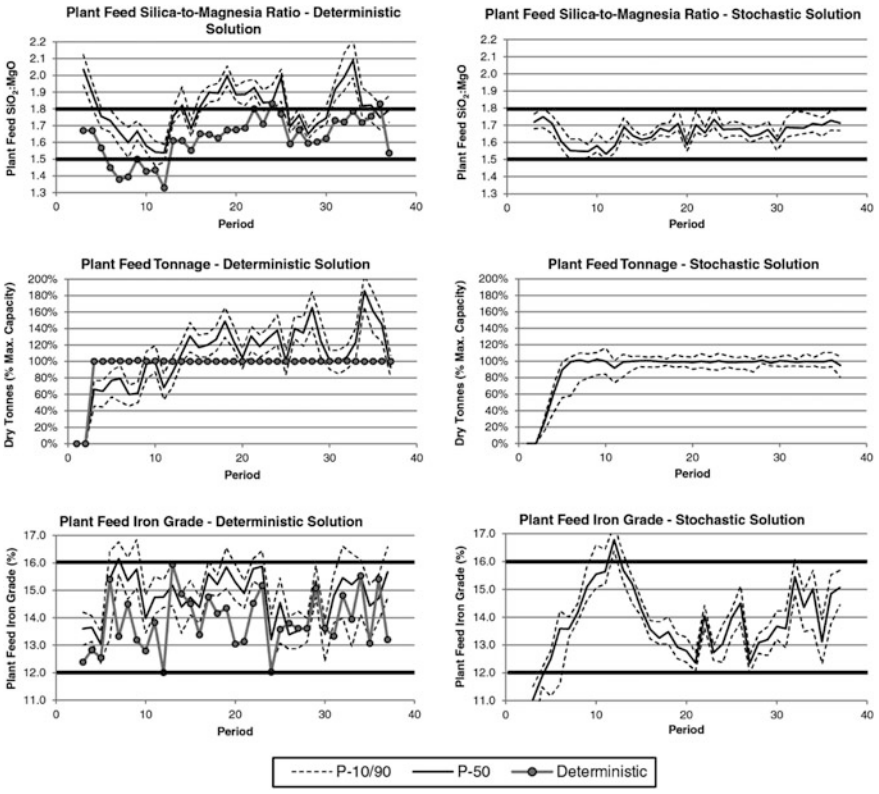

Fig. 3 Comparison of deterministic and stochastic risk profiles for the chemistry and tonnage at the processing plant

pile) decision variables for each of the scenarios. The results are summarised on the same figure using a risk profile, which indicates the P-10, P-50 and P-90 exceedance probabilities (i.e. the value for which 10, 50 or 90% of the simulations lie below). While the destination policies generated for the estimated orebody models are able to satisfy the blending and production constraints, the risk analysis indicates that these policies are not adequate when considering the spatial variability and uncertainty in the saprolite layers, along with the variability of the primary attributes of interest. As a result, this destination policy does not provide a feed to the processing plant that satisfies the blended quality constraints, and generally misclassifies ore and waste materials, which causes the plant feed tonnages to be under or over the target tonnage. This is simply a result of the difference between the distributions of the estimated and simulated orebody models, where a simulated model is better able to capture the variability in the univariate distributions and the spatial auto- and cross-correlations. It is noted, however, that this result does not relate to the performance of the optimiser or the quality of the solution generated. The risk profiles highlight the need to adopt stochastic approaches when optimising mining complexes, particularly for operations that have multiple elements and a large amount of variability, both in terms of materials and metal content.

A stochastic optimiser works with all geological simulations simultaneously, and attempts to find a single destination policy, and the scenario-dependent processing stream (stockpile) decision variables. Figure 3 (right) shows a summary of the risk profiles for a stochastic design. It is noted that, unlike the risk profiles from the deterministic design, the stochastic design is able to satisfy the key constraints of interest, namely, the SiO_2:MgO ratio, iron grade and plant feed tonnage. It is interesting to note that in the first ten periods, there is more variability in tonnage than in the later periods; this is largely attributed to two factors: (i) prioritizing a consistent SiO_2:MgO ratio over tonnages; and (ii) developing the quantities of materials in the stockpiles, which act as a buffer between the highly variable in situ saprolite material and the material sent to the processing plant. Not only is the stochastic destination policy able to satisfy critical blending constraints, thus is much more practical and realistic, the NPV (not shown for confidentiality purposes) is 3% higher than the deterministic-equivalent depicts with the estimated orebody model.

Application 2—Global Optimisation for a Copper-Gold Mining Complex

The second application is related to the stochastic global optimisation of a copper-gold open pit mining complex, which considers simultaneous production scheduling, destination policies and processing stream decisions. Figure 4 provides an overview of the material flows through the mining complex. The key destinations of interest are the sulphide mill, which has a capacity of 3 Mtpa, and the

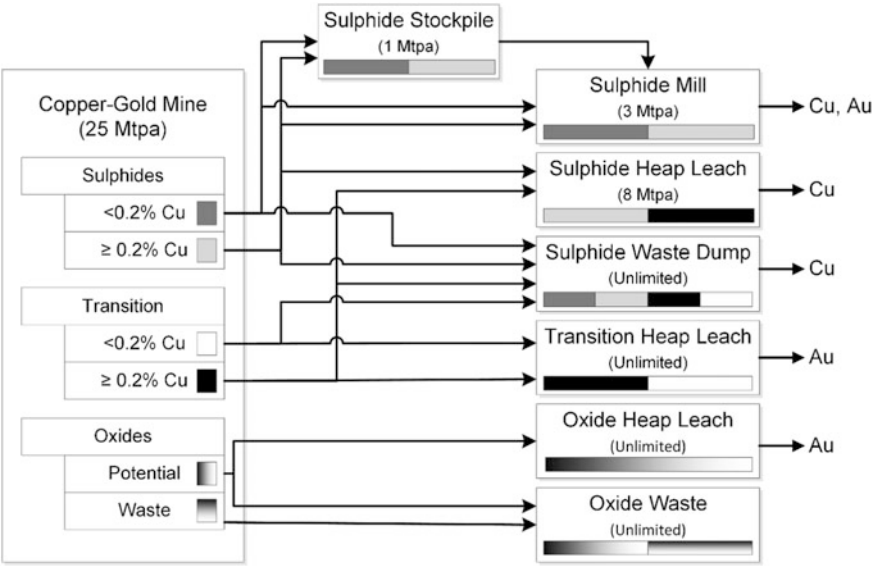

Fig. 4 Material flow through the copper-gold mining complex

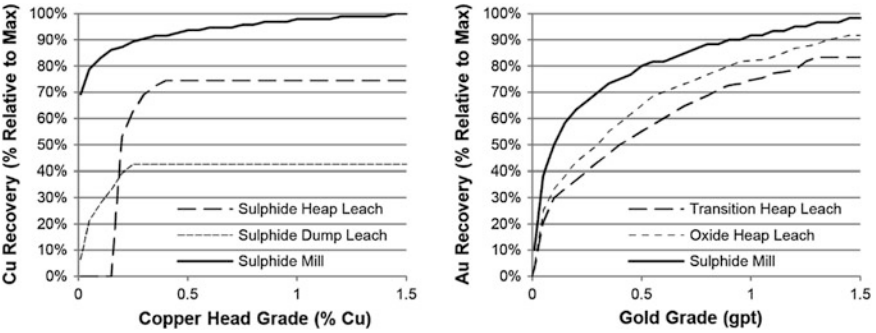

Fig. 5 Non-linear grade-recovery curves for copper (left) and gold (right), based on the head grade from the mine

sulphide heap leach, which has a capacity of 8 Mtpa. A stockpile may be used to store additional sulphide material that is sent to the mill. All other locations are considered to have an unlimited capacity. An interesting aspect of this study is the use of non-linear grade-recovery curves (Fig. 5) for the copper and gold head grades at the respective processing stream. Rather than specifying the recovery for each block in each simulation, which assumes that each block is processed independently, this approach considers the blended feed of all materials received from the mine. The primary objectives of the optimisation are defined as follows, in order of importance:

1. Maximise NPV.
2. Meet sulphide mill production target (3 Mtpa) and minimise associated risk.
3. Meet sulphide heap leach production target (8 Mtpa) and minimise associated risk.
4. Obey mine production capacity constraint (25 Mtpa).
5. Obey end-of-year stockpile capacity constraints (1 Mtpa).

A set of 35 geological simulations and an E-type model (deterministic) have been generated in order to compare the deterministic and stochastic designs. First, a conventional design is generated using a commercial mine planning suite to generate an initial design. A "deterministic-equivalent" design, generated using the proposed method, is then used to demonstrate the advantages of using the global

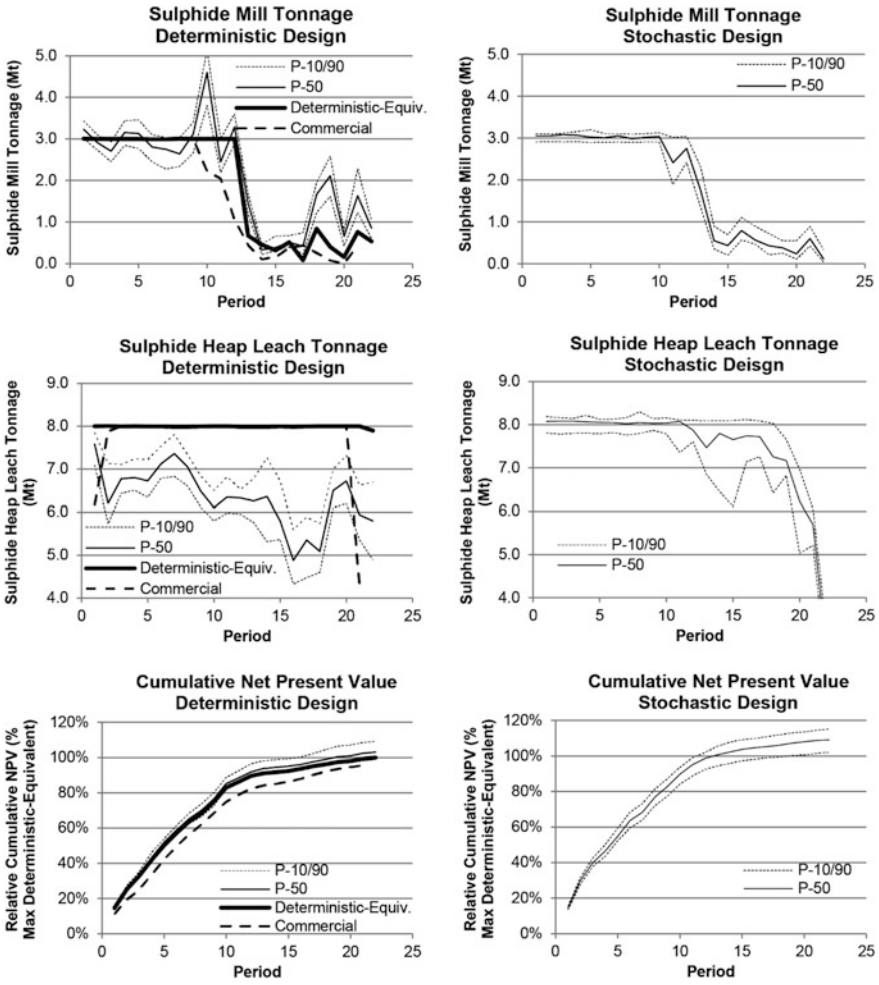

Fig. 6 Comparison of risk profiles deterministic designs and stochastic design for the copper-gold mining complex

optimisation approach. Figure 6 (left) shows a comparison of the commercial, deterministic-equivalent and the risk analysis for the deterministic-equivalent design for the sulphide mill and sulphide heap leach tonnages and the cumulative NPV. First, it is noted that the deterministic-equivalent design has an additional year of mining, and is better able to meet the sulphide mill and heap leach production targets. As a result, the deterministic-equivalent has a 4.5% higher NPV than the design generated using commercial software, which is mostly a result of an increase in tonnes sent to the sulphide mill and sulphide heap leach. However, when testing the deterministic-equivalent design with a set of geological simulations, the risk profiles indicate a substantial amount of risk related to meeting production targets at both destinations. Despite this risk, the risk profiles for this design indicate a 3% higher NPV than the deterministic model indicates, which is caused by a slightly inflated given the excess amount of sulphide material in period 11 and the difference in grade-tonnage distributions between the simulated and E-type orebody models.

The stochastic optimiser generates a single LOM production schedule, destination policy and optimises the use of the stockpile using all simulations. Figure 6 (right) shows the risk profiles of this stochastic design using the 35 simulations. Unlike the risk profiles from the deterministic design, it is apparent that the stochastic design is better able to meet the production targets at the sulphide mill and sulphide heap leach, and simultaneously reduce the risk in terms of the quantities sent. As a result of being able to control ore production, particularly for materials sent to the sulphide heap leach, the NPV of the stochastic design is 6.1% higher than the risk profiles indicate from the deterministic-equivalent design (measured from the P-50 values).

Conclusions

This paper discusses developments in the stochastic optimisation of mineral value chains, with two applications. First, a generalised modelling methodology is discussed, which may be adopted and modified in order to create an accurate and highly detailed model of a mining complex, including non-linear aspects such as stockpiling, blending and non-linear processing transformations. Similarly, a generalised optimisation model is provided, which can be tailored to suit the objectives, priorities and constraints that are unique to each operation. In this implementation, these models are optimised using a combination of two metaheuristics: simulated annealing and particle swarm optimisation.

Two applications are discussed. The first application is related to the definition of a destination policy for a nickel laterite complex that has multiple stockpiles and blending constraints. The results highlight the fact that ignoring the geological uncertainty related to material and grades can lead to a sub-optimal policy that may lead to severe deviations from product quality requirements. A stochastic approach is better able to manage this risk, and is able to generate a blending policy that

satisfies stringent constraints. The second application for a copper-gold mining complex integrates LOM production scheduling with destination policies and stockpile management. In this example, the deterministic-equivalent of the proposed global optimiser is able to generate a design that is 4% higher than a commercial design. When comparing the risk profiles between the deterministic design and a stochastic design, the stochastic approach is better able to meet production targets and manage the associated risk, while simultaneously generating a 6.1% higher NPV than the deterministic design. Future work will seek to test the methods developed herein on mineral value chains with more complex down-stream (post-extraction) aspects.

Acknowledgements This work is funded from the National Science and Engineering Research Council of Canada, Collaborative R&D Grant CRDPJ 411270-10 with AngloGold Ashanti, Barrick Gold, BHP Billiton, De Beers, Newmont Mining and Vale.

References

Albor Consuegra FR, Dimitrakopoulos R (2010) Algorithmic approach to pushback design based on stochastic programming: method, application and comparisons. Min Technol 119(2):88–101

Arthur D, Vassilvitskii S (2007) K-means++: the advantages of careful seeding. In: Proceedings of the eighteenth annual ACM-SIAM symposium on discrete algorithms, Society for Industrial and Applied Mathematics, Philadelphia, pp 1027–1035

Audet C, Brimberg J, Hansen P, Le Digabel S, Mladenović N (2004) Pooling problem: alternate formulations and solution methods. Manage Sci 50(6):761–776

Benndorf J, Dimitrakopoulos R (2013) Stochastic long-term production scheduling of iron ore deposits: integrating joint multi-element geological uncertainty. J Min Sci 49(1):68–81

Birge JR, Louveaux F (2011) Introduction to stochastic programming, 2nd edn. Springer, New York, p 485

Bley A, Gleixner AM, Koch T, Vigerske S (2012) Comparing MIQCP solvers to a specialized algorithm for mine production scheduling. In: Bock HG, Hoang XP, Rannacher R, Schlöder JP (eds) Modeling, simulation and optimization of complex processes. Springer, Berlin, pp 25–39

Boland N, Dumitrescu I, Froyland G (2008) A multistage stochastic programming approach to open pit mine production scheduling with uncertain geology, Optim Online. Available from: http://www.optimization-online.org/DB_FILE/2008/10/2123.pdf (26 Aug 2014)

Boucher A, Dimitrakopoulos R (2009) Block simulation of multiple correlated variables. Math Geosci 41(2):215–237

Caccetta L, Hill SP (2003) An application of branch and cut to open pit mine scheduling. J Global Optim 27(2–3):349–365

Dagdelen K (1985) Optimum multi period open pit mine production scheduling, Ph.D. thesis (unpublished), Colorado School of Mines, Colorado

Dimitrakopoulos R, Jewbali A (2013) Joint stochastic optimisation of short and long term mine production planning: method and application in a large operating gold mine. Min Technol 122 (2):110–123

Dimitrakopoulos R, Farrelly CT, Godoy M (2002) Moving forward from traditional optimization: grade uncertainty and risk effects in open-pit design. Min Technol 111(1):82–88

Geman S, Geman D (1984) Stochastic relaxation Gibbs distributions, and the Bayesian restoration of images. IEEE Trans Pattern Anal Mach Intell 6(6):721–741 (IEEE Computer Society, Washington)
Godoy M (2002) The effective management of geological risk in long-term production scheduling of open pit mines, PhD thesis (unpublished), University of Queensland, Brisbane
Goodfellow R, Dimitrakopoulos R (2013) Algorithmic integration of geological uncertainty in pushback designs for complex multiprocess open pit mines. Min Technol 122(2):67–77
Hoerger S, Hoffmann L, Seymour F (1999) Mine planning at Newmont's Nevada operations. Min Eng 51(10):26–30
Johnson T (1968) Optimum open pit mine production scheduling, Ph.D. thesis (unpublished), University of California, Berkley
Kennedy J, Eberhart R (1995) Particle swarm optimization. IEEE Int Conf Neural Networks 4:1942–1948
Khalokakaie R, Dowd PA, Fowell RJ (2000) Lerchs-Grossmann algorithm with variable slope angles. Min Technol 109(2):77–85
Kirkpatrick S, Gelatt CD, Vecchi MP (1983) Optimization by simulated annealing. Science 220 (4598):671–680
Lamghari A, Dimitrakopoulos R (2012) A diversified Tabu search approach for the open-pit mine production scheduling problem with metal uncertainty. Eur J Oper Res 222(3):642–652
Lamghari A, Dimirakopoulos R, Ferland JA (2015) A hybrid method based on linear programming and variable neighborhood descent for scheduling production in open-pit mines. J Global Optim 63(3):555–582
Leite A, Dimitrakopoulos R (2014) Mine scheduling with stochastic programming in a copper deposit: application and value of the stochastic solution. Min Sci Technol 24(6):755–762
Lerchs H, Grossmann IF (1965) Optimum design of open-pit mines. CIM Bull 58:47–54
Lloyd S (1982) Least squares quantization in PCM. IEEE Trans Inf Theory 28(2):129–137 (IEEE Press, Piscataway)
Meagher C, Abdel Sabour SA, Dimitrakopoulos R (2010) Pushback design of open pit mines under geological and market uncertainties. In: Dimitrakopoulos R (ed) Advances in orebody modelling and strategic mine planning I: old and new dimensions in a changing world. The Australasian Institute of Mining and Metallurgy, Melbourne, pp 297–304
Menabde M, Froyland G, Stone P, Yeates G (2017) Mining schedule optimization for conditionally simulated orebodies, in this volume
Montiel L, Dimitrakopoulos R (2013) Stochastic mine production scheduling with multiple processes: application at Escondida Norte Chile. J Min Sci 49(4):583–597
Montiel L, Dimitrakopoulos R, Kawahata K (2017) Simultaneously optimizing open pit and underground mining operations under geological uncertainty, in this volume
Picard J-C (1976) Maximumal closure of a graph and applications to combinatorial problems. Manage Sci 22(11):1268–1272
Ramazan S, Dimitrakopoulos R (2013) Production scheduling with uncertain supply: a new solution to the open pit mining problem. Optim Eng 14(2):361–380
Stone P, Froyland G, Menabde M, Law B, Pasyar R, Monkhouse, PHL (2017) Blasor—blended iron ore mine planning optimisation at Yandi, Western Australia, in this volume
Tolwinski B, Underwood R (1996) A scheduling algorithm for open pit mines. IMA J Math Appl Bus Ind 7:247–270
Urbaez E, Dagdelen K (1999) Implementation of linear programming model for optimum open pit production scheduling problem. Trans Soc Min Metall Explor 297:1968–1974
Whittle G (2007) Global asset optimization. In: Dimitrakopoulos R (ed) Orebody modelling and strategic mine planning: uncertainty and risk management models, 2nd edn. The Australasian Institute of Mining and Metallurgy, Melbourne, pp 331–336
Whittle J (2017) The global optimizer works—what next?, in this volume

Sensor Based Real-Time Resource Model Reconciliation for Improved Mine Production Control—A Conceptual Framework

J. Benndorf, M. Buxton and M. S. Shishvan

Abstract The flow of information and consequently the decision making along the chain of mining from exploration to beneficiation typically occurs in a discontinuous fashion over long time spans. In addition, due to the uncertain nature of the knowledge about the deposit and its inherent spatial distribution of material characteristics actual production performance in terms of produced ore grades and quantity and extraction process efficiency often deviate from expectations. Reconciliation exercises to adjust mineral reserve models and planning assumptions are performed with timely lags of weeks, months or even years. With the development of modern Information and Communication Technology over the last decade, literally a flood of data about different aspects of the production process is available in a real-time manner. For example, sensor technology enables online characterisation of geochemical, mineralogical and physical material characteristics on conveyor belts or at working faces. The ability to utilise the value of this additional information and feed it back into reserve block models and planning assumptions opens up new opportunities to continuously control the decisions made in production planning to increase resource recovery and process efficiency. This leads to a change in paradigm from a discontinuous to a near real-time reserve reconciliation and model updating, which calls for suitable modelling and optimisation methodologies to quantify prior knowledge in the reserve model, to process and integrate information from different sensor-sources and accuracy, back propagate the gain in information into reserve models and efficiently optimise operational decisions real-time. This contribution introduces the concept of an integrated closed-loop framework for *Real-Time Reserve management* (RTRM) incorporating

J. Benndorf (✉)
Technische Universität Bergakademie Freiberg, Institute of Mine Surveying and Geodesy, Freiberg, Germany
e-mail: Joerg.Benndorf@mabb.tu-freiberg.de

M. Buxton · M. S. Shishvan
Department of Geosciences and Engineering, Delft University of Technology, Stevinweg 1, 2628CN Delft, The Netherlands

R. Dimitrakopoulos (ed.), *Advances in Applied Strategic Mine Planning*,
https://doi.org/10.1007/978-3-319-69320-0_42

sensor based material characterisation, geostatistical modelling under uncertainty, modern data assimilation methods for a sequential model updating and mining system simulation and optimisation. The effectiveness of the framework and the value added will be demonstrated in an illustrative case study.

Introduction

Successful planning and operations management in mineral resource extraction is based on a solid understanding of the spatial distribution of ore tonnages and grades in the deposit. The knowledge about the deposit is often based on exploration data and typically captured in a digital 3D resource model. Exploration data are gathered in campaigns prior to operation, often undertaken decades ago. The sample spacing is designed to capture major features of the deposit with the anticipated level of accuracy while minimising expenditure. Although resource models are created using sophisticated geostatistical modelling techniques, such as different types of Kriging or conditional simulation (e.g. Chiles and Delfiner 2012), they can locally exhibit significant deviations from in situ resource characteristics.

Short-term production scheduling in mining operations is based on the resource model and aims to define an extraction sequence that meets short-term production targets in terms of ore tonnage produced and associated grades. The scale of short-term production targets can be as small as a train load in the order of 1000t that is shipped to the customer; such a scale is not supported by data, gathered during exploration. The consequences can be unexpected deviations from production targets which may have significant economic impacts. Therefore the understanding of short scale variability of ore characteristics is critical to control the operation and to meet production targets.

As demonstrated in various case studies (e.g. Benndorf 2009; Zimmer 2012; Benndorf 2013), short scale variability and uncertainty in prediction can be modelled by conditional simulation and propagated through a transfer function to assess the expected performance of a short-term mine plan. Although this methodology allows the recognition of the magnitude and frequency of potential deviations, it does not lead to an increase in knowledge, since no additional data are included in the decision making process.

With the recent developments in Information- and Communication technology (ICT) over the past decade, online data capturing of production performance provides an alternative source of information. Literally a flood of data is available. Sensor technology for detecting the characteristics of raw materials on a conveyor belt has been proven in industrial field tests in some operations. Documented studies refer to the application of specific sensor technologies such as Near Infra Red (e.g. Goetz et al. 2009) or Dual Energy X-Ray Transmission (Jong et al. 2003). The application of sensors provides a high density of information on a short time

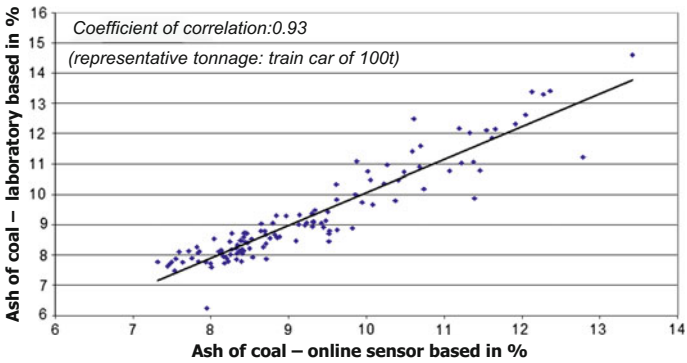

Fig. 1 Correlation between sensor-based measurements and lab analysis in coal samples

scale with a reasonable precision. The example in Fig. 1 compares lab analyses and sensor based measurements for coal ash content of train-car loads of approximately 100t. The correlation coefficient of 0.93 suggests high information content of the sensor data.

To date sensor information are mainly utilised in feed forward loops applied for downstream process control, such as supporting dispatch decisions, material sorting or blending on stockpiles (e.g. Scholze and Köhler 2012; Sládková et al. 2011). An immediate feedback of sensor information into the resource and planning assumptions to continuously increase its certainty in prediction does not occur. However, the ability to feed data back suggests a significant potential for improvement an operational efficiency. With increased certainty of prediction of grades for reserve blocks the frequency of misclassification and unfavourable dispatch decisions is expected to decrease. Buxton and Benndorf (2013) quantified this value in the order of $5 Mio. per annum for an average sized operation. A breakthrough towards a "self-learning mine" utilising all available data for real-time feedback control and process optimisation requires fast integration and processing of data, a back-propagation of process information into the models and a real-time decision support. A similar framework was recently developed in petroleum reservoir management (Jansen et al. 2009) and demonstrated increased process efficiency in the order of 6–9%.

This contribution introduces a new and innovative framework for real-time reconciliation and optimisation for extractable reserves in continuous mining operations. It consists of a closed-loop approach (Fig. 2), which feeds back sensor-data into resource models and optimises operational decisions to account for the gained information during production in real-time. First the concept is described and the recent developments in the major pillars of the framework are documented. Later selected aspects of the framework are demonstrated in an illustrative case study.

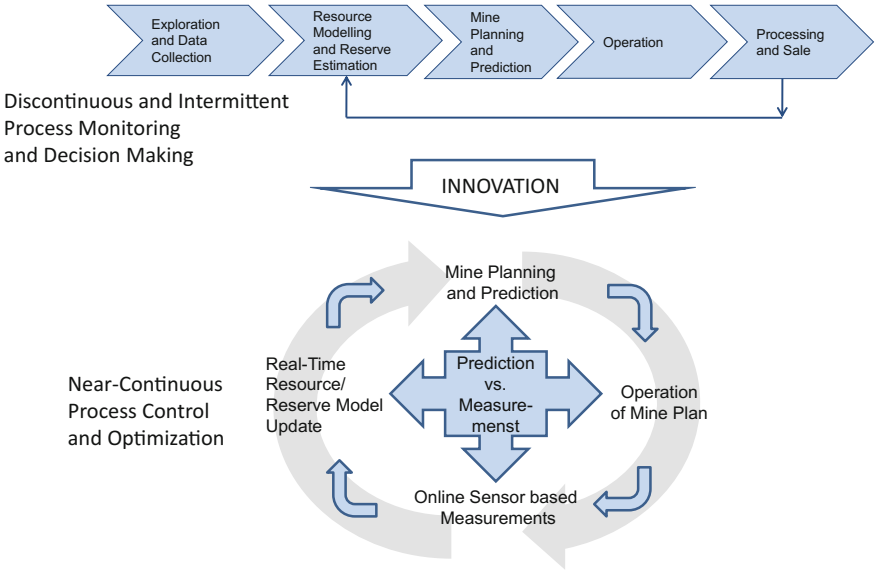

Fig. 2 Closed-loop concept for near-continuous process control and optimisation

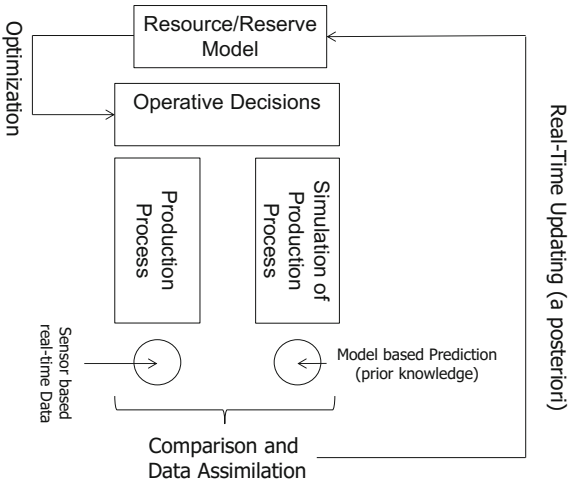

Fig. 3 Flow chart of real-time reserve management (RTRM)

Moving Towards Real-Time Reserve Management (RTRM) —The Closed Loop Concept

Figure 3 illustrates the closed-loop-concept for Real-Time Reserve Management (RTRM), which is defined by following steps.

(1) Based on available exploration data a resource model is generated and reserves are assessed as the basis for short-term mine planning and production control. This model is referred to as *prior* model. In general, techniques can involve geostatistical estimation as well as simulation.
(2) Short-term mine planning and operational decisions are optimised to ensure that production targets are achieved most efficiently. These optimisation tasks may be performed using mathematical optimisation techniques such as Mixed Integer Programming or Stochastic Programming, meta-heuristic methods or techniques of simulation based optimisation for more complex systems.
(3) Based on these optimised decisions and utilising the resource/reserve model, model based expected process efficiency indicators and material characteristics can be predicted at different locations in the extraction and material handling process.
(4) When executing the mine plan sensor derived measurements about the process efficiency and material quality can be taken generated at these different locations.
(5) Differences between model-based prediction (Step 3) and actual measurements (Step 4) may have two different causes, a resource/reserve model error and a measurement error. Modern techniques of data assimilation are used to separate the influence of these two causes and utilise this information of the difference to update the prior resource/reserve model (Step 1) to obtain a *posterior* model.
(6) Go back to step 2 and optimise short-term and operational decisions based on the updated *posterior* resource/reserve model.

The proposed concept of RTRM is the subject of current research and technical development. Its maturation for industrial application requires further development in three main pillars:

- sensor based material characterisation,
- a real-time feedback loop of sensor data for resource/reserve model updating and
- simulation based optimisation for short-term production scheduling and production control.

The following three subsections provide an overview of recent developments in the areas of the three main pillars and propose algorithmic solutions and areas for future development.

Online Sensor Based Raw Material Characterisation

For real-time updating of the reserve model and mine optimisation, sensor-derived data are required to identify and discriminate raw material properties such as texture, mineralogy, geochemistry and physical properties prior to and during mining. Specific sensor techniques that have the potential to be used to satisfy these

requirements include Laser Induced Breakdown Spectroscopy (LIBS) (e.g. Death et al. 2008), Visible Near Infra-Red (VisNIR), Short Wave Infra-Red (SWIR) imaging for determining textures and mineralogy, X-Ray Fluorescence (XRF) for geochemistry and thermal, Mid Wave Infra Red (MWIR) or Long Wave Infra-Red (LWIR) (e.g. Harris et al. 2010) for assessing silica content. Imaging techniques are required for size, volume and shape determination. These can contribute towards mass and density determination. Infra red (VisNir, SWIR, LWIR), XRF, RAMAN and LIBS methods require no pre-preparation of sample.

Infrared spectral techniques can be used to determine mineralogical parameters for geological material by use of different spectral ranges including VisNir (wavelength range 0.4–0.7 μm) and SWIR (wavelength range 0.7–2.6 μm). The SWIR is an important range for providing mineral identification for hydroxyl, water and carbonate bearing minerals. Commercial applications are available including airborne scanners, real-time assessment of materials on conveyor belts and monitoring of material during scheduling. Technologies such as the CSIRO HyLogger suite have been developed to provide voluminous and automated point data. These systems capture infrared data from drill core or chip samples. In a static mode, hyperspectral imaging systems for logging of drill cores have been developed such as the SisuRock system by Spectral Imaging Ltd. (SPECIM) in Finland. The LWIR (wavelength range 6–14 μm) is one of the most important regions for mineralogy since direct detection and identification of rock forming silicates is possible. Hyperspectral LWIR imaging systems for mineral detection are commercially available for airborne scanners and static imagers. Applications for use in high throughput environments have not yet been developed.

LIBS can be used for the analysis of solid, liquid and gaseous samples. An analysis can be performed in a few tenths of μs simultaneously for all chemical elements whose spectral lines lie in the detected spectral range of the spectrometer. Using modern data acquisition electronics, up to 1000 LIBS measurements per second are possible (Bette et al. 2005).

Mineral characterisation using Raman is well established. However, because Raman spectroscopy is a molecular technique, it is seldom used to characterise whole rocks such as those extracted during mining. With respect to Raman spectroscopy instrumentation, commercially available state-of-the art handheld instrumentation are designed for a specific task, which is in most cases pharmaceutical or homeland security. Although the hardware may be applicable to whole rock samples from mines, the software is not. Issues regarding resolution and optical quality in complex polymineralogical applications are not resolved.

Raman and LIBS can be combined to provide complementary detection solutions. The combination is attractive for remote mineralogical characterisation and has been increasingly studied by NASA and ESA for lunar and Mars exploration (e.g. Sharma et al. 2003; Escudero-Sanz et al. 2008). LIBS shows high sensitivity in detecting cations and trace elements but is less sensitive in detecting anions. Raman can identify the anion groups in the crystals and crystal forms from Raman active lattice modes (Sharma et al. 2007). LIBS/RAMAN combinations also have potential for the mapping of heterogeneous minerals (Hoehse et al. 2009). But

there is a technology gap between the highly portable systems designed for space exploration, which are excessively expensive and highly overspecified for applications in a terrestrial industrial scenario and the current state-of-the-art bulky laboratory systems. A portable combined Raman and LIBS system for high throughput mining applications does not currently exist but is clearly required for practical measurements in an operational environment.

For all sensor types, imaging techniques may be required for size, volume and shape determination. These will contribute towards mass and density determination. Sensor resolution and the ability to discriminate differ for each of the different sensor types. Different sensor types generate different data outputs in terms of response, precision, accuracy and format. One specific sensor cannot satisfy all requirements.

There is no current application that integrates combinations of these sensors for comprehensive material characterisation and discrimination in a highly variable and large throughput environment. Current research and development activities of such technology will enable real-time feed-back loops for reserve updating.

Real-Time Feed Back Loop for Reserve Model Updating

The part of the RTRM is designed as a back-propagation of process information into the resource/reserve model. To account for different data originating from different sources with a different data quality, density and support, the currently used methods in geostatistical modelling and data fusion have to be extended. Different data, e.g. from exploration holes and lab analysis, online responses of sensors, GPS measurements of actually mined raw material or geodetic survey data have to be integrated consistently to update the reserve model in a Bayesian fashion. In addition, the material characterised at sensor locations may represent a blend of material originating from multiple phases and locations of extraction. In order to feed back the sensor information the influence of material originating from each extraction face has to be separated.

To solve these challenges multiple solutions are possible. This contribution proposes a modification of Kalman-Filter techniques. These are designed to sequentially estimate the system states, in this case the local grades at excavation locations, recursively on the basis of noisy measured input data. Kalman (1960) introduced a method in the context of system and control theory describing a recursive solution to estimate the state of a stochastic process Z^{t+1} at time $t + 1$ (Kalman 1960) based on a prior model of the state $\mathbf{Z}^{t}$ at time t and observations l at time t.

To update a spatial resource model, the system state is put in a spatial context and represents the block model estimate $(\boldsymbol{x})$. The observations correspond to sensor measurements during a production period of a certain time span, e.g. 5 min or 1 h.

The idea is to update the resource model, denoted with $\boldsymbol{Z}^{t+1}(\boldsymbol{x})$ as a linear combination of the prior block model $\boldsymbol{Z}^{t}(\boldsymbol{x})$ and the difference between model based prediction and the vector of sensor based measurements $\boldsymbol{l}$ (Eq. 1).

$$\boldsymbol{Z}^{t+1}(\boldsymbol{x}) = \boldsymbol{Z}^{t}(\boldsymbol{x}) + \boldsymbol{K}(\boldsymbol{l} - \boldsymbol{A}\boldsymbol{Z}^{t}(\boldsymbol{x})) \tag{1}$$

Matrix $\boldsymbol{A}$ is a design matrix and captures the contribution of each reserve block per time interval to the raw material flow produced and observed at a sensor station. The term $\boldsymbol{A}\boldsymbol{Z}^{t}(\boldsymbol{x})$ represents the model-based prediction and integrates the operative decisions (digging capacity and location of excavators at each time) in $\boldsymbol{A}$ and the prior resource/reserve model $\boldsymbol{Z}^{t}(\boldsymbol{x})$. The objective is to determine the matrix $\boldsymbol{K}$, which is the unknown updating factor (Kalman-Gain) as a best linear and unbiased estimator. A detailed derivation is out of scope for this paper and the reader is referred to literature (e.g. Welsh and Bishop 1997; Benndorf 2014). It can be shown that

$$\boldsymbol{K} = \left(\boldsymbol{A}^{T}\boldsymbol{C}_{ZZ}^{t}\boldsymbol{A} + \boldsymbol{C}_{ll}\right)^{-1}\boldsymbol{A}^{T}\boldsymbol{C}_{ZZ}^{t} \tag{2}$$

An interpretation of Eq. (2) reveals the integrative character of the Kalman-Gain. The first term is the inverse of two error sources: (a) the model prediction error, represented by the covariance matrix of the prior resource model $\boldsymbol{C}_{ZZ}^{t}$, which is propagated through the mining system by the design matrix and (b) the measurement error, represented by the covariance matrix of the sensor-based measurement $\boldsymbol{C}_{ll}$. The second term represents again the error source of the model-based prediction. A comparison of potential magnitudes of the two error terms reveals that:

- if the model error is large and the measurement error small, the Kalman-gain $\boldsymbol{K}$ tends towards 1. The application to Eq. (1) shows that the full difference between model-based prediction and sensor-based measurement is taken into account to update the resource/reserve model.
- if the model error is small and the measurement error large, the Kalman-gain $\boldsymbol{K}$ tends towards 0. The application to Eq. (1) indicates that the difference between model-based prediction and sensor-based measurement is not taken into account to update the resource/reserve model. The precision of the sensor is too low to add value to estimation of resources and reserves.

It is intuitive that with the integration of sensor-data in the resource/reserve model the prediction uncertainty decreases. This is not only the case for reserve blocks, which are currently excavated but as well for adjacent blocks to be excavated, because these are spatially correlated. It can be shown that the improvement in model prediction can be quantified by

$$\boldsymbol{C}_{ZZ}^{t+1} = \boldsymbol{C}_{ZZ}^{t} - \boldsymbol{K}\boldsymbol{A}\boldsymbol{C}_{ZZ}^{t}. \tag{3}$$

Where C_{ZZ}^{t+1} is the updated posterior model covariance matrix, which is by definition smaller than the prior model covariance matrix C_{ZZ}.

Due to the storage and propagation of the error covariance matrix, Kalman Filter based approaches suffer from computational efficiency especially when applied to large systems. To handle large problems with potential nonlinear dynamics, the Ensemble Kalman Filter (EnKF) offers a solution (Evensen 2003). Instead of propagating the covariance matrix in time using Eq. (3), a finite set of so called ensemble members is generated representing realisations z(**x**) of the spatial random function Z(**x**). Each ensemble member is an equally probable representation of the spatial random field at time t. The initial set of ensemble members can be generated using techniques of conditional simulation in geostatistics (e.g. Chiles and Delfiner 2012). Using Eq. (1) all ensemble members are propagated separately in time when new data **y** are available (Fig. 4).

Instead of storing the complete Covariance matrix C_{ZZ}, only a finite set of ensemble members is kept. If the number of ensemble members is sufficiently large, the Covariance matrix can be approximated by

$$\boldsymbol{C}_{\boldsymbol{ZZ}}^{t+1} \cong \frac{1}{\mathrm{N}} \sum_{\mathrm{i}=1}^{\mathrm{N}} \left(\mathbf{z}(\mathbf{x_i}) - \overline{\mathbf{z}(\mathbf{x})} \right) \cdot \left(\mathbf{z}(\mathbf{x_i}) - \overline{\mathbf{z}(\mathbf{x})} \right)^{\mathrm{T}} \tag{4}$$

Note that in order to maintain the variance and covariance structure of the ensemble members, the observations have to be treated as random variables. For this reason an error $\boldsymbol{\omega_r}$ has to be added to the observations **l** used to update the several ensemble members r with r = 1,…,N.

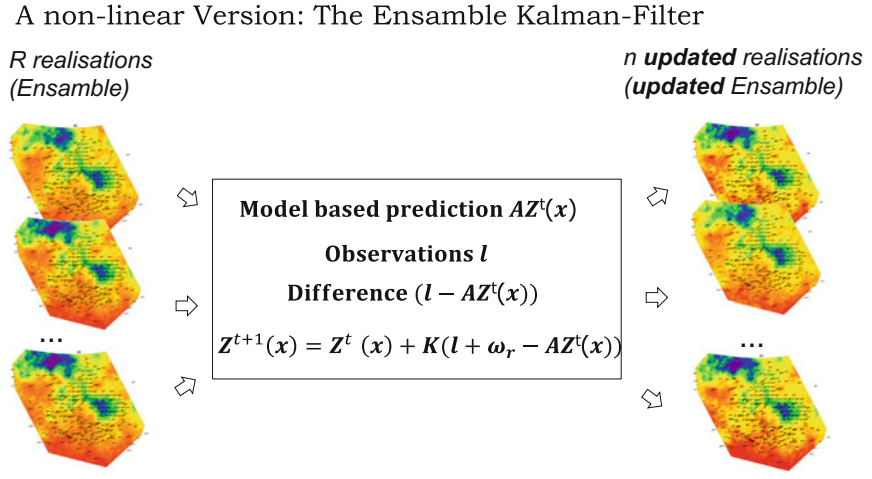

Fig. 4 The concept of the Ensemble-Kalman Filter (reproduced after Evensen 2003)

Simulation Based Optimisation for Short-Term and Operative Decisions

The updated model will lead to possibly new decisions in short-term operation management such as production sequencing, digging capacity control or stock-pile management. Methods of mathematical programming, such as Dynamic Programming or Mixed Integer Programming, are well acknowledged in the field of mine planning optimisation (e.g. Ramazan and Dimitrakopoulos 2004). Recent research was successfully performed to integrate geological uncertainty (e.g. Dimitrakopoulos and Ramazan 2008; Benndorf and Dimitrakopoulos 2013) leading to an increase of 24% in NPV while reducing the risk of not achieving production targets. Jewbali (in Jewbali and Dimitrakopoulos 2011) introduced a short-term production scheduling optimisation based on geological uncertainty and updateable models and demonstrates the benefit in the Australian gold mining industry. The previous mentioned applications are small or moderate in size. Short-term production scheduling in large open pit mines represents a problem, which is typically complex and involves many interdependencies. These are difficult to model in a closed form.

Most of the mathematical programming approaches are limited by the amount of decision variables, as applications become large and suffer from reduced computational efficiency. In leading manufacturing process industries, such as aerospace, chemical industry or petroleum engineering, the simulation approach is applied to support making expensive decisions and optimisation during design and operation of processes (e.g. Young Jung et al. 2004; Schulze-Riegert and Shawket 2007; Subramaniam and Gosavi 2007). Simulation based optimisation methods (Fig. 5), such as Response Surface Methods or Learning Automata Search, have been proven to result in near optimal solutions for decision problems and are especially applicable for scheduling complex and computationally large systems (Goshavi 2003), such as continuous mining operations. The concept of simulation based optimisation is shown in Fig. 5. Using general system simulation techniques the

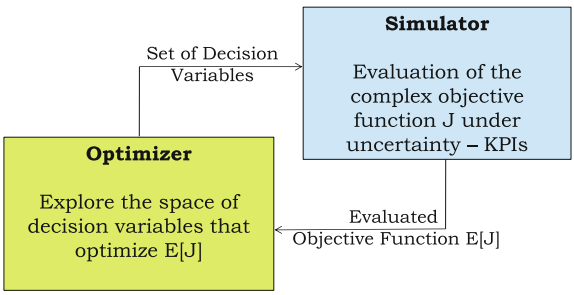

Fig. 5 The concept of simulation based optimisation

objective value *J* of a complex objective function can be evaluated for a given set of decision variables. The optimisation part, such as response surface methods in combination with gradient descent methods will explore the space of decision variables to obtain a near to optimal set of these.

Stochastic process simulation, whether discrete, continuous or combined (Kelton and Law 2000), provides a powerful tool for measuring performance indicators summarised in an objective function of complex systems. In essence the simulator assesses a complex objective function *J*. Hall (2000) presented the requirement for successful simulation modelling, advantages and disadvantages of simulation as well as pitfalls for mining related application in two case studies. The results showed that simulation can be a powerful tool for the mining engineer. When used in proper applications it is able to provide insights into complex system behaviour. (Baafi and Ataeepour 1996) and (Askara-Nasab et al. 2012) used discrete event simulation to investigate a truck-shovel system of discontinuous open pit mines. The process simulation method is used to optimise the truck fleet size for the system. For short-term mine planning (Soleymani Shishvan and Benndorf 2013) presented for the first time a simulation based approach for continuous mining applications integrating geological uncertainty. The objective is to evaluate the performance in terms of producing the target quantity and quality in a large open pit coal operation and assess the efficiency for alternative production schedules. Different sets of decision variables are tested, including a shift schedule, block sequencing and defined production rates. Results demonstrated the stochastic approach provides the mine planning engineer with a valuable tool to foresee critical situations affecting the continuous supply of raw material to the customers and system performance. Comparing the outcome of different sets of decisions provides a tool for improved decision making.

Having available powerful simulation tools for mining systems, the impact of a set of short-term or control decision variables can be evaluated. Simulation based optimisation is based on an iterative perturbation of decision variables and the mapping of the corresponding objective value J. Utilising the Response Surface Method the objective value can be mapped as a function of decision variables, even if not all possible combinations are tested. The efficient exploration of combinations of decision variables can be supported by stochastic gradient descent methods. The maximum of the resulting response surface of the objective values leads to optimal decision variables. Salama et al. (2014) used a combination of discrete event simulation and Mixed Integer Programming (MIP) as a tool to improve decision making in underground mining. The proposed method uses the simulation approach to evaluate the operating costs of a set of different haulage system scenarios and obtained the cash flows for input into the MIP model.

Further work is required to extend current applications to continuous production control variables such as effective digging rates and include the short-term sequencing problem in the optimisation phase.

An Illustrative Example for Model Updating

The subsequent example investigates the performance of the proposed updating methodology for different mining system configurations and sensor precisions. For deeper insights into the continuous mine system simulation for short-term planning and decision control under geological uncertainty, the reader is referred to Soleymani Shishvan and Benndorf (2013). Here an artificial test case is presented, which is built around the well-known and fully understood Walker Lake data set (Isaaks and Srivastava 1989). The data set (Fig. 6) is interpreted as a quality parameter of a coal deposit, e.g. as calorific value. It is sampled irregularly at a spacing corresponding to an average of two reserve block length. The blocks were defined with a dimension of 16 m × 16 m × 10 m. The block—variogram is given with a spherical structure, range 50 m, nugget effect 0.4 and sill 0.6.

With an assumed density of 2t/m^3, one mining block represents a tonnage of 5.120t. Ordinary Kriging was used to generate a resource block model and the prior error covariance matrix, Generalised Sequential Gaussian Simulation was used to derive the realisations or ensemble members for the EnKF application. For simplicity, no dilution and losses were applied resulting in the reserve model being equal to the resource model. The resulting block model (Fig. 6) was used as the prior model.

Without loss of generality the artificial block model will be mined with a continuous mining system, which consists initially of two bucket-wheel excavators positioned at separate benches (Fig. 7). Figure 6 shows the extraction sequence for the case of two excavators. Different digging rates were applied: Excavator one mines at a rate of 500t/h and excavator two at 1.000t/h. The material is discharged on belt-conveyors positioned on the benches, which are combined to one material flow at the central mass distribution point. The belt speed is assumed to be constant at 6 m/s.

The combined material flow of both excavators is scanned by a sensor positioned above a central conveyor feeding the stock- and blending yard. Since no real sensor data are available, virtual sensor data were generated. The artificial sensor data represent a 10 min moving average (corresponding to about 250 t production) and are composed of three components. Component one is the true block grade taken

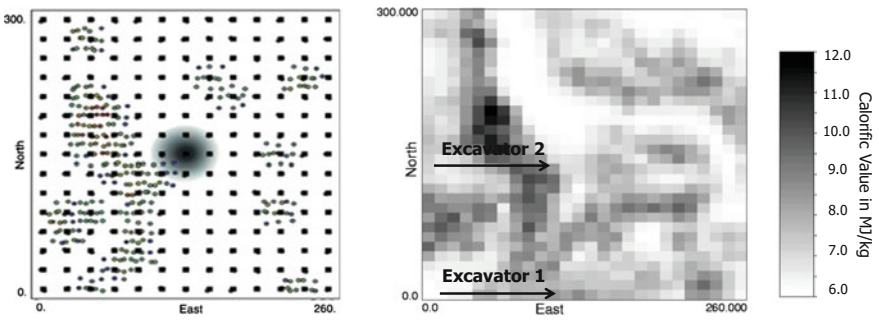

Fig. 6 Set up for illustrative case study

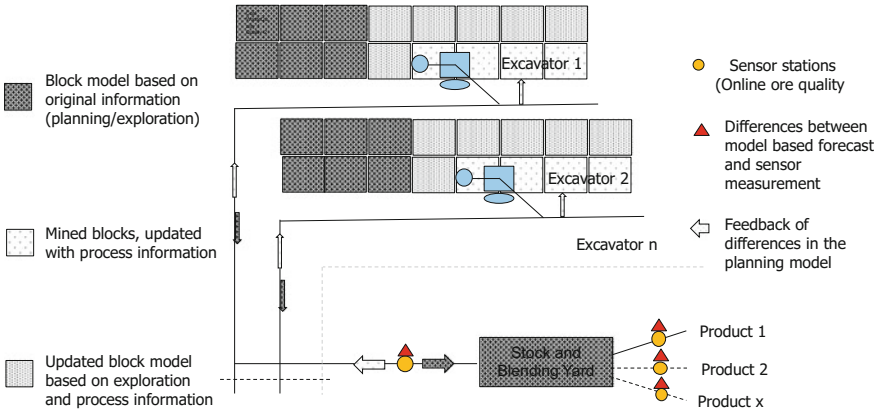

Fig. 7 Continuous mining system used in illustrative test case

from the exhaustively known data set. Component two captures the volume variance relationship and corrects the smaller sensor-measurement support of 250 t to the mining block support of 5120 t by adding the corresponding dispersion variance. The third component mimics the precision of the sensor. For this case study the relative sensor error is varied between 1%, 5% and 10%.

Evaluation Measures

The performance of the proposed Kalman-Filter approach will be evaluated using two measures. The first measure is the mean square difference or mean square error (MSE) related to the true block value. Here, the difference between estimated block value $\mathbf{z}^{t+1}(\mathbf{x})$ and real block value $z(\mathbf{x})$ from the exhaustive data set is compared. The MSE is an empirical error measure and can be calculated according to

$$MSE = \frac{1}{N}\sum_{i=1}^{N}\left(z^{t+1}(\boldsymbol{x}_i) - z(\boldsymbol{x}_i)\right)^2 \tag{5}$$

As second measure the theoretical block variance BV is used, which can be calculated using Eq. (3) for the Kalman-Filter and for the Ensemble Kalman Filter empirically based on the updated ensemble members.

Results and Discussion

To evaluate the performance for different system configurations and different sensor precisions, following cases were investigated:

- operating only one excavator using KF (Case A),
- operating two excavators simultaneously using KF and EnKF (Case B) and
- operating three excavators simultaneously using KF (Case C).

Table 1 summarises the parameters used in this example. In order to guarantee linear independency of rows in the production matrix ***A,*** a cyclic component was added to the extraction rates in the cases of two and three excavators. This cyclic behaviour is typical for continuous mining equipment and is observed in practice.

Figures 8, 9, 10 summarise the results for applying the Kalman-Filter to the Cases A, B and C. Figure 11 shows the results the Ensemble Kalman Filter applied to Case B. Each figure shows both measures, the MSE and BV, which are separately calculated for already mined blocks, blocks, directly adjacent to the mined blocks and blocks, which are two block-lengths away from mined blocks.

Figure 8 clearly demonstrates the ability of the Kalman-Filter based approach to decrease the uncertainty of predicting block values by updating based on sensor data. Considering the MSE, the following observations can be made:

- For mined blocks, the uncertainty almost vanishes. This is expected because in the case of one excavator the sensor measurements can be unambiguously tracked back to the source block. Residual uncertainties remain due to the sensor precision.
- Adjacent blocks are updated resulting in a significant improvement compared to the prior model. For high precision sensors this improvement leads to an about 40% decrease of the MSE. This improvement is due to the positive covariance between two adjacent blocks. In addition, the sensor clearly influences the result.
- Blocks in the second next row are still updated. Due to the larger distance and the corresponding smaller covariance. The effect is less obvious compared to directly adjacent blocks. It is, however, still significant.

The comparison between the empirical error measure MSE and the theoretical error measure BV reveals that the theoretical error measure reflects realistically the true error. Observed BV's are quantitatively very similar to the MSE. Slight differences occur and are mainly due to the limited amount of blocks tested.

Table 1 Equipment parameter and model approach used

Case	Extraction rate	Extraction mode	Sensor Precision	Method
One excavator	E_1: 500t/h	Constant	1%, 5%, 10%	KF
Two excavators	E_1: 500t/h E_2: 1000t/h	Cyclic	1%, 5%, 10%	KF and EnKF
Three excavators	E_1: 500t/h E_2: 1000t/h E_3: 2000t/h	Cyclic	1%, 5%, 10%	KF

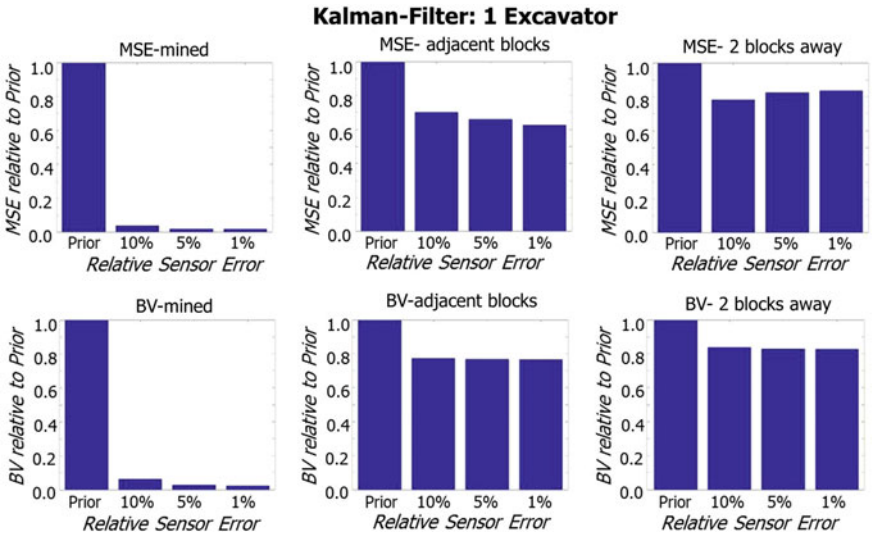

Fig. 8 Performance of the KF for updating the resource model in case A

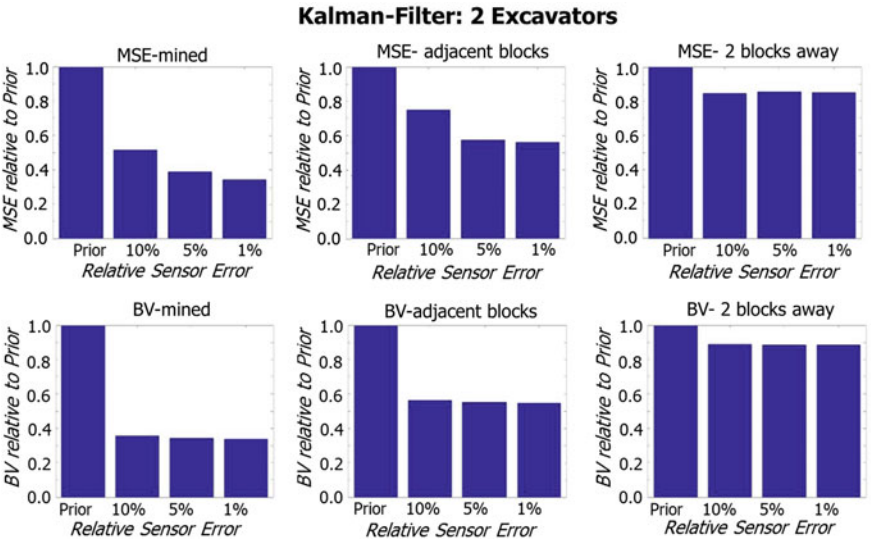

Fig. 9 Performance of the KF for updating the resource model in case B

Figures 9 and 10 show the increased difficulty of the filter to track back the differences between the sensor measurements and model based predictions for combined material flow to the source blocks. The MSE and BV for mined blocks do not vanish completely; the remaining uncertainty can be interpreted as the limit of

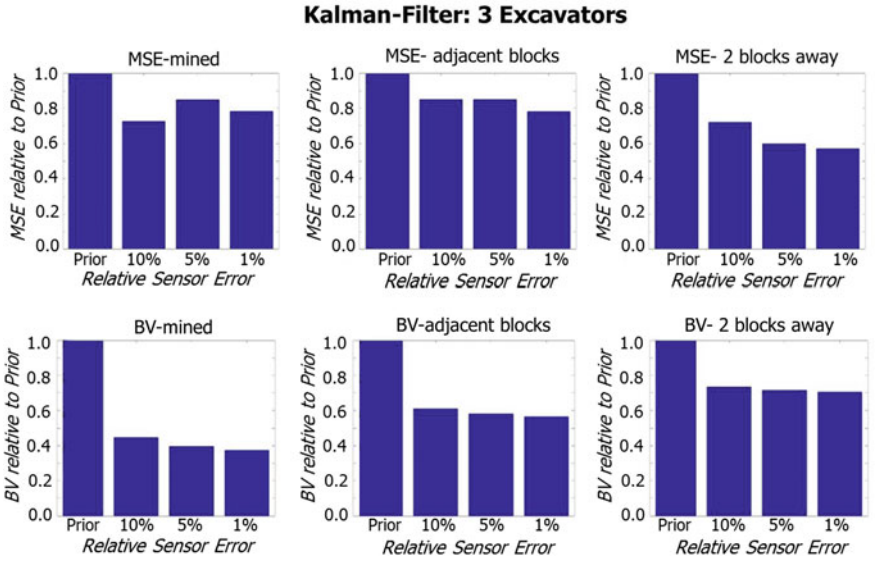

Fig. 10 Performance of the KF for updating the resource model in case C

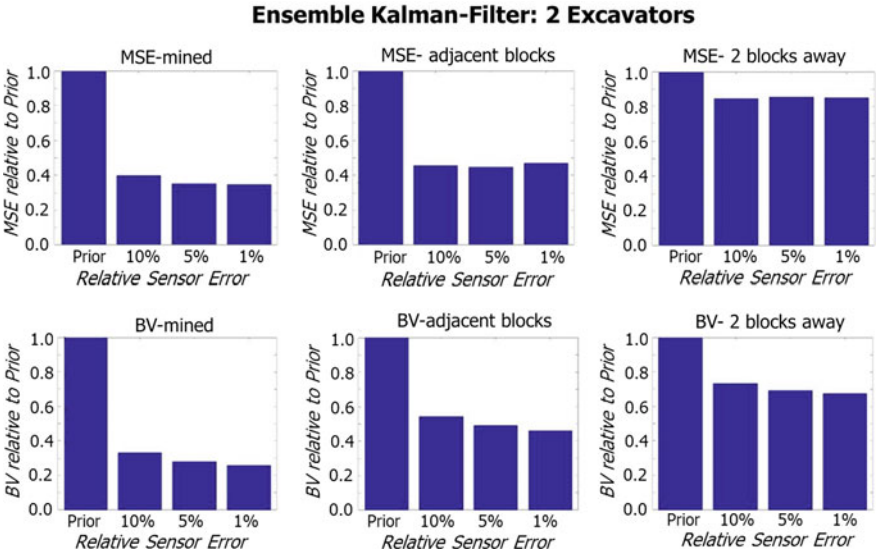

Fig. 11 Performance of the EnKF for updating the resource model in case B

the filter for this specific application. It is expected, that with increased sensor sampling, for example every 2 or 5 min instead of 10 min, the performance can be improved. Nevertheless, there is still a significant improvement in prediction for

directly adjacent blocks and the next row of blocks. Again, MSE and BV behave similarly. Differences are again due to local anomalies of grades in the tested blocks and locally varying sample data configuration (Fig. 6).

Figure 11 shows the example of the EnKF applied to case B. Results are very similar to the Fig. 9 and demonstrate the validity of using the EnKF. Due to the limited problem size, observations concerning computational efficiency cannot be regarded as representative.

Results demonstrate a significant level of improvement by incorporating sensor data, in this case about 15–40% relative compared to solely relying on exploration data. This improvement could be interpreted as magnitude of frequency reduction of being out of spec for delivery coal to customers. The significant positive economic impact is obvious.

Conclusions, Value of RTRM and Future Outlook

The ability to incorporate online sensor data, derived during the production process, into resource/reserve models and a subsequent near real-time optimisation of short-term or operational decision variables promises a large potential for improvement in efficiency in any type of mining operation. This is especially the case when the variability of grades or quality parameters inherent in the deposit is medium to large. The economic effect of such a RTRM and mining process control can be quantified by a profit function J, which was adapted from (Engel 2007)

$$\begin{aligned}\Delta J = {} & J(u_{prior}, d = 0) - J(u_{prior}, d = d_i) + J(u_{prior}, d = d_i) - J(u_{opt}, d = d_i) \\ & + J(u_{opt}, d = d_i) - J(u_{posterior}, d = d_i)\end{aligned} \tag{6}$$

The first term is the loss due to the difference d_i between actual and expected production targets, if decision variables u_{prior} are fixed at their values based on the prior resource/reserve model. The second term represents the difference between actual production targets achieved and the potential optimum resulting from an optimal adaptation of the decision variables u_{opt} to the real conditions. The third term represents the compensation which is achieved by model updating and improved production decisions $u_{posterior}$. It represents the residual uncertainty. This equation offers the means to evaluate, if real-time optimisation I of any value. For example, if the first term in (6) is much larger (in absolute value) than the second one, or if all terms are relatively small, then a variation of the decision variables offers no advantage. This can be the case at highly varying grades, where an adaption to real-time data corresponds to the adaption of noise. Real-time control aims to decrease the third term and should be designed at a timely resolution to decrease this difference to an anticipated level.

The presented framework of RTRM is a concept, which is currently further developed from a level of experimental proof of concept to a level of system

prototype demonstration in an operational environment to prove industrial viability. The particular focus lies on the maturation of sensor technologies, overcoming limits of the feedback algorithms in terms of convergence as function of system complexity and available data. In addition to grades or quality parameters, efficiency and recovery influencing parameters can also be integrated in the reserve model, e.g. by using GPS sensors and energy consumption recordings at excavators. This will require efficient data fusion algorithms. Simulation based optimisation techniques will be developed further for efficient real-time optimisation of mine production control variables as new data become available.

With an implemented framework further questions can be answered, such as: "What is an efficient monitoring network for the system?" or "What implications does the knowledge gained have on the long-term planning and necessary level of exploration?" In particular the last question is interesting as it investigates the utilisation of additional sensor data for mine planning and suggests that the level of "traditional" exploration may be decreased in future. New exploration strategies for a "self-learning-mine" have to be developed that incorporate the time-effect of available information and maximise the use of it.

References

Askara-Nasab H, Torkamani E, Badiozamani M, Tabesh M (2012) Alignment of short-term and operational plans using discrete event simulation, SME Annual Meeting, 19–22 February 2012, Seattle-Washington

Baafi E, Ataeepour M (1996) Simulation of a truck-shovel system using ARENA, Chapter 24 of 26th Proceedings of the application of computers and operations research in the mineral industry, 153–159

Benndorf J (2009) Evaluation of lignite deposits using conditional simulation in geostatistics (published monograph at the Department of Geotechnik and Markscheidewesen of the TU Clausthal, Germany)

Benndorf J (2013) Application of efficient methods of conditional simulation for optimising coal blending strategies in large continuous open pit mining operations. Int J Coal Geol 112(2):141–153

Benndorf J, Dimitrakopoulos R (2013) Stochastic long-term production scheduling of iron ore deposits: integrating joint multi-element geological uncertainty. J Min Sci 49(1):68–81

Benndorf J (2014) A method for sequential teal-time updating of mineral resource models utilising Online Sensor Data, Mathematical Geosciences, paper accepted

Buxton M, Benndorf J (2013) The use of sensor derived data in real time mine optimisation: a preliminary overview and assessment of techno-economic significance. Paper presented at the 142nd SME annual meeting and exhibit, Denver, Colorado

Bette H, Noll R, Müller G, Jansen HW, Nazikkol C, Mittelstädt H (2005) Highspeed scanning LIBS at 1000 Hz with single pulse evaluation for the detection of inclusions in steel. J Laser Appl 17(1):183–190

Chiles JP, Delfiner P (2012) Geostatistics, modelling spatial uncertainty. Wiley, New York

Death DL, Cunningham AP, Pollard LJ (2008) Multi-element analysis of iron ore pellets by laser-induced breakdown spectroscopy and principal component regression. Spectrochima Acta, Part B 63(1):763–769

Dimitrakopoulos R, Ramazan S (2008) Stochastic integer programming for optimising long-term production schedules of open pit mines: methods, application and value of stochastic solutions. IMM Trans Min Technol 117(4):155–160

Engell S (2007) Feedback control for optimal process operation. J Process Control 17(3):203–219

Escudero-Sanz I, Ahlers B, Bazalgette Courrèges-Lacoste G (2008) Optical design of a combined Raman–laser-induced-breakdown-spectroscopy instrument for the European Space Agency ExoMars Mission. Opt Eng 47(3):033001. http://dx.doi.org/10.1117/1.2896453

Evensen G (2003) The ensemble Kalman filter: theoretical formulation and practical implementation. Ocean Dyn 53(4):343–367

Goetz AFH, Curtiss B, Shiley DA (2009) Rapid gangue mineral concentration measurement over conveyors by NIR reflectance spectroscopy. Miner Eng 22(1):490–499

Gosavi A (2003) Simulation-based optimisation: parametric optimisation techniques and reinforcement learning. Springer, New York

Hall BE (2000) Simulation Modelling of Mining Systems, paper presented at Massmin 2000. The Australasian Institute of Mining and Metallurgy, Melbourne

Harris P, Linton P, Buxton M, Pendock N, Bars R (2010) Applications of near infrared core imaging. In: Proceedings of ‚3D mineral spectroscopy of the earth's skin—the 1st national virtual core library symposium July 8–9th 2010, Australian Earth Science Convention

Hoehse M, Mory D, Florek S, Weritz F, Gornushkin I, Panne U (2009) A combined laser-induced breakdown and Raman spectroscopy Echelle system for elemental and molecular microanalysis. Spectrochim Acta, Part B 64(11):1219–1227

Isaaks EH, Srivastava RM (1989) Applied geostatistics. Oxford University Press, Oxford

Jansen JD, Douma SD, Brouwer DR, van den Hof PMJ, Bosgra OH, Hemink AW (2009) Closed-Loop Reservoir management, Paper SPE 119098 presented at the 2009 SPE reservoir simulation symposium, The Woodlands, USA, 2–4 February

Jewbali A, Dimitrakopouos R (2011) Implementation of conditional simulation of successive residuals. Comput Geosc 37(1):129–142. doi:http://doi.org/10.1016/j.cageo.2010.04.008

Jong TPR, Dalmijn W, Kattentid HUR (2003) Dual energy X-Ray transmission imaging for concentration and control, paper presented at IMPC 2003. Cape Town, South Africa

Kalman RE (1960) A new approach to linear filtering and prediction problems. J Basic Eng 82 (1):35–45

Kelton WD, Law AM (2000) Simulation modeling and analysis. McGraw Hill, Boston

Scholze P, Koehler U (2012) Complex control functions and management systems in the opencast mines of Vattenfall Europe Mining AG. World of Min GdmB 2012:31–39

Schulze-Riegert R, Shawket G (2007) Modern techniques of history matching, paper presented at 9th international forum on reservoir simulation, Abu Dhabi

Salama A, Nehring M, Greberg J (2014) Operating value optimisation using simulation and mixed integer programming. Int J Min Reclam Environ 28(1):25–46

Sharma AK, Lucey PG, Ghosh M, Hubble HW, Horton KA (2003) Stand-off Raman spectroscopic detection of minerals on planetary surfaces. Spectrochim Acta Part A Mol Biomol Spectrosc 59 (1):2391–2407

Sharma AK, Misra AK, Lucey PG, Wiens RC, Clegg AM (2007) Combined remote LIBS and Raman spectroscopy at 8.6 m of sulfur-containing minerals, and minerals coated with hematite or covered with basaltic dust. Spectrochim Acta Part A Mol Biomol Spectrosc 68(1):1036–1045

Sládková D, Kapica R, Vrubelm H (2011) Global navigation satellite system (GNSS) technology for automation of surface mining, Taylor and Francis. Int J Min Reclam Environ 25(3): 284–294

Soleymani Shishvan M, Benndorf J (2013) Performance optimisation of complex continuous mining system using stochastic simulation. In: Proceedings of the 4th international conference on engineering optimisation, in Lisabon (paper in print)

Subramaniam G, Gosavi G (2007) Simulation-based optimisation for material dispatching in vendor-managed inventory systems. Int J Simul Process Model 3(4):238–245

Ramazan S, Dimitrakopoulos R (2004) Recent applications of operations research in open pit mining. SME Trans 316(1):73–78

Welsh G, Bishop G (1997) An Introduction to the Kalman Filter, Online document of Department of Computer Science University of North Carolina at Chapel Hill

Young Jung J, Blau G, Pekny JF, Reklaitis GV, Eversdyk D (2004) A simulation based optimisation approach to supply chain management under demand uncertainty, Comput Chem Eng 28(3)

Zimmer B (2012) Continuous mining equipment vs. complex geology challenges in mine planning. Paper presented at 11th international symposium of continuous surface mining 2012, the University of Miskolc

On the Joint Multi Point Simulation of Discrete and Continuous Geometallurgical Parameters

K. G. van den Boogaart, R. Tolosana-Delgado, M. Lehmann and U. Mueller

Abstract Geometallurgical parameters are descriptions of the mineralogy and microstructure of the ore determining its mineralogical and microstructural characteristics. From a conditional geostatistical simulation of such properties, a processing model can compute recovery, equipment usage, processing costs, and thus the monetary value for mining and processing a block with certain processing parameters. The output can be used for optimising mining sequences or finding optimal processing parameters by solving the corresponding stochastic optimisation problem. The approach requires two properties of the simulation not provided by established geostatistical techniques:

(1) Many relevant geometallurgical parameters are from non-Euclidean statistical scales such as (mineral) compositions, (grain size) distribution, (grain) geometry, and (stratigraphic type) categorical which might produce nonsensical values (for example, negative proportions, negative facies probabilities, planar grains) when simulated with standard geostatistical techniques.
(2) Due to the nonlinearity of processing, the entire conditional distribution of the geometallurgical parameters is relevant, not only its mean and variance. The

K. G. van den Boogaart (✉)
Modelling and Valuation, Helmholtz Institute Freiberg for Resource Technology, 34 Halsbrueckerstr, 09599 Freiberg, Germany
e-mail: boogaart@hzdr.de

K. G. van den Boogaart · M. Lehmann
Institute for Stochastics, Technical University Bergakademie Freiberg, 9 Prüferstr, 09599 Freiberg, Germany
e-mail: m.lehmann@student.tu-freiberg.de

R. Tolosana-Delgado
Modelling and Evaluation, Helmholtz Institute Freiberg for Resource Technology, 34 Halsbrueckerstr, 09599 Freiberg, Germany
e-mail: r.tolosana@hzdr.de

U. Mueller
Edith Cowan University, 270 Joondalup Drive, Joondalup WA6027, Australia
e-mail: u.mueller@ecu.edu.au

R. Dimitrakopoulos (ed.), *Advances in Applied Strategic Mine Planning*,
https://doi.org/10.1007/978-3-319-69320-0_43

geostatistical simulation needs to reproduce the joint conditional distributions of all the geometallurgical parameters.

The multi-point conditional geostatistical simulation technique discussed here allows for jointly simulating dependent spatial variables from various sample spaces. The technique combines an infill simulation, similar to the one used in multi-point geostatistics (MPS), with a new form of distributional regression to estimate conditional distributions of arbitrary scales from different information sources, including training images, training models and observed data. The distributional regression is based on a generalisation of logistic regression and is related to both Bayesian Maximum Entropy (BME) geostatistics and high order cumulants. The method ensures that simulated data reside in the set of possible values and honour the characteristics of the joint distribution to be reproduced. The computational effort is substantial, but affordable for a useful application with standard problems: from processing-aware block value prediction and block processing optimisation as shown in the test application to a mathematically completely defined simulated model situation with a complex processing model.

Introduction

Geometallurgical parameters describe the mineralogical and microstructural characteristics of the ore. The conditional geostatistical simulation of geometallurgical parameters enables one to construct a processing model for computing recovery, equipment usage, processing costs, and other relevant economic parameters and thus the monetary value for mining and processing of a block with certain processing parameters. The processing model could be used for optimising mining sequences or finding optimal processing parameters by solving the corresponding stochastic optimisation problem.

An ideal geostatistical simulation procedure for geometallurgical applications should have two properties which are not met by established geostatistical techniques. First, many relevant geometallurgical parameters are data from non-conventional scales such as (mineral) compositions, (grain size) distribution, (grain) geometry, and (lithotype) categorical data, which might produce impossible values when simulated with standard geostatistical techniques. Second, as processing implies a nonlinear transformation of the material properties, the entire conditional distribution of the geometallurgical parameters is relevant and not only its mean and variance. Thus a geostatistical simulation needs to reproduce the joint conditional distributions of all relevant geometallurgical parameters.

This contribution presents a multi-point conditional geostatistical simulation framework which provides a description of the joint conditional distribution of several spatial variables from various sample spaces. The framework combines an infill simulation scheme, similar to the multi-point simulation (MPS) algorithms, with a new form of distributional regression to estimate conditional distributions of

arbitrary scales from different information sources, including training images, training models and observed data. The distributional regression is a generalisation of logistic regression and generalised linear models.

Existing Methods

Brief Description of SNESIM

Consider a categorical variable s with K levels whose spatial distribution is to be modelled. Following Strebelle (2002), given a training image, a template $\tau_n = \{h_\alpha, \alpha = 1, \ldots, n\}$ is specified such that $\{x_\alpha = x + h_\alpha : \alpha = 1, \ldots, n\}$ defines the grid nodes within the search neighbourhood $W(x)$ centred at x.

Next denote by d_n the data event associated with τ_n composed of the values at the n conditioning data $s(x_\alpha) = k_\alpha$, $\alpha = 1, \ldots, n$ considered jointly. The probability that the value of the categorical variable s at the central location x is k, given that the data event for the neighbourhood of x is d_n is estimated by

$$\pi(x, k|\tau_n) \cong \frac{c_k(d_n)}{c(d_n)}$$

where $c(d_n)$ and $c_k(d_n)$ are the number of replicates $c(d_n)$ of the data event d_n in the training image, and the number of replicates of the data event d_n with central value $s(x) = k$ respectively.

The above estimation of the probability of occurrence of a value of k at the central location x relies on the categorical information being available at each location of the search neighbourhood, however the conditioning information might only be available at a subset of the possible nodes, motivating the introduction of a sub-template. Let $\tau_{n'}$ $(n' \leq n)$ be a sub-template of τ_n and $d_{n'}$ the associated data event. The number of replicates $c(d_{n'})$ of $d_{n'}$ is given by

$$c(d_{n'}) = \sum_{d_n, d_{n'} \subset d_n} c(d_n)$$

and the number of replicates of $d_{n'}$ with central value $s(x) = k$ is

$$c_k(d_{n'}) = \sum_{d_n, d_{n'} \subset d_n} c_k(d_n).$$

As before the probability distribution conditional to the data event $d_{n'}$ is estimated as

$$\pi(x, k|\tau_{n'}) \cong \frac{c_k(d_{n'})}{c(d_{n'})}.$$

The standard procedure of SNESIM (single normal equation simulation) then makes use of the sub-templates as follows:

1. Scan the training image and retain only those conditional probability distribution functions (cpdf) associated with τ_n that can be inferred from the training image.
2. Assign the conditioning data to grid nodes and define a random path visiting all unsampled nodes exactly once.
3. At each unsampled location x retain the conditioning data present and identify the corresponding sub-template $\tau_{n'}$ and compute $\pi(x, k|(n'))$, if $n' = 1$, use the marginal probabilities of occurrence of the categories.
4. Draw a value $s(x)$ from the cpdf constructed in step 3 and add the node and its value to the conditioning information.
5. Repeat until all nodes are simulated.

A Logistic Regression View of MPS

The estimation of the cpdf in the SNESIM algorithm uses a simple counting approach, which requires a large training image in order to obtain reliable estimates of the local probabilities. An alternative approach (Stien and Kolbjørnsen 2011) is the estimation of the cpdfs via multinomial logistic regression. This assumes that at an unsampled location x the categorical variable follows a multinomial distribution with probability parameter $\boldsymbol{\pi} = [\pi_1, \pi_2, \ldots, \pi_K]$. This vector is modelled through a log-odd linear expression as

$$\ln\left(\frac{\pi_k(x|\tau_n)}{\pi_K(x|\tau_n)}\right) = \sum_{q=1}^{Q} g_q(x, \tau_n)\left(\boldsymbol{\beta}_q\right)_k, \tag{1}$$

where Q depends on the complexity of the interactions considered, and is the number of *influence functions* $g_q(x, \tau_n)$ which the analyst wishes to take into account. Each vector $\boldsymbol{\beta}_q$ is a vector of size $K - 1$ which gives the increments of the log-odds for each category with respect to the category K due to the q-th influence function. An influence function is either an indicator function or a product of indicator functions depending on some of the points in the template chosen. The basic indicator function of category k at location x is

$$i(x, k) = \begin{cases} 1 & s(x) = k \\ 0 & else \end{cases}.$$

Thus the first $1 + n(K - 1)$ functions in the sum are the model intercept and the indicators

$$g_q(x,\tau) = i(x_\alpha, k), \quad 1 \le k \le K, \quad 1 \le \alpha \le n$$

where, as before, x_α is one of the locations relative to the template $\tau_n = \{h_\alpha, \alpha = 1, \ldots, n\}$ as defined in SNESIM: Since for each location the indicator of one of the categories is redundant (one of them can always be calculated as 1 minus the sum of all the other indicators), it can be dropped, so that the number of first order indicators is $n(K-1)$. Two-point and three-point interactions are built as products of these first-order indicators,

$$g_q(x,\tau) = i(x_\alpha, k) \cdot i(x_{\alpha'}, k'),$$
$$g_q(x,\tau) = i(x_\alpha, k) \cdot i(x_{\alpha'}, k') \cdot i(x_{\alpha''}, k'').$$

They describe the occurrence of pairs (triples) of categories at pairs (triples) of locations relative to the unsampled location x. There are respectively $(n \cdot (K-1))^2$ and $(n \cdot (K-1))^3$ of these functions. Similarly, M-order interactions ($M \le n$) are of the form

$$g_q(x,\tau) = \prod_{m=1}^{M} i(x_{\alpha^{(m)}}, k^{(m)}),$$

and there are $(n(K-1))^M$ of them. If all possible interactions are taken into account, there are $K^n - 1$ Influence functions. The counting approach of MPS is equivalent to considering all these functions, resulting in having to estimate $K^{n+1} - 1$ parameters. As a consequence the training images would have to be impractically large to deliver enough information for this estimation problem. For this reason, Stien and Kolbjørnsen (2011) suggest using only some sets of influence functions. The proposed approach in this paper is to restrict the order of the interactions to a small number $M \ll n$, but without necessarily reducing the size of the pattern. In both cases, the model of Eq. (1) can be estimated by maximum likelihood using training images of reasonable size as data. The optimal trade-offs between the number of points in the pattern, the order of selected interactions, and the size of the training image depends on the actual joint distribution of the parameters. They should thus be selected by the user for each simulation task depending on the assumed spatial dependence. Some regression diagnostics might help in this choice.

Generalisation

Extension to Compositional Covariates

The regression approach described in the previous section opens up the ability to extend the MPS model by including additional predictive variables such as

quantitative covariates available at the conditioning locations of the pattern, or even at the simulation location itself. This is done via additional influence functions. A particular case is the consideration of the available compositional information at the pattern locations $\mathbf{z}(x_\alpha) = [z_1(x_\alpha), z_2(x_\alpha), \ldots, z_D(x_\alpha)],\ \alpha = 1, \ldots, n$, where the component $z_i(x_\alpha)$ represents the mass of the i-th component at location x_α, and $z_1(x_\alpha) + z_2(x_\alpha) + \cdots + z_D(x_\alpha) = 100\%$ at each location. It is known that compositional data carry only relative information (Aitchison 1986), which implies that the influence functions to include in Eq. (1) should be in the form of log-ratios (Aitchison 1996)

$$g_{q(\ldots)}(x, \tau_n) = \ln \frac{z_k(x_\alpha)}{z_D(x_\alpha)}, =: (alr(\mathbf{z}(x_\alpha)))_k. \tag{2}$$

The expression in (2) gives the definition of the *additive log-ratio transformation* (alr; Aitchison 1986) of a composition. If no second or higher order interactions are desired, then compositional information can be accounted for with one influence function for each alr score and each location in the template, resulting in as many as $n(D-1)$ additional functions. The specific choice of the denominator of the log-ratio transform (additive, centered or isometric log-ratio transforms, Aitchison 1986; Egozcue et al. 2003) is irrelevant, since they are linear transforms of one another and compensated by the linear structure of the model. Accordingly the parameter vector $\boldsymbol{\beta}_q$ obtained from maximum likelihood estimation depends on the choice of log-ratio transform, but it can be transformed to the parameter vector that would be derived through the use of a different transform by a linear transformation so that the same predicted conditional probabilities are delivered. In the examples presented here alr is chosen for simplicity. In order to model more complex dependencies it is possible to add interaction terms including categorical information and compositional information at conditioning locations.

With this extension it is possible to introduce other spatial variables from other layers of the dataset as covariates into the prediction of the conditional probability in step 3 of the SNESIM algorithm. This might be categorical (with indicators as regressors), real (as non-transformed regressors), ratio (for example with log transformed data as regressors) or compositional (with alr -transformed data as regressors) data. Replacing the single normal equation approach by a logistic regression further provides the additional flexibility of choosing models with fewer parameters, allowing the use of smaller training images.

The approach thus assumes multiple layers of different scales and can use information from all other layers in the conditional simulation of the binary layers.

Characterisation of a Probability Distribution via an Exponential Family

Logistic regression is a particular case of a set of models known as generalised linear models (GLMs). The framework of GLMs allows the transfer of the preceding models from the simulation of categorical variables to the simulation of many other kinds of variables. The only condition to be satisfied by these variables is that the probability distribution $p(\mathbf{z})$ of the random variable $\mathbf{Z}(x)$ to be predicted can be described as an exponential family, that is

$$p(\mathbf{z}|\boldsymbol{\theta}) \propto \exp\left(\sum_{i=1}^{d} T_i(z)\theta_i\right) \times p_0(\mathbf{z})$$

where d is the dimension of the vector of parameters of the exponential family, for each i, $1 \leq i \leq d$ the function $T_i(\mathbf{z})$ is a known function of the random variable Z, θ_i is a natural parameter of the distribution and $p_0(\mathbf{z})$ is a reference probability distribution. This specification is sufficiently flexible to include most commonly used models of probability distributions. For instance, for a lognormal distribution with logarithmic mean μ and variance σ^2, two functions and two parameters are required: the parameters are $\theta_1 = \mu/\sigma^2$ and $\theta_2 = (\sigma^2 - 1)/2\sigma^2$, the functions $T_1(\mathbf{z}) = \ln(z)$ and $T_2(\mathbf{z}) = \ln^2(z)$, and the reference distribution is the standard lognormal distribution. The multinomial distribution is obtained with the parameterisation $\theta_i = \ln(\pi_i/\pi_K)$, the functions $T_i(\mathbf{z}) = z_i - z_K$, and the reference distribution $p_0(\mathbf{z})$ is the discrete uniform distribution on the set of unit vectors in $\mathbf{R}^K$. For a D-part additive logistic normal random composition (ALN) with alr mean vector and covariance matrix $\boldsymbol{\mu}$ and $\boldsymbol{\Sigma}$, the parameters are $\boldsymbol{\theta}_1 = \boldsymbol{\Sigma}^{-1}\boldsymbol{\mu}$ and $\boldsymbol{\theta}_2 = (\mathbf{I} - \boldsymbol{\Sigma}^{-1})/2$, the functions are $alr_i(\mathbf{z})$ and $alr_i(\mathbf{z})alr_j(\mathbf{z})$ with $i,j = 1,2,\ldots D-1$, and the reference distribution is the standard ALN distribution. A random composition $\mathbf{Z}$ is said to have an ALN distribution (Aitchison 1986) if and only if its transform alr $(\mathbf{Z})$ is $(D-1)$-variate normally distributed. In theory all finite functions are admissible choices for the T_i resulting in great flexibility in the shape of the conditional distributions.

Extension of MPS to Predict a Compositional Output

From the concept of exponential family described in the preceding section, it can be concluded that Eq. (1) (and thus MPS) is just a way to estimate the natural parameters of a multinomial regionalised categorical variable. It is therefore possible to consider the prediction of the probability distribution of a continuous property (in this case, the composition) by establishing a GLM linking the natural parameters of the target distribution (Egozcue et al. 2013; van den Boogaart et al.

2014) to a linear combination of the existing influence functions $\{g_q(x,\tau_n);\quad q=1,2,\ldots,Q\}$. In the case of compositional information, the conditional distribution can be taken to be of the ALN family, in which case the GLM will imply predicting the vector $\boldsymbol{\theta}_1$ and the matrix $\boldsymbol{\theta}_2$, where

$$\boldsymbol{\theta}_1 = \sum_{q=1}^{Q} g_q(x,\tau_n)\boldsymbol{\beta}_q^{(1)},$$
$$\boldsymbol{\theta}_2 = \sum_{q=1}^{Q} g_q(x,\tau_n)\boldsymbol{\beta}_q^{(2)}.$$

Note that the parameters $\boldsymbol{\beta}_q^{(1)}$ are vectors of the same length as $\boldsymbol{\theta}_1$, while $\boldsymbol{\beta}_q^{(2)}$ are matrices of the same size as $\boldsymbol{\theta}_2$. From the predicted values of these parameters, the covariance matrix and mean vector of the alr transformed composition conditional to all available information can be recovered respectively as $\hat{\Sigma} = (\mathbf{I} - 2\hat{\theta}_2)^{-1}$ and $\hat{\mu} = (\mathbf{I} - 2\hat{\theta}_2)^{-1}\hat{\theta}_1$. Having estimated these two parameters, they can easily be used to obtain a random realisation of a multivariate normal distribution $\mathbf{y} \sim N(\hat{\mu}, \hat{\Sigma})$, which would then be back-transformed to a composition by the inverse alr transformation,

$$alr^{-1}(\mathbf{y}) = 100 \times \frac{\exp(\mathbf{y})}{1 + \mathbf{1}^t \exp(\mathbf{y})}. \tag{3}$$

Ensuring a Valid Conditional Covariance

Mean vectors do not pose any problem to the proposed methodology, as all possible results of these equations give a valid measure of the central value of the conditional random composition. But as is the case with conventional two-point kriging techniques, it must be ensured that the resulting covariance matrices are positive (semi)definite, which implies that the algorithms fitting the several $\boldsymbol{\beta}_q^{(2)}$ should be able to solve an optimisation problem constrained to the condition that $\boldsymbol{\Sigma}$ is positive (semi)definite for all possible values of the influence functions. To avoid this, most commonly used GLM implementations assume a constant covariance matrix. Alternatively, if one desires that the spread of the composition also adapts to the existing conditioning information, it is necessary to impose some conditions on the values of $\boldsymbol{\beta}_q^{(2)}$.

When the only conditioning information is of categorical nature, then all influence functions are valued either as zero or one, and $\boldsymbol{\theta}_2$ is just a sum of some of the $\boldsymbol{\beta}_q^{(2)}$. Thus, the following are different sufficient conditions yielding valid covariance matrices:

- all $\boldsymbol{\beta}_q^{(2)}$ are negative semidefinite; or
- for any indicator $i(x_\alpha, k)$ the sum of the $\boldsymbol{\beta}_q^{(2)}$ associated with the set of influence functions $\{g_q(x, \tau_n)\}$ should be negative semidefinite. This condition should be satisfied for all elemental indicators, i.e. for each point x_α and each category k.

These conditions are sufficient but not necessary, as the form $\hat{\Sigma} = (\mathbf{I} - 2\hat{\theta}_2)^{-1}$ would allow $\hat{\theta}_2$ to have some small positive eigenvalues (all smaller than 1, though).

For the case where conditioning information is compositional as well, no solution exists that ensures negative semidefiniteness of $\hat{\theta}_2$ for all possible conditioning values if the influence function is of the form in Eq. (2), as such an influence function is linear and will surely grow to $\pm\infty$ for some values of the conditioning $\mathbf{z}(x_\alpha)$. A partial solution is to assume that the compositional conditioning information has no influence on $\boldsymbol{\theta}_2$ but retain it for $\boldsymbol{\theta}_1$. A second solution is to consider bounded influence functions scaled to lie between 0 and 1 only, in which case the same conditions as with indicator functions would apply, i.e. ensuring all $\boldsymbol{\beta}_q^{(2)}$ to be negative semidefinite would be sufficient. The simplest way to have bounded compositional influence functions is to use the composition expressed in proportions, without any log-ratio transformation. For instance, the additive planar transformation (apt, van den Boogaart and Tolosana-Delgado 2008), would be a valid choice,

$$(apt_i(\mathbf{z}(x_\alpha))) := \frac{z_i(x_\alpha) - z_D(x_\alpha)}{z_1(x_\alpha) + z_2(x_\alpha) + \cdots + z_D(x_\alpha)}. \tag{4}$$

This transformation could then be used to define an influence function, for example $g_q(x, \tau_n) = 0.5 + 0.5 \cdot (apt_i(\mathbf{z}(x_\alpha)))$, which has monotonous behaviour, i.e. identifying some linear combination of the components at the conditioning locations whose value increases/decreases the spread of the composition at the target location. On the other hand, if quadratic influence functions are considered, for example $g_q(x, \tau_n) = (apt_i(\mathbf{z}(x_\alpha)) - 1)(apt_{i'}(\mathbf{z}(x_\alpha)) - 1)$, then the restriction on $\boldsymbol{\beta}_q^{(2)}$ to be negative definite would mean that the spread of the target composition would increase when some of the components of the conditioning compositions decrease.

Step-by-Step Procedure

This section summarises the approach via a brief step by step description of the proposed procedure:

1. Setting:
   1.1. data aspects: choice of the transformations that will be applied to each layer (most probably, alr/apt—Eqs. (2) resp. (4)—for compositional data, indicators for categorical data)
   1.2. algorithm aspects: choice of the largest template $\tau_n = \{h_\alpha, \alpha = 1, \ldots, n\}$ to consider; definition of all plans to use, given the data distribution and the chosen template
   1.3. model aspects: choice of the influence functions $\{g_q(x, \tau_n)\}$ to be used for each natural parameter $\boldsymbol{\theta}_i$ of each layer (e.g. how deep will be the interactions considered?); choice of the reference probability distribution $p_0(\mathbf{z})$ for each layer
2. Model Fitting: for each plan,
   2.1. fit the parameters $\{\boldsymbol{\beta}_q\}$ of the generalised linear model
3. Simulation: for each scale of the grid to simulate, from the coarsest to the finest:
   3.1. set a random path through the grid nodes to be simulated
      3.1.1. for each grid node on the random path
         3.1.1.1. identify available conditioning data, including „actual“ data and previously simulated data
         3.1.1.2. select the plan that uses all the available data
         3.1.1.3. using the fitted model for that plan, obtain the estimated conditional probability distribution
         3.1.1.4. draw a random value from that distribution (in general, with acceptance/rejection techniques)
      3.1.2. go to the next grid node
      3.1.3. once the categorical variable has been simulated at all grid nodes repeat the procedure to simulate the log-ratio variables; back-transform simulated log-ratios to compositions by Eq. (3) in a step 3.1.1.5
   3.2. go to the next grid scale.

Example Application

The Simulation Procedure

The proposed method will be tested with an illustration toy study, loosely inspired by the characteristics of a Ni/Co-lateritic deposit like Murrin-Murrin (WA). A simulated example is used, since this allows checking the performance of the method with a fully known ore body. In this sense, the method proposed in this

contribution can be considered as a first step towards answering the questions posed by Mueller et al. (2014). In this toy study, three lithotypes are considered (FZ: washed zone, MZ: mineralized zone and UM: fresh rock), with a relatively complex contact geometry. Figure 1 shows such zoning as an illustrative example from the motivating deposit (adapted from Markwell 2001). The spatial domain will be considered a 2D planar cut to ensure simple graphic representation. Four mineralogical components will be considered: a value mineral A and three different types of other minerals B, C and D with different separation characteristics in different processing steps. For the unconditional simulation of a test example the domain geometry has been simulated by taking independent random fields with a Gaussian covariance of uncorrected range 0.7 km for each of the lithotypes and to select the lithotype with the maximum value in its random field. This generates a lithology with continuous boundaries, for which each lithotype has the same proportion of occurrence. Conditionally to that the mineral composition has been simulated in log-ratio scores with a universal kriging trend model and isotropic covariance structure given by independent log-ratio scores each following an exponential semivariogram with uncorrected range 0.7 km, a sill of 0.2 plus a small nugget of 0.02. The trend was given by different compositional means for the three regions, given in Table 1. The resulting geometry of the region and mineral proportion maps for the components are shown in Fig. 2. Although the entire simulation procedure is possible using just 2-point statistics in a 2-layer hierarchy, the whole set obtained cannot be modelled any longer with conventional semivariogram-based geostatistics, because the estimation of the semivariograms would depend on knowing the average composition at each facies, and to estimate the facies knowledge of the semivariogram would be required (a typical problem of UK). In contrast, the proposed methodology should be able to model this double dependence correctly by considering all compositional-indicator, compositional-compositional and indicator-indicator 2-point interactions.

A regular grid (as depicted in Fig. 3) of observation locations was chosen. The category and the composition at these locations were used as conditioning data for

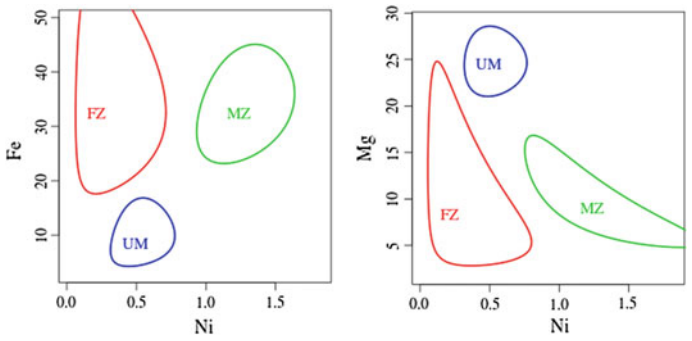

Fig. 1 Schematic representation of the three zones considered in the toy example (simplified from Markwell 2001)

Table 1 The compositional means of the three lithotypes in the toy example

	Mineral A	Mineral B	Mineral C	Mineral D
Lithotype 1	0.077	0.077	0.077	0.769
Lithotype 2	0.154	0.077	0.462	0.308
Lithotype 3	0.181	0.364	0.091	0.364

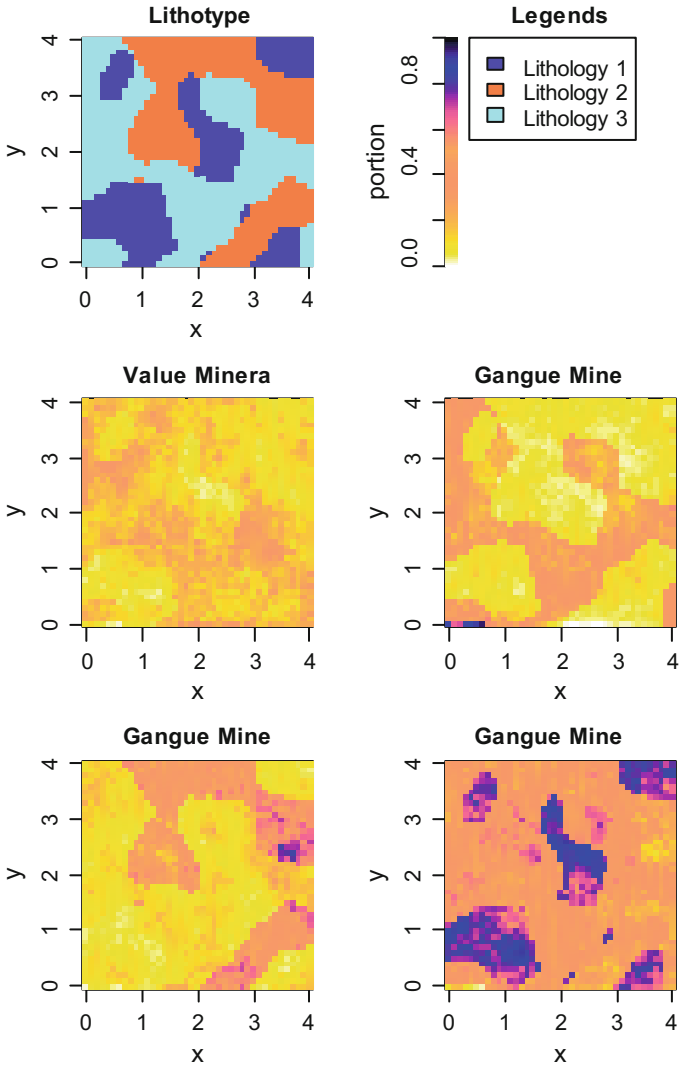

Fig. 2 A simulated scenario serving as training image and conditioning situation

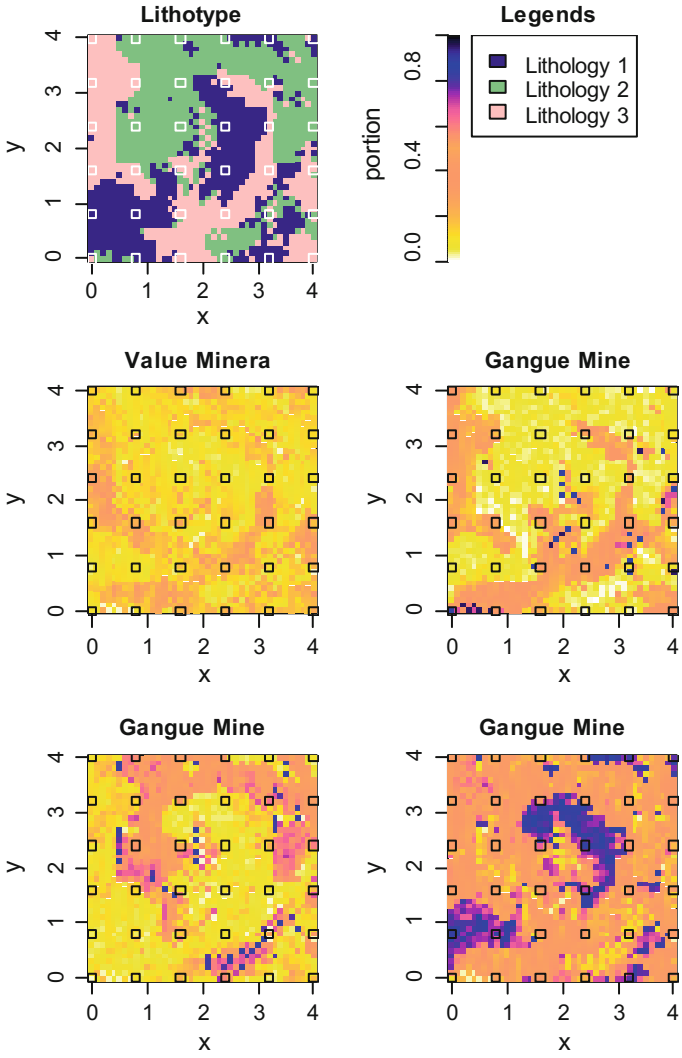

Fig. 3 A conditional simulation of the training image produced by the new algorithm. White squares mark the conditioning locations

the algorithm. The original unconditional simulation was used as a training image to exclude any problem with the size of the training image and its ability to represent the conditional distribution in the dataset from the analysis. Based on this, a sequence of simulation points was chosen covering every location in every layer exactly once (following the idea of snesim of denser and denser grids). At each point first the categorical, and then the conditional variable was scheduled for simulation. For each step in the simulation sequence the relative locations of

observed or already simulated data were determined and those data were included in the plan for conditioning points if they were at a distance of less than $\sqrt{2}$ times the current grid spacing. This was done to include all diagonal neighbours. Larger neighbourhoods require larger training images and more computer time, but can be used too. For practical reasons, in this application the original set of observation locations was chosen on the grid in order to keep the number of plans small (a plan is a sub-template produced by eliminating some of the conditioning points of a template, previously scaled to simulate at a certain grid scale). The resulting plans were then compared and the set of all combinations of conditioning data with the layer to be simulated were computed. The 36 different combinations for the given scenario are shown in Fig. 4.

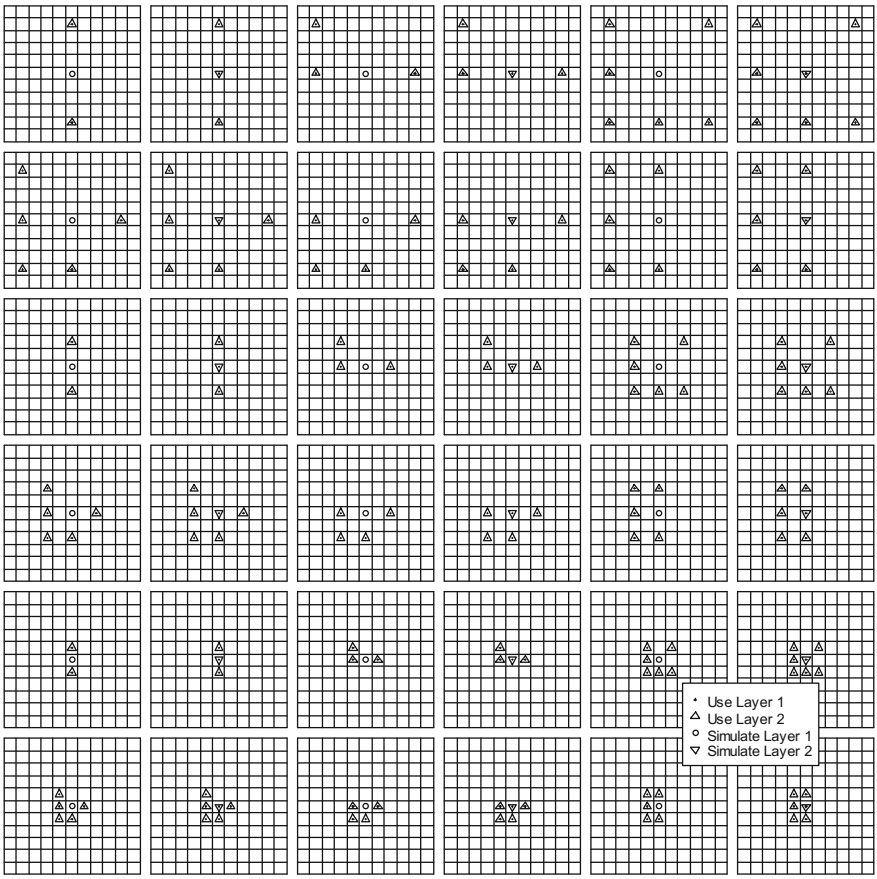

Fig. 4 The 36 plans for conditioning points used in the toy example. A plan is the combination of three elements: the scale of the grid (i.e. of 9 × 9, 5 × 5 or 3 × 3), the sub-template (built from the template by removing conditioning data points), and the layer that is being simulated

For each of the combinations a GLM was fitted to data read from 120 locations of the training image and their respective neighbourhoods according to the plan. The locations were chosen at random, subject to the condition that all necessary information (the dependent variable and the conditioning locations) is inside the training image. The generalised linear model was defined for both layers in the following way: The reference measure was taken as the empirical distribution of the data in the training image. This allows a start from completely non Gaussian reference distributions, while still weighting the different parts of the distribution by the neighbourhood given by the exponential part of the GLM. The sufficient statistics $T(x)$ for the multinomial layer were given by its first two indicators (the choice of which 2 indicators from the possible 3 is irrelevant) as usual in multinomial logistic regression. The sufficient statistics $T(x)$ for the compositional layer were given by the alr transform and the monomials of order 2 (i.e. products and squares) of the apt transform. The influence functions $g_j(x, \tau)$ were selected to be simply all monomials up to order 2 in all available indicators and apt transforms for the conditioning data points. The method was thus effectively a 3 point procedure. The GLMs represent one of the simplest possible regression model choices according to this contribution. The resulting GLMs were fitted with a straightforward Fisher scoring, with a simple step size control, starting from all $\beta_q^{(i)} = 0$. The fitting step takes several hours with an R/C++ implementation on a standard 4 core Intel(R) Core(TM) i7-2640 M CPU @ 2.80 GHz.

The simulation algorithm then uses the conditioning data points, the simulation sequence, the plan for the conditioning points, and the fitted β-parameters for each of the plans to compute for each of the simulation points the conditional distribution according to the GLM. A new value is then realised by rejection sampling. This is repeated until all points are simulated. Such a conditional simulation of both layers simultaneously is shown in Fig. 4. The simulation step runs in O(n) time and needs less than 5 s per simulation on the same machine, which is indeed faster than the Cholesky decomposition based marginal simulation used to generate the compositional training image (>20 s).

Geometallurgical Optimisation

The aim of such simulation procedures is geometallurgical optimisation, leading to optimal processing choices for each mining block. It is assumed that for each known set of geometallurgical parameters of the ore (for example lithotype and mineral composition) and for each known set of processing parameters one can compute material streams, recovery and the costs along the processing chain. In the toy example this situation was modelled by a conceptual model of a processing chain, which was given by known recoveries and costs for several optional processing steps measured in costs units (cu; monetary unit per mass unit):

1. Mining ("mine or leave"-choice for each mining block), mining costs depend on lithotype (10cu, 20cu, 15cu). Every block mined will be processed further. No mining is the typical choice for poor ore from any of the lithologies.
2. Density separation comes at a cost of 100cu and recovers 95% A, 10% B, 5% C, 0.2% D. Density separation is the typical choice for rich ore from lithology 1 as it removes the dominating gangue D effectively.
3. Flotation comes at a cost of 100cu and recovers 95% A, 5% B, 1% C, 5% D. Flotation is the typical choice for rich ore from lithology 2 as it removes both materials C and D effectively.
4. Metallurgy comes at a cost of 100cu and recovers 0.95% of the metal content of A, 20% of the metal content of B, 5% of the metal content of C, and 5% of the metal content of D. Metallurgy is always necessary, since otherwise there are unsellable minerals. It is assumed that the metals in the minerals B, C, D are not desired in the final product.
5. Upgrading, a metallurgical step at 20 cu recovering 0.95% of the metal from A, 0.2% of the metal from B, and 80% of the metal from C and D. This step is potentially necessary to remove high contents of B in the metal product. Flotation followed by upgrading can be a good choice for ore from lithology 3.
6. It is assumed that the resulting metal can be sold on the world market at a price of 4000cu if metal A content is 99% or higher. Nearly all material can reach this concentration, when all three processing steps are applied, however this generates costs and lowers recovery substantially.

This model thus implies four simple yes/no processing choices: mining, density separation, flotation, and upgrading, resulting in $1 + 2^3 = 9$ possible choices (as ore not mined does not require any further choices). The optimal choice can be estimated for each mining block of the training image by finding which of the 9 choices provides the maximum value. The result is given in Table 2 and the left panel of Fig. 5. It shows that the optimal processing choice does not only depend on lithology, but also on the actual composition. Following van den Boogaart et al. (2013b), this will be called the omniscient choice since it depends on the complete knowledge of all relevant parameters. However, in reality the lithology and mineral composition are not known at every location, but only at the observation locations. According to van den Boogaart et al. (2013a) the optimal processing given the available data is the choice maximising the conditional expectation of the gain, i.e. the cashflow resulting from the choice. This conditional expectation has been approximated by averaging over 100 simulations from the conditional simulation algorithm. The result, called the conditional choice, is presented in Table 3 and the right panel of Fig. 5. As usual for conditional simulations the result of both choices is the same at all observation locations. Both choices mine roughly the same area. Analogous to the smoothing effect of kriging, the conditional choice shows a smoother structure than the omniscient choice. The conditional choice also shows some artefacts resulting from the grid structure of the algorithm. Table 4 compares different choices, including the omniscient choice, the conditional choice and all non-adaptive choices, which in this case would not make the mine economic at all.

Table 2 Number of blocks classified by dominant facies and optimal processing according to the processing model, computed for each block of the training image

Lithology	1	2	3
No mining	399	382	308
Flotation + upgrading	0	1	116
Density + flotation	22	27	243
Flotation only	3	129	21
Density sep. only	23	6	1

This is the best choice, however it would require full knowledge of the true lithology and mineralogical composition, hence the name "omniscient"

The huge difference between the omniscient choice and the conditional choice suggests that in this situation more data should be acquired.

Discussion

This new approach of conditional simulation of several layers of different data types (*data scales* in Statistics) simultaneously has a lot of inbuilt flexibility. The general structure of exponential families allows the inclusion of many kinds of data as predictors. The maximum likelihood estimation for exponential families solves likelihood equations, which can be formulated such that the expected value of the product of the sufficient statistics T and g -functions in the regressors fit on average the observed mean of this same product in the training dataset. The generated conditional distribution thus fits the corresponding high order moments defined by the chosen exponential family and the regression model. In this way the method is related to the high order cumulants in the sense that it selects a special case of conditional distributions fitting specified higher order moments. If all moments up to a given degree fit, the cumulants up to this degree will fit also. In addition, the method is closely related to Bayesian maximum entropy methods, as exponential families maximise the entropy with respect to certain constraints.

The method is also related to classical multiple point statistics approaches in the sense that it can generate the same conditional distributions, when saturated models are used (i.e. with all interactions considered). However the method provides additional flexibility. Different scales and data layers can be incorporated. The choice of conditioning functions is robust with respect to the particular definition of moments considered, cumulants or other polynomial functions of the moments. The use of arbitrary reference measures, such as empirical distributions from the training images, enables the reproduction of complex distributions, such as multimodal distributions, in the conditional simulation.

The trade-off between the precision of parameter estimation and the size of the training image has to be handled by user choices regarding the conditioning neighbourhood and model choices, like the statistics used and the degree of interaction selected. This trade-off is always present in multiple point geostatistics

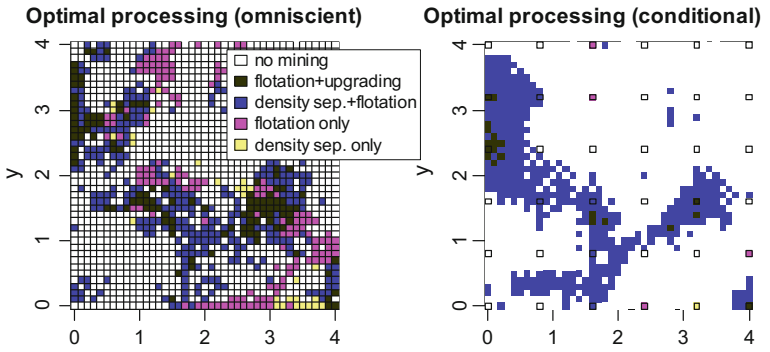

Fig. 5 Comparison of the optimal choice based on known geometallurgical parameters (omniscient) and the computed choice conditional to the observed data. Theory expects the conditional choice to be much smoother than the omniscient choice. Black outlines show the data needed for the choice. In the left panel, this is an exhaustive sampling along the grid

Table 3 Number of blocks classified by dominant facies and optimal processing according to the processing model, computed for each block using the conditional expectation of the gain for each processing choice based on the simulated conditional distribution of the properties

Lithology	1	2	3
No mining	373	512	367
Flotation + upgrading	0	0	20
Density + flotation	73	29	302
Flotation only	0	4	0
Density sep. only	1	0	0

This is the best choice anticipating our lack of knowledge, however approximated by conditional simulations rather than the unknown full conditional distribution. In contrast to the omniscient choice in Table 2 more often the conservative choices of no mining and both separation techniques are preferred

methods, either explicitly or hidden to the user. The difference is merely that in the framework presented here it must be treated explicitly. The selection of the precise form of the regression models for the various plans requires some understanding of the properties of the resulting exponential families, as inconsistent models can be constructed, for example models with parameters corresponding to negative variances. In our experience such inconsistencies typically result in numeric errors or non-convergence of the fitting algorithms. Some mathematical skills and a good understanding of the spatial dependence structure are yet needed to select the generalised linear models (GLMs) used in the simulation algorithm. Currently the algorithm only uses GLMs with the so-called natural link. Eventually future extensions towards other link functions might simplify model building. The numerical fitting of the multivariate and high parametric GLMs with the current general algorithm (relying on sample based integration) requires a substantial amount of computing power. The algorithm is thus only recommended, when

Table 4 Total gain for various processing choice strategies on the training image

Choice	Sum realised values of all mining blocks in thousand monetary units
Omniscient choice	30
Conditional choice	4
No mining	0
Complete processing	−80
Flotation + upgrading	−80
Density sep. +upgrading	−63
Upgrading only	−195
Density sep. + flotation	−26
Flotation only	−168
Density separation only	−199
Metallurgy only	−161

All non-adaptive choices result in losses. This is mainly due to an insufficient choice of an ultimate pit. This decision is however difficult to take as it depends on both parameters, lithotype and the mineral composition, as the different gangue minerals behave differently during processing

powerful computer servers are available. The simulation itself however is extremely fast, so that many realisations can be computed once the GLMs have been fitted.

An interesting aspect is that classical geostatistical methods can likewise be understood in terms of a linear model (i.e. regression). Simple kriging is known (Stein and Corsten 1991) to be closely related to usual regression models and the conditional distribution in SNESIM corresponds to a saturated multinomial logistic regression model, although both are computed with different algorithms. Sequential Gaussian Simulation and SNESIM likewise are based on such sequences adding points iteratively on a selected simulation path through the simulation grid. The method can thus be seen as a joint generalisation of sequential Gaussian simulation and MPS.

The first test of the model with the toy example processing suggests that the simulation approach is fit for purpose with respect to geometallurgical optimisation choices. Unlike other methods it can produce joint simulations of all parameters relevant for processing honouring information on other data layers, and it can consider bidirectional dependence (i.e. each layer depends on the other). It has enough flexibility to model complex dependencies and complex conditional distributions. It has inbuilt flexibility to tackle the trade-off between the precision of fitting based on finite training images and the approximation error introduced by unsaturated models. And unlike other models it can honour restricted sample spaces such as positive numbers, compositions or any other kind of restricted sample spaces, by selecting the reference measure accordingly. On the other hand, the present implementation it is not foolproof and requires substantial user choices and further research. The representation of the conditional distribution in terms of GLMs might help with that, since all the standard methods for this type of

regression analysis can be used for these decisions. These include tests or confidence intervals on the influence parameters $\boldsymbol{\beta}_q$, diagnostic graphics and global goodness-of-fit statistics.

The paper has not discussed standard complexity issues in geostatistics like change of support, how to define a good training image or how to find a best possible prediction of the conditional distribution at a location. This is left for further research, and the reader should be aware that more would need to be said about this.

Conclusions

A new approach was proposed for the joint simulation of various data scales, as required if geometallurgical processing models are to be incorporated into mine planning. The approach provides a high degree of flexibility, which will have to be explored, but is also quite promising for solving several problems of geostatistical simulation simultaneously, including: managing several scales, constraint spaces, multivariate joint simulation, limited training images, precision in simulation and complex dependence structures.

References

Aitchison J (1986) The statistical analysis of compositional data. Chapman & Hall Ltd, London

Egozcue JJ, Pawlowsky-Glahn V, Mateu-Figueras G, Barceló-Vidal C (2003) Isometric logratio transformations for compositional data analysis. Math Geol 35(3):279–300

Egozcue JJ, Pawlowsky-Glahn V, Tolosana-Delgado R, Ortego MI, van den Boogaart KG (2013) Bayes spaces: use of improper distributions and exponential families. Rev de la Real Acad de Cienc Exactas, Físicas y Naturales, Serie A Matemáticas 107:475–486

Markwell T (2001) Murrin Murrin Ni/Co resource estimation: MME resource modelling report. Anaconda

Mueller U, Tolosana-Delgado R, van den Boogaart KG (2014) Simulation of compositional data: a Nickel-Laterite case study. In: Dimitrakopoulos R (ed) Orebody modelling and strategic mine planning, symposium, Perth, WA, 24–26 Nov 2014. The Australasian Institute of Mining and Metallurgy, pp 61–72

Stein A, Corsten LCA (1991) Universal kriging and cokriging as a regression procedure. Biometrics 47(2), pp 575–587

Stien M, Kolbjørnsen O (2011) Facies modelling using a Markov mesh model specification. Math Geosci 43:611–624

Strebelle S (2002) Conditional simulation of complex geological structures using multiple-point statistics. Math Geol 34:1–21

van den Boogaart KG, Tolosana-Delgado R (2008) "Compositions": a unified R package to analyze compositional data. Comput Geosci 34(4):320–338

van den Boogaart KG, Konsulke S, Tolosana Delgado R (2013a) The challanges of adaptive processing to geostatistical prediction, 23rd world mining congress, 11. 15 Aug 2013, Montreal, Canada

van den Boogaart KG, Konsulke S, Tolosana-Delgado R (2013b) Nonlinear geostatistics for geometallurgical optimisation, GeoMet 2013. In: Proceedings of the second AusIMM international geometallurgy conference, 30 Sept–2 Oct

van den Boogaart KG, Egozcue JJ, Pawlowsky-Glahn V (2014) Bayes Hilbert spaces. Austr N Z J Stat 56:171–194

Geologically Enhanced Simulation of Complex Mineral Deposits Through High-Order Spatial Cumulants

H. Mustapha and R. Dimitrakopoulos

Abstract Earth sciences and engineering phenomena such as geologic units, grade content and other properties of a mineral deposit, as well as attributes of other natural phenomena, represent complex geological systems distributed in space. Their spatial distributions are currently predicted from finite measurements and second-order spatial statistical models, which are limiting, as geological systems are highly complex, non-Gaussian and exhibit non-linear patterns of spatial connectivity. Non-linear and non-Gaussian high-order geostatistics is a new area of research based on higher-order spatial connectivity measures and spatial cumulants. Key elements of a high-order spatial stochastic modelling framework are developed herein, starting with the definitions of high-order spatial statistics and, more specifically, the definition and properties of spatial cumulants, and the inference and interpretation of high-order anisotropic cumulants. Spatial cumulants are shown to capture the directional multiple-point periodicity and spatial architecture of geological processes. It is further shown that only a subset of all the cumulant templates has to be computed to characterize complex spatial patterns. The second key element of high-order geostatistics is the simulation of complex mineral deposits using a nonparametric Legendre series approximation with coefficient calculated in terms of spatial cumulants. Examples show that the approach works very well.

H. Mustapha (✉)
COSMO—Stochastic Mine Planning Laboratory, Department of Mining and Materials Engineering, McGill University, Montreal, QC H3A 2A7, Canada
e-mail: hussein.mustapha@mcgill.ca

R. Dimitrakopoulos
FAusIMM, COSMO—Stochastic Mine Planning Laboratory, Department of Mining and Materials Engineering, McGill University, Montreal, QC H3A 2A7, Canada
e-mail: roussos.dimitrakopoulos@mcgill.ca

R. Dimitrakopoulos (ed.), *Advances in Applied Strategic Mine Planning*,
https://doi.org/10.1007/978-3-319-69320-0_44

Introduction

In earth sciences and engineering, measurements of phenomena under study represent complex non-Gaussian systems distributed in space. Frequently, it is required that geo-environmental attributes are modeled and their spatial distributions predicted from a limited set of measurements. Random field models and stochastic data analysis, termed geostatistics, have long been established and used as the key approach to modelling and predicting natural phenomena in a variety of earth sciences and engineering fields (e.g. Matheron 1971; David 1977, 1988; Journel and Hijbregts 1978; Journel 1989, 1994; Ripley 1987; Cressie 1993; Kitanidis 1997; Hohn 1999; Goovaerts 1997; Chilès and Delfiner 1999). Despite the considerable developments over the past three decades, modelling approaches are based on second-order statistics, and the spatial information these contain. Concerns articulated during the last decade suggest that current modelling frameworks are limited in their ability to account for the spatial complexity of the natural phenomena being modelled, that are critical to modelling and predicting spatially-distributed, location-dependent data (e.g. Guardiano and Srivastava 1993; Journel 1997). Several attempts to develop new techniques dealing with spatial complexity include the multiple-point approach (Strebelle 2002; Zhang et al. 2006; Journel 2000), new Markov random field based approaches (Daly 2005; Tjelmeland and Eidsvik 2005; Tjelmeland 1998), and others. These developments replace the two-point covariance with a training image so as to account for high-order dependencies. Although these are novel approaches, there is a need for a well-defined spatial stochastic modelling framework capable of dealing with the complexity of geo-environmental phenomena. The approach advocated herein is based on cumulants, which are combinations of moment statistical parameters allowing the complete characterization of non-Gaussian random variables. In multiple point statistics, training images are used as a model for high order joint distributions. However this model does not necessarily represent the true joint distribution of the random field under consideration. The multiple-point is a particular case of the high-order moment and does not infer from a concrete statistical theory. While cumulants that have statistical advanced properties compared to the moments are explored in this paper and will be essential in a future work. Spatial cumulants are a new concept and it is introduced here because cumulants completely characterize non-Gaussian stationary and ergodic spatial random fields, thus can provide a new consistent framework in addressing issues mentioned above. Related works on cumulants of one-dimensional random function models have been developed to deal with the identification, analysis and testing of non-linear signals (e.g. Billinger and Rosenblatt 1966; Mendel 1991; Swami et al 1990; Nikias and Petropulu 1993).

In the following sections, this paper first outlines basic definitions, summarizes approaches to calculating anisotropic spatial cumulants, shows examples, and comments on relations between cumulants and geological process. Then, the simulation of mineral deposits with complex non-Gaussian and non-linear geological patterns is outlined based on the use of spatial cumulants in the high-dimensional space of Legendre polynomials (Lebedev 1965). Examples from simulating a

complex channel system illustrate the practical aspects of high-order simulations based on spatial cumulants. Conclusions and comments follow.

High-Order Statistics of Non-gaussian Spatial Random Functions

Let $(\Omega, \Im, P)$ be a probability real space. A spatial real random field $Z(x)$ is a family of random variables $\{Z(x_1), Z(x_2), \ldots\}$ at locations $x_1, x_2, \ldots$, where each random variable is defined on $(\Omega, \Im, P)$ and takes real values.

Assuming $Z(x)$ is a zero-mean ergodic stationary random field, then the cumulants of the random field $Z(x)$ are defined from the MacLaurin expansion of the cumulant generating function:

$$\widetilde{\Psi}(v) = \ln\left(E\left\{\exp(jv^T Z)\right\}\right)$$

If its moments up to order r exist, then:

$$Mom[Z(x)Z(x+h_1), \ldots, Z(x+h_{r-1})] = E\{Z(x)Z(x+h_1) \ldots Z(x+h_{r-1})\}$$

The moments depend only on the vectors $h_1, h_2, \ldots, h_{r-1}$.

Similarly, the rth-order cumulants of $Z(x)$ can be denoted as:

$$c_r^z(h_1, h_2, \ldots, h_{r-1}) = \text{Cum}[Z(x), Z(x+h_1), \ldots, Z(x+h_{r-1})]$$

For example, the second-order cumulant of a non-centered random function $Z(x)$ known as the covariance is given by:

$$c_2^z(h) = E\{Z(x)Z(x+h)\} - E\{Z(x)\}^2$$

Its third-order cumulant is given by:

$$\begin{aligned} c\frac{z}{3}(h_1, h_2) &= E\{Z(x)Z(x+h_1)Z(x+h_2)\} \\ &- E\{Z(x)\}E\{Z(x+h_1)Z(x+h_2)\} \\ &- E\{Z(x)\}E\{Z(x+h_1)Z(x+h_3)\} \\ &- E\{Z(x)\}E\{Z(x+h_2)Z(x+h_3)\} + 2E\{Z(x)\}^3 \end{aligned}$$

where:

h_3 is the difference between vectors h_1 and h_2.

It may be computationally convenient to consider zero-mean random functions as some of the terms vanish. In addition, note that the cumulants of orders higher than three of a zero mean random function are related to their moments of lower orders and a combination of their moments of order two.

Calculating Experimental Anisotropic Spatial Cumulants

In this section, the definitions and implementation details of the calculations of experimental cumulants from exhaustive and sparse data sets are described.

Definitions

Spatial cumulants are defined in terms of distances in space. Existing cumulant calculations assume regularly sampled data and/or a regularly sampled training data set. In general, however, geological data are available only on irregularly spaced borehole locations. Similarly to anisotropic experimental variograms, it is possible to restrict the calculation of cumulants to a given direction. For this purpose, the concept of spatial template for calculating cumulants is introduced here. A spatial template T is defined as a particular geometry of points in space; more formally, given a set of directional vectors $\left\{\vec{h}_1, \vec{h}_2, \ldots, \vec{h}_r\right\}$, supported by the direction angles $\{\theta_1, \theta_2, \ldots, \theta_r\}$, the associated spatial template of order $(n+1)$ is defined (considering a spatial location x as a reference) as:

$$T_{r+1}(x, \vec{h}_1, \vec{h}_2, \ldots, \vec{h}_r, \theta_1, \theta_2, \ldots, \theta_r) = \left\{x, x+\vec{h}_1, x+\vec{h}_2, \ldots, x+\vec{h}_r\right\}$$

For example, the $r = 3$ order cumulant with the given template T_3 is computed from:

$$C_{h_1,h_2}^{T_3} = \frac{1}{N^2}\sum_{i=1}^{N}\sum_{j=1}^{N} Z(x)Z(x+\vec{h}_i)Z(x+\vec{h}_j), \quad \{x; x+\vec{h}_i; x+\vec{h}_j\} \in T_3.$$

Figure 1 shows an example of a template associated to a third-order experimental cumulant.

Implementation on Regular Grids

In the case of regular grids, the calculations are straightforward for particular templates that are in the same Cartesian system as the grid. In this case, the distances and angles are defined in terms of grid increments. For example, the template

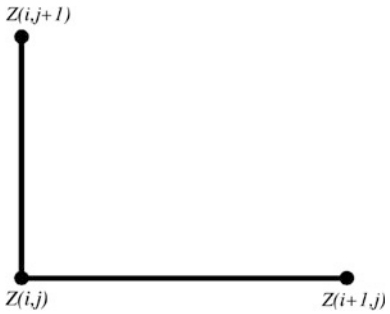

Fig. 1 L-shape template for cumulant calculation on regular grid data

shown in Fig. 1 can be easily implemented in a finite difference way. If the orthonormal basis of the grid is defined with the supporting unit vector $\vec{i}$ and $\vec{j}$. For example, the experimental third-order cumulant associated with the template T shown in Fig. 1 is given by:

$$C^{T_3}_{h_1,h_2} = \frac{1}{N^2}\sum_{i=1}^{N}\sum_{j=1}^{N} Z(x)Z(x+\vec{h}_i)Z(x+\vec{h}_j), \quad \{x; x+\vec{h}_i; x+\vec{h}_j\} \in T_3$$

Then, the algorithm is summarized as follows:

1. Choose a template T by defining $\vec{h}_i$ and $\vec{h}_j$. The angles are defined by the grid: 0.45 or 90°. Start with closest grid node $(i + 1, j)$, $(i, j + 1)$.
2. Loop until all possible triplets are multiplied.
3. Average the products.
4. Increase grid node separation and go back to step 2.

Implementation on Irregular Grids

For irregular grids, the situation is computationally more complex. Computations involve angles and distances calculations, that is, the grouping of points in terms of angles and distances. In practice, the directional neighbourhood search is equivalent as computing several directional variograms, with given angles and ranges as shown in Fig. 2.

The algorithm for third-order irregular experimental cumulant calculations (see Figs. 2 and 3 for complementary information) can be summarized as:

1. Choose a template by defining $\vec{h}_i$ and $\vec{h}_j$. The angles a_1 and a_2 can be anything between 0 and 360°. Choose tolerance angles Ta_1 and Ta_2 for each of the vectors. If angle equal to 90°, omnidirectional cumulants are calculated.
2. Choose a tolerance distance Th_1 and Th_2 for each direction.

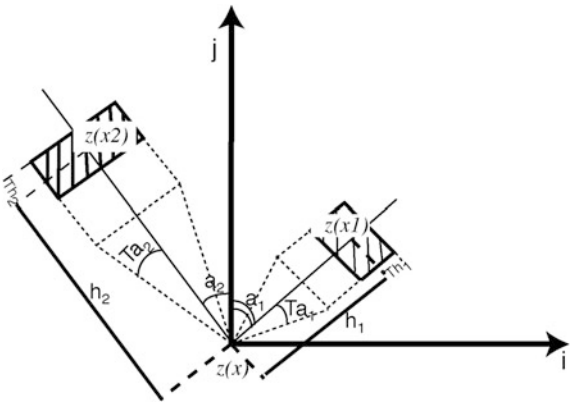

Fig. 2 Irregular template for 3rd order cumulant calculation. h_2 and h_1 are the distances with Th_1 and Th_2, tolerance distances respectively. a_1 and a_2 are the angles with tolerances Ta_1 and Ta_2, respectively. (i, j) is the basis of the cartesian coordinate system

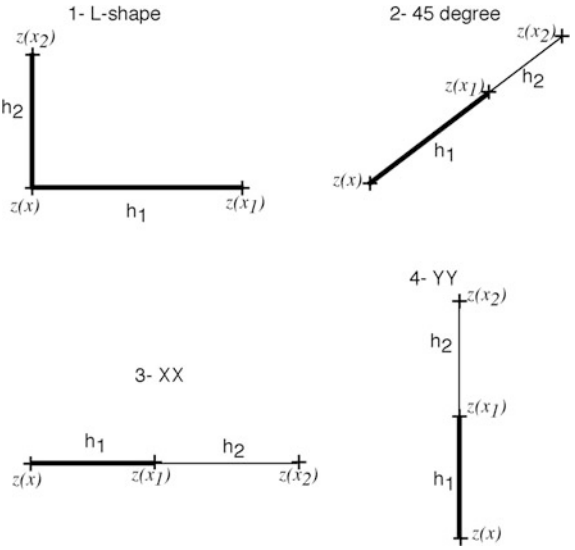

Fig. 3 The four experimental third-order cumulant templates used in the following examples. (1) L-shape, (2) 45°, (3) XX and (4) YY. h_1 is the distance between x and x_1 and h_2 is the distance between x and x_2

3. Find the points inside the cone angle for each vector (Fig. 2).
4. Calculate all the possible products between points inside dashed boxes and supporting point at the origin $\{Z(x), Z(x_1), Z(x_2)\}$.
5. Classify the products in terms of both distances $||\vec{h}_1||$ and $||\vec{h}_2||$ and average in every lag.

Sequential Simulation with High-Order Spatial Cumulants

Approximation of a Joint Probability Density Using Legendre Series

This section discusses the approximation of continuous densities using Legendre series. A squared integrable and real piecewise smooth function f defined on $D = [-1, 1]$ can be formally written in a series of Legendre polynomials

$$f(z) = \sum_{m=0}^{\infty} L_m \frac{P_m(z)}{||P_m||}, \tag{1}$$

where $P_m(z)$ is the mth-order Legendre polynomials, with norm $||P_m||$, defined as (Lebedev 1965)

$$P_m(z) = \frac{1}{2^m m!}\left(\frac{d}{dz}\right)^m \left[\left(z^2 - 1\right)^m\right] = \sum_{i=0}^{m} a_{i,m} z^i, \quad \text{and } -1 \le z \le 1. \tag{2}$$

The Legendre polynomials $P_m(z)$ obey the following recursive relation

$$P_m + 1(z) = \frac{2m+1}{m+1} x P_m(z) - \frac{m}{m+1} P_{m-1}(z) \tag{3}$$

where $P_0(z) = 1$, $P_1(z) = z$, and $m \ge 1$. The set of Legendre polynomials $\{P_m(z)\}_m$ forms a complete orthogonal basis set on the interval $[-1, 1]$. The orthogonality property is defined as

$$\int_D P_m(z) P_n(z) dx = \begin{cases} 0 & m \ne n \\ \frac{2}{2m+1} & m \ne n \end{cases} \tag{4}$$

The discrete Legendre polynomials also satisfy

$$\sum_{i=1}^{k} P_m(z_i) P_n(z_i) \Delta z = \frac{2}{2m+1} \delta_{mn}, \quad \forall\, m, n \ge 0, \tag{5}$$

where

$$\begin{aligned} \Delta z = z_i - z_{i-1} = 2/k & \quad \textit{is a space step} \\ k & \quad \textit{is the number of steps} \\ \{z_i\} & \quad \textit{is a uniform discretisation of} [-1, 1] \\ \delta_{mn} & \quad \textit{is the delta Dirac function} \end{aligned} \quad <!\textit{endaligned}>$$

To avoid numerical instability in polynomial computation, we normalized the Legendre polynomials by utilizing the square norm. The set of normalized Legendre polynomials is defined as:

$$\overline{P}_m(z) = \sqrt{\frac{2m+1}{2}} P_m(z).$$

In this case, the orthogonality condition given in Eq. 4 becomes:

$$\sum_{i=1}^{k} \overline{P}_m(z_i)\overline{P}_n(z_i)\Delta z = \delta_{mn}, \quad \forall m, n \geq 0. \tag{6}$$

The coefficients L_m in Eq. 1 of the Legendre series, the so-called Legendre cumulants, can be determined using the orthogonality property in Eq. 4 as:

$$L_m = \int_D \overline{P}_m(z) f(z) dz = g_m(c_i), i = 0, \ldots m \quad \text{and} \quad m = 0, 1, 2, .. \tag{7}$$

where c_i is the ith-order cumulant of f. Theoretically, the series 1, with coefficients L_m calculated from Eq. 7, converges to $f(z)$ at every continuity point of $f(z)$ as demonstrated by Lebedev (1965). Finally, if only cumulants of order smaller than or equal to ω are given, then the function $f(z)$ in Eq. 1 can be approximated as follows:

$$f(z) \approx \tilde{f}_\omega(z) = \sum_{m=}^{\omega} L_m \overline{P}_m(z) \tag{8}$$

The above is detailed for three-dimensional spaces in Mustapha and Dimitrakopoulos (2010a).

A High-Order Simulation Method

This section describes the high-order conditional simulation method (*hosim*) based on spatial cumulants. A sequential procedure simulating values at unsampled locations that are randomly visited is used here. The Legendre series approximation is used to estimate the cpdfs (Mustapha and Dimitrakopoulos 2010a). This expression uses Legendre polynomials which are orthogonal on the finite interval $[-1, 1]$. Then, the training image (TI) and the data values [Fig. 4(1)] and the data values [Fig. 4(2)] are first scaled to $[-1,1]^d$, where d is the dimension of the problem (i.e., d = 1, 2 or 3).

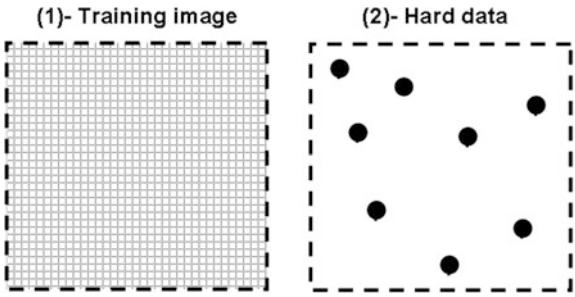

Fig. 4 (1) Training image; hard data locations in (2)

The hosim method first combines the TI used and the samples (Fig. 5) to infer the high-order spatial cumulants. A global calculation procedure is performed based on a given maximal template size (*TEMP*) [Fig. 5(2)]. This step consists of calculating all the spatial cumulants needed by the Legendre series approximation.

The main steps of *hosim* method are as follows:

1. Scan the training image and the sample data [Fig. 5(1)] and store the spatial cumulants in a global tree.
2. Define a random path visiting once all unsampled nodes.
3. Define the template shape T for each unsampled location x_0 using its neighbours. The conditioning data available within *TEMP* are then searched (Fig. 5). The high-order spatial cumulants are read from the global tree in Step 1, and are used to calculate the coefficients of the Legendre series. These coefficient are used to build the cpdf of Z_0.
4. Draw a uniform random value in [0, 1] to read from the conditional distribution a simulated value, $Z(x_0)$, at x_0.

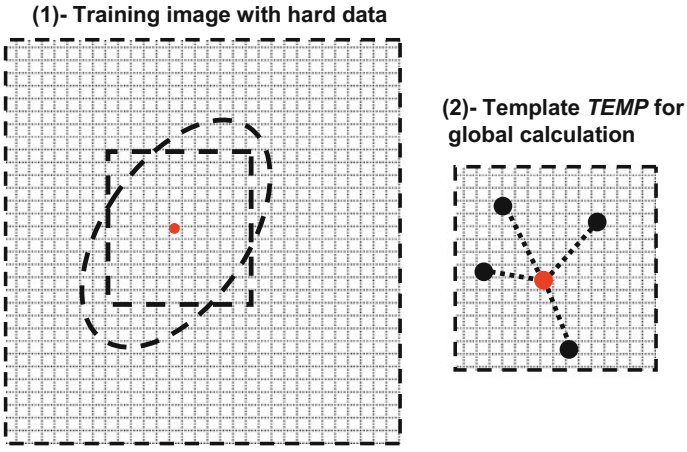

Fig. 5 Training image in (1). The template in (2) is used for a global calculation of the spatial cumulants

5. Add x_0 to the set of sample hard data and the previously simulated values.
6. Repeat Steps 3 and 5 for the next points in the random path defined in Step (3).
7. Repeat Steps 2 to 6 to generate different realizations using different random paths.

The random path defined in Step 5 concerns only the unsampled locations. Thus, the final realization obtained in after Step 8 honours the conditioning data.

Spatial Cumulants: Examples, Calculation and Geological Interpretations

Examples of third-order cumulants calculated on two- and three-dimensional data sets are presented in this section. Results are interpreted so as to understand their use as a pattern recognition tool. The data sets utilised represent complete images and the regular grid approach described in a previous section is followed. It should be noted that, the covariance is a measure of the periodicity between pairs of points separated by given distances; similarly, the higher-order cumulant is also a measure of periodicity but in the direction of the symmetry axis of template used, that is, the multiple point symmetry. In the examples that following, cumulants are computed on zero mean data sets.

Spatial Templates

In the following example, the covariance map and four directional experimental cumulants are presented, unless otherwise specified. Fourth- and fifth-order cumulants are, respectively, computed with the and xy(−x)(−y) templates as shown in Fig. 6.

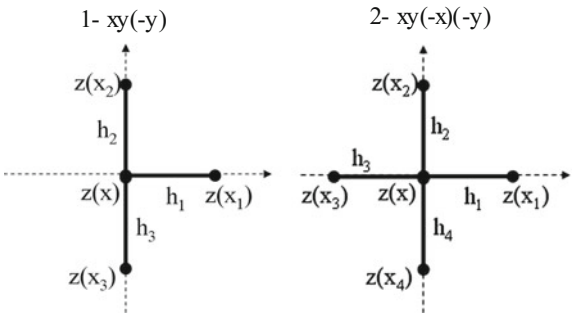

Fig. 6 Examples of fourth-order cumulant templates (1) and fifth-order cumulant templates (2)

Training Image

In Fig. 7(2), (3) we consider an interpretation of a diamond baring kimberlite pipe of the Ekati mine, NT Canada (Nowicki et al. 2004), and its translation to a 3D binary training image (76,055 nodes are used). The geological interpretation of the pipe geometry is seen as two parts: one on the top and another one on the bottom as shown in Fig. 7. The part on the bottom is close to a three-dimensional cone geometric shape. The base of this cone or the intersection between the two parts of the pipe is a horizontal section of size 150 m along x and 200 m along y (Figs. 7 and 11). (For more details, see Dimitrakopoulos et al. 2010 and Mustapha and Dimitrakopoulos 2010b). Results for high-order cumulants are presented first. Then, a discussion follows.

The third-order cumulant maps provide approximations of the pipe shape as shown in Fig. 8(1), (3). The fourth-order xyz cumulants average the objects and translate them to the origin.

For example, the pipe, considered as the only object in Fig. 7(3), is translated to the origin as shown in Fig. 9(1). From this figure, 2D cross-sections are shown in Fig. 9(2), (3). These cross-sections provide, approximately, the results obtained by the third-order cumulant maps in Fig. 8. This conclusion is justified by the fact that the pipe shape is approximately reflected, in a specific plane, by using orthogonal shapes (xy or L-shape, xz or yz) cumulants, while it is fully characterized using xyz cumulants. These observations show, not surprisingly, the ability of the higher order cumulants to include key relations seen in lower orders. More generally, relations between cumulants can be extended for an order higher than four and, in particularly, order five. The fifth-order cumulant maps are based on four directions, and placed in four-dimensional space. Then, cross-sections are used as detailed before. For example, Fig. 10 shows a 3D cross-section of the xyz(−z) fifth-order cumulant map. This figure translates the pipe to the origin and reflects the results of the fourth-order and, consequently, the third-order results are reflected too. The pipe shape varies strongly between the bottom and the top along the vertical

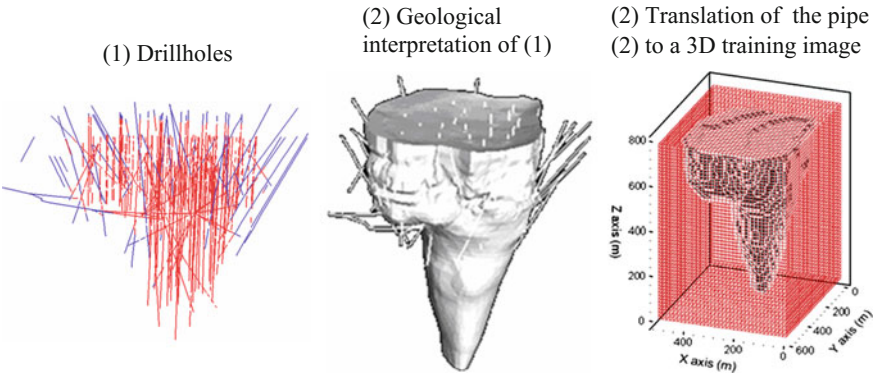

Fig. 7 A geological interpretation of a kimberlite pipe, (1) drillholes; (2) a geological interpretation of (2); (3) regular block approximation of the pipe surrounding rock

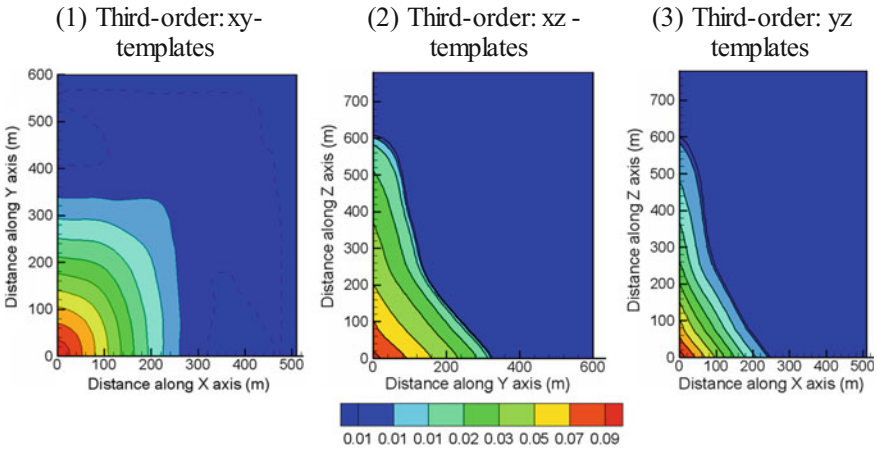

Fig. 8 Third-order cumulants. (1)–(3) are third-order cumulants for the Fox kimberlite pipe, NT in Fig. 7(3), using xy, xz and yz templates

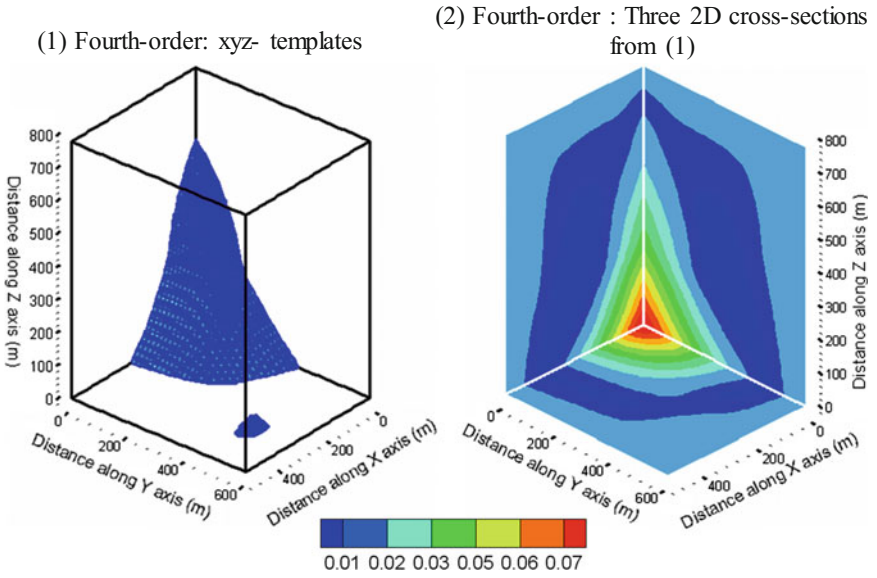

Fig. 9 Fourth-order cumulants. (1) is a fourth-order cumulant map for the Fox kimberlite pipe, NT in Fig. 7(3), using xyz templates; (2) are three 2D cross-sections from (1)

axis (z) while the variations are less along the horizontal axis (x and y) as shown in Fig. 11. Figure 12 shows results of the third-, fourth- and fifth-order with a different way. Figure 12(1.a)–(3.a) present third-order cumulant maps using lines contours from Fig. 8.

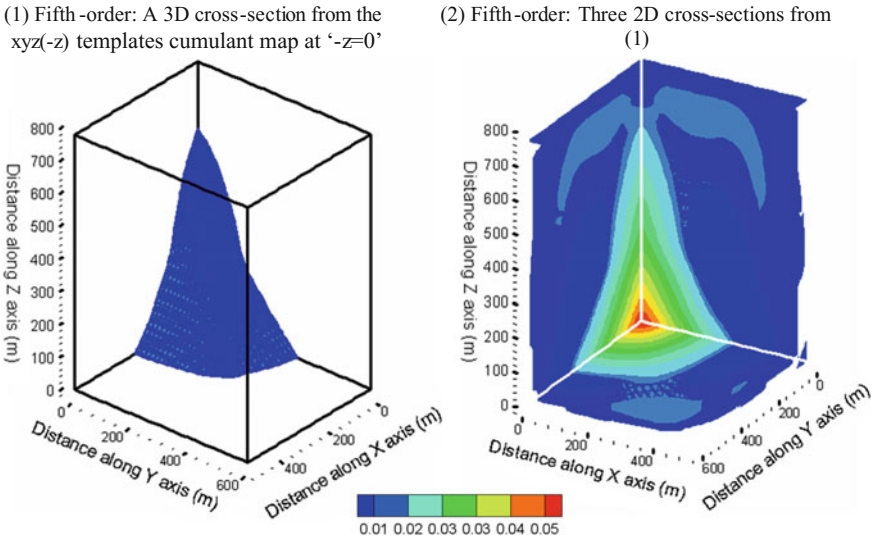

Fig. 10 Fifth-order cumulants. (1) is a 3D cross-section at $-z = 0$ of the five-dimensional xyz(−z) template cumulant map; (2) are three 2D cross-sections from (1)

Several 2D cross-sections, along x, y and z directions, are selected from the fourth-order cumulant maps in Fig. 9. The fronts from 2D cross-sections of Fig. 10 are selected as shown in Fig. 12(1.c)–(3.c). The third-order cumulant map in Fig. 12(1.a) shows a regular shape of the horizontal sections of the pipe while the fourth- and fifth-order cumulant maps, in Fig. 12(1.b)–(1.c), reflect some horizontal irregularity of the pipe. The main raison comes from the variation of the pipe size along the vertical axis.

This variation is more described by the fourth- and the fifth-order cumulants because they manipulate points in more than two directions. For example, four points are considered for the fourth order-cumulant and one of the points varies along the z direction. The variations along x and y axis are less than the variation along z axis. The third-order cumulant maps in Fig. 12(2.a)–(3.a) show, approximately, results close to those obtained from fourth- and fifth-order maps as shown in Fig. 12(2) and (3). The fourth- and fifth-order maps detect with more precision the size along x (150 m) and y (200 m) of the intersection between the two parts of the pipe.

Drill Hole Data

The cumulant maps calculated on the 3D training image provide good interpretation for the pipe's shape. In the following, cumulants are calculated on the original data obtained from the pipe drill holes in Fig. 7(1). Figures 13, 14 and 15 show the obtained results. In these figures, the red lines represent the borders of the set of high values in the cumulants maps. These borders reflect the shape of the pipe along x and y directions which is approximately similar to the results obtained on the 3D

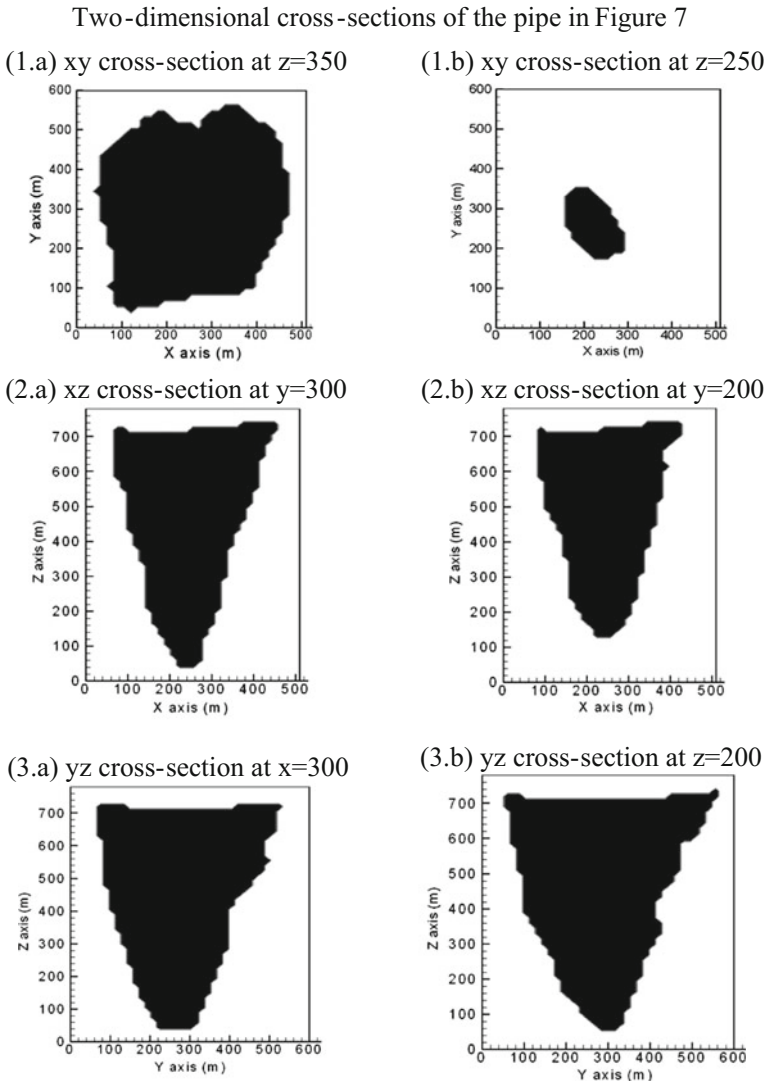

Fig. 11 Different horizontal and vertical 2D cross-sections of the pipe in Fig. 7

training image (Fig. 12). The top part of the pipe is better detected then the bottom part and that because most of the data points are in the top part, until 300 m depth, as the pipe drill holes show in Fig. 7(1). In Fig. 13 the fourth- and fifth-order cumulants maps calculated on data provide better description of the horizontal sections than the third-order map. They show irregularity between $400 < x < 500$ and along y as detected with the fourth- and fifth-order maps from the 3D training image.

THIRD-ORDER

(1.a) $\{\vec{x}, \vec{y}\}$ cumulant map

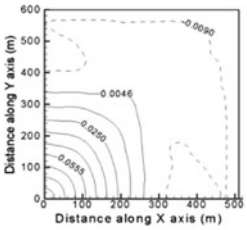

(2.a) $\{\vec{x}, \vec{z}\}$ cumulant map

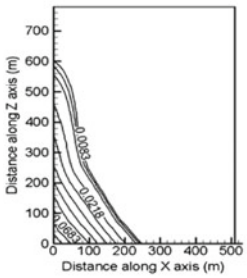

(3.a) $\{\vec{y}, \vec{z}\}$ cumulant map

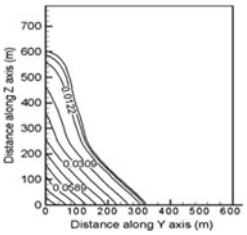

FOURTH-ORDER

(1.b) 2D cross-sections along z from the map in Figure 9 (1)

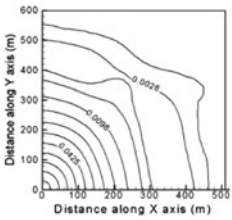

(2.b) 2D cross-sections along y from the map in Figure 9 (1)

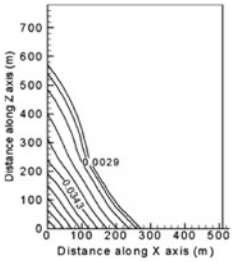

(3.b) 2D cross-sections along x from the map in Figure 9 (1)

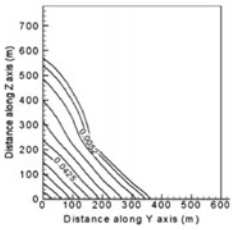

FIFTH-ORDER

(1.c) 2D cross-sections along z from the map in Figure 10 (1)

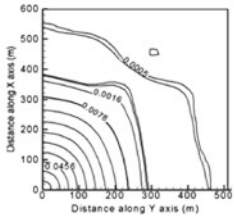

(2.c) 2D cross-sections along y from the map in Figure 10 (1)

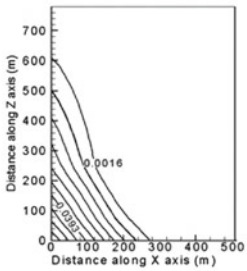

2D cross-sections along x from the map in Figure 10 (1)

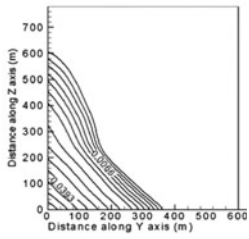

Fig. 12 Third-, fourth- and fifth-order cumulant maps for the pipe (3D training image) in Fig. 7

Conditional Simulation Using Cumulants and Training Images

In this section, the simulation of a two-dimensional exhaustive image [Fig. 16(1)] is shown so as to illustrate the high-order conditional simulation using spatial cumulants. The example presented herein uses 25 sample data [Fig. 16(2)], the training image in Fig. 16(3) and the conditional simulation algorithm discussed above.

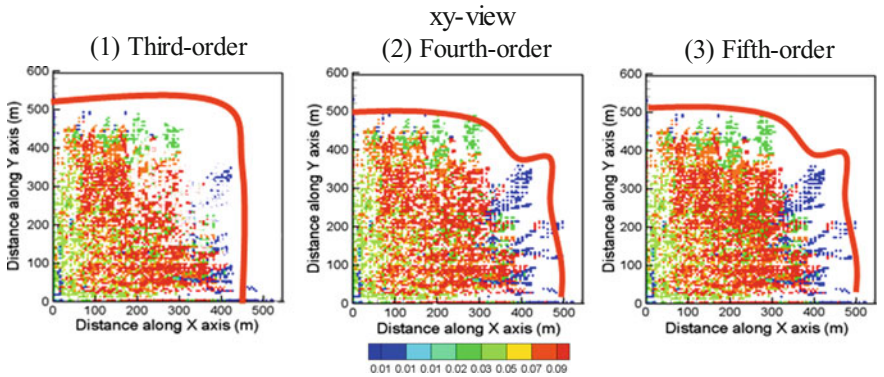

Fig. 13 xy views of the third-, fourth- and fifth-order cumulant maps calculated using the data from drill holes in Fig. 7(1)

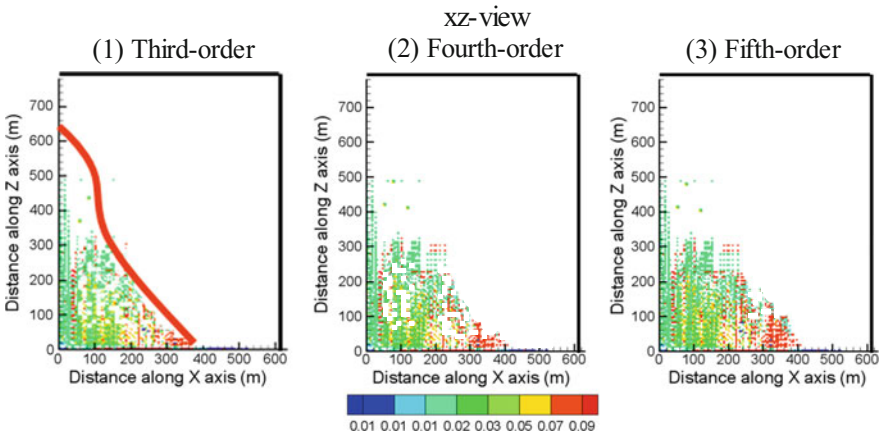

Fig. 14 xz views of the third-, fourth- and fifth-order cumulant maps calculated using the data from drill holes in Fig. 7(1)

Different realizations are presented as shown in Fig. 17. This figure shows that the main characteristics of the exhaustive image are reproduced using a sparse data set (about 0.85% of the total number of points). The 2D sections presented here have particular and complex distributions as shown by the bimodal histogram in Fig. 18(1). This figure shows the comparison between the generated realizations histograms and the data set histogram. In addition, the realizations reproduced the variograms along the EW and NS directions of the data set as shown in Fig. 18(2) and (3). The developed method is also validated by comparing the high-order statistics of the data set, exhaustive image and the different realizations obtained. For example, the third-order spatial cumulant maps of the exhaustive image, data set, realizations (1) and (2) are very close as shown in Fig. 19. This last result is

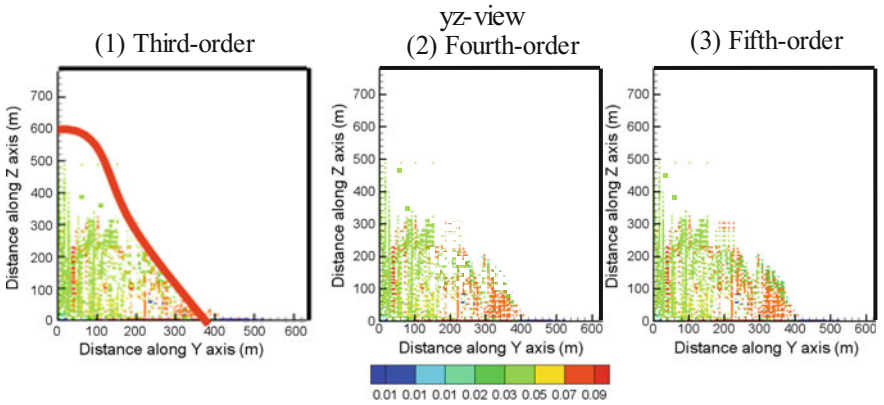

Fig. 15 yz views of the third-, fourth- and fifth-order cumulant maps calculated using the data from drill holes in Fig. 7(1)

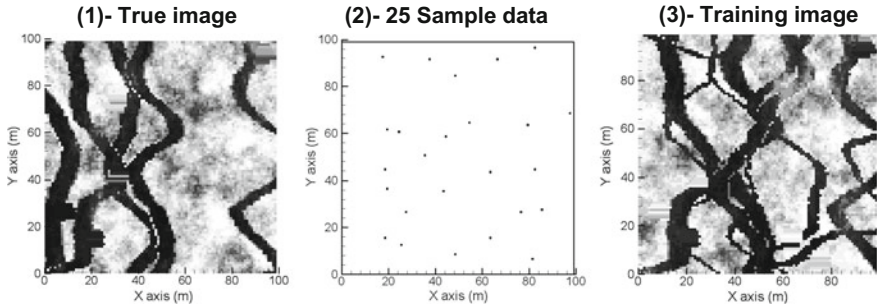

Fig. 16 Simulation of a horizontal 2D section of a fluvial reservoir. (1) Exhaustive image: true image, (2) 25 sample data, and (3) a training image

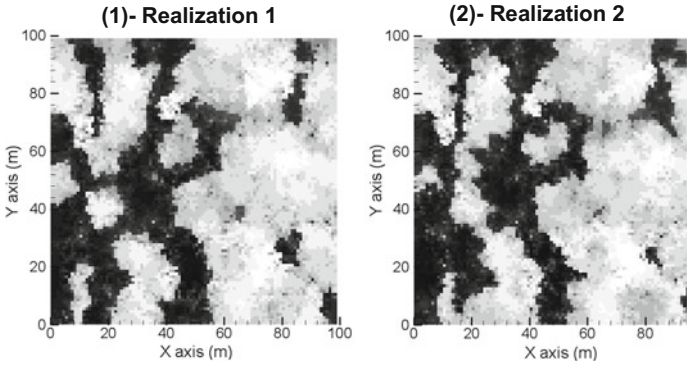

Fig. 17 Realizations (1) and (2) obtained by the hosim

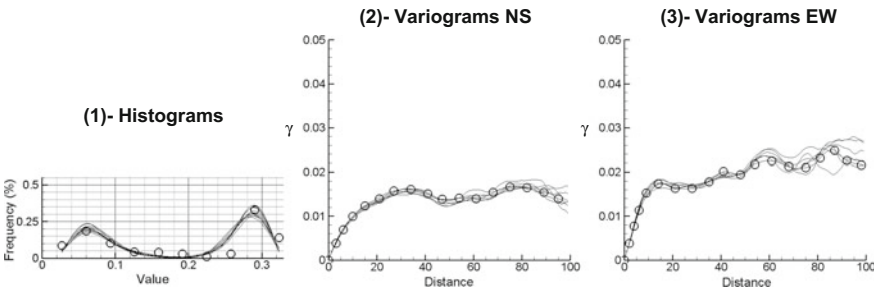

Fig. 18 Histograms (1), NS (2) and EW (3) variograms of 10 hosim realizations. The circles refer to the data set 1 and the solid lines refer to the realizations

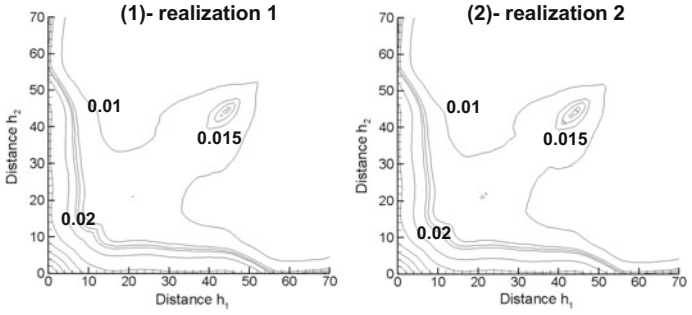

Fig. 19 Third-order spatial cumulant maps of the realizations 1 and 2, respectively

obtained because the new conditional simulation algorithm uses different cumulants orders in the Legendre series and this will guaranty the reproduction of not only the histogram and variograms of the sample data, but also their high-order statistics.

Conclusions

This paper presented developments towards a new alternative approach to modelling complex, non-linear, non-Gaussian earth sciences and engineering data, as required in most applications. The new alternative framework is founded upon concepts from high-order statistics that are introduced herein in a spatial context. Mathematical definitions of non-Gaussian spatial random functions and their high-order spatial statistics are described in detail, stressing the notion of spatial cumulants. The calculation of spatial cumulants, including anisotropic experimental cumulant calculations using spatial templates are introduced, and examples of three-dimensional images presented and their characteristics analyzed to assess the relations between cumulants and geological patterns. The simulation of a complex

image of channels is presented using a new high-order sequential simulation method which is based on the concept of high-order spatial. The results showed a good reproduction of the main features of the exhaustive image using a small data set. The realizations generated reproduced the histogram, variogram and high-order statistics of the data set. A key aspect of the simulation method based on spatial cumulants is the compliance of the simulated realizations with all statistics (any order) of the available data and avoid possible conflicts between training images and dense data sets commonly available in mining studies.

Acknowledgements The work in this paper was funded from NSERC CDR Grant 335696 and BHP Billiton, as well NSERC Discovery Grant 239019. Thanks are in order to Brian Baird, Peter Stone, and Gavin Yates, as well as BHP Billiton Diamonds and, in particular, Darren Dyck, for their support, collaboration, data from Ekati Mine, and technical comments.

References

Billinger DR, Rosenblatt M (1966) Asymptotic theory of kth-order spectra. In: Harris B (ed) Spectral analysis of time series. Wiley, New York, pp 189–232

Chilès JP, Delfiner P (1999) Geostatistics: modeling spatial uncertainty. Wiley, New York

Cressie NA (1993) Statistics for spatial data. Wiley, New York

Daly C (2005) Higher order models using entropy, Markov random fields and sequential simulation. In: Geostatistics Banff. Springer, pp 215–225

David M (1977) Geostatistical ore reserve estimation. Amsterdam, Elesevier

David M (1988) Handbook of applied advanced geostatistical ore reserve estimation. Amsterdam, Elsevier

Dimitrakopoulos R, Mustapha H, Gloaguen E (2010) High-order statistics of spatial random fields: exploring spatial cumulants for modeling complex non-Gaussian and non-linear phenomena. Math Geosci 42(1):65–97

Goovaerts P (1997) Geostatistics for natural resources evaluation. New York, Oxford

Guardiano J, Srivastava RM (1993) Multivariate geostatistics: beyond bivariate moments. In: Soares A (ed) Geosatistics Tróia '92, vol 1. Dordrecht, Kluver, pp 133–144

Hohn ME (1999) Geostatistics and petroleum geology. New York, Kluwer

Journel AG (1989) Five leassons in geostatistics. AGU, San Francisco

Journel AG (1994) Modeling uncertainty: some conceptual thoughts. In: Dimitrakopoulos R (ed) Geostatistics for the next century. Dordrecht, Kluwer

Journel AG (1997) Deterministic geostatistics: a new visit. In Baafy E, Shofield N (eds) Geostatistics Woolongong '96. Dordrecht, Kluwer, pp 213–224

Journel AG (2000) Stochastic imaging of channels from seismic data using mp statistics. SCRF, report 13. Stanford University

Journel AG, Huijbregts CJ (1978) Mining Geostatistics. Academic Press Inc, New York, 600 p

Kitanidis PK (1997) Introduction to geostatistics—applications in hydrogeology. Cambridge University Press, New York

Lebedev NN (1965) Special functions and their applications. New York, Prentice-Hall Inc, p 308 P

Matheron G (1971) The theory of regionalized variables and its applications. Cahier du Centre de Morphologie Mathematique, Number 5, Fointanebleau

Mendel JM (1991) Use of high-order statistics (spectra) in signal processing and systems theory: theoretical results and some applications. IEEE Proc 79:279–305

Mustapha H, Dimitrakopoulos R (2010a) High-order stochastic simulations for complex non-Gaussian and non-linear geological patterns. Math Geosci 42(5):457–785

Mustapha H, Dimitrakopoulos R (2010b) A new approach for geological pattern recognition using high-order spatial cumulants. Comput Geosci 36(3):313–334

Nikias CL, Petropulu AP (1993) Higher-order spectra analysis: a nonlinear signal processing framework. Upper Saddle River, PTR Prentice Hall, p 538 p

Nowicki T, Crawford B, Dyck D, Carlson J, McElroy R, Oshust P, Helmstaedt H (2004) The geology of the kimberlite pipes of the Ekati property, Northwest Territories, Canada. Lithos 76:1–27

Ripley BD (1987) Stochastic simulation. Wiley, New York

Strebelle S (2002) Conditional simulation of complex geological structures using multiple point statistics. Math Geol 34:1–22

Swami A, Giannakis GB, Mendel JM (1990) Linear modelling of multidimensional non-Gaussian processes using cumulants. Multidimension Syst Signal Process 1:11–37

Tjelmeland H (1998) Markov random fields with higher order interactions. Sacndinavian J Stat 25:415–433

Tjelmeland H, Eidsvik J (2005) Directional metropolis: hastings updates for posteriors with nonlinear likelihoods. In: Geostatistics Banff. Springer, pp 95–104

Zhang T, Switzer P, Journel AG (2006) Filter-based classification of training image patterns for spatial simulation. Math Geosci 38:63–80

Optimising a Mineral Supply Chain Under Uncertainty with Long-Term Sales Contracts

J. Zhang and R. Dimitrakopoulos

Abstract A two-stage stochastic mixed integer non-linear program is formulated for a mining complex to optimize strategic and tactical plans. The objective is to find the near optimal decisions for a mineral supply chain in the context with uncertainties in both ore supply and the commodity market (price and demand). The endogenous spot price in the commodity market and long-term sales contracts are considered in the formulation of the mining complex's optimization model and an ad hoc heuristic is developed to deal with the throughput- and head-grade-dependent recovery rate in processing plants. Numerical results indicate that the proposed heuristic is effective and efficient in numerical tests. Based on the proposed model and heuristic, a long-term contract design strategy is proposed for making decisions on the contract price and strategic investments. A shadow price based method is also proposed to evaluate the existing mining schedule.

Introduction

A mining supply chain is an end-to-end supply chain including all value-added production operations from the procurement of raw materials to the delivery of final products (or commodity). A typical mining supply chain in the contex of a "mining complex", consists of mines, waste dumps, ore stockpiles, processing plants, product warehouses and fleet vehicles for product transportation (Montiel and Dimitrakopoulos 2015; Goodfellow and Dimitrakopoulos 2016). When mining complexes are considered, integrated mining supply chains are formed to provide comprehensive mine-to-port supply of materials/commodities, including mining and processing ore, generating products (gold bullion, copper concentrate, iron supply, and so on) and transportation. In this work, stochastic modelling and solving techniques are used to find the near optimal decisions for a mining complex

J. Zhang (✉) · R. Dimitrakopoulos
COSMO—Stochastic Mine Planning Laboratory, McGill University, Montreal, QC, Canada
e-mail: jian.zhang9@mail.mcgill.ca

R. Dimitrakopoulos (ed.), *Advances in Applied Strategic Mine Planning*,
https://doi.org/10.1007/978-3-319-69320-0_45

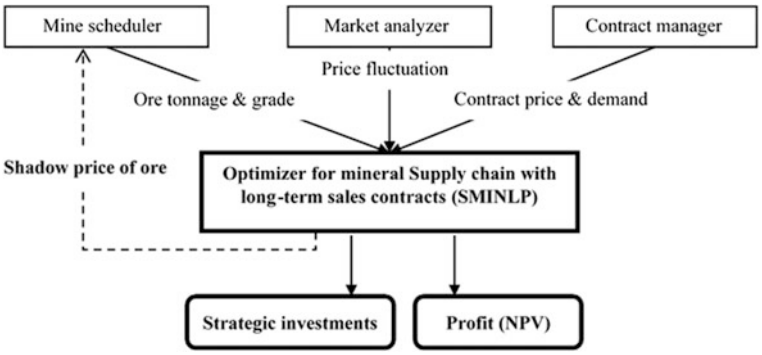

Fig. 1 The decision support system for mineral supply chain optimization with long-term sales contracts

to maintain its profitability in the context with uncertainties in both ore supply and the commodity market. Research todate focusses only on ore supply and related uncerrainty (Montiel and Dimitrakopoulos 2015, 2017 in this volume; Goodfellow and Dimitrakopoulos 2016, 2017 in this volume).

The mineral supply chain optimisation model proposed herein, as shown in Fig. 1, uses the data obtained from three program modules, i.e., mine scheduler, market analyser and contract manager, which are assumed already available. The spot market and contracted customers are considered in the proposed model. The dynamic recovery rate that depends on the head grade of the feeding material and the throughput of a processing plant is also considered. A sales contract designing strategy is proposed using the proposed model and heuristic.

The remainder of this paper is organized as follows. In Sect. "Notation and Planning Assumptions", the notation and assumptions for the optimization model are provided. In Sect. "Model and Heuristic", a stochastic mixed integer nonlinear program is formulated and the corresponding solving heuristic is developed. A series of numerical tests are conducted in Sect. "Model and Heuristic" to show the accuracy and the efficiency of the proposed heuristic. In Sect. "Designing Long-term Sales Contract", a long-term sales contract design strategy based on the proposed model and heuristic is proposed. Section "Conclusions" contains the remarks of conclusions and future work.

Notation and Planning Assumptions

The mining complex's planning horizon is T time periods, and $t \in \{1, \ldots, T\}$ is the period index. The uncertainty of the mining complex as considered here includes metal (geological) uncertainty and commodity price (market) uncertainty represented by scenarios. Each scenario combines both sources of uncertainty. Let S be the total number of scenarios that account for the uncertainties of both mineral deposits and

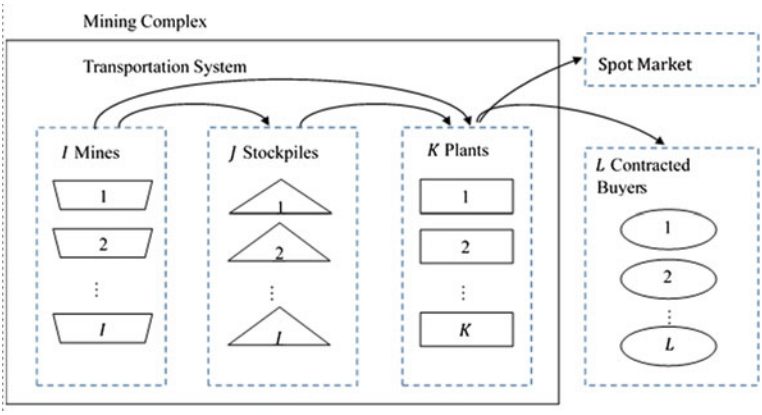

Fig. 2 The structure of the mineral supply chain studied in this work

commodity markets, and $s \in \{1, \ldots, S\}$ is the scenario index. The mining complex includes a number of mines, stockpiles, processing plants and fleet vehicles for transporting material and products (as shown in Fig. 2). The detailed assumptions for each facility in a mining complex are described below.

Mines A mining complex consists of I mines each of which is indexed by $i \in \{1, \ldots, I\}$. For each mine, the mining schedule is predetermined and hence the tonnage and the grade of the extracted material are treated as exogenous. Because of the geological uncertainty, the tonnage and the grade of ore extracted in each period are stochastic. Because the mine production schedule is assumed to be predetermined in this work, the tonnage and the grade of the ore eactracted in each period can be simulated. The tonnage and the grade of ore extreacted in each period are denoted by $o_{its} \in [0, +\infty)$ and $g^M_{its} \in (0, 1)$, respectively, where the superscript M indicates that the symbol is associated with a "Mine". After the material is extracted from a mine, it can be sent to either a processing plant or a stockpile.

Stockpiles The mining complex has J stockpiles each of which is indexed by $j \in \{1, \ldots, J\}$. A stockpile only accepts the material of a particular type which is determined by certain parameters such as grade, hardness, composition, etc. A waste pile can also be treated as a special stockpile if the wate is treated special ore of which the grade is below the cutoff grade for waste. For clarity, a binary parameter, denoted by $a_{ijts} \in \{0, 1\}$ is used to indicate if stockpile j accepts material extracted from mine i in scenario s and period t. Because a material stockpile is not homogeneous and it is usually the case that only the surface is accessible for grade test (Holmes 2004), the grade of the material from a stockpile can only be tested when it is being moved. Thus, the grade of the material from a stockpile is treated as exogenous and stochastic. Let $g^H_{jts} \in (0, 1)$ be the grade of material from stockpile j, where the superscript H indicates that the symbol is associated with a "Stockpile". The tonnage of material stocked in stockpile j is denoted by

$v^H_{jts} \in [0, +\infty)$. The flow from mine i to stockpile j is denoted by $x^{MH}_{ijts} \in [0, +\infty)$, and the cost of transporting a unit tonnage material is denoted by $c^{MH}_{ij} \in [0, +\infty)$. Because c^{MH}_{ij} can also capture other costs incurred at stockpile j, we do not use an additional parameter to denote the rehandling cost.

Processing plants The mining complex has K processing plants each of which is indexed by $k \in \{1, \ldots, K\}$. For any plant k, the head grade of the feeding material is denoted by $g^P_{kts} \in (0, 1)$, where the superscript P indicates that the symbol is associated with a "Processing plant". The head grade should satisfy $g^P_{kts} \in \left[\underline{g}^P_{kts}, \bar{g}^P_{kts}\right]$ to meet the requirements of the processing method employed by plant k. The unit processing cost for plant k is denoted by $c^P_{kts} \in [0, +\infty)$. The throughput in plant k, denoted by $v^P_{kts} \in [0, +\infty)$, is constrained by plant k's processing capacity $\bar{v}^P_{kts}$. The recovery rate in a processing plant is dynamic depending on the throughput and the head grade. Plant k's recovery rate function is denoted by $f^P_k\left(v^P_{kts}, g^P_{kts}\right)$ which is decreasing in v^P_{kts} and increasing in g^P_{kts} based on the observations by Hadler et al. (2010) and Splaine et al. (1982). The material flow from mine i to plant k is denoted by $x^{MP}_{ikts} \in [0, +\infty)$, and $c^{MP}_{ik} \in [0, +\infty)$ is the unit transportation cost. Similarly, the material flow from stockpile j to plant k is denoted by $x^{HP}_{jkts} \in [0, +\infty)$, and $c^{MH}_{ik} \in [0, +\infty)$ is the unit transportation cost.

The spot market and the contracted buyers The mining complex sells its commodity to contracted buyers at contract prices or to "uncontracted" buyers in the spot market at the *spot price*. The spot price fluctuates and is influenced by the mining complex's commodity supply. Let x^U_{kts} be plant k's commodity supply to the spot market, and c^U the expected transaction cost of selling a unit tonnage of commodity to the spot market, where the superscript U indicates that the symbol is associated with the "uncontracted" spot market. The spot price is obtained as $p^U_{ts} - \eta_{ts} \sum_{k=1}^{K} x^U_{kts}$ where p^U_{ts} and η_{ts} are random parameters reflecting market status. η_{ts} is the spot price's sensitivity to the mining complex's commodity supply and depends on the mining complex's market share. In the literature, similar assumptions can be found in the articles reviewed by Yano and Gilbert (2004). The mining complex has L contracted buyers each of which is indexed by $l \in \{1, \ldots, L\}$. The contract price and demand for buyer l are denoted by $p^C_l \in [0, +\infty)$ and $d^C_{lt} \in [0, +\infty)$, respectively, where the superscript C indicates that the symbol is associated with a "contract" buyer. If buyer l's contract demand is not fulfilled by the mining complex, a penalty of $\bar{p}^U_{ts} - p^C_l$ is incurred for each unit of shortage to ensure the contracted buyer to find an alternative supply. The quantity of the unfulfilled demand is denoted by $d^-_{lts} \in [0, +\infty)$ for buyer l. The commodity flow from plant k to buyer l is denoted by $x^{PB}_{klts} \in [0, +\infty)$, and the unit transportation cost is denoted by $c^{PB}_{kl} \in [0, +\infty)$.

Transportation system Without loss of generality, the mining complex's transportation system is simplified to two subsystems: *internal* and *outbound* subsystems. The internal subsystem transports material between mines, stockpiles and processing plants, and the outbound subsystem transport commodity from processing plants to buyers. The internal and outbound transportation capacities are determined by the number of trucks $\bar{y}^{INT} \in \{0, 1, \ldots\}$ and $\bar{y}^{OUT} \in \{0, 1, \ldots\}$ denote the numbers of existing internal and outbound trucks, respectively. $u \in [0, +\infty)$ is the transportation capacity of each truck. The mining complex can expand the capacity of its internal and/or outbound transportation system by adding $y^{INT} \in \{0, 1, \ldots\}$ and/or $y^{OUT} \in \{0, 1, \ldots\}$ trucks at a cost of $\tau \in R_{[0,+\infty)}$. for each.

The profit of a mining complex is evaluated by its net present value (NPV) that accounts for the time value of the cash flows in all planning periods. The rate of

Table 1 List of notation

Symbol	Description[a]
Indices:	
$s \in \{1, \ldots, S\}$	Scenario index
$t \in \{1, \ldots, T\}$	Period index
$i \in \{1, \ldots, I\}$	Mine index
$j \in \{1, \ldots, J\}$	Stockpile index
$k \in \{1, \ldots, K\}$	Plant index
$l \in \{1, \ldots, L\}$	Contracted buyer index
Parameters:	
$\gamma \in R_{[0,+\infty)}$	The mining complex's rate of return
$o_{its} \in R_{[0,+\infty)}$	Ore tonnage extracted from mine i
$g^M_{its} \in R_{(0,1)}$	Ore grade extracted from mine i
$a_{ijts} \in \{0, 1\}$	Indicate if mine i's material is acceptable to stockpile j
$g^H_{its} \in R_{(0,1)}$	Material grade obtained from stockpile j
$c^{MH}_{ij} \in R_{[0,+\infty)}$	Unit transportation cost from mine i to stockpile j
$\underline{g}^P_k, \bar{g}^P_k \in R_{[0,+\infty)}$	Plant k's lower and upper limits for acceptable head grade
$c^P_k \in R_{[0,+\infty)}$	Plant k's unit processing cost
$\bar{v}^P_k \in R_{[0,+\infty)}$	Plant k's processing capacity
$\alpha_k \in R_{(0,1)}, \beta^V_k, \beta^G_k \in R_{[0,+\infty)}$	Parameters of plant k's recovery function
$c^{MP}_{ik} \in R_{[0,+\infty)}$	Transportation cost from mine i to plant k
$c^{HP}_{jk} \in R_{[0,+\infty)}$	Transportation cost from stockpile j to plant k
$p^U_{ts} \in R_{[0,+\infty)}$	Spot price without the mining complex's commodity supply
$\eta_{ts} \in R_{[0,+\infty)}$	Spot price's sensitivity to the mining complex's total commodity supply
$c^U \in R_{[0,+\infty)}$	The expected unit transaction cost of selling in the spot market

(continued)

Table 1 (continued)

Symbol	Description[a]
$p_l^C \in R_{[0,+\infty)}$	Buyer l's contracted price
$d_{lt}^C \in R_{[0,+\infty)}$	Buyer l's contracted demand
$u^{INT}, u^{OUT} \in R_{[0,+\infty)}$	Capacities of an equipment for internal and outbound transportation
$\bar{y}^{INT}, \bar{y}^{OUT} \in Z_{[0,+\infty)}$	Quantities of the existing internal and outbound trucks
$\tau^{INT}, \tau^{OUT} \in R_{[0,+\infty)}$	Cost of a unit internal and outbound trucks
Strategic variables:	
$y^{INT}, y^{OUT} \in Z_{[0,+\infty)}$	Quantities of new internal and outbound trucks
Tactical variables:	
$x_{ijts}^{MH} \in R_{[0,+\infty)}$	Material flow from mine i to stockpile j
$x_{ikts}^{MP} \in R_{[0,+\infty)}$	Material flow from mine i to plant k
$x_{jkts}^{HP} \in R_{[0,+\infty)}$	Material flow from stockpile j to plant k
$x_{klts}^{PB} \in R_{[0,+\infty)}$	Commodity flow from plant k to buyer l
$x_k^U \in R_{[0,+\infty)}$	Plant k's supply to the spot market
Intermediate variables:	
$v_{jts}^H \in R_{[0,+\infty)}$	Stockpile j's tonnage
$v_{kts}^P \in R_{[0,+\infty)}$	Plant k's throughput
$g_{kts}^P \in R_{[0,+\infty)}$	Plant k's head grade
$d_{lts}^- \in R_{[0,+\infty)}$	Buyer l's unfulfilled demand
Function:	
$f_k\left(v_{kts}^P, g_{kts}^P\right)$	Compute plant k's recovery rate from its throughput and head grade

[a]The descriptions for subscripts t and s, representing period- and scenario-dependant, are omitted

return for each planning period is denoted by γ. For clarity, the notation defined in this section is listed in Table 1.

Model and Heuristic

In this section, the problem is formulated as a 2-stage stochastic mixed integer nonlinear program (SMINLP) and a constructive heuristic is developed following the model.

Model

The mining complex's objective function is to maximize its expected profit over the planning horizon as

$$\begin{aligned} \textit{Maximize}\ \frac{1}{S}\sum_{s=1}^{S}\sum_{t=1}^{S}\frac{1}{[1+\gamma]^t}\Bigg[& \underbrace{\left[p_{ts}^{U}-\eta_{ts}\sum_{k=1}^{K}x_{kts}^{U}-c^{U}\right]\sum_{k=1}^{K}x_{kts}^{U}+\sum_{l=1}^{L}\sum_{k=1}^{K}p_{l}^{C}x_{klts}^{PB}}_{(i)} \\ & -\Bigg[\underbrace{\sum_{j=1}^{J}\sum_{i=1}^{I}c_{ij}^{MH}x_{ijts}^{MH}+\sum_{k=1}^{K}\sum_{i=1}^{I}c_{ik}^{MP}x_{ikts}^{MP}+\sum_{k=1}^{K}\sum_{j=1}^{J}c_{jk}^{HP}x_{jkts}^{HP}+\sum_{l=1}^{L}\sum_{k=1}^{K}c_{kl}^{PB}x_{klts}^{PB}}_{(ii)}\Bigg]-\sum_{k=1}^{K}\underbrace{c_{k}^{P}v_{kts}^{P}}_{(iii)} \\ & -\underbrace{\sum_{l=1}^{L}\left[p_{t}^{U}-p_{l}^{C}\right]d_{lts}^{-}}_{(iv)}\Bigg]-\underbrace{\tau^{INT}y^{INT}-\tau^{OUT}y^{OUT}}_{v}. \end{aligned} \tag{1}$$

In the objective function (1), (i) computes the gross profit from the spot market and the contracted customers, (ii) computes the total transportation cost, (iii) computes the total processing cost incurred in processing plants, (iv) computes the total penalty incurred for not fulfilling contract demands, and (v) computes the total strategic investment considered in this work. As noted earlier, any scenario s contains a combination of simulated parameters that account for the uncertainties in both geology and commodity market, and the expected profit is obtained by averaging the profit obtained in each scenario.

The constraints of the model are formulated as follows.

Mine constraint:

$$o_{its}=\sum_{j=1}^{J}x_{ijts}^{MH}+\sum_{k=1}^{K}x_{ikts}^{MP},\quad \forall i,t,s. \tag{2}$$

(2) constrains that at any mine j, the total amount of flows to stockpiles and processing plants equals to mine j's yield.

Stockpile constraints:

$$x_{ijts}^{MH} \le a_{ijts} M \quad \forall i, j, t, s. \tag{3}$$

$$v_{jts}^{H} = v_{j,t-1,s}^{H} + \sum_{i=1}^{I} x_{ijts}^{MH} - \sum_{k=1}^{K} x_{jkts}^{HP}, \quad \forall j, t, s. \tag{4}$$

(3), where M is a large constant, determines whether the material extracted from mine i is acceptable to stockpile j. (4) computes the stock level in stockpile j in each period.

Plant constraints:

$$v_{kts}^{P} = \sum_{i=1}^{I} x_{ikts}^{MP} + \sum_{j=1}^{J} x_{jkts}^{HP}, \quad \forall k, t, s. \tag{5}$$

$$g_{kts}^{P} = \frac{\sum_{i=1}^{I} g_{its}^{M} x_{ikts}^{MP} + \sum_{j=1}^{J} g_{jts}^{H} x_{jkts}^{HP}}{v_{kts}^{P}}, \quad \forall k, t, s. \tag{6}$$

$$\underline{g}_{k}^{P} v_{kts}^{P} \le \sum_{i=1}^{I} g_{its}^{M} x_{ikts}^{MP} + \sum_{j=1}^{J} g_{jts}^{H} x_{jkts}^{HP} \le \bar{g}_{k}^{P} v_{kts}^{P}, \quad \forall k, t, s. \tag{7}$$

$$\left[\sum_{i=1}^{I} g_{its}^{M} x_{ikts}^{MP} + \sum_{j=1}^{J} g_{jts}^{H} x_{jkts}^{HP} \right] f_k\left(v_{kts}^{P}, g_{kts}^{P}\right) = x_{kts}^{U} + \sum_{l=1}^{L} x_{klts}^{PB}, \quad \forall k, t, s. \tag{8}$$

$$v_{kts}^{P} \le \bar{v}_{k}^{P}. \quad \forall k, t, s. \tag{9}$$

(5) and (6) compute the throughput and the head grade of plant k, respectively. (7) constrains the material fed to plant k to meet plant k's requirements on head grade. (8) computes the plant k's commodity output based on its material input and recovery rate function, and the commodity is sent to contracted customers and the spot market. (9) constrains plant k's throughput to be within its processing capacity.

Transportation constraints:

$$\sum_{j=1}^{J} \sum_{i=1}^{I} x_{ijts}^{MH} + \sum_{k=1}^{K} \sum_{i=1}^{I} x_{ikts}^{MP} + \sum_{k=1}^{K} \sum_{j=1}^{J} x_{jkts}^{HP} \le u\left[\bar{y}^{INT} + y^{INT}\right], \quad \forall t, s. \tag{10}$$

$$\sum_{l=1}^{L} \sum_{k=1}^{K} x_{klts}^{PB} \le u\left[\bar{y}^{OUT} + y^{OUT}\right], \quad \forall t, s. \tag{11}$$

(10) and (11) constrain the transportation to be within an expandable capacity. Because the transport distance is usually in proportion to the unity transportation cost, here the unit transportation cost is used as the transport distance without loss of generality.

***Penalty constraint*:**

$$\sum_{k=1}^{K} x_{klts}^{PB} + d_{lts}^{-} = d_{lt}^{C}, \quad \forall l, t, s. \tag{12}$$

(12) computes the unfulfilled demand for each contracted buyer in any period t and scenario s.

Solution Heuristic

From the model above, it can be observed that because the recovery rate function in a processing plant, in (8), depends on throughput and head grade, the mining complex has to solve a nonconvex nonlinear program, which is difficult to solve using general methods. Hence, a heuristic is developed to solve the proposed program.

Because our heuristic is iteration-based, for clarity, we use a hat mark, "ˆ", to label a constant parameter equal to optimal solution of the corresponding variable obtained in the previous iteration. The main idea for modifying the program is removing the non-convexity by fixing the inputs of the recovery rate function. Thus, in each iteration, constraints (6), (8) and (9) are substituted with

$$F_k\left(0, \hat{g}_{kts}^{P}\right) + v_{kts}^{P} F_k'\left(0, \hat{g}_{kts}^{P}\right) + \kappa_{kts}^{G1} z_{kts}^{G} \geq x_{kts}^{U} + \sum_{l=1}^{L} x_{klts}^{PB}, \quad \forall k, t, s. \tag{13}$$

$$F_k\left(v_{kts}^{\prime P}, \hat{g}_{kts}^{P}\right) + \left[v_{kts}^{P} - v_{kts}^{\prime P}\right] F_k'\left(v_{kts}^{\prime P}, \hat{g}_{kts}^{P}\right) + \kappa_{kts}^{G2} z_{kts}^{G} \geq x_{kts}^{U} + \sum_{l=1}^{L} x_{klts}^{PB}, \quad \forall k, t, s. \tag{14}$$

$$z_{kts}^{G} = \sum_{i=1}^{I} g_{its}^{M} x_{ikts}^{MP} + \sum_{j=1}^{J} g_{jts}^{H} x_{jkts}^{HP} - \hat{g}_{kts}^{P} v_{kts}^{P}, \quad \forall k, t, s. \tag{15}$$

$$\Delta^{G} v_{kts}^{P} \leq z_{kts}^{G} \leq \Delta^{G} v_{kts}^{P}, \quad \forall k, t, s. \tag{16}$$

$$v_{kts}^{P} \leq v_{kts}^{\prime P}, \quad \forall k, t, s. \tag{17}$$

In the modified constraints above, $F_k\left(v, \hat{g}_{kts}^{P}\right)$ can be obtained as

$$F_k\left(v, \widehat{g}_{kts}^P\right) = \widehat{g}_{kts}^P \times v \times f_k\left(v, \widehat{g}_{kts}^P\right),$$

And $F_k'\left(v, \widehat{g}_{kts}^P\right)$ is the first-order derivative of $F_k\left(v, \widehat{g}_{kts}^P\right)$ with respect to v.

The throughput in the recovery function is set to 0 and $v_{kts}'^P$ in (13) and (14), respectively, for outer linearization. Additional terms, $\kappa_{kts}^{G1} z_{kts}^G$ and $\kappa_{kts}^{G2} z_{kts}^G$, are introduced in the left-hand side of (8) to correct the error incurred by fixing head grade.

Because for any k, t and s, the optimal setting of $v_{kts}'^P$ in the recovery function always makes (17) bind, in our heuristic, $v_{kts}'^P$ for all k, t and s are gradually reduced from its maximum value, $\overline{v}_k^P$, until the slack of constraint (17) is small enough for any k, t and s.

Numerical Test

The proposed heuristic is tested through a series of numerical experiments. The parameters of the mining complex's optimization problem are simulated as in Table 2. To test the accuracy of the proposed heuristic, the proposed heuristic is first compared with Lingo Global Solver, which is capable of solving general nonlinear program, through a small-scale problem with a planning horizon of 2 periods. For Lingo global solver, the limit of computation time is set to 2 h. The objective value obtained by Lingo global solver and the proposed heuristic are displayed in Fig. 3. It can be observed that within reasonable computation time, the solutions found by Lingo global solver are worse than the ones found by the proposed heuristic, and the proposed heuristic requires much less computation time to solve the test problems at different scales

Table 2 Parameters settings in the hypothetical case

Category	Parameter settings
Mines	$I = 2$, $o_{its} \sim U(2500, 3000)$, $g_{its}^M \sim U(0, 1)$
Stockpiles	$J = 2$, $\underline{g}_j^H = [j-1]/2$, $\bar{g}_j^H = j/2$, $g_{jts}^H \sim U\left(\underline{g}_j^H, \bar{g}_j^H\right)$
Processing plants	$K = 2$, $\underline{g}_k^P = U(0.1, 0.5)$, $\bar{g}_k^P = \underline{g}_k^P + 0.5$, $c_k^P \sim U(0.5, 1)$, $\bar{v}_k^P = 3000$, $f_k\left(v_{kts}^P, g_{kts}^P\right) = \beta_k^0 - \beta_k^1 v_{kts}^P + \beta_k^2 g_{kts}^P$ where $\beta_k^0 \sim U(0.6, 0.7)$, $\beta_k^1 \sim U(0.00005, 0.0001)$ and $\beta_k^2 \sim U(0.2, 0.3)$
Contracted buyers	$L = 3$, $p_l^C \sim U(8, 10)$, $d_{lt}^C \sim U(500, 1000)$
Spot market	$\bar{p}_{ts}^U \sim U(15, 25)$, $\eta_{ts} \sim U(0, 0.001)$, $c^U = 1$
Transportation	$c_{ij}^{MH} \sim U(0.5, 1)$, $c_{jk}^{HP} \sim U(0.5, 1)$, $c_{ik}^{MP} = min_j\left[c_{ij}^{MH} + c_{jk}^{HP}\right] - 0.1$, $c_{kl}^{PB} \sim U(0.5, 1)$, $\bar{y}^{INT} = \bar{y}^{OUT} = 0$, $u^{INT} = u^{OUT} = 50$, $\tau^{INT} = \tau^{OUT} = 100$
Other	$\gamma = 0.01$

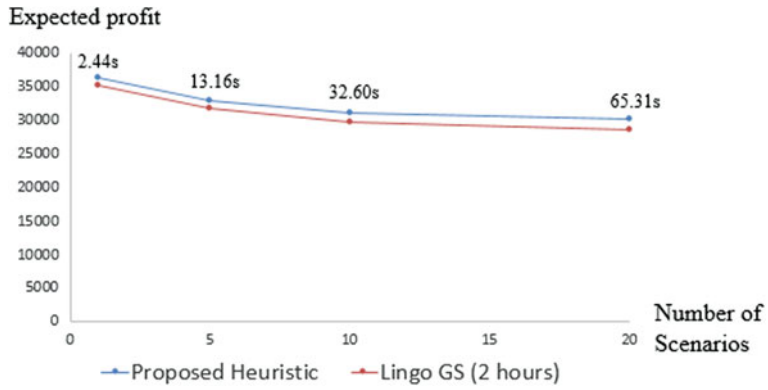

Fig. 3 Results of small-case test

The efficiency of the proposed heuristic is tested for larger problem with 24 periods and the 100 scenarios. Because the Lingo Global Solver cannot solve the modified program at this scale, the heuristic is programed using CPLEX OPL script. It takes 1498.74 s for the proposed heuristic to solve the problem. Figure 4a and Fig. 4b shows the averages of $v'^{P}_{kts} - v^{P}_{kts}$ and $\left|g^{P}_{kts} - \widehat{g}^{P}_{kts}\right|$ for all k, t and s, and Fig. 4c shows the change of the obtained objective value as the heuristic progresses.

Designing Long-Term Sales Contract

A long-term sales contract specifies the price and the purchase quantity of the commodity produced by the mining complex. For clarity, we use "principal buyer" ($l = 1$) to refer to the buyer that is currently signing a long-term sales contract with the mining complex. In the contract negotiating phase, a common assumption is made that the principle buyer's preference on the contracted demand is price-sensitive, which reflects a practice that the contract demand increases with quantity discount. A good review of the operations literature on quantity discounts can be found in Viswanthan and Wang (2003). Without loss of generality, the relationship between the price quote and the principal customer's contracted demand is simplified to be linear as

$$d^{C}_{1t}\left(p^{C}_{1}\right) = \bar{d}_{1t} - \alpha_{1t} p^{C}_{1}$$

where $\bar{d}_{1t}$ and α_{1t} represents the principal buyer's willingness to buy and demand-price sensitivity, respectively. The mining complex's maximum expected profit can be estimated using the proposed model and heuristic if the contract is signed at any contract price p^{C}_{1}. The worst-case profit, which is the lowest possible profit that can be obtained from the scenarios considered in the optimization model,

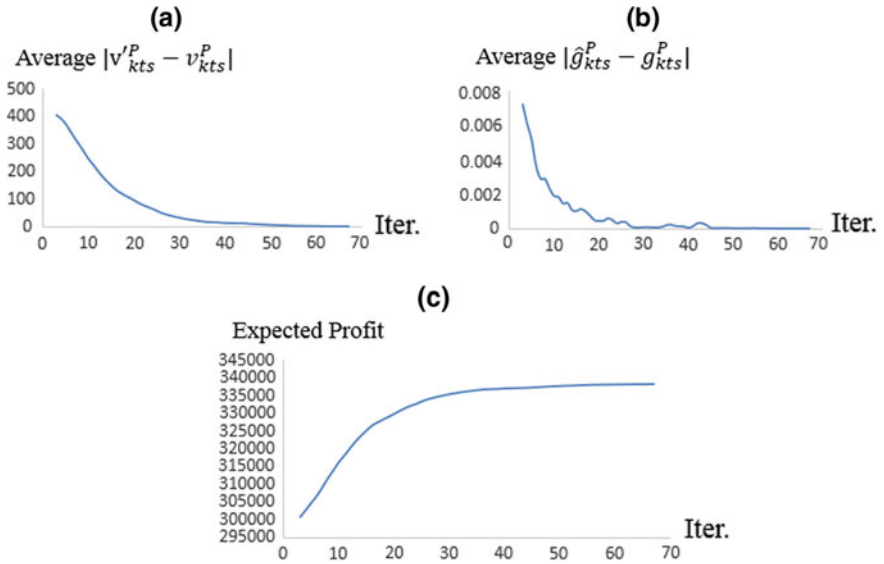

Fig. 4 Convergence curve for solving a large-scale problem ($T = 24$, $S = 100$)

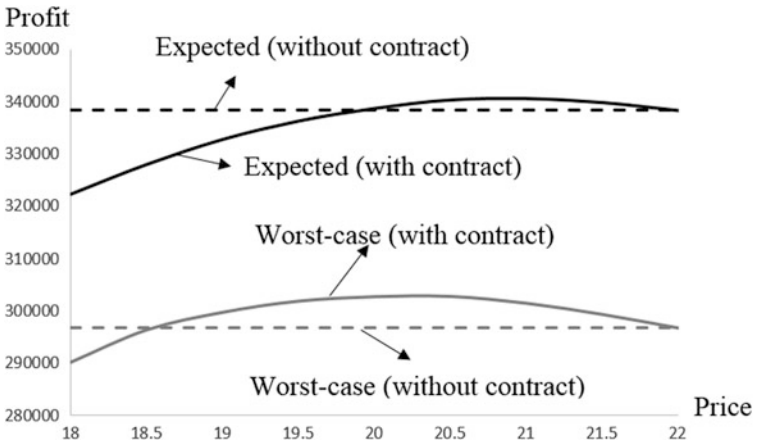

Fig. 5 The mining complex's expected profit and worst-case profit at different contract prices

is also evaluated as a consideration factor to decide if a contract offer should be accepted. The worst-case scenario usually includes parameters with low yield of ore tonnage and grade, and low market price and demand. We demonstrate the implementation of the proposed contract design strategy by a hypothetical case with the identical settings as in Sect. 3. Without loss of generality, the principal buyer's parameters are set to $\bar{d}_{1t} = 2200$ and $\alpha_{1t} = 100$ for all $t \in \{1, \ldots, 24\}$. Figure 5 shows the mining complex's expected profit and the worst-case profit at different

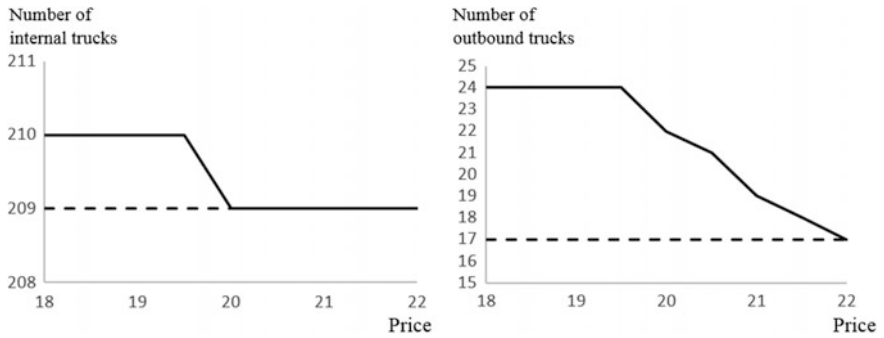

Fig. 6 Optimal strategic investment at different contract prices

contract prices. The dashed line shows the mining complex's expected profit and the worst-case profit if the contracted demand is 0, which is equivalent to the case without the present contract. It can be observed that when the contract price is over 19.5, the contract brings positive profit to the mining complex, and the mining complex's expected profit is maximized if the contract can be signed at $p_1^C = 21$. When the contract price is lower than 20 but higher than 18.5, the risk-averse mining complex still has an incentive for signing the contract because the worst-case profit with the present contract is higher than the one obtained without the present contract.

Figure 6 shows the mining complex's optimal strategic investments, which are the expansions of internal and outbound transportation capacities, at different contract prices, and the dashed lines are the mining complex strategic investment without the present contract. It can be observed that the requirement for internal transport capacity is not significantly changed as the contracted demand is increasing because the mining complex reduces the sales quantity to spot market to honour contracted demand. When the contracted demand increases to a certain level, the production capacity in the processing plant becomes the bottleneck of the supply chain so that there is no need to continue to increase the outbound transportation capacity and the penalty for undelivered demand is increased to reduce the mining complex's expected profit.

Conclusions

For a mining supply chain, the uncertainties in mineral deposits (material types, ore grade and tonnage) and the commodity market (price and demand) should be considered in making strategic decisions to maximize the profit of the entire supply chain. In this work, a stochastic nonlinear mixed integer programming model is proposed to help a mining complex to make decisions in signing a long-term sales contract to deal with the uncertainties existing in both ends of a mineral supply chain. Due to the complexity in solving the proposed nonconvex and nonlinear

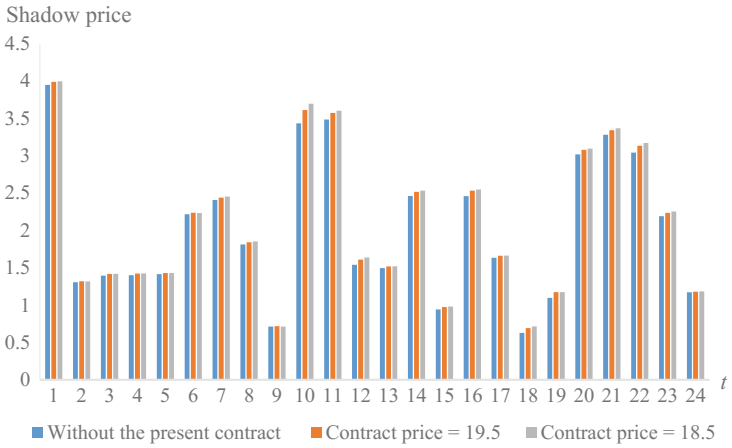

Fig. 7 The shadow price of ore extracted at different periods

model, a heuristic is developed and tested by a number of numerical experiments. The result shows that can find a near optimal solution efficiently.

As a suggestion for the future research, methodology in mining scheduling based on ore shadow prices (or dual price) will be studied, and the shadow-price-based mine production scheduling method will account for the cost, the profit and the uncertainty incurred in mineral resource supply chain regardless of the complex structure of the supply chain. (Figure 7)

References

Goodfellow R, Dimitrakopoulos R (2016) Global optimization of open pit mining complexes with uncertainty. Appl Soft Comput 40:292–304

Goodfellow R, Dimitrakopoulos R (2017) Simultaneous stochastic optimisation of mineral value chains: developments and applications with technical risk management, in this volume

Hadler K, Smith C, Cilliers J (2010) Recovery vs. mass pull: the link to air recovery. Miner Eng 23 (11):994–1002

Holmes RJ (2004) Correct sampling and measurement the foundation of accurate metallurgical accounting. Chemometr Intell Lab Syst 74(1):71–83

Montiel L, Dimitrakopoulos R (2015) Optimizing mining complexes with multiple processing and transportation alternatives: an uncertainty-based approach. Eur J Oper Res 247:166–178

Montiel L, Dimitrakopoulos R (2017) Simultaneously optimizing open pit and underground mining operations under geological uncertainty, in this volume

Splaine M, Browner S, Dohm C (1982) The effect of head grade on recovery efficiency in a gold-reduction plant. J S Afr Inst Min Metall 82(1):6–11

Viswanthan S, Wang Q (2003) Discount pricing decisions in distribution channels with price sensitive demand. Eur J Oper Res 149:571–587

Yano CA, Gilbert SM (2004) Coordinated pricing and production/procurement decisions: a review. In: Managing business interfaces, Springer, pp 65–103